به نام خدا

مرکز دانلود رایگان
مهندسی متالورژی و مواد

---

www.Iran-mavad.com

Handbook of Extractive Metallurgy

Edited by Fathi Habashi

Volume I: The Metal Industry
Ferrous Metals

WILEY-VCH

Weinheim · Chichester · New York · Toronto · Brisbane · Singapore

Professor Fathi Habashi
Université Laval
Département de Mines et de Métallurgie
Québec G1K 7P4
Canada

Editorial Directors: Karin Sora, Ilse Bedrich
Production Manager: Peter J. Biel
Cover Illustration: Michel Meyer/mmad

Library of Congress Card No. applied for
A CIP catalogue record for this book is available from the British Library

Die Deutsche Bibliothek – CIP-Einheitsaufnahme
Handbook of extractive metallurgy / ed. by Fathi Habashi. –
Weinheim ; New York ; Chichester ; Brisbane ; Singapore ; Toronto :
WILEY-VCH ISBN 3-527-28792-2

Vol. 1. The metal industry, ferrous metals. – 1997

Vol. 2. Primary metals, secondary metals, light metals. – 1997

Vol. 3. Precious metals, refractory metals, scattered metals, radioactive metals, rare earth metals. – 1997

Vol. 4. Ferroalloy metals, alkali metals, alkaline earth metals; Name index; Subject index. – 1997

Composition: Jean François Morin, Québec, Canada
Printing : Strauss Offsetdruck GmbH, D-69509 Mörlenbach
Bookbinding: Wilhelm Oswald & Co., D-67433 Neustadt/Weinstraße

Printed in the Federal Republic of Germany

Preface

Extractive metallurgy is that branch of metallurgy that deals with ores as raw material and metals as finished products. It is an ancient art that has been transformed into a modern science as a result of developments in chemistry and chemical engineering. The present volume is a collective work of a number of authors in which metals, their history, properties, extraction technology, and most important inorganic compounds and toxicology are systematically described.

Metals are neither arranged by alphabetical order as in an encyclopedia, nor according to the Periodic Table as in chemistry textbooks. The system used here is according to an economic classification which reflects mainly the uses, the occurrence, and the economic value of metals. First, the ferrous metals, i.e., the production of iron, steel, and ferroalloys are outlined. Then, nonferrous metals are subdivided into primary, secondary, light, precious, refractory, scattered, radioactive, rare earths, ferroalloy metals, the alkali, and the alkaline earth metals.

Although the general tendency today in teaching extractive metallurgy is based on the fundamental aspects rather than on a systematic description of metal extraction processes, it has been found by experience that the two approaches are complementary. The student must have a basic knowledge of metal extraction processes: hydro-, pyro-, and electrometallurgy, and at the same time he must have at his disposal a description of how a particular metal is extracted industrially from different raw materials and know what are its important compounds. It is for this reason, that this *Handbook* has been conceived.

The *Handbook* is the first of its type for extractive metallurgy. Chemical engineers have already had their Perry's *Chemical Engineers' Handbook* for over fifty years, and physical metallurgists have an impressive 18-volume *ASM Metals Handbook*. It is hoped that the present four volumes will fill the gap for modern extractive metallurgy.

The *Handbook* is an updated collection of more than a hundred entries in *Ullmann's Encyclopedia of Industrial Chemistry* written by over 200 specialists. Some articles were written specifically for the *Handbook*. Some problems are certainly faced when preparing such a vast amount of material. The following may be mentioned:

- Although arsenic, antimony, bismuth, boron, germanium, silicon, selenium, and tellurium are metalloids because they have covalent and not metallic bonds, they are included here because most of them are produced in metallurgical plants, either in the elemental form or as ferroalloys.
- Each chapter contains the articles on the metal in question and its most important inorganic compounds. However, there are certain compounds that are conveniently described together and not under the metals in question for a variety of reasons. These are: the hydrides, carbides, nitrides, cyano compounds, peroxo compounds, nitrates, nitrites, silicates, fluorine compounds, bromides, iodides, sulfites, thiosulfates, dithionites, and phosphates. These are collected together in a special supplement entitled *Special Topics*, under preparation.
- Because of limitation of space, it was not possible to include the alloys of metals in the present work. Another supplement entitled *Alloys* is under preparation.
- Since the largest amount of coke is consumed in iron production as compared to other metals, the articles "Coal" and "Coal Pyrolysis" are included in the chapter dealing with iron.

I am grateful to the editors at VCH Verlagsgesellschaft for their excellent cooperation, in particular Mrs. Karin Sora who followed the project since its conception in 1994, and to

Jean-François Morin at Laval University for his expertise in word processing.

The present work should be useful as a reference work for the practising engineers and the students of metallurgy, chemistry, chemical engineering, geology, mining, and mineral beneficiation. Extractive metallurgy and the chemical industry are closely related; this *Handbook* will therefore be useful to industrial chemists as well. It can also be useful to engineers and scientists from other disciplines, but it is an essential aid for the extractive metallurgist.

Fathi Habashi

Table of Contents

Part One

The Metal Industry

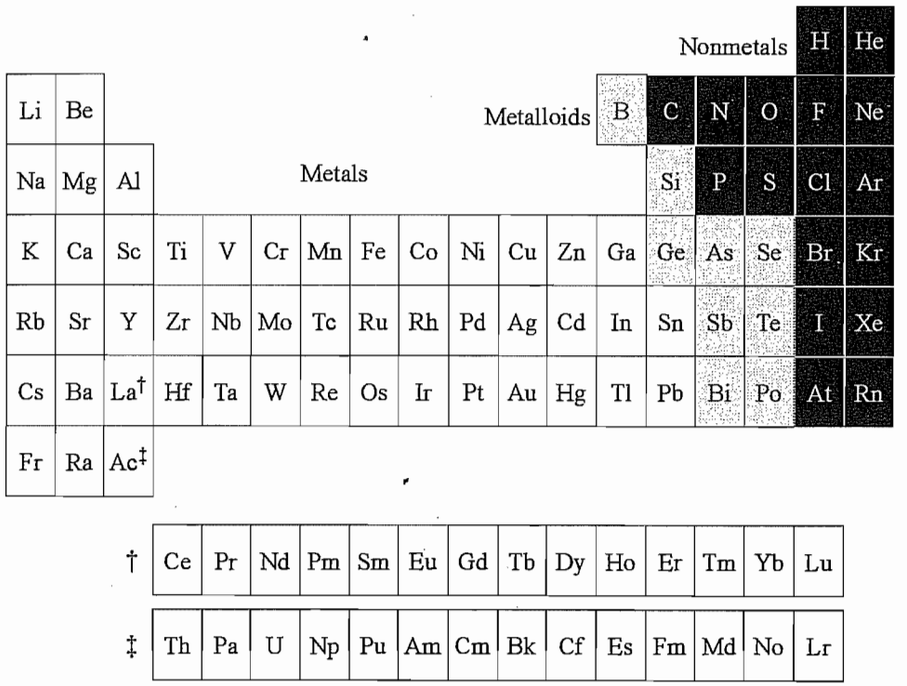

1 The Economic Classification of Metals

FATHI HABASHI

1.1 Introduction

While the Periodic Table classifies metals, metalloids, and nonmetals according to their chemical properties, it does not indicate their relative economic value. The fact that iron and its alloys, e.g., steel, are by far the most important metals from the point of view of production and use, has resulted in the classification of metals as ferrous (iron and its alloys) and nonferrous (all other metals and metalloids). This classification is well justified: the annual production of iron in one year exceeds the production of all other metals combined in ten years.

1.2 Ferrous Metals

Iron produced in the blast furnace (pig iron) is converted into the following commercial products: Steel, wrought iron, cast irons, and pure iron. Table 1.1 shows typical analysis of these products; steel is the most important product. Chemically pure iron is prepared on a small scale because of its limited use.

1.2.1 Steel

Steel is made on a large scale by blowing oxygen and powdered lime through molten iron to oxidize the impurities. According to their use, steels are divided into three main groups:

Constructional Steel. This is used for the manufacture of machine parts, motor cars, building elements, sky scrapers, ships, bridges, war instruments (cannons, tanks, etc.), and containers. It can be carbon or alloy steel. The mechanical properties of alloy steel are considerably higher than those of carbon steel. Chromium and nickel are the main alloying elements used in this category.

Tool Steel. This is used for the manufacture of tools (lathe knives, chisels, cutters, etc.). It is either carbon (0.7–1.2% C), or chromium, manganese, silicon, or tungsten alloy steel. Manganese alloy steels are used to make machines such as rock crushers and power shovels, which must withstand extremely hard use.

Table 1.1: Typical analysis of ferrous materials.

	Pig iron	Cast iron	White cast iron	Steel	Wrought iron
C	3.5–4.25	2.50–3.75	1.75–2.70	0.10	0.02
Si	1.25	0.50–3.00	0.8–1.20	0.02	0.15
Mn	0.90–2.50	0.40–1.00	< 0.4	0.40	0.03
S	0.04	0.01–0.18	0.07–0.15	0.03	0.02
P	0.06–3.00	0.12–1.10	< 0.02	0.03	0.12
Slag	0	0	0	0	3.00

Special-Quality Steel. These include corrosion-resisting, stainless, acid-resisting, and heat-resisting steels. Stainless steel, which contains chromium and sometimes nickel and manganese, is a hard, strong alloy that resists heat and corrosion. Stainless steels are used for such things as jet engines, automobile parts, knives, forks, spoons, and kitchen equipment.

1.2.2 Wrought Iron

Wrought iron was known since antiquity and was the major ferrous material produced until the nineteenth Century; it is produced now in limited amounts. Wrought iron is practically pure iron, low in carbon, manganese, sulfur, and phosphorus, but contains an appreciable amount of slag in mechanical admixture. Its desirable properties are due to the fibrous structure of this slag which gives it excellent resistance to shock and vibration, making it particularly suitable for the manufacture of such products as engine bolts, crane hooks, lifting chains and couplings. Wrought iron is readily welded, and the presence of slag makes it self-fluxing. It is readily machinable and cuttings are sharp and clean because the chips crumble and clear the dies instead of forming long spirals. Wrought iron is made from pig iron by melting in a furnace lined with ferrous oxide. Under these conditions, the entire carbon content of the pig iron is oxidized and removed, as well as most of the other impurities while silicon forms slag. As a result, the melting point of the mass increases and a sticky lump is obtained saturated with slag. the lump, which weighs about 200 kg is removed from the furnace then put through a squeezer to remove as much slag as possible.

1.2.3 Cast Irons

Cast iron is a series of iron-carbon alloys containing more than 1.5% C, together with silicon, manganese, phosphorus, and sulfur which are impurities from the raw material and are not alloying elements. The form in which carbon is present in the cast iron determines its properties.

Grey Cast Iron. Produced by melting pig iron, scrap iron, and steel mixture to give the cast iron composition. The slow cooling and the high silicon content favors the decomposition of cementite into iron and free carbon in the form of flakes. Gray cast iron is characterized by its power to damp vibrations and by the wear resistance imparted by the lubricating effect of graphite. Both properties make it a useful material for the construction of machinery by casting. It is readily machinable (due to graphite flakes) and is an economic material since it has a low melting point of about 1200 °C. It has, however, poor toughness and limited tensile strength.

White Cast Iron. Produced by melting pig iron and steel scrap. After solidification no carbon is precipitated but remains in combination as iron carbide. It is hard, brittle, and unmachinable. It is used for making grinding balls, dies, car wheels, but mostly used for making malleable cast iron.

Malleable Cast Iron. Prepared from white cast iron by annealing for several days, whereby iron carbide is decomposed into iron and graphite in form of nodules. It is more ductile and more resistant to shock than grey cast iron. It is used in large quantities for such materials as pipes and pipe fittings and the automative industry requiring higher mechanical properties.

Ductile Cast Iron. It is a high-carbon ferrous product containing graphite in the form of spheroids. The spheroid is a single polycrysalline particle, whereas the nodule is composed of an aggregate of fine flakes. Ductile cast iron has all the advantages of cast iron, e.g., low melting point, good fluidity and castability, ready machinability, and low cost, plus the additional advantages of high yield strength, high elasticity, and a substantial amount of ductility. It is used by the automotive, agricultural instruments and railroad industries, pumps, compressors, valves, and textile machinery. Ductile cast iron is produced from any cast iron by introducing a small amount of magnesium (in form of a magnesium–nickel alloy containing 50–80% Ni), or cerium into the molten iron while in the ladle, shortly before casting. This addition catalyzes the decomposition of carbon into spheroids and not flakes.

1.2.4 Pure Iron

High-purity iron possesses temporary magnetism, i.e., when the magnetic field is removed, the magnetism disappears. Carbon–iron alloys on the other hand, show permanent magnetism. For this as well as for other reasons, e.g., studying the physical properties of the metal, the preparation of high-purity iron is of scientific interest. Preparation of pure iron is a tedious process that requires special techniques and numerous operations.

1.3 Nonferrous Metals

The nonferrous metals are divided into numerous groups according to their production, properties, use, and occurrence (Table 1.2). This classification is arbitrary since one metal may be placed in two groups, e.g., titanium is both a light and a refractory metal, rhenium is both scattered and refractory; similarly hafnium. The term "rare metals" is sometimes applied to the refractory, scattered, radioactive, and the lanthanides collectively. This terminology is misleading because such metals are not rare; it may be the difficulty in their extraction and uncommon utilization that give the impression that they are rare.

1.3.1 Primary Metals

While iron is the most widely used metal, it lacks important properties such as corrosion resistance. From the beginning of the Nineteenth Century, copper, nickel, lead, zinc, and tin and their alloys found use as substitutes for iron in industrial applications that required particular properties in which cast irons and steels were lacking. That is one reason why these metals are known as primary metals. (Table 1.3).

Table 1.2: Commercial classification of nonferrous metals and metalloids.

Group	Metals	Remarks
Primary	Cu, Pb, Zn, Sn, Ni	Extensively used; second in importance to iron.
Secondary	As, Sb, Bi, Cd, Hg, Co	Mainly by-products of primary metals but also form their own deposits. Used in almost equal amounts (10–20 thousand tons annually).
Light	Be, Mg, Al, Ti	Low specific gravity (below 4.5), used mainly as material of construction.
Precious	Au, Ag, Pt, Os, Ir, Ru, Rh, Pd	Do not rust; highly priced.
Refractory	W, Mo, Nb, Ta, Ti, Zr, Hf, V, Re, Cr	Melting points above 1650 °C. Mainly used as alloying elements in steel but also used in the elemental form. Some resist high temperature without oxidation.
Scattered	Sc, Ge, Ga, In, Tl, Hf, Re, Se, Te	Do not form minerals of their own. Distributed in extremely minute amounts in the earth's crust.
Radioactive	Po, Ra, Ac, Th, Pa, U, Pu	Undergo radioactive decay. Some of them (U, Pu, and Th) undergo fission. Plutonium prepared artificially in nuclear reactors.
Rare earths	Y, La, Ce, Pr, Nd, Sm, Eu, Gd, Tb, Dy, Ho, Er, Tm, Yb, Lu	Always occur together, similar chemical properties. Not rare as the name implies.
Ferroalloy metals	Cr, Mn, Si, B	Were once mainly used as alloying elements to steel, but now also used in elemental form.
Alkali	Li, Na, K, Rb, Cs	Soft and highly reactive.
Alkaline earths	Be, Mg, Ca, Sr, Ba	Higher melting point and less reactive than the alklali metals

Table 1.3: Typical uses of primary metals.

Metal	Use	%
Copper	Electrical	50
	Buildings	20
	Engineering and transport	25
	Other	5
		100
Lead	Batteries	35
	Pipes, sheets	15
	Gasoline additive	12
	Cable sheathing	10
	Pigments, chemicals	10
	Alloys, solder	10
	Other	7
		100
Zinc	Galvanizing	40
	Die casting	27
	Alloys	18
	Sheet, wire, etc.	8
	Zinc compounds	5
	Other	2
		100
Tin	Tinplate	50
	Solder	20
	Alloys	15
	Chemicals	3
	Other	12
		100
Nickel	Stainless steel	28
	Cast irons and alloy steels	20
	Nonferrous alloys	20
	High-temperature alloys	12
	Electroplating	16
	Catalysts	1
	Other	3
		100

Copper. The high heat conductivity of copper makes it a suitable material of construction for heat conducting devices such as heating or cooling coils, boiling kettles, and other parts of chemical engineering apparatus. Because of its high electrical conductivity it became the chief material for conductors, contacts, and other electroconductive parts. It is used only as a pure metal since traces of impurities greatly reduce this property. However, pure copper is too soft for structural components of machines and apparatus. Its alloys with other metals are much stronger and many of them surpass copper in other properties, e.g., in corrosion resistance.

Alloys of copper with 10 to 40% Zn are called brass. They are cheaper then pure copper, can readily be shaped and machined, and are strong, hard and resistant to corrosion. They find extensive application in chemical and general machine-building, ship-building and military engineering. Bronze is an alloy of copper with 6 to 20% tin that found extensive use because of its excellent mechanical, antifriction, and anticorrosion properties. Alloys similar to bronze are prepared by admixing metals other than tin to copper, e.g., aluminum (5–11%), lead (25–33%), silicon (4–5%), and beryllium (1.8–2.3%). Aluminum bronzes with additions of lead are suitable for bearings while beryllium bronzes are used in the manufacture of springs. Copper–nickel alloys (5–35% Ni) and German silver (5–30% Ni and 13–45% Zn) are particularly resistant to attack by aggressive media. They are used to make medical instruments, home appliances, and works of art. Copper was the first among nonferrous metals in world output until 1958 when it was moved to second place by aluminum. In electrical engineering, copper is more and more being replaced by aluminum, which is less electroconductive, but lighter.

Nickel. As compared to other heavy nonferrous metals, nickel is stronger, harder, more refractory and more corrosion resistant. Similar to iron and cobalt, it is ferromagnetic. It is relatively expensive and its consumption as a pure metal is low. Nickel is used for plating metals with a view to protect then against corrosion and for ornamental purposes. Nickel sheets, pipes, and wire are used for special components of apparatus and instruments in the chemical industry. Nickel is also required for the manufacture of certain types of batteries which are lighter, more compact and dependable in operation than lead batteries. Nickel catalysts find their application in many chemical processes.

More than half of nickel is consumed in the manufacture of nickel–iron alloys. Chromium–nickel, stainless, and acid-resistant steels, commonly containing up to 8% Ni and with admixtures of chromium and other metals, are widely used in the chemical industry, machine tool manufacture, building of durable

structures, general machine building, and military engineering. Strong and wear-resistant nickel cast irons, alloyed with chromium, molybdenum, and copper, are necessary for the manufacture of heavy internal combustion engines for locomotives and of special machine tools and dies.

Many nickel alloys are chemically resistant and can withstand temperatures up to 600 °C. They are used for turbines of jet aircraft, gas turbine power plants, and in nuclear reactors. Nichrome (75–85% Ni, 10–20% Cr, the balance iron) and other similar thermoelectric nickel alloys are not only refractory, but possess high electrical resistance and are suitable for wire or strip resistor heaters. Strongly, magnetic alloys of nickel with iron (permalloys) and other similar alloys find extensive application in electrical and radio engineering. Alloys of nickel with copper have been mentioned earlier.

Lead. Lead was used to make coins, ornaments, miscellaneous vessels, and water pipes. With the invention of gun powder, it found use for the manufacture of case-shot, bullets, and shot. Abilities of lead to resist attack by dilute sulfuric and hydrochloric acids and many other chemicals have made the metal the chief material for the chemical industry in the 19th century. Lead is amenable to rolling: sheets 2 to 10 mm thick are suitable for anti-corrosion coating of various apparatus. Sheaths of electric cables intended for prolonged underground service, in water or moist surroundings are made from lead blended with small amounts of other metals to enhance its plasticity. Lead storage batteries are necessary to start internal combustion engines. About half of the lead produced is used in the manufacture of electric cables and storage batteries. In nuclear engineering, lead serves as a shield against γ-rays.

Lead alloys differ from the pure metal either by greater strength and hardness or by antifriction properties, and most of the alloys are resistant to corrosion. Printing alloys for casting type contain antimony, tin, and copper in addition to lead. Antimony makes the alloys hard, while tin greatly improves their castability. Alloys of lead and antimony, hard and corrosion-resistant, find extensive use in chemical engineering. In soldering alloys, or solders, lead may partly replace tin.

Zinc. Zinc protects iron against corrosion in the air and in cold water. More than half of zinc output is consumed for this purpose. Zinc-plating (galvanizing) is considerably cheaper than tin-plating or nickel-plating. Another important field of application is the manufacture of alloys, inclusive of the already mentioned brases and German silver. Zinc-based alloys, partly employed instead of bronzes and low-friction alloys in bearings, contain aluminium (8–11%), copper (1–2% and magnesium (0.03–0.06%). Identical components, but in a different ratio to zinc, are contained in printing alloys, similar in properties to lead–antimony alloys.

Tin. Used in tin-plating, solders, bronze and other alloys. At one time was used for wrapping purposed in form of tinfoil.

1.3.2 Secondary Metals

This group includes the metals cadmium, cobalt, and mercury and the metalloids arsenic, antimony, and bismuth. They are mainly by-products of the primary metals but also form their own deposits. They are used worldwide in almost equal amounts of about 20 000 tons annually (Table 1.4).

Cadmium. Cadmium is used in the metallic form in electroplating and alloying. Cadmium compounds are used in paints and pigments; cadmium sulfide is yellow, and cadmium selenide is red. Cadmium compounds are toxic and therefore care must be taken during processing cadmium and its compounds to avoid inhalation or dispersal of cadmium fumes and dust or the release of cadmium-bearing effluents into the environment.

Cobalt. This metal is used principally in heat and corrosion-resistant alloys, in jet engine parts, and in magnets. It also serves as a binder material in tungsten and other carbide cutting

tools, and in hardfacing alloys. Nonmetallic applications (paint drier, ceramics, and catalysts) account for about 20% of its consumption.

Table 1.4: Typical uses of secondary metals.

Metal	Use	%
Antimony	Batteries	47
	Pigments, chemicals	18
	Fire retardants	11
	Rubber, plastics	8
	Glass, ceramics	6
	Bearing alloys	4
	Other	6
		100
Cadmium	Cadmium plating	50
	Plastics stabilizer	20
	Pigments	15
	Ni–Cd batteries	7
	Other	8
		100
Cobalt	Alloys	45
	Magnets	30
	Paint driers	10
	Ceramics	5
	Catalysts	5
	Other	5
		100
Mercury	Caustic-chlorine cells	35
	Batteries, electrical	28
	Biocidal paints	14
	Instruments	10
	Dental	5
	Agriculture	3
	Other	6
		100

Mercury. In older times mercury was principally used for the recovery of gold and silver from their ores by amalgamation, a process that is now obsolete because of the poisonous nature of the metal vapor. It is now used as a liquid cathode in chlorine and sodium hydroxide manufacture. The mercury lamps use and electric discharge tube that contains mercury vapor; they are more efficient as a light source. Mercury is also used in electrical switching devices, in thermometers and barometers, as an alloy with silver and tin for dental applications. Nonmetallic applications include mercuric oxide in batteries, in certain organic preparations as fungicide, bactericide, or preservative.

Arsenic. Arsenic is regarded as a troublesome impurity in smelting and refining and must be removed during the recovery of the primary metals. Its compounds are toxic and therefore their handling in a plant is costly because of the strict anti-contamination measures. Its consumption in the metallic form is only 3% of the total; it is mostly used as compounds. As metal, it is used as a minor additive in nonferrous alloys (copper and lead based) to improve their strength, and sometimes to improve corrosion resistance. In the electronic industry, high-purity arsenic is combined with gallium and/or indium for making semiconductors, solar cells, infrared detectors, light-emitting diodes, and lasers. Arsenic compounds are mainly used as herbicides and insecticides.

Antimony. Antimony is mainly used as an alloying constituent of lead, e.g., to harden lead for storage batteries, and as alloying element in bearings, type metal, and solder. In compound form antimony trioxide is used in ceramic enamels in plastics, as a white pigment, and as flame retardant.

Bismuth. Bismuth is mainly used for the manufacture of low-melting alloys (m.p. as low as 60 °C) which are used for making safety plugs.

1.3.3 Light Metals

These are beryllium, aluminum, magnesium, and titanium. They are used in pure state and in alloys, characterized by light weight and high strength hence they are valuable materials of construction (Table 1.5). They are reactive metals and difficult to prepare and became known in the metallic state relatively recent.

Beryllium. Beryllium is an expensive metal used in small and specialized industries. Its dust and fumes as well as vapors of its compounds are poisonous to inhale. It is fabricated by powder metallurgy techniques because coarse grains tend to develop in the castings causing brittleness and low tensile strength. About 10% of the metal is used in the metallic

form, 80% in form of beryllium–copper alloys (containing about 2% Be), or other master alloys, and the remaining 10% is used as a refractory oxide. In the metallic form it is used as a moderator to slow down fast neutrons in nuclear reactors because of its low atomic weight and low neutron cross section. As an alloy with copper, it is particularly important in springs because such alloys possess high elasticity and great endurance.

Table 1.5: Typical uses of light metals.

Metal	Use	%
Beryllium	Electric industry	37
	Electronic industry	16
	Nuclear reactors	20
	Aerospace	18
	Others	9
		100
Aluminum	Buildings	30
	Transportation (automotive, aircrafts)	20
	Electrical	15
	Packaging	15
	Others (reducing agent, paint)	20
		100
Titanium	Jet engine	84
	Chemical industry	16
		100
Magnesium	As metal and alloy (reducing agent)	65
	As oxide for refractories	7
	Fertilizer, paper, etc.	28
		100

Aluminum. Pure aluminum often replaces copper in electrical engineering. Although its electrical conductivity is only 65% that of copper, the density of aluminum is almost three times as less (Cu 8.95, Al 2.7). This means a lesser consumption of the metal. Also suspension of aluminum conductors requires fewer poles than that for copper. Pure aluminum is soft, but, if alloyed with small additions of other elements its mechachical strength increases. Aluminum alloys combine strength, lightness, and corrosion resistance. Its large scale production started in the first quarter of this century when aeronautics was then making its first steps. Today it finds wide application in building construction. Aluminum alloys containing silicon are used in casting, cylinders, pistons, and other parts of aircraft and automotive engines as they readily reproduce mould configuration; they are also light and strong.

The surface of aluminum and of its alloys is always coated by a thin but strong layer of Al_2O_3 which protects it against further oxidation. The film is extra strong if it is obtained by anodic oxidation. The film can readily be dyed in many colors and this is widely used. The strength of the surface films and its harmlessness to users make aluminum suitable for the manufacture of various equipment in the food industry. In the form of foil it is used for packing foodstuffs. Aluminum powder is also used in the manufacture of paint. The strong affinity of aluminum makes it suitable for preparing metals from their oxides. Because of its abundance in the Earth's crust, the metal is more likely to be used as a substitute to wood, plastics, and other construction materials. Nonmetallic applications of aluminum account for about 10% of the element. Bauxite and alumina are used as refractories, fused alumina is used in abrasives, aluminum sulfate is used in water treatment.

Magnesium. Magnesium is lighter than aluminum resists poorly the action of atmospheric air, particularly when moist but its alloys with aluminum, zinc, and manganese are adequately corrosion resistant. These alloys, readily castable and machinable, have a wide application in the manufacture of aircraft, automotive industry, and in rockets. The high affinity of magnesium for oxygen allows its use as a reducing agent for metallothermic reactions, e.g., production of titanium and uranium. The high affinity of magnesium for oxygen and its ability to burn in the air with evolution of large quantities of heat and light makes it suitable in the manufacture of incendiary shells and flares. The main application of magnesium at present is an oxide used as a refractory brick for furnace lining. A large amount of this material is prepared from sea water.

Titanium. Titanium is somewhat heavier than magnesium and aluminum, but it is stronger and very resistant to corrosion. Titanium and

its alloys resist heat up to 450 °C, whereas aluminum and magnesium alloys tend to fail at about 300 °C. That is why titanium alloys became the basic materials for jet aircraft. Titanium alloys are used for the manufacture of jet engines, rockets, and shells of satellites. The largest application of titanium is an oxide used as a white pigment.

1.3.4 Precious Metals

This group of metals is composed of gold, silver, and the six platinum group metals: platinum, osmium, iridium, ruthenium, rhodium, and palladium. They are all common in that they do not rust, and are highly priced (Table 1.6).

Table 1.6: Typical uses of precious metals.

Metal	Use	%
Gold	Jewelry and arts	70
	Dental	9
	Space and defence	8
	Other	13
		100
Silver	Silverware	29
	Photography	28
	Electrical	22
	Brazes, solder	10
	Silver batteries	3
	Other	8
		100
Platinum	Catalysts	60
	Electrical	17
	Glass forming	9
	Dental, medical	5
	Jewelry, etc.	4
	Other	5
		100

Gold. A large part of the world's gold supply is held by governments and central banks, to provide stability for paper currency, and as a medium for settling international trade balances. The unit of gold purity is called karat, it is 1/24[1]. A 22-karat gold, for example, is an alloy containing 22 parts gold and 2 parts other ingredients, usually silver; hence it contains 91.67% gold and 8.33% silver. A large part is also used in jewellery, arts, in dentistry, and in coins.

[1] A carat is also the unit of trade (200 mg) of diamonds.

- All the gold ever mined in the world would fit into a store room measuring 17 metres long, 17 metres high, and 17 metres wide.
- The American Federal Reserve Bank on Wall Street is the biggest repository of gold in the world: some 13 000 tons of gold are kept behind 90 ton steel doors in vaults blasted out of solid granite.
- Gold is used in the electronics industry to make more than 10 billion tiny electrical contacts every year.
- Of the estimated 100 000 tons of refined gold in the world – bullion, jewellery, coin – no less than 40 000 tons, or 40% was mined in South Africa since 1886.
- Over 50 tons of gold are used every year by the world's dentists.
- Italy is by far the biggest user of gold for the manufacture of jewellery: about 250 tons annually, enough to make 100 million wedding rings.

Silver. Pure silver is too soft for many applications and an alloy of silver and copper is commonly used. Silver is used as an ornamental metal for tableware and in coins. It is also commonly used in plating articles made of cheaper metals, in fabricating mirrors, and in preparation of silver salts used in photography.

Platinum. Platinum is an important contact catalyst in the chemical industry e.g., oxidation of ammonia. It has also important uses in the electrical industry, in dentistry, in jewellery, and in laboratory ware.

1.3.5 Refractory Metals

This group of metals is composed of the transition metals tungsten, molybdenum, niobium, tantalum, titanium, zirconium, hafnium, vanadium, rhenium, and chromium. All these metals have high melting points. For example, tungsten melts at 3380 °C, rhenium at 3180 °C, molybdenum at 2610°C. They are mainly used as alloying elements in steel but also are used in the elemental form. Some resist high temperature without oxidation, and some are very hard, having excellent wear and abrasion resistance (Table 1.7).

Table 1.7: Typical uses of refractory metals.

Metal	Use	%
Vanadium	Ferrous alloys	80
	Nonferrous alloys	10
	Catalyst (V_2O_5)	10
		100
Chromium	Metallurgical (stainless steel)	58
	Refractories (oxide)	30
	Chemical industry (tanning of leather, electroplating)	12
		100
Molybdenum	Steel industry	80
	Chemicals	20
		100
Tungsten	Tungsten carbides	53
	Alloy steels	23
	Electrical lamps	13
	Chemicals	4
	Other	7
		100

Tungsten. Tungsten has the highest melting point of all metals; it also has one of the highest densities. When combined with carbon, it becomes one of the hardest man-made materials. While the tungsten filaments for light bulbs are widely used, its most common and most valuable use is in metal cutting, mining, and oil drilling tools. Although tungsten can be used at high temperatures, an oxide film forms which is volatile above temperature of approximately 540 °C. So, for use at extremely high temperatures, tungsten parts must be coated, used in a vacuum, or be surrounded by a protective atmosphere. Typical uses involving protective atmospheres – or vacuum – include incandescent lamp filaments, electron tube electrodes, and various types of heating elements. Silicide coating and noble metal cladding are effective oxidation-resisting coatings, for example, cladding the tungsten with a platinum gold alloys.

Tungsten is resistant to many severe environments which readily attack other metals. It resists nitric, sulfuric, and hydrofluoric acids at room temperatures. It is only subject to slight attack by hot alkaline solutions such as potassium, sodium, and ammonium hydroxides. Tungsten also has good resistance to several liquid metals including sodium, mercury, gallium, and magnesium; to oxide ceramics such as alumina, magnesia, zirconia and thoria. It is often used for crucibles to melt these materials in an inert atmosphere.

Molybdenum. Molybdenum is hard with respect to tensile stresses. Its electric and heat conductivities are somewhat lower than those of tungsten. When heated without access of air, it is readily amenable to mechanical working and can be drawn into a thin wire. It retains strength up to temperatures of about 1000 °C. It is used in parts of vacuum apparatus, e.g., hooks for filaments in electric bulbs, targets of X-ray tubes, heaters of high-temperature furnaces, plates of generator and rectifier tubes. Molybdenum steels posses a high mechanical strength, wearability and impact strength. Because molybdenum oxidizes rapidly at about 600 °C in air, a protective coating is needed in hot air applications. Many coatings involve formation of a thin layer of $MoSi_2$ on the surface of the molybdenum part. The compound has outstanding oxidation resistance up to about 1650 °C. In vacuum, uncoated molybdenum has a virtually unlimited life at high temperature.

Vanadium is mainly used as an alloying element in steel, in titanium alloys, and in some high-temperature alloys. In form of V_2O_5 it is used as a catalyst for oxidation reactions (SO_2 to SO_3).

Niobium. The major use of niobium is as an alloying element for steel. It also offers lower density and low thermal neutron cross section compared to other refractory metals, which makes niobium useful in atomic reactors. At ordinary temperatures niobium will resist attack by all mineral acids, with the exception of hydrofluoric acid, and it is not affected by mixed acids such as aqua regia.

Tantalum. Tantalum is one of the most corrosion resistant materials available. It forms stable anodic oxide films which make excellent electronic capacitors.

Rhenium. Rhenium has a melting point exceeded only by tungsten, density exceeded

only by osmium, iridium, and platinum. It is unique among refractory metals in that it does not form carbides. It is highly desirable as an alloying addition with other refractory metals. The addition of rhenium greatly enhances the ductility and tensile strength of these metals and their alloys. Rhenium alloys are gaining acceptance in nuclear reactors, semiconductors, thermocouple, gyroscopes and other aerospace applications. Tungsten–rhenium alloys are used to surface molybdenum targets in X-ray tube manufacture. Other rhenium alloys (with tungsten or molybdenum) are used for filaments, grid heaters, and ignitor wires in photo-flash bulbs. Rhenium has found important applications in catalysts for reforming in conjunction with platinum and in selective hydrogenation. It is resistant to hydrochloric acid and shows good resistance to salt water corrosion.

1.3.6 Scattered Metals

This group of metals and metalloids is composed of scandium, germanium, gallium, indium, thallium, hafnium, rhenium, selenium, and tellurium. They do not form minerals of their own but occur in very small amounts in the ores of other common metals. Thus gallium occurs with aluminum in bauxite, selenium and tellurium in copper and nickel sulfide ores, etc. (Table 1.8). As a result of processing a large tonnage of ores each year, these metals are enriched in certain fractions and are usually recovered.

1.3.7 Radioactive Metals

These metals have the highest atomic weights in the Periodic Table starting from polonium, and include radium, actinium, thorium, protactinium, uranium, and the transuranium metals which do not occur in nature[1]. They undergo spontaneous nuclear disintegration due to the repulsion of the protons within the nuclei of those atoms as a result of their increased number. In this process a helium ion (composed of two protons and two neutrons) is ejected. The helium ion (called alpha particle) possesses extraordinary cohesion.

Naturally-occurring radioactive metals form three series, each element in the series being produced when the one before it disintegrates, with the successive radioactive disintegrations stopping when a stable isotope of lead is formed. The three series are formed from uranium 238, uranium 235 (an isotope of uranium occurring in uranium ores to the extent of 0.7%), and thorium 232 (Figure 1.1). During their disintegration radium 226, 223, and 224 are formed respectively. These disintegrate in turn to the radioactive inert gas radon 222 and its isotopes radon 219 (called actinon), and radon 220 (called thoron), respectively. They then disintegrate to different polonium isotopes. Being gases with short half lives, radon and its isotopes represent a serious health hazard during the treatment of ores containing radioactive metals.

[1] Potassium 40 is a very weak naturally occurring radioactive element; it emits beta particles.

Table 1.8: Parent ores of scattered metals.

Metal	Parent ore	Concentration in ore, %	Major use
Gallium	Bauxite	0.01	Semiconductor
Germanium	Zinc sulfide	Trace	Semiconductor
Hafnium	Zircon sand	1	Nuclear reactors, control rods
Indium	Zinc sulfide	Trace	Semiconductor
Rhenium	Molybdenite concentrates from porphyry copper ores	0.07	Refractory metal
Scandium	Uranium and thorium	Trace	
Selenium	Copper sulfides	Trace	Photoelectric cells
Tellurium	Copper sulfides	Trace	
Thallium	Zinc sulfide	Trace	

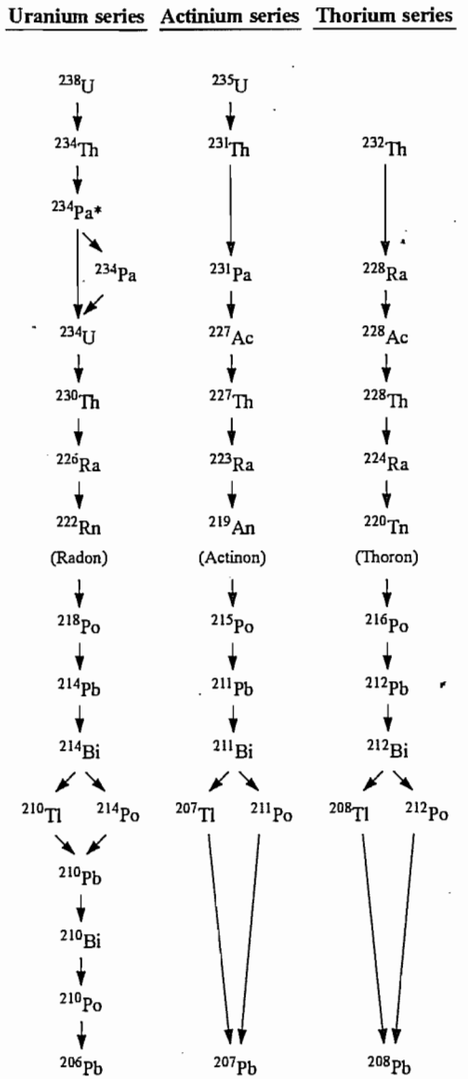

Figure 1.1: Radioactive metals.

Uranium 235 undergoes fission when bombarded by thermal neutrons; it breaks apart into two smaller elements and at the same time emitting several neutrons and a large amount of energy (Figure 1.1):

$$^{235}_{92}U + {}^{1}_{0}n \rightarrow {}^{89}_{36}Kr + {}^{144}_{56}Ba + 3{}^{1}_{0}n + 200\ \text{MeV}$$

$$\downarrow \qquad \downarrow$$

$$^{89}_{39}Y + 4e^{-} \qquad {}^{144}_{56}Ba + 3e^{-}$$

Uranium 238 absorbs neutrons forming uranium 239 which is a beta emitter with a short half life; its daughter neptunium 239 also emits an electron to form plutonium 239.

$$^{238}_{92}U + {}^{1}_{0}n \rightarrow {}^{239}_{92}U \rightarrow {}^{239}_{93}Np + e^{-}$$

$$\downarrow$$

$$^{239}_{94}Pu + e^{-}$$

Plutonium 239 (half life 2.4×10^4 years) is an alpha emitter, it undergoes fission with the emission of several neutrons and can maintain a chain reaction. Thus, a nuclear reactor using uranium as a fuel, not only produces energy, but also produces another nuclear fuel. Under certain conditions it is possible to generate fissionable material at a rate equal to or greater than the rate of consumption of the uranium. Such a reactor is known as a *breeder reactor.*

Thorium absorbs neutrons and is transformed to uranium 233:

$$^{232}_{90}Th + {}^{1}_{0}n \rightarrow {}^{233}_{90}Th \rightarrow {}^{233}_{91}Pa + e^{-}$$

$$\downarrow$$

$$^{233}_{92}U + e^{-}$$

Uranium 233 also undergoes fission; and can be used to operate a breeder reactor according to the scheme:

$$^{233}_{92}U + {}^{1}_{0}n \rightarrow \text{Fission products} + \text{Energy} + \text{one neutron that is captured by } {}^{232}_{90}Th \text{ to continue chain reaction}$$

$$^{232}_{90}Th \rightarrow {}^{233}_{90}Th \rightarrow {}^{233}_{91}Pa + e^{-} \rightarrow {}^{233}_{92}U + e^{-}$$

Uranium is the base of nuclear power reactors and nuclear weapons. Non-energy applications (ceramic glazes, catalysts) account for

approximately 10% the industrial demand. At the beginning of this century, shortly after the discovery of radioactivity, uranium ores were exclusively treated for their radium content to be used for medical purposes while uranium was rejected. It was only after the discovery of fission that this tendency was reversed. Highly enriched uranium, used for weapons needs, has more than 90% ^{235}U.

1.3.8 Rare Earths

This group of 13 metals always occur together and have similar chemical properties. These are cerium, praseodymium, neodymium, samarium, europium, gadolinium, terbium, dysprosium, holmium, erbium, thulium, ytterbium, and lutecium. Another member of this group is promethium, whose position in the Periodic Table is between neodymium and samarium does not occur in nature but is found in the fission products of uranium. To this group is always added lanthanum and yttrium because they also have similar properties and are associated with these metals in nature. These metals are not rare – they are widely distributed in nature and it is preferable to call them the lanthanides in reference to the first member of the group. They form their own ore deposits and also occur in phosphate rock, in iron ores, and others.

The annual consumption of lanthanides is about 30 000 tons. They are finding use as deoxidizers, in alloys, in the production of cast iron and steel, as catalysts, in lighter flints and flares, in the glass and ceramic industry, in optical glass as well as glass polishers, in the manufacture of ferrites for use as magnetic materials for electric motors, electronic circuits, and computers. Europium and yttrium are used in the manufacture of phosphors, producing the bright reds and greens of color television. Because of neutron-absorption properties they are used in the manufacture of control rods in nuclear reactors. they have many other applications, e.g., in the production of more efficient fluorescent lighting, portable X-ray sources, better X-ray screens, fiber optics, quick-drying paints, synthetic gems, and others.

1.3.9 Ferroalloy Metals

This group of metals is composed of chromium, manganese, silicon, and boron. They were once mainly used as alloying elements to steel in form of ferroalloys but now are also used in the elemental form. Thus chromium is used as a protective coating by electroplating on iron, silicon is used in the preparation of semiconductors and to convert energy from the sum directly into electricity. Manganese is used as an alloying element with aluminum and copper. Manganese dioxide is a powerful oxidizing agent. Boron carbide and boron nitride are hard materials second only to diamond.

1.3.10 Alkali Metals

This is the first group in the Periodic Table. Their name is derived from fact that when reacted with water they form alkalies. Soft and highly reactive, usually not used as metals except lithium as an alloying element for aluminum, sodium as a reducing agent either alone or as an amalgam, and an alloy of 50% Na and 50% K known as NaK is used as a coolant in nuclear reactors. Sodium salts have a variety of applications, e.g., NaCl is a source of chlorine, potassium salts are used as fertilizers.

The economic deposits of the alkali metals are mainly found in nature as salt deposits or in surface and subsurface waters except lithium which may also be found as a silicate; the last member of the group, francium, does not occur in nature. At one time sodium carbonate was recovered from the ashes left after burning wood by leaching with water, while potassium carbonate was recovered similarly but from ashes left after burning seaweeds. One of potassium isotopes that is naturally occurring is radioactive.

$$^{40}_{19}K \rightarrow {}^{40}_{19}Ca + e^-$$

1.3.11 Alkaline Earth Metals

This is the second group of the Periodic Table whose name originates from the fact that these metals form stable oxides (earths) that have alkaline reaction. For example, calcium forms the oxide CaO which dissolves in water to form calcium hydroxide. The first two members beryllium and magnesium are of useful mechanical properties and being light, are used as light metals. The last member, radium is radioactive and of no importance as a metal. At the beginning of this century, radium salts were used for treating cancer and for painting phosphorescent watch dials. Of the remaining three, calcium is the most important being used sometimes as a reducing agent. Calcium compounds $CaCO_3$ (limestone), $CaSO_4 \cdot 2H_2O$ gypsum, and $Ca_{10}(PO_4)_6F_2$ (fluorapatite, the main component of phosphate rock) occur in nature in great amounts and the first two are widely used as material of construction while the third is a source of fertilizers. The pyramids of Egypt were constructed of limestone.

Magnesium is like calcium in forming large deposits, for example, dolomite and magnesite. It is also found in relatively large amounts in sea water. Besides being a light metal it is also used as a reducing agent. Strontium and barium on the other hand, are of limited use.

1.4 References

1. F. Habashi, *Metallurgical Chemistry*, American Chemical Society, Washington, DC, 1987. Audio course (5 cassettes, 5 hours playing time) and manual.
2. F. Habashi, *Principles of Extractive Metallurgy*, volume 1: "General Principles" (1969, reprinted 1980); vol. 2: "Hydrometallurgy" (1970, reprinted 1980); vol. 3: "Pyrometallurgy" (1986, reprinted 1992). Gordon & Breach, Langhorne, PA.
3. N. Sevryukov, B. Kuzmin, Y. Chelishchev, *General Metallurgy*, translated from Russian, Mir Publishers, Moscow 1969.
4. A. Zelikman, O. E. Krein, G. V. Samsonov, *Metallurgy of Rare Metals*, translated from Russian, Israel Program for Scientific Translations, Jerusalem 1966.
5. N. L. Weiss (ed.): *SME Mineral Processing Handbook*, Society of Mining Engineers, AIME, New York 1985.

2 Metal Production

FATHI HABASHI

2.1 The Logarithmic Law

There is usually a gradual increase in the production of most metals. This is due to new ore discoveries, increased population, and the natural development in society.

For most metals, the rate of increase of production follows a logarithmic law (Figures 2.1 and 2.2) and is constant within a certain period of time:

$$\log W_2 - \log W_1 = k(t_2 - t_1)$$

where W_2 and W_1 are the weights of metal produced in time t_2 and t_1 respectively, and k is a constant. This logarithmic law is the same as population growth (Figure 2.3) which is derived from the relation: rate of increase of population at a certain moment is proportional to the number of people at that moment:

$$\frac{dN}{dt} = kN$$

$$\int_{N_1}^{N_2} \frac{dN}{N} = k\int_{t_1}^{t_2} dt$$

$$2.303 \log \frac{N_2}{N_1} = k(t_2 - t_1)$$

Statistical information on metal production are useful in projection of future needs. some facts can also be deducted from these curves:

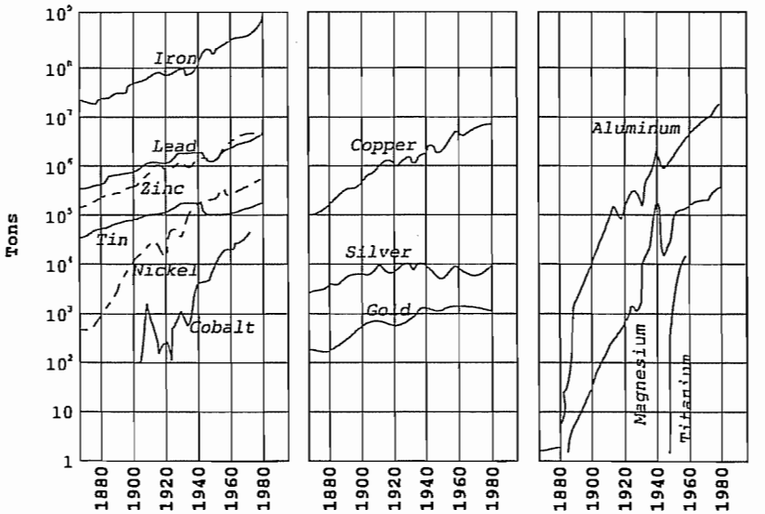

Figure 2.1: Production of metals.

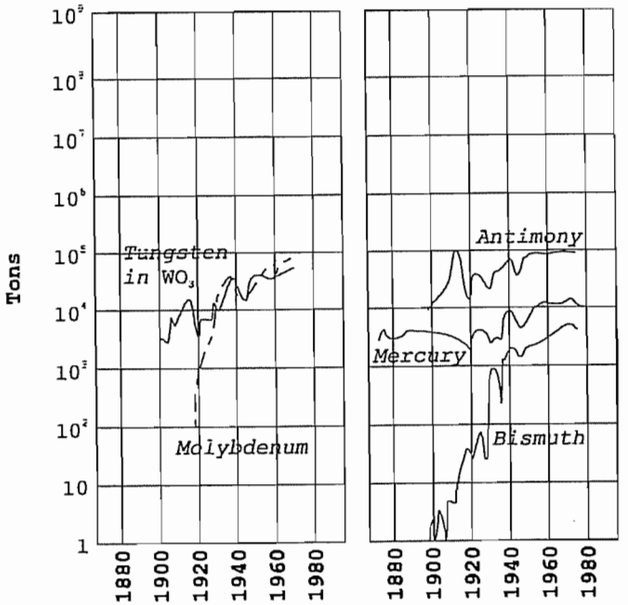

Figure 2.2: Production of metals (continued).

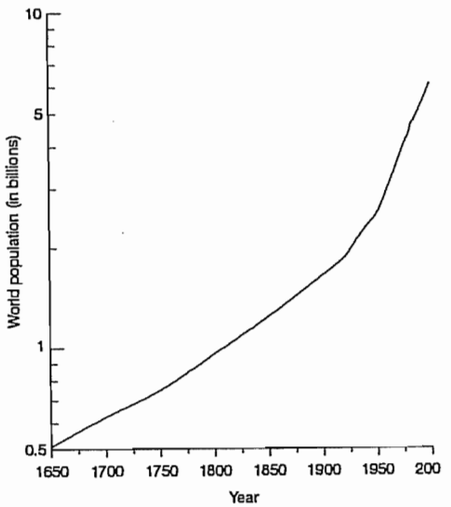

Figure 2.3: World population.

2.1.1 Growth Rate

The constant $k \times 100$, which is the slope of the curves shown in Figures and during a certain period, is called the *growth rate* and is expressed in percent. For example, the growth rate of copper during the period 1870 to 1910 was 5%, i.e., copper production increased by 5% every year during the period mentioned. The growth rate for metals are not the same; some metals, especially the new ones grow at a faster rate than the old metals. For example:

- The growth rate of nickel is higher than that for lead. The reason for this is that an old metal like lead, once used extensively for constructing equipment for chemical plants, e.g., lead chambers in sulfuric acid plants, is now giving way to the new metal, nickel, which is finding increasing use in the form of stainless steels and for constructing corrosion resistant equipment.
- The growth rate of aluminum is higher than that for copper. The two metals are good electrical and heat conductors, easily worked or machined, and resistant to atmospheric corrosion. Aluminum became cheaper than copper after World War II and is now replacing it in power cables.

2.1.2 Doubling Period

Another way of expressing the rate of growth is the *doubling period*, Δt, i.e., the time required for a certain metal to double its production. This is related to the growth rate by the relation:

$$\Delta t = \frac{2.303 \log 2}{k} = \frac{0.69}{k}$$

Thus, is the case of copper mentioned above, a growth rate of 5%, i.e. $k = 0.05$ means that copper production doubles every 14 years ($\Delta t = 0.69/0.05 \approx 14$) during that period.

2.2 Production Patterns

The maxima in the curves in Figures 2.1 and 2.2 are due to the exceptionally high production rates in time of wars to meet military needs and for stockpiling. On the other hand in time of crises, the curves show exceptionally low production rates, e.g., 1921 and the early 1930s.

With the exception of iron ores and aluminum ores, most ores are complex, i.e., they may yield more than one metal. As a result, the production pattern of a certain metal may also be complex. Table 2.1 shows the production pattern for silver. It can be seen that only 20% of the world's silver comes from silver ores and the rest is by-product of lead, copper, copper–nickel, gold, and tin ores.

Table 2.1: Sources of silver produced worldwide.

Origin	%
Silver ores	20
Lead ores	45
Cu, Cu–Ni ores	18
Gold ores	15
Tin ores	2
	100

A metal may follow the production pattern of another if both occur together in ores. For example:

- Gold and silver usually follow each other because a large part of silver is a by-product of gold production.

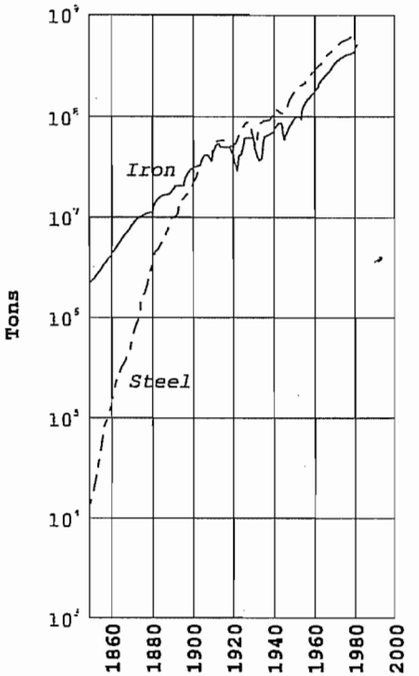

Figure 2.4: World production of iron and steel.

- Lead and zinc have nearly the same production level (as well as the same price). The two metals are closely related in the sense that they always occur together in ores; thus a zinc plant usually produces lead as by-product and vice versa.

Production patterns of metals change as a result of the following factors:

- *Changing technology.* Steel was produced in small amounts until the discovery of the Bessemer Process in 1850s (Figure 2.4). Similarly, the production of aluminum increased rapidly after the discovery of the electrolytic process in 1886, and that of gold after the discovery of the cyanidation process in 1887.
- *Changing application.* The curve for silver shows a slight decrease in production during the past 40 years. It is not so much used as a coinage metal since the introduction of nickel. Otherwise it has the same growth rate as gold.

2.3 Prices

Prices of metals vary from few cents/kg, e.g., iron, aluminum, and lead, to tens of thousands of dollars/kg, e.g., gold and platinum. The price of a metal varies also with the purity, the form whether in powder, ingot, pellets, etc., and the amount sold. There are many factors that control the price of a metal. For example:

Availability of rich deposits. Large iron deposits containing 60% iron are common, while a gold deposit is usually 0.001%. It would, therefore, be expected that iron is cheaper than gold.

Easiness in extraction. A metal that can be extracted by reduction with carbon is usually cheaper than metal that must be extracted by reduction with metallic magnesium (or other metal). For example, lead oxide is reduced by coke while beryllium fluoride is reduced by magnesium. Evidently, lead will be cheaper than beryllium.

Easiness in refining. A metal that can be refined from aqueous solution or can be handled in air when molten will be usually cheaper than a metal that must be refined from fused salts or must be handled in inert atmosphere because of its reactivity. Thus nickel, for example, is cheaper than titanium.

However, there are many exceptions to the above. For example:

- Copper is actually easier to produce than aluminum, yet it is more expensive.
- Tellurium occurs in ores in nearly the same concentration as gold, yet, it is much cheaper.
- Lead is more difficult to refine than nickel, yet, it is cheaper.
- Sodium is more difficult to handle than zinc, yet, it is cheaper.

All these factors combine to give a simple relation: The price of a metal varies inversely with its production. Metals produced in large tonnage are less expensive than those produced in small tonnage. Iron is the cheapest metal while the platinum metals are the most expensive. Expressed in a different way, cheaper metals are consumed in greater quantities than more expensive ones. Many other commodities fall on the same straight line.

This straight line cannot be explained by the law of supply and demand because if a metal is in great demand its price should rise. This is not the case: iron is in great demand yet its price is the lowest of all metals. The law of supply and demand, however, applies temporarily within certain periods when the production level of a metal is changed. For example, a shut down in the steel industry may lead to an increased price of the metal because of the temporary shortage in supply. When the price reaches a certain high level, production is resumed. This is usually the case when there is a labor conflict. The price of the metal, however, usually does not come back to its original level before the conflict because of the increased cost of its production. Soon after, other industries follow suite, and the prices adjust themselves.

A natural phenomenon in pricing metals is that new metals start with high price, and their price gradually decreases as time goes on due to development in the extractive processes, and also to increase in its production due to increased demand. For example, aluminum started as a very expensive metal, now it is a cheap metal.

The price of the lanthanides (rare earths) requires some clarification. There metals always occur together. To separate a member of the group it is necessary to separate all the others and stock pile them. The cost of producing a desired member is therefore very high. If for instance a use is found for the stock piled material, then price would decrease.

Once the price of an expensive metal is reduced and approaches another metal, substitution for a particular use becomes possible without sacrificing a loss in the end use. For example, aluminum foil replaced tin foil in wrapping, aluminum busbars replaced copper in electrical industry, and aluminum beverage cans replaced tinned steel.

The price of copper was once about three times that of either lead or zinc. In the last 30 years it has only been double their price. this can be explained when comparing the production patterns; it was only 30 years ago that copper production approached that of lead or zinc and started to surpass them.

2.4 Metal-Producing Associations and cartels

A great demand for a metal causes a shortage in the market, and as a result, the price tends to rise. To meet the shortage and hold the price constant, cartels are formed. These can be either private or government sponsored. For example, the tin cartel which was composed of seven producing countries as members and controlled 94% of the production in the Western World fixed the price of the metal by creating a stock of the metal furnished by the members. Should the price of the metal increases, the cartel offers its stock for sale thus lowering the price and vice versa: should the price decrease the cartel buys metal from the market until the price is stabilized at the desired value. The tin cartel, however, broke down few years ago because a non-member producing country increased its production of the metal and the cartel was unable to buy a large stock of the metal available on the market.

Associations are usually formed between producers of a certain metal world-wide. For example:

- Aluminum Association
- Cobalt Development Institute
- International Copper Association
- International Lead–Zinc Research Organization
- Nickel Development Institute
- Tantalum–Niobium International Study Center

The purpose of these associations is to promote the use of the metal in question through diffusing information, subsidizing research in potential applications, etc. Metal producing companies participate by paying the cost of operations. They also sponsor holding conferences and publish bulletins about their activities.

2.5 References

1. *Canadian Minerals Yearbook*, Communications Canada, Ottawa 1996.
2. *Minerals Yearbook*, volume 1: "Metals and Minerals"; volume 2: "Area Reports"; volume 3: "International Review". US Bureau of Mines, Washington, DC, 1992.

3 Recycling of Metals

FATHI HABASHI

3.1 Introduction

Recovery of a metal from scrap requires much less energy than starting from ore. For example, the remelting of steel scrap to produce reusable steel saves about 74% of the energy that would be required to produce the same quantity of steel from iron ores. In the case of aluminum, it is even higher – it reaches 96% (Table 3.1). Recycling of metals has two important effects on society.

- Conservation of natural resources
- Decreasing pollution of the environment.

As a result, there is a great effort nowadays to collect and recycle old metals.

Table 3.1: Energy savings through recycling of metals.

Metal	Energy saving, %
Aluminum	96
Copper	87
Iron and steel	74
Zinc	63
Lead	60

3.2 Ferrous Metals

There are small-scale steel plants that operate solely on scrap; these usually use electric furnaces for melting. Other steelmaking processes based on raw iron as a starting material also use scrap to a variable degree (Figure 3.1). The use of scrap in certain steelmaking processes is necessary because it is used to control the temperature in the converter during steelmaking. As a result of oxidizing the impurities in the pig iron, the temperature rises because of the exothermic nature of the reaction. To prevent the rapid deterioration of refractories, scrap is added to cool down the change. On the average, the steel industry consumes 50% raw iron and 50% scrap. Steel scrap for steelmaking comes from two main sources:

- **Local.** This is scrap produced locally in a steelmaking plant during shaping. In a steel plant, about one third of the steel produced is returned as scrap.
- **External.** This is old automobiles, farm equipment, railroad rails, ships, etc., that is purchased from outside sources.

Steel scrap in form of tin cans is usually sold to the copper industry to be used for precipitating copper from leach solutions by the reaction:

$$Cu^{2+} + Fe \rightarrow Cu + Fe^{2+}$$

It is first heated to remove tin by volatilization before use (detinning).

A shortage of scrap is expected in the future as a result of introducing continuous casting method which produces less local scrap. This shortage, however, can be overcome by producing a certain quantity of iron by "direct reduction" methods. This iron is not produced in the blast furnace but in less expensive equipment such as a rotary kiln, a static bed, or a fluidized bed. It differs from blast furnace iron in being not subjected to melting, and is suitable as a substitute for scrap. Usually steel produced from such iron is made in electric furnaces (Figure 3.1).

3.3 Nonferrous Metals

Great efforts are now being made to collect and recycle scrap of aluminum (e.g., beverage cans), copper (e.g., electric wires), lead (e.g., old automobile batteries), silver (e.g., used photographic films, table ware), nickel from hydrogenation catalysts, platinum from auto-

mobile exhaust gas catalyst and ammonia oxidation catalyst, etc. As a result, new technologies are constantly emerging for treating and purifying such scrap.

3.4 References

1. S. A. Bortz, R. S. De Cesare, *Accomplishments in Waste Utilization*, Information Circular 8884, U.S. Bureau of Mines, Washington, DC, 1982.
2. S. A. Bortz, K. B. Higbie (eds.): *Materials Recycling*, Information Circular 8826, U.S. Bureau of Mines, Washington DC, 1980.
3. R. K. Collings, *Mineral Waste Resources of Canada*, a series of reports issued by CANMET, Ottawa 1977–1980.
4. P. Mehant et al. (eds.): *Resource Conservation and Environmental Technologies in Metallurgical Industry*, Canadian Institute of Mining, Metallurgy, and Petroleum, Montréal 1994.
5. S. R. Rao et al., *Waste Processing and Recycling in Mining and Metallurgical Industries*, Canadian Institute of Mining, Metallurgy, and Petroleum, Montréal 1992.
6. S. R. Rao, T. J. Veasey, *Second International Symposium on Waste Processing and Recycling in the Mining and Metallurgical Industries*, Canadian Institute of Mining, Metallurgy, and Petroleum, Montréal 1995.
7. R. F. Rolsten (ed.), *Materials: Dispose or Recycle?*, Wright Company, Dayton, OH, 1977.
8. M. Sittig, *Metal and Inorganic Waste Reclaiming Encyclopedia*, Noyes Data Corporation, Park Ridge, NJ.
9. M. J. Spendlove, *Recycling Trends in the United States*, Information Circular 8771, U.S. Bureau of Mines, Washington, DC, 1976.
10. M. J. Spendlove, *Bureau of Mines Research on Resource Recovery*, Information Circular 8750, U.S. Bureau of Mines, Washington, DC, 1977.
11. P. R. Taylor, H. Y. Sohn, N. Jarret (eds.), *Recycle and Secondary Recovery of Metals*, The Minerals, Metals and Materials Society, Warrendale, PA, 1985.
12. K. J. Thome-Kozmiensky (ed.), *Recycling International: Recovery of Energy and Material from Residues and Waste*, Freitag-Verlag, Berlin 1982.

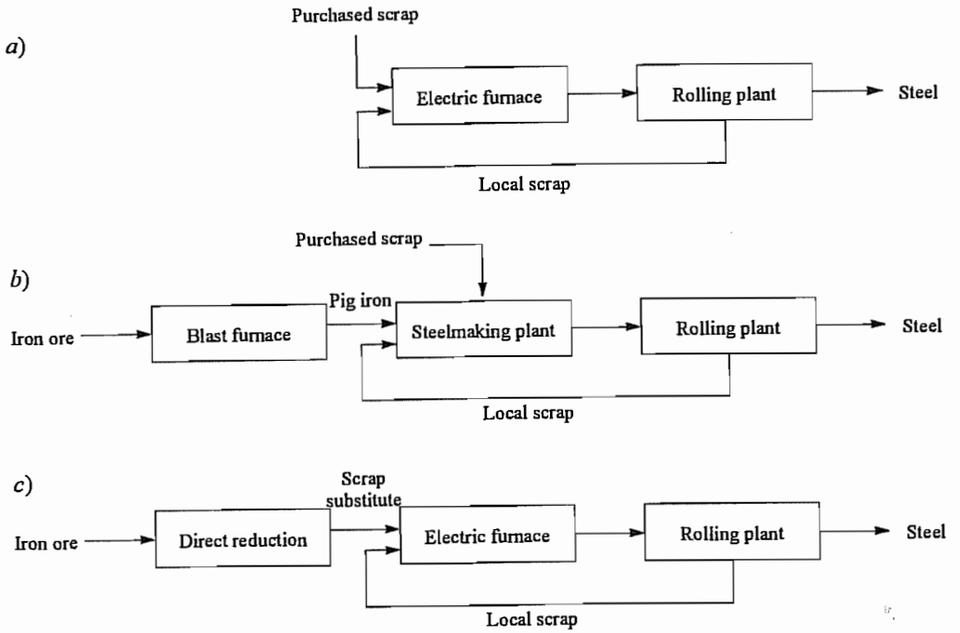

Figure 3.1: The role of scrap and scrap substitutes in the steel industry: (*a*) Steel industry based solely on scrap; (*b*) Steel industry based on ≈ 50% raw iron and ≈ 50% scrap; (*c*) Steel industry based on scrap substitutes.

4 By-Product Metals

FATHI HABASHI

4.1 Introduction

It is often possible to recover certain metals as by-products during the processing of ores. This is often aided by the fact that metals found in exceedingly small amount in a feed material to a chemical or a metallurgical process are enriched in certain fractions during processing i.e.g. dust, slimes and residues and therefore can be economically recovered as by-products. In some cases this may be a means to conserve the natural resources, in others it may be an essential purification step.

4.2 Uranium from Phosphate Rock

Phosphate rock contains on the average 150 ppm uranium. During the processing of the rock for fertilizer manufacture, uranium is enriched in the phosphoric acid produced as an intermediate product and is usually recovered as a by-product without interfering with the manufacturing process (Figure 4.1).

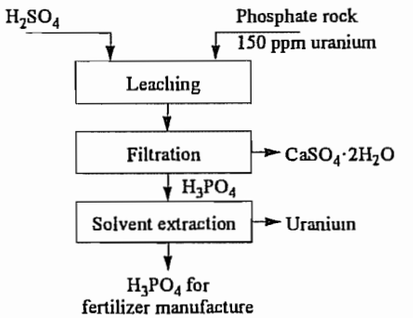

Figure 4.1: Recovery of uranium from phosphate rock.

4.3 Vanadium from Fuel Oil

Fuel oil contains on the average 100 ppm vanadium. During burning in boilers to generate steam, the dust collected in the gas treatment section is rich in vanadium (Figure 4.2).

4.4 Precious Metals from Copper Ores

A copper ore containing 1 to 2% Cu that may be beneficiated to a concentrate containing 20 to 40% Cu, when smelted yields raw metal containing about 97% Cu. During the electrolytic refining step to get 99.9% Cu, the impurities behave differently: some remain in solution and can be crystallized, for example nickel sulfate, while the others remain at the botton of the tank as insoluble residue called slimes (Figure 4.3). These are an important source of the precious metals as well as selenium and tellurium originally present in the ore.

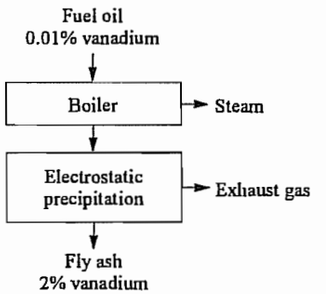

Figure 4.2: Recovery of vanadium from fuel oil.

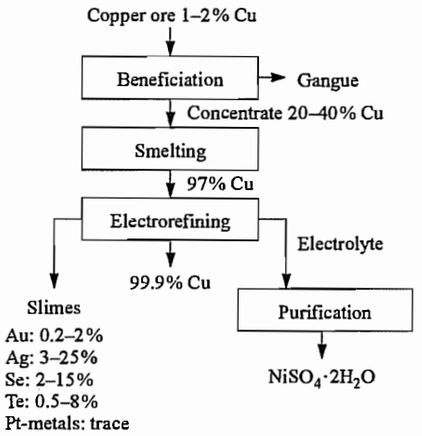

Figure 4.3: Enrichment of traces of metals present in copper ore during the production of the metal.

4.5 Rhenium from Porphyry Copper Ores

Chalcopyrite concentrate from porphyry copper ores contains on the average 0.05% molybdenite. This is usually separated by selective flotation. The molybdenite concentrate obtained contains about 700 ppm rhenium which is enriched in the dust fraction during oxidation (Figure 4.4). This is the principal source of rhenium.

4.6 Cadmium from Zinc Concentrates

During the production of zinc by the hydrometallurgical route small amounts of cadmium are present in the leach solution and these must be removed before the electrowinning step (Figure 4.5). This is an important source of cadmium. At the same time germanium, indium, and thallium are retained in the leach residue and are recovered.

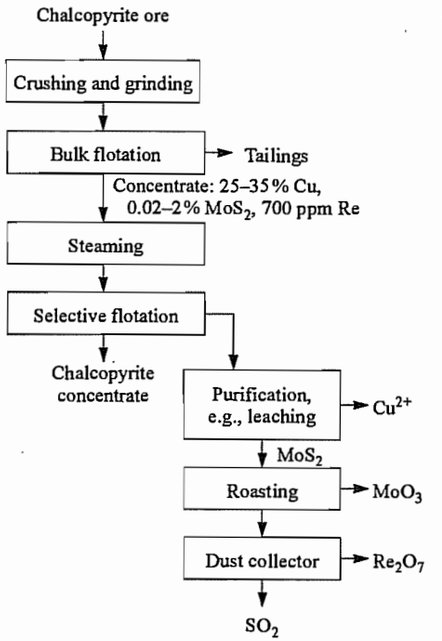

Figure 4.4: Chalcopyrite – a major source of rhenium.

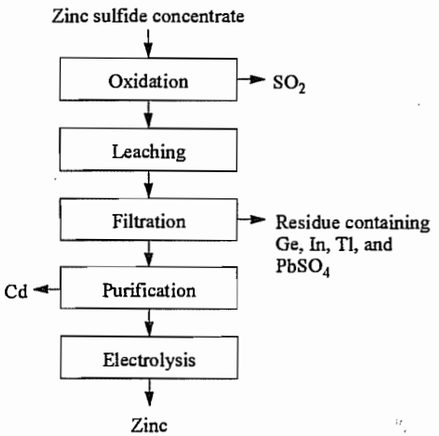

Figure 4.5: Recovery of cadmium as a by-product of the zinc industry.

4.7 Gallium from Aluminum Ores

Traces of gallium found in bauxite, the principal source of aluminum, are usually recovered from a bleed of the aluminate leach solution (Figure 4.6).

4.8 References

1. W. Schreiter, *Seltene Metalle*, 3 volumes, VEB Deutscher Verlag für Grundstoffindustrie, Leipzig 1961–1963.
2. R. Kieffe, G. Jangg, P. Ettmayer, *Sondermetalle*, Springer-Verlag, Vienna 1971.
3. A. Patrick et al., *The Economics of By-Product Metals*, 2 parts, US Bureau of Mines Information Circulars 8569, 8570 (1973).
4. J. G. Parker, *Occurrence and Recovery of Certain Minor Metals in the Smelting–Refining of Copper*, US Bureau of Mines Information Circular 8778 (1978).
5. L. A. Haas, D. R. Weir (eds.): *Hydrometallurgy of Copper, its By-Products, and Rarer Metals*, Society of Mining Engineers AIME, New York 1983.

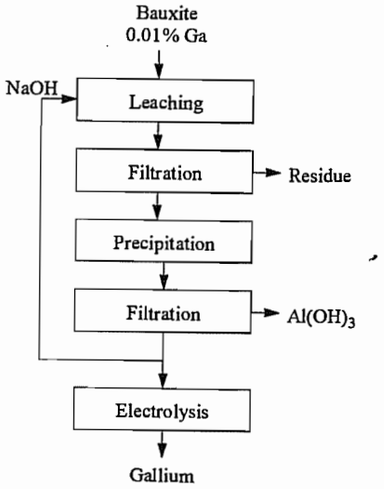

Figure 4.6: Recovery of gallium from bauxite as a by-product of the aluminum industry.

Part Two

Ferrous Metals

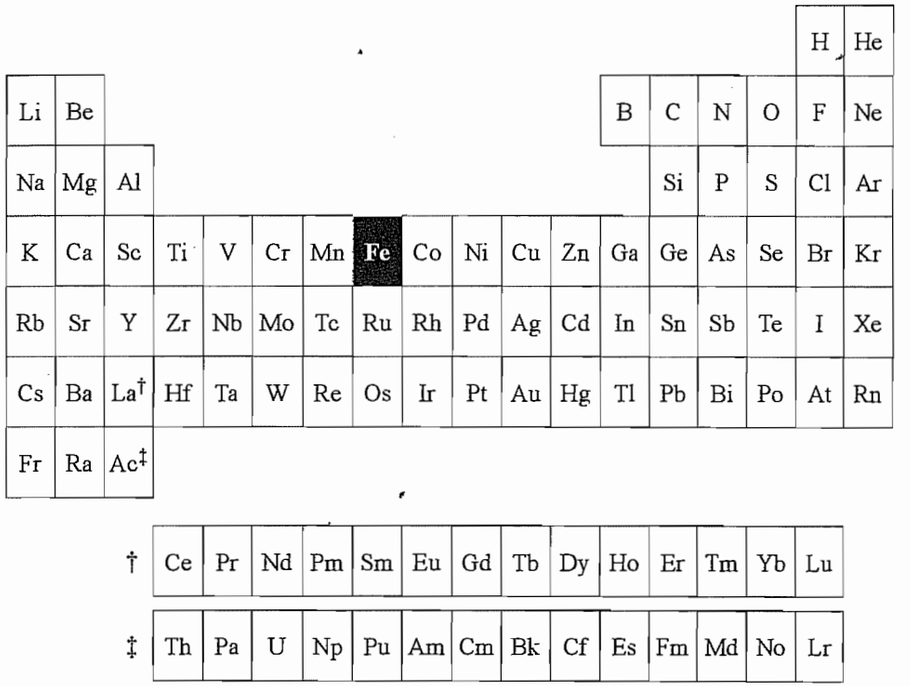

5 Iron

FATHI HABASHI (§§ 5.1, 5.2, 5.4–5.6 EXCEPT 5.5.6–5.5.11, 5.8–5.9 EXCEPT 5.9.1, 5.14–5.16, 5.17.1, 5.18–5.19); HEINRICH MEILER (§ 5.3); JUN-ICHIRO YAGI (§§ 5.5.6–5.5.11); ANDREAS BÜHR, MANFRED KOLTERMANN (§ 5.7); LOTHAR FORMANEK, FRITZ ROSE (§ 5.10 EXCEPT 5.10.1); KLAUS WESSIEPE (§ 5.10.1); JÜRGEN FLICKENSCHILD, ROLF HAUK (§ 5.11); GERNOT MAYER-SCHWINNING, REINER SKROCH (§ 5.12); HEINZ-LOTHAR BÜNNAGEL, HANS-GEORG HOFF (§ 5.13); EGON WILDERMUTH (§§ 5.17.2–5.17.3); HANS STARK (§§ 5.17.4–5.17.5); FRANZ LUDWIG EBENHÖCH (*RETIRED*), GABRIELE FRIEDRICH (§ 5.17.6); BRIGITTE KÜHBORTH (§ 5.17.6, TOXICOLOGY AND OCCUPATIONAL HEALTH); JACK SILVER (§ 5.17.7); RAFAEL RITUPER (§ 5.20); GUNTER BUXBAUM, HELMUT PRINTZEN (§ 5.21.1); HORST FERCH, WILFRIED MAYER, KLAUS SCHNEIDER, HEINRICH WINKELER (§ 5.21.2); HENDRIK KATHREIN, LUTZ LEITNER (§§ 5.21.3.1–5.21.3.3); HELMUT JAKUSCH, MANFRED OHLINGER, EKKEHARD SCHWAB, RONALD J. VEITCH (§ 5.21.3.4); GÜNTER ETZRODT (§ 5.21.4); RALF EMMERT, KLAUS-DIETER FRANZ, HARTMUT HÄRTNER, KATSUHISA NITTA, GERHARD PFAFF (§ 5.21.5); HARALD GAEDCKE (§§ 5.21.6–5.21.7); JOHN C. CRELLING (§§ 5.22.1–5.22.4, 5.22.9–5.22.11); DIETER SAUTER (§§ 5.22.5, 5.22.8); DIETER LEININGER † (§ 5.22.6); UDO BERTMANN, BERNHARD BONN (§ 5.22.7); RAINER REIMERT (§ 5.22.8); WOLFGANG GATZKA (§ 5.22.12); SEMIH ESER, RASHID KHAN, LJUBISA R. RADOVIC, ALAN SCARONI (§ 5.22.13)

5.1 Introduction[1]

Iron is an Anglo-Saxon word; the symbol, Fe, comes from Latin *ferrum*. The French term *sidérurgie*, i.e., iron technology, comes from σιδηρος the Greek word for iron. Also *sideritis* is the Latin work for lodestone.

The use of iron has been known since the earliest times; it was prepared by the so-called bloomery hearth, or Catalan forge. Iron ores were heated in a shallow trench with a large excess of wood charcoal, fanned by bellows. Lumps (blooms) of wrought iron were obtained, and were welded together by hammering. As technology advanced during the Middle Ages, the trench was replaced by a small shaft furnace, and from this the present day blast furnace has developed. The use of water power to operate the blast was introduced during the 14th century. The consequent considerable increase in furnace temperature resulted in the production of iron with a much higher carbon content than formerly, namely cast iron. This was not malleable but it was soon discovered how this might be converted into malleable iron by a second heating in an ample supply of air (refining). The iron industry received a great impetus at the end of the 18th century, when the demand for iron began to increase as a result of the invention of the steam engine and the railway. The shortage of wood charcoal led to the introduction of coke, as fuel and as reducing agent. Coke was first used in the blast furnace by Abraham Darby, in 1732. The refining process underwent fundamental improvements during the 19th century, through the introduction of the blast refining method (Bessemer process, 1855; Thomas–Gilchrist process, 1878) and of regenerative heating (Siemens–Martin process 1865). Later, smelting in the electric furnace has been introduced for the production of certain high-grade steels.

Iron is the cheapest and most widely used metal. Its annual production exceeds by far that of all other metals combined. It comprises approximately 93% of the tonnage of all the metals used.

[1] For *History of Iron*, see Secction 6.2.

5.2 Occurrence

Iron is a relatively abundant element in the universe. It is found in the sun and many stars in considerable quantity. Iron is found native as a principal component of a class of meteorites known as siderites. The core of the earth is thought to be largely composed of iron. The metal is the fourth most abundant element in the earth's crust: about 5% is iron. Iron is a vital constituent of plant and animal life, and appears in hemoglobin.

5.2.1 Native Metal

Iron occurs in the native state in two forms [1]:

Telluric Iron. This form of iron is known as telluric iron, i.e., terrestrial, to distinguish it from meteoric, i.e., coming from outer space. The difference in nickel, cobalt, carbon, and basalt content clearly distinguishes one from the other (Table 5.1). Although both types may look alike and may occur as large boulders 20 to 80 tons, there is another way to distinguish between the two, besides chemical analysis, is the Widmanstätten structure that appears in meteoric iron when a piece is polished, etched and examined by the optical microscope. The large crystals indicating slow cooling is characteristic of meteoric iron. The major occurrence of telluric iron is in association with the basalts[2] of Western Greenland. Large boulders are on exhibit at the Natural History Museums in Stockholm, Copenhagen, and Helsinki. Telluric iron is found also as small millimeter-sized pea-shaped grains disseminated in the basalt, characterized of their low carbon content, usually less than 0.7%. These were extracted from the basalt by the natives by crushing and then cold-hammering the collected metallic particles into coin-sized

[2] Basalt is a heavy dark grey or black basic igneous rock composed mainly of finely divided pyroxene, feldspar, and sometimes olivine.

flakes to insert them into groves in bone and use them as knives.

Table 5.1: Typical analysis of telluric and meteoritic iron.

	Telluric, %	Meteoric, %
Nickel	0.5–4	5–20
Cobalt	0.1–0.4	0.5–0.7
Carbon	0.2–4.5	0.03–0.10
Basalt	5–10	nil

Ferronickel. Ferronickel is an iron–nickel alloy that occurs in nature as the mineral awaruaite, $FeNi_3$ (named after Awarua Bay in New Zealand, where it was first discovered), and josephinite, $FeNi_2$ (named after Josephine County, Oregon where it was first discovered). Both minerals contain cobalt, usually in the ratio Ni:Co = 10:1. Ferronickel also occurs as microscopic lamellæ in association with asbestos, as microscopic crystals in association with serpentine, or as microscopic particles associated with the minerals pentlandite, (Fe, Ni)S, and hazelwoodite, NiS, in serpentine rocks (Figure 5.1). Thus it occurs in most asbestos formations and can be recovered from the asbestos tailings by magnetic methods.

5.2.2 Oxide Minerals

Iron ores of sedimentary origin account for nearly 80% of the world's reserves; the remaining 20% is of magmatic origin such as magnetite. The most important oxide minerals are the following:

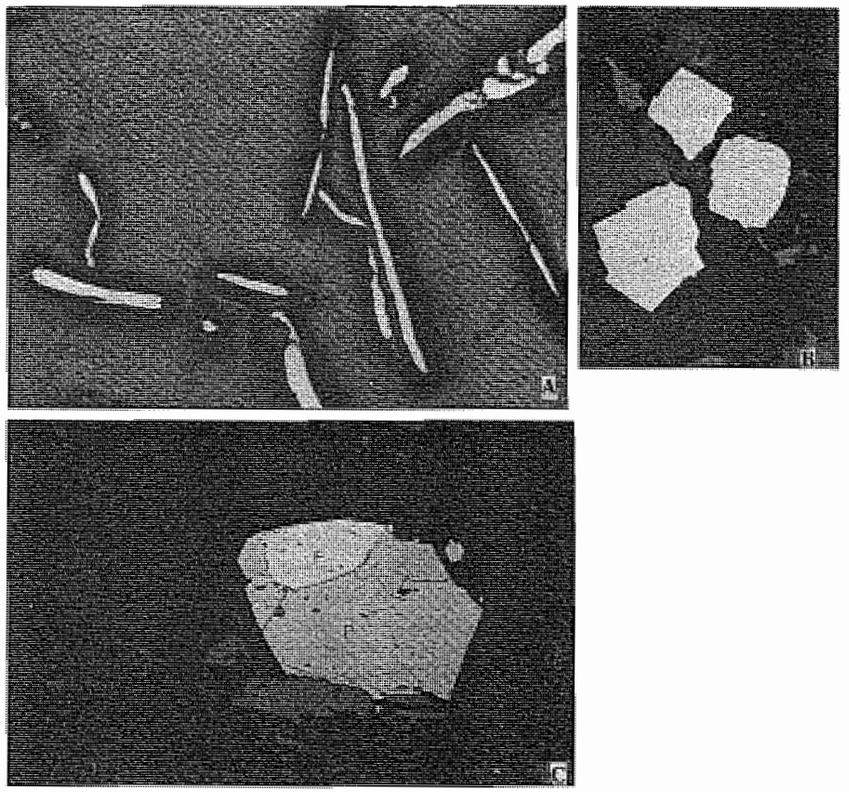

Figure 5.1: Photomicrograph of polished sections. A) Lamella of ferronickel in asbestos deposit 0.05–0.5 mm in size (70 ×); B) Microscopic crystals of ferronickel (560 ×); C) Microscopic particles of ferronickel (F) cemented with pentlandite (P) from serpentine rock (210 ×).

- Hematite, Fe_2O_3. Occurs in nature in the following forms:
  - Specular hematite: black to steel grey crystals with metallic luster
  - Micaceous hematite: occurs in thin flakes resembling mica; they may be so thin as to be translucent and they are then deep red
  - Common red hematite is dark red in massive, granular or earthy (red ocher) form
  - Magnetic. This is the γ-Fe_2O_3 which occurs in the Ural as the mineral maghemite. It is like Fe_2O_4, a cubic spinel type.
- Magnetite, Fe_3O_4. It is brittle with a dark grey to black opaque color, with metallic luster, strongly magnetic.

Geological Terms

- Limonite is a geologic term signifying certain deposits of hydrated iron oxides which vary in color from brown to yellow. It is formed by the weathering and alteration of other iron-bearing compounds. When present in a loose, porous and earthy deposits in swamps, it is known as bog iron ore. When mixed with clay it forms what is known as yellow ocher. Most limonite ores require washing to remove clay, and drying to remove moisture, before shipping or reduction.
- Taconite is another geological term signifying an iron ore deposit consisting of fine grains of hematite and magnetite embedded in a matrix of silica. It is difficult to drill and blast but easy to grind. Large deposits of this type occur in the Lake Superior region containing 25–35% Fe. Enrichment can be effected by magnetic methods to separate magnetite, and flotation to separate hematite to achieve a concentrate containing 63% Fe.
- Laterite is a limonite containing 1–2% Ni and about 0.1% Co. At present these are used as nickel and not as iron ore, e.g., in Cuba.
- Oolitic ironstone is iron carbonate which has replaced the $CaCO_3$ of an oolitic limestone retaining the texture of the original rock. The rock consists of small round grains resembling the roe of fish.

Table 5.2: Complex oxides of iron.

Chromite	$Cr_2O_3 \cdot FeO$
Columbite	$Nb_2O_5 \cdot (Fe, Mn)O$
Tantalite	$Ta_2O_5 \cdot (Fe, Mn)O$
Ilmenite	$TiO_2 \cdot FeO$
Wolframite	$WO_3 \cdot FeO$

5.2.3 Complex Oxides

Iron occurs in combination with other metals in form of complex oxides (Table 5.2). It is only recovered from ilmenite concentrates as a by-product of the manufacture of titanium slag, e.g., Sorelslag used for making TiO_2 pigment.

5.2.4 Carbonates

Siderite, $FeCO_3$. When occurring in economic deposits it represents a low-grade iron ore since the pure mineral contains only 48.3% Fe. It crystallizes in rhombohedra like calcite, which dissolves in water containing carbonic acid, with the formation of iron(II) hydrogen carbonate, $Fe(HCO_3)_2$. Such waters rapidly deposit iron(III) oxide hydrate when exposed to air, since the excess carbon dioxide escapes, the carbonate deposited is hydrolyzed, and is oxidized by atmospheric oxygen.

5.2.5 Sulfides, Disulfides, and Complex Sulfides

Iron(II) sulfide occurs in nature as pyrrhotite, FeS, iron(II) disulfide as pyrite and marcasite, FeS_2. It also occurs in combination with arsenic as the mineral arsenopyrite, FeAsS. Iron(III) sulfide occurs in the form of double sulfides, especially with copper(I) sulfide — e.g., chalcopyrite, $CuFeS_2$ or $Cu_2S \cdot Fe_2S_3$, and bornite, Cu_3FeS_3 or $3Cu_2S \cdot Fe_2S_3$. These are the major copper minerals.

Iron monosulfide (ferrous sulfide), FeS. Iron sulfide, crystallized in the hexagonal system, is magnetic. The iron sulfide occurring in meteorites, with the same crystal structure, is called troilite. Pyrrhotite almost always contains nickel, and is therefore of importance as a nickel ore. The sulfur content of pyrrhotite is usually 1 to 2% higher than corresponds with

the formula FeS, the excess sulfur being built into the crystal lattice. Its ability to take up a certain excess of sulfur arises from the fact that a proportion of the positions which should be occupied by Fe atoms may remain vacant. The density of FeS varies between 4.5 and 5.

Pyrite (iron disulfide), FeS_2. Pyrite is widely distributed in nature. The ore is not a source of iron but a source of sulfur. However, the residue of roasting from the manufacture of sulfuric acid is smelted for iron, after the impurities which are undesirable for this purpose, although often valuable in themselves, have been removed in special refineries: silver and gold are present as well as copper and zinc. The disulfide also occurs as marcasite.

Pyrite and marcasite have a brassy yellow color and metallic luster. They differ in their crystal structures. Pyrite, which is commonly found in well formed large crystals (usually cubes or pentagonal dodecahedra, or combinations of these forms), belongs to the pentagonal hemihedral class of the cubic system. Marcasite is orthorhombic.

Pyrite and arsenopyrite are different from other sulfide minerals since they contain the disulfide ion, S_2^{2-}; arsenopyrite contains in addition the diarsenide ion, As_2^{2-}. In pyrite, FeS_2, the iron atoms are in a face-centered cubic arrangement with pairs of the sulfur atoms located on the cube diagonals. In arsenopyrite, FeAsS, the iron atoms are also in a face-centered cubic arrangement like in pyrite but half of the diagonal positions are occupied by pairs of the sulfur atoms and the other half by pairs of arsenic atoms.

Pyrite and arsenopyrite have received great attention recently because in some gold ores called "refractory", they entrap gold in their crystal structure and render the metal unextractable by cyanide solution unless the mineral structure is destroyed by thermal or aqueous oxidation prior to cyanidation. Pyrite is also the major sulfur-bearing impurity mineral in coal. Attempts to upgrade the coal include the aqueous oxidation of the pyrite.

5.2.6 Phosphates

Vivianite. Hydrated iron(II) orthophosphate, $Fe_3(PO_4)_2 \cdot 8H_2O$, is the main source of phosphorus impurity in iron ores.

Table 5.3: Important minerals in iron ores.

Mineral	Chemical formula	Density, g/cm³	Hardness (Ⅰ)	Specific susceptibility (order of magnitude)
Iron (for comparison)	Fe	7.88	4–5	
Magnetite	Fe_3O_4	5.2	5.5	10^{-1}–1
Specularite ("hematite")	Fe_2O_3	5.2–5.3	6.5	10^{-4}
Limonite				
Needle ore	α-FeOOH	4.3	5–5.5	10^{-6}–10^{-5}
Ruby mica	β-FeOOH	4.0	5	10^{-6}–10^{-5}
Siderite	$FeCO_3$	3.7–3.9	4–4.5	10^{-6}
Pyrite	FeS_2	5.0–5.2	6–6.5	10^{-6}
Pyrrhotite	FeS	4.6	4	10^{-3}–10^{-4}
Chalcopyrite	$CuFeS_2$	4.1–4.3	3.5–4	10^{-5}–10^{-6}
Apatite	$Ca_5F(PO_4)_3$	3.2	5	-10^{-6}
Vivianite	$Fe_3(PO_4)_2 \cdot 8H_2O$	2.6–2.77	3	
Quartz	SiO_2	2.65	7	-10^{-6}
Orthoclase	$KAlSi_3O_8$	2.55	6	10^{-6}
Plagioclase	$NaAlSi_3O_8/CaAl_2Si_2O_8$	2.6–2.8	2–2.5	10^{-2}–10^{-5}
Kaolinite, dickite	$Al_4(OH)_8Si_4O_{10}$	2.6	1	
Muskovite	$KAl_2(OH,F)_2[AlSi_3O_{10}]$	2.6–2.8	2–2.5	10^{-2}–10^{-5}
Pyrolusite	MnO_2	5	1–6	10^{-6}
Calcite	$CaCO_3$	2.6–2.8	3	-10^{-6}
Ilmenite	$FeTiO_3$	4.5–5	5–6	10^{-4}

5.3 Ores [2, 3]

Iron is found in high concentration in ore deposits, where it occurs mainly as oxide. Table 5.3 lists the iron minerals of greatest industrial importance (along with some accompanying gangue minerals) and their relevant properties.

The only minerals of worldwide importance are hematite (specularite, Fe_2O_3), magnetite (Fe_3O_4) and limonite (FeOOH). Siderite ($FeCO_3$) finds limited use on a local basis. Other ores such as chamosite (an iron magnesium aluminosilicate) or pyrite are virtually not important for iron production anymore.

5.3.1 Ore Deposits

Of the variety of classification systems that have been proposed for iron-ore deposits, the one from the United Nations Survey is used here [4]. The criterion is the physical appearance of the deposit; the main types are bedded (A), massive (B), residual (C), by-product (D) and other (E)

A Bedded Deposits
A-1 *Iron formation*
Lake Superior Type
Chiefly Precambrian; primarily as sedimentary deposits, heavily metamorphosed (itabirite, taconite, jaspilite or quartz-banded ore); enriched by weathering processes (Mesabi, Minas Gerais, Carajas, Venezuela, Labrador and Quebec, Krivoi Rog)
Algoma Type
Primarily as thinly-banded quartzite with interlayers of iron ore; enriched as limonite hematite weathering ore
A-2 *Ironstone formation*
Mainly marine sedimentary deposits of minette type; Clinton, Wabana; chiefly mesozoic, with limonite as the most important mineral
A-3 *Other Iron-Ore Sedlments*
Examples: clastic deposits, ferruginous sandstone, and iron shale; also alluvial deposits and unconsolidated clastic sediments
B Massive Deposits
B-1 *Bilbao Type*
Deposits from weathering of siderite rock, with limonite and hematite in the weathering zone
B-2 *Magnitnaya Type*
Contact-metasomatic replacement deposits
B-3 *Kiruna Type*
Magnetite intrusion, usually with apatite
B-4 *Taberg Type*
Syngenetic titanomagnetite bodies and deposits of finely intergrown ilmenite ores
C Residual Deposits
C-1 Laterite and iron-ore caps as a result of weathering of underlying iron-bearing rocks
C-2 Fluvial deposits and bog ore
C-3 Other residual ores, e.g., caps of sulfide ore deposits (gossan, "iron hat"), unconsolidated clastic deposits
D By-products
Recoverable values in by-product iron oxide
E Other Types of Deposits
e g, Iode-type deposits (Siegerland)

Bedded deposits are stratigraphic members enriched in iron by a factor of ca. 4–12 above average. They occur in all geologic ages; including ores which originate from them, they account for ca. nine-tenths of potential iron reserves. Names applied to Precambrian metamorphic ore beds are itabirite, taconite, Lake Superior type, quartz-banded ore, jaspilite, magnetite quartzite, hematite quartzite, etc. More recent formations are known as minette (Jurassic), Salzgitter type, and other local names. In general, the term bedded deposits is used for iron–mineral enrichments in which ore minerals are more or less closely laminated with quartz, jasper or carbonate rock and the iron-bearing sediments lie conformably to the under- and overlying beds of igneous or metasedimentary rock. Thus, iron formations can be chemical rocks, clastic sediments, or rock beds that have been replaced by iron mineral during diagenesis or in their subsequent history.

Massive iron-ore deposits are ore bodies of irregular shape, discordantly embedded in the enclosing rock. They include:

- Replacement deposits in carbonate rocks (Bilbao type) with siderite, hematite or limonite (the last two in the weathering zone above the water table)
- Contact-metasomatic deposits in the contact region of acidic intrusive rocks with magnetite and, to a lesser extent, hematite, siderite, pyrite, pyrrhotite and copper sulfide (Magnitnaya type)
- Magnetite intrusions in acidic magmatic rock (Kiruna type)
- Massive or intergrown titanomagnetite or ilmenite concentrations in basic rock (Taberg type).

The most important type of *residual deposit* is laterite, which occurs as a cap overlying a

wide variety of rocks. It is the product of weathering in tropical and subtropical climatic regions. The iron content of these ores is usually low (limonite, hematite), the alumina content high, and undesirable accessory constituents such as chromium, phosphorus, and nickel are frequently present (e.g., at Vogelsberg, Germany). Thus, laterite has largely ceased to be an important iron ore except where the lateritic caps of other iron ore deposits have secondary enrichments of up to 69% iron. On the other hand, nickel-bearing laterites are the most important nickel ores of the future (Cuba, New Caledonia, the Philippines). Extended fluvial deposits, such as the Robe River deposit in Western Australia, should also be mentioned. Bog ores, in contrast, form deposits of small extent that were formerly locally important. They are precipitation products from iron-containing solutions. The weathering cap of sulfide deposits (gossan or "iron hat"), which are usually separated from the primary sulfides by an indistinct boundary, are of some importance.

5.3.2 Supply of Iron Ore

Until about the 1950s, ironworks were mainly supplied from their own deposits; ore and concentrate were transported over short distances. Since that time a fundamental change has occurred as a result of (1) the greater demand because of increased production, (2) the drop in the cost of overseas transport because of larger ship capacities, and (3) the need for higher productivity because of continually rising labor and energy costs. The iron ore demand of the most important steel-producing regions is essentially met by a few large ore-producing regions.

Medium-sized and small ironworks located at deposit are now found only in case of large deposits (northeast India, the Ukraine and other areas of the former Soviet Union, northeast China). Table 5.4, listing world iron-ore reserves, also shows, from the tonnage standpoint, that only a few countries play important roles in ore supply. The short descriptions below are limited to the most important deposit areas and supplier countries.

Production figures for iron ore, ore concentrate, and ore agglomerate appear in Table 5.5.

Table 5.4: World iron ore reserves [5].

	Reserves, $t \times 10^6$	Iron content, %
Former Soviet Union	110 750	25.4
China	42 000	30.0
Brazil	34 540	56.9
Canada	26 417	31.6
United States	25 400	20.7
Australia	17 781	60.0
India	13 500	61.5
South Africa	6 300	59.1
France	4 064	40.2
Sweden	3 353	59.1
Venezuela	2 337	54.4
Liberia	1 668	39.5
Other	2 235	28.4
World total	290 235	35.4

Table 5.5: World iron ore production, ore, concentrate and agglomerate (1975–1986) ($t \times 10^6$) [6].

	1975	1980	1986	1993
North America	132.0	127.1	82.8	96.0
Canada	46.9	48.8	36.1	32.3
Mexico	5.1	7.6	7.3	8.0
United States	80.1	70.7	39.4	55.7
South America	134.3	146.1	164.7	189.8
Brazil	89.9	114.7	132.0	159.4
Chile	11.0	8.6	7.0	7.0
Peru	7.8	5.7	5.0	5.2
Venezuela	24.8	16.1	19.1	15.5
Europe	355.5	335.3	313.6	184.2
Austria	3.8	3.2	3.1	1.4
France	49.6	29.0	12.4	3.5
Germany	3.3	1.9	0.7	0.1
Norway	4.1	3.9	3.7	2.2
Spain	7.6	9.2	6.1	2.5
Sweden	30.9	27.2	20.5	18.7
Soviet Union/CIS	232.8	244.7	249.9	154.0
United Kingdom	4.5	0.9	0.3	—
Former Yugoslavia	5.2	4.5	6.7	0.3
Asia	122.7	122.8	151.9	303.8
China	65.0	68.1	90.0	224.7
India	41.4	41.9	47.8	56.0
North Korea	9.4	8.0	8.0	10.0
Turkey	2.4	2.6	4.0	5.1
Africa	57.7	60.8	55.8	44.2
Algeria	3.2	3.5	3.4	2.6
Liberia	24.0	18.2	15.3	—
Mauretania	8.7	8.9	8.9	9.2
South Africa	12.3	26.3	24.5	29.4
Oceania	99.9	99.2	92.5	123.7
Australia	97.6	95.5	90.0	121.4
New Zealand	2.3	3.6	2.4	2.3
World total	902.0	891.3	861.3	941.7

It is striking that the most important supply sources are type A deposits (bedded), and among these the metamorphic deposits of Itabira type (under that or some other local name), chiefly of Precambrian age.

Especially important are the enrichment or weathering zones of these deposits, where the mobilization of silica and alumina has produced rich ores that can be forwarded to ironworks without preliminary beneficiation. Table 5.5 also shows that ores expensive to produce and those whose beneficiation does not yield concentrates with at least ca. 60% iron have lost much of their importance. In fact, most of them will no longer be in production after a few years. Examples are the Mesozoic deposits in France, Belgium and Luxembourg (minettes), in the United Kingdom (home ore), and in Germany (Salzgitter, Siegerland, Lahn–Dill, Oberpfalz).

The important producer countries rank as follows by tonnage output (1993 production, tonnes $\times 10^6$):

China	224.7
Brazil	159.4
Former Soviet Union	154.0
Australia	121.4
India	55.0
United States	55.7
Canada	32.3
Sweden	18.7
Venezuela	17.5

5.3.3 Most Important Iron-Producing Countries [4–8]

Brazil. Brazil is currently the biggest producer of ore for *overseas shipment*. Two ore districts are now in production. The "iron quadrangle" ("Quadrilatero ferrifero") in Minas Gerais state is the more important. It supplies several local ironworks, but most of the product is exported.

The ores occur in three successive beds, Precambrian in age and strongly metamorphosed, called (from shallowest to deepest) Rio das Velhas, Minas Gerais, and Italcolomi [4]. The ore is thought to consist of marine sedimentary deposits. The ore beds contain 35%–60% iron.

Various ore types are distinguished:

- Hematite enrichments (lump to powder ore), > 64% iron
- Silica-rich hematite ore, 60–64% iron
- Itabirite, 35–60% iron, occurring in compact, soft and powder forms and typical of the Minas Gerais series
- Canga, (60–68% iron), a conglomerate-like ore that often consists of rounded fragments in a limonite matrix

Capacity is ca. 130×10^6 t/a of ore shipped; about a tenth is shipped as lump ore, 24×10^6 t/a as pellets, and the remainder as sinter fine ore ("sinter feed").

The second large ore district is Carajas, with a production target of 35×10^6 t/a, 10–20% of this being lump ore. The Carajas ore also lies within Precambrian beds and has been enriched by secondary processes to 60–67% iron.

Venezuela [4, 8]. The most important iron-ore district is the Imataca belt, including the well-known Cerro Bolivar, El Pao, and San Isidro deposits. The belt is part of the Precambrian Guyana Shield. The ores occur in a sequence of metamorphic rocks with gneiss, shales, and taconite-like iron-banded quartzite. Secondary processes have created rich ore deposits, partly through the precipitation of iron hydroxide in cavities. At the surface, a hematite-rich laterite cap, 1–50 m thick has formed; this is still the main source of ore. In 1987, ore output was 17.2×10^6 t, of which 5.5×10^6 t was consumed domestically.

Lump ore, sintered fine ore and pellet feed containing 62–67% iron, 0.6–6% silica, 2% alumina and 2–5% loss on ignition are produced. To meet the needs of direct reduction units (Midrex, HyL) at the Matanza ironworks, a 6 600 000 t/a pellet plant has been erected.

Canada. The Labrador geosyncline is the most important ore district. Precambrian deposits of the Lake Superior type are regarded genetically as continental shelf deposits that have undergone various degrees of metamorphosis. There are weathered rich ores containing over 60% Fe and having high limonite

contents; weathered, relatively coarse-grained magnetite hematite ores containing 20–50% quartz; and unweathered banded ore.

United States—Lake Superior. Most of the known iron-ore reserves in the United States are found in the Lake Superior area, in Minnesota, Wisconsin, and Michigan. About three-quarters of U.S. ore production comes from this region; the output goes to ironworks south of the Great Lakes (Ohio, Pennsylvania). The deposits occur in Lower and Middle Precambrian strata. Iron oxide, carbonate, silicate and sulfides are thinly banded with gel quartz and other gangue minerals. The thickness is between 15 and 300 m. Fine-grained magnetite and hematite are the principal ore minerals.

In weathering zones locally enriched lump ores exist containing ca. 60% Fe; these consist of hematite and limonite. Mining is limited to these rich ores and magnetite-bearing beds, which are relatively easy to beneficiate by magnetic separation.

Australia. The large iron-ore reserves of this continent are concentrated in the north of Western Australia, in the Pilbara district. The Precambrian banded itabirite ores contain magnetite, quartz, carbonate, and stilpnomelane. The near-surface region includes hematite and limonite weathering ores. Besides these in situ enrichments, conglomerate and residual ores are also found; the latter have a high limonite content and occur chiefly in old Tertiary riverbeds.

India. In India the most important ore deposits are enclosed in the strata of a Precambrian geosyncline, which runs parallel to the east coast over a significant part of the subcontinent. The ore is mainly of itabirite type; lateritic weathering has produced rich ore with a high alumina content in the gangue, which extends to a considerable depth. Locally, quartz-banded lean ore and similar primary ores have also been exploited. Hematite ore containing > 60% iron is worked; it is partly lump ore and partly sinter fine ore. Hematite-limonite ore also occurs. The lateritic hard-ore cap is often underlain by blue dust. This ore consists of medium- to fine-grained primary specularite, martite and, locally, primary magnetite as weathering residue, and contains only small amounts of quartz, kaolin minerals, and gibbsite as gangue.

China. China has many isolated ore deposits, most of which form the basis for local iron and steel industries. The largest concentration of reserves, however, is in the provinces of Liaoning (northeast China) and Hebei (eastern central China). The ores are of itabirite type, mainly with hematite–quartzite ores containing 50% iron. Large rich ore reserves are obviously nonexisting in China. Of the ores now being mined, it is known that beneficiation is often difficult and costly. Exceptions are the various magnetite deposits of Magnitnaya type. Some ores contain undesirable secondary constituents such as tin, fluorspar and finely intergrown apatite. Despite the potential reserves, cost considerations may cause China to import iron-rich ore; the recently observed construction of steelworks at coastal sites is an indication of this policy.

Former Soviet Union. The former Soviet Union has more than 20 iron-ore regions. The most important reserves are in the regions of Kursk, western Siberia, and the Ukrainian crystalline shield. The first two areas account for ca. 30% each, the last for some 10% of the Soviet Union's total reserves [4]. The most important production region is the Ukrainian Shield, with the Krivoi Rog syncline as its center ("Krivbas"). The Precambrian strata here contain both magnetite–quartzite and hematite–martite quartzite ores.

In the area of the *Kursk Magnetic Anomaly*, three basins are distinguished: Belgorod in the west, Kursk-Orel in the center, and Staryi Oskol in the east. Near-surface rich ore with hematite and martite has been exploited for some time. The horizontal quartzite magnetite beds are of increasing economic importance. From the geological standpoint, the iron-bearing beds form part of the Precambrian basement of the Central Russian shield.

In the *western Siberian* ore province, three districts exist. However, only the *Kuznetsk–Sayan area* has acquired economic importance. It consists of a large number of contact-metasomatic magnetite ore bodies of slight and moderate thickness, which also contain iron sulfide and zinc sulfide. The deposits are thought to have originated in the time of the Caledonian orogenesis.

The *Gornyi Altai* district has limited reserves in Clinton-type deposits (sedimentary deposits with partial secondary enrichment), which date from the Variscan orogenesis.

The western Siberian district, in a narrower sense, has considerable reserves of minette-type sedimentary ore deposits that have not been much explored; these had their genesis as marine coastal deposits in the Upper Cretaceous and the Eocene.

Sweden. For a long time, Sweden was the most important ore supplier for the Central European and, in part, the Western European iron industry. Quartz-banded magnetite-hematite ores of the Lake Superior type were mined in central Sweden. However, the chief source of ore for export is northern Lapland, in a district centered around Kiruna and Malmberget, where Kiruna-type magnetite deposits (massive intrusions in granite-like enclosing rock, with a relatively high apatite content) occur. Reserves are more than 2×10^9 t, with ca. 60% iron and 0.04–5% phosphorus. The phosphorus content is reduced to 0.04% by beneficiation, because hardly any Bessemer pig iron is produced in western Europe anymore.

5.3.4 Beneficiation of Iron Ore

The purpose of beneficiation is to render the ore more suitable for transport and for various reduction and smelting processes in the production of pig iron or steel.

The only processing steps used for ores mined from rich deposits (rich ores) are crushing and screening. Such ores come mainly from the weathering zones of itabirite deposits. At some mines, washing is combined with the screening of fines (< 6–8 mm) for sintering; very fine material containing kaolin is thus separated, and the alumina content is reduced. Low-grade ore is concentrated to lower transport costs and bring about a chemical composition suitable for the subsequent reduction step. In this enrichment process, the gangue is reduced and, in many cases, its composition improved. Current reduction and smelting processes require a basic slag ($CaO : SiO_2 > 1$), but the gangue, of nearly every type of iron ore, is "acidic", that is, it contains an excess of silica. Beneficiation lowers the silica level to 5–8% in the concentrate.

Harmful components present in the ore must be removed. Such components include phosphorus, arsenic, chromium, copper, vanadium, alkali, sulfur and titanium; these either make metallurgical processing more difficult or degrade the iron and steel quality. A small quantity of titanium (< 0.5%) is, however, added to the burden at some ironworks, because it has been found to increase the life of the blast-furnace brickwork.

The basic methods of beneficiation for iron ores are usually the same as for nonferrous ores and industrial minerals. Naturally some peculiarities exist because of the mineralogy and the type of intergrowth.

Crushing. Conventional equipment is employed for crushing. Primary crushing takes place in gyratory crushers (up to 3500 t/h) or jaw crushers. Mobile versions of the latter are now employed directly at the mines. Cone crushers are common for the second and third stages of crushing. They are however, increasingly replaced by semiautogenous grinding (SAG). Here steel balls, 100 mm or greater in diameter are added in a quantity of up to 6 vol% to aid the comminuting action. Autogenous mills are tumbling mills of large diameter and relatively short length, roughly 0.4–1.2 times the diameter. Fine grinding takes place in rod and ball mills, usually in a closed circuit with classification by hydrocyclones. Both dry and wet comminution are practiced; the wet process is more common when this step is followed by concentration.

Another option is autogenous or semi-autogenous primary crushing followed by fine grinding in a pebble mill; a tumbling mill which does not contain steel balls but lumps of ore of ca. 75–30 mm in diameter. This is possi-

ble only with hard ore that yields enough "pebbles" in the first crushing stage. This process has the advantage that no grinding balls are needed, but the energy requirement for grinding often increases if the conditions in the mill are not optimal.

Screening. Vibration screens with elliptical or linear oscillations have been widely adopted for screening. Multilevel screens of the Mogensen design are increasingly used.

Concentration. The concentration of iron ore is generally based on physical differences between the iron-bearing and gangue minerals (Table 5.3). *Flotation* and *electrostatic concentration* utilize physicochemical differences. The iron minerals have a higher specific gravity than the gangue minerals, so in many cases *gravity* or *centrifugal concentration* is possible. The *dense-media separation* process for coarse particles (≥ 3 mm) in drum or tank separators is also used. For medium-sized material, ca. 15–0.5 mm, cyclone separators or the cylindrical "Dyna Whirlpool" can be employed. Both use a centrifugal force field for separation. Gravity separators for fines (roughly 2–0.075 mm) include the Humphreys' spiral concentrator and the Reichert cone separator.

The Reichert cone separator has been adopted in the past two decades mainly for the beneficiation of placer ore, but it is used more and more for fine-grained weathering iron ores.

The *magnetic concentration* of magnetite ore takes place in drum-type separators with a low-intensity magnetic field. Dry separators are fed from the top and discharge the nonmagnetics, in wet separation the ferromagnetics are picked up from the feed pulp (underfeed). Ferrite-based permanent magnets have almost completely replaced ALNICO and electromagnets. The magnetic flux density is up to 0.15 T. Wet separators include drums up to 1500 mm in diameter and 3600 mm wide, with throughput capacities of 50–200 t/h. The drums, with up to five poles, are arranged in appropriately designed tanks for cocurrent or countercurrent operation. In addition, high-intensity wet magnetic separators have been employed since ca. 1970 in the concentration of weakly magnetic ore. The Jones design is most common. Here the separating elements are arranged in a ring which rotates carousel-fashion through a strong field generated by electromagnets. The magnetic flux density in the separation zone is 0.1–0.5 T; because of the tip configuration of the separating elements, it is concentrated at the tips to much higher values with a strong convergence of the field lines. The carousel design permits semicontinuous operation.

High-intensity dry magnetic separators are generally not used in beneficiation any longer. Electrostatic drum type separators are employed only for the recleaning of the concentrate, where they remove mainly quartz-bearing gangue. The process is restricted to grain sizes in the range of 1–0.05 mm.

Flotation has been used for iron-ore beneficiation since ca. 1950. The first two systems in Michigan were built for "direct" flotation (values in froth) of fine-grained specularite ore. Tall oil and diesel oil were added as collectors. "Hot flotation" enabled concentrates to float with only a few percent of silica. The rougher concentrate in pulp form was heated to > 90 °C, then recleaned in several stages after cooling. "Indirect" or "reverse" flotation is most commonly used today; the gangue goes into the froth and the iron ore into the underflow. Conditions are controlled so as to prevent the ore from flotation. As depressants for iron ore, starches or dextrin are used in conjunction with a basic pH. The collectors employed for gangue depend on the gangue minerals: oleic acid or oleates (e.g., for apatite) or amine salts (for quartz and feldspar). In general, the goal is first to enrich the ore as much as possible by less expensive means (gravity, magnetic separation), using relatively expensive flotation only for the final beneficiation stage. In the case of rich ores, however, flotation can also be employed as the sole concentration process when only a little gangue is to be removed.

A process of limited importance is *magnetizing roasting* followed by low-intensity magnetic separation. The iron minerals are

thermally converted to magnetite with solid, liquid or gaseous reducing agents. The process is used in shaft furnaces in China and rotary kilns in the former Soviet Union.

A *thermal* beneficiation process is the roasting of siderite ore. The purpose of this process is to save weight for transport and to relieve the blast furnace of the carbon dioxide load. Shaft furnaces or sintering machines are employed. In the latter case, agglomeration is combined with calcination.

Figure 5.2 presents a general flowsheet for the beneficiation of iron ore. Currently almost all the crude ore comes from large-scale open pit mines with capacities between 10 000 and 100 000 t/d. Only in Swedish Lapland, the former Soviet Union and China are high-capacity underground mines operated. Depending on the iron content and other requirements, the ore is processed into lumps, sinter or pellets; Table 5.6 lists the fractions of these products in blast furnace burdens in several areas. Table 5.7 gives some analyses of ores that are of commercial importance.

The beneficiation of an Indian laterite ore is shown schematically in Figure 5.3. The ore is a decomposition product containing limonite and hematite values along with kaolin, quartz and alumina minerals as gangue. By washing in a drum and then removing the finest fraction, the iron content is elevated by ca. 3% units and the Al_2O_3 content is lowered from 3–4% to < 1.7%.

Table 5.6: Lump ore and agglomerate in blast-furnace charge, 1986, % [8].

	Germany	Western Europe	Japan	United States	Total
Lump ore	9.8	12.1	16.8	5.3	12.5
Sinter	64.4	70.5	73.6	22.5	62.4
Pellets	25.8	17.4	9.6	72.2	25.1
Total	100.0	100.0	100.0	100.0	100.0

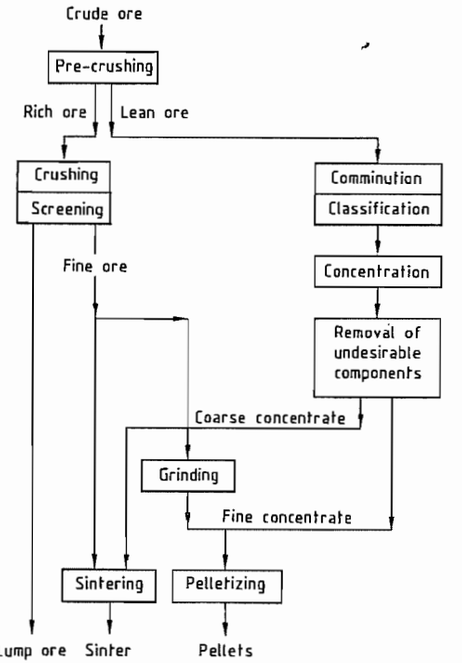

Figure 5.2: Schematic diagram of iron-ore processing.

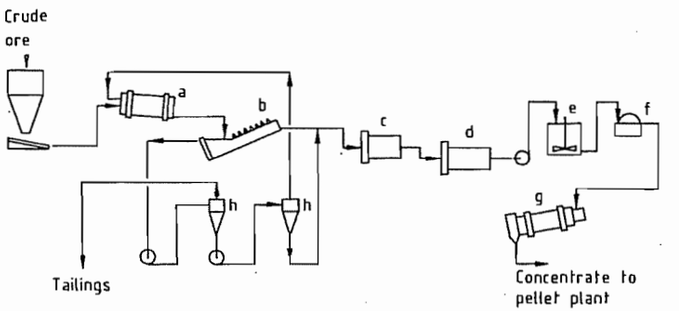

Figure 5.3: Flowsheet of Pale beneficiation plant, India: a) Washing drum; b) Spiral classifier; c) Rod mill; d) Ball mills; e) Slurry tank; f) Disk filter; g) Rotary dryer; h) Hydrocyclones.

Table 5.7: Analyses of iron ores [9, 10].

	Fe_{tot}	SiO_2	Al_2O_3	CaO	MgO	Ignition loss
Lump ores						
Hamersley Iron	65.0	2.9	1.6	0.1	0.1	2.7
Mt. Newman Mining	65.7	3.4	1.2	0.1	0.1	1.5
CVRD-Itabira	67.7	1.1	1.0	0.0	0.0	0.4
CVRD-Carajas	67.6	0.7	1.1	0.1	0.0	1.3
Ferteco Feijao	67.3	1.8	1.0	0.1	0.0	0.9
MBR-Aguas Claras	68.4	0.6	0.7	0.1	0.1	0.8
Chowgule	60.1	3.5	2.8	0.0	0.0	not known
Bellary-Hospet	66.9	2.1	1.9	0.1	0.1	0.8
SNIM-Mauretania	63.1	6.8	1.3	0.0	0.0	not known
ISCOR-Sishen	66.5	3.1	1.1	0.1	0.1	0.6
ISCOR-Thabazimbi	64.0	6.0	1.0	0.2	0.4	1.2
Cerro Bolivar	64.2	1.3	1.0	0.1	0.1	5.5
Fine ores						
Hamersley Iron	62.5	4.4	2.6	0.1	0.1	3.2
Mt. Newman	62.6	5.5	2.4	0.0	0.0	4.7
Robe River	57.2	5.6	2.7	0.1	0.1	9.2
CVRD-Sinter Fines	64.4	5.0	1.2	0.1	0.1	1.5
CVRD-Carajas	67.9	0.6	0.7	0.1	0.1	1.4
Ferteco-Fabrica	64.3	3.1	1.9	0.1	0.1	2.7
Romeral	65.4	4.4	0.9	0.9	1.0	0.8
Mifergui-Nimba	67.5	2.3	1.0	0.1	0.0	1.0
Sesa Goa	60.6	3.5	4.2	0.1	0.1	3.8
NMDC-Bailadila	65.4	2.1	1.9	0.0	0.0	not known
Carol Lake	65.8	4.5	0.1	0.5	0.4	0.3
Bong Mining Co.	64.7	7.5	0.3	0.2	0.3	0.3
LAMCO	64.7	4.7	1.0	0.0	0.0	1.7
LKAB–Kiruna KBF	69.7	1.2	0.2	0.6	0.5	0.2
LKAB–Kiruna KDF	62.0	4.6	0.8	3.6	1.2	0.6
Co. Andaluza de Minas	55.0	4.4	1.1	4.3	0.4	not known
ISCOR–SISHEN	65.5	3.7	1.6	0.1	0.1	0.7
C.V.G.–El Pao	64.5	3.7	1.4	0.1	0.1	1.9
Pellets						
Evelth Mines	65.6	4.9	0.1	0.8	0.4	
Kiruna	66.1	2.5	0.3	0.3	2.0	
Malmberget	66.7	2.2	0.8	0.2	1.6	
CVRD	65.3	2.8	0.5	3.0	0.1	
Ferteco	65.0	3.3	0.9	2.5	0.0	
Samarco	65.1	2.6	1.2	2.2	0.2	
Kudremukh	66.1	2.8	0.3	2.3	0.1	
Carol Lake	65.6	4.9	0.3	0.5	0.3	
Cartier Mining Co.	65.2	5.2	0.5	0.4	0.3	
Wabush Lake	65.8	3.0	0.4	0.1	0.0	
Bong Mining Co.	64.1	7.0	0.3	0.3	0.3	
Las Encinas	66.8	1.5	0.7	1.6	0.8	
Empire CCI.	65.3	5.6	0.4	0.2	0.3	
Empire CCI.	59.5	5.3	0.4	7.0	1.9	
Minntac	65.6	5.4	0.2	0.2	0.3	

This simple way of improving the composition of iron-rich fine ore is often used in India and Brazil. A basically similar process with washing troughs or log washers was formerly used for high-alumina ores in many other regions (Salzgitter, Ilsede, Mesabi Range). If much of the alumina present is associated with limonite, a rod mill is employed instead of a washing drum. Applying 3–4 kWh/t on comminution frequently results in satisfactory removal of alumina. Figure 5.4 illustrates the beneficiation of a magnetite ore from a Magnitnaya-type deposit. Secondary and tertiary crushing and primary grinding are replaced by an autogenous mill.

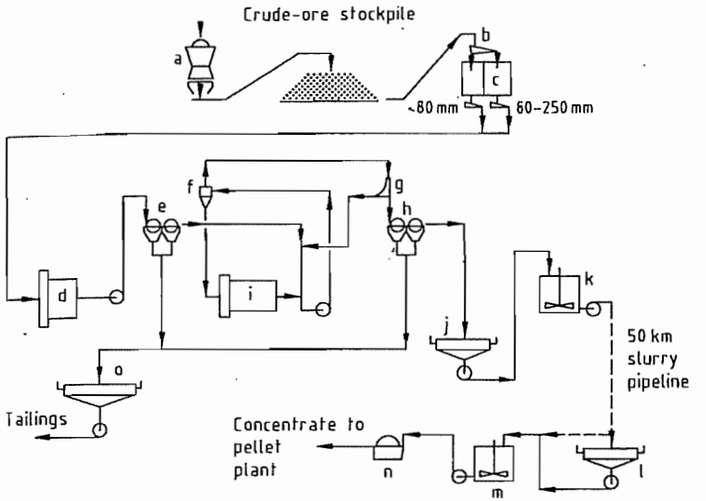

Figure 5.4: Flowsheet of Pena Colorada beneficiation plant, Mexico: a) Primary crusher; b) Crude-ore screen; c) Crude-ore bins; d) Autogenous mill; e) Primary magnetic separation; f) Hydrocyclones; g) Sieve bend; h) Secondary magnetic separation; i) Ball mill; j) Concentrate thickener; k) Slurry tank; l) Concentrate thickener; m) Slurry tanks; n) Disk filter; o) Tailings thickener.

The concentrate has ca. 69% iron; with a particle-size distribution of ca. 80% < 0.045 mm, which is fine enough for pipeline transportation and pelletizing. Numerous beneficiation plants for magnetite ore from other deposit types have been designed in a similar way, for example in the former Soviet Union (Krivoi Rog, Kursk, Olenogorsk), in the Lake Superior area, and in northern Sweden. Older installations still employ conventional comminution (three stages of crushing and two to three stages of grinding).

For hematite ore, the first grinding stage is followed by gravity separation or, in the case of fine grained ore, further grinding is followed by high-intensity wet magnetic separation or flotation. In many cases, however, the principal iron minerals in such ores from weathering zones include not only hematite but martite (which is only a little less magnetizable than magnetite) with residual magnetite. In this case, complex flowsheets must be adopted, including low- and high-intensity magnetic separation, flotation, classification and slurry treatment for dewatering of the concentrate. This is also the case if undesirable constituents are present (e.g., apatite).

Finally, the *selective dispersion* process should be mentioned. In one Michigan plant, this operation is a preliminary to flotation. After grinding to the liberation size, sodium hydroxide and starch are added to the ore pulp (sodium hydroxide to disperse aluminous and limonitic constituents, starch to flocculate the specularite) and the flocculated agglomerates are separated from the dispersed minerals in a hydroseparator. The downstream flotation removes coarse quartz which is discharged in a conventional manner, with amine salts as collectors.

5.3.5 Agglomeration

In present-day smelting technology, very fine material is undesirable in the reduction equipment. The blast furnace is the dominant type of equipment for the production of iron metal. Only in exceptional cases (small furnaces with capacities up to ca. 100–150 t/d of pig iron) is unscreened crude ore used (after primary crushing if necessary). Modern high-performance blast furnaces require physical and metallurgical preparation of the burden. Formerly agglomeration was used in a purely

physical way, as a process of size enlargement aimed at improving the permeability of the blast-furnace burden; however, developments hl recent years have shifted part of the slagging into the fine-ore or concentrate sh1tering step. On the other hand, the requirements for physical and chemical quality of the blast furnace burden have become more stringent, and mining companies that supply ore to several ironworks (as the large ones generally do) now prepare a variety of concentrate or fine ore qualities from the same or similar crude ores.

As a rule, blast-furnace burden contains lump ore, sinter, and pellets. Pellets are made from both concentrate and iron-rich fine ore. If the beneficiation process yields very fine-grained concentrates (e.g., < 0.1 mm), these are usually converted to pellets at the mine and transported in this form. Sinter is generally produced at the ironworks. The varying loads imposed on material during transport to the blast furnace mean that pellets must satisfy stringent mechanical strength requirements. Pellets are also nearly always made from one well-defined ore or concentrate, whereas sinter is produced from predesigned mixtures of ores and additives. There are exceptions, such as pellets made at ironworks from mixed ore, or sinter made from a single ore or concentrate quality where an ironworks uses ore from a single deposit. Blast furnaces are also sometimes operated with lump ore alone, sinter alone, or pellets alone. Sponge iron plants are generally fed with a single iron source.

Sinter and pellets differ in the way the particles are bound into the agglomerate. In pellets, the ore particles are connected chiefly by bridges of ore. When magnetite is oxidized at temperatures > 900 °C during hardening of pellets, these bridges arise through mobilization of lattice constituents during recrystallization into the hematite lattice. In the case of hematite ores, mobilization is less pronounced, because the crystal lattice structure does not change. The formation of iron oxide bridges is supported by additional slag bridges; it must be remembered that the quantity of slag in many pellet qualities is only 3–4% (corresponding to 6–7 vol%).

Sinter consists of a calcium ferrite matrix, with siliceous and aluminous constituents dissolved and primary hematite embedded in it. Whereas pellets are thoroughly oxidized (a maximum of 0.5% FeO), sinter contains 4–6% FeO, which is linked to silica and alumina in the matrix.

Pellets are burned at a temperature below the melting points of the constituents. Their strength gain is adequate only when the reaction temperature is controlled to ±10 °C over long time periods. For this reason, hot gas is used to supply heat; it can be generated by the combustion of fuel gas, oil, or even coal. In sintering, on the other hand, the constituents of the mixture are melted. This happens at temperatures so high that the reaction itself goes to completion within minutes, but in a thin layer that continuously advances through the material bed cocurrently to the gas. The fuel is coke breeze, or occasionally non-gassing coal fines, evenly distributed in the sinter mixture.

Pelletizing. Iron-ore pellets are made in two steps. The concentrate to be pelleted must have a sufficiently fine particle-size distribution (65–85% < 0.045 mm) and a specific surface area of at least 1600 cm^2/g as measured by a permeability method (Blaine, Fisher Subsieve Sizer).

Spherical *green pellets* (green balls) of appropriate size (ca. 9–16 mm in diameter) are formed by a pelletizing disk or drum. The particles are bound together by capillary forces acting through water bridges between them. This means that green pellets can be obtained only at a narrow range of moisture content. If the water content in the fine ore (which is usually recovered as a filter cake) is too high, water-absorbent materials such as bentonite can be used to correct it within narrow limits. If the water content is low (ideal case) it is useful to hold it in the filter cake ca. 0.5–1% lower than the green pellet moisture content to suppress the premature formation of undersize pellets ("micropellets") in the granulator.

Prior to (or during) the formation of green pellets, substances are added to the fines to render them stable against the stresses that occur in the hardening process. In addition to bentonite, whose active constituent is strongly water-absorbent montmorillonite, organic binders such as Peridur have come into use recently. The latter are advantageous in that they can be burned off during hardening, whereas bentonite elevates the silica and alumina content of the pellets.

Purchasers usually prescribe the gangue composition of pellets to fit the operating requirements of the particular blast furnace and the chemical composition of the other iron sources to be used. This composition, which also governs the chemical and metallurgical properties of the pellets, is controlled with additives, the most important being slaked lime, limestone, dolomite and olivine. These are added in a grain size corresponding to that of the fines.

The second operation is the thermal *hardening* of the pellets at 1200–1320 °C. Nonthermal hardening is employed only in a few unimportant cases. Three distinct heat hardening systems exist: the traveling grate (Figure 5.5), the combination of preheating traveling grate and rotary kiln (grate–kiln) (Figure 5.6), and the shaft furnace. The shaft furnace is mainly suitable for magnetite concentrates and low capacities (up to ca. 500 000 t/a) and has lost much of its market share in the past 15 years. The traveling grate and the grate–kiln combination each share ca. 50% of the market.

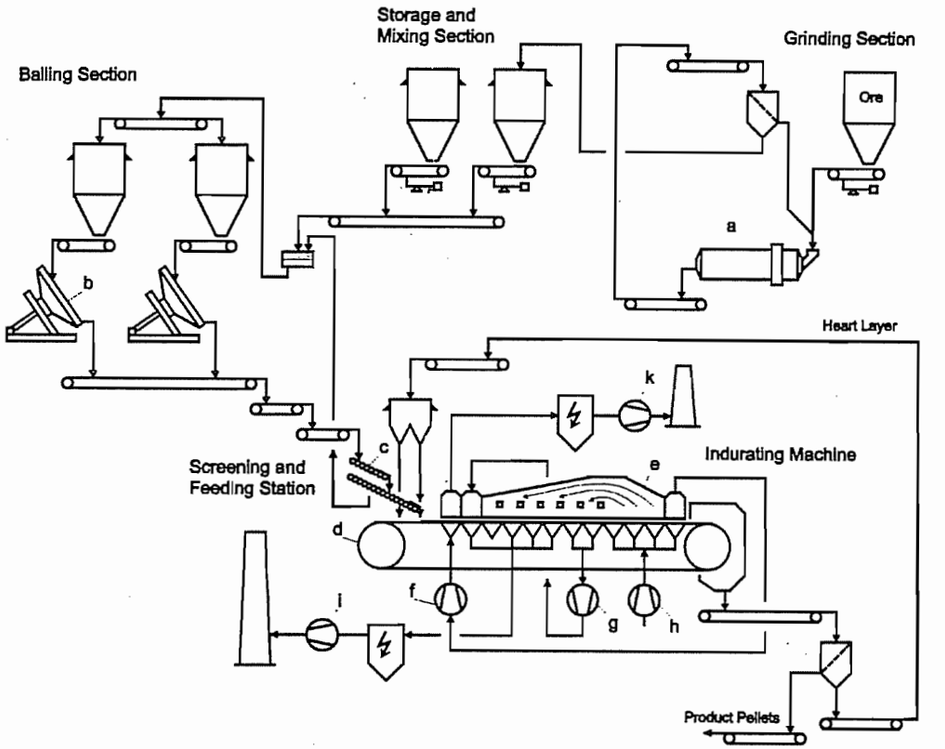

Figure 5.5: Flowsheet of Lurgi–Darvo travelling grate pelletizing process: a) Grinding mill; b) Pelletizing discs; c) Roller feeders; d) Travelling grate; e) Firing hood; f) Updraft Drying fan; g) Recuperation fan; h) Cooling air fan; i) Waste gas fan; k) Hood exhaust fan.

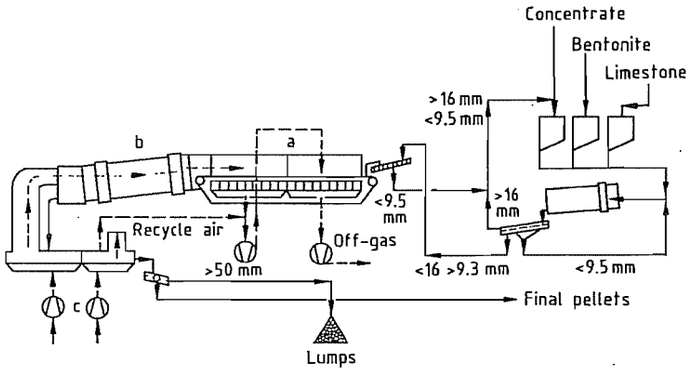

Figure 5.6: Flowsheet of combined traveling grate/rotary kiln ("grate kiln") process: a) Traveling grate; b) Rotary kiln; c) Annular coolers.

The "basicity" of the final pellets, expressed as the ratio $(CaO + MgO):(SiO_2 + Al_2O_3)$, is < 0.1 for "acid pellets" or up to 1.3 for "basic pellets". Each range of values offers certain advantages and disadvantages with respect to mechanical strength and metallurgical qualities.

After a number of years of declining pellet production and the shutdown of several plants, the western world had, at the end of 1987, a pellet capacity of roughly 163×10^6 t/a (100 units using the three hardening processes).

According to present information, the former Soviet Union has 20 traveling-grate plants and 5 grate–kiln plants. The first group has a total reaction area of ca. 6500 m^2, which might correspond to a pellet capacity of ca. 50×10^6 t/a. Grate–kiln plants add an estimated capacity of ca. 107 t/a.

While the former Soviet Union has a large number of pellet plants, up to now this has not been the case for China.

For the assessment of the mechanical and metallurgical properties of burned pellets, a number of parameters are determined in more-or-less standardized tests. The most important are:

- Cold Compression Strength
  Individual pellets 10–12 mm in diameter are compressed to failure between two plane or slightly concave faces of a hydraulic press, and the crushing force is measured (values found in practice are usually > 3000 N per pellet).
- Abrasion Resistance
  The abrasion resistance is determined in the ISO tumble test. Under standardized conditions, pellets are tumbled in a drum and the > 6.3 mm and < 0.6 mm fractions are determined. The values should be at least 95% and at most 4%, respectively.
- Low-Temperature Disintegration test
  This test indicates how the pellets will behave, for example, in the blast furnace in the critical range of temperatures around 500 °C. In an electrically heated rotary kiln, pellets are heated to 500 ± 10 °C and held at this temperature for 60 min under reducing conditions. After cooling, the pellets are screened to determine the > 6.3 mm and < 0.5 mm fractions. The degree of reduction is determined. The values for the > 6.3 mm fraction are usually between 60 and 80%; those for < 0.5 mm usually 10–20%.
- Free Swelling
  In a vertical tubular furnace, 18 pellets are reduced with a carbon monoxide hydrogen mixture at 1000°C. The weight loss during reduction yields the degree of reduction. The volume change in the pellets indicates the swelling, which should be 20% at maximum. The compression strength measured in a hydraulic press should be > 500 N per pellet.

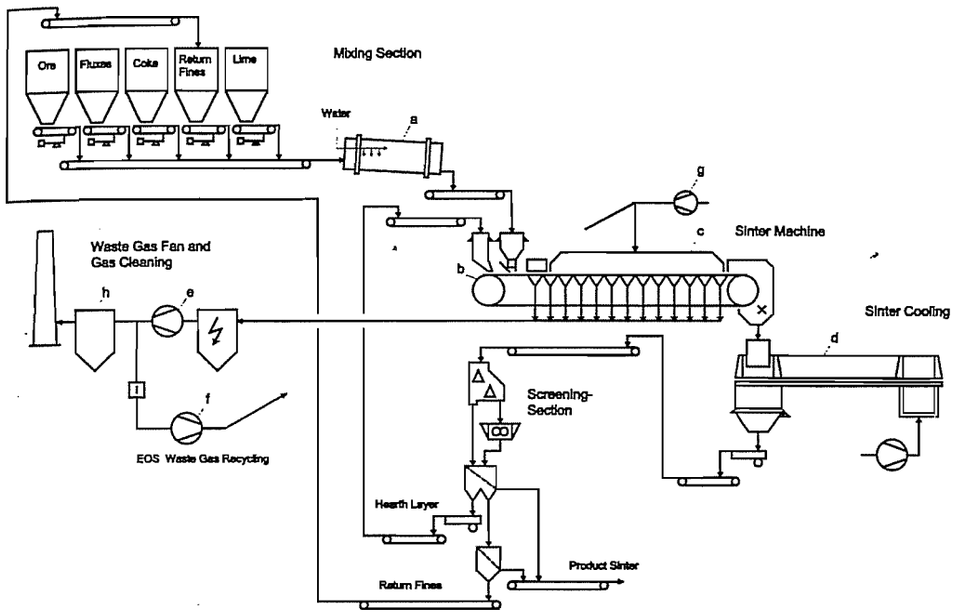

Figure 5.7: Flowsheet of sintering: a) Mixing drum; b) Travelling grate; c) Gas distribution hood (EOS only); d) Annular cooler; e) Waste gas fan; f) EOS recycling gas fan; g) Fresh air blower (EOS only); h) Waste gas final cleaning.

- Reduction under Load (RUL)
  In an upright retort, pellets are heated to 1050 °C, placed under a mechanical load of 5 N/cm^2, and exposed to a reducing atmosphere. The pressure drop of the reducing gas across the bed and the reduction rate are determined. A low pressure drop indicates pellets stable in reduction. The pressure drop should not exceed 100 Pa.

The reduction rate at 40% reduction is an important parameter of reducibility; dR/dt_{40} should be at least 1% per minute.

Special test methods have been devised for pellets used in various direct-reduction processes (HyL reduction test in an upright retort, Midrex test, and testing for the SL/RN process in an electrically heated laboratory rotary kiln). In the test for the SL/RN process, pellets and reducing agent (usually coal) are investigated at the same time. A number of different or modified test procedures are employed in individual countries or at individual ironworks.

Sintering. Iron ore sinters are virtually all produced in travelling-grate installations (Figure 5.7). The rotary kiln and pan-sintering processes formerly in use are no longer important. Likewise, cooling of the hot sinter at the last section of the grate has become obsolete. Standard is now the straight-grate "Dwight–Lloyd-Process". Straight-grate as well as annular coolers are in use. Quite some efforts are being made to reduce solid and gaseous contaminants contained in the sintering off-gas (dust, SO_2, NO_x). A new development recently introduced by Lurgi in industrial plants is "EOS" (Emission Optimised Sintering") process. It is characterized by recirculating approximately half of the off-gas of the sintering grate back to the gas distribution hood, where it is mixed with fresh air and used as oxygen carrier and for heat transportation through the sinter bed. The advantages are reduction of the final waste gas volume (allows for smaller gas cleaning facilities), and substantial reduction of waste gas pollutants (dust, SO_2, NO_x, dioxines, furanes). Fuel consumption is reduced by

about 5 kg/t of sinter, whereas the electric energy consumption is increased by about 1.5 kWh/t.

As a rule, several ores are processed in one unit; a "monosinter" from just one ore is the exception. Along with ore and concentrate, the mixture for sintering also contains recycle material from the ironworks, provided no buildup of undesirable or detrimental substances results. Undersize sinter from the screening step is also recycled. The basicity of the sinter has been substantially increased in recent years. Originally sintering was considered only as a means to deal with fine ore with respect to improved handling and permeability of the blast furnace burden ("physical burden processing"). The overall chemical composition of the blast furnace feed (including coke ash) was adjusted by addition of suitable materials in the form of lumps (limestone, dolomite, manganese ore if necessary). Thus, the basicity of sinter and lump ore generally was < 1 (exception minette ore with high calcite content of the gangue).

Today these additives are generally added to the sinter mix as fines (< 5 mm) and sometimes precalcined (burnt lime instead of limestone). The basicity of the sinter is generally higher than that of the blast furnace slag to compensate (1) for the "acid" coke ash, (2) the gangue of the lump ore, and (3) slag components of the iron-ore pellets.

Increasing the basicity also improves the quality of the basic sinter as well as the heat economy. Many plants today produce sinter with a basicity of > 1.5. The slag analysis is controlled by addition of limestone or burnt lime, dolomite (to control CaO and MgO), olivine (to control MgO and SiO_2), and quartz sand. The most common fuel is coke breeze. To ignite the mixture gas or oil heating is applied. The total heat consumption for an iron-rich basic sinter is between 1.3 and 1.7 MJ per tonne of final sinter. When low-iron ore mixtures (e.g., those containing minettes) or ores containing high levels of alumina (2–4% Al_2O_3) are sintered, the heat consumption is higher (up to 2.5 MJ/t). Analyses of sinter from German ironworks fall in the following approximate ranges (in %):

Fe_{tot}	55.5–55.8
Fe(II)	4.5–6
SiO_2	5–6
CaO	9–11
MgO	1.2–3.2
Al_2O_3	1.2–2
$CaO:SiO_2$	1.4–1.9

Ironworks in *Germany* use imported ores almost exclusively; some heat-consumption and analysis figures for other European ironworks differ from the ones cited, because low-iron domestic ores still are processed there. In contrast, sintering plants in *Japan* operate under conditions similar to those in Germany. The basicity of the sinter in Japan, however, is nearly always > 1.8.

In the *United States*, the fraction of sinter in the burden is only 22.5% (1986; Table 5.6), much lower than in Europe and Japan. The fraction of pellets, on the other hand, is very high (72.2%). Thus, in the United States improvement in pellet quality, above all in metallurgical properties, have been the focus of attention, with the result that basic pellets with $CaO:SiO_2$ ratios of ca. 1.5 have been sought.

Few details are known about current sintering technology in the former *Soviet Union* and *China*. Rich fine ores are rare in both countries, and agglomerates are made chiefly from concentrates. In some works, blast furnaces are operated on 100% sinter. Since the basicity of the sinter in these cases must be adapted to the requirements for blast-furnace operation, the basicity values are often too low for a sinter of truly good quality. One remedy might be to pellet part of the concentrate at a low basicity and raise the basicity of the sinter to 1.6–1.8.

A variety of test methods are used for sinter quality control; some of the techniques are similar to the ones for pellets. The methods include:

- Shatter Test
  The shatter test has been standardized only in Japan. At Lurgi, 150 kg of sinter (grain size > 8 mm) is dropped three times from a height of 2 m onto a steel plate; then the > 20 mm, 20–8 mm, 8–2 mm, and < 2 mm fractions are determined.
- Tumble Test
  The shatter test is often replaced by the tumble test, which follows the same guidelines as described above for pellets The fraction < 6.3 mm should be at least 70%; at German ironworks it is between 70 and 85%.
- Low-Temperature Disintegration
  This test is not one of the standard ones; it is performed in a similar way to the test on pellets.
- Reduction Degradation Index (RDI)
  The reduction degradation index is now regarded as the most important quality criterion for sinter. In the test, 500 g of sinter (grain size 20–16 mm) in a stationary bed is reduced for 30 min at 550 °C by a gas mixture comprising 30 vol%, carbon monoxide and 70 vol% nitrogen.
  After cooling, the sample is placed in a drum (130 mm in diameter and 200 mm long and provided with two lifters) and subjected to 900 revolutions at 30 rpm. The material is then screened at 6.3 mm, 3.15 mm and 0.5 mm. The RDI is the fraction < 3.15 mm. This should be 35% if possible; at ironworks, in Germany it is between 30 and 40%.
- Relative Reducibility
  Ironworks use very different methods for the relative reducibility test. A sample is reduced at 900 °C using a carbon monoxide nitrogen mixture similar to RDI. The index reported is the degree of reduction at the end of the test. In addition, a test as set forth in ISO 4695 is carried out to determine the reduction rate at 40%, reduction, which is usually ca. 1.5% per minute.

5.4 Reduction of Iron Oxides [11]

5.4.1 Chemical Aspects

The reduction of iron oxide ores takes place at an appreciable rate only at temperatures above 900 °C. Below this temperature, a dark porous mass is obtained having the same shape as the original lumps or particles, and reduction is usually incomplete. Figure 5.8 shows a particle of Fe_2O_3 before and after reduction by hydrogen at 700 °C showing the porous nature of the product. In general, reduction follows the scheme

$$Fe_2O_3 \rightarrow Fe_3O_4 \rightarrow FeO \rightarrow Fe$$

If reduction is conducted below 570°C, the reaction follows the scheme

$$Fe_2O_3 \rightarrow Fe_3O_4 \rightarrow Fe$$

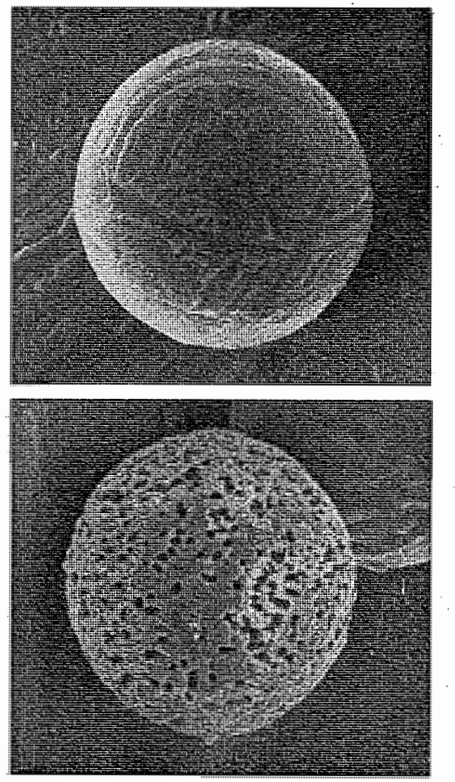

Figure 5.8: A 20-µm Fe_2O_3 sphere before and after reduction by hydrogen at 700 °C (2500 ×).

since FeO is unstable below 570 °C. When a hard dense oxide is reduced, metallographic examination usually shows a layered structure: Fe_2O_3 in the core, surrounded by Fe_3O_4, FeO, and finally Fe as can be seen in Figure

5.9. For porous oxides, however, no distinct interfaces are observed, except a gradual transformation from Fe on the outside to Fe_2O_3 in the center. This is because the reducing gas can penetrate faster than it can react at any oxide interface.

Between 950 and 1000 °C complete reduction in a reasonable length of time usually takes place. At 1000 °C, sintering of the particles starts and a product having the form of a sponge is obtained. At about 1200 °C a pasty porous mass is formed due to the presence of impurities. If reduction is carried out in the presence of carbon, the iron absorbs it rapidly and the product begins to melt at 1300 °C. Iron containing 4.5% carbon melts at 1125 °C which is far below the melting point of pure iron (1530 °C). Table 5.8 summarizes these points.

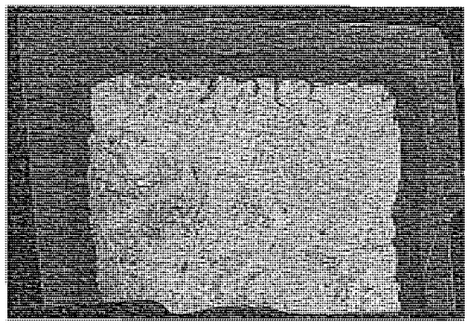

Figure 5.9: Cross section of a partially reduced dense iron ore in hydrogen at 850 °C for 35 minutes. Sample etched to show the multilayer structure of products.

Table 5.8: Effect of temperature on the reduction of iron oxide ores.

Temperature, °C	Product
900	Dark grey porous mass has the same shape as the original particles; reduction usually incomplete.
950–1000	Complete reduction in a reasonable length of time.
1000	Sintering of product starts; the product has the shape of a sponge.
1200	A pasty porous mass is formed.
1300	If reduction is carried out in presence of carbon, the iron absorbs it rapidly and the product begins to melt.

Ferric oxide, Fe_2O_3, is generally reduced with a higher velocity than Fe_3O_4. Also, hydrogen is more effective than CO as a reducing agent. Like any other heterogeneous reaction, the rate of reduction is influenced by the stagnant boundary layer of gas which surrounds each oxide particle (the Nernst boundary layer). This factor depends on the rate of flow of the reducing gas past the oxide particle, i.e., it is a function of the design and operation of the apparatus used for reduction. The resistance of the boundary layer may be eliminated by increasing the rate of flow of gas, but this way may not be economically feasible because unreacted gas will escape in the stack, or the carry over of dust particles will be excessive.

Swelling or shrinkage may accompany the reduction. Swelling is due to the formation of whiskers which in turn is related to the phenomena of nucleation and crystal growth. Shrinkage is due to volume change when the oxide is reduced to metal as well as due to sintering. Both are influenced by impurities. Calcium oxide, for example, was found to prevent swelling and to increase the rate especially when conducted at or below 700 °C. The width of the FeO layer formed when Fe_2O_3–CaO mixture is reduced is much less than when pure Fe_2O_3 is reduced, all other conditions being equal. It seems that FeO reacts with CaO forming Fe and a ferrite according to

$$3FeO + CaO \rightarrow Fe + CaFe_2O_4$$

Calcium ferrite formed is then reduced directly to Fe and CaO without producing FeO. Calcium carbonate increases the rate of reduction in the same way as CaO with the added advantage that during sintering prior to reduction, CO_2 is given off thus creating a porous product which enhances reduction. Small amounts (0.1–1%) of Na_2CO_3 or K_2CO_3 cause extensive swelling.

5.4.2 Technical Aspects

It was not until the 14th century that furnaces were developed that could not only produce iron but at the same time melt it so that the product called pig iron could be tapped

from the furnace in a molten form, thus allowing large scale production and continuous operation. Such a furnace is called a blast furnace because of the blast of air introduced. Figure 5.10 shows a typical view of a blast furnace plant. At present, most pig iron is transferred in molten state to steelmaking plants and in this form it is referred to as hot metal. Sometimes, it is required in solid form for convenient handling and therefore is cast into molds where it solidifies to form what is referred to as pigs. Processes taking place in the furnace are:

- Reduction of the iron compounds present in the ore
- Separation of the resulting iron from the slag.

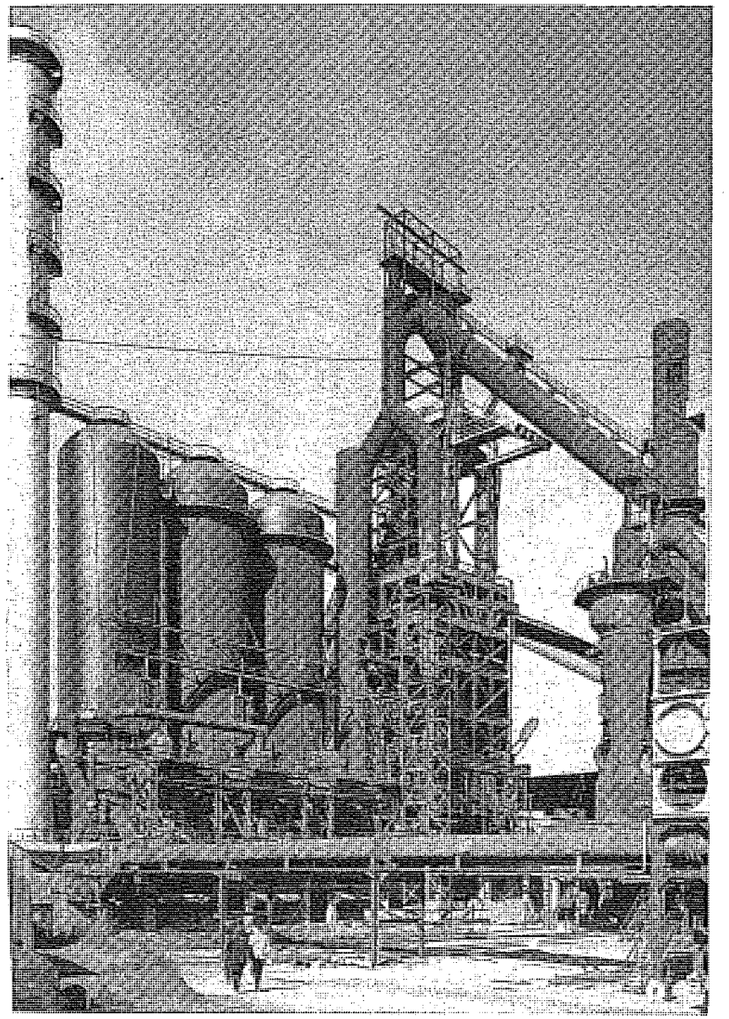

Figure 5.10: Typical view of a blast furnace plant. The blast furnace at the center, the three towers on the left are the stoves.

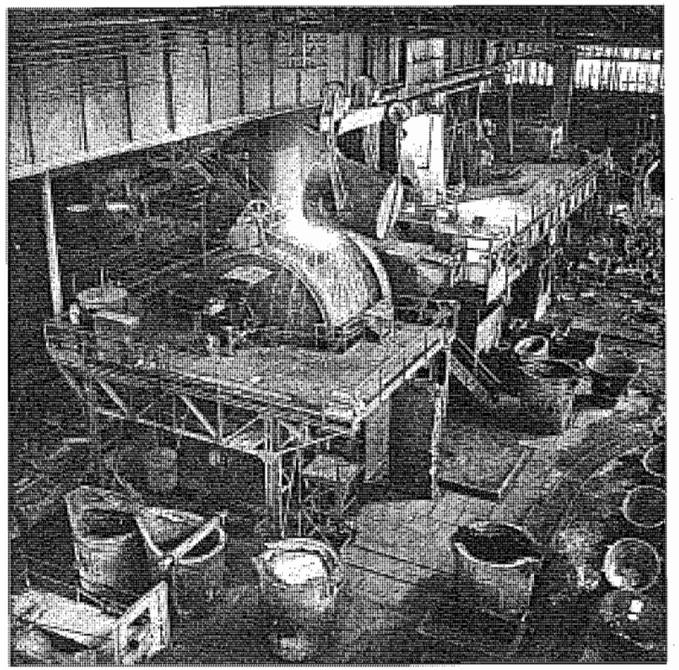

Figure 5.11: Hot metal mixer.

Steel is the most important commercial form of iron because of its high tensile strength. Molten pig iron from the blast furnace is usually stored in a hot-metal mixer before transferring it to the steelmaking plant (Figure 5.12). A hot-metal mixer is a cylindrical vessel up to 1500 tons capacity, lined with fire bricks (about 0.6 m thickness) and mounted horizontally such that it can be tilted to pour the desired amount of metal into a transfer ladle for transport to the steelmaking plant (Figure 5.11). The functions of the hot-metal mixer are therefore the following:

- To conserve the heat in pig iron, keeping it molten for long periods.
- To promote uniformity of iron by mixing the products of several blast furnaces. This permits delivery of iron of more uniform compositions and temperatures.
- To permit independent operations between the blast furnaces and the steelmaking plant because of its large capacity.

Table 5.9 shows the raw materials and the products of a modern blast furnace.

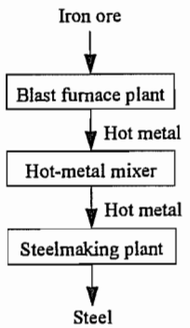

Figure 5.12: Schematic representation for the flow of raw material for steelmaking.

5.4.3 Raw Materials

Iron ores are the most important raw material charged to blast furnace. Other minor material are the following:

- Mill scale (Fe_3O_4 by-product of hot-rolling)

Table 5.9: Raw materials and products of a blast furnace per ton of pig iron (in tons).

Raw materials	
Ore	1.7
Coke	0.5–0.65
Flux (limestone)	0.25
Air	1.8–2.0
Products	
Pig iron	1.0
Slag	0.2–0.4
Flue dust	0.05
Blast furnace gas	2.5–3.5

Table 5.10: Typical analysis of Lake Superior ore.

	%
Fe	55.6
SiO_2	5.9
Mn	0.2
P	0.6
Al_2O_3	3.6
CaO	1.2
MgO	0.9
SO_3	0.06
$Na_2O + K_2O$	trace
TiO	0.02
H_2O	12.1

- Blast furnace flue dust after sintering
- Pyrite cinder after leaching away of the non-ferrous metals it contained

5.4.3.1 Iron Ores

High-grade ores contain 60–70% Fe, medium-grade 40–60% Fe, and low-grade < 40% Fe. The world's main supply of iron is obtained from ores containing hematite; those containing magnetite supply only about 5% of the world's iron and the most important source of such ores is Sweden and the Urals. The most important ore containing siderite is in Erzberg, Austria. A typical analysis of an iron ore is shown in Table 5.10.

5.4.3.2 Coke[1]

Coke in the blast furnace has two functions:

- As a fuel producing the heat required for reduction and melting the iron.
- To supply the reducing agent (mainly CO).

[1] For the manufacture of coke, see Section 5.22.

Table 5.11: Typical analysis of coke.

	%
C	90.0
SiO_2	4.4
Fe	1.3
Mn	0.07
P	0.03
Al_2O_3	2.8
CaO	0.3
MgO	0.2
S	0.9
H_2O	1.5

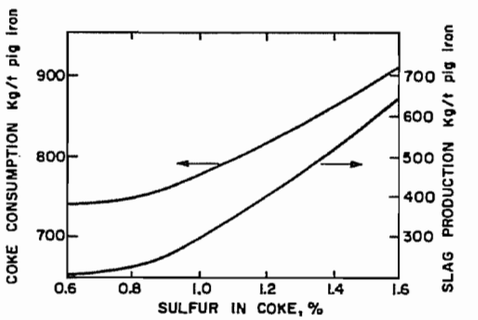

Figure 5.13: Effect of sulfur in coke on coke consumption and slag volume.

Besides, a small amount of carbon dissolves in the hot metal, thus lowering its melting point. Main requirement for coke are: high calorific value, high mechanical strength, and low impurities. A typical analysis of coke is given in Table 5.11. Coke burns intensively near the tuyères; temperatures in this region reach 1700 °C. At this temperature, CO_2 reacts immediately with carbon to form CO:

$$C + O_2 \rightarrow CO_2$$

$$C + CO_2 \rightarrow 2CO$$

Sulfur in the coke accounts for about 90% of the total sulfur entering the blast furnace. About half of this sulfur is volatilized as H_2S or COS when the coke is burned and leaves with the blast furnace gas. The remaining sulfur is partially eliminated in the slag, and a small amount enters the metal. When coke contains excess sulfur, large amounts of limestone must be added to insure that the sulfur content of the pig iron is maintained at a low level. This will result in a large volume of slag, and a correspondingly large consumption

of coke because the decomposition of limestone is an endothermic reaction, as shown in Figure 5.13. Furthermore, the productivity of the furnace decreases.

5.4.3.3 Limestone

The function of limestone is to render the gangue in the ore and the ash of the coke, mainly SiO_2 and Al_2O_3 which have high melting points, easily fusible. In the blast furnace, limestone is decomposed starting at 800 °C as follows:

$$CaCO_3 \rightarrow CaO + CO_2$$

It is used in pieces 5–10 cm in size; a typical analysis is shown in Table 5.12.

Table 5.12: Typical analysis of limestone.

	%
CaO	51.5
MgO	1.7
CO_2	41.4
SiO_2	3.4
Fe	0.3
Mn	0.1
P	0.006
Al_2O_3	0.9
SO_3	0.06
$Na_2O + K_2O$	trace
H_2O	0.5

5.4.3.4 Air

Air for the blast furnace has to be preheated to 500–1000 °C and compressed to 200–300 kPa to burn the necessary amount of coke to furnish the required temperature for the reaction:

$$C + {}^1/_2O_2 \rightarrow CO$$

Air always contains a certain amount of moisture depending on the atmospheric humidity. Near the tuyères zone, any moisture in the air will react with coke as follows:

$$C + H_2O \rightarrow CO + H_2$$

Since this reaction is endothermic, variation in atmospheric humidity greatly affects the thermal balance of the furnace to such an extent that it would cause wide variation in the chemical composition of the iron produced. Some plants installed units to separate the moisture from the air by refrigeration before entering the furnace.

Table 5.13: Typical analysis of pig iron.

	%
C	3.5–4.25
Si	≈ 1.25
Mn	0.9–2.5
S	≈ 004
P	0.06–3.00
Fe	≈ 94

5.4.4 Products

5.4.4.1 Pig Iron

Pig iron is transferred molten as hot metal or molded in pig-machine. A typical analysis of pig iron is given in Table 5.13. The hearth temperature influences the carbon content in pig iron.

5.4.4.2 Slag

Slag formed in the blast furnace serves two purposes:

- To collect the impurities in the molten metal
- To protect the metal from oxidation by the furnace atmosphere

Analysis of a typical blast furnace slag is given in Table 5.14. About 1% of the slag containing about 60% Fe is recovered by magnetic separation and is returned to the blast furnace. Molten slag from a blast furnace is usually treated in one of the following ways:

- It is poured into a pit and after solidifying and cooling it is excavated, crushed, and screened. The product is called air-cooled slag and is used in concrete and railroads.
- It is either allowed to run directly into a pit of water producing a coarse, friable product, or a stream of molten slag is broken up by a high-pressure water jet as it falls into the pit. The product in both cases is called granulated slag and is used in making building blocks.
- If limited amounts of water are applied to the molten slag, a dry cellular lump of product called lightweight expanded slag is formed. In this case the amount of water should be less than that required for granulation. This slag has a relatively high structural strength with good insulating and acoustical properties and is therefore used in making acoustical tile and for other structural purposes.
- Slag fines are used as filling material in road construction since they have excellent binding properties with bitumen.

Table 5.14: Analysis of a typical blast furnace slag.

	%
SiO_2	35
CaO	44
Al_2O_3	15
MgO	3
FeO	1
MnO	1
S	1
Total	100

Table 5.15: Typical analysis of blast furnace gas.

	vol%
CO	27
CO_2	12
N_2	60
H_2	1
$(CN)_2$	trace
Total	100

5.4.4.3 Gas

Gas coming out of furnace top is more than that introduced at the bottom due to the gasification of carbon. A typical analysis of the gas is given in Table 5.15. The CO content in the gas is due to the reaction:

$$CO_2 + C \rightarrow 2CO$$

About 20% of the total fuel requirement is consumed in this manner. This reaction not only consumes coke but also consumes heat since it is endothermic. Carbon dioxide is a product of ore reduction and $CaCO_3$ decomposition. Because of its CO content, the blast furnace gas is used as a fuel to preheat the air blast and to generate power (boilers, etc.). The gas leaves the furnace at 120–370 °C.

During the manufacture of iron in the blast furnace, some hydrogen cyanide, HCN, and cyanogen gas, $(CN)_2$, are formed as a result of the reaction of nitrogen in the blast with coke. These gases are extremely poisonous. Their formation is thought to be catalyzed by alkali oxides:

$$H_2O + 3C + N_2 \rightarrow 2HCN + CO$$

Blast furnace gas contains 200–2000 mg/m^3 of these cyano compounds. In the dust collecting system, the gases are scrubbed with water and some of this water finds its way in waste disposal. Before discharging this water, cyanide compounds dissolved in it must be destroyed.

5.4.4.4 Flue Dust

This material is composed of about 15% carbonaceous material, 15% gangue, and 70% Fe_3O_4 though only Fe_2O_3 may have been charged; the reason is that the reaction at the top of furnace is

$$3Fe_2O_3 + CO \rightarrow 2Fe_3O_4 + CO_2$$

Flue dust is collected as a mud in the venturi scrubbers and Cottrell precipitators; it contains about 40% solids. It is transferred to thickeners where it is thickened to 60% solids, then filtered. The filtrate returns to the thickeners and the filter cake containing about 25% moisture is transferred to the sintering plant where it is agglomerated into a product suitable for charging to the furnace.

5.4.5 Behavior of Impurities

Impurities in the raw materials play an important role in the blast furnace because they influence the quality of the product and the life of the refractory lining. Although some of these impurities may be in trace amounts, yet they will represent hundreds of thousands of tons when considering the continuous operation of the furnace for 5 to 7 years through which millions of tons of ore have been reduced. The behavior of impurities varies considerably and can be divided as follows:

- Unobjectionable impurities are those which are not reduced, e.g., Al_2O_3 and MgO. They are also valuable fluxes.
- Impurities that completely enter the pig iron; these are phosphorus, copper, tin, nickel, and vanadium. The reduction of the

compounds of these elements takes place readily. Of these the most serious is phosphorus since it has to be completely removed to make an acceptable steel.

- Impurities that partially enter the pig iron: these are manganese, silicon, titanium, and sulfur. The reduction of MnO_2, SiO_2, and TiO_2 takes place only at high temperatures. Therefore, the presence of the respective metals in pig iron will be a function of the temperature in the hearth; usually about 70% of these metals enter the pig iron. Titanium is especially undesirable because its presence in the slag, even in small amounts, increases its viscosity. Manganese, silicon, and sulfur have to be removed later in the steelmaking process.
- Impurities that accumulate in the furnace: these are the alkali metals and zinc. Compounds of these metals are readily reduced. As the charge descends into the hotter region of the furnace they are reduced to metals; these metals are volatile under the conditions of operations in the furnace. As vapors, they travel upward, where they react with CO_2 and deposit as oxides on the surfaces of the cooler particles of the charge and are again returned to the hotter region of the furnace as the charge descends. The process is repeated and thus these metals will never leave the furnace. They accumulate in large amounts and the vapors penetrate the refractories and partially condense in the pores and cracks thus causing their disintegration. To minimize difficulties in furnace operation such as fluctuating hot metal temperature or sulfur content and to avoid the build-up of alkali in the furnace, the amount of alkali entering the furnace is carefully monitored and maintained at a fixed low level. Slag basicity and hot metal temperature are also adjusted to ensure maximum removal of alkali in the slag. The tendency is approximately as follows:
  - As the alkali content increases, slag basicity should be decreased for any given temperature of iron.
  - As the temperature of molten iron increases, slag basicity should be decreased for any given alkali loading.

These conditions are opposite to those needed for hot metal sulfur content, and therefore a compromise has to be made.

5.5 The Blast Furnace

5.5.1 General Description [11–14]

The blast furnace is composed of a hearth and a stack on the top. Such furnace is also known as a shaft or a vertical furnace (Figure 5.14). The name is due to the fact that air is blown or "blasted" through the charge. The furnace has the following characteristics:

- The charge enters at the top of the stack and the products get out at the bottom. Any gases formed are discharged from the top.
- Heating is conducted by burning coke which is incorporated in the charge. It is ignited by air blown in near the bottom of the furnace. The hot gases pass upward through the descending cold charge.
- The charge must consist of coarse material that is strong enough to withstand the static pressure in the shaft without crumbling into powder. Powders are objectionable because they will be easily blown outside the furnace by the gases. Also, they cause channelling to take place in the furnace, i.e., the reacting gases will go only through certain channels in the bed thus decreasing greatly the furnace efficiency. The charge must be permeable so that the rising gases can pass freely through all of its parts.
- At one time, the top of the furnace was left open causing great heat loss. Later, it was closed and opened only during charging. Today furnaces have at the top the double bell system which keeps the furnace closed at all times thus preventing the escape of gases even during charging. This system (Figure 5.15) is composed of two bells: one small and one large. When both are in the closed position, the charge is dumped in the hopper above the small bell. The large bell remains closed while the small bell is opened to admit the charge to the large bell hopper. The small bell is then closed to prevent the escape of gas into the atmosphere, and the large bell is opened to admit the charge to the furnace. The large bell is again closed and the process repeated. It should be noted that the rod supporting the large bell passes through a hollow rod supporting the small bell, thus permitting the independent operation of bells. The opening and closing of the bells is fully automated.
- High temperature can be attained in a furnace without damaging the refractory lining by inserting hollow wedge-shaped plates in the outer side of the refractory lining which are water-cooled.

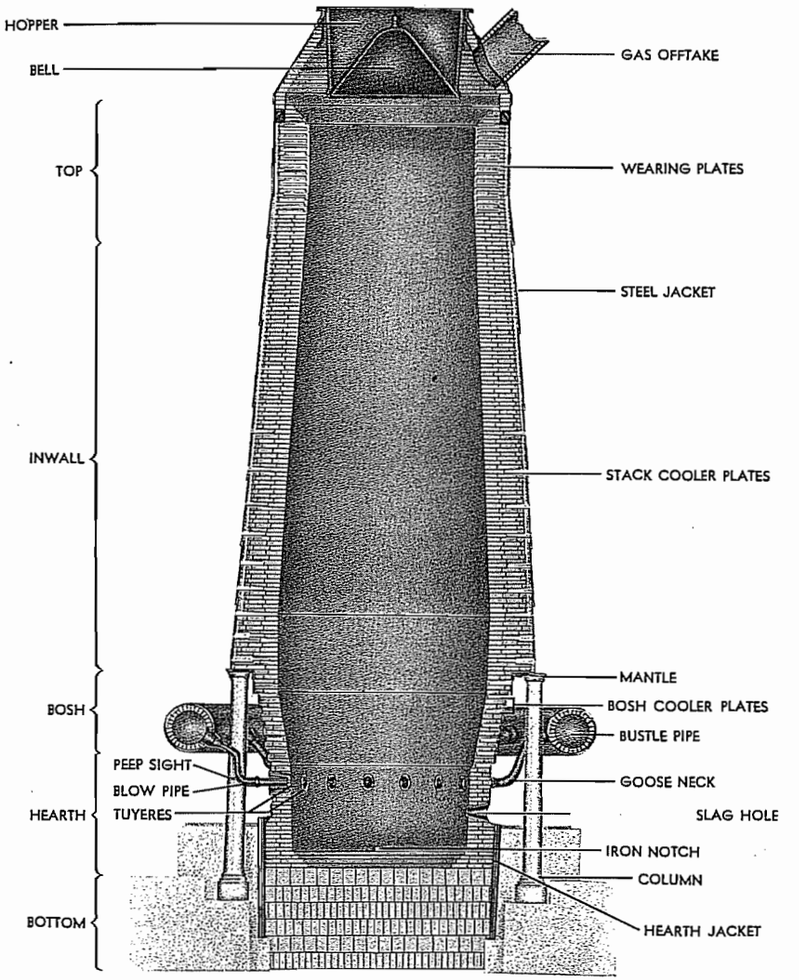

Figure 5.14: A vertical furnace — the iron blast furnace.

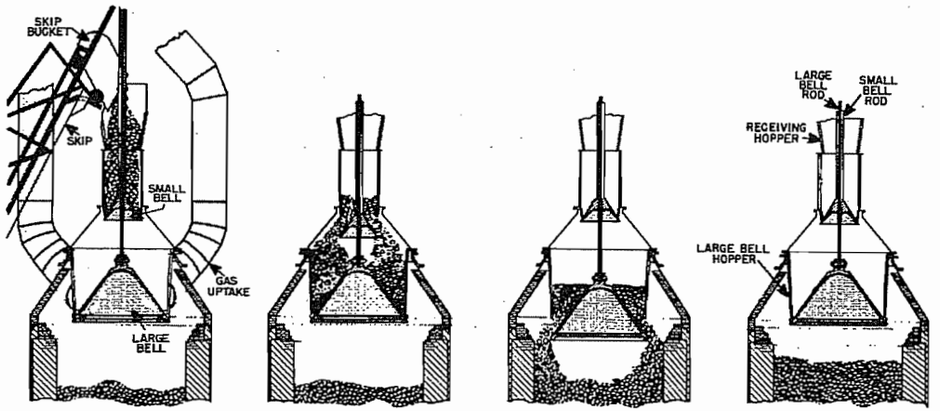

Figure 5.15: Double bell system for charging a blast furnace without permitting an escape of gases.

- Air for the furnace is introduced at the lower part. Figure 5.16 shows a section through the bosh and upper part of the hearth wall showing details of connections between the tuyère and the bustle pipe in a large blast furnace. The bustle pipe is a large circular, refractory-lined pipe that encircles the furnace at about the mantle level and distributes the air blast from the hot-blast main to the furnace. The blowpipe, a horizontal, ceramic-lined steel pipe about 1.5 m long, carries the hot blast from the bustle pipe through the tuyère stock and gooseneck to the tuyères. The tuyères are nozzle-like copper castings about 20 in number, spaced equally around the hearth about 30 cm below the top of the hearth. Each tuyère fits into a tuyère cooler casting through which cold water circulates. The gooseneck is lined with fire brick, and has a small opening closed by the tuyère cap through which a small rod may be inserted to clean out the tuyères without removing the blow pipe. A small glass-covered opening called the peep sight is placed in front of the tuyères to allow the inspection of the interior of the furnace directly.
- The furnace acts as a countercurrent heat exchanger: the cold charge is descending while the hot gases are ascending in the furnace. Thus, coke will be preheated in the upper part of the furnace so that when it reaches the lower portion and comes in contact with the hot air blast at the tuyères, it will burn with great intensity. In the upper part of the furnace, the ore also loses its water content and is preheated.
- The liquid products formed settle to the bottom from where they can be removed. New material is charged at the top in quantities sufficient to keep the charge level relatively constant.
- Tapping a molten material from the furnace, e.g., a molten metal is usually conducted in the following way. The notch which is closed with clay is opened by drilling into the clay with a pneumatic drill until the skull of metal is met, then an oxygen lance is used to form a hole through it. The metal flows into the main trough which has a skimmer located near its end. The skimmer separates any slag flowing with the metal and drives it into the slag ladles. The metal continues to flow down the main runner from which it is diverted at intervals into the metal ladles by means of gates. At the end of tapping, the hole is closed by means of the clay gun. The nose of the gun enters the metal notch and clay is forced from the gun by a plunger or a screw operated electrically or by steam. The slag notch can be opened or closed by means of a steel cone-shaped knob on the end of a long steel bar. Figure 5.17 shows a section through the slag notch.

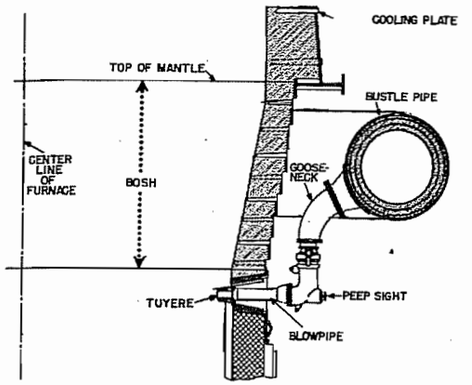

Figure 5.16: Section through the bosh and upper part of the hearth wall of a blast furnace.

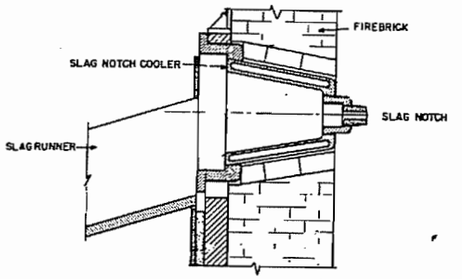

Figure 5.17: Section through slag notch of a blast furnace.

- The furnace is lined with refractory materials which must have a high melting point to withstand high temperatures. Alumina–silica refractories are usually used for lining the stacks. The percentage of Al_2O_3 in the bricks increases in the lower part of the stack. Graphite is one of the most refractory substances known but oxidizes slowly at high temperatures; it is usually used for lining the hearth.
- The furnaces are fully automated and may produce 10 000 tons of iron per day. They are huge structures over 60 m high. The column of material inside the furnace is about 25 m high that varies in temperature between 190 and 1760 °C. A furnace is designed to operate continuously for 5–7 years with a total production of about 14 million tons.
- To support a large furnace, a reinforced concrete pad about 3 m thick and 18 m diameter is built. A circular heat-resistant concrete pad about 6 cm thick is laid over the foundation (Figure 5.18). A large furnace requires 8–10 supporting columns which are anchored to the concrete foundation. A heavy, horizontal steel ring 5–10 cm thick called mantle rests on the top of the supporting columns. It supports the furnace shell and brickwork so that, when necessary, the hearth and bosh brickwork may be removed without much trouble.

5.5.2 Operation

Starting a New Furnace. Bringing a newly built furnace into routine operation is called "blowing-in". This process requires the skill and cooperation of a large number of people, and it takes probably more than a month to achieve this goal. Once a furnace goes into operation it is expected to continue for 5 to 7 years during which about 8 million tons of iron are produced before a major shutdown. The steps involved are:

- Drying the lining of furnace and stoves. This operation is carried out for the following reasons:
  - To drive off the vast amount of water absorbed by the brick during construction, and contained in the slurry used in bricklaying.
  - To avoid as much as possible thermal shock to the structure. Drying is carried out by burning natural gas or wood in the stoves and circulating the hot gases to the furnace. Heating should be increased gradually and it usually takes 10 to 14 days. During this stage intensive checking of pipes, connections, etc., takes place.
- *Filling the furnace.* Usually the hearth and bosh are filled with coke, then about an equal charge of coke, limestone, and siliceous material are mixed together and added on top. Then comes a charge composed of a small amount of ore and coke.

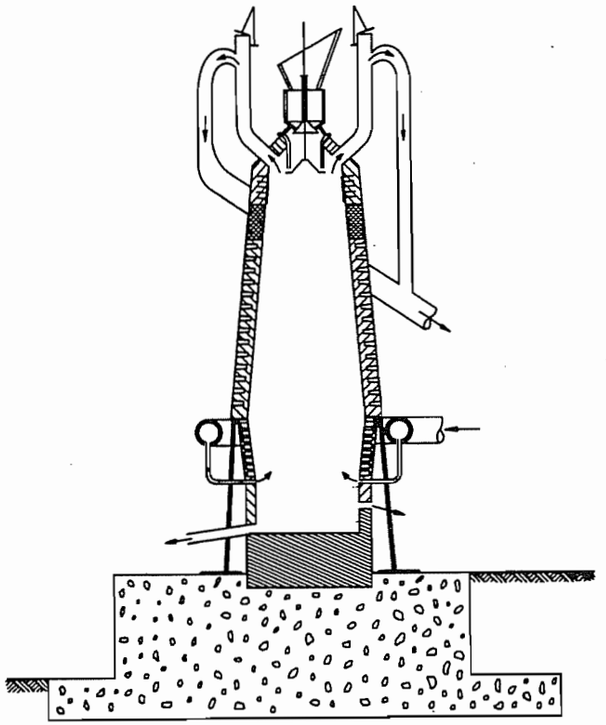

Figure 5.18: General view of the iron blast furnace showing top details and concrete foundation.

- *Lighting the charge.* This is done by blowing small volumes of hot blast at 1000 °C.
- *First stages of operation.* Once the coke in the furnace is ignited, it is important to ignite the gas leaving the furnace otherwise it will cause a health hazard to the environment due to the CO content. Gradually the hot blast volume entering the furnace is increased. After the initial coke charge is consumed, slag will begin to accumulate in the hot hearth. Charging at the top continues and at the same time the percentage of the ore is gradually increased. Once there is indication that enough slag accumulated, the slag notch is closed. Tapping of slag takes place 6 to 8 hours after the air was blown in, while iron tapping takes place after 24 to 28 hours. It takes 5 to 6 days until the iron produced is according to the specifications.

5.5.3 Operating Difficulties

An important difficulty in operation is when the charge in the upper part of the stack is cemented together into a large impervious mass (bridge) while the material underneath continues to move downward thus creating a void. The void tends to increase until the bridge collapses, causing a sudden downward movement of the charge which is known as "slip". In severe cases, this causes a sudden increase in gas pressure and an effect like an explosion. Reasons for this slip may be due to alkali vapors that condense at the top of the furnace and cement the solid material together, or it may be due to fine carbon depositions which results from the reaction

$$2CO \rightarrow CO_2 + C$$

5.5.4 Shutdown

Temporary shutdown for an emergency or otherwise is called "banking", and it involves reducing the combustion rate, thus preserving the charge for future use. The air blast is stopped, the blowpipes are dropped, and the tuyères openings are plugged with clay. If the shutdown is planned for a few days, coke may be charged without flux, and charging continues, until the coke descends to the bosh. The final tapping is made and then air is cut off. A heavy blanket of ore is dumped in the furnace to cover the upper burden surface and reduce the natural draft. At the conclusion of the tapping, the tapping holes are plugged and the furnace isolated. In this way the charge in the furnace can be kept for an indefinite time until blowing-in is required.

Extended shutdown is called "blowing out" and usually takes place when the lining is worn. Sometimes, however, business conditions may necessitate that production is no more required and an extended shutdown is necessary. Subsequent to blowing out and when the furnace is to be completely relined, the hot metal must be completely drained. A hole is drilled into the furnace bottom below the hearth staves, and a runner for iron is installed. A long oxygen lance is inserted in the hole to open the remaining brick and allow the iron to flow. This residual iron is called "salamander", and may be 400 to 600 tons.

Starting an empty furnace from cold is generally faster and requires less effort than starting it from a shutdown. However, the cost of blowing out, raking out, and cleaning prior to starting is more expensive than a temporary shutdown.

5.5.5 Efficient Operation and Improvements

In the past 50 years blast furnace production increased from an average of 800 t/day to 8000 t/day with some furnaces operating at 10 000 t/day. It seems, however, that the size of a blast furnace is limited by two factors:

- The large capital cost which will be difficult to raise
- The limited mechanical strength of coke to withstand the static pressure of a tall furnace.

The great increase in the blast furnace output is due to the following:

Beneficiated Feed. A feed to a blast furnace should fulfill the following conditions:

- Uniform size to allow gases to flow through without channelling.
- Mechanically strong to withstand handling, the high temperature, and the high static pressure in the furnace without crushing or disintegration.
- Free from fines to minimize the dust blown out of the furnace.
- Fairly permeable to enhance the reduction process.

For these reasons high quality coke sized to about 50 mm is usually used. Ore is also prepared and sized between 10 and 25 mm. Powdered feed material is compacted and sized before charging. Since high temperatures are usually applied in the compaction process, a part of the limestone required for the charge to the furnace is incorporated into the compacted material. In this way, the calcination $CaCO_3$ takes place outside the furnace, thus increasing its capacity and at the same time decreasing the volume of the exit gases. This process is known as "self fluxing sinter".

Increased Blast Temperature. When the air blast temperature is increased by preheating, the coke consumption will decrease and as a result the furnace capacity will increase. Since a certain amount of heat enters the furnace with the preheated air, the furnace efficiency increases. The higher the air temperature the higher the economy will be for the following reasons:

- The amount of coke required per unit metal produced is reduced.
- As a result of decreased fuel consumption, the air volume per unit metal produced will also decrease.

- As a result of the previous two points, the volume of gas leaving the furnace per unit metal produced will also decrease. This results in the decreased size of gas ducts and dust collecting system, etc.
- The reaction rate is increased as a result of increased air temperature, thereby lowering the reaction time of the process, i.e., increased productivity.

Oxygen Enrichment. Air is composed of 21% oxygen and 79% nitrogen. The advantages gained by using pure oxygen or oxygen-enriched air in oxidation processes offsets the cost of liquefaction of air and separating the nitrogen. The reasons for that are the following:

- Nitrogen acts as a diluent and absorbs large amounts of the combustion heat. When oxygen or oxygen-enriched air is used, the amount of heat lost by nitrogen is therefore decreased. As a result, the temperature of the furnace rises, and consequently production is increased. Or, coke consumption/ton of material processed is reduced.
- The total volume of gases passing through the furnace would be considerably less than in normal practice. Therefore, the erosion of the refractories should be reduced and the size of furnace and dust-collecting units reduced.
- High-melting-point slags can be used, i.e., slags containing lime. In this case sulfur can be eliminated.

Nitrogen-Free Operation. Instead of using a high temperature air blast it has been suggested to use cold oxygen. In this way the temperature in the furnace could be kept high and the inconveniences due to nitrogen could be eliminated. The cold tuyères facilitate the injection of coal in the furnace and in this way coke will be used only as a reducing agent and not as a fuel, which represents a great saving. Further, the top gas could be cleaned, treated to remove CO_2, and the remaining CO recycled for use as a fuel.

Fuel Injection. When a sufficiently hot blast is available, a portion of a cheap fuel (pulverized coal, fuel oil, natural gas) can be injected to replace some of the expensive coke. This results in increased production because it permits the removal of some coke from the charge. It is also a means for controlling the flame temperature since the fuel is injected cold. Generally, when tuyère-injected fuels are used, the moisture content of the blast must be decreased. The choice of the fuel depends on its cost and also on the cost of equipment for its injection. The equipment for gas injection is the least expensive and that for pulverized coal is the most.

Blast Humidity Control. By adding moisture to the blast in the form of steam, it is possible to control the flame temperature and to achieve a smooth furnace operation because the reaction of steam with coke is endothermic:

$$H_2O + C \rightarrow H_2 + CO$$

The products of this reaction are themselves reducing agents.

Pressure Operation. There is a recent tendency to operate the blast furnace under a slight pressure. This results in increased furnace capacity and decreased coke consumption. Operating under pressure, however, results in several difficulties. The furnace must be air tight at the top. Also charging equipment must have a special mechanism to allow the bell to be lowered. On the other hand, flue gases, being at high pressure, may be recovered in a turbine to be used, for example, in blast blowing.

Operating the blast furnace under pressure can be achieved by introducing a throttling valve in the gas system. This results in the following advantages:

- Larger amounts of air can be blown and consequently increased production rate.
- Increased pressure shifts the equilibrium of the following reaction to the left:

$$CO_2 + C \rightleftharpoons 2CO$$

This reaction is responsible for the consumption of unnecessary amounts of coke. As a result, operating a furnace at 200 kPa results in a decreased coke consumption of about 10%.

- As a result of decreased coke consumption, the available volume in the furnace will increase and more ore can be reduced.

5.5.6 Engineering Aspects

The iron produced in the blast furnace is saturated with carbon and is in the molten state. Depending on burden composition and operation technique of the blast furnace, the molten iron produced contains varying amounts of other elements such as silicon, manganese, phosphorus and sulfur. The blast furnace can produce pig iron but not steel.

The blast furnace is operated to achieve the following three major objectives:

- *Lowest energy consumption*, particularly the lowest coke rate;
- *Highest productivity*, i.e., highest production rate per unit volume of the furnace;
- *Composition and temperature* of the molten pig iron produced must meet the requirements of the steel shop and must be constant.

Table 5.16 shows the simplified mass and heat balances of the reactions that proceed sequentially during the descent of the burden in the blast furnace. All figures in the table are based on 1 mol Fe_2O_3, 1/4 mol $CaCO_3$ as a flux, and k mol of coke as fuel and reductant.

Hematite is first reduced via magnetite to wustite by the gas. Because the heat requirement of the reactions are small, the heat content of the gas is sufficient for heating the burden (see Figure 5.20). The gas composition prevailing in the upper part of the furnace (below 1000 °C) has the reducing potential for hematite and magnetite as depicted in Figure 5.21. Only a portion x of the wustite is reduced to iron because of kinetic limitation. The deviation of the gas composition from the Boudouard equilibrium above 650 °C is due to the low reactivity of coke. Thus, carbon dioxide is not adequately converted to carbon monoxide. Deviation below 650 °C is caused by suppression of the carbon deposition reaction, $2CO \rightleftharpoons CO_2 + C$. For coke saving, the former deviation from equilibrium is desirable, however, the latter undesirable.

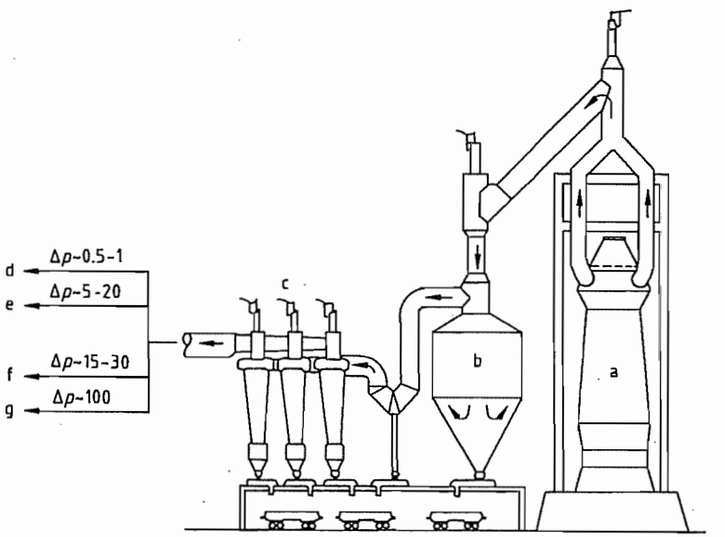

Figure 5.19: Top gas cleaning system [15]: a) Blast furnace; b) Dust catcher; c) Cyclone; d) To electric precipitator; e) To hurdle scrubber; f) To bag filter; g) To venturi scrubber.

Table 5.16: Simplified mass and heat balances in the blast furnace as a counter-current reactor [21]: increase (+), decrease (–).

		C	Fe_2O_3	FeO	Fe	$CaCO_3$	CaO	CO	CO_2	O_2	N_2	Heat[a]
1	Charge consisting of 1 mol Fe_2O_3, $^1/_4$ mol $CaCO_3$, k mol carbon	$+k$	+1			$+^1/_4$						
2	Indirect reduction hematite → wustite $Fe_2O_3 + CO \rightarrow 2FeO + CO_2$		–1	+2				–1	+1			negligible
3	Indirect reduction wustite → iron $x(2FeO + 2CO \rightarrow 2Fe + 2CO_2)$			–2x	+2x			–2x	+2x			negligible
4	Decomposition of limestone					$-^1/_4$	$+^1/_4$		$+^1/_4$			ΔH_k for 1 $CaCO_3$ = 67.2 kJ at > 700 °C
5	Direct reduction of remaining wustite $(1-x)(2FeO + 2C \rightarrow 2Fe + 2CO)$	$-2(1-x)$		$-2(1-x)$	$+2(1-x)$			$+2(1-x)$				ΔH_{CO} for 2 FeO = 315(1 – x) kJ at 1100 °C (heat of reaction)
6	Melting of iron and slag											ΔH_{ss} for 2 Fe = 42 kJ at 1300 °C
7	Combustion of carbon $y(C + {}^1/_2O_2 + 2N_2 \rightarrow CO + 2N_2$	$-y$						y		$-^y/_2$		ΔH_C for 1 C = –111 kJ
8	Hot blast $^1/_2y$ mol									$+^y/_2$	$+2y$	ΔH_L for 5/2 mol air = – $0.084(t_b - t_R)$ kJ[b]
	Input at top	$+k$	+1			$+^1/_4$				$+^y/_2$	$+2y$	
	Input at bottom			0				$y + 1 - 4x$	$1.25 + 2x$		$+2y$	
	Output at top			0	+2	0	$+^1/_4$					
	Output at bottom	$k - 21 - x - y = 0$	0	0								

[a] Heat of reaction not based on reaction temperature.
[b] t_b = Hot blast temperature; t_R = Temperature at which the direct reduction is assumed to proceed.

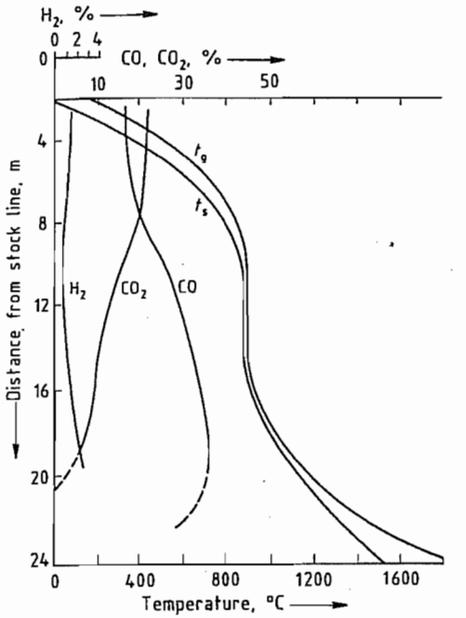

Figure 5.20: Schematic profile of temperature and gas composition in the longitudinal direction of the blast furnace.

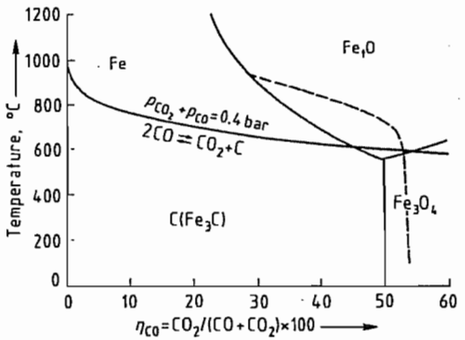

Figure 5.21: Variation of temperature and gas composition in a typical operation of the blast furnace superimposed on the reduction equilibrium diagram of iron oxide.

During descent of the burden, limestone starts to decompose at ca. 700 °C. This reaction requires heat and releases carbon dioxide, therefore the gas is cooled and its carbon dioxide content increases. Consequently, the reduction rate of iron oxide decreases and the value of x in Table 5.16 decreases. A lower value of x corresponds to a higher coke rate according to the balance shown in Table 5.16. The wustite that has not yet been indirectly reduced by the gas to iron must be reduced directly with carbon. This reaction requires a great amount of heat. For simplicity it has been assumed in Table 5.16 that direct reduction of wustite proceeds at 1100 °C. This zone of the furnace is critical for the completion of the entire process. The amount of oxygen which must still be removed from the ore in this part of the furnace depends on the degree of reduction achieved in its upper part. Therefore the residual amount of oxygen depends on the reducibility of the ore. On the other hand, the amount of oxygen which can be removed from the ore in this zone depends on the enthalpy that is delivered by the gas at 1100 °C. This enthalpy, in turn, depends on the amount of coke that is available for combustion in front of the tuyères.

If *excess heat* is available, a higher top-gas temperature is found. However, the utilization degree of the gas η_{CO} decreases because the excess heat is supplied by combustion of coke to carbon monoxide. This phenomenon can be controlled by decreasing the coke rate of the burden materials fed at the top of the bed. However, the action will only be effective after 4–6 h when the burden charged at new rates comes to the tuyère zone. An immediate effect is obtained if the heat input to the lower part of the furnace is decreased by increasing the moisture content or decreasing the temperature of the blast.

It is more difficult to compensate an *enthalpy shortage* in the lower part of the furnace. An increase in the coke rate is effective only after several hours. It is often not possible to increase the temperature of the blast because the blast temperature is usually at its maximum for economic reasons. The maximum blast temperature is limited by the capacity of the stoves and also by the maximum allowable temperature of the blast furnace. A short-term solution to compensate an enthalpy shortage is to inject fuels such as hydrocarbons, natural gas, oil, or pulverized coal together with an oxygen enrichment of the blast.

Upon further descent of the burden, the enthalpy $\Delta H_{E,S}$ needed to melt iron and slag must be supplied. For simplicity, they are assumed to melt down at 1300 °C (see column 6 in Table 5.16).

The various heat sinks are compensated by the equal amount of heat supplied from the combustion of the coke and from the hot blast as described in columns 7 and 8 in Table 5.16. This requirement almost determines the coke rate for various conditions. This is an approximate calculation because the coke requirement for the reduction of molten wustite, silica, and manganese oxide as well as that for the carbon dissolved in the metal has not been taken into account. To consider the heat and mass balances, the furnace is divided into two parts by a boundary line which is drawn in the thermal and chemical reserve zone. In this zone, the temperature is almost constant (ca. 900 °C) and no reduction of iron ores occurs.

The coke rate is determined by the enthalpy requirement of the lower furnace. The quantity of carbon y (mol of carbon per moles of hematite to be reduced) needed to supply the heat is given by Equation (1) (for symbols see Table 5.16):

$$y = -\Delta H_{E,S} + \frac{(1-x)\Delta H_{CO}}{\Delta H_C + \Delta H_L} \quad (1)$$

The total amount of carbon required k is given by (see Table 5.16):

$$k = y - 2x + 2 \quad (2)$$

The amount of carbon required for direct reduction is:

$$k - y = -2x + 2$$

Substitution of the figures listed in Table 5.16 gives the carbon rate as a function of the hot blast temperature t_B and the amount of wustite reduced indirectly x, assuming that the direct reduction proceeds primarily at t_R = 1100 °C

$$k = \frac{357}{111 + 0.084(t_B - 1100)} - \frac{2 + 315}{111 + 0.084(t_B - 1100)}x + 2$$

The coke rate Q is then given by:

$$Q = 118k$$

on the basis of a carbon content of the coke of 85% and on iron content of the hot metal of 93.5%.

The *fraction of indirect reduction* r_{CO} indicates how much oxygen has been removed from the ore by indirect reduction. Taken together with the fraction of direct reduction r_C, the sum should be equal to unity:

$$r_{CO} + r_C = 1 \quad (3)$$

For reduction of hematite, the following relation is valid (Table 5.16, columns 2 and 3):

$$r_{CO} = \frac{O_{removed}}{O_{total}} = 1 + \frac{2x}{3} \quad (4)$$

On the basis of the *balance* shown in Table 5.16, it is not possible to assign a value to x (amount of wustite indirectly reduced). The maximum value of x can be determined thermodynamically. If the value of x is given, then r_{CO}, is obtained from Equation (4). In fact, the value of x is determined by the rate of the indirect reduction of iron ore and by the reactivity of the coke which, in turn, determines the degree to which the Boudouard reaction proceeds. The value of x can be evaluated from the composition of the top gas if the operational data are available. The gas utilization factor is defined by Equation (5):

$$\eta_{CO} = \frac{\%\ CO_2}{\%\ CO_2 + \%\ CO} \quad (5)$$

Substitution of the values in Table 5.16 provides the following Equation:

$$\eta_{CO} = \frac{1 + 2x}{2(1-x) + y} \quad (6)$$

Since y depends only on the enthalpies and x for a given blast temperature (see Equation 1), the value of x can be determined if the decomposition of limestone is neglected. In practice, r_{CO} is between 0.45 and 0.65 and the corresponding values of x are between 0.175 and 0.475.

The *amount of air* l required per mole of hematite and the *amount of off-gas* generated g_G, are obtained from Table 5.16:

$$l = \frac{5y}{2} \quad \text{(amount of air)} \quad (7)$$

$$g_G = 3y - 2x + 2 \quad \text{(amount of off-gas)} \quad (8)$$

These equations are approximate expressions and should be improved for more accurate calculations—particularly when the calculated results are to be used for furnace control to keep the composition and temperature of the hot metal constant. For this purpose it is necessary to formulate the heat and mass balances on hydrogen from water vapor and hydrocarbons and on the solutes in the iron (e.g., carbon, silicon, manganese, and phosphorus).

5.5.7 Effective Utilization of Energy

The high thermal efficiency of the blast furnace (Table 5.17) directly leads to a low coke rate. Heat losses through the wall amount to ca. 5%. Additionally 2–5% of thermal energy is lost in the form of off-gas enthalpy. These values decrease with increasing furnace size so that the total loss of thermal energy is < 6%. Compared to the low *thermal energy loss* of the blast furnace, the *chemical energy* of the off-gas is rather large and amounts to ca. half of the thermal energy used effectively in the furnace.

Table 5.17: An example of enthalpy balance for the modern blast furnace (no. 6BF at Chiba works of Kawasaki Steel Corp.).

Enthalpy	¥ 103 kJ per ton of pig iron	%
Input		
Raw materials	519	3
Coke	14 412	83
Blast	1 411	8
Electricity	1 093	6
Total	17 439	100
Output		
Top gas	5 389 (chemical: 4966; thermal: 423)	31
Pig iron	9 697	56
Slag	908	5
Dust	255	1
TRT's recovery[a]	536	3
Wall, heat loss	653	4
Total	17 439	100

[a] TRT: Top-gas pressure recovery turbine.

The thermal energy supplied by the hot blast (Table 5.17) should be partly subtracted from the total energy required for the blast furnace operation because the blast is primarily heated by the off-gas. Even in modern blast furnaces ca. 30% of the primary energy supplied by coke leaves the process in the form of carbon monoxide and hydrogen in the off-gas. A heat loss of 3–7% is caused by *slag enthalpy*. With these considerations in mind, lowering of the energy requirement can be accomplished as follows:

- use the chemical energy of the off-gas as efficiently as possible in the process system,
- decrease the specific slag volume,
- prepare the burden (operation of the stack), i.e., carry out dehydration and decarbonization outside the blast furnace by utilizing inexpensive energy sources.

Additionally, efforts exist to replace metallurgical coke by other inexpensive energy sources because of high cost and shortage of coking coal.

Blast Furnace Operation and Physical Properties of Burden Materials. The heat required to produce 1 t of hot metal substantially depends on the physical properties of the iron ores. In modern blast furnace operation, processed ores like sinter and pellets are usually fed to the furnace to conduct stable operation for pursuing higher productivity and lower coke rate. Physical properties which significantly affect the blast furnace operation are reducibility and reduction disintegration. *Higher reducibility* contributes to the increase in indirect reduction in the stack region thereby increasing the utilization factor η_{CO} and decreasing the coke rate because of a decrease in direct reduction. *Reduction disintegration* directly affects the gas permeability of the burden beds and may cause flow maldistribution which negatively affects the reduction of iron ore and gas utilization. Therefore, the physical properties of the sinter should be controlled appropriately. A lower FeO content in the sinter enhances the reducibility, however, a higher content improves the reduction disintegration as shown in Figures 5.22 and 5.23.

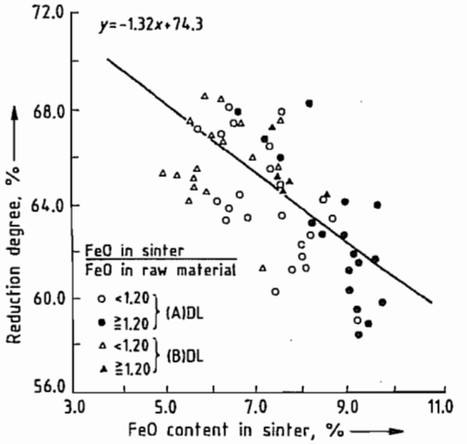

Figure 5.22: Influence of FeO content in sinter on the reducibility [22] (Courtesy of The Iron and Steel Institute of Japan).

A low gangue content of the burden materials also contributes significantly to the coke savings by decreasing the slag volume.

Chemical Energy of the Off-Gas. Burden materials with a high reducibility and a low reduction disintegration provide a low coke rate, but a high gas utilization factor η_{CO}. A better burden preparation allows the use of higher blast temperatures which results in the use of a larger portion of the off-gas for heating the blast. These circumstances significantly decrease the waste energy that leaves the blast furnace process in the form of off-gas. Figure 5.24 illustrates the decrease in the coke rate in Germany and in Japan by improving the physical properties of the burden materials and utilization of the off-gas. Figure 5.24 also shows the effect of replacing coke by oil and pulverized coal on the coke rate. The theoretical limits of the coke rate for a fully oxidized burden and a burden that has been 60% and 100% prereduced are also indicated in this diagram. When 100% prereduced burden is used, the blast furnace is operated as a melting furnace like a cupola that produces cast iron. In this case, a gas with a very high calorific value is produced because the blast furnace works as an iron and gas producer.

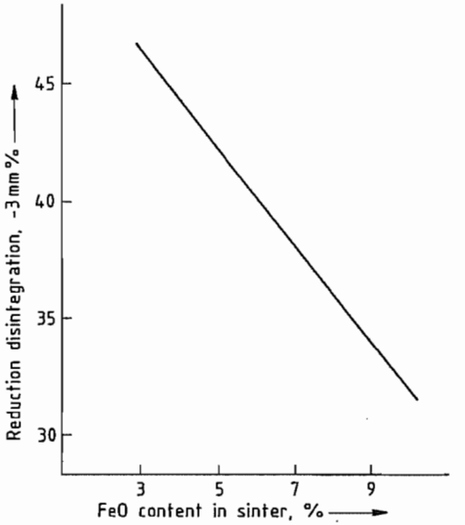

Figure 5.23: Relation between FeO content in sinter and reduction disintegration degree [23] (Courtesy of The Iron and Steel Institute of Japan).

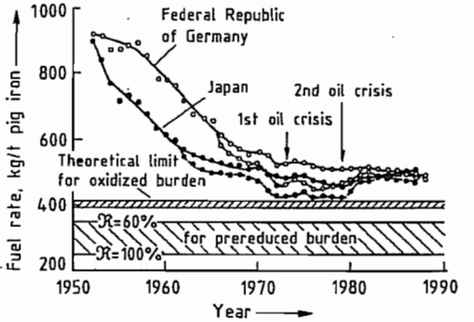

Figure 5.24: Specific fuel rate for the production of 1 t hot metal in Japan and Germany: — Fuel rate; – – Coal rate.

Figure 5.25 shows that the calorific value of the off-gas decreases with decreasing coke rate, which favors the cost effective operation of the blast furnace. On the other hand, it may be necessary to increase the calorific value of the off-gas by increasing the coke rate when the calorific value of the off-gas is not sufficient to heat other furnaces in the steep plant or the hot blast stoves and when a cheaper energy source is not available. In the case, the blast furnace also has a function as a gas producer.

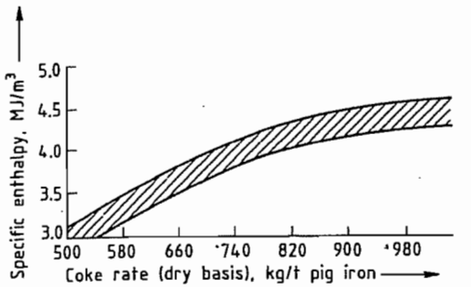

Figure 5.25: Relationship between specific enthalpy of top gas and coke rate [24] (Courtesy of Verlag Stahleisen mbH).

In spite of the successful efforts to decrease the coke rate and to use substitutive fuels since the 1950s, the problem to what limit the coke rate can be lowered is still not solved. Sufficient coke must be present in front of the tuyères to form a dead man through which the gaseous products can ascend. In addition, the coke consumed in the dead man must be replaced. If the quantity of coke required for these portions of the process is not available, then the characteristics of the process change and it can no longer be called a blast furnace process.

Figure 5.26 gives a schematic illustration of the processes occurring in the combustion zone in front of the tuyères [24]. According to direct observations, coke particles are entrained in the turbulent air flow immediately in front of the tuyère opening and fly on circular trajectories within the raceway.

The coke particles are primarily gasified in the raceway. According to the gaseous composition distribution in the raceway shown in Figure 5.27, coke burns with the gas at first forming carbon dioxide, and then carbon dioxide is reduced to carbon monoxide in an area near the coke-filled bed. A typical gas composition change from the tuyère via the raceway to the packed bed calculated by a two-dimensional model [27] is shown in Figure 5.28. From this figure the gasification reaction has almost gone to completion in the raceway region, therefore a very small quantity of CO_2 is left for the coke packed bed around the raceway.

Moreover, the direct observations indicate that a shower of iron and slag droplets descends in front of the tuyères, together with coke particles falling through the air flow In addition, in no other part of the raceway roof was the burden observed to descend. On the basis of these observations it is assumed that the molten iron and slag trickles down in the space between the individual tuyères and within the dead man. This phenomenon has been proven by dissection of blast furnaces [28, 29].

Fluid flow studies have shown that the adequate quantity of gas cannot flow through the cohesive layers or through the layers which hold up the molten materials unless a sufficient volume of coke bed (which has a high permeability) is present inside the furnace.

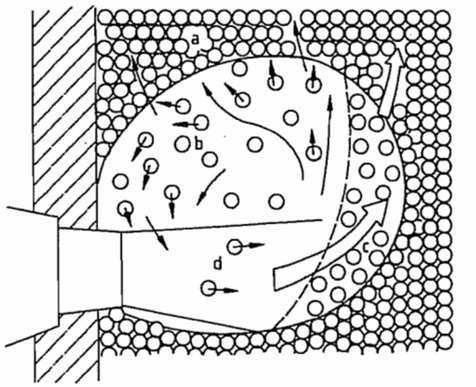

Figure 5.26: Movement of coke particles in front of the tuyère and location of combustion zone: a) Packed zone; b) Coke fluidizing zone; c) Coke slow moving zone; d) Blast jet.

Basic Concept to Improve Blast Furnace Performance. The following technologies or their combinations have been principally approved to decrease the coke rate and to increase the productivity of the blast furnace:

- Pretreatment of iron ores improves the reducibility and permeability and hence, increases the gas utilization η_{CO}. Examples are *sintering* or *pelletizing* of the ore and screening to separate the fines.

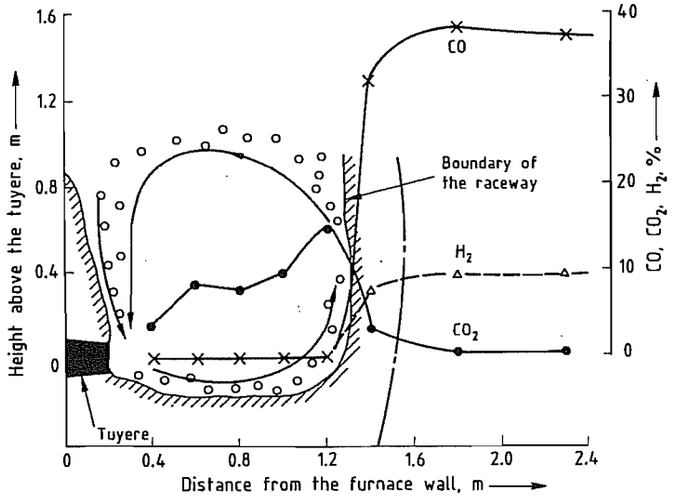

Figure 5.27: Combustion of coke in the raceway [25] (Courtesy of The Iron and Steel Institute of Japan).

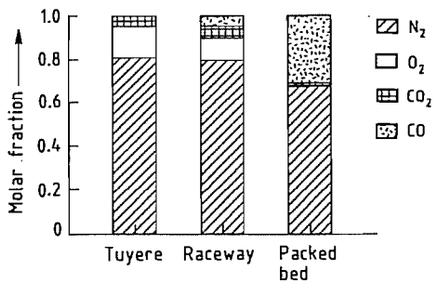

Figure 5.28: Change of gas composition from the tuyère to the packed bed.

- Injection of *auxiliary fuels* such as hydrocarbons, oil, and pulverized coal replaces coke for heating and reduction purposes.
- Oxygen enrichment of the blast together with fuel injection decreases the amount of blast; this decreases the amount of off-gas per tonne of coke and increases the furnace efficiency.
- *Increase in the blast temperature* reduces the amount of coke required for heating.
- *High pressure operation* allows the introduction of a larger amount of blast per unit time.
- *Reducing gas injection* in the lower part of the stack lowers the amount of coke required for reduction.
- The use of *partially reduced ore* results in a decrease in the coke rate and an increase in the productivity of the furnace.

The effect of these various technologies on the coke rate and their limits of applicability can be summarized with the aid of the extended Rist diagrams shown in Figures 5.29, 5.30 and 5.32.

Table 5.18 lists quantitative results obtained from operational data concerning the technologies applied to decrease the coke rate on the basis of the Rist diagram and to increase the productivity.

Curve 1 in Figure 5.29 represents the conditions in a blast furnace without additional technologies. Heat is liberated during the oxidation of carbon (coke for heating) by the hot blast (E to F). The segment FG represents the reduction of elements dissolved in iron and segment GK corresponds to direct reduction. The indirect reduction is represented by the segment AK. The diagram allows the determination of the amount of carbon required per mole of iron (C/Fe) and the amount of coke (85% C) required per tonne of hot metal (93.4% Fe). For this purpose, the operating line 1 is shifted to the line 1a which goes through the origin. The intersection of 1a with the abscissa in the upper part of the diagram

together with curves I or II gives the carbon consumption (C/Fe) on the ordinates I or II on the left side, while the coke consumption can be read from the ordinate on the right. The lower abscissa (0–100%) is valid for the segment between E and K. It shows the coke consumption for heating (EF), for reduction (GK), and for the reduction of minor constituents in the burden (FG). For the blast furnace operation in accordance with line 1 the coke rate is 550 kg per tonne of hot metal which is equivalent to a C:Fe ratio of 2.3. The consumption ratio is 60% for heating, 25% for direct reduction, and 15% for the reduction of the minor constituents in the burden.

Lines 2 and 3 are theoretical operating lines for obtaining the limits of the coke rate. *Line 2* (no coke used for reduction) is based on the assumption that the reactivity of the coke is so poor that the Boudouard reaction and the direct reduction are suppressed completely. However, it is also assumed that a gaseous composition is reached which corresponds to the reduction equilibrium from wustite to iron (point W). In this case the entire quantity of carbon monoxide required for the reduction must be generated by the combustion of coke. This condition causes the extremely high coke rate (line 2a) of ca. 1000 kg per tonne of hot metal, a lower gas utilization η_{CO} as well as higher temperatures of off-gas and molten iron.

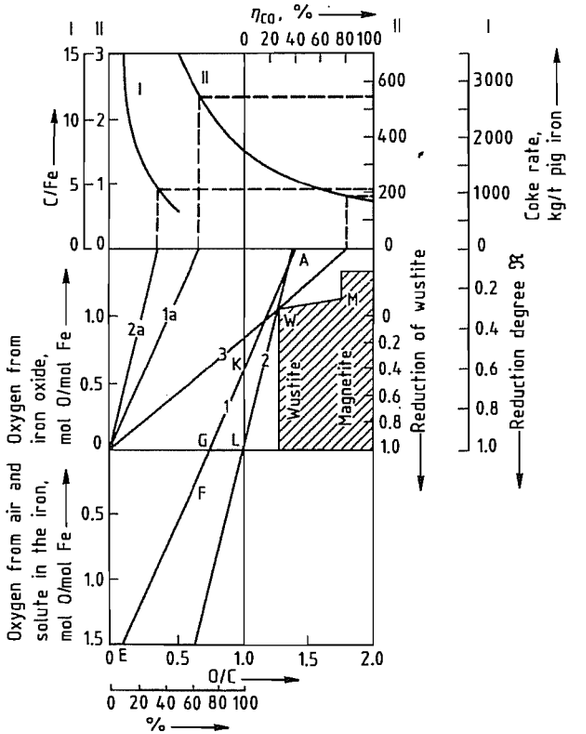

Figure 5.29: Extended Rist diagram [20]. Line 1: normal blast furnace operation (standard); Lines 2 and 3: hypothetical operation (Line 2: coke for reduction = 0, line 3: coke for heating = 0).

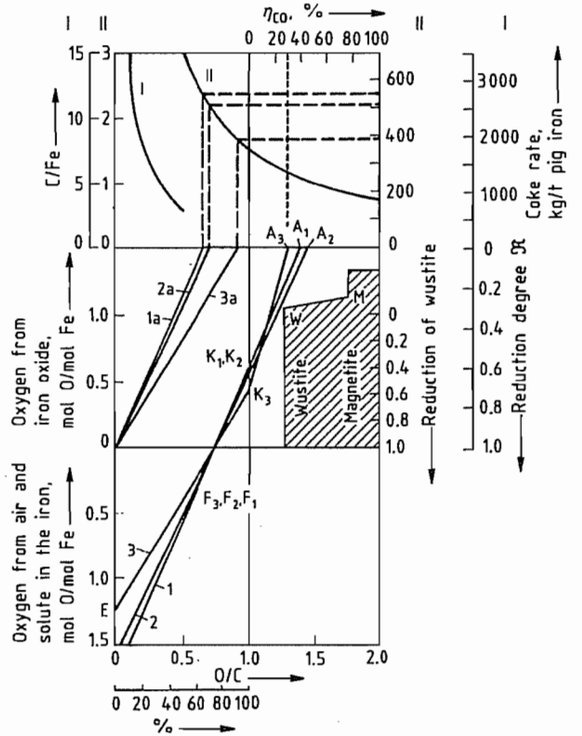

Figure 5.30: Effect of measures to decrease the coke rate and to increase the productivity of the blast furnace estimated by the Rist diagram [20]. Line 1: normal blast furnace operation (standard); Line 2: improvement in gas permeability and reducibility; Line 3: improvement in indirect reduction (K_3) by injecting reducing gas into the stack.

Line 3 is based on the assumption that no coke is required for heating and that the total heat required is supplied by a hot inert gas. In that case the coke rate would be ca. 200 kg per tonne of hot metal while the gas utilization would be 80%.

Line 2 in Figure 5.30 shows the decrease of the coke rate caused hy the improvement of gas permeability and reducibility compared with the standard case (line 1). Line 2 gives an improvement of 5% in gas utilization thereby close approaching the equilibrium point W in the wustite field. In addition, the degree of direct reduction (K_2) decreases which leads to a coke saving of 30 kg per tonne of hot metal (thm). The reducibility of various burdens are shown in Figure 5.31, which were measured according to Japanese industrial standard.

It is evident from Figure 5.30 that improvement in the physical properties of burdens does not result in a large decrease in the coke rate but can probably contribute much to the stable operation of the blast furnace. A lower coke rate (i.e., a lower slope of the operating line in Figure 5.30) could only be achieved if it were possible to increase the degree of direct reduction together with the gas utilization. This method would lead to an increase in the heat requirement that must he supplied by a hotter blast if coke is to be saved. However, the hot blast temperatures have already reached their technological limit.

Table 5.18: Effect of various parameters on the coke rate and the productivity of the blast furnace, based on 1 t of hot metal [21].

Parameter	Range	Change	Effect on coke rate kg per tonne of hot metal
Slag volume, kg/t	250–350	–100	–15 to 25
Partially reduced pellets[a], % of burden	0–30	+10	–1.5 to 2.0
Fully reduced pellets[b], kg/t.	0–20	+10	–2 to 3
Scrap, kg/t		+10	–4
Gas velocity in stack[c], m/s	2.5–5.0	–0.1	–2.5 to 3.0
Hot metal silicon, %	0.5–1.5	–0.1	–4 to 7
Fines in burden, % < 5 mm	0–7	–1	–4 to 7
Crushed ore, % of burden			
8–40 to 8–30 mm	0–40	40	–10 to 13
8–30 to 10–25 mm	0–40	40	–5 to 7
Coke ash content, %	6–12	–1	–5 to 10
Pellet content of burden, %	0–100	+10	–5 to 10
Sinter content of burden, %	0–100	+10	–5 to 10
Blast moisture content[d], g/m³		–10	–6 to 10
Blast temperature, °C	900–1350	+100	–8 to 20
Oil injection, kg/t	50–100	+1	–0.9 to 1.4
Blast oxygen enrichment, %		+1	+2 to 3%[e]
Top gas pressure, kPa	10–250	+10	+1 to 2%[e]

[a] With 68% Fe, 40% metallic iron.
[b] Fully metallized.
[c] With respect to empty stack (superficial velocity).
[d] Air at standard conditions.
[e] Increase in melting rate.

Fuel injection through the tuyères (e.g., pulverized coal or hydrocarbons) can supply a part of the heat requirement. In some cases, the blast is also enriched with oxygen to increase the combustion efficiency. The best record achieved up to now with the blast furnace in the Kimitsu Works of Nippon Steel are shown by line 2 in Figure 5.32. The coke rate is 390 kg/t for a heavy oil addition of 60 kg/t (gas utilization of ca. 45%, indirect reduction of ca. 75%). There is a slight break in the line at K_2 which indicates that the quantity of reducing gas is larger as a result of the oil addition than in the case of carbon gasification alone.

Auxiliary fuels injected into the blast furnace can replace coke only up to a certain limit. In the raceway the hydrocarbons are only combusted to carbon monoxide and hydrogen, liberating less heat than coke per equal quantity of oxygen.

Natural gas

$$CH_4 + {}^1/_2O_2 \rightarrow CO + 2H_2 \quad \Delta H_{298} = -36\ \text{kJ/mol} \qquad (9)$$

Oil

$$-CH_2- + {}^1/_2O_2 \rightarrow CO + H_2 \quad \Delta H_{298} = -90\ \text{kJ/mol} \qquad (10)$$

Coke

$$C + {}^1/_2O_2 \rightarrow CO \quad \Delta H_{298} = -111\ \text{kJ/mol} \qquad (11)$$

Thus a given quantity of heating coke can only be replaced by a larger quantity of hydrocarbons if the same amount of heat has to be generated. In other words, the replacement ratio, defined by hydrocarbons:coke is > 1. However, twice to three times the amount of reducing gas including hydrogen is produced per mole of combustion air (Equations 9 and 10) compared to the combustion of coke (Equation 11).

The addition of hydrocarbons increases the degree of indirect reduction because the reduction rate of hydrogen is higher than that of carbon monoxide. Thus, the degree of direct reduction and its enthalpy requirement decrease. Consequently, the overall effect of hydrocarbon injection on the replacement ratio increases, thereby giving an overall hydrocarbon coke replacement ratio < 1. The enthalpy deficiency which suppresses further increase of indirect reduction becomes increasingly noticeable whenever more coke is replaced by increasingly larger amounts of hydrocarbons.

The advantage of the lower fuel cost, therefore, becomes gradually less. However, a more serious problem is the decrease in the furnace productivity. Fuel injection can be made more cost-effective by increasing the oxygen enrichment of the blast or the hot blast temperature. Modern practice makes use of the theoretical and actual flame temperatures to control the replacement ratio. Japanese furnaces are operated on the basis of a theoretical flame temperature of ca. 2200 °C.

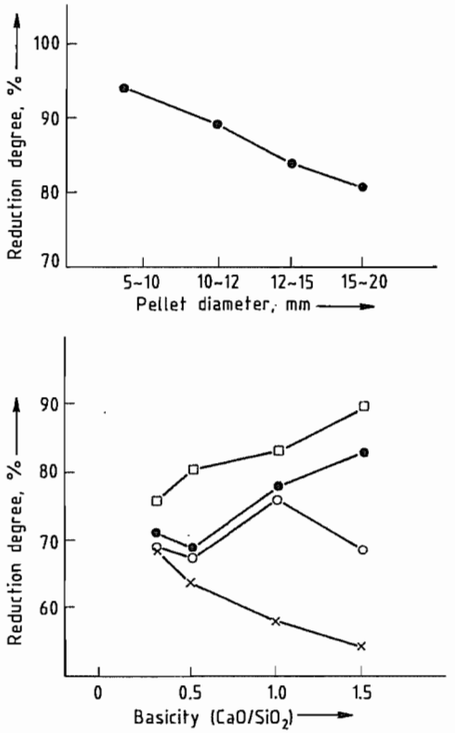

Figure 5.31: Influence of basicity and pellet diameter on reduction degree [31] (Courtesy of The Iron and Steel Institute of Japan): —□— 1200 °C; —●— 1250 °C; —○— 1300 °C; —×— 1350 °C.

Cost effectiveness considerations should take into account the fact that the sulfur content of the hot metal increases as a result of oil injections. This leads to a cost increase associated with the desulfurization of hot metal. Additions of up to 70 kg/t have been tried and were technically feasible. However, the oil crises of 1973 and 79 made oil very expensive. Therefore almost all blast furnaces operated in Japan changed the injection fuel from oil to pulverized coal. Figure 5.33 illustrates the replacement ratio of coke by pulverized coal. Pulverized coal is more difficult to inject into the blast furnace than oil because it is in the solid not in the fluid state and it contains ash. A successful technology for pulverized coal injection has been developed to inject up to 150 kg/t by using low ash coal crushed to < 200 mesh (74 μm) [33]. However oil or natural gas injection is also conducted depending on local energy conditions all over the world.

Line 3 in Figure 5.30 shows a break which represents the operation of *injecting a reducing gas* into the stack to promote indirect reduction. This leads to the heating and reducing coke requirement of 390 kg/t (line 3a). However, inherent to the low coke rate is a low gas utilization η_{CO} of only 30%. The break in line 3 at K_3 is the result of an increase in the quantity of the gas at the poin1t of injection. This technology has not been accepted for widespread application because of the poor gas utilization and the large amount of top gas. However, the reducing gas injection in the stack region is an important technology for the operation of the blast furnace with pure oxygen [34], which is currently being developed for the super high productivity of the blast furnace process.

Line 3 in Figure 5.32 represents a blast furnace operation using *prereduced ore* with a metallization degree of 50%. This procedure leads to a decrease in the coke rate to 310 kg/t. In this case, gas utilization is only ca. 30%. Therefore, such an operation is only recommended when the blast furnace capacity is insufficient to satisfy a sudden increase in hot metal demand. The productivity of the blast furnace increases significantly by using prereduced material although it is more expensive.

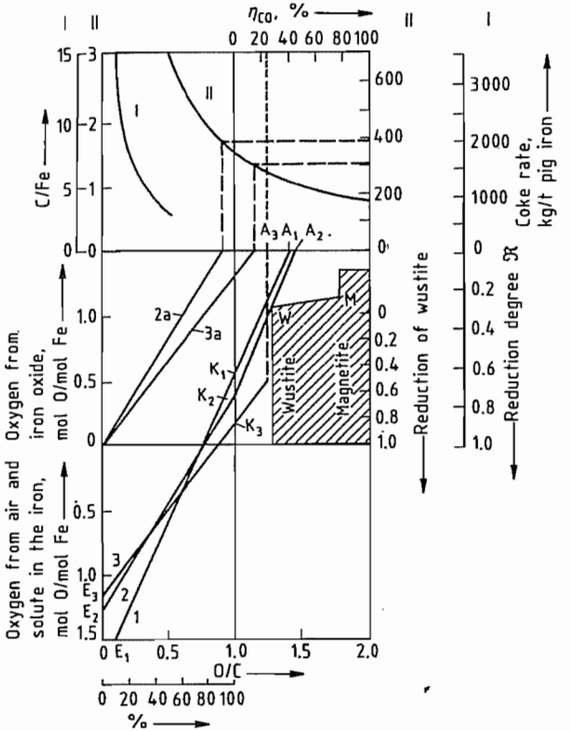

Figure 5.32: Effect of measures to decrease the coke ratio and to increase the productivity of the blast furnace estimated by the Rist diagram [20]. Line 1: blast furnace operation (standard); Line 2: decrease in the coke ratio through injection of inexpensive energy (best values achieved with Japanese furnaces); Line 3: operation with prereduced ore.

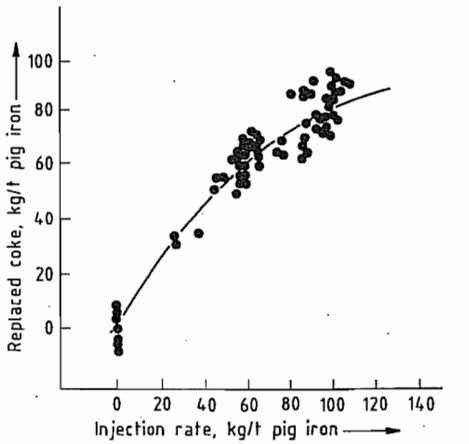

Figure 5.33: Coke replacement with pulverized coal injection [32] (Courtesy of The Iron and Steel Institute of Japan).

Slag Practices. The slag must meet the following requirements:

- It should absorb all unreduced non-volatile components of the burden and remove them from the blast furnace.
- It should be a liquid of low viscosity.
- It should be able to absorb the sulfur primarily contained in the fuels and it should contain as little iron oxide as possible to increase the yield of hot metal.
- The slag volume should be as low as possible without impairing the desulfurization.
- The temperature range where the burden components become cohesive should be narrow to ensure better permeability of the burden column.
- Finally, the slag should be converted to salable material.

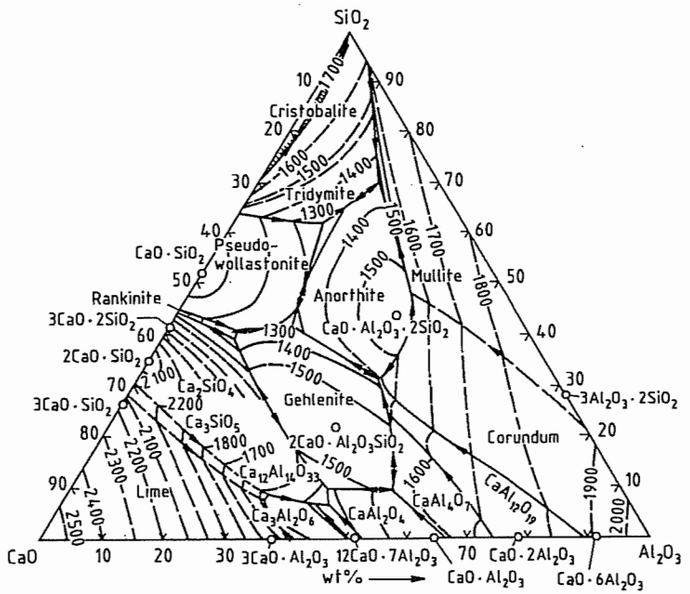

Figure 5.34: Phase diagrams of the system $CaO–Al_2O_3–SiO_2$ [35].

These requirements are in part complementary and in part mutually exclusive. It is therefore necessary to state priorities.

About 95% of the slag consists of SiO_2, CaO, MgO, and Al_2O_3. The requirement of low viscosity can be met by a variety of components in this quaternary system. Ignoring the presence of MgO, the phase diagram of the ternary system $CaO–Al_2O_3–SiO_2$ illustrated in Figure 5.34 shows a low melting temperature region which is parallel to the $CaO–SiO_2$ binary for low Al_2O_3 content. This region extends from high SiO_2 content to the saturation isotherm for $2CaO·SiO_2$ and then for essentially constant CaO content toward high Al_2O_3 content. The MgO content of the slag does not substantially affect the relative position of the low melting temperature region and only affects the absolute values of the melting temperatures. The compositions of blast furnace slags as encountered under various operating conditions are shown in Figure 5.35.

The desulfurization of the hot metal increases with slag basicity, i.e., with increasing CaO and/or MgO content. *Region 1* in Figure 5.35 can, therefore, be used only for processing low sulfur burden (e.g., in Brazil where very low sulfur content charcoal is often used as reductant). Because the gangue constituents usually form a low basicity slag, region 1 largely represents the slag composition without addition of fluxes. The furnace can be operated at a relatively low temperature because of the low melting points. *Region 2* is reached for low *iron content burden with acid gangue* constituents. This mode of operation prevails, for example, in Salzgitter and requires extensive desulfurization of the hot metal outside of the blast furnace. The attainment of a basicity that would result in adequate desulfurization within the furnace would require a large lime addition which leads to a high slag volume and consequently to higher coke rate. *Region 3* represents the worldwide preferred slag compositions for *large blast furnaces*. In this case, depending on the alumina content, dolomite must be added to satisfy the required MgO contents (see Table 5.19).

Slags with higher basicities B as shown in Table 5.19 would favor *optimum softening*

conditions. The softening and melting range of the gangue constituents is ca. 80–130 °C for $B = 0.5$ and ca. 20–50 °C for $B = 2.0$. Because of the higher melting temperature of the highly basic slag and of extra energy required due to the larger quantity of flux addition, hence, the slag basicity is maintained at ca. 1.2.

Table 5.19: Optimum composition of blast furnace slag in % [35].

Al_2O_3	CaO	MgO	SiO_2
5	43	16	36
10	44	14	32
15	44	12.5	28.5
20	45	11	24
25	48	8	19
30	56	5	9
35	54	4	7

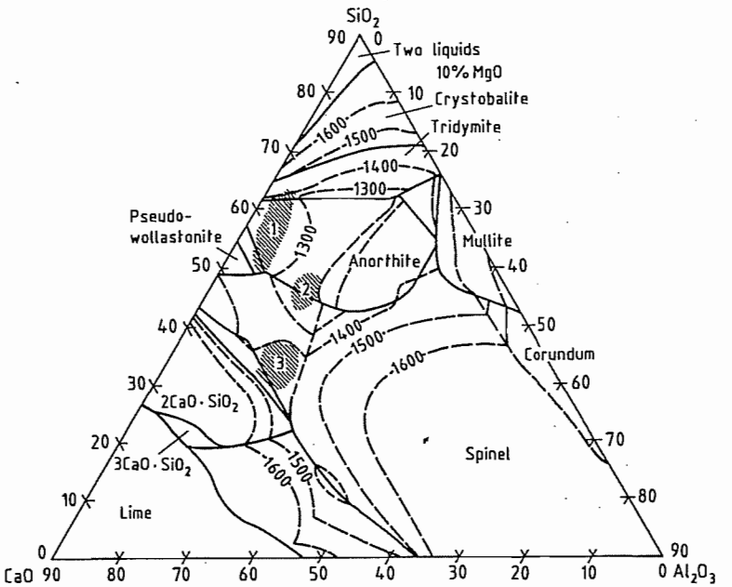

Figure 5.35: Composition of typical blast furnace slags on the $CaO–Al_2O_3–SiO_2$ phase diagram (see Figure 5.34) [20] (for explanation of regions 1, 2, and 3 see text).

5.5.8 Blast Furnace Productivity Criteria

The production rate P (t/d) of a blast furnace has been linked in various ways with the constructive data of the blast furnace and with metallurgical properties of the burden to give the specific furnace productivity. To date, no consensus has been reached to define a parameter which characterizes the furnace size and can be used in the calculation of the productivity. The characteristic parameters proposed up to now are (1) the hearth diameter, (2) the hearth bustle area that determines the depth of penetration of the blast in front of the tuyères, (3) the square of the hearth diameter, (4) the hearth area, and (5) the working volume of the furnace. In Germany the hearth area is mostly used as a characteristic parameter for the furnace size, whereas in Japan the inner volume of the furnace is often used.

To compare various furnaces, the coke consumption with respect to the hearth diameter is often used. The coke consumption is a criterion (typical parameter) to express the productivity in the furnace which is operated in a given mode. The amount of coke consumed in the furnace is determined stoichiometrically by the constant blast volume blown. If the quantity of blast exceeds the limit, unfavor-

able phenomena such as hanging of the burden or variations in hot metal composition occur. The following relations have been proposed between hearth diameter and coke consumption:

$$D = \sqrt{4Q/\pi R}$$

$$Q = 30.673 \times 1.829(D - 1.829 - 2L_p)$$

$$Q = \gamma D^2 \qquad (12)$$

$$\log Q = 2.59 \times \log d + 0.73$$

$$Q = 9.06D^{2.22}$$

where γ is the productivity factor, D is the hearth diameter and R a constant. The production of hot metal P is related to coke consumption per day Q (t coke per day) by the coke rate K (t of coke consumed for producing 1 t of hot metal) and is indirectly evaluated from the quantity of blast blown or the coke consumed:

$$P = Q/K \qquad (13)$$

Blast furnaces which are well operated have a specific hot metal production rate $p = P/A$ of 65 $tm^{-2}d^{-1}$ at a coke rate of 470 kg/thm, a slag volume of 300 kg/thm, a superficial gas velocity at the top of 3 m/s and a blast temperature of 1100 °C. In Japan specific production rates of 80 $tm^{-2}d^{-1}$ together with slag volume of 180 kg/thm have been achieved. Productivities based on the hearth area should be interpreted carefully, because the hearth diameter increases during the course of a furnace campaign by the wear of the lining. Therefore, the productivity should be evaluated by using the actual hearth area.

The coke consumption Q is shown as a function of the hearth diameter in Figure 5.36 for a productivity factor γ between 10 and 25. The daily production rate of some blast furnaces, as a function of the hearth diameter is shown in Figure 5.37. Curves for the specific hot metal productivity p are also shown for comparison. In practice it has been observed that the specific iron productivity does not increase proportionally for extremely high coke rates because for hard driven furnaces the coke rate K in Equation (13) increases with decreasing gas utilization.

Table 5.20: Values of constants in Equation (14) [39] (Courtesy of The Iron and Steel Institute of Japan).

	l	m	n
$P_t \leq 1000$	0	2.0	500
$1000 < P_t \leq 1500$	0.10	1.5	1000
$1500 < P_t \leq 2000$	0.175	1.2	1500
$2000 < P_t$	0.235	1.0	2000

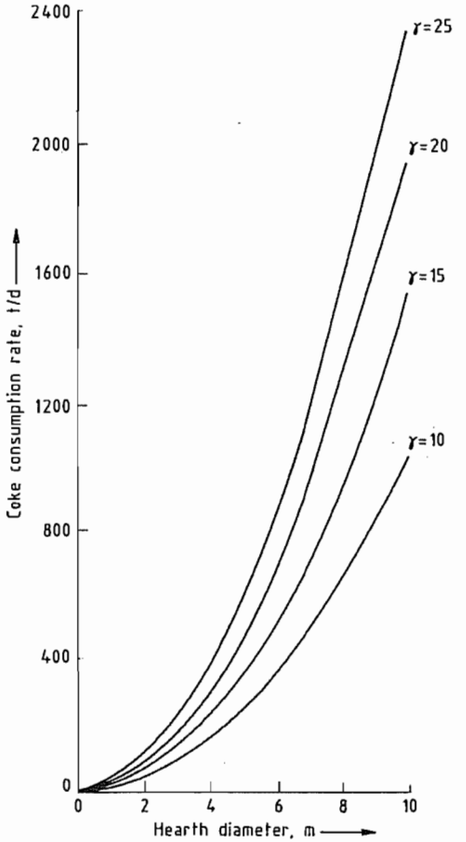

Figure 5.36: Change of coke consumption with the hearth diameter D and productivity factor γ [37].

Formulæ for the *calculation of the productivity* based on empirical observation of operating furnaces have been derived with the aid of regression analysis [38]. These formulæ are used to compare various furnaces or for the design of new furnaces. A regression formula on productivity is given for the blast furnace which produce pig iron for steelmaking.

Table 5.21: Characteristic data for modern large blast furnaces.

	Japan		Germany	France
	No: 2 Oita NSC	No. 5 Fukuyama NKK	No. 1 Schwelgern Thyssen Stahl AG	No. 4 Dunkerque SOLLAC
Blown in date, month-year	10-1976	02-1986	02-1973	1I-1987
Hearth diameter, m	14.8	14.4	13.6	14.0
Working volume, m^3	5070	4664	3596	3648
Number of tuyères	40	42	40	40
Number of tap holes	5	3	4	4
Number of cinder notch	0	0	0	0
Bell and hopper arrangement[a]	2B + V	4B	PW	PW
Top gas pressure, kPa	max. 300	230	330	max. 250
Hot blast stoves (number-type)[b]	4/ECS	4/ECS	3/ECS	4/ECS
Blast blower	electr.	electr.	electr.	electr.
Gas cleaning[c]	DC/2VS	DC VS EP	DC C VS	DC VS C
Production, t/d	10 150	9295	8700	8250
Load on hearth area, $tm^{-2}d^{-1}$	59.0	57.1	60.7	54
Net burden weight, kg/thm[d]	—	1640	1600	1631
Slag weight, kg/thm	321	309	255	314
Coke rate (dry), kg/thm	493	512	337	345
Pulverized coal injection (dry), kg/thm	0	0	145	127
Blast temperature, °C	1097	995	1150	1185
Blast volume (standard conditions), m^3	1110	1151	1100	1062
Oxygen enrichment, %	0	1.05	0	0

[a] B = bell; V = valves; PW = Paul Worth top without a bell.
[b] ECS = extemal combustion stack.
[c] DC = dust catcher; VS = venturi scrubber; EP = electric precipitator; C = cyclone.
[d] thm = tonne of hot metal.

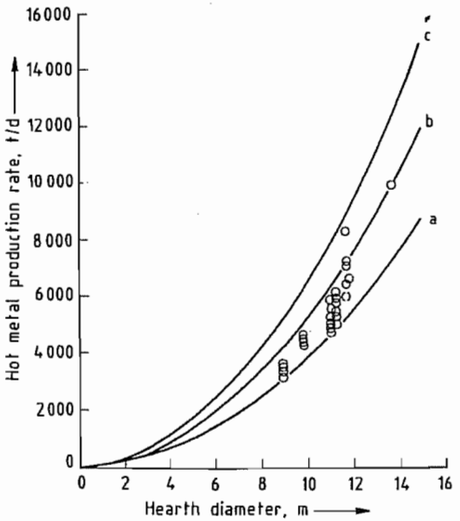

Figure 5.37: Relationship between hot metal production rate and the hearth diameter. The curves are for different specific hot metal production rates [38]. a) 50 $tm^{-3}d^{-1}$; b) 68 $tm^{-3}d^{-1}$; c) 85 $tm^{-3}d^{-1}$.

$$P = A \frac{\left[9241 + \left[(4.5(O_2 - 2.20))/100 + \left(l + \frac{(m/100)(P_t - n)}{100}\right)\right]\right]}{\left[\begin{array}{c} 489 - 0.10(t_b - 1132) + 10(\text{Ash} - 10.8) \\ 0.2(\text{SV} - 304) - 0.9[(\text{SR} - \text{SFPe}) - 71.7] \\ -0.5(\text{OPe} - 91) \end{array}\right]} \qquad (14)$$

where P is the productivity ($td^{-1}m^{-3}$); A a constant (0.85–1.15) O_2 the oxygen enrichment of the blast (%); P, the top-gas pressure (gf/cm^2 = gram force per square centimeter = 98.0665 Pa); l, m, n are constants given in Table 5.20, t the blast temperature (°C); Ash the ash content in coke (%); SV the slag volume, (kg per tonne of pig iron); SR the sinter ratio (%); SFPe the self fluxing pellet ratio (%), OPe the acid pellet ratio (%).

The disadvantage of this formula is that it is entirely empirical. It does not predict productivity increases with technological improve-

ments. Important operational data for some large blast furnaces are summarized in Table 5.21.

5.5.9 Use of Blast Furnace Products

Hot metal, slag and top gas are the products of the blast furnace.

Hot Metal. Most of the hot metal is processed to *steel* by means of the LD (Linz Donawitz) oxygen top-blowing processes. The hot metal used for the LD or open hearth (Siemens–Martin) steelmaking process is known as *low-phosphorus* hot metal. It is characterized by low phosphorus and low sulfur contents. *High phosphorus* hot metal (Thomas iron) can also be refined to steel by means of the oxygen steelmaking (LD/AC) process Other types of hot metal are further processed in foundries to *cast iron* or are used as alloys in the steel shop or in the foundry because of their high alloy content (e.g., manganese, silicon). The composition of the common types of hot metal are listed in Table 5.22. The Bessemer (Thomas) and open hearth processes have been replaced by the oxygen top-blowing processes.

Slags. Depending on the conditions during solidification, the slags produced by the blast furnace are further processed to:

- Air-cooled slag (solidification in slag pots or pouring pads),
- Granulated slag (spraying of the liquid slag with water),
- Pumice slag (foaming with water), or
- Slag wool (blowing of the liquid slag with air or steam)

Granulated slag can be in the form of pebbles or can have a porous structure depending on the granulation process. The different structure affects the hydraulic-bonding properties, the grindability, and the strength. Granulated slag is used as a material for making blast furnace cement by mixing it with Portland cement after pulverization. It is also used as a fertilizer.

Pumice slag is used in porous form as an insulation and filler material in heavy concrete and as a replacement for other bulk additions.

Air-cooled slag is either ground, such as granulated slag, or crushed and screened to be used as ballast or aggregate.

Slag wool is used in the form of pads for thermal insulation.

The relative quantities of the various products made from blast furnace slag for the various application are listed in Table 5.23 [40].

Table 5.22: Average composition of various kinds of hot metal (%) [36].

	C	Si	Mn	P	S
Low phosphorus iron	3.8–4.5	0.5–1.0	1.5–5.0	0.05–0.12	< 0.05
LD hot metal	3.8–4.4	1.0	0.8–1.2	0.01	< 0.04
Thomas (Bessemer) iron	3.5–3.9	ca. 0.3	ca. 0.8	ca. 1.8	< 0.055
Hematite hot metal	3.5–4.2	1.5–3.5	0.7–1.0	< 0.12	< 0.04
Foundry iron I	3.5–4.5	1.5–3.5	1.0	0.5–0.7	< 0.04
Foundry iron III	3.5–4.5	1.5–3.5	1.0	0.7–1.0	< 0.06
Foundry iron IV A	3.5–4.5	1.5–3.5	0.7	1.0–1.4	< 0.06
Foundry iron IV B	3.5–4.5	1.5–3.5	0.7	1.4–2.0	< 0.06
Specialty and malleable cast iron	3.4–4.3	0.3–4.0	0.2–1.0	0.05–0.10	< 0.05
Specialty metal (high carbon)	4.0–4.8	< 2.5	0.3–0.6	0.08–0.15	< 0.05
Specialty metal for the production of nodular cast iron	2.8–4.3	< 2.0	< 0.2	< 0.06	< 0.02
Siegerland specialty metal	2.8–3.4	2–3.5	2–4	< 0.1	< 0.05
Spiegel iron	4.0–5.0	< 1.0	6–30	0.1–0.15	< 0.04
Ferro manganese (75%)	6.0–7.0	< 1.0	70–80	< 0.25	< 0.03
Ferro silicon	1.4–2.2	8–13	0.5–0.7	< 0.15	< 0.04
Charcoal hot metal	3.6–4.2	0.25–2.75	< 1.0	ca. 0.03	ca. 0.015

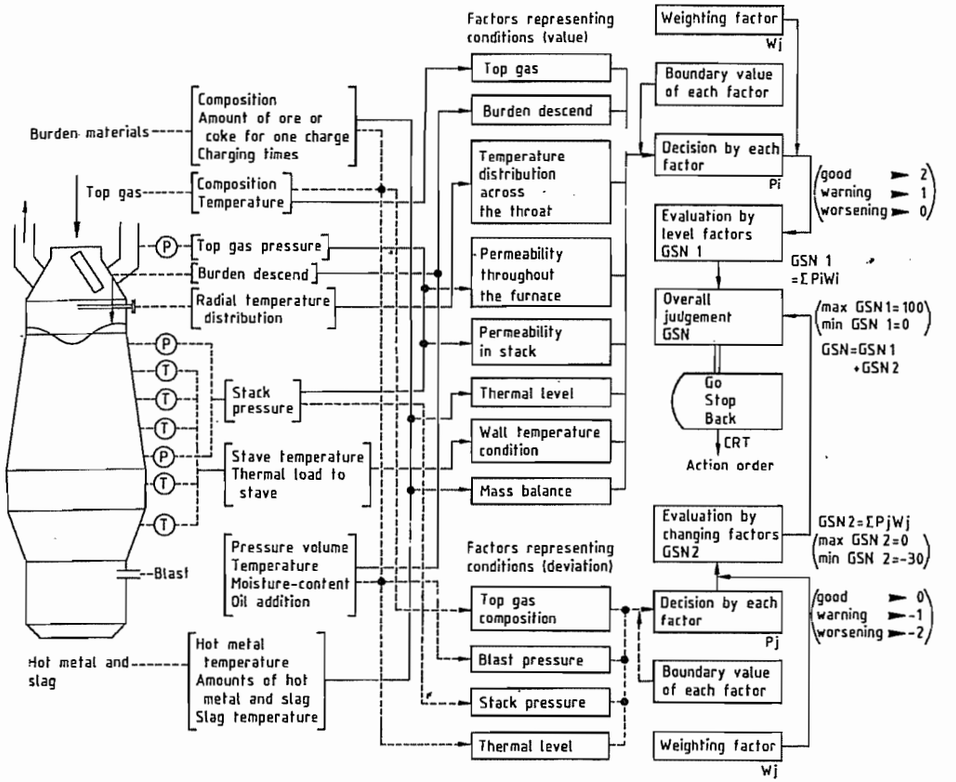

Figure 5.38: A control system of blast furnace developed by Kawasaki Steel Corp. [41] (Courtesy of The Iron and Steel Institute of Japan).

Table 5.23: Slag production and use in Japan in 1987 [40].

	10^3 t	%
Slag production from blast furnace	23 842	
Slag use		
Road-bed construction	6 328	26.54
Improvement of grand	174	0.73
Engineering works	1 666	6.99
Cement	12 064	50.60
Concrete	1 496	6.27
Manure and improvement of soil	423	1.77
Building	603	2.53
Others	1 088	4.56

Top-Gas. The top-gas consists mainly of N_2, CO_2, CO and H_2. The utilization degree of the top gas is usually ca. 50% therefore it is a lean gas whose calorific value is between 2850 and 3560 kJ/m³ (STP). This value is very low compared to those of coke oven gas and LD gas. Almost all the top gas is used in the iron and steel plant itself which has been extensively discussed (see Figures 5.7, 5.20, and 5.25).

5.5.10 Process Control

Thirty years ago, the blast furnace process was operated completely by manual control. Relatively few measuring devices were available for process monitoring purposes. since the 1950s the productivity of a typical furnace has increased by ca. 20 times. This improvement in operation increased the importance of the process control. Modern blast furnaces are, therefore, equipped with a sophisticated system of measuring and controlling devices, and are directly linked to the process computer

(Figure 5.38). The latter is often incorporated into the total control system of the whole plant via a larger business computer.

The computer control of the blast furnace process for the optimization of the quality and costs started ca. twenty years ago. Research in this area is still being carried out. Much information can be obtained about the process by measuring the in- and outflows of mass and energy and also about many phenomena taking place inside the furnace. However, the basic problem is to convert these informations into control variables to serve the control circuit. The algorithm to evaluate the control variables from the measured values are based on various mathematical models.

Static and Dynamic Models Based on Statistics. In these models the blast furnace is considered to be a black box. The effect of certain deliberate changes in the input variables (e.g., coke addition, pulverized coal injection, moisture content of the blast, back pressure at the top) on productivity, hot metal composition, top gas utilization, etc. is evaluated. With the aid of statistical models, this leads to regression expressions containing the desired algorithms for the determination of the control variables. These statistical blast furnace models that have already been applied successfully do not, in principle, require any knowledge concerning the phenomena occurring inside the blast furnace. An example of such a regression expression is the productivity formula (see Equation 14) which should only be used for control purposes based on the values of a particular furnace and not based on values collected from various furnace operations. Although it is relatively simple to derive such an expression representing a blast furnace model from operational data, its application is limited. If such a model is applied to new operating conditions, then its predictions deviate from reality, the more the new operating conditions deviate from those which are described by the statistical data. Optimization of the operating conditions becomes stringently conservative when applying statistical models.

Static models based on statistics allow predictions concerning the steady state of the furnace only. *Dynamic models* based on statistics allow predictions concerning the behavior during a transient when passing from one steady state condition to another.

Models Based on Overall Balances. Models derived by taking overall balances represent the internal phenomena of the blast furnace on the basis of two-stage heat and mass balances. The procedure is principally similar to that described in section 5.5.6 in which the application of the Rist diagram and the heat and mass transfer phenomena (Table 5.16) were discussed. However, the models are more exact and detailed. A disadvantage of these blast furnace models is that they are unable to predict time-dependent phenomena in the furnace, although data concerning phenomena occurring in the blast furnace are evaluated. For the evaluation of the control variables it is, therefore, necessary to make assumptions concerning the *thermal equilibrium* between gas and solids in the thermal reserve zone and the *chemical equilibrium* between gaseous components (CO and CO_2) and solid component (iron and wustite), in the chemical reserve zone. The assumption corresponds to point W in the Rist diagram.

In the overall balance model, a *direct* relationship exists between input and output variables. This is a definite difference to the statistical model. The overall balance model has only one apparent degree of freedom which is the *degree of indirect reduction*. The existence of this apparent degree of freedom is caused by a lack of knowledge and will disappear when the internal phenomena of the blast furnace can be measured exactly and incorporated in the model. Under the fixed technological boundary condition the function of the blast furnace is *determined* by these phenomena in combination with certain pretreatment of ore and coke as well as a given hot metal composition.

Kinetic-Dynamic Model. The kinetic-dynamic model in its most extensive form is based on a knowledge of all phenomena that

constitute the entire blast furnace process. The phenomena include thermodynamic equilibrium and the kinetic relationships that govern the momentum, heat and mass transfer. The model is also based on the knowledge of the behavior of burden materials (e.g., size distribution at the top of the furnace, descending movement, softening and melting), coke gasification, and gas permeability. The model can simulate the behavior of a blast furnace for any given situation with a large computer. All the data required for the model can be determined in the laboratory and essentially need not be corrected with data based on actual operating conditions. The model thus constructed has proved to be advantageous for the study of new processing conditions and the predictions of the operating results without performing costly experiments with the blast furnace. Its disadvantage is the requirement of great amount of expenditure to complete information on all the important phenomena occurring in the furnace. For routine blast furnace control, the model must be simplified to reduce computer loads.

The most important kinetic phenomena for constructing the mathematical model by taking differential balances around a control volume are the chemical reactions (e.g., reduction of iron oxide, coke gasification, water gas shift reaction, and reduction of silica). The reduction rate of iron oxide by carbon monoxide or hydrogen can be expressed in terms of the three-interface unreacted-core shrinking model which is represented in Figure 83. Rate and equilibrium constants needed for the rate equation are given in reference [42]. For *silica reduction*, a mechanism via the intermediate formation of SiO gas has recently been proposed [43]. A rate equation has been derived for the transfer of silicon from the SiO gas to the hot metal in accordance with the mechanism as described by Equation (15).

$$\frac{d[\%Si]}{dt} = k_c(A/M)P_{SiO} \qquad (15)$$

where k_c designates the reaction rate constant, A/M the specific area, and P_{SiO} the partial pressure of SiO.

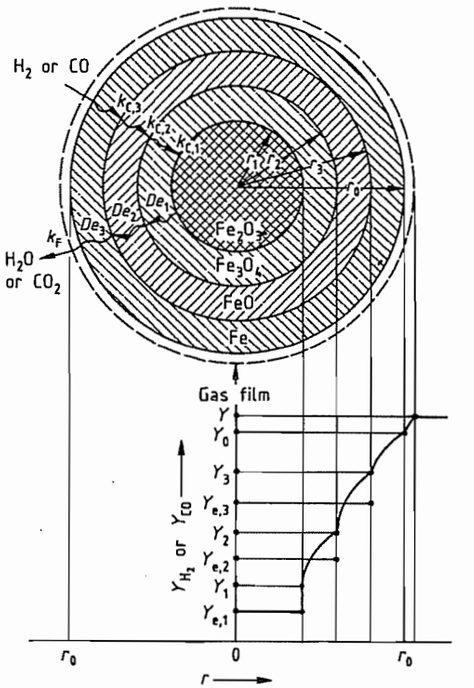

Figure 5.39: Three-interface unreacted core model [41] (Courtesy of The Iron and Steel Institute of Japan): De_i = intraparticle diffusivity in i-th phase; k_{ci} = rate constant of i-th chemical reaction; k_F = mass transfer coefficient through gas film; r = radial coordinate; Y = molar fraction of gas.

This mechanism has been found to give excellent simulation results when it is incorporated into the mathematical model.

The *heat transfer* between the different phases in a packed bed is usually expressed in the form of convection heat transfer. The estimation of the heat transfer coefficient is mainly based on the Ranz Equation [45]:

$$Nu = 2.0 + 0.6(9Re_p)^{1/2}Pr^{1/3} \qquad (16)$$

where Nu, Re_p, and Pr designate Nusselt, particle Reynolds, and Prandtl numbers.

However, this equation sometimes gives an inappropriate value. The rate of heat exchange in a packed bed is currently being studied. *Flow maldistribution* of gas in a packed bed can be estimated by using the Ergun equation,

a *potential flow mechanism* is often applied to the solid flow [46].

On the basis of the principal concepts mentioned above, *one-dimensional* [47], or *two-dimensional* [46, 48, 49] mathematical models were derived. On the other hand, dynamic changes in the internal situation of a blast furnace were also simulated by an unsteady-state mathematical model [50, 51].

Even if a supercomputer is available for the simulation computation of a whole blast furnace, it is still quite difficult to obtain detailed results which include all the phenomena occurring in a blast furnace. Mathematical models presenting some specified phenomena in a blast furnace are effective when detailed information is requested. Such models are developed for analyzing burden distribution at the top of a blast furnace [52], gas flow and heat transfer in the cohesive zone [53], raceway phenomena [27], fluid flow in the hearth [54] and so on.

Some examples of the simulation results are shown in Figures 5.40, 5.41, and 5.42. Figure 5.40 depicts a onedimensional distribution of process variables such as temperature, pressure, concentration, and fractional reduction for two different top-gas pressure.

Temperature and gas-concentration distributions reveal the existence of thermal and chemical inactive zones and characteristic distribution of CO concentration which shows maximum value at the position where the CO_2 concentration is zero. The simulation results agree well with the principal behaviors of the process variables previously shown in Figure 5.20.

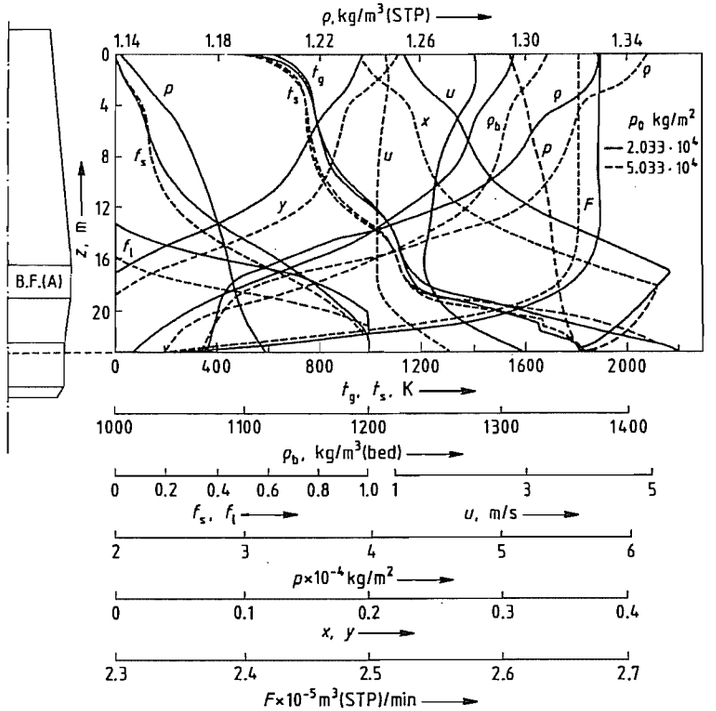

Figure 5.40: Longitudinal distribution of process variables in blast furnace (A) for the case of high-pressure operations [46] (Courtesy of The Iron and Steel Institute of Japan): t_g, t_s = temperatures of gas and solid; f_s = fractional reduction of iron oxide; f_l = fractional decomposition of limestone; u = superficial gas velocity; p = gas pressure; p_0 = top gas pressure; x, y = molar fraction of CO and CO_2; F = volume flow rate of gas; ρ = gas density; ρ_b = bulk density of burden bed.

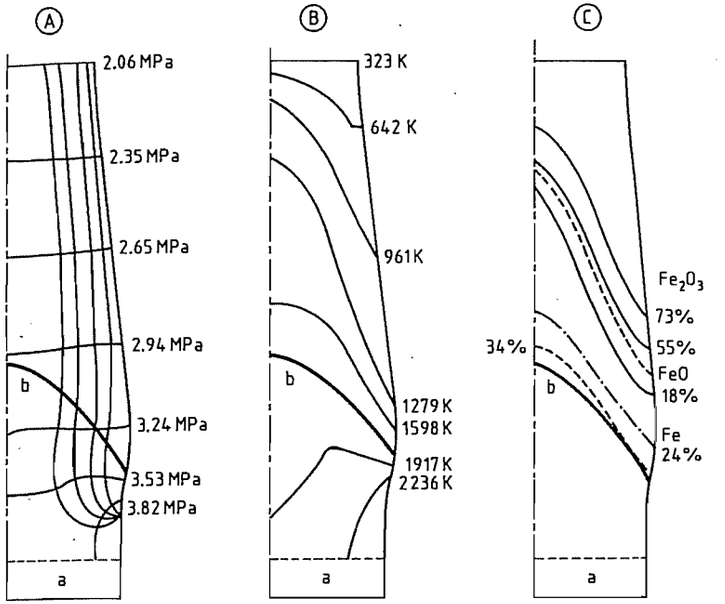

Figure 5.41: Two dimensional simulation results by finite difference method [48] (Courtesy of The Iron and Steel Institute of Japan): A) Streamlines and isobars; B) Isotherms of solid; C) Reduction of ore; a) Liquid; b) Fusion zone.

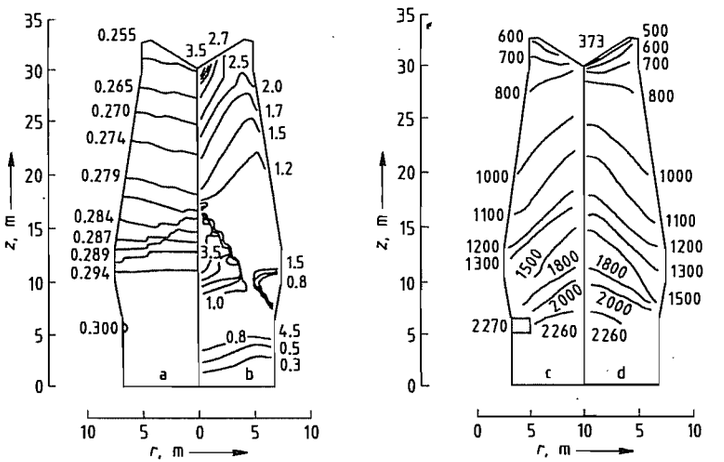

Figure 5.42: Two dimensional simulation result by finite element method [46] (Courtesy of The Iron and Steel Institute of Japan): a) Isobars (P in MPa); b) Contour lines of average mass velocity of gas ($kgm^{-2}s^{-1}$); c) Isotherms of gas (t_g ion K); d) Isotherms of solid (t_s in K).

Figure 5.41 shows the streamline of gas, as well as the radial distribution of pressure, temperature and reduction degree, which show a considerable nonuniformity One of the important problems is how to control or utilize the nonuniformity to improve productivity.

Figure 5.42 shows computed radial profiles of pressure, gas velocity, and temperatures of

gas and solids. In this computation, the layer-by-layer structure of the packed beds and the radial particle size distribution were considered, which markedly affect the gas permeability and then gas flow and temperature distributions.

Complete measurement of the internal state of a blast furnace is very difficult because of its huge size. Simulation technology in combination with operating and some measured data is very important to understand the behavior of the blast furnace.

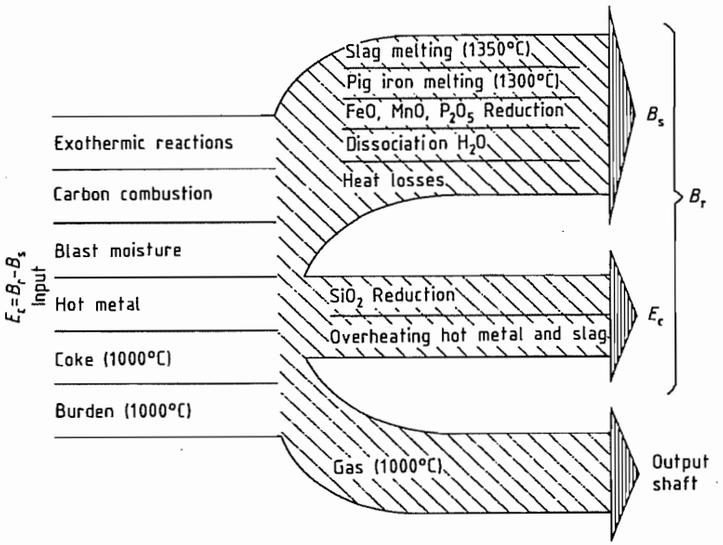

Figure 5.43: Heat balance for calculating value of E_c-heat required for the reduction of silicon and for the overheating of iron and slag [55] (Courtesy of The Institution of Mining and Metallurgy).

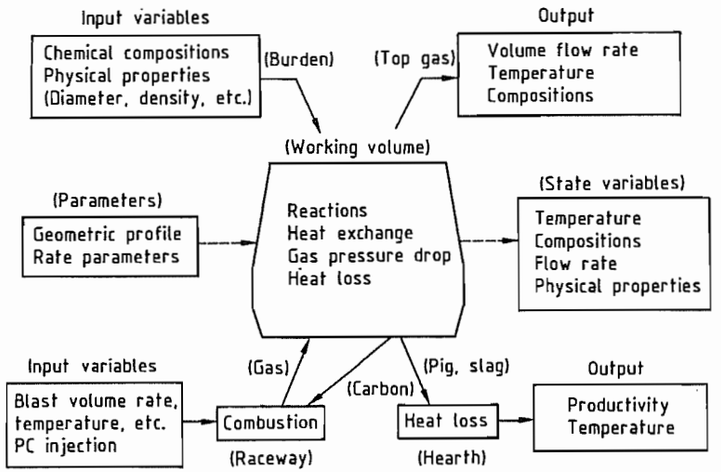

Figure 5.44: Schematic diagram of a dynamic simulation model of blast furnace [51] (Courtesy of The Iron and Steel Institute of Japan).

Application of the Models. The purpose of the blast furnace control during continuous operation is the increase in productivity by stabilizing the furnace operation and the production of high quality pig iron of appropriate temperature and composition. The control variables are (1) ore: coke ratio and burden distribution at the top of the furnace, (2) flow rate and temperature of blast, water vapor addition, and oxygen injection, pulverized coal, oil and fine ore injection.

Originally, attention was paid to the *thermal condition* in the *lower part* of the blast furnace for the stable operation. The so-called *Wu model* was proposed by the Institut de recherches sidérurgiques (IRSID) in France. In the model, the heat input into the lower part of the furnace is calculated from blast volume and composition, tuyère injection, and the off-gas analysis. The amount of heat Wu is that required for the melting of iron and slag, the reduction of the alloying elements, and compensation for heat loss. The value of Wu can be calculated by subtracting the heat consumed by direct reduction of the iron oxides from the total heat supplied to the lower part of the furnace. By maintaining Wu at a constant set value pig iron of a constant composition can be produced.

At the Centre de recherches métallurgiques (CNRM) in Belgium, a somewhat different model of the same basic type was developed for automatic regulation of the thermal condition of the furnace. In this model, the heat input per ton of pig iron into the high-temperature zone of the furnace was calculated from the temperature and composition of the top gas, the blast volume, blast temperature, and blast composition. The value obtained is called the heat requirement. The term E_c, was defined as the difference between the actual (B_r) and the standard heat requirements (B_s). The latter quantity represents the amount of heat needed to produce a pig iron at 1300 °C containing 0% Si.

The value of E_c corresponds to the heat required for silica reduction and for overheating slag and metal. The heat balance to calculate E_c is shown in Figure 5.43.

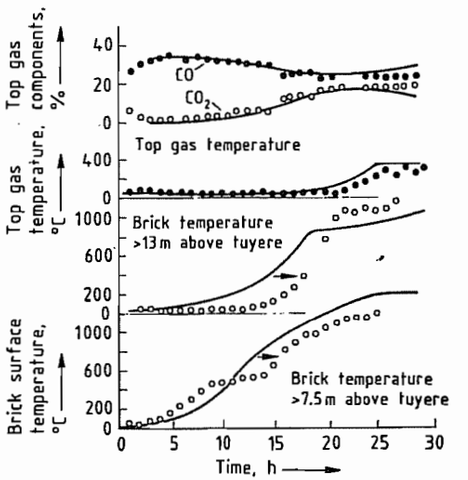

Figure 5.45: Comparison between measured and simulated changes of process variables in blow-in operation of Kokura no. 2 blast furnace, Sumitomo Metal Industries, Ltd. [51] (Courtesy of The Iron and Steel Institute of Japan): — Predicted; ● ○ Measured.

A *one-dimensional dynamic model* was applied to the *unsteady-state* blast furnace operation such as the shut down, the blow-in, and the blow-out together with a *two-dimensional gas flow* model. A schematic diagram is shown in Figure 5.44. Figure 5.45 shows the simulation results for the blow-in operation of the blast furnace according to the scheduled increase in blast volume and temperature as shown in Figure 5.46. The initial condition given to the mathematical model was obtained from the actual filling condition of coke and burden before the start of the blow-in. The results confirm the effectiveness of the model application to the planning of the blow-in operation of the blast furnace. Another successful example for the application of a dynamic model to the actual operation has been reported for the blow-out of the blast furnace. The content of the blast furnace was blown out with the decrease of stock level from the top to the upper bosh under the schedule predicted by the mathematical model. Actual changes of the operation conditions are shown in Figure 5.47 in comparison with the scheduled ones. The actual results are in reasonable agreement with the schedule (see Table 5.24). Some im-

provements to the mathematical model are necessary for obtaining a satisfactory agreement. However, principally such a kinetic-dynamic model is found to be effective not only for steady-state but also for unsteady-state operations.

The most precise mathematical model of a blast furnace to date is the two-dimensional steady-state kinetic model developed by SUGIYAMA et al. [57] (Nippon Steel Corp:). It includes models tor operational design, burden distribution, gas, solid and liquid flow, for the reaction rate of seven chemical reactions, for heat transfer and a total combination model. When operational conditions and a blast furnace profile are given, this model provides (1) streamlines of gas, liquid and solids, (2) pressure distribution, (3) reduction degree of iron oxides, (4) gas, solid and liquid temperature, and (5) location of the cohesive zone.

An integrated process computer system in the entire ironmaking department is being developed for increasing flexibility and productivity in the ironmaking systems which consist essentially of coke ovens, sintering machines, hot stoves, and blast furnaces.

The three-layer hierarchical system shown in Figure 5.48 is used for integrated control. In the system, *microcomputers* can accept the operating data directly from the plant and can control it. A *process computer* which eventually controls the overall ironmaking system is installed to provide sufficient information to the operator for realizing effective operation. Finally, a central *business computer* is connected to the process computers for optimal control of the overall iron and steel production system. Chiba works of Kawasaki Steel Corp. constructed this three layers system for two sintering plants and achieved effective operational control.

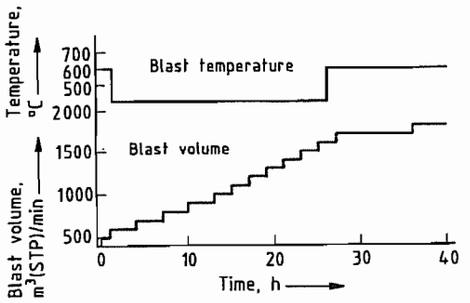

Figure 5.46: Schedule of the blow-in operation for the Kokura no. 2 blast furnace based on a dynamic model [51] (Courtesy of The Iron and Steel Institute of Japan).

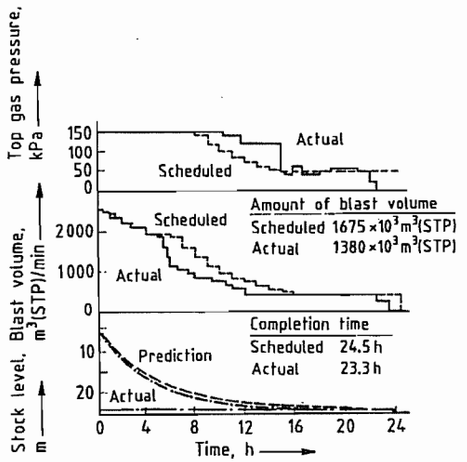

Figure 5.47: Results of the empty blow-out operation of the Kokura no. 2 blast furnace [56] (Courtesy of The Iron and Steel Institute of Japan).

Table 5.24: Results of the empty blow-out operation of the Kokura no. 2 blast furnace in Sumitomo Metal Industries [56] (Courtesy of The Iron and Steel Institute of Japan).

	Actual results	Schedule	Difference, %
Blow-out operation time, h	23.3	24.5	–5
Accumulated amount of blast volume, $m^3 \times 10^3$ (STP)	1380	1675	–18
Accumulated amount of water-spray, t	694	716	–3
Pig iron produced during blow-out, t	880	998	–12
Amount of total coke consumption, t	550	690	–20
Coke consumption per blast volume, $t/m^3 \times 10^3$ (STP)	0.40	0.41	–2

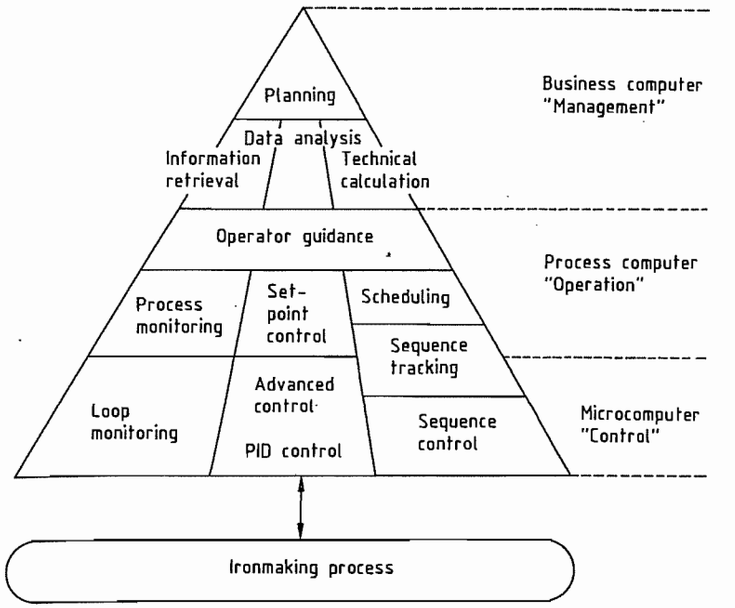

Figure 5.48: Functional hierarchy of the ironmaking information system [57] (Courtesy of The Iron and Steel Institute of Japan).

Table 5.25: Summation of net exergy losses in the blast furnace ironmaking system [60] (Courtesy of The Iron and Steel Institute of Japan).

Process	Case A-1			Case A-2, MJ/thm		
	Inflow	Outflow	Net loss	Inflow	Outflow	Net loss
Blast furnace	17 054	15 175	1 879 (20.8%)	16 920	14 736	2184 (24.1%)
Coke oven	22 657	18 580	4 077 (45.1%)	20 110	16 491	3619 (39.9%)
Hot stove	1 983	1 276	707 (7.8%)	2 100	1 423	677 (7.5%)
Sintering machine	3 014	764	2250 (24.9%)	3 074	733	2341 (25.8%)
Rotary kiln	138	33	105 (1.2%)	339	79	260 (2.9%)
Curing of nonfired pellets	190	170	20 (0.2%)			
Total	45 036	35 998	9038 (100%)	42 543	33 462	9081 (100%)

Although great progress has been made in the computer control of blast furnaces by introducing mathematical models, control is still incomplete. Recently, artificial intelligence has been introduced into blast-furnace control. The principal strategy of this technology is based on operational data [59]. Therefore, the question how to accumulate the operating data is most important. Some trials have been made to couple the artificial intelligence (Expert system) with a mathematical model.

Energy Recovery. After the oil crisis, energy cost increased drastically. Therefore in high-energy consuming industries, energy saving has been examined from various points of view. In Japan 1.9×10^7 kJ energy is currently consumed to produce 1 t crude steel in the blast furnace ironmaking process. This value is 20% lower than 10 years ago. The energy savings are still conducted in each ironmaking process. Tn the blast furnace, a lot of energy is saved by using top-pressure recovery turbines. Figure 5.49 illustrates the development of energy savings in the ironmaking department of NSC during the last 15 years.

To pursue further energy savings, an exergy analysis was conducted on the basis of actual

operation data of a blast furnace ironmaking system which produced ca. 7000 t pig iron per day. Very high net exergy losses occur in the coke oven and the sintering machine (see Table 5.25). Compared to these processes the blast furnace destructs less exergy. Net exergy losses in the conventional blast furnace, the direct reduction electric furnace, and the smelting reduction systems are compared in Figure 5.50. The exergy analysis for the conventional and the direct reduction iron-electric furnace systems was performed on the basis of operation data but in case of the smelting reduction system, the data were obtained by taking heat and material balances. However, no definite difference among the net exergy losses were found. Further energy savings will probably lower exergy losses even further.

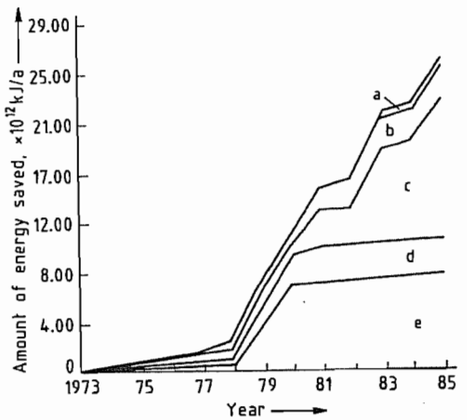

Figure 5.49: Chronological change in the amount of energy saved by main waste heat recovery process in Nippon Steel Corp. [60] (Courtesy of The Japan Iron and Steel Institute): a) Recovery of sensible heat from coke oven gas; b) Recovery of waste heat from sinter cooler; c) Coke dry quenching; d) Recovery of sensible heat from hot stove; e) Top gas pressure recovery turbine.

5.5.11 Hot-Metal Desulfurization

The sulfur content of the hot metal produced depends on the sulfur content of the fuels, the slag basicity, the slag volume, and the silicon content of the hot metal. The sulfur transfer mechanism in the blast furnace is shown schematically in Figure 5.51. After the hot metal is separated from slag, the former is desulfurized by gas metal and slag–metal reactions. However, in the upper part of the cohesive zone, the sulfur compounds present in the gas phase are absorbed partly by solid iron ores.

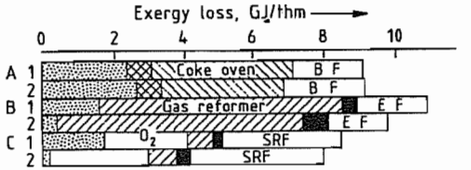

Figure 5.50: Summation of net exergy losses in different ironmaking systems [61] (Courtesy of The Iron and Steel Institute of Japan): A) Blast furnace ironmaking (1 = standard, 2 = pulverized coal injection); B) Direct reduction-electric furnace ironmaking (1 = fired pellet, 2 = nonfired pellet); C) Smelting reduction ironmaking (1 = shaft furnace, 2 = fluidized bed). O2 = oxygen production; BF = blast furnace; EF = Electric furnace; SRF = Smelting reduction furnace. □ Pretreatment, agglomeration of raw materials; ■ Shaft furnace, fluidized beds; ▨ Hot stove.

The steelmaking process requires a sulfur content of the hot metal of < 0.025–0.035%, because desulfurization is difficult in the steelmaking process. Except for the desulfurization of the coke, sulfur can be removed in the blast furnace, between the blast furnace and the steel shop, and in the steel shop. The cost is reported to be the lowest for desulfurization between the blast furnace and the steel shop [62].

Desulfurization in the *blast furnace* requires an increase in the limestone additions. This leads to the additional costs associated with the limestone itself and the increased coke rate because more heat is needed for melting the slag and for decomposing the limestone. In addition to this, the carbon dioxide generated from limestone must be compensated.

Desulfurization in the *steel-producing vessel* requires a large slag volume even for highly basic slags because of the unfavorable sulfur distribution ratio under oxidizing conditions. Iron losses to the slag increase because of the large slag volume.

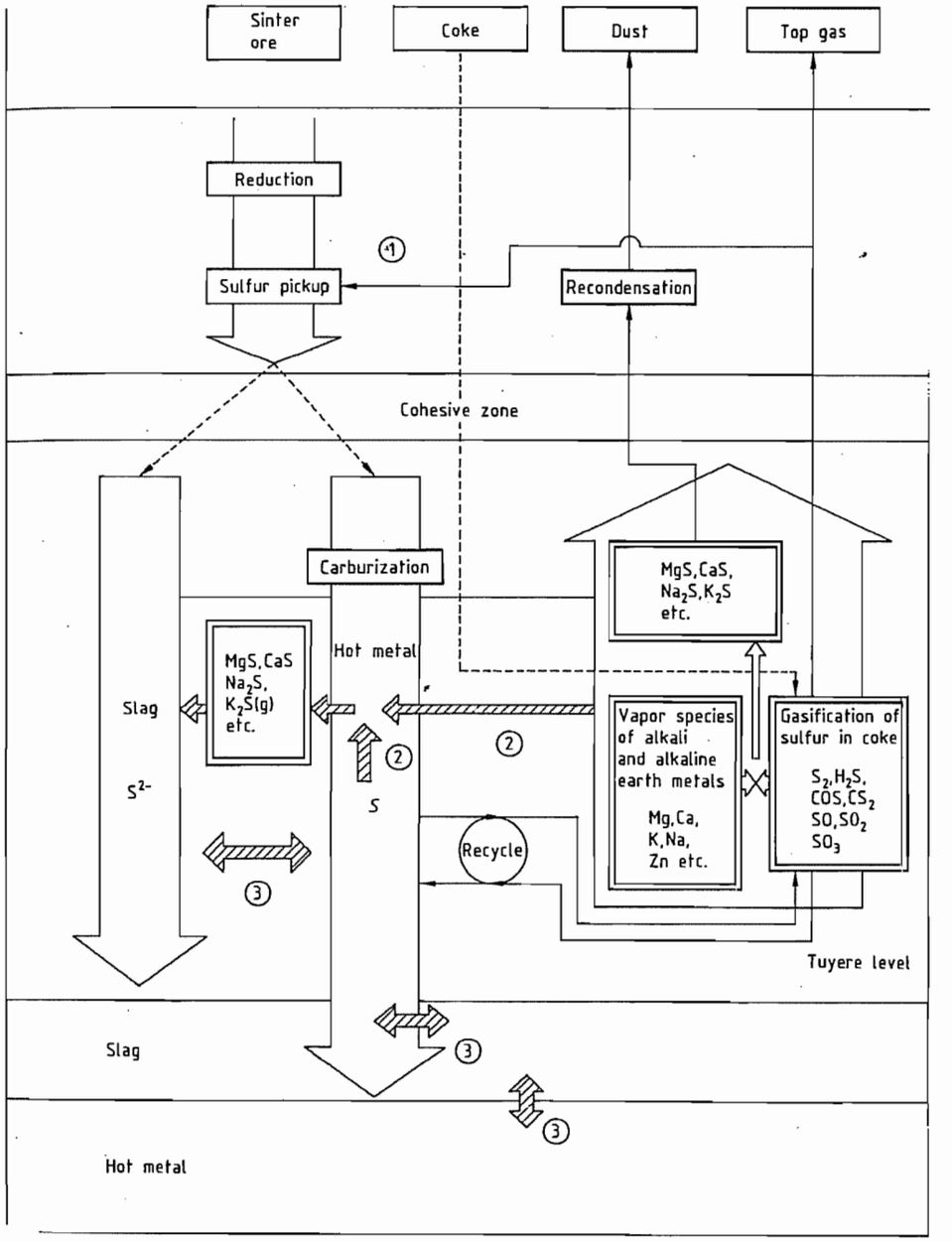

Figure 5.51: Schematic representation of sulfur transfer routes in the blast furnace [65] (Courtesy of The Iron and Steel Institute of Japan).

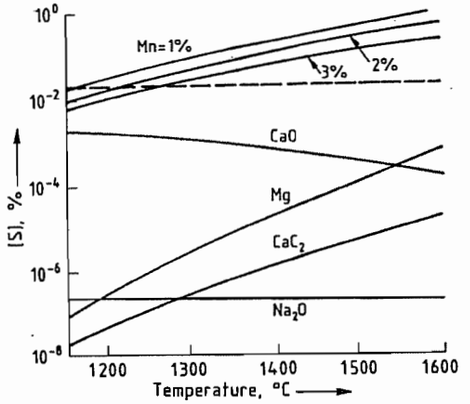

Figure 5.52: Temperature dependence of equilibrium sulfur content of carbon-saturated hot metal [63] (Courtesy of The Iron and Steel Institute of Japan).

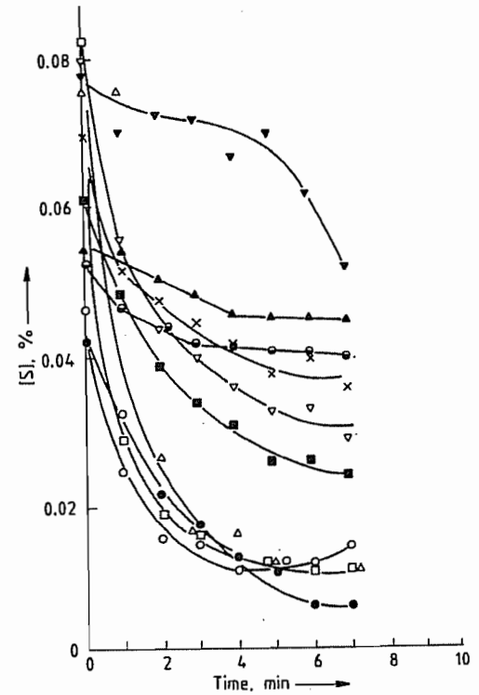

Figure 5.53: Changes of sulfur content with time in bottom-blowing ladle desulfurization process for variable fluxes (amount of flux addition 10 kg/thm) [63] (Courtesy of The Iron and Steel Institute of Japan): ● CaC_2; ▲ CaO; ■ $Ca(CN)_2$; □ Na_2CO_3; △ NaOH; □ KOH; × NaCl; ▽ NaF; ▼ CaF_2; ● Na_3AlF_6.

At present, it is advantageous to desulfurize at least a portion of the hot metal during *transportation to the steel shop*. After mixing with hot metal which is not desulfurized outside the blast furnace, an input sulfur content of ≤ 0.02% can be delivered to the steel shop.

Desulfurizing Fluxes include calcium compounds which are in the solid state or half melting conditions at the hot metal temperature (e.g., CaO, CaC_2, $Ca(CN)_2$, and CaF_2), alkaline compounds in the liquid state (e.g., KOH, NaCl, and NaF), and magnesium and its alloys in the gaseous state.

Their desulfurization ability is remarkably affected by treatment conditions such as (1) mixing, (2) atmosphere (oxidizing or reducing), (3) composition of hot metal, and (4) property and amount of blast furnace slag. Figure 5.52 shows the equilibrium sulfur content obtained by each desulfurizing flux. Actual desulfurization curves for the *bottom blowing* method with nitrogen are shown in Figure 5.53.

According to these figures, desulfurization degree, method, cost, and workability should be considered when selecting of a desulfurizing flux in addition to its desulfurizing ability.

The equation for the desulfurization reaction with *soda ash* [64] and of concurrent reactions are as follows (Equations 17–19):

$$(Na_2CO_3) + [S] + [Si] \rightarrow (Na_2S) + (SiO_2) + CO \quad (17)$$

$$(Na_2CO_3) + (FeS) + [Si] \rightarrow (Na_2S) + (SiO_2) + [Fe] + CO \quad (18)$$

$$(Na_2CO_3) + [Si] \rightarrow (Na_2O \cdot SiO_2) + C \quad (19)$$

Furthermore, Na_2CO_3 reacts easily with SiO_2 from the refractories forming $2Na_2O \cdot SiO_2$, $Na_2O \cdot SiO_2$, and $Na_2O \cdot 2SiO_2$. The vaporization loss of Na_2CO_3 is ca. 6% at 1250 °C. This value increases to 35% at 1350 °C, therefore the effect of desulfurization decreases sharply at temperatures > 1300 °C. The disadvantages of desulfurization with soda ash are its corrosive action to the vessel lining and the environmental problems related to discarding slags which contain high alkaline contents. Environmental problems arise from sodium oxide-containing fumes and from the reaction

of the sodium sulfide contained in the slag with water to produce hydrogen sulfide and sodium hydroxide.

The desulfurization reactions of hot metal with *calcium carbide* are as follows:

$$\langle CaC_2 \rangle + [S] \rightarrow (CaS) + 2[C] \quad (20)$$

$$\langle CaC_2 \rangle + {}^1/_2\{O_2\} \rightarrow \langle CaO \rangle + 2[C] \quad (21)$$

$$\langle CaC_2 \rangle + {}^1/_2[O] \rightarrow \langle CaO \rangle + 2[C] \quad (22)$$

$$C + {}^1/_2O_2 \rightarrow CO \quad (23)$$

As calcium carbide is easily oxidized (see Equations. 21 and 22) the desulfurization should take place under controlled atmosphere. The reaction product CaS which has a high melting temperature of 2450 °C forms the solid slag. The diffusion of sulfur in the hot metal to the boundary between hot metal and calcium carbide is the rate-determining step of the desulfurization reaction. In the sulfur-transfer mechanism, mixing strongly affects the degree of desulfurization. When calcium carbide particles are injected with an inert carrier gas, a calcium sulfide layer grows at the outer surface of the particle as the reaction proceeds. The reactivity of each particle decreases with increasing thickness of this layer. Thus, the efficiency of this flux is relatively low. Its advantage is that a very low residual sulfur content of the hot metal can be achieved irrespective of its initial sulfur content.

When *lime* is used, the following desulfurization reactions proceed:

$$4CaO + 2[S] + [Si] \rightarrow 2CaS + 2CaO \cdot SiO_2 \quad (24)$$

$$2CaO + 2[S] + [Si] \rightarrow 2CaS + SiO_2 \quad (25)$$

The reaction given by Equation (25) occurs at 1300 °C even if the silicon content of the hot metal is only 0.05%. If the silicon in the hot metal is oxidized to silicon dioxide in this process, it reacts with lime to form $2CaO \cdot SiO_2$. This reaction decreases the amount of lime available for desulfurization. Therefore oxidation of silica should be prevented by using the inert or reducing atmospheres or airtight vessels.

Magnesium is sometimes used as a desulfurizing flux because it has a very strong affinity for sulfur. Equations (26), (27), and (28) represent the desulfurization by magnesium and the oxidation of magnesium which occurs in the desulfurization process.

$$\{Mg\} + [S] \rightarrow MgS \quad (26)$$

$$\{Mg\} + [O] \rightarrow MgO \quad (27)$$

$$\{Mg\} + {}^1/_2O_2 \rightarrow MgO \quad (28)$$

The vaporization temperature of magnesium is relatively low (1107 °C). Therefore, magnesium evaporates upon contact with the hot metal and the desulfurization efficiency decreases. It is therefore necessary to control the vaporization (see below).

Table 5.26: Typical desulfurization processes outside the blast furnace [18] (Courtesy of The Iron and Steel Institute of Japan).

Method	Process
Soda-ash paving	soda-ash paving process reladling process ladle with siphon process
Shaking ladle	shaking ladle process DM converter process rotating drum process
Stirrer	Demag-Östberg process Rheinstahl process KR process
Injection	(ladle process) (torpedo-car process)
Gas bubbling	bottom blowing process top blowing process
Gas-lift mixing reactor	GMR process
Desulfurization with magnesium	injection process plunging bell process
Continuous desulfurization in the blast-furnace runner	turbulator process powder injection process paddle-type stirrer process electromagnetic stirrer process

Desulfurization Processes. To produce low-sulfur or ultra-low sulfur steel, a number of desulfurization processes have been developed. Typical processes for desulfurization *outside* the blast furnace are listed in Table 5.26. Tn each process, acceleration of the desulfurization reaction is achieved by increasing the contact area between the desulfurizing fluxes and the hot metal. This is carried out by employing improved stirring techniques. The other requirements for the processes are as follows: (1) inexpensive desulfurizing fluxes, (2) high reproducibility with regard to the de-

gree of desulfurization, (3) small decrease of the hot metal temperature, (4) low iron loss to the slag, and (5) an easy and inexpensive disposal of the slag.

Desulfurization in the *blast-furnace runner* is not widely accepted at present despite the favorable surface:volume ratio and the low degree of technical expenditure required. The reasons are the corrosive attack of the slag on the runner material, the hazardous exposure of the workers to alkaline fume, and the poor reproducibility with respect to the degree of desulfurization.

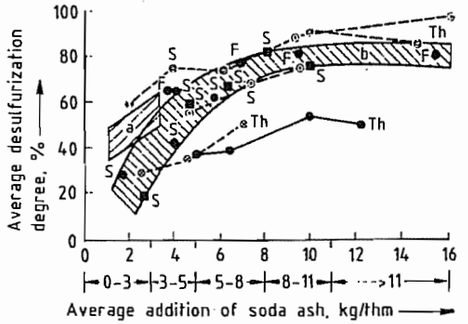

Figure 5.54: Effect of the amount of soda ash addition on the desulfurization of hot metal in various desulfurization processes [66] (Courtesy of Verlag Stahleisen mbH): ○ Blast-furnace runner; ■ Transportation ladle; ⊗ Mixer–ladle; ⊙ Mixer–ladle-ladle; ⊖ Torpedo car ladle, ladle with siphon. S = pig iron for steelmaking; Th = Thomas pig iron; F = pig iron for foundry. a) Ladle with siphon; b) furnace-runner and transportation ladle.

The soda-ash paving method is frequently used for desulfurization in the *transport ladle* because of its simplicity. The transport ladle is used to transport the hot metal from the blast furnace to the hot-metal mixer located in the steel shop. In this method, the desulfurizing flux is placed in the ladle prior to filling it with hot metal. Good mixing is achieved by formation of carbon dioxide and by the falling hot-metal stream. The slag is removed from the filled ladle. Figure 5.54 illustrates the relationship between the final degree of desulfurization and the amount of soda ash added. The final desulfurization degree increases with increasing soda-ash addition up to a value of 80%, which is obtained at 8 kg "soda-ash addition" per ton of hot metal. After that the desulfurization degree in most cases reaches a plateau level.

Efforts to improve the mass transfer of the sulfur by moving the vessel containing the hot metal involved trials with rotating drums (Kalling–Domnarvet process [67]) and *shaking* or *rotating ladles*. In the shaking ladle, the ladle axis rotates around a circular path at ca. 70 rpm. By reversing the direction of the movement, the mixing effect can be enhanced (Kobe Steel process [65]).

Figure 5.55 shows desulfurization processes with mechanical stirrers. The stirrer proposed by Östberg (see Figure 5.55A) has a *hollow* stirrer which discharges the *hot metal* through horizontal tubes by centrifugal forces and absorbs hot metal from the bottom of the vertical tube. The simple stirrer proposed by Kraemer in Rheinstahl Hüttenwerk (Figure 5.55B) is made of refractory. This stirrer mixes in *desulfurizing fluxes* into the hot metal. The stirrer developed by Nippon Steel (Figure 5.55C) is an impeller which produces eddy flow of the *hot metal*. Results of plant experiments for this stirrer are shown in Figure 5.56. According to this figure the process is highly effective for desulfurization. The stirrer method is widely used in North America, Europe, and Japan for the production of low-sulfur steel or ultra-low sulfur steel.

The *injection method* of hot metal desulfurization is widely accepted for the desulfurization in a ladle or a torpedo-car. In this method the flux powder of desulfurization is injected with a gas stream. As flux powder CaC_2, $Ca(CN)_2$, CaO and soda ash are widely used. Currently magnesium is also used. The injection lance is better for dipping into the hot metal bath. The dipping depth should be 1/2 to 3/4 of the bath depth. NSC [76] and TSAG [77] developed the respective process for desulfurization by using the injection method.

In the *gas-bubbling* method, the desulfurizing flux is at first added to the surface of the hot metal and then mixing is started by the injection of gas into the hot metal. The injection is made through the lance dipped into the hot metal (top-blowing method) or through the porous plug at the bottom (bottom-blowing

method). Figure 5.57 represents schematically the bottom-blowing desulfurization ladle. Ultra-low sulfur steel containing 0.001–0.002% S can only be produced by this method if the second addition of calcium carbide is made after the slag of the first treatment is removed.

The *gas-lift mixing reactor* method (GMR method) was proposed by Kobe Steel. The basic principle of this method is to use the buoyancy force of the gas injected at the bottom of the riser as driving force for a circulatory motion of the hot metal as illustrated in Figure 5.58. This method removes sulfur in hot metal to < 0.002% by adding 5 kg of CaC_2 per tonne of hot metal.

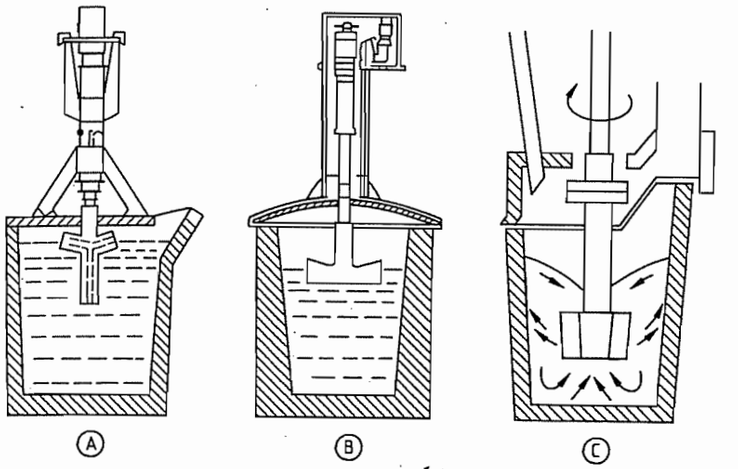

Figure 5.55: Stirrers for desulfurization of hot metal [75] (Courtesy of The Iron and Steel Institute of Japan): A) Demag-Östberg process; B) Rheinstahl process; C) KR process.

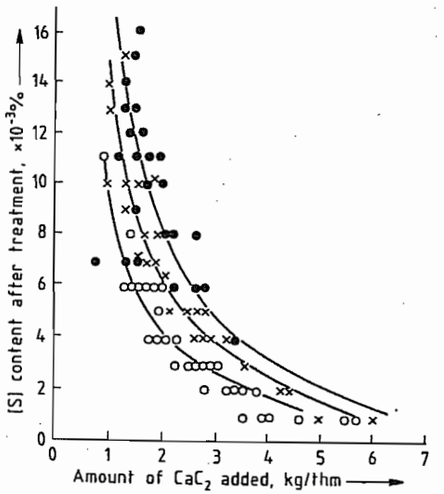

Figure 5.56: Relation between amount of CaC_2 added and [S] content after treatment [75] (Courtesy of The Iron and Steel Institute of Japan). [S] content before treatment (1350 °C): ○ 0.02%; × 0.03%; ● 0.04%.

If magnesium is used as a desulfurizing flux, magnesium–coke [80], a plunging bell [80–82] injection of a magnesium aluminum alloy, surface-coated magnesium, or a mixture of CaO and Mg with gas [83–85] are used to suppress the vaporization loss of magnesium.

Since some problems remain unsolved in magnesium desulfurization (such as violent scattering of hot metal and resulfurization which requires a too long treatment time) the operation techniques must be improved. The advantages of this method in comparison to other methods are the very small amounts of flux required, ca. 1 kg/t, and the easy disposal of the slag.

It is very difficult to compare the various desulfurization processes for the pretreatment of hot metal, because many factors such as facility cost, operation cost, amount and cost of desulfurizing flux, degree of desulfurization, workability, and iron loss must be considered.

Figure 5.59 shows the relationship between degree of desulfurization and operation cost. To reduce the cost of desulfurization, effective and inexpensive desulfurization fluxes and desulfurization processes requiring less flux must be developed.

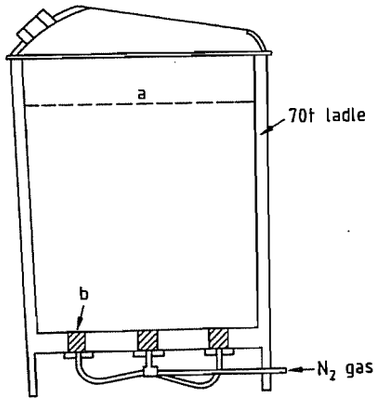

Figure 5.57: Desulfurization ladle with porous plugs [78] (Courtesy of The Iron and Steel Institute of Japan): a) Surface of hot metal; b) Porous plugs.

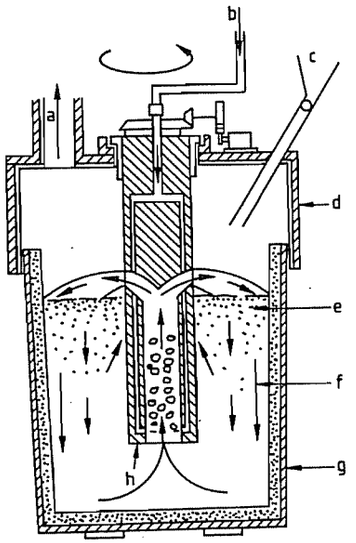

Figure 5.58: Schematic diagram of the gas lift mixing reactor for desulfurization [79] (Courtesy of The Iron and Steel Institute of Japan): a) Dust collecting duct; b) Compressed nitrogen; c) Inlet of flux; d) Cover for dust catch; e) Desulfurizing flux; f) Hot metal; g) Ladle; h) Main part of gas-lift mixing reactor.

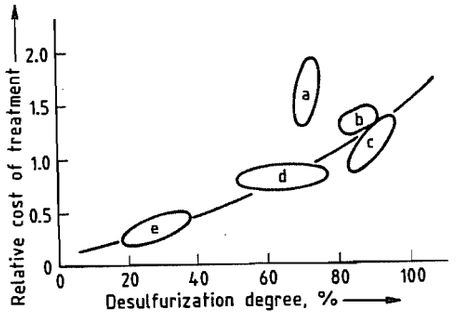

Figure 5.59: Relation between desulfurization degree and relative cost of treatment [76] (Courtesy of Dept. of Materials Science and Engineering, McMaster University, Hamilton, Canada). Sulfur content before treatment: 0.030%. a) Mag-coke process; b) Porous plug process; c) KR process; d) Top blowing process; e) Soda-ash pouring process.

5.6 Plant Layout

A blast furnace plant consists of numerous units beside the furnace itself (Figure 5.60). The most important units are the following:

5.6.1 Dust-Recovery System

The blast furnace gas may contain up to 170 kg of dust per ton of pig iron produced. This dust must be captured for two reasons:

- To recover its valuable metal content
- To prevent pollution of the environment.

Gas cleaning is conducted in two steps:

- Removal of large particles in dust catchers followed by cyclones.
- Removal of fine particles in spray towers, venturi scrubbers, or electrostatic precipitators.

5.6.1.1 Dust Catchers

The gas is allowed to pass through a large chamber to reduce its velocity and cause the dust to drop out by gravity. To enhance the separation, the direction of gas flow is reverse. A typical gravity chamber is shown in Figure 5.61. It is a 10–12-m diameter, brick-lined vessel.

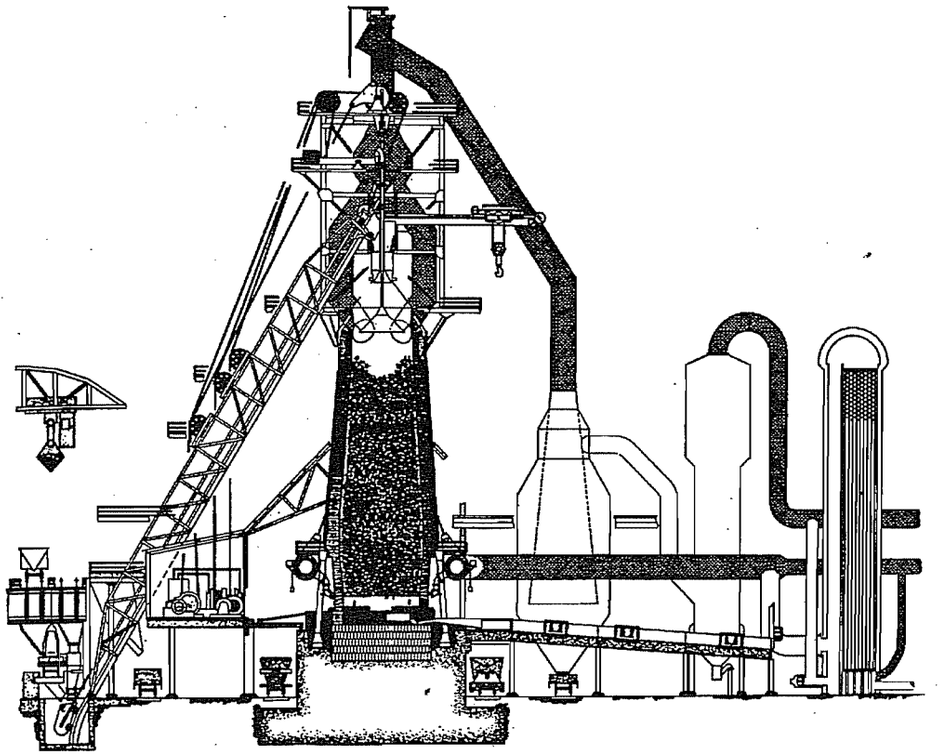

Figure 5.60: Blast furnace plant.

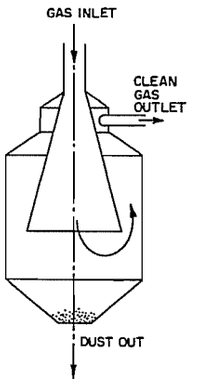

Figure 5.61: Dust catcher.

5.6.1.2 Cyclones

This equipment is more efficient than the previous type and occupies less space. The dust-laden gas enters a cylindrical or conical chamber tangentially. The centrifugal force causes the dust particles to travel outward to the wall of the chamber, where they collide and fall downward to a receiver at the bottom, while the gas escapes from an opening at the top (Figure 5.62).

5.6.1.3 Spray Towers

In these towers (Figure 5.63) the gas passes upwards countercurrent to a descending spray of water. To increase the contact between the two phases, the tower is packed with wooden grates, ceramic tiles, or metal spirals. The part of the tower above the water spray is for separating the water droplets from the exit gases. A typical unit consists of a contact zone where the dust laden gas and the water are brought together, followed by a separation zone where

the gas is separated from the wetted slurry. In the contact zone, the particles increase their weight and size and adhere together when they are moistened thus making their separation easy.

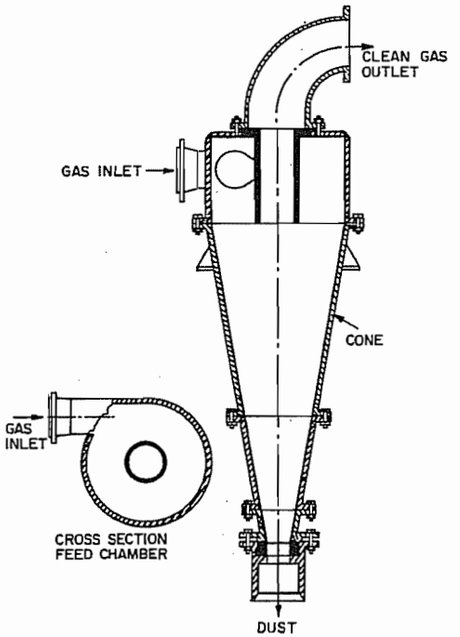

Figure 5.62: Dust-collecting cyclone.

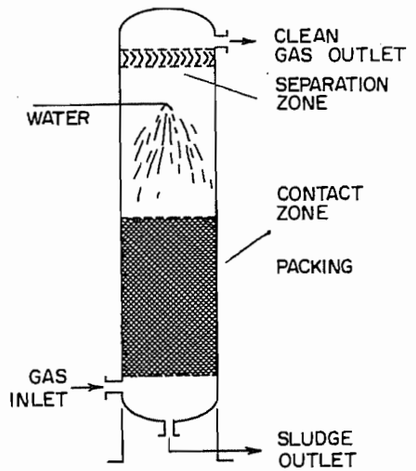

Figure 5.63: Spray towers for dust removal.

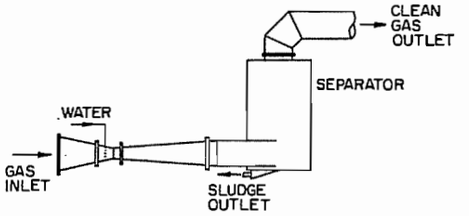

Figure 5.64: Venturi scrubber.

5.6.1.4 Venturi Scrubbers

In this system, water is introduced at the throat of a venturi perpendicular to gas flow and is atomized into tiny droplets; thus a large surface area is created. The venturi is followed by a separating section usually in the form of a centrifugal eliminator for the removal of the entrained droplets and collected dust particles (Figure 5.64).

5.6.1.5 Electrostatic Precipitators

Dust separation in this equipment is based on the fact that if the solid particles carried in a gas are given an electrical charge, they will be attracted to a collection device carrying the opposite charge. The type most commonly employed consists of a series of ionizing electrodes and an oppositely charged series of collecting electrodes housed in a chamber through which the exhaust gas is routed (Figure 5.65). The ionizing electrodes are rods while the collecting electrodes are grounded plates or shells that have a large surface area compared to the ionizing electrodes. A high voltage of 50 000 to 80 000 volts is applied across the two sets of electrodes to maintain the highest electrostatic field without sparking.

Under the influence of the electrostatic field, the gas molecules get electrically charged and move away from these electrodes toward the collecting electrodes. As the suspended dust particles collide with these molecules, the electric charge is transferred to the dust.

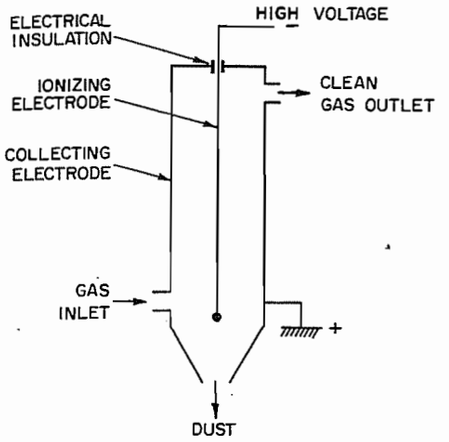

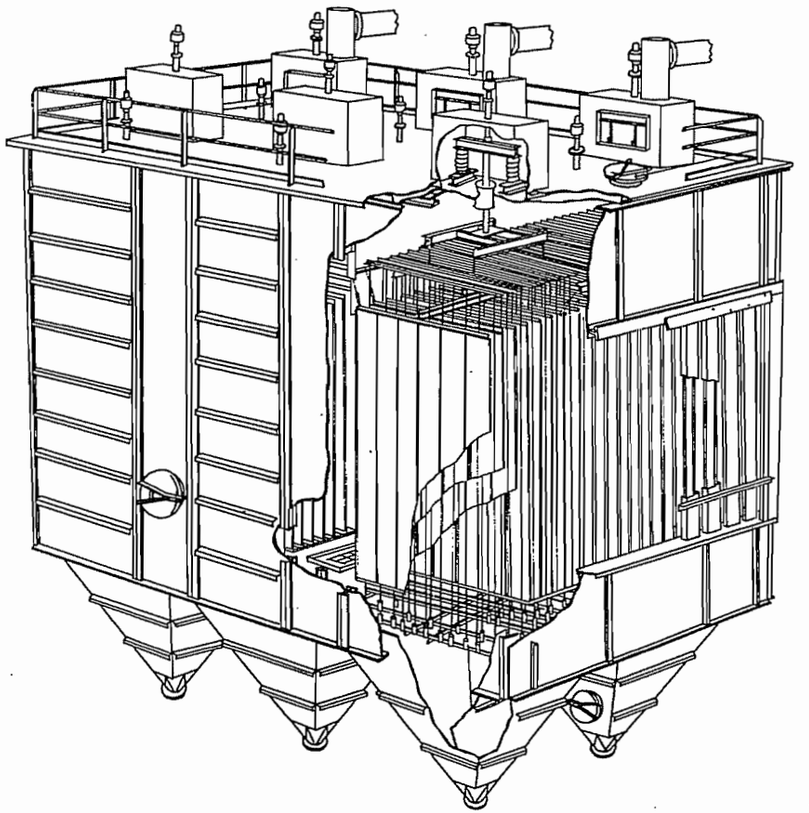

Figure 5.65: Electrostatic precipitator. A) Principle; B) Industrial installation.

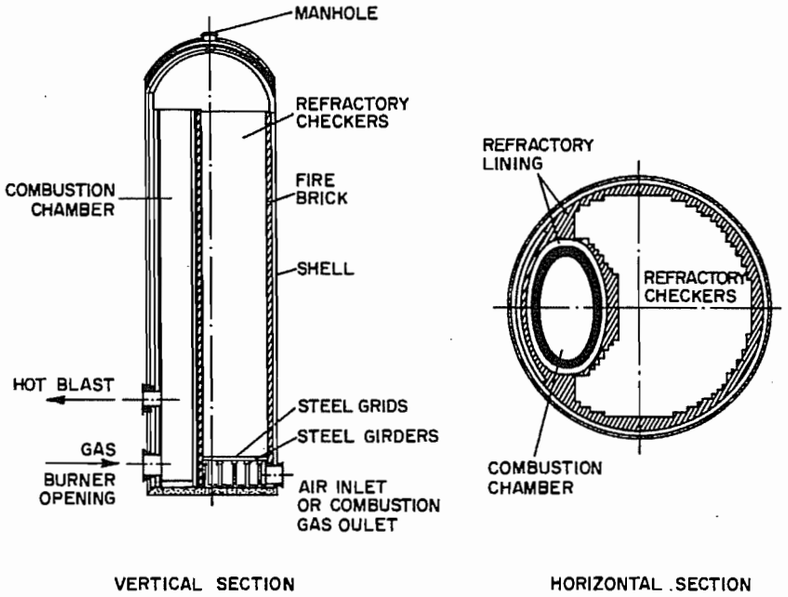

Figure 5.66: Stoves for heat recovery from blast furnace gas.

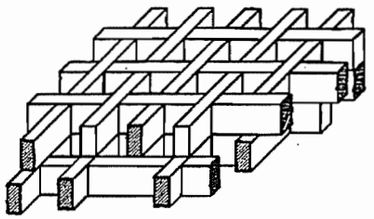

Figure 5.67: Arrangement of refractory brick in a regenerator.

The particles are then attracted to the collecting electrodes, where they lose their charge and fall into hoppers below, or become dislodged by automatic intermittent tapping. Electrostatic precipitations are expensive but efficient equipment.

5.6.2 Heat Economy System

Gases leaving a blast furnace are not at high temperature but have a high calorific value due to their CO content. The gases after being purified of their dust content are then burned in stoves and the heat of combustion is used to heat fire brick chambers. Once the chambers are hot, the blast furnace gas is switched over to another stove and air is introduced in the hot chamber to take away the heat before entering the furnace. The cycle is then repeated. A typical unit is 7–9 m diameter and about 36 m high with a dome-shaped top and consists of two parts (Figure 5.66):

- The combustion chamber where the blast furnace gas is burned.
- The refractory chamber where the hot combustion gases pass before their exit (Figure 5.67).

The heating surface in the chambers is usually 22 000–25 000 m^2. There are usually 3 units per furnace, and they are provided with a common stack. The air blast for the furnace passes through the heated stove countercurrent to the gas. One stove is "on blast" for 1 to 2 hours at a time while the other two stoves are "on gas" for 2 to 4 hours. This is achieved by means of automatic valves. With the advancement of gas cleaning, the use of refractory bricks with small openings became feasible, thus resulting in a high efficiency.

5.7 Refractory Materials

Refractory materials must meet the following requirements:

- Mechanical stability under load at high temperatures (up to and beyond 1800 °C, depending on quality),
- Resistance to slags and dusts at high temperature, and
- Specific thermal properties, such as thermal conductivity, specific heat, and resistance to sudden temperature changes, depending on application.

These properties can be tested in the laboratory under conditions similar to the service conditions. Some methods are internationally standardized (PRE, i.e., Fédération européenne de produits réfractaires and ISO recommended test methods) [86]. Refractories are classified by chemical-mineralogical criteria and by process requirements. The basic distinction is between shaped products (bricks) and unshaped ones (mixtures, mortars, castables). Another basis for classification is the type of binding. Here a distinction must be made between fired products (firing temperatures 800–1800 °C) and unfired, chemically bonded refractories (phosphate binders, resin binders, refractory cements, water glass, magnesium sulfate).

In the iron and steel industry in Germany, the classification of the "Steel and Iron Material Data Sheets" (Stahl–Eisen-Werkstoffblätter) is used.

Table 5.27 shows the consumption of refractory materials (kg per tonne of crude steel) for Germany and Japan in 1970, 1980, 1990, and 1993. The steep decline is mainly accounted for by new steelmaking technologies (oxygen-injection process replacing the Siemens–Martin furnace, introduction of continuous casting) and by improvements in refractory qualities.

This progression is also clear from Table 5.28, which lists the outputs of the main qualities of refractory bricks in Japan. The 1970 and 1993 figures show the decrease in fireclay brick and silicate brick production and the increase in high-grade refractories (magnesia–carbon, high-alumina castable).

The world steel industry is the principal consumer of refractories (ca. 60%).

Pig-iron production includes (1) blast furnaces with hot blast stoves, and (2) torpedo ladles, with a molding capacity of 150 600 t of molten pig iron, as transport containers from the blast furnace to the steelworks. This sector employs mainly the following refractory qualities: carbon and graphite bricks, silicon carbide bricks, materials containing more than 50% alumina, fireclay, and silica.

In *steelworks* the most important qualities are magnesia–carbon bricks, bricks and mixtures based on magnesia and dolomite, zircon material, and high-alumina castables.

Table 5.27: Consumption of refractories in Germany and Japan (kg per tonne of crude steel).

	Germany				Japan			
	1970	1980	1990	1993	1970	1980	1990	1993
Bricks	19	12.9	8.8	7.1	24	9.5	5.5	4.9
Mixtures	16	10.5	5.9	6.3	5	5.8	6.0	6.4
Total	35	23.4	14.7	13.4	29	15.3	11.5	11.3

Table 5.28: Production of refractories in Japan in 1000 t.

Bricks	1970	1980	1990	1993
Fireclay	1800	829	325	200
50% Al_2O_3	191	173	155	125
Silica	260	66	7	5
Chrome–magnesia	284	278	126	99
Magnesia–carbon		52	123	107
Dolomite–magnesia	251	104	13	8
Zircon	61	91	52	31
Silicon carbide		53	27	18
Insulants	88	55	27	15
Others	75	44	35	37
Unshaped Products (Mixtures)	570	907	836	845

Blast Furnaces. Molten pig iron and slag are present in the lower part of the blast furnace (bottom and hearth). Repairs cannot be made to this part of the furnace during operation. Chemical and mechanical attacks on the refractory material occur here. Graphite and carbon bricks are the most important structural refractories for this portion of the blast furnace. Carbon bricks have a higher cold-crushing strength than graphite bricks and those containing some graphite (part-graphite and semi-graphite bricks). Carbon bricks have a

lower porosity than graphite bricks. Microporous carbon and part-graphite bricks with additions of alumina and silicon have higher alkali and pig-iron resistance [91, 98].

The current state of the art is the "ceramic cup", which comprises sintered mullite bricks placed in front of the carbon on the bottom, and large-size prefabricated panels of corundum concrete in front of the carbon on the wall. This type of lining protects the carbon bricks and prolongs their service life greatly. In the other zones of the blast furnace (bosh, belly, stack), a variety of brick qualities are used. These include bricks containing over 50% alumina, corundum bricks, and silicon carbide bricks with various binders. Hard fireclay bricks are usually employed in the stack. Furnaces often differ greatly in their refractory linings. The properties of some refractory structural materials are given in Table 5.29.

Runner and Taphole Mixtures. Tar-free unshaped products containing > 50% alumina, silicon carbide, and carbon are used in cast, vibrated or rammed form. Numerous and very different mixtures are in use, including spinel ($MgAl_2O_4$)-containing material in the metal level and mixtures up to 80% SiC in the slag level.

Hot Blast Stoves. The standard lining consists of silica bricks in the dome (temperatures up to 1500 °C), bricks with > 50% alumina in the combustion chamber, and silica and fireclay bricks (depending on thermal stress) in the checkerwork shaft.

Torpedo Ladles [90, 99]. In the lining design, the following factors relating to stresses on the refractory must be considered: temperature of pig iron (1450–1520 °C), distance transported, slag composition, and metallurgical reactions such as desiliconization, dephosphorization and desulfurization in the ladle.

Lining bricks mostly contain > 50% Al_2O_3 (andalusite and bauxite bricks). If the slag has a $CaO:SiO_2$ ratio > 1, unfired pitch-bonded dolomite bricks can also be used with success. The increase in metallurgical reactions in torpedo ladles has led to new types of lining, which have been adopted in an attempt to extend the service life (100 000–400 000 t pig iron transported). In zone lining, resin-bonded corundum–carbon–silicon carbide bricks are used in the slag zone (especially in Japan), with resin-bonded andalusite carbon bricks in the bottom. Linings differ from plant to plant, depending on service conditions.

5.8 Iron from Pyrite Cinder

[74]

Pyrite is mainly used for the manufacture of sulfuric acid. It is oxidized in fluidized bed reactors whereby the following reaction takes place:

$$2FeS_2 + {}^{11}/_{2}O_2 \rightarrow 4SO_2 + Fe_2O_3$$

While SO_2 can be readily converted to SO_3 and then to H_2SO_4, iron oxide (called cinder) cannot be used directly for manufacturing iron because of the presence of impurity metals. Table 5.30 shows analysis of cinder. As a result, methods have been developed to purify the cinder and at the same time to recover the nonferrous metals present. The recovery of nonferrous metals from the cinder is achieved by two routes: the chloride and the sulfate processes.

5.8.1 The Chloride Route

In this route, the nonferrous metals are transformed into water-soluble chlorides by heating with a solid chloride. At low temperature the chlorides remain in the residue while at high temperature they are volatilized.

Table 5.29: Properties of blast-furnace lining bricks.

	Carbon	Microporous carbon (10% Al_2O_3, 15% Si)	Graphite	Mullite (70% Al_2O_3)	Corundum concrete (90% Al_2O_3)
Bulk density, g/cm³	1.53–1.57	1.63–1.73	1.55–1.60	2.45	3.30
Open porosity, %	14–18	14–18	25–28	15–18	9–12
Micro porosity > 1 µm, %	8–11	≤ 2			
Ash, %	< 7	35–40	< 1		
Cold compression strength, N/mm²	30–40	60–90	15–25	70	60
Thermal conductivity, $Wm^{-1}K^{-1}$,					
at 20 °C	3–8	5–7	130	2	5
at 500 °C	5–12	8–10	95	1.8	4
at 1000 °C	8–14	11–13	65	1.7	3

Table 5.30: Typical analysis of pyrite cinder.

Main components, %		Trace metals, ppm	
Fe	54–58	Co	300–1500
Gangue	6–10	Ag	25–50
Cu	0.8–1.5	Au	0.5–1.5
Zn	2.0–3.5	Cd	40–100
S	2.5–4.0	Ni	15–1500
Pb	0.3–0.7	Mn	300–3000

Table 5.31: Data on the treatment of pyrite cinder by Kowa–Seiko process.

	Dry pellets, %	Heated pellets, %	Volatilization, %
Cu	0.47	0.04	91
Pb	0.18	0.01	92
Zn	0.59	0.01	97
As	0.05	0.05	—
S	0.61	0.03	96.5
Fe	59.2	61.5	—
Au (g/t)	0.94	0.05	95
Ag (g/t)	33.6	7.00	80

DK Process. This process has been used in Germany for nearly a century at the Duisburger Kupferhütte in Duisburg (operations ceased in 1980s). The pyrite cinder is mixed with NaCl and heated continuously in a multiple hearth furnace at 800 °C to transform nonferrous metals into water-soluble chlorides. Each batch requires about 2 days for leaching in vats. The concentrated leach solution obtained in the first 15 to 20 hours is sent for copper and other metals recovery, while that subsequently obtained, being poor in metal content, is recycled. The residue, called purple ore, now a high-grade iron ore (61–63% Fe), is sintered and delivered to the blast furnace.

Kowa–Seiko Process. This is a Japanese process in which the cinder is mixed with calcium chloride, pelletized, then heated in a rotary kiln at 1100 °C to volatilize nonferrous metal chlorides (Table 5.31). These are scrubbed in water from the exit gases and the solution treated for metal recovery.

5.8.2 The Sulfate Route

This route is mainly used for the recovery of cobalt from the cinder. It is based on a careful temperature control during the oxidation of pyrite. If the temperature is kept at 550 °C, cobalt in the pyrite will be converted to sulfate and therefore can be leached directly from the cinder with water. At least two plants are using this process:

- At the Bethlehem Steel plant, Sparrows Point, Maryland, the hot pyrite cinder is quenched with water to give a slurry containing 6–8% solids. When the solids are filtered off, the solution contains 20–25 g/L Co; it is processed further for metal recovery. In the cinder the Fe:Co ratio is 50:1; in solution it is 1:1. This plant supplies the only domestic source of cobalt in USA.
- In Finland at the Outokumpu Company plant, the sulfated pyrite cinder contains 0.8–0.9% Co and other nonferrous metals. It is leached with water to get a solution at pH 1.5 analyzing 20 g/L Co, 6–8 Ni, 7–8 Cu, 10–12 Zn, and trace amounts of iron, which is treated for metal recovery.

5.9 Iron from Ilmenite [11]

Ilmenite, $FeTiO_3$, is the major titanium mineral. It represents 90% of the world titanium ore reserves while rutile, TiO_2, accounts for the remaining 10%. Ilmenite occurs either

as massive deposits, e.g., in the Province of Quebec, or as sand at the mouth of rivers, e.g., in India. The Quebec deposits are one of the largest in the world. However, when compared with other ilmenite ores, the Quebec ore is a low-grade ore (Table 5.32). It is beneficiated by physical methods to a concentrate containing 36.8% TiO_2, 41.8% Fe (total), and a small amount of sulfur.

Table 5.32: Analysis of ilmenite ores.

	%
TiO_2	43–59
FeO	9–38
Fe_2O_3	5–25
SiO_2	0.4–4
Al_2O_3	1.3–3.3
MgO + CaO	0.1–1.4
V	0.4–2

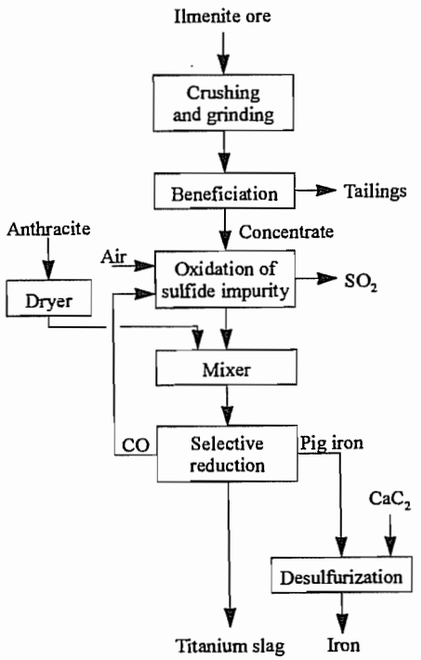

Figure 5.68: Selective reduction of ilmenite.

The concentrate is mixed with a certain amount of carbon which is just enough to reduce the iron oxide component of the ore, then charged in an electric furnace at 1650 °C where iron oxide is reduced to metal while titanium is separated as a slag (Figure 5.68). This method is used by the QIT Fer et Titane incorporation at its plant in Sorel near Montréal and at Richards Bay in South Africa. It is also used in Ukraine at Zaporozhye and in Japan.

A small amount of TiO_2 is reduced to Ti_2O_3 and will be found in the slag. The slag is mainly titanates of iron, magnesium, and calcium together with some calcium and aluminum silicates; its titanium dioxide content varies between 72 and 98%. The analysis of iron produced at Sorel is given in Table 5.33. The slag is high in titanium and low in iron and is therefore preferable to ilmenite in manufacturing TiO_2 pigment or titanium metal.

5.10 Direct Reduction Processes

The name "direct reduction" is misleading, because these reduction processes do not constitute a "more direct" route to steel than does the blast furnace. Nor does the term have anything to do with direct reduction in the blast furnace. Despite all these objections, however, the term has become accepted in international usage.

Table 5.34 lists the plants for direct reduction of iron ore that were in operation or under construction in 1995, together with their locations and the processes employed.

Table 5.33: Analysis of iron produced from Quebec ilmenite at Sorel (also known as Sorelmetal).

	%
C	1.8–2.5
S	0.11
P_2O_5	0.025
MnO	trace
V_2O_5	0
Cr	0.05
Si	0.08
TiO_2	trace

Table 5.34: World direct reduction plants (plant list is correct as of December 31, 1995) [102] This list does not include plants that are inoperable or have been dismantled..

Process	Plant	Location	Capacity, Mt/year	Modules	Start-up	Status[a]
Midrex	Georgetown Steel	Georgetown, SC, USA	0.40	1	1971	O
	Hamburger Stahlwerke	Hamburg, Germany	0.40	1		O
	Sidbec Dosco 1	Contrecœur, QC, Canada	0.40	1	1973	O
	SIDERCA	Campana, Argentina	0.40	1	1976	O
	Sidbec Dosco 2	Contrecœur, QC, Canada	0.60	1	1977	O
	SIDOR I	Matanzas, Venezuela	0.35	1		O
	ACINDAR	Villa Constitución, Argentina	0.60	1	1978	O
	Qatar Steel Co.	Umm Said, Qatar	0.40	1		O
	British Steel	Hunterston, Scotland	0.80	2	1979	I
	SIDOR II	Matanzas, Venezuela	1.27	3		O
	CIL	Point Lisas, Trinidad & Tobago	0.84	2	1980–1982	O
	Delta Steel	Warri, Nigeria	1.02	2	1982	O/I
	Hadeed I	Al-Jubail, Saudi Arabia	0.80	2	1982–1983	O
	OEMK	Stary Oksol, Russia	1.67	4	1983–1988	O
	Amsteel Mills	Labuan Island, Malaysia	0.65	1	1984	O
	ASCO	Ahwaz, Iran	1.20	3	1985–1992	O
	ANSDK I	El Dikheila, Egypt	0.72	1	1986	O
	LISCO	Misurata, Libya	1.10	2	1989–1990	O
	Essar Steel I & II	Hazira (India)	0.88	2	1990	O
	MINORCA (OPCO)	Puerto Ordaz, Venezuela	0.83	1		O
	VENPRECAR	Matanzas, Venezuela	0.66	1		O
	Essar Steel III	Hazira, India	0.44	1	1992	O
	NISCO	Mobarakeh, Iran	3.20	5	1992–1994	O
	Hadeed II	Al-Jubail, Saudi Arabia	0.65	1	1992	O
	HDIL	Raigad, India	1.00	1	1994	O
	ANSDK II	El Dikheila, Egypt	0.80	1	1997	C
	Hanbo Steel	Asan Bay, South Korea	0.80	1		C
	IMEXSA	Lázaro Cárdenas, Mexico	1.20	1		C
	Total		24.08	45		
HyL-III	Hylsa 2M5	Monterrey, Mexico	0.25	1	1979	O
	Hylsa 3M5	Monterrey, Mexico	0.50	1	1983	O
	IMEXSA	Lázaro Cárdenas, Mexico	2.00	4	1988–1990	O
	Grasim	Raigad, India	0.75	1	1993	O
	PT Krakatau Steel	Kota Baja, Indonesia	1.35	2	1993–1994	O
	PSSB	Kemaman, Malaysia	1.20	2	1993	O
	Usiba	Salvador, Bahia, Brazil	0.31	1	1994	O
	Hylsa 2P5	Puebla, Mexico	0.61	1	1995	O
	Total		6.97	13		
HyL-I	Tamsa	Veracruz, Mexico	0.28	1	1967	I
	SIDOR I	Matanzas, Venezuela	0.36	1	1976	O
	Hylsa 2P	Puebla, Mexico	0.63	1	1977	O
	PT Krakatau Steel	Kota Baja, Indonesia	1.68	3	1978–1982	O/I
	SIDOR II	Matanzas, Venezuela	1.70	3	1980–1981	O
	ASCO	Ahwaz, Iran	1.03	3	1993–1995	O
	Total		5.68	12		
SL/RN	Piratini	Charquedas, Brazil	0.06	1	1973	I
	SIIL	Paloncha, India	0.03	1	1980	O
	Siderperu	Chimbote, Peru	0.09	3		O
	ISCOR	Vanderbijlpark, South Africa	0.72	4	1984	O
	BSIL I	Chandil, India	0.15	1	1989	O
	Prakash Industries I	Champa, India	0.15	1	1993	O
	Nova Iron & Steel	Bilaspur, India	0.15	1	1994	O
	Prakash Industries II	Champa, India	0.15	1	1996	C
	BSIL II	Chandil, India	0.15	1	1998	C
	Total		1.65	14		

Process	Plant	Location	Capacity, Mt/year	Modules	Start-up	Status[a]
Jindal	Jindal Strips	Raigarh, India	0.40	4	1993–1995	O
	Monnet Ispat I	Raipur, India	0.10	1	1993	O
	Jindal Strips	Raigarh, India	0.20	2	1996–1997	C
	Monnet Ispat II	Raipur, India	0.10	1	1997	C
	Total		0.80	8		
DRC	Scaw Metals I	Germiston, South Africa	0.18	2	1983–1989	O
	Tianjin Iron & Steel	Tianjin, China	0.30	2	1996	C
	Scaw Metals II	Germiston, South Africa	0.15	1		C
	Total		0.63	5		
Codir	Dunswart	Benoni, South Africa	0.15	1	1973	O
	Sunflag	Bhandara, India	0.15	1	1989	O
	Goldstar	Mallividu, India	0.22	2	1992	O
	Total		0.52	4		
Fior	Fior de Venezuela	Matanzas, Venezuela	0.40	1	1976	O
OSIL	OSIL	Keonjhar, India	0.10	1	1983	O
	Lloyd's Steel	Ghugus, India	0.30	2	1996–1997	C
	Total		0.40	3		
Purofer	ASCO	Ahwaz, Iran	0.33	1	1977	O
SIIL	SIIL	Paloncha, India	0.06	2	1980–1985	O
	Bellary Steels	Bellary, India	0.06	2	1992–1993	O
	HEG	Borai, India	0.06	2	1992	O
	Kumar Met.	Nalgonda, India	0.03	1	1993	O
	Raipur Alloys	Raipur, India	0.03	1		O
	Tamilnadu Sponge	Salem, India	0.03	1		O
	Aceros Arequipa	Pisco, Peru	0.06	2	1996	C
	Total		0.33	11		
Iron Carbide	Nucor Steel	Point Lisas, Trinidad & Tobago	0.30	1	1994	O
Tisco	Ipitata I	Joda, India	0.12	1	1986	O
	Ipitata II	Joda, India	0.12	1	1998	C
	Total		0.24	2		
Dav	Davsteel	Cullinan, South Africa	0.04	1	1985	O
Kinglor–Metor	No. 3 Mining Enterprise	Maymo, Burma	0.04	2	1981–1984	O

[a] Status codes: O = operating; I = idle; C = under construction.

Table 5.36 contains technical data for the direct reduction processes described in this chapter and certain other processes. The stated capacities should be regarded as approximate, as some of the processes have been further developed. The annual plant outputs often vary from the original design capacity. In particular, the demand of the client (i.e., of the electric steel mill), a low scrap price, or a shortage of spare parts may lower the annual output.

In most direct reduction processes, up to 92–95% of the iron oxide is reduced to metallic iron. The degree of metallization $Fe_{metallic}/Fe_{total}$ in % is an important variable for characterizing the direct-reduced iron (DRI) produced by the process in question.

5.10.1 Fuels and Reducing Agents

[103, 104]

A considerable amount of heat input is required in the production of iron, because essentially all the processes involved are pyrometallurgic. Part of the heat is used to heat up the raw materials to be processed and part of it is required for endothermic chemical reactions. The majority of this energy is obtained by combustion of fossil fuels. Approximately one-quarter of the annual output of steel is derived from scrap in electric arc furnaces which pose a correspondingly high demand for thermoelectric energy.

Fuels. Fossil fuel, especially in the form of coke constitutes the primary reducing agent in blast furnaces; this coke cannot be replaced arbitrarily by substitutes such as coal. Coke functions both as a support material and as a matrix through which gas circulates in the stock column. A portion of the fuel can be introduced into the tuyère along with the air supply. Figure 5.69 provides detailed insight into the demand for the fossil fuels in iron manufacture, indicating its percentage distribution by various fuel types and consumers.

The illustration is based on an integrated production facility in which all the coke and a portion of the required electrical energy is produced on site, the extent of the latter being a function of the availability of excess off-gas [105].

All energy data in Figure 5.69 relate to total energy input, including that from external sources of electricity. Approximately 88% of the imported energy is derived ultimately from coal, 83% of which is converted into coke. Gas is derived as a by-product: 15% from the coke ovens, 20% from the blast furnace, and 4% from the steel mill. This gas is in turn processed in the coke oven plant and distributed to power plants and other appropriate units within the facility for subsequent processing.

A number of requirements must be met by coke that is intended for use in iron manufacture:

- The ash, moisture, and sulfur content should be as low as possible, and should show little variation.
- Coke strength should be consistently high with the lowest possible variation.
- The coke should be as unreactive as possible, in particular toward carbon dioxide and steam.
- Particle size should be kept in the range of 40–80 mm, but at least in the range of 20–80 mm.

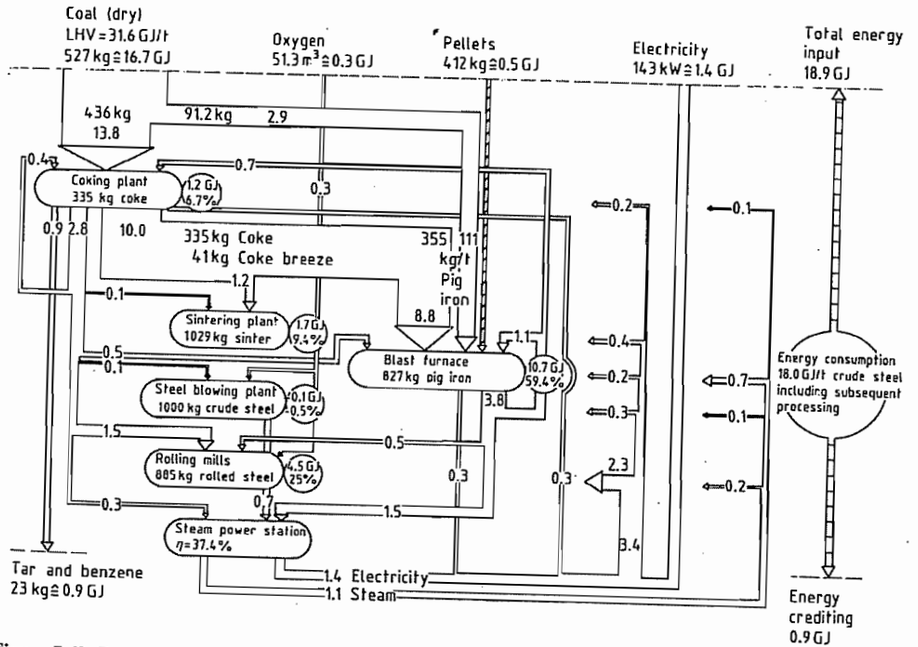

Figure 5.69: Energy demand distribution in an integrated steel mill based on 1 t of crude steel.

Table 5.35: Important characteristics of coke.

	Blast furnace coke
Drum index[a] (%)	> 90
Dust M 10[a] (%)	< 6
Moisture (%)[b]	< 5
Ash (%)[b]	< 10
Sulfur (%)[c]	< 1
Volatiles (%)[c]	

[a] Based on DIN 51 717, equivalent to ISOIR 556.
[b] % of crude weight.
[c] Of dry weight.

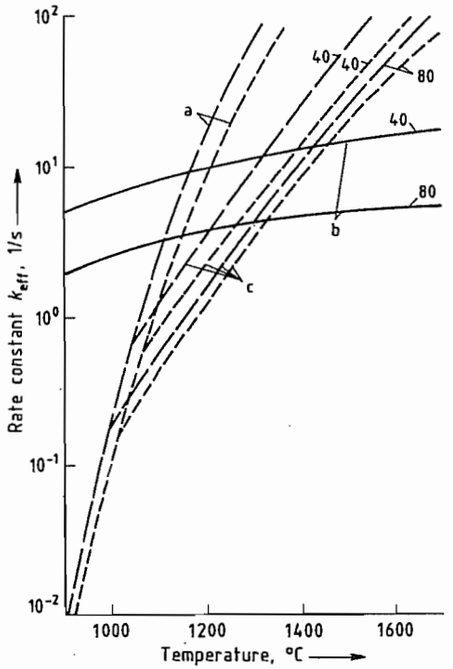

Figure 5.70: Limiting curves for the effective rate constant in the Boudouard reaction shown for two types of coke; — — coke type a; – – – coke type b (the curve parameter is the grain diameter in mm): a) Chemical surface reaction; b) Boundary layer diffusion; c) Pore diffusion.

Coke *characteristics* are the subject of numerous norms, including ISOIR 556, DIN 51 717–51 719, DIN 51729, and DIN 51730. Typical values for coke intended for iron manufacture (reflecting these norms) are presented in Table 5.35.

Coke *reactivity* is determined on the basis of the norm ST/ECE/Cool/12. Specifications supplied with respect to ash and sulfur content are applicable not only to coke but also to injection coal.

Depending on coke temperature and particle size, the principal determinant in the rate of the Boudouard reaction

$$C + CO_2 \rightleftharpoons 2CO \qquad (29)$$

is the varying resistance to reactivity In the case of blast-furnace coke with a particle size between 40 and 80 mm, and at low temperature (< 1050 °C), the limiting factor is the resistance of the interfacial reaction. For particles < 8 mm in diameter the resistance of the interfacial reaction is rate-limiting up to ca 1200 °C. Between 1050 and ca. 1350 °C the resistance of pore diffusion becomes the rate-determining factor in the Boudouard reaction. Above 1350°C the rate of reaction is governed by the diffusion of carbon dioxide through the gaseous layers adhering to the coke particles. The corresponding relationships are illustrated in detail in Figure 5.70.

Carbon conversion r_e in $mol\,m^{-3}s^{-1}$ may be computed on the basis of the rate constant k_{eff} derived from Figure 5.70 [103]

$$r_e = \frac{dn_c}{dt} = k_{eff}(n^0_{CO_2} - n^{eq}_{CO_2}) \qquad (30)$$

where $n^0_{CO_2}$ is the CO_2 concentration in the gas phase (mol/cm^3) and $n^0_{CO_2}$ the CO_2 concentration in equilibrium with C and CO (Boudouard reaction).

Furthermore

$$k_{eff} = k_m \cdot m_C \cdot \eta \qquad (31)$$

where m_C is the mass of carbon (g) per cubic meter of charge and η the pore utilization factor according to Thiele. Within the temperature range in which the interfacial reaction is rate determining

$$k_m = H_C \cdot e^{-360/RT}\ g^{-1}s^{-1} \qquad (32)$$

where H_C is the reactivity factor. Moreover, because $n = 1$

$$k_{eff} = m_C \cdot H_C \cdot e^{-360/RT}\ s^{-1} \qquad (33)$$

The activation energy of 360 kJ/mol is uniformly applicable with respect to any fuel [86]. Depending on reactivity and charge size,

the product $m_C \times H_C$ may range from $0.4 \times 10^{13}\ s^{-1}$ to $0.4 \times 10^{15}\ s^{-1}$.

Gaseous and liquid fuels used in iron manufacture are described elsewhere.

Reducing Agents. Assuming that iron oxide is present in the solid state, industrial-scale reduction of iron ore with carbon monoxide or hydrogen takes place according to

$$FeO_n + n(CO, H_2) \rightarrow Fe + n(CO_2, H_2O) \qquad (34)$$

If iron oxide is present as a liquid, a second reaction is also possible:

$$FeO_n + nC \rightarrow Fe + nCO \qquad (35)$$

Carbon monoxide is produced in the blast furnace from the reaction of oxygen in the blast air with hot coke and other reducing agents such as injected coal or oil

$$C + {}^1/_2O_2 \rightarrow CO \qquad (36)$$

Carbon monoxide is also the product of the Boudouard reaction

$$C + CO_2 \rightleftharpoons 2CO \qquad (29)$$

Carbon dioxide required by Equation (29) is formed during the reduction of iron oxide according to Equation (34). In some cases, coal is utilized as the reducing agent, which means that the gases actually responsible for reduction arise both from coal pyrolysis and from coal gasification inside the reduction reactor.

Coal pyrolysis may lead to varying quantities of hydrogen and hydrocarbons, which in turn serve partly as reducing agent and partly as fuel. The majority of the reducing gas in such a case originates from the solid carbon contained in the coal, where ore reduction and the Boudouard reaction are linked through Equations (29) and (34).

Gaseous reducing agents other than those formed in the reduction reactor itself are derived from natural gas, oil, or coal. Stoichiometrically, the large number of processes that are actually suitable for gas production, is limited significantly because a low content of steam and carbon dioxide as well as a specific hydrogen:carbon monoxide ratio is required in the reducing gas.

An appropriate gas for reduction above the decomposition temperature of carbon monoxide is that produced by steam reforming, with a composition of 73% hydrogen, 13% carbon monoxide, 1% water, 8% carbon dioxide, and 5% methane:

$$CH_4 + H_2O \rightarrow CO + 3H_2$$

In the *Midrex process* a 1.5:1 ratio of hydrogen and carbon monoxide is required. This ratio is achieved by reaction of natural with blast furnace top gas which results in a better utilization of input energy (composition after condensation of steam: 20% CO_2 with the balance being CO and H_2O at equal ratios):

$$CH_4 + CO_2 \rightarrow 2CO + 2H_2$$

Reduction gas should contain as little steam and carbon dioxide as possible. Even relatively small amounts of these substances drastically limit the utility of the gas, because according to Equation (34) the reduction of iron oxide itself produces carbon dioxide and water. Their presence in the reduction gas would therefore shift the equilibrium to the side of iron oxide. At the temperatures normally employed for converting iron oxide to iron, the ratio $CO:CO_2$ or $H_2:H_2O$ must not fall significantly below 2.3. In addition, reduction gas should contain as little undecomposed hydrocarbons as possible.

The use of fossil fuels in iron manufacture is currently the subject of careful reevaluation, and new reduction techniques are in the development stage. It is quite likely that coal will come to play an increasingly important role as a source of reduction gas. This can be accomplished by partially combusting coal with oxygen in an iron bath. The resulting hot gas is then used to reduce iron oxide in a separate vessel (see the equations above). Then the reduced iron is itself transferred to the iron bath where it is melted. Gas generation on the basis of nuclear energy is expected to remain economic for many years, although some effort is currently being directed toward the use of a plasma arc for converting carbon sources into reduction gas.

5.10.2 Shaft Furnace Processes for Direct Reduction

Wiberg–Söderfors Process. The oldest shaft furnace process for direct reduction of iron ore, the Swedish Wiberg process, is based on a patent issued in 1918. Up to the end of the 1950s, it was technologically improved and adapted to changed conditions on the ore and fuel markets. Nowadays, the Wiberg process is only of historical significance.

The development of the process was promoted above all by the growing shortage of very low-sulfur charcoal pig iron, the raw material for swedish high-quality steel. In addition, it was intended that coke would only be used for the reduction process, the process heat being supplied by cheap electricity available because of the geographical location.

In the Wiberg process (Figure 5.71) the iron ore is preheated in the top section of the furnace (a) to the reduction temperature of ca. 950 °C by hot gases generated by combustion of part of the so-called excess gas. In the zone immediately below, the ore is reduced to wustite with ca. one third of the reducing gas volume. The reduction to metallic iron takes place in the bottom section of the furnace at ca. 950 °C with ca. 1300 m³ (STP) gas/t DRI.

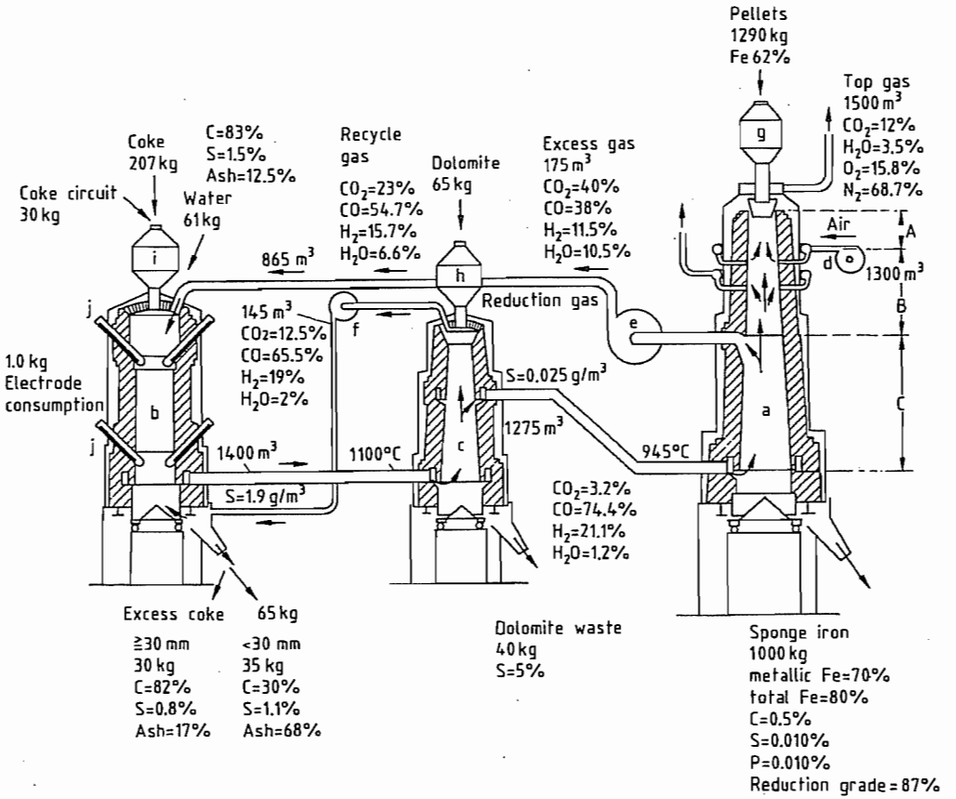

Figure 5.71: Flow Sheet and material balance (based on 1 t sponge iron) of the Wiberg process. All volumetric values of the gases refer to standard conditions [101]. a) Reduction shaft; b) Carburetor; c) Desulfurization shaft; d, e, f) Fans; g, h, i) Charging bins for pellets, dolomite, and coke; j) Electrodes; A) Preheating zone; B) Pre-reduction zone; C) Main reduction zone.

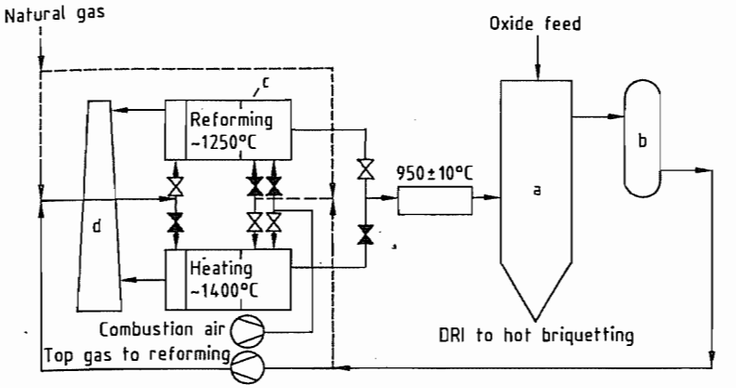

Figure 5.72: Schematic of the Purofer process: a) Shaft furnace; b) Top-gas scrubber; c) Gas reformer; d) Stack.

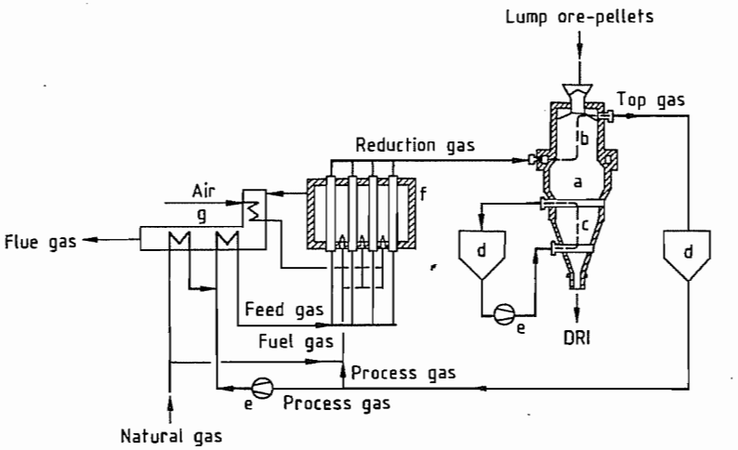

Figure 5.73: Schematic of the Midrex process: a) Shaft furnace; b) Reduction zone; c) Cooling zone; d) Scrubber; e) Gas compressor; f) Gas reformer; g) Recuperator.

Table 5.36: Typical consumption figures for direct reduction processes.

Process	Reductant	Consumption, GJ/t DRI	Electrical energy, kWh/t DRI	Metallization, %
Midrex	natural gas	10.0	100	92–94
HyL I	natural gas	18.9		85
HyL III	natural gas	10.5		90–93
Purofer	natural gas, oil	14.3	93	95
Nippon steel	natural gas	10.5		90–92
Fior	natural gas	16.0		90
SL/RN	coal	14.8	80	93

Two thirds of the reducing gas is withdrawn by means of a hot gas fan (e) and regenerated in the carburetor (b) over a hot column of coke. The energy required for the endothermic reactions

$$CO_2 + C \rightarrow 2CO$$
$$H_2O + C \rightarrow CO + H_2$$

is supplied by resistance-heating electrodes.

The gas, which is contaminated with sulfur from coke, is passed through dolomite in a shaft furnace for desulfurization (c). The reducing gas contains 95% carbon monoxide and hydrogen in a ratio of ca. 3:1.

The Wiberg process, which was developed for the special conditions of the Swedish iron industry, was a pioneering technology. The

high cost of coke and electrical energy to generate the reducing gas is the reason why this process is no longer in use.

The principle of generating the reducing gas by a chemical reaction between the off-gas of the reduction shaft (the top gas) and natural gas has been applied in two processes: the Purofer and the Midrex process.

Purofer Process. This process (Figure 5.72) was developed at Hüttenwerke Oberhausen (later Thyssen Niederrhein); the ICEM process developed by the Romanian Research Institute for Metallurgy is similar to it. The ore (preferably pelletized) passes vertically downward through the shaft furnace in countercurrent to the hot reducing gas. The gas is used for heating the charge and for reduction. The reducing gas is generated catalytically in regenerative-type gas generators. After cooling and purification, the top gas is used partly for heating up the gas generators and partly for chemical conversion of the natural gas at 900–1000 °C to reducing gas according to the equations

$$CH_4 + CO_2 \rightarrow 2CO + 2H_2$$
$$CH_4 + H_2O \rightarrow CO + 3H_2$$

The carbon from methane reforming that is deposited on the catalyst of the regenerator during reducing-gas production is burned off during heating-up. This regenerative phase causes slight variations in reducing gas temperature and composition. In the Purofer process, the DRI is discharged hot and can be transported in containers either directly to an electric steel mill or to a hot briquetting plant.

In addition to the pilot plant in Oberhausen (capacity 500 t/d), one plant was built in Brazil (but with a Texaco heavy-oil gasifier as gas generator) which is now dismantled. The only plant in operation in Iran is designed for operation with natural gas.

Midrex Process. The most successful gas-based direct reduction process is the Midrex process developed by Midland-Ross Corp. of Toledo, Ohio (Figure 5.73) [107].

In this process, natural gas continually undergoes catalytic conversion to hydrogen and carbon monoxide (ratio ca. 1.5:1) at ca. 900 °C using a partial stream (ca. 2/3) of the top gas, which is cleaned and cooled to lower its water-vapor content. Reduction is accomplished in the cylindrical part of the shaft furnace at 780–900 °C, depending on the temperature at which sintering ("sticking") of the reduced ore or the pellets occurs. In the conical discharge section of the shaft furnace, the DRI is cooled to ca. 45 °C by recirculated cooling gas. Here the carbon content of the product can also be adjusted to between 1.2 and 2.5%. There are also Midrex plants featuring hot discharge followed by hot briquetting.

One third of the top gas is used to heat the gas reformer, whereas the hot flue gases serve to preheat the combustion air and the feed gas mixture prior to reforming.

With increasing heat recovery in the recuperator and reduction temperatures of ca. 900 °C, energy consumption per tonne of DRI may fall to 9.6 GJ in the Midrex process.

The reducing gas can also be generated by *steam reforming* of natural gas. The first shaft furnace direct-reduction process to employ steam reforming was the *Armco process*. Here natural gas undergoes continuous catalytic conversion with excess steam according to the reaction:

$$CH_4 + xH_2O \rightarrow CO + 3H_2 + (x-1)H_2O$$

After removal of the water vapor, the top gas is used as cooling gas.

Only one commercial plant was ever built because of the difficulty of achieving complete mixing of the cooling gases entering the lower part of the shaft with the hot top gases from the reduction zone, the low reducing potential of the gases, and a range of technical problems.

Nippon Steel (NSC) Process. The reducing gas containing over 95% carbon monoxide and hydrogen is generated by steam reforming with only a slight excess of water vapor and addition of top gas freed from water and carbon dioxide (see Figure 5.74). Like the Purofer process, the NSC process has a hot discharge facility, from which DRI can be filled into containers and taken either directly

to a steel mill or to a hot briquetting plant. Only one plant in Malaysia with a design capacity of 1000 t/d has been built which was later modified into an HyL-III plant.

HyL-III Process. Hojalata y Lamina S.A. (HyL) of Mexico has also developed a shaft-furnace process based on steam reforming of natural gas (HyL-III process, Figure 5.75). This process represents a further development of HyL's retort process (see Section 5.10.3). Because of the large quantity of excess steam produced in continuous catalytic conversion of the natural gas, the generated gas must first be cooled to remove the excess water vapor. After addition of water- and carbon dioxide-free top gas and indirect heating to ca. 850 °C, the reducing gas is fed into the reduction shaft. In the bottom section of the shaft furnace, the DRI is cooled down to < 50 °C as in the Midrex process. HyL-III plants can also be operated with hot discharge and hot briquetting.

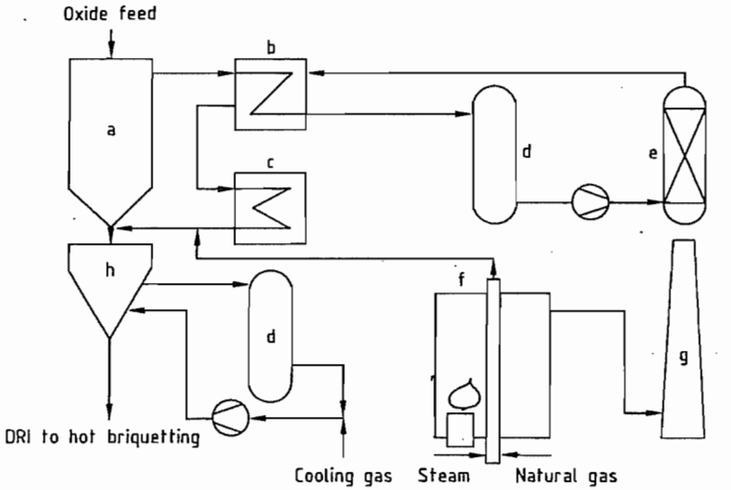

Figure 5.74: Schematic of the Nippon Steel process: a) Shaft furnace; b) Heat exchanger; c) Gas heater; d) Dust remover; e) CO_2 scrubber; f) Reformer; g) Stack; h) Cooling zone.

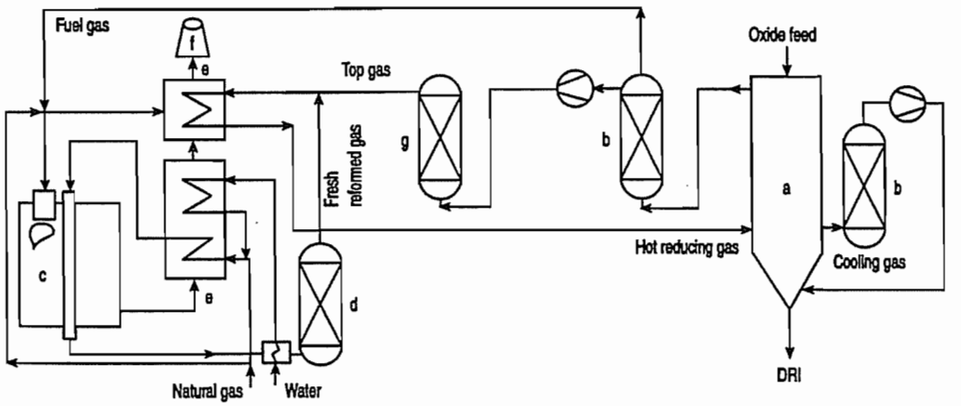

Figure 5.75: Schematic of the HyL-III process: a) Shaft furnace; b) Gas scrubber; c) Reformer; d) Cooler; e) Recuperator; f) Stack; g) CO_2 scrubber.

The degree of metallization of the DRI produced by the various shaft furnace processes ranges from 92–95%. The carbon content is usually 1.5–2%.

5.10.3 Retort Processes

HyL Process (HyL-I Process). A number of plants employing this process were built up to 1975 before the shaft-furnace processes became established. The development of this process began in 1951 at Hojalata y Lamina S.A., Monterrey (Mexico). It operates with four reactors simultaneously, each one being at a different point in the reduction cycle at a particular time. Figure 5.76 shows the stage at which product DRI is cooled with cold reducing gas in retort 1. At this point, the carbon content of the DRI is adjusted to ca. 2%. After cooling and water-vapor condensation, the off-gas from this retort is reheated to reduction temperature and passed through retort II, where pre-reduced material is fully reduced. The gas is then recooled to remove any newly formed water vapor, reheated and fed to retort III containing freshly charged ore, which is then pre-reduced. The off-gas from this stage is cooled and freed from water vapor; it is then available for use as fuel gas for steam raising. Retort IV is simultaneously emptied from DRI and charged with ore.

As lump ore or pellets are stationary in the retorts during reduction, the risk of sticking is high. Sophisticated removal devices are required for emptying the retorts.

The degree of metallization of the DRI is often lower at the bottom of the retorts than in the upper layers. Thus the target average degree of metallization is often only ca. 86%. As gas generation is carried out with a large excess of steam and cooling and reheating of each retort is very costly, an energy consumption of ca. 21 GJ per tonne DRI must be taken into account.

Höganäs Process. This process has been in operation since 1911 and has undergone no significant technical modifications since the 1950s, nor has its use become any more widespread. In this process, iron ore is reduced with coal in hermetically sealed crucibles with indirect heating (by combustion of the carbon monoxide escaping from the crucibles). The sulfur content of the DRI is minimized by adding limestone or dolomite to the charge mix and rapidly cooling the product. It is thus suitable for use in powder metallurgy or stainless-steel production. The capacity of plants operating on the Höganäs process is relatively low, ca. 35 000 t/a.

Kinglor–Metor Process. This process occupies a category between the shaft furnace and the retort processes. The development of this process (Figure 5.77) by Co. Kinglor–Metor S.p.a., Mineraria & Metallurgica, Italy, began in 1971 but was based on the Echeverria process which had been in operation in Spain since 1957 [108]. Like the rotary kiln processes (see Section 5.10.5) and in contrast to the gas-based direct reduction processes described so far, it uses a solid carbon-containing reductant, which is charged together with the ore (6–25 mm size) and, where applicable, limestone or dolomite is used for desulfurization. The heat for the strongly endothermic reaction

$$FeO_x + xC \rightarrow Fe + xCO$$

which in this case takes place at ca. 1050 °C, is supplied through the wall of the shaft furnace, which must therefore have a high thermal conductivity. Silicon carbide satisfies the requirements as to thermal conductivity, heat resistance, and abrasion resistance. The shaft heating burners are designed for gaseous and liquid fuels. The reduced material is indirectly cooled with gas in the bottom zone of the shaft. Commercial plants consist of a group of six reduction chambers, each with a capacity of ca. 20 t/d DRI.

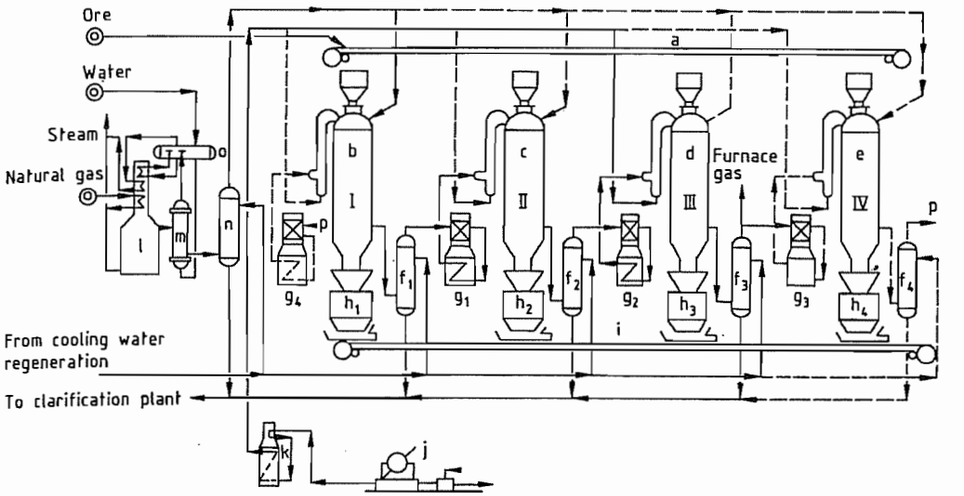

Figure 5.76: Flow sheet of the HyL-I process: a) Ore conveyor belt; b) Retort I at cooling stage; c) Retort II at final reduction stage; d) Retort III at pre-reduction stage; e) Retort IV at discharging and charging stage; f_1–f_4) Cooler; g_1–g_4) Gas preheating; h_1–h_4) Intermediate container for sponge iron; i) Conveyor belt for sponge iron; j) Air compressor; k) Air preheating; l) Reduction gas generator; m) Superheated steam generator; n) Cooler; o) Saturated steam generator; p) Connection between cooler f_4 and preheater g_4.

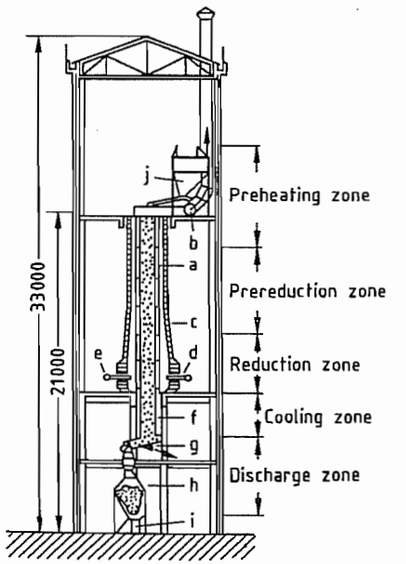

Figure 5.77: Shaft furnace of the Kinglor-Metor process (dimensions in mm): a) Silicon carbide shaft; b) Gas discharge pipe; c) Fireclay outer wall; d) Burner; e) Gas or oil pipe; f) Air cooling; g) Extruding screw discharge; h) Hopper; i) Sponge iron discharge; j) Charging hopper.

5.10.4 Fluidized-Bed Processes

Fluidized-bed processes for direct reduction exploit the lower cost of fine ores compared with lump ores and pellets. However, the disadvantages of these processes are that (1) the fine ores have a tendency towards sticking above ca. 700 °C and that (2) below 600 °C the susceptibility to reoxidation of the DRI is so high that it must be stored under inert gas or hot-briquetted.

Fluidized-bed processes that operated with pure hydrogen were the *Novalfer process* and the *H-Iron* process; however, they did not attain any major technological significance. In the *HIB-process*, reduction was carried out in several stages with a gas containing ca. 85% hydrogen. The ore of 0.2 mm size underwent only ca. 65% metallization and was then hot-briquetted. The sole commercial plant has been converted by Midrex Corp. into a shaft furnace plant with hot discharge/hot briquetting.

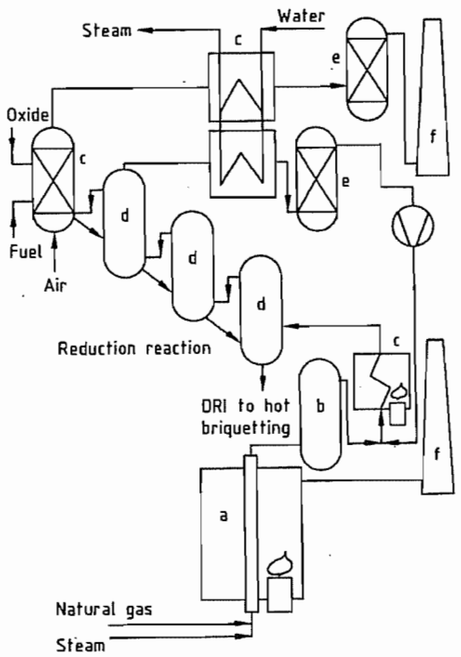

Figure 5.78: Schematic of the Fior process: a) Reformer; b) Gas cooler; c) Heater; d) Fluidized-bed reactor; e) Scrubber; f) Stack.

Fior (Fluidized Iron Ore Reduction) Process. Development of the Fior process (Figure 5.78) started in the 1950s at Esso Research and Engineering in collaboration with Arthur D. Little. Following the building and operation of a 300 t/d pilot plant in Dartmouth, Nova Scotia, from 1965 to 1969, a 400 000 t/a commercial plant operating on this process was built in Puerto Ordaz, Venezuela.

After drying and preheating to ca. 880 °C, the fine ore (mostly < 5 mm) is metallized to a degree of ca. 92% in a three-stage fluidized bed. The reducing gas is generated by steam reforming of natural gas in continuously operating catalytic reformers. The reduced fine ore is hot-briquetted, the briquettes being cooled and shipped to the end-users without further passivation.

The Finmet process is a further development of the Fior process, taking advantage of the experience gained in more than 10 years of Fior plant operation.

Iron Carbide Process (Figure 5.79) [109]. In NUCOR's Iron Carbide process, fine iron oxide (0.1–1 mm) is reduced by a hydrogen- and methane-containing gas to iron carbide according to:

$$3Fe_2O_3 + 5H_2 + 2CH_4 \rightarrow 2Fe_3C + 9H_2O$$

The iron oxide is heated to 700 °C prior to feeding into the fluidized bed reactor in which the reduction of the iron oxide and the formation of iron carbide occurs at a temperature of approx. 570 °C and at a pressure of approx. 3 bar(g).

In the fluidized bed reactor baffles are arranged, which cause the solids to move from the inlet to the outlet. The relatively low reduction temperature required to form iron carbide results in a retention time of about 16 hours in the first 900-t/day plant built in Trinidad. At a gas-to-solids ratio of about 10 000 Nm^3/t oxide, the gas volumes to be handled are very high compared to shaft-furnace processes.

The fines carried over with the reduction gases are partially recovered in a cyclone and recycled into the reactor. After heat exchange with the cold reduction gas, the off-gases are scrubbed, cooled for water condensation, compressed, and recycled via heat exchanger and a gas heater. Make-up gas is hydrogen. The reduction gas consists of 60% CH_4, 34% H_2, 2% CO, 1% H_2O, and minor amounts of CO_2 and N_2. The iron carbide formed in NUCOR's plant contains 90% Fe total (90% as Fe_3C, 8% as FeO, 2% as Fe metal), 6.2% C, 2% gangue.

Iron carbide is listed as a nonpyrophoric material, therefore handling and shipping do not require briquetting or other treatment to avoid reoxidation.

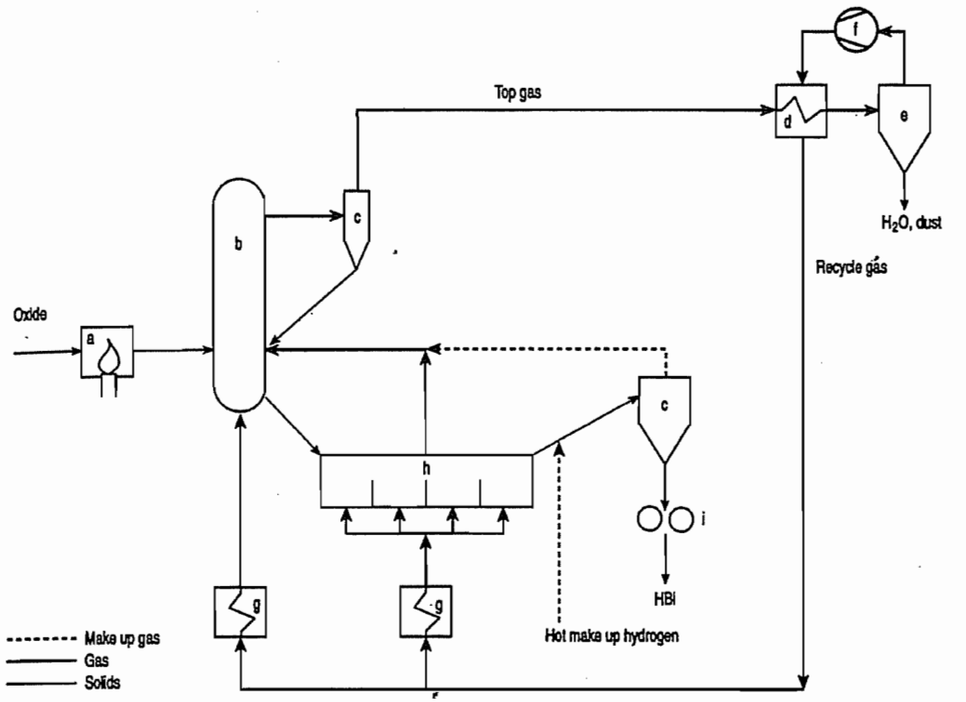

Figure 5.79: Flowsheet of the Iron Carbide process: a) Oxide heater; b) Reduction reactor; c) Cyclone; d) Heat exchanger; e) Scrubber/cooler; f) After-cooler; g) Compressor; h) Gas heater; i) Product cooling.

Circored® Process (Figure 5.80) [110]. In Lurgi's Circored® process fine iron oxide ores (0.1–1 mm) are reduced by hydrogen according to:

$$Fe_2O_3 + 3H_2 \rightarrow 2Fe + 3H_2O$$

The ore, preheated to approx. 800 °C, is first prereduced to about 65% metallization in a circulating fluidized-bed reactor (CFB) within 20 minutes.

The final reduction to 90–93% metallization is achieved in a following fluidized-bed reactor (FB) with several compartments at lower gas velocities over a period of up to 4 hours — depending on the desired metallization and the reducibility of the oxides.

The reactors are operated at temperatures generally below 650 °C to avoid sticking. The off-gases from the final reduction step in the FB as well as make-up hydrogen are passed into the CFB reactor. Most of the solids in the off-gases from the CFB are recovered in the recycle cyclone.

The gases are then passed through a heat exchanger, dedusted, cooled for water vapor condensation, and compressed to the plant pressure of approx. 4 bar(g). After heat exchange with the hot off-gases from the CFB the reduction gas is heated to 750 °C before being reintroduced into the two reduction reactors.

Hot make-up hydrogen is first used to transport and further heat up the reduced fines from the FB into a briquetting plant before being passed into the CFB. The reduced DRI fines are hot briquetted if the product is intended for export. It is also possible to directly charge it into smelting furnaces.

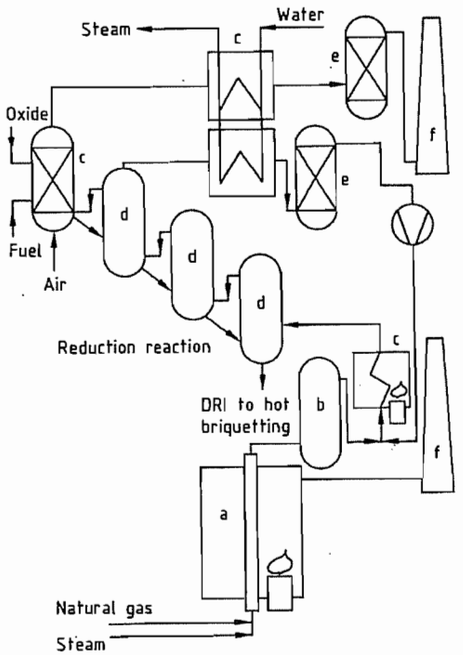

Figure 5.78: Schematic of the Fior process: a) Reformer; b) Gas cooler; c) Heater; d) Fluidized-bed reactor; e) Scrubber; f) Stack.

Fior (Fluidized Iron Ore Reduction) Process. Development of the Fior process (Figure 5.78) started in the 1950s at Esso Research and Engineering in collaboration with Arthur D. Little. Following the building and operation of a 300 t/d pilot plant in Dartmouth, Nova Scotia, from 1965 to 1969, a 400 000 t/a commercial plant operating on this process was built in Puerto Ordaz, Venezuela.

After drying and preheating to ca. 880 °C, the fine ore (mostly < 5 mm) is metallized to a degree of ca. 92% in a three-stage fluidized bed. The reducing gas is generated by steam reforming of natural gas in continuously operating catalytic reformers. The reduced fine ore is hot-briquetted, the briquettes being cooled and shipped to the end-users without further passivation.

The Finmet process is a further development of the Fior process, taking advantage of the experience gained in more than 10 years of Fior plant operation.

Iron Carbide Process (Figure 5.79) [109]. In NUCOR's Iron Carbide process, fine iron oxide (0.1–1 mm) is reduced by a hydrogen- and methane-containing gas to iron carbide according to:

$$3Fe_2O_3 + 5H_2 + 2CH_4 \rightarrow 2Fe_3C + 9H_2O$$

The iron oxide is heated to 700 °C prior to feeding into the fluidized bed reactor in which the reduction of the iron oxide and the formation of iron carbide occurs at a temperature of approx. 570 °C and at a pressure of approx. 3 bar(g).

In the fluidized bed reactor baffles are arranged, which cause the solids to move from the inlet to the outlet. The relatively low reduction temperature required to form iron carbide results in a retention time of about 16 hours in the first 900-t/day plant built in Trinidad. At a gas-to-solids ratio of about 10 000 Nm^3/t oxide, the gas volumes to be handled are very high compared to shaft-furnace processes.

The fines carried over with the reduction gases are partially recovered in a cyclone and recycled into the reactor. After heat exchange with the cold reduction gas, the off-gases are scrubbed, cooled for water condensation, compressed, and recycled via heat exchanger and a gas heater. Make-up gas is hydrogen. The reduction gas consists of 60% CH_4, 34% H_2, 2% CO, 1% H_2O, and minor amounts of CO_2 and N_2. The iron carbide formed in NUCOR's plant contains 90% Fe total (90% as Fe_3C, 8% as FeO, 2% as Fe metal), 6.2% C, 2% gangue.

Iron carbide is listed as a nonpyrophoric material, therefore handling and shipping do not require briquetting or other treatment to avoid reoxidation.

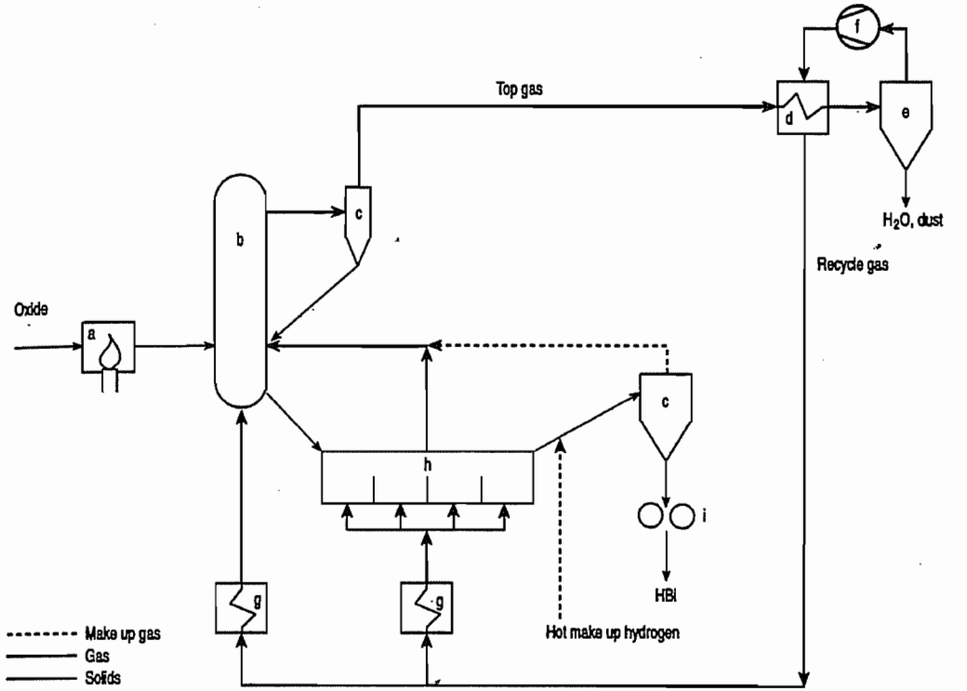

Figure 5.79: Flowsheet of the Iron Carbide process: a) Oxide heater; b) Reduction reactor; c) Cyclone; d) Heat exchanger; e) Scrubber/cooler; f) After-cooler; g) Compressor; h) Gas heater; i) Product cooling.

Circored® Process (Figure 5.80) [110]. In Lurgi's Circored® process fine iron oxide ores (0.1–1 mm) are reduced by hydrogen according to:

$$Fe_2O_3 + 3H_2 \rightarrow 2Fe + 3H_2O$$

The ore, preheated to approx. 800 °C, is first prereduced to about 65% metallization in a circulating fluidized-bed reactor (CFB) within 20 minutes.

The final reduction to 90–93% metallization is achieved in a following fluidized-bed reactor (FB) with several compartments at lower gas velocities over a period of up to 4 hours — depending on the desired metallization and the reducibility of the oxides.

The reactors are operated at temperatures generally below 650 °C to avoid sticking. The off-gases from the final reduction step in the FB as well as make-up hydrogen are passed into the CFB reactor. Most of the solids in the off-gases from the CFB are recovered in the recycle cyclone.

The gases are then passed through a heat exchanger, dedusted, cooled for water vapor condensation, and compressed to the plant pressure of approx. 4 bar(g). After heat exchange with the hot off-gases from the CFB the reduction gas is heated to 750 °C before being reintroduced into the two reduction reactors.

Hot make-up hydrogen is first used to transport and further heat up the reduced fines from the FB into a briquetting plant before being passed into the CFB. The reduced DRI fines are hot briquetted if the product is intended for export. It is also possible to directly charge it into smelting furnaces.

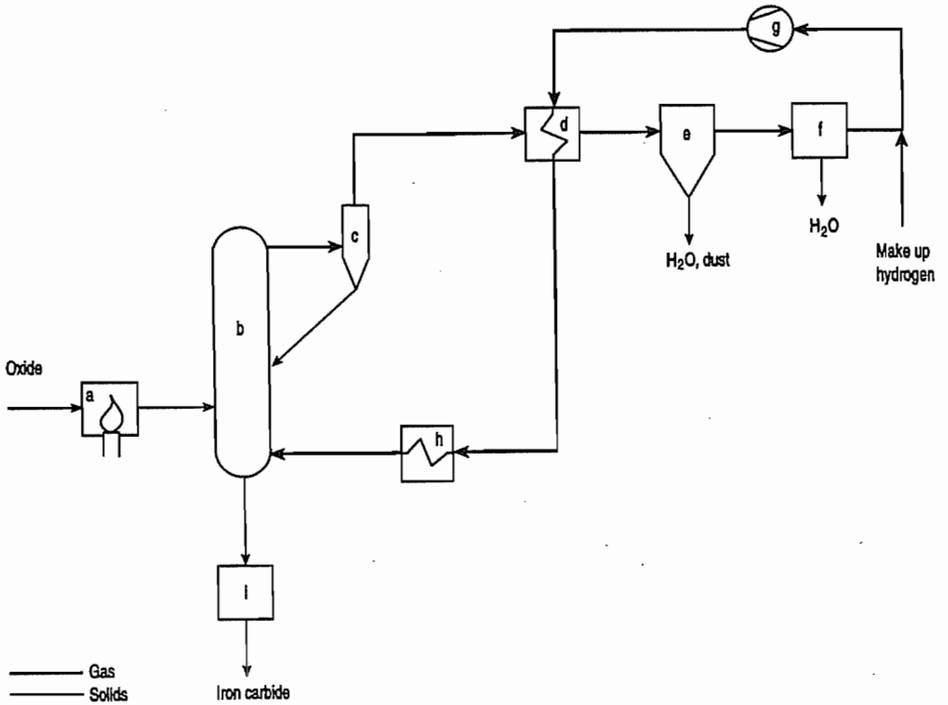

Figure 5.80: Flowsheet of the Circored® process: a) Oxide heater; b) Circulation in fluidized bed; c) Cyclone; d) Heat exchanger; e) Scrubber/cooler; f) Compressor; g) Gas heaters; h) Fluidized bed; i) Briquetting machine.

A 500 000-tpy Circored® plant is under construction in Trinidad. By using a CO/CH_4-containing reduction gas, the Circored® process can also be applied for production of a carbon containing HBI with approx. 1–3% C or iron carbide with approx. 6.5% C.

Circofer® Process (Figure 5.81). Another fluidized bed process developed by Lurgi Metallurgie operating with a CFB prereduction and a final FB reduction step is based on coal as the basic energy source. Fine coal is partially burned in a "gasifier/heater" and the semicoke produced is used as a heat carrier into the CFB as well as to prevent sticking of the iron particles at the reduction temperature of > 900 °C. The final reduction is achieved at lower temperatures in the FB with recycled off-gases from the CFB. The gas treatment is rather similar to the Circored® process, however, a CO_2-absorber step had to be included as the reduction is achieved mainly with CO-containing gases No commercial plant has been built so far.

5.10.5 Rotary Kiln Processes

The internal kiln temperature is continuously recorded by thermocouples installed along the entire length of the kiln and projecting into the kiln freeboard. The power supply to the shell fans and the transmission of the data recorded by the individual thermocouples is accomplished by means of slip rings mounted on the kiln shell. Devices for taking samples of material during operation are also mounted on the kiln shell.

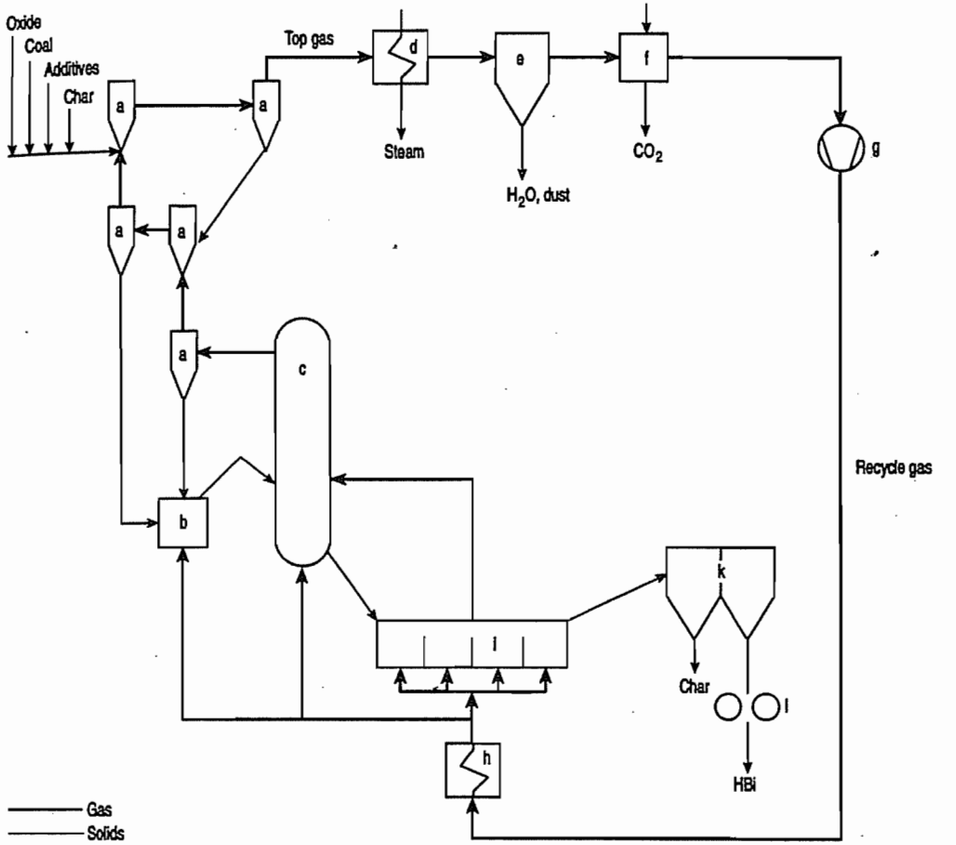

Figure 5.81: Flowsheet of the Circofer® process: a) Preheating cyclone system; b) •••; c) Circulating fluidized bed; d) Heat exchanger; e) Scrubber/cooler; f) CO_2 removal; g) Compressor; h) Gas heater; i) Fluidized bed; k) Magnetic separation; l) Briquetting machine..

Rotary kiln processes for direct reduction of iron oxides are based on coal as reductant. Typical features of rotary kiln processes are their high flexibility with regard to feedstocks and their capability for economic production of even small quantities of DRI. All non-caking coals ranging from lignite through bituminous coals up to anthracite or coke breeze are suitable as reductants. In addition to the pellets and lump ores that are the main iron-bearing materials, iron sands, and ilmenite concentrates are also industrially used.

Of the various rotary kiln processes [111], the *Krupp Codir process* and the *Lurgi SL/RN process* have attained the greatest technological significance. The two processes operate according to similar principles. As most of the DRI currently produced in rotary kilns worldwide is manufactured by the SL/RN process (see Table 5.36), the principle of the rotary kiln processes will be explained with reference to this process.

The SL/RN process was developed in 1964 out of the combination of two separate processes: the Stelco-Lurgi (SL) process for producing DRI from *high-grade ores* and the Republic Steel National Lead (RN) process for beneficiation of *low-grade ores*.

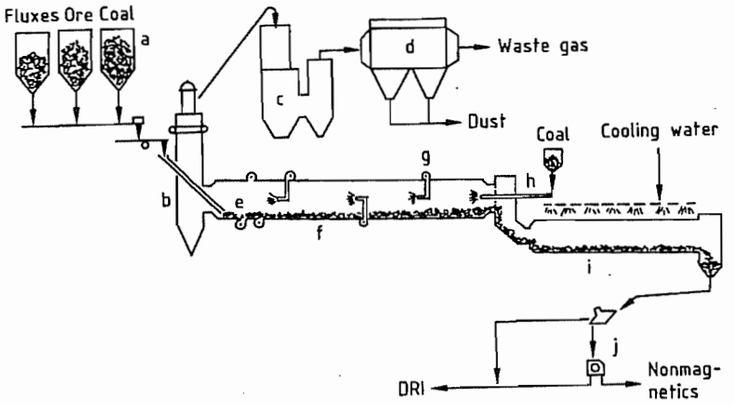

Figure 5.82: Lurgi SL/RN process: a) Bins for raw materials; b) Afterburning chamber; c) Waste-heat boiler; d) Gas cleaning; e) Underbed air injection; f) Rotary kiln; g) Air tubes; h) Injection coal; i) Rotary cooler; j) Product separation.

In the SL/RN process (Figure 5.82), reduction of iron oxide is carried out in a refractory-lined rotary kiln (f) inclined from the feed to the discharge end. The slope of the kiln is ca. 1.5–2.5% depending on the feed materials.

The kiln is equipped at both ends with special seals between the rotating kiln and the fixed feed and discharge heads. These seals essentially prevent inleakage of air and thus reoxidation. A number of fans are installed on the shell of the kiln; these supply the necessary process air via so-called air tubes or via air injection nozzles in the feed zone of the rotary kiln.

The *central burner* installed at the kiln discharge end is used to dry out the refractory kiln lining during the initial start-up and to heat up the system after a shutdown. Under normal operating conditions, only air without fuel is fed through the central burner. However, if low-reactivity coals (anthracite) are used, it may be necessary to continuously fire a small amount of supplementary fuel via the central burner to satisfy the overall heat requirement.

Fresh coal, recycle carbon, ore or pellets, and dolomite or limestone as desulfurizing agent are charged in a predetermined ratio at the kiln feed end by a gastight charging system.

Up to ca. 35% of the total fresh coal required is fed into the kiln from the discharge end with a special pneumatic injection system (h). This improves the utilization of the energy contained in the coal volatiles and prevents depletion of carbon in the material bed, especially in the case of very long kilns.

The charge passes through the kiln in ca. 8–12 h. The retention time mainly depends on the slope, degree of filling, and the rotational speed of the kiln. For each combination of iron-bearing material and reductant, a minimum retention time is necessary to achieve the desired degree of metallization; this is determined with laboratory tests.

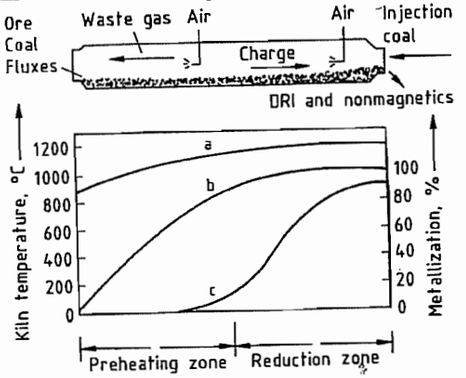

Figure 5.83: Temperature and degree of metallization as a function of the location in the kiln: a) Gas temperature; b) Charge temperature; c) Metallization.

Table 5.37: Iron ores and coals processed in SL/RN plants.

Plant	City	Country	Iron ore Type	Iron ore Analysis %, dry Fe	SiO_2	CaO	Others	Coal Type	Coal Analysis %, dry Fixed carbon	Volatile matter	Ash	Sulfur
Highveld[a]	Witbank	South Africa	Mapochs lump ore	54	2.1		13.2 TiO_2 1.7 V_2O_5	Greenside	54	31	15	0.6
NZS	Glenbrook	New Zealand	Iron sand	58	1.1	0.2	8 TiO_2	Huntly	51	43	6 35	0.3
Piratini	Charqueadas	Brazil	Itabira pellets	67	2.4	1.6		Charqueadas	40	25	18	0.4
Siderperu	Chimbote	Peru	Marcona pellets	66	2.2	1.0		Coke Breeze	81	3	25	0.7
SIIL	Paloncha	India	Bayarani lump ore	63	4.5	0.1		Singareni	44	31	14	0.3
Iscor	Vanderbijlpark	South Africa	Sishen lump ore	66	2.5	0.2		Van Dyksdrift	59	26	25	0.6
BSIL	Chandil	India	Bihar lump ore	67.4	1.5	0.1		Ray Bachara	51	24		0.7

[a] Prereduction only.

For example, the necessary retention time for a combination of "porous" pellets and highly reactive lignite is low, whereas that for "compact" lump ores and low-reactive anthracite is high.

In simplified terms, the rotary kiln can be divided into a preheating and a reduction zone (Figure 5.83).

In the preheating zone, the feed materials are dried, and coal volatiles escape, and the charge is heated to reducing temperature (ca. 950–1100 °C).

An overview of the coals and ores used in SL/RN plants is given in Table 5.37. The usual grain sizes of the feed materials are < 15 mm for the reductant, < 25 mm for the iron-bearing materials and < 3 mm for the desulfurizing agent.

The charge is heated through exchange of heat with the kiln waste gases flowing counter-currently to the charge. The energy is supplied by the sensible heat of the waste gases from the reduction zone, by the partial combustion of the coal volatiles, and by direct burning of carbon in the preheating zone.

If high-volatile coals are used, injection of air into the charge can bring about partial combustion of the volatiles within the charge, which accelerates preheating.

In the preheating zone, a certain degree of prereduction is accomplished through the coal volatiles. However, the greater part of the reduction occurs in the *reduction zone* at near-constant temperature according to

$$Fe_xO_y + CO \rightarrow Fe_xO_{y-1} + CO_2$$

The carbon dioxide formed during reduction reacts within the charge with fixed carbon according to the Boudouard reaction

$$C + CO_2 \rightarrow 2CO$$

and forms the carbon monoxide required for the reduction process.

The necessary heat in the reduction zone is supplied through combustion of the surplus carbon monoxide from reduction, of the volatiles in the injected coal, and of fixed carbon.

The desired temperature profile is established by controlled addition of combustion air along the length of the kiln.

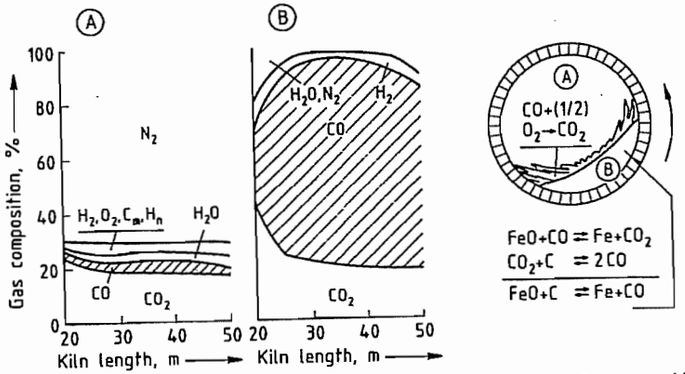

Figure 5.84: Gas composition in the kiln freeboard (A) and kiln charge (B) measured in an industrial kiln of 50 m length.

Inside the kiln, an *oxidizing atmosphere* above the charge and a *reducing atmosphere* within the charge prevail in close proximity (Figure 5.84). Accordingly, the reactions occurring above the charge in the kiln freeboard are exothermic and those taking place in the material bed are endothermic. Separation of the two atmospheres is ensured by the gas generated in the material bed, which also prevents reoxidation of particles of DRI at the charge surface.

After leaving the rotary kiln, the DRI is cooled to ca. 100 °C together with the excess coal in an indirectly cooled rotary cooler. The DRI is separated from the nonmagnetic kiln discharge material by *screening* and *magnetic separation*.

The > 3 mm fraction of the *magnetic portion* can be directly used for steel production, the < 3 mm fraction is normally briquetted before further use.

The > 3 mm fraction of the *nonmagnetic portion* is mostly char and can be recycled to the process. The < 3 mm fraction, containing ash, calcined desulfurizing agent, and char, is disposed of.

In particular cases, e.g., if the ash content of the coal is very low, it is advantageous to charge the entire kiln discharge material directly into a downstream electric furnace without cooling and separation. This brings considerable savings in electric energy for the melting down process.

The waste gases leave the kiln at the feed end at ca. 850–1000 °C. They pass through a dust-settling chamber to remove coarse dust and enter an afterburning chamber, where combustible gases and carbon particles are burnt off. The waste gases are then cooled, cleaned and discharged to the atmosphere. Alternatively, the sensible heat of the gases leaving the afterburning chamber may be recovered in a downstream steam boiler for generation of process steam or combined for production of steam and electric power.

Since 1984, a four-strand SL/RN plant with a capacity of 600 000 t/a DRI and waste-heat recovery has been in operation at the Vanderbijlpark Works of ISCOR in South Africa. Approximately 1.9 t of process steam (1.6 MPa, 260 °C) per tonne of DRI are generated for the steel mill.

Taking into account a variety of reducing agents, the energy requirement (without char recycling) referred to as the lower heating value of the coals, is ca. 19.3 GJ/t DRI for lignite briquettes (A), ca. 18.4 GJ for bituminous coal (B), and ca. 17.8 GJ for a mixture consisting of 70% anthracite (C) and 30% bituminous coal (B) [112]. The analyses of these coals are shown in Table 5.38.

If a combination C:B = 50:50 with recycled char is used, the energy requirement is only 14.8 GJ/t DRI [112].

Further typical consumption figures are given below:

Ore or pellets (Fe_{tot} 67%)	1.42–1.44 t
Fixed carbon	380–475 kg
Electric power	70–90 kWh
Water	1.5–2.5 m^3
Manpower	0.4–0.6 man hours
Repair and maintenance	$8–10

In addition to DRI production, SL/RN rotary kilns are commercially used for prereduction of iron ore at Highveld Steel in Witbank, South Africa (13 units with an ore capacity of 200 000 t/a each, 30–35% metallization) and for reduction of ilmenite concentrates at Westralian Sands Ltd. in Capel, Western Australia (one unit, ilmenite throughput 180 000 t/a, 95–97% metallization).

Table 5.38: Coal analyses.

Coal	A	B	C
Fixed carbon, %	44	59	88
Volatile matter, %	51	27	8
Ash, %	5	14	4
Lower heating value (dry), GJ/kg	23.3	27.0	32.7

5.11 Smelting-Reduction Processes

Smelting-reduction processes are multistage processes where hot metal is produced directly with coal, particularly noncoking coal.

The main reasons for developing smelt-reduction processes (since 1970) was to find processes which produce *liquid iron* economically at low capacity and use *coal directly*. The processes should be more flexible regarding raw material and operation and should cause less pollution than a blast furnace.

The ore, fine ore, or lump ore is prereduced with the gas produced in the melting vessel. The prereduced ore (sponge iron) is melted down in a melting vessel where melting energy is generated by oxidation of coal. Some processes use also electrical energy in the melting stage.

Simulations with computer models were performed for different smelt reduction process configurations [113–115] to find an optimum process and to estimate the influence of postcombustion and prereduction on coal consumption. (Postcombustion is defined as the partial oxidation of a gas previously generated in the melting vessel, whereby the energy produced by this combustion is transferred to the bath with high efficiency.) Economical and technical comparison can be found in the literature [116–118].

Characteristics of Coals for the Smelting-Reduction Processes. The most important property of the coal for the smelting reduction processes is its volatile content, because this determines the gasification temperature of the reaction

$$\text{coal} + O_2 \rightleftharpoons CO + H_2$$

Coals with *low volatile* content generate a high temperature when gasified with oxygen, the released energy being used for sponge iron melting. Gasification of coals with a high volatile content such as lignite results in a low temperature because the volatile hydrocarbons must be cracked before gasification can occur.

Figure 5.85 shows the calculated adiabatic gasification temperature (gasification to CO + H_2) as a function of the H:C and O:C molar ratio of the coal. The higher the gasification temperature the better the coal is suited for smelt reduction process, i.e., the lower is the coal consumption. The classification of coals by the aforementioned molar ratio is more accurate than by volatile content because coals with the same volatile content can show remarkable differences in their gasification temperature. The coal rank classification shown in Figure 5.85 gives only a rough estimation.

For *converter-type* melters the degree of postcombustion must be increased when using highvolatile coal, but there are some limitations with respect to the movement of the bath. For processes with countercurrent flow of coal and gas, besides energetic limitation, problems with tar formation can also occur.

The *ash content* of the coal is less critical than its volatile content. The mainly acidic ashes of the coal must be compensated for by additives so that basic slags can be formed. Thus, processes which require a high slag basicity are more sensitive to the ash content. The additives (limestone, dolomite) enter the melter stage in most cases in the calcined form. Otherwise the influence of the ash con-

tent on the coal consumption is too high and extra energy for calcining the additives and for the endothermic Boudouard reaction is needed.

The *moisture content* of the coal (ca. 10%) decreases the gasification temperature drastically because of the endothermic water-gas reaction. Hence, most of the processes use dried coal.

Other properties of the coal such as the melting behavior of the ash, the swelling index, or the reactivity are of little or no concern. The Hardgrove index influences the grinding cost when grinding is necessary (converter processes).

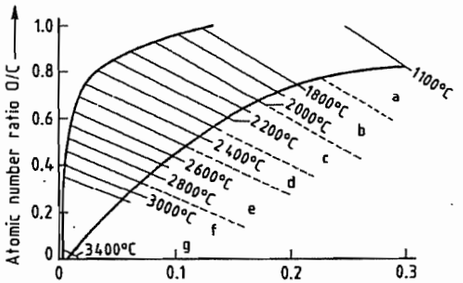

Figure 5.85: Adiabatic gasification temperatures (H_2 + CO) for coals in dependence on the atomic number ratio: a) Lignite; b) Subbituminous coal; c) High volatile bituminous coal; d) Medium volatile bituminous coal; e) Low volatile bituminous coal; f) Anthracite; g) Coke.

The *sulfur content* of the coal should be of course as low as possible (≤ 1%). However, the tolerable range must be evaluated for each smelt reduction process separately.

Classification of Smelting-Reduction Processes. The first developments in smelting reduction on a laboratory scale failed in the 1960s because the conversion of coal and fine ore in a melting vessel was tried without prereduction [119]. The next development was in Sweden in the 1970s, where the energy was introduced into the melting vessel in the form of *electrical energy*. Further developments were the *converter processes* with and without postcombustion. Processes which are closest to the blast furnace are those with a char-or coke-bed melter–gasifier (Table 5.39).

Processes which only modify the blast furnace technique such as the oxygen-coal blast furnace of BSC and NKK or the plasmaheated blast furnace Pirogas [117] are not discussed here.

In the case of processes using fine ore generally only the smelting reactor is developed. The integration of the fine-ore reduction into the process and therefore directly into the smelting reactor has not yet been realized in any of the existing pilot plants.

5.11.1 Processes Using Electrical Energy

These processes were developed in Sweden and consist of a prereduction stage of the fine ore and a final reduction which use electrical energy. The electrical energy is introduced via plasma burners (Plasmamelt), electric arc (Elred), or electric resistance heating (Inred). The only process which has a technical application is the Plasmamelt process in a modified form (Plasmadust and Plasmachrome). Because of the high electricity consumption these processes can only be considered for iron production in countries with cheap electricity.

Plasmamelt. The Plasmamelt process [142, 137] was developed by SKF Steel Engineering AB. The flow sheet is shown in Figure 5.86. Fine ore is prereduced with a reduction gas generated in the smelting reduction stage. The prereduced material (reduction degree 50–60%) is injected together with powdered coal into a coke-filled shaft furnace (melter) provided with plasma generators. Recycled process gas is used as injection gas. The final reduction and melting occur inside the coke column which also protects the refractory. A proportion of the spent reduction off-gases is combusted to dry and preheat the ore fines.

The Plasmamelt process requires a low coke intake (consumption 50–100 kg per tonne of hot metal), 1100 kWh of electricity and 200 kg coal per tonne of hot metal. The prereduction stage was developed separately in a 1 t/h pilot plant. Integrated operation of melting and reduction has not yet been tested.

Table 5.39: Smelting-reduction processes [118].

Process	Ore type	Fuel	Prereduction (reduction degree)	Final reduction	Development stage	References
Char or coke bed melter–gasifier						
Corex	lump	lump coal	shaft furnace (90%)	fluidized bed	1000 t/d	[120–123]
Sumitomo SC	lump	coke (30%) fine coal	shaft furnace (60%)	cupola	8 t/d	[124, 125]
Kawasaki XR	fine	lump coal	circulating fluidized bed (40–80%)	fluidized bed	10 t/d	[126, 127]
Converter with postcombustion						
HIsmelt (CRA)	fine	fine coal	fluidized bed	horizontal cylindrical converter (C-injection)	10 t	[128–130]
MIP and melting cyclone	fine	fine coal	hot and melting cyclone (30%)	horizontal cylindrical converter (C-injection)	20 t	[131]
NKK	fine	fine coal	fluidized bed (15%)	converter (C-top blowing)	5 t	[132, 133]
NSC	fine	fine coal	circulating fluidized bed (30%)	converter (C-top blowing)	5 t	[134]
Kobe Steel	lump	fine coal, CH_4	shaft furnace	converter (C-injection)	0.5 t	[117]
Without postcombustion						
Coin (Krupp)	fine	fine coal	circulating fluidized bed (> 90%)	converter (C-injection)	3 t	[135–137]
CBF (British Steel/Hoogovens)	lump	fine coal	shaft furnace (> 90%)	two-stage converter (C-top blowing)		[117]
Process with electrical energy						
ELRED (ASEA)	fine	fine coal	circulating fluidized bed	d.c. arc furnace	8 t/h melting, 0.5 t/h red.	[138, 139]
Inred (Boliden)	fine	fine coal	melting chamber	arc furnace	8 t/h	[140, 141]
Combismelt (Lurgi)	lump	lump coal fine coal	rotary kiln	submerged electric furnace		
Plasmamelt (SKF)	fine	coke fine coal	fluidized bed	shaft furnace	8 t/h melting	[142, 143]

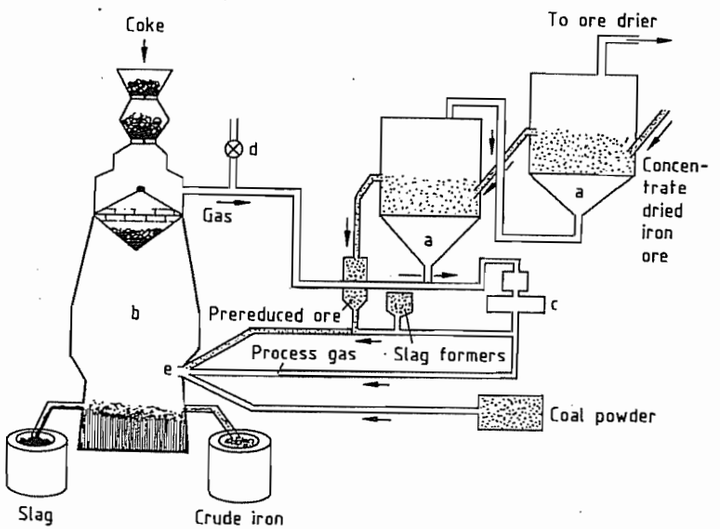

Figure 5.86: The Plasmamelt process: a) Prereduction; b) Shaft furnace; c) Compressor; d) Pressure control; e) Plasma generator.

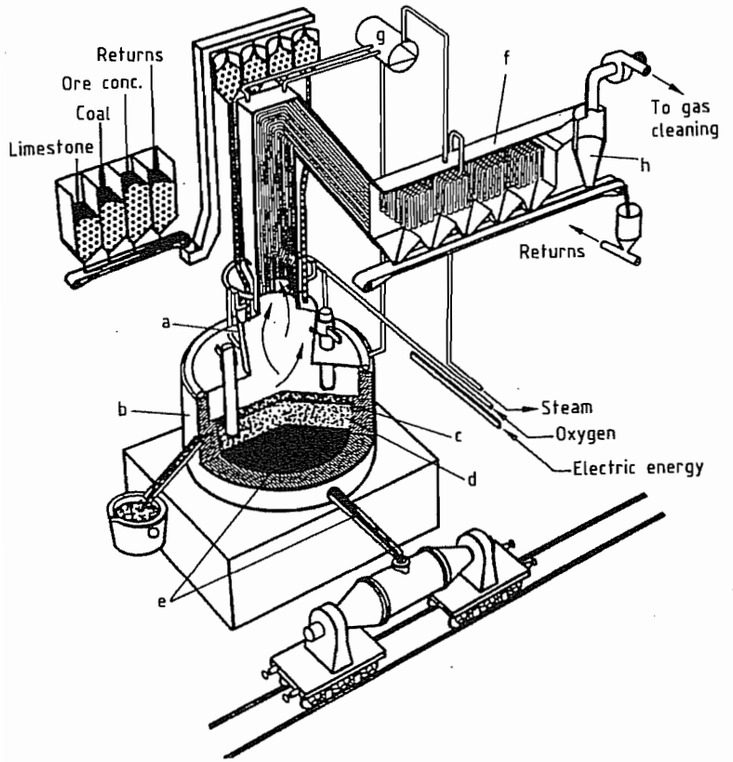

Figure 5.87: The Inred process: a) Flash-smelting chamber; b) Submerged-arc furnace; c) Coke bed with sponge iron and slag; d) Slag; e) Iron; f) Waste-heat boiler; g) Boiler drum; h) Cyclone.

A melter with a capacity of 8 t/h is integrated in a modified process (Plasma dust) where waste oxides from steelworks are processed in Southern Sweden.

The *Inred process* [140, 141] was developed by Boliden and tested from 1982–1984 in a pilot plant with a capacity of 8 t/h. Fine ore, coal, and fluxes are fed together with oxygen in a *flash-melting chamber* giving temperatures of 1900 °C. Superheated liquid FeO together with some coal char fall into the *electric furnace* with submerged arc, where final reduction takes place (Figure 5.87). Because of the high FeO content in the slag (7–8%) a sulfur content of 0.15–0.2% must be expected for a commercial plant.

In the *Elred process* [138, 139] fine ore is prereduced to 60–70% in a single-stage fast-fluidized bed at 950–1000 °C before being melted down in an electric arc furnace (hollow Söderberg electrode). The reducing gas is produced by partial combustion of coal with air within the fluidized bed. The prereduction pilot plant was built by Lurgi with a capacity of 500 kg/h and the electric arc furnace by ASEA (capacity 8 t/h) (Figure 5.88). Up to now this process has found no technical application for iron production.

The *Combismelt process* combines the Lurgi prereduction rotary kiln and a submerged electric arc furnace (DEMAG). The electric energy is generated by waste heat and off-gas.

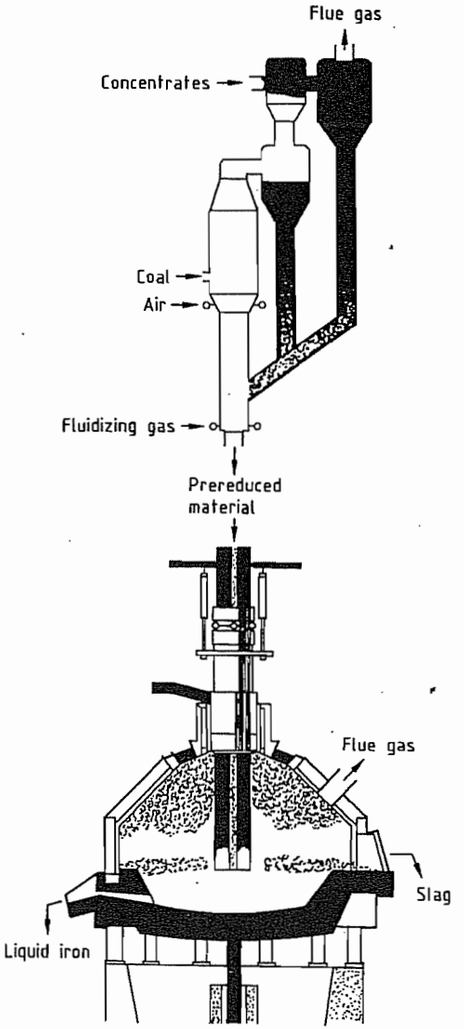

Figure 5.88: The Elred process.

5.11.2 Char–Coke-Bed Melter–Gasifiers

In these processes the melting stage is a fixed bed or fluidized bed of char or coke. Prereduction is performed in a shaft furnace (Corex, Sumitomo) or fluidized bed (Kawasaki).

The Corex process (formerly called KR process) is the most advanced smelting reduction process with a 1000 t/d plant in operation in South Africa since 1988 [120–123]. This process was developed by Deutsche Voest-Alpine Industrieanlagenbau (formerly Korf Engineering) and its parent company Voest-Alpine in Austria to a 60 000 t/a pilot plant from 1981 to 1987.

The Corex process (Figure 5.89) separates the iron-ore reduction and melting steps into two reactors:

- Generation of reducing gas and liberation of energy from coal for melting occur in the *melter–gasifier.*
- Reduction of iron ore occurs in a *shaft furnace.*

The Corex process is designed to operate under elevated pressure, up to 0.5 MPa.

Coal is fed into the gasifier (a) where it comes into contact with a reducing gas atmosphere at a temperature of ca. 1000–1100 °C. Instantaneous drying and degasification of the coal particles occur in this upper portion of the melter–gasifier. Reducing gas is generated in a fluidized bed, by the partial oxidation of coal.

At first carbon is oxidized to carbon dioxide. Then, carbon dioxide reacts with free carbon to form carbon monoxide. The gas temperature in the fluidized bed is in the range of 1600–1700 °C. The temperature conditions in the freeboard zone above the fluidized bed guarantee production of a high-quality reducing gas which contains ca. 65–70% carbon monoxide, 20–25% hydrogen, and 2–4% carbon dioxide. The remaining constituents are methane, nitrogen and steam.

After leaving the melter–gasifier, the hot gas is mixed with cooling gas to obtain a temperature suitable for direct reduction, ca. 850–900 °C. The gas is then cleaned in hot cyclones (d) and fed to the shaft furnace as reducing gas. A small amount of the cleaned gas is converted to cooling gas in a gas cooler. The fines captured in the hot cyclone are reinjected into the melter–gasifier.

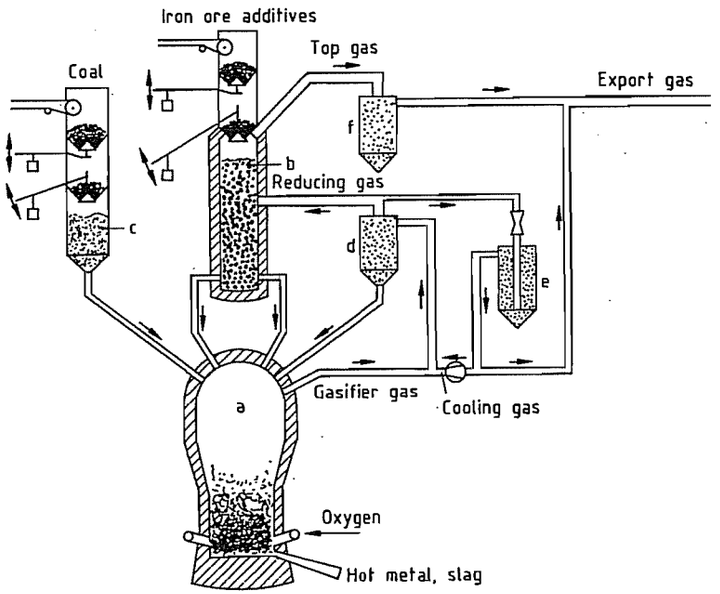

Figure 5.89: The Corex process, basic flow sheet with export gas: a) Melter–gasifier; b) Reduction shaft furnace; c) Coal feed system; d) Hot dust cyclone; e) Cooling-gas scrubber; f) Top-gas scrubber.

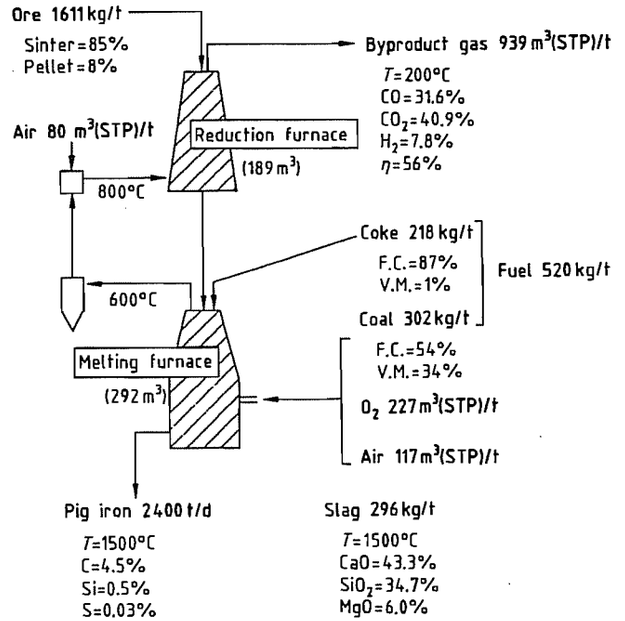

Figure 5.90: Expected material flow sheet for a Sumitomo SC commercial plant (F.C. = fixed carbon; V.M. = volatile matter).

The reducing gas is fed into the reduction furnace and countercurrently ascends through the iron burden.

The iron ore, charged into the shaft furnace through a lock hopper system, descends by gravity. The reduction reaction in the shaft furnace, using gas with ca. 70% carbon monoxide and 25% hydrogen is exothermic, leading to temperatures in the burden which are above the reducing gas temperature. Because of carbon monoxide decomposition, carbon deposits will form on the iron and act as a lubricant. Formation of Fe_3C occurs as well and cluster formation is avoided. The top gas is cleaned and cooled in a scrubber, and is then available for various purposes. Metallization of the DRI averages 90–95%, and its carbon content is in the range of 3–5%, depending on the raw material used and operating conditions.

The continuous transfer of the hot DRI (temperature 800–900 °C) from the reduction furnace to the melter gasifier is carried out by a special controllable transport system which discharges into connected downcomers. The velocity of the descending sponge iron particles is lowered in the fluidized bed, further reduction is completed, heating and melting occurs. Hot metal and slag drop to the bottom of the melter–gasifier. Analogous to the practice in the blast furnace hot metal and slag are discharged by conventional tapping procedures. Tapping is carried out every 2.5–3 h on an average. For a good desulfurization a slag basicity > 1 is required.

Temperature and silica content of the hot metal can be adjusted by various process parameters, i.e., coal particle size, height of the fluidized bed, system pressure, and rate of hot metal production.

The melter–gasifier may generate a certain amount of surplus gas depending on the coal selected. This surplus gas becomes part of the cooling gas stream, and can be either used separately or mixed with the top gas from the shaft furnace. When using a high volatile bituminous coal, the resulting gas mixture (export gas) approximates 1800 m^3 (STP) per tonne of hot metal with a lower heating value of ca. 8000 kJ/m^3 (STP).

According to the composition and quality of the coal, the specific oxygen consumption is ca. 450–550 m^3 (STP) per tonne of hot metal. The energy for the oxygen production can be supplied from about one third of the export gas of the Corex plant. The coal consumption depends on the coal quality and is ca. 0.5–0.7 t fixed carbon per tonne of hot metal.

If the export gas cannot be used economically, it is converted to reducing gas by removal of carbon dioxide and recycled. This process route offers the advantage of a lower coal and oxygen consumption.

The *Sumitomo SC process* [124–125] uses a combination of two shaft furnaces (Figure 5.90), the reduction furnace which produces DRI from lump ore and a coke-bed melting furnace which generates the reducing gas. Oxygen, air, and pulverized coal are blown into the coke bed. Low-grade coke is charged at the top of the melting furnace which corresponds to the lower part of a blast furnace or a cupola.

The gas coming out of the melting furnace with a temperature of 600 °C is cleaned in a cyclone, then it must be heated up by partial combustion with air to the reducing temperature of 800 °C.

The *melting furnace* was developed in a pilot plant with a capacity of 8 t/d in 1982. In 1984 the *reduction furnace* was integrated. Expected consumption figures (Figure 5.90) for a commercial plant are given on the basis of the result obtained by the pilot plant. The expected coke consumption of 218 kg per tonne of hot metal (in the pilot plant much higher) is nearly as high as that of a modern blast furnace with a high coal-injection rate. So the goal of a cokeless process is not achieved.

Kawasaki developed a smelting reduction process for ferrochrome production on the basis of a *coke-bed melter* with two-stage tuyères, the *XR process* [126, 127]. Powdered ore was prereduced in a fluidized-bed reactor and injected into the furnace through the upper tuyère. For iron production, this process was

modified to feed coal from the top as schematically shown in Figure 5.91.

Small-size degassed coal forms a fluidized bed in the upper part of the furnace and the lumpy char forms a packed bed in the lower part. The pilot plant for the XR process with a capacity of 10 t/d was started 1987. It is planned to reduce the fines in a circulating fluidized bed to a reduction degree of 80%.

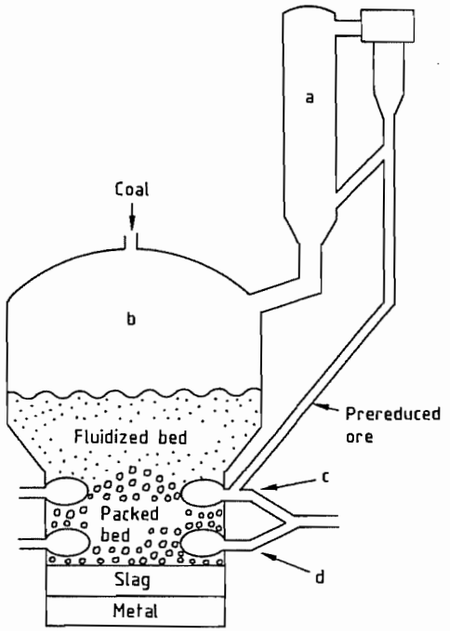

Figure 5.91: The Kawasaki XR process: a) Fluidized bed prereduction furnace; b) Coke-bed melter; c) Upper tuyère; d) Lower tuyère.

5.11.3 Converter-Type Melters

The converter-type melters are under development from the experience of the oxygen LD-BOF converter for steelmaking. Coal is injected with or without oxygen in a liquid iron bath.

In most of the processes the carbon monoxide hydrogen gas mixture coming out of the melt is partially combusted (postcombusted) to generate heat (up to 1900 °C) which is transferred to the bath. Processes using fine ore prereduce the ore in fluidized beds to a reduction degree of 15–90%. In most cases the process pressure is low (ca. 50 kPa). At present only the melting stage is developed for most of the processes. *Integrated operation* of melting and reduction has not been tested. Apart from the latter the most critical areas of these processes are refractory lifetime, gas-handling system (accretions), and foaming and splashing of the melt. Because of the high FeO-content in the slag the sulfur content of the hot metal is higher and the silicon content lower than in the blast furnace process.

Processes with Postcombustion. The most advanced converter process has been developed by Klöckner, Germany, and CRA, Australia, since 1981 [128–130]. After pretests a pilot 10 t-converter started operation in 1984 with a capacity of 4 t/h where especially postcombustion was investigated. The prereduction stage was not tested in this plant. In 1987 Klockner was bought out and CRA formed a joint venture with Midrex to further develop the process under the name *HIsmelt*. The flowsheet of the HIsmelt process is shown in Figure 5.92. Coal is injected from the bottom into the melt. The energy for melting and final reduction is generated by partial combustion of the converter gas with preheated air. The converter off-gas is used for prereduction of the fine ore. Because of the high oxidation degree of the gas it is only possible to reduce the ore to iron(II) oxide which is separated in a cyclone and fed to the converter. The main problem of this process is whether the high postcombustion degrees, up to 65% depending on coal quality, and reduction degree can be maintained for continuous operation and whether the huge amount of hot gas can be handled.

The *NKK process* [132, 133] is another converter type process which also operates with a high postcombustion degree (see Figure 5.93). Coal and oxygen are blown in from the top to the bath. The fine ore is prereduced only to a low degree.

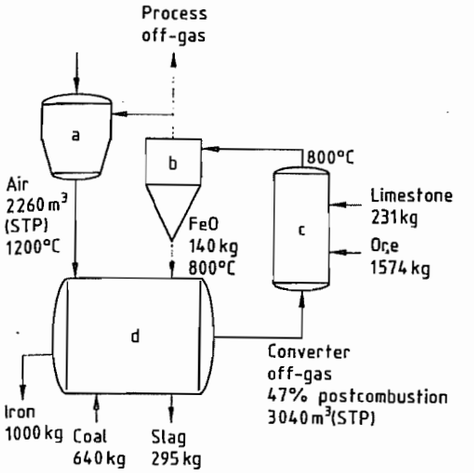

Figure 5.92: Flowsheet of HIsmelt process for the case 47% postcombustion and reduction to FeO: a) Air preheaters; b) Cyclone; c) Prereducer; d) HIsmelt converter.

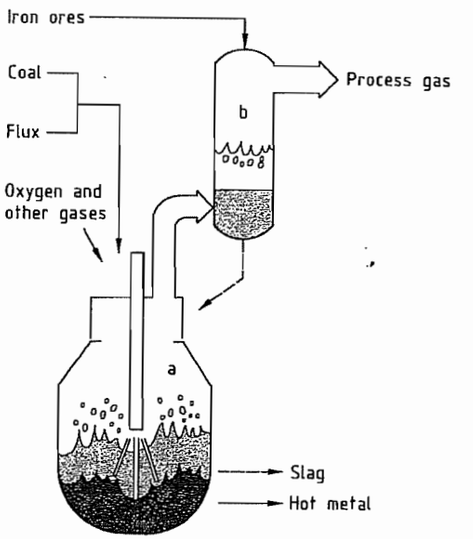

Figure 5.93: The NKK's smelting reduction process for ironmaking: a) Smelting reduction furnace; b) Preheating and prereduction furnace.

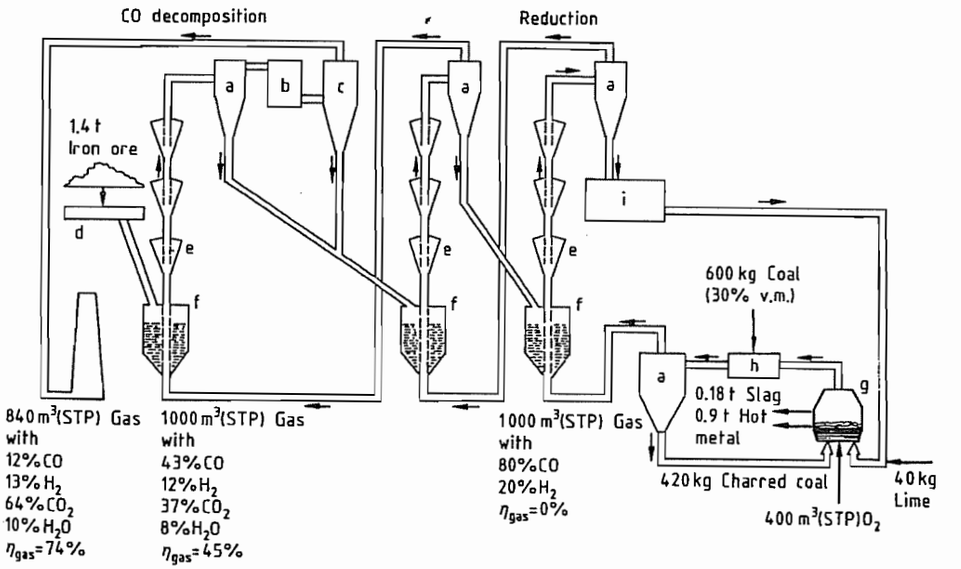

Figure 5.94: COIN concept of a coal-based smelting reduction process for iron ore fines: a) Hot cyclone; b) Gas cooler; c) Bag filter; d) Screw conveyor; e) Whirl box; f) Pneumatic conveyor; g) Melter–gasifier; h) Charring; i) 1 t directly reduced iron and 85 kg carbon.

Since 1986 tests have been performed in a 5 t-converter. In 1988 a prereduction stage was integrated in the pilot plant with a capacity of 100 t/d.

Processes Without Postcombustion. The Coin process [135–136] developed by Krupp operates without post combustion and with a high reduction degree. In the first published flow sheets the prereduction stage was a shaft furnace. The latest one (see Figure 5.94) shows a multistage prereduction of fine ore which was tested separately in a pilot plant. The prereduction stage is a combination of entrained-bed and fluidized-bed reactors.

The converter pilot plant is a 3 t-converter. To achieve a high degree of metallization a high reduction temperature is needed. Sticking of the ore is prevented by carbon monoxide decomposition in a prereduction stage at 500–600 °C. Oxygen and degassed coal is blown into the bath from the bottom. As no postcombustion delivers energy, the coal (especially high volatile coal) must be preheated and charred by injecting in the converter off-gas and recycling via a cyclone. The process is very complex and integration of the multistage prereduction, the coal devolatilizer, and the converter is not easy.

5.12 Aspects of Environmental Protection

In the recent past, the rapidly increasing environmental consciousness has led to considerably tightened environmental standards in many countries. In Germany, for instance, a limiting value for dust emissions of 150 mg/m^3 (STP) was stipulated as early as 1974 in the TA Luft for the prevention of air pollution. The amendment to the TA Luft in 1986 further reduced dust emissions in waste gases to 50 mg/m^3 (STP) [144]. This limit applies to *total* dust emissions. Lower limits have been set for *individual* components, such as heavy metals, e.g., 0.2 mg/m^3 (STP) for cadmium, mercury, and thallium; 1 mg/m^3 (STP) for arsenic, cobalt, nickel, selenium, and tellurium; and 5 mg/m^3 (STP) for antimony, lead, chromium, manganese, vanadium, and copper as well as cyanide and fluoride. Urged by stringent requirements, the steel industry has made substantial investments in environmental technology in recent years [145]. In Germany, for instance, from 1975 to 1984 ca. 2.4×10^9 DM (10% of the steel industry's resources for new investments) were spent on environmental protection. The lowering of dust emissions from 10 kg per tonne of raw steel in 1960 to the present value of 1.4 kg per tonne of crude steel serves as an example for the success of new techniques in controlling air pollution [146].

The endeavors towards pollution control are not limited to the *air pollution control*, but also include *water pollution control*, *reduction of noise*, and *waste management*. The division of capital expenditure between the individual areas in Germany (1975–1984) is as follows:

Air pollution control	67.7%
Water pollution control	21.4%
Noise reduction	9.5%
Waste management	1.4%
Total	2354×10^6 DM

It can be seen that the investment in air-pollution control represents two thirds of the total capital expenditure.

Apart from the *direct measures* taken to control pollution, the *saving* or *recovery* of *energy* also has a favorable effect on the environment because the corresponding amounts of energy can only be produced at the expense of the environment. The most important examples of these measures are (1) the reduction of the specific fuel consumption during sintering by half since the 1950s, (2) the expansion of blast-furnace top gas in turbines and its utilization for heating, (3) dry coke quenching, and (4) CO gas recovery.

Pollution-control techniques being currently employed in pig-iron production and in related auxiliary plants will be described with a series of examples. However, in view of the diversity of processes available, a complete survey cannot be presented here.

5.12.1 Air Pollution Control

Virtually all areas of ironworks make use of gas dedusting techniques. Apart from mechanical and filtering dust separators and scrubbers, electrostatic precipitators are frequently used today [147–149].

Sintering Plants. In the past, dust separation from off-gases in iron-ore sintering plants was carried out with cyclones. Today's demands are essentially fulfilled by three-field horizontal dry electrostatic precipitators, which are operated on the suction side of the sinter waste-gas fan. The waste-gas flow rate of a sinter belt with a reaction area of e.g., 400 m^2 is in the range of 1.8×10^6 m^3/h. As shown in Figure 5.95, the waste-gas dedusting in that case is achieved in two parallel electrostatic precipitators.

The electrical resistance of sinter dust, which in most cases is very high, frequently impedes electrostatic dust precipitation [150]. Increasing the humidity of the gas, by adding water either to the off-gas or to the sinter belt, can improve dust separation by reducing the *electrical resistance* of the dust. Dust emission can be reduced by 20–50% of the starting values by conditioning the waste gas with sulfur trioxide [149]. In this process sulfur dioxide, obtained, e.g., by combustion of sulfur, is oxidized to sulfur trioxide and added to the waste gas in front of the electrostatic filter. A level of 10–30 ppm of sulfur trioxide in the waste gas is sufficient to reduce the electrical resistance of dust and thus cause the improvement in dedusting efficiency mentioned above. The required amount of sulfur trioxide is so low that only ca. 33 kg/h of sulfur are needed to produce e.g., 20 ppm of sulfur trioxide for the conditioning of the waste gas of a 400 m^2 sinter belt. Extra sulfur trioxide emission does not occur because it is bound to the dust by chemisorption (sulfate formation). The effect of this process depends on the basicity of the sinter feed and on the composition of the raw material.

Simple housings at feeding points, at the sinter discharge end, at screening machines and at numerous transport devices cannot effectively prevent the escape of dust into the surroundings. For this reason, *suction hoods* are installed that are connected by means of branched ducts to a central dedusting system, which is often an electrostatic precipitator. The schematic of a so-called room dedusting system of this type is presented in Figure 5.96. In many cases, the dust-laden off-gas from the sinter cooler is passed through the room dedusting plant, however, it may sometimes be led to a separate electrostatic precipitator.

Blast Furnace. A blast furnace with an open top is not used any longer. Dedusting systems have allowed the cleaning of top-gas to dust loading values of < 10 mg/m^3 (STP), and thus have permitted the utilization of the energy contained in this gas in turbines and for the heating of hot blast stoves. Apart from the direct protection of the environment brought about by top-gas purification compared to an open top, an indirect effect is achieved by saving energy which would have to be produced at the expense of the environment.

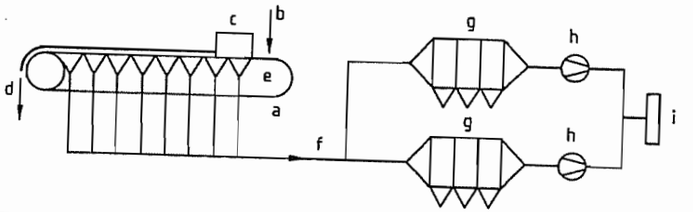

Figure 5.95: Sinter plant waste-gas dedusting: a) Sintering machine; b) Feed point; c) Igniter; d) Sinter; e) Wind boxes; f) Manifold; g) Electrostatic precipitator; h) Fan; i) Stack.

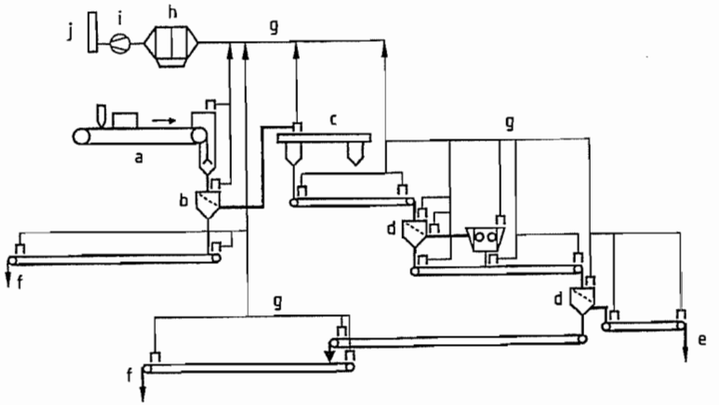

Figure 5.96: Sinter plant room dedusting: a) Sintering machine; b) Hot screening; c) Cooler; d) Cold screening and crushing; e) Sinter product; f) Return fines; g) Suction system; h) Electrostatic precipitator; i) Fan; j) Stack.

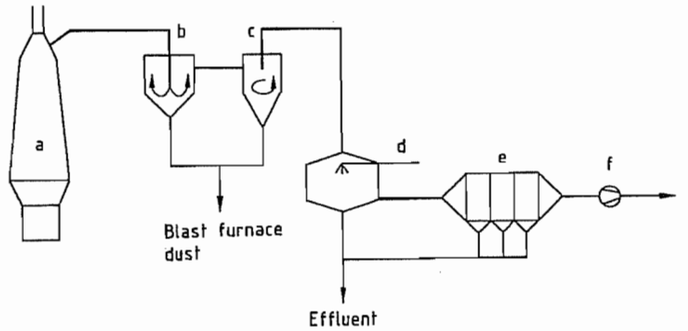

Figure 5.97: Top-gas cleaning: a) Blast furnace; b) Gravity dust catcher; c) Cyclone; d) Scrubber; e) Wet electrostatic precipitator; f) Fan.

The top-gas leaving the blast furnace (a) is loaded with 10-40 g/m^3 (STP) of dust. The volumetric flow rate of a blast furnace that has, e.g., an output of 5000 t of hot metal per day is ca. 420 000 m^3/h (STP). Figure 5.97 shows the components of the top-gas purification plant of a blast furnace that is operated at a *slight overpressure*. The larger particles of dust are first separated in a gravity dust catcher (b), i.e., a settling chamber with flow deflection, and subsequently in a cyclone (c). Further cleaning of the blast-furnace gas occurs in a single- or multiple-stage scrubber (d) and in a wet electrostatic precipitator (e), which carries out both fine purification as well as removal of droplets. If the top-gas volumetric flow rates are very high, several purification plants are installed in parallel.

The top-gases from blast furnaces that are operated at *higher pressures* can be freed from dust to the desired degree of purity by using a pressure difference of ca. 20 kPa in high performance scrubbers without an electrostatic precipitator. Another method of top-gas dust separation, which has been repeatedly and successfully used recently, is dry dust removal in electrostatic precipitators. This method has the advantage of involving low pressure losses and consequently has a lower energy requirement for gas transport and, in addition, water and sludge treatments are no longer necessary. Dry top-gas purification represents the latest technological development.

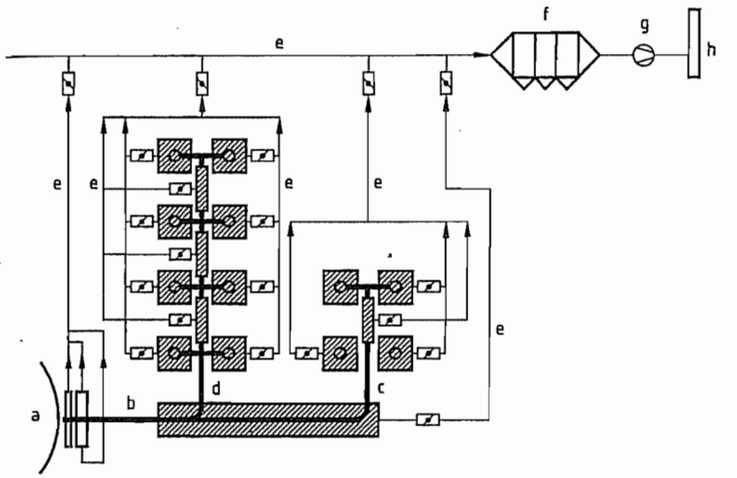

Figure 5.98: Cast house dedusting: a) Blast furnace, area of tapping hole; b) Main runner with skimmer; c) Hot metal runner with transfer points; d) Slag runner with transfer points; e) Suction lines; f) Electrostatic precipitator; g) Fan; h) Stack.

In the area of raw material handling a room dedusting plant prevents dust emissions. The burden bunkers and conveyors are connected by a suction system to a bag filter or an electrostatic precipitator.

The smoke that arises during the tapping of the blast furnace represents a minor environmental problem as far as emission protection is concerned. However, it is a nuisance for the operating personnel and makes working conditions on the casting platforms very difficult. *Cast house dedusting* is being carried out for some years now to improve working conditions. In fact, even older blast furnaces are being equipped with dedusting systems [151, 152]. The enclosing of the skimmer, iron, and slag runners and their points of transfer with easily removable hoods having fire-proof linings is characteristic for a casting house dedusting plant. The enclosed areas are connected to suction lines, which are preferably installed below the casting platform. The region of the tapping hole cannot be enclosed because it has to remain accessible to the drilling and plugging machines. In this case, smoke is usually caught with a suction hood placed near the tapping hole and then led to the precipitator. The flow diagram of the main, hot metal, and slag runners on a casting platform as well as the suction system is shown in Figure 5.98. The hatched parts of the diagram represent the enclosed areas. It can be seen that each suction point has a damper. When the plant is in operation, only the suction points at which smoke is to be trapped are opened. For instance, if no slag is discharged in the first phase of tapping, all the dampers on the slag runner remain closed.

In blast furnace tapping, the flow volume that has to be trapped, dedusted, and transported is 500 000–800 000 m^3/h. The power consumption of a casting house dedusting system can reach 0.8 MW, hence, modern plants are automatically controlled. Control dampers in the suction lines and variable-speed blowers draw off as little air as necessary. For example, a minimum amount of air is withdrawn during tapping pauses and maximum amounts at the start and termination of tapping. Bag filters or electrostatic precipitators are employed as dust collectors. The advantages of electrostatic precipitators are the substantially lower pressure loss and the fact that they can be operated during tapping pauses with minimal power input.

Dry Coke Quenching. As mentioned above, dry quenching of coke also has a positive effect on the environment, because of the fact that, in contrast to wet quenching, the waste heat of the coke is utilized and no cooling clouds are produced. The heat is removed from the coke with the help of recirculating gas and used for steam generation in a waste-heat boiler. In an ironworks in Germany, two 70 t/h dry coke quenching plants produce 36 t/h of steam each, which is then used as a fuel substitute in a neighbouring power plant [153]. The fuel saved in this way contributes to environmental protection. An equivalent of > 20 MW of electrical power is produced.

Direct Reduction Plants. In direct reduction plants the waste gases leaving the furnace are freed from dust in an electrostatic precipitator, bag filter or scrubber, depending on the requirements in the operational areas. Electrostatic precipitators or bag filters are used for room dedusting plants.

Regarding the emissions of the dust components mentioned above, cadmium, lead, and possibly manganese can be of relevance in the making of pig iron, however, the limiting values for these metals are generally adhered to.

5.12.2 Prevention of Water Pollution

In the course of pig iron production, modern ironworks cause practically neither water pollution, nor warming up of waters. Only small amounts of water are required in *sintering plants* for rolling the burden and, if necessary, for sinter cooling or gas conditioning. The water used is released into the atmosphere in the gaseous state through the waste gas stack. Generally, direct *reduction plants* do not produce wastewater.

Blast furnaces, on the other hand, have a considerable water requirement for cooling. In the past, up to 60 m^3 of water were consumed per tonne of pig iron [154]. Another water-consuming process pertaining to the blast furnace is wet top-gas purification. It is becoming increasingly rare today that the wastewater of this process is released into the atmosphere. In fact, the introduction of a closed water circulation with the appropriate water conditioning plant [155, 156] for top-gas purification and blast furnace cooling contributes to the marked decrease in the water requirement for steelmaking, which is today ca. 30 m^3 per tonne of raw steel [146].

Blast-furnace cooling with a closed circulation requires water-cooling plants. Usually the circulation water is evaporated in the blast furnace coolers and condensed and cooled in cooling towers.

The essential components of a scrubber/precipitator effluent for top-gas purification are shown in Figure 5.99. The clarification of the effluent can be carried out in a thickener and the dewatering of the sludge in a filter press. However, other dewatering machines, such as drum or rotary disk filters may be applied.

5.12.3 Noise Reduction

As in other industrial plants, numerous sources of noise exist in ironworks, which contribute to the total noise emission. Many of these noise sources are not specific to the production of pig iron. These include fans, compressors, pumps and ore-dressing plants. The noise abatement measures consist of, e.g., the use of low-vibration motors, the enclosing of machines or other apparatus, or even entire parts of the plant, such as the sinter waste-gas fans [157].

Special measures are required to dampen the feeding and expansion noises at hot blast stoves. Considerable noise reduction can be achieved here by covering the valves and the expansion line with a sound-absorbing material and by using sound absorbers or perforated disks in the blowoff line [158]. Emission values of ca. 40 dB(A) can be achieved at a distance of 1000 m from a blast furnace or sintering plant if noise damping measures are used consistently [159].

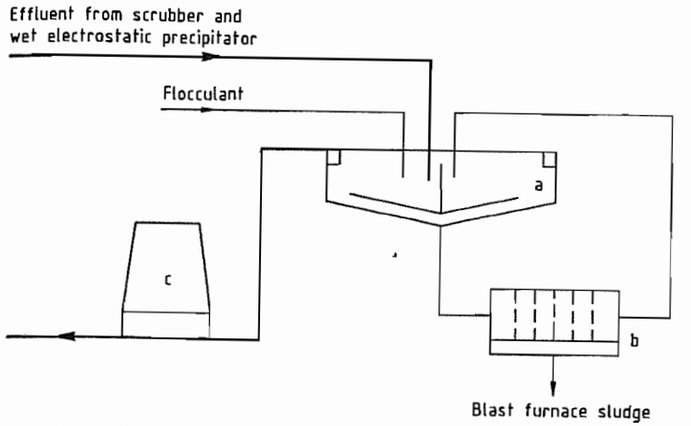

Figure 5.99: Effluent treatment for top-gas cleaning: a) Thickener; b) Filter press; c) Cooling tower.

5.12.4 Waste Management

Blast furnace slag is quantitatively the most important waste material created in the production of pig iron. This material is completely utilized. About two thirds of the total amount is employed in road construction. The remainder is used by the cement industry for the production of blast furnace cement [160].

The recycling of the *dry dust* obtained in top gas purification also causes no problems because it can be recycled to the sintering plant. However, *blast furnace sludge* is for the most part still being dumped, in amounts of 130 000 t/a in Germany [161]. The reason for this is the high content of lead, zinc, and alkali found in the sludge. If the sludge were recirculated, these substances would accumulate in the blast furnace. Today, various processes are available which reduce the environmental impact caused by these dumps by allowing the recycling of blast furnace sludge and other waste containing lead and zinc.

One way of expelling the unwanted accompanying substances is the reprocessing of dusts and sludge in rotary kilns [162–165]. The product thus obtained consists essentially of metallic iron, which can, e.g., be briquetted and returned to the pig iron production [166].

Most of the dust separated in the waste-gas precipitators of sintering plants can usually be led back into the process. Only the dust arising in the last field of the electrostatic precipitator must be removed from the circulation because of alkali enrichment.

The prime goal is always the avoidance or minimizing of residual substances. For example the specific amount of slag has decreased from 800 kg/t at the beginning of the 1950s to 300–350 kg/t of pig iron today. In a modern steel plant, ca. 90% of the total amount of waste products is recycled.

5.13 Economic Aspects

Pig Iron. The conventional and by far the most common approach to iron manufacture involves reducing and smelting the iron ore in a blast furnace together with coke, the immediate product being pig iron. Pig iron, in turn, is the principal raw material for the manufacture of commercial iron and steel. Production of a tonne of steel requires ca. 700 kg of pig iron in addition to scrap and flux.

World production of pig iron in 1988 reached a level of 532×10^6 t, derived from ca. 960×10^6 t of iron ore (Tables 5.40 and 5.41) [167]. The European Community alone produced 93.7×10^6 t of pig iron in 1988, using 142×10^6 t of ore and sinter together with 44×10^6 t of coke [168]. The major cost factors in pig iron manufacture are related to raw materials (41%), fuel (34%), and processing (25%).

Table 5.40: Iron ore production and fraction of world output, reported by country.

Country	Fe content, %	Production, 10^6 t			% of World Output		
		1986	1987	1988[a]	1986	1987	1988[a]
France	30	12.6	11.3	10.0	1.3	1.2	1.0
United Kingdom	28	0.3	0.3	0.2	0	0	0
Germany	30	0.7	0.2	0.1	0.1	0	0
Spain	46	6.1	3.3	3.9	0.6	0.4	0.4
Sweden	64	20.5	19.6	20.4	2.1	2.1	2.1
Turkey	57	4.0	4.5	4.8	0.4	0.4	0.5
Norway	64	3.5	3.1	2.6	0.4	0.4	0.3
Austria	30	3.1	3.1	2.3	0.3	0.3	0.2
Finland	59	0.7	0.7	0.6	0.1	0.1	0.1
United States	62	39.6	47.0	57.4	4.1	5.1	6.0
Canada	64	37.3	37.8	40.2	3.9	4.1	4.2
Brazil	65	129.5	134.0	145.0	13.6	14.5	15.1
Venezuela	64	16.7	17.2	18.2	1.7	1.9	1.9
Mexico	62	8.0	7.0	8.5	0.8	0.8	0.9
Peru	67	5.3	5.4	4.3	0.6	0.6	0.4
Chile	60	6.3	6.2	7.3	0.7	0.7	0.8
Argentina	39	0.6	0.7	0.7	0.1	0.1	0.1
Other Latin America		0.4	0.6	0.6	0	0.1	0.1
South Africa	64	24.5	22.0	22.7	2.6	2.4	2.4
Liberia	60	15.6	13.8	12.8	1.6	1.5	1.3
Mauretania	61	9.2	9.0	9.7	1.0	1.0	1.0
Algeria	50	3.4	3.4	3.5	0.4	0.4	0.4
Egypt	44	2.0	2.0	2.0	0.2	0.2	0.2
Tunisia	50	0.3	0.3	0.3	0	0	0
Morocco	63	0.2	0.2	0.1	0	0	0
Zimbabwe	64	0.8	0.9	1.0	0.1	0.1	0.1
India	63	48.8	48.4	52.5	5.1	5.3	5.5
Iran	46	0.3	0.3	0.5	0	0	0.1
South Korea	48	0.5	0.5	0.8	0.1	0.1	0.1
Japan	50	0.3	0.3	0.2	0	0	0
Other Asia		0.3	0.3	0.3	0	0	0
Australia	62	97.3	104.6	95.4	10.2	11.3	9.9
New Zealand	57	2.6	2.3	3.0	0.3	0.3	0.3
Former Soviet Union	60	250.0	251.0	250.4	26.2	27.2	26.1
China	60	142.5	157.0	153.8	14.9	17.0	16.0
North Korea	48	8.0	8.0	8.0	0.8	0.9	0.8
Yugoslavia	35	6.8	4.2	5.6	0.7	0.5	0.6
Rumania	26	2.0	2.0	2.0	0.2	0.2	0.2
Bulgaria	33	2.1	1.9	2.1	0.2	0.2	0.2
Former Czechoslovakia	26	1.8	1.8	1.8	0.2	0.2	0.2
Hungary	24						
Albania	50	0.8	0.8	0.8	0.1	0.1	0.1
EEC		19.7	16.5	14.2	2.1	1.8	1.5
Western nations		501.1	495.2	535.5	52.5	53.7	55.8
Socialist nations		433.7	426.7	424.5	45.4	46.3	44.2
World total		954.5	921.9	960.0	100	100	100

[a] Preliminary figures, in some cases estimates.

Table 5.41: Pig iron production and fraction of world output, by country.

Country	Production, 10^6 t			% of World Output		
	1986	1987	1988[a]	1986	1987	1988[a]
EEC	85 324	85 603	93 681	17.45	16.94	17.62
Germany	29 018	28 517	32 453	5.94	5.64	6.11
Belgium/Luxembourg	10 724	10 559	9 182	2.19	2.09	1.73
France	13 982	13 449	14 786	2.86	2.66	2.78
United Kingdom	9 812	11 914	13 235	2.01	2.36	2.49
Italy	11 886	11 355	11 376	2.43	2.25	2.14
The Netherlands	4 628	4 575	4 994	0.95	0.91	0.94
Portugal	463	431	445	0.09	0.08	0.08
Spain	4 811	4 804	4 691	0.98	0.95	0.88
Finland	1 978	2 063	2 173	0.41	0.41	0.41
Norway	570	370	367	0.12	0.07	0.07
Austria	3 349	3 451	3 664	0.69	0.68	0.69
Sweden	2 435	2 314	2 494	0.50	0.46	0.47
Switzerland	65	70	70	0.01	0.01	0.01
Turkey	3 666	4 068	4 437	0.75	0.81	0.83
United States	39 772	43 917	50 457	8.14	8.68	9.49
Canada	9 249	9 719	9 486	1.89	1.92	1.78
Japan	74 651	73 418	79 295	15.27	14.53	14.92
Australia	5 853	5 579	5 723	1.20	1.10	1.08
OECD Nations	232 181	230 497	251 837	47.50	45.61	47.38
Former Soviet Union	113 600	113 900	114 000	23.24	22.53	21.45
German Democratic Republic	2 625	2 743	2 750	0.54	0.54	0.52
Bulgaria	1 600	1 656	1 650	0.33	0.33	0.31
Poland	10 200	10 023	10 000	2.09	1.98	1.88
Rumania	9 500	9 500	9 500	1.94	1.88	1.79
Former Czechoslovakia	9 600	9 788	9 800	1.96	1.94	1.84
Hungary	2 075	2 109	2 050	0.42	0.42	0.39
Comecon Nations	149 200	149 770	149 750	30.52	29.64	28.17
Former Yugoslavia	3 067	2 868	2 912	0.64	0.57	0.55
South Africa	5 774	6 317	6 112	1.18	1.25	1.15
Zimbabwe	644	560	545	0.13	0.11	0.10
Argentina	1 639	1 752	1 610	0.34	0.35	0.30
Brazil	15 838	21 335	23 627	3.24	4.22	4.44
Chile	591	617	778	0.12	0.12	0.15
Colombia	319	326	310	0.07	0.06	0.06
Mexico	3 728	3 698	3 642	0.76	0.73	0.69
Peru	216	179	202	0.05	0.04	0.04
Venezuela	491	471	506	0.10	0.09	0.10
China	47 000	50 200	51 000	9.62	9.93	9.59
India	10 509	10 920	11 709	2.15	2.16	2.20
North Korea	5 750	5 900	5 900	1.18	1.17	1.11
South Korea	9 003	11 057	12 585	1.84	2.19	2.36
World	488 836	505 514	531 575	100	100	100

[a] Preliminary figures, in some cases estimates. Source for EEC data: SAEG; for all other nations: IISI.

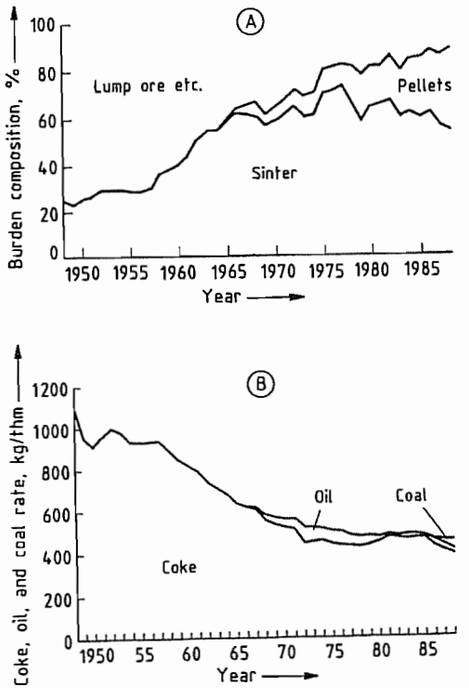

Figure 5.100: Development of blast furnace burden composition (A) and fuel rate (B) in Germany since 1950 for basic pig iron.

In view of the massive requirements for raw material and energy, and investment costs, the potential for savings through optimization of scale and exploitation of more economical sources of raw material is extremely attractive. Environmental protection measures have also come to play an increasingly important economic role in iron manufacture in recent years.

Careful organization and quality control on the input side of pig iron production is also important with respect to the properties of the principal end product—steel—and consequently on the market picture as it relates to steel vs. alternative materials. Economic factors and quality are therefore closely linked.

Several recent developments deserve special mention as determinants of the competitiveness of steel, especially from the standpoint of cost reduction:

- Increased emphasis on major sources of ore displaying a high iron content, a consideration which helps to minimize fluctuations in ore quality.
- Significant improvement in the facilities for *handling* and *transporting* ore in increasingly large unit amounts. Intercontinental marine ore transport today involves units as large as 350 000 dwt (i.e., dead weight), representing a three-fold increase in maximum load in the course of 20 years.
- Steady improvement in the *preparation of the furnace charge* in terms of ore classification, sintering, and pelleting. For example, the use of lump ore has decreased in Germany from 35% in 1970 to < 10% currently. Sinter input, on the other hand, has increased to 60%, and pelletized ore—virtually unknown before 1965—now represents 30% of the charge (Figure 5.100).
- Significant reduction in *fuel consumption* and more variety in the nature of the fuel employed for reduction.

Fuel consumption has dropped by a total of ca. 20% over the last 20 years, now amounting to only 480 kg per tonne of pig iron. Coke continues to constitute the major source of fuel (415 kg/t), although since about 1986 inexpensive coal has increasingly been used as a coke substitute (40 kg/t). Petroleum fuel currently accounts for ca. 25 kg/t.

By far the largest part of the pig iron output goes into *steel production*: ca. 91 × 10^6 t (97%) in the case of the EEC with an additional 2 × 10^6 t consumed by foundries. About 0.7 × 10^6 t in the form of spiegel eisen and high-carbon ferromanganese are being used for the production of alloyed steel.

In Europe essentially *no open market* exists for basic pig iron, because the steel industry is effectively self-supporting. Iron of this type is purchased only rarely and in times of shortage, as when demand is particularly strong or some industrial mishap causes supply problems. By contrast, there is a lively trade in such products as *foundry iron*, *hematite iron*, and *spheroidal pig iron*. The list price of foundry iron, for example, remained steady in the range of

55–75 $/t for nearly 20 years. It finally began to climb at the time of the 1974 oil crisis as a result of increasing energy prices, subsequently reaching a level of 190–260 $/t.

The largest exporter of pig iron, and by a wide margin, is *Brazil* at 2 × 10^6 t/a, followed by *Canada* and *Germany* with ca. 0.5 × 10^6 t/a each (Table 5.42) [169].

Sponge Iron. The direct reduction process (see Section 5.10) has recently provided the market with a new form of pig iron: sponge iron, available in significant quantity since the 1970s and produced from lump ore or pellets. Current world output of sponge iron is estimated at 14 × 10^6 t/a.

Table 5.42: Development of import and export of pig iron (worldwide).

Country	1981	1982	1983	1984	1985	1986	1987	1988
Import[a]								
EEC[b]	1550	1672	1430	1541	1698	1885	1906	2363
Germany	285	303	279	295	348	379	364	324
Belgium/Luxembourg	172	132	89	135	160	159	182	309
Denmark	52	66	31	38	61	77	79	113
France	435	399	385	447	505	413	424	325
United Kingdom	148	165	168	102	124	148	119	233
Ireland	1	2	1	1	1	1	1	3
Italy	348	437	319	400	335	475	530	745
Netherlands	51	50	39	64	62	61	60	72
Greece	17	14	17	7	14	25	21	
Spain	41	104	102	52	88	147	126	8
Austria	95	89	51	66	67	52	42	62
Sweden	64	83	61	64	69	77	62	25
Switzerland	65	74	72	71	78	42	34	46
Former Czechoslovakia	843	901	780	745	869	809	717	685
Japan	1068	1337	952	777	604	921	1443	2917
United States	857	633	456	925	307	603	378	811
Poland	1449	1273	1135	1188	1354	1323[c]	1338	
Hungary	291	235	295	281	321	255	263	
Former Yugoslavia	71	99	65	75	57	57[c]	27	
Export[a]								
EEC[b]	1420	1013	996	1145	1281	690	697	713
Germany	821	622	497	590	705	542	540	464
Belgium/Luxembourg	19	17	16	27	26	23	30	38
Denmark		1						
France	538	332	389	475	451	12[d]	54	55
United Kingdom	35	31	60	34	59	33	43	31
Ireland			2			1		
Italy	1	3	22	10	22	61	20	37
Netherlands	6	5	12	9	18	18	10	4
Norway	280	213	183	160	212	185	191	134
Austria					1	1	7	
Sweden	45	30	27	3	7	10	3	12
Australia	158	300	350	150				
Japan	12	61	341	285	1083	1058	51	30
Canada	523	526	389	449	654	602	523	388
United States	33	59	14	61	40	50	53	70
Hungary			5	21				
Brazil	714	693	1801	2473	2476	2369	2445	2532

[a] Pig iron including spiegel iron and blast furnace ferromanganese.
[b] Including internal exchange, 1988 without Greece.
[c] Preliminary.
[d] Export not totally broken down because of security reasons.

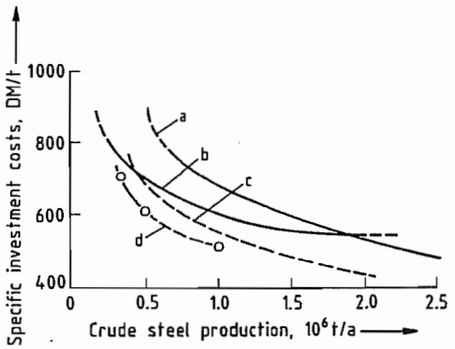

Figure 5.101: Specific investment costs for steel mills based on coal.

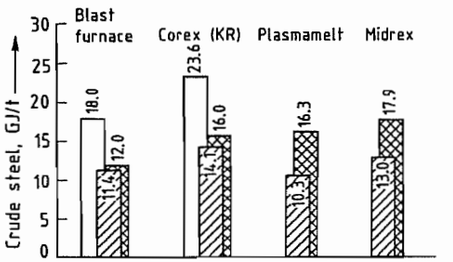

Figure 5.102: Comparison of specific gross energy consumption (□), net energy consumption (▨), and consumption of primary energy referred to net energy (▨) for different production processes (for the production of 1 t of crude steel based on ore).

This newer production method represents a significantly more economical route to pig iron than that involving coke when alternative forms of energy are available in abundance (e.g., natural gas, as in the case of Indonesia, Malaysia, the Middle East, Mexico, and Venezuela). Indeed, sponge iron can often be produced for 120$/t under appropriate conditions, and most of the direct reduction facilities currently in operation are located in the regions cited [170].

Sponge iron is devoid of elemental silicon and phosphorus, and it contains only little carbon i.e., it lacks any source of energy for the subsequent conversion to steel. In this sense it is comparable to steel scrap, and it is highly priced as a charge for electric furnaces where these can be operated economically.

Alternative Production Methods. So far, no other alternative routes to iron manufacture have achieved any significance. The current trend in technical innovation is suggested by the Corex method utilizing a melter–gasifier which was developed in Germany and first introduced in South Africa in 1988. One important advantage of the process is a significant reduction in environmental pollution, and it also avoids the expensive construction of coking pelletizing, and sintering facilities. The potential cost saving has been estimated at as much as 30%.

Size of the Production Facility. One way of classifying the various manufacturing methods is in terms of dimension (scale, capacity). For example, *blast furnaces* today may be as large as 15 m in diameter, with a working volume of 5580 m^3 (Cherepovets, Novolipetsk). Nevertheless, massive facilities such as these are not always optimal from an economic standpoint, nor do they necessarily match the needs in a given situation. Local factors and a desire for flexibility may well dictate smaller units. Thus, the average blast furnace in Japan has a diameter of 12 m, while in Germany 9 m is more typical.

For technical reasons, *direct reduction* facilities are much smaller, with a typical maximum annual output of 600 000 t. The first *smelting reduction* Corex units are currently producing only ca. 300 000 t/a.

Lower investment costs are responsible for the fact that smaller steel mills in particular (i.e., those with an annual output $< 1 \times 10^6$ t) tend to utilize a direct-reduction or smelting-reduction iron process (Figure 5.101) in contrast to the blast furnaces at larger integrated steel mills, where the *lower fuel consumption* associated with a conventional blast furnace is the decisive factor [171] (Figure 5.102).

The principal economic factors addressed here with respect to iron intended as a precursor to steel—performance of the production unit, investment costs, energy consumption, advantages of scale—all suggest that the blast furnace will continue to retain its primacy over the long term. Only where unusual local conditions favor other sources (through cheap sources of energy or limited demand) is the otherwise efficient and economical blast furnace likely to be displaced.

5.14 Pure Iron [172, 173]

The pure metal is not often encountered in commerce, but is usually alloyed with carbon or other metals. Chemically pure iron can be prepared either by the reduction of pure iron oxide (best obtained for this purpose by heating the oxalate in air) with hydrogen, or by the electrolysis of aqueous solutions of iron(II) salts, e.g., of iron(II) ammonium oxalate. On the technical scale, pure iron is prepared chiefly by the thermal decomposition of iron pentacarbonyl. The so-called "carbonyl iron" prepared in this way initially contains some carbon and oxygen in solid solution. These impurities can be removed by suitable after treatment.

Table 5.43: Some physical properties of iron.

Density at 20 °C, g/cm³	7.874
Thermal expansion coefficient at 20 °C	11.7×10^{-6}
Lattice constant, cm	2.861×10^{-8}
Melting point, °C	1539
Boiling point, °C	≈ 3200
Temp. of α,γ transformation (A_3) on heating, °C	910
Temp. of γ,δ transformation (A_4) on cooling, °C	1400
Resistivity at 20 °C, Ωcm	9.7×10^{-6}
for commercial iron	11×10^{-6}
Temperature coefficient of resistance	0.0065
Compressibility, cm²/kg	0.60×10^{-6}
Specific heat, cal g^{-1} K^{-1}	0.105
Heat of fusion, cal/g	64.9
Heat of α,γ transformation, cal/g	3.86
Heat of γ,δ transformation, cal/g	1.7
Linear correction at α,γ on heating	0.0026
Linear correction at γ,δ on heating	0.001–0.003
Modulus of elasticity, lb/in²	30×10^6
dynes/cm²	21×10^{11}
Modulus of rigidity, lb/in²	12×10^6
Proportional limit for annealed iron, lb/in²	19×10^3
Tensile strength, lb/in²	$25–100 \times 10^3$
Brinell hardness number (annealed)	50–90

Pure iron is a lustrous, rather soft metal (hardness 4.5). Some of its physical properties are given in Table 5.43. Iron is ferromagnetic, i.e., it is strongly magnetized when placed in a magnetic field. Unlike iron which contains carbon, pure iron has a very low remanence, i.e., it instantly loses its magnetization when the applied electric field is removed. For this reason it finds certain applications in electrotechnology, e.g., for electric motors and transformers, in which rapid fluctuations must occur in the magnetism of an iron core. In the solid state, iron can have several allotropic forms depending primarily on its temperature. These are:

- α-Iron: magnetic and stable to 768 °C, crystallizes in a body centered cubic lattice, i.e., iron atoms are arranged at the centre and the apexes of unit cubes. It dissolves very little carbon (0.025% at 721 °C). Alpha iron with the carbon traces dissolved in it is called *ferrite*.
- β-Iron: it is a form stable between 768 and 910 °C. It is alpha iron that has lost its magnetism. It does not dissolve carbon.
- γ-Iron: this form is stable between 910 and 1390 °C. The crystallographic appearance is a face centered cubic lattice, i.e., iron atoms are arranged at the apexes and centers of the sides of unit cubes. It is nonmagnetic and dissolves 2% carbon at 1102 °C. Gamma iron with carbon in solution is called *austenite*.
- δ-Iron: the last of the allotropic forms, it is nonmagnetic and stable between 1391 and 1537 °C, melting point. The crystallographic arrangement is in the form of a body-centered cubic lattice.

The physical properties of iron are changed by the presence of foreign elements (metalloids or metals) in very small amounts.

Iron has a great affinity for oxygen. It rusts in moist air, i.e., the surface gradually becomes converted into iron oxide hydrate. Compact iron reacts with dry air only above 150 °C. When heated in air it forms the intermediate oxide, Fe_3O_4, which is also formed during the forging of red hot wrought iron. In a very finely divided state — such as is obtained, for example, when iron oxalate is heated in hydrogen — iron is pyrophoric.

Iron objects are protected from rusting by covering them with coatings of other metals (e.g., zinc, tin, chromium, nickel) or with paint (red lead). A particularly effective protection from rust can be achieved by converting the iron superficially to iron(II) phosphate ("phosphatizing"). This is done by treatment with a solution of acid manganese or zinc phosphate, $Mn(H_2PO_4)_2$ or $Zn(H_2PO_4)_2$. Iron dissolves in dilute acids with the evolution of hydrogen and the formation of iron(II) salts. The normal potential of iron in contact with iron(II) salt solutions is +0.440 V at 25 °C, relative to the normal hydrogen electrode. If iron is dipped into a copper sulfate solution, it becomes covered with metallic copper:

$$Fe + Cu^{2+} \rightarrow Fe^{2+} + Cu$$

At ordinary temperature, iron is hardly attacked by air-free water. If air has access, however, the porous iron(III) oxide hydrate is formed, and corrosion goes on continuously as a result. Concentrated sodium hydroxide attacks iron, fairly strongly, even in the absence of air, especially at high temperatures, since the $Fe(OH)_2$ goes into solution through the formation of hydroxo salts.

Iron combines energetically with chlorine when heated, and also with sulfur and phosphorus, but not directly with nitrogen. It has a strong tendency, however, to unite or alloy with carbon and silicon. These alloys are most important for the properties of technical iron. Oxygen is dissolved by molten iron, as FeO; some of this is retained in solid solution on cooling (δ-iron can dissolve up to 0.12%, α-iron only up to 0.04% of O in solid solution). The oxygen content of iron reduces its workability when hot. Nitrogen is absorbed from the air by molten iron only in minimal amounts. However, if iron is heated in ammonia gas, an iron–nitrogen compound, Fe_2N, is formed, which displays a considerable solubility in solid iron, and confers great hardness. This property is utilized in the surface-hardening of iron articles, by heating them in ammonia (nitriding process). In addition to the foregoing, there is a second compound, Fe_4N, with a rather narrow range of homogeneity. Above 660 °C, this is transformed without change of composition into crystals of Fe_2N, in which only one half of the available lattice positions are occupied by nitrogen atoms.

Hydrogen is also absorbed by iron at a red heat. The amount absorbed is small, and is proportional to the square root of the pressure. Electrolytic iron, however, may contain larger amounts of hydrogen, which make it hard and brittle. The hydrogen is driven off on heating, and the iron then becomes ductile.

5.15 Iron–Carbon System

A variety of textural constituents can be distinguished in solidified iron containing carbon. The most important are the following:

Austenite, a solid solution of carbon in iron (more precisely, in γ-iron). The formation of austenite depends on the fact that carbon atoms can take up positions at the center and in the middle of the cell edges of the unit cube of γ-iron (Figure 5.103). If these sites were occupied in every unit cell, a compound FeC, with 50 atom% C, would be produced. However, the crystal lattice of austenite is stable only below 8 atom% C. The C atoms thus built into the crystal lattice distribute themselves statistically between the cell centers and cell edges, and austenite has the characteristics of a "solid solution". The crystal lattice of γ-iron is expanded uniformly in all directions by the incorporation of the C atoms, but the expansion is small.

Martensite, a metastable conversion product of austenite, formed by rapid cooling, can be regarded as a (supersaturated) solid solution of carbon in α-iron. Like all supersaturated solutions, it is unstable (or metastable). As shown in Figure 5.103, only a fraction of the sites available for C atoms is occupied in the martensite structure also. If all lattice positions were occupied, a compound FeC would result in this case also. As compared with the α-iron structure, the crystal lattice of martensite has undergone tetragonal distortion; it is stretched in one direction, and contracted a little in the two others.

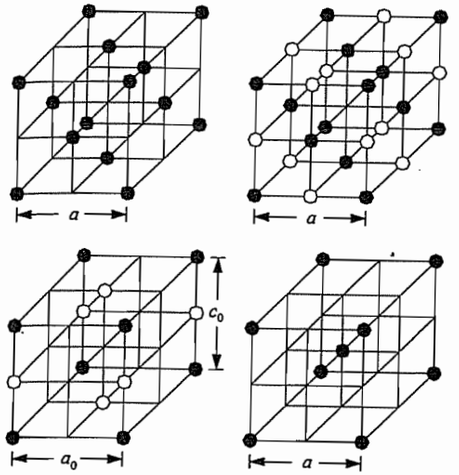

Figure 5.103: Detailed structure of the textural constituents in iron–carbon system. γ-iron: $a = 3.59$ Å (extrapolated to room temperature); austenite: $a = 3.63$ Å (for 8 atom% C); martensite: $a_0 = 2.84$, $c_0 = 3.00$ Å (for 6 atom% C); α(δ)-iron: $a = 2.86$ Å.

Cementite, a compound of iron and carbon, Fe_3C (contains 6.68% C), has a considerably more complex structure; the Fe atoms form prisms, with the C atoms located at their midpoints.

Ledeburite, an eutectic mixture of cementite with austenite (saturated with carbon). An eutectic is formed by the cooling of a melt.

Pearlite, am eutectoid mixture of ferrite and cementite. An eutectoid is applied to a mixture which is formed in the solid state.

Figure 5.104 represents the phase diagram of the iron–carbon system up to a content of 5% by weight of C. The melting point of iron is first lowered by the addition of carbon, from A to E, and is then raised again with further increase of carbon content. The eutectic point E corresponds to 4.2% C, and a temperature of 1140 °C. A melt of iron containing 4.2% of carbon solidifies in the form of ledeburite. From melts with a lower carbon content, mixed crystals of γ-iron with carbon (austenite) first separate. The mixed crystals have a lower carbon content than the melt, so that a melt having the composition corresponding to the point b on the liquidus curve AE is in equilibrium with mixed crystals having the composition given by the point a on the solidus curve AC. The melt is thus enriched in carbon through the deposition of austenite. At the same time, the concentration of carbon in the austenite deposited rises continuously until, at the point C, with a carbon content of 1.7% C, this phase is saturated with carbon. The melt has then reached the point E, and the remaining melt solidifies as ledeburite.

Melts containing up to 1.7% of carbon therefore yield only austenite, and those with a higher content (up to 4.2%) give ledeburite as well. Austenite, however, is only stable at high temperatures. When the alloy is slowly cooled, it undergoes transformation into a mixture of ferrite and pearlite, at temperatures between F (the transformation temperature of γ-iron into δ-iron) and H (or D), depending on its carbon content (G is the transformation temperature of δ-iron into α-iron). Martensite, which is characterized by its extreme hardness, is formed as an intermediate product in this transformation, and persists at ordinary temperature if cooling is effected rapidly ("quenching"). Under microscopic examination on a polished section, martensite stands out clearly in the form of dark needles from the light, not yet transformed austenite.

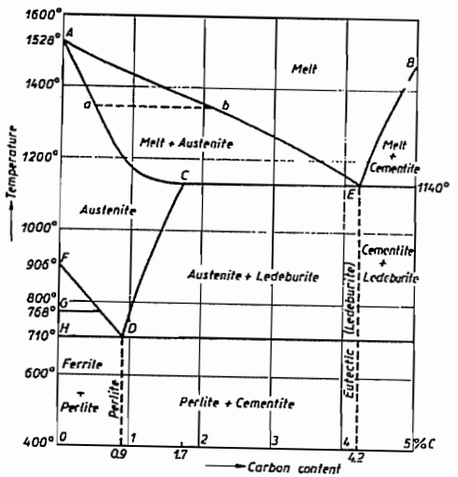

Figure 5.104: Phase diagram of iron–carbon alloys (simplified).

On passing to a melt with more than 4.2% of carbon, cementite, Fe_3C, first separates on rapid cooling. When the carbon content of the residual melt has thereby been reduced to 4.2%, the rest solidifies as ledeburite. If cooling is allowed to take place slowly, however, graphite crystallizes out, for the most part, in place of cementite. This is because, at temperatures below the melting point, a mixture of iron and graphite is more stable than a mixture of iron and cementite. Hence the latter is slowly converted into the former at about 1000 °C. As a result of this transformation within the solid alloy, the graphite is deposited in an extremely finely divided state ("temper carbon"). This fact, as already mentioned, is taken advantage of in malleabilizing.

5.16 Technical Varieties of Iron

Ordinary technical iron contains silicon, manganese, and other impurities, as well as carbon, and the properties of the iron–carbon alloys may be modified to a considerable extent by these other constituents. Thus silicon represses the formation of cementite and favors the deposition of graphite, whereas manganese acts in the opposite manner. The influence of silicon, manganese, etc. on the range of existence of the various modifications of iron, becomes practically important only when these elements are present in considerable concentration, as in the special steels.

Pig Iron or Cast Iron. This is iron which contains more than 2.3%, and usually 5–10% of foreign constituents, with a carbon content of 2–5%. It melts without previous softening, and therefore cannot be forged, but it casts well, since it fills the molds sharply. The melting point of pig iron lies between 1100 and 1200 °C. Pig iron is brittle at ordinary temperature. Ordinary grey cast iron contains the carbon chiefly in the form of graphite (typically 0.9% "combined carbon", 2.8% graphite). White cast iron, contains its carbon essentially as cementite (e.g., 3% "combined carbon", 0.1% graphite). Since it is harder and more brittle than grey cast iron, it is less suitable for castings (except for malleable cast iron), and is used almost exclusively as raw material for the production of malleable iron.

Malleable iron has a lower carbon content than pig iron, and contains fewer impurities. The carbon content is usually between 0.04 and 1.5%. Malleable iron melts at a higher temperature than pig iron. It softens gradually at high temperatures, and can therefore be forged and welded, as well as rolled or stretched into wires.

Soft Iron. This iron contains 0.5% of carbon at the most. It is tough and relatively soft, and can therefore be worked particularly well. It approaches pure iron in its properties, but differs from the latter in that, when magnetized, it loses its magnetism with a greater or less delay (hysteresis).

Steel. Steel has a higher carbon content than soft iron — usually between 0.5 and 1%. It can be forged and welded less readily than soft iron. It is also harder than the latter, and not tough but elastic at ordinary temperature. The most important characteristic of steel is that it may be hardened. If it is heated to bright redness, and suddenly cooled (by plunging it into water or oil), it becomes extraordinarily hard and brittle. The brittleness can be removed without any reduction in hardness, by "tempering" the steel — that is, by hearing it carefully for a short time to a moderately high temperature (250–300 °C).

The possibility of hardening steel is based on the fact that iron–carbon alloys with a carbon content below 1.7% can be converted into austenite by heating them. When this is suddenly cooled ("quenched") it passes over, partially or completely, into the very hard martensite. As follows from the phase diagram (Figure 5.104), the temperature necessary for hardening varies, according to the carbon content of the steel. It is usually about 900 °C. The effect of tempering is to release or diminish the internal strains that result from quenching.

If, in course of tempering, the temperature is raised higher, so that pearlite begins to separate out in a state of very fine subdivision, the hardness decreases to some extent but the tensile strength is increased. It is essential, however, that the heat treatment should not be continued so long that the martensite decomposes completely into pearlite, as the hardness and strength would then be lost once more.

5.17 Compounds

5.17.1 General

5.17.1.1 Ferrous Compounds

When iron is dissolved in nonoxidizing acids such as hydrochloric or dilute sulfuric, solutions containing ferrous ion are obtained.

$$Fe + 2H^+ \rightarrow Fe^{2+} + H_2$$

When a solution of a pure ferrous salt is treated with an alkali hydroxide, a white, gelatinous precipitate of ferrous hydroxide, $Fe(OH)_2$ is formed. In the presence of air, ferrous hydroxide quickly turns green, and then slowly becomes reddish-brown as it is oxidized to hydrous ferric oxide.

$$4Fe(OH)_2 + O_2 \rightarrow 2Fe_2O_3 + 4H_2O$$

Because of this fact it is difficult to obtain pure white ferrous hydroxide, and ferrous oxide, FeO, is prepared by the thermal decomposition of ferrous oxalate:

$$FeC_2O_4 \rightarrow FeO + CO + CO_2$$

rather than by the dehydration of ferrous hydroxide. Solutions containing ferrous ion have a pale green color. In the presence of air, ferrous ion is slowly oxidized to ferric. This oxidation takes place much more readily in alkaline than in acidic solution, as is indicated by the standard potentials for the following half-reactions:

$$Fe^{2+} \rightarrow Fe^{3+} + e^- \quad E = -0.77\ V$$

$$Fe(OH)_2 + OH^- \rightarrow Fe(OH)_3 + e^- \quad E = 0.56\ V$$

The most important ferrous compound is the sulfate, which crystallizes from aqueous solution as the heptahydrate, $FeSO_4 \cdot 7H_2O$. Because of the ease with which ferrous compounds are oxidized, particularly in alkaline solution, ferrous sulfate is widely used in chemical industry and in the laboratory as a reducing agent.

When equimolar proportions of ferrous sulfate and ammonium sulfate are brought together in aqueous solution, and the solution is evaporated until crystallization takes place, a double salt of the formula $(NH_4)_2SO_4 \cdot FeSO_4 \cdot 6H_2O$, known as Mohr's salt, is obtained. In the solid state, Mohr's salt is not oxidized by the air, and it is useful, therefore, as a dependable source of ferrous ion free from ferric.

The ferrous halides are most readily prepared by the action of solutions of the corresponding hydrogen halides upon metallic iron. The chloride crystallizes as the green hydrate $FeCl_2 \cdot 4H_2O$ when its solution is evaporated out of contact with the air.

Ferrous sulfide, FeS, is obtained either by direct union of iron and sulfur or by the action of hydrogen sulfide on neutral or basic solutions of ferrous ion. The black precipitate of FeS obtained in this reaction is readily soluble in even weakly acidic solutions. A black precipitate is obtained by the action of S^{2-} ions on iron(III) salt solutions. This is practically insoluble in water, but is soluble in dilute acids, and has a composition corresponding to the formula Fe_2S_3. It decomposes readily in air when it is moist, with the formation of iron oxide hydrate and the deposition of sulfur. Sulfur is also deposited when the precipitate is treated with hydrochloric acid:

$$Fe_2S_3 + 4HCl \rightarrow 2FeCl_2 + 2H_2S + S$$

5.17.1.2 Ferric Compounds

The iron atom has only two electrons in its outer (4*s*) shell. It may, however, lose or share in addition an electron from the incomplete 3*d* subshell, thereby attaining an oxidation state of 3+. Solutions of many ferric salts contain the hydrated ferric ion, $Fe(H_2O)_6^{3+}$. Because of the small size and high charge on the ferric ion, the hydrated ion reacts with water to give acid solutions.

$$Fe(H_2O)_6^{3+} + H_2O \rightarrow Fe(H_2O)_5(OH)^{2+} + H_3O^+$$

When solutions of ferric salts are boiled, basic ferric salts or hydrous ferric oxide may be precipitated. The yellow color of solutions of ferric salts is due to complex hydrated ions or to colloidal hydrous ferric oxide. When a solution of a ferric salt is treated with ammonia, or with a soluble hydroxide, a red-brown gelatinous precipitate of hydrous ferric oxide is obtained which readily goes into the colloidal condition. Since its composition varies with the method of preparation. It is best represented as $Fe_2O_3 \cdot xH_2O$. Hydrous ferric oxide does not dissolve in basic solutions.

When hydrous ferric oxide is strongly heated, it loses all its water and yields the anhydrous oxide, Fe_2O_3. This oxide exists in a number of crystalline modifications, the particular form depending upon the method by which it is obtained. As the mineral hematite, ferric oxide occurs in large quantities in the earth's crust. Finely divided ferric oxide obtained by the burning of pyrite is used as a red pigment or as a mild abrasive under the names of Venetian red. When ferric oxide is heated to a very high temperature, or when iron burns in oxygen or is heated in steam, ferroxoferric oxide, Fe_3O_4, is obtained. This compound occurs naturally as the ore called magnetite, some samples of which are highly paramagnetic and are known as lodestones. This oxide may also be regarded as ferrous ferrite, and its formula accordingly may be written $Fe(FeO_2)_2$.

The most important salt of ferric ion is ferric chloride. It is a true salt only when hydrated; the physical properties of the anhydrous form indicate that it is covalent. Anhydrous ferric halides are obtained by the passage of a current of the corresponding halogen gas over heated iron. Under these conditions, ferric chloride, for example, crystallizes in black crystals in the cold parts of the tube. The density of the vapor formed when these crystals are volatilized (280 °C) indicates that the compound is Fe_2Cl_6. Anhydrous ferric chloride dissolves readily in water to yield a yellow solution of the hydrated compound. Several solid hydrates are obtainable, the most familiar being $FeCl_3 \cdot 6H_2O$.

On evaporation of solutions containing equimolar proportions of ferric sulfate and the sulfate of an alkali metal or ammonium, violet-colored ferric alums are obtained, e.g., $(NH_4)_2SO_4 \cdot Fe_2(SO_4)_3 \cdot 24H_2O$. Ferric nitrate, also, may be obtained in violet-colored crystals, having the formula $Fe(NO_3)_3 \cdot 9H_2O$.

5.17.1.3 Complex Compounds

Iron in both the 2+ and 3+ oxidation states forms many complex compounds. Of these, the complex cyanides, because of their high stability, are particularly important.

When solutions containing ferrous ion are treated with an excess of cyanide ion, the pale yellow complex ferrocyanide ion is obtained. This ion is so stable that solutions of ferrocyanides have none of the properties either of ferrous or of cyanide ion:

$$Fe^{2+} + 6CN^- \rightarrow Fe(CN)_6^{4-}$$

The most familiar ferrocyanides are the readily soluble sodium and potassium salts, $Na_4Fe(CN)_6 \cdot 10H_2O$ and $K_4Fe(CN)_6 \cdot 3H_2O$. Likewise, when solutions containing ferric ion are treated with an excess of cyanide ion, the very stable red ferricyanide complex is obtained:

$$Fe^{3+} + 6CN^- \rightarrow Fe(CN)_6^{3-}$$

The most important ferricyanide is the potassium salt $K_3Fe(CN)_6$, which is obtained industrially by the oxidation of the ferrocyanide with chlorine:

$$2K_4Fe(CN)_6 + Cl_2 \rightarrow 2K_3Fe(CN)_6 + 2KCl$$

These complex cyanide ions form precipitates with a number of metal ions and are therefore useful in analytical chemistry. When a solution of a ferrocyanide reacts with a soluble ferric salt, a dark blue precipitate of complex structure, called Prussian blue, is obtained. Likewise, when a solution of a ferricyanide is treated with a soluble ferrous salt, a complex dark blue precipitate known as Turnbull's blue is obtained. The compositions of these precipitates vary considerably with the conditions under which the reaction is carried out. The important fact, however, is that ferrous ion reacts with ferricyanide ion to give a dark blue precipitate, whereas ferric ion reacts with ferrocyanide ion to give a precipitate of practically identical color. On the other hand, pure ferrous ion forms a white precipitate with ferrocyanide ion, and ferric ion reacts with ferricyanide ion to yield a brown solution containing a complex of unknown composition. These reactions provide a convenient method for testing for ferrous and ferric ions and for distinguishing between them.

The addition of a solution containing thiocyanate ion, SCN^-, to a solution containing ferric ion produces a deep red color. More than one colored complex ion is formed but in each of these complexes, thiocyanate ions are coordinated to the ferric ion. This reaction constitutes a very sensitive test for ferric.

5.17.2 Iron(II) Sulfate

Properties. Iron(II) sulfate heptahydrate, ferrous sulfate, copperas, green vitriol, $FeSO_4 \cdot 7H_2O$, *mp* 64 °C, ρ 1.898 g/cm³, crystallizes from aqueous solution as green, monoclinic crystals, which are readily soluble in water and glycol but insoluble in alcohol, acetone, and methyl acetate. On being heated to 60–70 °C, 3 mol of water is driven off to form the tetrahydrate, $FeSO_4 \cdot 4H_2O$. In the absence of air, at ca. 300 °C, iron(II) sulfate monohydrate, a white powder, is formed. When heated to ca. 260 °C in the presence of air, the monohydrate is oxidized to iron(III) sulfate. Decomposition of iron(II) sulfate begins at about 480°C. Iron(II) sulfate is efflorescent in dry air. In moist air, the surface of the crystals becomes covered with brownish basic iron(III) sulfate. Aqueous solutions of iron(II) sulfate are slightly acidic due to hydrolysis. The rate of oxidation by air increases in alkaline solution and on raising the temperature. Iron(II) sulfate reduces copper(II) ions to copper(I) ions and gold or silver ions to the corresponding metal. With univalent cations (e.g., K, Rb, Cs, NH_4, and Tl) and divalent cations (e.g., Cd, Zn, Mn, and Mg), double salts (alums) are readily formed; an example is Mohr's salt, iron(II) ammonium sulfate, $FeSO_4(NH_4)SO_4 \cdot 6H_2O$. This green salt is soluble in water, easily purified, and more stable to oxidation than iron(II) sulfate heptahydrate.

Production. Iron(II) sulfate is produced by dissolving scrap iron in dilute sulfuric acid or by oxidizing moist pyrites in air.

Iron(II) sulfate is also obtained as a byproduct from steel pickling and from the production of titanium dioxide (sulfate process, with ilmenite a s raw material). It is recovered from pickling liquors in a relatively pure form. The purity of iron(II) sulfate from the production of titanium dioxide depends on the source of the ilmenite. A typical composition is 87–90% $FeSO_4 \cdot 7H_2O$, 6–7% $MgSO_4 \cdot 7H_2O$, 0.6–0.7% $TiOSO_4$, 0.2% $MnSO_4 \cdot 7H_2O$, 3–6% water, and depending upon the type of ilmenite used, traces of nickel, chromium(III), vanadium, copper, zirconium, and others.

Uses. Iron(II) sulfate is used for the preparation of other iron compounds. It is employed to a lesser extent in writing inks, wood preservatives, desulfurizing coal gas, and the production of Turnbull's blue, Prussian blue, and other iron pigments; as an etchant for aluminum; for process engraving and lithography; and as an additive to fodder.

As sensitivity to environmental protection increased, other uses had to be found for iron(II) sulfate, because the above mentioned applications did not consume the amounts available as a byproduct from industrial processes. Large amounts of iron(II) sulfate are used for the clarification of community effluents. With an additional clarification step, up to 90% of the phosphate in the effluent can be eliminated. Sludge formed in clarification tanks may be used as fertilizer [174–175]. Iron(II) sulfate can also be recycled. After drying to the monohydrate, it is decomposed in a calciner:

$$4FeSO_4 \rightarrow 2Fe_2O_3 + 4SO_2 + O_2$$

Sulfur dioxide is converted by the contact process to sulfuric acid [176]. The conversion of iron(II) sulfate to gypsum and iron(II) chloride

by treatment with calcium chloride has also been proposed. The iron(II) chloride is then decomposed to iron(III) oxide and hydrochloric acid [177]. To convert surplus iron(II) sulfate to a product that can be disposed on a dump site, it can be neutralized with one equivalent of calcium hydroxide. The conversion is reportedly 97% [178]. To regulate the setting characteristics of cement, gypsum can be replaced by iron(II) sulfate [179]. As an additive to cement, iron(II) sulfate can reduce the content of water-soluble chromates substantially [180]. Iron(II) sulfate solutions can be used to eliminate chlorine in waste gases [181]. Effluents containing cyanides and chromates may be decontaminated with iron(II) sulfate [182]. Iron(II) sulfate can be used to combat chlorosis, a disease of vines [179]. It is also used to treat alkaline soil and to destroy moss [179].

Toxicology. If swallowed, iron(II) sulfate can cause disturbances of the gastrointestinal tract. Ingestion of large quantities by children may cause vomiting, hematemesis, hepatic damage, and peripheral vascular collapse [183].

The acute oral toxicity (LD50) of iron(II) sulfate in the rat is 1389–2778 mg/kg, and the in rabbit, 2778 mg/kg [184].

5.17.3 Iron(III) Sulfate

Properties. Anhydrous iron(III) sulfate, ferric sulfate, $Fe_2(SO_4)_3$, is a yellowish-white solid. It dissolves in water, hydrolyzing at the same time, to yield a brownish solution. Basic iron(III) sulfate precipitates when the solution is boiled. With alkali metal (M) sulfates, iron(III) sulfate forms alums, $M^IFe(SO_4)_2 \cdot 12H_2O$. Alums are almost colorless but normally have a violet tinge.

Production. Iron(III) sulfate is prepared by treating iron(II) sulfate with boiling concentrated sulfuric acid, or by evaporating a mixture of iron(III) oxide and sulfuric acid. Iron(III) sulfate solutions are produced industrially by injecting chlorine gas into an iron(II) sulfate solution [185]. The solution thus obtained contains a mixture of iron(III) sulfate and iron(III) chloride.

Uses. Ferric sulfate is used to prepare alums and iron oxide pigments, and as a coagulant for the treatment of liquid effluents. Ammonium ferric sulfate is used for tanning. Solutions of iron(III) compounds are used to reduce the volume of sludge from effluent treatment plants. By using a mixture of iron(III) sulfate, iron(III) chloride, and calcium hydroxide it is possible to achieve a dry-matter content of the sludge, after filtration, of at least 35% [186].

5.17.4 Iron(III) Chloride

Iron(III) chloride, ferric chloride, is a by-product of some metallurgical and chemical processes, such as the chlorinating decomposition of iron-bearing oxide ores. Its ready availability and the cheap feeds used to produce it (iron and chlorine) have made iron(III) chloride, especially its aqueous solution, a significant feed stock for many industries, in particular, water treatment and the production of iron oxides or other iron compounds.

Properties. Iron(III) chloride, $FeCl_3$, sublimation temperature ca. 305 °C, *bp* 332 °C [2.1]; ΔH_f^0 (25 °C) –399.67 kJ/mol [187], ρ (25°C) 2.89 g/cm^3 [188], is an almost black crystalline solid.

It is dimeric (Fe_2Cl_6) in the gas phase up to about 400 °C, dissociates at higher temperature, and is monomeric at 750 °C in the presence of excess chlorine. If chlorine is not present in excess, the compound decomposes to iron(II) chloride and chlorine above 200 °C [189].

Anhydrous iron(III) chloride has a hexagonal layer structure and forms dark, almost black, microcrystalline platelets with a metallic luster. The strongly hygroscopic crystals form a series of hydrates in humid air ($FeCl_3 \cdot xH_2O$, $x = 6, 3.5, 2.5, 2$) [190] and deliquesce on absorbing more moisture. The crystalline commercial product is iron(III) chloride hexahydrate, $FeCl_3 \cdot 6H_2O$, *mp* ca. 37 °C. It forms yellow crystals and occurs as $[FeCl_2(H_2O)_4]^+Cl^- \cdot 2H_2O$.

Iron(III) chloride is very soluble in water: 430 g of $FeCl_3$ per kilogram of solution at 0 °C, 480 g/kg at 20 °C, and 743 g/kg at 40 °C [191]. The enthalpy of solution of anhydrous iron(III) chloride is 95 kJ/mol for the formation of a 40% solution at 20 °C. The aqueous solution is strongly acidic. If a solution of iron(III) chloride is diluted and neutralized slowly with alkali, $[Fe(H_2O)_6]^{3+}$ is deprotonated to give yellow $[Fe(OH)(H_2O)_5]^{2+}$ and dimeric $[Fe_2(OH)_2(H_2O)_8]^{4+}$. Brown, colloidal β-FeOOH is formed upon further neutralization; at higher temperature, iron hydroxide precipitates [192].

Iron(III) chloride is readily soluble in liquids having donor properties, such as alcohols, ketones, ethers, nitriles, amines, and liquid sulfur dioxide, but only sparingly soluble in nonpolar solvents such as benzene and hexane. The reaction of iron(III) chloride with hydrochloric acid or chlorides yields the tetrachloroferrates $[FeCl_4]^-$ and $[FeCl_4(H_2O)_2]^-$. Because complexes are also formed with donor solvents, iron(III) chloride can be extracted from aqueous solutions in the presence of hydrochloric acid by using ether [193].

Iron(III) chloride is a strong oxidizing agent. Thus, many metals (for example, Fe, Cu, Ni, Pd, Pt, Mn, Pb, and Sn) are dissolved by aqueous iron(III) chloride, with the formation of iron(II) chloride; magnesium dissolves with evolution of hydrogen. Iron(III) chloride solution liberates carbon dioxide from alkali-metal carbonates. When iron(III) chloride is heated in air, iron(III) oxide and chlorine are produced. Above 200 °C, iron(III) chloride is rapidly reduced by hydrogen to iron. It is also reduced by coal.

Production. Anhydrous iron(III) chloride is produced industrially by reaction of dry chlorine with scrap iron at 500–700 °C [194]. The process is known as direct chlorination. Preheated scrap is charged into the top of a water-cooled iron shaft furnace, while chlorine (or a mixture of chlorine and nitrogen) is admitted at the bottom. To prevent formation of iron(II) chloride, a 10–30% excess of chlorine is used. Iron scrap is added continuously at a rate depending on the reaction temperature and the amount of chlorine remaining in the exit gas. The iron(III) chloride vapor produced passes through water- or air-cooled condensation chambers. The crystals obtained are removed continuously from the walls by vibration or knocking. They are then ground, screened, and packaged with exclusion of moisture. Chlorine in the waste gas is removed either by scrubbing with iron(II) chloride solution, to give iron(III) chloride, or by reacting with sodium hydroxide solution, to yield sodium hypochlorite and sodium chloride.

In another process, carried out in a reactor with an acid-resistant liner, iron scrap and dry chlorine gas react in a eutectic melt of iron(III) chloride and potassium or sodium chloride (e.g., 70% $FeCl_3$ and 30% KCl) [195]. First, iron scrap is dissolved in the melt at 600 °C and oxidized to iron(II) chloride by iron(III) chloride. Iron(II) chloride then reacts with chlorine to yield iron(III) chloride, which sublimes and is collected in cooled condensation chambers.

The advantages of direct chlorination include higher space time yields, lower capital cost, and less waste. The melt process gives a purer product because impurities remain largely in the melt; however, for this reason the melt must be changed and disposed of frequently.

Iron(III) chloride solutions are prepared by dissolving iron in hydrochloric acid and oxidizing the resulting iron(II) chloride with chlorine. In a continuous, closed-cycle process, iron(III) chloride solution is reduced with iron and the resulting iron(II) chloride solution is reoxidized with chlorine. Iron(III) chloride solution is also produced by solving iron(III) oxide in hydrochloric acid. Solid iron(III) chloride hexahydrate is crystallized by cooling a hot concentrated solution.

Quality Specifications and Analysis. Commercial forms of iron(III) chloride include sublimed anhydrous iron(III) chloride (≥ 99% $FeCl_3$), iron(III) chloride hexahydrate (ca.

60% $FeCl_3$), and iron(III) chloride solution (ca. 40% $FeCl_3$). Iron(III) chloride for potable water treatment must comply with DIN 19602 (February 1987).

Trivalent iron is determined by iodometric titration with sodium thiosulfate; chloride ion is determined by argentometry.

Occupational Health. Iron(III) chloride irritates the skin and, especially, eyes. Therefore, workers handling it must wear protective glasses, facial protection, and rubber gloves. The TLV for iron(III) chloride is that for soluble iron salts: 1 mg of iron per cubic meter.

Storage and Transportation. Anhydrous iron(III) chloride can be stored in standard steel containers. It is shipped airtight in sheet-iron drums or plastic barrels, and loose in tank trucks. Moist iron(III) chloride and iron(III) chloride solutions attack ordinary metals. The following materials are suitable for containers to hold iron chloride solutions: rubberized steel; plastics such as polyethylene, poly(vinyl chloride), and polytetrafluoroethylene; fiber-reinforced plastics; glass; stoneware; porcelain; and enamel. The only suitable metallic materials are titanium, tantalum, and Hastelloy C.

The transport classification for anhydrous iron(III) chloride is UN No. 1773, RID–ADR Class 8.11c and for iron(III) chloride solution, UN No. 2582, RID–ADR Class 8.5c.

Iron(III) chloride spilled by accident must be collected and forwarded to a sewage plant for disposal. Contaminated soil must be cleaned with a large amount of water and neutralized with lime. Iron(III) chloride is a Class 1 hazard to water quality.

Uses. Anhydrous iron(III) chloride is used in organic chemistry as a chlorinating agent for aliphatic hydrocarbons and for aromatic compounds. It also acts as a catalyst in Friedel–Crafts syntheses and condensation reactions. Iron(III) chloride is also used occasionally as an oxidizing agent [196, 197].

Because solutions of iron(III) chloride dissolve metals such as copper and zinc without troublesome evolution of hydrogen, they are used for the etching or surface treatment of metals (e.g., in the manufacture of electronic printed circuits, copperplate rotogravure printing, textile printing rolls), and for making signs. Iron(III) chloride solutions are also used in leaching the copper ore chalcopyrite.

Iron(III) chloride is used as a starting material in the preparation of other iron compounds, particularly oxides and hydroxides. However, most iron(III) oxide pigments obtained by hydrolysis of iron(III) chloride at high temperature have weak colors and a bluish cast, so these processes have not achieved commercial importance.

The largest use of iron chloride is in the form of dilute solutions that are employed as flocculating and precipitating agents in water treatment [198]. In processing surface waters into potable and process water, 5–40 g of iron(III) chloride is added to 1 m^3 of crude water at pH 6–7. The precipitated iron(III) hydroxide adsorbs finely divided solids and colloids (e.g., clays and humic acids). If decarbonization or the precipitation of heavy metals is to be carried out at the same time, slaked lime is added to adjust the pH to 9–11.

In municipal and industrial wastewater treatment, iron(III) chloride is particularly effective because it precipitates heavy metals and sulfides, whereas contaminants such as oils and polymers, which are difficult to degrade, are adsorbed on the iron hydroxide flocs. Phosphates are also lowered to a level of ca. 1 mg of phosphorus per liter of water in the clarifier discharge. Preliminary treatment with iron(III) chloride can increase the capacity of overloaded clarifier plants.

Sludge conditioning with iron(III) chloride and lime improves the dewatering of filter sludge, so that drier sludges, better suited to disposal or incineration, are obtained.

Consumption of iron(III) chloride in the United States in 1994 was as follows [199]:

Sewage and wastewater treatment: 65%
Water treatment: 25%
Catalyst, etchant, and other: 10%

Solutions of iron chlorosulfate, $FeClSO_4$, obtained by chlorinating iron(II) sulfate, are also used extensively as flocculents in water treatment [201].

Economic Aspects. Of the few anhydrous iron(III) chloride producers worldwide, the most important in Europe is BASF. Most of the iron(III) chloride is obtained as a by-product when iron-bearing raw materials are chlorinated or when steels are pickled with hydrochloric acid; the major commercial form is the 40% solution.

Outputs (by year, as 100% $FeCl_3$) and major producers are

Europe (1994)	estimated 150 000 t (Solvay, Atochem, BASF, SIDRA)
USA (1994) [199]	200 000 t (Du Pont, PVS, Imperial West Chem.)
Japan (1987) [200]	322 000 t

The most important European producers of iron chlorosulfate are Kronos Titan and Thann et Mulhouse SA.

5.17.5 Iron(II) Chloride

Iron(II) chloride, ferrous chloride, is much less important industrially than iron(III) chloride. The etching of steel with hydrochloric acid yields large amounts of iron(II) chloride, which is chlorinated in solution or thermally decomposed to iron oxide and hydrochloric acid. A solution of iron(II) chloride is also obtained as a by-product from the chloride process for the production of titanium dioxide.

Properties. Iron(II) chloride, $FeCl_2$, *mp* 677 °C, *bp* 1074 °C, ΔH_f^0 (25 °C) –342.1 kJ/mol, ρ (25 °C) 3.16 g/cm^3, forms pale green, rhombohedral crystals which are readily soluble in water, alcohol, and acetone, but only sparingly soluble in ether and benzene. The compound occurs naturally as the mineral lawrencite. It forms several hydrates, $FeCl_2 \cdot xH_2O$ ($x = 1, 2, 4, 6$).

When heated in air, iron(II) chloride forms iron(III) chloride and iron oxides. Iron(II) chloride solution undergoes virtually no hydrolysis; it is oxidized readily by air.

Production. Anhydrous iron(II) chloride is produced from iron filings heated to red heat in a stream of hydrogen chloride or from iron and chlorine at 700 °C. The product is obtained as a sublimable white mass. Iron(II) chloride can also be prepared by passing hydrogen over heated iron(III) chloride.

Solutions of iron(II) chloride are prepared by dissolving iron in hydrochloric acid or by reducing iron(III) chloride solutions with iron. When a hot saturated solution is cooled to 0 °C, pale green, monoclinic crystals of the hexahydrate are obtained; cooling to room temperature yields the blue-green tetrahydrate. If the solution is concentrated at 90 °C, the green dihydrate is obtained; above 120 °C or on vacuum evaporation, the dihydrate is converted to the monohydrate, $FeCl_2 \cdot H_2O$. In the absence of air, the monohydrate is converted to anhydrous iron(II) chloride at 230 °C [202].

Quality Specifications. Iron(II) chloride is sold as an anhydrous powder (≥ 96% $FeCl_2$), as the dihydrate (> 75% $FeCl_2$), as the tetrahydrate (> 60% $FeCl_2$), and as an aqueous solution (ca. 30% $FeCl_2$).

Transportation. Solid iron(II) chloride is shipped in sheet-iron drums, plastic bags, or glass containers, and its solution is transported in rubberized containers or plastic barrels.

Uses. Iron(II) chloride is used as a reducing agent and for the production of other iron compounds. Increasingly, iron(II) chloride solution serves as a precipitating and flocculating agent with reducing properties for use in water treatment; it is especially effective with wastewater containing chromate, for example.

Pure iron(II) chloride solution is an important starting material for the preparation of acicular goethite, α-FeOOH, and lepidocrocite, γ-FeOOH, which are further processed to γ-Fe_2O_3 magnetic pigments. Pure iron(II) chloride is also employed in the preparation of pure iron.

5.17.6 Iron Pentacarbonyl

Metal carbonyls are complexes in which carbon monoxide is coordinated to the central metal atom. Of the iron carbonyls, only iron pentacarbonyl, $Fe(CO)_5$, is economically significant.

M. Berthelot [203] and, independently, L. Mond and L. Quincke [204] discovered iron pentacarbonyl in 1891 [205]. Only after BASF had developed high-pressure technology for ammonia synthesis was its industrial production feasible. In 1925, a large plant was built in Germany by BASF to make iron pentacarbonyl which had proved to be a very effective antiknock agent for gasoline engines. When the compound was replaced shortly afterwards by lead alkyls, which were beneficial to motors, the production of iron powder from iron pentacarbonyl came to the fore.

In 1940, GAF began producing the pentacarbonyl in the United States under license from BASF. A BASF plant was moved to the Soviet Union in 1945. Plants built in England (1944) and France (1952) have ceased production. In addition to iron powder, BASF has been producing pure iron oxide from the carbonyl since about 1930.

Physical Properties. Iron pentacarbonyl is a clear, yellow, mobile liquid with an indistinctive odor. The molecule has a trigonal-bipyramidal structure [206].

Endothermic decomposition to iron and carbon monoxide begins at ca. 60 °C. Although decomposition becomes marked at the boiling point, iron pentacarbonyl can be distilled at atmospheric pressure with slight losses.

Some physical properties of iron pentacarbonyl are as follows:

mp	–20 °C
bp	103 °C
Critical temperature	285–288 °C
Critical pressure	2.90 MPa
Heat of fusion	69.4 kJ/kg
Heat of vaporization	190 kJ/kg
Specific heat (20 °C)	1.2 $kJkg^{-1}K^{-1}$
Viscosity (20 °C)	76 mPa·s
Surface tension (20 °C)	0.022 N/m
Coefficient of linear expansion (20 °C)	0.00125
Refractive index (n_D^{22})	1.518
Thermal conductivity	0.139 $Wm^{-1}K^{-1}$
Enthalpy of dissociation (vapor)	994 kJ/kg
Heat of combustion (to CO_2 and Fe_2O_3)	–8200 kJ/kg
Density, g/cm^3	
at 0 °C	1.495
at 20 °C	1.457
at 40 °C	1.419
at 60 °C	1.380
Vapor pressure, kPa	
at 20 °C	3.49
at 60 °C	21.33
at 100 °C	87.58

Iron pentacarbonyl is completely miscible with petroleum ether, hexane, benzene, pentanol and higher alcohols, ethyl ether, acetone, acetic acid, and ethyl acetate. It is partially miscible with paraffin oil and lower alcohols up to butanol [207].

Water solubility data for iron pentacarbonyl are contradictory; a value of 50–100 mg/L can be assumed [208]. The solubility of water in iron pentacarbonyl is 200–400 mg/kg.

The most complete documentation on iron pentacarbonyl is given in [209]; for earlier literature, see [210].

Chemical Properties. Iron pentacarbonyl is an easily combustible substance. It does not react with water or with weak or dilute acids. With concentrated acids, the corresponding iron salts are formed with the evolution of carbon monoxide and hydrogen. Reactions with halogens yield iron halides. Iron pentacarbonyl also reduces organic compounds; for example, nitrobenzene is reduced to aniline; a ketone, to an alcohol; and indigo, to indigo white. The Hieber base reaction yields iron carbonyl hydride or its salts [212–216]:

$$Fe(CO)_5 + 4NaOH \rightarrow Na_2Fe(CO)_4 + Na_2CO_3 + 2H_2O$$

The salt $Na_2Fe(CO)_4$ is a strong reducing agent.

Visible-light photolysis of pure iron pentacarbonyl or its solutions yields diiron nonacarbonyl, which precipitates as golden hexagonal platelets [217, 218]:

$$2Fe(CO)_5 \rightarrow Fe_2(CO)_9 + CO$$

The trinuclear iron carbonyl $Fe_3(CO)_{12}$ is also known [219–224].

As a highly reactive and readily available compound, iron pentacarbonyl is used for the preparation of many complexes, but these are not very significant industrially [211].

The most important industrial reactions of iron pentacarbonyl are thermal decomposition in the absence of air, yielding iron powder and carbon monoxide, and combustion to iron(III) oxide, Fe_2O_3.

Table 5.44: Equilibrium data for the formation of iron pentacarbonyl.

T, °C	p_{CO}, bar	$Fe(CO)_5$, vol% (at equilibrium)	$K = \frac{p_{CO}^5}{p_{Fe(CO)_5}}$	
			Observed	Calculated
60	0.69	22.4	0.86	0.363
80	1.47	21.8	20.1	3.39
160	38.83	9.0	2.4×10^7	1.0×10^5
200	132.68	5.7	5.5×10^9	1.26×10^5

Production. Although nickel carbonyl can be obtained from nickel and carbon monoxide at atmospheric pressure and moderate temperature, the production of iron pentacarbonyl requires a pressure of 5–30 MPa, a temperature of 150–200 °C, and the presence of reactive iron.

Values reported for the reaction equilibrium are not in good agreement with those calculated [225–228]. Table 5.44 lists experimental data for the equilibrium constant along with values calculated from the Nernst approximation [228].

Even at high temperature and pressure, massive iron reacts sluggishly with carbon monoxide, so iron sponge, with its greater surface area, is used as starting material [229]. Better yields are said to be obtained with iron quenched and granulated from the melt and containing 2–4% sulfur [230], which has a catalytic action [231]. For the reaction kinetics, see [232].

The exothermic reaction

$$Fe + 5CO \rightarrow Fe(CO)_{5(l)} \quad \Delta H = -226.92 \text{ kJ/mol}$$

is carried out in high-pressure batch equipment with a vertical reactor charged with iron. The gas, circulated by a pump, is preheated and admitted to the reactor. It leaves the reactor hot and loaded with iron pentacarbonyl which is condensed in a heat exchanger and allowed to expand into the unpressurized purification system under low pressure. To maintain the pressure in the system, the carbon monoxide used is replaced with fresh gas. Most of this is obtained when the carbonyl is decomposed to iron powder. This closed operating cycle removes carbonyl from the reaction equilibrium [233].

Carbon monoxide pressure, temperature, and flow rate are controlled carefully throughout the batch to avoid spontaneous decomposition of carbon monoxide, which would result in a sharp temperature increase and the deposition of carbon black [234].

The liquid carbonyl contains some lubricating oil (from the pump), water, and iron dust. Depending on the starting material, volatile carbonyls of nickel, chromium, molybdenum, and tungsten may also be present. These are removed by distillation.

The batch process is rather expensive and requires inert gas purging at the beginning and end of each batch. Nonetheless, other approaches have not been implemented. In a wet process, carbon monoxide was reacted with solutions of iron(II) salts in aqueous ammonia at 11.5 MPa and 80 °C, giving iron pentacarbonyl in yields of 40–50% [235, 236]. A solution of iron(II) chloride in methanol containing a sulfur compound and Mn powder is said to form iron pentacarbonyl on reaction with carbon monoxide [237]. Another process uses three fluidized beds in series, for iron ore (e.g., hematite) reduction, high-pressure carbonylation, and carbonyl decomposition; however, the process has not been adopted commercially [238, 239].

Quality Specifications and Analysis. Commercial pure iron pentacarbonyl is brought to high purity by double distillation. The levels of contaminants, metals that form volatile carbonyls, and sulfur are at or below the threshold of detectability [208].

To test for trace contaminants, a sample is solidified by cooling, treated with excess bromine, and brought slowly to room temperature. After the reaction stops, the residue is dissolved in dilute nitric acid. Techniques suitable for analyzing the solution (e.g., for Cr, Ni, Mo, or Pb) are atomic absorption spectroscopy and emission spectroscopy with inductively coupled plasma. Iron pentacarbonyl can be analyzed in a similar fashion after being dissolved in concentrated nitric acid.

Iron pentacarbonyl in gases, including air, can be oxidized with a hydrogen peroxide

methanol mixture and analyzed as iron hydroxide [208]. Bromine water and concentrated nitric acid are also suitable as oxidizing agents. The exposure of individual workers to iron pentacarbonyl is measured using a personal air sampler, consisting of a charcoal-filled tube and a small battery operated gas pump. The iron pentacarbonyl is catalytically oxidized on the activated charcoal to give iron oxide, which can be determined as iron after combustion of the charcoal. The average content of iron pentacarbonyl in the air is then calculated.

Indoor air can be continuously monitored by radiometry with ionization detectors. Iron pentacarbonyl is atomized to an aerosol in a measuring chamber at 150 °C; the aerosol diminishes the ionization current generated by a radioactive source. The change in current is a measure of the carbonyl concentration. The detection threshold is ca. 0.1 ppm [240].

Gas chromatography with an electron-capture detector has been used to determine iron pentacarbonyl and nickel tetracarbonyl in synthesis gas. The limit of detection for nickel tetracarbonyl has been found to be 0.001 ppm and that for iron pentacarbonyl somewhat less [241].

Safety. Two potential hazards must be considered in relation to iron pentacarbonyl: toxicity and combustion. These can be controlled only if the product is handled in sealed equipment [208]. The fire hazard can be summarized as follows:

Flash point	< –15 °C
Ignition point	< 65 °C
Lower explosion limit	2.6–4.5 vol%

On substances with a high surface area, such as activated charcoal, ignition is possible even at room temperature.

Because the heat of combustion of iron pentacarbonyl is only one-fifth that of fuel oil, iron pentacarbonyl fires are easy to extinguish. The best extinguishing agent is water, which removes heat and forms an airtight cover. Water that has been used to extinguish tires must not be discharged into natural waters.

Iron pentacarbonyl burns completely to iron(III) oxide and carbon dioxide only when it is atomized with air. Open combustion (e.g., in a dish) does not go to completion, and carbon monoxide is formed.

The best protection against the occurrence of iron pentacarbonyl concentrations that might present a danger of poisoning or explosion is continuous air monitoring. Carbon monoxide alarms respond only at much higher, toxic concentrations.

Storage. At industrial plants, iron pentacarbonyl is stored and processed in the absence of air in metallic (usually steel) equipment. Suitable seals and fittings are recommended by the carbonyl producer [208].

In unpressurized tanks, the carbonyl is covered with a protective gas (CO, N_2, Ar, CO_2). Tanks are connected to a gas reservoir so that the pressure does not drop below atmospheric even when the tank is cooled.

When the product is stored in pressurized vessels, the liquid is withdrawn through a submerged tube, not through valves in the tank bottom.

Tanks and pumps are installed in liquid-tight collecting basins.

Cleaning of Equipment and Disposal. Process equipment can be cleaned before opening by flushing with steam and then condensing the iron pentacarbonyl and water.

Carbonyl residues are collected and reused whenever possible. Because of the density difference, the product can easily be separated from water.

Laboratory carbonyl residues can be collected in a bottle partly filled with water. Glassware is washed several times with a small amount of acetone, which is poured into water for phase separation.

Small amounts of iron pentacarbonyl can be disposed of by burning in a sheet-metal tub. The presence of carbon monoxide in the off-gas must be taken into account.

Transportation. Because of fire and toxicity hazards, stringent regulations apply to the transportation of iron pentacarbonyl. Containers must be airtight and stable.

In Germany, the same regulations apply as in the case of nickel carbonyl. Both substances are assigned to Class 6.1, No. 3 under RID and GGVE for rail shipment, and under ADR and GGVS for road shipment. These regulations allow pressurized containers up to 250 L rated at 1 MPa. They are subject to inspection as pressure vessels (e.g., by TÜV) before being placed in service and at five-year intervals thereafter. The contents are limited to 1 kg of iron pentacarbonyl per liter of capacity. Every pressurized container must bear a nameplate with the following information: name of substance, owner, empty weight, year of first inspection and year of most recent inspection, inspector's stamp, maximum filling weight, and rated pressure.

The largest producer of iron pentacarbonyl, BASF, sells it in 20- and 250-kg pressurized containers. Each container has two valves or a double valve, so that liquid can be withdrawn through a submerged tube.

Also used as nonreturnable packaging in Europe are 1-L pressurized aluminum bottles, with a rated pressure of 1 MPa and a filling weight of 1 kg.

For international shipment by sea, iron pentacarbonyl is classified as follows: UN No. 1994, Class 6.1, IMDG Code. Air shipment and mailing are forbidden.

Similar regulations now apply in the United States. Although iron pentacarbonyl is a Poison B, because of the risk of inhalation it must be packaged in gas containers under pressure as prescribed for a Poison A under DOT Hazardous Materials Regulations. The containers hold 300 pounds of carbonyl.

Carbonyl Iron Powder. By far the largest use of iron pentacarbonyl is for the production of carbonyl iron powder. The equilibrium reaction

$$Fe(CO)_{5(g)} \rightleftharpoons Fe + 5CO, \quad \Delta H = +194.7\ kJ/mol$$

goes from left to right at standard pressure above 200 °C. The iron deposited on hot surfaces is brittle hard, and not commercially usable. In hot liquids such as paraffin oil, finely dispersed iron is obtained [242]. The only process that has become industrially important is decomposition in cavity decomposers, which yields spherical iron particles of 1–10 μm diameter [243].

The decomposer is a pipe, externally heated by electricity or gas, into which iron pentacarbonyl vapor is admitted from the top. The carbonyl decomposes not on the wall, which is heated to > 300 °C, but on iron particles circulating in the gas stream. These particles grow to 3–8 μm and are then discharged along with the carbon monoxide generated. Carbon and oxygen produced by the decomposition of carbon monoxide are incorporated in the iron. Addition of ammonia reduces the carbon and oxygen content but leads to incorporation of nitrogen in the iron particles.

The cavity decomposer, invented by BASF in 1924, has not changed fundamentally. A variety of practices have been adopted to control the product, above all its particle size. Zinc particles are obtained by admitting oil vapor into the decomposer [244], by diluting the carbonyl vapor with recycled carbon monoxide gas [245], or by applying a temperature gradient from the top to the bottom of the decomposer [246]. Fine particles result if the rate of flow of iron pentacarbonyl is high; larger ones, if the rate is low [247]. Inlet velocity is also a factor [248].

Carbon, nitrogen, and oxygen can be largely eliminated from the iron powder by treatment with hydrogen at ca. 450 °C [249]. The spheres, which were previously very hard (Vickers Lardness 800–900), become soft (100–150 Vickers) and can be deformed by pressure. Hard and soft types are marketed for diverse applications [250].

Carbonyl iron powder is made into magnetic cores for electronic components [251, 252]. In powder metallurgy, pure iron and iron alloys are made into parts by pressing [253, 254] and by metal injection molding [255, 256], carbonyl iron powder being an important component of powders and feedstocks [257, 258]. Carbonyl iron powder is also employed for the fortification of foods such as

white bread and in the production of iron-containing pharmaceuticals. It is used as a reducing agent in organic chemistry, and is incorporated in rubber or plastic sheets that are used for microwave attenuation [259–261]. For preparation, use, particle-size distribution, and behavior on heat treatment, see [262–266].

Carbonyl Iron Oxide. Only BASF converts iron pentacarbonyl to iron oxides. The processes are harmless to the environment, because the only by-product is carbon dioxide, and no pollution of the wastewater with salts occurs, unlike when iron oxides are precipitated from solutions of iron salts.

Red iron oxide, in a finely divided form similar to carbon black, is obtained by atomizing iron pentacarbonyl and burning it in an excess of air [267]. By varying temperature and residence time in the reactor, transparent or highly transparent red pigments can be produced [268–270]. The highly transparent pigments are nearly X-ray amorphous and have BET surface areas of 80–160 m^2/g. The less transparent grades have surface areas of 10–35 m^2/g and clearly show a hematite structure. The iron oxide is used to make high-quality ferrites and similar ceramic materials. Because the content of other metals and electrolytes is extremely low and little energy is needed for dispersion, the oxide is particularly suitable for use as a lightfast, UV-blocking red pigment for paints, wood varnishes, fiber dyeing, and color printing.

Water injection [271] and passage through an intense centrifugal force field [272] during production improve both separation and compactibility.

Air oxidation of iron pentacarbonyl to magnetite is possible at higher temperature [273]. At 100–400 °C, magnetic black Fe_3O_4 or brown γ-Fe_2O_3 can be obtained, as desired. The carbon monoxide formed undergoes virtually no oxidation if the reaction takes place in a mechanically agitated fluidized bed of product oxide [274]. Finely dispersed γ-Fe_2O_5 pigments and Fe_3O_4 pigments (particle size 2 to 200 nm) are produced by BASF to be used in aqueous suspension as contrasting agents in nuclear magnetic resonance tomography [275].

To obtain mixed oxides with iron as primary component, iron pentacarbonyl is atomized together with a compound of the other metal (in liquid or dissolved form) that is converted to the oxide at high temperature. For example, by atomizing the carbonyl with an aqueous solution of chromic acid, iron chromium oxide can be obtained for use as a catalyst or as a brown pigment [276, 277].

Other Uses. Polycrystalline iron whiskers can be made by decomposing iron pentacarbonyl in a magnetic field [278–288]. The whiskers are remarkably strong and said to be suitable for making composites or for catalysts. Another process for producing iron whiskers employs an empty space decomposer at temperatures higher than 360 °C for thermal decomposition of iron pentacarbonyl [289].

Novel effect pigments ranging from bright yellow to brilliant red are prepared in a fluidized bed of aluminum powder, which is coated with iron oxide when iron pentacarbonyl vapor and air are admitted [290, 291]. Novel brilliant pigments are produced by coating aluminum flakes with nanometer films of hematite deposited from iron pentacarbonyl and optionally a second layer of colorless metal oxide [292]. Other pigments are made on a mica base [293]. These pigments are lightfast and corrosion resistant and are therefore suitable for use in automobile paints.

Carriers for the toner in photocopiers are obtained by coating fine spherical particles of iron or glass [294], respirable plastics [295], or porous silico-containing material [296]. Colored single component toner powders are made of dispersions of carbonyl iron powder, reflecting pigments or dyes and other substances in a binder [297, 298].

Suspensions of finely divided iron [299] or its alloys [300] are prepared by decomposing iron pentacarbonyl in solution. This process can be used to produce magnetic liquids [301].

If iron pentacarbonyl is decomposed on, for example, gold ore, the iron deposits preferentially on the metal, which could then be recovered by magnetic separation [302].

Iron pentacarbonyl is not an important industrial catalyst [303]; for its use as a catalyst in organic chemistry, see [304]. Iron pentacarbonyl has been described as a catalyst for the hydrogenation of coal [305, 306]. The catalysis of partial subsurface combustion of heavy crude oil by iron pentacarbonyl, with the aim of lowering the viscosity, has been reported [307, 308].

The complex $Na_2Fe(CO)_4$ formed in solution by the Hieber base reaction [309], recommended long ago for reducing vat dyes [310], has met with renewed interest. For example, chlorate can be removed from diaphragm-cell caustic soda with this product [311]. The use of $Na_2Fe(CO)_4$ to reduce organic compounds has been described [312]. Operation of a fuel cell using iron pentacarbonyl and an aqueous alkali hydroxide of pH < 9 has been proposed [313].

If iron carbonyl is added during thermal degradation of hydrocarbons to carbon fibers, subsequent high-temperature treatment gives a higher yield of better graphitized, more conductive fibers [314].

Pyrite films are obtained from iron pentacarbonyl and sulfur or hydrogen sulfide by chemical vapor deposition. The films are photoactive and can be used to make solar cells [315].

Economic Aspects. Three companies produce iron pentacarbonyl: BASF (Germany) with a capacity of over 9000 t/a, GAF (Huntsville, Alabama) with an estimated 1500–2000 t/a, and a plant in the former Soviet Union.

These plants also produce carbonyl iron powder, with capacities of ca. 1500 t/a (BASF) and 500 t/a (GAF). The BASF plant has an iron oxide capacity of ca. 1000 t/a.

Consumption of the carbonyl for other purposes is insignificant compared to inplant consumption.

Toxicology and Occupational Health. Based upon the limited data that is available from laboratory animal studies, iron pentacarbonyl must be classified as highly toxic.

The first laboratory study demonstrated that a 45.5 min inhalative exposure to 0.025 vol% (250 ppm) of iron pentacarbonyl is fatal to rabbits [316]. Studies by BASF showed that 30-min exposure to 40 ppm of iron pentacarbonyl is already lethal to rabbits [317]. Cats reacted with considerably less sensitivity and survived exposure to 300 ppm. In guinea pigs, rats, and mice, fatalities began after exposure to 140 ppm. After 30-min exposure, LC_{50} values of 2.190 mg/m^3 (275 ppm) for mice and 910 mg/m^3 (115 ppm) for rats were found in later acute toxicity studies [318]. The four-hour median lethal concentration was determined to be 10 ppm in rats [319].

The oral LD_{50} of iron pentacarbonyl is 0.012 mL/kg (0.018 mg/kg) in rabbits and 0.22 mL/kg (0.033 mg/kg) in guinea pigs [320]. After percutaneous application, the LD_{50} in rabbits is 0.24 mL/kg [320]. In BASF experiments, the following LD_{50} values were determined for acute oral toxicity: rabbit, 20 mg/kg; rat, 25 mg/ kg; mouse, 100 mg/kg; cat, 100 mg/kg. Iron pentacarbonyl was found to be not mutagen in an Ames test. No skin and eye irritation was observed in OECD 404, OECD 405 tests [317].

Depending on carbonyl concentration, lethargy, respiratory symptoms, and lung edema were found in rats in further inhalation experiments [321]. No data are available on the chronic toxicity of iron pentacarbonyl. Only one six-month feeding study with rats, in which 13 mg/d did not lead to any toxic effects, has been reported [322]. The clinical symptomatology of iron pentacarbonyl intoxication is similar to that of nickel carbonyl poisoning. It is marked by immediate onset of disorientation and vomiting. Fever, coughing, and difficulty in breathing occur after 12–36 h. Fatalities usually occur 4–11 d after exposure to a lethal dose. Pathological lesions are found in the lungs and in the vascular and nervous systems [323]. Although iron pentacarbonyl and nickel carbonyl intoxications have similar symptoms, iron pentacarbonyl is probably less toxic (see Table 5.45) [324]. Furthermore, the use of iron pentacarbonyl should result in less

exposure than nickel carbonyl because of its lower vapor pressure.

Safety precautions are, however, required when working with iron pentacarbonyl to prevent oral, inhalatory, and dermal exposure, because of the relatively high acute toxicity. The MAK value for iron pentacarbonyl is 0.1 ppm. The TLV-TWA is 0.1 ppm (0.8 mg/m^3), as Fe.

Table 5.45: Acute rat inhalation toxicity.

Substance	LC_{50}, mg/m^3	Exposure time, min
$Ni(CO)_4$	240	30
$Fe(CO)_5$	910	30

5.17.7 Iron Compounds, Miscellaneous

Iron Acetates. When scrap iron reacts with acetic acid, it dissolves to form acetate salts [325]. If the initial black solution is concentrated to 12%, solid iron acetate can be obtained. This salt is a mixture of iron(II) and iron(III) oxidation states of indefinite proportions best formulated as $Fe_x(CH_3COO)_y$. It is used as a catalyst for acetylation and carbonylation reactions.

Iron(II) acetate, $Fe(C_2H_3O_2)_2$, is colorless. It is used in textile dyeing as an iron base for dark brown, dark blue, and black colors.

Iron(III) acetate, $Fe(C_2H_3O_2)_3$, is prepared industrially by reacting scrap iron with acetic acid, followed by oxidation of the solution with air; it is very sensitive to light. Iron(III) acetate is used for dyeing and printing textiles, as a mordant in dyeing, as a catalyst in organic oxidation reactions, and in dyeing chamois leather.

Basic iron(III) acetate, $Fe(OH)(C_2H_3O_2)_2$, is obtained by boiling a solution of iron(III) acetate and allowing the hydroxy salt to precipitate. This brownish-red compound is used as a mordant in dyeing, for weighting silk and felt, as a conservation additive for timber, and as a colorant for leather.

Iron(II) carbonate, $FeCO_3$, forms as a white precipitate when solutions of alkali-metal carbonate salts are added to solutions of iron(II) salts. It is used as a supplement in animal diets and as a flame retardant [325].

Iron Citrates. Iron citrate is a complex of indefinite formula, containing both iron(II) and iron(III). *Iron(II) citrate* and *iron(III) citrate* are also of indefinite stoichiometry. *Iron(III) citrate* (1 : 1 Fe–citric acid) is also known. Iron citrates are readily soluble in hot water and exhibit complex solution chemistry. These compounds have been used as supplements to animal diets and to soil.

Iron(III) ammonium citrate also has an indefinite formula. The brown hydrated form contains 16.5–18.5% iron, ca. 9% ammonia, and 65% citric acid, whereas the green hydrated form contains 14.5–16% iron, ca. 7.5% ammonia, and 75% citric acid [325]. Iron ammonium citrates are very soluble in water but insoluble in ethanol. They are used as iron additives in food for human consumption (e.g., bread and milk) and for the treatment of iron deficiency in small animals and cattle. They are sensitive to light and are used in light-sensitive paper [325].

Iron Halides. The iron(II) halides (fluoride, bromide, and iodide) are used as catalysts for fluorination, bromination, and iodination in organic reactions. Iron(II) iodide is used as a source of iron and iodine in veterinary medicine.

Iron(III) fluoride is used as a catalyst in organic reactions. Iron(III) bromide is used in the catalytic bromination of aromatic compounds.

Iron Nitrates. *Iron(II) nitrate hexahydrate*, $Fe(NO_3)_2 \cdot 6H_2O$, mp 60.5 °C, forms green, rhombohedral crystals. It is prepared by dissolving iron in cold nitric acid ($d < 1.034$ g/cm^3). With increasing density, a greater proportion of iron is oxidized to iron(III). Iron(II) nitrate is used as a catalyst for reductions.

Iron(III) nitrate nonahydrate, $Fe(NO_3)_3 \cdot 9H_2O$, forms colorless or pale violet monoclinic crystals. It is made by dissolving iron in nitric acid ($d > 1.115$ g/cm^3).

Iron(III) nitrate hexahydrate, $Fe(NO_3)_3 \cdot 6H_2O$, forms colorless, cubic crystals (*mp* 35 °C). Iron(III) nitrate is used as a mordant, in tanning, and as a catalyst for oxidation reactions.

Iron(II) phthalocyanine is synthesized from 1,2-dicyanobenzene and an iron(II) complex in refluxing 1-chloronaphthalene and is purified by sublimation at 450 °C. This green compound is insoluble in most solvents. Because it can exist in many oxidation states, iron(II) phthalocyanine is used as a catalyst for a variety of chemical and electrochemical redox reactions. It is also an important pigment [326].

Iron Compounds for the Treatment of Anemia [327, 328]. Sufficient iron in the diet of humans and animals is essential for tissue growth. Iron is found at the active site of many important proteins in the human body. These include hemoglobin (oxygen transport), myoglobin (storage of oxygen), cytochrome c oxidase (converts oxygen to water), cytochrome P450 (hydroxylation of poisonous or unwanted chemicals), and other cytochromes such as cytochrome c (part of the electron-transport system). In addition, iron is necessary for the biosynthesis of iron–sulfur proteins such as rubedoxin.

Although a sufficient amount of iron can usually be found in the diet, the level of absorption of this element from food is generally low. Therefore, the supply of iron can become critical in a variety of conditions. Iron-deficiency anemia is commonly encountered in pregnant women and may also be a problem in the newborn, especially in animal species such as the pig. Some diseases (e.g., rheumatoid arthritis, hemolytic diseases, and cancer) result in poor distribution of iron in the body and thus lead to chronic anemia.

More than 34 iron-containing preparations are used as hematinics for the treatment of iron-deficiency anemia [328]. Oral iron therapy is usually the preferred method of treatment unless good reasons exist for using another route. The daily oral dosage of elemental iron should be 100–200 mg. Iron(II) salts are more commonly used than iron(III) salts because they are assumed to be more soluble in the pH range 3–7. Solubility is essential if the compound is to permeate cell membranes. The rate of regeneration of hemoglobin appears to be independent of the salt used, provided sufficient iron is given. Factors affecting the choice of preparation are the incidence of side effects and the cost. If side effects occur, an alternative iron preparation or a reduced dosage can be tried. The main iron compounds used in iron supplements are iron(II) fumarate, iron(II) gluconate, iron(II) sulfate, iron(II) succinate, iron(III) chloride solution, and iron(III) ammonium citrate. In addition, iron dextran and iron sorbital are used in injectable hematinics. Iron(II) sulfate is often preferred because it is the cheapest form and is at least as effective as any other. A number of oral preparations contain ascorbic acid (vitamin C) to stabilize the iron(II) state. However, the therapeutic advantage is minimal and the cost may be increased. Folic acid is used in conjunction with an iron salt for the prevention of anemia in pregnant women.

Iron(II) complexes have a major disadvantage, however, in that they are sensitive to oxidation, especially in aqueous environments. This can be hindered initially by protectively coating iron(II) compounds in tablet form. However, when they dissolve in the gut, oxidation still occurs to give insoluble iron(III) salts (containing hydroxide). These frequently cause irritation and gastrointestinal distress. Such side effects are often severe, because large doses are necessary to ensure that enough iron is absorbed. Nausea and epigastric pain may occur and are said to be dose-related, although the relationship between altered bowel behavior (constipation) and dosage is unclear [328].

Soluble iron(III) complexes are thus preferred (because oxidation is not a problem). Unfortunately, such complexes are likely to be charged (which is unsatisfactory for passive membrane diffusion). Even if these complexes were neutral, they may still be toxic.

The ideal properties of an iron(III) chelation complex for treating iron-deficiency anemia are: (1) solubility in the pH range 6–9, (2) a ligand with a high affinity for iron(III), (3) a neutral iron(III) complex, and (4) nontoxicity. Furthermore, after absorption into the body the complex must enter into an equilibrium

with transferring (the iron-transport protein) so that iron is available for utilization in metabolic pathways. This means that the chelator must be metabolized rapidly to ensure that iron is freshly available.

One such complex currently under trial is iron(III) maltol, [FeL_3] (maltol(HL) = 3-hydroxy-2-methyl-4H-pyran-4-one). Recently, iron(III) maltol and similar complexes [328–332] have been shown to possess the desirable properties outlined above for the treatment of iron-deficiency-related diseases.

Another iron-related disease in humans is severe tissue iron overload. This may occur during the treatment of anemia, mainly as a result of a large number of blood transfusions. This condition is treated by injections of desferrioxamine mesylate, which is a good chelating agent for iron(III), and is also used to treat cases of accidental iron poisoning.

5.18 Relationships Between the Different Forms of Iron Oxides

Fe_2O_3 loses oxygen on heating at about 1390 °C to give Fe_3O_4:

$$3Fe_2O_3 \rightarrow 2Fe_3O_4 + {}^1/_2O_2$$

Fe_3O_4 can be considered as a compound of ferrous oxide, FeO, and ferric oxide, Fe_2O_3. It crystallizes in the cubic system and can be obtained by heating iron fillings in air. it is also formed during the forging of red hot wrought iron. In pure water in the absence of oxygen, steel forms a film of Fe_3O_4 at about 50 °C:

$$Fe + 2H_2O \rightarrow Fe(OH)_2 + H_2$$

$$3Fe(OH)_2 \rightarrow Fe_3O_4 + H_2 + H_2O$$

It is a black powder, insoluble in dilute acids, strongly ferromagnetic, and has a high electrical conductivity. That is why it is sometimes used as electrodes.

It was once thought that synthetic Fe_3O_4 behaves differently from natural magnetite on oxidation in that an intermediate phase γ-Fe_2O_3 is observed in the synthetic sample but not in the natural mineral:

$$Fe_3O_{4(synthetic)} \rightarrow \gamma\text{-}Fe_2O_3 \rightarrow \alpha\text{-}Fe_2O_3$$

$$Fe_3O_{4(natural)} \rightarrow \alpha\text{-}Fe_2O_3$$

This was later resolved when it was found that the oxidation is dependent on the particle size of Fe_3O_4; only extremely fine particles 3000 Å yield γ-Fe_2O_3.

Ferrous oxide, FeO, is known as the wüstite phase, $Fe_{1-x}O$, after its discover Fritz Wüst. It has a cubic lattice of NaCl type, and unstable below 570 °C when it decomposes as follows:

$$4FeO \rightarrow Fe_3O_4 + Fe$$

However, it can be cooled rapidly to prevent the decomposition. It can be obtained as a black pyrophoric powder in the following ways:

- Heating ferrous oxalate in the absence of air:

  $$(COO)_2Fe \rightarrow FeO + CO + CO_2$$

- Heating stoichiometric amounts of Fe and Fe_3O_4 in an inert atmosphere at 1100 °C, then cooling rapidly:

  $$Fe + Fe_3O_4 \rightarrow 4FeO$$

Iron(II) hydroxide, $Fe(OH)_2$ or $FeO \cdot H_2O$, is formed by treating iron(II) salts with alkali hydroxide in absolutely air-free solution. It precipitates as a white flocculent material which has a great affinity for oxygen. It thereby turn green, which progressively darkens and eventually passes into the red brown color of iron(III) oxide hydrate. The green color may be an intermediate product such as $Fe(OH)_2 \cdot FeOOH$. Pure $Fe(OH)_2$ when washed and dried in the absence of air decomposes at 200 °C to give FeO with some Fe_3O_4. It is slightly soluble in concentrated NaOH forming sodium hydroxoferrate, $Na_2[Fe(OH)_4]$. If oxygen is passed through a strongly alkaline suspension of $Fe(OH)_2$, α-FeOOH is produced.

Iron(III) hydroxide, $Fe(OH)_3$, is formed by adding ammonia to iron(III) salt solutions, as a red-brown slimy precipitate which yields a gel of variable water content when it is dried. When freshly precipitated, it is amorphous to x-rays. It dissolves readily in dilute acids, and also dissolves to some extent in hot concentrated NaOH forming sodium ferrite, $NaFeO_2$.

As aging takes place, the diffraction pattern characteristic to FeOOH develops but is never complete:

$$Fe^{3+} + 3OH^- \rightarrow Fe(OH)_3$$

$$Fe(OH)_3 \rightarrow FeOOH + H_2O$$

Two types of iron oxide hydroxide can be obtained in this way: α-FeOOH from sulfate, nitrate (Figure 5.105), and β-FeOOH from chloride and fluoride solutions (Figure 5.105).

Freshly precipitated ferric hydroxide when filtered and washed, then examined by differential thermal analysis shows endothermic peak at low temperatures (100–250 °C) due to the loss of water, followed by exothermic peak at about 300 °C. X-ray diffraction before 300 °C shows no pattern, but after 300 °C shows that of α-Fe_2O_3, thus indicating that the exothermic peak is due to the crystallization of α-Fe_2O_3:

$$\alpha\text{-}FeOOH \rightarrow \alpha\text{-}Fe_2O_{3(amorphous)} \rightarrow \alpha\text{-}Fe_2O_{3(crystalline)}$$

A sample aged for 28 months showed similar behavior, but the transition amorphous to crystalline took place at about 400 °C and is less defined, demonstrating that during aging only partial crystallization took place.

If the oxide hydrate is prepared at room temperature by precipitation, the transition temperature of crystallization is about 300 °C as indicated previously; but, if prepared at 90 °C by hydrolysis, the transition temperature is about 450 °C. Electron micrographic studies showed that the transition process amorphous–crystalline is accompanied by an increase in the particle size from below 50 Å to about 300 Å. This phenomena is not restricted to iron oxides but to other oxides as well.

β-FeOOH is obtained as a light brown deposit when a ferric solution containing Cl^- ion is hydrolyzed by boiling. It entraps variable amounts of Cl^- ions within its crystal structure which can be partly washed with water. The amount of Cl^- has an important influence on the thermal behavior of the material and its infrared spectrum but not on the x-ray diffraction pattern.

γ-FeOOH occurs in nature to a minor extent as the mineral lepidocrocite. When heated below 500 °C it loses water giving γ-Fe_2O_3:

$$2\gamma\text{-}FeOOH \rightarrow \gamma\text{-}Fe_2O_3 + H_2O$$

It is artificially prepared by adding NaOH to dilute $FeSO_4$ solutions until pH 6 followed by blowing air through the solution for 2 hours and is then allowed to age for 2 days. The differential thermal analysis pattern of γ-FeOOH shows an endothermic dehydration peak at 330 °C followed by the exothermic transformation of γ-Fe_2O_3 to α-Fe_2O_3 at 535 °C. At room temperature and in weak acid or neutral medium, FeS is oxidized slowly to γ-FeOOH as follows:

$$4FeS + 3O_2 + 2H_2O \rightarrow 4\gamma\text{-}FeOOH + 4S$$

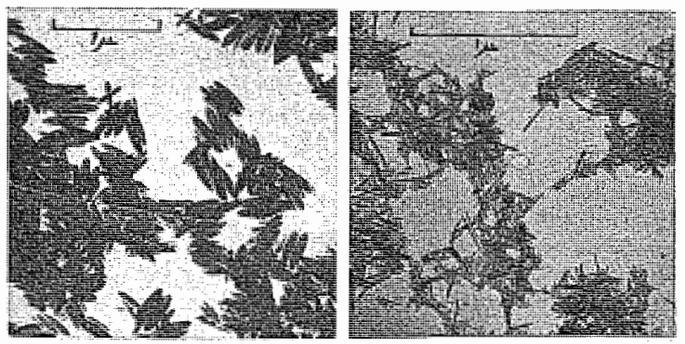

Figure 5.105: Left: α-FeOOH obtained by aging iron hydroxide gel for 155 days (precipitation took place at pH 10); Right: β-FeOOH.

Oxidation of Fe_3O_4 below 400 °C also yields γ-Fe_2O_3.

δ-FeOOH is obtained from $Fe(OH)_2$ by rapid oxidation with an excess of H_2O_2 or ammonium persulfate. It is a brown strongly magnetic material that loses about 10% of its water at 100 °C and is partially transformed to hematite; complete transformation takes place at 200 °C.

$FeCO_3$ can be formed artificially when $(NH_4)_2CO_3$ is added to a ferrous solution. Freshly precipitated ferrous carbonate when oxidized by excess H_2O_2 is transformed to $Fe(OH)_3$; however, this hydroxide is dark yellow instead of red brown. It also undergoes crystallization during aging to α-FeOOH. Ferrous carbonate reacts with NaOH to form a surface layer of $Fe(OH)_2$ which on oxidation results in the formation of magnetic iron oxides:

$$FeCO_3 + 2NaOH \rightarrow Fe(OH)_2 + Na_2CO_3$$

$$2Fe(OH)_2 + {}^1/_2O_2 \rightarrow \gamma\text{-}Fe_2O_3 + 2H_2O$$

$$3Fe(OH)_2 + {}^1/_2O_2 \rightarrow Fe_3O_4 + 3H_2O$$

This is the basis of a beneficiation method for low-grade siderite ore, whereby the magnetic iron oxides formed are separated from the gangue minerals by magnetic methods.

5.19 The Aqueous Oxidation of Iron Sulfides [333]

The behavior of pyrite and arsenopyrite during leaching is different from other sulfides due to the presence of the disulfide ion, S_2^{2-}. Arsenopyrite contains in addition, the diarsenide ion, As_2^{2-}. The presence of the disulfide ions is manifested on heating the minerals in absence of air: pyrite loses an atom of sulfur, while arsenopyrite loses an atom of arsenic:

$$FeS_2 \rightarrow FeS + S$$

$$FeAsS \rightarrow FeS + As$$

5.19.1 Pyrite

Pyrite dissociates in water as follows:

$$FeS_{2(s)} \rightleftharpoons Fe^{2+}_{(aq)} + S^{2-}_{2(aq)}$$

When the disulfide ion reacts further, the equilibrium is shifted to the right, and more pyrite goes into solution. Disulfide ion is similar to peroxide ion, O_2^{2-}, which may undergo autooxidation[1] to elemental sulfur and sulfide ion:

$$S_2^{2-} \rightarrow 2S + 2e^-$$

$$S_2^{2-} + 2e^- \rightarrow 2S^{2-}$$

Overall reaction:

$$S_2^{2-} \rightarrow S + S^{2-}$$

Hence, three paths may arise depending on the conditions:

- High acidity and the absence of oxygen. In this case H_2S is formed:

$$S^{2-} + 2H^+ \rightarrow H_2S$$

or

$$FeS_2 + 2H^+ \rightarrow Fe^{2+} + S + H_2S$$

- High acidity and low oxygen concentration. In this case, elemental sulfur is formed:

$$S^{2-} \rightarrow S + 2e^-$$

$${}^1/_2O_2 + 2H^+ + 2e^- \rightarrow H_2O$$

Overall reaction:

$$S^{2-} + {}^1/_2O_2 + 2H^+ \rightarrow S + H_2O$$

or

$$FeS_2 + {}^1/_2O_2 + 2H^+ \rightarrow Fe^{2+} + 2S + H_2O$$

In this case, the aqueous oxidation of pyrite may be considered to take place by an electrochemical mechanism like other sulfides in acid medium and can be represented by:

Anodic reaction: $FeS_2 \rightarrow Fe^{2+} + 2S + 2e^-$

Cathodic reaction: ${}^1/_2O_2 + 2H^+ + 2e^- \rightarrow H_2O$

- In neutral medium and high oxygen concentration: In this case, it seems that the autooxidation of the disulfide ion does not take place because in neutral medium, thiosulfates and other lower oxidation products were identified. Thiosulfates may, therefore, form directly from the disulfide ion by the following reaction:

[1] The autooxidation of peroxide ion is as follows:
$O_2^{2-} \rightarrow O_2 + 2e^-$ $\quad O_2^{2-} + 2e^- \rightarrow 2O^{2-}$
Overall reaction:
$2O_2^{2-} \rightarrow O_2 + 2O^-$ or $2H_2O_2 \rightarrow O_2 + 2H_2O$

$$S_2^{2-} + {}^3/_2O_2 \rightarrow S_2O_3^{2-}$$

which oxidizes further to sulfate:

$$S_2O_3^{2-} + 5H_2O \rightarrow 2SO_4^{2-} + 10H^+ + 8e^-$$

$${}^1/_2O_2 + H_2O + 2e^- \rightarrow 2OH^-$$

$$H^+ + OH^- \rightarrow H_2O$$

The overall reaction in this case is:

$$S_2O_3^{2-} + 2O_2 + H_2O \rightarrow 2SO_4^{2-} + 2H^+$$

which leads to the global oxidation reaction of pyrite in neutral medium

$$S_2^{2-} + {}^7/_2O_2 + H_2O \rightarrow 2SO_4^{2-} + 2H^+$$

or

$$FeS_2 + {}^7/_2O_2 + H_2O \rightarrow Fe^{2+} + 2SO_4^{2-} + 2H^+$$

Two points should be noted from the above scheme:

- Pyrite takes up one eighth of its oxygen required for oxidation to sulfate from the water and the remaining from molecular oxygen. This was confirmed experimentally by using radioactive oxygen in following up the reaction.
- Under certain conditions hydroxyl ions are formed during the oxidation. This was confirmed when pyrite was in contact with water containing agar-agar thus minimizing the diffusion of OH^- ions. Cathodic regions form on pyrite whereby oxygen is reduced according to:

$${}^1/_2O_2 + H_2O + 2e^- \rightarrow 2OH^-$$

while at the anodic zone the following reactions would take place:

$$FeS_2 \rightarrow Fe^{2+} + S_2^{2-}$$

$$S_2^{2-} + {}^3/_2O_2 \rightarrow S_2O_3^{2-}$$

$$S_2O_3^{2-} + 5H_2O \rightarrow 2SO_4^{2-} + 10H^+ + 8e^-$$

The presence of thiosulfates in waste solutions raises an environmental problem because these are usually not precipitated by standard methods like sulfates, e.g., when adding $Ca(OH)_2$. Hence they escape the mine site and may contaminate surface waters. This topic was the subject of an extensive research project in Canada.

Sulfites were also identified in deaerated solutions. The relation between disulfide, thiosulfate, sulfites, and sulfate ions is shown schematically below:

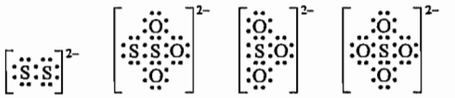

5.19.2 Arsenopyrite

Arsenopyrite may dissociate in water as follows:

$$2FeAsS_{(s)} \rightleftharpoons 2Fe^{2+}_{(aq)} + As^{2-}_{2(aq)} + S^{2-}_{2(aq)}$$

The behavior of disulfide ion is probably the same as in the case of pyrite in acid and in neutral medium, while the diarsenide ion forms arsenic acid:

$$As_2^{2-} + 3O_2 + 2H^+ + 2H_2O \rightarrow 2H_3AsO_4$$

The overall reactions are:

- In acid medium:

$$4FeAsS + 7O_2 + 8H^+ + 2H_2O \rightarrow 4H_3AsO_4 + 4Fe^{2+} + 4S$$

- In neutral medium:

$$4FeAsS + 13O_2 + 6H_2O \rightarrow 4H_3AsO_4 + 4Fe^{2+} + 4SO_4^{2-}$$

Ferrous ion formed in the above reactions oxidizes further to form ferric arsenate precipitates:

$$2Fe^{2+} + {}^1/_2O_2 + 2H^+ \rightarrow 2Fe^{3+} + H_2O$$

$$Fe^{3+} + H_3AsO_4 + 2H_2O \rightarrow FeAsO_4 + 2H_2O + 3H^+$$

5.19.3 Pyrrhotite

Pyrrhotite is slowly solubilized in water at 110 °C and 200 kPa oxygen pressure as ferrous sulfate:

$$FeS + 2O_{2(aq)} \rightarrow FeSO_{4(aq)}$$

If, however, the reaction is conducted in presence of dilute acid (0.1 M), the formation of elemental sulfur and ferric oxide takes place:

$$2FeS + {}^3/_2O_{2(aq)} \xrightarrow{H^+} Fe_2O_3 + 2S$$

It will be also observed that the acid initially added will be present unchanged at the end of reaction. In fact the acid is consumed at the initial stage of the reaction and then regenerated later. The reason is that the oxidation of

ferrous ion to ferric is possible only in presence of acid:

$$2Fe^{2+} + 2H^+ + {}^1/_2O_2 \rightarrow Fe^{3+} + H_2O$$

Hydrolysis of ferric ion then follows with generation of acid:

$$Fe^{3+} + 3H_2O \rightarrow Fe(OH)_3 + 3H^+$$

$$2Fe(OH)_3 \rightarrow Fe_2O_3 + 3H_2O$$

That is why FeS suspended in water will yield only a solution of $FeSO_4$ when oxidized but in presence of acid the formation of Fe^{3+} becomes possible. Because of hydrolysis, Fe_2O_3 is formed and the acid is regenerated. It should be observed that the oxygen utilization in the presence of acid is less than in the first case.

5.20 Regeneration of Iron-Containing Pickling Baths

In Germany in 1987, the output of rolled steel products from base, high-grade, and stainless steels averaged 2.0×10^6 t per month. Approximately 60% of this is pickled at least once.

Pickling removes the oxide layer that adheres to the steel surface. The oxide layer arises as scale in heat-treatment processes or as rust through the corrosive action of water, with its load of dissolved susbstances, or through humid atmospheric corrosion.

Whereas rust consists largely of Fe_2O_3, scale is made up of the three iron oxides (wustite FeO, magnetite Fe_3O_4, and hematite Fe_2O_3) in a ratio that depends on steel composition, annealing conditions (temperature, heating time, furnace atmosphere), final temperature of rolling, and rate of cooling after rolling.

The "picklability" of a steel and the acid consumption for pickling also depend on many factors: adherence of scale, composition of the steel, mode and magnitude of mechanical working, type and composition of pickling solution, and pickling conditions. The selection of pickling acid is dictated by the required surface quality and by economic factors. The most important pickling acids for iron and steel are sulfuric and hydrochloric. Phosphoric, nitric, and hydrofluoric acids are used for special purposes and stainless steels.

Iron(III) ions that dissolve during pickling are reduced by metallic iron, so that the pickling acid contains primarily iron (II) salts. The quantity of iron dissolved during pickling is called chemical pickling loss; it accounts for 0.2–1.2% of the iron or steel being pickled and accounts for approximately three-quarters of the weight loss during pickling.

If iron salts are removed from the pickling liquor, the unconsumed pickling solution can be returned to the pickling unit after the addition of an amount of acid equivalent to the quantity of salts precipitated.

The acid consumed in pickling can also be completely regenerated from the iron salts. The pickling liquor recycled between the pickling tanks and the regeneration unit is thus not consumed, apart from evaporation losses.

5.20.1 Sulfuric Acid Pickling Solutions

When steel is pickled with sulfuric acid, the scale oxides dissolve to give iron sulfates. The rate of dissolution of the three oxides in sulfuric acid increases in the order Fe_2O_3, Fe_3O_4, FeO. The reaction of sulfuric acid with metallic iron to give iron(II) sulfate and hydrogen is inhibited by pickling additives (inhibitors).

Two processes are employed to regenerate sulfuric acid pickling liquor, whose description follows.

5.20.1.1 Crystallization

In industrial plants, spent pickling solution is usually cooled by using brine. The cooling effect depends strongly on the cleanness of the cooling surface, on which salt crust can easily form. These systems, therefore, require very careful upkeep. Frequent shutdowns must be expected.

Vacuum Crystallization (Figure 5.106). A vacuum equal to the vapor pressure of water at the desired final temperature is maintained in the crystallization vessel.

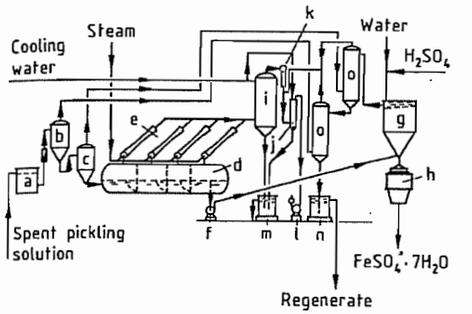

Figure 5.106: Vacuum crystallization (Keramchemie/Lurgi): a) Suction tank; b, c) Precoolers; d) Crystallizer; e) Steam-jet compressor; f) Salt-slurry pump; g) Thickener; h) Centrifuge; i) Direct-contact condenser; j) Auxiliary condenser; k) Steam-jet venting device; l) Vacuum pump; m) Water receiver; n) Pickling solution receiver; o) Acid direct-contact condensers.

Part of the pickling solution is pumped continuously from the pickling tank to the vacuum crystallizer, where it is cooled evaporatively to 5 °C and then to 0 °C to crystallize iron(II) sulfate. Water vapor flows directly, or after compression in a high-performance steam-jet apparatus, to a direct-contact condenser. The salt–liquid mixture is removed continuously by a salt-slurry pump and separated in a centrifuge. After the mother liquor has been freshened with concentrated sulfuric acid and water, it is returned to the pickling tank. The vacuum in the evaporator is maintained by a vacuum pump connected to the direct-contact condenser.

A modified design omits the steamjet apparatus; therefore, only electrical energy is needed for its operation, which may be an economic advantage because in this case no fuel is required for steam generation.

Cyclone Crystallization (Figure 5.107). In the cyclone crystallizer (b), fine droplets of spent pickling solution are sprayed countercurrent to a stream of air. In this way, rapid evaporation and cooling are accomplished. If the iron content of the pickling solution is to be kept low, a second cooling stage is added. Indirect cooling with water or brine takes place in the cooling vessel (c). A blower injects air to prevent the crystals from settling and forming a crust on the vessel wall. Iron(II) sulfate crystals are separated in the centrifuge (d); the filtrate (regenerate) is returned to the pickling plant.

The iron(II) heptahydrate can be used in the production of cyanoferrates, as a flocculent in wastewater treatment, in the production of gas adsorbents, as a pesticide, as a chemical fertilizer, and in the production of iron-oxide pigments.

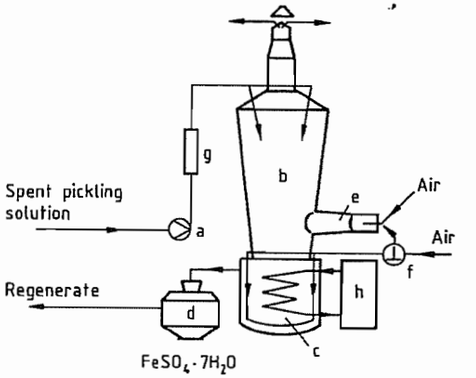

Figure 5.107: Cyclone crystallizer (Andritz-Ruthner): a) Acid pump; b) Cyclone crystallizer; c) Cooling vessel; d) Centrifuge; e) Vent; f) Blower; g) Pickling liquor tank; h) Cooling system.

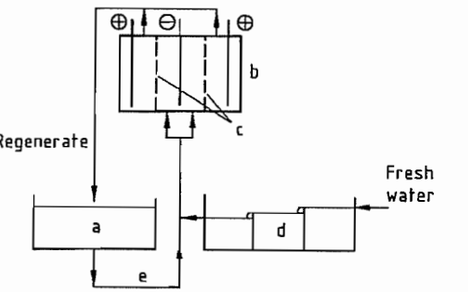

Figure 5.108: Regeneration by electrolysis: a) Pickling tank; b) Electrolysis cell; c) Diaphragms; d) Cascade rinsing; e) Spent pickling solution.

The heptahydrate can also be converted to the monohydrate. A continuous apparatus for the preparation of very pure monohydrate is built by Mannesmann Anlagenbau/Messo-Chemietechnik.

The heptahydrate is dehydrated to the monohydrate at a well-defined acid concentration at ca. 90 °C. After separation of the crys-

talline monohydrate in a centrifuge, iron sulfate-poor mother liquor is returned to the reactor. The water vapor resulting from the dehydration is removed from the cycle.

5.20.1.2 Electrolysis

An electrolytic process has recently been developed [334]. Cathode and anode compartments are separated by a diaphragm (Figure 5.108). Metallic iron is deposited at the cathode; sulfuric acid and oxygen are produced at the anode. Electrolysis is facilitated by addition of an electrolyte, which is not consumed and does not affect the pickling process, but allows iron to be recovered most effectively from the acidic solution. Sulfuric acid either flows directly from the anode compartment back to the pickling tank or is detained temporarily in a holding tank.

Evaporation and electrochemical decomposition result in a continual loss of water. Using multiple countercurrent cascade rinsing after pickling allows the quantity of water to be adjusted so that no wastewater is produced. The unit is marketed by Keramchemie.

5.20.2 Hydrochloric Acid Pickling Solutions

Because of its technical advantages, hydrochloric acid has largely replaced sulfuric acid in pickling baths, especially in large plants.

Hydrogen is produced when iron is dissolved. Iron(III) chloride, formed by dissolution of Fe_3O_4 and Fe_2O_3, is reduced by the hydrogen to yield $FeCl_2$, so that virtually the only chloride present in the pickling liquor is iron(II) chloride. Spent pickling solution can be regenerated completely by thermal decomposition. Iron chloride is converted to iron oxide and hydrochloric acid:

$$4FeCl_2 + 4H_2O + O_2 \rightarrow 2Fe_2O_3 + 8HCl$$

Gas or oil is used as fuel. The heat consumption is ca. 3 MJ for the simultaneous regeneration of 1 L of pickling solution and 1 L of rinse liquor.

In large-scale operations, the two processes that have found widespread application are (1) the fluidized-bed process and (2) the spray-roasting process.

Each is employed in more than 100 industrial plants. The efficiency of the acid recovery is ca. 99%.

Fluidized-Bed Process. In the Lurgi–Keramchemie fluidized-bed regeneration process [335] (Figure 5.109), spent pickling solution is led via the settling tank and the venturi loop into the fluidized bed in the reactor. The bed consists of granulated iron oxide. Residual acid and water are evaporated at 850 °C, and iron chloride is converted to iron oxide and hydrogen chloride. Growth and new formation of iron oxide grains in the fluidized bed are controlled so that a dust-free granulated product is obtained, with a particle diameter of 1–2 mm and a bulk density of ca. 3.5 g/cm³. The granular product is discharged continuously at the bottom of the reactor and transported by a vibrating cooling chute and a vibrating spiral conveyor to the storage bin. In smaller units, the granular product can also be discharged directly into shipping containers.

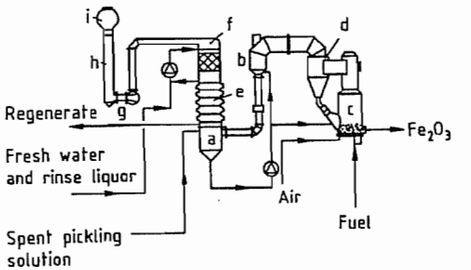

Figure 5.109: Fluidized-bed process for regeneration of hydrochloric acid pickling solutions: a) Separating tank; b) Venturi scrubber; c) Reactor; d) Cyclone; e) Absorber; f) Scrubbing stage; g) Off-gas blower; h) Stack; i) Mist collector.

The hot gases from the reactor contain hydrogen chloride and a small amount of iron oxide dust, which is collected in the cyclone and returned to the fluidized bed. In the venturi scrubber, the off-gas is then cooled to ca. 100 °C. The thermal energy of the off-gases is used to concentrate the pickling solution by evaporation before it is fed to the reactor. Fine dust particles in the gas stream are removed by scrubbing.

From the venturi scrubber, the cooled gas stream goes to the absorber, where hydrogen chloride is absorbed adiabatically with rinse liquor and fresh water. The hydrochloric acid thus produced has a concentration of ca. 18%. It is recycled to the pickling unit or held in a storage tank. After passing through a scrubbing stage and a mist collector, the off-gas is virtually free of hydrochloric acid and is released to the atmosphere.

Spray-Roast Process. The spray-roast process is often employed for the recovery of metal oxides from metal chloride solutions. It can also be used for the regeneration of iron chloride-laden hydrochloric acid solution [336]. The pure spray-roast oxide obtained in this way is used in the ferrite industry (150 000 t in 1987).

As shown in Figure 5.110, spent pickling solution goes to the venturi scrubber where hot gases concentrate it hy evaporation of water. In the next step, the highly concentrated pickling liquor is injected into the spray-roast reactor at a pressure of 0.3–0.5 MPa as a fine spray either cocurrent or countercurrent to hot combustion gases. The cocurrent arrangement is common for pickling acids that contain zinc and lead, because their chlorides have high vapor pressures and are separated after a shorter retention time.

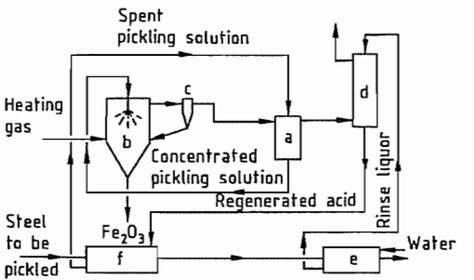

Figure 5.110: Spray-roast process for regeneration of hydrochloric acid pickling solutions: a) Venturi scrubber; b) Spray-roast reactor; c) Cyclone; d) Absorber; e) Rinse tanks; f) Pickling tanks.

The temperature of the roasting gas outlet from the spray tower is about 400 °C. The gases proceed to the cyclone. Fine iron oxide powder, together with the oxide collected in the cyclone, is discharged continuously (bulk density 0.3–0.4 g/cm³).

When some silicon-rich steels are pickled, the silicon dioxide content of the pickling solution does not permit the iron(III) oxide product to be used in the ferrite industry. The quantity of silica can be reduced in an additional precleaning step [337], in which silica is selectively removed from the pickling solution.

After passing through the cyclone, the roasting gases are cooled and scrubbed in the venturi scrubber before going to the absorber, where hydrogen chloride is absorbed to produce 18–20% hydrochloric acid. The acidic iron chloride solution, which is generated when the pickled steel is rinsed, is used as the absorption liquor. Hydrochloric acid is recycled to the pickling tank. Residual gases, with a low hydrochloric acid content, are discharged to the atmosphere.

Spray-roast plants have unit capacities of 0.3–25 m³/h of pickling acid and a similar amount of rinse liquor.

The Fe_2O_3 generated in the thermal decomposition process can be used as raw material in various industries. The most important options are the production of magnetic materials (e.g., soft and hard ferrites), the production of iron powder for the fabrication of sintered parts and welding electrodes, and use as an additive in the manufacture of magnetic tapes, abrasives, tiles, glass, cosmetics, and pigments.

5.20.3 Nitric and Hydrofluoric Acid Pickling Solutions

Stainless and acid-resistant steels are usually pickled with a mixture of nitric and hydrofluoric acids. Nitric acid serves as an oxidizing agent, whereas hydrofluoric acid forms complexes with metal ions. In contrast to the pickling of carbon steel, the permissible iron concentration in a pickling solution for special steels is limited by the tendency of iron and the alloy components to form fluoride complexes and thus reduce the concentration of fluoride ions in solution. Severe inhibition of the pickling process occurs at a total metal

concentration of 50 g/L, so that pickling solutions must be topped up with fresh hydrofluoric acid, and eventually neutralized and discarded, even though only about half the acid content has been consumed.

When the pickling bath is neutralized with calcium hydroxide, the resulting metal hydroxides and calcium fluoride form a sludge that can be disposed of without treatment, but nitrates remain in solution and contribute to eutrophication in receiving waters.

The following regeneration processes have been devised in recent years.

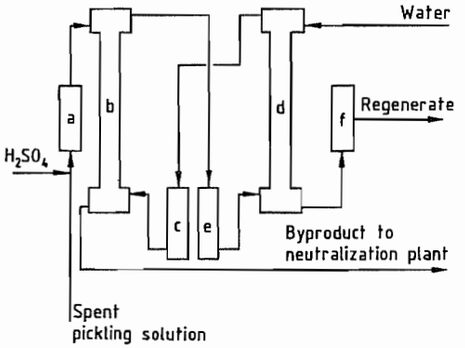

Figure 5.111: Regeneration of HF–HNO_3 pickling liquors by liquid–liquid extraction: a) Heat exchanger; b) Extraction column; c) Storage tank; d) Reextraction column; e) Storage tank; f) Adsorber.

Liquid–Liquid Extraction. Liquid–liquid extraction [338] makes use of the fact that nitric and hydrofluoric acids form adducts with tributyl phosphate that are soluble in hydrocarbon solvents. Addition of sulfuric acid also renders extractable acid anions bound in the form of metal salts. Around 93% of the nitric acid and 60% of the hydrofluoric acid can be recovered. The flow sheet for the process is shown in Figure 5.111.

After sulfuric acid has been added to the spent pickling solution and the mixture has been cooled, it is directed to the top of an extraction tower; the organic phase enters at the bottom. The aqueous raffinate, containing sulfuric acid, is discharged at the bottom. From the top of the tower, the organic phase, laden with extracted acid, goes to the foot of a re-extraction tower. The water inlet at the top washes out the acids. The organic phase discharged at the top goes back to the extraction tower. In an adsorber, traces of tributyl phosphate are removed from the aqueous regenerate before it is returned to the pickling tank. The tributyl phosphate is returned to the tank (c).

Fluoride-Crystallization. In this process, the recovery of nitric acid is ca. 90% (Figure 5.112) and that of hydrofluoric acid, 55%, despite the fact that metals precipitate as fluorides, so that corresponding amounts of hydrofluoric acid are consumed. The filter residue can be employed as a feedstock for the production of hydrofluoric acid or for the recovery of nickel.

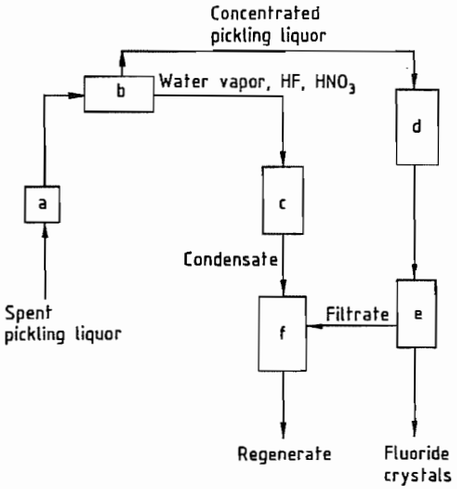

Figure 5.112: Regeneration of HNO_3–HF pickling solutions by fluiride crystallization: a) Particle collector; b) Flow-through evaporator; c) Condenser; d) Crystallization tanks; e) Filter; f) Storage tank.

Spent pickling solution is led through a particulate collector and a flow-through evaporator, where it is evaporated within minutes to about half its volume by electrical heating. The water vapor, which contains part of the nitric and hydrofluoric acids, is condensed by indirect cooling. The sparingly soluble fluorides of iron and of the alloy constituents precipitate from the concentrated, supersaturated solution in crystallization tanks and are removed periodically by filtration. The filtrate is led to a storage vessel where it is combined with condensate from the condenser. After addition of fresh nitric and hydrofluoric acid, the liquor is returned to the pickling tank.

Bipolar Membrane Process. In the bipolar membrane process [339] (Figure 5.113), the free acids are first recovered in an electrodialysis cell and then returned to the pickling tank. Metal ions are then precipitated as metal hydroxides by neutralization with potassium hydroxide. Metal hydroxide sludge is collected in the downstream filter press. The filtered salt solution (potassium fluoride and potassium nitrate) goes to a bipolar membrane module where HF, HNO_3, and KOH are separated from the potassium salts. The acid mixture is returned to the pickling tank, whereas potassium hydroxide is reused for neutralization. The dilute salt solution (KF, KNO_3) is desalted by reverse osmosis. Part of it is used as wash liquor for the filter press, and the rest is recycled to the membrane unit to obtain the highest possible yield of acids and potassium hydroxide. The residue from the filter can be reused as raw material in iron and steel works, depending on its content of metal hydroxides.

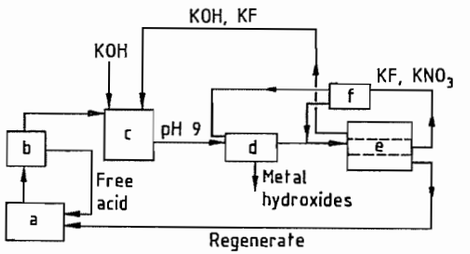

Figure 5.113: Regeneration of HNO_3–HF pickling solutions in a bipolar membrane cell: a) Pickling tank; b) Electrodialysis cell; c) Neutralization; d) Filter press; e) Bipolar membrane module (Aquatech cell); f) Reverse osmosis.

Retardation Process. The retardation process can generally be employed for separating strong inorganic acids from their salts. By loading a strongly basic ion-exchange resin with spent pickling solution and then eluting with water, separation into a high-salt fraction and a subsequent high-acid fraction is achieved. The flow sheet for the process is shown in Figure 5.114.

Acid retardation can probably be accounted for by diffusion of undissociated acid into the ion-exchange resin grains so that upon elution with water, it must diffuse back out; the result is that elution of acid is retarded [340].

For nitric and hydrofluoric acid pickling solutions, most of the free acids can be recovered in this way. Partial regeneration of pickling solutions reduces disposal costs.

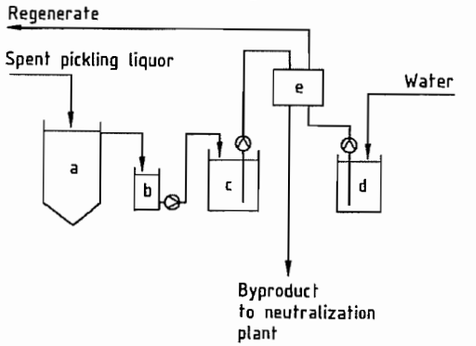

Figure 5.114: Regeneration of HNO_3–HF pickling solutions by acid retardation: a) Sedimentation tank; b) Buffer tank; c) Pickling-liquor metering tank; d) Water metering tank; e) Resin bed.

5.21 Pigments

5.21.1 Iron Oxide Pigments

The continually increasing importance of iron oxide pigments is based on their nontoxicity; chemical stability; wide variety of colors ranging from yellow, orange, red, brown, to black; and low price. Natural and synthetic iron oxide pigments consist of well-defined compounds with known crystal structures:

- α-FeOOH, goethite, diaspore structure, color changes with increasing particle size from green-yellow to brown-yellow
- γ-FeOOH, lepidocrocite, boehmite structure, color changes with increasing particle size from yellow to orange
- α-Fe_2O_3, hematite, corundum structure, color changes with increasing particle size from light red to dark violet

- γ-Fe_2O_3, maghemite, spinel super structure, ferrimagnetic, color: brown
- Fe_3O_4, magnetite, spinel structure, ferrimagnetic, color: black

Mixed metal oxide pigments containing iron oxide are also used. Magnetic iron oxide pigments and transparent iron oxide pigments are described later.

5.21.1.1 Natural Iron Oxide Pigments

Naturally occurring iron oxides and iron oxide hydroxides were used as pigments in prehistoric times (Altamira cave paintings) [341]. They were also used as coloring materials by the Egyptians, Greeks, and ancient Romans.

Hematite (α-Fe_2O_3) has attained economic importance as a red pigment, goethite (α-FeOOH) as yellow, and the umbers and siennas as brown pigments. Deposits with high iron oxide contents are exploited preferentially. Naturally occurring magnetite (Fe_3O_4) has poor tinting strength as a black pigment, and has found little application in the pigment industry.

Hematite is found in large quantities in the vicinity of Málaga in Spain (Spanish red) and near the Persian Gulf (Persian red). The Spanish reds have a brown undertone. Their water-soluble salt content is very low and their Fe_2O_3 content often exceeds 90%. The Persian reds have a pure hue, but their water-soluble salt content is disadvantageous for some applications. Other natural hematite deposits are of only local importance. A special variety occurs in the form of platelets and is extracted in large quantities in Kärnten (Austria). This micaceous iron oxide, is mainly used in corrosion protection coatings.

Goethite is the colored component of yellow ocher, a weathering product mainly of siderite, sulfidic ores, and feldspar. It occurs in workable amounts mainly in South Africa and France. The Fe_2O_3 content gives an indication of the iron oxide hydroxide content of the ocher, and is ca. 20% in the French deposits and ca. 55% in the South African.

Umbers are mainly found in Cyprus. In addition to Fe_2O_3 (45–70%), they contain considerable amounts of manganese dioxide (5–20%). In the raw state, they are deep brown to greenish brown and when calcined are dark brown with a red undertone (burnt umbers).

Siennas, mainly found in Tuscany, have an average Fe_2O_3 content of ca. 50%, and contain < 1% manganese dioxide. They are yellow-brown in the natural state and red-brown when calcined [342].

The processing of natural iron oxide pigments depends on their composition. They are either washed, slurried, dried, ground, or dried immediately and then ground in ball mills, or more often in disintegrators or impact mills [343].

Siennas and umbers are calcined in a directly fired furnace, and water is driven off. The hue of the products is determined by the calcination period, temperature, and raw material composition [344].

Natural iron oxide pigments are mostly used as inexpensive marine coatings or in coatings with a glue, oil, or lime base. They are also employed to color cement, artificial stone, and wallpaper. Ocher and sienna pigments are used in the production of crayons, drawing pastels, and chalks [345].

The economic importance of the natural iron oxide pigments has decreased in recent years in comparison with the synthetic materials.

5.21.1.2 Synthetic Iron Oxide Pigments

Synthetic iron oxide pigments have become increasingly important due to their pure hue, consistent properties, and tinting strength. Single-component forms are mainly produced with red, yellow, orange, and black colors. Their composition corresponds to that of the minerals hematite, goethite, lepidocrocite, and magnetite. Brown pigments usually consist of mixtures of red and/or yellow and/or black; homogeneous brown phases are also produced, e.g., $(Fe, Mn)_2O_3$ and γ-Fe_2O_3, but quantities are small in comparison to the mixed materials. Ferrimagnetic γ-Fe_2O_3 is of great importance for magnetic recording materials.

Several processes are available for producing high-quality iron oxide pigments with controlled mean particle size, particle size distribution, particle shape, etc. (Table 5.46):

- Solid-state reactions (red, black, brown)
- Precipitation and hydrolysis of solutions of iron salts (yellow, red, orange, black)
- Laux process involving reduction of nitrobenzene (black, yellow, red)

The raw materials are mainly by-products from other industries: steel scrap obtained from deep drawing, grindings from cast iron, $FeSO_4 \cdot 7H_2O$ from TiO_2 production or from steel pickling, and $FeCl_2$ also from steel pickling.

Iron oxides obtained after flame spraying of spent hydrochloric acid pickle liquor, red mud from bauxite processing, and the product of pyrites combustion are no longer of importance. They yield pigments with inferior color properties that contain considerable amounts of water-soluble salts. They can therefore only be used in low-grade applications.

Solid-State Reactions of Iron Compounds. Black iron oxides obtained from the Laux process (see below) or other processes may be calcined in rotary kilns with an oxidizing atmosphere under countercurrent flow to produce a wide range of different red colors, depending on the starting material. The pigments are ground to the desired particle size in pendular mills, pin mills, or jet mills, depending on their hardness and intended use.

The calcination of yellow iron oxide produces pure red iron oxide pigments with a high tinting strength. Further processing is similar to that of calcined black pigments.

High-quality pigments called copperas reds are obtained by the thermal decomposition of $FeSO_4 \cdot 7H_2O$ in a multistage process (Figure 5.115). If an alkaline-earth oxide or carbonate is included during calcination, the sulfate can be reduced with coal or carbon-containing compounds to produce sulfur dioxide, which is oxidized with air to give sulfuric acid [346–349]. The waste gases and the dissolved impurities that are leached out in the final stage present ecological problems, however.

Table 5.46: Reaction equations for the production of iron oxide pigments.

Color	Reaction			Process
Red	$6FeSO_4 \cdot xH_2O + {}^3/_2O_2$	→	$Fe_2O_3 + 2Fe_2(SO_4)_3 + 6H_2O$	copperas process
	$2Fe_2(SO_4)_3$	→	$2Fe_2O_3 + 6SO_3$	
	$2Fe_3O_4 + {}^1/_2O_2$	→	$3Fe_2O_3$	calcination
	$2FeOOH$	→	$Fe_2O_3 + H_2O$	calcination
	$2FeCl_2 + 2H_2O + {}^1/_2O_2$	→	$Fe_2O_3 + 4HCl$	Ruthner process
	$2FeSO_4 + {}^1/_2O_2 + 4NaOH$	→	$Fe_2O_3 + 2Na_2SO_4 + 2H_2O$	precipitation
Yellow	$2FeSO_4 + 4NaOH + {}^1/_2O_2$	→	2α-$FeOOH + 2Na_2SO_4 + H_2O$	precipitation
	$2Fe + 2H_2SO_4$	→	$2FeSO_4 + 2H_2$	Penniman process
	$2FeSO_4 + {}^1/_2O_2 + 3H_2O$	→	2α-$FeOOH + 2H_2SO_4$	
	$2Fe + {}^1/_2O_2 + 3H_2O$	→	2α-$FeOOH + 2H_2$	
	$2Fe + C_6H_5NO_2 + 2H_2O$	→	2α-$FeOOH + C_6H_5NH_2$	Laux process
Orange	$2FeSO_4 + 4NaOH + {}^1/_2O_2$	→	2γ-$FeOOH + 2Na_2SO_4 + H_2O$	precipitation
Black	$3FeSO_4 + 6NaOH + {}^1/_2O_2$	→	$Fe_3O_4 + 3Na_2SO_4 + 3H_2O$	1-step precipitation
	$2FeOOH + FeSO_4 + 2NaOH$	→	$Fe_3O_4 + Na_2SO_4 + 2H_2O$	2-step precipitation
	$9Fe + 4C_6H_5NO_2 + 4H_2O$	→	$3Fe_3O_4 + 4C_6H_5NH_2$	Laux process
	$3Fe_2O_3 + H_2$	→	$2Fe_3O_4 + H_2O$	reduction
Brown	$2Fe_3O_4 + {}^1/_2O_2$	→	3γ-Fe_2O_3	calcination
	$3Fe_3O_4 + Fe_2O_3 + MnO_2 + {}^1/_2O_2$	→	$(Fe_{11}Mn)O_{18}$	calcination

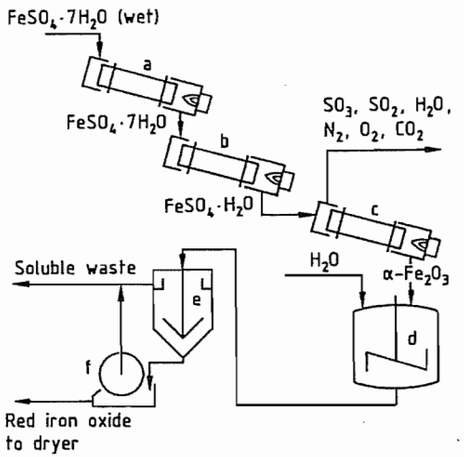

Figure 5.115: Production of copperas red: a) Dryer; b) Rotary kiln (dewatering); c) Rotary kiln; d) Tank; e) Thickener; f) Filter.

Lower quality products can be obtained by single-stage calcination of iron(II) sulfate heptahydrate in an oxidizing atmosphere. The pigments have a relatively poor tinting strength and a blue tinge. Decomposition of iron(II) chloride monohydrate in air at high temperatures also yields a low-quality red iron oxide pigment [350].

In a new process, micaceous iron oxide is obtained in high yield by reacting iron(III) chloride and iron at 500–1000 °C in an oxidizing atmosphere in a tubular reactor [351].

Black Fe_3O_4 pigments with a high tinting strength can be prepared by calcining iron salts under reducing conditions [352]. This process is not used industrially because of the furnace gases produced.

Controlled oxidation of Fe_3O_4 at ca. 500 °C produces a single-phase brown γ-Fe_2O_3 with a neutral hue [353].

Calcination of α-FeOOH with small quantities of manganese compounds gives homogeneous brown pigments with the composition $(Fe, Mn)_2O_3$ [354]. Calcination of iron and chromium compounds that decompose at elevated temperatures yields corresponding pigments with the composition $(Fe, Cr)_2O_3$ [355].

Precipitation Processes. In principle, all iron oxide hydroxide phases can be prepared from aqueous solutions of iron salts (Table 5.46). However, precipitation with alkali produces neutral salts (e.g., Na_2SO_4, NaCl) as by-products which enter the wastewater.

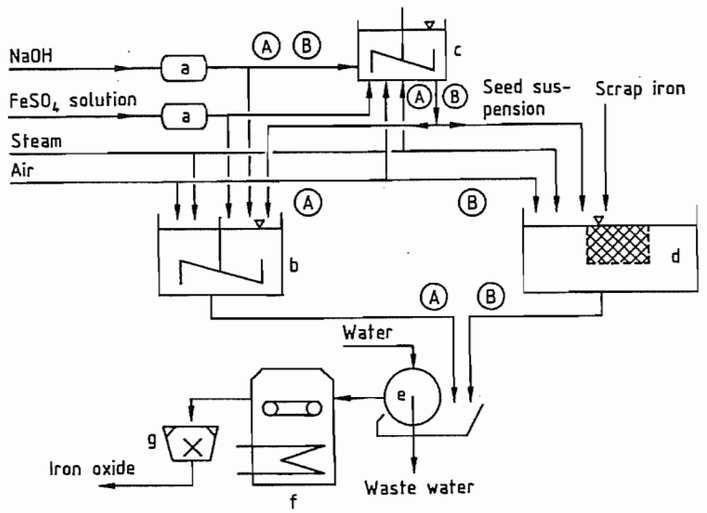

Figure 5.116: Production of yellow iron oxide by the precipitation (A) and Penniman (B) processes: a) Tank; b) Pigment reactor; c) Seed reactor; d) Pigment reactor with scrap basket; e) Filter; f) Dryer; g) Mill.

Precipitation is especially suitable for producing soft pigments with a pure, bright hue. The manufacture of α-FeOOH yellow is described as an example. The raw materials are iron(II) sulfate ($FeSO_4 \cdot 7H_2O$) or liquors from the pickling of iron and steel, and alkali [NaOH, $Ca(OH)_2$, ammonia, or magnesite]. The pickle liquors usually contain appreciable quantities of free acid, and are therefore first optionally neutralized by reaction with scrap iron. Other metallic ions should not be present in large amounts, because they have an adverse effect on the hue of the iron oxide pigments.

The solutions of the iron salts are first mixed with alkali in open reaction vessels (Figure 5.116 Route A) and oxidized, usually with air. The quantity of alkali used is such that the pH remains acidic. The reaction time (ca. 10–100 h) depends on the temperature (10–90 °C) and on the desired particle size of the pigment. This method yields yellow pigments (α-FeOOH) [356, 357]. If yellow nuclei are produced in a separate reaction (Route A in Figure 5.116, tank c), highly consistent yellow iron oxide pigments with a pure color can be obtained [358].

If precipitation is carried out at ca. 90 °C while air is passed into the mixture at ca. pH ≥ 7, black iron oxide pigments with a magnetite structure and a good tinting strength are obtained when the reaction is stopped at a $FeO:Fe_2O_3$ ratio of ca. 1:1. The process can be accelerated by operating at 150 °C under pressure; this technique also improves pigment quality [359]. Rapid heating of a suspension of iron oxide hydroxide with the necessary quantity of $Fe(OH)_2$ to ca. 90 °C also produces black iron oxide of pigment quality [360, 361].

Orange iron oxide with the lepidocrocite structure (γ-FeOOH) is obtained if dilute solutions of the iron(II) salt are precipitated with sodium hydroxide solution or other alkalis until almost neutral. The suspension is then heated for a short period, rapidly cooled, and oxidized [362, 363].

Very soft iron oxide pigments with a pure red color may be obtained by first preparing α-Fe_2O_3 nuclei, and then continuously adding solutions of iron(II) salt with atmospheric oxidation at 80 °C. The hydrogen ions liberated by oxidation and hydrolysis are neutralized by adding alkali and keeping the pH constant [364]. Pigment-quality α-Fe_2O_3 is also obtained when solutions of an iron(II) salt, preferably in the presence of small amounts of other cations, are reacted at 60–95 °C with excess sodium hydroxide and oxidized with air [365].

The Penniman process is probably the most widely used production method for yellow iron oxide pigments [366, 367]. This method considerably reduces the quantity of neutral salts formed as by-products. The raw materials are iron(II) sulfate, sodium hydroxide solution, and scrap iron. If the sulfate contains appreciable quantities of salt impurities, these must be removed by partial precipitation. The iron must be free of alloying components. The process usually consists of two stages (Route B in Figure 5.116).

In the first stage, nuclei are prepared by precipitating iron(II) sulfate with alkali (e.g., sodium hydroxide solution) at 20–50 °C with aeration (c). Depending on the conditions, yellow, orange, or red nuclei may be obtained. The suspension of nuclei is pumped into vessels charged with scrap iron (d) and diluted with water. Here, the process is completed by growing the iron oxide hydroxide or oxide onto the nuclei. The residual iron(II) sulfate in the nuclei suspension is oxidized to iron(III) sulfate by blasting with air at 75–90 °C. The iron(III) sulfate is then hydrolyzed to form FeOOH or α-Fe_2O_3. The liberated sulfuric acid reacts with the scrap iron to form iron(II) sulfate, which is also oxidized with air. The reaction time can vary from ca. two days to several weeks, depending on the conditions chosen and the desired pigment. At the end of the reaction, metallic impurities and coarse particles are removed from the solid with sieves or hydrocyclones; water-soluble salts are removed by washing. Drying is carried out with band or spray dryers (f) and disintegrators or jet mills are used for grinding (g). The

main advantage of this process over the precipitation process lies in the small quantity of alkali and iron(II) sulfate required. The bases are only used to form the nuclei and the relatively small amount of iron(II) sulfate required initially is continually renewed by dissolving the iron by reaction with the sulfuric acid liberated by hydrolysis. The process is thus considered environmentally friendly. The iron oxide pigments produced by the Penniman process are soft, have good wetting properties, and a very low flocculation tendency [366–374].

Under suitable conditions the Penniman process can also be used to produce reds directly. The residual scrap iron and coarse particles are removed from the pigment, which is then dried [375] and ground using disintegrators or jet mills. These pigments have unsurpassed softness. They usually have purer color than the harder red pigments produced by calcination.

The Laux Process. The Béchamp reaction (i.e., the reduction of aromatic nitro compounds with antimony or iron) which has been known since 1854, normally yields a black-gray iron oxide that is unsuitable as an inorganic pigment. By adding iron(II) chloride or aluminum chloride solutions, sulfuric acid, and phosphoric acid, LAUX modified the process to yield high-quality iron oxide pigments [376]. Many types of pigments can be obtained by varying the reaction conditions. The range extends from yellow to brown (mixtures of α-FeOOH and/or α-Fe_2O_3 and/or Fe_3O_4) and from red to black. If, for example, iron(II) chloride is added, a black pigment with very high tinting strength is produced [376]. However, if the nitro compounds are reduced in the presence of aluminum chloride, high-quality yellow pigments are obtained [377]. Addition of phosphoric acid leads to the formation of light to dark brown pigments with good tinting strength [378]. Calcination of these products (e.g., in rotary kilns) gives light red to dark violet pigments. The processes are illustrated in Figure 5.117.

The type and quality of the pigment are determined not only by the nature and concentration of the additives, but also by the reaction rate. The rate depends on the grades of iron used, their particle size, the rates of addition of the iron and nitrobenzene (or another nitro compound), and the pH value. No bases are required to precipitate the iron compounds. Only ca. 3% of the theoretical amount of acid is required to dissolve all of the iron. The aromatic nitro compound oxidizes the Fe^{2+} to Fe^{3+} ions, acid is liberated during hydrolysis and pigment formation, and more metallic iron is dissolved by the liberated acid to form iron(II) salts; consequently, no additional acid is necessary.

The iron raw materials used are grindings from iron casting or forging that must be virtually free of oil and grease. The required fineness is obtained by size reduction in edge runner mills and classification with vibratory sieves. The iron and the nitro compound are added gradually via a metering device to a stirred tank (a) containing the other reactants (e.g., iron(II) chloride, aluminum chloride, sulfuric acid, and phosphoric acid). The system rapidly heats up to ca. 100 °C and remains at this temperature for the reaction period. The nitro compound is reduced to form an amine (e.g., aniline from nitrobenzene) which is removed by steam distillation. Unreacted iron is also removed (e.g., in shaking tables, c). The pigment slurry is diluted with water in settling tanks (d) and the pigment is washed to remove salts, and filtered on rotary filters (e). It may then be dried on band, pneumatic conveyor, or spray dryers to form yellow or black pigments, or calcined in rotary kilns (h) in an oxidizing atmosphere to give red or brown pigments. Calcination in a nonoxidizing atmosphere at 500–700 °C improves the tinting strength [379]. The pigments are then ground to the desired fineness in pendular mills, pin mills, or jet mills, depending on their hardness and application.

The Laux process is a very important method for producing iron oxide because of the coproduction of aniline; it does not generate by-products that harm the environment.

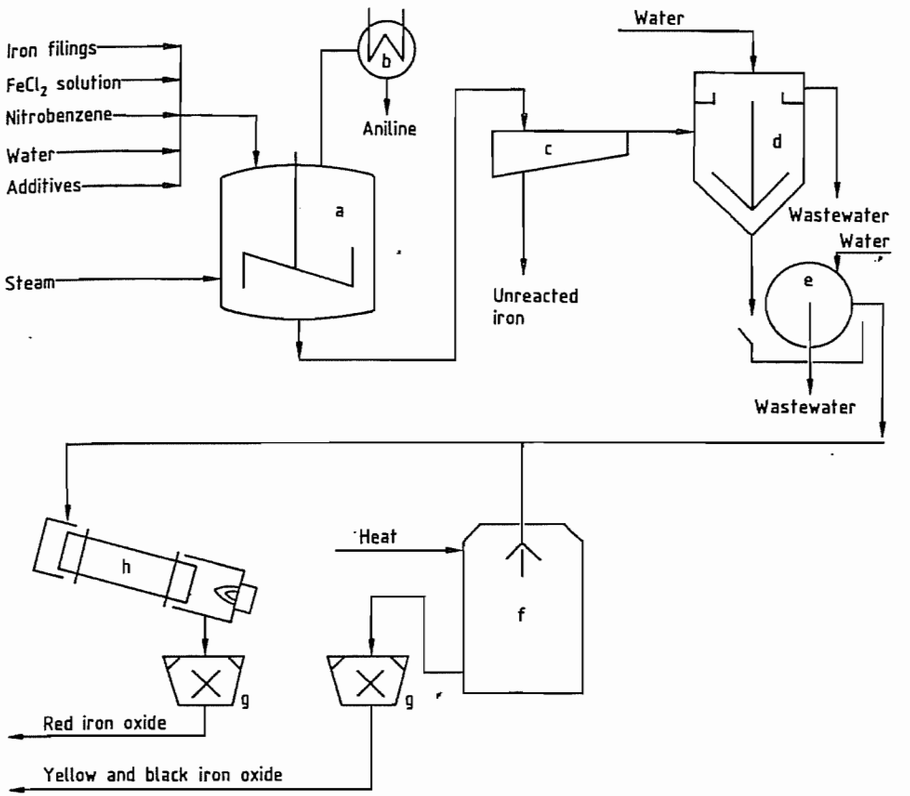

Figure 5.117: Production of iron oxide pigment by the Laux process: a) Reactor; b) Condenser; c) Classifier; d) Thickener; e) Filter; f) Dryer; g) Mill; h) Rotary kiln.

Other Production Processes. The three processes already described are the only ones that are used on a large scale. The following processes are used on a small scale for special applications:

- Thermal decomposition of $Fe(CO)_5$ to form transparent iron oxides [380]
- Hydrothermal crystallization for the production of α-Fe_2O_3 in platelet form [381]

5.21.1.3 Toxicology and Environmental Aspects

The Berufsgenossenschaft der Chemischen Industrie (Germany) has recommended that all iron oxide pigments should be classified as inert fine dusts with an MAK value of 6 mg/m³. This is the highest value proposed for fine dusts.

Iron oxide pigments produced from pure starting materials may be used as colorants for food and pharmaceutical products [382]. Synthetic iron oxides do not contain crystalline silica and therefore are not considered to be toxic, even under strict Californian regulations.

5.21.1.4 Quality

The red and black iron oxide pigments produced by the methods described have an Fe_2O_3 content of 92–96%. For special applications (e.g., ferrites) analytically pure pigments with Fe_2O_3 contents of 99.5–99.8% are produced.

The Fe_2O_3 content of yellow and orange pigments lies between 85 and 87% corresponding to FeOOH contents of 96–97%. Variations of 1–2% are of no importance with respect to the quality of the pigments. Pigment quality is mainly determined by the quantity and nature of the water-soluble salts, the particle size distribution (hue and tinting strength are effected) and the average particle size of the ground product. The hue of red iron oxide is determined by the particle diameter, which is ca. 0.1 μm for red oxides with a yellow tinge and ca. 1.0 μm for violet hues.

The optical properties of the yellow, usually needle-shaped, iron oxide pigments depend not only on the particle size, but also on the length to width ratio (e.g., length = 0.3–0.8 μm, diameter = 0.05–0.2 μm, length: diameter ratio = ca. 1.5–8). In applications for which needle-shaped particles are unsuitable, spheroidal pigments are available [383]. Black iron oxide pigments (Fe_3O_4) have a particle diameter of ca. 0.1–0.6 μm.

Some iron oxide pigments have a limited stability on heating. Red iron oxide is stable up to 1200 °C in air. In the presence of oxygen, black iron oxide changes into brown γ-Fe_2O_3 at ca. 180 °C and then into red α-Fe_2O_3 above 350 °C. Yellow iron oxide decomposes above ca. 180 °C to form red α-Fe_2O_3 with liberation of water. This temperature limit can be increased to ca. 260 °C by stabilization with basic aluminum compounds. The thermal behavior of brown iron oxides produced by mixing depends on their composition.

5.21.1.5 Uses

All synthetic iron oxides possess good tinting strength and excellent hiding power. They are also lightfast and resistant to alkalis. These properties are responsible for their versatility. The principle areas of use are shown in Table 5.47.

Iron oxide pigments have long been used for coloring construction materials. Concrete roof tiles, paving bricks, fibrous cement, bitumen, mortar, rendering, etc. can be colored with small amounts of pigment that do not affect the setting time, compression strength, or tensile strength of the construction materials. Synthetic pigments are superior to the natural pigments due to their better tinting power and purer hue.

Natural rubber can only be colored with iron oxides that contain very low levels of copper and manganese (Cu < 0.005%, Mn < 0.02%). Synthetic rubber is less sensitive.

In the paint and coating industries, iron oxide pigments can be incorporated in many types of binders. Some reasons for their wide applicability in this sector are pure hue, good hiding power, good abrasion resistance, and low settling tendency. Their high temperature resistance allows them to be used in enamels.

The use of iron oxide as a polishing medium for plate glass manufacture has decreased now that other methods of-glass production are available.

Table 5.47: Main areas of use for natural and synthetic iron oxide pigments.

Use	Amount, %		
	Europe	United States	World
Coloring construction materials	64	37	60
Paints and coatings	30	48	29
Plastics and rubber	4	14	6
Miscellaneous	2	1	5

5.21.1.6 Economic Aspects

Accurate production figures for natural and synthetic iron oxide pigments are difficult to obtain, because statistics also include non-pigmentary oxides (e.g., red mud from bauxite treatment, intermediate products used in ferrite production). World production of synthetic iron oxides in 1985 was estimated to be between 500 000 and 600 000 t; production of natural oxides was ca. 100 000 t. The most important producing countries for synthetic pigments are Germany, the United States, the United Kingdom, Italy, Brazil, and Japan. The natural oxides are mainly produced in France, Spain, Cyprus, Iran, Italy, and Austria.

The most important manufacturers are Bayer, Deanshanger, SILO (Europe); Columbian Chemicals, Harcross, Miles (USA); Globo (Brazil); and Toda (Japan).

5.21.2 Iron Blue Pigments

The term iron blue pigments as defined in ISO 2495 has largely replaced a variety of older names which were either related to the place where the compound was produced or represented particular optical properties, e.g., Berlin blue, Bronze blue, Chinese blue, Milori blue, Non-bronze blue, Paris blue, Prussian blue, Toning blue, and Turnbull's blue. These names usually stood for insoluble pigments based on microcrystalline Fe(II)Fe(III) cyano complexes which do not differ significantly in their composition; many were associated with specific hues. A standardized naming system has been demanded by users and welcomed by manufacturers, and has led to a reduction in the number of names [384].

Iron blue, C.I. Pigment Blue 27:77510 (soluble blue is C.I. Pigment Blue 27:77520), was discovered in 1704 by Diesbach in Berlin by a precipitation reaction, and can be regarded as the oldest synthetic coordination compound.

Milori was the first to produce it as a pigment on an industrial scale in the early nineteenth century [385].

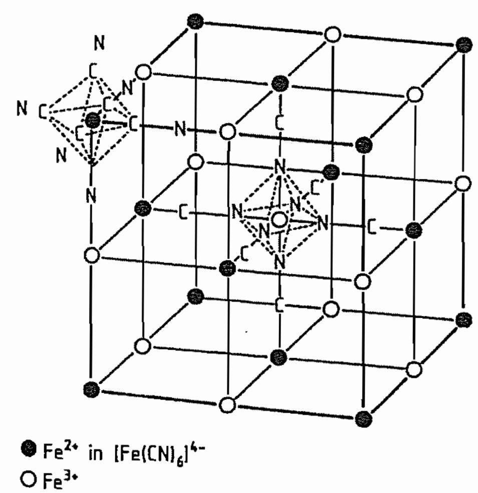

Figure 5.118: Crystal structure of iron blue [388].

5.21.2.1 Structure

X-Ray and infrared spectroscopy show that iron blue pigments have the formula $M^IFe^{II}Fe^{III}(CN)_6 \cdot H_2O$ [386]. M^I represents potassium, ammonium, or sodium, of which the potassium and ammonium ions are preferred because they produce excellent hues in industrial manufacture.

The crystal structure of the $Fe^{II}Fe^{III}(CN)_6$ grouping is shown in Figure 5.118. A face-centered cubic lattice of Fe^{2+} is interlocked with another face-centered cubic lattice of Fe^{3+} to give a cubic lattice with the corners occupied by iron ions. The CN^- ions are located at the edges of the cubes between each Fe^{2+} ion and the neighboring Fe^{3+}; the carbon atom of the cyanide is bonded to the Fe^{2+} ion and the nitrogen atom is coordinatively bonded to the Fe^{3+} ion. According to [387] the deep blue colour is the result of electron transfer from iron(II) and iron(III) with the absorption of light energy ("Charge Transfer Complex").

The wide-mesh lattice of the crystal contains relatively large spaces which can be occupied alternately by alkali ions and water molecules. In order to retain the crystal structure — and also the optical properties — water molecules must be present. Loss of water beyond a certain limit brings about fundamental changes in the pigment properties. A bonding mechanism for the coordinating water molecules assumes that both zeolitic and adsorptive states are possible.

Many investigations helped to elucidate the structure of iron blue [390–393].

5.21.2.2 Production

Iron blue pigments are produced by the precipitation of complex iron(II) cyanides by iron(II) salts in aqueous solution. The product is a whitish precipitate of iron(II) hexacyanoferrate(II) $M_2^IFe^{II}[Fe^{II}(CN)_6]$ or $M^{II}Fe^{II}[Fe^{II}(CN)_6]$, (Berlin white), as an intermediate stage, which is aged and then oxidized to the blue pigment [388].

Potassium hexacyanoferrate(II) or sodium hexacyanoferrate(II) or mixtures of these salts

are usually used. When the pure sodium salt or a calcium hexacyanoferrate(II) solution is used, the pigment properties are obtained by adding a potassium or ammonium salt during the precipitation of the white paste product or prior to the oxidation stage.

The iron(II) salt used is crystalline iron(II) sulfate or iron(II) chloride solution. The oxidizing agent can be hydrogen peroxide, alkali chlorates, or alkali dichromates. Industrial precipitation is carried out batchwise in large stirred tanks by simultaneous or sequential addition of aqueous solutions of potassium hexacyanoferrate(II) and iron(II) sulfate to a dilute acid. The filtrate from the white paste product must contain a slight excess of iron. Temperature, pH, and concentration of the starting solutions have a decisive influence on the size and shape of the precipitated particles. The suspension of white paste is aged by heating. The ageing period varies in length and temperature depending on the required properties of the finished pigment. This is followed by the oxidation to form the blue pigment by adding hydrochloric acid and sodium or potassium chlorate [394]. Finally, the suspension of the blue pigments is pumped into filter presses either immediately or after having been washed with cold water and decanted. After filtering, it is washed until free of acid and salt.

Depending on the pigment type, the filter press-cakes (35–60% solids) are either moulded into cylindrical pellets and dried to a finished dust-free product, or liquefied and spray dried, or dried and then ground to form a powder pigment.

Dispersibility can be improved by adding organic compounds to the pigment suspension before filtering to prevent the particles from agglomerating too strongly on drying [395, 396]. In another method (the Flushing process), the water in the wet pigment paste is replaced by a hydrophobic binder [397]. Although these and other methods of pigment preparation produce fully dispersible products consisting mainly of iron blue and a binder [398–400], they have not become established on the market.

A "water-soluble" blue can be manufactured by adding peptizing agents (the latter improve the water solubility via an emulsifying action). This forms a transparent colloidal solution in water without the use of high shear forces [388].

5.21.2.3 Properties

Hue, relative tinting strength, dispersibility, and rheological behavior are the properties of iron blue pigments with the most practical significance. Other important properties are the volatiles content at 60 °C, the water-soluble fraction, and acidity (ISO 2495). Pure blue pigments are usually used singly (e.g., in printing inks) and do not need any additives to improve them. Finely divided iron blue pigments impart a pure black tone to printing ink.

Owing to their small particle size (see Table 5.48 and Figures 5.119 and 5.120), iron blue pigments are very difficult to disperse. A graph of particle size distribution is given in Figure 5.121 for a commercial quality iron blue and for a micronized grade with similar primary particle size. The micronized grade gives greater tinting strength in dry mixtures than the blues obtained from standard grinding. The average size of the aggregates in the micronized material is ca. 10 μm compared with ca. 35 μm for the normal quality product.

Iron blue pigments are thermally stable for short periods at temperatures up to 180 °C, and therefore can be used in stoving finishes. The powdered material presents an explosion hazard, the ignition point is 600–625 °C (ASTM D 93-52). The pigments are combustible in powder form, ignition in air being possible above 140 °C [388].

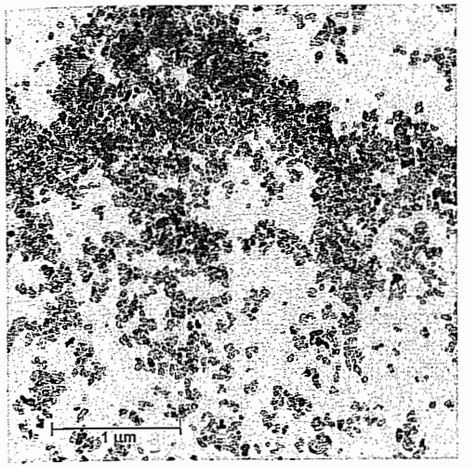

Figure 5.119: Electron micrograph of an iron blue pigment of small particle size (Manox Blue® 460 D).

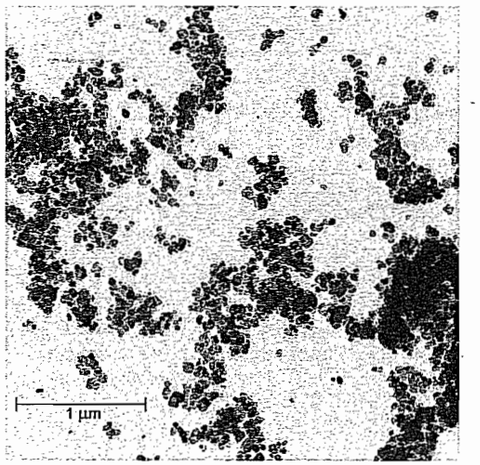

Figure 5.120: Electron micrograph of an iron-blue pigment of normal particle size (Vossen Blau® 705).

Table 5.48: Physical and chemical properties of iron blue pigments (Vossen-Blau® and Manox® grades).

Type	Vossen Blau® 705	Vossen Blau® 705 LS[a]	Vossen Blau® 724	Manox® Blue 480 D	Manox Easisperse® HSB 2
Colour Index Number	77510	77510	77510	77510	77510
Colour Index Pigment	27	27	27	27	27
Tinting strength[b]	100	100	100	115	95[c]
Hue	pure blue	pure blue	pure blue	pure blue	pure blue
Oil absorption[d], g/100 g	36–42	40–50	36–42	53–63	22–28
Weight loss on drying[e], %	2–6	2–6	2–6	2–6	2–6
Tamped density[f], g/L	500	200	500	500	550
Density[g], g/cm^3	1.9	1.9	1.9	1.8	1.8
Mean diameter of primary particles, nm	70	70	70	40	80
Specific surface area[h], m^2/g	35	35	35	80	30
Thermal stability, °C	150	150	150	150	150
Resistance to acids	very good	very good	very good	very good	very good
Resistance to alkalis	poor	poor	poor	poor	poor
Resistance to solvents	very good	very good	very good	very good	very good
Resistance to bleeding	very good	very good	very good	very good	very good

[a] LS = Luftstrahlmühle (air jet mill).
[b] DIN ISO 787/XVI and DIN ISO 787/XXIV.
[c] Surface-treated easily dispersible type.
[d] DIN ISO 787/V, ASTM D 281, or JIS K 5101/19 (JIS: Japanese Industrial Standard).
[e] DIN ISO 787/II, ASTM D 280, or JIS K 5101/21.
[f] DIN ISO 787/XI or JIS K 5101/18.
[g] DIN ISO 787/X or JIS K 5101/17.
[h] DIN 66131.

Iron blue pigments have excellent light- and weatherfastness. When mixed with white pigments, these properties can disappear [401]. Recent investigations have shown that a topcoat (as commonly applied in automobile manufacture) overcomes this problem [402]. Figure 5.122 shows changes in residual gloss and color after a short weathering period. The pigments are resistant to dilute acid and oxidizing agents, and do not bleed. They are decomposed by hot, concentrated acid and alkali. Other properties are listed in Table 5.48.

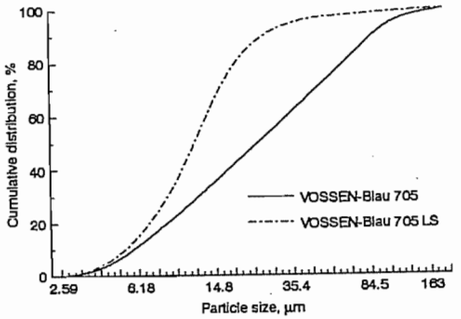

Figure 5.121: Cumulative particle size distribution curve of a normal (705) and a micronized (705 LS) iron blue pigment of equal primary particle size. LS = Luftstrahlmühle (air jet mill).

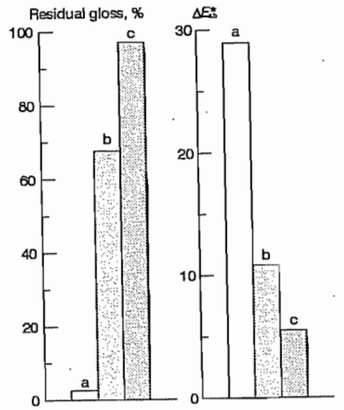

Figure 5.122: Residual gloss and ΔE^*_{ab} values for isocyanate-cross-linked polyacrylate resins that contain 15% Vossen-Blau® 2000 (older pigment type which has been replaced by Manox® Blue 460 D) relative to the binder and 15% TiO_2 (rutile) relative to the iron blue pigment after 1000 h fast exposure to UV [402]: a) Without clearcoat; b) With clearcoat but without UV protection; c) With clearcoat and UV protection.

5.21.2.4 Uses

Total production of iron blue in 1975 was ca. 25 000 t/a, but in 1991 it was only ca. 15 000 t/a. The main consumer in Europe and the United States is the printing industry. The second largest use in Europe, especially of micronized iron blue pigments, is for coloring fungicides, but use in the paint industry is decreasing.

Printing Ink Industry. Iron blue pigments are very important in printing, especially rotogravure, because of their deep hue, good hiding power, and economic cost/performance basis. Iron blue is often mixed with phthalocyanine pigments for multicolor printing. Another important use is in controlling the shade of black printing inks. Typical amounts used are 5–8% for full-shade rotogravure inks and 2–8% for toning black gravure and offset inks.

Iron blue pigments are used in the manufacture of single- and multiple-use carbon papers and blue copying papers, both for toning the carbon black and as blue pigments in their own right [388].

Toning of Black Gravure Inks. For the toning of black gravure inks, for example, 2 to 6% of Vossen-Blau 705 are used together with 6 to 12% of carbon black. Combinations with red pigments with a blue undertone are also common. When using organic pigments, resistance to solvents must be taken in account. Because of the poor dispersibility of iron blue compared with carbon black it is both economical and practical to disperse the blue pigment in a separate step.

While the visual judgement of black is influenced by the individual ability of the observer to distinguish small colour differences in deep black, it is possible, with the help of photometric measurements, to graphically interpret objective evaluations by means of physical data [389].

Figure 5.123 illustrates the colour changes of a low structure LCF-type carbon black by addition of Pigment Blue 27 (Vossen-Blau 705) and Pigment Violet 27 or by toning with a 4:1 combination of Pigment Blue 27 and Pigment Red 57:1. A mixture of asphalt resin, calcium/zinc resinate and phenol resin was used as a binder. The pigment concentration for all was 13.2%. The toner was added in 2.2% steps up to 6.6% with a simultaneous reduction from 13.2 to 6.6%.

Toning of Black Offset Printing Inks. The basic requirements for the successful use of iron blue as a toning agent in offset printing inks are resistance to damping or "fountain"

solutions and good dispersibility. "Resistance" is understood here as the hydrophobic characteristics of the pigment.

This property prevents wetting of the pigment by water and therefore its peptization. Non-resistant iron blue can render the ink useless by adsorbing water to above the normal content. A negative side-effect of peptization is the "dissolution" of the blue pigment from the printing ink and the resulting blue colouration of the fountain solution with the familiar problems of printing-plate contamination, also known as scumming or toning.

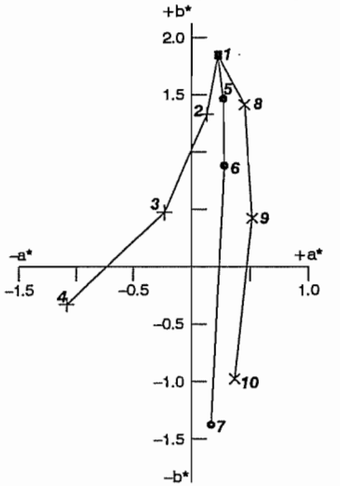

Figure 5.123: Colour coordinates of black gravure inks with different toning. + 2–4: Pigment Black LCF*/Vossen-Blau 705; ● 5–7: Pigment Black LCF/[VB 705–Pigment Red 57:1(4:1)]; × 1–10: Pigment Black LCF*/[VB 705 Pigment Violet 27 (2:1)]; ■ 1: Pigment Black LCF = Printex 35.

The combined dispersion of pigments is only practical with colourants of similar dispersibility. Toning agents with a considerable higher resistance to dispersion than carbon black are therefore delivered by the manufacturer in the form of a predispersed paste or must be ground separately by the user.

Developments in the fields of iron blue technology have overcome these problems. A new generation of pigments has been generated which covers both the demand for a sufficient resistance against damping solutions and the request for a good dispersibility. Easily dispersible iron blue is preferred to be used for combined dispersion with carbon black in the so-called "Co-Grinding" process.

In the following section, the coloristic effects of those iron blue pigments are described, as obtained in toning experiments involving a LCF-type carbon black, in comparison with Pigment Blue 15:3 and Pigment Blue 61.

The pigment concentration of the inks is 24%, i.e. the amount of carbon black was reduced correspondingly with the addition of 3, 6, or 9% of blue pigment. Black inks containing 15 to 24% of carbon black are excluded from this experiment, and are presented to give an additional coloristic description of "pigment" black as regards the development of the hue when used as a self-colour pigment in increasing concentrations.

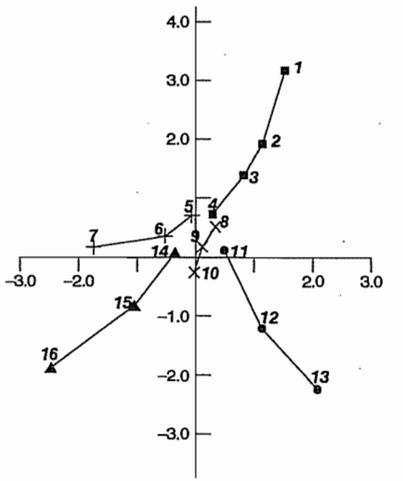

Figure 5.124: Colour locations of black offset printing inks with different toning. ■ 1–4: Pigment Black LCF (= Printex 35); + 5–7: Pigment Black LCF/Manox Easisperse; × 8–10: Pigment Black LCF/[Manox Easisperse/Pigment Red 57:1(4:1)]; ● 11–13: Pigment Black LCF/Pigment Blue 61; ▲ 14–16: Pigment Black LCF/Pigment Blue 15:3.

In the visual and the colorimetric evaluation the colour location change of the carbon black when used as a self-colour pigment is noticeable since there is a tendency to a black with a blue undertone at higher pigment concentration, even without the addition of toning

agent. In Figure 5.124 these are the colour locations 1–4, starting with 15% carbon black and in increasing additions in steps of 3% to a maximum concentration of 24%.

However, it is also clear that without the addition of a blue pigment the achromatic point cannot be achieved.

By adding various toning agents the desired colour hue is achieved - although with varying red/green spread. Iron blue (Manox Easisperse 154) brings about a clear shift towards green with a relatively small shift in the blue direction (see colour locations 5–7). The required target is more successfully achieved by the use of a mixture of iron blue an Pigment Red 57:1 in the ratio 4:1. The colour locations 8–10 illustrate useful ways of approaching the achromatic point with the addition of 3%, 6%, and 9% of the mixture.

The addition of 3% of Pigment Blue 61 already results in a significant step towards blue/red and shows almost identical incremental changes with further additions (see colour locations 11–13). In addition, the bronze effect occurs which intensifies with increasing distance from the achromatic point. With Pigment Blue 15:3 in numerically equivalent increments, the hue of the black ink moves towards blue/green in the opposite direction from the achromatic point and with a negative shift (colour locations 14–16).

Agriculture. Since ca. 1935 and especially in Mediterranean countries, blue inorganic fungicides based on copper and used for treating vines have largely been replaced by colorless organic compounds. Micronized iron blue pigments are used to color these fungicides (normally at a concentration of 3–8%), so that even small amounts become visible due to the high color intensity, and precise control is possible. The fungicide is usually milled or mixed with a micronized iron blue pigment [403].

A welcome side effect of treating fungi (e.g., *peronospora plasmopara viticola*) with iron blue is the fertilizing of vines in soils that give rise to chlororsis. Leaf color is intensified, aging of the leaves is retarded, and wood quality ("ripeness") is also improved [404–406]. Iron is necessary for chlorophyll synthesis, which improves grape quality and yield. Other iron salts do not have this effect [405].

Paints and Coatings. Iron blue pigments are used in the paint industry, especially for full, dark blue colors for automotive finishes. A full shade with good hiding power is produced by 4–8% iron blue pigments.

Paper. Blue paper can be produced by adding "water-soluble" iron blue pigment directly to the aqueous phase. Alternatively, a suitable iron blue pigment can be ground together with a water-soluble binder, applied to the paper, dried, and glazed (quantity applied: ca. 8% in the finished product).

Pigment Industry. The importance of iron blue in the production of chrome green and zinc green pigments has greatly increased worldwide (see Section 46.10.2.3).

Medical Applications. Iron blue has become important as an agent for decontaminating persons who have ingested radioactive material. The isotope ^{137}Cs which would otherwise be freely absorbed via the human or animal digestive tract exchanges with the iron(II) of the iron blue [407, 408] and is then excreted in the feces [409]. Gelatin capsules containing 500 mg iron blue are marketed as Radiogardase-Cs (Heyl). Thallium ions have been found to behave similarly [410–412]. The gelatin capsules for this purpose are sold as "Antidotum Thalii" (Heyl) [413].

5.21.2.5 Toxicology and Environmental Aspects

Blue pigment compounds show no toxicity in animal studies therefore it is not expected to cause any adverse effects on human health. No toxic effects were reported in humans when blue pigment compounds were used experimentally or therapeutically.

Toxikokinetic studies showed, that the adsorption of iron blue pigments is very low. Following intravenous injection of a ^{59}Fe-radio labelled iron blue pigment, the $[^{59}Fe(CN)_6]^{4-}$ ion was rapidly and virtually completely excreted with the urine. After oral administration of ferric cyanoferrate (^{59}Fe) approx. 2% of the labelled hexacyanoferrate ion was absorbed by the gastro-intestinal tract [414]. Most of the substance is excreted with the feces [415] and there was no evidence of its decomposition.

The decomposition of blue pigment salts to toxic cyanide in aqueous systems is very low. The CN-release of $KFe[Fe(CN)_6]$ in artificial gastric or intestinal juice was 141 or 26 µg/(g · 5 hours) respectively and in water 37 µg/(g · 5 hours). The corresponding figure of $Fe_4[Fe(CN)_6]$ were 64, 15 and 22 µg/(g · 5 hours) [416].

In the breath of rats after i.p. injection of ^{14}C-labelled $KFe[Fe(CN)_6]$ less than 0.01% (detection limit) was found, whereas in another study 0.04–0.08% of the orally administered dose was found in the exhaled air [417]. It can be concluded, that the hexacyanoferrate(II) complex disintegrates only to a small extent in the intestinal tract after oral administration. This is confirmed by the results of acute oral toxicity studies which show in high doses no clinical symptoms or lethality. The LD_{50} values are above 5000–15 000 mg/kg (limit tests) [418–420].

In primary irritation tests no or only slight effects were seen at the skin or in the eyes of the treated rabbits respectively [420, 421]. No skin sensitisation occurred in a Guinea pig maximisation test [418].

The subchronic (90–120 days) consumption of iron blue pigments at concentrations of 1–2% in the food or drinking water influenced slightly the body weight gain, but no other clinical signs or histopathologial changes were observed [422–425]. After the administration of daily doses of 200 or 400 mg/kg for ten days to dogs the body weight gained and the general condition remained unaffected [426].

In a bacterial test system (ames test) no increase of mutagenicity was detected without or in presence of a metabolic system [420].

In human volunteers who received 1.5 or 3.0 g ferric cyanoferrate for up to 22 days apart from a slight obstipation no effects were reported [426, 427].

$Fe_4[Fe(CN)_6]$ can bind cesium therefore iron blue pigments are used in clinical practice as an antidote for the treatment of humans contaminated with radioactive cesium (see also section 5.21.2.4). Clinical use of iron(III) ferrocyanide in doses up to 20 g/d for decontaminations of persons exposed to radio cesium has not been associated with any reported toxicity [428].

Blue pigment salts are also used as an effective antidote for thallium intoxications. Ferric cyanoferrate interferes with the enterosystemic circulation of thallium ions and enhances their faecal excretion [429].

In a semistatic acute fish toxicity test (Leuciscus idus, melanotus, fresh water fish) a saturated solution with different blue pigment compounds (with unsolved material on the bottom or filtrated solution) no death occurred within 96 hours. Based on the quantity weighed the *No Observed Effect Level* (NOEL) is greater than 1000 mg/L (nominal concentrations) [430].

The bacterial toxicity was measured according DEV, DIN 38 412, L3 (TTC [2,3,5-triphenyl-2*H*-tetrazolium chlorid] test). The result gives an EC_{50} (effective concentration) varying between 2290 and 14 700 mg/L, and estimated NOEC values in the range of < 10 to 100 mg/L [431].

There are no harmful effects on fish, but the toxic effects on bacteria constitude a slight hazard when iron blue pigments are present in water.

5.21.3 Iron Magnetic Pigments

5.21.3.1 Iron Oxide Magnetic Pigments

Ferrimagnetic iron oxide pigments are used in magnetic information storage systems such as audio and videocassettes, floppy disks, hard disks, and computer tapes. Cobalt-free iron(III) oxide and nonstoichiometric mixed-phase pigments have been used since the early

days of magnetic tape technology. Currently, γ-Fe_2O_3 and Fe_3O_4 (the latter in small amounts) are mainly used in the production of low-bias audio cassettes [iron oxide operating point IEC I standard (International Electrotechnical Commission)], and studio, broadcasting, and computer tapes.

Production. The shape of the pigment particle is extremely important for ensuring good magnetic properties. Isometric iron oxide pigments produced by direct precipitation are seldom used. Since 1947, needle-shaped γ-Fe_2O_3 pigments have been prepared with a length to width ratio of ca. 5:1 to 20:1 and a crystal length of 0.1–1 µm [432].

Anisometric forms of Fe_3O_4 with the spinel structure or γ-Fe_2O_3 with a tetragonal superlattice structure do not crystallize directly. They are obtained from iron compounds that form needle-shaped crystals (usually α- and γ-FeOOH) [433–435]. The oxyhydroxides are converted to Fe_3O_4 by dehydration and reduction. Reducing agents may be gases (hydrogen, carbon monoxide) or organic compounds (e.g., fatty acids). The particle geometry is retained during this process.

Since the pigments are subjected to considerable thermal stress during this conversion, the FeOOH particles are stabilized with a protective coating of sintered material (usually silicates [436], phosphates [437], chromates [438], or organic compounds such as fatty acids [439]).

Finely divided stoichiometric Fe_3O_4 pigments are not stable to atmospheric oxidation. They are therefore stabilized by partial oxidation or by complete oxidation to γ-Fe_2O_3 below 500 °C.

In an alternative process, the starting material consists of needle-shaped particles of α-Fe_2O_3 instead of FeOOH pigments [440, 441]. The synthesis is carried out in a hydrothermal reactor, starting from a suspension of $Fe(OH)_3$, and crystal growth is controlled by means of organic modifiers.

Properties. Magnetic pigments with very different morphological and magnetic properties that depend on the field of application and quality of the recording medium, are used. The largest particles (length ca 0.6 µm) are used in computer tapes. The noise level of the magnetic tape decreases with decreasing particle size. Fine pigments are therefore being used increasingly for better quality compact cassettes.

The magnetic properties may be determined by measurement of hysteresis curves on the powder or magnetic tape.

Table 5.49: Some quality requirements for iron oxide and metallic iron magnetic pigments.

Field of application	Pigment type	Approximate particle length, mm	Specific surface area, m^2/g	Coercive field strength H_c, kA/m	Saturation magnetization M_s, $mT \cdot m^3/kg$	M_r/M_s
Computer tapes	γ-Fe_2O_3	0.60	13–17	23–25	y	0.80–0.85
Studio radio tapes	γ-Fe_2O_3	0.40	17–20	23–27	85–92	0.80–0.85
IEC I compact cassettes standard (iron oxide operating point)	γ-Fe_2O_3	0.35	20–25	27–30	87–92	0.80–0.90
high grade	Co-γ-Fe_2O_3	0.30	25–37	29–32	92–98	0.80–0.90
IEC II compact cassettes (CrO_2 operating point)	Co-γ-Fe_2O_3, Co-Fe_3O_4	0.30	30–40	52–57	94–98	0.85–0.92
IEC IV compact cassettes (metal operating point)	metallic iron	0.35	35–40	88–95	130–160	0.85–0.90
Digital audio (R-DAT)[a]	metallic iron	0.25	50–60	115–127	130–160	0.85–0.90
½" Video	Co-γ-Fe_2O_3, Co-Fe_3O_4	0.30	25–40	52–57	94–98	0.80–0.90
Super-VHS video	Co-γ-Fe_2O_3	0.20	45–50	64–72	94–96	0.80–0.85
8-mm video	metallic iron	0.25	50–60	115–127	130–160	0.85–0.90

[a] R-DAT: rotary digital audio tape.

Table 5.49 shows some quality requirements for the most important applications of magnetic pigments. Column 4 gives the coercive field strength (H_c) required for information storage materials. The coercive field is the magnetic field required to demagnetize the sample.

The saturation magnetization M_s is a specific constant for the material and for magnetic iron oxides is principally determined by the Fe^{2+} ion content. The ratio of remanent magnetization to saturation magnetization (M_r/M_s) for the tape depends mainly on the orientation of the pigment needles with respect to the longitudinal direction of the tape, and should approach the theoretical maximum value of unity as closely as possible.

Apart from the morphological and magnetic properties, usual pigment properties such as pH value, tap density, soluble salt content, oil absorption, dispersibility, and chemical stability are of great importance for the manufacture of magnetic recording materials.

Producers of magnetic iron oxides include BASF and Bayer (Germany); Ishihara, Sakai, Showa Denko, Titan K., and Toda K (Japan); 3M, Magnox (USA); and Saehan Media (Korea).

World production of cobalt-free magnetic iron oxides in 1990 was ca. 24 000 t, of which ca. 74% was used in compact cassettes and audio tapes, and ca. 25% in computer tapes.

5.21.3.2 Cobalt-Containing Iron Oxide Pigments

Cobalt-containing iron oxides form the largest proportion (ca. 60%) of magnetic pigments produced today. Due to their high coercivity they can be used as an alternative to chromium dioxide for the production of video tapes, high-bias audio tapes (CrO_2 operating point), and high-density floppy disks.

Production. The iron oxide pigments described above are either doped or coated with cobalt:

- Body-doped pigments contain 2–5% cobalt that is uniformly distributed throughout the hulk of the pigment particles. It is either incorporated during production of the FeOOH precursor or precipitated as the hydroxide onto one of the intermediate products [442] using cobalt(II) salts as the cobalt source.
- Cobalt-coated pigment particles (2–4% Co) consist of a core of γ-Fe_2O_3 or nonstoichiometric iron oxide phase, and a 1–2 nm coating of cobalt ferrite with a high coercivity [443]. The coating can be produced by adsorption of cobalt hydroxide, or epitaxial precipitation of cobalt ferrite in a strongly alkaline medium [444, 445]. Surface-coated pigments show better magnetic stability than doped pigments.

Properties. Pigments with a coercive field strength of 50–56 kA/m are used in video cassettes, high-bias audio cassettes (chromium dioxide operating point IEC II), and high-density floppy disks. Depending on the quality of the tape, the particle size varies between 0.2 and 0.4 µm (Table 5.49).

Pigments with a higher coercive field strength (ca. 70 kA/m) and smaller particle size (particle length ca. 0.15–0.2 µm) are used for super VHS cassettes.

Pigments treated with only small amounts of cobalt (0.5% Co, coercive field strength ca. 31 kA/m) are used as an alternative to cobalt-free γ-Fe_2O_3 pigments for high-quality low-bias audio cassettes.

Cobalt-containing pigments are mainly produced by the magnetic iron oxide producers. World production for 1990 was 45 000 t, of which the highest proportion (ca. 85%) was used for video tapes.

5.21.3.3 Metallic Iron Pigments

The magnetization of iron is more than three times higher than that of iron oxides. Metallic iron pigments can have a coercive field strength as high as 150 kA/m, depending on particle size. These properties are highly suitable for high-density recording media. Oxidation-resistant products based on metallic pigments first became available in the late 1970s.

Production. Metallic iron pigments are commercially produced by the reduction of acicular (needle-shaped) iron compounds [446]. As in the production of magnetic iron oxide pigments, the starting materials are iron oxide hydroxides or iron oxalates, which are reduced to iron in a stream of hydrogen either directly or via oxidic intermediates.

Due to their high specific surface area, metallic pigments are pyrophoric, so that passivation is necessary. This can be achieved by slow, controlled oxidation of the particle surface [447].

Properties. The coercive field strength of metallic iron pigments is primarily determined by their particle shape and size, and can be varied between 30 and 150 kA/m. Pigments for analog music cassettes ($H_c \approx 90$ kA/m) usually have a particle length of 0.35 μm (Table 5.49). The length to width ratio of the pigment needles is ca. 10:1. Finely divided pigments (particle length ca. 0.25 μm) with a coercive field strength of 120 kA/m are used for 8-mm video and digital audio cassettes (R-DAT), tapes used by television organizations (ED Beta, Betacam SP MP, M II, Digital Video D2), and for master video cassettes (mirror master tapes). In the field of data storage, a small quantity is used in micro floppy disks.

Metallic pigments have a higher specific surface area (up to 60 m^2/g) and a higher saturation magnetization than oxidic magnetic pigments. Their capacity for particle alignment corresponds to that of the oxides (Table 5.49).

Economic Aspects. The largest producers of metallic iron pigments are Chisso, Dowa Mining, Kanto Denka K., Mitsui Toatzu, and Nissan Chemicals (Japan).

World consumption in 1990 was ca. 1000 t, of which ca. 75% was used in the manufacture of video tapes and ca. 25% for audio tapes. Consumption is expected to increase.

5.21.3.4 Barium Ferrite Pigments

Barium ferrite pigments have been considered for several years for high-density digital storage media [448, 449]. They are very suitable for preparing unoriented (e.g., floppy disks), longitudinally oriented (conventional tapes), and perpendicularly oriented media. In the latter the magnetization is oriented perpendicular to the coating surface. They are required for perpendicular recording systems which promise extremely high data densities, especially on floppy disks. Barium and strontium ferrites are also used to prevent forgery of magnetic stripes, e.g., in cheque and identity cards.

Properties. Hexagonal ferrites have a wide range of structures distinguished by different stacking arrangements of three basic elements known as M, S, and Y blocks [450]. For magnetic pigments, the M-type structure (barium hexaferrite $BaFe_{12}O_{19}$) is the most important. The magnetic properties of M-ferrite can be controlled over a fairly wide range by partial substitution of the Fe^{3+} ions, usually with combinations of di- and tetravalent ions such as Co and Ti. Barium ferrite crystallizes in the form of small hexagonal platelets. The preferred direction of magnetization is parallel to the c-axis and is therefore perpendicular to the surface of the platelet. The specific saturation magnetization of the undoped material is ca. 72 Am^2/kg and is therefore somewhat lower than that of other magnetic oxide pigments. In banum ferrite the coercive field strength is primarily determined by the magnetocrystalline anisotropy and only to a limited extent by particle morphology. This is the reason why banum ferrite can be obtained with extremely uniform magnetic properties. Barium ferrite pigments have a brown color and chemical properties similar to those of the iron oxides.

Production. There are three important methods for manufacturing barium ferrite on an industrial scale: the ceramic, hydrothermal, and glass crystallization methods. The main producers are Toshiba and Toda.

Ceramic Method. Mixtures of barium carbonate and iron oxide are reacted at 1200–1350 °C to produce crystalline agglomerates which are ground to a particle size of ca. 1 μm.

This method is only suitable for the high-coercivity pigments required for magnetic strips [451].

Hydrothermal Method. Iron [Fe(III)], barium, and the dopants are precipitated as their hydroxides and reacted with an excess of sodium hydroxide solution (up to 6 mol/L) at 250–350 °C in an autoclave. This is generally followed by an annealing treatment at 750–800 °C to obtain products with the desired magnetic properties. Many variations of the process have been described [452–456], the earliest report being from 1969 [457]. In later processes, hydrothermal synthesis is followed by coating with cubic ferrites, a process resembling the cobalt modification of iron oxides. The object is to increase the saturation magnetization of the material [458–460].

Glass Crystallization Method. This process was developed by Toshiba [461]. The starting materials for barium ferrite production are dissolved in a borate glass melt. The molten material at ca. 1200 °C is quenched by pouring it onto rotating cold copper wheels to produce glass flakes. The flakes are then annealed to crystallize the ferrite in the glass matrix. In the final stage the glass matrix is dissolved in acid. In a variation of this process, the glass matrix is produced by spray drying [462].

Magnetic Recording Properties. Typical values of physical properties of barium ferrite pigments used in magnetic recording are given in Table 5.50.

Barium ferrite is highly suitable for high-density digital recording mainly because of its very small particle size and its very narrow switching field distribution. It also has a high anhysteretic susceptibility and is difficult to overwrite [463]. This is partly explained by positive interaction fields between particles in the coating layer [464]. The high anhysteretic susceptibility makes barium ferrite media particularly suitable for the anhysteretic (bias field) duplicating process [465]. Unlike many other magnetic materials used in high-density recording, barium ferrite, being an oxide, is not affected by corrosion [466]. Processing of the pigment can be problematic, e.g., applying orienting fields can easily lead to unwanted stacking of the particles which has adverse effects on the noise level and the coercive field strength of the magnetic tape. A marked temperature dependence of the magnetic properties was a problem in the early days, but this can be overcome by appropriate doping [467].

Table 5.50: Typical properties of barium ferrite pigments.

Application	Specific surface area, m^2/g	Platelet diameter, nm	Platelet thickness, nm	H_c, kA/m	M_s/ρ, Am^2/kg
Unoriented (floppy disk)	25–40	40–70	15–30	50–65	50–65
Oriented	25–60	40–120	10–30	55–100	50–65
Magnetic strips	12–15	100–300	50–100	220–440	60–70

5.21.4 Iron Phosphide

Commercial iron phosphide anticorrosive pigments usually consist of Fe_2P with traces of FeP and SiO_2. The pigment is a powder with a metallic gray color and contains 70% Fe, 24% P, 2.5% Si, and 3.0% Mn. The density is 6.53 g/cm^3 and the mean particle size is ca. 3–5 μm.

Iron phosphide anticorrosive pigments are recommended by manufacturers as replacement materials for zinc dust to reduce the price of zinc-rich paints [468].

A *trade name* for iron phosphide is Ferrophos (Hooker Chemicals & Plastics Corp., USA).

5.21.5 Iron Oxide–Mica Pigment [469–474]

Mica can be coated not only with TiO_2 but also with other metal oxides that are deposited from hydrolyzable metal salts [469–474]. Iron(III) oxide is highly suitable because it combines a high refractive index (metallic luster) with good hiding power and excellent weather resistance [475].

Aqueous precipitation reactions are used for production of commercial Fe_2O_3–mica pigments, starting from Fe^{2+} or Fe^{3+} with subsequent calcination at 700–900 °C.

Pigments can also be produced by a direct CVD fluidized-bed process based on oxidation of iron pentacarbonyl and deposition of Fe_2O_3 on mica and other platelet substrates [476, 477].

Brilliant, intense colors are obtained with 50–150 nm layers of Fe_2O_3 (hematite) on muscovite. Absorption and interference colors are produced simultaneously and vary with layer thickness. Especially the red shades are more intense than those of TiO_2–mica pigments because interference and absorption enhance each other. An intense green-red flop with different viewing angles is possible at a Fe_2O_3 layer thickness producing green interference [478]. A theoretical investigation is given in [479, 480].

On account of their good hiding power, high chemical inertness, lack of toxicity, and brilliant intense color in the bronze, copper, and red ranges, these pigments are becoming increasingly important in sophisticated end uses such as automotive coatings and cosmetics.

5.21.6 Transparent Iron Oxides

Transparent yellow iron oxide has the α-FeO(OH) (goethite) structure; on heating it is converted into transparent red iron oxide with the α-Fe_2O_3 (hematite) structure. Differential thermogravimetric analysis shows a weight loss at 275 °C. Orange hues develop after brief thermal treatment of yellow iron oxide and can also be obtained by blending directly the yellow and red iron oxide powders.

Production. *Transparent yellow iron oxide*, C.I. Pigment Yellow 42:77492, is obtained by the precipitation of iron(II) hydroxide or carbonate with alkali from iron(II) salt solutions and subsequent oxidation to FeO(OH). On an industrial scale, oxidation is usually carried out by introducing atmospheric oxygen into the reaction vessel. Important factors for good transparency are high dilution during precipitation, a temperature of < 25 °C during oxidation, and short oxidation times (< 5 h). Oxidation can be carried out under acidic or basic conditions [481, 482]. The best results are obtained by using 6% iron(II) sulfate solutions and precipitation with ca. 85% sodium carbonate as a 10% solution. The starting material is usually crystalline $FeSO_4 \cdot 7H_2O$, obtained as a by-product from ilmenite in the pickling of iron or in the production of titanium dioxide according to the sulfate procedure. In order to improve pigment properties, the suspension is matured for about a day before filtration. It is then filtered, dried, and carefully ground to a powder. The primary particles are needle-shaped and have an average length of 50–100 nm, a width of 10–20 nm, and a thickness of 2–5 nm.

Transparent red iron oxide, C.I. Pigment Red 101:77491, is obtained by heating the yellow pigment (e.g., in a cylindrical rotary kiln) at 400–500 °C (Figure 5.125).

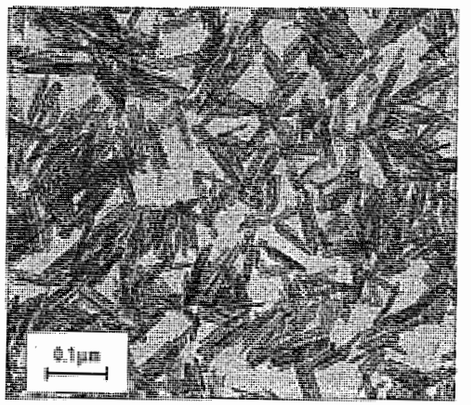

Figure 5.125: Electron micrograph of a transparent red iron oxide pigment (Sicotrans Red 2815).

Transparent red iron oxides containing iron oxide hydrate can also be produced directly by precipitation. A hematite content of > 85% can be obtained when iron(II) hydroxide or iron(II) carbonate is precipitated from iron(II) salt solutions at ca. 30 °C and when oxidation is carried out to completion with aeration and seeding additives (e.g., chlorides of magnesium, calcium, or aluminum) [483]. Transparent iron oxides can also be synthesized by heating finely atomized liquid pentacarbonyl iron in the presence of excess air at 580–800 °C [484, 485]. The products have a primary particle size of ca. 10 nm, are X-ray amorphous, and have an isometric particle form. Hues ranging from red to orange can be obtained with this procedure, however, it is not suitable for yellow hues.

Transparent brown iron oxides are produced by precipitating iron(II) salt solutions with dilute alkali (sodium hydroxide or sodium carbonate) and oxidizing with air. Only two-thirds of the precipitated iron hydroxide, oxide hydrate, or carbonate is oxidized. Alternatively, the iron oxides can be produced by complete oxidation of the precipitate iron compounds and subsequent addition of half the amount of the initial iron salt solution and precipitation as hydroxide [486, 487]. However, these products have the composition $FeO \cdot Fe_2O_3$ and are ferromagnetic; they are not of practical importance.

Properties and Uses. As far as resistance to light, weather, and chemicals is concerned, transparent iron oxides behave in a similar manner to the opaque iron oxides. In addition, they show a high UV absorption, which is exploited in applications such as the coloring of plastic bottles and films used in the packaging of UV-sensitive foods [488, 489].

Worldwide consumption of transparent iron oxides is 2000 t/a. They are mainly used in the production of metallic paint in combination with flaky aluminum pigments and in the coloring of plastics for bottles and fibers.

Toxicology. Special toxicological studies on transparent iron oxides have not yet been carried out. The results of opaque iron oxides are applicable.

Trade names and producers include Capelle (Gebroeders Cappelle N.V., Belgium), Fastona Transparent Iron Oxide (Blythe Colours Ltd., UK), Sicotrans (BASF and BASF Lacke + Farben, Germany), and Trans Oxide (Hilton Davis, USA).

5.21.7 Transparent Iron Blue

Iron blue, C.I. Pigment Blue 27:77520 (Milori blue), also occurs in finely dispersed forms (primary particle size < 20 nm, specific surface area 100 m^2/g) that are more transparent than the conventional iron blue pigments. They are generally produced by the same procedure as the less transparent iron blue pigments but a higher dilution factor is used. The transparency of these pigments is exploited solely in the production of printing inks (illustration gravure).

Trade names include Manox Iron Blue (Manox, UK), and Vossen-Blue 2000 (Degussa, Germany). Transparent iron blue pigments are also produced by Dainichiseika (Japan).

5.22 Coal and Coal Pyrolysis

5.22.1 Coal Petrology

Coal Characterization. Coal is an extremely heterogeneous, complex material that is difficult to characterize. Coal is a rock formed by geological processes and is composed of a number of distinct organic entities (macerals) and lesser amounts of inorganic substances (minerals). Each of the coal macerals and minerals has a unique set of physical and chemical properties; these in turn control the overall behavior of coal. Although much is known about the properties of minerals in coal, for example, the crystal chemistry, crystallography, and magnetic and electrical properties, surprisingly little is known about the properties of individual coal macerals. Even though coal is composed of macerals and minerals, it is not a uniform mixture of these substances. The macerals and minerals occur in distinct associations called lithotypes, and each lithotype has a set of physical and chemical properties that also affect coal behavior.

Coal seams, the basic units in which coal occurs, are in turn composed of layers of coal lithotypes, and individual coal seams may also have their own sets of physical and chemical properties. For example, even if two coal

seams have the same maceral and mineral composition, the seams may have significantly different properties if the maceral associations in lithotypes in the two seams are different. The enclosing rocks immediately adjacent to a coal seam can also affect the properties of the coal. This aspect is particularly important in mine design, production, and strata control. The compositional characterization of a coal seam must cover the nature of the macerals, the lithotypes, the entire seam, and the association of the seam with the neighboring strata.

In addition to compositional factors, coal properties also change with the rank or the degree of coalification of a given sample of coal. Coal is part of a metamorphic series ranging from peat, through lignite and subbituminous and bituminous coal, to anthracite. Temperature, pressure, and time alter the original precursors of coal through this metamorphic series. As the rank of the coal changes, the properties of the coal macerals change progressively and, therefore, so also do the properties of lithotypes and the entire seam.

Because of these factors, coal characterization requires a detailed knowledge of both the maceral composition and the rank of the coal. All coal properties are ultimately a function of these two factors.

The Maceral Concept. The term maceral was introduced by STOPES to distinguish the organic components of coal (macerals) from the inorganic components (minerals) [490]. The term is now interpreted in two conflicting ways. The interpretation of the International Committee for Coal Petrology (ICCP) is that a maceral is the smallest microscopically recognizable component of coal [491]. This conception, generally held by most European coal petrographers, is based on morphology and other criteria such as size, shape, botanical affinity, and occurrence. The ICCP concept implies that the properties of the macerals change with rank. Thus, the same maceral, vitrinite, can exist in a bituminous coal as well as in an anthracite.

In contrast, the maceral concept of SPACKMAN (commonly held in North America) is based on the idea that macerals are substances with distinctive sets of properties [492]. Thus, vitrinite in a bituminous coal is viewed as a different maceral than vitrinite in an anthracite because the two materials have different properties.

The basis of the petrographic study of coal composition is the idea that coal is composed of a number of distinct macerals. The entire body of coal petrographic literature supports this idea and is in direct contrast to the earlier chemical concept of coal being composed of a single unique molecular substance. Although the concept and the term "coal molecule" may once have been useful, modern chemical studies of coal recognize coal's heterogeneous maceral composition.

Maceral Types and Properties. A large number of different macerals have been named and classified in various systems. The ICCP system is given in part in Table 5.51. Although this system is useful for some purposes, it is impractical for routine maceral analysis because of the large number of terms. For such routine analysis, classification systems with a limited number of terms are needed. In the standard method for maceral analysis D 2799 of the American Society for Testing and Materials (ASTM), only six terms are required, although some additional terms are defined in ASTM Standard D 2796 (see Table 5.52).

Although there is no standard method for the analysis of fluorescent macerals, some additional terms, listed in Table 5.52, are used for this type of analysis.

As shown in Table 5.52, coal macerals fall into three distinct groups: vitrinite, liptinite, and inertinite. Vitrinite macerals are generally the most abundant, commonly making up 50–90% of North American coals. This group is not as abundant in coals that originate in the southern hemisphere.

Table 5.51: Survey of the macerals of hard coal, according to the ICCP system.

Maceral group	Maceral	Maceral type[a]	Maceral variety[a]	Kryptomaceral[a]
Vitrinite	telinite		cordaitotelinite	
			fungotelinite	
			xylotelinite	kryptotelinite
	collinite	telocollinite		kryptocorpocollinite
		gelocollinite		
		desmocollinite		
		corpocollinite		
	vitrodetrinite			
Exinite	sporinite		tenuisporinite	
			crassisporinite	
			microsporinite	kryptoexosporinite
			macrosporinite	kryptointosporinite
	cutinite			
	resinite			
	alginite			
	liptodetrinite			
Inertinite	micrinite			
	macrinite			
	semifusinite			
	fusinite	pyrofusinite		
		degradofusinite		
	sclerotinite		plectenchyminite	
			corposclerotinite	
			pseudocorposclerotinite	
	inertodetrinite			

[a] Incomplete, can be arbitrarily extended.

Table 5.52: Classification of macerals, according to the ASTM system, for routine analysis.

Maceral group	Maceral ASTM D 2799	Additional ASTM D 2796	Terms used in fluorescence analyses
Vitrinite	vitrinite	pseudo-vitrinite	fluorescing vitrinite
Liptinite	exinite	sporinite	fluorinite
	resinite	cutinite	bituminite
		alginite	exudatinite
Inertinite	micrinite	macrinite	
	semifusinite	sclerotinite	
	fusinite		

Most vitrinite macerals are derived from the cell wall material (woody tissue) of plants. Although the details of the vitrinization process are not well understood, it is generally believed that during the coalification process the plant cell wall material is chemically altered and broken down into colloidal particles that are later deposited and desiccated. This process commonly homogenizes the components so that the resulting macerals are structureless. The variation in vitrinite macerals is usually thought to be due to differences in the original plant material or to different conditions of alteration at the peat stage or during later coalification.

Under the microscope, vitrinite macerals have a reflectance (brightness) between that of the liptinite and inertinite macerals. Because the reflectance of the vitrinite macerals shows a more or less uniform increase with coal rank, reflectance measurements for the determination of rank are always taken exclusively on vitrinite macerals. The reflectance of vitrinite macerals is also anisotropic, so that in most orientations a particle of vitrinite will display two maxima and two minima with complete rotation. Two types of vitrinite are usually distinguished in North American coals. Normal vitrinite is almost always the most abundant maceral present and makes up the groundmass in which the various liptinite and inertinite macerals are dispersed. It has a uniform gray color and is always anisotropic. With UV excitation, some normal vitrinites will fluoresce. Pseudovitrinite always has a slightly higher reflectance than normal vitrinite in the same coal. It also tends to occur in large particles that are usually free of other macerals and py-

rite. Pseudovitrinite particles commonly show brecciated corners, serrated edges, wedge-shaped fractures, and slitted structures. Pseudovitrinite does not fluoresce under UV light.

In international practice, the terms desmocollinite, heterocollinite, and vitrinite B are used to describe normal vitrinite, and telocollinite, homocollinite, and vitrinite A are used for pseudovitrinite.

Liptinite macerals are derived from the waxy and resinous parts of plants, i.e., the spores, cuticles, and resins. This group generally makes up 5–15% of most North American coals, although it dominates some unusual types of coal such as cannel and boghead. In any given coal, liptinite macerals have the lowest reflectance. Liptinite macerals arc the most resistant to alteration or metamorphism in the early stages of coalification; thus, the reflectance changes are slight up to the rank of medium-volatile coal. In this range the reflectance of liptinite macerals increases rapidly until it matches or exceeds the reflectance of vitrinite macerals in the same coal and, thus, essentially disappears. Sporinite is the most common of the liptinite macerals and is derived from the waxy coating of fossil spores and pollen. It generally has the form of a flattened spheroid with upper and lower hemispheres compressed until they fuse. The outer surfaces of the sporinite macerals often show various kinds of ornamentation. In Paleozoic coals, two sizes of spores are common. The smaller ones, usually < 100 μm in diameter, are called microspores, and the larger ones, ranging up to several millimeters in diameter, are called megaspores. Cutinite, found as a minor component in most coals, is derived from the waxy outer coating of leaves, roots, and stems. It occurs as long stringers, which often have one fairly flat surface and another that is crenulated. Cutinite usually has a reflectance equal to that of sporinite. Occasionally the stringers of cutinite are distorted. Resinite is also common in most coals and usually occurs as ovoid bodies with a reflectance slightly greater than that of sporinite and cutinite but still less than that of vitrinite. Some of the larger pieces of resinite may appear to be translucent with an orange color. In some coals, particularly in those from the western United States, a number of different forms of resinite may be distinguished by using fluorescent microscopy. Alginite is derived from fossil algæ colonies. It is rare in most coals and is often difficult to distinguish from mineral matter. However, in UV light it fluoresces with a brilliant yellow color and can display a distinctive flower-like appearance.

Newly Defined Fluorescent Macerals. With the use of fluorescence microscopy, TEICHMULLER defined three new macerals: fluorinite, bituminite, and exudatinite [493]. Although these macerals have some characteristic features in normal white-light microscopy, they can be properly identified only by their fluorescence properties.

Fluorinite usually occurs as very dark lenses that may show internal reflections. Fluorinite is also commonly associated with cutinite. Fluorinite fluoresces with a very intense yellow color.

Bituminite is difficult to detect in white light and is often mistaken for mineral matter. It is common in vitrinite-poor detrital coals. It occurs as stringers and shreads and fluoresces weakly with an orange to brown color. This material is similar to what organic petrologists call amorphous organic matter (AOM).

Exudatinite is a secondary maceral which appears as an oil-like void filling. It has no shape of its own, and can usually only be detected by its weak orange to brown fluorescence in UV light.

The *inertinite* maceral groups are derived from plant material, usually woody tissue, that has been strongly altered by charring in a forest fire or by biochemical processes such as composting either before or shortly after deposition. These macerals can make up 5–40% of most North American coals, with the higher amounts occurring in Appalachian coals. In southern hemisphere coals, this group commonly is more abundant than vitrinite. The inertinite macerals have the highest magnitude and greatest range of reflectance of all the macerals. They are distinguished by their relative reflectances and by the presence of cell texture.

Fusinite is seen in most coals and has a charcoal-like structure. It is always the highest reflecting maceral present and is distinguished by a cell texture that is commonly broken into small shards and fragments.

Semifusinite has the cell texture and general features of fusinite except that it is of lower reflectance. In fact, semifusinite has the largest range of reflectance of any of the various coal macerals. Semifusinite is also the most abundant of the inertinite macerals in most coals.

Macrinite is a very minor component of most coals and usually occurs as structureless ovoid bodies with the same reflectance as fusinite.

Micrinite occurs as very fine granular particles of high reflectance. [t is commonly associated with the liptinite macerals and sometimes gives the appearance of actually replacing the liptinite.

5.22.2 Coalification

A unique and often troublesome feature of coal that distinguishes it from other fuels and bulk commodities is its property of rank. All coal starts out as peat, which is then changed into progressively higher ranks of coal. This transformation is generally divided into two phases. The first, which occurs in the peat stage, is called diagenesis or biochemical coalification. In this phase most of the plant material making up the peat is biochemically broken down. Specifically, most of the cellulose in the plant material is digested away by bacteria, and the lignin in the plant material is transformed into humic acids and humic compounds, humins. Some plant material is also thermally altered by partial combustion or biochemical charring. Still other plant material, such as spores and pollen, survive the diagenesis stage without much change. After diagenesis is complete and the altered peat is buried, geological forces begin to act in the geological or metamorphic phase of coalification.

Because of the common occurrence of high-rank coals in geologically deformed areas, for example, anthracite in the eastern Appalachian Mountains and low-volatile bituminous coal in the folded and faulted Canadian Rocky Mountains, it was assumed that tectonic pressure was responsible for the high rank of most coals. However, this position has now lost most of its support because recent studies in the folded coal seams of the Ruhr Basin show that isorank lines (isovols) follow the folds in the seams [495]. This shows that the coal achieved its rank before the structural deformation and was not altered during or after such deformation. Similar studies of stratigraphic relationships in the Canadian Rocky Mountains showed that the higher rank coals correlated with increasing depth of burial and not tectonism [496]. Laboratory experiments using increased confining pressure have not led to increased coalification [497].

The majority of the geological evidence suggests that temperature is the major factor in coalification and that the temperature range in which most coalification takes place is 50–150 °C. The depth at which these temperatures occur is a function of the natural geothermal gradient (dT/dZ), which ranges from 0.8 °C/100 m to 4 °C/100 m. Therefore, at these two geothermal gradient extremes, the depth at which 150 °C would be reached, if a surface temperature of 20 °C is assumed, is 16.25 km (53 300 feet, 10.1 miles) for the lowest gradient and 3.25 km (10 700 feet, 2.02 miles) for the highest. The major lines of evidence for the importance of temperature in coalification are as follows:

- An increase in coal rank and temperature with depth is confirmed by thousands of bore holes.
- Lines of equal rank contour igneous intrusions and show an increase in rank in the direction of the intrusion. In some cases, natural coke is found at the contact of a coal seam with an intrusion.

- Laboratory experiments show that wood can be coalified by heating in an inert atmosphere. Increasing the pressure alone has no effect on the coalification of wood.
- When thermodynamic factors are considered, it is clear that temperature should have more of an effect than pressure While an increase in temperature will encourage most coalification reactions by increasing the available energy, an increase in pressure may often inhibit such reactions by raising the energy requirements for such reactions to take place.

It was long thought that time was not a factor in coalification, and the example of the Russian paper coals of lignite rank and Carboniferous age was often cited as evidence. However, it is now believed that if the peat has been buried deeply enough to effect coalification, then time does have a "soaking effect". For example, in Venezuela there is a subbituminous coal of Eocene age that has been buried at a depth of 1120–1220 m at 125 °C for (10–20) × 10^6 years. In Germany there is a coal that has been at the same depth and temperature for 300 × 10^6 years and is of anthracite rank [495]. Numerous other examples have been found and a number of correlation charts relating depths of burial, temperature, rank, and time are based on this type of data.

Changes in the coal rank correspond to changes in most of the properties of the coal. For example, as rank increases, moisture, volatile matter, and ultimate oxygen and hydrogen decrease, whereas fixed and ultimate carbon, calorific value, and reflectance increase. All of these measurements and even some combinations of these have been used as measures of coal rank. However, with the exception of reflectance, they all suffer from two major drawbacks. First, none actually change uniformly across the rank range of coal. Second, they are all bulk properties of coal and, thus, can be significantly affected by changes in maceral composition having nothing to do with rank. For example, a coal with a higher-than-normal content of liptinite macerals can have a higher-than-normal hydrogen content and, therefore, appear to have a lower rank than it actually does on the basis of a rank parameter independent of composition such as reflectance. The reflectance parameter of coal is based on the amount of light reflected from the vitrinite macerals in a coal compared to a glass standard of known refractive index and reflectance. The vitrinite reflectance of coal changes uniformly across most of the coal rank range. However, it is not very sensitive in the lowest rank range (lignite to lower subbituminous).

5.22.3 Occurrence

Coal Seam Occurrence. Although coal particles are scattered throughout many rock units, most coal occurs in seams, which can range in thickness from a few millimeters to over 30 m. In North America and, indeed, most of the world, anthracite and bituminous coals occur in thinner seams of 1–2 m while the lower rank coals, lignite and subbituminous, commonly occur in thicker seams of up to 20–30 m. While many seams, even minable seams, are of a limited size area, some seams continuously underlie large areas. The Pittsburgh coal seam extends over 77 700 km^2 in Pennsylvania, Ohio, West Virginia, and Maryland, and it is of minable thickness for over 15 540 km^2.

Although there are hundreds of named coal seams in the United States, relatively few are of the quality, thickness, and size of area to be extensively exploited commercially. In the Appalachian anthracite region, the Mammoth seam is the major source of production. In the northern Appalachian field, the major minable seams are the Pittsburgh, Lower Kittanning (No. 5 Block), Upper Freeport, Campbell Creek (No. 2 Gas), Upper Elkhorn (No. 3), Fireclay, Pocahontas, and Sewell seams. All of these seams are suitable for use in making coke. In the southern Appalachians, the Sewanee, Mary Lee, and Pratt seams are the most important, and the latter two are used extensively as coking coals. In the Illinois Basin, the Harrisburg Springfield No. 5 and the Herrin No. 6 are of a minable thickness of over 38 800–51 800 km^2. In the Oklahoma, Kansas, Missouri, and Arkansas region, the Weir–Pittsburg and Lower Hartshorne seams are the most important. In the Powder River Basin, the Anderson–D–Wyodak seam is continuously exposed for 193 km and is estimated to contain at least 91 Gt of coal. In Utah the Lower Sunnyside and Hiawatha seams have produced the most coal. The former is of coking quality, and the latter is characterized by a high resinite content, which itself has been exploited. In Colorado the Wadge, Raton–Walsen, and Wheeler A, B, C, and D are the most important coal seams and some production from the Raton–Walsen and Wheeler seams has been used for coking. Finally, in Washington state the Roslyn (No. 5) is the most mined coal seam. Production from these seams accounts for ca. 75–80% of the cumulative past United States coal production [499].

Coal Seam Structures. All coal seams have a number of structural features, including partings, splits, rolls, cutouts, cleats, faults. folds, and alterations caused by igneous intrusions. These features strongly affect the mining and economical recovery of the coal. *Partings* are layers of rock, usually shale or sandstone, that occur within a coal seam and were caused by an influx of sediment into the original coal swamp. In commercial seams, the partings must, of necessity, be few and thin (a few centimeters). However, even in such seams the partings can be very extensive. For example, near the base of the Herrin No. 6 seam, there is a parting known as the blue band that is found throughout the entire Illinois Basin. When the thickness of a layer of rock within a seam increases to the point where it is no longer practical to mine the parting with the coal, the seam can be considered to have *split*. Although some seams like the Hiawatha in Utah split into three or more minable seams, the splitting of one seam into multiple seams can present serious problems in mining, including correlation (i.e., tracing a given seam across a zone, e.g., a valley, where it is missing) and loss of minable thickness.

In addition to partings and splits within the coal seam, the upper and lower surfaces of a seam often pinch and swell to change the coal seam thickness. Such features have been called *pinches*, *rolls*, *horsebacks*, and *swells*, and their occurrence at the base of a seam is usually attributed to differential compaction. Roof rolls are common and the protrusion of rock into the coal causes some serious problems with mine roof stability. *Cutouts* or stream washouts are the extreme cases where the protrusion actually eliminates the coal seam. These features are clearly the result of nondeposition or erosion by ancient streams associated with the coal swamps.

Another important feature of coal seams, especially in bituminous coals, is the presence of closely spaced fractures within the coal. These fractures, called *cleats*, are usually perpendicular to the bedding plane of the coal and commonly occur in two sets perpendicular to each other. This gives the coal a tendency to break into blocks. The cleat controls the ease with which the coal breaks up, and it has long been used in coal mining. The most prominent cleat is called the face cleat because the working face of a mine is often parallel to it. The other cleat is called the butt cleat. Cleats give coal high permeability to gas and groundwater and also act as sites of mineral deposition. Calcite and pyrite are the most common cleat-filling minerals, although other minerals including gypsum can occur.

Faulting and *folding* of coal seams by geological forces can also be important features. Seams that are faulted or folded usually cannot be mined by surface methods and are more expensive to mine than flat seams. When faulting is extensive, even thick seams of high quality may be too discontinuous to mine. On the other hand, folding can double the minable thickness of some seams, thereby increasing their value, as with the anthracite seams in eastern Pennsylvania.

The *alteration* of coal seams by igneous intrusions is widespread and is a serious problem in some coal fields, such as those in the Rocky Mountains of the United States. The alteration is thermal and causes an increase in carbon content and a decrease in hydrogen, moisture, and volatile matter. In the contact

zone, the coal may be transformed into natural coke. Although such contact zones are usually small, extensive amounts of natural coke are known and have been commercially exploited in some areas such as the Raton Mesa of Colorado.

Coal Seam Distribution. Although coal seams are found in rocks of all geologic ages since the Devonian, the age distribution is not even. Major coal deposits of Carboniferous age occur in eastern and central North America, in the British Isles, and on the European continent. Major deposits of Permian age occur in South Africa, India, South America, and Antarctica. In Jurassic times the major coal accumulation was in Australia, New Zealand, and parts of Russia and China. The last great period of coal deposition was at the end of the Cretaceous period and the beginning of the Tertiary period. Coals originating at this time are found in the Rocky Mountains of North America, in Japan, Australia, New Zealand, and in parts of Europe and Africa. Because they are younger, these coals tend to be of lower rank, usually subbituminous, than the Carboniferous coals. Since the Cretaceous some coal has been deposited in scattered locations more or less continuously and tends to be lignite or brown coal.

The distribution of coal seams throughout the world is also not uniform. As shown in Figure 5.126, most of the world's coal is located in only three countries, the United States, the former Soviet Union, and China. Although the figures vary from source to source, each of these countries has about 25% of the total coal resources, while the rest of the world shares the remaining 25%. In the United States, bituminous coal seams are concentrated in the Appalachian and Illinois Basins. Most of the subbituminous coal occurs in the various smaller basins in the Rocky Mountain region, and the lignite seams are concentrated in the northern Great Plains and the Gulf Coast area.

Figure 5.126: Geographic location of the world's coal.

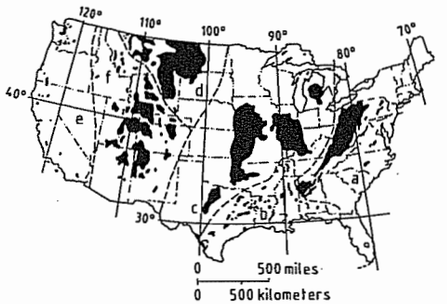

Figure 5.127: Coal provinces of the conterminous United States: a) Eastern; b) Gulf; c) Interior; d) Northern Great Plains; e) Pacific Coast; f) Rocky Mountains.

5.22.4 Classification

Coal is combustible and should be composed of more than 50% carbonaceous material [500]. Commercially, coal is classified in a number of ways on the basis of:

- The original plant or maceral composition, sometimes called coal type
- The degree of maturity or metamorphism, called coal rank
- The amount of impurities such as ash or sulfur, called coal grade
- The industrial properties such as coking or agglomeration.

One of the main classifications by composition used by the United States Bureau of Mines is based on the relative amounts of petrographic entities detected in thin-section analysis, including anthraxylon (translucent material roughly equivalent to vitrinite), translucent attritus (roughly equivalent to liptinite), and opaque attritus and fusain (roughly equivalent to inertinite) [501, 502]. Under this system, coals are divided into two groups: **banded coals**, with > 5% anthraxylon, and **nonbanded coals**, with < 5% anthraxylon. The banded coals are subdivided into three types: *bright coal*, consisting mainly of anthraxylon and translucent attritus with < 20% opaque matter; *semisplint coal*, consisting mainly of translucent and opaque attritus with 20–30% opaque matter; and *splint coal*, consisting mainly of opaque attritus with > 30% opaque matter. The nonbanded coals are divided into *cannel coal*, consisting of attritus with spores, and *boghead coal*, consisting of attritus with algæ.

The various bands or layers in coal evident to the unaided eye have also been classified into four types [503]. *Vitrain* layers appear bright and vitreous; *clarain* appears as relatively less bright, striated layers; *durain* is dull and featureless; *fusain* layers are dull gray and like charcoal. Although these terms (all ending in ain) are megascopic terms meant to be applied to hand-specimen samples, they do have some compositional implications at the microscopic level. For example, vitrain layers contain mainly vitrinite macerals, fusain layers contain mainly inertinite macerals, and clarain and durain are mixtures of all three maceral types.

The most important classification for commercial purposes in the United States is the ASTM classification by rank. It is the basis on which most of the coal in the United States is bought and sold. This classification, ASTM Standard D 388 shown in Table 5.53, divides coals into 4 classes, anthracite, bituminous, subbituminous, and lignitic, which are further subdivided into 13 groups on the basis of fixed carbon and volatile matter content, calorific value, and agglomerating character. The fixed carbon and volatile matter values are on a dry, mineral-matter-free basis and the calorific values are on a moist, mineral-matter-free basis. In this system, coals with ≥ 69% fixed carbon are classified by fixed carbon content and those with < 69% fixed carbon content are classified by calorific value.

Table 5.53: Classification of coal by rank. This classification does not include a few coals, principally nonbanded varieties, which have unusual physical and chemical properties and which come within the limits of fixed carbon or caloric value of the high-volatile bituminous and subbituminous ranks. All of these coals either contain < 48% dry, mineral-matter-free fixed carbon or have > 15 500 Btu/lb moist, mineral-matter-free.

Class	Group	Fixed carbon limits, % (dry mineral-matter-free basis)		Volatile matter limits, % (dry, mineral-matter-free basis)		Calorific value limits, Btu/lb (moist, mineral-matter-free basis)[a]		Agglomerating character
Anthracite	metaanthracite	≥ 98	—	—	≤ 2	—	—	non-agglomerating
	anthracite	≥ 92	< 98	> 2	≤ 8	—	—	
	semianthracite[b]	≥ 86	< 92	> 8	≤ 14	—	—	
Bituminous	low-volatile bituminous coal	≥ 78	< 86	> 14	≤ 22	—	—	commonly agglomerating[d]
	medium-volatile bituminous coal	≥ 69	< 78	> 22	≤ 31	—	—	
	high-volatile A bituminous coal	—	< 69	> 31	—	≥ 14 000[c]	—	
	high-volatile B bituminous coal	—	—	—	—	≥ 13 000[c]	< 14 000[c]	
	high-volatile C bituminous coal	—	—	Ö	—	≥ 11 500	< 13 000[c]	
						≥ 10 500	< 11 500	agglomerating
Subbituminous	subbituminous A coal	—	—	—	—	≥ 10 500	< 11 500	non-agglomerating
	subbituminous B coal	—	—	—	—	≥ 9 500	< 10 500	
	subbituminous C coal	—	—	—	—	≥ 8 300	< 9 500	
Lignitic	lignite A	—	—	—	—	≥ 6 300	< 8 300	
	lignite B	—	—	—	—	—	< 6 300	

[a] Moist refers to coal containing its natural inherent moisture but not including visible water on the surface of the coal.
[b] If agglomerating, classify in low-volatile group of the bituminous class.
[c] Coals having 69% or more fixed carbon on the dry, mineral-matter-free basis shall be classified according to fixed carbon, regardless of caloric value.
[d] It is recognized that there may be nonagglomerating varieties in these groups of the bituminous class, and there are notable exceptions in high-volatile C bituminous group.

Thus, all lignitic and subbituminous coals and the lower rank bituminous coals are classified by their calorific value. It is also important to note that not all coals can be fitted into this system. This is especially true of coals with a high liptinitic maceral content, such as cannel and boghead types.

The other important classification system is the international system of the ISO. In this system, coals are divided into two types: hard coals with greater than 23.86 MJ/kg (10260 Btu/lb) and brown coals and lignites with calorific values less than that amount. In the hard coal classification shown in Table 5.54, the coals are divided into classes, groups, and subgroups. The classes are similar to ASTM groups and based on dry, ash-free volatile matter and moist, ash-free calorific value. The classes are numbered as 0 to 9. The classes are divided into four groups, numbered 0 to 3 on the basis of the swelling properties (free-swelling index, also called crucible swelling number, and Roga index). These groups are further broken down into six subgroups numbered 0–5 on the basis of their Audibert–Arnu dilatation number and Gray–King coke type. The system is set up in such a way that all coals are classified with a three-digit number, in which the first digit is the class, the second digit is the group, and the third digit is the subgroup.

The lignites and brown coals are only divided into classes and groups. The classes, numbered from 1 to 6, are based on ash-free moisture; the groups, based on dry, ash-free tar yield, are numbered from 0 to 4. This classification is shown in Table 5.55.

Although the ASTM and International Systems are different, there is a reasonable correspondence between the ASTM group names and the International System class numbers. This is shown in Table 5.56.

5.22.5 Chemical Structure of Coal

The organic components of coal consist of a complex mixture of macromolecular carbon compounds of varied chemical constitution. The heterogeneity of coal is well-known from optical studies of thin coal sections. The microscopically distinct and distinguishable maceral groups of vitrinite, liptinite, and inertinite, their proportions, and the association of macerals of several groups with each other are essentially responsible for the physical, chemical, and technological properties of a particular coal. Preformed macerals derived from transformation of the original lipidic, woody, and waxy plant matter under varying oxidizing and reducing conditions and processes are present in peat and soft lignites. Temperature-induced chemical changes of these macerals and increased pressures influencing the physical structure of the material undergoing coalification have led to the formation of lignitic, subbituminous, bituminous, and anthracitic coals, forming the basis of coal classification by rank [504, 505].

The minerals of coal play a considerable part in the industrial use of coals of all ranks. The mineral content, its distribution within the coal and its composition may affect carbonization, gasification, combustion, and liquefaction processes by modifying the process of coal depolymerization and influencing hydrogenation and the thermal behavior of the resulting ash under both oxidizing and reducing conditions.

Besides microscopically unidentifiable plant ash, coals contain varying amounts of *syngenetic* and *epigenetic* minerals, which entered the organic coal substance during the first or second phase of coalification, respectively. They have either grown together with the organic substance or are physically separable. Generally, medium to high ash coals contain epigenetic minerals. Structure and hardness bear considerable influence on the distribution in the various fractions of the crushed coal from coal preparation plants.

Table 5.54: International classification of hard coal by type. Where the ash content of coal is too high to allow classification according to the present system, it must be reduced by laboratory float-and-sink method (or any other appropriate means). The specific gravity selected for flotation should allow a maximum yield of coal with 5–10% of ash.

Group (caking properties)			Code numbers[a]							Subgroups (coking properties)		
Group number	Free-swelling index	Roga index								Subgroup number	Dilatation number	Gray–King
					435	535	635			5	> 140	> G_8
				334	434	534	634			4	50–140	G_5–G_8
3	> 4	> 45		333	433	533	633	733		3	0–50	G_1–G_4
				332[a]	432	532	632	732	832	2	≤ 0	E–G
				323	423	523	623	723	823	3	0–50	G_1–G_4
2	2.5–4	20–45		322	422	522	622	722	822	2	≤ 0	E–G
				321	421	521	621	721	821	1	contraction	B–D
1	1–2	5–20		212	312	412	512	612	712	812	2	≤ 0	E–G
				211	311	411	511	611	711	811	1	contraction	B–D
0	0–0.5	0–5		100	200	300	400	500	600	700	800	900	0	nonsoftening	A
Class number[c]			0	1A	1B	2	3	4	5	6	7	8	9			
Class parameters	Volatile matter, % (dry, ash-free)		0–3	3–6.5	6.5–10	10–14	14–20	20–28	28–33	> 33	> 33	> 33	> 33			
	Calorific parameter[d]		—	—	—	—	—	—	—	> 13 950	12 960–13 950	10 980–12 960	10 260–10 980			

[a] First digit class, second digit group, third digit subgroup.
[b] 332a: volatile matter 14–16% and 332b: volatile matter 16–20%.
[c] Approximate volatile matter content 33–41% (class 6), 33–44% (class 7), 35–40% (class 8), and 42–50% (class 9).
[d] Gross calorific value on moist ash-free basis (30 °C, 96% relative humidity) in Btu/lb.

Table 5.55: Classification of brown coal according to ISO 2950-1974-(E).

Group parameter: yield of tar on a dry, ash-free basis, %	Group number	Code number				
> 25	4	14	24	34	44	54	64
20–25	3	13	23	33	43	53	63
15–20	2	12	22	32	42	52	62
10–15	1	11	21	31	41	51	61
≤ 10	0	10	20	30	40	50	60
Class number		**1**	**2**	**3**	**4**	**5**	**6**
Class parameter: total moisture content of mined coal on an ash-free basis, %		≤ 20	20–30	30–40	40–50	50–60	60–70

Table 5.56: Comparison of class numbers and boundary lines of the International System with group names and boundary lines of the ASTM system.

International classification class number	0	1	2	3	4	5	6	7	8	9
ASTM classification group name	metaanthracite	anthracite	semianthracite	low-volatile bituminous coal	medium-volatile bituminous coal	high-volatile A bituminous coal	high-volatile B bituminous coal	high-volatile C bituminous coal and subbituminous A coal	subbituminous B coal	
Volatile-matter parameter[a]	5	10	15	20	25	30				
Calorific-value parameter[a]						14 000[b]	13 000	12 000	11 000	10 000

[a] Parameters in the International System are on ash-free basis; in the ASTM system, they are on mineral-matter-free basis.
[b] No upper limit of calorific value for class 6 and high-volatile A bituminous coals.

The mineral structure of coal ash is extremely difficult to determine. Low-temperature combustion in oxygen plasma produces an ash that can be analyzed by X-ray diffraction and IR absorption spectrometry. Deductions must also be made from the chemical analysis of the oxides present in the ash. The major constituents of coal ash as determined by this chemical analysis are SiO_2, Al_2O_3, Fe_2O_3, and CaO, in addition to MgO, Na_2O, K_2O, BaO, TiO_2, P_2O_5, and SO_3.

These oxides may be derived from minerals of the following types originally present in the coal: kaolinite, illite, and bentonite as major clay minerals; calcite or siderite as major carbonates; pyrite or marcasite as the sulfides; and many other minor minerals such as apatite, hematite, rutile, quartz, etc.

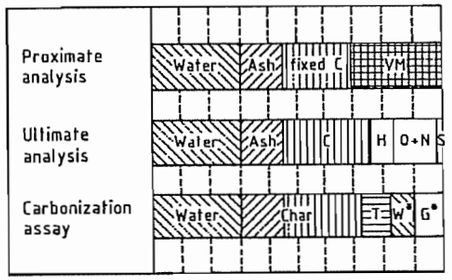

Figure 5.128: Comparison of proximate and ultimate analysis with carbonization assay. C, H, O, N, S = elements; T = tar; W* = decomposition water; G* = carbonization gas; VM = volatile matter.

5.22.5.1 Characterization of Coals

Standard Analytical Methods

Coals are characterized by various chemical and physical methods that have been established as national and international standards. These include proximate analysis, carbonization assay, ultimate analysis, heating value (calorific value) determination, sulfur distribution, caking and coking behavior, ash composition, and fusibility.

The above tests are carried out on representative prepared coals, using either as-received (by the laboratory) or predried samples. The results are commonly expressed on an as-received, dry (d), dry ash-free (daf), or dry mineral-matter-free (dmmf) basis.

Figure 5.128 shows the comparison and relationship between the proximate and ultimate analyses as well as the carbonization assay.

In Figure 5.129 the sulfur forms occurring in coals are illustrated. Figure 5.130 shows selected typical distributions of mineral components.

The coalification series, expressed by plotting atomic ratios of H/C vs. O/C, is graphically represented in Figure 5.131. As one moves from right to left, i.e., from peat to bituminous coals, the diagram shows only a slight shift to somewhat lower H/C ratios while the O/C ratios steadily decrease.

At an O/C level of ca. 0.05, a steep decline in the H/C ratio occurs when the anthracitic coals are reached. Examples of actual compositions of various coals of different degrees of coalification are given in Table 5.57.

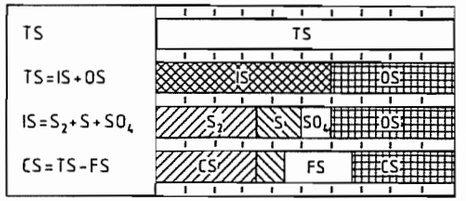

Figure 5.129: Scheme of sulfur distribution in coal. TS = total sulfur; IS = inorganic sulfur; OS = organic sulfur; S_2 = pyrite sulfur; S = sulfide sulfur; SO_4 = sulfate sulfur; CS = combustible sulfur; FS = fixed sulfur.

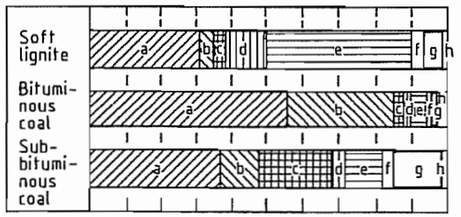

Figure 5.130: Distribution of mineral components of ash: a) SiO_2; b) Al_2O_3; c) Fe_2O_3; d) MgO; e) CaO; f) Na_2O + K_2O; g) SO_3; h) Balance.

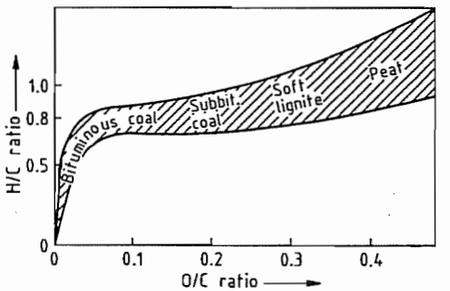

Figure 5.131: Coalification series: atomic ratios H/C vs. O/C.

Laboratory and Bench-Scale Simulation Tests

Because of the complex structure of coal and its vastly varying composition, its depolymerization, liquefaction, and combustion characteristics in thermal and extractive applications are somewhat unpredictable. In commercially operated processes, they depend very much on the prevailing conditions, such as heating and flow rates, pressure, and gas or solvent composition.

Table 5.57: Analytical data for coals of different degree of coalification.

Analytical parameter	Peat	Soft lignite	Lignite	Subbituminous coal	Bituminous coal	Anthracite coal
Moisture (as received), %	> 75	56.7	38.7	31.2	3.7	1.0
Ultimate analysis (daf)						
Carbon, %	58.20	70.30	71.40	73.40	82.60	92.20
Hydrogen, %	5.63	4.85	4.79	4.86	4.97	3.30
Nitrogen, %	1.94	0.74	1.34	1.16	1.55	0.15
Sulfur, %	0.21	0.27	0.60	0.31	1.50	0.98
Oxygen (difference), %	34.02	23.84	21.87	20.27	9.38	3.37
Elemental ratio						
H/C	1.15	0.82	0.80	0.79	0.72	0.43
O/C	0.44	0.25	0.23	0.21	0.09	0.03
Heating value (dry, ash-free), kJ/kg	23 500	27 500	28 500	29 400	30 600	35 700

Therefore, it is often necessary to evaluate coal properties further by subjecting samples to thermal, extractive, and mechanical tests, assessing on a small scale the expected behavior and at the same time providing for study of the types and compositions of specific reaction products.

Such experiments that yield fragmental decomposition compounds can also be employed for the structural identification of coals.

The determinations include, e.g., pyrolytic or progressive devolatilization tests, extraction or solubility studies, performance of selected coking tests, reactivity measurements on specially prepared cokes, grain stability evaluation, and ash slagging behavior.

Petrographic Studies

The determination of the petrographic composition of coals by maceral group analysis is a valuable tool for assessing structural aspects and predicting coal behavior. Usually it also incorporates the determination of the degree of coalification by measuring the reflectance of the vitrinite as the most important and abundant group of macerals. This method allows a ranking or classification of coals by their degree of coalification and, hence, identifies the type of coal. It also reveals specific phenomena that may have induced structural coal changes within the geochemical stage of coal formation, such as aging or contact coalification due to inflowing magma.

5.22.5.2 Structural Deductions from Analytical and Bench-Scale Data

The results of coal analyses predict thermal decomposition products (proximate analysis, carbonization assay, caking and coking tests) and the element composition (ultimate analysis). Furthermore, the moisture level of run-of-mine coals is indicative of the capillary structure, allowing a first tentative classification of a particular coal. The lack of moisture holding capacity of highly coalified coals is proof of an increasingly densified structure. The element ratio, particularly that of H/C and its change to lower values as coalification progresses, points toward the aromatization of structural groups. Likewise, the dramatic decrease in oxygen within the series peat to anthracite strongly suggests the loss of functional end groups.

The softening properties of bituminous coals (caking and coking tests) reveal the mobility of fragmented decomposition products, observed particularly in coals with high hydrogen and, hence, high vitrinite and liptinite contents. On the other hand, oxygen-rich coals, i.e., low-rank coals with an associated appreciable inertinite content or highly aromatic coals with a high degree of cross-linkage, yield recondensed solid depolymerization products. The tar and gas composition (carbonization assay, devolatilization, caking, and coking tests) shows that hydrogen preferentially enters liquid and gaseous components due to rearrangement [506].

Stable fragments, obtained from specific pyrolysis or hydropyrolysis studies, indicate the major types and the volatility of aromatic molecules present in a particular coal. Liquid-phase treatment produces larger unit fragments, which can be determined analytically. A petrographic survey permits selective composition analyses and structural identification of individual major maceral groups such as vitrinite.

5.22.5.3 Bonding of Elements in Coal

Thermal depolymerization by controlled slow or flash pyrolysis of coals, oxidation, hydrogenation, liquefaction of coals, supercritical and selective solvent extraction, as well as the application of modern physical techniques such as X-ray diffraction, IR spectroscopy, nuclear magnetic resonance, or pyrolysis mass spectrometry have furnished extensive data on the bonding of elements in coals. Major findings from these investigations are [507]:

Carbon: The aromaticity increases from 40–50% C in subbituminous coals to 70–80% C in bituminous coals and is over 90% C in anthracites.

Hydrogen: Aromatic bonding to carbon and as aliphatic hydrogen in, e.g., methylene ($-CH_2-$) and methyl ($-CH_3$) groups occurs.

Oxygen: Major functional groups are hydroxyl (–OH), carboxyl (–COOH), carbonyl (>C=O), etheric (–O–) and heterocyclic oxygen.

Sulfur: Bonding is predominantly as thiophenes, also in the thiolic form (R–SH), decreasing with higher rank coals; up to ca. 25% S is present as aliphatic sulfides (R–S–R). Heterocyclic sulfur compounds are also known to exist.

Nitrogen: Very little information on organic nitrogen bonding is available. It appears to occur in heterocycles.

5.22.5.4 Structural Evidence of Coals

Much data on the structural aspects of coal has been accumulated and published by numerous authors, with the aid of the chemical and physical techniques available to modern science [508, 509].

The overall picture, however, is still very incomplete. The difficulty is that coal is a highly heterogeneous mixture and, as such, is not a clearly defined macromolecular aromatic compound of uniform molecular mass and structure. Thus, evaluated structural parameters refer to isolated fragments, components (vitrinite), or constituents. According to the current level of understanding, however, coal may be described structurally as a three-dimensional skeleton of generally four to five highly stable condensed aromatic and hydroaromatic units with cross-linkage by weaker short-chain aliphatic groups. Reactive functional end groups and aliphatic structures are attached to the aromatic skeleton. The average molecular mass distribution is ca. 500–800 for low-rank coals, increasing to ca. 3000–6000 for bituminous coals, and possibly values in excess of 100 000 for anthracites.

Various overall models for the complex organic structure of coals, combining available experimental data on structural fragment analysis, have been tentatively proposed. However, none as yet fully accounts for all the phenomenological characteristics [507].

5.22.6 Hard Coal Preparation

The ROM (run of mine) coal brought to the surface contains various types of accompanying minerals and interstratifications, which must be removed to obtain a coal that complies with market demands for the different types and grades. Grain size, ash content, and moisture content can be controlled within a narrow range by applying mechanical and physical cleaning methods. The ROM coal is subjected almost exclusively to mechanical wet treatments that are more difficult and expensive if the feed is intimately intergrown.

5.22.6.1 Preliminary Treatment and Classification of Raw Coal

The upper grain size of raw coal is defined by the dimensions of the coal cleaning equipment. Before being fed to that equipment, the coal is subjected to preliminary screening and crushing to a diameter of 120–150 mm; foreign matter is simultaneously removed. Coarse dirt is normally reduced in particle size along with the coal, and only in exceptional cases is it removed by preliminary treatment. Such preliminary removal of coarse dirt is done exclusively in drum or inclined separators. Dual eccentric and resonance screens are used for lump coal; each of these machines has a throughput of up to 2 kt/h.

After preliminary screening and removal of foreign matter, the coal in the 0–150 (or 0–120) mm diameter range is defined as raw feed coal. To an increasing extent, this coal is fed to a storage and homogenization plant without further treatment. Homogenization then produces a consistent grain size and uniform contents of moisture, dirt, and volatile materials. The uniform quality of the coal feed makes possible a uniform product and optimal utilization of the washery capacity [510].

Homogenization of the raw feed coal can be carried out in blending silos or on blending yards. Figure 5.132 shows the homogenization results of a silo. A critical factor in homogenization is the size of the storage location for containing one day's output.

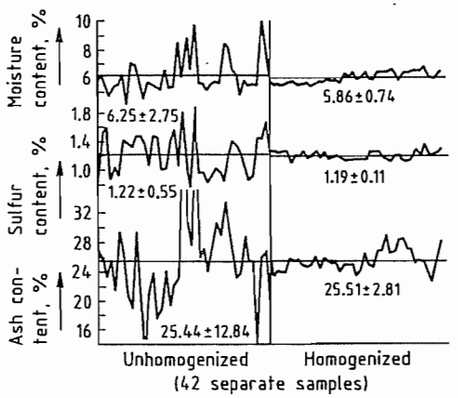

Figure 5.132: Homogenization of raw coal in a blending silo.

In the washery the coal is first classified to ensure optimal utilization of the subsequent cleaning equipment for coarse coal and smalls. Normally the raw feed coal is screened off between 10 and 12 mm and subdivided into coarse raw coal and raw smalls. Such classification is carried out either on vibrating screens or on tensioned screens equipped with varying types of bottoms of perforated plate or tissue. The throughput for a unit may be as high as 1 kt/h [511]. The raw coarse fraction is then subjected to wet mechanical cleaning, which completely removes adhering smalls and ultrafines by spraying.

Prior to cleaning of the raw smalls 0–12 (or 0–10) mm, the ultrafines are removed by a complex method. Normally an air separation method, e.g., dry classifying, or wet desliming on screens is used. Among the air separators, cyclone separators with mechanical dust discharge have proven to be most successful. These are designed for throughputs of up to 700 t/h. Vibrating separators are used in some exceptional cases where dust must be removed from all of the raw feed 0–150 (or 0–120) mm [512]. With some rare exceptions, the separator dust is added unscreened to the saleable products; in the future, however, an increasing proportion of the dust will need to be cleaned.

5.22.6.2 Wet Treatment

Cleaning of the raw feed is done by wet treatment in jigs and dense-medium separators, which separate according to differences in density or flotation (surface) properties.

Cleaning in Jigs

Almost all of the jigs used in Germany are of the air-pulse type or, in exceptional cases, of the wash-box type [513, 514]. They usually yield three products. Separation is accomplished by density, under the action of a pulsating flow of water. Pulsation may be applied either by a simple stroke or a superimposed double stroke.

During recent years, the Batac jig with compressed air chamber underneath the bed proved to be the most successful machine. With such a system, all of the machine width, including the chamber width, is available for jigging. An electronic valve control or a mechanical rotational valve is used to adjust the compressed-air load. Air pulsation coupled to the hydraulic inductive discharge controls enables the operator to modify the cut point by simply actuating a selector. This allows the cleaning of two different coal types successively in the same jig. The jigs usually accept coarse coal 10–150 (or 10–120) mm in diameter and smalls < 10 mm.

Cleaning in Dense-Media Separators

The coarse fraction is also cleaned by dense media, particularly in star-wheel extractors or inclined separators [515].

Whereas previously baryte, clay, ultrafine dirt, loess, and pyrite were used as dense media, the more recent equipment runs almost exclusively on magnetite and ilmenite. Selection of the dense medium depends on the method of regeneration (magnetic separation or gravity). The regeneration method also depends on the grain size of the dense medium.

A jig can be controlled by using either floaters or a layer of a given weight. It can also be fully automatic, controlled by gamma-ray counters. Dense-media equipment is controlled by maintaining the densities constant via automatic addition of the dense liquid. This adjustment can be set so precisely that it approximates separation by a true solution. While the cut point with dense-media cleaning is, in general, more precise than that with jigs, the latest achievements in jig cleaning have resulted in the widely expanded use of jigs within Germany because the coal normally is highly amenable to jig cleaning and because machine expenditure and costs are lower.

Cleaning by Flotation

Currently, some 14% of the raw coal feed in Germany is subjected to flotation. The diverging degrees of wettability of different mineral components allow cleaning of very fine particles by means of air bubbles. The bubbles are created by dispersion of the air feed in the dense medium; they remove the coal particles that have been rendered hydrophobic by flotation agents [516]. Flotation is applied to slurries if they contain an excessive percentage of mineral components so that their inclusion in the high-grade product is economically impossible.

Flotation plants consist of five to seven separate cells or flotation troughs with the corresponding number of stirrers. Each cell is between 5 and 14 m^3 and has a throughput up to 100 t/h particulate matter corresponding to 1000 m^3/h of pulp. Flotation is done either in one or two steps. The current flotation agent is of the collecting and foaming type. A ton of particulate matter requires 0.3–0.8 kg of flotation agent for the process.

Other Cleaning Methods

Cleaning on tables and in dense-media cyclones has been used in certain cases to reduce the sulfur content of the product and to obtain a coal extremely low in ash.

5.22.6.3 Dewatering

Moisture must be removed after wet cleaning [516–519]. There are static and dynamic methods. Among the dynamic methods are screen dewatering of nut-size coal and preliminary dewatering of small products on stationary screening tables or in refuse elevators. The static methods are being replaced by dynamic ones (centrifuge, vacuum, and pressurized dewatering) because of the demand for low final moisture content. The concurrent higher ultrafine and moisture contents in the raw coal have necessitated additional process steps.

Smalls are normally dewatered on vibrating screen centrifuges. Several improvements in their design particularly the conversion from vertical to horizontal arrangements have allowed high throughputs and easy repair and maintenance. Centrifuges with drum diameters of 1.3 m and rated capacities of 250 t/h (water-free) are the best. The smalls are dewatered down to 5 or 7% at centrifugal forces of 80–100 g, depending on grain size distribution.

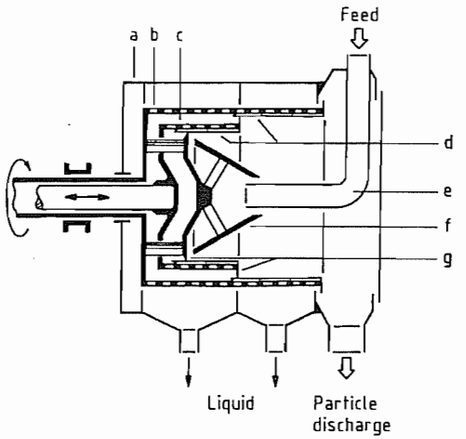

Figure 5.133: Two-step pusher screen: a) Enclosure; b) External screen drum; c) Internal screen drum; d) Slot screens; e) Feed pipe; f) Vortex; g) Pusher rings.

Coarse slurries are dewatered in pusher screens where the centrifuge forces (400–500 g) are higher than in vibrating screen centrifuges and where residences are considerably longer. Figure 5.133 shows a pusher screen. A

first (comparatively short) step provides preliminary dewatering and an even distribution of particles on the drum periphery. This is followed by the secondary dewatering step. Recent pusher screen designs have drum diameters up to 1.2 m with a rated throughput of coarse slurrying of more than 40 t/h. The coarse slurry is dewatered to 9–15%, depending on grain size distribution.

Drum filters with surface areas up to 120 m^2 and disk filters of up to 500 m^2 are available for ultrafine dewatering. With this equipment, specific feed rates of 100–800 $kgm^{-2}h^{-1}$ (wf) and moisture contents of 18–28% are attainable.

The flotation concentrate is also dewatered by means of a solid-bowl screen centrifuge where a solid-bowl section is followed by a cylindrical screen section, which dewaters the pre-thickened feed under favorable conditions independent of the particle concentration in the feed medium. Such a solid-bowl centrifuge is depicted in Figure 5.134. Flotation tailings are dewatered either by chamber filter presses or by solid-bowl centrifuges. More recently, screen belt presses have also been used. The selection of these alternatives depends on the desired moisture content of the waste.

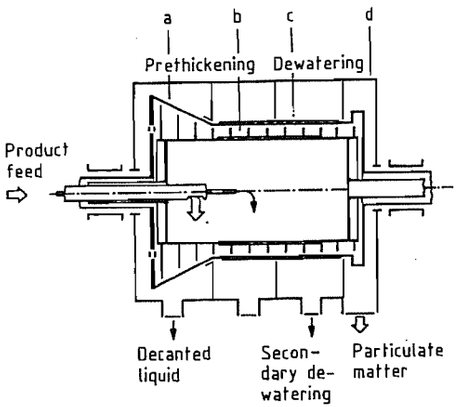

Figure 5.134: Solid-bowl centrifuge: a) Solid bowl; b) Conveyor screw; c) Screen bowl; d) Enclosure.

5.22.6.4 Decantation and Thickening of the Process Water

Wet-type coal preparation plants involve a number of particle-water circuits where up to 6000 m^3/h medium are circulated. If the water is to be reused for further cleaning steps, the particulate matter must be removed from it as far as possible. Decantation units, which usually consist of circular thickeners with diameters up to 40 m, are used. Rectangular thickeners are used less often. Water circulation varies, depending on the mechanical equipment, and can be as high as 6 m^3 per ton of raw feed coal. Water consumption oscillates near 0.2 m^3/t feed for a closed circuit. It can rise to as high as 1 m^3/t feed if, e.g., salt content is excessive or if the flotation waste must be discharged to an external disposal site.

The decantation units are meant to bring about simultaneously a desirable degree of thickening for subsequent dewatering or cleaning procedures. Thickener outputs fluctuate between final concentrations of 120 g/L for flotation feed and 650 g/L for pusher screen dewatering. About 0.5 g of organic sedimentation accelerators are added per cubic meter to promote sedimentation for wash-water decantation.

5.22.6.5 Dosing and Blending

The products from coal preparation (nuts, dewatered smalls, air separation dust, flotation concentrate, and middlings, i.e., product that has a high content of intergrown material) are stored separately in bunkers. The demand for nut-size particles has been declining, and they are reduced to < 10 mm diameter by impact or hammer mills. They then serve as a constituent of high-grade coals. The cleaned products are withdrawn from the bunkers and blended according to a set program. During this operation, the ash contents can be monitored or adjusted by automatic rapid-measuring instruments. The addition of those components that are highest in ash (air separation dust) is adjusted, depending on the measurements, so that the final product is brought to the desired ash content. Instruments for rapid and continuous measurement of moisture content will soon be introduced. Other mechanical equipment used for dose-feeding and blending includes filling-level indicators, dose-feeding devices, and belt weighers.

5.22.6.6 Removal of Pyritic Sulfur

Sulfur may be present in hard coal as elementary sulfur, sulfate, organic sulfur, or sulfide (pyrite).

Pyritic sulfur is removed by modern cleaning procedures [520, 521]. The raw coal is screened off at ca. 40 mm. The dirt of the > 40 mm product is removed in a jig. The jig floatings are reduced to < 40 mm, fed along with the < 40 mm product from sizing to a blending yard, and homogenized. The product is then cleaned in another jig; the coal and intergrowth of this step are reduced to a diameter of < 10 mm and fed to dense-media cyclones to yield, at low separation density, a raw coal low in sulfur. The intergrowth from the cyclone is reduced to a diameter < 3 mm and then classified in cyclones at 0.063 mm and subjected to secondary cleaning on tables. The < 0.063 mm product is then subjected to flotation. Dewatering of the intermediate products is done in vibrating screen centrifuges, pusher screens, and solid-bowl screen centrifuges.

5.22.6.7 Thermal Drying

Thermal drying is restricted to a few special cases in the treatment of coking and power station coals because the procedure involves high costs. The continuing increase of the ultrafine proportion, which is difficult to dewater, and the increasingly stringent quality demands necessitate more advanced dissociation and cleaning of ultrafines, as well as novel techniques of coal extraction, haulage, and treatment. These factors have led to increasing reliance on thermal drying in the aforementioned sectors [521].

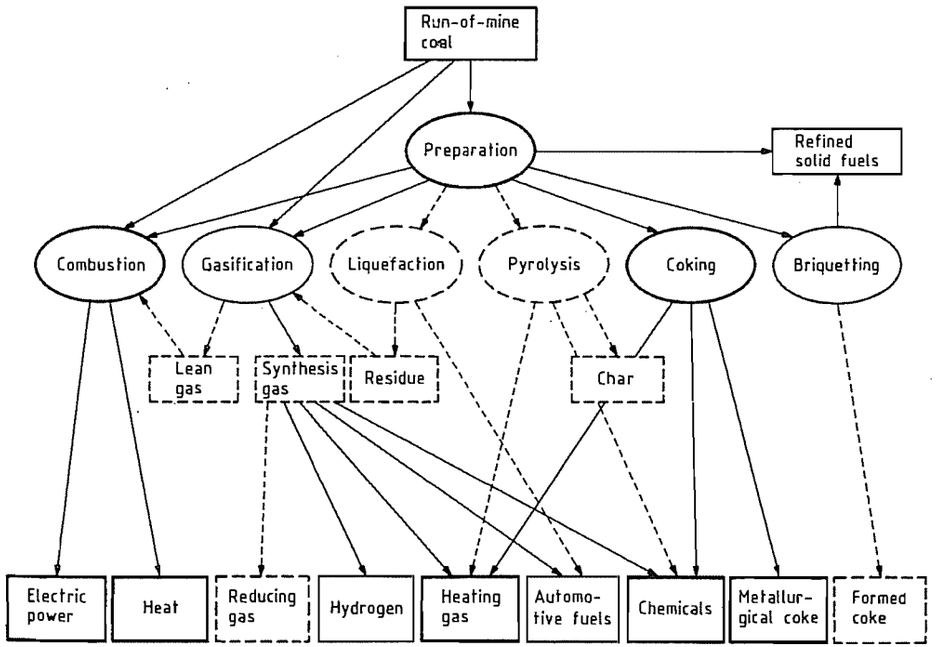

Figure 5.135: Coal conversion processes and end uses.

Drum-type dryers are usually superior to the gas suspension dryers in terms of energy balance. The current quality requirements for coals for coking and power stations require that only part of the coal volumes be dried to stay within the moisture tolerances required for the final smalls product. Less drying also reduces problems of dust.

5.22.7 Coal Conversion (Uses)

Coal conversion processes may be divided into three groups. *Mechanical conversion processes* include coal preparation and briquetting. *Processes for transforming coal into secondary fuels* include coking, gasification, liquefaction, and combustion. *Processes for the conversion of coal for purposes other than the generation of energy* include the recovery of by-products during coking, the production of active carbon, and the preparation of coal-based materials.

In Figure 5.135 the individual conversion processes are shown by ellipses, and the intermediates and end products are depicted by rectangles. Because there are so many variations of the processes, only the most important routes are depicted. The dark lines show processes and common applications. The thinner lines represent less common routes, and the broken lines show those that are still under development or have not yet found commercial application.

5.22.7.1 Preparation

Coal preparation is part of the colliery operation and is intended to turn the raw coal into more saleable products with defined characteristics. The choice of preparation process depends on the *raw material* and its technological properties, the *market requirements* for quantity, type, and quality, and *economic* and *environmental considerations*.

Coal preparation is used to differing extents in different countries. In Germany, all of the coal obtained by underground mining is subjected to preparation, whereas ca. 85–90% of the lignite, which is obtained exclusively by open-cast mining, is used for power generation without preparation. The lignites and subbituminous coals in the United States and Australia are also used without preparation. These two countries only submit coal to full preparation if it is to be used for coking. Probably about half of the coal used throughout the world undergoes preparation.

The water, ash, and sulfur contents, the size, and the volatile constituents are all important properties of coal that can be affected by preparation. Reduction of the sulfur content is especially significant because there is a worldwide concern about pollution.

Comminution, screening, grading (the true focal point of the preparation process), dewatering, settling, thickening, storage, proportioning, and mixing to blend the finished products are all important preparation processes.

The production and stabilization of suspensions of coal in water and coal in oil, which can be used to replace fuel oil in power stations and industrial boilers, are not considered to lie within the normal scope of preparation. The application of suspensions of coal in water to the transport of coal in pipelines is being examined as an alternative to other types of transport [523–525].

5.22.7.2 Briquetting

Lignites or low-volatile coals of a particle diameter < 6 mm that are not suitable for coking and are not used in power stations can be burned in grate stokers only if they are converted to lump form. This can be carried out commercially by briquetting. Binding agents are used for low-volatile coals, but these are not required for lignites. Less common methods of compacting include hot briquetting, in which a coking coal is used as the binding agent, and pelletizing. With some exceptions, such as in the former German Democratic Republic, briquetting is of only minor significance in the sales of coal to private and industrial users. Since the mid-1950s, oil and natural gas have effectively replaced coal as a

means of heating in other countries because of their cost and convenience.

5.22.7.3 Carbonization and Coking

Low-temperature carbonization and coking involve heating of coal with the exclusion of air. This process removes the condensable hydrocarbons (pitch, tar, and oil), gas, and gas liquor, leaving a solid residue of coke. Low-temperature carbonization (up to 800 °C) and coking (> 900 °C) are differentiated by the final temperature. The two processes also differ sharply in the rate of heating of the coal and in the residence time in the reactor. These parameters have a direct effect on the product yields. Low-temperature carbonization produces fine coke and fairly large quantities of liquid and gaseous products, whereas high-temperature coking is used primarily for the production of a high-temperature lump coke. After the oil crisis of 1973, attempts were made to submit the coal used in power stations to preliminary low-temperature carbonization. The coal by-products were then to be refined while the coke was used for firing. However, the process could not be made profitable.

Currently, high-temperature coking of coal is carried out entirely in batch-operated coke ovens, of which the majority are of the horizontal chamber type. The feedstock is a coking coal of given size composition. The coking properties depend chiefly on softening and resolidification temperatures and on swelling behavior. Coking takes place at a temperature of 1000–1400 °C. The coking time of 15–30 h depends on the operating conditions and type of oven. The main product is metallurgical coke required for the production of pig iron. It is characterized by its suitable size and high resistance to abrasion even under blast furnace conditions. Coke oven gas and liquid by-products are also produced. In Western Europe, these have considerable influence on the economy of coking and, therefore, are reprocessed. However, in many coke oven plants in the United States, the by-products are burned.

Considerable technical improvements in coke production have occurred in recent years. These have led to greater cost effectiveness. They include mechanization and automation of oven operation, reduction of coking time and increase of specific throughput by the use of thinner bricks of higher thermal conductivity, and increased oven sizes.

Coking in horizontal chamber ovens is becoming increasingly difficult for the long term due to the deteriorating quality of coal feedstocks. Therefore, coking technology must be assisted with additives and auxiliary technology. Potential additives include petroleum coke, bitumen, and oil. Among the auxiliary technologies to be considered are the ramming operation, such as is used in Germany and some East European countries, and the various modifications of coal preheating, which are used in Western Europe, the United States, and Japan.

Dry cooling of coke has recently found increased use in Western Europe to recover stored heat. For climatic reasons this technique has been used for a considerable time in the former Soviet Union. Dry cooling of coke leads to considerable savings in energy and pollution, especially when used in combination with preheating.

At the start of the 1960s, many countries considered developing a continuous production process for formed coke in expectation of a further worldwide increase in demand for coke for steel production. Numerous process developments, such as briquette coking or hot briquetting of a mixture of char and caking coal, have been demonstrated on an industrial scale. Even so, these processes have not been able to gain acceptance. This is partly because unexpected improvements in chamber coking have been realized and partly because the steel industry has been having difficulty for more than a decade, and thus, the anticipated shortage of coking coal has not yet occurred.

5.22.7.4 Pyrolysis

Pyrolysis includes carbonization and coking. It is also the starting reaction in gasifica-

tion, combustion, and direct liquefaction processes. As the modern coal conversion processes have come to involve higher pressures, e.g., to increase the reaction rates and reduce the vessel dimensions, pyrolysis under pressure and in different gas atmospheres has been systematically studied.

Laboratory-scale trials show that under high hydrogen pressure, coal can be converted to gaseous and liquid products, especially BTX aromatics (benzene, toluene, and xylene), with good yield. In addition, the process results in a residue char that must be either burned or gasified. The technology is called *hydropyrolysis*. It is classified as gasification or liquefaction, according to temperature and pressure (800 °C, 100 MPa). An extended research and development program on hydropyrolysis is funded by the International Energy Agency. After successful laboratory trials, a process development unit has begun operation.

5.22.7.5 Coal Liquefaction

Coal liquefaction can be accomplished in two ways. Treating coal suspended in suitable oils with hydrogen in the presence of a catalyst or with hydrogenating solvents yields oil products and some unreactive residue. This technology is called *direct liquefaction* or *coal hydrogenation*. In addition, coal can be gasified with steam and oxygen to yield a mixture of hydrogen and carbon monoxide (synthesis gas) from which liquid products can be synthesized. This technology is usually called *indirect liquefaction*. Both routes were developed into industrial-scale processes during the 1930s. However, (indirect) coal liquefaction is currently employed on an industrial scale only in South Africa (Sasol plants I, II, and III). Further developments took place in 1975–1985 mainly in Germany, the United States, and Japan.

Direct Liquefaction

Coal hydrogenation is a hydrogenating digestion of the coal molecule. Hydrogenation using a solvent brings about depolymerization at ca. 15 MPa and 430–460 °C to yield an asphalt-like product. This product can have the ash removed, e.g., by hot filtration, and it can serve as a boiler fuel or as a feedstock, e.g., for the production of high-quality carbon products. However, many development schemes went on to further hydrogenate the extract in a separate stage and thereby produce a synthetic oil that can be distilled and refined into marketable products [527, 528]. New examples of this technology are the American EDS (Exxon donor solvent) [529] and SRC (solvent refined coal) [530] processes and several Japanese developments on a pilot-plant scale [531]. In the new American development of ITSL (integrated two stage liquefaction), extraction and further hydrogenation are combined in one process [532].

Catalytic hydrogenation of coal usually requires a pressure of tens of megapascals and a temperature of 450–480 °C. These strong reaction conditions yield a light oil fraction that can be further refined. This technology is used, e.g., in the Kohleöl process (Germany), in the H-Coal process (United States), and in Japanese developments. For the Kohleöl process a demonstration plant of 200 t/d coal throughput has been in operation since 1981. The Japanese are just completing a demonstration plant in Australia. These new processes surpass the prewar Bergius–Pier process by increased selectivity and yield of useful liquid products, by a considerable reduction in operating pressure to 20–30 MPa from ca. 70 MPa, by increased volumetric reactor throughput, by improved availability of the plant, and last but not least, by having the unreacted residue conditioned in such a way as to make it accessible to steam gasification for hydrogen production. The very recent German development of integrated raffination in which part of the downstream processing of the Kohleöl has been incorporated into the hydrogenation process has led to further substantial improvements and may even constitute an entirely new liquefaction process.

Direct liquefaction also reduces the sulfur and nitrogen contents of the liquid products compared to those of the reactant feed coal. Thus, extractive hydrogenation is also considered as a means of obtaining a clean boiler fuel from coal. However, the economic prospects that complete hydrogenation will produce a synthetic crude oil are more promising. Further refinement into light fuel oil, automotive fuels, and chemical feedstocks essentially follows petrochemical technology although coal oils require an adaptation of the refining catalysts.

Indirect Liquefaction

The synthesis of hydrocarbons from synthesis gas is called indirect liquefaction. This technology is also named the Fischer Tropsch synthesis after its discoverers. The process was developed in prewar Germany and was used extensively during World War II. After the war, the process could not compete with cheap oil from the Middle East. New capacity was erected only in South Africa, where it was set up downstream of Lurgi fixed-bed coal gasifiers. In the Sasol I plant, two different Fischer Tropsch process technologies are employed, the fixed-bed Arge process (Lurgi Ruhrchemie) and the entrained-flow Synthol process (Kellogg–Sasol). The Arge process produces mainly gasoline, fuel oil, and waxes, whereas the Synthol process yields a larger fraction of gasoline and low molecular mass products (methane and propylene). The Sasol II and III plants, built in the late 1970s, use only the Synthol process. On an energy basis the total liquid product yield obtained by indirect liquefaction of coal in the Sasol II plant is ca. 32%.

5.22.7.6 Coal Gasification

Systematic development of coal gasification began in the first half of the 19th century. A mixture of carbon monoxide and hydrogen was produced. This was generally used for chemical purposes, which remained the main application of coal gasification for nearly 100 years. Many communities relied on coke oven gas to supply town gas for illumination, cooking, and heating into the second half of this century. However, coal or coke gasification was also employed mainly for peak shaving in large gas schemes and also for the supply of gas to industrial furnaces. These applications provided strong development incentives. Natural gas and mineral oil in large amounts and at low cost replaced gas manufactured from coal not only in the heating market, but also in the chemical industry in most countries. The oil crisis of 1973–1974, with its sudden steep increase in prices of mineral oil and natural gas and the subsequent supply shortages, triggered new interest in coal gasification.

Gasification can be accomplished by reacting coal with oxidizing or reducing agents. Using oxygen (or air) and steam as gasifying agents yields water gas.

$$C + H_2O \xrightarrow{O_2} CO + H_2$$

The composition chosen for the blast depends on individual process conditions and governs the carbon monoxide: hydrogen ratio of the product. Varying the steam:oxygen ratio in the blast is a very sensitive and convenient means of controlling the reaction temperature.

Gasification with hydrogen (hydrogasification) leads primarily to methane.

$$C + 2H_2 \rightarrow CH_4$$

However, hydrogasification is usually incomplete and produces a char residue, which cannot economically be converted with hydrogen. Thus, reductive gasification is considered as only a preliminary step in the complete gasification of coal. However, it is a very favorable step if a gas with a high heating value, e.g., substitute natural gas (SNG), is to be produced. Hydrogasification is also involved in most fixed-bed countercurrent-flow gasification processes, contributing to the methane content of the product. Several other reactions take place simultaneously, including the Boudouard reaction, complete combustion of carbon, and methane formation from carbon monoxide and hydrogen.

In coal gasification processes, it is necessary to optimize heat transfer, mass transfer,

and chemical reaction conditions between huge flows of solid and gaseous agents and to achieve a high throughput and optimal energy economy at the same time. Many varieties of coal gasification processes have been developed, reflecting compromises of the many constraints and conditions.

First consideration must be given to the intended use of the product gas. Current interest focuses on the preparation of the following:

- A gas with a high heating value, e.g., SNG
- A fuel gas, e.g., a clean boiler or turbine fuel
- Synthesis gas, for the production of commodity chemicals
- Hydrogen, for ammonia production or for energy purposes
- Reducing gas, for direct reduction of iron ore

A second, equally important, consideration applies to the available coal. Of particular importance are coal rank, grain size, caking properties, ash content, and ash melting behavior. Third, environmental regulations, site specific infrastructure, etc. have to be taken into account. Considering all these factors, a decision in favor of fixed-bed, fluidized-bed, or entrained-flow gasification can be made.

In a *fixed-bed* gasifier, coal and blast are usually contacted in countercurrent flow. This leads to the splitting of the overall gasification reaction into several zones with favorable conditions for the various reaction steps involved. Fixed-bed gasification usually results in excellent carbon utilization and high efficiency. It is applicable to coals of all ranks. However, it requires lump, noncaking or weakly caking coal with a high ash softening temperature. The product contains tars and other liquid byproducts that complicate the gas treatment. Atmospheric fixed-bed gasifiers of various design are still occasionally found in small-scale industrial use. On a large scale, some Lurgi fixed-bed pressurized gasification plants are operating commercially, e.g., in South Africa (Sasol I, II, and III).

Fluidized-bed gasification, invented in 1922 by WINKLER at BASF, has the advantage of fairly simple reactor design and very high reactor throughputs even at atmospheric pressure. However, reaction temperature is limited by the need to avoid ash agglomeration so that fluidized gasification is restricted to very reactive fuels such as subbituminous coals or lignite. Winkler gasifiers operating at atmospheric pressure produce synthesis gas in the former German Democratic Republic and in India. In Germany, further development to Winkler gasification at high pressure has taken place, and a first demonstration unit has been completed [533, 534].

Entrained-flow gasification takes place in a flamelike reaction zone, usually at a very high temperature to produce a liquid slag. For economical operation, a high-standard heat recovery system is mandatory, but the product gas is free of methane, tars, etc., thereby considerably simplifying gas and water treatment.

Entrained-flow gasifiers of the Koppers–Totzek design operated at atmospheric pressure are used industrially in many countries to produce hydrogen or synthesis gas. The Texaco partial-oxidation process recently has been adapted to coal gasification in a pressurized entrained-flow reactor. Industrial-scale plants operate or are under construction in the United States, Germany, and Japan.

Apart from these well-established or highly developed processes, further intense development is under way on existing processes, as well as on new concepts. During the last decade most of the existing processes have been modernized or modified by incorporating new process engineering, materials, and control technology. Such new concepts as pressurized gasification in various modes, hydrogasification, multistage processes, slag bath and molten iron processes, and allothermal processes, e.g., using process heat from gas-cooled nuclear reactors, have been proposed and tested [535–540].

Some of the new development projects have subsequently been terminated or shelved because of the present availability of mineral oil and natural gas. However, the long-term incentive of securing and diversifying the world energy supply is still valid. Environmental considerations may favor converting coal into a clean fuel gas that can be used either conventionally or in highly efficient technologies like fuel cells or combined cycle power plants. Furthermore, low-quality coals, which are located in remote places and are therefore not marketable as such, can be gasified and converted on site into transportable products such as commodity chemicals or hydrocarbons and thereby contribute to worldwide supplies.

5.22.7.7 Coal Combustion

In combustion the energy content of the fuel is completely released and can be recovered as sensible heat. The combustion products are usually considered to be useless waste products. Therefore, coal combustion is not classically considered to be a coal conversion or refining process, but rather an energy conversion process. However, modern combustion systems, e.g., two-stage combustion or low-nitrogen oxide burners, involve clearly distinguishable reaction steps such as pyrolysis and partial oxidation (gasification), which are classical conversion reactions. In the fluidized-bed combustion of coal, sulfur dioxide is removed from the flue gas during the combustion process by adding limestone sorbent to the feed coal. This enables low-grade coal to be burned cleanly, eliminating the need for preliminary upgrading steps.

5.22.7.8 Conversion of Coal for Purposes Other Than the Generation of Energy

Coal Tar Chemical Industry

Considerable quantities of aromatic chemical feedstocks are still prepared by reprocessing the coal tar that is produced during coking at a worldwide rate of ca. 16 Mt/a (tar and pitch). The tar components are reprocessed into dyes, pesticides, varnishes, vitamins, and textile auxiliaries. Tar oils are used for the production of carbon black, e.g., for tire manufacture, and for the production of impregnating oils. Special pitches recovered from coal tar are used for the production of special coke, e.g., that used for electrodes.

Until the early 1950s, industrial production of aliphatic hydrocarbons was based on acetylene produced from calcium carbide. This coal-based chemical feedstock was subsequently replaced by the more economical ethylene produced from crude oil. Research into the production of acetylene is again being carried out worldwide, and new methods using carbide and plasma arcs are being investigated. Special attention is given to reducing the high energy requirement.

Production and Use of Activated Carbon

Precise thermal and chemical treatment of lignite or coal can produce activated carbon with a specific pore system. Activated carbons made from coal are particularly noted for their high ignition temperatures and good resistance to abrasion. Therefore, they are suitable for use in industrial processes for removing sulfur and nitrogen compounds from the flue gases emitted by coal-fired power stations, for wastewater purification, for separation of various mixtures of gases, and for solvent recovery, etc.

5.22.8 Agglomeration

Numerous industrial processes require coal in its coarse state for handling and transportation and as a feed for such thermal applications as combustion, gasification, iron ore reduction, and carbonization. However, highly mechanized mining operations, coal preparation, and beneficiation yield a high proportion of fines. Upgrading of such coal fines by agglomeration is frequently applied and considered [541–546].

The choice of agglomeration process and of a possible binder depends very much on the degree of coalification of the coal and the intended application.

The agglomeration ability of a coal is mainly influenced by its moisture-holding capacity, ash content and composition, hydro-

phobicity, size distribution, and plastic or elastic behavior.

Fundamental coal agglomeration methods are grouped into

- Briquetting and extrusion [542, 546–550];
- Balling and tumbling [542, 544, 545, 551–554].

In the processes of the first group, a compressive force is applied to a prepared coal or a coal and binder mixture.

The double-roll hydraulic press and extrusion presses of various designs are the most common mechanical devices used. Binderless briquetting or extrusion requires that a high pressure be exerted on the coal. Therefore, its applicability is generally limited to predried peat or soft lignites sized to particle diameters < 1 or 0.5 mm that exhibit defined plastic properties. Ash contents should be low to prevent excessive erosion [550].

Binder briquetting or extrusion exercised at low to medium pressures is applied to coal with insufficient plastic properties, but essentially elastic properties, i.e., subbituminous, bituminous, and anthracitic coals usually of particle sizes < 3 mm. Organic binders such as pitch, bitumen, starch, molasses, lignosulfonates, or inorganic additives, e.g., clay minerals, are used in quantities of 2–8%. Briquettes produced with water-soluble binders require a subsequent drying step to attain final strength [546, 555, 556].

Hot briquetting techniques utilizing the softening of bituminous coals at a temperature of 350–450 °C are employed for the production of hot briquettes from mixtures of coal and coke.

Balling of finely ground prepared coal generally smaller than 0.315 mm in particle diameter with 2–6% of organic or inorganic binders has only recently evolved as a commercially viable coal agglomeration technique by using pelletizing disks designed for light bulk materials [544, 554, 557]. Both moist and dry pellets may be used industrially. Although the disk produces pellets of almost uniform size, tumbling in, e.g., rotary drums or mixers yields pellets of a wide size distribution. This mode of agglomeration is preferentially applied to subbituminous, bituminous, and anthracitic coals of both low and high ash contents, but predried lignites can also be pelletized [542, 551, 552]. Drying and thermal treatment of these pellets, however, cause severe cracking and significant losses in strength and stability.

Coal agglomerates must withstand mechanical and thermal treatment when used in industry. The type and severity of stress depend on the particular use and mode of treatment which mainly include transportation, drying, thermal shock, pyrolysis, gasification, and combustion [546, 549, 551]. Suitable procedures for the agglomeration step may be developed and selected from bench-scale simulation studies. Subsequent handling and thermal experiments with these agglomerates lead to a final, optimized product, which may be tested on a larger scale in pilot or commercial plants.

5.22.9 Transportation

The large amount of coal that is mined every year is a major commodity for the transportation industry and one that requires a significant capital investment. In the United States, ca. 50% of the 700–800 Mt of coal produced per year is shipped by rail; 18% is shipped by river barges; and the rest is handled by trucks, conveyor belts, and pipelines. The actual cost of long-distance shipping is usually quite modest, but the loading and unloading of the coal adds greatly to the total cost of shipping. In a typical surface mining operation, for example, coal is moved from the mine by truck or conveyor belt to a nearby preparation plant, where it is loaded onto a unit train for rail shipment to a utility or port facility. At the port it may then be loaded onto river barges or ocean-going bulk carriers.

Although some of the coal transported by *rail* is shipped at single car or bulk rates, most is carried at lower rates in unit trains of up to 100 cars that travel continuously to a single destination and return. The unit train carries only coal and each car can carry up to 100 t.

The cars are of either the bottom-dumping or roll-over type, and each car can be unloaded in 1.5–5 min in modern processing facilities, which have a capacity of 2000–6000 t/h.

The least expensive means of transporting coal is by *river barges*, whereby the cost is as low as $0.005 per mile ($0.003 per km). The barges have open tops and commonly hold up to 1000–1500 t each. They are moved in groups or tows of 20–30 barges powered by a single towboat. Although there can be some problems with delivery schedules due to congestion, the ease and economy of river transport are major factors in the location of many coal-burning utilities along inland waterways in the United States and in Europe.

In the United States, ca. 12% of coal production is carried by *trucks*. Much of this is done at surface mines, where the coal is hauled from the working face to preparation plants. This is usually done with dedicated high-capacity vehicles; however, significant amounts of coal are hauled by trucks on public highways. *Conveyor belts* are also used for transporting coal from mines to preparation plants, as well as for short cross-country hauls of over 10 miles (16 km) to loading points. Because they are dependable and economical, conveyor belts are also widely used for in-mine coal transport.

Although > 80% of the coal mined in the United States is used domestically as steam coal, some of the metallurgical coal production is shipped overseas. This coal is shipped in dry bulk carriers that can be loaded and unloaded in modern port facilities at rates of up to 100 000 t/h. These ocean-going ships are usually in the 60 000 t range, although some are larger. In addition, some smaller vessels in the 30 000 t range that are self-unloading are also in service. These ships have the advantage of being able to use a much greater number of ports.

The transportation of coal by *slurry pipeline* has been demonstrated to be dependable and economical, even though there are only a few such pipelines in use around the world. In this technique the coal is reduced to a diameter of < 1 mm, treated with chemicals to prevent corrosion and improve flow characteristics, and mixed with water. It is then pumped as a slurry at a velocity of 1.5–2 m/s. The fact that pipelines can be built above ground or buried eliminates some environmental problems, but their high water requirements can be a serious drawback. Sustained delivery rates of > 600 t/h have been demonstrated.

5.22.10 Coal Storage

The use of any bulk commodity requires the storage of sufficient material to ensure efficient operations. In the case of coal, this requirement varies from a few days supply at the mine to a few months supply at a power plant. Although some covered storage in bins or silos is practical at mines and small operations, most of the larger volumes of coal are stored in open piles, where it is exposed to the air and precipitation. When coal is exposed to air, it loses moisture and begins to oxidize. This oxidation can degrade coal quality, and more important, it can cause spontaneous combustion that destroys the coal. The main coal properties that influence oxidation are the particle size, pyrite content, and rank. Coal oxidation leading to spontaneous combustion is enhanced as the particle size decreases and as the pyrite content increases. Low-rank coals such as lignite and subbituminous coal are very difficult to store because of their strong tendency toward spontaneous combustion, and care must be taken even with the lower rank bituminous coals. Repeated wetting and drying also exacerbate oxidation. The continued oxidation generates more heat than can be dissipated, and this leads to hot spots, which eventually ignite.

In a stockpile even mild oxidation can lead to a degradation of coal quality. For steam coals there can be some loss in calorific value, but in coking coals there can be a total loss of quality. The fluid properties can be destroyed, and the heat transfer properties and coke production yields can also be reduced. The quality of coke made from oxidized coal is also seriously altered. The prime coke property, coke strength or stability, is reduced, and this

can result in the loss of iron production in the blast furnace. Oxidized coal also increases the reactivity of coke and leads to higher coke consumption in the blast furnace. Because all of the effects of oxidation are undesirable, every effort should be made to prevent it.

The main steps to prevent oxidation involve limiting the access of air and protection from wind and precipitation. Stacking the coal to eliminate size segregation and compaction of the pile with earth-moving equipment to reduce pore space have proven helpful. Coating the pile with a sealant also helps protect it from air and moisture, although this may be expensive. Another costly but useful step is to provide the storage piles with some kind of wind protection. The wind not only enhances oxidation, but it also removes the fine particles from the coal pile and can thereby create environmental problems.

Another aspect of coal storage is the need to mix and blend the stockpile coal to homogenize the product coal reclaimed from it, so that a consistent, uniform product can be delivered to the plant. This can be a serious concern in cases where coal is coming into an operation from a number of sources. The usual way to solve this problem is to develop a bedding and blending system. A typical system consists of a plan to build a stockpile with long, thin layers of the various incoming coals and to reclaim the coal from the pile with vertical cuts across these layers. The key design factors are the variability of a target blending parameter such as ash or sulfur content and the desired degree of homogeneity. These are evaluated to determine the necessary pile parameters such as individual layer thickness.

5.22.11 Quality and Quality Testing

Because coal is so variable in its maceral and mineral composition, its suitability for a given use must be determined by a variety of tests. Although some tests such as chemical analysis are quite general in nature, others such as ash fusion are specific for particular uses.

Chemical Analyses. Although coal is composed of a large number of organic chemical components, no true standard organic chemical test exists for coal. The two major kinds of chemical analyses used are the proximate analysis and ultimate analysis, which are standard tests defined by the American Society for Testing and Materials.

The *proximate analysis* (ASTM D 3172) consists of a determination of the moisture, ash, and volatile matter, and a calculation of the fixed carbon value. The *moisture* is determined by heating the sample at 104–110 °C to a constant weight. The percent weight loss is reported as the moisture value. The *ash* in this analysis is the incombustible residue after the coal is burned to a constant weight. It should be noted that the ash value is not a measure of the kinds or relative amounts of the minerals in the coal. The *volatile matter* is a measure of the amount of gas and tar in a coal sample. It is reported as the weight loss minus the moisture after the coal is heated in the absence of air at 950 °C for 7 min. The *fixed carbon* is not a distinct chemical entity. It is reported as the difference between 100% and the sum of the moisture, ash, and volatile matter values. While the proximate analysis as described above is a rather simple assay of the chemical nature of coal, its value as a quality parameter is well established and is widely used in commerce.

The *ultimate analysis* (ASTM D 3176) consists of direct determinations of ash, carbon, hydrogen, nitrogen, sulfur, and an indirect determination of the oxygen. The ash is determined as in the proximate analysis, and because all of the values are reported on a moisture-free basis, moisture must also be determined.

Both proximate and ultimate analyses are reported in a number of different ways, and care must be taken to be certain of the method of reporting. On the "as-received" basis, the results are based on the moisture state of the coal sample as it was received for testing. With the "dry" basis, the results are calculated back to a condition of no moisture, and with the "dry, ash-free" basis, the results are calculated to a condition of no moisture and no ash. These calculations are done so that different coals can be compared on their inherent organic nature. The reporting basis can cause significant changes in the values reported, and it is essential that a target value and the value of a sample in question be on the same basis. For example, for a given coal with a moisture of 10%, an ash value of 15%, a volatile matter of 30%, and a fixed carbon content of 45%, the volatile matter content would be 33.3% on a dry basis and 40% on a dry, ash-free basis. The corresponding fixed carbon values are 50% and 60%, respectively.

Because some components of the minerals such as water from the clays and carbon dioxide from calcite are lost in the high-temperature ashing process, the ash value determined is less than the actual mineral matter in the raw coal. A number of corrections for this loss are in use, but the one most used in the United States is the Parr formula, where the corrected mineral matter is equal to 1.08 times the ash percentage plus 0.55 times the sulfur percentage. Results reported with this correction are considered to be on a dry, mineral-matter-free basis.

Mineral Matter. The mineral matter content of a coal is the actual weight percent of the minerals present. It is the best measure of the inorganic content of a coal, but it is difficult to determine. Although there is no standard test for mineral matter, low-temperature ashing (< 150 °C) with an oxygen plasma device is widely used for this purpose. The X-ray diffraction analysis of the low-temperature ash is used to identify the actual minerals in the ash. However, with present techniques it is impossible to accurately determine the amounts of the various minerals present in a given coal.

Although a large number of different minerals have been identified in coal, the four most common are clays, pyrite, calcite, and quartz. The minerals get into the coal in a variety of ways. Some can be part of the original plant material itself. Silica (quartz) is present in some of the saw grasses of modern swamps, and similar types of plants are known from ancient swamps. Certainly much of the mineral matter is transported into the coal-forming swamp from the environment. Much of the clays and quartz minerals were brought into the coal swamp as clastic material in streams or in airborne dust. Most of the common minerals could be chemically precipitated from solution under conditions that can exist in swamps. Some minerals such as calcite and pyrite can also be precipitated into cleats and fractures in coal after it has formed and coalified beyond the peat stage.

The presence of sulfur in coal is of great interest because of the problems it causes in utilization, especially air pollution. There are three commonly recognized forms of sulfur in coal. Pyrite sulfur is the sulfur tied up in the mineral pyrite, FeS_2; it is determined by leaching with nitric acid. Sulfate sulfur is of minor importance and thought to be formed by the weathering of pyrite; it is determined by leaching with hydrochloric acid. Organic sulfur is that portion of the total sulfur that is organically bound with the various coal macerals; it is determined indirectly by difference. There also may be some minor elemental sulfur present in coal. The forms of sulfur are determined in accordance with the ASTM standard D 2492.

The occurrence of pyrite in coal is of special interest because it is the only form of sulfur that can usually be removed by mechanical cleaning methods and because it is a major source of air and water pollution. Although some pyrite is formed by the chemical combination of the sulfur and iron that occur naturally in peat, most of the pyrite found in coal is thought to form from Fe(III) ions absorbed on clay minerals that are transported into coal swamps, and from sulfate ions that are introduced into the swamp in seawater. Marine water usually has about two orders of magnitude more sulfate ions than fresh water. In the swamp the ferric Fe(III) is reduced to Fe(II), which combines with the sulfur in the sulfate ions to form pyrite. While this process is clearly not the only way that pyrite can form in coal seams, it is a good model for many United States coal seams, especially those in

the Illinois Basin. In these seams it is reported [558–560] that both the total sulfur and pyritic sulfur contents are controlled by the nature of overlying rocks; they are both high under marine rocks and low under nonmarine rocks.

Pyrite can occur in coal in a number of forms such as single crystals, void fillings, irregular and dendritic masses, and framboids (raspberry-like clusters). The most significant forms are the more massive ones, which are easier to remove from the coal by washing, and the framboidal forms, which are more chemically active because of their high surface area. When pyrite is exposed to air and water, it oxidizes in a series of chemical reactions that generate sulfuric acid and cause acid mine drainage. In fact, the reaction of 1 mol of pyrite with air and water results in the generation of 2 mol of sulfuric acid.

Thermal Properties. The most widely used thermal property is the calorific value, which is a measure of the heat produced by combustion of a unit quantity of coal under given conditions (ASTM D 3286). It is usually reported on a moist, mineral-matter-free basis and is used this way in the ASTM classification of coals by rank. The major use of the calorific value is in the evaluation of coals for use in steam generation. In many utility company contracts, coal is bought on the basis of total calorific value per unit mass.

5.22.12 Economic Aspects

5.22.12.1 World Outlook

Reserves. The world's proven recoverable reserves of coal are an estimated 520×10^9 t of hard coal (anthracite and bituminous) and 512×10^9 t of brown coal (subbituminous and lignite). Proven reserves are those which geological and engineering information indicate with reasonable certainty can be recovered in the future from known deposits under existing economic conditions.

Production. Total production of hard coal (anthracite and bituminous) worldwide has remained on the same level since 1988. However, the individual regions of production have developed to different extents. For instance, production in Europe has been reduced, while the coal output of countries such as Australia, China, India, Indonesia, and South Africa has increased, in some areas considerably. In 1994, production of hard coal reached 3.2×10^9 t (Table 5.58). World production of brown coal (subbituminous and lignite) has been increasing continuously, and in 1994 output amounted to ca. 1.3×10^9 t (Table 5.59). This amount yields approximately the same heat as 0.9×10^9 t of hard coal.

Consumption. Approximately 20% of the 3.2×10^9 t of hard coal used in the world is allocated to coking coal and 80% to steam coal. Virtually all brown coal is used in power stations. The largest growth in both production and consumption in the period 1984 to 1994 has been in Australia and Asia.

Trade. Most coal is consumed in the regions of production. World trade in hard coal amounts to only 12% of world production. Nevertheless, since some important consumer countries are without adequate resources of their own, trade in hard coal has assumed worldwide proportions (Table 5.61). Australia, North America, and South Africa are the main net exporting regions, Japan, Western Europe, and Korea are the main importing regions. Brown coal is not traded over long distances.

Table 5.58: Proven recoverable world coal reserves as of end 1994 [561].

Region	Quantity, Mt	
	Anthracite and bituminous	Subbituminous and lignite
Africa	60 405	1 267
Canada & United States	111 004	138 177
Latin America	6 509	4 899
Asia	133 173	94 599
Eastern Europe[a]	135 422	180 091
Western Europe	27 476	47 529
Australia & New Zealand	45 369	45 690
Total	519 358	512 252

[a] Including the former Soviet Union.

5.22.12.2 Some Major Coal-Producing Countries

United States of America

Reserves. The United States possess economically recoverable hard coal reserves of ca. 107×10^9 t — one fifth of the total world reserves. For brown coal the respective figures are 134×10^9 t and 25%.

Table 5.59: World hard coal production in 1994 [562].

Region or country	Quantity, $\times 10^6$ t	Proportion, %
Africa		
South Africa	195.3	6.1
Others	7.9	0.3
Africa total	203.2	6.4
Americas		
United States	605.0	19.0
Canada	36.6	1.2
Brazil	4.4	0.1
Colombia	23.5	0.7
Mexico	6.7	0.2
Others	6.3	0.2
America total	682.5	21.4
Asia		
China	1110.0	34.9
India	248.0	7.8
Indonesia	30.5	1.0
Japan	6.9	0.2
South Korea	7.4	0.2
Pakistan	3.1	0.1
Turkey[a]	5.0	0.2
Others	51.5	1.6
Asia total	1462.4	46.0
Europe		
Bulgaria	0.2	0.0
Czech Rep. & Slovakia	17.4	0.5
Hungary	1.0	0.0
Poland	133.6	4.2
Romania	4.3	0.1
Former Soviet Union[b]	369.2	11.7
Other Eastern Europe	0.2	0.0
Eastern Europe total	525.9	16.5
France	7.5	0.2
Germany	52.0	1.7
Spain	14.4	0.5
United Kingdom	48.0	1.5
Other Western Europe	0.6	0.0
Western Europe total	122.5	3.9
Europe total	648.4	20.4
Australia & New Zealand	184.7	5.8
World	3181.2	100.0

[a] Includes the part in Europe.
[b] Includes the part in Asia.

Production. The United States have maintained a high level of production for decades, producing one fourth of the world's coal. Long-wall mining accounts for an increasing proportion of underground coal production.

Consumption. Domestic coal consumption, which absorbs nearly 90% of the production, has varied little in the past few years, with power stations being the main consumers. Exports have fallen due to heavy competition from newcomers.

Australia

Reserves. Australia possesses economically recoverable reserves of 45×10^9 t of hard coal and 45×10^9 t of brown coal, each representing 9% of world reserves.

Table 5.60: World brown coal production in 1994 [562].

Region or country	Quantity, $\times 10^6$ t	Proportion, %
America		
United States	330.0	26.0
Canada	36.2	2.8
America total	366.2	28.8
Asia		
China	100.0	7.8
India	19.0	1.5
Turkey[a]	45.0	3.5
Others	38.4	3.0
Asia total	202.4	15.9
Europe		
Bulgaria	28.6	2.2
Czech Rep. & Slovakia	65.8	5.2
Hungary	12.4	1.0
Poland	66.8	5.3
Romania	36.3	2.9
Former Soviet Union[b]	105.8	8.3
Other Eastern Europe	53.6	4.2
Eastern Europe total	369.3	29.1
Austria	1.4	0.1
France	1.5	0.1
Germany	207.1	16.4
Greece	57.3	4.5
Italy	0.5	0.0
Spain	15.7	1.2
Western Europe total	283.5	22.3
Europe total	652.8	51.4
Australia & New Zealand	48.8	3.9
World	1270.2	100.0

[a] Includes the part in Europe.
[b] Includes the part in Asia.

Table 5.61: World trade in hard coal in 1983. [563].

Country	Quantity, $\times 10^3$ t	
	Exports	Imports
United States	67 603	6 631
Canada	28 225	8 402
Colombia	18 400	
Venezuela	3 600	
China	18 000	1 350
India	99	6 278
Indonesia	18 833	251
Israel		5 381
Japan		111 404
Korea		35 977
Turkey		5 640
Belgium	645	11 894
Czech Republic	5 301	1 939
Denmark	24	10 467
Finland		5 933
France	622	14 231
Germany	970	13 090
Italy		14 299
Netherlands	2 242	15 121
Poland	22 968	129
Russia	27 400	28 300
Spain		12 726
Ukraine	4 126	8 930
United Kingdom	1 095	18 400
South Africa	42 650	
Australia	128 405	
Others	37 692	101 933
Total	428 900	438 706

Production. Coal production has risen steadily during the last few decades and is expected to do so in future.

Consumption. The high-quality coals found in Queensland and New South Wales are of value as steam and metallurgical coals, and most of production is for export. In 1984 Australia became the world's foremost hard-coal exporter with 61×10^6 t. In 1993 exports even doubled these figures. Production from Western Australia, Victoria, and South Australia (bituminous and subbituminous coal, lignite) is geared to local thermal electricity generation.

Germany

Reserves. Due to its very large deposits of brown coal, unified Germany possesses nearly 8% of the world's economically recoverable coal reserves.

Production. Output of hard coal has fallen from a peak of 150×10^6 t in 1957 to 52×10^6 t in 1994, and further reductions are planned. Brown-coal production dropped continuously with the closure of mines in the eastern Länder. Nevertheless, with > 200×10^6 t, Germany is still the second largest producer of brown coal in the world.

Consumption. The majority of the hard coal (65%) and nearly all of the brown coal is channeled into the generation of electricity. The second largest consumer is the steel industry. Hard-coal imports have not varied much in recent years.

Poland

Reserves. Polish recoverable coal reserves amount to 29×10^9 t of hard coal and 13×10^9 t of brown coal.

Production. Poland boosted its production for export reasons for a long period. In mid-1980s government officials expected to increase hard-coal output to 205×10^6 t and its brown coal output to 100×10^6 t by the year 2000. Instead, production in 1994 fell to 133×10^6 t of hard coal and 67×10^6 t of brown coal.

Consumption. Inland consumption decreased every year from 1984 to 1994 and may decrease even further. In the meantime, Poland tried to maintain its exports. In 1984, when it was able to export 45×10^6 t, thereby attaining a 14% share of world trade, Poland set its intermediate export goal at 42×10^6 t/a of hard coal. During the last years, exports reached only 20×10^6 t.

South Africa

Reserves. South Africa has recoverable reserves of ca. 55×10^9 t of hard coal, which at current production levels would last 300 years.

Production. Production has remained fairly constant at ca. 190×10^6 t/a.

Consumption. The slight increase in production in the last years was initiated by higher internal demand. Coal is the main primary energy for the generation of electricity (95%). In addition, South Africa still uses coal as a raw material for the production of liquid and gaseous fuels. Exports are estimated at a rather constant 43×10^6 t/a.

China

Reserves. China accounts for ca. 11% of world recoverable coal reserves. Hard-coal reserves are concentrated in the north and northwest of the country. Substantial lignite deposits are distributed throughout the country.

Production. Production has been increased steadily, so that China is now the world's largest producer (1994: 1110×10^6 t hard coal; 100×10^6 t lignite and brown coal).

Consumption. China is very dependent on its vast coal reserves. In the period 1984 to 1994 China's coal demand has increased by 50% and now accounts for ca. 75% of primary energy requirements. Transportation of coal is a major problem, with a significant proportion of production being in the north, but with the most rapidly growing demand in the southern and eastern regions. Therefore, China is investigating the transport of coal by pipeline. High-capacity electricity transmission to the south is another option under consideration. Only minor quantities (20×10^6 t/a) of coal are exported, the bulk being used internally for electricity and heat generation.

India

Reserves. India possesses ca. 7% of world reserves, mostly bituminous coal.

Production. Coal is the main source of energy and vital for India's economic development. Efforts to develop the industry have resulted in a steady increase of production to ca. 250×10^6 t of hard coal.

Consumption almost doubled in the period 1984 to 1994. Despite increased production, some coal is imported, mainly for quality reasons.

Indonesia

Reserves. Indonesia has vast resources of high-quality accessible coal. In terms of tonnage, southern Sumatra contains the highest proportion although much of it is lignite. The coal from Kalimantan includes some deposits of very high quality (low ash and sulfur, high volatile matter).

Production. In the period 1984 to 1994, production has risen dramatically.

Consumption. A major export market has developed and exports are expected to grow and to gain a substantial market share for high-quality coals in Europe, the Far East, and possibly the United States. However, Indonesia is expected to become a net importer of oil early in the 21st century. The national policy is therefore to expand internal use. The target is for 80% of electricity to be generated from coal-fired plants.

United Kingdom

Reserves. In its 1992–1993 annual accounts, British Coal estimated that 190×10^9 t of coal resources lie under the United Kingdom in seams over 0.6 m thick and less than 1200 m deep, of which 2×10^9 t were regarded as economically recoverable. A reasonable estimate for lignite resources in Northern Ireland is ca. 10^9 t.

Production. Due to the high cost of extracting the coal, production had to be steadily reduced and will be cut even further.

Consumption. The United Kingdom is still among the major consumers of coal in the world, but with competition from other energy resources, especially oil and gas from the North Sea, a further decline is expected.

Former Soviet Union

Reserves. With 241×10^9 t of recoverable coal reserves, 104×10^9 t of which hard coal, the

former Soviet Union accounts for 25% of the total world reserves.

Production. Due to its vast resources the Soviet Union ranked third among world producers. The political changes were followed by major economic disruptions which affected coal production in particular. In 1994 coal production in Russia reached only 65% of the 1984 level. The Ukrainian production dropped by 40%.

Consumption. Coal consumption has mirrored reduced production. Major changes will depend on future political developments.

5.22.13 Coal Pyrolysis

Coal pyrolysis is the heating of coal to produce gases, liquids, and a solid residue (char or coke). Pyrolysis occurs in all coal utilization processes, i.e., combustion, gasification, liquefaction, and carbonization. The nature of pyrolysis and of the products is intimately related to the operating conditions and to the composition and properties of the coal. Consequently, control of pyrolysis is important in coal utilization processes.

The thermal decomposition (or devolatilization) of coal is illustrated using WISER's model of coal structure (Figure 5.136) [564]. This model, one of many in the literature, represents the types of structures found in coals. Although it does not necessarily depict the structure of a particular coal, it is consistent with current knowledge of coal physics and chemistry.

Pyrolytic rupture of functional groups attached to aromatic and hydroaromatic units of the coal structure leads to the formation of gases (CO, CO_2, H_2O, CH_4, C_2H_4, etc.). In addition the cross-links (indicated by arrows in Figure 5.136) break and release reactive free radicals (fragments). The fate of these radicals controls the overall yield and distribution of products. Stabilization of the fragments with hydrogen gives primary volatile products and favors a high yield of gases and liquids (Figure 5.137). Some primary products are also obtained by release of low molecular mass species (the so-called mobile phase), which are believed to be trapped within the coal network [565]. However, if the fragments undergo secondary cracking, polymerization, or condensation reactions, part of the primary product is converted to char.

The four fundamental aspects of this complex process are the following:

- The thermoplastic behavior of some coals;
- The yield and distribution of pyrolysis products;
- The temperature and time dependency (kinetics) of the pyrolysis process;
- The source of hydrogen for the stabilization of reactive fragments.

5.22.13.1 Thermoplastic Properties of Coal

When bituminous coal is heated, it undergoes marked chemical and physical changes, which are influenced by rank, petrographic composition, particle size, heating rate, temperature, and the atmosphere in which pyrolysis occurs. Bituminous coal softens and melts at 350–400 °C. In contrast, lignite, subbituminous coal, and anthracite do not soften when heated. Fusion and agglomeration may produce a fluid mass. Concurrently, thermal decomposition may liberate gases and vapors, producing a foamlike material with significant volume change. At some point, the foam solidifies.

These macroscopic changes are accompanied by microstructural rearrangements within the fluid phase, which govern the properties of the resulting coke. Development of the coke microstructure often involves formation of an intermediate phase called carbonaceous mesophase.

Volume changes (expansion and contraction) occur in some bituminous coals on heating. Initial softening at temperature T_s produces a fluid. As softening increases, pores and voids are eliminated and the material undergoes volume contraction, reaching a minimum V_c at temperature T_c. At this point, rapid gas evolution leads to expansion, producing a maximum V_s at temperature T_e. With a further increase in temperature, the fluid coal resolidifies at temperature T_r; the corresponding volume is V_r. These phenomena, i.e., softening, swelling, and resolidification are collectively referred to as the *thermoplastic properties* of a coal, otherwise called the softening, plastic, fluid, agglomerating, caking, and coking properties of coal.

The terms "caking" and "coking" are sometimes used incorrectly as synonyms. In a strict sense, caking describes softening and agglomeration of coal on heating, without any implications about the nature of the resulting solid. Coking coals, on the other hand, are those that form strong, coherent solids (metallurgical cokes) on softening and resolidifying in conventional coke ovens. In other words, all coking coals exhibit caking behavior, but not all caking coals can be coked. Coal that does not become fluid when heated is generally termed nonswelling or noncaking.

Continued heating of a semicoke, i.e., a solid residue still containing appreciable volatile matter, to ca. 1000 °C leads to further decomposition with formation of a solid residue termed coke. Coke contains little or no volatile matter and undergoes little further volume change when heated. The volume changes occurring during the transformation of a coal into a semicoke depend on the fluidity of the plastic mass and its resistance to the escape of gases and vapors.

An understanding of the thermoplastic behavior of coal is important for nearly all coal conversion and coke-making processes. For example, plasticity development and agglomeration may create severe operating difficulties in gasifiers.

In a *moving-bed gasifier*, as the coal proceeds down the (sometimes pressurized) reactor, it devolatilizes at relatively low heating rates (25–65 °C/min) in the presence of a reducing atmosphere. Under these conditions, bituminous coal undergoes, in varying degrees, thermoplastic transformations that can lead to the formation of coke masses. These are detrimental to the flow of gases and solids, resulting in poor operation of the gasifier. In the extreme, coke agglomerates can completely plug the reactor.

In a *fluidized-bed gasifier*, an agglomerated mass may disrupt the fluidization. As a complicating factor, highly swollen coke may greatly reduce the bed density and lower the throughput. As a further complication, a highly swollen coke mass tends to disintegrate when it is fluidized, producing excessive fines that are carried from the bed and must be separated from the exhaust gas.

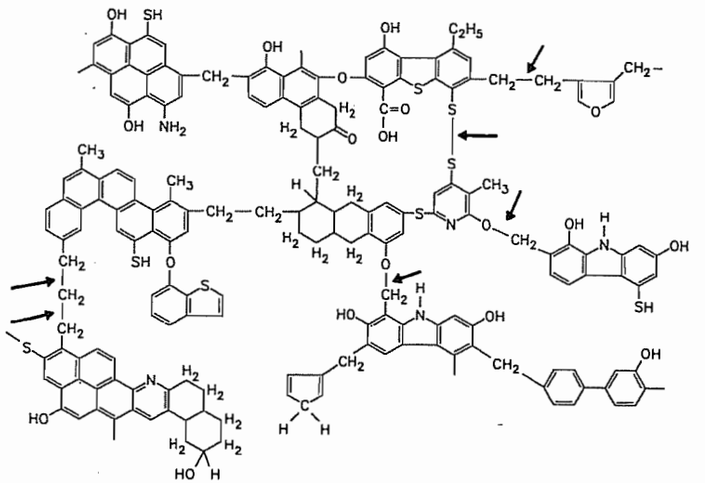

Figure 5.136: WISER's model of coal structure [564].

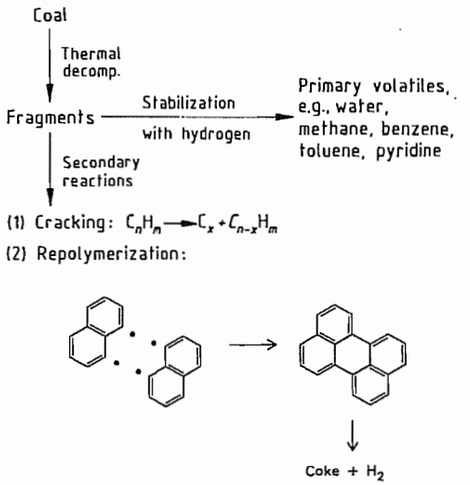

Figure 5.137: Primary and secondary reactions in coal pyrolysis.

In contrast to the general objectives in gasification and combustion, extensive plasticity development is essential during carbonization to produce metallurgical coke. The main objective of the coking industry is to produce coke for blast furnace operation. In this context, recent research has focused on the identification of coke microconstituents and the mechanism of their formation. The improvement of coke microstructure depends largely on the ability to modify the thermoplastic properties of the coal feedstocks and the associated mesophase. This is of particular significance because of the interest in the plastic behavior of weakly caking coal as a supplement to the reserves of prime coking coal.

Experimental Techniques

The industrial importance of the thermoplastic properties of coal is reflected in the many methods available for its characterization [566]. A common objective of these techniques is to predict the behavior of coal in various processes.

The *free-swelling index* (Gray–King) provides a visual comparison of cokes carbonized under well-defined conditions. The method is inexpensive, rapid, and reproducible, but lacks flexibility. *Hot-stage optical microscopy* permits the visual observation of morphological changes caused by heat. The *Foxwell gas flow method* measures the resistance to the flow of a highly purified gas through a bed of coal during continuous heating; the pressure drop indirectly measures the fluidity of the plastic mass. The *constant torque plastometer* records the velocity, as a function of temperature, of a rotating shaft passing through a bed of coal. In the variable torque plastometer, the velocity is kept constant and the required torque measured as a function of temperature. The resulting measurements of fluidity provide a sensitive index of oxidation or weathering, but not of swelling. The heating rate is limited to ca. 3 °C/min. In the *dilatometer*, the volume change on solidification is measured as a function of temperature. This is applicable over a wide range of heating rates and provides data on dilation parameters and transition temperatures, but not on fluidity changes.

These empirical tests require that experimental conditions be specified when results are reported. Furthermore, these tests measure different aspects of thermoplastic behavior; therefore, there is no single best method or technique that can predict the changes which occur in all industrial processes. Selection of a test method depends on the utilization process.

Experimental Variables

The thermoplasticity of a coal is a complicated phenomenon. It is affected by softening and rheological properties and by formation of gas bubbles [570], which are strongly influenced by pyrolysis conditions and feedstocks.

Coal Rank and Petrographic Composition

The thermoplastic properties of coal vary widely as a function of rank. Moreover, the plastic properties of some bituminous coals serve to differentiate them from others of similar rank. A number of attempts have been made to *correlate plastic properties with rank*. Swelling, measured by dilatometry, exhibits a maximum for a volatile-matter content of ca. 25–28%; the Gieseler fluidity reaches a maximum at ca. 28–32% of volatile matter [568]. Correlation of the free-swelling index (FSI) with the maximum Gieseler fluidity is poor, which is not surprising; rather, it illustrates the heterogeneity of coal [567]. Some variations can be expected because of the obvious differences in test conditions. In the FSI test, a 1-g sample of coal (250 µm particle size or 60 mesh) is heated in a silica crucible at 820 ± 2 °C for 2.5 min; the swelling is compared to that of a standard. The Gieseler fluidity test measures the rotary speed (in dial division per minute, ddpm) of a stirrer under a constant torque in a compacted 5-g charge, heated at 3 ± 0.1 °C/min from 300 °C until it resolidifies. However, the FSI does not increase monotonically with increasing Gieseler fluidity. In any case, the data support the concept of an optimum fluidity that is essential for maximum swelling.

The principal maceral responsible for coal plasticity is *vitrinite*, the predominant petrographic constituent of most United States coals. Exinite differs from vitrinite of the same rank by containing more hydrogen and volatile matter. Exinite exhibits a lower softening temperature, wider plastic range, greater Gieseler fluidity, and higher dilatometric swelling than vitrinites (Figure 5.138) [566].

Inertinite is infusible and inert, regardless of coal rank. It is distinguished from vitrinite of the same rank by its higher density and lower hydrogen and volatile matter contents [568].

Plasticity usually reflects the properties of the constituent macerals, but it also depends on the dispersion of exinite and inertinite within the vitrinite. This dispersion determines the degree of interaction between the different macerals. Consequently, predicting the thermoplastic behavior of a coal from its petrographic (maceral) analysis alone is impossible.

Heating Rate

The thermoplasticity of coals increases as the heating rate is increased [569]. Shock heating rates (above 100 °C/min) significantly increase the maximum swelling [569]. However, beyond a limiting heating rate (100–300 °C/min) a further increase does not increase swelling. On the other hand, at a low heating rate (below 3 °C/min), even a highly plastic coal may not soften or swell.

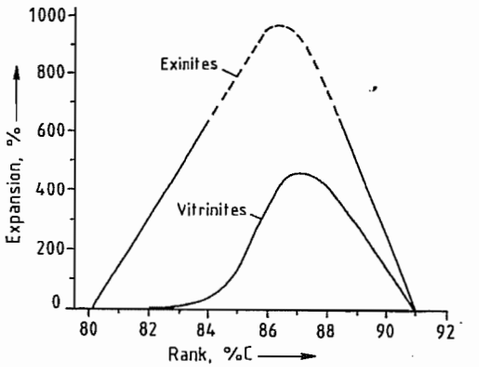

Figure 5.138: Expansion of vitrinites and exinites [566].

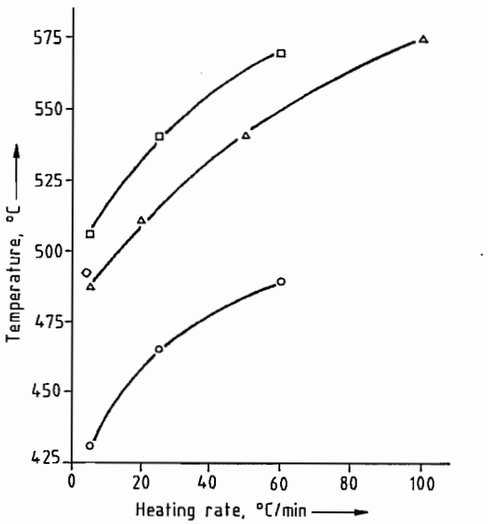

Figure 5.139: Effect of heating rate on the characteristic temperatures of a low-volatile bituminous coal (particle size: –74 µm; pressure: 101.3 kPa of He) [567]. ○ Softening temperature; △ Temperature of maximum devolatilization; ◇ Temperature of maximum fluidity [570]; □ Temperature of maximum swelling (dilatometry).

The effect of heating rate can be explained in terms of a competition between evolution of volatile matter and thermal decomposition. At

a higher heating rate, reactive components of the volatile matter, which would otherwise be lost before plasticity develops, can participate in secondary reactions that promote fluidity.

With an increase in heating rate, the characteristic temperatures (for softening, maximum swelling, and maximum fluidity) increase, as measured by plastometry or dilatometry (see Figure 5.139). Because these temperatures do not shift to the same extent, the temperature range over which the coal is plastic is generally widened.

An important effect of heating rate on the thermoplastic properties of coals is related to the maximum rate of devolatilization [566]. As the heating rate increases from ca. 1 to ca. 7 °C/min, the maximum swelling, maximum Gieseler fluidity, and maximum devolatilization rate all increase [567]. An increase in the heating rate produces a linear increase in the maximum rate of devolatilization. In addition, the maximum swelling increases with increasing heating rate, although this parameter is dependent on particle size. The maximum rate of devolatilization is slightly lower for the larger fraction.

The sequence of events occurring during coal pyrolysis is a function of heating rate. Softening is preceded by a rapid increase in evolution of volatile matter. Within the same temperature range, the viscosity of the sample reaches a minimum [570]. In response to this rapid rise in formation of volatile substances the coal particles and coal bed expand, producing the maximum swelling, determined by dilatometry, and the maximum rate of devolatilization, determined by thermogravimetric analysis [567].

Particle Size

The effect of particle-size variations on the thermoplastic properties of coal has not been widely reported. The data published before 1980 conflict. A few investigations have suggested that extremely fine grinding of the coal particles reduces thermoplastic properties. However, these results are possibly due to increased ease of weathering and oxidation of the more finely ground coal, or to maceral and mineral segregation that occurs during grinding.

Experimental data on particle size must be interpreted with caution. Studies conducted in a Hoffmann dilatometer, which accommodates coarse samples, have shown that the effect of particle size varies according to coal type and petrographic constituents [568].

The effect of particle size is dependent on heating rate [567]. At a high rate (60 °C/min), a considerable decrease in the particle size resulted in a significant increase in swelling. This confirmed earlier findings that, at a higher heating rate, the maximum swelling was greatest for the smallest size fraction [571, 572]. The behavior at 60 °C/min has been explained as follows: the smaller coal particles, with their greater surface: volume ratio, fuse more easily with the neighboring particles and produce a homogeneous mixed phase [567]. In contrast, the larger coal particles tend to maintain their individuality [567, 569].

With slower heating (5 °C/min), the swelling parameter for the smaller fraction (–74 μm) was less than that at 60 °C/min. This was attributed to slower devolatilization at 5 °C/min, resulting in a lower swelling pressure, i.e., the pressure generated inside the particles. In addition, the diffusion distance (the distance traveled by the volatile substances before escaping) is shorter for smaller particles. Therefore, an increase in particle size with slower heating results in greater swelling.

A particle-size effect is also noted in the contraction parameter. In general, the initial contraction of the coal particles is significantly greater for the smallest fraction [567, 571, 572]. This is explained by the suggestion that larger coal particles fuse less than smaller ones because of their lower surface: volume ratios.

Pressure

Until recently, little work had been published on the effects of inert gas pressure on the thermoplastic properties of coal. In the absence of data at elevated pressure, the behavior of coal under typical gasification conditions (elevated pressure and reducing atmosphere) has generally been extrapolated from data obtained at atmospheric pressure. However, this treatment has serious deficiencies.

Several investigations have shown that pressure increases the coke and gas yields at the expense of tar production. This has been attributed to an increased residence time of volatile and plasticizing substances in the coal melt and to a corresponding effect on rheological behavior. Pyrolysis of bituminous coal at elevated pressure has also been shown to increase the Gieseler fluidity (Figure 5.140) [573].

Swelling of coal in dilatometers results from a balance between opposing forces and occurs when the internal (intraparticle or intrabed) gas pressure (swelling pressure) generated in the plastic state is higher than the applied forces that tend to contain it. This internal pressure depends on the coal type, particle size, heating rate, and temperature. Consequently, at elevated pressure, coal swelling depends largely on experimental conditions. For a range of bituminous coals, the rank dependency of the effect of pressure on the maximum swelling parameters was highly variable [567]. In addition, the extent of maximum swelling varied markedly.

Other observed effects of pressure, irrespective of coal rank, were an increased contraction parameter and an expanded plastic range. In contrast, with vacuum pyrolysis, maximum swelling, contraction, and plastic range were significantly reduced [567]. The effects of pressure can be explained qualitatively by invoking the concept of optimum fluidity, which is essential for high expansion. If the melted coal is very fluid, swelling is not extensive because the volatile substances escape easily. At the other extreme, minimum fluidity is essential for the material to fuse and entrap volatile material. This implies that an optimum fluidity exists, which is necessary to permit a high degree of swelling. Under vacuum, for example, volatile and plasticizing components are readily removed before sufficient fluidity or swelling pressure can develop. Hence, thermoplastic behavior is inhibited [567].

Production of volatile matter during pyrolysis is a necessary but insufficient condition for a coal to become plastic and swell. The combined effects of the generated volatile matter and the rheological properties of coal determine thermoplastic behavior [567, 572, 574].

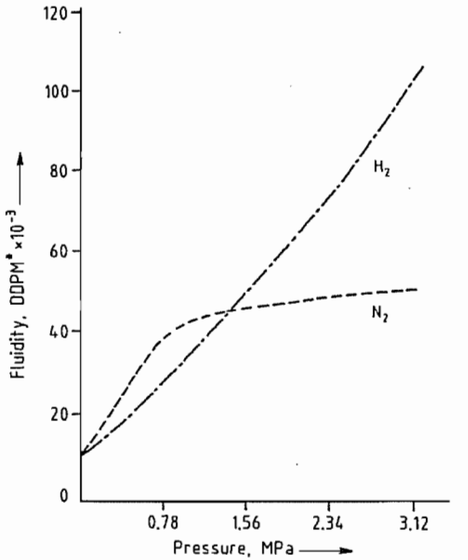

Figure 5.140: Effect of pressure on the Gieseler fluidity of a bituminous coal [573]. *DDPM = dial divisions per minute.

Gaseous Atmosphere

The effects of a gaseous atmosphere on the thermoplastic properties of coal are of interest because in many processes devolatilization occurs in the presence of reactive gases, e.g., H_2, CO/H_2, or CO_2.

The effects of H_2 and He depend on the conditions. However, an increase in the maximum swelling parameter can be correlated with the degree of hydrogenation. At heating rates above 60 °C/min in a high-pressure microdilatometer, the thermoplastic properties of

a low-volatile bituminous coal were not significantly different in atmospheres of H_2 or He [567]. The total loss of mass during pyrolysis at ca. 630 °C in these two gases was similar, indicating little hydrogenation at high heating rates.

In contrast, at a low heating rate of 5 °C/min, the maximum swelling is significantly greater at elevated H_2 pressure compared to He. The loss of mass during pyrolysis is also significantly greater in H_2 than in He, indicating some hydrogenation at this heating rate [567].

The maximum Gieseler fluidity (heating rate, 5 °C/min) of a weakly swelling coal (FSI = 0.5) at atmospheric pressure was markedly greater in H_2 than in He or N_2 [573, 575].

Preoxidation

In many processes, thermoplastic behavior of bituminous coals can have undesirable consequences. Caking can be reduced or eliminated by low-temperature (below the softening point) preoxidation, which can destroy thermoplastic properties [568, 569, 576, 577]. In addition, carbonization of preoxidized bituminous coal produces a char with a higher gasification reactivity and surface area than coke produced from untreated coal [578].

Although many studies have been conducted on oxidized or weathered coals, oxidation mechanisms are still poorly understood. Small amounts of oxygen (0.01–0.02%) can produce substantial changes in coal plasticity [579]. The first stage of oxidation was postulated as peroxide formation; however, this has not been confirmed experimentally. It was further suggested that the peroxide is unstable above 70 °C and decomposes to yield more stable coal oxygen complexes with evolution of CO_2, CO, and H_2O.

Another proposed mechanism was that oxidation increases hydroxyl, carboxyl, and carbonyl content [566]. As the temperature rises the hydroxyl groups can condense with the liberation of water:

$$Ar\text{–}OH + Ar\text{–}OH \rightarrow Ar\text{–}O\text{–}Ar + H_2O$$

where Ar is an aromatic radical.

Fourier transform infrared (FTIR) studies suggest that in the early stages of oxidation, the main functional groups formed are carbonyl and carboxyl [580]. At higher degrees of oxidation, evidence indicates a significant increase in ether, ester, and phenolic groups. Loss of plastic properties on oxidation is attributed to the formation of ether and ester cross-links. The decline in fluid behavior on oxidation can be correlated to a reduction in the aliphatic hydrogen content [581].

The swelling of a highly fluid coal increased on mild oxidation [568, 569, 571]. More severe oxidation sharply reduced swelling.

Little work has been done on carbonization of preoxidized coal under the pressure of a reducing gas. Successful operation of fixed- and fluidized-bed processes depends on the behavior of preoxidized coal when it is devolatilized under these conditions.

A preoxidized coal shows a higher loss of mass during pyrolysis in H_2 than in N_2 [567]. The thermoplastic properties of preoxidized coal are highly dependent on pressure, and maximum swelling increases significantly at an elevated pressure of H_2 or He [567, 582, 583]. This suggests that if preoxidized coal is used as a feed material for a pressurized process, where devolatilization occurs in a reducing atmosphere, the effects of preoxidation are reduced.

Although oxidation is an inexpensive technique for reducing the plastic behavior of coal, deleterious consequences have been reported [567]. Preoxidation results in an overall loss of carbon (as CO_2) and hydrogen (as H_2O); hence, the heating value is significantly reduced. Consequently, other means of reducing thermoplastic properties are being investigated.

Additives

Inorganic additives are an alternative to preoxidation. They reduce the caking of coal carbonized at atmospheric pressure (Table 5.62); however, they have economic and operational drawbacks.

Table 5.62: Effects of additives on thermoplastic behavior of coal [584].

Additive	Concentration	Pretreatment	Caking index[a]	Changes in caking index	
				Before	After
Dry sand	20%	dry mixed	FSI	4.5	4.1
NaOH	20%	dry mixed	FSI	4.5	1.0
Na_2CO_3	20%	dry mixed	FSI	4.5	1.8
Na_2CO_3	10%	dry mixed	FSI	4.5	3.0
Na_2CO_3	5%	dry mixed	dpm	275	15
K_2CO_3	20%	dry mixed	FSI	7.0	1.5
Boric acid	2%	dry mixed	BS swelling no.	8.0	0.5
NaCl	1 *N* solution	20 g of coal in 200 mL of solution dried at 105 °C for 40 min	FSI	4.5	2.0
Na_2CO_3	1 *N* solution		FSI	4.5	1.3
$NaHCO_3$	1 *N* solution		FSI	4.5	1.5
NaOH	1 *N* solution		FSI	4.5	1.0
BF_3	0.25 mmol BF3/100 g	gravimetric gas sorption at saturated pressure	FSI	8.0	2.0
			FSI	8.0	2.0
BF_3	0.27		FSI	9.0	2.0
BF_3	0.21		FSI	7.0	2.5
$AlCl_3$, $(CH_3)_2CHCl$[b]	—	—	coke inspection	agglomerated	powder
HCl	not stated	1 h at 150 °C	coke inspection	agglomerated	powder
Excess tri-*n*-butyl borate	—	—	BS swelling no.	8.0	0
Phosphorylation[c]	—	—	BS swelling no.	8.0	0.5
Acetylation[c]	—	—	BS swelling no.	8.0	2.5
NH_3 solution with Ni catalyst	3–3.5% Ni	autoclaved with liquid NH_3 at 120 °C for 4 h	swelling no.	2.2	1.1

[a] FSI = Free Swelling Index; dpm = Divisions per minute as determined by a Gieseler plastomer; BS = British Standard.
[b] Friedel–Crafts alkylation.
[c] Esterification of phenolic hydroxyl groups.

The mechanism of decaking is not known. In general, an additive may function as an inert diluent or in a more active role by chemically interacting with the softened coal. Some inert additives may provide sites for complex reactions of the coal. Some inert additives reduce fluidity by adsorbing primary decomposition products. Removal of 2–3% of the extractable bitumen prevents caking completely [568].

Additives may also increase the permeability to gas flow and, therefore, reduce swelling in the coal melt. Compounds like SiO_2, however, serve simply as diluents.

Additives may also react chemically with the pyrolysis products. Substances, such as K_2CO_3, KOH, CaO, Fe_2O_3, Fe_3O_4, HCl, and BF_3, reduce the swelling of coal at atmospheric pressure.

The effectiveness of additives in decaking under gasification conditions has been examined [567, 585, 586]. Compounds of K, Ca, or Fe significantly reduced thermoplasticity under most conditions. Although K_2CO_3 and KOH are effective decaking agents, KCl is not. Similarly, CaO and $Ca(OCOCH_3)_2$ were more effective than $CaCO_3$. Both Fe_2O_3 and Fe_3O_4 destroyed thermoplasticity at 0.1 MPa (H_2 or He), even at ca. 5%.

Effective additives may promote char formation during pyrolysis. Pyrolysis at elevated hydrogen pressure usually increases V_s. This was attributed to a reduction of char-forming reactions, thereby increasing fluidity of the system [567].

Development of Thermoplasticity

Softening

Although thermoplastic properties of coal have been studied for many years, softening still lacks a satisfactory explanation. However, a general pattern has been established.

Direct microscopic observations are revealing Between 325 and 450 °C, depending on coal rank and experimental conditions, visible softening is manifested as follows [569]:

- Coal particles become mobile and fill the bed space. Larger particles, which soften less than smaller ones, fuse with the smaller particles.
- So-called fusion pores begin to form as softening continues, depending on particle size and nature of the coal. However, with further softening, the material becomes more homogeneous, making distinction between pores formed by fusion and those formed by devolatilization difficult. As softening continues, viscosity decreases, particle boundaries disappear, and gas evolution increases.
- With a further increase in temperature, viscosity increases until resolidification occurs, pore volume and vitrinite reflectance increase, and in some cases, anisotropy increases.

Softening can be measured in a dilatometric test by the onset of contraction when a bed of coal is heated under a weighted plunger. A more precise measurement is given by the attainment of a specific degree of fluidity within the plastometer. In all theories of plasticity, it is acknowledged that a fusible material is formed during softening, but differences of opinion exist as to the origin, nature, and function of this material [572].

The homogeneous-melt theory, for example, proposes that coal undergoes pastelike melting throughout the entire mass, but decomposes at the same time, giving rise to gas and an infusible solid [587, 588]; the composition of this mixture depends on time and temperature. Resolidification is observed when the transformation to infusible material is complete. If decomposition proceeds too rapidly before the inception of softening, fusion does not occur and char is formed. On the other hand, if softening occurs before the evolution of volatiles, a coal fuses and swells to form a coke.

According to the *partial-melt theory*, only a fraction of the coal melts and the remainder is plasticized. The fusible fraction, the coking principle or bitumen, has been identified in benzene and chloroform extracts.

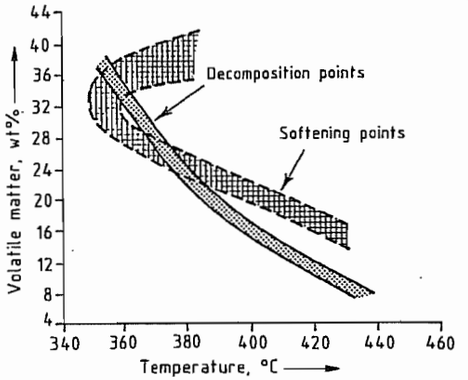

Figure 5.141: Relationship of volatile matter content to softening points and decomposition points of coal [589].

In the *thermobitumen theory*, softening is defined as a consequence of pyrolysis that transforms coal into fluid products. The appearance of these fluid products causes softening and plasticity. Their disappearance by evaporation or thermal decomposition results in resolidification. The fluid products are termed metaplast or thermobitumen, implying that they are the products of pyrolysis.

The *physical and physicochemical theory* proposes that thermal softening is initially a physical process of partial melting of the coal substance to a fluid mass. However, the rheological properties of this mass are subsequently modified by chemical reactions during decomposition. Therefore, development of fluidity is believed to be the result of both physical and physicochemical processes.

In noncaking coal, the decomposition point is lower than the softening point. The rank dependency of these temperatures is illustrated in Figure 5.141, which shows that plastic coals occupy only a narrow range of rank. Other theories suggest that the fraction of a coal that fuses plasticizes the remainder [589–598].

Thermal softening of coal is apparently not related to physical melting but instead to kinetic phenomena [566, 599]. The development of fluidity may be the result of physical and physicochemical processes without appreciable rupture of covalent bonds during pyrolysis. After melting of the mass, the properties are modified by pyrolytic reactions [594]. This mechanism is consistent with three conditions that have been proposed as being necessary and sufficient for plasticity development [600]:

- Lamellar bridging structures that can be thermally broken
- A supply of hydroaromatic hydrogen
- Intrinsic ability of micelles and lamellæ to become mobile, i.e., ability of the coal to melt independent of thermal bond rupture.

Swelling

Investigators agree that the softening of coal particles is caused by the melting or solvation of low molecular mass substances or by primary pyrolytic decomposition [568]. Softening causes swelling and the formation and liberation of gas. The gas cannot escape rapidly because of the low permeability of the plastic mass. Hence, gas bubbles are formed with high internal pressures. In response to this internal pressure, the viscous plastic mass swells like baker's dough. The formation of an impermeable plastic mass is a precondition for swelling.

Swelling can be observed in coal particles individually or collectively. *Intraparticle* (single-particle) *swelling* results from the formation of a plastic mass that eliminates the fissures and macropores through which gas could escape. The resulting internal pressure swells the plastic mass. Swelling of particle beds, i.e., *interparticle swelling*, is caused similarly when the plastic mass fills the interparticle spaces, preventing gas from escaping.

The importance of each type of swelling depends on the particle size and the nature of the coal. Intraparticle swelling is only important for weakly coking coal. For coal to form a coherent and strong coke, interparticle swelling is necessary. In highly plastic coal distinction between the two types of swelling is often impossible [585].

The extent of swelling depends on the rate of devolatilization [566, 567]. A minimum fluidity is essential to reduce the permeability of the plastic mass to gas flow and generate swelling pressure. However, if the plastic mass is too fluid, gas bubbles escape at low pressure.

Swelling has been viewed as a process independent of softening [596, 597, 601]. In this light, swelling is a consequence of the pore structure of the starting coal. It is caused by the pressure of the evolved gas trapped within the micropores.

Porosity exhibits a minimum for the higher rank bituminous coals, for which swelling is at a maximum. This mechanism explains intraparticle swelling, but not interparticle swelling. Because microporosity is a prominent feature of agglomerating coal, an empirical relationship between swelling and porosity may exist without necessarily implying that swelling is a consequence of porosity. In fact, swelling and porosity may be consequences of a third factor, such as cross-linking density.

Resolidification

Resolidification is usually attributed to a series of cracking reactions followed by condensation and polymerization. A large number of free radicals and small molecules are generated by cracking. This is consistent with the observation that the original solvating agent, the bitumen, decomposes at ca. 480 °C, before resolidification of the coal to form a semicoke [594]. Because of the loss of hydrogen-donating and solvating agents, which would otherwise stabilize the free radicals, the solid material polymerizes forming semi-coke. This viewpoint is supported by the fact that the semicoke is deficient in hydrogen compared to the precursor.

Coke Microstructure and Mesophase Formation

The properties of cokes are determined by their microstructural characteristics. The structure property relationship is, however,

difficult to establish for coke because of its extreme heterogeneity in chemical constitution and physical structure. Nevertheless, considerable progress has been made since the 1920s, primarily with the aid of optical microscopy.

The most significant industrial use of coke is in the production of iron and steel. Only prime coking coal produces coke appropriate for blast furnaces, where reactivity and stability under thermal stress are required [602, 603]. These requirements are met by metallurgical coke.

In general, the principal feature of the coke microstructure is the anisotropy of the organic coke substance as observed by optical microscopy [604–608]. The critical role of an intermediate plastic phase (carbonaceous mesophase) in the development of the characteristic anisotropic structures was first recognized in 1965 [609, 610]. Subsequent research has been devoted to the significance of mesophase formation during the carbonization of coking coal [611], the effect of coal rank and chemical constitution on mesophase formation [612–616], the use of optical and scanning electron microscopy [617], and the chemistry of mesophase formation [618–622]. These investigations may help to improve coke manufacture by modifying the microstructure through the development of a carbonaceous mesophase.

Microscopic Characterization

Optical microscopy is the principal means of analyzing coke morphology and anisotropic structures [617, 620]. The resolution limit of the optical microscope is ca. 0.2 μm. Optical anisotropy is an expression of structural anisotropy on the same scale [623].

For microscopic examinations, polished coke sections are viewed in plane-polarized light [624]. The appearance of the polished surface is termed the optical texture. Isotropic and anisotropic structures can be distinguished on the basis of different behavior [625, 626]. A common technique employs *reflection interference colors* [626]. These are yellow, blue, and dark purple for anisotropic materials and light purple for isotropic materials. Thus, cokes can be characterized by color and the shape and size of the isochromatic areas [617].

Differences in optical activity between isotropic and anisotropic cokes are due to differences in the range of crystallographic order [618]. The crystallographic order of isotropic coke is considered to be only small in scale; i.e., the parallelism of associated constituent lamellar molecules extends over short distances (ca. 1–5 nm). Although the structure can be claimed to be anisotropic for 1–5 nm, it is essentially isotropic to the light beam because this range is far below the resolution of the optical microscope (ca. 200 nm). However, for anisotropic coke, the range of crystallographic order extends from 0.3 to ca. 200 μm; in the light beam, the material has bulk anisotropy [618].

An optical microscopic classification of the organic solid residues derived from the hydrogenation of bituminous coal can be applied to coke obtained by carbonization. Table 5.63 includes the type of macerals and the transient phases responsible for coke microstructures. The formation of the transient, fluid phases (vitroplast and mesophase) is indicative of fusion (or plasticity) during carbonization and is limited to certain bituminous coals.

The term *vitroplast* designates a plastic or formerly plastic carbonization product of vitrinite that, unlike the starting material, is optically isotropic. In coke it is characterized by flow structures and spherical morphologies.

The semifusinite maceral can also make a small contribution to the formation of spherical vitroplast. Further alteration of vitrinite and the spherical vitroplast derived from it is seen in the development of cenospheres. This term was first used to designate structures formed by rapid heating of pulverized coal [628, 629]. A cenosphere is defined as a reticulated hollow sphere composed of ribs or frames and windows. Cenospheres are formed by the gas liberated within vitroplast spheres during the plastic stage [627].

Table 5.63: Optical microscopic classification of solid carbonization products [627].

Classification	Optical nature	Intermediate fluid phase	Maceral precursor
Vitroplast (VP[a])	isotropic	vitroplast	vitrinite, semifusinite
Cenosphere (CS[a])	isotropic and anisotropic	vitroplast	vitrinite
Semicoke (SC[a])	anisotropic	mesophase	vitrinite, semifusinite
Unreacted or slightly altered			
vitrinite (UV[a])	anisotropic	—	vitrinite
fusinite (FS[a])	isotropic	—	fusinite

[a] Abbreviation.

In contrast to vitroplasts, the mesophase is optically anisotropic and represents the main route for the formation of anisotropic structures in coke. It is considered to be a unique, ordered, fluid system consisting of high molecular mass, planar molecules.

The solid product formed via a mesophase is called a semicoke, a term used in a more general sense for the solid products of low-temperature (500–600 °C) carbonization of coking coals or heavy hydrocarbon feedstocks, such as coal-tar and petroleum pitches.

Both vitroplasts and cenospheres may develop intrinsic anisotropic structures (depending on the conditions of carbonization) while retaining their characteristic morphology. Another type of anisotropy in coke is associated with the unreacted vitrinite fragments. The distinction among these anisotropic microconstituents has a significant bearing on coke properties [627].

Scanning electron microscopy (SEM) is also useful for examining the microstructural characteristics of solids [630]. Its high resolution (ca. 3 nm) and depth of focus permit characterization of surface topography at very low and high magnifications (up to × 200 000). Specimens are examined by sweeping a finely focused electron beam across the surface. The resulting signals include secondary electrons, backscattered electrons, and characteristic X-rays.

In the examination of coke, the most useful signal is the variation in secondary electron emission with changing surface topography. Optical microscopy and SEM are complementary techniques for coke characterization, providing structural and topographical information, respectively [618].

Carbonaceous Mesophase

The important properties of cokes, including mechanical strength and reactivity, are governed by the arrangement of the constituent carbon atoms. The principal features of the atomic arrangement are the alignment and size of *carbon crystallites*. The highest degree of alignment is seen in natural graphite crystals, which consist of extended layers of fused hexagonal rings of carbon atoms. This structure, with an interlayer spacing of 0.3354 nm, is approached by certain carbons manufactured from coal tar and petroleum pitches and by polynuclear aromatic hydrocarbons on heating at 2500–3000 °C. Depending on their behavior when heat-treated, carbonaceous solids can be classified as graphitizing or nongraphitizing, e.g., coke and char, respectively, in the case of coal-derived solids.

Although the crystallite alignment in carbonaceous solids is only observable after heating at 1000 °C, crystallite alignment starts during carbonization over a narrow temperature range near 450 °C [620]. This stage, coincident with plasticity development, is characterized by the formation of carbonaceous mesophase, which leads to the anisotropic structures found in cokes. The shape and size of these anisotropic structures usually determine the behavior of the coke [631]. Substances that form graphitizing coke via a mesophase include the vitrinites of medium-volatile coking coal, coal-tar and petroleum pitches, polymers such as poly(vinyl chloride), and polynuclear aromatic compounds such as anthracene.

Lignites, thermosetting resins, polymers such as poly(vinylidene chloride), and hydrocarbons such as biphenyl do not form me-

sophase; instead, they produce isotropic nongraphitizing coke commonly referred to as *char* [620].

An outstanding characteristic of carbonaceous mesophase is the prevailing *molecular order*, which represents an intermediate state between totally isotropic liquids and anisotropic solid crystals. A crystal is characterized by long-range order. Isotropic liquids, on the other hand, possess no long-range order [632]. In liquid crystals, some but not all of the long-range order is maintained. The state is neither crystalline nor strictly liquid, and in 1922 the term mesophase was proposed [633–635]. The plastic, anisotropic phase formed during carbonization is designated interchangeably as liquid crystal or (carbonaceous) mesophase.

Of the several types of *liquid crystals*, the nematic (threadlike) type is the most relevant to carbonaceous mesophase [636]. Nematic liquid crystals separate from the isotropic liquid as anisotropic spherical droplets that eventually coalesce to give nematic domains. The molecular arrangement is envisaged as rod-shaped, similarly sized molecules lying parallel to each other but with no stacking order.

The parallel alignment of the molecules in carbonaceous mesophase and the separation from the isotropic liquid in the form of spheres suggest the behavior of nematic liquid crystals. The molecular units of carbonaceous mesophase are, however, disk-shaped and widely varied in size [637]. Furthermore, the formation of carbonaceous mesophase usually involves irreversible chemical processes, in contrast to the physical and reversible formation of nematic liquid crystals. Carbonaceous mesophase consists essentially of large polynuclear aromatic hydrocarbons [638]. Mesophase spheres formed during the carbonization of pitch may contain smaller molecules incorporated in the matrix of planar condensed-ring compounds (Figure 5.142) [637]. This gives a molecular mass distribution in the range of 400–3000 or even more.

The most commonly observed arrangement of molecules in mesophase spheres is the *Brooks–Taylor configuration*, in which layers of planar molecules lie parallel to the equatorial plane around the polar axis, but curve to reach the surface at an angle [620, 640]. Other configurations have been observed, especially in the presence of induced magnetic fields and solid particles, e.g., carbon black [641, 642]. These configurations apparently show no different properties.

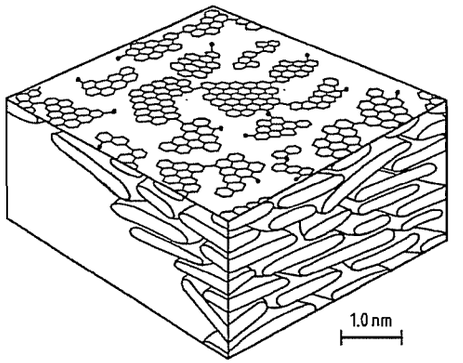

Figure 5.142: Nematic molecular order of carbonaceous mesophase comprised of methyl-substituted polynuclear aromatic compounds connected by methylene bridges and biaryl linkages [637, 639].

The uninhibited *formation and development of mesophase* occurs in three sequential stages: nucleation, growth, and coalescence. This progression, although clearly seen with the optical microscope in pitch and aromatic hydrocarbons, is not always observed during coal carbonization because of the inhibition of growth and coalescence or the very rapid formation of the final texture of the semicoke.

Nucleation is observed as the separation of anisotropic spheres from the isotropic melt, when they become sufficiently large (ca. 0.3 µm in diameter) to be visible. This is a homogeneous process that does not require a specific site. Under favorable conditions, the spheres can grow at the expense of the isotropic melt and coalesce to form large domains of ordered regions, which eventually solidify to semicoke. This type of extensive mesophase development (flow domains) leads to highly graphitizable coke.

If growth and coalescence are inhibited, irregularly shaped anisotropic spheres of small-scale order (0.3–10 µm grain size) are formed. These structures, frequently encountered in

coal carbonization, are termed *mosaics*. A widely used classification, based on the shape and size of the anisotropic structures found in coke, is as follows [614]:

Isotropic	no optical activity, uniform, light purple color on the surface
Anisotropic	
Via mesophase	dark purple, yellow and blue areas of varying shape and size
Fine-grained mosaics	irregularly shaped, isochromatic areas (ISIA), 0.5–1.5 µm long
Medium-grained mosaics	ISIA, 1.5–5.0 µm long
Coarse-grained mosaics	ISIA, 5.0–10 µm long
Coarse flow	rectangular, flow-type structures 30–60 µm long; > 10 µm wide
Flow domains	flow-type structures > 60 µm long; > 10 µm wide
Domains	isometric structures > 60 µm in diameter
Basic anisotropy	flat, featureless anisotropy associated with the parent unreacted (or slightly altered) vitrains from high-rank coals

The sequential formation of mesophase is apparently not the sole mechanism leading to anisotropic structures in coal-derived coke. *Vitrains* from high-rank coals behave somewhat differently from coking and caking coals [612]. The inherent (basic) anisotropy of vitrain, which is rather featureless, is unchanged or converted directly to flow-type anisotropy. In this respect, it does not follow the progressive development of flow-type anisotropy.

Mesophase formation results from extremely complex and interdependent *physical and chemical processes* occurring during carbonization. The first chemical process is the rupture of weak bonds, breaking down the molecular network and forming free radicals, followed by such reactions as cyclization, aromatization, and polymerization.

The *fluid carbonization medium* at this stage can be envisaged as a dynamic chemical system, with increasing molecular mass and size [618]. When the planar molecules reach a critical concentration and size, van der Waals forces become sufficiently strong to establish parallel orientation. The resultant anisotropic miscellæ separate from the isotropic fluid phase in the form of spheres. If the molecules are not sufficiently planar, parallel stacking is sterically hindered. The spherical shape of the separated anisotropic miscella results from the usual requirement of minimum surface area and surface energy at the interface of a two-phase system [618].

The principles governing mesophase formation can be summarized as follows:

- Heteroatoms and alkyl groups inhibit mesophase formation by cross-linking reactions, which impair planarity.
- Naphthenic hydrogen promotes mesophase formation via hydrogen-transfer reactions, which retard cross-linking and increase fluidity.
- Aromatic systems promote mesophase formation by virtue of their planarity and low reactivity.

These findings are based on studies of model compounds thought to resemble the building blocks of bituminous coal and petroleum feedstocks [619, 622, 643, 644]. In addition, mesophase formation depends on carbonization conditions.

The carbonization of coal of different rank produces coke with corresponding optical properties [616]. Low-rank coals (lignite and subbituminous) do not soften during carbonization, thus producing isotropic chars [617].

The size of the anisotropic structures in coke generally increases with increasing coal rank (Figure 5.143) [51]. Whole coal behaves like vitrain. Caking coal with high volatile content forms isotropic coke containing small amounts of fine-grained mosaics. With increasing rank up to the prime coking coals, these anisotropic structures become larger (5–10 µm) and more numerous.

In coke from prime coking coal, the optical texture (apart from inorganic and infusible organic petrographic components) is essentially and continuously anisotropic, with structures varying in size from fine-grained mosaics to coarse particles up to 20 µm. The anisotropic structures in coke from fusing coal (high-to-low-volatile-content bituminous) develop mostly via mesophase formation.

Semianthracites, anthracites, and some noncaking low-volatile bituminous coals

have no fluid stage during carbonization. The large anisotropic structures found in these cokes originate from the inherent anisotropy of the parent coal [612].

The variations in the optical texture of coke from coals of different rank reflect the differences in mesophase formation. These differences can be explained in terms of the variations in chemical constitution.

Coals become more aromatic with increasing rank, which is also associated with decreasing oxygen content and increasing incorporation of oxygen into cyclic structures [645–647].

In low-rank coal, most oxygen is in the form of carboxyl (–COOH) and hydroxyl (–OH) groups; both are reactive cross-linking agents. Oxygen in cyclic structures does not participate in cross-linking. In light of the principles discussed in this section, increasing aromaticity and decreasing oxygen content can explain the improvement in mesophase formation with increasing coal rank.

Carbonization conditions also affect mesophase formation. These effects are due to changes in the rate of chemical and physical processes [648, 649].

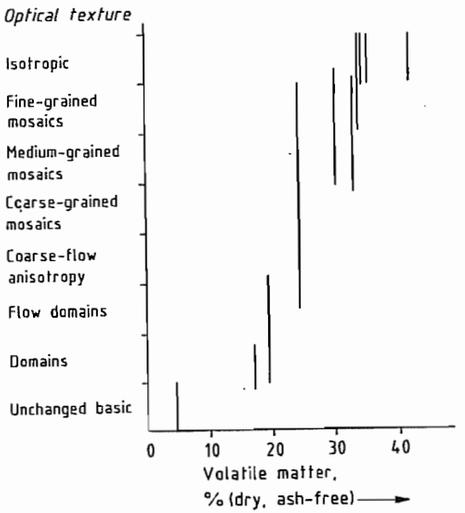

Figure 5.143: Variation of coke optical texture with volatile matter content of the parent vitrains [614].

Modification of Optical Texture and Properties

The most significant feature of the microstructure of metallurgical coke is the unique anisotropy that is associated with low porosity and takes the form of mosaics bridged by small flowtype structures in the pore wall [616]. Most macropores are hundreds of micrometers in size; the pore wall is of significant thickness [616]. The limited porosity provides a coke density suitable for blast furnace operations, whereas the bonding of the small growth units of the anisotropic structures strengthens the coke. In addition, the anisotropic and nonporous nature of the coke reduces reactivity toward carbon dioxide, as is desired in blast furnace operations.

Consequently, coke properties can be modified by altering the optical texture and morphology. This makes possible manufacture of metallurgical coke from the large reserves of noncoking coal of low rank.

Modification of mesophase formation has therefore, great value in improving coke. The cocarbonization of noncoking coal with coking coal or pitch is also useful [650, 651].

5.22.13.2 Yield and Distribution of Pyrolysis Products

Experimental Methods

The yield of pyrolysis products (gases, liquids, and solids) is determined by monitoring the loss of coal mass or the quantity of gas evolved. In the traditional determination of proximate volatile matter (e.g., ASTM or DIN), the yield is measured as the mass lost from a fixed bed at standard conditions. Deviations from these conditions can change mass losses significantly (Figure 5.144). Smaller samples in a standard crucible (shorter bed depths) and higher heating rates and temperatures increase volatile yield.

Yields are also increased by reducing gas pressure and particle size. Thus, the volatile-matter content is highly dependent on pyrolysis conditions and can exceed 150% of the

ASTM value (e.g., last line, Table 5.64). When volatile products are desired, increased yield is of great interest. Furthermore, factors that influence the product distribution are important because in many processes the liquids (not the gases) are of primary interest.

In contrast to coal gasification, for example, with its few and easily identified products, the prediction of yield and product distribution in coal pyrolysis is difficult. The extreme complexity of coal pyrolysis precludes accurate thermodynamic analysis. Moreover, the temperature and pressure are often ill-defined. In rapid pyrolysis, internal pressures as high as 100 MPa have been estimated [652]. The design of reactors and processes is usually based on experimental determination of the yield and product distribution as functions of temperature, heating rate, pressure, particle size, and coal rank [653].

Experimental Variables

Time and Temperature

The determination of temperature and residence time in entrained-flow reactors presents special problems. Particle temperature is usually estimated from measurements of gas temperature (by suction pyrometry) with the aid of a heat-transfer model. Particle residence time (≤ 1 s) is calculated from known or assumed trajectories by using an appropriate model for the fluid and solid dynamics. The total yield of volatile substances, when not obtained from material balances, is frequently determined from the mineral matter or ash in the coal or char. The distribution of volatile products is usually determined by gas chromatography or mass spectrometry.

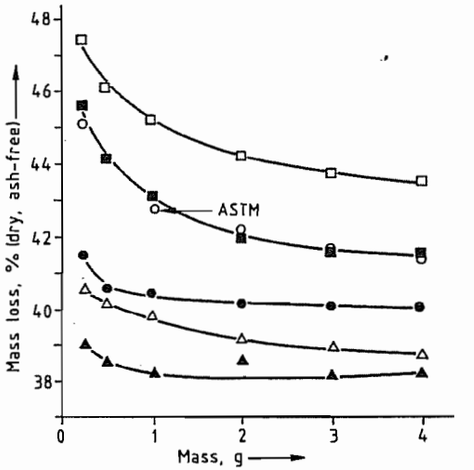

Figure 5.144: Effect of sample mass (bed depth), heating rate, and pyrolysis temperature on mass loss [652].

Symbol	Heating rate, °C/s	Temperature, °C
△	6	750
○[a]	14	950
□	22	1150
▲	0.5	750
●	0.5	950
■	0.5	1150

[a] Standard ASTM volatile matter test.

Table 5.64: Comparison of experimental pyrolysis yields with proximate volatile matter [653].

Conditions	Coal rank	Proximate analysis[a], *VM*, %	Experimental yield, *V'*, %	*V'*/*VM*[b]
Dry basis, heated to 950 °C at 600 °C/s	medium-volatile bituminous (mvb)	25.3	19	0.75
	high-volatile A bituminous (hvAb)	31.6	36	1.14
	high-volatile A bituminous (hvAb)	37.7	49	1.30
	subbituminous	40.7	48	1.17
	high-volatile bituminous (hvb)	44.0	41	0.93
Dry, ash-free basis, heated to 1000 °C at 10^3 °C/s	bituminous	46.2	53.7	1.16
	lignite	44.3	44.7	1.01
	bituminous	44.6	52.2	1.17
heated to 2000 °C at 10^5 °C/s	bituminous	42.5	65	1.53

[a] ASTM method.
[b] *V'* = total volatile matter; *VM* = proximate volatile matter.

Table 5.65: Distribution of volatile products in coal pyrolysis [653].

Method	Coal type	Volatile products, % (dry)			
		Tar[a]	Gas	Water	V[b]
Fischer assay, 600 °C	Furst Leopold	11.2	10.0	8.1	29.3
Stirred bed, 600 °C		18.7	7.0	7.5	33.2
Slow heating, 0.08 °C/s	Moscow brown coal	4.6	11.9	6.0	22.5
Rapid heating to 500 °C		4.0	8.1	9.6	21.7
Thin layer of particles heated to 1050–1100 °C at 1500 °C/s	Maigre Oignies no. 2	1.8	5.1	1.5	8.4
	Bergmannsgluck	41.7	5.9	3.0	23.6
	Emma fines	15.9	6.2	2.4	24.5
	Lens-Lievin no. 10	17.1	7.0	2.6	26.7
	Flenus de Bruay	25.2	9.6	4.4	39.2
	Wendell III	22.5	7.9	4.1	34.5
	Faulquemont	18.9	12.6	5.2	36.7
Entrained flow, 600 °C	West Virginia, mvb[c]	18.7	1.8	6.5[e]	27.0
	Illinois, mvb[c]	19.6	19.7	4.6[e]	43.9
	Pittsburgh, hvAb[d]	31.5	22.0	8.0[e]	61.5
	Wyoming, subbituminous B	11.0	26.4	5.6[e]	43.0
Fischer assay, 500 °C	Western Kentucky	16.3	5.0	9.4	30.7
Flow tube, 530–650 °C	hvBb[c]	33.0	6.6	1.7	41.3
Thin layer of particles heated to 1000 °C at 1000 °C/s	Pittsburgh, hvAb[d]	25.8	11.3	6.5	43.6
	Montana lignite	6.8	22.7	10.4	39.9

[a] Volatiles condensable at 20 °C.
[b] Combined volatiles from tar, gas, and water.
[c] See Table 5.64 for abbreviation.
[d] High-volatile A bituminous.
[e] Estimated as mass difference between original dry coal and combined tar, gas, and char yields.

Table 5.66: Composition of gaseous products in coal pyrolysis [653].

Conditions	Temperature, °C	Volatiles, %	Gas composition, vol% (dry)			
			CO_2	CO	H_2	CH_4
Thin layer of particles	105–1100 (at 1500 °C/s)	8.4	2.2	10.1	66.2	8.6
		18.1	1.6	5.0	67.2	21.4
		20.4	2.0	6.0	62.9	20.3
		24.4	3.8	9.6	64.2	21.0
		31.0	4.1	15.8	54.3	16.9
		33.9	2.4	10.0	52.8	21.8
		36.4	6.1	20.6	60.3	13.1
Fluidized bed	600	31	12.0	12.3	14.7	50.5
Fischer assay	600	31	10.3	8.7	22.4	54.2
Entrained flow	600	31.6	9.2	3.6	19.4	24.7
		34.6	11.7	0.0	23.0	40.7
		37.7	9.5	9.5	17.1	42.9
		40.7	16.0	10.5	25.6	33.9
Flow tube	530–650	41	10.6	4.9	25	42.3
Thin layer of particles	1000 (at 1000 °C/s)	39.5	3.2	9.9	57.8	17.8
		39.6	24.0	37.2	27.8	8.8

The yield of volatile products in the pyrolysis of coals of different rank under different heating rates increases continuously with increasing temperature. This results from the existence of a hierarchy of bond energies in the structure of coals (Figure 5.136). In most cases, even at heating rates as high as 10 000 °C/s in entrained-flow reactors, pyrolysis is complete at ca. 1000 °C. For a longer residence time, a lower temperature is needed to achieve a particular yield, in accordance with Arrhenius-type behavior. In particular, the yield is a sensitive function of temperature for short residence times in entrained-flow reactors.

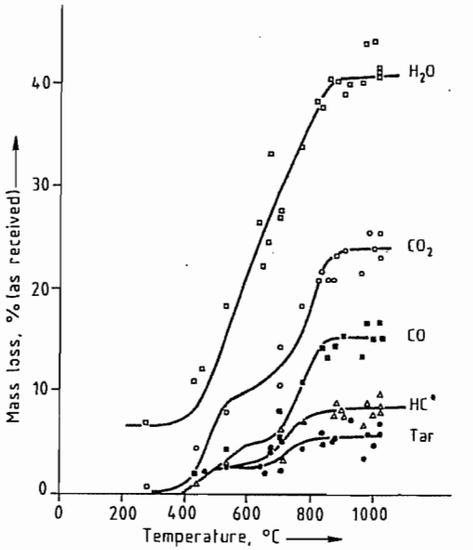

Figure 5.145: Effect of temperature on the distribution of volatile products from a lignite (pressure: 101.3 kPa of He; mean particle diameter: 74 mm; heating rate: 270–10 000 °C/s). □ Total; ○ Tar + HC gases and H_2 + CO + CO_2; ■ Tar + HC gases and H_2 + CO; △ Tar + HC gases and H_2; ● Tar [653]. * HC = Hydrocarbon.

The effect of temperature, the most important influence on product distribution, is illustrated in Tables 5.65 and 5.66, and Figures 5.145 and 5.146. The influence of temperature on the distribution of volatiles obtained from rapid pyrolysis of a lignite (270–10 000 °C/s) is clearly seen in Figure 5.145. The yield of tars reaches a low maximum at relatively low temperature. The hydrocarbon gases consist mainly of methane, ethylene, and hydrogen. The oxygen-containing products, water, carbon dioxide, and carbon monoxide, dominate the gas composition. A result of this temperature dependence is that the pyrolysis products have a range of heating values. This is illustrated in Figure 5.147 for lignite and is typical of the problems associated with obtaining clean-burning fuel from low-rank coals.

In contrast, a high yield of tar and other combustible matter is obtained by the rapid pyrolysis of bituminous coal (Figure 5.146). In both cases, as in all pyrolysis processes, the yield of char or coke is substantial, even at 1000 °C.

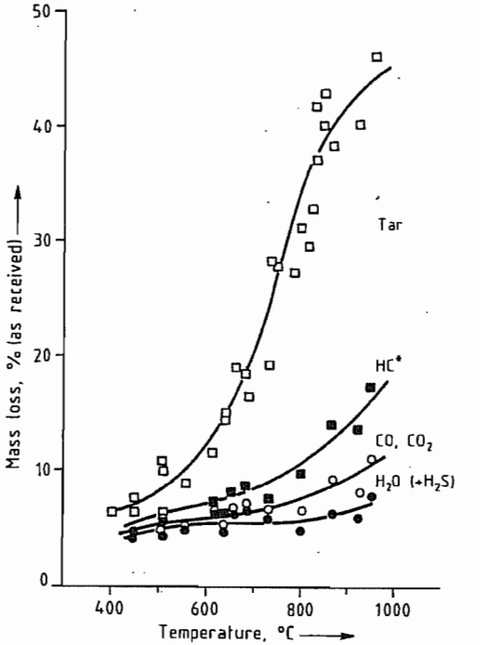

Figure 5.146: Effect of temperature on the distribution of volatile products from a bituminous coal (pressure: 101.3 kPa of He; mean particle diameter: 74 mm; heating rate: 1000 °C/s). □ Total; ■ HC gases and H_2 + CO and CO_2 + H_2O and H_2S; ○ CO and CO_2 + H_2O and H_2S; ● H_2O and H_2S [653]. * HC = Hydrocarbon.

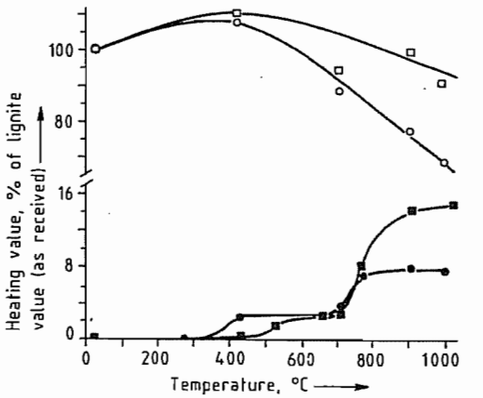

Figure 5.147: Effect of temperature on the distribution of heating value among the products of pyrolysis of a lignite (pressure: 101.3 kPa of He; heating rate: 1000 °C/s). □ Total; ○ Char; ■ Gas; ● Tar [653].

Table 5.67: Effect of heating rate on product distribution from bituminous coals [653].

Product	Yield, % (as received)		
	350–450 °C/s	1000 °C/s	13 000–15 000 °C/s
CO	2.4	2.4	2.3
CO_2	1.6	1.2	1.7
H_2O	7.6	7.8	7.7
CH_4	2.2	2.5	2.4
C_2H_4	0.40	0.83	0.66
C_2H_6	0.59	0.51	0.59
C_3S	1.1	1.3	1.2
Other HC gas	1.1	1.3	1.4
Light HC liquid	2.3	2.4	2.7
Tar	22.4	23.0	23.0
H_2	—	1.0	—
Char	54.0	53.0	53.0
Total	95.69	97.24	96.65
Error (loss)	4.3	2.8	3.3
Number of runs	3	20	2

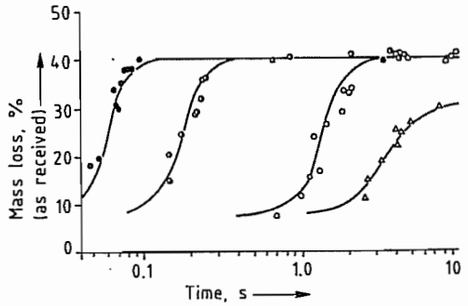

Figure 5.148: Effect of time on pyrolysis mass loss from a lignite (pressure: 101.3 kPa of He; final temperature (if attained): 1000 °C; mean particle diameter: 70 µm). ● 10^4 °C/s; ◑ 3000 °C/s; ○ 650 °C/s; △ 180 °C/s [653].

Heating Rate

The effect of heating rate on coal pyrolysis has often been misunderstood. If slow heating (e.g, 10 °C/min in fixed-bed reactors) is compared with rapid heating (e.g., 10 000 °C/s in entrained-flow reactors), the latter usually gives a better yield. In most such comparisons, however, the heating rate is not the only variable. A change from a fixed-bed reactor to an entrained-flow reactor involves a sharp decrease in the density of the pyrolyzing medium, with important implications for secondary char-forming reactions. However, when the only change is an increased heating rate (Table 5.67 and Figure 5.148), yield and product distribution are unaffected [653], but the time required to reach a given yield is reduced.

Pressure

In the rapid pyrolysis of bituminous coal yield usually decreases with increasing pressure (Figure 5.149). A drop in the yield of tar is not compensated by an increase in the yield of hydrocarbon gases, such as methane (Figure 5.150 and Table 5.68). Increased pressure evidently favors char-forming reactions, particularly cracking and polymerization.

Particle Size

As with heating rate, the effect of coal particle size has been difficult to determine. Changes in particle size are usually accompanied by changes in temperature and residence time. In entrained-flow systems, the calculated residence time is dependent on particle size. Obtaining identical temperature time histories for a range of sizes is difficult; therefore, reports in the literature are conflicting.

As might be intuitively expected (see Section 5.22.13.2), larger particles give a lower yield of volatiles. Increase in char formation (due to tar cracking or polymerization) is not compensated by increased yield of hydrocarbon gas (Figure 5.151 and Table 5.69).

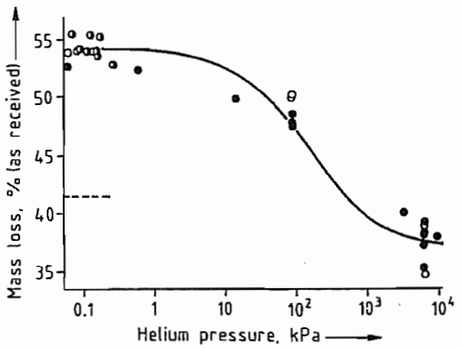

Figure 5.149: Effect of pressure on pyrolysis mass loss from a bituminous coal (final temperature: 1000 °C; mean particle diameter: 70 µm; residence time: 5–20 s). Nominal heating rate, °C/s: ● 650–750; ◑ 3 000; ○ 10 000. ----- Proximate volatile matter (ASTM).

Table 5.68: Effect of pressure on product distribution from lignite and bituminous coal [653].

Product	Yield, % (as received)					
	Lignite			Bituminous[a]		
	6.6 Pa of He[b]	0.1 MPa of He[b]	6.9 MPa of He[a]	6.6 Pa of He	0.1 MPa of He	6.9 MPa of He
CO	6.1	7.1	9.0	2.0	2.4	2.5
CO_2	7.6	8.4	10.6	1.4	1.2	1.7
H_2O[c]	17.7	16.5	13.4	6.8	7.8	9.5
H_2	—	0.50	—	0.75	1.0	—
CH_4	0.94	1.3	2.5	1.6	2.5	3.2
C_2H_4	0.43	0.56	0.55	0.45	0.83	0.46
C_2H_6	0.21	0.18	0.17	0.44	0.51	0.89
$C_3H_6 + C_3H_8$	0.46	0.37	0.38	0.71	1.3	0.71
Other HC[d] gases	0.60	0.47	0.21	0.98	1.3	1.6
Light HC[d] liquids	0.81		1.1	1.6	2.4	2.0
Tar	6.9	5.4	2.8	31.9	23.0	12.0
Char	55.2	58.7	59.0	48.5	53.0	62.4
Total	97.0	99.5	99.7	97.1	97.2	97.0
Error (loss)	3.0	0.5	0.3	2.9	2.8	3.0

[a] Final temperature: 850–1070 °C; mean particle diameter: 74 µm; heating rate: 1000 °C/s; residence time: 2–10 s.
[b] Final temperature: 900–1035 °C; no residence time.
[c] Includes coal moisture (lignite: 6.8%; bituminous: 1.4%); may include H_2S.
[d] HC = Hydrocarbon.

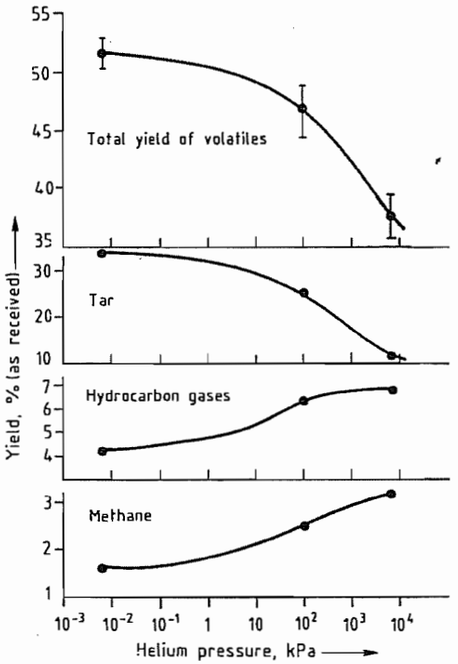

Figure 5.150: Effect of pressure on the yield and distribution of volatile products from a bituminous coal (final temperature: 1000 °C; mean particle diameter: 74 µm; heating rate: 1000 °C/s; residence time: 2–10 s) [653].

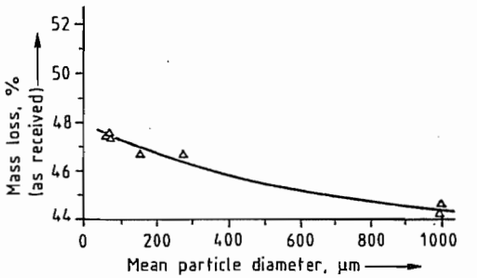

Figure 5.151: Effect of particle size on pyrolysis mass loss from a bituminous coal (pressure: 101.3 kPa of He; final temperature: 1000 °C; heating rate: 650–750 °C/s; residence time: 5–20 s) [653].

Coal Rank

Coals over a wide range of rank can give yields of pyrolysis products that are higher than their standard content of volatile matter (as determined by ASTM proximate analysis) (see Figures 5.145 and 5.146, Tables 5.65 and 5.70). The most important result is the high tar yield given by entrained-flow pyrolysis of bituminous coal.

Table 5.69: Effect of particle size on product distribution from a bituminous coal (pressure: 101.3 kPa of He; final temperature: 850–1070 °C; heating rate: 1000 °C/s; residence time: 3–10 s) [653].

Product	Yield, % (as received)			
	53–88 µm (average, 74 mm)	< 300 µm[a]	300–830 µm	830–900 µm
CO	2.4	2.7	3.2	3.0
CO_2	1.2	1.1	1.2	1.3
H_2O[b]	78	5.4	5.3	7.2
H_2	1.0	—	—	0.99
CH_4	2.5	2.9	3.0	3.2
C_2H_4	0.83	1.0	1.1	1.3
C_2H_6	0.51	0.50	0.55	0.63
C_3S	1.3	0.92	0.84	1.1
Other HC[c] gases	1.3	1.4	1.1	1.2
Light HC[c] liquids	2.4	2.5	2.6	2.7
Tar	23.00	24.2	21.3	18.4
Char	53.0	57.1	56.5	55.8
Total	97.2	99.7	96.7	96.8
Error (loss)	2.8	0.3	3.3	3.2
Number of runs	20	1	2	3

[a] 830–990-µm sample ground to pass 297-µm sieve (50 mesh).
[b] Includes coal moisture (1.4%); may include some H_2S.
[c] HC = Hydrocarbon.

Table 5.70: Effect of coal type on yields of gaseous pyrolysis products [653].

Element/compound	Composition, %		
	Lignite	Subbituminous	Bituminous
Coal analysis (as received)			
C[a]	71.2	73.5	77.7
H[a]	4.6	5.8	5.5
N[a]	1.1	1.2	1.5
S[a]	1.3	0.81	6.1
O[a], by difference	21.8	18.7	9.2
H_2O	6.8	34.7	1.4
Ash, dry	10.6	9.1	11.5
VM[a]	44.3	—	11.5
Product analysis[a]			
CO	8.5	5.8	2.8
CO_2	10.10	11.3	1.4
H_2O	11.6	—	7.4
H_2	0.60	1.1	1.2
N_2	—	—	—
CH_4	1.6	4.8	2.9
C_2H_4	0.67	0.24	0.95
C_2H_6	0.24	0.89	0.58
C_3H_8	0.17	0.47	1.5[b]
Total	33.5	24.6	18.7

[a] Dry, ash-free.
[b] Includes C_3H_6.

Mechanism

The objective of most coal pyrolysis processes, whether fuels or chemicals are being produced, is to maximize the yield of gaseous and liquid products (coke production is a notable exception). This is achieved by reducing secondary char-forming reactions (cracking and polymerization) of high molecular mass products.

Cracking and polymerization can occur within and between the coal particles. These reactions are usually subject to surface catalytic effects and to the nature of the medium to which the primary products are exposed [654].

Volatile material can be driven from the interior of a coal particle by increasing the internal pressure or by reducing the external (ambient) pressure. High pressure gradients accelerate volatilization, thus reducing residence time within the particle, which decreases the probability of secondary reactions and char formation. This explains the effect of external pressure (shown in Figure 5.149) and of high heating rates, which result in rapid heat transfer and a high rate of thermal decomposition. This higher rate of formation of volatiles increases the internal pressure and reduces char formation.

Minimizing interparticle secondary reactions also is important for a maximum yield of volatiles. This is achieved by minimizing particle loading. In entrained-flow reactors, particle loading is far lower than in fixed-bed reactors and the heating rate is far higher. Fluidized-bed reactors are intermediate between these two types.

When pyrolyzed, low-rank coal yields much less tar than bituminous coal. In part this is due to the presence of high molecular mass aromatic units in high-rank coal, which form liquid rather than gaseous products. Another factor is the presence of cations in low-rank coal. Acid washing removes these cations and substantially increases the yield of volatiles (Figure 5.152). This is attributed to a higher tar yield and the elimination of char-forming reactions catalyzed by the highly dispersed cations (principally Ca^{2+}).

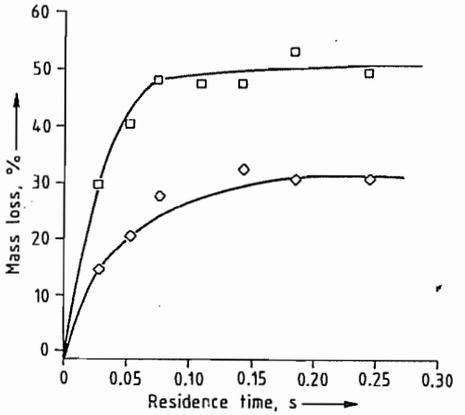

Figure 5.152: Effect of cations on pyrolysis mass loss from a lignite (pressure: 101.3 kPa of N_2; final temperature: 900 °C; mean particle diameter: 70 µm; heating rate: 104 °C/s). □ Acid-washed; ◇ As received [655].

Various options are available when selecting the operating conditions of a pyrolysis reactor [656]. Residence times of 0.1 s or less are attainable only in entrained-flow reactors; at the other extreme, residence times of 100 000 s or more are practical only in fixed-bed reactors. At low temperature (ca. 525 °C), the total yield of volatiles is low because thermal decomposition is incomplete. Entrained-flow conditions minimize secondary reactions and give the highest overall yield. Furthermore, high molecular mass products are stable at low temperature, and the product distribution favors liquids. At ca. 1000 °C, volatilization is complete, with a correspondingly high yield. Again, entrained-flow conditions reduce secondary reactions and increase overall yield. However, even under dilute conditions in entrained-flow reactors, high temperature causes substantial cracking and gives gas as the principal volatile product.

5.22.13.3 Kinetics

The practical importance of the kinetics of the processes described in section 5.22.13.2 depends on the reactor type [653, 657, 658]. In *fixed-bed reactors*, such as coke ovens where the heating rate is ca. 100 °C/min or less, kinetics are not important. The time required for complete pyrolysis is much less than the time required for heating to the final temperature, which determines yield and product distribution.

On the other hand, residence time at pyrolysis temperatures is important in *entrained-flow reactors*, such as pulverized-coal combustors and some modern pyrolysis reactors, which are increasingly important.

A simple kinetic treatment for determining the rate constants that define the size of a reactor or reaction zone is to assume first-order decomposition of the volatile matter in the coal:

$$\frac{dV}{dt} = k(V' - V) \qquad (37)$$

where k = late constant (s^{-1}), V = fraction of volatiles evolved at time t, and V' = total amount of volatiles in the coal.

The magnitude of the effect of coal rank is debatable. In one report the kinetics of pyrolysis were found to be insensitive to changes in rank from lignite to bituminous coal [657]. A possible explanation for this observation is that rapid pyrolysis rates are not determined by the chemical process of bond rupture, but by the physical processes of heat or mass transfer.

The modeling of the complex pyrolysis process by a single first-order reaction is an oversimplification. Many alternative kinetic schemes, proposed to represent more closely the actual mechanism of coal pyrolysis, range from 2 independent parallel reactions corre-

sponding to the postulated 2 components in coals [659], to 42 reactions of the postulated 14 different functional groups in coal [660].

A reasonable compromise, which incorporates process complexity and is a mathematically adequate yet physically reasonable kinetic model [661], is based on a hierarchy of bond energies in the coal structure (Figure 5.136). The pyrolysis is assumed to consist of a large number, i, of independent chemical reactions representing the rupture of various bonds within the coal structure:

$$\frac{dV_i}{dt} = k_i(V_i' - V_i) \tag{38}$$

where the symbols are analogous to those of Equation (37), with the subscript i denoting a particular reaction. The rate constants k_i are assumed to be of Arrhenius form and to differ only in the values of their activation energies. The number of reactions is assumed to be large enough to permit the activation energies E_i to be expressed as a continuous Gaussian distribution function

$$f(E) = \frac{1}{\sigma(2\pi)^{1/2}}\exp\left[-\frac{(E-E_0)^2}{2\sigma^2}\right]$$

with

$$\int_0^\infty f(E)dE = 1$$

where E_0 = mean activation energy and σ = standard deviation.

The term $f(E)dE$ represents the fraction of potential volatiles that have an activation energy between E and $E + dE$,

$$\frac{dV'}{V'} = f(E)dE \tag{39}$$

The total amount of volatiles remaining in the coal is obtained by combining the contribution from each reaction, i.e., by integrating Equation (38) over all values of E by using Equation (39):

$$\frac{V'-V}{V'} = \int_0^\infty \exp\left[-A\int_0^t\left(-\frac{E}{RT}\right)dt - \frac{(E-E_0)^2}{2\sigma^2}\right]dE \tag{40}$$

or

$$\frac{V'-V}{V'} = \frac{1}{\sigma\sqrt{2\pi}}\int_0^\infty \exp\left[-A\int_0^t e^{-\frac{E}{RT}}dt - \frac{(E-E_0)^2}{2\sigma^2}\right]dE \tag{41}$$

Equations (40) and (41) show that in addition to the temperature time history, four parameters are needed to correlate coal pyrolysis data. The total yield of volatiles, V', should be determined experimentally and is not necessarily equal to the ASTM volatile matter content.

This model represents a significant improvement over the single first-order reaction scheme. Curves drawn through the experimental points in Figures 5.145 and 5.146 were obtained by using this model.

If, for simplicity and convenience, the single first-order reaction model of coal pyrolysis is assumed, the treatment that in the past has been applied to complex continuous reaction mixtures [662] and more recently to model coal liquefaction [663] should be used. It results in a temporal distribution of activation energies rather than the spatial distribution just described. It considers coal to be composed of constituents C_i; pyrolysis results in products P_i,

$$\sum C_i \rightarrow \sum P_i$$

where the pyrolysis of each constituent is a first-order reaction:

$$-\frac{dC_i}{dt} = k_i(T)f(C_i)$$

Because C_i and P_i are not identifiable chemical species, a grouping procedure is used:

$$\sum C_i = V$$

The first-order rate expression, analogous to Equation (37), becomes [664]

$$-\frac{dV}{dt} = k(T, V)f(V)$$

Thus, the first-order rate constant k is not only a function of temperature, but also of the concentration of the volatiles, i.e., of conversion or time of pyrolysis. Limited experimental evidence [665] suggests that k decreases with conversion because of an increase in the observed activation energy. This can be interpreted as the intuitively reasonable initial predominance of the rupture of relatively weak bonds in the coal structure.

The main conclusion from this brief analysis is that some of the variation in rate constants can be attributed to the fact that the constants may not have been compared at the same level of conversion.

For optimization of product distribution, having rate parameters for the total yield of volatiles and for individual compounds is desirable. The principal issue is the number of reactions necessary to describe the pyrolysis. In particular, determination of tar evolution rates is difficult because the rates are dependent on the transport properties of the experimental system. In one report these rate constants seem to correlate equally well the pyrolysis of lignite, subbituminous coal, and bituminous coal [657]. This means that pyrolysis rates may be dependent only on the quantity of the various functional groups in the coal and not on its origin or type. This conclusion, if established as generally valid for chemically rather than physically controlled pyrolysis processes, would simplify the design of pyrolysis reactors.

5.22.13.4 Hydropyrolysis

Most coal conversion processes involve hydrogen transfer reactions; pyrolysis involves *hydrogen redistribution*. Free radicals formed by bond rupture usually capture hydrogen atoms (Figure 5.137). Under entrained-flow pyrolysis conditions, the total yield of volatiles is typically 20–40% higher than the ASTM volatile content of the coal, i.e., at least 30–40% of the product is a solid. The available hydrogen is used primarily to stabilize gaseous radicals, such as methyl or ethyl, leaving the higher molecular mass radicals to polymerize and form char.

To reduce char formation and increase volatile yield, the coal is pyrolyzed in the presence of hydrogen [666]. The effect is more pronounced at higher hydrogen pressure, but is not observed if pyrolysis in an inert atmosphere is followed by exposure to hydrogen. Coal can be converted completely to methane in a few seconds at 950 °C and 50 MPa of hydrogen [667]. These effects are not fully understood, but seem to resemble the effect of hydrogen in coal liquefaction, where external hydrogen stabilizes the free radicals formed by bond scission and inhibits char formation. Another possible role of hydrogen in hydropyrolysis is to attack the highly reactive, but transient nascent carbon sites. Aromatic carbon radicals are formed by cleavage of functional groups. Hydrogen reacts with these active sites eventually forming methane, and, thus, the overall yield of volatiles is increased.

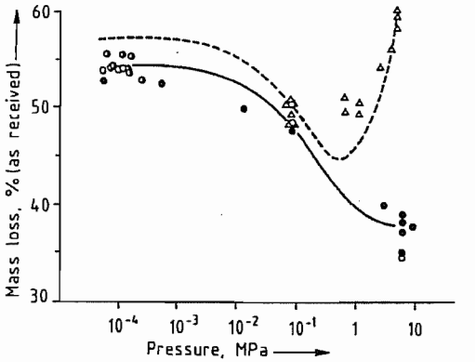

Figure 5.153: Effect of helium and hydrogen pressure on pyrolysis mass loss from a bituminous coal (final temperature: 1000 °C; mean particle diameter: 70 µm; residence time: 5–20 s). ○ He (104 °C/s); ◑ He (3000 °C/s); ● He (650–750 °C/s); △ H_2 (750 °C/s) [653].

The effects of hydrogen pressure on the yield and distribution of pyrolysis products is illustrated in Figures 5.153 and 5.154 (see also Table 5.71). As discussed previously, an increase in the pressure of an inert gas reduces the yield of volatiles. With hydrogen, however, the yield first drops (Figure 5.153), and then increases with an increase in pressure.

Table 5.71: Yields from pyrolysis and hydropyrolysis of bituminous coal (final temperature: 850–1070 °C; mean particle diameter: 74 µm; heating rate: 1000 °C/s) [653].

Product	Yield, % (as received)					
	0.1 MPa of He[a]		6.9 MPa of He[a]		6.9 MPa of H_2[b]	
	Bituminous[c]	Lignite[d]	Bituminous[c]	Lignite[d]	Bituminous[c]	Lignite[d]
CO	2.4	9.4	2.5	9.0	—	7.1
CO_2	1.2	9.5	1.7	10.6	1.3	8.5
H_2O	6.8	16.5	9.5	12.9	—	16.0
CH_4	2.85	1.3	3.2	2.5	23.2	9.5
C_2H_4	0.8	0.6	0.5	0.6	0.4	0.2
C_2H_6	0.5	0.2	0.9	0.2	2.3	1.4
$C_3H_6 + C_3H_8$	1.3	—	0.7	—	0.7	—
Other HC[e] gases	1.3	—	1.6	—	2.0	—
Light HC[e] liquids	2.4	—	2.0	—	5.3	—
Tar	23	5.4	12	3	12	8
Char	53.0	56.0	62.4	59.8	40.2	48.5

[a] Pyrolysis.
[b] Hydropyrolysis.
[c] Residence time: 2–20 s.
[d] Residence time: 3–10 s.
[e] HC = Hydrocarbon.

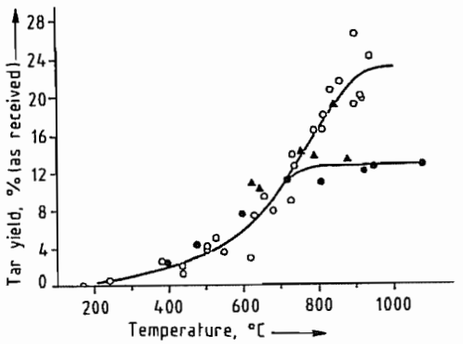

Figure 5.154: Comparison of tar yields from pyrolysis and hydropyrolysis of a bituminous coal (mean particle diameter: 74 µm; heating rate: 1000 °C/s). ○ 0.1 MPa of He; ● 6.9 MPa of He; ▲ 6.9 MPa of H_2 [653].

Experimental evidence suggests that the principal effect of H_2 is not in preventing secondary char-forming reactions (Figure 5.154). The yield of tar under the experimental conditions employed decreased under high hydrogen pressure. In this instance, the detrimental effect of a high external pressure overcame the beneficial stabilizing effect of hydrogen. In the case of a bituminous coal and a lignite, the overall yield enhancement was due to an increase in methane production (see Table 5.71).

On thermal decomposition, the pores of coal particles are filled with reactive (e.g., radicals) and less reactive volatiles. The latter escape unchanged, whereas the former are either quenched and escape, are cracked, or polymerize. Active char (or coke) contains active sites that react with H_2 to give methane. The deactivated sites contribute little or nothing to the overall volatile yield. The corresponding kinetic expressions are given below [653]:

Pyrolysis:

$$V' = V_{mr}'' + V_r'' \frac{K_c}{K_c + k_1} = V_{mr}'' + V_r'' \frac{1}{1 + k_1 P / k_c}$$

Hydropyrolysis:

$$V' = V_{mr}'' + V_r'' \frac{K_c + k_2 P_{H_2}}{K_c + k_2 P_{H_2} + k_1} + k_3 P_{H_2}$$

The curves in Figure 5.153 were obtained by using these expressions.

5.22.13.5 Pyrolysis Processes

Pyrolysis and hydropyrolysis give gaseous, liquid, and solid products; a further hydrogenation step may be required. Fixed-bed processes (low heating rate) give the highest quality coke. They predominate commercially and are often referred to as carbonization processes. Dilute-phase fluidized-bed and entrained-flow processes (high heating rate), suitable for high yield of gaseous and liquid products, are at various stages of precommercial development.

Pyrolysis processes can be classified as early (Table 5.72) [668] or contemporary (advanced). The *early processes* generally involved low-cost systems and were intended to produce solids (coke or char) rather than liquids.

Table 5.72: Early pyrolysis processes [668].

Pyrolysis process	Final temp., °C	Products	Processes
Low temperature	500–700	more coke, high tar yield	Rexco (700 °C), cylindrical vertical retorts; coalite (650 °C), vertical tubes
Medium temperature	700–900	more coke, high gas yield, domestic briquettes	Town gas (obsolete) and coke, phurnacite, using low-volatile steaming coal, pitch-bound briquettes carbonized at 800 °C
High temperature	900–1050	hard, unreactive coke for metallurgical use	foundry coke (900 °C); blast furnace coke (950–1050 °C)

Table 5.73: Low-temperature batch processes [670].

	Process						
	Krupp–Lurgi	Brennstoff–Technik	Otto	Weber	Phurnacite	Parker retort	Rexco
Country (year)	Germany (1930s)	Germany (1940s)	Germany (1940s)	Germany (1940s)	United Kingdom (1940s)	United Kingdom (1920s)	United Kingdom (1920s)
Objective	char production	lumpy char from weakly coking coals	char and gas production	char production	smokeless domestic fuel	smokeless domestic fuel	smokeless domestic fuel
Plants (year)	Wanne-Eickel (1943)	Berlin-Neukollin (1944)	—	—	South Wales (1942)	Barnsley (1927), Bolsover (1936)	Nottingham, England (1936)
Yields							
Char	2.04×10^8 kg/a	0.75 kg/kg dry coal	—	—	0.7 kg/kg coal	—	—
Tar	1.2×10^6 kg fuel oil/a	0.1 L/kg dry coal	—	—	0.06 kg/kg coal	0.08 L/kg coal	0.08 L/kg coal
	1.9×10^6 kg motor fuel/a				—	—	—
Gas	105 L/kg coal	142 L/kg dry coal	—	—	—	125 L/kg coal	unknown
Gas HV[a]	—	$(2.5–3) \times 10^4$ kJ/m³	—	—	—	26 000 kJ/m³	5200 kJ/m³
Reactor	vertical fixed-bed retort	vertical fixed-bed retort	vertical fixed-bed retort	vertical fixed-bed retort	vertical fixed-bed retort	vertical fixed-bed retort	vertical fixed-bed retort
Capacity	270 kg/d	10^5 kg briquettes/d	3600 kg/d	unknown	11 340 kg/d	0.3 kg/kg charge	50 000 kg/d
Heating	indirect hot gas recycling	indirect hot gas recycling	indirect heating by gas burned in flues	unknown	indirect heating by recycling hot combustion gas	indirect radiant heat by combustion gas	direct heat by combustion gas
Temperature range	560–620 °C	650 °C	—	—	—	650 °C	650 °C
Residence time	2–3 h	2–4 h	—	—	4 h	4.5 h	13.5 h
Current status	—	semicommercial plant still may be operating in the former GDR[b]	closed	—	—	—	—

[a] HV = heating value.
[b] GDR = German Democratic Republic.

Table 5.74: Low-temperature continuous processes [670].

	Process			
	Coalite & Chemical Products	Lurgi–Spullgas	Disco	Koppers continuous vertical ovens
Country (year)	United Kingdom (1950s)	Germany (1930s)	United States (1930s)	Germany (1940s)
Objective	char, liquid fuels	char, automotive fuels	lump char	char
Plants (year)	Bolsover, England (1952)	Offleben, Germany, Japan (1941), New Zealand (1931), Lehigh, North Dakota (1940)	Pittsburgh, PA	Kattowitz (1945)
Yields				
Char	0.74 kg/kg coal	0.45 kg/kg briquette	6.8×10^5 kg/d	1.5×10^4 kg/d-retort
Tar	0.06 L/kg coal	0.125 kg/kg briquette	—	2.1×10^3 kg/d retort
Gas	111 L/kg coal	144 L/kg briquette	—	0.32 L/kgcoal
Gas HV[a]	26 000 kJ/m³	8380 kJ/m³	—	1.8×10^4 kJ/m³
Reactor	Parker vertical retort	continuous vertical retort	continuous rotating horizontal retort	continuous vertical retort
Capacity	0.3 kg coal charge	2.7×10^5 kg briquettes/d	1.4×10^5 kg/d	25 000 kg/d
Heating	radiant heat supplied by combustion gas	direct contact with combustion gas	indirect heating by circulating hot combustion gas through flues built in hearths	indirect and direct heating by passing hot gases alternately upward and downward through flues and regenerators
Temperature range	combustion chamber held between 600 and 700 °C	600–700 °C	550 °C	700 °C
Residence time	coal carbonized for 4 h	20 h	1.5 h	21 h/retort
Current status	in operation	—	closed	—

[a] HV = heating value.

Contemporary processes, on the other hand, have been designed to maximize production of liquid by using conditions (e.g., dilute phase, pressurized H_2, and rapid heating and quenching) that minimize secondary pyrolysis reactions. This requires more expensive equipment and severer operating conditions [656, 669].

Low-Temperature Pyrolysis Processes

Early Processes

Low-temperature pyrolysis (below 700 °C) was developed mainly to supply gas for public lighting and smokeless (devolatilized) solid fuel for home use. By-product tars were valuable as chemical feedstocks and could be converted to gasolines, heating oils, and lubricants. Commercial low-temperature coal pyrolysis was utilized extensively in Europe, but was almost abandoned after 1945 as oil and natural gas became widely available. Rising oil prices have reactivated interest in this process.

The many low-temperature processes developed in Europe can be classified as batch or continuous, vertical or horizontal, and directly or indirectly heated (Tables 5.73 [670] and 5.74).

Retorts or by-product coke ovens were employed. Horizontal retorts (D retorts), 2.5–6 m long, were usually grouped together to form a bank heated by flue gas, with manual loading and unloading. Vertical retorts, both batch and continuous, were preferred in the United States and Europe because they permit gravity loading and unloading [671].

Rates of heat-transfer and carbonization were increased by using steel refractories as materials of construction. Internal heating was sometimes necessary to accelerate heat transfer by circulating hot gas. Only noncaking or weakly caking coals were used in continuous vertical retorts because caking coal softens and flows, forming large masses of coke that stick to the retort walls.

Two noteworthy low-temperature pyrolysis processes are the Disco and Coalite processes. These were successful when most low-temperature processes failed [671, 672].

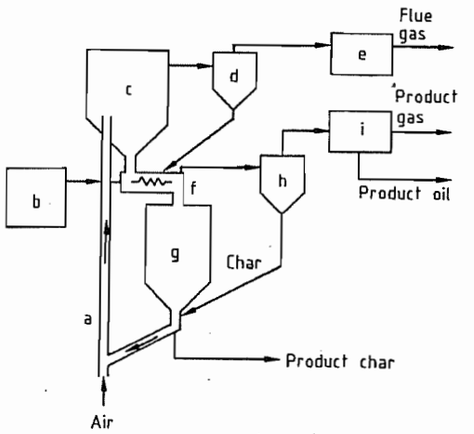

Figure 5.155: Lurgi–Ruhrgas process: a) Transport reactor and lift line; b) Coal preparation; c) Collecting bin; d) Cyclone; e) Heat recovery; f) Mixer–carbonizer; g) Surge hopper; h) Cyclone; i) Condenser.

Contemporary Processes

Lurgi–Ruhrgas Process. The Lurgi–Ruhrgas process (Figure 5.155) for the low-temperature production of liquids from low-rank coals is currently in commercial use in Europe.

Crushed coal is rapidly heated in a mixer (f) to 450–600 °C by contact with recirculating char particles that have been heated by partial oxidation in an entrained-flow reactor. The gas from the mixer is freed of particulate matter in a cyclone (h) and is passed through a series of condensers (i) to collect the liquid products, the latter are hydrogenated to yield stable products.

The char constitutes ca. 50% of the products, whereas liquid yield is ca. 18%; the remaining 32% is gas with a heating value of $(26–31) \times 10^6$ J/m³.

Toscoal Process. The Toscoal process, an adaptation of the Toscoal II oil–shale retorting process, was developed at a pilot plant near Golden, Colorado, with a capacity of 22.5 × 10^3 kg/d.

Crushed dry coal is preheated in lift pipes with flue gas from a ball heater and is fed to a rotating pyrolysis drum containing hot ceramic balls. Pyrolysis at ca. 500 °C produces char and hydrocarbon vapors. The char is separated by a trommel screen and withdrawn. The balls are reheated and returned to the drum. Pyrolysis products are cooled and condensed to recover light gases and coal liquids.

High-Temperature Processes (Coke-Making)

Coke Ovens

High-temperature carbonization is employed primarily to produce blast-furnace and foundry cokes for use in iron and steel manufacture. The process is carried out in coke ovens at ca. 900 °C.

In the 16th century, coke was found to burn hotter and cleaner than coal [673]. The earliest type of coke oven, the so-called *beehive oven*, was developed in the 1850s; its main characteristic is that the heat necessary for coking is produced by burning the volatile coal constituents within the oven [674, 675]. All the gaseous and liquid by-products are lost, together with large amounts of heat.

Beehive ovens have persisted well into the 20th century with progressive improvements in design and operation, such as heat recovery systems and vertical flues to supply process heat to the coking chamber.

A parallel development during the 19th century led to *slot ovens*. At first, these were simple rectangular firebrick structures holding a layer of coal ca. 1 m deep; later they were equipped with external heating flues [650]. In a further development, volatile by-products were collected and used as fuel.

By the 1940s, the basic design of *modern coke ovens* had been developed. The ovens were ca. 12 m long, 4 m high, and 0.5 m wide, equipped with doors on both sides. The air supply was preheated by the hot exit gas. The

recovery of the waste heat created higher temperatures and increased coking rates [676]. Since the 1940s, the process has been mechanized and the construction materials have been improved without significant design modifications. Current assemblies may contain up to 60 ovens as large as 14 m long and 6 m high. Because of heat transfer considerations, widths have remained 0.3–0.6 m. Each oven in the battery holds up to 30 t of coal and operates on a 15-h cycle [677].

The coking process illustrated in Figure 5.156. The coal is conveyed from storage bunkers (a) to blending (b) and crushing (c) units, and then to the coke oven bunker (d). The ovens are loaded from a mobile larry car (e) located on top of the battery. Coking takes place in completely sealed ovens (f). The by-product vapors and gases are collected and sent to recovery and processing units.

After carbonization, the oven doors are opened and the ram (g) pushes the red-hot coke into a quenching car. The coke is transported to the quenching unit (h) and then dumped on a sloping wharf (i) for cooling and drying. The dry coke is transferred to the screening and loading unit (j).

Coke Properties

The properties of coke depend on the coal and the processing conditions employed. The particle size, mineral matter, and moisture content, which can be controlled, affect the bulk density of the coal. Rank and maceral composition determine the fluidity of the plastic phase formed at intermediate temperatures. Significant process conditions include the wall temperature, coking time, and oven width; the heating rate and final temperature also affect coke structure.

The coal is prepared for coking by washing, drying, sizing, preheating, briquetting, and blending, with or without addition of pitch or breeze (fine coke particles) [674]. Foreign matter is removed mechanically and particle size is adjusted. Preheating (up to ca. 600 °C) increases production by ca. 50% and reduces coking time without loss of quality [674].

Briquetting, with or without binder, increases the strength of the coke produced and permits noncoking or poorly coking coals to be used to make metallurgical coke. Cold briquetting is performed below the softening point of the coal (ca. 400 °C) and hot briquetting above the softening point (450–520 °C) [676].

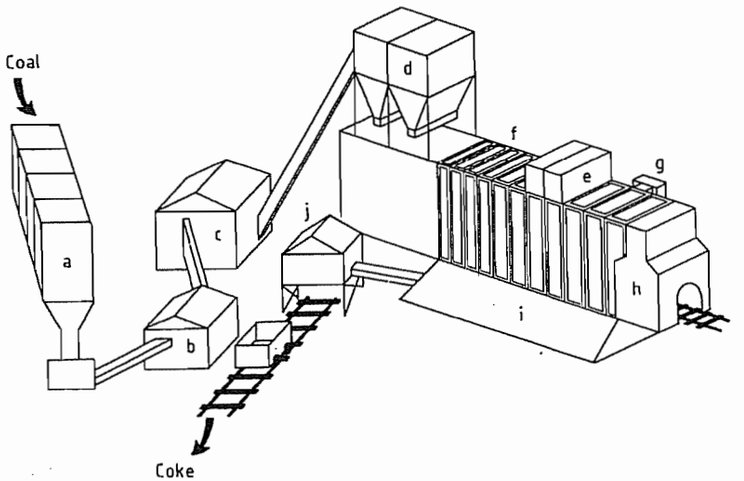

Figure 5.156: Coke-making process [650]: a) Storage bunkers; b) Blending plant; c) Crusher; d) Service bunker; e) Charging car; f) Coke oven; g) Ram machine; h) Cooling tower; i) Cooling wharf; j) Coke screen.

Coal blending improves coke properties and yield and permits the use of noncoking or weakly coking coals [678]. Blending may also prevent damage to ovens when high coking pressure develops.

By-Products

Carbonization by-products were important in the development of the organic chemicals industry, but their use has greatly diminished because of competition from petroleum-based products. The principal by-products are tar and coke-oven gas. Gas produced in the early slot ovens was used for domestic heating. Coal tar can be processed by petroleum-refining techniques. High-temperature tar can be fractionally distilled; three oil cuts are taken and a solid residue remains [596, 679]:

- *Light oil* (*bp* < 200 °C), composed primarily of benzene, toluene, xylenes, and styrene.
- *Middle oil* (*bp* < 370 °C), containing tar acids (phenols), tar bases (e.g., pyridine, anilines, and quinolines), and neutral oils (naphthalene).
- *Heavy oil* (*bp* < 550 °C), containing aromatic compounds, such as anthracene, phenanthrene, carbazole, and chrysene.
- *Coal tar pitch* (solid residue), consisting of a wide range of polycondensed aromatic compounds; it can be used as a binder for coal briquetting.

By-products that are obtained more cheaply from petroleum are no longer recovered exhaustively from coal tar.

Formed-Coke Processes

The preparation techniques and reactor configurations employed by some of the coking processes developed since the 1960s are different. Among these processes, the formed-coke ones have been the most successful (see Table 5.75). The term "formed coke" is used to describe cokes obtained by the carbonization of briquettes of weakly coking or noncoking coals. These processes provide the possibility of using weakly coking or noncoking coals, of controlling coke size to improve blast furnace operation, and of continuous operation in a contained system.

Blast furnace tests of these cokes have been successful. They are usually higher in moisture, volatile matter, sulfur, and reactivity to carbon dioxide, and lower in abrasion resistance than conventional metallurgical cokes [650].

Table 5.75: Formed-coke processes [650, 676, 680].

Process (country)	Raw materials	Process steps
FMC (USA)	noncoking or coking coals and tar	1) Oxidation and carbonization of coal in fluidized beds 2) cold briquetting of char with tar 3) preheating and carbonization of briquettes
DKS (Japan)	noncoking, coking coals and pitch	1) cold briquetting of coal with pitch 2) carbonization of briquettes
HPNC (France)	weakly coking, coking coals and pitch	1) cold briquetting of coal with pitch 2) carbonization of briquettes
BFL (Germany)	high-volatile noncoking coals and coking coals or pitch	1) carbonization of noncoking coal 2) hot briquetting of char with coking coal or pitch 3) carbonization of briquettes
ANCIT (Germany)	low-volatile noncoking coals and coking coals	1) flash heating of low-volatile noncoking coal 2) hot briquetting of char with coking coal 3) reheating of briquettes
Sapozhnikov (Russia)	high-volatile weakly coking coals and low-volatile weakly coking coals	1) flash heating of coal 2) hot briquetting 3) carbonization of briquettes
CCC-BNR (USA)	high-volatile noncoking coals and coking coals on pitch as binder	1) preheating of high-volatile coal 2) hot briquetting of char with binder 3) carbonization of briquettes

Environmental Aspects

Coking plants create environmental problems like other large installations producing dusty materials and gaseous and liquid effluents [649]. Gas and volatile emissions may arise from leaks. Coal and coke particulates may be discharged during loading and unloading, and water used for quenching may be contaminated.

Particulate, volatile, and gas emissions can be reduced by using sheds or traveling hoods with dust and fume collectors [650]. Polluted water must be treated in wastewater plants. In some plants, dry quenching is used instead of water quenching, and the coke is cooled by gas or steam in a closed system. A further advantage of this process is that energy can be recovered via sensible heat and combustible gases.

In addition to air pollution, machinery and working conditions are hazardous. Plant location and accident prevention require serious consideration.

Contemporary Hydropyrolysis and Pyrolysis Processes

The three processes shown in Table 5.76 illustrate the principles described in section 5.22.13.2. Their main objective is production of liquid hydrocarbons, for which entrained-flow conditions are the most favorable. However, char or coke is still the principal product in all three processes; its efficient use is one of the main issues in their economic analysis. The use of hydrogen in the Rockwell process reduces char production to some extent but as discussed in Chapter 5.22.13.4, this is achieved primarily by increasing the yield of gas, not liquids.

The *Coal Oil Energy Development* (*COED*) *process* (Figure 5.157), is a part of the COGAS process for complete conversion of coal to gases and liquids. The residual char from pyrolysis reacts with H_2O and O_2 in a fluidized-bed gasifier (g) to produce the hot synthesis gas, a mixture of CO and H_2. The synthesis gas serves as fluidizing and heat-transfer medium in the pyrolysis reactors (p_1–p_4).

The conditions in the gasifier do not permit complete conversion to gases. Part of the char that leaves is recycled to the pyrolysis section, where it provides additional heat for the endothermic devolatilization. The entrained fine particles and the remaining char are burned in a combustor (c). The hot flue gas is also recycled to the pyrolysis section to provide more heat.

This brief description illustrates the principal technical issues involved in the evaluation of pyrolysis processes: the type of contact between solids and fluids; the method of supplying heat; and the amount and fate of the residual char. In this context, several features of the COED process increase the production of liquids. The countercurrent flow of solids and gases (or vapors) and the increasing operating temperatures in the various pyrolysis stages help to reduce cracking by avoiding subsequent exposure to higher temperatures. The relatively dilute medium in the fluidized beds also helps to reduce the probability of secondary interparticle reactions.

The low final temperature favors production of liquids. However, the heating rates are relatively low and intraparticle secondary reactions may still occur. The use of internally generated and recirculated hot gas and char to provide energy for devolatilization has the advantage of efficiency but it introduces a degree of complexity.

Table 5.76: Characteristics of selected pyrolysis processes [656].

Process	Reactors	Temperature, °C	Pressure, MPa	Yield, % (dry)			
				Coke	Tar and oil	Gas	H_2O
COED	fluidized-bed	290–565	0.12–0.19	62	21	14	3
Occidental	entrained-flow	610	0.3	56	35	7	2
Rockwell	entrained-flow	845	3.5	46	38	16	—

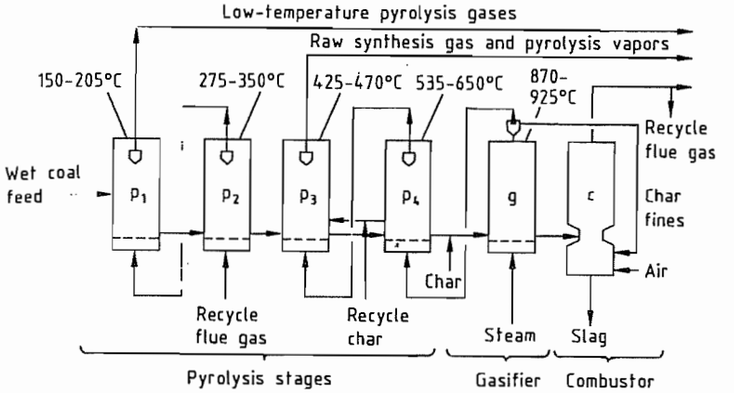

Figure 5.157: COED pyrolysis process [656]. p_1–p_4 = Pyrolysis reactors; g = Fluidized-bed gasifier; c = Combustor.

The complete internal utilization of the coal is a virtue of the COED/COGAS process. The relatively low final pyrolysis temperature forms a char that is highly reactive and, thus, suitable for gasification with steam. The resulting synthesis gas is a highly valuable and versatile product that can be converted, for example, to a natural gas substitute by methanation.

Entrained-flow reactors are favored by a new generation of coal-conversion processes for several reasons. Both fixed-bed and fluidized-bed reactors need auxiliary equipment to avoid difficulties in processing of agglomerating bituminous coal. The fusion of coal particles during pyrolysis can block these reactors. In the COED process (Figure 5.157), for example, where bituminous coal is the preferred feedstock because of its potentially high liquid yield, one of the stages (p_2) introduces oxygen cross-links into the coal structure and subsequently reduces or eliminates thermoplasticity, thus preventing agglomeration.

High throughputs are possible in entrained-flow reactors. The very dilute medium reduces the probability of particle agglomeration. Furthermore, rapid heating and a short residence time sharply reduce the importance of the plastic phase of pyrolysis of bituminous coals.

Finally, these conditions maximize the yield of volatiles and favor production of chars that may be sufficiently reactive to give valuable products, as in the COGAS process. Less reactive chars serve as fuel.

In the *Occidental process* (Figure 5.158) [681], the reactor operates at ca. 625 °C, thus maximizing production of liquids. Heat is supplied by mixing the coal with recirculated char that is made incandescent by partial combustion. The conditions for entrained flow require particles smaller than 200 µm (typically 80% passing through a 60 mesh screen) and, thus, pulverization is necessary in contrast to fixed-bed and fluidized-bed processes. The residual char is usually desulfurized for sale as "smokeless" fuel.

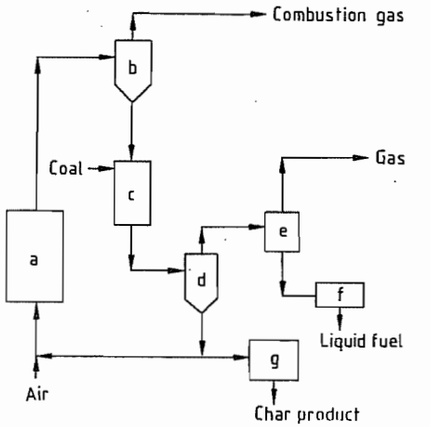

Figure 5.158: Occidental pyrolysis process [681]: a) Char burner; b) Cyclone; c) Reactor; d) Cyclone; e) Oil collection system; f) Liquid upgrading; g) Char desulfurization plant.

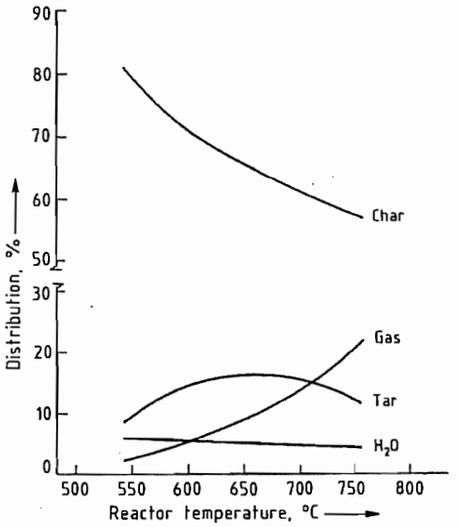

Figure 5.159: Effect of temperature on the distribution of products from a subbituminous coal in the Occidental process (pressure: 21 kPa of N_2; particle size: 80% passing a 250 µm screen, 60 mesh; residence time: 1.5 s) [681].

The effect of temperature and residence time on product distribution is shown in Figures 5.159 and 5.160.

The *Rockwell hydropyrolysis process* (Figure 5.161) incorporates the entrained-flow reactor as a minor component; other operations are similar to those encountered in petroleum refining. The hydrogen feed is preheated by partial combustion. After hydropyrolysis lasting 0.02–0.2 s, the products are rapidly quenched to prevent secondary char formation. A maximum liquid yield is obtained at an intermediate reactor temperature [682].

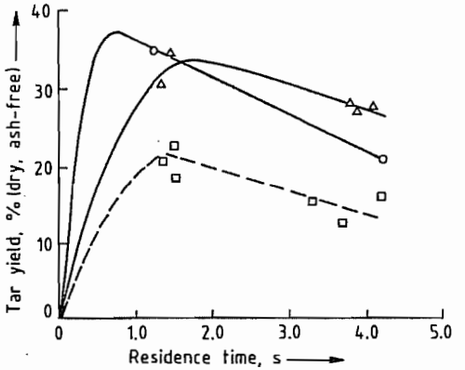

Figure 5.160: Effect of residence time on tar yield in the Occidental process (pressure: 21 kPa of N_2; particle size: 80% passing a 250 µm screen, 60 mesh). □ Subbituminous coal (649 °C); △ Bituminous coal (607 °C); ○ Bituminous coal (660 °C) [681].

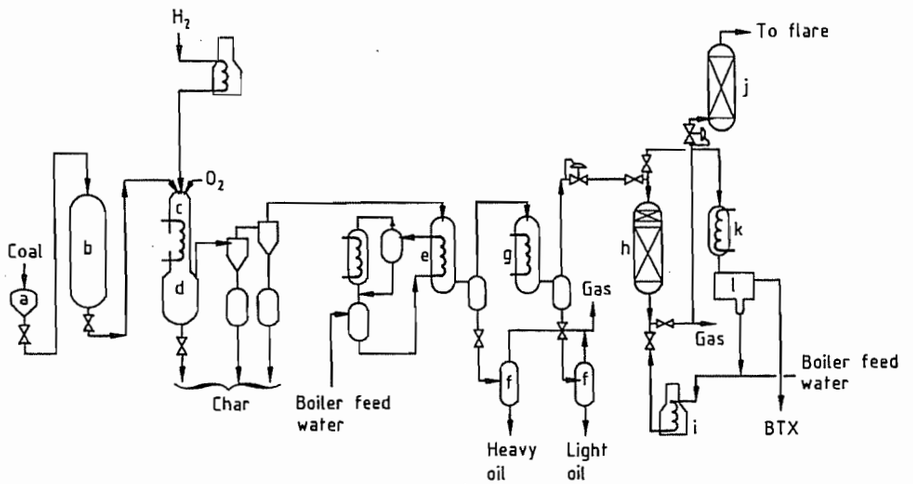

Figure 5.161: Rockwell hydropyrolysis process [682]: a) Loading feeder; b) Coal feeder; c) Reactor; d) Char–vapor separator; e) Heavy oil condenser; f) Flash drum; g) Light oil condenser; h) BTX adsorber; i) Boiler; j) Scrubber; k) BTX–steam condenser; l) Decanter.

Changing hydrogen pressure affects product distribution, but not the yield of liquids; very high pressure is apparently needed to stabilize the reactive fragments in the absence of a solvent [682].

5.23 References

1. F. Habashi, "Native Metals" in R. G. Reddy, R. N. Weizenbach (eds.), *International Symposium Extractive Metallurgy of Copper, Nickel, and Cobalt*, volume 1, The Minerals, Metals & Materials Society, Warrendale, PA, 1993, pp. 1147–1153.
2. United Nations Conference on Trade and Development Review of Iron Ore Statistics, GF.94-53266, 1994.
3. H. J. Werz et al.: *Environmental Protection in Iron Ore Sintering by Waste Gas Recirculation*, Stahleisen 1995, pp. 120–126.
4. United Nations, Survey of World Iron Ore Resources, New York 1970.
5. *Skillings Mining Review* **75** (1986) no. 39, 4.
6. *Iron Ore 1986*, American Iron Ore Association, Cleveland, OH *1987.*
7. *Skillings* Mining Review **77** (1988) no. 17, pp. 4–5, 17.
8. K. J. Pieper, *Handel und Verbrauchsentwicklung von Eisenerzpellets in der westlichen Welt*, lecture at VDEh Düsseldorf, 10.6.1987.
9. R. C. Anderson et al. *Skillings Mining Review* **76** (1987) no. 33, pp. 6–9.
10. Exploration und Berghau GmbH, personal communication 1988.
11. F. Habashi, *Principles of Extractive Metallurgy*, volume 3 — Pyrometallurgy, Gordon & Breach, New York 1986.
12. H. E. McGannon (ed.), *The Making, Shaping, and Treating of Steel*, United Steel, Pittsburgh, PA, 1964.
13. J.H. Strassburger et al. (editors), *Blast Furnace. Theory and Practice*, 2 volumes, Gordon & Breach, New York 1969.
14. Gmelin–Durrer, *Metallurgy of Iron/Metallurgie des Eisens*, volumes 1–4, Springer Verlag, Berlin 1964–1972.
15. Gmelin-Durrer: *Metallurgie des Eisens*, 4th ed. vols. 2a, b, Verlag Chemie, Weinheim 1964.
16. M. Higuchi, M. Iizuka, T. Shibuya: *Developments in Iromnaking Practice*, The Iron and Steel Institute, London 1973 p. 98.
17. G. Heynert, E. Legille, in [16] p. 109.
18. Iron and Steel Inst. Japan: *Handbook of Iron and Steel*, vol. 2, Maruzen Publishing Co., Tokyo 1979, p. 295.
19. in Ref. [18] p. 306.
20. *Ullmann*, 4th ed., **10**, 370.
21. M. Manes, J. S. Maikay, *J. Metal.* **14** (1962) 308–314.
22. in Ref. [18] p. 110.
23. in Ref. [18] p. 120.
24. G. Heynert, P. Ischebeck, W. V. Spee, *Eisen* **81** (1961) 1–12.
25. M. Nakamura, T. Sugiyama, T. Uno, Y. Hara, S. Kondo, *Tetsu to Hagane* **63** (1977) 28–36.
26. M. Hatano, B. Hiraoka, M. Fukuda, T. Masuike, *Trans. Iron Steel Inst. Jpn.* **17** (1977) 102–109.
27. M. Hatano, K. Kurita, T. Yanaka: *Int'l Blast Furnace Hearth and Raceway Symposium*, Newcastle AIMM 1981, p. 4.1–4.10.
28. K. Kanbara et al., *Trans. Iron Steel Inst. Jpn.* **17** (1977) 371–380.
29. K. Takeda et al., *Proc. Ironmaking Conf.* 46 (1987) 191–198.
30. H. Lackmann: *4. Dozentenseminar des Vereins Deutscher Eisenhüttenleute*, Gelsenkirchen 1973.
31. in Ref. [18] pp. 159, 160.
32. M. Iizuka: *116th and 117th Nishiyama Memorial Seminar organized by Iron Steel Institute Japan*, 1987, pp. 1–38.
33. J. Cappel, M. Geerdes, K. Hangner, H. B. Lüngen, *Stahl Eisen* **108** (1988) 459–468.
34. Y. Ohno et al., *7th Process tech. Conf. Proceedings*, Toronto 1988, pp. 195–201.
35. in [15] 1972, vols. 4a, b.
36. in [15] vols. 4a, b.
37. H. Schenk, *Stahl Eisen* **83** (1963) 1683–1690.
38. H. Wysocki, *Vorlesung Entwerfen von Hüttenwerksanlagen*. Techn. Univ. Berlin 1975.
39. in Ref. [18] pp. 278–300.
40. Japan Institute of Iron and Steel Slags: *Annual Report of Iron and Steel Slags Statistics* 1988.
41. M. Saino: *116th and 117th Nishiyama Memorial Seminar organized by Iron Steel Institute*, Japan 1987, pp. 237–278.
42. Y. Hara, M. Sakawa, S. Kondo, *Tetsu to Hagane* 62 (1976) 315–323.
43. Iron and Steel Inst. Japan: *Blast Furnace Phenomena and Modeling*, Elsevier, London 1987, pp. 121–127, pp. 132–133.
44. N. Tsuchiya, M. Tokuda, M. Ohtani, Tetsu to *Hagane* **58** (1972) 1927–1939.
45. W. E. Ranz, *Chem. Eng. Prog.* **48** (1952) 247–253.
46. J. Kudoh, J. Yagi, *Tetsu to Hagane* 73 (1987) 2020–2027.
47. J. Yagi, I. Muchi, *Trans. Iron Steel Inst. Jpn.* **10** (1970) 392–405.
48. M. Hatano, K. Kurita, *Tetsu to Hagane* **66** (1980) 1898–1907.
49. M. Kuwabara et al., *Proc. Joint Symp. of Iron Steel Inst. Jpn. and Australasian Institute* Mining and Metallurgy, Tokyo 1983, pp. 193–204.
50. S. Taguchi et al., *Tetsu to Hagane* **68** (1982) 2302–2310.
51. M. Hatano, K. Kurita, H. Yamaoka, T. Yokoi, *Trans. Iron Steel Inst. Jpn.* **25** (1985) 911–940.
52. Y. Okuno et al., *Tetsu to Hagane* **73** (1987) 91–98.
53. T. Sugiyama, J. Yagi, Y. Omori: *Proc. 3rd Int'l Iron Steel Congr.*, 1978 Chicago, pp. 479–488.
54. J. Ohno et al., *International Blast Furnace Hearth & Raceway Symposium*, Newcastle, Australia 1981, pp. 10–12.
55. A. Poos: *Heat and Mass Transfer in Process Metallurgy*, A. W. D. Hills, 1967, pp. 1–38.
56. M. Hatano, K. Kurita, H. Yamaoka, T. Yokoi, in [50] pp. 941–948.
57. T. Sugiyama et al., *Curr. Adv. Mater. Proc.* (in Japanese), **1** (1988) 22–25.

58. A. Kato, *Tetsu to Hagane* **73** (1987) 461–468.
59. J. Yagi, T. Akiyama, *Curr. Adv. Mater. Proc.* (in Japanese) **2** (1989) 2.
60. A. Nakagawa, *Tekkokai* (1986) no. 6, 5–9, issued by The Japan Iron and Steel Federation.
61. T. Akiyama, J. Yagi, *Process Tech.* **74** (1988) *Conf. Proc.* ISS-AIME, vol. 7, Toronto, 1988, pp 179–193.
62. M. Wahlster, H. P. Schulz, J. Thein, *Stahl Eisen* **89** (1969) 478–486.
63. in Ref. [18] p. 450.
64. W. Domalski, K. Fabian, D. Nolle, *Stahl Eisen* **88** (1968) 906–919.
65. in Ref. [18] p. 443.
66. H. P. Schulz, *Stahl Eisen* **89** (1969) 249–262.
67. S. Eketorp, B. Kalling, *Gießerei* **46** (1959) 905–912.
68. T. Okuro, *Tetsu to Hagane* **52** (1966) no. 2, 120–139.
69. in Ref. [18] p. 446.
70. H. Kajioka in W. K. Lu (ed.): *Symposium on External Desulphurizations of Hot Metal*, p. 15-1–15-35 McMaster Univ., Hamilton, Canada, 1975.
71. W. Meichsner, K. H. Peters, W. Ullrich, H. Knahl, *J. Met.* **26** (1974) no. 4, 55–58.
72. in Ref. [18] p. 441.
73. in Ref. [18] p. 448.
74. F. Habashi, *A Textbook of Hydrometallurgy*, Métallurgie extractive Québec, Sainte-Foy 1993.
75. Iron and Steel Inst. Japan: *Handbook of Iron and Steel*, vol. 2, Maruzen Publishing Co., Tokyo 1979, p. 446.
76. H. Kajioka in W. K. Lu (ed.): *Symposium on External Desulphurizations of Hot Metal*, p. 15-1–15-35 McMaster Univ., Hamilton, Canada, 1975.
77. W. Meichsner, K. H. Peters, W. Ullrich, H. Knahl, *J. Met.* **26** (1974) no. 4, 55–58.
78. in [75] p. 441.
79. in [75] p. 448.
80. H. Nashiwa, S. Yamaguchi, M. Takano, M. Iwami, *Sumitomo Kinzoku* **27** (1975) 207–211.
81. W. H. Duquette: *Open Hearth Conf. Proc.*, TMS-AIME, **56** (1973) 79.
82. P. F. Potocic, K. G. Leewis, *Gießerei* **46** (1959), pp. 3-1–3-19.
83. W. A. Voronova, *Steel USSR* **4** (1974) 261.
84. L. G. Nelson, *Proc. Ironmaking Conf.* **34** (1975) 451–459.
85. P. Koros, R. G. Petrushka, in [80], pp. 7-1–7-25.
86. Fédération européenne de produits réfractaires *PRE Refractory Materials*, PRE Administrative Secretariat, Rue de Colonies 18–24, Boîte 17, B 1000, Brussels.
87. *Stahleisen-Werkstoffblätter* 912 bis 917, Verlag Stahleisen, Düsseldorf 1984.
88. *Refractory Engineering — Materials, design, construction*, Vulkan-Verlag, Essen 1996.
89. M. Koltermann, "Refractories from the European View Point. Development and Trend of Refractories in the Steel Industry", *Taikabutsu Overseas* **4** (1984) no. 3, pp. 3–13.
90. Y. Naruse: *Future Trend and Development of Refractories Industry in Japan*, Proceedings of 2nd International Conference on Refractories, The Technical Association of Refractories Japan, Tokyo 1987, pp 3–60.
91. Institut für Gesteinshüttenkunde der RWTH Aachen, *Feuerfeste Werkstoffe für die Herstellung und den Transport von Roheisen*, 31. Internationales Feuerfestkolloquium, Aachen, 10.–11. Oktober 1988.
92. M. Koltermann, "Feuerfeste Stoffe für Hochtemperaturwinderhitzer", *Stahl Eisen* **95** (1975) 847–850.
93. M. Koltermann, "Torpedo ladle Refractories in West Germany", *Taikabutsu Overseas* **5** (1985) no. 2, 35–40.
94. M. Koltermann, "Feuerfeste Baustoffe 1980 bis 1990 — Rückblick und Prognosen", Stahl und Eisen 111 (1991) no. 8, 41–48.
95. M. Koltermann, "Steelplant Refractories — Tendency in Production, Consumption, Ladle Lining", *Proceedings of the 2nd International Symposium on Refractories*, Beijing, China, November 1992, 135–148.
96. N. Nameishi, B. Nagai, T. Matsumoto, "Overview of refractory technology in the nineties in Japan", *Proceedings of the 2nd International Symposium on Refractories*, Beijing, China, November 1992, 79–105.
97. S. Kataoka, "Refractories for steelmaking in Japan", *UNITECR Proceedings*, vol. 1, Kyoto 1995, 1–27.
98. H. Nakamura, "Carbon-containing bricks for blast furnaces", *Taikabutsu Overseas* **15** (1995) 13–18.
99. H. Nishio, A. Matsuo, "Al_2O_3–SiC–C bricks for torpedo car", *Taikabutsu Overseas* **15** (1995) 39–46.
100. "Statistics", *Taikabutsu Overseas* **16** (1996) no. 3, 58.
101. *Ullmann* 4th ed., **10**, 395.
102. Midrex Corporation, *Direct from Midrex*, vol. 21, no. 3, 2nd quarter, 1996, Charlotte, NC.
103. L. v. Bogdandy, H. J. Engell: *Die Reduktion der Eisenerze*, Springer Verlag, Berlin/Verlag Stahleisen mbH, Düsseldorf 1967.
104. Energie- und Betriebswirtschaftsstelle des Vereins Deutscher Eisenhüttenleute (eds.): *Anhaltszahlen für die Wärmewirtschaft in Eisenhüttenwerken*, 6th ed., Verlag Stahleisen mbH, Düsseldorf 1968.
105. *Energy and the Steel Industry*, International Iron and Steel Institute, Committee on Technology, Brussels 1982.
106. Fédération européenne de produits réfractaires *PRE Refractory Materials*; Recommendations 1985, PRE-Sekretariat, CH-8023 Zürich, Löwenstr. 31.
107. Midrex Corporation, *Direct from Midrex*, vol. 13, no. 4, 3rd quarter 1988, Charlotte, NC.
108. R. Ferrari, F. Colanti, *Iron Steel Eng.* **53** (1975) 57–60.
109. R. Garraway, *Iron & Steelmaker*, June 1996, pp. 27–30.
110. M. Hirsch, R. Husain, P. Weber, H. Eichberger, paper presented at the International Conference "Prereduced Products in Europe", Milan, Italy, Sept. 23–24, 1996.
111. R. L. Stephenson, R. M. Smailer: "Direct Reduced Iron, Iron and Steel" *AIME Annu. Meet. Proc. Sess.* (Warrendale, PA) 1980.
112. L. Formanek, H. Eichberger: *Direktreduktion im Drehrohrofen*, European economic community research project for coal and steel; Document no. 7210-BA/101, 1985.

113. F. Oeters, A. Saatci, *Proc. Tech. Proc. ISS* **6** (1986) 1021.
114. F Oeters, A. Saatci: *Stahl Eisen Report*, "Mass and Heat Balances", Verlag Stahleisen GmbH, Düsseldorf 1987.
115. R. J. Fruehan, K. Ito, B. Ozturk: "Analysis of bath smelting processes for producing iron", *Steel Res.* **60** (1989) no. 3/4, 129–137.
116. J. O. Edström: "Alternative Ironmaking Proccsses", *European Ironmaking Congress*, Aachen 1986.
117. R. B. Smith, M. J. Corbett: "Coal based iron making process", *7th Process Techn. Conf. Proc., AIME*, Toronto 1988, 147–178.
118. F. Oeters, R. Steffen: "Entwicklungslinien der Schmelzreduktion und des Einschmelzens", *4. Kohle-Stahl-Kolloquium*, TU Berlin 1989.
119. S. Eketorp: "Smelting reduction", Process Ironmaking Conference, *Metallurg. Soc. AIME* **27** (1968) 36–39.
120. G. Papst, R. Hauk, W. Kepplinger, F. Ottenschläger: "The Corex process", *Metal. Plant. Technol.* **9** (1986) no. 6, 24, 26, 28, 29.
121. R. Hauk, J. Flickenschild, F,. Ottenschläger: "KR-Process hot metal production on the basis of coals", *6th Process Techn. Conf. Proc., AIME*, Washington 1986, pp. 1031–1039.
122. H. Feichtner, W. Maschlanka, F. Helten: "The COREX-proccss", *Skilling's Min. Rev.* **78** (1989) no. 2, 20–27.
123. H. van der Merwe, W. Kepplinger, R. Hauk, B. Vuletic: "Operation results in the first commercial COREX-plant at ISCOR Pretoria Works", *International Congr. New developments in metallurgical processing Proc.*, vol. 1, VDEh, Düsseldorf 1989.
124. M. Hatano, T. Miyazaki, H. Yamaoka, Y. Kamei: "New Ironmaking process by use of pulverized coal and oxygen", *6th Process Techn. Conf. Proc., AIME*, Washington 1986 pp. 1049–1055.
125. T. Miyazaki, H. Yamaoka, Y. Kamei, F. Nakamura: "A new ironmaking process consisted of shaft type reduction, furnace and cupola type melting furnace", *Trans. Iron Steel Inst. Jpn.* **27** (1987) 618–625.
126. T. Hamada et al.: "Development of Kawasaki smelting reduction process for the reduction of iron and ferroalloys", *Proceedings of the pyrometallurgy 1987* London 1987, pp. 435–459.
127. H. Itaya et al.: "Development of the XR-process", *7th Process Techn. Conf. Proc., AIME*, Toronto 1988, pp. 209–216.
128. L. von Bogdandy, K. Brotzmann, K. Schäfer, H.-G. Geck: *Stahl Eisen* **104** (1984) no. 22, 1143–1148.
129. K. Brotzmann: "New concept and methods for iron and steel production", *70th Stee/making Conference Proceedings, ISS-AIME*; Pittsburgh 1987, pp.3–12.
130. J. A. Innes, J. P. Moodie, I. D. Webb, K. Brotzmann "Direct smelting of iron ore in a liquid iron bath – the HI-smell process", *Process Techn. Conf. Proc., AIME*, Toronto 1988, pp 225–231.
131. J. Barin, M. Lemperle, M. Modigell: "Smelting reduction of iron ore", *Steel Res.* **60** (1989) no. 3/4, 120–121.
132. K. Iwasa et al.: *Curr. Adv. Mat. Proc.* **1** (1988) no. 4, 1085.
133. K. Iwasaki, H. Kawata, K. Yamada, T. Kitagaw: "Integrated test plant work on smelting reduction ironmaking process", *International Congr. New Developments in Metallurgical Processing Proc.*, vol. 1, VDEh, Düsseldorf 1989.
134. N. Tokumitsu et al.: "Development of smelting reduction process using an iron bath", *7th Process Techn. Conf. Proc., AIME*, Toronto 1988, pp. 99–107.
135. J. Harlwig, D. Neuschütz, D. Radke, F. Seelig: "Entwicklung eines Einschmelzverfahrens mit kombinierter Direktreduktion unter Einsatz beliebiger Feinkohlen", *Stahl Eisen* **100** (1980), 535–543.
136. J. Hartwig, D. Neuschütz, D. Radke, W. D. Röpke: "The Krupp COIN Process Combined with Direct Reduction", *UNECE Seminar*, Noordwijkerhout, Netherlands, May 1983.
137. D. Neuschütz, T. Hoster: "Concept and present state of a coal-based smelting reduction process for iron ore fines", *Steel Res.* **60** (1989) no. 3/4, 113–119.
138. P. Collin, H. Stickler: "Ironmaking alternative paves the way to cheaper steel", *Iron Steel Int.* **53** (1980) 81–86.
139. H. Stickler: "Varianten des Elred-Verfahrens", *Stahl Eisen* **104** (1984) 539–541.
140. H. I. Elvander, R. A. Westman: *Iron Steel Eng.* **59** (1982) no. 4, 57–60.
141. H. Elvander, G. Omberg: "Das Inred-Iron-Verfahren für die Roheisenerzeugung", *Stahl Eisen* **104** (1984) 864–866.
142. H. G. Herlitz, B. Johansson, S. O. Santen: "A new family of reduction processes based on plasma technology", *Iron Steel Eng.* **61** (1984) 39–44.
143. J. Feinmann (ed.): *Plasma Technology in metallurgical processing*, Iron and Steel Society, Warrendale 1987, p. 111.
144. *Erste Allgemeine Verwaltungsvorschrift zum Bundes-Immissionsschutzgesetz* (Technische Anleitung zur Reinhaltung der Luft) 27. Febr. 1986.
145. D. Eickelpasch el al., *Stahl Eisen* **100** (1980) no. 6, 260–270.
146. J. A. Philipp et al., *Stahl Eisen* **107** (1987) no. 11, 507–514.
147. H. J. White: *Industrial Electrostatic Precipitation*, Addison-Wesley Publishing Company, Inc., Reading, MA 1963.
148. G. Mayer-Schwinning, R. Rennhack, *Chem. -Ing.-Techn.* **52** (1980) no. 5, 375–383.
149. S. Oglesby, Jr., G. B. Nichols: *Electrostatic Precipitation* (Pollution engineering and technology; 8), Marcel Dekker, New York 1978.
150. R. Bothe, *Stahl Eisen* **88** (1968) no. 25, 1414–1422.
151. H. Kahnwald, *Stahl Eisen* **104** (1984) no. 7, 351–356.
152. P. O. Spawn, T. J. Maslany, *JAPC* **31** (1981) 1060.
153. B. Bussmann et al., *Stahl Eisen* **105** (1985) no.3, 121–130.
154. R. Görgen, W. Theobald, *Stahl Eisen* **97** (1977) no. 14, 657–664.
155. W. Theobald, G. Schnegelsberg, *Berghüttenmann Monatsh.* **116** (1971) no. 9, 328–340.
156. G. Metcalf, G. Eddy: *Wastewater Engineering*, McGraw-Hill Book Company, Boston 1979.
157. L. L. Beranek: *Noise Reduction*, McGraw-Hill Book Company, London 1960.

158. K. Althoff, *Stahl Eisen* **107** (1987) no. 22, 1071–1075.
159. H. U. Haering et al., *Stahl Eisen* **102** (1982) no. 15/16, 749–754.
160. J. A. Philipp, H. Maas, *Stahl Eisen* **104** (1984) no. 8, 403–407.
161. E. Mertins, *Erzmetall* **39** (1986) no. 7/8, 399–404.
162. H. Serbent, *Techn. Mitt.* **71** (1978) no. 11/12, 569–575.
163. G. Meyer et al., *Stahl Eisen* **96** (1976) no. 24, 1228–1233.
164. H. Maczek, R. Kola, *J. Met.* **32** (1980) no. 1, 53–58.
165. G. Kossek et al., *Erzmetall* **32** (1979) no. 3, 135–139.
166. W. Kaas et al., *Stahl Eisen* **98** (1978) no. 24, 1277–1281.
167. *Statistisches Jahrhuch Stahl*, WV 1988, p. 292, 297.
168. K.-H. Peters, H.-B. Lüngen, *Stahl Eisen* **110** (1989) to be published.
169. Ref. [167] p. 318.
170. R. Steffen, H.-B. Lüngen, *Stahl Eisen* **108** (1988) no. 7, p. 67–71.
171. E. Steinmetz, R. Steffen, R. Thielmann, *Stahl Eisen* **106** (1986) no. 9, 37–45.
172. H. E. Cleaves and J. G. Thompson, *The Metal Iron*, McGraw-Hill, New York 1935.
173. H. Remy, *Lehrbuch der anorgischen Chemie*, volume 2, Akademische Verlagsgesellschaft, Leipzig 1961, pp. 299–344.
174. K. Mudrak, G. Stobbe: "Anwendung der Simultanfällung zur Phosphateliminierung", *Wasser Luft Betr.* **18** (1974) no. 5, 289–293.
175. K. I. Dahlquist, L. Hall, L. Bergmann: "Eliminierung von Phosphaten mit zweiwertigem Eisensulfat in der Kläranlage Käppala (S)", *Wasser Luft Betr.* **20** (1976) no. 5, 107–112.
176. A. Heitmann, P. Reher, *Chem. Ing. Tech.* **46** (1974) 592–593.
177. Standard Messo, DE-OS 30 30 964 A1, 1980 (H. D. Kutta).
178. Enteco Impianti SpA, DE-OS 29 37 131, 1979 (L. Piccolo, A. Paolinelli, A. Rovele).
179. K. H. Linder et al.: *Materialien*, "Rückstände aus der Titan Dioxid Produktion", vol. 2/76, Umweltbundesamt, Berlin 1982, pp. 96 ff.
180. Aktieselskabet Aalborg Portland Cement Fabrik, EP 01 60 747, 1981 (P. L. Rasmussen).
181. J. Latorezai, I. Nagy, I. Kalo, J. Mihaleczku, HU 24 384, 1979.
182. M. Munemori, T. Aoki, Y. Inove, in K. B. Pojasek (ed.): *Toxic and Hazardous Waste Disposal*, "Simultaneous removal of hazardous metals from waste water and disposal of the resultant sludge", Ann Arbor Science Publishers, Ann Arbor 1980, pp. 97–105.
183. *Dangerous Prop. Ind. Mater. Rep.* 7 (1987) no. 1, 55–60.
184. W. S. Spector: *Handbook of Toxicology*, vol. 1, W. B. Saunders Co., Philadelphia–London 1956.
185. Kronos Titan GmbH, DE 27 10 969, 1977 (A. Hartmann, A. Kulling, D. Schinkitz, E. Klein).
186. Kronos Titan GmbH, DE 30 30 558, 1980 (A. Hartmann, D. Schinkitz).
187. JANAF, *Thermochemical Tables*, NSRDS-NBS 37, 2nd ed., National Bureau of Standards, Washington, DC, 1971.
188. R. C. Weast et al.: *Handbook of Chemistry and Physics*, 68th ed., CRC Press, Boca Raton, FL, 1987–1988.
189. H. Schäfer, *Z. Anorg. Allg. Chem.* **266** (1951) 269–274.
190. Gmelin, System no. 59 "Eisen", part B, pp. 239–241.
191. R. K. Freier: *Daten für Anorg. und Org. Verb.*, vols. 1 + 2, "Wässrige Lösungen", Walter de Gruyter, Berlin – New York 1978.
192. W. Feitknecht, R. Giovanoli, W. Michaelis, M. Müller, *Helv. Chim. Acta* **56** Fasc. 8 (1973) no. 293, 2847–2856.
193. D. E. Chalkey, R. J. P. Williams, *J. Chem. Soc.* **1955**, 1920–1926.
194. BASF, DE 1 592 222, 1967 (K. Opp et al.).
195. BASF, DE 830 787, 1948 (H. Schlecht).
196. *Houben-Weyl*, "Halogenverbindungen", **V/3**.
197. *Synthetica Merck*, vol. I, Merck AG, Darmstadt 1969, pp. 182–189.
198. R. Klute, *Entsorgungspraxis* **11** (1987) 536–548.
199. *Chemical Economics Handbook*, SRI International, Nov. 1995.
200. *Jpn Chem. Week*, Sept. 9, 1987, p. 2.
201. G. von Hagel, *Korresp. Abwasser* **33** (1969) no. 10, 908–915.
202. DOW, US 1 938 461, 1932 (C. F. Prutton).
203. M. Berthelot, *C. R. Hebd. Seances Acad. Sci.* **112** (1891) 1343.
204. L. Mond, L. Quincke, *J. Chem. Soc.* **1891**, 604.
205. W. A. Herrmann, *Chem. Unserer Zeit* **22** (1988) no. 4, 113–122.
206. R. Boese, D. Blaeser, *Z. Kristallogr.* **193** (1990) nos. 3–4, 289–290.
D. Braga, F. Grepioni, A. G. Orpen, *Organometallics* **12** (1993) no. 4, 1481–1483.
207. Produkt-Merkblatt GAF 1977.
208. F. L. Ebenhöch: *Pentacarbonyl Iron Brochure*, BASF Aktiengesellschaft, Ludwigshafen 1988.
209. *Gmelin*, Eisenorganische Verbindungen, **B3**, pp. 1–247.
210. *Gmelin*, no. 59, Eisen, Teil **B**, pp. 486–498.
211. *Ullmann*, 4th ed., **10**, 417–418.
Greenwood–Earnshaw: *Chemie der Elemente*, VCH Verlagsgesellschaft, Weinheim 1988.
212. W. Hieber, F. Leutert, *Ber. Dtsch. Chem. Ges.* **64** (1931) 2831.
213. W. Hieber, F. Leutert, *Naturwissenschaften* **19** (1931) 360.
214. W. Hieber, F. Leutert, *Z. Anorg. Allg. Chem.* **204** (1932) 145.
215. W. Hieber, *Z. Anorg. Allg. Chem.* **204** (1932) 165.
216. Ch. Eischenbroich, A. Salzer: *Organometallchemie*, Teubner, Stuttgart 1986, pp. 243–245.
217. J. Dewar, H. O. Jones, *Proc. R. Soc. (London) Ser. A* **76** (1905) 558–577.
218. E. Speyer, H. Wolf, *Chem. Ber.* **60** (1927) 1424.
219. J. Dewar, H. O. Jones, *Proc. R. Soc. (London) Ser. A* **79** (1907) 66.
220. H. Freundlich, E. J. Cuy, *Chem. Ber.* **56** (1923) 2264.
221. P. Chini, *Inorg. Chim. Acta Rev.* **2** (1968) 31–51.

222. W Hieber, G. Brendel, *Z. Anorg. Allg. Chem.* **289** (1957) 324.
223. BASF, DE 928 044, 1953.
224. BASF, DE 948 058, 1952.
225. A. Mittasch, *Angew. Chem.* **41** (1928) 827.
226. H. Pichler, H. Walenda, *Brennst. Chem.* **21** (1940) 134.
227. L. W. Ross, F. H. Haynie, R. F. Hochmann, *J. Chem. Eng. Data* **9** (1964) 339–340.
228. H. E. Charlton, J. H. Oxley, *AIChEJ* **11** (1965) no. 1, 79–84.
229. BASF, DE 499 296, 1924 (A. Mittasch, M. Müller-Cunradi, A. Pross).
230. BASF, DE 634 283, 1934 (L. Schlecht, H. Naumann).
231. W. Hieber, O. Geisenberger, *Z. Anorg. Allg. Chem.* **262** (1950) 15.
232. E. M. Vigdorchik, R. A. Shvartsman, P. P. Shukvostov: *Issled. V. Obl. Metall. Nikelya i Kobalta*, Leningrad 1983, pp. 125–132.
233. BASF, DE 485 886, 1925 (A. Mittasch, C. Müller, L. Schlecht).
234. BASF, DE 442 718, 1925 (M. Müller-Cunradi).
235. W. Reppe, *Justus Liebigs Ann. Chem.* **582** (1953) 116.
236. BASF, DE 753618, 1940.
237. Montecatini, IT 728074, 1966.
238. C. Dufour-Berte, E. Pasero, IT 887 928, 1971.
239. C. Dufour-Berte, E. Pasero, *Chim. Ind. (Milan)* **49** (1967) no. 4, 347–354.
240. Mine Safety Appliances Comp., DE 1 086 460, 1957 (R. A. Morris, R. Heine-Geldern).
241. W. Schäfer, *Fresenius Z. Anal. Chem.* **335** (1989) no. 7, 785–790.
242. BASF, DE 493 874, 1926 (A. Mittasch, C. Müller, E. Linckh).
243. BASF, DE 500 692, 1924 (A. Mittasch, W Schubardt, C. Müller).
244. GAF, US 2 612 440, 1950 (G. O. Altmann).
245. GAF, US 2 914 537, 1957 (D. J. Randall).
246. V. G. Syrkin, I. S. Tolmasky, SU, 1 186 398, 1964.
247. BASF, US 2 851 347, 1956 (L. Schlecht, E. Östereicher, F. Bergmann).
248. BASF, DE 3 428 121, 1984; US 4 652 305, 1985 (F. L. Ebenhöch, R. Schlegel).
249. BASF, DE 528 463, 1927 (W. Meiser, W. Schubardt, O. Kramer).
250. BASF Broschüre, "*Carbonyleisenpulver*", Ludwigshafen 1994.
251. BASF, US 1 840 286, 1926 (E. Hochheim).
252. C. Heck: *Magnetische Werkstoffe und ihre technische Verwendung*, Heidelberg 1975, pp. 79–81, 397–415.
253. F. Durtschmid, L. Schlecht, W. Schubardt, *Stahl Eisen* **52** (1932) 845–849.
254. F. V. Lenel: *Powder Metallugy*, MPIF Princeton, NJ 1980.
255. L. F. Pease, *Metal Powder Report* **43** (1988) no. 4, 242–254.
256. M. Blömacher, D. Weinand, *Metal Powder Report* **43** (1988) no. 5, 328–330.
257. M. Blömacher, D. Weinand, M. Schwarz, E. Langer, *Powder Injection Molding, Advances in Powder Metallurgy & Particulate Materials — 1993*, Vol. 5, Metal Powder Industries Federation, Princeton, NJ.
258. E.-M. Langer, M. Schwarz, H. Wohlfrom, M. Blömacher, D. Weinand, *Prakt. Metallogr.* **33** (1996) 5.
259. Whittaker Corp., US 4 173 018, 1979 (M. Dawson, L. Saffredial).
260. The Dow Corp., US 4 414 339, 1982 (J. Sole, R. R. Harris).
261. H. Dominik, E. Eckert, *Nachrtechn. Z.* **41** (1988) 280–283.
262. A. Mittasch, *Angew. Chem.* **41** (1928) 827–833.
263. G. Böhm, (BASF) World Steel & Metalworking (1982/83).
264. F. L. Ebenhöch, *Prog. Powder Metall.* **42** (1986) 133–140.
265. F. L. Ebenhöch, *Metal Powder Report* **42** (1987) no. 1, 12–14.
266. GAF, *Metal Powder Report* **43** (1988) no. 5, 338–340.
267. BASF, DE 422269, 1924 (A. Mittasch).
268. BASF, DE 2210279, 1972 (F. L. Ebenhöch, K. P. Hansen, H. Stark).
269. BASF, DE 2344196, 1973 (W. Ostertag et al.).
270. W. Ostertag, F. L. Ebenhöch, K. Bittler, G. Wunsch, *Defazet Aktuell* (1979) no. 12, 434–435.
271. BASF, DE 1116643, 1959 (H. Klippel).
272. BASF, DE 2619084, 1976 (W. Ostertag et al.).
273. BASF DE 830946, 1949 (L. Schlecht, G. Trageser).
274. BASF, DE 3208325, 1982 (M. Appl, F. L. Ebenhöch, R. Schlegel, E. Völkl).
275. BASF, WO-A-96/06891, 1994.
276. BASF, DE 1953518, 1969 (F. L. Ebenhöch et al.).
277. BASF, DP 2517713, 1974 (W. Ostertag, G. Wunsch, F. Ebenhoch, E.. Völkl, G. Bock).
278. US 3 441 408, 1964 (H. J. Schladitz).
279. US 3 570 829, 1971 (H. J. Schladitz).
280. H. J. Schladitz, *Z. Metall.* **59** (1968) 18.
281. H. J. Schladitz, W. A. Jesser, D. S. Lashmore, *Z. Appl. Phys.* **48** (1977) 478.
282. Klöckner-Werke AG, US 3955962, 1975 (W. Dawihl, W. Eicke).
283. Klöckner-Werke AG, US 4002464, 1975 (W. Dawihl, W. Eicke).
284. Klöckner-Werke AG, DE-OS 2603951, 1976 (H. Schön, R. Gustke).
285. Fa. W. M. Müller, DE 3206838, 1982 (F. Unterreithmeier).
286. W. Dawihl, W. Eicke, *Powder Metall. Int.* **3** (1971) 75.
287. L. E. Mürr, O. T. Inal, *J. Appl. Phys.* **42** (1971) 3887.
288. H. G. F. Wilsdorf, O. T. Inal, L. E. Mürr, *Z. Metallk.* 69 (1978) no. 11, 701–705.
289. BASF, US 5085690, 1992.
290. BASF, FR 3003352, 1981 (W. Ostertag, K. Bittler, G. Bock).
291. W. Ostertag, N. Mronga, P. Hauser, *Farbe Lack* **93** (1987) no. 12, 973.
292. BASF, EP 05580022, 1992.
293. BASF, US 4344987, 1981 (W. Ostertag, K. Bittler, G. Bock).
294. Xerox Corp., US 4 238 558, 1980 (R. F. Ziolo).
295. XeroX Corp., US 4 245 026, 1981 (R. F. Ziolo).
296. Xerox Corp., GB 1 577 257, 1980 (R. F. Ziolo).
297. BASF, US 4803143, 1989.
298. Oce, US 4443527, 1984.
299. Xerox Corp., US 4 252 671, 1981 (T. W. Smith).

300. Hitachi Maxell Ltd., JP-Kokai 58/137202, 1983.
301. J. M. Ginder, *Encyclopedia of Applied Physics*, Vol. 16, VCH Publishers Inc., 1996.
302. Hazen Research Inc., US 4 229 209, 1980 (J. K. Kindig, R. L. Turner).
303. *Ullmann*, 4th ed., **10**, 417–418.
304. H. Alper in T. Wender, P. Pino (eds.): *Organic Syntheses via Metal Carbonyls*, vol. 2, Wiley Interscience, New York 1977, pp. 545–593.
305. T. Suzuki, O. Yamada, Y. Takahashi, Y. Watanabe, *Fuel Process Technol.* **10** (1985) no. 1, 33–43.
306. Pentanyl Corp., US 4451351, 1984 (C. R. Porter, H. D. Kaesz).
307. D. Racz, I. Lorincz, B Toth, A. Kassay, HU 15890, 1975.
308. P. Kolocsai, D. Danoczy, K. Heberger, D. Racz, HU 35768, 1983.
309. BASF, DE 441179, 1925 (M. Müller-Cunradi).
310. BASF, DE 486596, 1927 (A. Schneevoigt).
311. BASF, DE 3707713, 1988 (W. Kochanek, B. Leutner, D. Schläfer).
312. J. P. Collmann, *Acc. Chem. Res.* **8** (1975) 342–347.
313. BASF, DE 3837309, 1988.
314. Asahi Chem. Ind., JP 86/225320–225328, 1985 (K. Nahamura, Y. Komatsu).
315. H. Tributsch et al., *Mater. Res. Bull.* **21** (1986) 1481–1487.
316. H. W. Armit, *J. Hyg.* **8** (1908) 565.
317. Letter from BASF Corporation to USEPA submitting enclosed follow-up information concerning enclosed reports and studies on iron pentacarbonyl with attachments (1991) NTIS order No.: NTIS/OTS0529732.
318. F. W. Sundermann et al., *Arch. Ind. Health* **19** (1959) 11.
319. Initial submission: an acute inhalation toxicity study of iron pentacarbonyl in the rat (final report) with attachments and cover letter dated 022792 (1992) NTIS order No.: NTIS/OTS0535889.
320. W. B. Deichmann, H. W. Gerarde: *Toxicology of Drugs and Chemicals*, Academic Press, New York–London 1969, p. 335.
321. J. C. Gage, *Br. J. Ind. Med.* **27** (1970) 1–18.
322. P. V. Sacks, D. N. Houchin, *Am. J. Clin. Nutr.* **31** (1978) 566–573.
323. R. S. Brief et al., *Am. Ind. Hyg. Assoc. J.* **28** (1967) 21.
324. H. E. Stokinger in: *Patty*, vol. IIA, pp. 1797–1799.
325. *Kirk-Othmer*, **13**, 764–788.
326. *Ullmann*, 4th ed., **10**, 426–428.
327. A. B. Prasad (ed.): *British National Formulary*, British Medical Association and The Pharmaceutical Society of Great Britain, Norwich 1986, pp. 282–288.
328. M. T. Ahmet, C. S. Frampton, J. Silver, *J. Chem. Soc., Dalton Trans.* **1988**, 1159.
329. R. C. Hider, G. Kontoghiorghes, J. Silver, M. A. Stockham, GB-A 2117766, 1983.
330. R. C. Hider, G. Kontoghiorghes, M. A. Stockham, FP-A 107458, 1984.
331. R. C. Hider, H. Kontoghiorghes, J. Silver, M. A. Stockham, EP-A 138421, 1985.
332. R. C. Hider, G. Kontoghiorghes, J. Silver, M. A. Stockham, FP-A 138420, 1985.
333. F. Habashi, "The Aqueous Oxidation of Pyrite, Covellite, and Arsenopyrite" in *Process Mineralogy XII*, edited by R.D. Hagni, The Minerals, Metals & Materials Society, Warrendale, PA, 1995, pp. 343–350.
334. Keramchemie GmbH, DE 3206538, 1986 (H. J. Heimhard, H. J Simon).
335. H. J. Heimhard, G. Hitzemann, *Stahl Eisen* **105** (1985) 1222–1228.
336. G. Diez, P. Nieder, *Ind. Anz.* **87** (1965) no. 56, 1303–1311.
337. Andritz-Ruthner Division, AT 380675, 1984 (H. Krivanec, B. Wasserbauer, D. Gausriegler).
338. H. Mühlberg, J. Mensler, P. Björklund, *Stahl Eisen* **95** (1975) 639–642.
339. Company brochure, Allied Signal Inc. USA, 1987.
340. R. Rituper, *Metall* **43** (1989) no. 9, 854–858.
341. J. L. W. Jolly, C. T. Collins: "Natural Iron Oxide Pigments", *Iron Oxide Pigments*, part 2, Information Circular-Bureau of Mines 8813, Washington 1980.
342. H. Kittel: *Lehrbuch der Lacke und Beschichtungen*, vol. II, Verlag, W. A. Colomb Berlin 1974, p. 109.
343. E. Ack, *Farben Ztg.* 28 (1922/23) 493.
344. M. A. Bouchonnet, *Bull. Soc. Chim. Fr.* (1912) **9** 345.
345. H. Wagner, R. Haug: "Gelbe Eisenoxydfarben", **8d**, *Veröffentlichung des Fachausschusses für Anstrichtechnik bei VDI und VDCh*, VDI-Verlag, Düsseldorf 1934.
346. I. G. Farbenind, US 1813649, 1929 (P. Weise).
347. Minnesota Mining & Manuf. Co., US 2634193, 1947 (G. E. Noponen).
348. Minnesota Mining & Manuf. Co., US 2452608, 1941 (G. B. Smith).
349. Verein Österr. Eisen- und Stahlwerke, OE 176206, 1952 (E. Petzel).
350. The Nitralloy Corp., US 2592580, 1945 (H. Loevenstein).
351. E. V. Carter, R. D. Laundon, *J. Oil Colour Chem. Ass.*, 1990 (1) 7–15.
352. Bayer, DE 2653765, 1976 (B. Stephan, G. Winter).
353. Bayer, DE 3820499, 1988 (B. Kröckert G. Buxbaum, A. Westerhaus, H. Brunn).
354. Bayer, DE-AS 1191063, 1963 (F. Hund, H. Köller, D. Räde, H. Quast).
355. BASF, DE-OS 2517713, 1975 (W. Ostertag et al.).
356. Magnetic Pigment Co., US 1424635, 1919 (P. Fireman).
357. Ault & Wiberg Co., US 1726851, 1922 (E. H. McLeod).
358. Interchem. Corp., US 2388659, 1943 (L. W. Ryan, H. L. Sanders).
359. C. K. Williams & Co., US 3133267, 1934.
360. Reconstruction Finance Corp., US 2631085, 1947 (L. M. Bennetch).
361. Reymers Holms Gamla Ind., GB 668929, 1950 (T. G. H. Holst, K. A. H. Björned).
362. Glemser, DE 704295, 1937 (O. Glemser).
363. Pfizer, DE-OS 2212435, 1972 (L. M. Bennetch, H. S. Greiner, K. R. Hancock, M. Hoffman).
364. Hollnagel, Kühn, DL 26901, 1960 (M. Hollnagel, E. Kühn).
365. C. K. Williams & Co., US 2620261, 1947 (T. Toxby).

366. West Coast Kalsomine Co., US 1327061, 1917 (R. S. Penniman, N. M. Zoph).
367. National Ferrite Co., US 1368748, 1920 (R. S. Penniman, N. M. Zoph).
368. Frazee, US 1923362, 1927 (V. Frazee).
369. Magnetic Pigment Co., US 2090476, 1936 (P. Fireman).
370. C. K. Williams & Co., US 2111726, 1932 (G. Plews); US 2111727, 1937 (G. Plews).
371. Magnetic Pigment Co., US 2127907, 1937 (P. Fireman).
372. Bayer, DE 902163, 1951 (B. H. Marsh).
373. C. K. Williams & Co., US 2785991, 1952 (L. M. Bennetch).
374. Bayer, FR 1085635, 1953 (F Hund); DE 1040155 1954 (F. Hund).
375. Mineral Pigments, US 2633407, 1947 (D. W. Marsh).
376. I. G. Farbenind., DE 463773, 1925 (J. Laux).
377. I. G. Farbenind., DE 515758 1925 (J. Laux).
378. I. G. Farbenind. DE 551255, 1930 (U. Haberland).
379. Bayer, EP 0249843, 1987 (A. Westerhaus, K. W. Ganter, G. Buxbaum).
380. I. G. Farbenind., DE 466463, 1926 (W. Schubardt, M. Grote).
381. Bayer, EP0014382, 1980 (G. Franz, F. Hund).
382. R. C. Rowe, *Pharm. Int.* **9** (1984) 221–224.
383. Bayer, DE 3326632, 1983 (W. Burow, H. Printzen, H. Brunn, K. Nollen).
384. *Ullmann*, 4th ed. **18**, 623.
385. C. Clauss, E. Gratzfeld in H. Kittel (ed.): *Pigmente*, 3rd ed. Wissenschaftl. Verlags GmbH, Stuttgart 1960.
386. M. F. Dix, A.D. Rae, *J. Oil Colour Chem. Assoc*, **61** (1978) 69.
387. A.Ludi, "Berliner Blau", *Chemie in unserer Zeit* **4** (1988) 22.
388. Degussa *Vossen-Blau-Pigmente*, Frankfurt/M. 1973.
389. "Fotometrische Messung tiefschwarzer Systeme", *Schriftenreihe Pigmente* Nr. 24, Degussa AG, 60287 Frankfurt/M. 1989.
390. G. K. Wertheim et al., *J. Chem Phys.* **54** (1971) 3235.
H. Buser et al., *J. Chem. Soc. Chem. Commun.* **23** (1972) 1299.
391. M. L. Napijalo, V. Stefancic, *Fizika* (*Zagreb*) 8 Suppl. (1976) 16.
392. R. J. Emrich et al., *J. Vac. Sci. Techn. A* **5** (1987) 1307.
393. F. Herren et al., *Inorg. Chem.* **19** (1980) 956.
A. Ludi, *Chem. Unserer Zeit* **22** (1988) 123.
394. Degussa AG, DE 1188232, 1964 (E. Gratzfeld).
395. Degussa AG, DE 976599, 1952 (H. Verbeek, E. Gratzfeld).
396. Chem. Fabrik Wesseling AG, DE 1061935, 1955 (H. Verbeek, E. Gratzfeld).
397. Degussa AG, DE 233669, 1962 (E. Gratzfeld).
398. Degussa AG, DE-OS 1792418, 1968 (E. Gratzfeld, E. Clausen, E. Ott).
399. Degussa AG, DE 1937832, 1969 (E. Gratzfeld).
400. Degussa AG, DE 1949720, 1969 (E. Gratzfeld, E. Kühn).
401. L. Müller-Fokken, *Farbe + Lack* **84** (1978) 489.
402. H. Ferch, H. Schäfer: *18th AFTPV-Kongreßbuch*, Nice 1989, p. 315.
403. "Vossen-Blau zur Färbung von Fungiziden", Schriftenreihe Pigments Nr. 50, Degussa AG, Frankfurt/M. 1985.
404. W. Koblet, *Schweiz. Z. Obst Weinbau* **1** (1965) 8.
405. H. Wiedmer et al.: *Agro-Dok* no. D4341, Sandoz AG, Basel 1977.
406. R. Ciferri: "Le 4 Stagioni" (Montecatine) **4** (1963) no. 2, 2.
407. V. Nigrovic, *Int. J. Rad. Biol.* 7 (1963) 307.
408. V. Nigrovic, *Phys. Med. Biol.* **10** (1965) 81.
409. I. V. Tananayev, *Zh. Neorg. Khim.* **1** (1956) 66.
410. P. Dvorak, *Z. Gesamte Exp. Med.* **89** (1969) 151.
411. P. Dvorak, *Arzneim. Forsch.* **20** (1970) 1886.
412. P. Dvorak, *Z. Naturforsch. B* **26** (1971) 277.
413. V. Nigrovic, F. Bohne, K. Madshus, *Strahlentherapie* **130** (1966) 413.
414. P. Dvorak, *Z. ges. exp. Med.* **151** (1969) 89–92.
415. T. A. Shashina et al., *Gig. Tr. Prof. Zabol.* **1** (1991) 35–36.
416. J. M. Verzijl et al., *Clinical Toxicol.* **31** (1993) 553–562.
417. B. D. Nielsen et al., *Z. Naturforsch.* **45** (1990) 681–690.
418. Degussa AG, unpublished report: Degussa AG US-IT-Nr. 84-0074-DKT (1984) and 88-0083-DKT, 88-0084-DKT (1988a).
419. *NPIRI* (*National Printing Ink Research Institute Raw Materials Data Handbook*) **4** (1983) 21, Napim, New York.
420. Degussa AG, unpublished report: Degussa AG US-IT-Nr. 77-0069-FKT (1977).
421. Degussa AG, unpublished report: Degussa AG US-IT-Nr. 85-0081-DKT, 85-0080-DKT (1985a), 87-0038-DKT, 87-0039-DKT, 87-0040-DKT (1987) and 88-0085-DKT (1988b).
422. F. Leuschner, H. Otto, unpublished (1967); in: *Kosmetische Färbemittel*, Harald Boldt Verlag KG, Boppard 1977.
423. V. Nigrovic et al., *Strahlentherapie* **130** (1966) 413–419.
424. M. Günther, Kernforschungszentrum Karlsruhe, KFK 1326, Gesellschaft für Kernforschung m.b.H., Karlsruhe, unpublished report US-IT-Nr. 70-0001-FKT (1970).
425. P. Dvorak et al.; *Naunyn-Schmiedebergs Arch. Pharmak.* **269** (1971) 48–56.
426. K. Madshus et al., *Int. J. Radiation Biol.* **10** (1966) 519–520.
427. A. K. Madshus, A. Strömme, *Z. Naturforsch.* **A23** (1968) 391–392.
428. J. P. Mulkey et al., *Vet. Human Toxicol.* **35** (1993) 445–453.
429. V. Pai, *West Indian Med. J.* **36** (1987) 256–258.
430. Degussa AG, unpublished report: Degussa AG US-IT-Nr. 85-0082-DGO, 85-0085-DGO, 85-0088-DGO, 85-0078-DGO (1985b).
431. Degussa AG, unpublished report: Degussa AG US-IT-Nr. 79-0046-DKO, 79-0047-DKO, 79-0088-DKO (1979), 85-0079-DKO, 85-0083-DGO (1985c).
432. Armour Research Foundation, US 2694656, 1947 (M. Camras).
433. Bayer, DE 1061760, 1957 (F. Hund).
434. EMI, GB 765464, 1953 (W. Soby).
435. BASF, DE 1204644, 1962 (W Balz, K. C. Malle).

436. VEB Elektrochemisches Kombinat, Bitterfeld, DD 48590, 1965 (W. Baronius, F. Henneberger, W. Geidel).
437. Agfa-Gevaert, DE 1592214, 1967 (W. Abeck, H. Kober, B. Seidel).
438. Bayer, DE 1803783, 1968 (F. Rodi, H.Zirngibl).
439. Pfizer, US 3498748, 1967 (H. S. Greiner).
440. Sakai Chemical Industries, US 4202871, 1980 (S. Matsumoto, T. Koga, K. Fukai, S. Nakatani).
441. A. R. Corradi et al., *IEEE Trans. Magn.* **MAG-20** (1984) 33–38.
442. Bayer, DE 1266997, 1959 (W. Abeck. F. Hund).
443. Y. Imaoka, S. Umeki, Y. Kubota, Y. Tokuoka, *IEEE Trans. Magn.* **MAG-14** (1978) 649.
444. 3M, US 3573980, 1968 (W. D. Haller, R. M. Colline).
445. Hitachi Maxell, DE 2235383, 1972 (Okazoe, Akira).
446. G. Bate, *J. Appl. Phys.* **52** (1981) 2447.
447. M. Kishimoto, S. Kitahata, M. Amwmiya, IEEE *Trans. Magn.* **MAG-22** (1986) 732–734.
448. T. Fujiwara, *IEEE Trans. Magn.* **MAG-23** (1987) 3125.
449. D. E. Speliotis, *IEEE Trans. Magn.* **MAG-25** (1988) 4048.
450. H. Hibst, *Angew. Chem.* **94** (1982) 263.
451. H. Stäblein in F. E . Wohlfarth (ed.): *Ferromagnetic Materials*, vol. 3, North Holland Publ., Amsterdam, Oxford, New York, Tokyo 1982.
452. Toshiba, EP-A 39773, 1980 (H. Endo et al.).
453. Toda, EP-A 150580, 1983 (N. Nagai et al.).
454. Dowa Mining, DE-OS 3527478, 1984 (K. Aoki).
455. Sakai Chemical, DE-OS 3529756, 1984 (S. Jwasaki et al.).
456. Ishihara, EP-A 299332, 1987 (K. Nakata et al.).
457. Ugine Kuhlmann, DE-OS 2003438, 1969 (M. G. de Bellay).
458. Toda, EP-A 164251, 1984 (N. Nagai et al.).
459. Toda, EP-A 232131, 1986 (N. Nagai et al.).
460. Matsushita, EP-A 290263, 1987 (H. Toril et al.).
461. Toshiba, DE 3041960, 1979 (O. Kubo et al.).
462. BASF, DE-OS 3702036, 1987 (G. Mair).
463. R. E. Fayling, *IEEE Trans. Magn.* **MAG-15** (1979) 1567.
464. R. J. Veitch, *IEEE Trans. Magn.* **MAG-26** (1990) 1876.
465. Y. Okazaki et al., *IEEE Trans. Magn.* **MAG-24** (1989) 4057.
466. D. E. Speliotis, *IEEE Trans. Magn.* **MAG-26** (1990).
467. O. Kubo et al., *IEEE Trans. Magn.* **MAG-24** (1988) 2859.
468. Hooker Chemicals & Plastics Corp.: *Ferrophos*, company information, Niagara Falls, NY, and D. E. de Jong bv. Apeldoorn, Holland, 1976.
469. W. Bäumer, *Farbe + Lack* 79 (1973) p. 747.
470. L. M. Greenstein in *Pigment Handbook*, 2nd ed., Vol. 1, J. P. Wiley & Sons, New York 1988, p. 846.
471. K. D. Franz, H. Härtner, R. Emmert, K. Nitta in *Ullmann's Encyclopedia of Industrial Chemistry*, Vol. A20, VCH Verlagsgesellschaft mbH, Weinheim 1992, p. 353.
472. K. D. Franz, R. Emmert, K. Nitta, *Kontakte (Darmstadt)* **2** (1992) p. 3.
473. G. Pfaff, R. Maisch, *Farbe + Lack* **101** (1995) p. 89.
474. R. Glausch, M. Kieser, R. Maisch, G. Pfaff, J. Weitzel in *Perlglanzpigmente*, Curt R. Vincentz Verlag, Hannover 1996, pp. 42–46.
475. Merck KGaA, US 3926659, 1975 (R. Esselborn, H. Bernhard).
476. BASF, US 4344987, 1982 (W. Ostertag, K. Bittler, G. Bock).
477. W. Ostertag, *Nachr. Chem. Techn. Lab.* **42** (1994) p. 849.
478. G. Gehrenkemper, F. Hofmeister, R. Maisch, *Eur. Coat. J.* **3** (1990) p. 80.
479. P. Hauser, N. Mronga, W. Ostertag, *Adv. Org. Coat. Sci. Technol. Ser.* **13** (1991) p. 414.
480. C. Schmidt, M. Friz, *Kontakte (Darmstadt)* **2** (1992) p. 15.
481. US 2558302, 1951 (G. C. Marcot et al.).
482. US 2558304, 1951 (G. C. Marcot et al.).
483. Bayer, DE-OS 2508932, 1975 (F. Hund, G. Linde).
484. Bayer, DE 2210279, 1973 (F. L. Ebenhöch, K.-P. Hansen, H. Stark).
485. BASF, DE 2344196, 1973 (F. L. Ebenhöch, D. Werner, G. Bock).
486. BASF F + F AG, DE-OS 2228555, 1972 (H. Gaedecke, R. Bauer).
487. Magnetic Pigment Comp., US 1424635, 1922 (P. Fireman).
Reichard-Coulston Inc., US 2574459, 1947 (L. H. Bennetch).
488. F. Finus, *Farbe + Lack* 7 (1975) 604–607.
489. G. Narvuglio, R. F. Sharrock, R. J. Kennedy, *Oil J., Col. Chem. Assoc.* **61** (1978) 79–85.
490. M. C. Stopes: "On the petrology of banded bituminous coals", *Fuel* **14** (1935) 4–13.
491. International Committee for Coal Petrology: *Handbook of coal petrography*, 2nd ed., Centre national de la recherche scientifique, Paris 1963.
492. W. Spackman: "The maceral concept and the study of modern environments as a means of understanding the Nature of Coal", *Trans. N. Y. Acad. Sci.* **20** (1958) no. 5, 411–423.
493. M. Teichmuller: "Über neue Macerale der Liptinit-Gruppe und die Entstehung von Micrinit", *Fortschr. Geol. Rheinld. Westfalen* **24** (1974) 37–64.
494. W. H. Ode, W. H. Frederic: "I'he International System of Hard-Coal Classification and Its Application to American Coals", *U.S. Bur. Mines Rep. Invest.* **5435** (1958).
495. M. Teichmuller, R. Teichmuller: "Geological cause of coalification", in R. F. Gould (ed.): "Coal Science", *Adv. Chem. Ser.* **55** (1966) 133–163.
496. P. A. Hacquebard, J. D. Donaldson: "Rank studies of coal in the Rocky Mountains and Inner Foothills Belt Canada", in R. R. Dutcher, P. A. Hacquebard, J. M. Schopf, J. A. Simon (eds.): "Carbonaceous materials as indicators of metamorphism", *Spec. Pap. Geol. Soc. Am.* **153** (1974) 75–93.
497. E. Hryckowian, R. R. Dutcher, F. Dachille: "Experimental studies of anthracite coals at high pressures and temperatures", *Econ. Geol.* **62** (1967) no. 4, 517–539.
498. G. H. Wood, T. M. Kehn, M. D. Carter, W. C. Culbertson: "Coal resource classification system of the U.S. Geological Survey", *Geol. Surv. Circ.* **891** (1983) 65 p.

499. P. Averitt: "Coal resources of the United States", *U.S. Geol. Surv. Bull.* **1412** (1975).
500. J. M. Schopf: "A definition of coal", *Econ. Geol.* **51** (1956) 521–527.
501. R. Thiessen: "What is coal?", *Int. Circ. U.S. Bur. Mines* **7397** (1947) 48 p.
502. B. C. Parks, H. J. O'Donnell: "Petrography of American coals", *Bull. U.S. Bur. Mines* **550** (1956) 193 p.
503. M. C. Stopes: "On the four visible ingredients in banded bituminous coals", *Proc. R. Soc. London Ser. B* **90** (1919) 470.
504. M. L. Gorbaty, K. Ouchi (eds.): "Coal Structure", *Adv. Chem. Ser.* **192**, American Chemical Society, Washington, DC, 1981.
505. R. C. Neavel: "Origin, Petrography and Classification of Coal", in M. A. Elliot (ed.): *Chemistry of Coal Utilization*, 2nd suppl. vol., Chap. 3, J. Wiley & Sons, New York, Chichester, Brisbane, Toronto 1981, pp. 91–158.
506. D. W. van Krevelen: *Coal and Its Properties Related to Conversion*, Int. Conference on Coal Conversion, Pretoria, RSA, 16–20 August 1982.
507. R. M. Davidson: *Molecular Structure of Coal*, Rep. No ICTIS/TR 08, Jan. 1980, IEA Coal Research, London.
508. G. R. Gavalas, P. H.-K. Cheong, R. Jain, *Ind. Eng. Chem. Fundam.* **20** (1981) 113–122.
509. G. J. Pitt, G. R. Millward: *Coal and Modern Coal Processing*, An Introduction, Academic Press, London, New York, San Francisco 1979.
510. R. von der Gathen, K.-H. Kubitza, B. Bogenschneider: "Die Auswirkungen der Vergleichmäßigung von Rohförderkohle auf Kosten und Produkte der Aufbereitung", *Glückauf* **119** (1983) 22–27.
511. M. Hampel: "Großsiebmaschinen für die Vorklassierung in Steinkohlenaufbereitungsanlagen", *Glückauf* **113** (1977) 80–85.
512. K.-H. Kubitza, P. Wilczynski: "Trockene Feinstkornabscheidung in Sichtern: neuere Entwicklungen bei der Ruhrkohle AG", *Glückauf* **110** (1974) 480–484.
513. E. Fellensiek: "Das Setzverhalten unterbettgepulster Feinkorn-Großsetzmaschinen", *Glückauf-Forschungsh.* **39** (1978) 207–212.
514. E. Fellensiek: "Feinkornsortierung auf einer neuartigen, in Doppelfrequenz gepulsten Durchsetzmaschine", *Glückauf-Forschungsh.* **42** (1981) 130–136.
515. S. Heintges: "Die Entwicklung der Schwertrübesortierung von Steinkohlen in del Bundesrepublik Deutschland", *Glückauf* **109** (1973) 955–960.
516. M. Becker: "Der Weg zu den Großraumflotationsanlagen bei der Ruhrkohle AG", *Glückauf* **113** (1977) 952–955.
517. W. Blankmeister, B. Bogenschneider, K.-H. Kubitza, D. Leininger, L. Angerstein, R. Köhling: "Optimierung der Fein- und Feinstkohlenentwässerung im Bereich unter 10 mm", *Glückauf* **112** (1976) 758–762.
518. W. Erdmann: "Neuere Entwicklungen bei der Entwässerung von fein- und feinstkörnigen Steinkohlenerzeugnissen", *Aufbereit. Tech.* **26** (1985) 249–258.
519. D. Leininger, P. Wilczynski, R. Köhling, W. Erdmann, T. Schieder: "Behandlung und Verwertung von Flotationsbergen in der Bundesrepublik Deutschland", *Glückauf* **115** (1979) 467–472.
520. R. von der Gathen: "Möglichkeiten und Grenzen der Entschwefelung von Steinkohle", *Glückauf* **115** (1979) 112–118.
521. W. P. Bethe, G. Koch: "Neue Bauformen für Aufbereitungsanlagen", *Glückauf* **119** (1983) 368–373.
522. W. Erdmann: "Die thermische Trocknung in der Steinkohlenaufbereitung der Bundesrepublik Deutschland", *Aufbereit. Tech.* **19** (1978) 581–586.
523. D. Rebb: "Latest Design in Coal Pipelining", *Can. Min. J.* **104** (1983) no. 3, 20–22.
524. T. Wheeler: "Hydraulic Transport of Coal: Slurry Pipelines", *Mine Quarry* **14** (1985) 35–38.
525. J. R. Siemon: "Economic Potential of Coal–Water Mixtures", *IEA Coal Res.*, London, Sept. 1985.
526. S. Furfari: "Hydropyrolysis of Coal", *IEA Coal Res.*, London, Oct. 1982.
527. E. Ahland, F. Friedrich, I. Romey, B. Strobel, H. Weber, *Erdöl Erdgas* **102** (1986) no. 3, 148–154.
528. A. G. Comalli, J. B. MacArthur, H. H Stotler: "H-Coal Process Demonstrations, Development and Research Activities", *Prepr. Pap. Am. Chem. Soc. Div. Fuel Chem.* **27** (1982) no. 3/4, 104–113.
529. D. T. Wade, L. L. Ansell, W. R. Epperly: "Coal liquefaction", *CHEMTECH* **1982**, no. 4, 242–249.
530. W. G. Schützendübel: "SRC II", *Energie* **32** (1980) no. 6/7, 254–259.
531. K. Uesugi: "The Status of Coal Liquefaction Technology Development in Japan", *Int. Working Forum of Coal Liquefaction*, Atlanta, GA, Apr. 4–9, 1986.
532. J. M. Lee, R. V. Nalitham, C. W. Lamb: "Recent developments in Two-Stage Coal Liquefaction at Wilsonville", *Prepr. Pap. Am. Chem. Soc. Div. Fuel Chem.* **31** (1986) no. 2, 316–324.
533. G. Franken, W. Adlhoch, W. Koch, *Chern. Ing. Tech.* **52** (1980) 324–327.
534. K. A. Theis, E. Nilschke: "Make Syngas from Lignite", *Hydrocarbon Process.* **66** (1982) no. 9, 233–237.
535. H.-D. Schilling, B. Bonn, U. Krauß: *Kohlenvergasung*, 3rd ed., vol. 22: "Bergbau, Rohstoffe, Energie", Verlag Glückauf, Essen 1982.
536. H.-D. Schilling, B. Bonn, U. Krauß: "Coal Gasification", Graham & Trotmann, London 1981.
537. R. Specks, *Glückauf* **119** (1983) no. 23, 1147–1159.
538. P. Nowacki (ed.): "Coal Gasification Processes", *Energy Technology Review No. 70*, Noyes Data Corp., Park Ridge, NJ, 1981.
539. H. Teggers, H. Jüntgen, *Erdöl Kohle Erdgas Petrochem.* **37** (1984) no. 4, 163–173.
540. J. M. Caffin: "Industrial Coal Gasification; Technology, Applications and Economics", *Energy Prog.* **4** (1984) no. 3, 131–137.
541. M. Teper, D. F. Hemming, W. C. Ulrich, EAS-Report E2/80, London, January 1983.
542. S. A. Elmquist et al., DOE/FE/05147-1488, May 1983.
543. M. K. Schad, C. F. Hafke, CEP May 1983, 45–51.
544. K. V. S. Sastry, D. W. Fuerstenau, EPRI CS-2198, Project 1030-1, January 1982.
545. F. P. Calhoun, *Min. Congr. J.* **49** (1962) 38–39.
546. N. Galbenis, O. Abel, J. Lehmann, W. Peters, *Erdöl Kohle Erdgas Petrochem.* **34** (1981) 59–65.
547. F. H. Beckmann, *Stahl Eisen* **100** (1980) 803–813.

548. E. Dunger, P. Dittmann, H. Reißmann, *Neue Bergbautech.* **10** (1980) 427–430.
549. H. Krug, W. Naundorf, *Energietechnik* **31** (1981) 62–68, 228–232.
550. R. Kurtz, *Braunkohle (Düsseldorf)* **32** (1980) 368–372, 443–448.
551. A. F. Baker, R. E. McKeever, A. W. Deurbrouck, DOE, RI-PMTC-12 (82), March 1982.
552. M. A. Colaluca, TENRAC/EDF-043, July 1981.
553. H. P. Hudson, J. E. Landon, J. H Walsh: *The Canadian Mining and Metallurgical Bull. for January 1964*, Montréal, pp. 52–58.
554. K. V. S. Sastry, V. P. Mehrotra, 3rd Int. Symp. Agglomeration, Nürnberg, May 1981, H 36–38.
555. E. Ahland, J. Lehmann, *Erdöl Kohle Erdgas Petrochem.* **34** (1981) 402–407.
556. H.-G. Schäfer, 3rd Int. Symp. Agglomeration, Nürnberg, May 1981, S 53–55.
557. M. Schad, D. Sauter et al., BMFT-FB-T-85, Oct. 1985, pp. 108–109.
558. G. H. Cady, *Illinois Geological Survey Report of Investigations*, no. 35, 1935, pp. 25–39.
559. H. J. Gluskoter, J. A. Simon, *Illinois Geologual Survey Circular*, no. 432, 1968, p. 28.
560. C. N. Kravits, J. C. Crelling, *Int. J. Coal Geol.* **1** (1981) 195–212.
561. *Survey of Energy Resources*, World Energy Council.
562. *BP Statistical Review of World Energy*, June 1995.
563. *1993 Energy Statistics Yearbook*, United Nations, 1995..
564. D. D. Whitehurst, T. O. Mitchell, M. Farcasiu: *Coal Liquefaction*, Academic Press, New York 1980.
565. T. Green, J. Kovac, D. Brenner, J. Larsen in R. A. Meyers (ed.): *Coal Structure*, Academic Press, New York 1982, pp. 199–282.
566. D. W. Van Krevelen: *Coal: Typology-Chemistry-Physics-Constitution*, Elsevier, Amsterdam 1961.
567. M. R. Khan, Ph. D. Thesis, The Pennsylvania State Univ., 1985.
568. R. Loison, A. Peytavy, A. Boyer, R. Grillot in H. H. Lowry (ed.): *Chemistry of Coal Utilization*, Suppl. vol., J. Wiley & Sons, New York 1963, pp. 150–201.
569. D. Hebermehl, F. Orywal, H. Beyer in M. A. Elliott (ed.): *Chemistry of Coal Utilization*, 2nd Suppl. vol., J. Wiley & Sons, New York 1981, pp. 317–351.
570. J. T. Senftle, Ph. D. Thesis, The Pennsylvania State Univ., 1982.
571. D. J. Maloney, M. S. Thesis, The Pennsylvania State Univ., 1980.
572. M. R. Khan, M. S. Thesis, The Pennsylvania State Univ., 1985.
573. M. S. Lancet, F. A. Sim, *Am. Chem. Soc., Div. Fuel Chem., Prepr.* **26** (1981) no. 3, 167.
574. M. R. Khan, R. G. Jenkins, *Fuel* **63** (1984) 109–115.
575. M. Kaiho, Y. Toda, *Fuel* **58** (1979) 397.
576. D. J. Maloney, Ph. D. Thesis, The Pennsylvania State Univ., 1983.
577. A. F. Boyer: *Proc. International Conference on Chemical Engineering in Coal Industry*, Pergamon Press, Paris 1957, p. 141.
578. O. P. Mahajan, M. Komatsu, P. L. Walker, Jr., *Fuel* **59** (1980) 3.
579. B. S. Ignasiak, A. J. Szladow, D. S. Montgomery, *Fuel* **53** (1974) 12.
580. P. C. Painter, M. M. Coleman, R. W. Snyder, O. P. Mahajan et al., *Appl. Spectrosc.* **35** (1981) 106.
581. C. Rhoads, J. T. Senftle, M. M. Coleman, A. Davis et al., *Fuel* **63** (1984) 245–250.
582. M. R. Khan, R. G. Jenkins, *Fuel* **65** (1986) 1291.
583. M. R. Khan, R. C. Jenkins, *Fuel* **65** (1986) 1203.
584. S. K. Chakrabartty, S. Parkash, N. Berkowitz, *Fuel* **55** (1976) 270.
G. F. Crewe, U. Gat, V. Dhir, *Fuel* **54** (1975) 20.
A. C. Cunningham, W. F. Wyss, *Fuel* **46** (1967) 137.
W. R. Epperly, H. M. Siegel: *Proc. of 11th Symposium Intersociety Energy Conversion Engineering Conference*, State Line, Nevada, Sept. 12–17, 1976, pp. 249–267.
Y. Nishiyamo, Y. Tamai, *Fuel* **57** (1978) 559.
J. W. Patrick, F. H. Shaw, *Fuel* **51** (1972) 69.
R. H. Schlosberg, M. L. Gorbaty, R. L. Lang, *Fuel* **57** (1978) 424.
585. M. R. Khan, R. G. Jenkins: *Proc. International Conference on Coal Science*, Int. Energy Agency (IEA), Pittsburgh, PA, 1983, pp. 495–498.
586. M. R. Khan, R. G. Jenkins, *Fuel Process. Technol.* **8** (1984) 307–311.
587. E. Audibert, *Fuel* **5** (1926) 229.
588. E. Audibert, L. Delmas, *Fuel* 6 (1927) 131–140, 182–189.
589. J. G. Bennett, *J. Inst. Fuel* **14** (1941) 175.
590. S. R. Illingworth, *Fuel* **1** (1922) 3–6, 17–19, 33–35, 65–67.
591. R. Thiessen, *Ind. Eng. Chem.* **24** (1932) 1032.
592. R. G. Atkinson, R. E. Brewer, J. D. Davis, *Ind. Eng. Chem.* **29** (1937) 840–844.
593. H. L. Riley, H. E. Blayden, J. Gibson: *Proc. Conference Ultrafine Structure of Coals and Cokes*, British Coal Utilization Research Assn. (BCURA), London 1943, pp. 176–231.
594. H. R. Brown, P. L. Waters, *Fuel* **45** (1966) 17–41.
595. W. Hirst in [593], pp. 80–94.
596. N. Berkowitz: *An Introduction to Coal Technology*, Academic Press, New York 1979.
597. D. H. Bangham, F. A. P. Maggs: *Proc. Conference Ultrafine Structure of Coals and Cokes*, BCURA, 1944, p. 118.
598. I. G. C. Dryden, M. Griffith, *BCURA Rev.* **134** (1954) 62.
599. D. Fitzgerald, *Trans. Faraday Soc.* **52** (1956) 362–369.
600. R. C. Neavel in M. L. Gorbaty, J. W. Larsen, I. Wender (eds.): *Coal Science*, vol. 1, Academic Press, New York 1982, pp. 1–19.
601. P. H. Given: *Coal Agglomeration and Conversion Symposium*, Morgantown, WV, 1975.
602. L. Grainger: *Coke Oven Managers Association Yearbook*, Mexborough U.K., 1975, p. 282.
603. J. Dartnell, *Ironmaking Steelmaking* **1** (1978) 18–24.
604. P. Ramdohr, *Eisenhüttenwesen* **1** (1928) 669.
605. C. E. Marshall, *Fuel* **24** (1945) 120.
606. E. Stach in H. Freund (ed.): *Handbuch der Mikroskopie in der Technik*, vol. 2, Verlag Umschau, Frankfurt 1952, Part 1, p. 411.
607. C. Abramski, M. T. Mackowsky in [606], p. 311.
608. B. Alpern, *Brennst. Chem.* **37** (1956) 194.
609. G. H. Taylor, *Fuel* **40** (1961) 465.
610. J, D. Brooks, G. H. Taylor, *Carbon* **3** (1965) 185.

611. H. Marsh, *Fuel* **52** (1973) 205.
612. J. W. Patrick, M. J. Reynolds, F. H. Shaw, *Fuel* **52** (1973) 198.
613. H. Marsh, F. Dachille, M. Iley, P. L. Walker, Jr. et al., *Fuel* **52** (1973) 253.
614. A. Grint, U. Sweitlik, H. Marsh, *Fuel* **58** (1979) 642.
615. A. Grint, H. Marsh, *Fuel* **60** (1981) 1115.
616. H. Marsh, P. L. Walker, Jr., *Fuel Process. Technol.* **2** (1979) 61–75.
617. H. Marsh, J. Smith in C. Karr (ed.): *Analytical Methods for Coal and Coal Products*, vol . 2, Academic Press, New York 1978, pp. 371–414.
618. H. Marsh, P. L. Walker, Jr. in P. L. Walker, Jr., P. A. Thrower (eds.): *Chemistry and Physics of Carbon*, vol. 15, Marcel Dekker, New York 1979, pp. 229–286.
619. E. Fitzer, K. Müller, W. Schäfer, in P. L. Walker, Jr. (ed.): *Chemistry and Physics of Carbon*, vol. 7, Marcel Dekker, New York 1971, pp. 237–383.
620. J . D. Brooks, G. H . Taylor, *Chemistry and Physics of Carbon*, vol. 4, Marcel Dekker, New York 1968, pp. 243–286.
621. H. Marsh, R. C. Neavel, *Fuel* **59** (1980) 511.
622. I. C. Lewis, *Carbon* **20** (1982) 519.
623. W. J. Schmidt in H. Freund (ed.): *Handbuch der Mikroskopie in der Technik*, vol. 1, Verlag Umschau, Frankfurt 1957, Part 1, p. 147.
624. E. A. Rosauer: *Instruments for Materials Analysis*, Iowa State Univ. Press, Ames 1981.
625. J. L. White in J. O. McCaldin, G. Somorjai (eds.): *Progress in Solid-State Chemistry*, vol. 9, Pergamon Press, Oxford 1974, pp. 59–104.
626. R. A. Forrest, H. Marsh, *Carbon* **15** (1977) 348.
627. G. D. Mitchell, A. Davis, W. Spackman in R. T. Ellington (ed.): *Liquid Fuels from Coal*, Academic Press, New York 1977, pp. 255–270.
628. H. E. Newall, F. S. Sinnatt, *Fuel* **3** (1924) 424.
629. P. J. Street, R. P. Weight, P. Lightman, *Fuel* **48** (1969) 342.
630. M. Von Heimendahl: *Electron Microscopy of Materials – An Introduction*, Academic Press, New York 1980.
631. H. Marsh, C. Cornford in M. L. Deviney, T. M. O'Grady (eds.): *Petroleum Derived Carbons, Amer. Chem. Soc. Symposium Series 21*, Amer. Chem. Soc., Washington, DC, 1976, pp. 266–281.
632. J. N. Murrell, E. A. Boucher: *Properties of Liquids and Solutions*, J. Wiley & Sons, New York 1982, pp. 92–95.
633. F. Reinitzer, *Monatsh. Chem.* **9** (1888) 421.
634. O. Lehmann, *Z. Phys. Chem. (Frankfurt am Main)* **4** (1889) 462.
635. G. Friedel, *Ann. Phys. (Paris)* **18** (1922) 273.
636. F. D. Saeva (ed.): *Liquid Crystals*, Marcel Dekker, New York 1979.
637. I. Mochida, K. Maeda, K. Takeshita, *Carbon* **16** (1978) 459.
638. I. C. Lewis, *Carbon* **16** (1978) 503.
639. J. L. White in M. L. Deviney, T. M. O'Grady (eds.): *Petroleum Derived Carbons, Amer. Chem. Soc. Symposium Series 21*, Amer. Chem. Soc., Washington, DC, 1976, pp. 282–314.
640. J. Dubois, C. Agache, J. L. White, *Metallography* **3** (1970) 337–369.
641. T. Imamura, Y. Yamada, S. Oi, H. Honda, *Carbon* **16** (1978) 481.
642. K. J. Hüttinger, *Carbon* **10** (1972) 5.
643. I. C. Lewis, L. S. Singer in P. L. Walker, Jr. (ed.): *Chemistry and Physics of Carbon*, vol. 17, Marcel Dekker, New York 1981, pp. 1–88.
644. T. Yokono, H. Marsh in H. D. Shultz (ed.): *Coal Liquefaction Products*, vol. 1, J. Wiley & Sons, New York 1983, pp. 125–138.
645. Ref. [566], pp. 445–452.
646. I. G. C. Dryden in [568], pp. 262–268.
647. P. H. Given, *Fuel* **39** (1960) 147.
648. J. W. Patrick, M. J. Reynolds, F. H. Shaw, *Carbon* **13** (1975) 509.
649. F. Goodarzi, D. G. Murchison, *Fuel* **57** (1978) 273.
650. L. Grainger, J. Gibson: *Coal Utilization Technology, Economy and Policy*, Holsted Press, London 1981, pp. 137–150.
651. M. Forrest, H. Marsh in E. L. Fuller, Jr. (ed.): *Coal and Coal Products: Analytical Characterization Techniques, Amer. Chem. Soc. Symposium Series 205*, Amer. Chem. Soc., Washington, DC, 1982, pp. 1–25.
652. R. H. Essenhigh in C. Y. Wen, E. S. Lee (eds.): *Coal Conversion Technology*, Addison-Wesley, Reading, MA, 1979, Chapter 3.
653. J. B. Howard in [569], Chapter 12.
654. A. W. Scaroni, P. L. Walker, Jr., R. G. Jenkins, *Fuel* **60** (1981) 558.
655. M. E. Morgan, R. G. Jenkins in H. H. Shobert (ed.): *The Chemistry of Low-Rank Coals, Amer. Chem. Soc. Symposium Series 264*, Amer. Chem. Soc., Washington, DC, 1984, p. 213.
656. R. F. Probstein, R. E. Hicks: *Synthetic Fuels*, McGraw-Hill, New York 1982.
657. P. R. Solomon, D. G. Hamblen, *Prog. Energy Combust. Sci.* **9** (1983) 323.
658. H. Jüntgen, K. H. van Heek, *Fuel Process. Technol.* **2** (1979) 261.
659. N. Y. Nsakala, R. H. Essenhigh, P. L. Walker, Jr., *Combust. Sci. Technol.* **16** (1977) 153.
660. G. R. Gavalas, P. H. K. Cheong, R. Jain, *Ind. Eng. Chem., Fundam.* **20** (1981) 113.
661. D. B. Anthony, J. B. Howard, *AIChE J.* **22** (1976) 625.
662. R. Aris, G. R. Gavalas, *Philos. Trans. R. Soc. London. Ser. A* **260** (1966) 43.
663. A. Szladow, P. Given, *Ind. Eng. Chem. Process Des. Dev.* **20** (1981) 27.
664. S. V. Golikeri, D. Luss, *AIChE J.* **18** (1972) 277.
665. P. L. Walker, Jr., R. G. Jenkins, L. R. Radovic: "Importance of Active Sites for Char Gasification in Oxygen (Air) and CO_2", Final Report, Gas Research Institute, Chicago, Oct., 1982.
666. J. L. Johnson in [569], Chapter 23.
667. F. Moseley, D. Paterson, *J. Inst. Fuel* 40 (1967) 523.
668. G. J. Pitt, G. R. Millward (eds.): *Coal and Modern Coal Processing. An Introduction*, Academic Press, New York 1979, p. 152.
669. L. Seglin, S. A. Bresler in [569], pp. 785–846.
670. M. R. Khan, T. Kurata: "The Feasibility of Mild Gasification of Coal: Research Needs", U.S. Dept. of Energy, Morgantown Energy Technology Center, Technical Note TM-85/4019, 1985, NTIS DE 85013625.

671. P. J. Wilson, Jr., D. D. Clendenin in [568], Chapter 10.
672. G. S. Pound, *J. Inst. Fuel* **25** (1952) 355.
673. M. O. Holwatey in R. A. Meyers (ed.): *Coal Handbook*, Marcel Dekker, New York 1981, Chapter 9.
674. F. Denig in H. H. Lowry (ed.): *Chemistry of Coal Utilization*, vol. 1, J. Wiley & Sons, New York 1945, Chapter 24.
675. J. Speight in J. Falbe (ed.): *The Chemistry and Technology of Coal*, Marcel Dekker, New York 1983, Chapter 12.
676. E. Ahland, G. Nashan, W. Peters, W. Weskamp in J. Falbe (ed.): *Chemical Feedstocks from Coal*, J. Wiley & Sons, New York 1982, pp. 12–77.
677. A. E. Williams, L. O. Smith, K. A. König, K. A. Basciani, *Iron Steel Eng.* **60** (1983, May) 45.
678. N. Nakamura, Y. Togino, T. Adachi, *Ironmaking Steelmaking* **5** (1978) no. 2, 49–60.
679. T. F. Edgar: *Coal Processing and Pollution Control*, Gulf Publ. Co., Houston 1983, Chapter 6.
680. W. Eisenhut in [569], Chapter 14.
681. P. W. Chang, K. Durai-Swamy, F,. W. Knell, *Coal Process. Technol.* **6** (1980) 20.
682. C. L. Oberg, A. Y. Falk, *Coal Process. Technol.* **6** (1980) 159.

6 Steel

Dieter Schauwinhold (§§ 6.1, 6.7.1); Manfred Toncourt (§ 6.2); Rolf Steffen (§ 6.3.1); Dieter Janke (§ 6.3.2); Klaus Schäfer (§§ 6.3.3–6.3.4); Rudolf Hammer †, Hatto Jacobi (§§ 6.3.5.1–6.3.5.3); Robert Hentrich (§ 6.3.5.4); Lothar Kucharcik (§ 6.3.5.5); Roger Pankert (§§ 6.4–6.5); Hans Hougardy (§ 6.6.1); Hans-Jürgen Grabke (§ 6.6.2); Winfried Dahl (§ 6.6.3); Reinhard Winkelgrund (§ 6.7.2); Volker Brückmann, Heinz-Lothar Bünnagel (§ 6.8)

6.1 Introduction

Nowadays the term steel is understood to include not only all forgeable iron-based materials, but also all highly alloyed metallic materials in which the element iron is an important component, but which are not necessarily forgeable. With few exceptions, the carbon content is < 2%.

For over 3000 years, steel has made a major contribution to human development, e.g., in tools for cultivating the soil and processing stone and almost all other materials, as a construction material for steel and reinforced concrete structures, in transport technology, for the generation and distribution of energy, for the fabrication of machinery and equipment (including equipment for the manufacture of plastics), in the household, and in medicine. It remains, for the foreseeable future, by far the most important material for the maintenance and improvement of our quality of life.

The outstanding importance of steel is the result of its ready availability and its versatility. The earth's crust contains ca. 5% iron, making it the fourth most abundant element after oxygen (46%), silicon (28%), and aluminum (8%). Rich deposits of iron ores are available in many parts of the world. Moreover, the free energy required to isolate iron from its oxidic ores is less than half of that required for aluminum [1]. The versatility of steel is due to the polymorphism of the iron crystal and its ability to alloy with other elements, forming solid solutions or compounds. The microstructure of steel in a finished component can be adjusted by means of the chemical composition, the forming conditions and a wide variety of possible heat treatments. The attainable tensile strength ranges from ca. 300 N/mm^2 for deep-drawing sheet steel (e.g., for automotive body parts that are difficult to draw) to > 2000 N/mm^2 for critical components in aircraft. Tensile strengths as high as 2600 N/mm^2 are achieved in 0.15 mm diameter drawn wire for steel cord used in radial tires.

Cryogenic steels with high strength and good toughness at very low temperatures are used for the transport and storage of liquefied gases at temperatures of < –200 °C. Other steels with good properties at temperatures of 650–700 °C and above are used in power station equipment and gas turbines.

Highly developed soft magnetic steels are essential in the construction of transformers. Steel is also used to make permanent magnets. Nonmagnetizable steels have also been developed for use in electrical technology, shipbuilding, and physics research. Wear-resistant steels are used in rock-crushing machines and in industrial stirring equipment. Machine tools, used for metal cutting, require steels of the highest possible hardness to endow stability to the cutting edge. Other steels with very good machinability have been developed and are used for the economic manufacture of complex turned parts, or for mass production on high-speed automated equipment. Chemically resistant steels are essential in the chemical and foods industries, as well as in household equipment. For the majority of steel grades—more than 2500 are available today—very good welding properties are important, and here steel has an advantage over competing materials.

Modern knowledge of controlling the microstructure of steel, and hence its properties, offer opportunities to match steel products to new sets of requirements [2].

Unlike brick or concrete buildings, steel structures can be dismantled relatively easily. Furthermore, almost 100% of the steel can be recovered from steel-containing products and can be remelted to yield steels of similar or higher quality. In this respect, iron and steel are superior to all competitive materials.

The great importance of steel in the world's economy is also exemplified by production figures. In the early 1900s, total world production of steel was less than 35 × 10^6 t/a. In 1940 it was 140 × 10^6 t/a. The figures for the period after 1950 (Figure 6.1) indicate a surprisingly large growth in world crude steel production after World War II. Up to the mid-1970s, this was mostly due to those developed countries with the greatest rate of economic growth, such as Japan, the six founding countries of the European Community, and also the Soviet Union. In the United States, growth had already ceased by the mid-1960s due to market saturation.

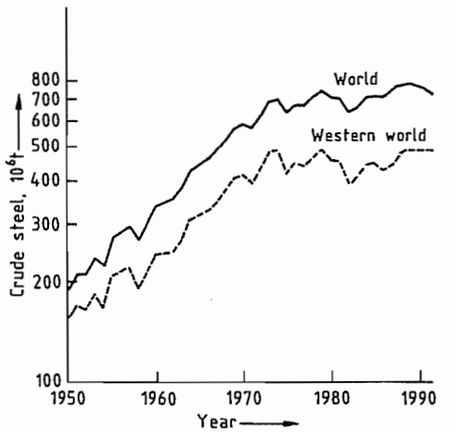

Figure 6.1: World crude steel production 1950–1991.

A rapid increase in steel production also took place in some Latin American countries, continuing until the mid-1980s. In many countries in Asia, Africa, and the Middle East, new steel industries were built up, or existing capacity was increased. The developments in some Asian countries during the last 16 years are remarkable (Table 6.1).

The relationship between total economic development and steel production can be seen clearly from these figures. Figure 6.1 also shows that world production of crude steel has stagnated since the mid-1970s, apart from the usual market fluctuations. A sharp rise in crude steel production in countries with rapidly increasing industrialization contrasts with zero or even negative growth in steel production in countries that are already highly industrialized (e.g., the United States). Several reasons can be suggested:

Table 6.1: Development of crude steel production in Asian countries (Source: International Iron and Steel Institute).

Country	Production, 10^3 t/a		
	1975	1985	1991
China	23 903	46 700	70 400
South Korea	1 994	13 539	26 000
Taiwan	680	5 088	11 000
India	7 991	11 140	17 100

The steel consumption of a country is determined by the "specific market demand", i.e., production plus imports minus exports of steel product s expressed in kilograms crude steel per capita. In industrialized countries, this reaches saturation at ca. 600 ± 100 kg, which can only be exceeded in special circumstances. If there are sections of industry with extremely high steel consumption (shipbuilding or automotive industries), and if these are strongly export oriented, a value of > 700 kg per capita can be reached because the exported finished products do not remain in that country. Figure 6.2 shows that the saturation value of 600 kg was reached as early as 1950 in the United States. Other industrialized countries reached this figure in the 1970s, and this reduced the growth of steel production. Also, the expansion of the steel industry in countries

which had been importing rolled steel made it impossible for steel exports from the industrialized countries to grow. Extrapolation of the Figure 6.2 into the 1980s is problematical because the figure "kilogram crude steel per capita" is now no longer comparable with figures up to ca. 1975 due to technical developments (described below) in rolled steel products.

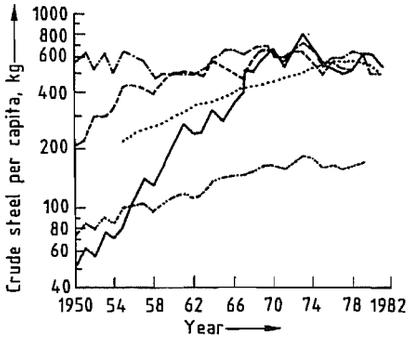

Figure 6.2: Specific market demand for crude steel (production + imports – exports) [1]: —·— = United States; — — = Germany; ····· = Former Soviet Union; — = Japan; –··– = World.

Table 6.2: Countries with a crude steel output > 10×10^6 t/a (1991 and 1992) with portion of continuously cast steel shown (Source: International Iron and Steel Institute, 1992).

Country	Production, 10^6 t/a		Portion of continuously cast steel, %	
	1991	1992	1991	1992
Soviet Union	132.8	116.8	17.7	17.1
Japan	109.6	98.1	94.4	95.4
United States	79.7	84.3	75.7	78.9
China	70.4	80.0	26.5	30.0
Germany	42.2	39.7	89.5	92.0
South Korea	26.0	28.0	96.4	96.8
Italy	25.1	24.9	95.1	96.1
Brazil	22.6	23.9	56.0	58.6
France	18.4	18.0	95.0	95.2
India	17.1	18.1	14.3	
United Kingdom	16.5	16.1	85.5	87.0
Canada	13.0	13.9	83.6	86.5
Spain	12.9	12.3	91.8	93.2
Czechoslovakia	12.1	11.1	17.0	21.9
Belgium	11.3	10.3	92.2	93.9
Taiwan	11.0	10.7	94.6	94.9
Poland	10.4	9.8	8.6	9.1

From the second half of the 1960s, use of the continuous casting process in steelworks increased, approaching 20% by 1975 worldwide. By 1991, the proportion of continuously cast steel reached 67% worldwide. This process gives an increase in yield of ca. 12–15% of crude steel for rolled steel products, compared with ingot casting. Hence, up to 15% less crude steel is required to produce the same amount of rolled steel product for the steel processing industry. Other improvements in yield productivity in steel plants and in steel-consuming industries also reduced the consumption of crude steel without jeopardizing the use of steel for a particular end product.

Table 6.2 lists all countries with a crude steel output of more than 10^6 t/a during 1991 and 1992 and gives the percentage of continuously cast steel.

In 1978, however, for the countries represented in Figure 6.2, the percentages of continuously cast steel were:

Former Soviet Union	9.5%
Japan	46.2%
United States	15.2%
Germany	38.0%

The large differences between the 1978 and 1991 figures, means that comparison of the number of kilograms crude steel per capita is of questionable value.

Below a continuously cast steel portion of ca. 85–90% "kilograms crude steel per capita" is an indication of the state of modernization of the steel industry of a country. Above this range, the production program and the proportion of steel products not produced by continuous casting (e.g., steel castings, heavy forgings) play an important part in crude steel production. Only countries with a crude steel output in 1991 of max. 10^6 t/a (e.g., Switzerland and New Zealand) produce 100% of their steel by continuous casting.

A further reason for the absence of the usual growth in crude steel production in the 1960s in the industrialized countries, must be attributed to the development of higher strength steel grades. In the last 15–20 years, these grades of steel have been increasingly used by steel processors. Especially in the motor vehicle industry, high-strength steels have been used to improve constructional design

through weight reduction. Consequently, there is a decrease in the amount of steel used, in addition to that achieved with the replacement of steel by competing materials such as aluminum or plastics.

When assessing the technological and economic significance of steel, it is interesting to examine the different finished steel products and how their share of the total production of rolled steel has changed over the years. There are two groups: "long products" (i.e., beams, steel shapes, steel bars, railway-track material, piling sections, and wire rod) and "flat products" (i.e., plates, sheets, strip-steel and universal-plate).

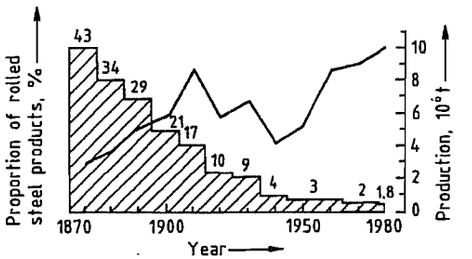

Figure 6.3: World production of steel for railway-track material lines. Solid line: total production of railway-track material; Hatched area: railway-track material as percentage of the total world production of rolled steel.

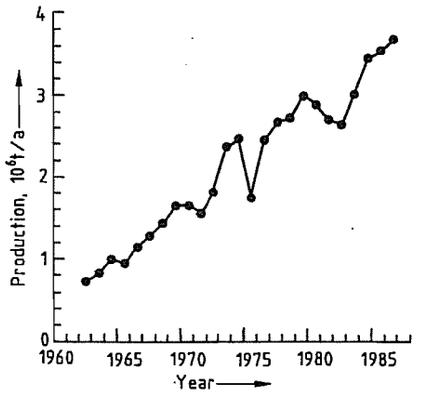

Figure 6.4: Production of cold-rolled stainless steel strip by western countries.

In 1870 3×10^6 t of railway-track material accounted for 43% of total world production of rolled steel products (Figure 6.3), while in 1991 the output of railway-track material, which underwent a threefold increase to 9×10^6 t, accounted for barely 1.2% of total production. In modern industrialized countries, 60–70% of rolled steel production consists of flat products, mainly hot- and cold-rolled strip and sheet, coated sheet, tinplate and electric sheet, all with thicknesses in the range of 0.15–3 mm. The production of cold-rolled stainless steel strip has increased sharply during the last 25 years, as shown in Figure 6.4.

There is intensive world trade in products of the steel industry, especially among major steel producing countries. Only in a few cases does this involve special products or special steel grades, for which some producers have a leading position. International competition is severe, and producers must offer consistently high-quality products. The large producers have therefore built up comprehensive quality assurance systems over many years, conforming to ISO Standard 9002 and local regulations such as ASME in the United States, Lloyds Register in the United Kingdom, and TUV in Germany. The aim is to control all steps of the manufacturing process, and to use statistical methods to ensure that the finished product has the desired properties, dimensional tolerances, and a defect-free surface finish. The intensive testing of finished products that was formerly carried out can then be largely dispensed with, and replaced by the testing of random samples, the results of which form part of the control loop.

Such quality-assured production is a prerequisite for the direct processing of sheet coils on automatic press lines without any inspection (even for exposed autobody parts).

A further important aid to international trade in steel is the existence of common standard specifications and terms of delivery. Specifications for steel products have been formulated by ISO over many years. However, these are often only the first steps toward harmonization of the various interpretations and technical possibilities. In Europe, since 1986, EN Standards for all steel products and testing methods have been compiled by the ECISS (European Committee for Iron and Steel Standardization). These standards must be adopted

via CEN (Comité européen de normalisation) into the national standards of all European nations. They will certainly achieve importance outside Europe, too.

6.2 History

6.2.1 From Prehistoric Times to the Middle Ages

6.2.1.1 Native Iron

Since the earliest times, humans have used iron, the second most abundant metal in the earth after aluminum. It was first discovered in the form of the native element, which occurs only rarely as tellurian iron of volcanic origin, and mainly as meteoric iron. The Egyptians, Sumerians, Khatti, and Hittites must have had knowledge of its origin, as they called it ore, or metal, from heaven. Meteoric iron can be identified from its high nickel content (ca. 5–25%), and the typical Widmanstätten structure, formed on solidification. The oldest known examples of worked meteoric iron are beads from Gerzeh (3500 B.C.) and a dagger from Ur (3000 B.C.).

6.2.1.2 Iron from Ores

It is not known when, where, or how iron was first deliberately produced from its ores. It is often said that the technique of extracting iron was developed from observations made during copper extraction, and that the idea suggested itself simultaneously in many places with a long tradition of copper smelting. A geographical analysis can be carried out from linguistic similarities, archeological finds, and documents. According to present knowledge, iron was first smelted in eastern Asia Minor and northern Mesopotamia around 2000–1500 B.C., and possibly also in the plains north of the Caucasus. As the Chinese were the first to produce a high-carbon, high-phosphorus (up to 7%) liquid castable iron, it is conceivable that they also succeeded in winning iron from its ores at a very early date. Around 500 B.C., knowledge of iron winning spread through Asia Minor to North Africa, parts of Asia, and all of Europe.

6.2.1.3 Technology of Iron Production

At first, the iron was smelted in a bloomery fire, later in a bloomery hearth furnace, and crucibles. The iron ore was charged with charcoal, and later, according to the type of gangue material, with other fluxes, into a hearth or the shaft of a furnace. The charcoal was burned by a blast caused either by a natural draught (convection) or by hand- or foot-operated bellows. The rising combustion gases dry the materials (Figure 6.5), and reduce the ore at ca. 900–1100 °C, forming a primary slag of wustite (FeO). From the gangue, a molten liquid slag forms, from which, in a further reduction stage, pure solid iron separates out, with formation of secondary slag. Since no appreciable carbonization of the iron takes place, it does not liquefy, even in the lower part of the furnace (temperature ca. 1200–1300 °C). The product, the so-called bloom, consists of iron with slag inclusions and residual charcoal. These were separated, and the blooms were reheated and forged into bars. Up to the late Middle Ages iron, or rather steel, was obtained exclusively by this process directly from the ore, except in China. As a result of improved bellow technology, the furnace volume grew. About 900 years ago, this development culminated in bloomery furnaces with reached heights of 4 m, thanks to the wind pressure from waterwheel-powered bellows.

In addition to the technique of iron winning, knowledge of the properties of iron and how to modify them also developed empirically and involved little understanding of cause and effect, even up to the 1700s. It was recognized at an early stage that iron could be hardened by heating (with carburization) followed by rapid cooling. As early as the 900s B.C. crucible furnaces were used for carburizing iron in Gerar, Palestine. Moreover, the technique of combining high- and low-carbon steels was used to achieve a desired combination of properties, such as toughness and hardness, e.g., in the production of Damascus steels.

6.2.2 From the Middle Ages to the 1800s

In the 900s, technology was revolutionized by the waterwheel, with far-reaching effects on iron production. Water power became more important than the availability of ore when choosing the location for iron smelters. Thus, the preferred smelter location changed from the mountains, with proximity to ore and wood, to the river valleys, with their availability of flowing water.

The blast produced by water-driven bellows enabled larger furnaces to be operated. These were originally bloomery furnaces, but became flowing furnaces in the 1100s and 1200s. Water power was also used to operate tail hammers, lift hammers, etc. This development took place almost simultaneously in the alpine regions, and in western and northern Europe, which is not surprising in view of the extensive trade in medieval Europe. The historical development of iron and steel production equipment, and the growth of total world steel production, is summarized in Figure 6.6.

6.2.2.1 Bloomery Furnaces

In principle, bloomery furnaces were simply an increase in furnace size. They were up to 6 m high, operated batchwise, and produced a bloom up to 100 kg after ca. 15 h operation. The earlier furnaces produced a bloom of only 20 kg. Refining the blooms is a two-stage operation: a metallurgical treatment in the refining furnace (slag removal, homogenization, and, if necessary, decarburization); followed by hammering into bars, and a mechanical mixing operation in which bars of steel of various qualities are hammered together, forming a fairly uniform product. Bloomery furnaces, like the small Corsican and Catalan forges that used the same principle, were still producing a small fraction of the total production up to the 1800s. The production of steel by the direct method is currently undergoing a renaissance.

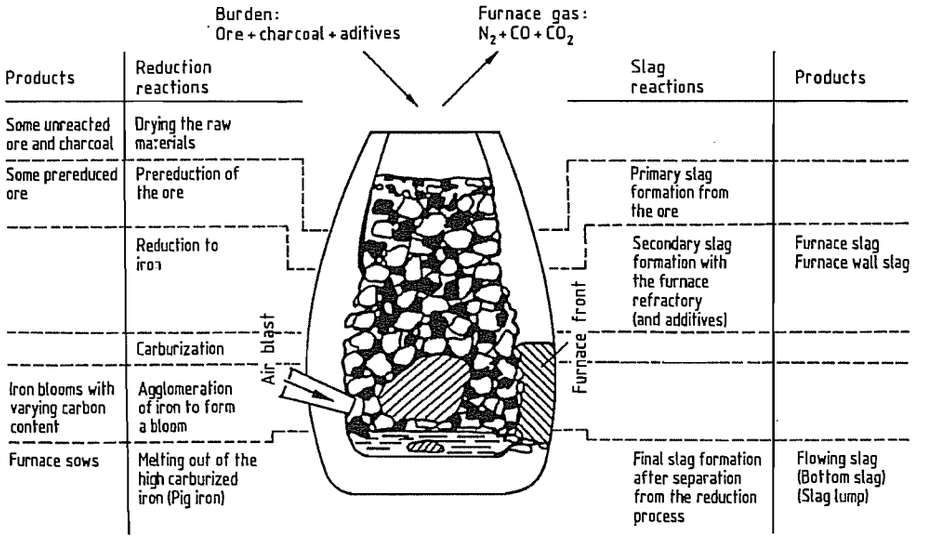

Figure 6.5: Furnace reactions for the production of iron by the direct method in a bloomery furnace (after D. HORSTMANN).

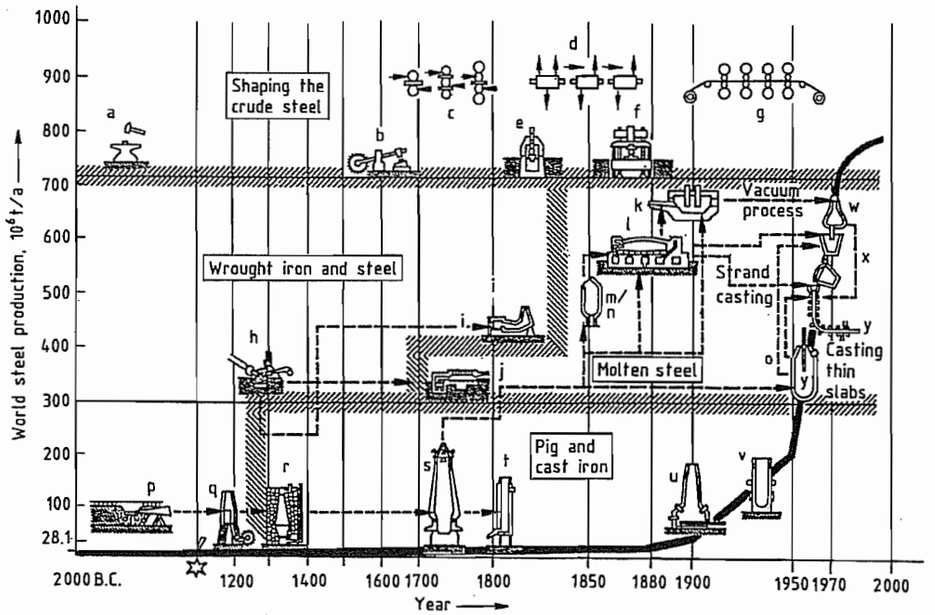

Figure 6.6: Development of steel production processes and forming, with a graph of annual steel production [13]: a) Hammer and anvil; b) Tail hammer; c) Two-, three-, and four-high rolling stands; d) Open rolling mill; e) Steam hammer; f) Forging press; g) Continuous rolling mill; h) Finery fire; i) Puddling furnace; j) Crucible furnace; k) Electric furnace; l) Open hearth furnace; m) Bessemer converter (acid lining); n) Thomas converter (basic lining); o) Oxygen steelmaking converter; p) Finery fire; q) Bloom furnace; r) Charcoal blast furnace; s) Coke blast furnace; t) Cupola furnace; u) Electric shaft furnace; v) Low shaft furnace; w) Vacuum degassing; x) Continuous casting; y) Thin slab casting.

6.2.2.2 Blast Furnaces

Together with the use of water power, the main revolution in iron smelting in Europe was the discovery of the two-stage indirect production of steel – the method still used today. In the first stage, liquid pig iron with a high carbon content is produced in the blast furnace. In the second stage, this pig iron is decarburized and refined to steel in a finery fire. The improved air pressure and flow rate enabled furnace temperatures > 1200 °C to be achieved. The furnace volume could be increased, leading to a longer dwell time for the burden as it passed down the furnace shaft. This led to improved reduction of the iron ore (the yield increasing from 50 to > 85%), and carburization of ca. 2.5–5.0%. The lowering of the melting point led to the production of liquid pig iron for the first time, and considerably improved output. The furnaces could be charged without interrupting the process, and the liquid iron was directly cast into finished products (furnace plates and cannon balls) or bars for sale or captive processing in the finery shown. Here, the crushed pig iron was smelted in the finery hearth and decarburized under an oxidizing slag. Steel blooms were formed from the molten metal as it thickened, and these were then hammer forged into semifinished products. The furnace workers were able in some degree to control the properties of the product, but their empirical knowledge was mainly limited to processing certain types of ore or pig iron. An example is Osemund iron, which was ductile and, therefore, used for wire production. Steel production and processing centers were established in Austria, France, Belgium, United Kingdom, Germany, Sweden, and Russia. Iron production in Europe increased from 20 000–30 000 t/a (when small blast furnaces were introduced in ca. 1200 A.D.) to ca. 150 000 t/a at the inception of coke-based metallurgy in the mid-1700s.

6.2.2.3 Metal Shaping

Up to the 1500s, iron was processed only by forging and drawing, but, as the indirect method of iron production became widespread, water-powered rolling mills came into use. However, production rates of the blast furnace, the finery fire, and the hammer forge were roughly comparable, and hot rolling was unable to produce a product comparable to forged steel. Therefore, hot rolling was only occasionally used for the treatment of forged material. Its most important application emerged later in the so-called iron-splitting works, in which strips were produced from steel sheet (e.g., for nail production). These operations were common in almost all iron-producing countries until the mid-1600s.

The range of rolled products increased during the early 1700s. In Sweden, Christoph Polhems was able to produce rolled steel with various profiles for knife blades and files. In England, John Hanbury produced thin steel sheet on a pillar rolling mill for tinplate manufacture. This type of equipment was being used for the manufacture of steel sheet for steam boilers by 1764 at the latest. In the same year, John Paynet obtained a patent for the preforming of flat bar by grooved rolls, and John Westwood was awarded a patent for cold rolling in 1783. In 1778, the Frenchman Fleur described a four-stand rolling mill with closed passes which he used for wire production. Proposals for continuous rolling were also published.

Apart from the iron bearings, rollers, cutting rings, and spacers, the rolling mills were constructed of wood. In the mid-1700s, gear wheels and pillars were all of cast iron. Energy was supplied by one or two waterwheels, depending on the size of the rolling mill. The upper and lower rolls were generally driven separately, but pinion stands were also used. The mechanical and thermal stresses on the rolls were large. At first the rolls were made by welding a hardenable steel sheet around the forged roll body. Later, cast iron rolls were used. A further development was the casting of steel around a bar which was used as roll neck.

Rolling mills did not yet replace hammer forges, as their use was limited by the quality of the engineering and the availability of power.

6.2.3 The Industrial Age

The 1700s saw the development of mechanical power (steam engines), transport (railways, bridges), and the increasing use of machinery, all of which was made possible only by the almost complete replacement of wood by steel as a construction material. The resulting enormous increase in demand provided the impetus for the development of new methods for bulk steel production.

Iron and steel were produced exclusively from charcoal up to the 1700s, but by the end of the century, processes had been developed that enabled charcoal to be replaced by coal. These were coke-based metallurgy and the crucible steel and puddling process, supplemented by the development of the hot rolling process. They formed the basis for the economic mass production of this universal construction material, which satisfied the broad requirements of the approaching industrial era.

During the preindustrial epoch, most of the improvements in steel production methods took place on the European mainland, but the inventions that led to the industrial revolution were made in Britain. These are linked with the following names:

- Abraham Darby II (1711–1763) who introduced the first true coke-based blast furnace (1735) and the first use of steam engines (1742) to steel production
- Benjamin Huntsman (1704–1776) – crucible steel casting (1742)
- Henry Cort (1740–1800) – development of the puddling process (1783–1784)

- Jean Beaumont Neilson (1792–1865) – hot air blast (1829)
- James Nasmyth (1808–1890) – steam hammers (1839), first installed at Creusot (1841)
- Henry Bessemer (1813–1898) – acid air refining process (1856–1860)
- Sidney G. Thomas (1850–1885) and Percy C. Gilchrist (1851–1935) – basic refining process (1878)
- Wilhelm Siemens (1823–1892) and Friedrich Siemens (1826–1904) – regenerative heating (1861)

Important innovators in other countries include:

- Faber du Faur (1786–1855) – blast heating (1832)
- Pierre-Émile Martin (1824–1915) – open hearth process (1864)
- Rainer Daelen (1813–1887) – universal mill stand (1848)
- Charles Morgan (1831–1911) – rolling mill technology (from 1865)
- George Bedson – continuous rolling mills (1860)
- Reinhard Mannesmann (1856–1922) and Max Mannesmann (1857–1915) – rolling seamless tubes (1890)
- Paul Héroult (1863–1914) electric arc furnace (1900)

These innovations were gradually introduced into the most important iron-producing countries, including the United Kingdom, Belgium, France, Germany, Austria, and the United States, all of which made their own contributions to the further development of iron and steel technology. Historically, the last pioneering inventions are the basic oxygen steelmaking process, secondary metallurgy, and continuous casting, which were developed in the 1940s and 1950s.

6.2.3.1 Pig Iron Production

The cradle of coke-based metallurgy was Coalbrookdale, where Abraham Darby I (1678–1717), who had invented the process of casting iron in sand molds in 1707, probably began the production of pig iron using coke in 1709. His son, Abraham Darby II, was the first to operate a blast furnace fueled entirely with coke in 1735. Coke-based metallurgy spread to the rest of the United Kingdom only slowly at first (in 1750, 3 of 74 blast furnaces were coke based; in 1760, 14 of 78; in 1791, 85 of 107). The real breakthrough came with the development of the puddling process for converting pig iron into steel, the production rate matching that of the iron-making process. In mainland Europe, these new technologies were adopted in a dilatory fashion. The first coke-based blast furnaces were operated in France by Creusot in 1785, and in Germany in Gleiwitz (1796). Whereas pig iron production in the U.K. was almost exclusively based on coke in the early 1800s, Germany reached this stage only at the end of the century.

From the early 1800s, coke-based metallurgy was accompanied by research and development, with increases in productivity and profitability. Developments were mainly concerned with the design and size of blast furnaces, including blast and power supplies, increasing the efficiency of energy utilization, and improving yield and quality through better understanding of the metallurgical processes, enabling the control of the blast furnace process to be improved, culminating in computer control. This development can be demonstrated by data for selected blast furnaces (Table 6.3).

6.2.3.2 Steel Production

After the invention of the pig iron furnace, forgeable and hardenable iron (steel) was produced both from almost carbon-free wrought iron and from highly carburized pig iron.

Wrought iron, in the form of soft iron bar, was carburized to steels with a higher carbon content from the early 1600s (originally in 1601 in Nuremberg by Paulus Hannibal) by heating in carbon-containing powders with exclusion of air. This so-called cemented steel had a wide range of uses, e.g., for springs, knives, and files. In the 1700s, the steel industry in Sheffield was founded on the use of this process for the treatment of imported Swedish iron bars. Here, 205 cementation furnaces produced almost 80 000 t steel in 1862. The last of these went out of production in 1951. This cemented steel (blister steel), which was inhomogeneously surface-carburized and blistered, was homogenized by hammering out (sometimes repeatedly) bundles of cemented steel rods to form "shear steel". Although this led to some equalization in material properties, this steel met the increasing quality requirements only to a limited extent.

Crucible Steel

The first decisive step toward production of nearly homogeneous and slag-free steel was taken by Benjamin Huntsman in 1740, with the production of liquid steel by melting together cement steel with added bar iron and glass in refractory crucibles. The productivity of this process was later increased by improvements to the crucible material (graphite). Crucible steel opened up completely new perspectives. The steel was both castable and forgeable. By pouring the contents of several crucibles into one mold, ingots and castings of large mass were produced for the first time. As alloying was possible, steel developed into a universal construction material. As this process was more economical than the production of shear steel, it spreads relatively rapidly.

Puddled Steel

Pig iron from the small furnaces that later developed into blast furnaces was cast, either directly or after remelting, in a cupola furnace to give finished products (e.g., machine parts, construction elements, household articles) or was decarburized to forgeable steel. The steel produced by decarburizing coke pig iron tended to be brittle (owing to sulfur and phosphorus) compared with that produced from charcoal pig iron. The low productivity of decarburization in open charcoal-fired finery fire became a problem, owing to the increasing rate of production of pig iron; steel producers sought a more effective fining process that would operate with coal or coke. The breakthrough was achieved by Henry Cort with his patented method (1783–1784) for producing wrought steel – the puddling process. This consisted of remelting the pig iron and fining with the combustion gases from the coal- or coke-fired reverberatory furnace (Figure 6.7), followed by mechanical slag removal and welding together of the lumps of steel by means of a steam hammer or squeezer to form blooms of very variable chemical analysis. These were rolled in a rolling mill to form "crude" flat iron. To produce a homogeneous rolled steel, fagots of flats were placed together, heated in a welding furnace, and rolled. This step could be carried out several times. The process met all requirements of the time, i.e., increase in productivity (tenfold), replacement of charcoal by coal, and reduction of production costs. It spread relatively rapidly into all iron-producing countries. In Germany, the first puddling plant was started in the Rasselstein iron works in 1824. The last puddling operation ceased in the 1940s.

Table 6.3: Development of blast furnaces.

Year and location	Hearth area, m^2	Coke consumption per tonne iron, kg	Iron output, t/d
1796 (Gleiwitz)	0.3	3500	1–2 (later 4)
1801–1815 (U.K.)		2500	5–7
1856 (Hasslinghausen)	3.6	1600	20–23
1880 (United States)	8.8	1510	120
1901 (United States)	15.3	1000	464
1929 (Bruckhausen)	33.2	740	1100
1993 (Schwelgern 2)	174.9	480[a]	10 600

[a] Fuel consumption.

Ingot Steel

With time the puddling process also became unable to meet the increasing demand for steel. In 1856, HENRY BESSEMER invented his autothermic air refining process, which made it possible for the first time in the history of iron production to convert pig iron directly into liquid steel, increasing productivity by a factor of 70 (Figure 6.8). In the Bessemer process, molten pig iron is blown with air from below in a tiltable converter. The molten metal is decarburized by oxidation, which also removes silicon and manganese. The heat liberated causes the temperature to rise well above the melting point. As the original lining of the converter was acidic, only low-phosphorus pig iron could be treated, and the use of the process was therefore limited. This problem was solved in 1878 by SIDNEY G. THOMAS and PERCY C. GILCHRIST by the use of basic dolomite as converter lining. Thus, phosphorus could be removed by means of a basic slag, which later became an important fertilizer (Thomas slag). The Thomas process was widely used, especially on the European mainland, where the ores, e.g., minette (oolitic iron ore), often have a high phosphorus content. In Germany, the first Thomas steelwork was operated in 1879. The last one was shut down only very recently.

Ingot steel production by air refining became the most important steel production process worldwide with the introduction of the basic oxygen (LD, Linz–Donawitz) process in 1952.

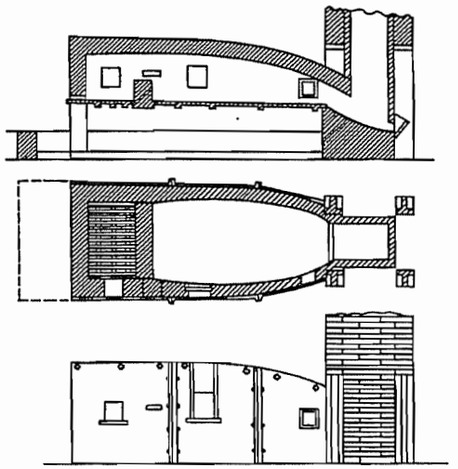

Figure 6.7: Puddling furnace with iron hearth and cast iron shell (1830) [14].

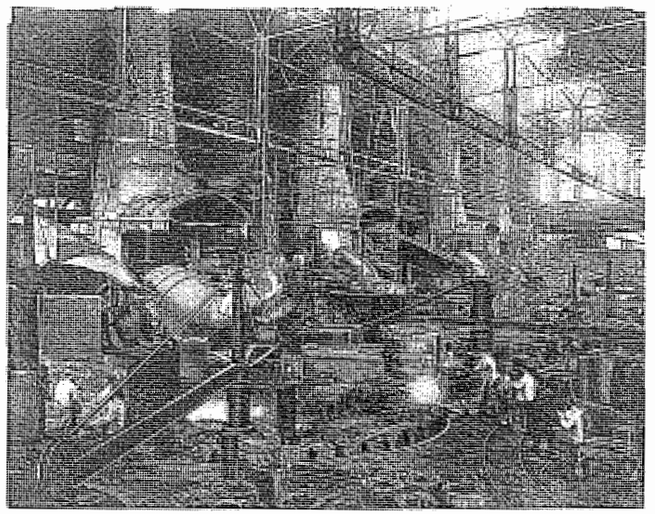

Figure 6.8: Bessemer steel works with circular casting pit (Friedrich Krupp, Historical Archive, 1970).

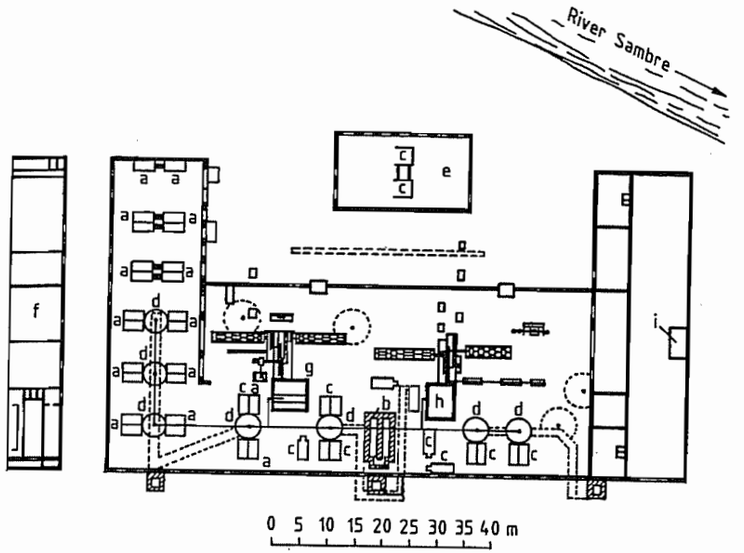

Figure 6.9: Ground plan of rolling mill at Couillet (1835) [15]: a) Puddling furnace; b) Coal-fired boiler; c) Welding furnaces; d) Waste heat boilers; e) Finishing drop; f) Workshops; g) Machine 1; h) Machine 2; i) Stores.

In parallel with the air-refining processes, the allothermic hearth process was also developed. In 1864, F. and W. SIEMENS together with E. and P. MARTIN succeeded in melting pig iron and steel scrap, using regenerative heating in a reverberatory furnace. The Siemens–Martin process at first achieved great importance for the recovery of scrap. Later, pig iron was melted with iron ore, with or without the addition of steel scrap. Until the breakthrough achieved by the oxygen refining process, this was the most important steel production process, accounting for up to 60% of all steel production.

After the 1850s, electrical energy became available, and attempts were made to build electric hearth melting furnaces. The electric arc furnace developed by HÉROULT was especially successful, and was first operated full-scale in Germany in 1906. Although it was initially used for the production of special steels, it is now increasingly used only for steel melting, owing to the availability of cheap electricity, and the introduction of secondary metallurgy.

6.2.3.3 Rolled Steel Production

Puddled Steel and Steam Power

Following the discovery of (1) the puddling process, which enabled iron to be converted to the finished product by a rolling operation; and (2) the introduction of the steam engine, the technology of the rolling mill became an integral part of steel production.

Although this new technology was quickly adopted and further developed in England, this only happened in a few places, owing to the high cost of steam engines. As early as 1784, J. WILKINSON started the first steam-driven rolling mill in his iron works in Bradbury, and replaced the hammer forge by a blooming mill with self-adjusting rolls. This was patented in 1792. There followed improvements in rolling equipment, by making it more powerful (the production of cast machine components of ever-increasing size, and the development of techniques for gearing and driving). This can be seen from the dimensions of the rolls, which reached diameters of 300 mm and body widths of 1200 mm.

On the basis of these new methods, England's iron and steel industry occupied a leading position throughout the 1800s. Continental iron producers were able to adopt the new technology only later, sometimes only by industrial espionage or by the enticement of specialist personnel. The major economic incentive was the immense demand for railway track.

The plan view (Figure 6.9) of the rolling mills at Couillet (1835) shows the layout of a typical works of that time. The puddling and rolling plants formed a single unit. The steam engines were at the heart of the ironworks. They drove the puddling plant and rail mill, the three-stand sheet mill, the six-stand bar mill, a two-stand mill for rolling-cutting, and an auxiliary plants. This works produced ca. 10 000 t rolled steel in 1840.

Ingot Steel and Mass Production

The further development of rolling mills took place against the background of the developing mass production of ingot steel. The first product became the cast steel ingot. Developments took place particularly in drive technology and the construction of specialized rolling stands and mills (and also auxiliary machinery and reheating furnaces which are not considered in this article). The realization of reversible operation of rolling stands driven by steam engines was the trigger for the further improvement of the driving machinery. In the 1870s, hydraulic friction coupling for reversible operation was successfully designed and constructed. However, almost 30 years of development were required before the problem of reversing the steam-driven rolling mill engine was solved by CLEMENS KISSELBACH in 1891. The use of electrical driving machinery, which began in 1900, increased, especially after the invention of the reversible electrically driven rolling mill engine by ILGNER in 1902.

The design and construction of rolling mills and plant was driven by the demand for mass production, with increasing throughput, size, and range of products. The American, JOHN FRITZ, in 1857, eliminated the need for reversible rolls by designing and successfully operating a three-high rolling stand for rail production. In 1848, RAINER DAELEN built the first universal rolling stand, which found wide application, especially in the United States. Using this equipment, finishing of I-beams was first achieved in 1866. In 1883, I. J. SEAMAN and H. SACK separately applied for patents for universal rolling mills for rolling beams. Wire and rod steel products were rolled in open rolling trains. The introduction of mechanical loopers in 1877 led to a considerable increase in performance. At the end of the 1860s, G. BEDSON constructed the first continuous finishing train for wire, with 16 alternately horizontal and vertical rolling stands. This type of train was further developed, mainly by C. MORGAN in the United States. In 1905, in Gary, Indiana, the first train operating completely continuously from ingot to finished product was commissioned. From the early 1800s, a large number of proposals for the production of seamless tubes by rolling were made. However, the breakthrough was an invention by M. and R. MANNESMANN, in which a hollow body was produced by skew rolling (1886), with subsequent expansion to form a seamless thin-walled tube in the Pilger step-by-step-type seamless tube rolling mill (1890). The development of flat rolling aimed to increase the dimensions of strip and sheet, the weight of charge, and productivity. The United States led the way, and the first continuous hot strip mill went into operation during the 1920s. These mills constitute as important a development for modern steel production as the oxygen steelmaking process, secondary metallurgy, and continuous casting.

6.3 Crude Steel Production

6.3.1 Raw Materials

The following iron-bearing materials are used for crude steel production (Table 6.4) [16]:

- Molten iron from blast furnaces (hot metal), mainly used for steel production by the basic oxygen furnace (BOF) process
- Scrap, sponge iron, and solidified blast-furnace iron (pig iron), mainly used for melting steel in electric furnaces

Another important raw material is lime for slag formation. Alloying elements, such as chromium, nickel, molybdenum, titanium, vanadium, and niobium, and elements used as deoxidizing agents (e.g., manganese, silicon, and aluminum) are not discussed in detail here.

The most important iron-bearing material is hot metal. Of the total world crude steel production of 770–720 t/a in the early 1990s, ca. 60% was produced from hot metal obtained by reducing iron ore, and ca. 40% from steel scrap. Steel scrap is of increasing importance as a raw material because of the lower primary energy consumption and lower CO_2 emissions, compared with the blast furnace–converter production route. Figure 6.10 compares the total specific primary energy consumption per tonne of steel produced from ore with that for steel produced from scrap [17].

Table 6.4: Properties of hot metal, sponge iron, and scrap [16].

	Hot metal	Sponge iron	Scrap
Raw materials	poor to rich ores, low or high in phosphorus	ores with low gangue content	internal scrap production scrap collected scrap
Availability	almost unlimited	limited to low gangue ores or pellets	depends on steel consumption and crude steel production
Production and processing	classification, sintering, pelletizing blast furnace	classification or pelletizing shaft furnace rotary furnace retort fluidized bed	shears (cutting–burning)
Primary energy consumption (GJ/t)	14	12 (shaft furnace)	0.6 (shredder)
State of aggregation	liquid	solid	solid
Storage and transport	severely limited	special techniques may be necessary (e.g., briquetting)	good
Type of furnace using this material	oxygen-blowing furnace (BOF) (electric furnace)	electric furnace (as cooling agent in oxygen furnace)	electric furnace Siemens–Martin furnace (as cooling agent in oxygen furnace)
Price	depends on production costs	depends on production costs, market price, or agreed price	market price
Chemical properties			
Composition	constant	constant	variable
Unwanted elements	sulfur phosphorus (depends on application)	none phosphorus (depends on application)	depends on process
Type of gangue		depends on ore	
Physical properties	liquid	bulk material	variable shredded scrap (in bulk)
Bulk density		> 12 t/m^3	fluctuates around 1.2 t/m^3 depending on type of scrap
Thermal conductivity		low	high

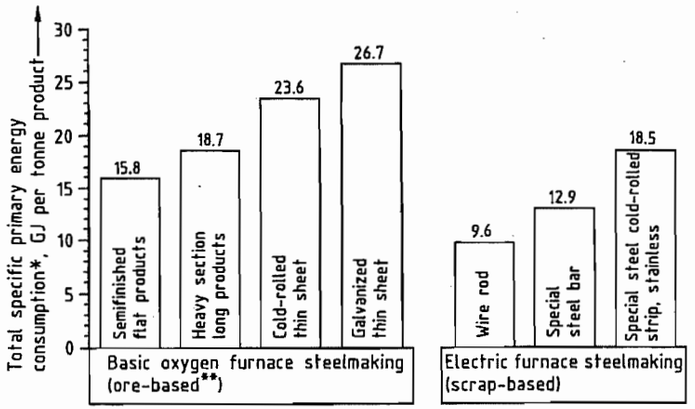

Figure 6.10: Comparison of total specific primary energy consumption for steel products made from ore and scrap [17]. * Including primary energy consumption for generating electricity in thermal power stations, and energy-intensive materials (oxygen, steam, compressed air, cooling water, etc.); ** Including added scrap for cooling.

Table 6.5: Characteristic compositions of grades.

Type of pig iron	C, %	Si, %	Mn, %	P, %	S, %
Low-phosphorus	4.0–4.5	0.30–0.70	0.20–0.70	0.05–0.12	0.03–0.06
High-phosphorus	3.2–4.0	0.30–0.70	0.25–1.20	1.50–2.20	0.03–0.06
Foundry	3.5–4.2	1.80–2.50	0.70–1.00	0.50–0.70	0.03–0.06

6.3.1.1 Hot Metal

Hot metal is produced by reduction of iron ore in a blast furnace. Modern furnaces produce 5000–12 000 t/d. Immediate transfer of the hot metal to the converter for refining to crude steel requires the blast furnace and the steelworks to be in close proximity.

Iron ore is charged to the blast furnace in lump form or as agglomerated fine ore (sintered or pelletized), and reduced. Coke and injected coal are used as reducing agents, and these react with the hot air blast, liberating energy. The molten product, known as hot metal, separates from the liquid slag. It can be pretreated before transfer to the steelworks, to reduce the content of undesired accompanying elements such as sulfur, silicon, and phosphorus.

Various types of hot metal are produced, depending on the composition of the ore fed to the blast furnace (burden) and the method of furnace operation. They include low-phosphorus hot metal, (Thomas) hot metal (high in phosphorus), and foundry hot metal (high in silicon). The chemical compositions of several grades of hot metal are listed in Table 6.5.

Low-phosphorus hot metal is important for steelmaking. Typical temperatures for tapping the blast furnace are 1350–1450 °C. Carbon content is typically high (4–4.5%), as is sulfur content, these elements being picked up from the coke and the injected coal. A pretreatment of the hot metal, e.g., with lime-magnesium mixtures, reduces the sulfur content from ca. 0.040% to < 0.010%.

Pig iron is also used to a limited extent as an iron-bearing material for steel production involving melting; the hot metal, after tapping from the blast furnace, is cooled in sand molds to form pigs which can be used like scrap in steel production.

Hot metal is produced not only by the blast furnace method, but also in coke-free processes in smaller units by smelting reduction, e.g., the Corex process, which produces 1000–2000 t/d [18].

6.3.1.2 Scrap

Steel scrap is traded worldwide [19]. It is mainly melted in electric furnaces, but to a limited extent is also added as a cooling agent to converters used in steel production by blowing processes. In 1992, ca. 350 × 10^6 t steel scrap was used worldwide for steel production, the specific scrap consumption being ca. 445 kg per tonne of crude steel. Specific scrap consumption differs widely between countries, depending on the structure of the steel industry [20, 21]. In Italy, where the proportion of electric steel production is 50%, the proportion of scrap used, ca. 650 kg per tonne of crude steel, is naturally larger than in Germany (ca. 380 kg/t), which has 21% electric steel production (Figure 6.11).

The total quantity of scrap handled on world markets is ca. 50 × 10^6 t/a. A survey of the most important exporting and importing countries is given in Table 6.6. The price of scrap fluctuates widely, depending on supply and demand. Figure 6.12 gives an example of the fluctuations in the price of a particular grade of scrap in the Ruhr region.

Scrap is classified according to its origin: internally recycled scrap; production scrap from the steel processing industry, also known as new scrap; and collected scrap, also known as old scrap.

Internally Recycled Scrap. Improvements in the utilization of materials and technological changes, e.g., the introduction of the strand casting process, have steadily reduced the availability of internally recycled scrap in recent years (Figure 6.13) [22].

New and Old Scrap. To meet the requirements of steelworks, internally recycled scrap is supplemented by the purchase of new and old scrap. To maintain steel production quality, the quality of these purchased materials is controlled by lists of scrap grades. Criteria include the metallic iron content (e.g., > 92%), the lump size, the bulk density (e.g., > 0.9 t/m^3), and the density of bundles (e.g., > 1.3 t/m^3).

Current proportions are ca. 50% from old scrap, 15–20% from new scrap, and 30–35% from internally recycled scrap.

The quantity of scrap available worldwide depends on the quantity of crude steel produced, although there is a time delay. Whereas internally recycled and new scrap are immediately returned to the system, an average of ca. 70% of used steel products are returned as old scrap after ca. 20 years [19, 20]. On the basis of this assumption, H. W. KREUTZER has shown how the total world supply of old scrap has changed with time (Figure 6.14). In line with steel production figures which increased steadily in former years, the availability of old scrap at first continues to increase, but then levels out after ca. 20 years.

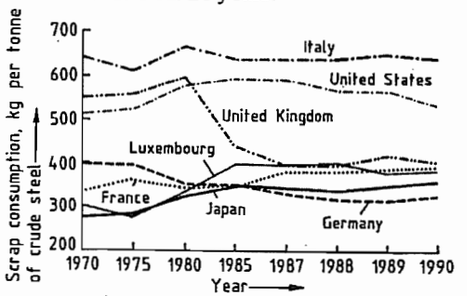

Figure 6.11: Average specific scrap consumption for crude steel production in various countries [21].

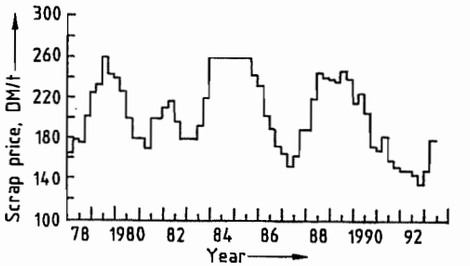

Figure 6.12: Variations in scrap prices since 1978 [20].

Table 6.6: Balance of exports and imports for several countries in 1991 [21].

	Export balance, 10^6 t	Import balance, 10^6 t
United States	8.28	
Germany	7.63[a]	
United Kingdom	3.12	
France	2.31	
Japan	1.48[a]	
European Community	1.96	
Taiwan		2.19
South Korea		3.49
Spain		4.27
Turkey		4.44
Italy		6.03
Developing countries		10.30

[a] Data for 1992.

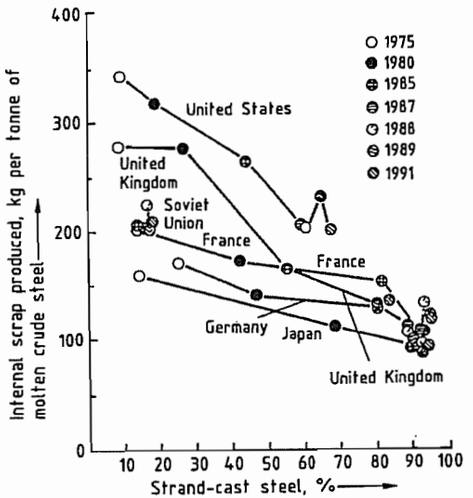

Figure 6.13: Variations in the specific amount of internal scrap produced in various industrialized countries as a function of the percentage of strand casting [22].

It is important that scrap should not introduce unwanted elements into the steel, thereby impairing its quality. Pretreatment of the scrap by size reduction and sorting, e.g., with the aid of a shredder, is therefore very important. It is essential not to introduce elements that cannot be removed from the crude steel, or whose removal is costly, e.g., copper, nickel, molybdenum, or tin. In some steel products, a copper content of 0.40% is tolerable, but in high-quality products, e. g., thin steel strip, the copper content is normally < 0.01%. Therefore, when recycling scrap automobiles, copper-containing components such as electric motors and cables must be stripped out before scrapping. On the other hand, when zinc-coated car bodies are recycled, the zinc becomes concentrated in the steelworks dust, and can be easily recycled, if the levels of zinc in the dust are high enough (ca. > 20%). So far, this has been achieved in electric steelworks owing to the high input of scrap [23]. The zinc is recovered from the dust in nonferrous metal smelting works.

Table 6.7 shows the maximum tolerable total content of Cu, Sn, Ni, Cr, and Mo for a number of steel products, and some typical concentrations of these elements in the raw materials pig iron, sponge iron, and five different types of scrap.

6.3.1.3 Sponge Iron

Another solid raw material for the steel industry is sponge iron, also known as DRI (direct reduced iron). Because of its purity and suitability for controlled feeding, it is becoming of increasing importance.

Table 6.7: Residuals in steel and its raw materials [24].

	Cu + Sn + Ni + Cr + Mo, %
Typical maximum residual limits of carbon steels	
Tinplate for draw and iron cans	0.12
Extra deep drawing quality sheet	0.14
Drawing quality and enameling steels	0.16
Commercial quality sheet	0.22
Fine wire grades	0.25
Special bar quality	0.35
Merchant bar quality	0.50
Typical residual content of charge materials	
Direct reduced iron	0.02
Pig iron	0.06
No. 1 factory bundles	0.13
Bushelling	0.13
No. 1 heavy melting	0.20
Shredded auto	0.51
No. 2 heavy melting	0.73

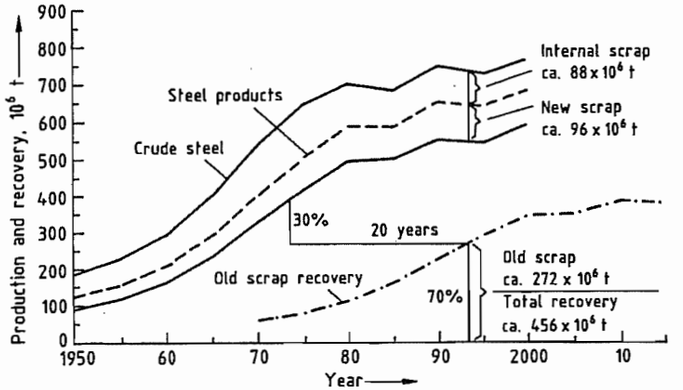

Figure 6.14: World crude steel production, with a forecast of old scrap availability up to 2015 [20].

Table 6.8: Processes for the direct reduction of iron ores.

Reduction by gases	Reduction by solids
Shaft furnace:	Rotary kiln:
Midrex	SL/RN
HyL III	Krupp–Codir
Fluidized bed:	Rotary hearth furnace:
FIOR	Inmetco
Iron carbide	Fastmet

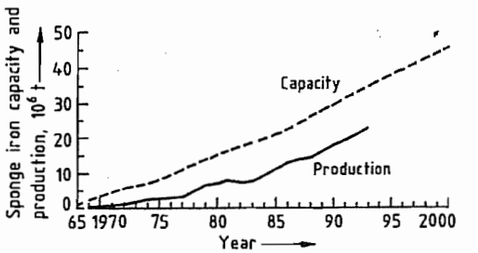

Figure 6.15: Growth of production capacity and production of sponge iron [25].

Sponge iron is produced by reduction of iron ore in the solid phase, by means of (1) reduction gas (obtained from natural gas with varying hydrogen and carbon monoxide content); or (2) coal. Of the direct reduction processes listed in Table 6.8, the Midrex and HyL processes are the most important. Gas reduction processes account for 92% of world sponge iron production. Direct reduction processes are operated where cheap energy is available (natural gas, coal), e.g., Mexico, Venezuela, Saudi Arabia, Iran, Malaysia, Indonesia, India, and South Africa.

Figure 6.15 shows the growth of the capacity and production rate of sponge iron [25]. In 1993, total production was 23.9 × 10^6 t while capacity was ca. 35 × 10^6 t, i.e., production plants were only 68% utilized. A further increase in world sponge iron capacity of at least 12 × 10^6 t/a is forecast for the year 2000.

The sponge iron produced is mainly melted in adjoining steelworks, so that amounts available on the world market are limited. Approximately 3.4 × 10^6 t sponge iron was exported in 1992 [26]. However, there is an increasing trend toward the construction of "merchant plants", e.g., in Malaysia and Venezuela.

These types of sponge iron could be of great interest for reducing levels of unwanted elements by replacing some of the scrap used in the production of scrap-based, high-grade steel products, especially flat products produced in minimills.

Because trade in these materials has so far been small, no lists of grades or general regulations exist for sponge iron supplies, such as apply to scrap. Important characteristics include the total iron content, the ratio of metallic iron to total iron, the gangue content, and the carbon content. As all the gangue constituents report to the sponge iron, ores low in gangue, or specially produced pellets, are used. Otherwise, additional energy must be used to melt the gangue when melting sponge iron. The metallic iron/total iron ratio should, therefore, preferably be > 92%. The carbon

content of sponge iron from the gas reduction process is 1–2.5%, which is higher than the typical value for sponge iron produced by the coal reduction process (0.1–0.2%). A high carbon content can help to reduce the consumption of electrical energy for melting if the carbon is burned with air or oxygen to form carbon monoxide, which is post-combusted in the melting plant. New developments in direct reduction involve the production of iron carbide, which should give a carbon content of > 5% of the DRI [27].

Table 6.9 gives typical figures for the composition of a Midrex sponge iron (gas reduction in a shaft furnace) and an SL/RN sponge iron (solid state reduction with coal in a rotary kiln). Table 6.10 gives typical figures for bulk density, lump density, and porosity of sponge iron produced from lump or pelletized ore, and for briquetted sponge iron [16].

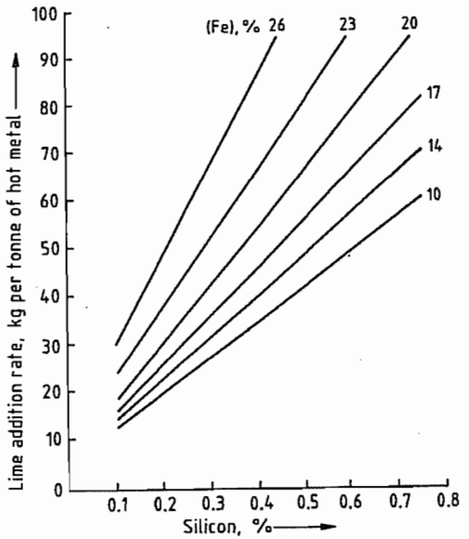

Figure 6.16: Required rate of addition of lime as a function of the silicon content of pig iron and iron content of slag [29].

When transporting and storing porous sponge iron, attention must be paid to its tendency to reoxidize exothermically, owing to the large surface: volume ratio. The heat given off can lead to ignition of the sponge iron and to a fire, e.g., during transport. This reoxidation behavior, typical of many types of sponge iron, can be characterized by determining the ignition temperature, the rusting behavior, and the evolution of hydrogen in a moist atmosphere. Safety precautions must always be taken for the transport, loading, unloading, and storage of sponge iron. Regulations and other information relevant to transport by sea have been published by insurance companies. The tendency to reoxidation can be reduced by passivation of the sponge iron. The best method of limiting transport hazards is briquetting.

Table 6.9: Chemical composition of sponge iron [25].

	Midrex	SL/RN
Fe, %	91–93	90.4–93.7
Metallic Fe/total Fe, %	92–95	92–93
SiO_2, %	2.0–3.5	2.4–5.8
Al_2O_3, %	0.5–1.5	1.8
CaO, %	0.2–1.6	0.05–0.3
MgO, %	0.3–1.1	≤ 0.05
C, %	1.0–2.5	0.1–0.2

Table 6.10: Properties of sponge iron [16].

Form	Bulk density, t/m³	Lump density, g/cm³	Porosity, %
Lumps	1.9	2–3.5	70–50
Pellets	1.7		
Briquettes	2.5	4.5–6	35–15

6.3.1.4 Lime

Lime is used as a reagent and slag former in steel production. It is the main constituent of the most metallurgically effective slags that combine with the unwanted elements in the steel.

Lime (CaO) is formed on calcination of limestone ($CaCO_3$) at ca. 1000 °C. Depending on the calcination temperature, calcination time, dwell time in the furnace, and type of gas flow through the furnace, various qualities of CaO can be produced, e.g., soft- or hard-burned lime [28]. The quality requirements of the steel industry include high purity (94–97% CaO), well-defined chemical composition, optimum grain size, and rapid dissolution in the slag. Calcined (soft-burned) dolomitic limestone is also used in steel production.

In steel production by top blowing with oxygen, the hot metal composition is of the greatest significance when determining the quantity of lime to be added for refining in the converter. The amount required to produce a slag that is slightly supersaturated with respect to lime is illustrated in Figure 6.16, which also shows the iron content of the slag [29]. As well as decreasing the silicon and sulfur content of hot metal, the changes brought about by the introduction of the combined blowing process in the mid-1980s had a further effect in reducing lime content [30, 31]. By bottom blowing with an inert gas to give agitation during oxygen blowing, the reactions approach equilibrium much more closely, and hence a better utilization of the slag is achieved. Figure 6.17 illustrates this trend toward a reduction in specific lime consumption, using German BOF steelmaking as an example. Between 1970 and 1990, specific lime addition was reduced from ca. 70 to ca. 45 kg per tonne of crude steel.

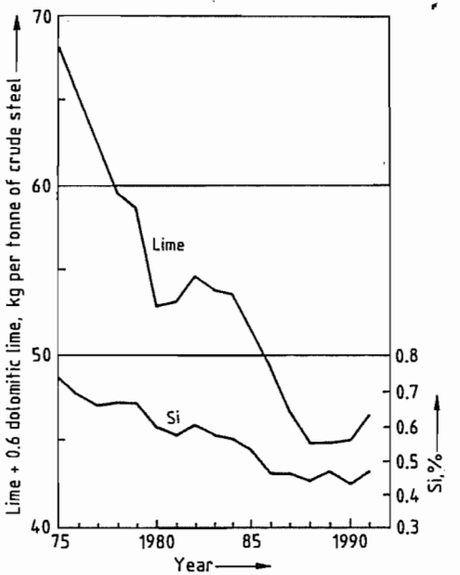

Figure 6.17: Variation in the specific consumption of lime and the silicon content of low-phosphorus pig iron in an oxygen steelmaking plant in Germany (1975–1990).

In electric steel production with scrap addition, the process in the 1970s was mainly to add an oxidizing slag, and then to change to a refining slag. Today, both low- and medium-alloyed steels are produced under one slag. The oxidizing treatment is followed by a reduction phase by the slag. All the other metallurgical operations have been moved to the later processing stages of the secondary metallurgy. Specific lime consumption in steel production in the electric arc furnace is currently 35–40 kg/t. Soft-burned lime usually has lump size 10–30 mm, and should have a sulfur content < 0.02%. With sponge iron instead of scrap, the amount of slag increases, because of the silica introduced with the gangue materials in the sponge iron. The amount of lime added depends on the amount of SiO2 that is to be reacted. The slag basicity (CaO/SiO_2) should be 1.5–2.

Modern developments in secondary metallurgy have led to new process steps in the operations that take place between the steelworks and the strand casting plant. Slags, which have become reactive contact phases, are now at the heart of metallurgical research and development. As there are many aims of secondary metallurgy, the slags used can differ widely. Lime-containing slags mostly consist of reactive $CaO–CaF_2–Al_2O_3$ mixtures for steel treatment in the ladle furnace, for intensive blowing in the ladle, or as a basic covering slag. The compositions of desulfurizing slags are ca. 55–60% CaO, 5–10% CaF_2 and Al_2O_3. Typical lime addition rates are therefore, 10–15 kg/t. As well as the intensive stirring process with synthetic slag, the injection of $CaO–CaF_2$ mixtures at the rate of 3–5 kg/t is common.

Metallurgical lime must fulfill special requirements for utilization of waste slag from the steelworks [32]. Steelworks slags, when used as hydratable components of building materials, should contain only such levels of lime and free magnesium oxide that volume stability can be absolutely guaranteed. For this reason the relevant specifications limit the free lime content to < 7% or < 4%, according to

the intended use (volume of intergranular free space).

The interests of the steelworks and the slag users coincide with respect to lime [32]. The steelworks require a readily soluble lime for metallurgical reasons. The slag user has problems with volume stability if the solid slag contains lime that failed to dissolve when it was liquid. Therefore, reactive, soft-burned lime should be used for slag utilization reasons.

6.3.2 Physical and Chemical Fundamentals

6.3.2.1 Thermodynamics

Metallic Systems Based on Iron

In steelmaking, the most common accompanying elements in molten iron are C, Si, Mn, P, S, and the gaseous elements H and N. In the reactions that take place when oxygen is brought into contact with the molten materials, the concentrations of the unwanted elements in the iron are reduced to the levels required in the steel produced. The thermodynamic data for metallic systems based on iron, such as solubility and activity, are of fundamental importance for the control of these reactions.

The state of carbon in Fe–C alloys can be seen from the phase diagram (Figure 6.18) [33]. Carbon dissolves in both molten and solid iron. Its solubility in the latter varies according to the crystal structure of the iron. Although carbon dissolves to only a very small extent in α-Fe and δ-Fe, its solubility in γ-Fe at 1153 °C is 2.1%. The solid solution of γ-Fe–C is known as austenite. The solubility of carbon in molten iron is given by the equation [34, 35]:

$$[\%C]_{max} = 1.30 \times 2.57 \times 10^{-3} t \quad (1)$$

$t = 1152–2000$ °C

The solubility of carbon in molten iron is also influenced by other elements present (Figure 6.19) [34].

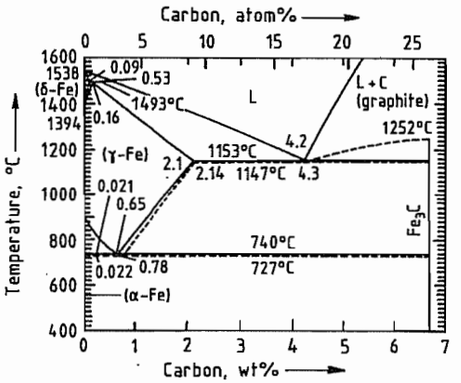

Figure 6.18: Phase diagram for Fe–C alloys.

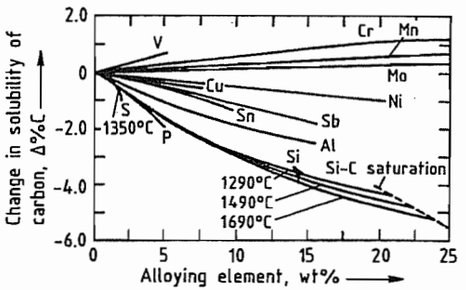

Figure 6.19: Effect of alloying elements on the solubility of carbon in molten iron alloys [34].

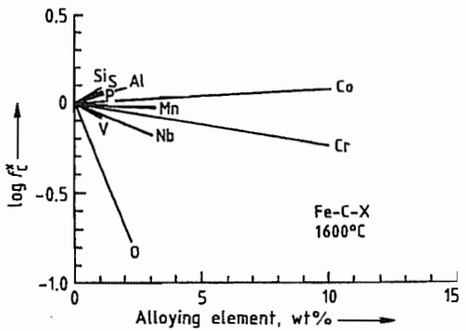

Figure 6.20: Effect of alloying elements on the activity coefficient of carbon in molten iron alloys [36].

The effect of other elements on the activity of the carbon in molten iron can be represented by the interaction parameters e_C^C and e_C^X. The value of e_C^C at 1600 °C is 0.14 [36]. The activity of the carbon is only slightly dependent on temperature. The effect of other elements on the activity coefficient of carbon is shown in Figure 6.20 [36].

The Fe–O phase diagram is shown in Figure 6.21 [37]. The liquid region, in which molten iron is in equilibrium with molten iron(II) oxide, is relevant to the steelmaking process. The solubility of oxygen in molten iron is limited by the precipitation of molten FeO in the reaction:

$$Fe_{(l)} + O \rightarrow FeO_{(l)}$$

The solubility of oxygen varies with temperature according to the equation [38]:

$$\log[\%O]_{max} = -\frac{6320}{T} + 2.734 \quad (2)$$

in the range 1530–1700 °C. Equation (2) corresponds to the line BB′ in Figure 6.21.

There have been many experimental determinations of oxygen activities in the system Fe–O and of the effect of other elements X in the system Fe–O–X. The temperature dependence of e_O^O is [36]:

$$e_O^O = -\frac{1750}{T} + 0.794 \quad (3)$$

The effect of various alloying elements and other additives on the activity coefficient f_O^X at 1600 °C is shown in Figure 6.22 [39].

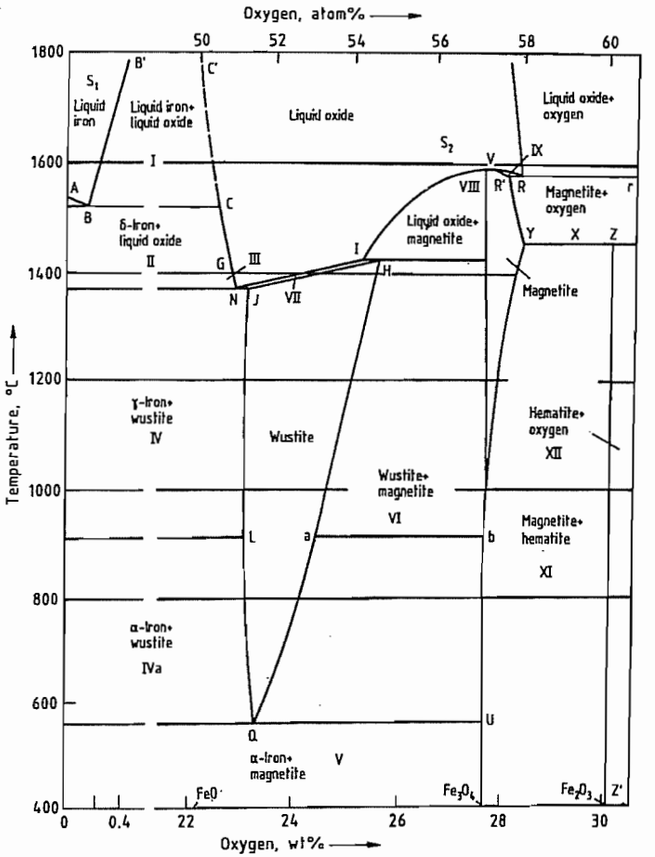

Figure 6.21: Phase diagram for Fe–O [37].

	T, °C	O_2, %	P_{CO_2}/P_{CO}
A	1536		
B	1528	0.16	0.209
C	1528	22.60	0.209
G	1400[a]	22.84	0.263
H	1424	25.60	16.2
I	1424	25.31	16.2
J	1371	23.16	0.281
L	911[a]	23.10	0.447
N	1371	22.91	0.282
Q	560	23.26	1.05
R	1583	28.30[b]	
R′	1583	28.07[b]	
S	1424	27.64	16.2
V	1597	27.64[c]	
Y	1457	28.36[b]	
Z	1457	30.04[b]	
Z′		30.06	

[a] Value for pure iron.
[b] $P_{O_2} = 0.1$ MPa.
[c] 5.75 kPa.

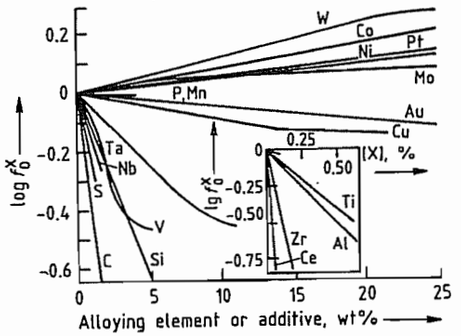

Figure 6.22: Effects of alloying elements and other additives on the activity coefficient of oxygen in molten iron alloys at 1600 °C [39].

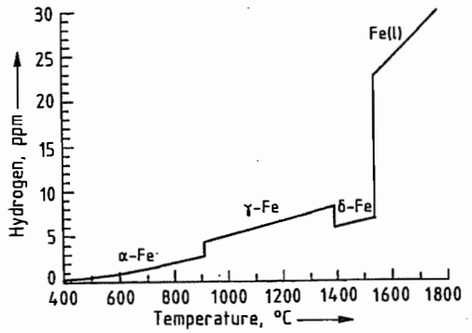

Figure 6.23: Effect of temperature on the solubility of hydrogen in pure iron at 0.1 MPa [40].

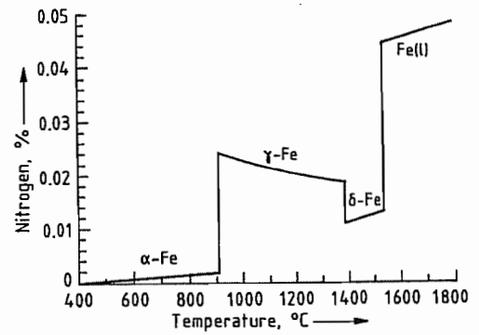

Figure 6.24: Effect of temperature on the solubility of nitrogen in pure iron at 0.1 MPa [40].

Hydrogen and nitrogen can have adverse effects on the properties of solid and liquid metals. During the process of steelmaking, hydrogen from atmospheric moisture usually enters the steel. The most important source of nitrogen during steelmaking is atmospheric air. Nitrogen is also absorbed during oxygen blowing, the N_2 content of the O_2 used being ca. 3%.

The solubility of H and N in iron obeys the Sievert square root law:

$$[\%H] = K_H\sqrt{p(H_2)} \quad (4)$$

$$[\%N] = K_N\sqrt{p(N_2)} \quad (5)$$

where p represents partial pressure.

The effect of temperature on solubility is reflected in variations of the equilibrium constants K_H and K_N. The solubility of hydrogen and nitrogen in pure iron at partial pressure 0.1 MPa (1 bar) is shown as a function of temperature in Figures 6.23 and 6.24 [40]. For hydrogen, the solution process is endothermic over the whole temperature range 400–1800 °C. Nitrogen dissolves exothermically in the γ-phase.

The solubility of hydrogen and nitrogen is changed by the presence of a third element, mainly by affecting the activity coefficient of the dissolved gas (Figures 6.25–6.28) [41–43].

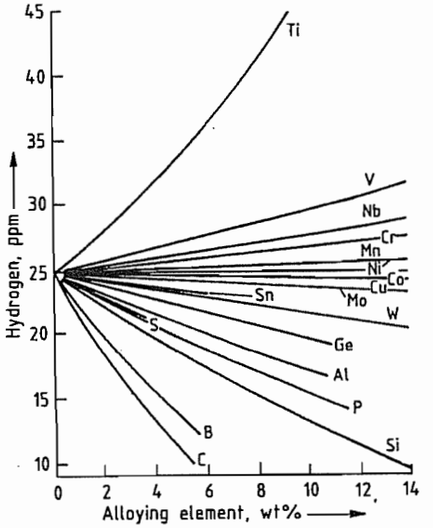

Figure 6.25: Effect of alloying elements on the solubility of hydrogen in iron alloys at ca. 1600 °C and $p(H_2) = 0.1$ MPa [41].

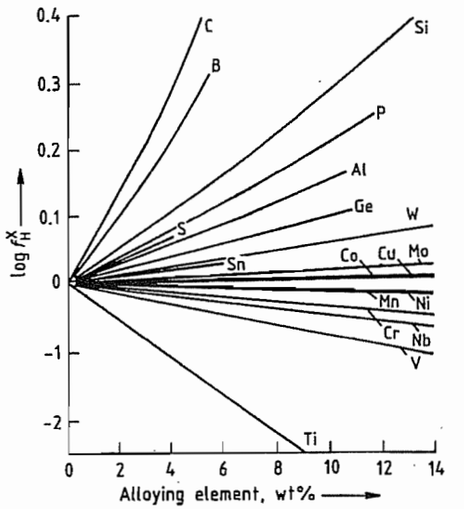

Figure 6.26: Effect of alloying elements on the activity coefficient of hydrogen in molten iron alloys at ca. 1600 °C and $p(H_2) = 0.1$ MPa [41].

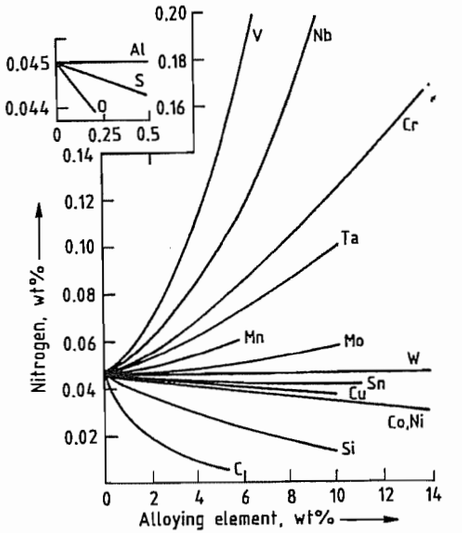

Figure 6.27: Effect of alloying elements on the solubility of nitrogen in molten iron alloys at ca. 1600 °C and $p(N_2) = 0.1$ MPa [42].

Slag Systems

In the steelmaking process, slags are formed as products of the refining reaction and by the addition of materials such as lime. It is extremely important that the slag forms quickly, enabling the important reactions between metal and slag, e.g., desulfurization and dephosphorization, to proceed until the required low levels of sulfur and phosphorus are obtained in the finished steel.

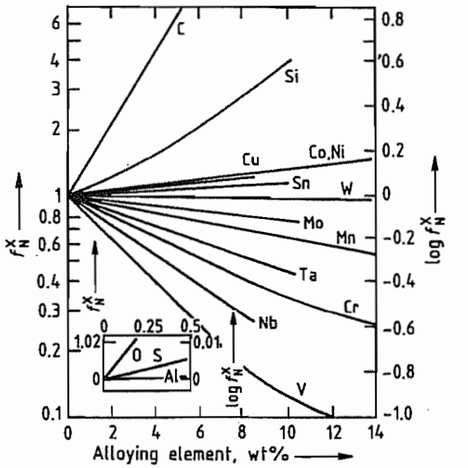

Figure 6.28: Effect of alloying elements on the activity coefficient of nitrogen in molten iron alloys at ca. 1600 °C and $p(N_2) = 0.1$ MPa [43].

Calcium silicate slags are important in the metallurgy of steelmaking when the raw materials have a low phosphorus content. The essential system is $FeO–CaO–SiO_2$ (Figure 6.29) [44]. In general, the total of these three components is > 80%, the remainder consisting mainly of MnO, with smaller amounts of P_2O_5, MgO, Al_2O_3, and Cr_2O_3. Figure 6.29 shows the solid phases in equilibrium with the melt at various surfaces of the precipitate. Continuous lines separate the saturation surfaces of individual solid phases from each other, at which more than one phase is precipitated on cooling. The isotherms are shown as broken lines. For steelworks slags, the most important region includes the stability zones of the liquid slags, dicalcium silicate, tricalcium silicate, and lime. An important isothermal diagram for steel manufacture is that at 1600 °C (Figure 6.30) [45], which shows lines of equal FeO activity for the equilibrium with

metallic iron. In the area a–b–c–d–e–f, the slags are liquid at 1600 °C. All other areas consist of more than two phases. The activity of FeO gives a measure of the tendency of the slag to oxidize, and from it the corresponding oxygen content of the melt can be deduced. The FeO activity is also important in desulfurization and dephosphorization.

Metal–Slag Reactions

Refining Reactions

In the refining treatment of molten pig iron to make steel, carbon is removed along with other elements, e.g., Si and Mn, by blowing the molten metal with oxygen. The thermodynamics of the reactions are independent of the process used; differences between the various processes affect only the kinetics of the individual reactions. Typical concentration changes in the steel melt during oxygen blowing in a basic oxygen converter are shown in Figure 6.31 [46]. The main aim is to reduce the carbon content to the desired value in the shortest possible time. However, the time must be long enough to enable the slag to form, the desired tapping temperature to be achieved, and phosphorus and sulfur to be removed from the system until the desired levels are reached.

Decarburization is achieved by the reaction:

$$C + O \rightleftharpoons CO \qquad (6)$$

The CO bubbles promote homogenization of the melt, and the elements H and N dissolved in the melt are picked up in the bubbles as they ascend. The equilibrium constant of the decarburization reaction [47] is given by:

$$\log K = \frac{1160}{T} + 2.003 \qquad (7)$$

In practical decarburization processes, a simplified expression for the equilibrium between C and O is used

$$[\%C][\%O] = 0.0025\,p(CO) \qquad (8)$$

at 1600 °C.

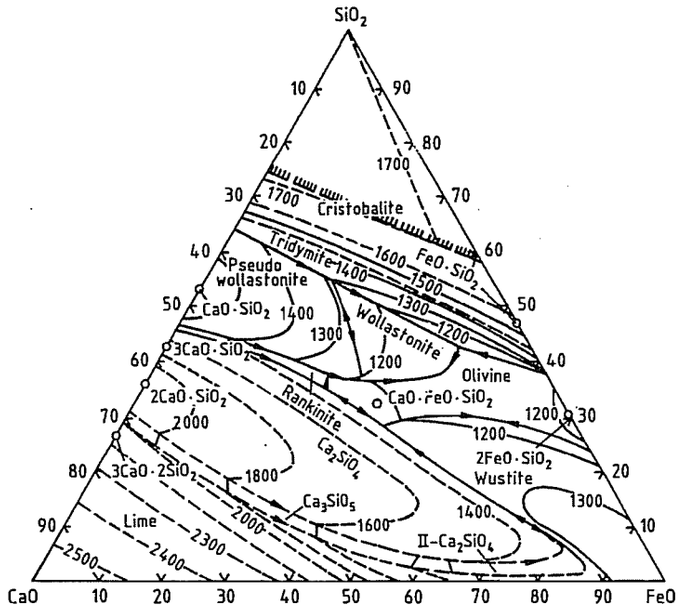

Figure 6.29: Phase diagram for CaO–FeO–SiO_2 [44].

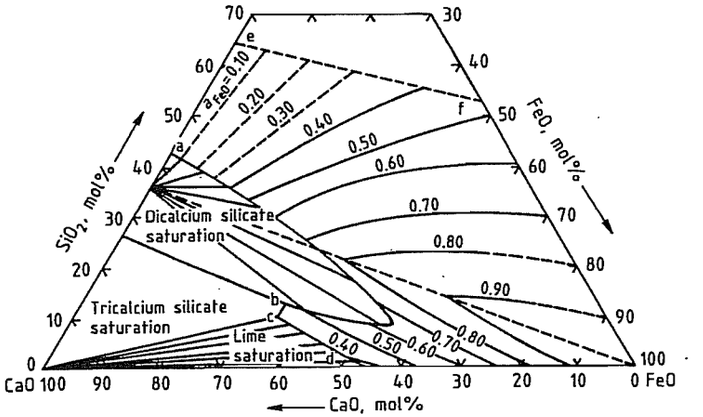

Figure 6.30: Phase diagram for CaO–FeO–SiO_2 with lines of equal activity for FeO at 1600 °C [45].

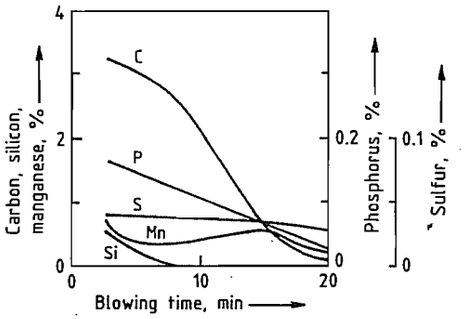

Figure 6.31: Changes in melt composition during the blow in a basic oxygen steelmaking converter (idealized) [46].

Silicon is rapidly removed during the oxidation process, owing to its high affinity for oxygen, and combines with the lime in the slag; oxidation takes place by the reaction:

$$Si + 2O \rightleftharpoons SiO_2 \qquad (9)$$

The equilibrium constant for this reaction is:

$$\log K = \log \frac{a_{SiO_2}}{a_{Si} a_O^2} = \frac{30\,110}{T} - 11.4 \qquad (10)$$

The exothermic oxidation of silicon provides a large proportion of the process heat. The oxidation product SiO_2, together with FeO, forms the first slag. This reduces the melting point of the added lime to such an extent that a reactive liquid slag can be formed. Therefore, the amount of CaO added and the amount of slag formed are mainly determined by the Si content.

Manganese is removed at the beginning of the oxidation process, mostly in parallel with silicon. Oxidation of manganese can be represented by the equation:

$$[Mn] + [O] \rightleftharpoons (MnO) \qquad (11)$$

The equilibrium constant is given by

$$\log K = \log \frac{a_{MnO}}{a_{Mn} a_O} = \frac{12\,590}{T} - 5.53 \qquad (12)$$

Toward the end of the silicon oxidation, the increased melt temperature leads to the reduction by carbon of the manganese oxide in the slag, according to the equation:

$$(MnO) + [C] \rightleftharpoons [Mn] + CO \qquad (13)$$

However, at the end of the blow, the manganese content decreases continuously, owing to oxidation of the manganese, mainly by FeO in the slag:

$$(FeO) + [Mn] \rightleftharpoons (MnO) + Fe_{(l)} \qquad (14)$$

Dephosphorization

The conditions in steelmaking processes favor dephosphorization of iron, which takes place by oxidation of phosphorus and combination with a basic slag. The reaction proceeds as follows:

$$2[P] + 5[O] + 4(CaO) \rightleftharpoons (4CaO \cdot P_2O_5) \qquad (15)$$

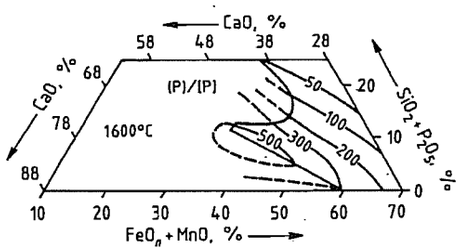

Figure 6.32: Lines of equal phosphorus distribution in the system $CaO–(SiO_2 + P_2O_5)–(FeO_n + MnO)$ [48].

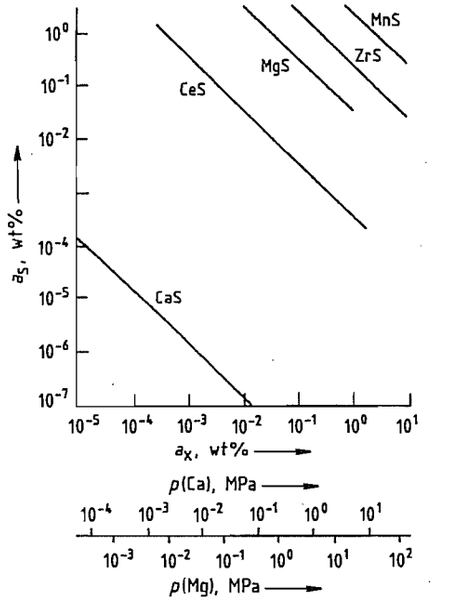

Figure 6.33: Equilibria between sulfur and various metallic elements in molten iron [49].

The equilibrium constant is given by:

$$\log K = \log \frac{a_{4CaO \cdot P_2O_5}}{a_{CaO}^4 a_{[P]}^2 a_{[O]}^5} = \frac{61\,100}{T} - 23.3 \qquad (16)$$

This expression shows that the conditions for oxidative dephosphorization are: (1) oxidizing slag (high FeO activity); (2) high activity of lime in the slag; and (3) low temperature, as reaction (15) is exothermic. These conditions are particularly well satisfied at the start of the process.

In low-phosphorus pig iron, the type most commonly produced today, the slag formed during steelmaking consists mainly of CaO, SiO_2, and FeO_n, with P_2O_5 content ca. 1–2%. The phosphorus equilibrium in this type of slag has been thoroughly investigated. In Figure 6.32, lines of equal phosphorus distribution at 1600 °C are shown for the system $CaO–(SiO_2 + P_2O_5)–(FeO_n + MnO)$, with 6% MnO and 2% MgO. As expected, the lines are approximately parallel to the lime saturation line.

Desulfurization

Unlike dephosphorization, desulfurization is a reduction reaction. Since the oxidizing conditions in the converter do not favor the removal of sulfur from the melt, desulfurization is mainly carried out by treatment of the pig iron or of the metal in the ladle.

Desulfurization can be carried out by means of the precipitation reaction that occurs when elements with a high affinity for sulfur are added, either by taking up the sulfur into the slag phase, or by transferring it into the gas phase.

The affinity for sulfur of a desulfurizing agent is indicated by the solubility product of its sulfide in molten iron (Figure 6.33) [49], the most stable of these being calcium sulfide. Although the alkaline earths and rare earths form relatively stable sulfides, their oxides are much more stable; the sulfides are formed only if the dissolved oxygen has been removed. The most commonly used desulfurizing agents are added to the steel in the form of alloys (CaSi, CaC_2, CaAl, etc.), by special techniques. The desulfurization reaction can be represented by the typical equation:

$$CaC_{2(s)} + [S] \rightarrow CaS_{(s)} + 2[C]$$

for which

$$\Delta G^0 = -359\,000 + 109.4T \text{ J/mol} \qquad (17)$$

Desulfurization by slag treatment is represented by the following equation, according to the ionic theory for slags:

$$(O^{2-}) + [S] \rightarrow (S^{2-}) + 2[O]$$

$$\Delta G^0 = 71\,965 - 38T \text{ J/mol} \qquad (18)$$

The most favorable thermodynamic conditions for slag desulfurization are: (1) high basicity of the slag; (2) low oxygen content in the slag or melt; and (3) high temperature.

Figure 6.34 shows the partition of sulfur between aluminum-containing steel and $CaO–Al_2O_3–SiO_2–MnO$ slag containing 5% MgO at 1625 °C [50]. Slags of this type are used for the desulfurization of steel in ladle metallurgy. The sulfur in pig iron can also be removed by Na_2CO_3. The desulfurization reaction is:

$$Na_2CO_3 + [S] + 2[C] \rightarrow (Na_2S) + 3CO_{(g)} \qquad (19)$$

or

$$Na_2CO_3 + [S] + [Si] \rightarrow (Na_2S) + CO_{(g)} + (SiO_2) \qquad (20)$$

The Na_2S formed can be oxidized by air:

$$2(Na_2S) + 2O_{2(g)} \rightarrow 2SO_{2(g)} + 2(Na_2O) \qquad (21)$$

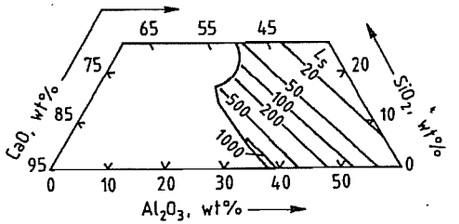

Figure 6.34: Sulfur partition coefficient L_S between aluminum-containing steel (a_{Al} = 0.07%) and $CaO–Al_2O_3–SiO_2–MgO$ slags containing 5% MgO at 1625 °C [50].

Deoxidation

At the end of the refining process, there is a considerable amount of oxygen dissolved in the molten steel; this can be removed by adding elements with a sufficient affinity for oxygen (precipitation deoxidation), or by slags which take up an amount of oxygen from the melt corresponding approximately to the equilibrium distribution (diffusion deoxidation).

The reaction between oxygen and a metal M in precipitation deoxidation can be represented by the equation:

$$x[M] + y[O] \rightarrow (M_xO_y) \qquad (22)$$

The equilibrium constant is:

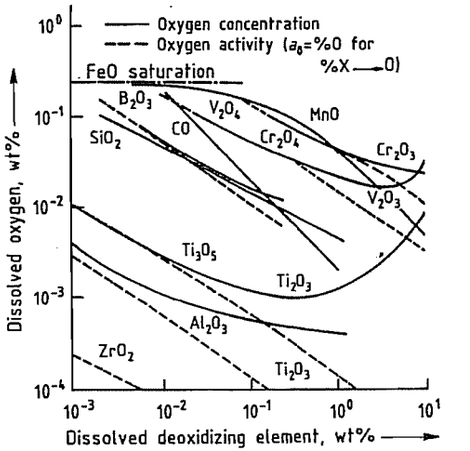

Figure 6.35: Deoxidation equilibria in molten iron at 1600 °C [51].

$$K = \frac{a_{M_xO_y}}{a_M^x a_O^y} \qquad (23)$$

In practice, either the deoxidation constant $K' = a_M^x a_O^y$ or the solubility product $K'' = [\%M]^x[\%O]^y$ is usually used. Small values of K' or K'' correspond to high deoxidizing power. The relative deoxidizing powers of various elements are shown in Figure 6.35 [51]. The activities, or concentrations, of oxygen are plotted against those of the deoxidation elements on a logarithmic scale. The three deoxidation elements most commonly used, in increasing order of effectiveness, are Mn < Si < Al. Aluminum is one of the most powerful deoxidation elements.

Deoxidation elements are often used in combination; the advantage of this lies partly in lowering the thermodynamic activity of the oxides formed, owing to compound formation, or dilution in the slag, and partly in the formation of oxidic slags with lower melting points, which separate more readily from the steel melt, or can be shaped at the rolling temperature. Figure 6.36 is a graphical representation of deoxidation with Al–Si. Various deoxidation products (alumina, mullite, and silicate) are formed, depending on the $[a_{Al}]/[a_{Si}]$ ratio.

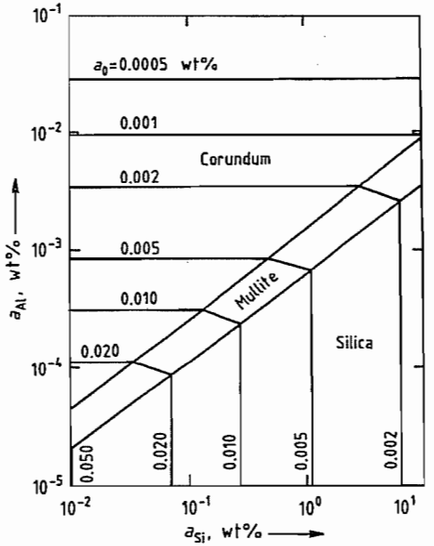

Figure 6.36: Deoxidation diagram for Al–Si–O at 1600 °C [49].

In diffusion deoxidation, no inclusions are formed in the melt, but long er reaction times are necessary to remove the oxygen. The reaction can be represented by:

$$[O] + Fe_{(l)} \rightarrow (FeO) \qquad (24)$$

Decreasing the FeO content of the slag leads to removal of oxygen from the melt. Diffusion deoxidation is being replaced by precipitation deoxidation.

Metal–Gas Reactions

If there is no slag on the surface of the molten metal, or if gas bubbles are formed within the melt, metallurgical reactions between the metal and gas phases take place. These include decarburization and degassing, either under reduced pressure, or by bubbling an inert gas such as argon through the melt.

As mentioned earlier, the concentrations of the gases dissolved in the iron depend on their partial pressures (Figure 6.37). Pressure reduction can cause hydrogen and nitrogen to be removed from the melt, but this is not the case with oxygen. Although the solubility of oxygen varies with pressure according to the equation:

$$[\%O] = K_O\sqrt{p(O_2)}$$

it is not feasible to remove oxygen simply by pressure reduction, as the required oxygen partial pressure is less than that attainable in vacuum vessels (10 Pa). However, it is possible to use vacuum in conjunction with reaction (6) in the melt between carbon and oxygen to form the gaseous deoxidation product CO. The equilibrium constant:

$$K = \frac{p(CO)}{a_C a_O}$$

explains the strong pressure dependence. Figure 6.38 shows the equilibrium between oxygen and carbon as a function of p(CO) [3.37]. A decrease in p(CO) leads to simultaneous decarburization and deoxidation.

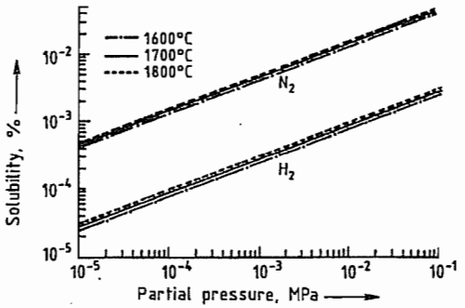

Figure 6.37: Solubility of nitrogen and hydrogen in molten iron [40].

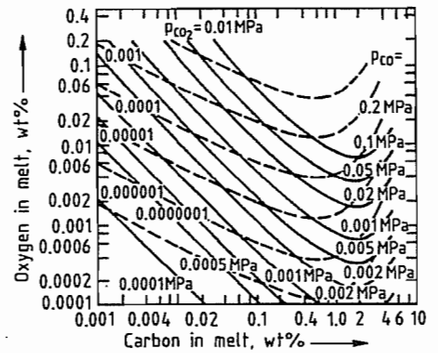

Figure 6.38: Equilibria between carbon and oxygen dissolved in molten iron with CO and CO_2 at various pressures and 1600 °C [52].

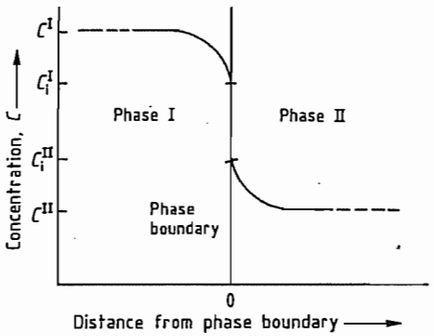

Figure 6.39: Schematic concentration profiles across a phase boundary.

Dissolved hydrogen and nitrogen can also be removed without vacuum degassing by bubbling an inert gas through the melt. As the partial pressures of the hydrogen and nitrogen in the bubbles of inert gas are almost zero, hydrogen and nitrogen diffuse from the melt into the bubbles, owing to the concentration difference, and ascend with them.

6.3.2.2 Kinetics and Mass Transfer

Kinetics of Heterogeneous Reactions

In the metallurgy of steel production, the kinetics of the heterogeneous reactions are of interest because the individual homogeneous phases are usually in local thermodynamic equilibrium, so that macroscopic reactions do not occur. Heterogeneous reactions occur between the various phases that are not in thermodynamic equilibrium with each other. Figure 6.39 shows the concentration profile of a substance in two phases in contact with each other. The total reaction is made up of several steps:

- Transport of the reactants to the phase boundary
- Chemical reaction at the phase boundary
- Transport of the reaction products from the phase boundary

The overall rate depends on the rate of the slowest step, known as the rate-determining step. If the overall process is considered, the mass flux density j is:

$$j = \frac{C^I - \frac{C^{II}}{K}}{\frac{1}{\beta_I} + \frac{1}{k} + \frac{1}{K\beta_{II}}} \qquad (25)$$

where C^I, C^{II} are concentrations in phases I and II, K is the equilibrium constant of the heterogeneous reaction, β_I, β_{II} are mass transfer coefficients, and k is the reaction rate constant. The equation:

$$\frac{1}{\beta_{tot}} = \frac{1}{\beta_I} + \frac{1}{k} + \frac{1}{K\beta_{II}} \qquad (26)$$

defines the overall mass transfer coefficient β_{tot}. Therefore, from Equation (25):

$$j = \beta_{tot}\left(C^I - \frac{C^{II}}{K}\right) \qquad (27)$$

The mass transfer coefficients β_I, and β_{II} are obtained from theory of mass transfer by using experimental data. The rate constant k is obtained from the chemical kinetics of phase boundary reactions for metallurgical systems. These rate constants are usually greater than the mass transfer coefficients of the transport processes that take place before and after the chemical reactions. The overall rate is therefore determined by mass transfer. Equation (27) gives the rate of mass transfer to a phase boundary when the mass transfer coefficient is known. To obtain an expression for the variation with time of the concentration of a dissolved substance in the mother phase, a mass balance must be carried out which takes account of the nature of the phase contact and the characteristic parameters for emulsified systems [53].

Flow and Mass Transfer Coefficients

Mass transfer into a phase is made up of diffusion and convection. In the interior of the phase, sufficient flow takes place to give a uniform concentration. Concentration gradients exist only near the phase boundary. As there is no flow at this boundary layer, mass

transport takes p lace by diffusion, and Fick's first law applies:

$$j = D\frac{C^{I} - C^{I*}}{\delta_N} \quad (28)$$

where the asterisk indicates the phase boundary.

If this is combined with the flow equation $j = \beta(C^{I} - C^{I*})$, the equation $\beta = D/\delta_N$ is obtained. Here, δ_N denotes the thickness of the boundary layer, and D the diffusion coefficient of the overlying material. To determine β, it is necessary to determine the boundary layer thickness, whose value depends on flow conditions. Theoretical analysis and experimental investigation of the various flow fields that occur in metallurgical processes yield a formula for calculating the mass transfer coefficient in dimensionless form.

Metal–Gas Phase Boundaries with Nonturbulent Flow

The flow field is represented in Figure 6.40. The flow from the interior of the melt is first deflected at a stagnation point, e.g., the top of a column of bubbles or the middle of an inductively agitated melt, flows parallel to the upper surface, and is again deflected at a later stagnation point, e.g., the wall, and flows back into the interior. In this way, the surface is continuously renewed. The diffusion process takes place between the gas phase and the metal flowing to the surface. A mean mass transfer coefficient for this condition can be calculated in the form of a Sherwood number *Sh*, as a function of the Reynolds number *Re* and the Schmidt number *Sc*:

$$Sh = \frac{2}{\sqrt{\pi}} Re^{1/2} Sc^{1/2} \quad (29)$$

where $Sh = \beta l/D$, $Re = ul/\nu$, $Sc = \nu/D$; β is the mean mass transfer coefficient (cm/s), l the flow length (cm), u the flow rate (cm/s), ν the kinematic viscosity of the melt (cm^2/s), and D the diffusion coefficient of the overlying material (cm^2/s).

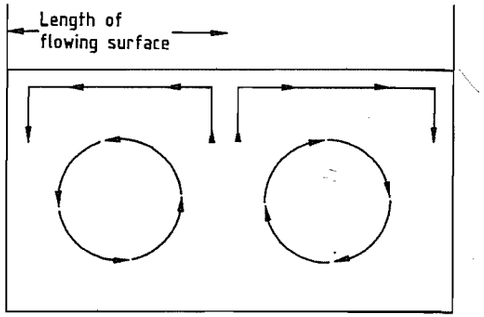

Figure 6.40: Mass transfer with continuous renewal of the free surface (schematic).

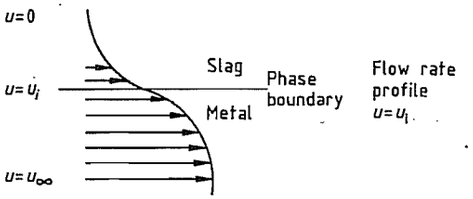

Figure 6.41: Flow field at a liquid–liquid phase boundary.

Metal–Slag Phase Boundaries with Nonturbulent Flow

This flow field is represented in Figure 6.41. Friction takes place between the slag and the metal. The phase boundary moves at a velocity u_i during mass transfer. In the determination of the mass transfer, momentum transfer due to friction must be taken into account. Equations for the flow film thicknesses on the metal and slag sides are first obtained. By including the condition that the shearing forces on each side of the phase boundary must be equal, the velocity of the phase boundary obtained and the mass transfer calculated.

Solid (Metal or Slag)–Liquid Phase Boundaries with Nonturbulent Flow

This condition represents, e.g., the processes of dissolution of alloys, or the solution abrasion of refractory materials. Mass transfer takes place on the liquid side. As shown in Figure 6.42, the flow rate, which is u_∞ within the melt, falls to zero at the boundary layer, and both the flow boundary layer and the diffusion boundary layer must be considered on the side of the melt. The mass transfer coefficient can be obtained by theoretical calculations from the equation:

$$Sh = 0.664 Re^{1/2} Sc^{1/3} \quad (30)$$

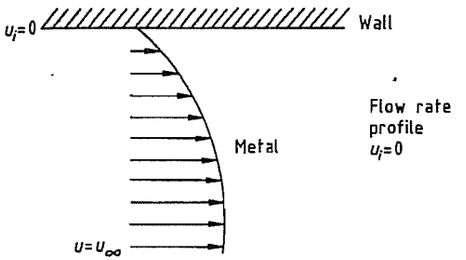

Figure 6.42: Mass transfer at a wall.

Mass Transfer with Turbulent Flow

In metallurgical vessels, turbulent flow is usually present, caused by ascending CO bubbles and/or blowing with oxygen. In turbulent flow, turbulence spheres at the phase boundary contribute additional mass transfer by their flow components perpendicular to the phase boundary. This mass transfer can be regarded as turbulent diffusion, leading to an increased value of the diffusion coefficient. To calculate the mass transfer at a solid wall with turbulent flow, the following equation can be used [54]:

$$Sh = 0.037 Re^{0.8} Sc^{0.2} \quad (31)$$

At free surfaces [53, 54]:

$$Sh = 0.32\left(\frac{D\rho u_\tau^3}{\sigma_{equiv}}\right)^{1/2} \quad (32)$$

where D is the diffusion coefficient, ρ the density of the melt, σ_{equiv} the equivalent interfacial tension of the melt, and u_τ the shearing force rate for turbulent flow.

The equivalent interfacial tension differs from the normal interfacial tension in that the back pressure, caused by the irregularity of the boundary surface, is expressed as the sum of the effects of interfacial and gravitational forces [54]. For steel melts, which have high interfacial tensions, σ_{equiv} can be assumed equal to the interfacial tension of the melt. The shearing force rate u_τ is a measure of the degree of turbulence. The value must be determined by turbulence measurements. For steel melts, this can at present only be investigated with the aid of mathematical models.

Equation (32) is also valid for metal–slag phase boundaries with turbulent flow, if there is no turbulence in the slags, and if the full weight of the stationary slag layer on the melt is considered when calculating the equivalent interfacial tension. If there is any turbulence in the slag, this should be included. However, it is often negligible.

6.3.3 Production Processes

Steel production depends on the availability of raw materials such as pig iron, scrap, and sponge iron. There are two fundamentally different methods (Figure 6.43) [55]: blowing oxygen into liquid iron (mainly pig iron), and smelting iron-containing materials, such as scrap and sponge iron.

A typical example of the first method is the oxygen converter. In the electric furnace, and (now of less importance) the open hearth furnace, large amounts of scrap and sponge iron can be melted together. Depending on local conditions, mixed methods can also be used, in which various proportions of scrap and pig iron are processed, e.g., the KMS (Klöckner–Maxhütte–Stahlerzeugungsverfahren, and EOF (energy-optimized furnace) processes.

The object of all steel production processes is the removal of unwanted metallic, nonmetallic, and gas-forming elements from the raw materials, and the controlled addition of alloying elements to obtain the required characteristics of the various grades of steel.

The growth of world crude steel production, and the proportional contributions of the various processes are shown in Figures 6.44 and 6.45 [56, 57].

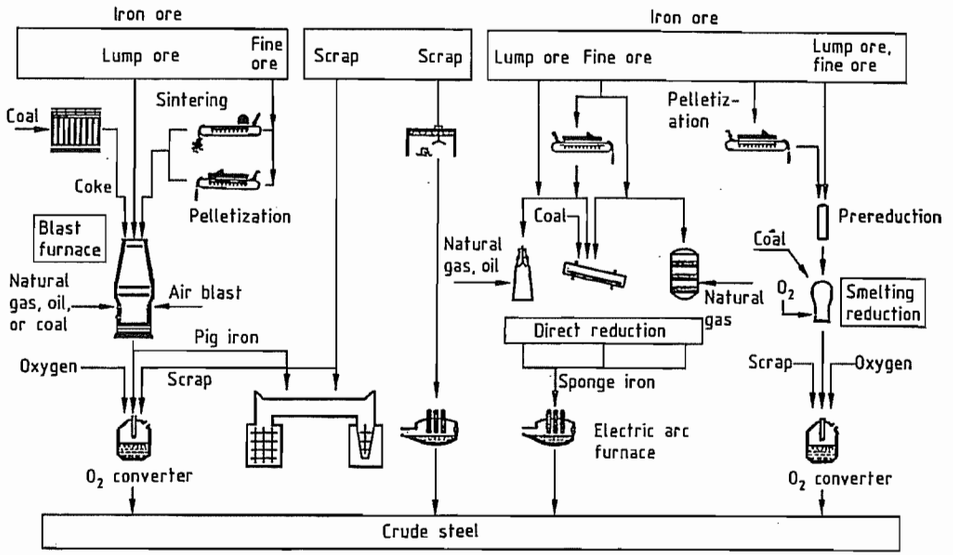

Figure 6.43: Crude steel production methods.

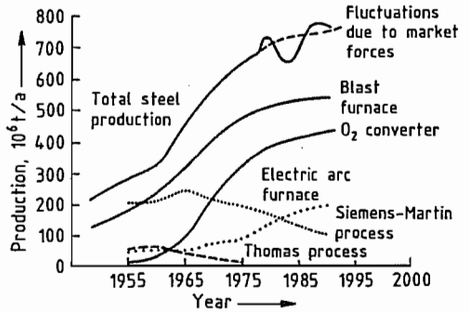

Figure 6.44: Growth of world pig iron and crude steel production by various processes.

6.3.3.1 Oxygen-Blowing Processes

Unwanted elements in pig iron (and sometimes in scrap), principally carbon, silicon, and phosphorus, are removed by the oxidation reactions and transferred into the gas or slag phases (decarburization).

The carbon monoxide produced is a source of thermal energy. After thorough purification, it is collected in gasholders and burned to provide heat for associated production plant. The oxides SiO_2 and P_2O_5 dissolve in the liquid slags formed from the added lime and the iron oxide produced during the oxidative decarburization processes.

The energy required to raise the temperature and melt the raw materials during the blowing process comes from the enthalpies of the oxidation reactions:

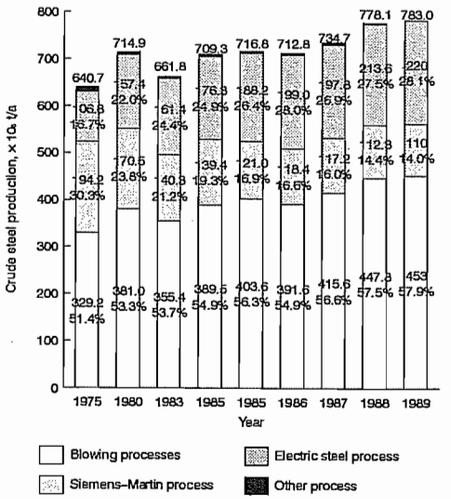

Figure 6.45: Growth of crude steel production, with contributions of the various production processes. * Estimated.

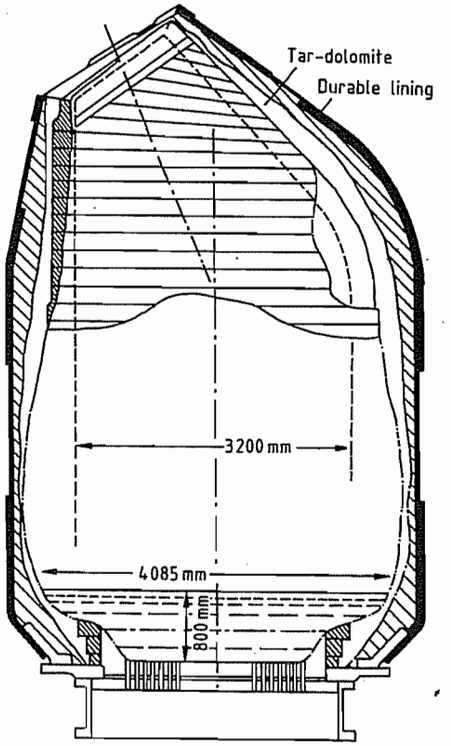

Figure 6.46: Section through a Thomas converter after 400 melts.

$2C + O_2 \rightarrow 2CO \quad \Delta H = -221$ kJ

$2Fe + O_2 \rightarrow 2FeO \quad \Delta H = -529$ kJ

$Si + O_2 \rightarrow SiO_2 \quad \Delta H = -878$ kJ

$2Mn + O_2 \rightarrow 2MnO \quad \Delta H = -771$ kJ

From ca. 1870, conversion of pig iron to liquid crude steel was carried out by blowing air, the oxidizing agent, through tuyères in the base of a bottom-blown converter (tiltable steel vessel with refractory lining) containing a 20–80 t charge. Steel production processes using air blowing can be subdivided into the Bessemer process (only for low-phosphorus pig iron) and the Thomas process (capable of removing phosphorus). In the Bessemer process, the converter was lined with silica bricks. It was not possible to use a lime-containing slag to combine with the P_2O_5, owing to the acidic lining. In the Thomas process (Figure 6.46), dolomite was used to line the converter, and a lime-based slag could then be used to treat phosphorus-containing pig iron [58].

The nitrogen in air dissolved to some extent in the liquid steel, and has a detrimental effect on its properties. Increasing quality requirements (aging stability, etc.) and the unfavorable economics of this process led to its discontinuation.

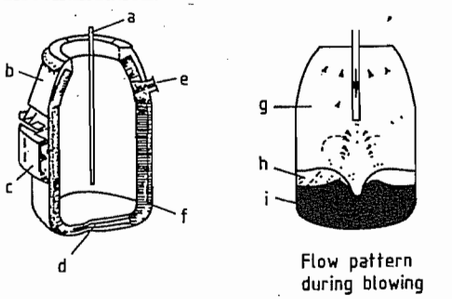

Figure 6.47: Top-blown oxygen converter: a) Oxygen lance; b) Converter top; c) Supporting ring; d) Converter bottom; e) Taping hole; f) Refractory lining; g) Gas space; h) Slag layer; i) Molten metal.

LD and OBM Processes

The first LD (Linz–Donawitz) converter, with a capacity of 30 t, was operated in Linz in 1952. The decarburization reaction is greatly speeded up by the use of pure oxygen, giving blowing times of 10–20 min. The oxidation enthalpies result in lower heat losses and enable more scrap or ore to be added. The converters have total charge 50–400 t, and are lined with dolomite or magnesite bricks [55].

Oxygen is injected from above through a water-cooled lance with several nozzles, onto the surface of the melt (Figure 6.47). The high-pressure jets of oxygen (up to 1.2 MPa) oxidize the iron, carbon, and other elements at rates depending on their affinity for oxygen. The gas reactions cause thorough mixing of the molten materials, and this is maintained after completion of the blowing process by purging bricks built into the base of the vessel. Temperatures of 2500–3000 °C are produced in the central reaction zone, and a reactive slag is rapidly formed from the added lime and the oxidized iron. The thermodynamic and kinetic

processes are described in Sections 6.3.2.1 and 6.3.2.2. The heat and mass transfer processes take place according to the rules given earlier.

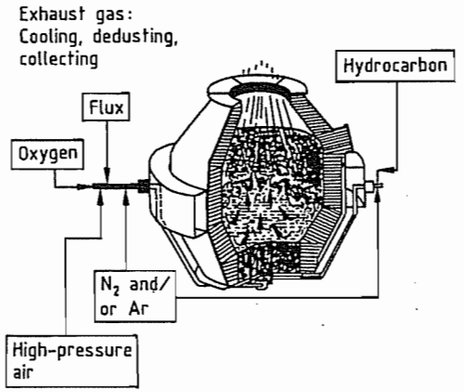

Figure 6.48: Section through an OBM converter. Oxygen is injected from below, through tuyères cooled by hydrocarbons blown into the melt.

The OBM (oxygen-blowing technique) (Figure 6.48), a modification of the air blast processes, was developed in 1968–1969 in Sulzbach-Rosenberg [55]. Pure oxygen is passed through bottom tuyères into the melt. These tuyères are highly stressed, and are stabilized by cooling them with hydrocarbons. The cooling effect is a result of the endothermic decomposition of the hydrocarbons by the hot melt. The OBM process causes more intensive mixing of the steel and the slag compared with the method of blowing in the oxygen from above. This gives improved reaction kinetics and yield, owing to the lower iron content of the slag. The advantages of the more rapid slag formation and the less violent blow can be enhanced by adding powdered lime through the bottom of the converter, along with the oxygen. However, the capacity of the OBM process for melting scrap is limited in comparison with the LD process, owing to the lesser extent of afterburning of the waste gases, and the smaller amount of iron oxidation.

The combined blowing technique in general use today (Figure 6.49) has been developed from the top-blowing process and past experience of the bottom-blowing process [55]. The combined process provides:

- Homogeneous melts due to rapid breakdown of the scrap
- Reduction of the blowing cycle time by 25%
- Higher yield of iron and alloying elements
- Better control of the chemical composition
- Improved purity
- Lower quantity of slag and reduced tendency for it to be ejected
- Increased lifetime of the converter lining
- More favorable conditions for the measuring systems for process control

Plant layouts do not differ greatly from one another. Figure 6.50 shows a side view of the converters and continuous casting plant of a steelworks [55].

Depending on the products required, the pig iron in the torpedo ladle car or filling pit is desulfurized by blowing with slag formers containing lime and/or magnesium. In Japan, for steel products with a very low phosphorus content, it is also usual to remove the silicon and phosphorus [59]. In this case, the converter simply removes carbon from the melt (Figure 6.51).

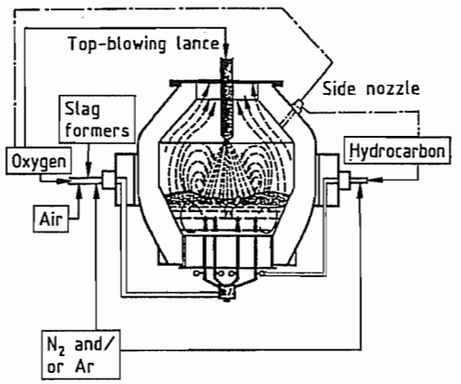

Figure 6.49: Combined blowing technique with top-blowing lance or side tuyère.

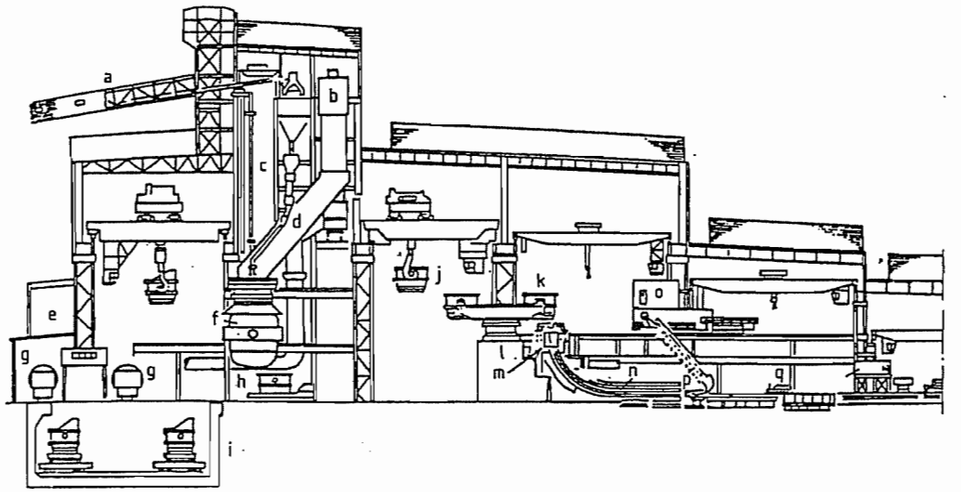

Figure 6.50: Converter and continuous casting plant: a) Feeder conveyor belt; c) High bunker; c) Blowing lance; d) Chute; e) Control room; f) 310 t converter; g) 600 t torpedo ladle car; h) Ladle transporter; i) Pig iron filling pit; j) Filled ladle; k) Pouring ladle; l) Ladle turret; m, n) Continuous casting machine; o) Continuous casting control room; p) Dummy bar; q) Cutting.

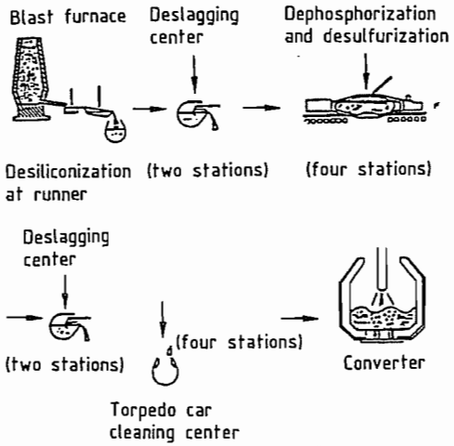

Figure 6.51: Hot metal pretreatment process at Mizushima works.

The mathematical model of the process calculates the quantities of pig iron, scrap, and lime for the melt (based on the composition and temperature of the raw materials); the nominal tapping temperature; and the analysis of the crude steel, and starts the oxygen addition after the scrap and pig iron have been charged. Distribution of the oxygen and control of the height of the lance are computer controlled. The course of the blowing operation is set by the dynamic process control, which requires occasional fine adjustments based on "sub-lance measurements", that give the temperature and the carbon and oxygen content of the melt. Other elements may also be determined if required. Figure 6.52 shows how the melt temperature and composition change during the blowing operation. Here, the final composition is 0.059% C, 0.031% Mn, 0.018% P, 0.019% S, 0.003% N, and 0.083% O. Figure 6.53 shows the corresponding changes in the composition of the slag [60].

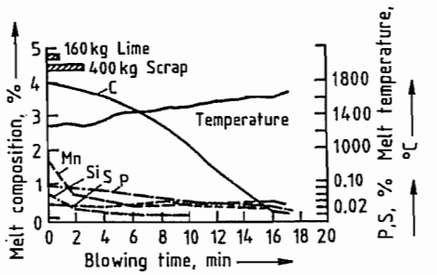

Figure 6.52: Changes in melt temperature and composition during blowing.

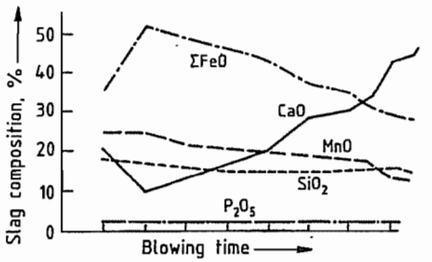

Figure 6.53: Changes in slag composition during blowing.

At the end of the oxygen treatment, the converter is tilted and the steel is tapped into a ladle (a steel container with bottom-pouring facility and refractory lining). The steel is separated from the slag during emptying of the converter by means of a floating stopper introduced into the tapping spout. This prevents the slag, which is of lower density, from running out. Alternatively, an electromagnetic measurement in the tapping system can give a signal for the emptying process to be stopped.

To prevent emission of dust in the waste gases, all sources of dust, such as the pig iron handling and charging operations, lime feeding equipment, etc., are linked to a filtering system, usually cloth filters. The physical and chemical heat of the converter waste gases are utilized by installing a waste heat steam boiler with associated electrostatic filter or scrubber. The waste gases, at 1400–1600 °C, supply heat to the steam generation system, and the cooled gases, calorific value ca. 7000 kJ/m^3, are collected in a gasholder after purification. The dust collected in the filters or scrubbers can be recycled to the process, after suitable treatment.

Other Developments

Steel production processes based on an air or oxygen blast are autothermic, i.e., the energy requirement is provided by the physical and chemical heat from the pig iron. The use of scrap is limited by the composition and temperature of the pig iron, and varies between 0 and 20%, depending on process variations and quality requirements.

Higher additions of scrap require the use of an allothermic process, with added fuel. In the KMS (Klöckner–Maxhütte–Steelmaking Process) process, additional energy is provided by adding hydrocarbons during scrap preheating, or powdered coal or coke during the blowing operation. This process is extremely flexible with regard to the metallic materials used, i.e., scrap, pig iron, and sponge iron.

In the KS process, the use of pig iron is completely eliminated. In the first phase, a carbon-rich melt is produced by melting scrap and adding carbon by a blowing process, together with an equivalent amount of oxygen. Heat transfer is optimized by afterburning the reaction gases. In the second phase, conversion of the carbon-rich melt to steel is completed by the further addition of scrap.

In the Tula process (developed in the former Soviet Union), a carbon-containing material in lump form is added from above to a combined blowing converter. This provides the energy required for melting the scrap.

The EOF furnace (energy-optimized furnace) uses combustion of the waste gas and continuous preheating of the scrap in the hot waste gas stream to minimize the additional fuel requirements for an increased proportion of scrap in the melt. This has enabled up to 60% steel scrap to be used.

6.3.3.2 Electric Steel Process

In the electric steel process, the heat required is obtained not by oxygen combustion of the accompanying elements in the pig iron, but from electrical energy. The conversion of electrical energy into heat can be achieved by an electric arc, induction, or plasma furnace. Electric steel processes are based on the use of scrap, with small amounts of solid pig iron. For a long time, the use of these processes was limited to the production of special steels, as energy consumption was high and the economics were unfavorable. Increases in the size of power stations and the capacity of electrical distribution systems have enabled batch weights to be increased, and the costs of energy, electrodes, refractory material, and capital investment to be reduced. Today, this process is second in importance only to the oxygen-blowing process in world crude steel production (Figure 6.47).

Over 90% of all electric steel produced is by the use of the a.c. electric arc furnace [61]. Three graphite electrodes carry the current through the furnace roof into the charge of metal. The electric arc formed melts the charge at temperatures up to 3500 °C. The furnace has the following essential components: the vessel or shell with a furnace door and a tapping hole; the roof which can be removed for charging; electrode arms which support the electrodes; tilting equipment for emptying the furnace; the furnace transformer; and the measuring and control equipment.

The melting procedure for the electric arc furnace comprises the following stages:

- Charging
- Melting
- Oxidization (decarburization), with an increase in temperature
- Tapping

The raw materials (scrap, sponge iron, pig iron, alloying elements, etc.) together with the required additives (lime, coal, ore, etc.) are loaded into special charging buckets which are then emptied into the furnace through a bottom opening. To fill the furnace, two or three charging operations are required, between which the scrap is partially melted.

The melting process begins with switching on the current and striking the arc. A supplementary blow with oxygen and fuel oxygen mixtures accelerates melting and reduces current consumption. The duration of the melting period is determined by the electric power limit and the maximum heat load of the furnace shell.

Oxidation of elements, such as silicon, manganese, carbon, phosphorus, and sulfur begins during the melting phase as the liquid reactants, steel and slag, react with the added oxygen. The gaseous carbon monoxide formed from the reaction between the iron oxide and the carbon causes bubbling in the melt and purges the hydrogen and nitrogen. Removal of the phosphorus as calcium phosphate in the slag during the oxidation phase is important, and all the other metallurgical processes take place during the reductive secondary metallurgical treatment in the ladle or ladle furnace.

After the steel has reached the required temperature, the tap hole is opened and the furnace is tilted to empty it into the ladle below.

The development of the modern electric steel process began early in 1960, using powerful transformers and blowing with oxygen (Figure 6.54) [62]. Modern furnace design and process control techniques have made it possible to increase the specific transformer power from 300–400 kVA/t to 800–1000 kVA/t. The electric furnaces of this new generation are operated at a power factor of 0.8–0.86, and enable tap-to-tap times of 50–80 min, and throughputs of > 100 t/h to be achieved (Figure 6.55).

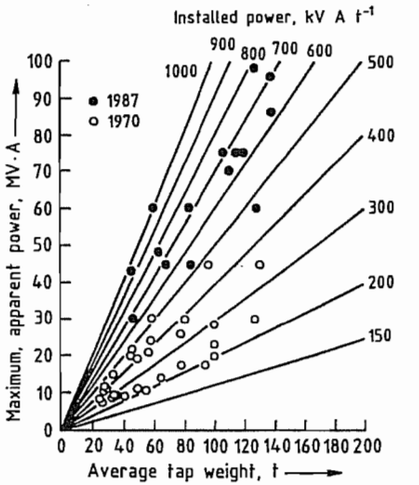

Figure 6.54: Development of specific installed power.

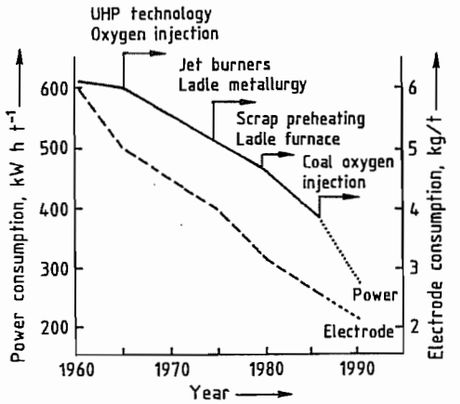

Figure 6.55: Effects of developments in electric arc furnace technology since 1965 on specific power and electrode consumption.

The essential characteristics of modern electric steel production are:

- Process automation
- Enclosure of the furnace
- Preheating of the scrap
- Water-cooled wall and roof elements
- Gas/oil–oxygen jet burners
- Foam slagging
- Current-carrying supporting arms for the electrodes
- Electrode cooling
- Facilities for charging through the furnace roof
- Bottom stirring devices
- Slag-free tapping (eccentric bottom tap hole)

Owing to their high energy input, modern electric furnaces produce considerable quantities of smoke and waste gas. To minimize environmental pollution, the furnaces are enclosed. Conditions in the workplace and surroundings can thus be maintained to a standard that meets legal requirements.

The waste gases produced in the furnace are extracted through an aperture in the furnace roof, and the dust from various sources in the furnace area is collected in the upper part of the housing. This is constructed from sound-insulating elements, and reduces the noise level from the furnace to 20–25 dB. The waste gas is passed through a cooler which can also serve to recover the heat, and is then dedusted by cloth filters. In some operating conditions, the dust from the electric furnace can contain considerable quantities of heavy metals, such as zinc and lead, and so it is worth recovering them.

The slags produced consist of calcium silicate with 10–15% iron oxide. These are quite stable, and can be used as fill for road and dam construction.

The very rapid development of the d.c. electric arc furnace began in the middle of 1985 (Figure 6.56) [63]. Important advantages are:

- Lower electrode consumption
- Savings in electrical energy
- Smaller effect on the electricity supply system
- Symmetrical distribution of heating in the melt
- Stirring effect on the melt

The central electrode becomes the cathode, and the melt the anode, the bottom of the furnace vessel being insulated from the wall. Current-carrying elements are built into the hearth, and provide an electrical connection to the melt.

The d.c. arc acts as a jet pump, directing the gases in and around the electric arc plasma toward the melt, causing efficient heat transfer from the electrode to the melt. The largest d.c. furnace operating has a capacity of 130 t, with a transformer power of 100 MV·A, and a steel output of 10^6 t/a.

An important feature of modern electric steel production is computer control. The supervision and control of the production units, combined with precise data collection, leads to improved material flow and more efficient utilization of energy and alloying metals, and ensures high and reproducible quality.

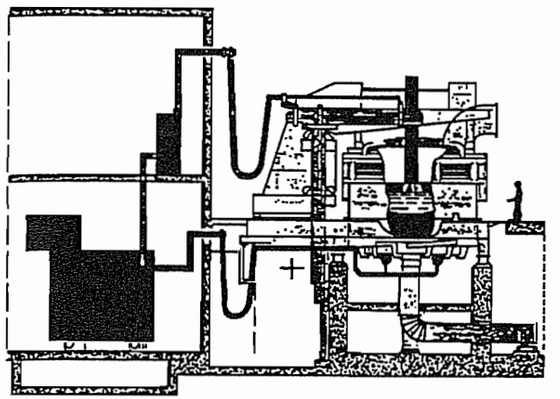

Figure 6.56: The bottom is made of electrically conducting refractory material to ensure reliable and durable continuity.

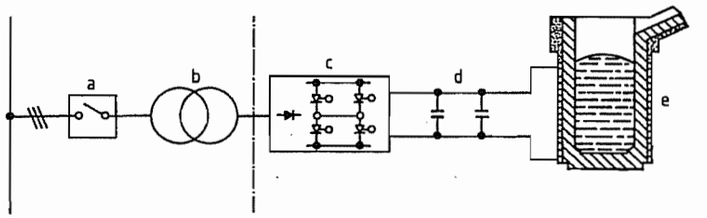

Figure 6.57: Electric induction furnace: a) Circuit breaker; b) Transformer; c) Frequency converter; d) Capacitor bank; e) Induction furnace. Melting capacities of 15 t/h can be achieved at current densities of 1 MW/t in an 8 t medium-frequency furnace.

Special Processes

In foundries, induction furnaces are widely used for melting and holding steel and nonferrous alloys [63]. The water-cooled, current-carrying coil surrounds a refractory-lined crucible (Figure 6.57) that holds the material to be melted. Electricity is supplied by a medium-frequency (MF) frequency converter, fed from a high- or low-voltage transformer. The current density can be 1 MW/t, and an output of 15 t/h can be obtained from an MF furnace with a capacity of 8 t.

Since the development of high-power plasma burners, it has become possible to use plasma melting furnaces for the production of special steels in 40 t batches. The energy is supplied by adjustable d.c. argon plasma burners, built into the furnace shell. The burner produces a plasma (ionized gas) in the electric arc, at temperatures 3000–5000 °C, and this melts the furnace contents. The use of inert gases for the plasma protects the melt against reactions with oxygen, nitrogen, hydrogen, etc., thereby ensuring a high yield of alloy. Carburization of the melt does not occur, as there are no graphite electrodes. Vacuum treatment of the steel is not necessary.

For the production of special alloys containing high proportions of alloying elements with a high affinity for oxygen (Al, Ti, etc.), it is common to use inductively heated or electron beam vacuum furnaces.

The Siemens–Martin Open Hearth Process

In 1960, the Siemens–Martin open hearth process (Figure 6.58) produced ca. 70% of the world's crude steel, but this rapidly declined following the growth of the oxygen-blowing

and electric steel processes, and ceased operation after a few years.

It was developed for melting scrap, and was characterized by its great flexibility with respect to the proportions of pig iron and scrap used. The tank-shaped furnaces are heated by fossil fuels such as gas or oil, burned in hot air. The regenerative air preheating invented by Siemens takes place in "checker chambers" that contain refractory bricks heated by the waste gas, and are situated under the furnace. The combustion temperatures achieved enable steel scrap to be melted.

The capacity of these furnaces is 50–1000 t. The use of air for the combustion leads to the production of large quantities of waste gas, whose purification, sometimes including desulfurization, is difficult and expensive. Additional oxygen, introduced through lances or burners (tandem furnaces), has been used to improve operation, but this leads to severe erosion of the refractory furnace lining. The open hearth process has in general lost its importance, as it cannot achieve either the output or flexibility of blowing processes.

6.3.3.3 Production of Stainless Steels

Although world steel production is subject to very severe fluctuations dictated by market conditions, the average growth rate of stainless steels (i.e., resistant to rust, acid, and heat) between 1950 and 1985 was 6%. In 1990, total output reached 10^7 t. Special metallurgical processes have been developed for steels with a chromium content 12–28% and low carbon content [65].

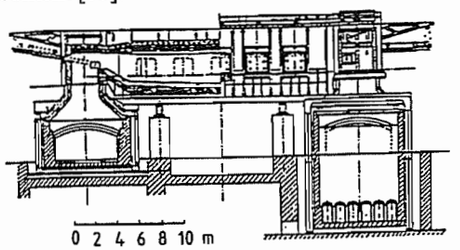

Figure 6.58: German–American design for a 250 t furnace for gas and oil firing [64].

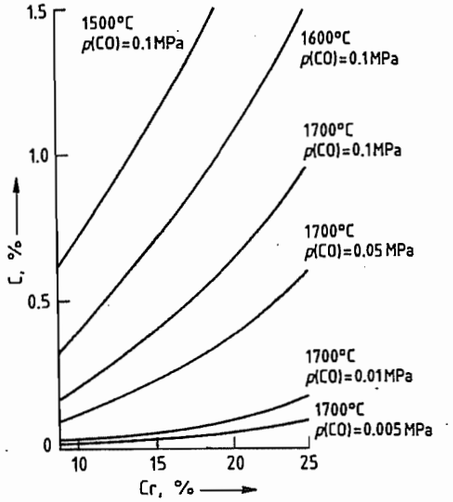

Figure 6.59: The Fe–C–Cr–O system.

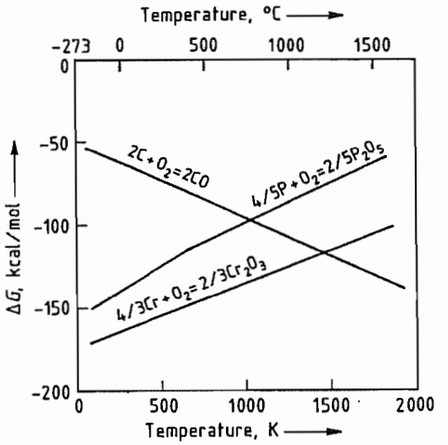

Figure 6.60: Free energy of oxidation of Cr, P, and C as a function of temperature.

Production conditions are determined by the thermodynamic equilibria of the reactions of oxygen with carbon and chromium (Figures 6.59, 6.60).

In the first process variation, which is mainly used in western countries, an electric furnace is used to melt scrap and alloying elements. The composition of the molten metal used corresponds approximately to that of the desired steel product, apart from the carbon

content. Decarburization and desulfurization are carried out, either in a converter or a ladle in vacuum, or in a combination of the two (Figure 6.61).

The converters are operated by the combined blowing technique (i.e., via top lance and bottom tuyères) to increase the rate of decarburization. Nitrogen is used as the protective gas for the bottom tuyères and to reduce the oxygen partial pressure. Argon is used to give low carbon contents and to avoid nitrogen pick up of the steel. After decarburization, the Cr_2O_3-containing slag is reduced with silicon, and the sulfur combines with the lime-based slag. In an alternative process, the premelt is poured from the electric furnace into a ladle placed in a vacuum chamber. Decarburization is then achieved by a stream of oxygen which enters via the lid of the vacuum chamber as the pressure is reduced, and is then blown through a lance into or over the melt.

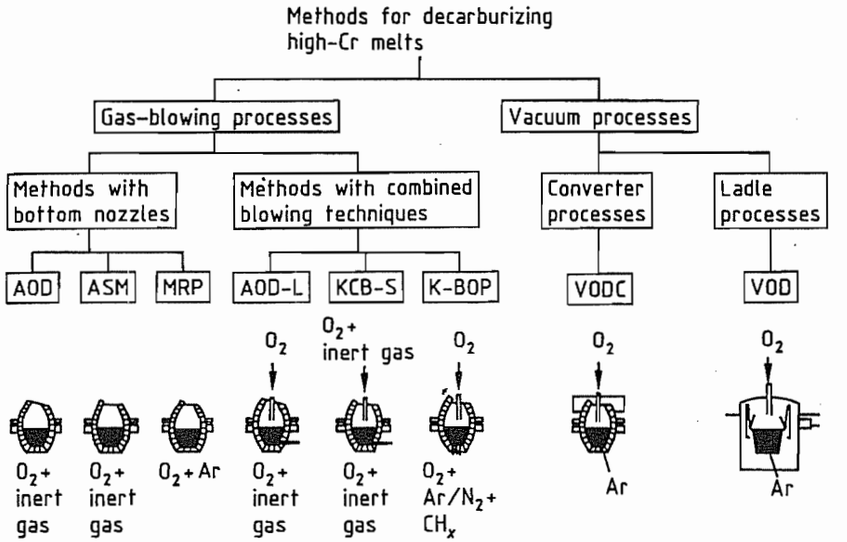

Figure 6.61: Methods for decarburizing high-chromium melts: AOD = argon–oxygen decarburization; ASM = argon secondary metallurgy; MRP = metal refining process; AOD-L = argon–oxygen decarburization lance; KCB-S = Krupp combined blowing stainless; K-BOP = Kawasaki basic oxygen process; VODC = vacuum–oxygen decarburization converter; VOD = vacuum–oxygen decarburization.

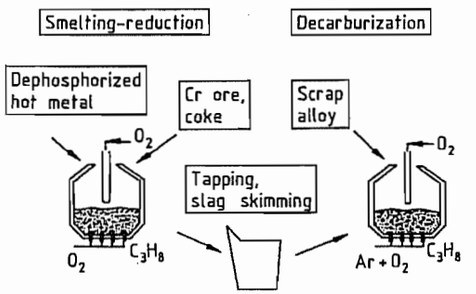

Figure 6.62: Two-stage stainless steel production (smelting–reduction) process.

In the vacuum process, the rate of decarburization reaches 0.03%/min, a considerably lower figure than that achieved by the converter processes. The latter give high productivity and favorable economics and are therefore, used for high-volume production of crude stainless steels. Vacuum processes are especially suitable for the production of special steels with very low carbon content (30 ppm), and low levels of nitrogen and hydrogen.

A combination of both processes utilizes the high decarburization rate of the converter in the high-carbon content region, and the low

carbon levels achievable by the vacuum process.

In Japan, a two-stage process is used for the melt reduction of chromium ores to produce stainless steels (Figure 6.62) [66]. Two 85 t combined blowing converters are used. In the first of these, chromium ore is added to a dephosphorized pig iron bath where it is reduced to chromium with coal and oxygen. The carbon-containing chromium melt is tapped and, after slag removal, charged to the second converter, where it is decarburized. The heat of reaction enables added scrap and alloying metals to be melted. The advantage of the combined blowing converter is that, as well as passing oxygen and argon through the bottom tuyères, it is also possible to decarburize with pure oxygen, as the tuyères are cooled with hydrocarbons.

6.3.4 Secondary Metallurgy

The steelmaking processes described earlier with the exception of plasma furnaces, take place in oxidizing atmospheres, and are designed to maximize the output and cost-effectiveness of crude steel production.

The secondary metallurgical treatment processes produce the specific properties required for the various applications of the steels concerned. They include:

- Adjustment of alloy composition
- Deoxidation
- Homogenization of temperature and composition
- Temperature adjustment
- Decarburization
- Desulfurization
- Degassing
- Control of inclusion shape
- Adjustment of purity

The processes take place in the steel ladle, so that the steel production equipment is not involved, and correspond to the quality program and the production plan (Figure 6.63) [55].

It is essential that the slag produced during the oxidation processes should be separated cleanly, and that the refractory lining of the ladle should not act as a source of oxygen during the reduction phase, or have a detrimental effect on the composition of the reaction slag.

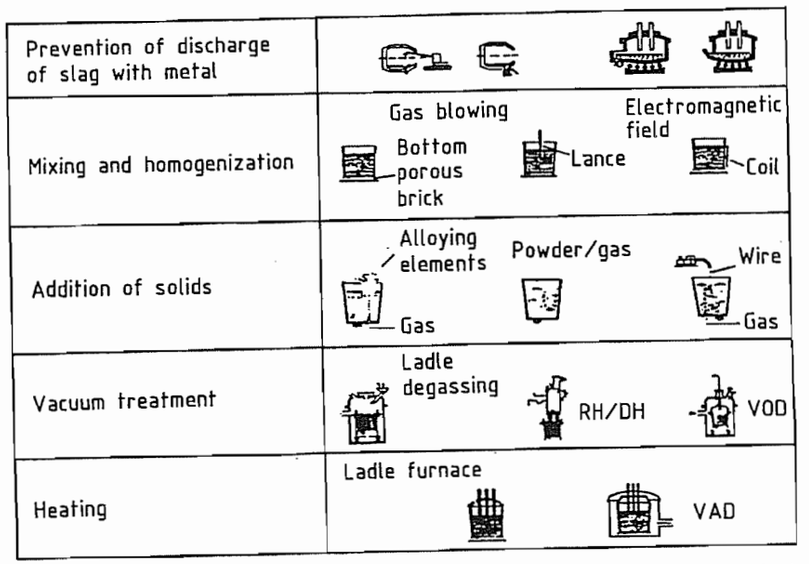

Figure 6.63: Secondary metallurgy processes in steel production. VAD = vacuum arc decarburization.

To hold back the slag formed during the oxygen-blowing process, floating stoppers are used to close off the tap hole. Their function depends on the different densities of the steel and slag; alternatively, mechanical or pneumatic devices can be used. In electric furnaces, there is a curved region or syphon near the tapping hole, or an oval hearth is provided so that no slag is discharged, provided that a residue of 15–20% steel is retained in the furnace.

6.3.4.1 Steel Treatment at Atmospheric Pressure

Secondary metallurgy requires mixing in the ladle. This is achieved by passing gases through porous bricks in the bottom of the ladle, or by injecting them through refractory-covered lances dipping into the melt, thus producing a rising stream of bubbles. A possible alternative is to use the stirring effect of electromagnetic fields acting through the nonmagnetic walls of the ladle. Depending on the amount of mixing energy generated, this can cause circulation and homogenization of the steel under the slag layer, or mixing of the steel with the slag with chemical reaction, e.g., desulfurization. If ladle covers are used, the steel can be protected from reoxidation and falling temperature.

The solid materials can be added in lump form through openings in the ladle lid, or injected in powder form through lances, using a gas as transport medium. For exactly measured additions, solid wire can be added (e.g., aluminum), or wire filled with other substances (e.g., CaSi), which can be added almost without loss of material.

Deoxidation

As well as alloy addition, deoxidation (removal of residual oxygen) i s necessary in the production of quality steels. Depending on the carbon content of the steel, it can contain 100–300 ppm dissolved oxygen, and this is removed by adding elements with an affinity for oxygen (e.g., silicon or aluminum, to form silica or alumina). These oxides are of lower density than steel, but their particle size also greatly affects their upward movement. The deoxidation products are encouraged to coagulate by agitating the steel in the ladle with argon or nitrogen. The ascending reaction products take up the liquid reactive ladle slag. The amount of these materials remaining in the steel determines its oxide content, and affects its mechanical properties. By using a combination of deoxidizing metals, a very low level of oxygen in the steel can be achieved (Figure 6.64) [68].

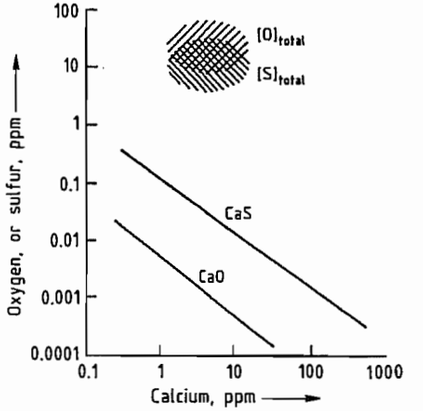

Figure 6.64: Equilibrium of calcium and sulfur or oxygen in liquid iron at unit activity of CaS and CaO [66, 67].

Desulfurization

For high rates of steel production, only a limited amount of desulfurization can be carried out in the blast furnace. When a blast furnace process is optimized for low fuel consumption, the sulfur distribution coefficient between the slag and the pig iron is 20, which, for current mass ratios, leads to a sulfur content of 500 ppm in the pig iron (Figure 6.65). Depending on quality requirements, the first step is the injection of lime and other calcium-magnesium compounds into the pig iron ladle. The relatively poor sulfur partition coefficient (ca. 5) in the oxygen injection steelmaking process is due to the oxidizing reactions. However, if the steel has a high enough aluminum content after deoxidation,

this gives good reducing conditions. If the correct desulfurizing agents are chosen (CaO, Mg, CaC_2, CaSi), or lime-saturated desulfurizing slags are used, sulfur distribution coefficients of 1000 can be achieved [69]. The desulfurization of the pig iron and steel, especially if both these processes are used, enables the required quality to be achieved flexibly and economically. The use of desulfurizing slags requires intensive mixing of the steel and the slag under reducing conditions.

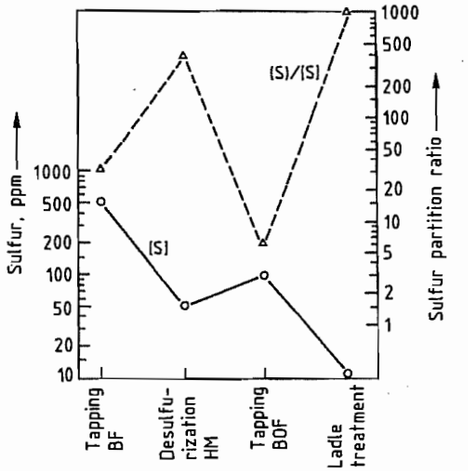

Figure 6.65: Process stages for adjustment of low sulfur content in liquid steel.

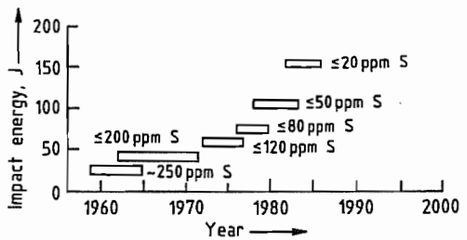

Figure 6.66: Development of toughness and sulfur content.

Figure 6.66 shows the changes in sulfur content in steel produced on a large scale over a number of years [68]. In this example, which refers to steel used for pipes, the development of toughness and sulfur content is shown. The use of calcium compounds under certain conditions leads to the formation of spheroidal inclusions that are not deformed during the rolling process. This has enabled high-strength steels with good toughness properties to be developed.

Dephosphorization

Phosphorus removal is carried out under oxidizing conditions during production of the crude steel, and is influenced by the lime saturation, the P_2O_5 content, and the temperature of the slag produced during decarburization (Section 6.3.3). The production of low-phosphorus steel requires low-P, low-Mn pig iron, and effective removal of the P_2O_5-containing slag produced during decarburization and before deoxidation.

Temperature Control

The temperature changes during steel production affect the course of the reaction (as shown by the example of dephosphorization), and also affect the economics (wear of the refractory linings of furnaces and ladles). The secondary metallurgical operations: alloying, desulfurization, degassing, etc., require time, and therefore involve heat losses. Without ladle heating, this would necessitate the use of unfeasibly high tapping temperatures. Electrically heated ladle furnaces are increasingly used in steelworks—initially in EF steel plants and then in BOF plants—to ensure an optimum temperature regime during the process.

Figure 6.67 illustrates the increasing use of ladle furnaces [67]. The furnaces consist of an assembly of two or three a.c. or d.c. electrodes, and a water-cooled roof, with fume extract ion equipment, and a working door for adding materials and for the control equipment (Figure 6.68) [69].

The transformer capacity is ca. 150 kV·A per tonne ladle contents, and gives a heating rate of 5 °C/min. The diameter of the pitch circle has been reduced to 600–700 mm in new designs to protect the refractory ladle lining. Agitation of the steel and slag to homogenize the steel, and to promote the steel–slag reactions, is very important in the operation of the

ladle furnace. The electricity consumption for treatment time ca. 40 min is 30–40 KWh/t, and the amount of electrode material consumed is 0.3 kg per tonne of steel. With a ladle furnace, the temperature at which the steel is tapped can be reduced by 100 °C without affecting the secondary metallurgical reactions.

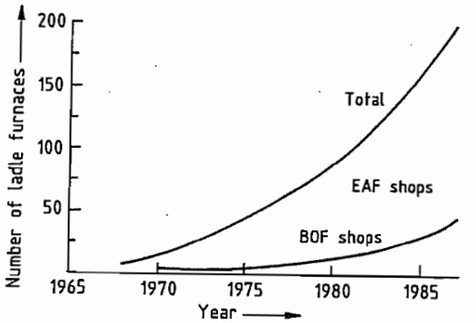

Figure 6.67: Ladle furnace development.

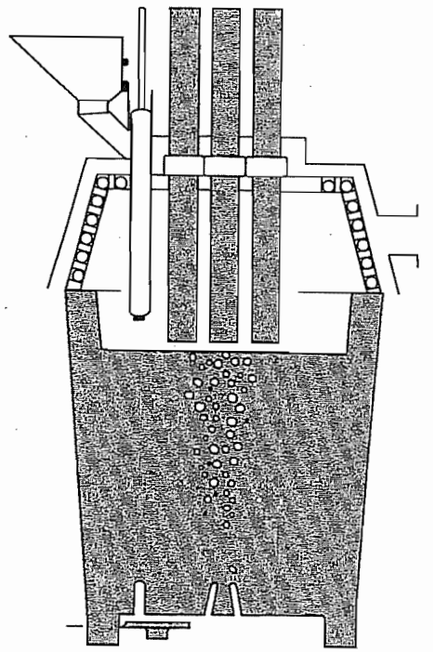

Figure 6.68: Typical layout for a ladle furnace.

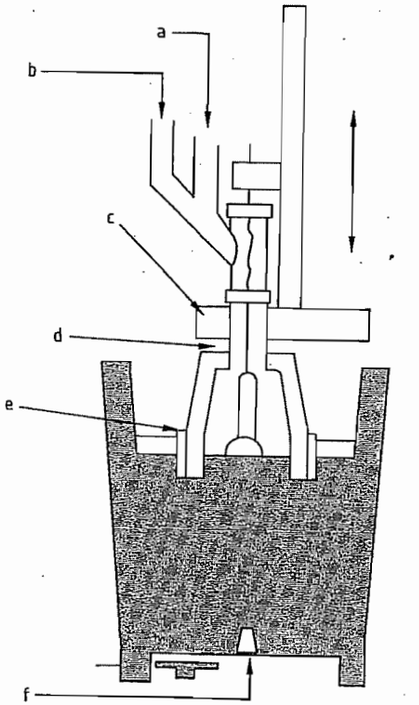

Figure 6.69: Equipment for the CAS process: a) Dust-collecting hood; b) Alloy chute; c) Snorkel raising and lowering unit; d) Oxygen lance; e) Bell; f) Porous plug.

An alternative to the ladle furnace is the CAS/CAS-OB (Composition Adjustment by Sealed Argon Bubbling) developed by Nippon Steel [69], the IR–UT (Injection Refining–Up Temperature) process proposed by Sumitomo. The heat evolved by the oxidation of aluminum or silicon is used to heat the steel, instead of electrical energy. The process is suitable for producing flat products that are insensitive to hydrogen. After the slag-free steel has been tapped, it is agitated by inert gas, and alloyed in a bell (Figure 6.69). If the temperature has decreased too much, the melt can be heated to the required pouring temperature by adding aluminum and oxidizing it with oxygen. The addition of O_2 at a rate of 11 $m^3h^{-1}t^{-1}$ gives a heating rate of 7 °C/min.

6.3.4.2 Vacuum Treatment

The vacuum treatment of steel is used increasingly owing to its versatility and special advantages, and is indispensable for removal of gases dissolved in the steel, such as hydrogen and nitrogen. The reactions proceed at very low pressure (0.5 hPa). The various processes are shown in Figure 6.70 [55]. They can be divided into three groups: recirculating treatment of small quantities of metal; ladle treatment; and treatment of a stream of molten metal.

The recirculating processes are characterized by high throughputs. In the RH plant, two refractory-clad snorkels dip into the steel being treated; in the DH plant only one snorkel is used. Whereas in the RH process, the steel is transferred into the vacuum vessel by blowing inert gas via a nozzle (gas lift), in the DH plant the movement of the steel in the vessel is achieved by the up-and-down motion of the vessel. In both processes, oxygen lances can be provided.

Decarburization

The decarburization reaction is strongly pressure dependent, so that when it is carried out under vacuum, fine decarburization is the result. As shown in Figure 6.71, carbon content < 50 ppm can be achieved reproducibly under optimal process conditions [68].

The required treatment time is strongly pressure dependent. A rapid decrease in pressure is only feasible if the vacuum vessel is fairly large, as the melt splashes severely. If the amount of oxygen dissolved in the steel is insufficient for the decarburization reaction, oxygen is blown in with a lance, liberating heat.

Nitrogen Removal

High nitrogen content has a detrimental effect on the deep-drawing properties of continuously annealed mild steel, and also reduces the resistance of tube steels to hydrogen-induced cracking (HIC). The change in nitrogen content during oxygen blowing is shown in Figure 6.72 [68].

If the nitrogen content in the pig iron is low, nitrogen levels of 30 ppm in plain carbon steels can be achieved. However, steel can pick up nitrogen if nitrogen-containing alloying elements are used, and nitrogen removal may then be necessary. This can be carried out by vacuum treatment under controlled conditions [68]. Nitrogen removal by ladle degassing (after desulfurization) can give a nitrogen content ca. 50 ppm (Figure 6.73). Sulfur interferes with nitrogen removal.

The ladle degassing operation gives intensive phase contact between the steel and the slag, which has a beneficial effect on desulfurization. With 10 ppm sulfur and low oxygen content, a nitrogen level of 30 ppm in the steel can be achieved, whether the starting level is 50 or 110 ppm.

Dehydrogenation

To avoid flaking (material separation) in the steel, the hydrogen content must be lower than its maximum solubility. For large cross sections, i.e., conditions favoring segregation, it is necessary to reduce the hydrogen content of the liquid steel to < 0.8 ppm. The diffusion reaction is controlled by the difference between the hydrogen partial pressure in the steel and that in the gas at the phase boundary, and therefore proceeds more rapidly as the pressure in the vessel decreases. The formation of new surfaces by intensive purging with inert gas, or otherwise agitating the steel in RH and DH equipment promotes hydrogen removal, as shown in Figure 6.74 [70].

The choice of steel production and secondary metallurgical processes depends on the product, the production rate, the raw material, and the energy situation. In Europe, high-quality flat products are produced by the route: blast furnace – oxygen blowing – RH or DH vacuum treatment – continuous casting. Long products are mainly produced by the route: electric furnace – ladle furnace – continuous casting. New developments such as COREX–EOF–KES and continuous casting to give

cast-to-shape products, promise technological and economic stimuli, especially with respect to the environment.

6.3.4.3 Fundamentals

All processes of casting and solidification depend on the basic processes of heat transfer, mass transfer, and interface kinetics. This applies not only to ingot casting, continuous casting, and foundry work, but also to remelting and spraying processes, crystal growth, the production of composite materials from a melt, and rapid solidification to give a crystalline or amorphous structure. These basic principles are valid for all metals and alloys, and the theory is very advanced [71–76].

Nevertheless, steel is special material, having its own characteristic casting and solidification properties that differ from those of both light and heavy nonferrous metals. The peculiarities of steel include: high melting point, low thermal conductivity, phase transformations of the iron, high density, and strong affinity for oxygen. The wide variety of alloy compositions of steel is also reflected in its solidification properties, i.e., the way in which the thermal processes and structure formation take place [77].

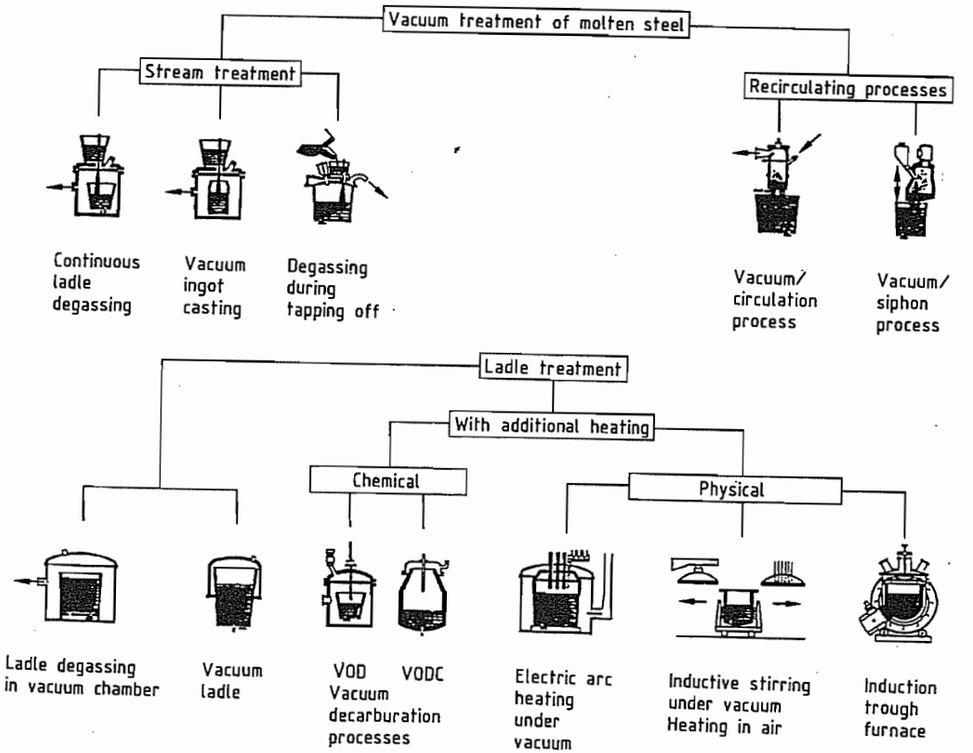

Figure 6.70: Vacuum treatment of steel.

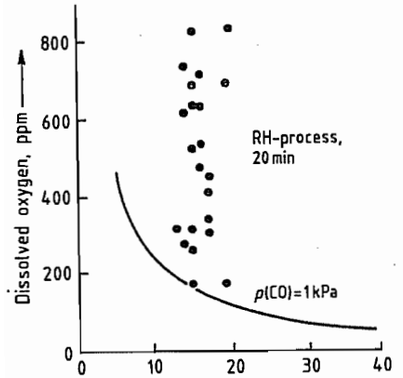

Figure 6.71: Final carbon content as a function of dissolved oxygen.

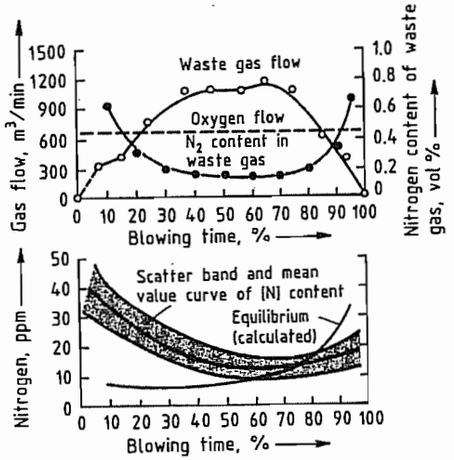

Figure 6.72: Nitrogen removal.

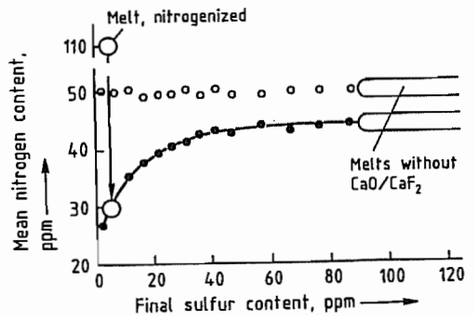

Figure 6.73: Mean nitrogen content before and after vacuum treatment. ○ = [N] before ladle degassing; ● = [N] after ladle degassing.

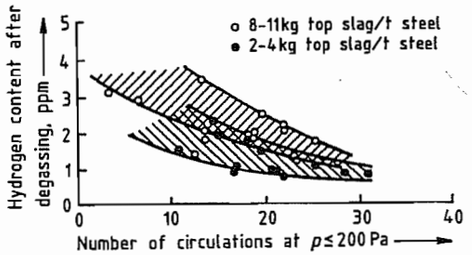

Figure 6.74: Hydrogen removal.

A rigorous scientific treatment of heat and mass transfer and interface kinetics cannot be given here, but their most important consequences are indicated, including solidification morphology, micro- and macrosegregation phenomena, sulfide precipitation, and the formation of inclusions by deoxidation. Thermal stress and mechanical deformation also merit consideration, as they particularly affect the quality of the product; processing techniques and mechanical engineering are tailored to suit them.

6.3.5 Casting and Solidification

Solidification Morphology of Steel. The general criteria for the stability of a nominally planar solidification front are: high superheat, convection, low rate of solidification, low content of alloying elements, and a high partition ratio. These conditions are seldom met in casting operations in the steel industry. Much more frequently, there is "constitutional undercooling" at the solidification front, so that steel almost always solidifies dendritically.

Figure 6.75 shows a scanning electron micrograph of a "quasi-decanted" dendritic solidification front from the central shrinkage cavity of a continuously cast billet of high-temperature steel.

The dendritic crystals consist of primary, secondary, and tertiary arms, all with crystallographic growth direction [100]. The dendritic growth mainly determines the spatial pattern of segregation.

Primary and secondary dendrite arm spacings in a typical continuously cast steel slab are shown in Figure 6.76. Plots of these spacings against distance from a surface of the slab are parabolic, with the widest spacings in the center of the slab.

By the method of steady-state unidirectional solidification, typical values for the growth variables affecting the dendrite arm spacings can be determined [78, 79]. In the equations:

$$\lambda = cR^m G^n$$

and

$$\lambda = c\theta_f^n$$

R represents the solidification rate, G the temperature gradient, and θ_f the local solidification time.

Figure 6.77 shows such a correlation for the primary arm spacings in a steel with 0.15% C and 1.44% Mn. Further values of these parameters for selected steels are given in Table 6.11. These show that high-alloy steels have a finer dendritic structure than low-alloy steels. Figure 6.78 shows that, for four low-alloy steels (I–IV), the data are in good agreement with equations of the form:

$$\lambda_2 = c\theta_f^n$$

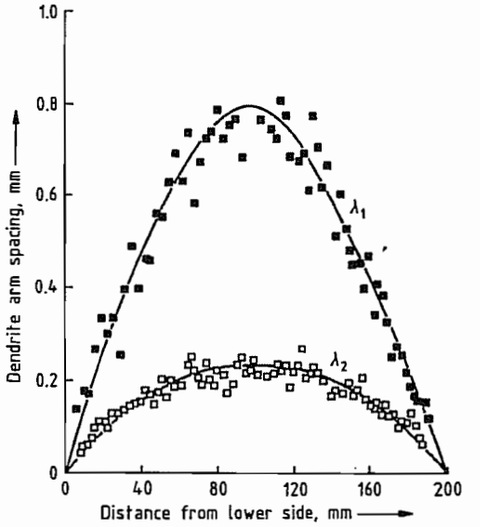

Figure 6.76: Variation of dendrite arm spacing in a continuously cast slab of steel, grade API X60, 0.14% C, 1.50% Mn.

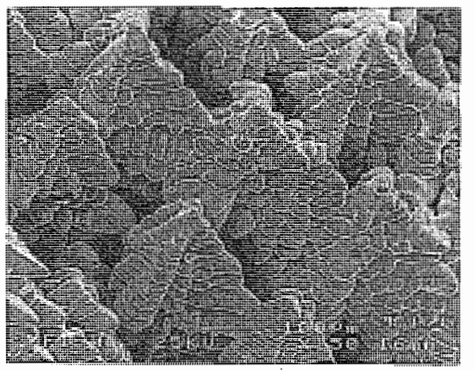

Figure 6.75: Dendrite morphology in center of a continuously cast billet of steel, grade 10 CrMo 910.

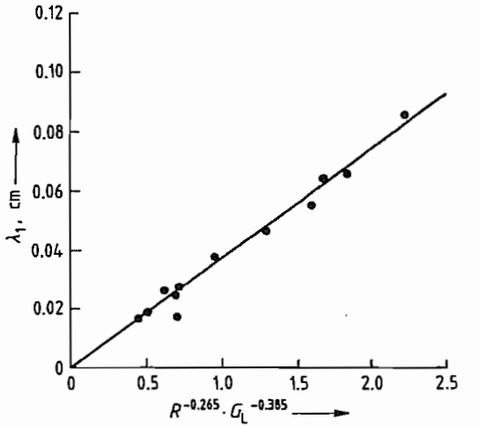

Figure 6.77: Correlation of primary arm spacing λ_1 with R and G_L for steel II with 0.15% C, 1.44% Mn. $\lambda_1 = 0.0368R^{-0.265}G_L^{-0.385}$; λ_1 in cm; R in cm/s; G_L (K/cm) is the temperature gradient at the liquidus temperature.

Table 6.11: Equations for dendrite arm spacings λ (cm) as a function of growth variables R (cm/s), G (°C/cm), and θ_f (s).

Type	Steel composition	Primary arms	Secondary arms	
I	0.09% C, 1.36% Mn	$\lambda_1 = 0.0367R^{-0.29}G^{-0.43}$	$\lambda_2 = 0.01487R^{-0.43}G^{-0.51}$	$\lambda_2 = 0.00280\theta_f^{0.507}$
II	0.15% C, 1.44% Mn	$\lambda_1 = 0.0368R^{-0.27}G^{-0.39}$	$\lambda_2 = 0.00645R^{-0.43}G^{-0.40}$	$\lambda_2 = 0.00168\theta_f^{0.43}$
III	0.59% C, 1.10% Mn	$\lambda_1 = 0.1900R^{-0.26}G^{-0.72}$	$\lambda_2 = 0.01500R^{-0.41}G^{-0.51}$	$\lambda_2 = 0.00158\theta_f^{0.447}$
IV	1.48% C, 1.14% Mn	$\lambda_1 = 0.2700R^{-0.24}G^{-0.72}$	$\lambda_2 = 0.01000R^{-0.49}G^{-0.51}$	$\lambda_2 = 0.00072\theta_f^{0.50}$
V	0.63% C, 24.9% Mn	$\lambda_1 = 0.0610R^{-0.17}G^{-0.36}$	$\lambda_2 = 0.00360R^{-0.41}G^{-0.37}$	$\lambda_2 = 0.00058\theta_f^{0.44}$
VI	0.68% C, 28.3% Cr	$\lambda_1 = 0.0280R^{-0.25}G^{-0.31}$	$\lambda_2 = 0.00320R^{-0.41}G^{-0.37}$	$\lambda_2 = 0.00052\theta_f^{0.39}$

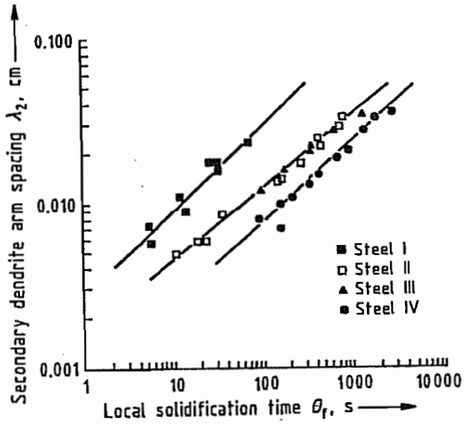

Figure 6.78: Correlation of secondary arm spacing λ_2 with local solidification time θ_f.

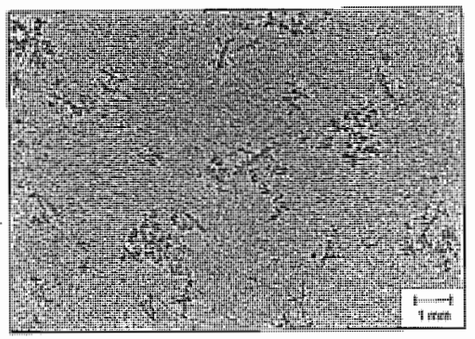

Figure 6.79: Formation of free crystals in a steel melt continuously cast with undercooling.

If R, G, and θ_f are known, the segregation spacings can be predicted. Conversely, local cooling rates can be found by measuring the segregation spacings.

If molten metal is undercooled during casting, free crystallites can be generated. This can take place by heterogeneous nucleation, or by the detachment of dendrite arms, which can be caused by a small degree of superheat, or by inoculation, stirring, jolting, or vibration.

A suspension of crystals in molten steel is shown in Figure 6.79. The crystallites can redissolve and become globular in form. The globulites settle out during casting and appear, e.g., at the bottom of an ingot or the lower side or central zone of a continuously cast strand. An advantage of this equiaxed structure is that its properties are isotropic.

Interdendritic Microsegregation. The thermodynamic basis for microsegregation is the change in concentration that accompanies a phase change from liquid to solid, and is expressed by the partition ratios k of the solute elements present in the iron. Kinetic factors include enrichment of the dissolved elements in front of the phase boundary, which depends on mass transfer in the liquid, and the extent of diffusional equilibration in the solid. The degree of concentration enrichment at the phase boundary C_S^*, in the case of layer crystal formation without diffusion in the solid, is given by:

$$C_S^* = kC_0(1-f_s)^{k-1}$$

where C_0 is the starting concentration, and f~ the extent of solidification in the dendritic volume element. The degree of solute rejection is, therefore, determined by k. Typical values of k for the more important elements found in steel are given in Table 6.12. The elements S, P, and C segregate strongly. With carbon, some concentration equilibration takes place by diffusion.

Table 6.12: Equilibrium partition ratio k of solute element at solid–liquid interface for δ- or γ-iron.

	$k^{\delta/l}$	$k^{\gamma/l}$
C	0.20	0.35
Si	0.77	0.52
Mn	0.75	0.75
P	0.13	0.06
S	0.06	0.025

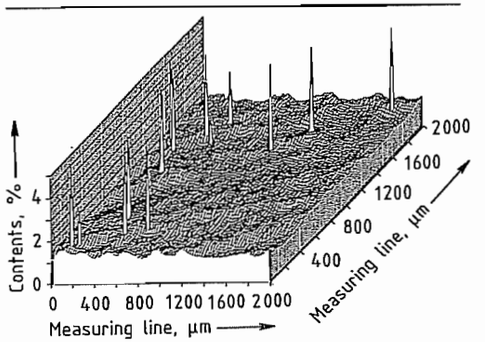

Figure 6.80: Concentration profile of the microsegregation of Mn in a 2.8 t ingot of steel, grade 25 CrMo 4.

Segregation can be measured over a large area by computer-controlled automatic electron beam microanalysis. For example, Figure 6.80 shows a three-dimensional relief map of the manganese concentration in a 25 CrMo 4 steel [80]. The scattered high peaks are caused by MnS inclusions.

Modern microanalytical techniques can produce up to 10^6 point measurements within 24 h. In a typical manganese determination, the area investigated can be 80 × 80 mm, the number of points measured 600 000, the time required 13 h, and the beam diameter 100 µm [81].

Formation of Macrosegregations. Macrosegregations extend over considerably greater distances than dendrite branches. Typical ranges are between the edge and the center or between the top and the bottom of an ingot. The distinction must be made between enrichment and depletion. A systematic discussion of segregration phenomena, including a theoretical treatment, is given in [82].

Positive A- and V-type segregations in cast ingots result from natural convection due to density differences in the enriched liquid over the cross section of the cast material. Stable flow channels can be formed. Sometimes, V-type segregation can also occur in the center of continuously cast strands with equiaxed solidification structure.

In the two-dimensional solidification of continuously cast billets, segregation can take place along the axis of the core. This is associated with shrinkage, and is caused by the growth of dendrites that periodically form bridges that partially seal off the lower part of the liquid metal. Owing to the volume deficit, a powerful suction force is produced toward the crater end. This type of flow restriction does not occur during the one-dimensional solidification of slabs.

Segregation can also be caused by deformation of the outer shell of a strand, e.g., by nonsteady-state bulging outward and rolling back again [83]. This causes a pumping effect in the remaining liquid metal, and leads to so-called central segregation in the slab. Tensile strains at the heterogeneous solidification front cause segregated internal cracking if critical stresses are exceeded. "Soft" or "hard" reduction, to densify the central zone must, therefore, not lead to overstressing of the material below the solidus.

If there is forced convection at the solidification front, e.g., caused by rimming action during ingot casting of unkilled steel or by electromagnetic agitation, a washing effect occurs. A depleted streaky layer is produced. With continuous casting, "white bands" are formed.

Depletion is also caused by sedimentation of suspended crystallites, as these are purer than the melt. The accumulation of a conical heap of crystals at the bottom of the ingot therefore leads to "negative" segregation, whereby the axial concentration of alloying elements increases toward the top of the ingot. This happens, e.g., with heavy forging grade ingots.

Sulfide Precipitation. With modern ladle metallurgical treatment, the sulfur content can be brought below 10 ppm, albeit at some cost, by transferring the sulfur into the slag. Any dissolved residual sulfur can be combined with calcium to form stable calcium sulfide, which has no harmful effects on the properties of the product.

However, it is not always necessary to have the lowest possible sulfur content, so desulfurization and calcium treatment of the steel can often be omitted. The sulfur then becomes concentrated in the interdendritic spaces, owing to its low k value, and eventually precipitates as MnS. The course of the reaction, and hence the form of the sulfide, are determined by the degree of deoxidation and alloy content of the melt, and the local processes of solute redistribution and mass transfer. The various sulfide types in the cast product are [84, 85]:

Type I. Globular oxysulfides that were originally liquid. Formation mechanism: monotectic degeneration. Steel grades: unkilled, semikilled.

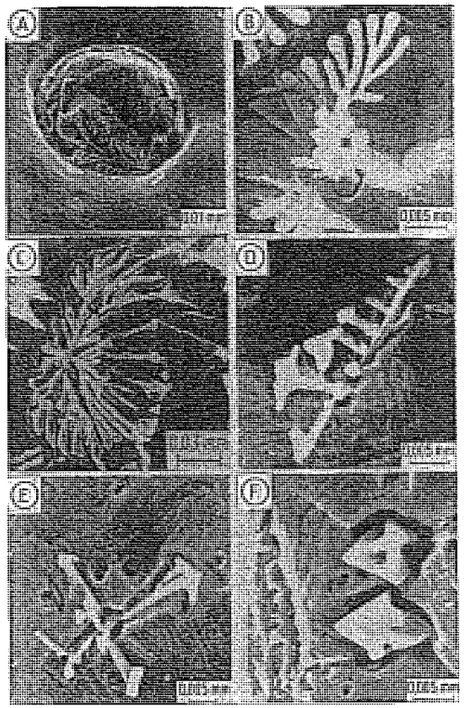

Figure 6.81: Variation of sulfide morphologies in as-cast steel: A) Type I; B, C) Type II; D, E) Transitional types; F) Type III.

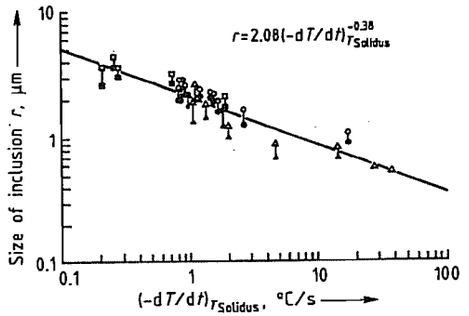

Figure 6.82: Mean size of sulfide inclusions in steel ingots with 0.55% C, 2.00% Mn, 0.009–0.039% S.

Type II. Coral-shaped chain-like sulfide colonies. Formation mechanism: eutectic. Steel grades: killed, low alloy.

Type III. Angular, crystalline sulfide particles. Formation mechanism: "divorced" eutectic. Steel grades: fully killed, high-alloy, containing C, Si, P, Cr, Zr.

The scanning electron micrographs in Figure 6.81 show typical examples of these morphologies. Types intermediate between II and III can have faceted shapes with branched dendrites.

The size of the sulfide inclusions depends on the local precipitation rate and hence indirectly on the rate of cooling at the solidus temperature. This correlation is illustrated by the log–log plot in Figure 6.82 [86].

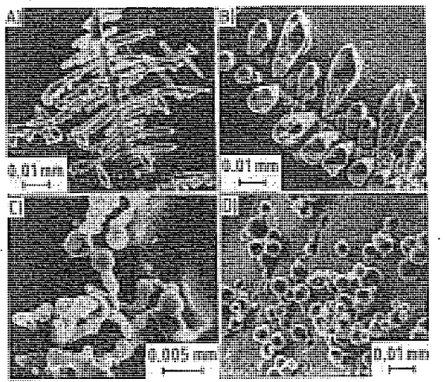

Figure 6.83: Growth morphologies of alumina inclusions in Al-killed steel.

Formation of Inclusions by Deoxidation. In contrast to sulfide formation during solidification, oxide inclusions are precipitated in the liquid steel at an earlier stage by deoxidation. The amount of dissolved oxygen is reduced to the equilibrium value in a few seconds after the addition of aluminum [87]. As deoxidation proceeds, the inclusions agglomerate or coagulate, and mostly go into the slag. This flotation leads to a reduction in so-called total oxygen.

When aluminum is used for deoxidation, alumina inclusions are formed with a spheroidal or dendritic morphology (Figure 6.83) [88]. The coral-like shapes are formed by agglomeration of particles, 2–5 µm in size. In steelworks these clusters are referred to as "nests" or "clouds".

The various growth shapes that can be formed under different supersaturation conditions and activities of the oxygen and aluminum are shown in Figure 6.84 [89]. From left to right, the oxygen level decreases and the aluminum activity increases. At low oxygen levels, the spheroidal oxides initially formed become covered with radiating, stalky, or compact nitrides.

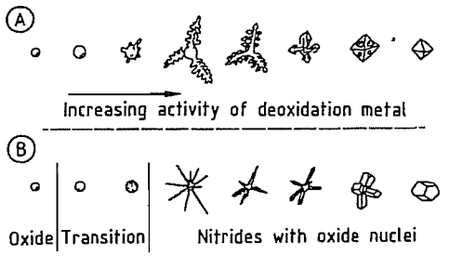

Figure 6.84: Schematic representation of oxide and nitride morphologies as a function of oxygen level.

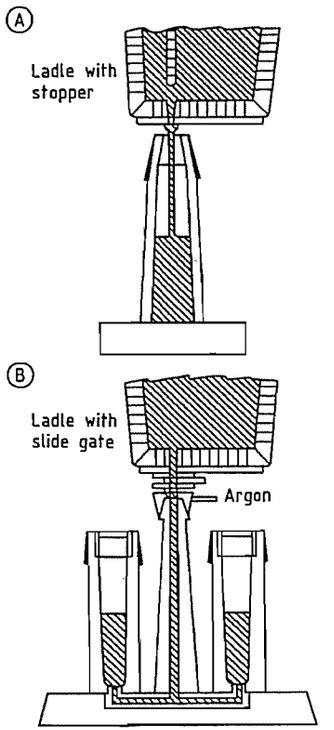

Figure 6.85: Top pouring (A) and bottom (B) pouring during ingot casting [90].

6.3.5.1 Ingot Casting

The transition of steel from liquid to solid is mainly achieved by continuous casting. Nevertheless, the older ingot casting process is still used in steelworks all over the world. The molten steel is poured into ingot molds, where it solidifies.

The steel is poured (teemed) from the refractory-lined ladle via a ceramic, closable outlet nozzle. There are two methods of filling the ingot mold. In the top-pouring method, the steel is poured from above directly into the mold, and in the bottom-pouring method, it passes down a central funnel, then through a system of refractory passageways built into a thick steel plate, and passes from below into the ingot molds standing on the plate (Figure 6.85) [90].

The molds can have a rectangular, square, circular, or polygonal interior cross section, depending on the cross section of the profile to be produced by rolling. To facilitate removal of the solid ingot, the mold tapers slightly outward, with the wider end either at the bottom (big-end-down molds) or top (big-end-up molds) (Figure 6.86) [91]. Ingots can be 0.1–40 t for rolled steel, and up to 500 t for forged steel.

Apart from the cross-sectional shape, the type of ingot mold, and the pouring method, ingots are also characterized according to the physical, thermodynamic, and chemical processes that take place during solidification. Several gases are present in solution in liquid steel. The solvent power of the steel decreases as the temperature decreases, and as the steel solidifies. In ingot casting, oxygen is of particular significance for the solidification process. If oxygen is liberated during solidification, it reacts with the carbon in the steel to form carbon monoxide. This can be partially or completely prevented by combining the oxygen with deoxidants such as aluminum, silicon, or titanium.

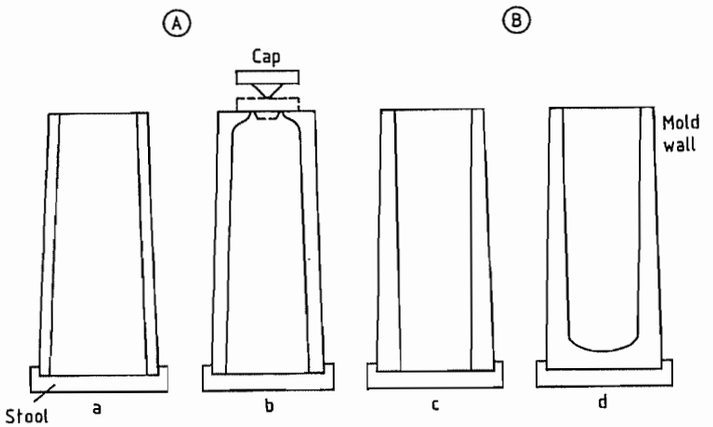

Figure 6.86: Cross sections (not to scale) of the principal types of ingot mold [91]. A) Big-end-down-molds: open top (a) and bottle top (b); B) Big-end-up-molds: open top (c) and closed top (d).

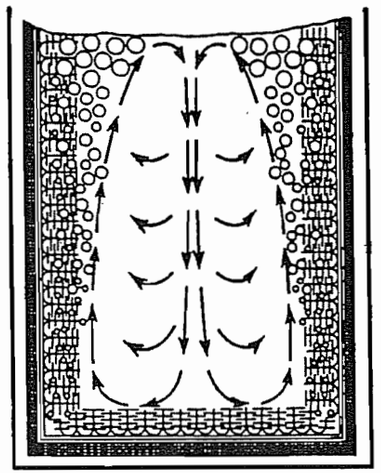

Figure 6.87: Flow pattern in a rimming steel ingot during solidification [97].

If the oxygen is allowed to react with the carbon, the steel product is known as rimming steel. Partial deoxidation leads to "semikilled" steel, and complete deoxidation to "killed steel". Deoxidation to semikilled or killed steel is carried out in the ladle. There is also a combined rimming and killed steel, obtained by first allowing the melt to solidify for some time, and then deoxidizing it in the mold, after which it solidifies completely like a killed steel. This produces "ingot-killed steel".

Rimming Steel. As soon as the liquid steel comes into contact with the walls of the mold and the bottom plate, a thin skin of solid steel is formed. This grows rapidly at first, as the cold mold and bottom plate rapidly absorb heat, and, much later, release it to the atmosphere. After a short time, this compact layer of steel becomes detached from the ingot wall as the solid steel contracts. The gap formed reduces the heat transfer rate from the steel to the mold, and hence the rate of loss of heat to the surroundings. Consequently, the steel solidifies more slowly [92–96].

As the steel changes from liquid to solid, the solubility of oxygen decreases, so that it is liberated and reacts with the carbon present to form carbon monoxide. In addition to the dissolved oxygen present at the start of the pouring process, atmospheric oxygen is picked up by the liquid steel during pouring, and during its subsequent solidification; this also reacts with the carbon in the steel. The CO gas bubbles are partly entrapped between the growing steel dendrites, forming so-called edge blow holes, but most of them ascend in the region of the solidification front, combining with other bubbles on their way up. This leads to the formation of a rim of bubbles at the edge of the steel, and an upward gas flow which causes an upward flow of the liquid steel. Thus, the steel in the ingot flows strongly upward at the solidification front and downward in the center (Figure 6.87) [97]. This rimming action has led to the name "rimming steel".

In the production of rimming steel, CO should be produced rapidly from the start of solidification, giving a strong flow. If the flow is weak, CO bubbles remain entrapped by the growing dendrites. This causes excessive formation of a ring of bubbles not far below the outer surface of the ingot, which results in the appearance of surface defects resembling cracks when the ingot is processed in the rolling mill.

Apart from oxygen, other elements that are less soluble in the solid state are released at the solidification front. This solute rejection is known as segregation (see Section 6.3.4.3). The elements that separate out are carried away by the flow of steel, and are concentrated in the remaining melt. This leads to a rim layer of greater chemical purity and enrichment of the segregated elements in the interior.

After a time, the process of gas release (rimming action) is deliberately stopped by placing a heavy steel cover on top of the ingot, or a steel plate, over which water is sprayed. The steel solidifies on the underside of the cover, and forms a dense cap. In the interior of the ingot, gas formation ceases, owing to the increase in gas pressure, and the flow of steel gradually subsides. In the part that still remains liquid, there are detached crystals of very pure iron, formed by redistribution of solute elements. These suspended solid particles sink to the lower part of the ingot, as their density is higher than that of the remaining liquid metal. This sedimentation results in an equiaxed zone, with a reduced level of impurity elements in the lower part of the ingot. At the top of the ingot, enrichment of elements occurs, e.g., phosphorus and sulfur, which can have a harmful effect on the properties of the rolled product. This marked concentration of elements at the top of the ingot is called macrosegregation.

The ring of gas bubbles formed during the rimming action, and those formed even after the ingot has been closed off, tend to compensate for the difference between the specific volume of the liquid and that of the solid steel. The walls of these cavities have a clean and bright metallic surface, and weld together during subsequent rolling.

These processes during solidification cause the ingot of rimming steel to have a clean edge zone, a rim of bubbles in the lower region, a chemically pure equiaxed region at the bottom end of the interior, and a strongly segregated upper region (Figure 6.88) [98].

Thus, the ingot of rimming steel has a very inhomogeneous structure. Owing to its clean edge region, it can be used in applications that require a good surface. However, it cannot be used for manufacturing components where a large amount of deformation is involved. This is due to its great inhomogeneity and its aging properties, owing to the residual nitrogen. It is also unsuitable if great importance is attached to welding properties [97–110].

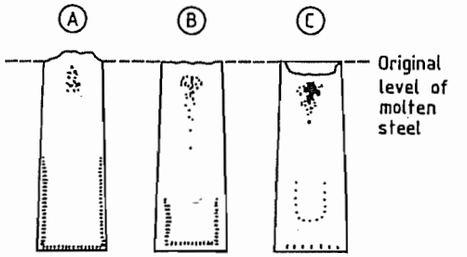

Figure 6.88: Distribution of bow holes in rimming steel ingots [98]. A) After slight rimming action: low oxygen content; B) After moderate rimming action: medium oxygen content; C) After vigorous rimming action: high oxygen content.

Killed Steel. If the dissolved oxygen content in the steel is reduced by deoxidation until it is significantly less than the carbon present, no carbon monoxide gas can form during solidification, and the steel is said to be killed. In killed steel, there is redistribution of those elements whose solubility in solid steel is lower than that in liquid steel. Some of these segregated elements are enclosed between the growing crystals (dendrites). This is termed microsegregation (see Section 6.3.4.3).

Convection of the molten metal also takes place during solidification of killed steel. However, this is considerably less intense than

in rimming steel, and takes place in the opposite flow direction. In front of the solidification interface, free crystallites move downward along with the liquid steel. The solid particles of steel settle at the bottom end of the ingot, while liquid steel flows upward in the center. As the descending crystals are chemically purer than the remaining liquid steel, a depleted conical heap forms at the bottom of the ingot. Here, the concentration of solute elements is lower than it was in the steel before pouring, whereas the concentration of the solute elements in the upper part of the ingot is correspondingly higher. Thus, there is so-called negative segregation in the lower part, and positive segregation in the upper part of the ingot. This is generally referred to as ingot segregation, and becomes more marked as the ingot cross section increases.

As well as ingot segregation, so-called A- or V-type segregation can take place when killed steel ingots solidify (see Section 6.3.4.3). Unsteady flow through the network of dendrites sometimes leads to the formation of channels, in which enriched liquid metal solidifies. On longitudinal cross sections of the ingot, these channels appear as A- or V-shaped segregation. The intensity of this type of segregation is dependent on the morphology of the solidified ingot. The finer the dendritic structure, the less marked is A- and V-type segregation.

To prevent the uncontrolled formation of shrinkage cavities in the interior of ingots of killed steel, the steel at the upper part of the ingot (the ingot head) is kept in the liquid state as long as possible. The liquid steel can then flow downward to compensate for the shrinkage of the solidifying region, and cavity formation is prevented.

The reservoir of liquid steel is maintained by reducing the heat transfer from the top part of the ingot to the mold by lining the latter with refractory, thermally insulating, and often slightly exothermic plates. The loss of heat in an upward direction to the atmosphere is reduced by applying an insulating and/or exothermic powder. Figure 6.89 shows typical longitudinal sections of steel ingots poured into normal big-end-up and big-end-down ingot molds, with and without a feeder head, or "hot top", of this type [91]. In big-end-down ingots, through-solidification occurs earlier in the upper part than in the lower part of the ingot. This produces axial porosity, which under no circumstance should connect with the outside atmosphere, as this leads to oxide formation in the interior, preventing welding during subsequent rolling operations. Unless the top of the ingot is thermally insulated (hot topping), ingots produced in big-end-up molds form shrinkage cavities which extend deep into the ingot, so that the yield of good material is poor. An ingot from a big-end-down mold without a hot top will have axial porosity.

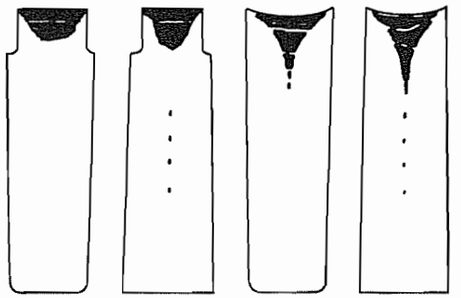

Figure 6.89: Types of killed ingot [91]. A) Big-end-up, hot-topped; B) Big-end-down, hot-topped; C) Big-end-up, not hot-topped; D) Big-end-down, not hot-topped.

When steels are to be used in applications that require an absolute minimum of interior defects, a hot top of adequate size is essential. For example, when heavy ingots are produced for forging, and are cast big-end-up, a feeder head of thermally insulating material is placed on top, with a volume large enough to prevent formation of a shrinkage cavity in the ingot. Segregation of the remaining molten material then takes place in the feeder head inside the hot top. This part is later separated from the good part of the ingot.

As killed steel is mostly used for demanding applications, there must be as few nonmetallic inclusions as possible. Modern ladle metallurgy, combined with a very high standard of pouring practice, have brought great improvements. If any nonmetallic inclusions remain entrapped, however, these consist mainly of oxidic and sulfidic materials. These can originate from the products of deoxidation, from insulating materials, or are formed during solidification by reactions of the segregation elements. Inclusions in killed steel are mainly found entrapped in the region of the cone of sedimented equiaxed material, at the bottom of the ingot [91, 111–119].

Semikilled Steel. In this type of steel, the ratio of oxygen to carbon content is set by controlled deoxidation, so that the ingot at first solidifies, like killed steel. After a time, the carbon and oxygen become enriched in the remaining liquid, so that the solubility product is exceeded and carbon monoxide is formed. Meanwhile, the ingot head has solidified and is therefore dense, so that blow holes are formed in the interior of the ingot, owing to shrinkage (Figure 6.90) [91].

Semikilled steels are not used for applications with high demands on internal purity and defect-free surface properties [91, 120–122].

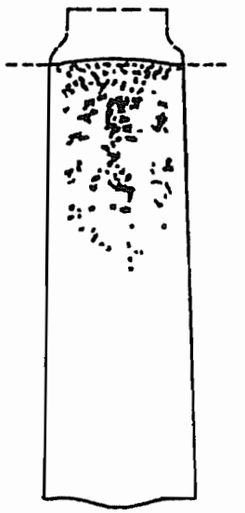

Figure 6.90: Longitudinal section through a semikilled steel ingot [91].

Ingot killed steel was developed to combine the clean surface of rimming steel with the low degree of macrosegregation and good aging stability of killed steel. The tops of the ingot molds are provided with insulating tiles, as with killed steel. The steel is poured undeoxidized into the mold until the insulated region contains a few centimeters of steel. A second and possibly a third mold is then filled in the same way. During this time, rimming takes place in the first mold, as well as solidification of an outer shell of steel, several centimeters thick, which consists of very clean unkilled steel, free of inclusions and segregation. The first ingot mold is then completely filled, while simultaneously adding aluminum in granular form to the stream of metal, thereby mixing it into the liquid part of the ingot. Carried by the central downward flow of rimming steel, the aluminum is transported to the lower part of the ingot. The dissolved aluminum reacts with the oxygen to form coarse Al_2O_3 particles, which rapidly ascend into the highest part of the ingot, owing to their low density. The ingot then solidifies like a killed steel. All the ingots from a heat are poured in this piecemeal fashion. This process produces an ingot with an outer layer of clean rimming steel, ca. 30 mm thick, and a larger inner region of nonaging killed steel with little macrosegregation (Figure 6.91) [123]. This steel can be used when a defect-free surface is required on a nonaging material [123].

6.3.5.2 Continuous Casting

In the historical development of continuous casting (strand casting), a breakthrough was achieved in large-scale production by S. Junghans with the invention of the oscillating mold in 1949. This became widely used during the 1970s [124, 125]. By definition, strand casting is a steady-state process in which a strand is continuously drawn out of a mold [126–130]. After the 1980s, development of the conventional continuous casting process virtually came to an end [131–143]. The rolled products produced from continuously cast strand sections are characterized by their extremely good finish and functional properties, are not subject to any particular limitations, and are suitable for a wide range of applications [144].

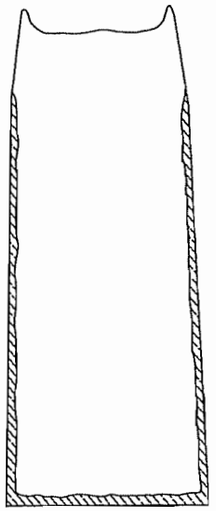

Figure 6.91: Longitudinal section through an ingot of steel killed in the mold [123].

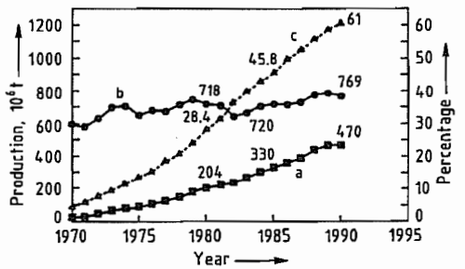

Figure 6.92: Development of world steel production, CC output and CC ratio 1970–1980: a) World CC-production; b) World crude steel production; c) Share of CC-production, %.

The Growth of Strand Casting

The growth of strand casting worldwide is illustrated in Figure 6.92. It has already reached > 60% of the total. Up to the 1980s, the competitiveness of steel producers was measured by the proportion of strand casting used. Today, many steelworks use the process exclusively. In many industrialized countries, the proportion is > 90%, but in some regions, it is only 20% [144].

The strand casting technique replaces individually cast ingots, blooming and slabbing mills, and semifinished mills. The yield of rolled products per tonne molten steel is increased by 10–18% (see section 6.1). This technological change has resulted in an excess of crude steel capacity, but has greatly contributed to energy savings.

Figure 6.93 shows the shapes and dimensions of some typical strands, with size ranges. Billets are used to manufacture wire or rod. Round bar products are used as the starting material for seamless tubes. Continuously cast blooms are used in the production of profile steel and rails. Case hardening and heat-treatable steels, cold-heading and cold-extruding steels, spring steels, chain steels, rolling bearing steels, and free cutting steels are routinely produced [145]. Slabs are converted into thick plate for pipeline or vessel construction, or processed into hot-rolled wide strip and products made from this, such as cold-rolled thin sheet, which may be surface treated for automobile construction or packaging applications.

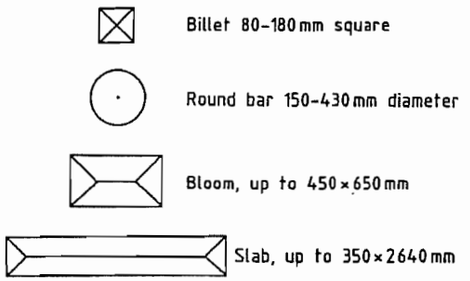

Figure 6.93: Typical cross sections and dimensions of continuously cast strands.

Productivity

If strand casting accounts for 100% of the total output of a steelworks, productivity rates become very important. The capacities of the melting, ladle treatment, and casting process must be matched as precisely as possible. If the mix of steel types produced is variable, it must be possible to react to changes with great flexibility.

Modern strand casting plants are characterized by high availability. The utilization ratio, i.e., the ratio of casting time to time available, is 40–90%. In sequential casting, one melt is cast immediately after another without interruption. The ladles are mounted on a turret which swivels, raises, and lowers the ladle (Figure 6.94). The molten steel passes through the following items of plant or process steps: ladle–tundish–mold–secondary cooling zone–straightening and withdrawal machine–runout rollers.

For high productivity, it is also necessary to have a high rate of withdrawal and a long length of the liquid pool. High outputs can only be achieved when bow type casters are used, where the strand, which still has a molten interior, is cast on a circular arc and then straightened to the horizontal position. Figure 6.95 shows the various types of plant used during the development of the process. Vertical plants (V) have a limited output, owing to the height required. The most usual system is the circular arc plant with a curved mold (CAC), with several straightening points. In a circular arc machine with straight mold (CAS), the strand, with its molten center, is first bent into an arc, and then straightened. The bending and straightening take place progressively. Extremely precise mechanical technology is used to minimize stressing of the cast material.

The production rate for a single strand depends on the format, dimensions, and casting speed (Figure 6.96) [144]. For slabs, a rate of 5.5 t/min is possible. This must be matched to the batch time of the basic oxygen furnace. For blooms and billets, the number of strands must be increased to four or six to match this batch time.

Plant availability can be improved by: insertion of the dummy bar from above; design of mold and runout rollers as a quick change unit; flying tundish changeover by means of a swivel device; uninterrupted casting of different steels me after the other without forming a mixed zone the old strand being joined to the new by a cage-and-anchor joint); and computer-controlled automatic width adjustment of the strand. A high standard of control technology and automations necessary in the casting plant. Regular inspection and preventive maintenance ensure problem-free casting.

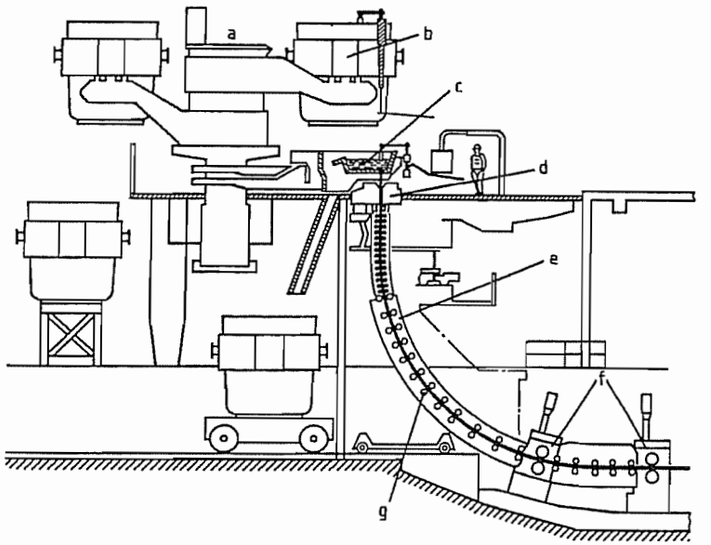

Figure 6.94: Blown caster with ladle turret: a) Ladle turret; b) Ladle; c) Tundish; d) Mold; e) Secondary cooling zone; f) Straightening and withdrawal; g) Guide rollers.

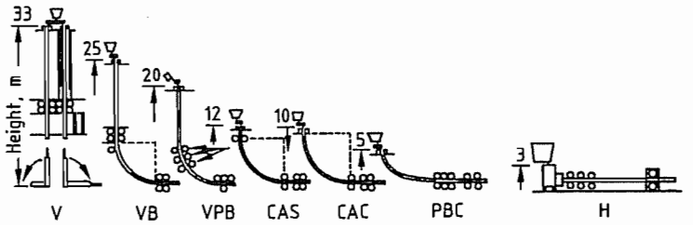

Figure 6.95: Principal types of continuous casting machines for steel: V = vertical; VB = vertical with bending; VPB = vertical with progressive bending; CAS = circular arc with straight mold; CAC = circular arc with curved mold; PBC = progressive bending with curved mold; H = horizontal.

With slabs and blooms, an average run of nine heats is usual, and with billets, five heats 144]. More flexibility in the production program is provided by a device for longitudinal cutting of slabs, especially for "jumbo" slabs, up to 2640 mm in width. Double and triple casting can also be provided for.

Mold Oscillation and Shell Formation

The most important invention in the technical development of strand casting was mold oscillation, which gives the product a good surface finish. Figure 6.97 shows how the molten steel from the tundish passes through a submerged entry nozzle into a slab mold. The steel flows sideways during slab casting, but vertically downward with square or round mold shapes. The pouring temperature is controlled within a very narrow range.

The oscillation of the mold is illustrated in Figure 6.98. The movement is usually sinusoidal. Stroke and frequency are so adjusted that the mold briefly overtakes the strand during the downward movement. During this so-called negative strip time, the skin of the casting is briefly upset. Any surface damage is completely healed. The negative strip time t_N (an important control parameter) is given by the following formula:

$$t_N = \frac{1}{\pi f}\arccos\frac{v_g}{\pi f h}$$

where t_N is in s, the frequency f is in s^{-1}, the casting speed v_g in mm/s, and the stroke h in mm. If $t_N \rightarrow 0$, tearing of the shell occurs, and if it is too large (> 0.2 s) deep oscillation marks are produced, and lubrication in the gap between the mold and the strand is impaired. When changes to the casting rate occur during unsteady phases, such as the start of casting or ladle changes, the frequency is adjusted. Amplitudes are kept constant at 2–6 mm, but frequencies vary around 6 s^{-1}. A curved mold oscillates precisely along the arc.

Molds are usually 700–900 mm long, and are made of high-strength, copper-based materials. To maximize operating life, the surface is coated with chrome (60–80 µm) or nickel (0.5–4.0 mm). For small cross sections, tube molds are usual, and for large cross sections, plates are mounted on stable steel frames. To accommodate the contraction of the steel, the molds taper inward. For plants with high casting rates for billets and blooms, very close geometrical tolerances must be adhered to. For sensitive steels with high sulfur content or wide solidification range, the casting speed is reduced.

Control of Molten Steel Level and Gap Lubrication

For problem-free strand withdrawal from the mold, the cycle must be optimized, the meniscus level of molten steel kept constant, and an appropriate casting powder must be used to lubricate the gap.

The flow of steel is controlled by sliding gates (Figure 6.97) or stoppers. The steel level is detected with the aid of radioactive sources, ^{60}Co or ^{137}Cs, or eddy current detectors, and is controlled within ±5 mm, or even ±2 mm, depending on the sophistication of the control equipment, the format of the strands, and the casting rate.

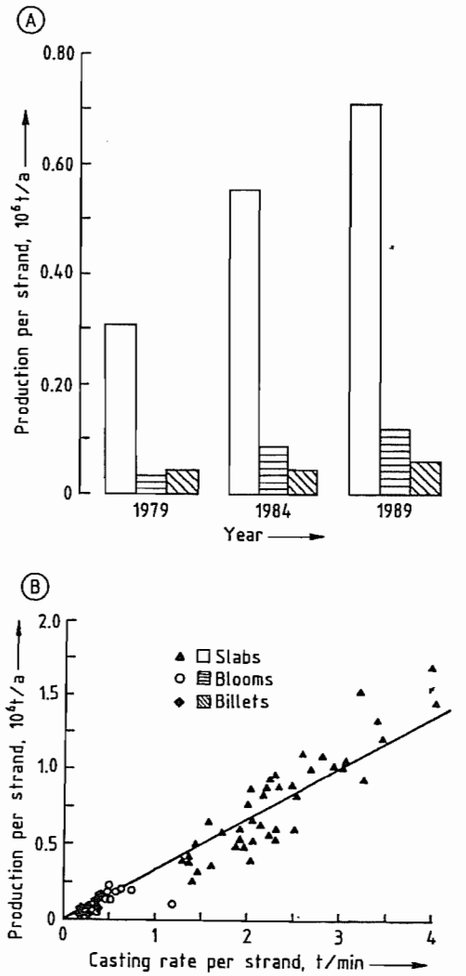

Figure 6.96: Annual production per strand of European casters (A) as a function of the casting rate per strand for different strand sections (B).

The casting powders used must be appropriate for the types of steel and the casting conditions. On contact with the surface of the steel, they should melt promptly at 1100–1200 °C, and form a lubricating film between the strand and the mold. Penetration into the gap plays a key role in the formation of the steel surface for high withdrawal speeds [145].

Casting powders consist of CaO, SiO_2, and Al_2O_3 CaF_2, Na_2O, or Li_2O are added to lower the viscosity. Carbon particles in the form of powdered coke or soot retard the melting. The basicity of the slags is given by:

$CaO/SiO_2 = 0.8\ 1.2$

The amount of casting powder required depends on the oscillation cycle, the casting speed, the geometry of the gap, and the viscosity. Slabs are cast by means of low-viscosity slags: 0.1–0.3 Pa·s (1300 °C). For blooms, viscosities must be somewhat higher: 0.4–1.5 Pa·s (1300 °C).

Casting powders protect the molten steel from radiation heat loss, prevent contact with atmospheric oxygen, and absorb oxide inclusions that rise to the surface, especially Al_2O_3. Powders and granules (nowadays preferred) can be added automatically in the fluidized state.

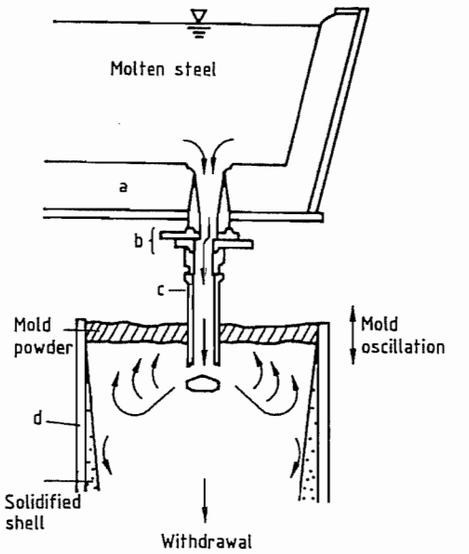

Figure 6.97: Steel flow from tundish into an oscillating slab mold: a) Tundish; b) Sliding gate; c) Submerged entry nozzle; d) Copper mold plate.

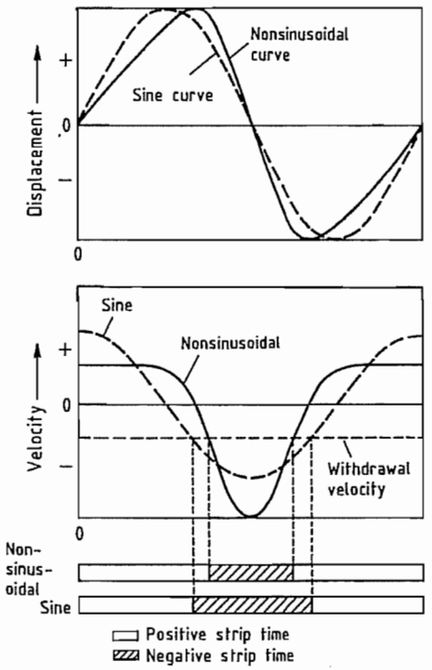

Figure 6.98: Mold oscillation with definition of positive and negative strip times.

Support Roller Apron and Secondary Cooling Zone

At the mold exit, the skin of the strand is sometimes quite thin, e.g., 10–12 mm, depending on the withdrawal velocity, and is ductile and deformable under the conditions of high temperature and ferrostatic pressure. Whereas billets and round bars are dimensionally stable, the wide faces of slabs and blooms tend to bulge, and must be supported by rollers [146].

To prevent excessive thermal stress on the rollers, they are cooled internally. The heliroller contain a spiral channel for circulating the water, and are stable and long-lasting [138]. Divided rollers with intermediate bearings are of smaller diameter and can accommodate narrower gaps between them. Where bending and straightening of the strand is carried out, deviation of the rollers from the ideal line must not exceed 1 mm. Loose-fitting and worn rollers must not cause this limit to be exceeded.

In the secondary cooling zone, the strand is cooled with water sprays. There are various jet systems to provide different flow rates of water impingement. In the extreme, the surface can be sprayed "black". In the early days, large quantities of water were used for fear of break-outs of molten steel. Since then, the water rate has been limited to the minimum required for the necessary cooling intensity. Air/water mixtures are used to achieve gentle and uniform cooling. Specific consumptions of spray water are 0.7 L per kilogram of steel for spray cooling, and 0.1–0.2 L/kg for air-mist cooling.

Automation

Today, almost all the functions of a casting machine are automatically controlled. Figure 6.99 gives an overview of the individual processes [132]. Secondary cooling is dynamically controlled. The spray water is adjusted according to the casting speed to prevent undercooling. Cooling water circulation, hydraulic, and lubrication systems are computer controlled. The rate of steel casting is measured by weighing, and cutting of the strand into lengths is optimized with respect to the heads and tail pieces.

Quality

The quality of continuously cast steel as a semifinished material for rolled steel production can be assessed by four criteria:

- Homogeneity of chemical composition
- Uniformity of steel structure
- Extremely high purity
- Defect-free surface

The above requirements are met if the process is trouble free. Solidification can be controlled to be columnar or equiaxed by means of temperature control and the stirring effect of electromagnetic fields, enabling the blooms and billets to have isotropic properties

throughout. With slabs, soft reduction is carried out by conical compression of the center.

Contact of air with the steel is prevented by shrouding systems and by covering the molten metal in tundish and mold with powder. Carry-over of slag along with the steel from the casting ladle is detected and prevented. The flow of steel in the tundish is controlled such that oxide inclusions separate out. It is also necessary to use stable refractory materials and refined pouring techniques to ensure a high-purity product. For high-output plants, a vertical part of 2–3 m in height enhances the flotation of inclusions and gas bubbles.

Materials technology has elucidated the high-temperature ductility of steel from its molten state to the γ–α transformation, and mechanical engineering has provided the necessary data on permissible material stresses during casting. By progressive bending and straightening, and suitable roller distances, tensile strain at the solidification front can be kept < 0.3%. Critical temperature zones susceptible to surface cracking are avoided by appropriate cooling. Harmful elements, e.g., N and S, are removed from the steel, or chemically combined to form stable compounds.

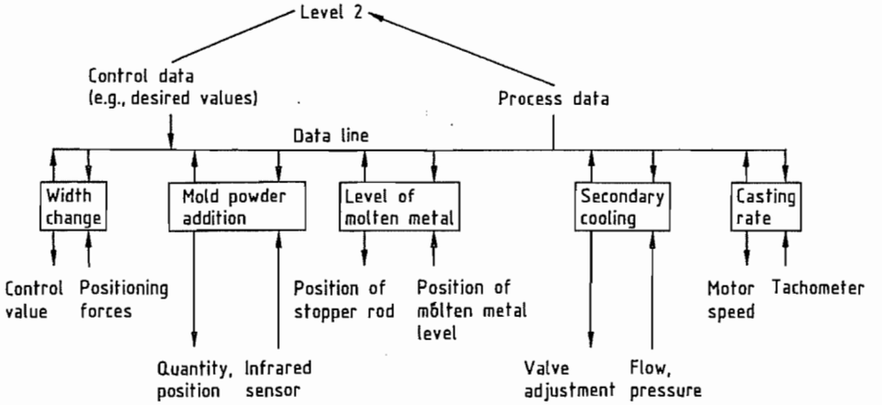

Figure 6.99: Instrumentation and automatic process control of a continuous casting machine.

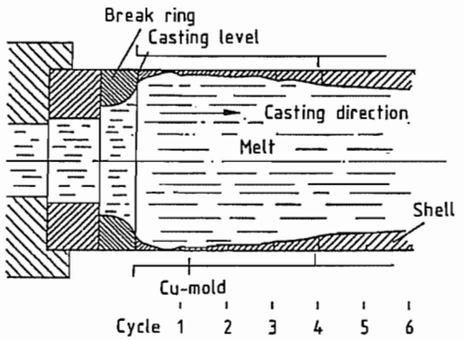

Figure 6.100: Creating an artificial meniscus during solidification in a horizontal casting mold.

Horizontal Strand Casting

Horizontal strand casting has replaced ingot mold casting for several types of steel which have hitherto been regarded as unsuitable for strand casting [137, 147]. The capital cost of a horizontal strand casting plant is small. The tundish and mold form a single unit, giving complete exclusion of air. The horizontal strand requires neither bending nor straightening.

The special feature of the process is the creation of an "artificial meniscus" at the break ring, where the skin of the casting first forms (Figure 6.100) [148]. The strand is withdrawn stepwise, and the short frozen sections are welded together. The cycle comprises three phases: pulling out, pushing back, and pause. The pushing-back stage allows healing to oc-

cur. The design of the machinery must enable the large mass of the strand to be moved with very high precision with respect to both distance and time [149, 150]. Typical round bar dimensions are 150–350 mm in diameter.

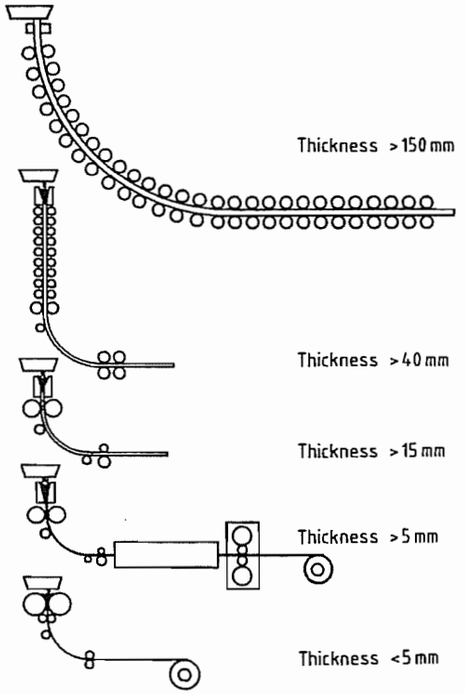

Figure 6.101: New processes for the production of thin slabs and hot strip.

The breaking ring is made of BN, and is not wettable. Useful lives for this item of 4–7 h have been reported. The formation of the solidified skin is precisely controlled with the aid of thermocouples. The casting parameters and mold taper must be precisely matched. Nevertheless, the process is flexible with regard to the formats and steel types. It is of interest for small-scale operations, e.g., 3000 t/month in 100 different grades of mild, stainless, or high-temperature steel [132, 149].

Hot Charging or Direct Rolling

Not only is conventional strand casting a fully developed process, guaranteeing a high productive capacity, but it offers the opportunity for energy savings by integration with the rolling mill, i.e., utilizing the heat of the strand by hot charging or direct rolling [139]. For this, the operation of the rolling mill must synchronize with the flow of material from the melting shop, the secondary metallurgical processes, and the strand casting plant. The temperature of the cast product is not allowed to fall below 1200 °C. The surface and the interior must be of high quality.

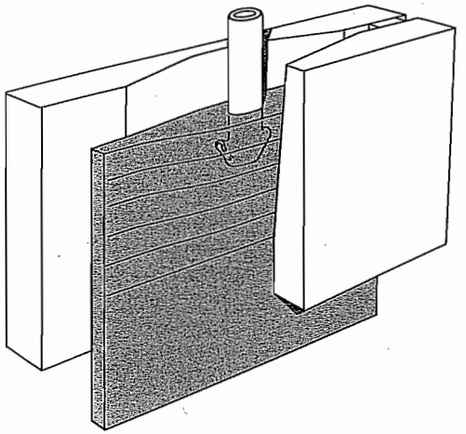

Figure 6.102: Schematic representation of casting mold for thin slabs.

Casting Thin Slabs

Under the heading "near net shape casting", the development of casting technology since 1983 has aimed to match the thickness of continuously cast slabs more closely to that of the end product [151, 152], i.e., to reduce the amount of metal forming required, and hence to economize on plant equipment [153–155]. Processes for the production of thin slabs or strip are illustrated schematically in Figure 6.101.

At the heart of thin slab technology is the funnel-shaped mold into which a narrow submerged entry nozzle with side exit openings is inserted (Figure 6.102) [153]. The shell of the strand is smoothly deformed in a controlled manner until it leaves the mold, and the gentle contours keep the bending stress small. The strand leaves the mold with plane parallel surfaces in its wide dimension. Thin slab technology is otherwise similar to conventional strand casting, e.g., control of the level of molten steel, supporting rollers, secondary cooling, etc.

New Processes for Hot Steel Strip Production

For integrated "mini-steelworks", various processes have been devised for the production of hot steel strip, based on thin slab casting technology. It is generally agreed that a direct link between casting and rolling to produce a finished product in an in-line, multistand rolling mill is impossible, because the casting and rolling speeds cannot be matched. A buffer can be provided between these processes by operating them in two stages.

A compact strip production (CSP) plant consists of a casting machine, a conveying and linking system designed as a roller hearth furnace, and a hot finish rolling mill [154, 155]. The casting machine is vertical, with bending facility. The casting format is 50 × 1600 mm; the casting speed is 5 m/min. The strand is cut into 45 m lengths, which are loaded at nearly 1100 °C into an annealing furnace, 162 m long. The final rolling temperature is 880 °C.

In-line strip production (ISP) is shown in Figure 6.103. The thin slab, with a liquid core, is softly reduced in thickness from 60 to 43 mm immediately after the mold [142, 156, 157]. After through-solidification, the strand passes through three graded stands of high-reduction rolling units. Its thickness is reduced to 15–25 mm, and it is made into 28 t coils. Before coiling, it can be reheated by inductive heating to a temperature of 1150 °C. The coils are kept hot in furnaces, ready for the finish rolling mills. The hot steel strip has a final thickness of 1.8–12.5 mm and can be intensively cooled.

The casting pressing-rolling (CPR) process (Figure 6.104), combines a conventional oscillating thin slab mold of the type described above, with a powerful pair of compression rollers to reduce the thickness of the strand, which has a liquid interior, to 15–25 mm in a single step [158]. The hot strand is then rolled to its final dimensions at 1300 °C in a four-high stand.

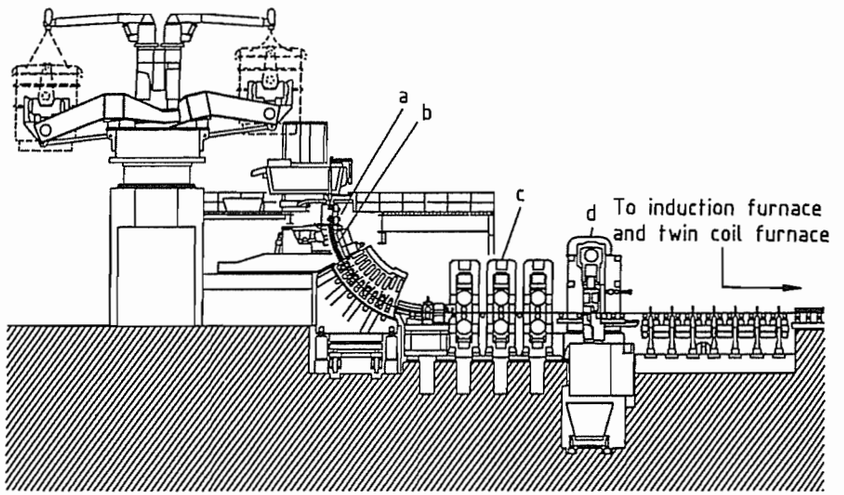

Figure 6.103: Caster for in-line strip production (ISP): a) Vertical bow-type mold; b) Soft reduction; c) High reduction (three stands); d) Pendulum shear.

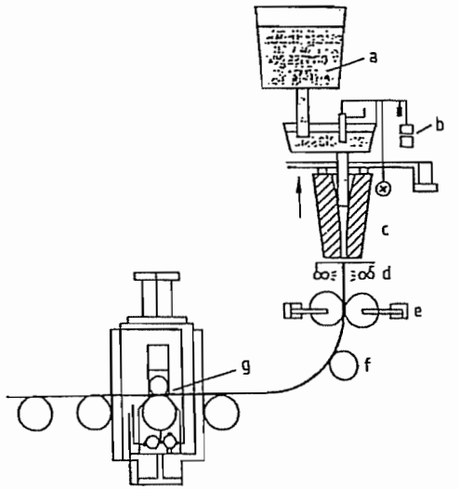

Figure 6.104: Casting–press–rolling process: a) Ladle; b) Tundish; c) Mold; d) Descaling; e) Press rollers; f) Bending roller; g) Straightening unit.

Rationalization

The new processes of hot steel strip production may replace some of the classical "thick slab hot strip steel mills", but not completely [155]. Hot strip steel produced by the standard method can be divided into: mild steel for cold forming and cold rolling (76.2%); weldable construction steels (10.5%); high-strength carbon steels (1.7%); microalloyed weldable fine grain and tube steels (6.4%); stainless steels (3.3%); and silicon steels for electric sheet (1.9%).

Assuming sufficiently good surface properties of the mild steels produced by the new casting-rolling processes, their suitability for cold forming and cold rolling is beyond question [155]. Of the total amount of hot steel strip listed above, 75% could be produced more economically. A considerable fraction of the total production could be transferred from large integrated steelworks to mini-steelworks. The forming properties of 21% of this total are difficult or critical. Further development work is needed; in particular, the alloy compositions of these materials must be matched to the new casting-rolling processes.

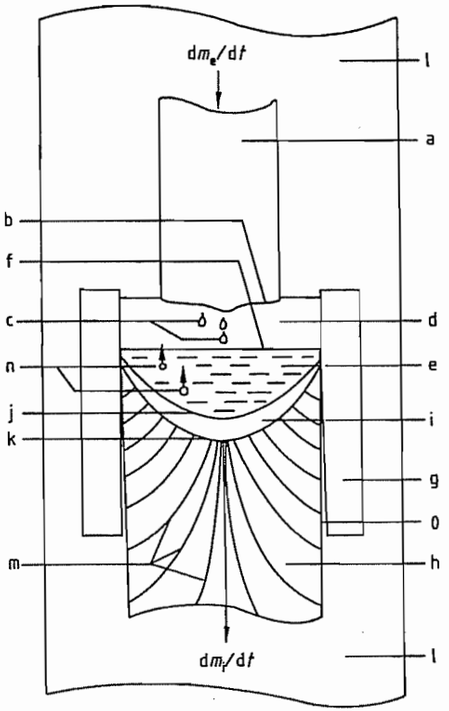

Figure 6.105: Consumable electrode remelting: a) Electrode = metal to be remelted; b) Electrode surface heated above *mp*; c) Metal droplets; d) Remelting environment (vacuum, liquid slag, plasma); e) Liquid metal pool; f) Surface of liquid metal pool; g) Crystallizer (water-cooled mold); h) Remelted ingot; i) Mushy zone; j) Liquidus isotherm; k) Solidus isotherm; l) External environment (vacuum, air, inert gas); m) Solidification direction; n) Inclusion in liquid pool.

6.3.5.3 Consumable Electrode Remelting Processes

Remelting processes are used for upgrading the quality of steels and Fe-, Co-, and Ni-based superalloys; conventionally made metal bars are transformed, by simultaneous remelting and resolidification, into new materials with superior properties.

Remelting Processes

Figure 6.105 outlines the remelting process for steel and superalloys. The metal to be remelted is first produced by primary melting, secondary refining, and casting processes, including vacuum induction (VIM) and plasma melting and casting. It is introduced into the remelting process as a so-called "electrode", which is normally shaped by direct ingot casting, with or without subsequent rolling or forging, or by continuous casting. Compound electrodes, such as bundles of bars or continuously cast billets may be used, as well as several individual electrodes to be remelted simultaneously. Addition of deoxidizers or alloying elements (e.g., Al wire, Ti strip, high-nitrogen alloy compacts) to an electrode, to form a compound electrode, is common.

The electrode is heated at one end above the liquidus temperature so that liquid metal droplets are formed. These fall through the reactive environment of the remelting zone to the liquid metal pool, the surface of which is also heated above the liquidus temperature. The liquid metal pool is confined by a heat-extracting crystallizer, usually a water-cooled copper (or steel) mold. Heat extraction causes the liquid pool to solidify slowly into a new ingot, the "remelted ingot". A "mushy zone" is maintained between the pool and the fully solidified ingot.

The remelting rate dm_e/dt of the electrode(s) practically equals the mold-filling rate dm_i/dt of the remelted ingot. This rate is one or two orders of magnitude smaller than in conventional ingot or continuous casting. A typical value for round remelted ingots of diameter D_i is:

$$dm_i/dt = (1000\ \mathrm{kg\,h^{-1}m^{-1}})D_i$$

A typical ingot for the rolling mill of mass 3000 kg and diameter 0.5 m thus needs a remelting time of 6 h, a big forging ingot (180 000 kg, 2.4 m) needs 75 h; the time is further increased by the necessary "hot topping" at the end of remelting.

General Aims of Remelting

Ingot Structure. One aim of remelting is improvement of ingot structure and homogenization of longitudinal and transverse mechanical properties.

Conventionally cast ingots and strands have a predominant direction of solidification, from the surface to the center, with consequent voids and center segregations. To achieve homogeneous and acceptable mechanical properties, high reduction during hot forming is necessary, which limits the final dimensions of the finished products. Because of their low solidification rate, remelted ingots solidify mainly from the bottom to the top (Figure 6.105), which presents center voids and segregations and leads to an extremely sound and homogeneous ingot structure. Less reduction is necessary to achieve a sound product, which increases the final dimensions attainable with a given hot forming device (rolling mill, forge).

Cleanliness. The second aim of remelting is the improvement of metal cleanliness, two mechanisms being effective:

- The heated metal surfaces and the droplets react with the reactive environment. If the reactive environment is high vacuum, degassing and vacuum deoxidation reactions take place, lowering the content of hydrogen, oxides, nitrides, and volatile metallic residual elements (Cu, Pb, Zn, etc.); if it is reactive slag, complex deoxidation, denitrogenation, and desulfurization take place, together with retention of inclusions from the electrode in the slag.
- Large inclusions, finding their way into the liquid pool, have time to rise slowly to the top, where they are eliminated by various mechanisms. By reaction with the liquid metal, many of the rising inclusions are reduced in size; below a certain particle diameter rising stops, and these inclusions are retained in the solidifying matrix. The remelted ingot has not only a lower total inclusion content, but the maximum inclusion size of the remaining inclusions is much lower than in the electrode material.

Other Aims. Through the introduction of remelting, these processes have often had the

special aim of making products previously not possible by conventional means. An important application is the production of high-nitrogen steels, with high-pressure nitrogen (e.g., 5 MPa) as the remelting environment. Another application is production of sound hollow ingots of steels which are difficult to hot-work, by remelting multiple electrodes into a common annular mold.

Remelting Apparatus

Table 6.13 lists the main processes. Most units for general applications are ESR units, followed by VAR units, EBR, PESR, VADER, and PAR are used for special applications. Details of remelting apparatus construction (electrode feeding; round, square, rectangular, and hollow molds; ingot withdrawal; slags; alloy addition devices; automation, etc.) and other processes are given in the references [159–166].

Results and Applications

The high cleanliness of remelted steels makes them useful for surgical implants, highly polishable pressing sheets for laminate production, etc. The homogeneity of mechanical properties is good for thick products of ultrastrength structural steels, tool steels, etc. The soundness of the ingot allows large forgings, up to 100 t or more, to be made from a much smaller ingot, compared with the conventional route. Some high-temperature alloys exhibit improved forgeability. High-nitrogen, fully austenitic PESR steels are used for production of large, nonmagnetic retaining rings for electrical power generators. Further applications are listed in [159–166].

During the last decade, steady improvements in conventional melting and casting technologies regarding cleanliness and soundness have taken over many applications; the more economic route of melting, secondary refining, and continuous casting is favored over remelting processes. For sound ingots of up to a few tonnes, the powder metallurgy route has become a competing, albeit more expensive process.

Table 6.13: Consumable electrode remelting processes.

Process	Name	Energy input	Remelting environment	External environment	References
ESR	electro-slag remelting	high-current a.c. (or d.c.) resistance heating of liquid slag	liquid slag of CaF_2–CaO–Al_2O_3 or similar type, heated above metal *mp*	air or inert gas	[159, 162, 163]
VAR	vacuum arc remelting	high-current d.c. arc between electrode and pool surface	low-vacuum plasma	high vacuum	[160–163]
EBR	electron-beam remelting	high-voltage electron beams hitting electrode tip and pool surface	high-vacuum plasma	high vacuum	[160, 162, 164]
PESR	pressure electro-slag remelting	see ESR	see ESR	high-pressure inert gas, mostly N_2 plus additions	[165]
VADER	vacuum arc double-electrode remelting	high-current d.c. arc between two electrodes	vacuum plasma	vacuum	[161–163]
PAR	plasma arc remelting	plasma beams from d.c. or a.c. plasma burner(s)	plasma gas	vacuum, normal or high-pressure inert or reactive gas	[162, 166]

6.3.5.4 Cast Steel and Cast Iron

Cast Steel

Many grades of steel, of various composition, are suitable for casting. The carbon content can be as high as 2%, but is usually 0.02–0.4%. Casting consists of pouring into refractory molds, and allowing to solidify.

In the production of steel castings, all types of molds and casting processes are used, including hand- and machine-made molds, shell molds, and ceramic molds. Other processes include precision casting by the lost wax process, the full mold process, and centrifugal casting. Castable steel is melted by methods similar to those for rolling and forging steel, mostly in electric arc furnaces lined with a basic refractory, and, less commonly, in induction-heated, crucible furnaces. The processes of secondary metallurgy in oxygen/argon converters or specially designed gas-purged ladles are increasingly important.

In Germany, of all the crude steel produced, 0.6% is cast. The proportion is similar in other industrialized countries.

Cast Steel for General Applications. These materials are used for components intended for use between –10 and 300 °C, which are subject to moderate dynamic and impact stresses, e.g., parts for general machinery, wheels and wheel bearings, rolling equipment, and ships' anchors. The most common material in this group is mild steel, though some low-alloy steels are also used. Steels with a low carbon content have good welding properties, which has ensured a wide range of applications for steel castings. It is common to improve the welding properties by reducing the carbon content, and to compensate for this by increasing the manganese content.

Figure 6.106 shows the temperature dependence of the mechanical properties of unalloyed cast steel.

Cast Steel for Special Applications. Cast steel was formerly at a disadvantage compared with forged and rolled steel for welded construction, in that high-strength grades with adequate welding properties were unavailable. Metallurgical advances in steel production, especially secondary metallurgy, have enabled the production of steels which, after casting and heat treatment have tensile strengths of ca. 800 N/mm². They are thus equivalent to rolled and forged steels, and can be welded to them (Figure 6.107).

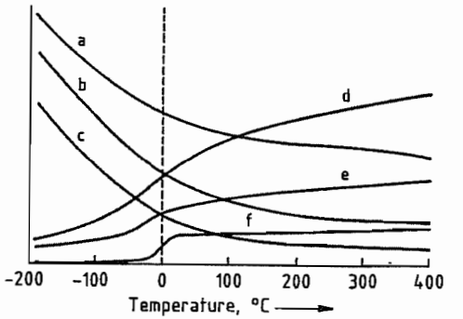

Figure 6.106: Mechanical properties of unalloyed cast steel as a function of temperature: a) Tensile strength; b) 0.2% yield strength; c) Flexural fatigue strength; d) Constriction; e) Elongation; f) Notched impact strength.

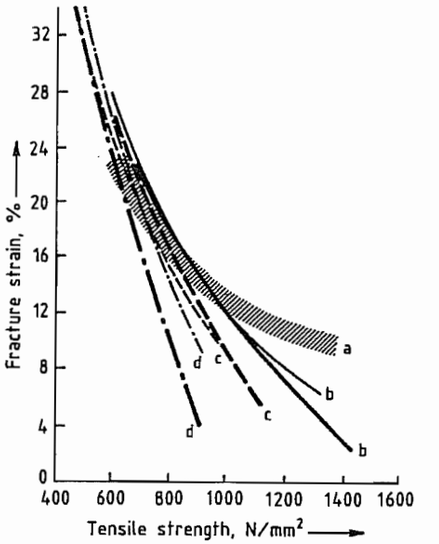

Figure 6.107: Correlation between fracture strain and tensile strength of tempered cast steel compared with rolled and forged steels: a) Steel values from DIN 17200; b) Tempered structure; c) Mixed structure; d) Ferritic–pearlitic structure. —— = Cast steel valves from Steel Castings Handbook; ▬ = Experimental cast steel valves.

With these properties, the high-strength weldable and castable grades of steel now available are suitable for welded designs in many areas of engineering. Grades suitable for turbines and steam power stations can be used to make castings up to 100 t.

Alloying costs are not high, but they need to have a carbon content of ca. 0.2% for good

welding properties. To ensure that components of all types will have the properties desired, including welding properties, martensitic and lower bainitic structures must be produced, for uniform strength and toughness.

For plain carbon steel castings, the limit of the wall thickness for through-tempering is ca. 20 mm. By the use of suitable alloying elements, this can be extended to ca. 500 mm, although the welding properties are somewhat affected.

Hot-strength, low-temperature, and stainless grades of cast steel, including austenitic and duplex steels, are produced in a similar way to the rolling and forging steels.

The tendency of low-temperature nickel steels to give a coarse-grained structure on solidification makes them less suitable for casting. It is, therefore, recommended that Cr–Mo or Ni–Cr–Mo alloy steels should be used, if possible.

Typical grades of steel for casting have heat and abrasion-resistance properties which cannot be matched by rolling and forging steels.

Cast steel is regarded as a high-temperature steel if it effectively resists the scaling effect of gases at > 600 °C. Heat-resistant steels can be divided into ferritic and austenitic grades, and alloys based on nickel and cobalt. Ferritic steels are alloys containing 7–28% Cr and 1.7% Si, and austenitic steels contain 18–30% Cr and 10–37% Ni. High-temperature steels (Figure 6.108) are used for components that are highly stressed, both thermally and mechanically, and are subjected, either continuously or intermittently, to corrosive gases at ca. 600–1150 °C. These materials have made the continuous operation of industrial furnaces an economic possibility. Other areas of use include ore treatment (roasting furnaces), and the cement, petroleum, and petrochemical industries. Heat-resistant cast steel is used for valve cages, and combustion chambers in diesel engines.

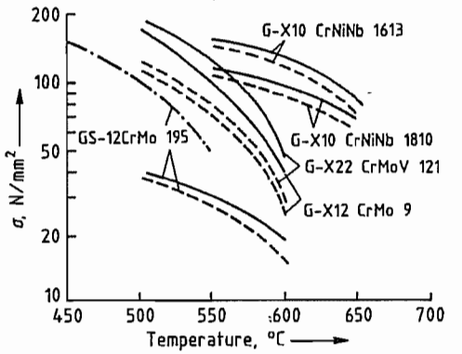

Figure 6.108: High-temperature cast steel for working temperatures above 540 °C. — = $\sigma_{B/100\,000}$; —— = $\sigma_{1/100\,000}$; —·— = DVM (Deutscher Verband für Materialprüfung der Technik) creep limit.

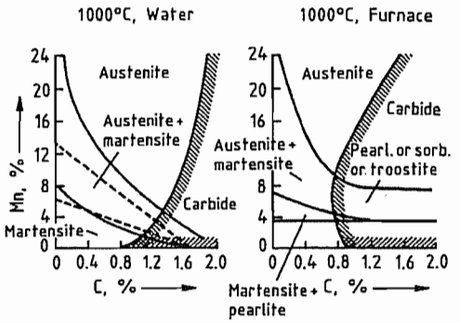

Figure 6.109: Structure of cast hard manganese steel as a function of cooling rate.

Cast hard manganese steel (Figure 6.109), which contains 1.0–1.4% C and 12% Mn, was first described in 1888, and has retained its importance up to the present day. In order to develop its maximum abrasion-resistance properties, a cold-hardening process is required, e.g., by impact or pressure working, which can increase the hardness of the abrasion-resistant surfaces from 250–300 to 500 HB (Brinell hardness scale). Good toughness properties can be produced by a solution annealing process at 1050 °C, with water quenching.

Hard manganese steel is unsatisfactory under conditions of abrasive wear without impact and pressure work hardening, as under these conditions no cold hardening occurs.

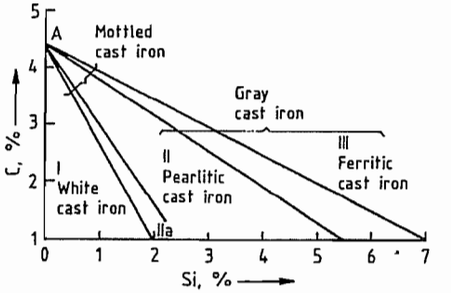

Figure 6.110: Structure zones of cast iron.

Tempering steels are used where components and workpieces undergo mainly abrasion, but are also subjected to impact stress.

Abrasion-resistant cast hard chrome steels have the highest abrasion resistance of all cast steels. They contain 2.5–3.5% C and 15–27% Cr, and attain their highest abrasion resistance after hardening at 900–1050 °C, with either accelerated or static air quenching. This group has the lowest toughness of all the abrasion-resistant materials. Components made of this material must not be subjected to transverse stress. Hard chromium steel is used under conditions of predominantly frictional abrasion, and where impact and pressure stresses are small.

Cast Iron

Cast iron includes iron carbon alloys with carbon content ca. 2.8–4%. The carbon is for the most part not chemically bonded to the iron, but is present in elemental form.

Gray Iron. Cast iron with flake graphite, also known as gray iron, is an iron-based material in which the carbon is nearly all in the form of microscopic graphite flakes with a ferritic–pearlitic structure (Figure 6.110). In Germany, this material falls under the DIN 1691 standard, which specifies tensile strengths of 150–350 N/mm^2. In the United Kingdom, BS 1452 applies, and in the United States, ASTM A48.

Formation of the graphite and its primary structure, and hence the strength and hardness of the product, depend very much on the cooling and solidification rate, and hence on the wall thickness. However, heat treatment of gray iron is not normally practicable, so this relationship is less important than the correct choice of chemical composition. For gray iron components, the design can only specify the wall thicknesses and the required strength the choice of chemical composition must be left to the foundry.

Cast iron is poured at ca. 1300–1450 °C. When molten, it can completely fill complicated thin-walled molds, reproducing pattern details exactly. Other important characteristics include its property of damping vibration, its good resistance to corrosion by weathering, and its good machining properties.

The amount of cast iron exceeds that of all other cast materials; ca. 40% is used in the automobile industry. Other applications include mechanical engineering, the building industry (radiators, boilers, sanitary ware, pipes), chemical plant, shipbuilding, and mining. The former demand by steelworks for cast iron ingot molds has been greatly diminished by the introduction of the continuous casting process.

Spheroidal Graphite (SG) Cast Iron. In spheroidal graphite, also known as ductile iron or nodular iron, the free graphite in the ferritic-pearlitic matrix is almost completely in spheroidal form. This is achieved by treating the melt with magnesium. The formation of spheroidal graphite gives very good ductility, unlike the brittle properties of gray iron.

This material, first produced in 1948, is now the subject of the German DIN 1693, BS 2789 in the United Kingdom, and ASTM A 536 in the United States. Its hardness can be increased by heat treatment and tempering. Its mechanical and physical properties place it between lamellar cast iron and cast steel, though it more closely resembles cast steel.

A large consumer of SG iron is the gas and water pipe industry, which produces centrifugally cast pressure pipes and special pieces (elbows, Y-pieces, T-pieces, etc.). The automobile and general engineering industries have an even greater and increasing demand. Rollers, ingot molds, and heavy, thick-walled

storage containers for the disposal of radioactive waste are manufactured from SG iron.

A special development, austempered ductile iron (ADI), also known (somewhat inappropriately) as "bainitic" cast iron, has interesting mechanical properties. When its tensile strength is 900 N/mm^2, its breaking elongation is 5–12%; when its tensile strength is 1400 N/mm^2, its breaking elongation is 1–2%. These materials also have very good abrasion properties. The bainitic hardening is carried out in a salt bath at ca. 300–500 °C for 20 min to ca. 2 h. As yet there is no standard specification in Germany, the United States, Japan, or Sweden. A European standard is in course of preparation.

Cast Iron with Vermicular Graphite. In this type of cast iron, the graphite that separates out is mainly in vermicular form. The connection between this type of cast iron and the mineral vermiculite, a magnesium aluminum silicate, is only conceptual. On heating and expanding, vermiculite swells up to worm-like shapes (Latin: *vermis*, worm). Expanded vermiculite is used in the building industry as a sound, and thermal insulator, and has no connection with cast iron.

The basic structure of cast iron with vermicular graphite can be ferritic, pearlitic, or a mixed structure. The mechanical properties of the material lie somewhere between those of gray iron and SG iron. Vermicular graphite has been known since the discovery of spheroidal graphite in 1948. Any vermicular graphite in the SG iron structure was regarded as having a harmful effect on properties. Its occurrence indicated the presence of troublesome elements (principally titanium), which limited the formation of spheroidal graphite if the standing time of the melt was inadequate or excessive. This led to fading of the effects of the magnesium treatment, and imperfect formation of the graphite in the interior of thick-walled SG iron castings.

There is no German standard for this material, but local standards exist.

Alloyed Cast Iron. The properties of cast iron can be modified within wide limits by adding elements such as nickel, chromium, manganese, copper, and silicon, which change the metallic structure. Corrosion-resistant and high-temperature grades are used, e.g., in the chemical industry, in furnaces, and in the automobile industry. The cryogenics industry uses low-temperature grades that do not become brittle at temperatures far below 0 °C. The electrical industry has wide-ranging requirements for nonmagnetic materials, and materials with high electrical resistivity.

In Germany, these materials are covered by DIN 1694 (austenitic cast iron) and DIN 1695 (abrasion-resistant alloyed cast iron), in the United Kingdom by BS 3468, and in the United States by ASTM A439.

White Cast Iron and Roll Casting. In these special grades of cast iron, the carbon in the structure is not graphite, but iron carbide. White cast iron is extremely resistant to abrasion by frictional and grinding effects. These grades are used in a wide range of rolling operations, and in grinding and mixing processes. As these materials are normally not heat treated, the mechanical properties depend only on the chemical composition, even for very heavy and thick-walled components (rolls).

Malleable Iron. Malleable iron castings acquire their special properties by a tempering heat treatment. Malleable iron is formed from an iron–carbon alloy (DIN 1692) whose chemical composition is such that, after solidification, the carbon in the metallic structure of the casting is not free graphite, but chemically combined as iron carbide, Fe_3C. In this condition, the material is hard and brittle, and almost useless. The tempering process causes a transformation of the white iron by decomposition of the iron carbide at the high temperature used. Elemental carbon is precipitated, and is then present in the structure as compact nodules or flakes.

Depending on the heat treatment, two types of malleable iron can be produced: "white heart" malleable iron in which the heat treatment removes the carbon (Figure 6.111), and

"black heart" malleable iron in which it does not.

Malleable iron can be produced only in castings of limited mass and wall thickness. Mass varies between a few grams and ca. 100 kg. The good machining properties and especially the uniformity and consistency of the useful properties of malleable iron make it highly suitable for production foundries.

Most of the malleable iron castings produced (65%) go to the automobile industry. In second place comes the building industry (fittings and pipe connectors). Other consumers include the general engineering and electrical industries, and manufacturers of locks.

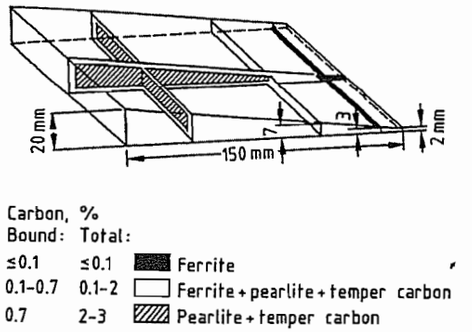

Figure 6.111: Distribution of carbon and development of the structure in white heart malleable iron of various wall thicknesses.

Melting of Cast Iron. The oldest and most widely used melting furnace in iron foundries is the cupola furnace. It was developed from the early charcoal furnaces, which were sometimes provided with a cover to keep off snow and rain.

The modern cupola furnace is a shaft furnace with height approximately six times its diameter. The inside diameter is ca. 800–3000 cm. Most cupola furnaces have melting capacities of 6–12 t (Figure 6.112), but the largest cupola furnaces produce 80 t/h. Pig iron, alloying elements, scrap castings, and steel scrap, together with coke (the fuel) and limestone to liquefy the slag and combine with the sulfur in the coke, are all charged in weighed batches into the cupola furnace.

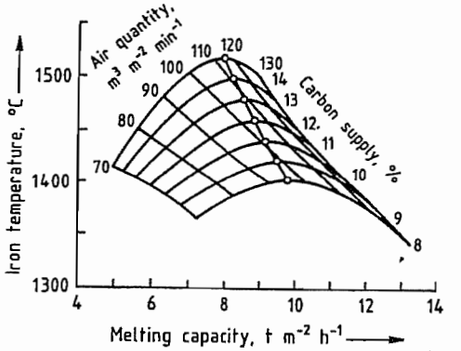

Figure 6.112: Iron temperature and melting rate as a function of air blast and available carbon for a cupola furnace with specific cross-sectional area 1 m^2.

The cupola furnace consists of a strong cylindrical steel sheet outer cover, lined with a thick layer of refractory bricks and rammed refractory material. In the bottom part of the furnace shaft, ring-shaped nozzles (tuyères) blow air into the incandescent layers of coke, iron, and other materials.

In the melting zone, the metallic raw materials, selected so that the molten cast iron has the desired composition when it flows from the furnace, are mixed. Molten cast iron at ca. 1500 °C and molten slag are then tapped from separate openings into separate containers. The cast iron is usually collected in a large, refractory-lined holding vessel in front of the cupola furnace. The casting ladles can then be filled from this as required. The slag flows into a cast iron skip, and, after solidification, is disposed of on a waste tip. It is sometimes granulated by adding water, or is used to produce slag wool, used as an insulating material.

Modern cupola furnaces use the hot blast system, in which the combustion air is preheated and sometimes enriched with oxygen. This increases the temperature and melting capacity.

In another type of cupola furnace, firing is by gas or oil. The furnace is provided with burners instead of tuyères. The column of metal is supported in the shaft by a water-cooled grate, located above the burner zone. Ceramic spheres on the grate increase heat transfer by convection, and the molten iron

passes over these and drips into the hearth. The cupola furnace is an economic method of melting large amounts of iron of constant or slightly varying composition. The molten iron can be continuously removed from the furnace. To an increasing extent, induction crucible furnaces are used in iron foundries, usually operating at mains frequency (50 Hz) with iron capacities up to 80 t, although most are in the range 3–25 t. Furnaces of this type do not absorb electrical energy when empty, and absorb very little when charged with material in small pieces, because no appreciable induced current is produced under these circumstances. Hence, low-frequency crucible furnaces must always have a quantity of molten metal in the furnace (25% of the total crucible capacity). To start up the furnace, a precast starting block that matches the shape of the crucible is placed in the crucible by means of a crane.

Medium-frequency induction crucible furnaces, operated at 500–1000 Hz, are similar to the mains frequency furnaces, except that their capacities are considerably less for electrical reasons. Medium-frequency furnaces are used if rapid melting and heating, melting without starting blocks, or frequent changes of metal grade are required.

6.4 Forming

Metals, including steel, can be subjected to plastic deformation in the solid state by the application of external forces, i.e., they can be formed into new permanent shapes. Here, the term "forming" or "metal forming" means the intentional and controlled change of the geometry of a workpiece, usually from a simple geometry to a complex one with regard to the shape, size, accuracy and tolerances, appearance and properties. The mass, composition, and state of the material remain unchanged. If, however, the plastic limit is exceeded so that the change in geometry is not controlled, forming with defects occurs, and the desired product is not obtained.

For many applications, the products of hot rolling are unsatisfactory, e.g., with respect to cross section, surface quality, dimension al accuracy, and general finish, so that cold rolling is necessary, i.e., reduction of the thickness of the hot-rolled strip between two working rolls without additional heating. Cold rolling of steel is mainly used in the production of light-section, thin sheet, and stainless steel sheet of thickness 0.1–3.0 mm.

The production cycles in a cold rolling mill differ considerably from those in a hot rolling mill. The raw material is first descaled, rolled, and then heated. Further steps are slitting, coiling, inspection, skin-pass rolling and packing.

6.4.1 Pickling

Hot-rolled steel sheet always has a layer of scale of variable structure on its surface, depending on the hot rolling conditions (Figure 6.113). The method of descaling depends on the composition of the scale. For high-grade steels, chemical descaling is carried out in hydrochloric or sulfuric acid, while stainless steels are normally pickled in a nitric acid mixture. Purely chemical descaling is often a long process, but it can be accelerated by preliminary mechanical descaling, e.g., stretching, leveling abrasive blasting, or rolling. Effective descaling requires the scale to be broken down.

Pickling is carried out in continuously operating plants (Figure 6.114). There are usually two pay-off reels from which the strip is run. It is first cut by cropping shears to form the beginnings and ends of the strips, and the start of the band is machine welded to the end of the previous band. Great care must be taken in the production of the weld bead, as this is rolled in the cold rolling mill, and must not be torn off. So that the actual pickling process can take place continuously during this interruption to the flow, there is a storage looper between the welding machine and the pickling plant. After welding, the storage looper is refilled at ca. 2.5 times the pickling speed.

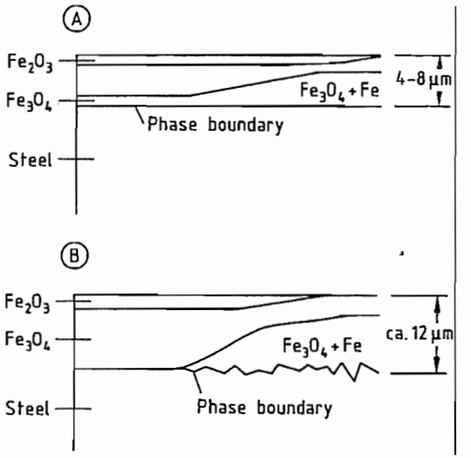

Figure 6.113: Structure of the scale layer on hot-rolled unalloyed or low-alloyed steel: A) Coil temperature ca. 570 °C; B) Coil temperature ca. 750 °C.

Before the actual pickling process, there is usually a stretcher bend-leveling device which also causes mechanical descaling. This preliminary descaling is very important, as there must be a certain percentage of free iron surface in the pickling bath, so that pickling can start. Normal steels are usually pickled in 20–25% sulfuric acid at 95–100 °C, or 15–20% hydrochloric acid at 60–70 °C in three or four fully enclosed pickling baths. For strip speed 240 m/min, the dwell time in the bath is ca. 20–30 s. The pickling time depends not only on the steel composition and hot rolling conditions, but is also a function of acid concentration, temperature, and concentration of iron(II) salt, which increases as the dissolution of scale proceeds.

The chemical reactions during pickling are described in the literature [175–179]. Individual pickling reactions are given in Table 6.14.

Table 6.14: Pickling reactions.

$Fe_2O_3 + Fe + 3H_2SO_4 \rightarrow 3FeSO_4 + 3H_2O$
$Fe_3O_4 + Fe + 4H_2SO_4 \rightarrow 4FeSO4 + 4H_2O$
$FeO + H_2SO_4 \rightarrow FeSO4 + H_2O$
$Fe + H_2SO_4 \rightarrow FeSO4 + H_2$
$Fe_2O_3 + Fe + 6HCl \rightarrow 3FeCl_2 + 3H_2O$
$Fe_3O_4 + Fe + 8HCl \rightarrow 4FeCl_2 + 4H_2O$
$FeO + 2HCl \rightarrow FeCl_2 + H_2O$
$Fe + 2HCl \rightarrow FeCl_2 + H_2O$

As the area of the clean steel surface increases, the pickling time decreases until a point known as the critical free surface is reached. For hydrochloric acid, this is ca. 15%, and for sulfuric acid, ca. 2%.

After leaving the acid baths, the strip is washed, dried, oiled, and coiled to form rolls of the required mass. The storage looper compensates for interruptions to the process. All pickling plants are provided with trimming shears, normally located at the exit, though in some plants at the inlet.

The used acid can be regenerated, in the case of sulfuric acid by precipitating iron sulfate as its heptahydrate in a crystallizer (see Section 5.20).

Hydrochloric acid can be regenerated by decomposing the iron chloride to hydrochloric acid and iron oxide, by a spray process at 450 °C, or in a fluidized bed at 850 °C [180].

6.4.2 Rolling

After pickling, the descaled hot-rolled strip is cold rolled, reducing its thickness (1.5–5 mm) by up to 90%. Many types of stands are used in the production of cold-rolled strip, e.g., two-high, four-high, or larger. In reversing stands, one roll pass can be immediately followed by another by reversing the direction of the rollers. Reversing stands with many rolls exert a high pressure on the strip because the diameters of the working rolls are small. These stands are therefore mainly used for steels with work-hardening properties, e.g., stainless steels and electric sheet steels.

Some 4-6 four-high stands can be installed one after the other to form a so-called tandem cold rolling mill (Figure 6.115). These mills have the advantage that the strip reaches its final thickness by going in one pass from the pay-off reel through all the stands. Strip speeds at the exit can reach 2400 m/min.

The gap is lubricated with an oil-water emulsion to enable a high degree of deformation (thickness reduction) to be achieved at high rolling speeds. The oil provides lubrication, and the water absorbs the heat produced in the rolling process.

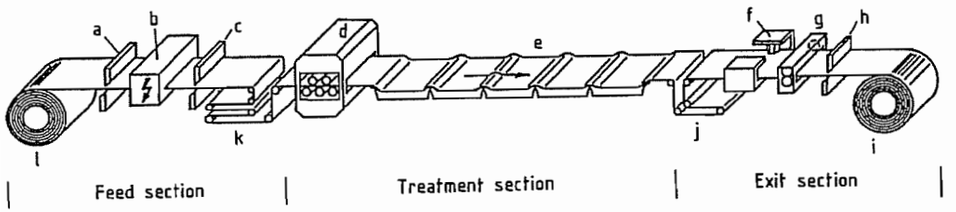

Figure 6.114: Continuous pickling plant: a) Cropping shears 1 (head); b) Welding/planing machine; c) Cropping shears 2 (foot); d) Stretch–bend–leveling device; e) Pickling/washing; f) Stamping device; g) Trimming shears; h) Cropping shears; i) Take-up reel; j) Exit hooper; k) Entry looper; l) Pay-off reel.

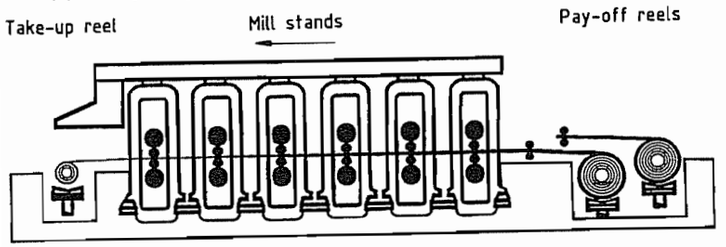

Figure 6.115: Six-stand tandem cold rolling mill.

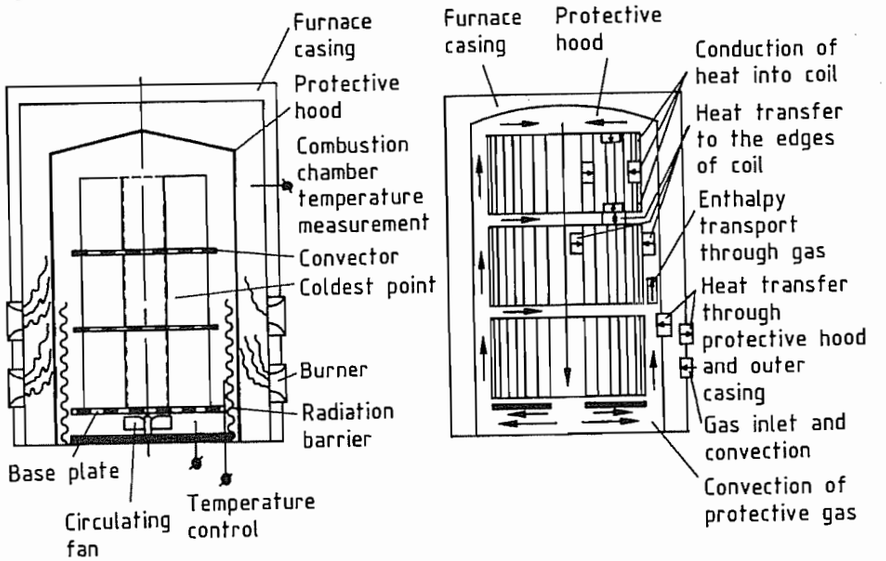

Figure 6.116: Hood furnace with heat transfer and gas flow indicated.

Experiments have shown that it is not possible to change the profile in a cold rolling mill, so the hot-rolled strip profile must be produced to close tolerances. If the shape of the gap between the rolls does not correspond to the profile of the strip being rolled, flatness defects can occur (differences in the length of individual fibers) [181].

The control elements usually used to adjust the flatness are:

- Curved working rolls, both positively and negatively. Gap correction up to 180 µm can be achieved.
- Adjustable intermediate rolls. This system requires six stands.
- Thermal changes to the crowning of the roll. The degree of thermal expansion of the roll body can be changed locally by adjusting the cooling, but this can only produce extremely small changes.
- Continuously variable crown systems (universal profile control). The rolls can be adjusted to produce a convex or concave gap; the range of control here is ca. 400 µm.

With the aid of precisely controlled strip tensions between the stands and highly developed measuring and automation technology, it is possible to provide a gap shape appropriate for the shape of the strip. With this system, flat cold-rolled strip with thickness variations of only a few thousandths of a millimeter and high-quality surface finish can be produced.

Cold rolling causes work-hardening of the steel. This is reduced by an annealing stage.

6.4.3 Annealing

The cold-rolled coiled strip is stacked in a hood furnace for annealing (Figure 6.116). The combustion chamber is heated by oil or gas burners. The heat passes through the protective hood into the space where the steel coils are stacked. A circulating fan provides as uniform a temperature distribution as possible. The atmosphere in conventional plants is usually HNX gas (a nitrogen–hydrogen mixture in which the hydrogen content is close to the flammability limit).

The heat passes into the coils through their outer edges, so that these areas are always hotter than the inner windings, especially during heating up.

This heat treatment causes the organic residues of the emulsion to burn off without leaving a residue, in accordance with the reactions given in Table 6.15 [182–184]. The strip is then heated to the recrystallization temperature, and annealed under the protective gas at ca. 700 °C. This treatment produces a complete recrystallization of the cold-rolled steel. The coils are cooled by removing the outer casing. As the annealing space is then hotter than its surroundings, heat passes out of the protective hood in the reverse direction. The outer windings of the coil cool more quickly than the inner windings. If the cooling is too rapid, tensions due to shrinking occur, and these can cause diffusion welding of the windings (stickers).

Table 6.15: Annealing reactions.

$CO_2 + C \rightleftharpoons 2CO$	Boudouard reaction
$CO + H_2O \rightleftharpoons CO_2 + H_2$	Water gas reaction
$Fe + xCO_2 \rightleftharpoons FeO_x + xCO$	Oxidation of iron due to CO_2/Co ratio
$Fe + xH_2O \rightleftharpoons FeO_x + xH_2$	Oxidation of iron due to H_2O/H_2 ratio
$C + 2H_2 \rightleftharpoons CH_4$	Methane reaction

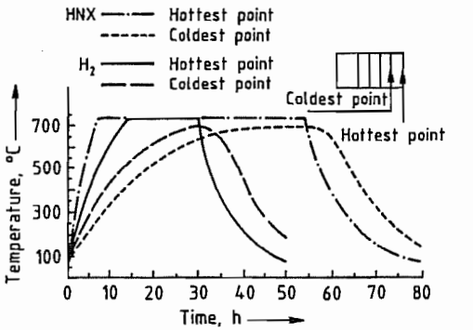

Figure 6.117: Comparison of annealing times in a hood furnace under HNX and H_2 atmospheres.

Annealing in this type of furnace was formerly very slow. Another serious limitation was the limited rate of cooling attainable, so that certain grades of steel were very difficult to produce in this furnace. An annealing process in a 100% hydrogen atmosphere with improved convection has been developed in recent years. This gives shorter annealing times (mainly owing to the rapid cooling), and more uniform mechanical properties. The hydrogen easily diffuses into the coil windings, and its conductivity is a factor of seven greater. Moreover, the smaller H_2 molecules

enable more rapid circulation of the atmosphere (high convection, Figure 6.117).

The continuous strip annealing process was developed in Japan in the 1970s (Figure 6.118). At the feed end there are: a double-feeder pay-off reel, a welding machine, a cleaning zone, and a storage looper (required if coils need to be welded together to give continuous operation). The strip then passes through the heat treatment zone: heating chamber, annealing chamber, cooling unit, tempering zone, and second cooling chamber. These are followed by the exit looper, the skin pass mill, the side-cutting shears, the inspection area, the cut-to-length line, and the double-coiling reel. As the treatment time for the material is short (ca. 10 min), the annealing temperature is higher than in the batch annealing process.

There are four continuous annealing processes which compete worldwide, differing mainly in the cooling equipment used, and the cooling rates achieved [185].

The recrystallizing annealing process eliminates the hardening produced by cold working, but the mechanical properties of the annealed strip are poor: low tensile strength, low yield point, high fracture strain, etc. Annealed thin strip has a marked upper yield point and a large extension at the lower yield point.

There are two basically different annealing cycles for continuous annealing furnaces (Figure 6.119). In the first, the strip is heated to the annealing temperature, held at this temperature, cooled to the dwell temperature, held again, and then cooled to room temperature. The other alternative consists of heating to the annealing temperature, cooling with gas jets to an intermediate temperature, and quenching in water to room temperature. The strip is then brought up to the aging temperature, and finally cooled again to room temperature. Treatment at the aging temperature is not necessary for dual-phase steels.

Quenching is produced by the rapid cooling of the strip in the continuous annealing process, so that the carbon remains in solution. For this reason, continuous annealing is very suitable for producing high-strength, dual-phase, and IF (interstitial-free) steels.

6.4.4 Skin-Pass Rolling

As stated above, the annealed material must be rolled (skin-pass rolling) to prevent flow lines owing to the distinct upper and lower yield points. This also produces the roughness which customers require. This is of great importance for deep drawing or coating the steel. For example, if complex deep-drawn parts are required, e.g., for automobile construction, the surface of the steel should be rough in order to retain the lubricant. Good coating properties require a surface with a large number of peaks, which should be randomly distributed.

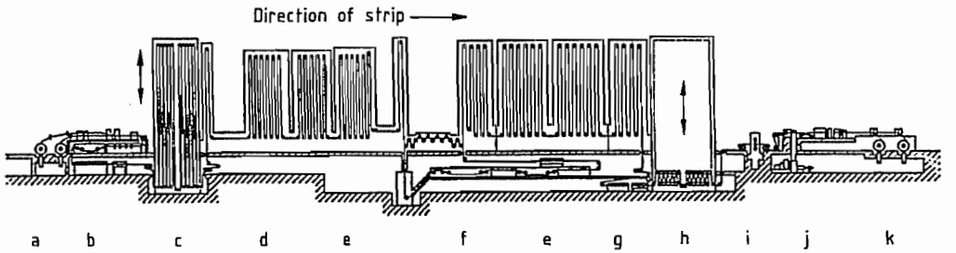

Figure 6.118: Continuous annealing plant: a) Pay-off reel; b) Strip cleaning; c) Entry looper; d) Heating zone; e) Tempering zone; f) Reheating zone; g) Cooling; h) Exit looper; i) Skin-pass rolling; j) Inspection/oil treatment; k) Take-up reel.

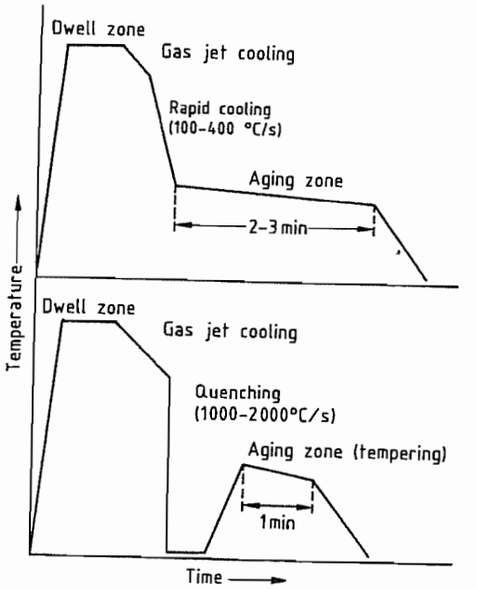

Figure 6.119: Heating cycles of continuous annealing.

Various steel grades can be produced in these two annealing cycles.

6.4.5 Stainless Steels

The processing of stainless steel in a cold rolling mill is quite different (Figure 6.120). Austenitic stainless steel behaves differently from ferritic stainless steel. The hot-rolled strip is first annealed. This is necessary because, after the hot rolling process, the strip cools slowly, and carbon tends to precipitate at the grain boundaries, owing to its reduced solubility at lower temperature. Annealing causes the carbon to go back into solution. Rapid cooling of the strip then prevents the carbon from precipitation by diffusion. Although the annealing time required to bring the carbon into solution is short for austenite, a long time is necessary for ferritic steels, so that batch annealing is necessary. In the continuous furnace, annealing is carried out in an oxidizing atmosphere to produce a scale with a high oxygen content, thereby assisting the pickling process. This does not apply to high-grade steels. The strip is then quenched, by air-water cooling.

Annealing in the hood furnace is successful because of the increase in throughput obtainable under the reducing atmosphere. Considerable increases in throughput have been achieved by the use of hydrogen, even though its concentration is only 25%.

A high proportion of the scale is removed by abrasive blasting. Although the abrasive particles are mainly spheroidal, a high degree of roughness is produced. This must be removed by rolling, another cause of the high deformation strain in high-grade steel mills.

Sodium sulfate is used in electrolytic pickling. The electrolytic pickle liquor is in effect self-regenerating.

Conventional pickling is carried out with a mixture of nitric (12–14%) and hydrofluoric acid (2–4%). Pickling temperatures are usually 40–60 °C. Unlike sulfuric acid or hydrochloric acid pickling solutions, regeneration is not possible, so that the spent acids must be rendered harmless and disposed off.

After pickling, the strip is usually rolled on "Sendzimir" rolling mills (more rarely on four- and six-high stands).

The strip is then annealed to convert the steel from the work-hardened state produced by cold rolling into a recrystallized and stress-relieved state, to enable further treatment of the strip to be carried out.

Stainless steels are to an increasing extent being annealed in bright annealing plants [186], as this process enables the bright surface produced by cold rolling, and typical of special steels, to be retained (Figure 6.121).

The strip is finally rolled again (skin-pass rolling).

6.4.6 Future Developments

The extent of automation in cold rolling mills has raised the possibility of linking the individual process steps. For instance, attempts are being made to link the pickling stage with the tandem rolling operation. This requires the outputs of the two operations to match. In Japan, a cold rolling mill is being

operated in which pickling, rolling, and continuous annealing have been combined, despite the fact that the outputs of the continuous annealing process and the rolling mill do not correspond. The maximum economic output of a continuous annealing plant is 800 000 t/a, while tandem rolling mills can easily achieve twice this production rate.

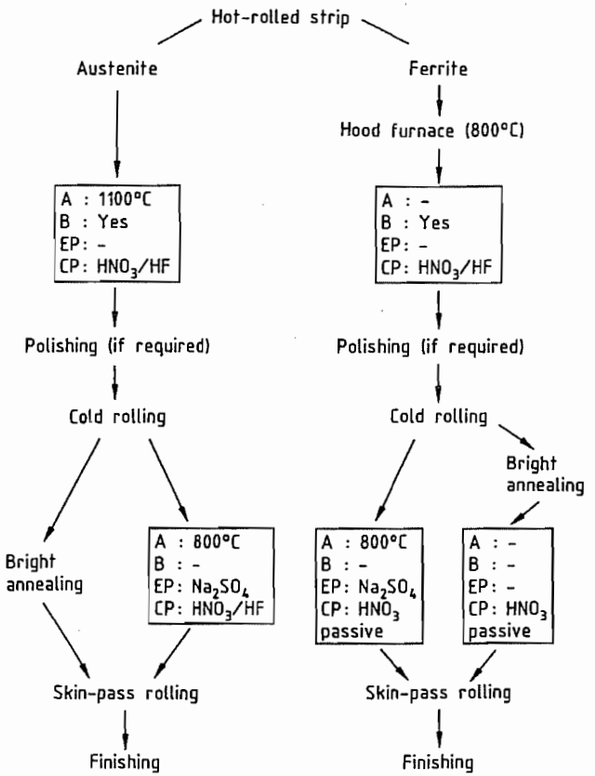

Figure 6.120: Flow diagram of a combined annealing/pickling line. A = annealing; B = abrasive blasting; EP = electrolytic pickling; CP = chemical pickling.

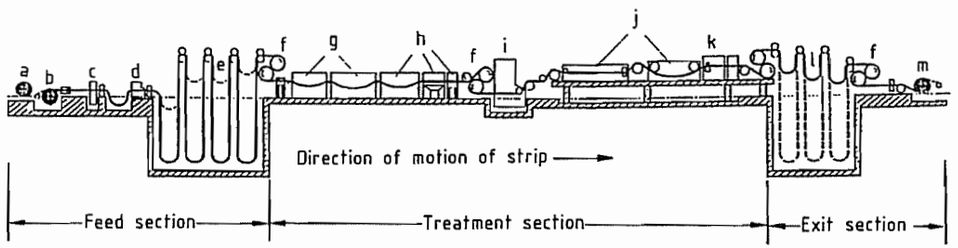

Figure 6.121: Annealing/pickling line for stainless steel: a) Pay-off reel 1; b) Pay-off reel 2; c) Welding machine; d) Trimming shears; e) Looper 1; f) Roll stand; g) Furnaces; h) Cooling zone; i) Abrasive blasting; j) Pickling; k) Spray washing; l) Looper; m) Take-up reel.

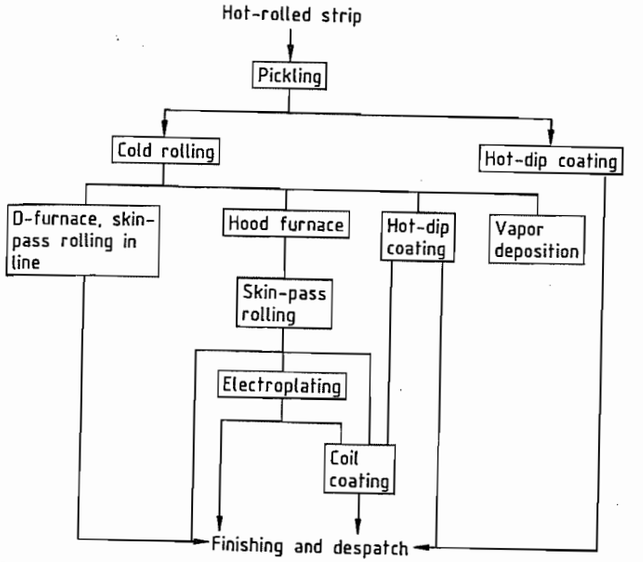

Figure 6.122: Surface coating in relation to other production processes.

6.5 Surface Coating

6.5.1 Introduction

Technical developments in recent years have greatly increased the output of surface-coated steel strip. The demand for improved corrosion protect ion is not the only driving force. The properties of coated strip, such as the yield point, expansion properties, and cold workability needed to be improved before these products could be used, e.g., in the automotive industry. New processes had to be developed to improve welding and paint application properties for large-scale industrial manufacture. These involved close cooperation between the producers and consumers of coated steel sheet. Within the steel industry the continuous surface coating processes used include hot dipping, electrolytic techniques, vapor treatment, and coil coating.

The status of surface coating in relation to other production processes within the steel industry is shown in Figure 6.122.

The design of surface coating plants for wide steel strip essentially consists of the mechanical entry section, the process itself, and the exit section. The input and output sections are provided with pay-off reels, coiling reels, leveling machines, shears, welding machines, loopers, regulating and pulling rolls, etc.

This equipment produces a continuous strip, and enables treatment to be carried out at constant strip speed, under stable process conditions. Inspection areas for quality assurance are usually situated at the exit end.

As well as coated strip, the steel industry also produces clad steel sheet. This is a composite material that combines the properties of a carrier material which is usually cheap (e.g., carbon steel) with those of a metal more suitable for the conditions of use (e.g., corrosion-resistant steel).

6.5.2 Hot-Dip Coating

6.5.2.1 Plant and Processes

In the hot-dip coating process, the steel strip is continuously passed through molten metal. An alloying reaction between the two

metals takes place, leading to a good bond between coating and substrate.

Cold-rolled wide strip is usually used for hot-dip coating, but this is contaminated with rolling lubricant emulsion and of abraded iron fines. To ensure a good bond between the metal coating and the substrate, the surface of the strip must be thoroughly cleaned before dipping in the molten metal.

The important parts of the hot-dip coating process (Figure 6.123) are [187]: the continuous furnace; the treatment zone where the metal coating is applied; cooling and final treatment.

Older plants usually have a horizontal continuous furnace which comprises a directly heated preheating furnace and indirectly heated reduction and holding zones with reducing H_2/N_2 atmospheres, followed by cooling zones. In the preheating furnace, the strip is rapidly heated to > 550 °C, and is cleaned by burning off the oil emulsion residues. In the reduction and holding zones, the strip is heated to cause recrystallization or normalization, according to the grade of steel, to give the cold-rolled, work-hardened substrate material the desired mechanical properties.

For normal grades of thin steel strip, temperatures are 700–750 °C, and for IF (interstitial free) steels > 800 °C.

The strip is cooled in the cooling zones to a temperature slightly above that of the molten metal, with static cooling elements and rapid coolers.

After leaving the continuous furnace, the cleaned and heated strip, under a protective gas, is fed by means of a so-called snout into the molten metal (Figure 6.124), which is contained in a heated metal or ceramic vessel. Immediately after this, jet processing is carried out by blowing a gaseous medium through a slit, of the same length as the width of the strip, onto the upper and lower sides of the strip. This enables different coatings to be produced on the two sides. The coating thickness (7–45 µm, or 50–300 g/m^2) is a function of gas pressure, strip speed, nozzle–strip distance, nozzle aperture, jet angle, and the viscosity and density of the metal being removed.

The thickness of the metal coating is continuously monitored, and controlled by adjustments to the jet processing equipment.

After jet processing, the liquid metal coating passes through air cooling equipment, so that it solidifies before it comes into contact with the first roller that deflects it from the vertical.

The strip then passes through more processing equipment. It is rolled in the finishing stand to improve its technical properties or to give a uniform surface appearance. The flatness of the strip is then improved by stretch–leveling equipment.

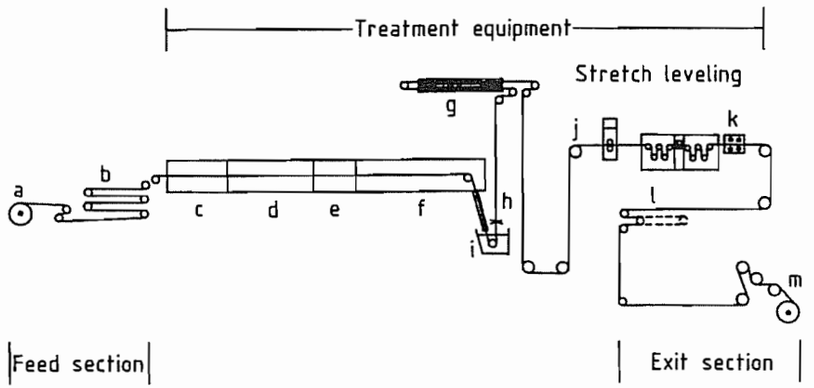

Figure 6.123: Hot-dip coating plant: a) Pay-off reel; b) Entry looper; c) Preheater; d) Reduction zones; e) Holding zone; f) Cooling zones; g) Strip cooling; h) Nozzle; i) Molten metal bath; j) Skin-pass rolling; k) Final chemical treatment; l) Exit looper; m) Take-up reel.

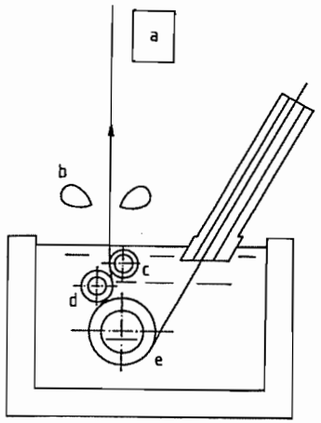

Figure 6.124: Control of coating thickness: a) Coating thickness measurement; b) Jet processing nozzle (slit); c) Pass line roll; d) Stabilizing roll; e) Bottom roll.

Further chemical treatment—chromate passivation and/or oil treatment, for temporary protection of the surface against "white rust" is sometimes carried out.

In new plants (Figure 6.125), the continuous furnace is usually vertical, which reduces the number of contacts between the easily damaged strip and the carrier rollers. These Plants also have alkaline cleaning equipment, with brushing and rinsing zones to remove both the emulsion residues and most of the particles of abraded iron. The preheater in these plants is usually indirectly heated, as the emulsion residues are removed in the alkaline cleaning.

6.5.2.2 Other Coating Processes

Up to the late 1960s, only zinc and aluminum were used to coat steel. Corrosion resistance and working properties were later improved by using coatings based on a composite zinc–aluminum system. Table 6.16 lists the most important coatings, with compositions, coating thicknesses, and bath temperatures.

Zinc in the presence of moisture provides cathodic protection of the steel substrate. This is effective, even in the region of the uncoated edges, up to a steel thickness ca. 1 mm.

Aluminum has a dense outer oxide layer which reduces loss rates in various atmospheres, and gives better corrosion protection, especially at higher temperatures. The zinc–aluminum combination is selected to give the best coating properties for each application.

In the hot-dip zinc coating process, when the oxide-free steel surface is dipped, a multilayer Fe–Zn diffusion zone is formed which is then covered with a layer of zinc on removing the sheet from the bath. In batch galvanizing, uncontrolled growth of the Fe–Zn layer leads to a thick and very brittle coating with several component layers (Figure 6.126) that does not readily undergo forming processes. On the other hand, a continuous zinc coating process involves short contact times between the strip and the molten zinc. Aluminum is added to reduce the speed of the Fe–Zn reaction, leading to a relatively thin alloy layer. Compared with batch processes, this composite system permits an extreme degree of deformation without detachment of the coating.

When the zinc coating solidifies, the well-known zinc spangle appears, caused by lead in the zinc bath (usually 0.10–0.15%). Hot zinc-coated thin strip with good forming and paint application properties must have zinc crystals that are as small and uniform as possible over the length and width of the strip. Crystal size can be controlled by nucleation or by the composition of the bath.

Control of the number of nuclei by the introduction of foreign nuclei has been used for some years (Figure 6.127). Nuclei in the form of water, water vapor, water-soluble salts, or zinc dust are blown onto the liquid coating surface. The success of the operation depends on uniformity over the whole width of the strip.

The third method of reducing zinc spangle is to reduce the lead content (Figure 6.128). As the solubility of lead in the zinc crystals is low, separate crystals tend to appear. If the lead content is < 0.05%, the crystals are hardly visible macroscopically.

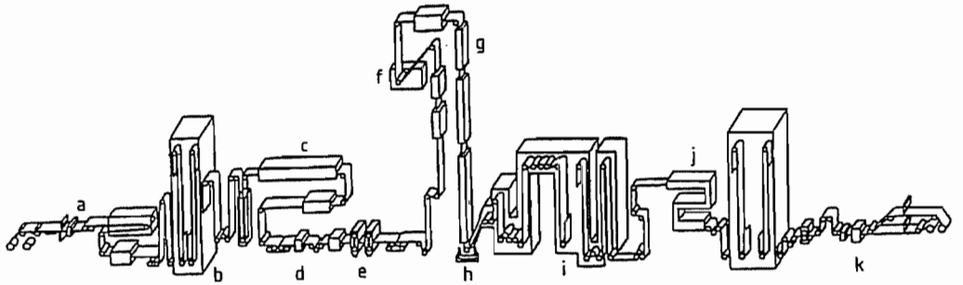

Figure 6.125: Hot-dip zinc coating plant at the Kawasaki Mizushima works: a) Exit section; b) Chromate passivation; c) Iron flash (electrolytic); d) Stretcher–roller leveling equipment; e) Measurement and control equipment; f) Skin-pass rolling; g) Zinc bath; h) Galvannealing furnace; i) Furnace; j) Pretreatment; k) Entry section.

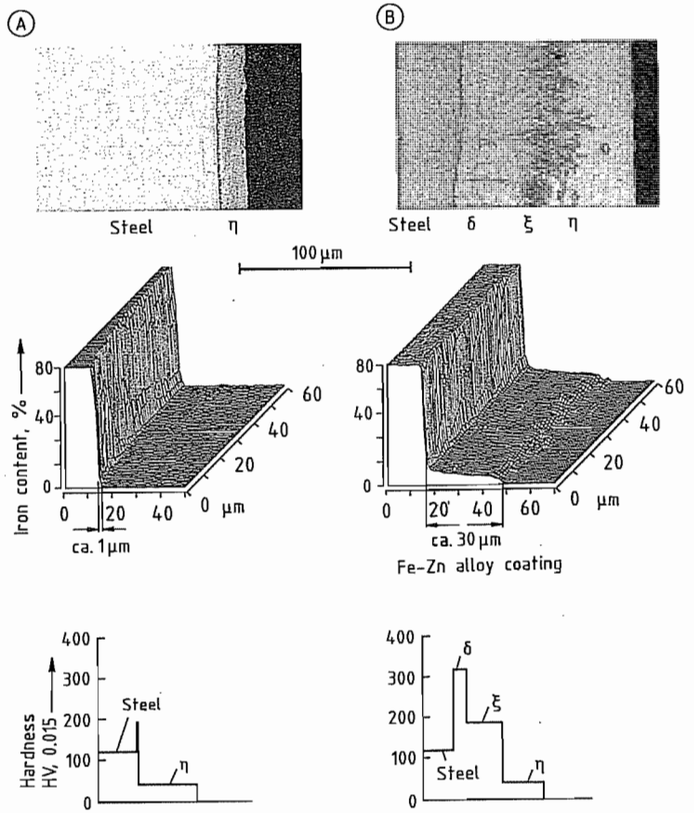

Figure 6.126: Coating structure, Fe content, and hardness of hot-dipped steel: A) Continuous galvanization; B) Batch galvanization.

Table 6.16: Composition and temperature of hot-dip coating baths and coating thicknesses produced.

Coating	Zn, %	Al, %	Si, %	Bath temperature, °C	Coating thickness, µm
Zinc coating					7–45
Monogal	99.5	0.12–0.30		450–480	7–15
Galvannealed					7–15
Galfan	95	5		420–450	7–25
Galvalume	43.4	55	1.6	600–620	13–28
Aluminum coating (type 1)		90	10	660–680	17–45

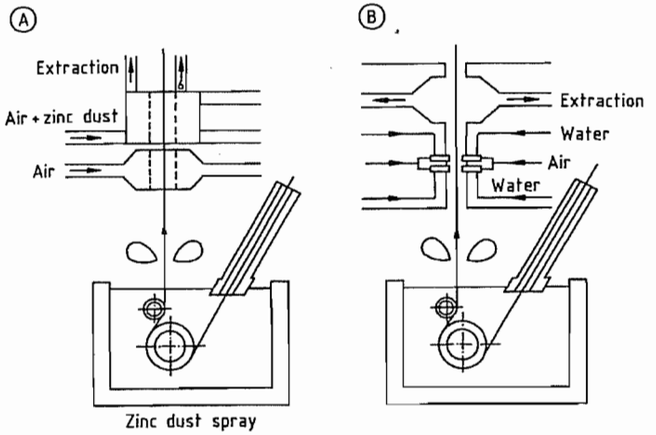

Figure 6.127: Control of crystal size in hot-dip zinc coatings by adding foreign nuclei: A) Zinc dust spray; B) Water–air spray.

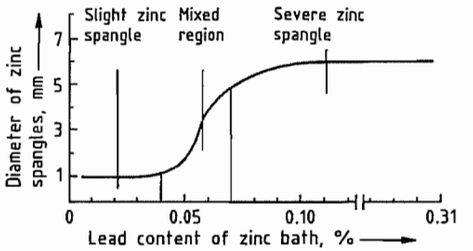

Figure 6.128: Zinc spangle diameter as a function of lead content of the coating bath.

Steel strip coated with zinc on one side only, the other side having similar properties to those of cold-rolled strip, is required in small amounts by the automotive industry.

In the process shown in Figure 6.129, liquid zinc is transferred to the strip under a nitrogen atmosphere by means of a carrier roll. In the Monogal process, the zinc coating is removed from one side of the strip by brushing in the opposite direction with a metal brush (Figure 6.130), and is removed by a fume extraction system. A residual layer remains on the brushed side, consisting of ca. 10 g/m^2 material in the form of an Fe–Zn layer. The result resembles material that has been coated by applying a hot melt to one side only.

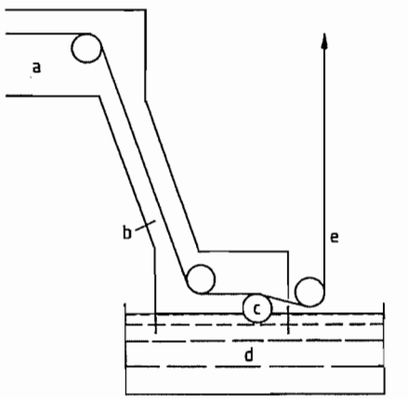

Figure 6.129: Coating steel strip on one side only (Nippon Steel): a) Furnace; b) N_2 atmosphere; c) Coating roller; d) Zinc bath; e) Stripping nozzle.

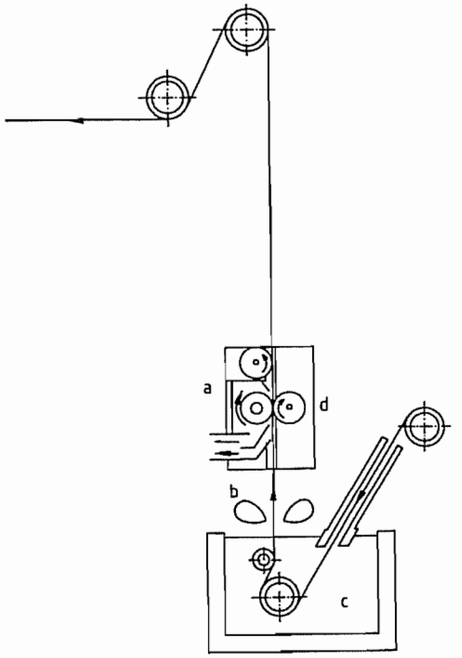

Figure 6.130: Hot-dip zinc coating by the Monogal process: a) Reverse-direction metal brush with zinc dust extraction; b) Nozzles; c) Zinc bath; d) Pass line roller.

In the Galvannealed process (Figure 6.131), on-line treatment of the strip is carried out immediately after zinc coating. After solidification, the coating (30–90 g/m^2, 5–12 µm) is heated briefly at 460–600 °C, inductively or with gas. This converts the zinc coating to a penetrating Fe–Zn alloy layer, which should have Fe content 9–11% for maximum forming properties. Compared with a pure zinc coating, Fe–Zn alloy coating gives improved welding and paint adhesion properties. If the Galvannealed strip is not painted, its corrosion resistance is less good.

A coating with the trade name Galfan was developed by the Centre de recherches métallurgiques in 1980. The zinc is alloyed with ca. 5% aluminum to give a eutectic composition with melting point ca. 380 °C. Wettability of the steel strip is improved by including small amounts of cerium and lanthanum in the melt bath. The Galfan coating has a lower loss rate and improved forming properties (for comparable coating thicknesses) when used without a paint coating in an industrial atmosphere.

An Al–Zn alloy (ca. 55% Al, ca. 43% Zn, and 1.6% Si) was introduced by Bethlehem Steel in 1963 under the trade name Galvalume. It has a low loss rate, especially in maritime climates.

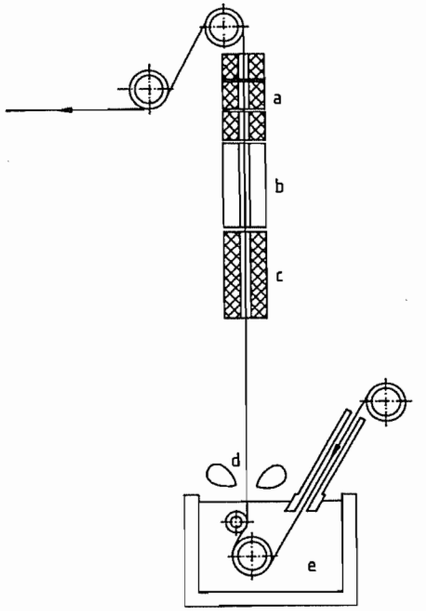

Figure 6.131: Hot-dip zinc coating by the Galvannealed process: a) Cooling zone; b) Holding zone; c) Heating zone; d) Nozzles; e) Zinc bath.

6.5.3 Electrolytic Coating (Electroplating)

6.5.3.1 Plant and Processes

In electrolytic coating (electroplating), the steel strip, which has been annealed and rolled (skin-pass rolling), is continuously passed through an aqueous electrolyte containing zinc ions (Figure 6.132) [188]. An electric current causes the zinc ions to be deposited on the steel strip, which forms the cathode. The process takes place at 55–75 °C, so that there is no alloying with the steel strip, and the mechanical properties of the substrate are not affected. The desired coating thickness is achieved by controlling current and strip speed.

In a electroplating plant (Figure 6.133), the equipment at the feed end is similar to that used for hot-dip coating, and only those features that differ from hot dipping are described here.

The surface of the cold-rolled strip must be clean so that an adherent, optically defect-free metallic coating is produced. Electrolytic coating plants have facilities for cleaning the strip, normally a combination of spray, brush, and electrolytic cleaning with alkaline cleaning solutions at 80 °C.

In cleaning facilities that use chemical solutions, multistage rinsing with brushing equipment is always provided, so that residues from the treatment solutions are removed as completely as possible.

After cleaning, many plants include stretch–leveling equipment to ensure that the strip is flat. This is necessary so that the distance between the anode and the strip can be kept small, while avoiding contact between the two (short circuits), thus minimizing electricity costs.

In the electrolytic pickling process, the strip is activated before the zinc coating stage. After cleaning and pickling, the strip enters the coating facility, in which the number of electrolytic cells is sufficient to enable the production rate to match that of the rest of the plant.

The strip can be treated to give additional temporary corrosion protection, most commonly by phosphating and/or chromate passivation.

A strip drier is always provided at the exit end of the treatment zones of an electrolytic coating plant. In the discontinuous part of the exit area, there are usually trimming shears to ensure the correct strip width.

6.5.3.2 Electroplating Cells

In steel strip electroplating plants, coating takes place in the electroplating cells. The strip is connected to the negative pole of a rectifier, and forms the cathode. The conduction rollers have a highly wear-resistant cladding of special steel, and have to be cooled, owing to the high current which they carry. Compression rollers ensure good electrical contact. The anodes are situated on both sides of the strip, as near the strip as possible.

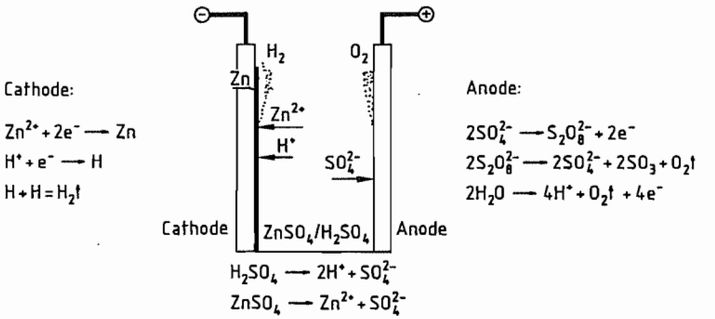

Figure 6.132: Electrolytic coating with zinc.

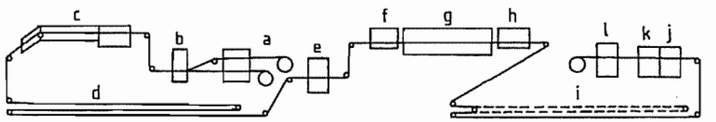

Figure 6.133: Electrolytic coating plant: a) Pay-off reels; b) Welding machine; c) Alkaline cleaning; d) Entry looper; e) Stretch-leveler; f) Pickling; g) Electroplating; h) Aftertreatment; i) Exit looper; j) Trimming shears; k) Oil treatment; l) Take-up reel.

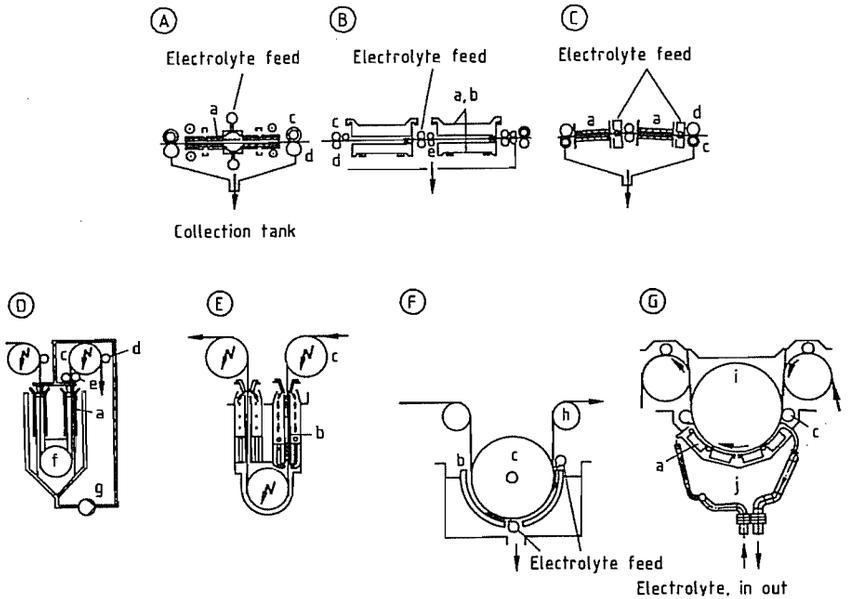

Figure 6.134: Electroplating cells: A) LCC-H (insoluble electrode, sulfate electrolyte; horizontal cell); B) NKK (soluble/insoluble anode; chloride/sulfate electrolyte; horizontal cell); C) Krupp/SEH (insoluble anode, sulfate electrolyte, horizontal cell); D) Gravitel (insoluble Ti anode, sulfate electrolyte, vertical cell); E) HS (soluble anode, sulfate electrolyte, vertical cell); F) Carosel (soluble anode, chloride electrolyte, radial cell); G) KC (insoluble anode, sulfate electrolyte, radial cell). a) Insoluble anode; b) Soluble anode; c) Current-carrying roller; d) Pressure roller; e) Squeeze rollers; f) Dipping rollers; g) Pump; h) Deflecting roller; i) Top roller; j) Edge mask.

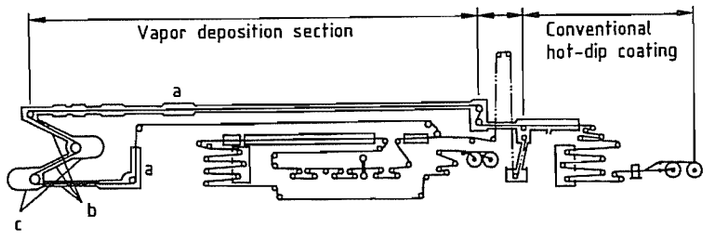

Figure 6.135: Zinc vapor deposition plant at the Nisshin Sakai works: a) Gas jet cooler; b) Vacuum system; c) Vaporization chambers.

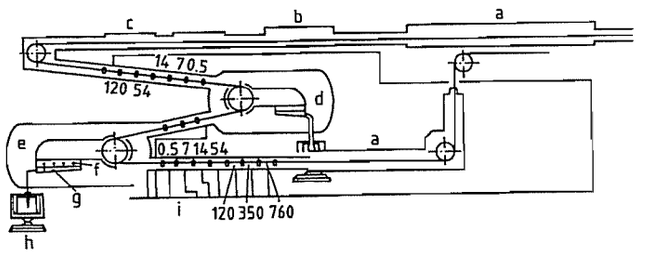

Figure 6.136: Vacuum system for the zinc vapor deposition plant: a) Gas jet cooler; b) N_2 gas; c) Edge heater; d, e) Vaporization chambers (2.66 Pa); f) Heating coils; g) Vaporizer; h) Zn melt; i) Vacuum pumps.

There are two types of anode:

- Solid anodes of the metal being coated dissolve at a rate proportional to the current and must be replaced at regular intervals.
- With insoluble anodes made of lead alloys, or titanium plates coated with noble metals. Zinc solutions must be added to the electrolyte.

To produce zinc or alloy coatings, sulfuric or hydrochloric acid electrolytes and soluble anodes are most often used. Addition of conducting salts, e.g., Na_2SO_4 or $(NH_4)_2SO_4$, ensures high conductivity, with current densities > 100 A/dm^2.

Three types of cell can be used for electroplating (Figure 6.134); horizontal and vertical cells are used for coating one or both sides, while radial cells coat one side only.

6.5.3.3 Coating Types

Zinc Electroplated Thin Steel Strip. Corrosion protection increases with increasing coating thickness, but workability and weldability deteriorate. A coating thickness of ca. 7.5 µm represents a good compromise.

Zinc–Nickel Coatings with 11 ± 1% Nickel. This material has good corrosion properties, but mechanical properties are sometimes inferior to those of pure zinc coatings. Sealed Zn–Ni coatings (Durasteel) give improved workability.

Zinc–Iron Coatings. These give cathodic protection up to an iron content of 85% in the coating. Anticorrosion and workability properties are good with iron content 15–25%, while good paint application properties are obtained with iron content > 50%. This has led to the development of a two-layer coating, the first with 10–25% Fe, (the rest being Zn), the outer coating containing > 60% Fe.

As well as these established types of coating, Zn–Co and Zn–Mn alloys are being investigated. Cobalt also shows interesting properties, even at low concentration, and can be plated at high current densities. Manganese is of great interest owing to the formation of a protective surface layer of Mn_2O_3.

Tin and Lead–Tin Coatings. Lead–tin coatings containing 10% Sn (Terne) are mainly used to plate steel sheet for gasoline tanks. It has indifferent electrochemical behavior towards chemicals, but displays good corrosion behavior as well as good paint application properties for selected paint systems.

Tinplate is steel strip, 0.1–0.5 mm thick, with a tin coating of ca. 2.4 g/m^2. A solution of tin fluoroborate can be used as electrolyte. The thin strip, which forms the cathode, is passed between two rows of thin anodes. After coating, the strip is heated above 232 °C (*mp* tin), and quenched in water to give the brilliant luster of electrolytically produced tinplate. Strip speeds > 650 m/min can be reached. Tinplate is used in packaging (painted, foil-covered, or printed).

Electrolytic chromium-coated steel (ECCS) is a special type of chromium-plated thin steel strip, and is produced in a similar process. In many applications, ECCS has replaced tinplate.

6.5.4 Vacuum Vapor Deposition

6.5.4.1 Plant and Processes

In the vacuum vapor deposition process, the coating metal is deposited onto the "cold" steel strip from the vapor phase [189]. Vacuum vapor deposition is not yet established on a large scale in the steel industry, and is operated at only one location so far, where a hot-dip plant has been converted to a vapor deposition plant (Figures 6.135, 6.136).

Vaporization is simply carried out in the zinc melting vessel. The plant has only a directly heated preheater, without alkaline cleaning. This degree of cleanliness of the strip is often adequate for the vapor process. Coating takes place in two chambers, both operating at 2.66 Pa; the vaporization capacity of the first is 350 kg/h, and that of the second chamber is 500 kg/h. Molten zinc at 460 °C is pumped into the vaporization chamber where it immediately vaporizes at the low pressure. The strip must be cooled to ca. 250 °C in the

vacuum chamber so that the zinc precipitates onto the cold strip. The operating pressure is reached by successive reduction of the atmospheric pressure by squeeze rollers.

While the hot-dip process is mainly suitable for producing zinc coatings with thickness > 60 g/m^2, zinc vaporization produces coatings with thickness ca. 30 g/m^2, often more cheaply than the electrolytic process.

6.5.4.2 Further Developments

[190, 191]

Vacuum vapor technology is mainly suitable for coating with pure metals, alloys, chemical compounds, and composite layers that cannot be produced by hot-dip or electrolytic coating. Potential coating materials under investigation are listed below:

Metals
- Zinc
- Aluminum
- Chromium
- Titanium
- Nickel
- Copper
- Silicon

Alloys
- Nickel chromium
- Zinc alloys, e.g., Zn–Mg, Zn–Cr, Zn–Al, Zn–Ni, Zn–Ti

Chemical compounds
- TiN, TiC
- Al_2O_3
- SiO_x

Composites
- Al–Ti, Al–Cr
- TiN–Cr
- Zn–Al
- Zn–Zn alloys

With a sufficient number of vaporizing chambers vapor coating could be carried out at rates of 350–400 m/min. A vaporizing plant could be incorporated into an existing continuous annealing furnace, adding to the production capacity for coated steel strip. As only one side is coated in each chamber, it would be possible to coat either one side or both.

6.5.5 Coil Coating

6.5.5.1 Plant and Processes

In the production of coil-coated thin sheet [192], the substrate material can be cold-rolled strip, zinc-coated thin sheet (hot-dip or electroplated), aluminum strip, or special steel strip. Liquid paint or foil is applied to these carrier materials by rolling.

A coil coating plant (Figure 6.137) consists of the feeding equipment, strip cleaning, chemical pretreatment, coating areas for primer and topcoat with the associated drying ovens, and the exit equipment. The strip is cleaned by methods similar to those used in zinc electroplating, but in this case the surface is then phosphated or chromated. For this, the solutions are sprayed at ca. 40 °C, under pressure. The strip is then cooled with deionized water and passivated. The chromate or phosphate coating provides corrosion protection for the whole system, and improves adhesion of the polymer coating. Before the strip is introduced into the coating station, this precoat is dried with hot air.

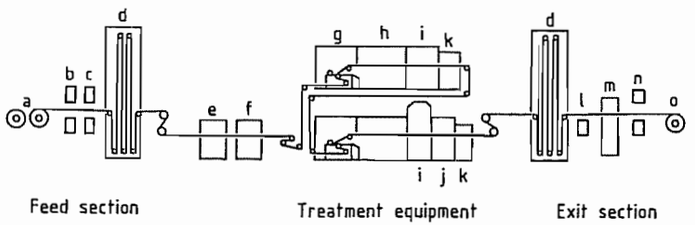

Figure 6.137: Coil coating plant: a) Pay-off reel; b) Cropping shears; c) Tack welding machine; d) Storage looper; e) Strip cleaning; f) Chemical pretreatment; g) Coating equipment; h) Furnace; i) Lamination equipment; j) Air cooler; k) Water quenching; l) Inspection table; m) Protective foil application; n) Edging shears; o) Coiling reel.

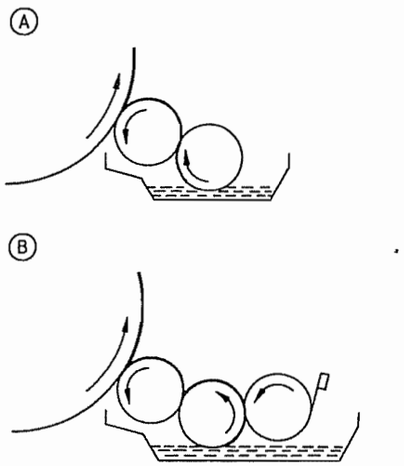

Figure 6.138: Typical coil coating systems: A) Two rollers, reverse rotation; B) Three rollers, complete reverse rotation.

Primer or undercoat is applied at the first coating station (Figure 6.138). The paint is usually applied by typical rolling machines, running in the opposite direction to the strip, one on each side of the strip, each paint roller having two or three feed rollers, depending on the coating material. As a rule, a chromium-plated dipping roller supplies the paint from a tank to a rubber-coated roller running in the opposite direction to the strip, and applies a paint film at a rate controlled by a special roller. The primer can be applied to the upper and lower side of the strip. The strip then usually passes into the first drying oven in which it hangs freely, and is heated to ca. 200–240 °C, depending on the coating system. The strip with its coat of primer is then cooled by air and water, and passes to the second coating station. The topcoat is applied on one or both sides, usually only the upper side. The coating is then backed in the second drying oven at ca. 240–260 °C. Before the strip passes to the air or water cooling area, it can be provided with a decorative and/or protective film. These laminates are applied under very precise conditions of temperature and pressure. If a decorative foil is used, an adhesive is applied instead of the top coat in the second coating station.

Table 6.17: Coating materials and thickness ranges of coating films.

Coating materials	Abbreviation	Usual range of film thickness, µm
Liquid coating materials		
Standard systems		
Polyesters	SP	5–25
Acrylics (resin)	AY	5–25
Silicone-modified polyesters	SP–SI	15–25
Epoxy resins	EP	3–15
Polyurethanes	PUR	10–25
Poly(vinylidene fluoride)	PVDF	20–25
Poly(vinyl chloride) organosol	PVC(O)	30–60
Poly(vinyl chloride) plastisol	PVC(P)	80–400
Special systems		
Weldable zinc dust primer	ZP	10–20
Heat-resistant nonstick system	HRNS	5–15
Film coatings		
Polyacrylate	PMMA(F)	50–75
Poly(vinyl chloride)	PVC(F)	100–300
Poly(vinyl fluoride)	PVF(F)	38
Polyethylene	PE(F)	100–300

Coating thicknesses, which depend on the coating system, are continuously monitored over short distances by integrating thickness measuring equipment, and are maintained within very close tolerances by varying the rotation speed or the application pressure of the coating rollers.

6.5.5.2 Coating Systems (Figure 6.139, Table 6.17)

The liquid coatings used are paints, based on polyester and acrylic resins, poly(vinyl chloride) plastisols, and poly(vinylidene fluoride). More recently, polyurethane paint systems have been used in special applications. Zincrometal and Inmozinc consist of thin steel sheet coated with zinc dust colors. Printed or single color poly(vinyl chloride) films are applied by rolling with an adhesive activated by hot air, and the same process is used for poly(vinyl fluoride) films. The coated or laminated material can be provided with additional protection against handling and assembly operations by means of adhesive polyethylene

protective films, applied hot or cold. Coating thicknesses are usually 15–300 µm.

6.5.6 Roll-Bonded Cladding

[193, 194]

6.5.6.1 Principles

In roll-bonding (cladding), two or more materials, which are usually flat, are pressure welded together. The process can be carried out with cold or preheated materials (cold roll-bonding or hot roll-bonding).

In continuous cold pressure welding of strip material, two metallic solids are bonded strongly together by high pressure, which causes plastic deformation. The adhesive bond can only be assured if the surfaces are clean and have a well defined surface structure (roughness).

The surfaces must be brought together under pressure until their distance apart is of the order of interatomic distances. As surfaces of technical quality are always covered with a very thin oxide layer, these layers must be broken by deformation. In roll-bonding, it is therefore necessary to stretch the surface, with exclusion of gas, so that new reactive surfaces are exposed by plastic flow. These are then brought into contact at interatomic distances, so that a strong bond can be formed by adhesion. The bond strength is increased by subsequent annealing homogenization.

6.5.6.2 The Process (Figure 6.140)

In the production of roll-bonded steels, surface pretreatment is very important. The necessary conditions are:

- Complete absence of grease
- A clean, freshly activated metal surface
- A roughened surface, produced by stretching

After pretreatment, the freshly brushed steel is fed, with the cladding material, into the roll nip, and deformed in one roll pass, the extent of deformation being 50–70%.

6.5.6.3 Variations

In roll-bonding, a composite material is produced which often combines the special properties of the individual components in an ideal manner. For cost effectiveness, a cheap substrate material is often plated with an expensive, corrosion-resistant, acid-resistant, or heat-resistant material (Table 6.18).

Table 6.18: Substrate cladding materials for cold roll-bonding.

Substrate materials	Cladding materials
Iron	Corrosion-resistant steels
Steel	High-temperature steels Ni and Ni alloys Cu and Cu alloys Aluminum Noble metals Special metals (Ti, Ta, Mo)

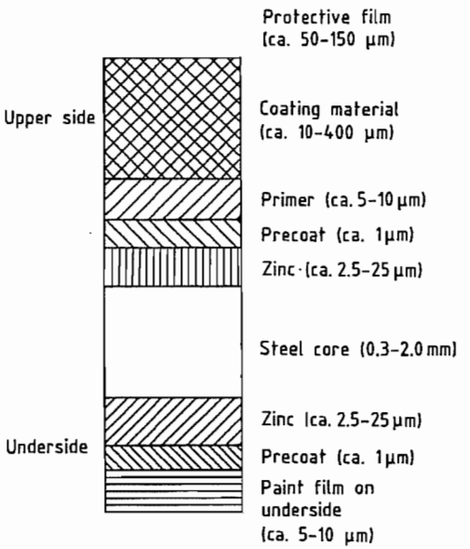

Figure 6.139: Cross section of coated steel strip.

6.5.7 Summary

Surface-coated thin steel strip was developed to improve, e.g., the corrosion properties of the steel, or to provide a decorative appearance. The user must consider a range of properties, such as workability, welding properties, adhesive properties, and paint application properties. Each type of surface treatment has strengths and weaknesses compared with competitive processes.

Other surface treatment methods are likely to become available, including electro- and plasma polymerization, electrolytic deposition of Al and Ti from organic solutions, plasma spraying, ion implantation, and cathodic sputtering.

6.6 Uses

6.6.1 Introduction

(Section 6.6.1 is reprinted from Ullmann's Encyclopedia of Industrial Chemistry, 5th Edition)

"At room temperature, pure iron has a body-centered cubic structure. The solubility of carbon is < 0.001% in this phase, which is known as α-iron. On heating, α-iron is transformed at 911 °C into the face-centered cubic γ-phase. This γ-iron can dissolve ca. 2% carbon as a solid solution. On cooling this, transformation of γ-iron to α-iron occurs and carbon is precipitated as carbide Fe_3C. In the heat treatment of transformable steels, they are heated until the γ-phase is formed, so when this is cooled more or less quickly, metastable states may be produced, and the precipitation of Fe_3C, which in equilibrium is associated with the formation of α-phase, is more or less suppressed. The range of applications of steel depends on the fact that heat treatment can induce all the transitions between the metastable states, and those states effectively correspond to equilibrium conditions, so that a large number of microstructures and combinations of properties can be produced [195, 196]. Another method of modifying steel consists of adding alloying elements to stabilize the α-phase up to the melting point, or conversely to cause the γ-phase to be stable down to room temperature. These possibilities are mainly used to improve corrosion resistance or to achieve particular physical properties."

6.6.2 Chemical Properties

6.6.2.1 Introduction

Iron is the most widely used metallic material and, alloyed with different elements, it is the basis of a wide variety of steels, with a range of mechanical properties and chemical stability. Iron itself is rather reactive, readily forming oxides, hydroxides, sulfides, etc. It undergoes an electrochemical reaction with humid air (rusting) which can rapidly consume unprotected unalloyed steel. The rust layer is not protective, unlike the thin, dense oxide layer on aluminum or zinc, but similar behavior can be attained by alloying Fe with Cr (> 12% Cr gives stainless steels).

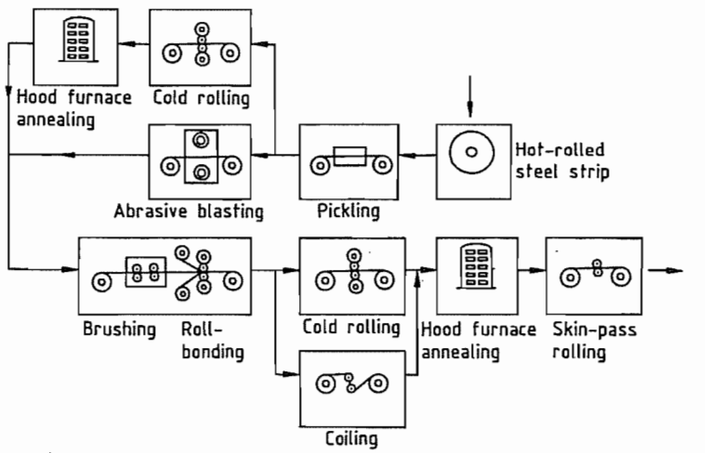

Figure 6.140: Production of roll-bonded steel strip.

Iron is also very susceptible to oxidation or sulfidation at high temperature; FeO and FeS show a wide homogeneity range, correlated to high concentrations of lattice defects (cation vacancies), high diffusivities in the lattice, and high growth rates. Alloying can lead to high oxidation resistance; Cr steels or Ni–Cr steels with ca. 20% Cr can be used up to 1000 °C, and Fe–Cr–Al alloys at even higher temperatures, since they form slow-growing oxide layers, which also give limited protection in environments which are sulfidizing, carburizing, or chloriding (heat exchangers in combustion or gasification atmospheres).

The chemical behavior of iron and steels is of greatest interest in connection with corrosion problems; in the following, reactions and corrosion processes are described only briefly, emphasizing the special points of chemical behavior of iron and steels.

6.6.2.2 Uniform Corrosion

Corrosion of iron in aqueous electrolytes results from the anodic dissolution process:

$$Fe \rightarrow Fe^{2+} + 2e^- \quad (33)$$

and the simultaneous, independent cathodic reduction of an oxidizing agent, in most cases either hydrogen ions:

$$2H^+ + 2e^- \rightarrow 2H_{ad} \rightarrow H_2 \quad (34)$$

or oxygen molecules dissolved in the electrolyte:

$$[O_2] + 2H_2O + 4e^- \rightarrow 4OH^- \quad (35)$$

The potential dependence of reactions (33) and (34) is described by the Volmer–Butler equation, an exponential relation; oxygen reduction is mostly controlled by diffusion of molecular oxygen to the metal surface, independent of potential. The overlap of anodic and cathodic reactions is shown in Figure 6.141. The corrosion potential U_k is established at a negative value, where the current density of anodic dissolution i_a and oxygen reduction i_k are equal. The anodic dissolution is further dependent on the concentration of defects in the metal surface, and especially for iron, is enhanced with increasing concentration of OH^- [198], and also SH^- or NH_4^+ [199].

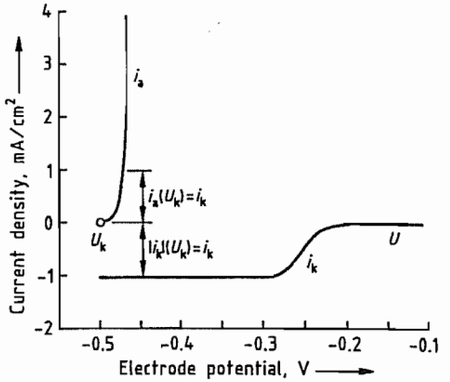

Figure 6.141: Electrochemistry of iron corrosion.

The reduction of H^+ occurs in several steps; electron transfer occurs by the Volmer reaction:

$$H^+ + e^- \rightarrow H_{ad} \quad (36)$$

The adsorbed H_{ad} atoms can react to H_2, according to the Tafel reaction:

$$2H_{ad} \rightarrow H_{2(g)} \quad (37)$$

or the Heyrowski reaction:

$$H_{ad} + H^+ + e^- \rightarrow H_{2(g)} \quad (38)$$

Adsorbed H atoms also can enter the metal, which leads to hydrogen-induced cracking (HIC) or hydrogen-induced stress corrosion cracking (HISCC).

In neutral water, the corrosion rate is determined by H^+ diffusion to the metal surface, and the anodic dissolution rate is restricted to 0.2 μA/cm², corresponding to 2×10^{-4} cm/a. Since the exchange current densities i_0 of the Volmer and Tafel reactions are very low, and since that of the Heyrowski reaction is negligibly small [200], iron does not corrode in neutral water free of oxygen. In contrast, the corrosion of iron in neutral water saturated with oxygen (in equilibrium with air) is rapid—the calculation assuming rate-controlling O_2 diffusion in a slowly flowing electrolyte yields 0.15 mA/cm², corresponding to a corrosion loss of 0.15 cm/a. This high value is not reached under natural conditions, since

rust is formed, and the oxygen must diffuse through the pores of this corrosion product.

6.6.2.3 Atmospheric Corrosion

In corrosion by oxygen-containing electrolytes, Fe^{2+} is oxidized to Fe^{3+}, and oxides and oxyhydrates are precipitated on the metal surface:

$$4Fe^{2+} + 3O_2 + 2H_2O \rightarrow 4FeOOH \quad (39)$$

$$6Fe^{2+} + O_2 + 12OH^- \rightarrow 2Fe_3O_4 + 6H_2O \quad (40)$$

These reactions occur on the surface of the solid corrosion products and not in the electrolyte. Atmospheric corrosion (rusting) in the presence of a liquid electrolyte film [201] on the metal leads to Fe_3O_4 at the iron surface, and FeOOH and Fe_2O_3 at the phase boundary with the atmosphere. With restricted oxygen access, when all pores of the rust are filled with water, Fe^{2+} formed at the inner phase boundary [202] can react with FeOOH:

$$Fe^{2+} + 2FeOOH + 2OH^- \rightarrow Fe_3O_4 + 2H_2O \quad (41)$$

On drying the rust layer, allowing better access of oxygen, Fe_3O_4 is oxidized again to FeOOH. Atmospheric corrosion can be retarded by certain alloying elements: Cu, P, Cr, and Ni, which are added to rust-resistant steels, e.g., Corten. Sulfur dioxide strongly accelerates rusting of steels by initiating the reaction sequence [203]:

$$4Fe + 4SO_2 + 2O_2 + 4H_2O \rightarrow 4FeSO_4 + 4H_2 \quad (42)$$

$$4FeSO_4 + 6H_2O + O_2 \rightarrow 4FeOOH + 4H_2SO_4 \quad (43)$$

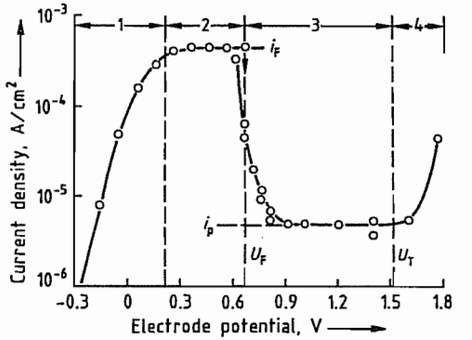

Figure 6.142: Electrochemistry of passivation of iron in HCl 1 mol/L at 25 °C. U_T = transpassivation potential.

In this reaction sequence, one SO_2 molecule can transfer 15–150 Fe atoms into the rust [204] by its catalytic action, until the reaction is stopped by formation of insoluble basic iron sulfates.

6.6.2.4 Passivation

The passivation behavior of iron is shown in Figure 6.142 [205]. In region 1, the current–potential curve describes active anodic dissolution; according to the Butler–Volmer equation, the increase in current is exponential. In region 2, the increase is limited since the solubility limit of $FeSO_4$ is approached at the metal surface—corrosion is controlled by outward diffusion of the Fe^{2+} through the diffusion boundary layer, independent of potential. At the passivation (Flade) potential UF the current density abruptly decreases, owing to formation of a passive layer, i.e., a very thin oxide layer, most probably γ-Fe_2O_3 [206], a few nanometers thick, depending on potential and temperature. In the passive region 3, a steady state of continuous film growth and dissolution is established, at current density i_p ca. 10^{-5} A/cm², corresponding to a corrosion rate 0.1 mm/a. In the transpassive region 4, enhanced iron dissolution and oxygen formation occur simultaneously. For the passivation potential of iron in the acidic region (in V):

$$U_F = 0.5 - 0.005pH \quad (44)$$

Iron is passivated at pH > 10 by oxygen in the electrolyte, this is important for the use of reinforcing steel in concrete, because the electrolyte in the pores of the concrete is saturated with $Ca(OH)_2$ at pH 12.5. Iron can also be passivated in strong oxidizing acids such as HNO_3.

The current-voltage curve for nickel [207] is similar to that for iron; for chromium [208] the passivation potential is shifted to more negative potentials, and current density in the passive state is < 10^{-7} A/cm² (Figure 6.143). In the passive region, Cr^{3+} is formed and very slowly dissolved, in the transpassive region, formation of chromate and dichromate with hexavalent Cr begins. This behavior is re-

flected in the passivation of Fe–Cr and Fe–Ni–Cr steels [209]; with increasing Cr content the passivation potential is shifted to lower values and the current density in the passive region is decreased, so stainless steels are passive over a wide range of conditions. The breakthrough potential at which Cr^{6+} formation starts, is virtually independent of Cr content.

6.6.2.5 Pitting Corrosion

If a passive layer is destroyed locally, the layer may heal under passivating conditions or, in the presence of halide ions, pitting may occur, i.e., local attack with formation of hemispherical pits. During pitting, active and passive regions are stable in the immediate neighborhood. The active areas are stabilized by the potential drop, caused by a high dissolution current through the electrolyte in the pit (the bottom of the pit is at potentials below passivation potential and the surrounding passive film is at a higher potential) [210]. Pitting occurs if the value of the pitting potential U_p is exceeded, and if the corrosive ions have a critical concentration c_L. For Fe–Cr and Fe–Ni–Cr steels, the pitting potential increases with Cr and Mo content (Mo is more effective than Cr). Since then, N has been found to be even more effective [211]. Pitting can start in Cr-depleted zones, e.g., after carbide precipitation at grain boundaries [212].

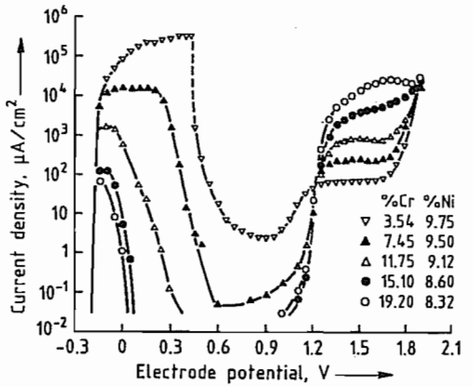

Figure 6.143: Electrochemistry of iron passivation at various concentrations of Cr and Ni.

6.6.2.6 Crevice Corrosion

If there are crevices between a metal and a second phase, or in the metal itself, the onset of corrosion is often observed in the crevice, owing to retardation of the electrolyte exchange into and out of the crevice. When the transport of oxidizing agent into the crevice is retarded, leading to depletion of, e.g., dissolved oxygen, the potential may fall below the passivation potential and iron and low-alloy steels may start to corrode. Also, the transport of corrosion products out of the crevice is inhibited, and their hydrolysis may lower the pH, e.g., by the reaction:

$$Cr^{3+} + 3H_2O = Cr(OH)_3 + 3H^+$$

The increasing acidity reduces the activation and pitting potentials, so active corrosion or pitting may start [213, 214].

6.6.2.7 Intergranular Corrosion of Stainless Steels

Ferritic chromium steels and austenitic Cr–Ni steels are susceptible to intergranular corrosion after sensitization, i.e., after precipitation of carbides at 450–750 °C. Precipitation at grain boundaries [215, 216] leads to chromium depletion nearby. If the potential is in the range between the passivation potentials of the steel and iron, rapid dissolution of the metal phase occurs along the grain boundaries. Potentials in this range are established in the Strauss test [217], where the sample is in contact with Cu and immersed in $CuSO_4$–H_2SO_4 solution, so that sensitized materials undergo intergranular disintegration. In the temperature–time diagram, the conditions for sensitization are limited by curves for the onset of carbide precipitation, which tends to shorter times at higher C concentration and longer times at lower temperature, and by curves for the end of carbide precipitation, which also needs shorter times at higher temperature. After the end of precipitation, the chromium concentration equalizes and the material becomes corrosion resistant again.

This intergranular corrosion of stainless steels can be suppressed by very low carbon

concentrations < 0.01% (Figure 6.144), or by addition of stabilizing elements, such as Ti and Nb, which tie up carbon in very stable carbides [218, 219]. Precipitation of TiC and NbC can be induced by heat treatment at 900–950 °C (stabilization), where the chromium carbides dissolve and the solubility of TiC and NbC is still very low; such treatment is important after welding of steels.

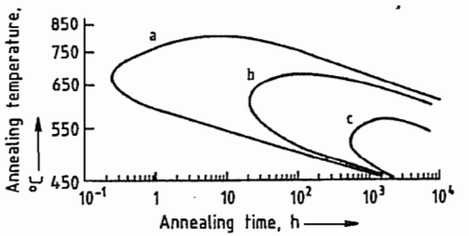

Figure 6.144: Annealing behavior of steel at various carbon concentrations: a) 0.04% C; b) 0.02% C; c) 0.01% C.

6.6.2.8 Stress Corrosion Cracking

The preconditions for stress corrosion cracking (SCC) are: (1) the stress causes a shear or strain of the material; and (2) the electrolyte induces formation of a passive or protective layer [220, 221]. The strain leads to failure of the passive layer at a slip step; there the free material is rapidly attacked under anodic dissolution. Repeated failure at this spot initiates crack growth. The electrolyte forms a new protective film at the walls of the crack and only the crack tip stays active, leading to deep cracks. Strain rate and passivation rate must obey certain relations to obtain SCC; if, for example, the passivation rate is too high, this leads to immediate passivation of the whole crack and termination of crack growth, whereas too slow passivation leads to strong truncation of the crack, or widening to a deep groove. SCC is observed in the following cases:

- Austenitic steels in chloride solutions—transgranular crack growth [222–226]
- Ferritic and ferritic–pearlitic structural steels in hot concentrated alkali carbonate and nitrate solutions—intergranular crack growth [227–231]

The latter type of SCC is enhanced by the presence of impurity elements, such as P, at grain boundaries, similar to the intergranular corrosion of iron and ferritic steels in nitrates at elevated potentials [231]. Under stress conditions, the selective corrosion of the crack tip causes SCC at low P concentrations and without anodic polarization.

6.6.2.9 Hydrogen Absorption and Hydrogen Embrittlement

On the surface of iron or steel, immersed in aqueous solution, the interplay of reactions (33)–(38) establishes coverage with adsorbed hydrogen H_{ad}, which may correspond to a high hydrogen activity ($a_H = 1$ at $p(H_2) = 100$ kPa), depending on electrochemical potential E and pH:

$$\log a_H = E\frac{F}{2.3RT} + \text{pH} = \frac{E}{0.059} + \text{pH} \qquad (45)$$

especially if the Tafel reaction (37) is poisoned by inhibitors, such as arsenic acid in the electrolyte. In a neutral NaCl solution free of oxygen, the corrosion potential E of iron is –0.6 V, and hydrogen activity can reach 10^3. Correspondingly, hydrogen is absorbed into the iron matrix in much higher concentration than its solubility at $p(H_2) = 100$ kPa, which at 25 °C is ca. 3 atoms per 10^8 iron atoms [232, 233]. Not all hydrogen in steels is dissolved, i.e., distributed on interstitial sites; most is in special sites (traps) where its energy is decreased, owing to stress fields in the lattice around dislocations, inclusions, etc. [234]. High hydrogen concentration in steels causes hydrogen embrittlement, i.e., decrease of toughness and brittle fracture. This effect of hydrogen is explained by H enrichment at the crack tip, where it weakens the Fe–Fe bonds in the already strained regions at the tip, and decreases the surface energy of the newly formed surface in the crack [235]. By this mechanism the presence of hydrogen can cause hydrogen-induced cracking (HIC), and aggravate stress corrosion cracking (HISCC). High-strength steels are especially susceptible.

6.6.2.10 Oxidation of Iron

Iron forms three oxides, hematite Fe_2O_3, magnetite Fe_3O_4, and wustite FeO which is stable only above 570 °C [236–238]. FeO has a wide range of homogeneity, due to cation vacancies V_{Fe}^{2-}, for which the concentration is dependent on oxygen pressure. Oxidation of iron at temperatures > 570 °C yields fast-growing oxide layers composed of an outer layer of Fe_2O_3, then Fe_3O_4, and a thick inner layer of FeO [239, 240]. The oxides grow mainly by outward diffusion of iron via cation vacancies, which move inward. Since the cation vacancy concentration is highest in FeO, the diffusivity of Fe^{2+} is high, and the growth rate is most rapid.

Owing to the high oxide growth rate, unalloyed steels cannot be applied at temperatures > 570 °C, but perform reasonably well at lower temperatures, since the scale of hematite and magnetite grows slowly enough. In CO_2–CO and H_2O–H_2 mixtures at high temperatures, oxygen partial pressures are effective at which only FeO or a Fe_3O_4/FeO layer is formed. Under such conditions, the growth rate of FeO up to a thickness of about 100 µm is controlled by the phase boundary reaction on the outer surface [241–243], where the oxygen is transferred from the gases:

$$CO_2 = CO + O_{ad} \quad (46)$$

$$H_2O = H_2 + O_{ad} \quad (47)$$

In this stage of oxidation, a linear rate law applies for the increase of scale thickness:

$$\frac{dx}{dt} = k_l \quad (48)$$

where the linear rate constant k_l is a function of the partial pressures, the oxygen activity at the surface, and the distance from equilibrium [243–245]. There is a gradual transition from phase boundary reaction control to diffusion-controlled growth, where the rate is inversely proportional to the thickness x:

$$\frac{dx}{dt} = \frac{k_p}{x} \quad (49)$$

This results in the parabolic law:

$$x^2 = 2k_p t \quad (50)$$

which leads to growth rate decreasing with time. Such parabolic behavior is characteristic of most metals and alloys used at high temperatures, the lower the value of k_p the slower the growth of the scale. Values of k_p can be deduced according to the theory of C. WAGNER [246] from data on the diffusivities of cations and anions or electric conductivity and transference numbers of the ions.

6.6.2.11 Oxidation of Carbon Steels and Low-Alloy Steels

On heat treatment and hot rolling, steels are oxidized and decarburized [247–249]. Oxidation is described by a linear law in CO_2 and a parabolic law in O_2; both reactions behave additively. At first only iron is oxidized and carbon is enriched in the metal below the scale. With continued scale growth, vacancies condense at the interface to form voids in which CO_2 and CO are formed in equilibrium with FeO. This gas diffuses outward through cracks and pores of the scale, which leads to carbon loss. Carbon diffusion through the solid oxide is impossible. After some time, a steady state is established in which the carbon supply to the interface is controlled by diffusion in the metal. Thus, after a brief oxidation, carbon enrichment is observed, but after long-term oxidation, the steel is always decarburized.

Some other more noble alloying (or impurity) elements in steels, e.g., Ni, Co, Cu, Sn, Pb, As, and Sb also enrich beneath the scale during oxidation. Enrichment of Cu, Sn, As, or Sb decreases the melting point, which can lead to difficulties in hot rolling. Specifically Cu, sometimes in combination with Sn, causes "hot shortness" by formation of a melt which penetrates into grain boundaries. If other elements are enriched beneath the scale, the iron must diffuse through this zone to the oxide-metal interface before it is oxidized. Especially for Fe–Ni and high-Ni steels [250–252], this causes inward growth of protrusions from the oxide into the metal which leads to a rugged, strongly interlocked interface; the oxide scale is strongly adherent to the metal and difficult to remove, e.g., after hot rolling. With increasing Ni content, enhanced temperature and oxygen partial pressure, the formation of FeO on Fe–Ni alloys is suppressed in favor of the more slowly growing spinel $(Fe,Ni)_3O_4$.

6.6.2.12 High-Temperature Steels

Steels to resist heat and oxidation must be alloyed with sufficient concentrations of Cr and/ or Al. The slowly growing oxides Cr_2O_3 or Al_2O_3, which have a small degree of disorder, can form a protective scale. Iron–chromium alloys are the base materials for many ferritic steels. The oxidation behavior as a function of Cr content is shown in Figure 6.145 [253]. At Cr concentrations < 2%, the oxidation rate is increased since dissolution of Cr_2O_3 in FeO may even increase the amount of cation vacancies (Wagner–Hauffe doping effect); trivalent Cr replaces divalent Fe, this is equalized by negatively charged vacancies. With increasing Cr content wustite formation is suppressed, the spinel $(Fe,Cr)_3O_4$ is formed, for which the growth rate decreases with Cr content. At Cr content 15–30%, the mixed oxide $(Fe,Cr)_2O_3$ is formed on the metal surface, its growth rate shows a minimum at 20–25% Cr in the alloy [254]. Many ferritic steels have Cr content 17–25%; they are oxidation resistant, but there may be chromium depletion beneath the scale, and if the scale is damaged outgrowth of wustite may occur with formation of "rosettes".

This effect is suppressed in the Cr–Ni steels where, instead of wustite, a Fe,Ni spinel is formed. Such austenitic steels, with 20–27% Cr and 12–32% Ni, are widely used for high-temperature processes, since, in contrast to ferritic Fe–Cr steels, they have higher mechanical strength and do not show embrittlement by σ-phase formation. Additional alloying with 12% Si improves resistance to oxidation and especially carburization, since an inner film of SiO_2 below the Cr_2O_3 retards oxidation and carburization.

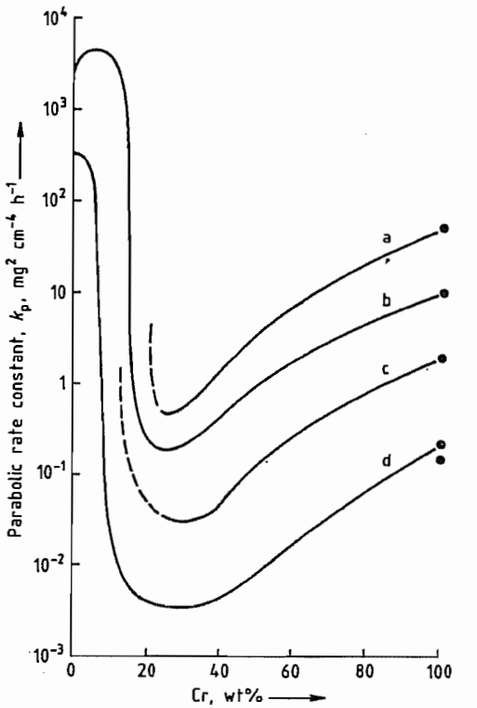

Figure 6.145: Oxidation kinetics as a function of Cr content: a) 1200 °C; b) 1100 °C; c) 1000 °C; d) 900 °C.

Iron–aluminum alloys need 6–8% Al to form a protective Al_2O_3 layer [255, 256], but only at temperatures > 900 °C is the most protective α-Al_2O_3 generated. Formation of Al_2O_3 and suppression of internal oxidation is favored by chromium; Fe–Cr–Al alloys with ca. 20% Cr and 4–5% Al are used for heating elements and other highly oxidation-resistant components. The lifetime of the heating elements is greatly increased by small additions of rare earths, e.g., Ce, Y, La, which strongly improve the adherence of the Al_2O_3 scale. The use of such additives also helps to improve other high-temperature alloys, in terms of nucleation, stability, and adherence of protective scales.

Silica layers may also serve as protective scales, but Fe–Si alloys are not used as high-temperature materials. Formation of Fe_2SiO_4 and an inner layer of SiO_2 plays a role in the

annealing of silicon sheet for electrical applications.

6.6.2.13 Effects of Chlorine in Oxidation

The presence of chlorine may cause acceleration of oxidation, so-called "active oxidation" [257–260]. Especially in waste PVC and NaCl-containing coal incineration, HCl and chlorides from combustion react with the oxide scale on steels to form chlorine

$$2HCl + {}^1/_2O_2 = H_2O + Cl_2 \quad (51)$$

$$2NaCl + Fe_2O_3 + {}^1/_2O_2 = Na_2Fe_2O_4 + Cl_2 \quad (52)$$

The chlorine penetrates the scale and reacts at the oxide–metal interface to form $FeCl_2$ which evaporates and oxidizes according to

$$2FeCl_{2(g)} + {}^3/_2O_2 \rightarrow Fe_2O_3 + 4Cl_2 \quad (53)$$

The chlorine partially diffuses inward and reacts again, thus establishing a circuit, in which Cl_2 catalyzes the "active corrosion" (active, since no dense oxide layer passivates the steel). This process causes problems in waste incineration and other processes in oxidizing, chloridizing atmospheres. Not only are low-alloy steels strongly attacked, but also chromia-forming high-alloy steels, due to the reaction

$$4NaCl + Cr_2O_3 + {}^5/_2O_2 \rightarrow 2Na_2CrO_4 + 2Cl_2 \quad (54)$$

The chlorine produced penetrates the scale and causes formation of volatile chlorides of the alloy components.

6.6.2.14 Sulfidation of Iron and Steel

The main sulfidation products of iron in sulfidizing environments are pyrrhotite FeS and pyrite FeS_2. Pyrrhotite, like FeO, is highly nonstoichiometric, owing to cation vacancies, their concentration being dependent on sulfur partial pressure and temperature [261, 262]. Accordingly, the diffusivity of Fe in FeS is high and the FeS growth rate is very rapid, even at relatively low temperature. As in the case of FeO, the linear rate law (Equation 47) applies for growth in H_2S–H_2 atmospheres [263, 264]; k_l depends on $p(H_2S)$ and is inversely proportional to the sulfur activity on the sulfide surface. The rate-controlling step is transfer of S_{ad} from H_2S to the surface, which is retarded with increasing sulfur activity. Upon sulfidation, rate control gradually changes to solid-state diffusion and to the parabolic rate law [265]. Corrosion by H_2S is a problem in the petrochemical and chemical industries, and is not easily suppressed. Even steels with Cr content up to 17% do not behave much better than low-alloy steels [266].

During corrosion of iron in SO_2 or Ar–SO_2 mixtures at 600–1000 °C, the phases FeO and FeS grow simultaneously on the metal surface [267–269], if the transport in the gas phase or the phase boundary reaction is rate determining. Owing to the high diffusivities of cations in FeS, lamellæ of FeO and FeS grow side by side up to a layer thickness of ca. 150 µm, following a linear law. In the application of steels in flue gases, a scale of Fe_2O_3/Fe_3O_4 is stable on the steel surfaces and SO_2 should have no effect on oxidation. However, if SO_2 penetrates the scale, at the interface sulfides can be formed. The mass action law for the reaction $SO_2 = {}^1/_2S_2 + O_2$ predicts that very high sulfur pressures are possible at the oxide–metal interface, since $p(O_2)$ is very low there. This is especially dangerous in high-Ni alloys, since Ni–Ni_3S_2 forms a liquid eutectic at 645 °C, and the presence of such melts strongly aggravates corrosion.

Sulfidation of heat exchangers is a problem in coal gasifiers; chromia-forming steels have been tested at 700–800 °C [270–274] but fail after lifetimes of some hundreds or thousands of hours. Preoxidation has been used to improve protection, but the chromia layers generated can also fail after similar lifetimes, either by external sulfidation, i.e., growth of sulfides of Fe, Ni, and Mn on the chromia scale, or by internal sulfidation, formation of sulfides of Cr and Mn beneath the scale.

6.6.2.15 Carburization

Carburization in gas atmospheres is a technical process for case hardening of steels, a specified carbon content is established in the surface and the carburized components are quenched in oil for hardening [275, 276]. Carburization can also be an unwanted process in the high-temperature corrosion of materials, e.g., cracking tubes in petrochemistry, and heating tubes or grates in industrial furnaces. In this process, carbon diffuses into the alloy and carbides are precipitated, mainly chromium carbides M_7C_3 and $M_{23}C_6$, with loss of both ductility and oxidation resistance [277, 278].

In both cases, the carbon transfer is by reactions in which CO, CH_4 or hydrocarbons decompose on the metal surface [279, 280], the transfer is very fast by the reaction:

$$CO + H_2 = C + H_2O \quad (55)$$

less fast by:

$$2CO = C + CO_2 \quad (56)$$

and very slow by:

$$CH_4 = C + 2H_2 \quad (57)$$

Rate equations and rate constants for these reactions have been determined for iron and binary iron alloys. The reactions are strongly retarded by sulfur [281].

In gas carburization for case hardening, the process is jointly controlled by the phase boundary reaction and inward diffusion of carbon; this has been studied in detail, and can be controlled well, to obtain certain penetration profiles of carbon in different steels and corresponding hardness profiles [282].

The unwanted carburization of cracking tubes [277, 278, 283] is generally suppressed, or at least retarded, by the oxide layer on the high-Cr–Ni steels used, only small amounts of carbon are transferred through pores or cracks formed on creep of the tubes. However, failure occurs if the tubes are heated above 1050 °C; the coke in the tubes reacts with Cr_2O_3 to chromium carbides which are no longer protective, and relatively fast carburization takes place [278]. This may happen during decoking of the tubes in H_2O–H_2 mixtures, when the temperature is not sufficiently controlled. Under these conditions, materials with 1–2% Si are resistant because of the protective effect of an inner SiO_2 layer beneath the chromia layer. Small amounts of sulfur in the atmosphere can also retard carburization.

Metal dusting [284–288] is the disintegration of steels into a dust of metal particles and carbon, occurring in atmospheres of $a_C > 1$ (carbon activity $a_C = 1$ means equilibrium with graphite) and in recent years has become problematic. The reaction sequence: (1) supersaturation of the metal with dissolved C; (2) formation of metastable carbide at $a_C > 1$; (3) deposition of graphite on this carbide ($a_C \rightarrow 1$); (4) decomposition of the carbide to carbon and metal particles; and (5) deposition of further graphite from the atmosphere on the metal particles. This leads to metal wastage and the formation of the loose corrosion product "coke", which is easily removed by fast gas flow in the plants, leaving pits and holes. Protection is possible by the chromia layer on high-alloy steels—their resistance depends on their ability to form oxide layers and healing. Furthermore, sulfur can protect since adsorbed sulfur effectively poisons steps (1), (3), and (5) of the reaction sequence, however, addition of sulfur is not possible with synthesis gas ($CO + H_2$) for the production of methanol, hydrocarbons, etc.

6.6.2.16 Nitriding

Similar to carburization, there is a technical process of nitriding for surface hardening, and an unwanted corrosion process at high temperatures which leads to nitride formation in steels and losses in ductility and oxidation resistance.

The nitrogen transfer can be from N_2, NH_3–H_2 mixtures, or by plasma nitriding in a glow discharge. The latter process is performed since N_2 is rather inert; nitrogen transfer:

$$N_2 = 2N_{(dissolved)} \quad (58)$$

is slow, with high activation energy [289]. Much faster is:

$$NH_3 = N_{(dissolved)} + {}^3/_2H_2 \quad (59)$$

So NH_3–H_2 mixtures can be used for nitriding and nitrocarburizing (with CO) at relatively low temperature. Their nitrogen partial pres-

sures are [289] very high as calculated from the mass action law; the equilibrium values are of the order of 10^5 kPa N_2. This may lead to deterioration of the nitrided case, by void formation with condensation of dissolved N at lattice defects to molecular N_2, which can develop high pressure, corresponding to the N_2 partial pressure of the NH_3–H_2 mixture, and form small bubbles in the material.

Nitriding for surface hardening leads to a layer of ε-nitride on the steels.

Nitriding of high-alloy steels happens only at high temperature > 1000 °C, e.g., on burner tubes [290, 291] and after failure of the oxide scale by cracking or spalling; mainly chromium nitrides Cr_2N are formed in the metal matrix.

6.6.2.17 Decarburization, Denitriding, and Hydrogen Attack

Thorough decarburization of steel is necessary for several applications, e.g., sheet for single-layer enameling, deep drawing steels, and silicon steels for use in generators and transformers. Decarburization is performed at 700–900 °C in wet hydrogen, and is controlled by carbon diffusion to the surface. The product $c_c D_c$ (solubility × diffusivity) is critical, and has a maximum at ca. 800 °C [292, 293]. The surface reactions are the formation of CO and CH_4, i.e., the back reactions of Equations (55) and (57), CH_4 formation being negligible.

Denitrogenation [294, 295] is also important for deep drawing and electric sheet, this is also conducted in wet H_2 at ca. 750°C, and occurs by NH_3 formation and N_2 desorption, the back reactions of Equations (54) and (55). The presence of some H_2O accelerates the rate of NH_3 formation [296, 297], but electric sheet with Si cannot be denitrogenated in wet hydrogen since SiO_2 formation retards the process.

In processes which involve high hydrogen partial pressures at elevated temperatures (hydrogenation reactions, ammonia synthesis), considerable amounts of atomic hydrogen enter the walls of steel vessels, and the cementite in unalloyed steels is attacked and methane is formed. Dissolution of the Fe_3C and precipitation of CH_4 and H_2 at interfaces and defects in the steel cause weakening and embrittlement of carbon steels. The more stable carbides in low-alloy Cr and Cr–Mo steels are resistant to hydrogen attack in the usual temperature range for the processes in question; the stability ranges of different steels as functions of temperature and hydrogen partial pressure are compiled in Nelson diagrams [298].

6.6.3 Physical Properties

Knowledge of the physical properties of steel is important for controlling its structure, and hence its properties. In this Section, the physical properties of pure iron are described first, followed by those of the solid solutions of the various iron modifications, and finally some other factors that influence structure [299].

6.6.3.1 Pure Iron

Crystal Structure. Iron occurs both in body-centered cubic (bcc) and face-centered cubic (fcc) structures. The bcc α-phase, which is stable at lower temperatures, is ferromagnetic up to the Curie temperature T_c = 1041 K, and is transformed into the paramagnetic state at higher temperatures (above the A_2 point). At 1184 K, the A_3 point, α-iron is transformed into the fcc form, γ-iron. The stability range extends up to 1665 K (A_4 point). Between 1665 and 1807 K, iron has a bcc structure, again δ-iron. Pure iron melts at 1807 K.

The crystal structures of α- and γ-iron are shown in Figure 6.146. The number of atoms in the unit cell is 2 in the bcc structure and 4 in the fcc structure. The number of nearest neighbors is 8 and 12 respectively, and of next nearest neighbors 6. The lattice constant of α-iron at room temperature a_{RT} = 0.28662 nm. Thermal expansion data are shown in Figures 6.147 and 6.148. In Figure 6.147, the difference in the *y*-axis scales for the bcc and fcc structures is due to the difference in the number of atoms per unit cell. The calculated density is ρ = 7.876 g/cm³.

The coefficient of linear thermal expansion α (Figure 6.149) increases with increasing temperature, and is higher for the fcc than for the bcc phase. The hatched area between the measured and calculated curves is due to a magnetostrictive effect in the region of the Curie temperature.

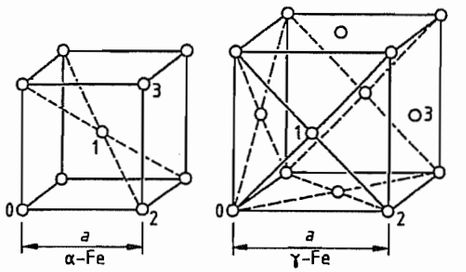

Figure 6.146: Crystal structure of α- and γ-iron.

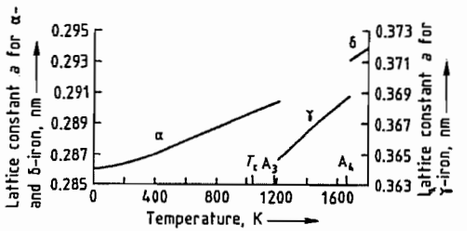

Figure 6.147: Effect of temperature on the lattice constant of iron.

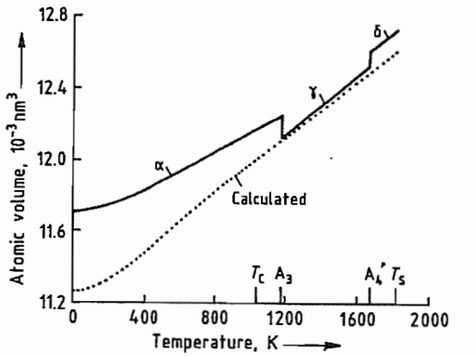

Figure 6.148: Effect of temperature on the atomic volume of iron.

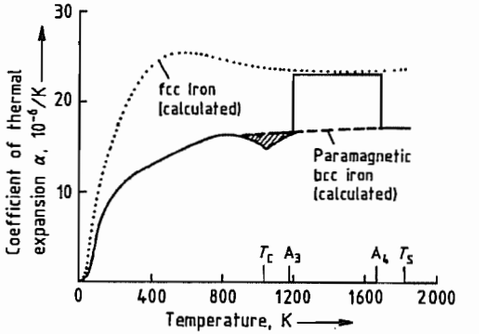

Figure 6.149: Effect of temperature on the thermal expansion coefficient of iron.

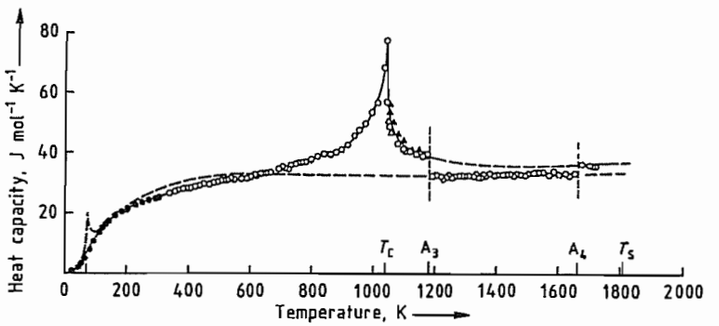

Figure 6.150: Effect of temperature on the molar heat capacity of iron. Solid line, most probable values; dashed line, values calculated for the instability ranges of α- and γ-iron. ● According to [301]; △ According to [302]; ▲ According to [303]; ○ According to [304].

Specific Heat Capacity. The specific heat capacity of a substance is the heat required to increase the temperature of unit mass by 1 K. The effect of temperature on its value is of fundamental importance, as the specific heat capacity is used in the calculation of enthalpy and entropy. The results of recent determinations are plotted in Figure 6.150, with the most

probable values indicated by a continuous curve [300]. The broken curves refer to the region of instability of the bcc and fcc phases.

The heat capacity is the sum of various components. There is a sharply defined maximum in bcc iron in the region of the Curie temperature. This represents the magnetic component, due to the energy required to destroy the magnetic ordering that occurs during the ferromagnetic–paramagnetic transition.

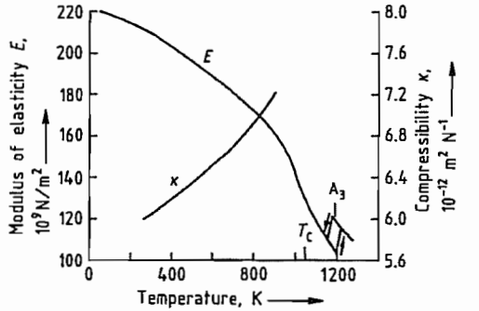

Figure 6.151: Moduli of elasticity and compressibility of iron [305].

Elastic Properties. The modulus of elasticity (Young's modulus E) represents the relationship between the elastic extension or strain and an applied tension or stress σ. This obeys Hooke's law $\sigma = E\varepsilon$. The effect of temperature on E is illustrated in Figure 6.151 (the values were determined for polycrystalline iron). In single crystals, the modulus of elasticity is strongly dependent on the crystallographic orientation of the sample (anisotropy). This anisotropy is also apparent in materials with a well-defined texture.

Volume changes under hydrostatic pressure are described by the compressibility κ, shown as a function of temperature in Figure 6.151.

Magnetic Properties. Individual iron atoms have a permanent magnetic moment. At temperatures above the Curie temperature, the directions of the magnetic moments are randomly distributed, and the material is paramagnetic. There is a linear relationship between field strength and polarization, represented by the volume susceptibility.

Below the Curie temperature, the magnetic moments of neighboring atoms in the bcc lattice are arranged parallel to each other, and the iron is ferromagnetic. Within the Weiss zones (magnetic domains) the moments are all in the same direction. This direction may differ from the direction within neighboring domains, so that they cancel each other.

The properties of a ferromagnetic material can be represented by the magnetization curve (Figure 6.152). With increasing field strength H, the polarization increases as the number of favorably oriented magnetic domains increases, and the magnetic moments align in the direction of the applied field. The maximum value is the saturation polarization. If the applied field is removed, the residual polarization at $H = 0$ is the remanence. The coercive field strength is the applied field which reduces the polarization to zero.

The saturation polarization varies with temperature, and disappears at the Curie temperature [306, 307]. The magnetization curve for single crystals varies with crystal orientation, being steepest in the [100] direction, and considerably less steep in the [111] direction. This effect is utilized in the manufacture of textured electroplated steel.

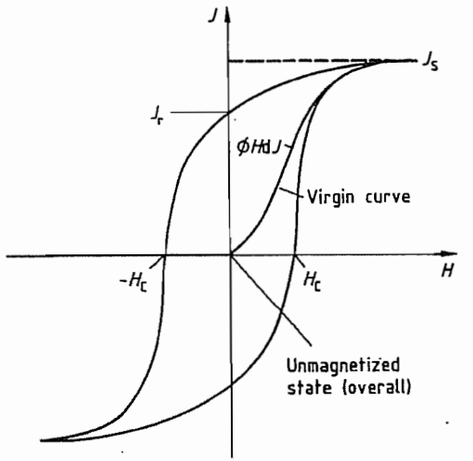

Figure 6.152: Magnetization curve of a ferromagnetic material. H = field strength; J = polarization ($B = J + \mu_0 H$ = induction); J_s = saturation polarization; J_r = remanence; H_c = coercive field strength; $\oint H dJ$, the area of the hysteresis loop, gives the amount of energy liberated as heat on reversal of the direction of magnetization. This is the hysteresis loss, quoted per unit mass.

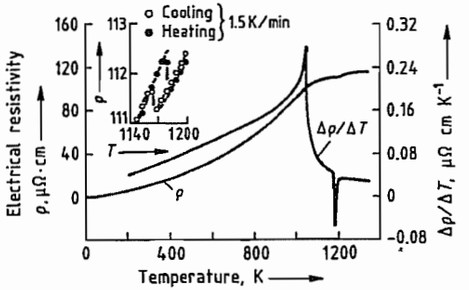

Figure 6.153: Effect of temperature on the electrical resistivity of pure iron.

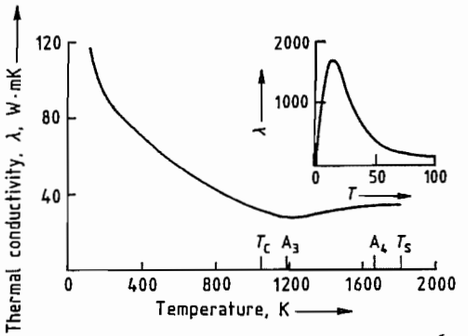

Figure 6.154: Effect of temperature on the thermal conductivity of pure iron.

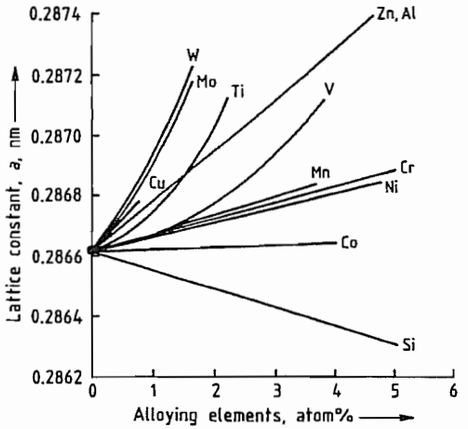

Figure 6.155: Effect of alloying elements on the lattice constant of α-iron.

Electrical Properties. The high electrical conductivity of iron is due to the great mobility of the free electrons, but their movement is scattered by deviations from the periodic lattice potential or by the electrons of unfilled shells. All crystal defects, e.g., holes, dislocations, stacking faults, impurity atoms, and precipitates, lead to energy losses by the motion of free electrons, and hence to an electrical resistance that falls to the so-called residual resistance at absolute zero. According to the Matthiessen rule, resistance is made up of a temperature-dependent part, due to lattice vibrations, and a residual resistance which is independent of temperature. The effects of the magnetic and the α–γ transitions can also be seen in Figure 6.153.

At high temperatures, thermal conductivity is a result of the same processes that lead to electrical conductivity. The thermal conductivity–temperature curve is similarly affected by the magnetic transformation as shown in Figure 6.154 [300, 308]. According to the Wiedemann–Franz–Lorenz law, the ratio of thermal conductivity to electrical conductivity is directly proportional to temperature. From this relationship, thermal conductivity can be calculated from electrical conductivity even at high temperatures when direct determination is difficult.

6.6.3.2 α-Iron Solid Solutions

Alloying elements can be divided into those that restrict the γ-region, and those that stabilize the γ-phase and extend its limits [309]. The effect of alloying additives on the transformation behavior of steel can be understood only from knowledge of the effect on various properties. Almost all alloying elements cause a volume increase. Figure 6.155 shows their effect on the lattice constant of α-iron. Only silicon leads to a contraction. Electrical resistance increases in proportion to the concentration of the alloying element (Figure 6.156). The most significant effect of alloying elements on magnetic properties is on the Curie temperature, as this affects the temperature of the transformation from γ- to α-iron. Figure 6.157 shows the effects of various elements. The large increase caused by cobalt is of special interest.

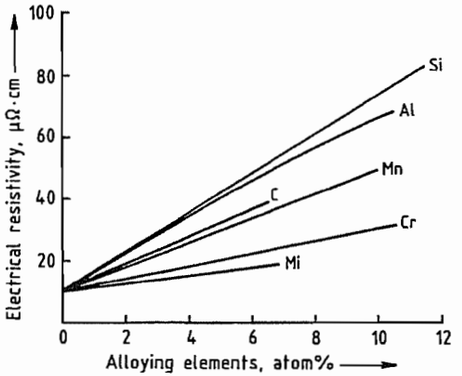

Figure 6.156: Increase in the decimal resistivity of α-iron by alloying elements.

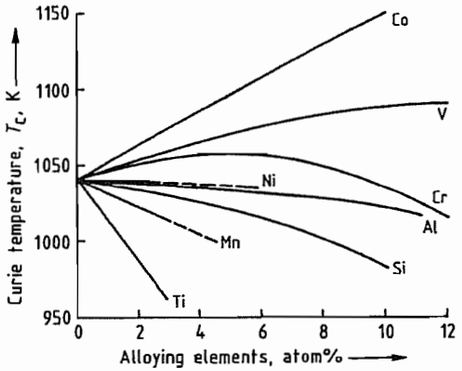

Figure 6.157: Effect of alloying elements on the Curie temperature of α-iron.

The temperature dependence of the physical properties of α-iron mixed crystals is closely linked to their magnetic behavior, and is not significantly different from that of pure iron. For example, the heat capacity of iron–chromium alloys is essentially constant if the temperature scale is based on the Curie temperature.

Ferritic iron–silicon alloys are of special importance, as these have low magnetization losses [306, 310]. Silicon addition increases electrical resistance, and hence reduces eddy current losses. The crystal anisotropy energies and the consequent hysteresis losses are reduced. Addition of > 4.5% Si prevents the α–γ transformation, and enables a coarse grain structure to be produced. Texturing allows the magnetic anisotropy to be exploited.

6.6.3.3 γ-Iron Solid Solutions

The magnetic properties of austenitic iron alloys are complex—as ferromagnetism, antiferromagnetism, and paramagnetism can occur. Iron-manganese [311], iron–nickel [312], and iron–nickel–manganese alloys [313] are of industrial importance.

The thermal expansion coefficients of paramagnetic γ-alloys (e.g., iron–manganese–nickel and iron–nickel–chromium alloys) are relatively high at room temperature. This is utilized in bimetallic systems [314]. Conversely, a large volume magnetostriction in magnetically ordered alloys compensates for thermally induced changes to the lattice dimensions; only a small amount of thermal expansion takes place over a certain temperature range [315]. Iron alloys containing 35% nickel are examples of Invar alloys of this type.

6.6.3.4 Other Effects of Structure

In general, physical properties are influenced by lattice defects. Density is somewhat decreased by lattice defects. All lattice defects increase the residual electrical resistance, whereas lattice vibrations are the main cause of resistance at high temperatures. Spontaneous magnetization and the Curie temperature depend mainly on lattice structure and composition. However, the magnetization curve is strongly influenced by the structure; lattice defects tend to prevent movement of the domain walls, and hence increase the remanence and coercive field strength.

In multiphase structures, the different properties of the phases must also be considered. These properties combine in proportion to the volume ratios in only the simplest cases, e.g., density, heat capacity, heat of transformation, and heat of formation, provided that the phases are in a coarse state of subdivision. A systematic treatment is not yet possible. Probably the most important industrial application is represented by the "hard" or permanent magnetic materials, with high coercive field strengths and a high BH value.

6.7 Environmental Protection

6.7.1 Environmental Aspects of Steel Production and Processing

6.7.1.1 Production of Steel and Steel Products

Large quantities of raw additive and auxiliary materials are used in the production of crude steel and rolled steel products, and large amounts of energy are used in these processes. Substances in the solid, liquid, and gaseous states are potential sources of environmental pollution.

For reasons of economy, the steel industry, especially in Europe, has always attempted to use as little primary energy as possible, to limit the consumption of auxiliary materials, e.g., water, by means of complex recycling systems, and to utilize or recycle by-products or residues, e.g., slags and mill scale. From the early 1900s, integrated steel plants, in close association with coking plants and rolling mills, have optimized the use of CO-containing blast furnace top gas according to the current state of technology. The use of blast furnace slag for cement and for road construction is very much older than the general interest in environmental pollution. In the last 20–30 years, the ever-increasing severity of environmental controls have led to technological developments within the steel industry which have been very successful [318]. However, some of the regulations imposed demand additional capital investment and operating costs whose justification may be dubious, especially when in some countries the regulations imposed are different and, thereby, distort competition. The following discussion is based mainly on available data for the steel industry, and particularly, individual steel plants in the western part of Germany.

Environmental aspects of the production of pig iron in a blast furnace have already been described. Further numerical data on developments during the last 30 years are given here. Figure 6.158 shows the considerable decrease in the consumption of carbon for reduction purposes in pig iron production [318]; Figure 6.159 shows the continuous decrease in the specific amount of blast furnace slag, and its 100% use in various applications [319]. The generation of electrical energy from expansion turbines running on blast furnace top gas (Figure 6.160) is a further contribution to environmental protection [320].

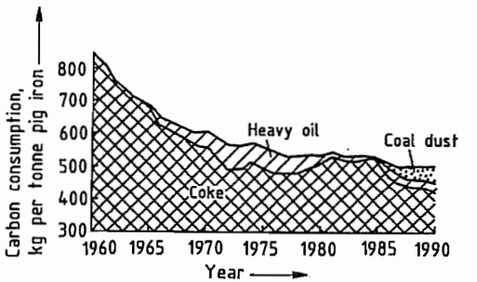

Figure 6.158: Carbon consumption in pig iron production.

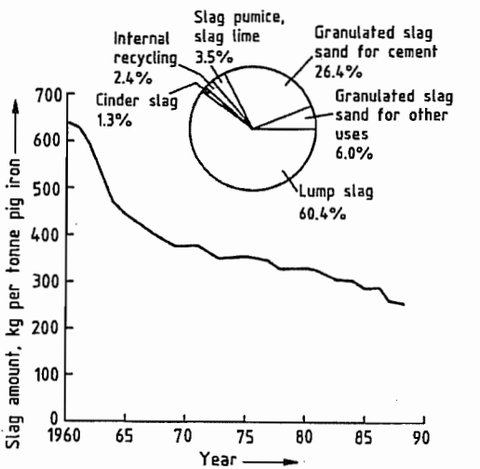

Figure 6.159: Development of the specific amount of blast furnace slag and its utilization.

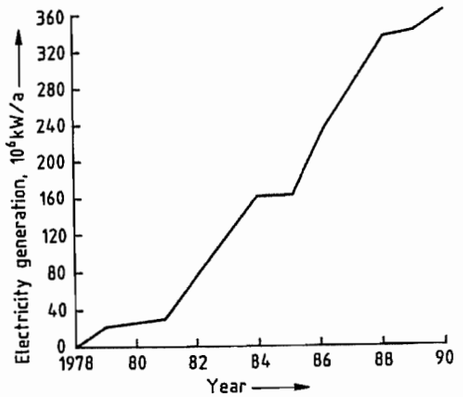

Figure 6.160: Electricity generation by expansion turbines from blast furnace top gas.

In a steel melting shop, the amount of dust formed and the possibility of its recovery depend very much on the different steel melting processes, which have undergone many changes (Section 6.3.3). The changeover to the oxygen blast process and improvements in dedusting equipment, including secondary dedusting, have led to an emission rate of only 0.7 kg per tonne crude steel in the melting shops of the German steel industry (Figure 6.161) [321]. Secondary dedusting, comparable to the "cast house dedusting" at the blast furnace, involves the additional dedusting equipment at different operation points located before and after the converters, e.g., pig iron transfer pit, mixers, deslagging stands; the dedusting equipment consists of stationary or movable hoods and skirts. Figure 6.162 illustrates the complexity of this additional dust collection in a steel melting shop with three converters [322].

A comprehensive study has shown that the total quantity of dust and sludge collected in the steel plants in North Rhine/Westphalia is 41 kg per tonne crude steel (Figure 6.163), of which more than 80% is reused [320].

The hot waste gas formed in an oxygen converter is used to produce steam in a waste heat boiler in the primary dedusting installation [321, 322]. After further purification and cooling (Figure 6.164), it is collected so that its high CO content (68–70%) can be used sometimes after mixing with other gases. Figure 6.165 shows the significant energy generation which has been achieved in Germany [319].

Slag, an inevitable by-product in steelworks has been further reduced in recent years, reaching 121 kg per tonne crude steel in 1991, of which 87.5% was utilized [320].

The mill scale occurring in hot rolling mills is a pure iron oxide, and can be reused in sintering plants. However, oil-containing mill scale sludge must be pretreated. Rotary kiln installations to be used for this purpose are in the experimental stage [322].

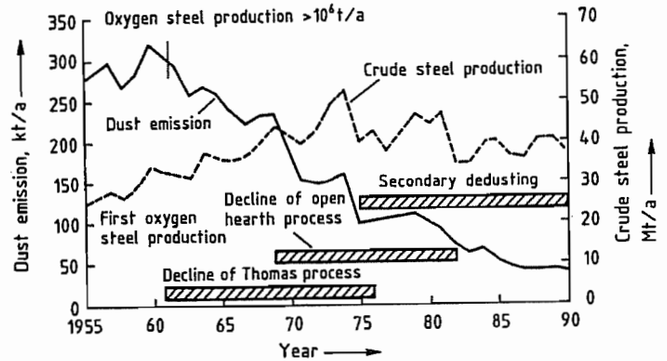

Figure 6.161: Development of crude steel production and dust emission by the German steel industry.

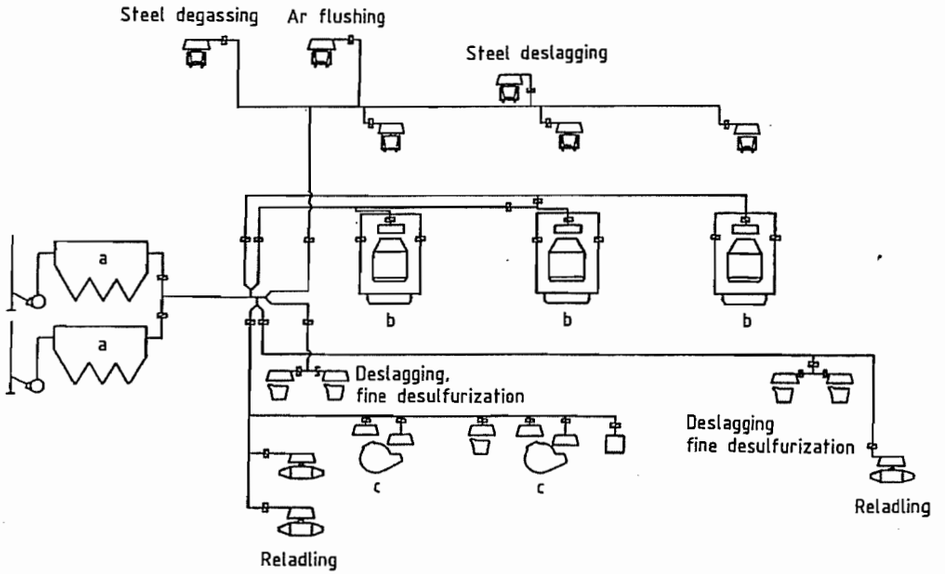

Figure 6.162: Dust collection in a three-converter steelshop: a) Electrostatic precipitator; b) Converters; c) Mixers.

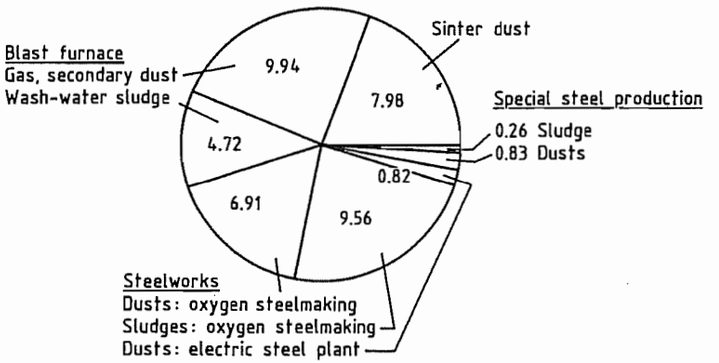

Figure 6.163: Origins of dusts and sludges in pig iron and steel production in North Rhine/Westphalia. Amounts in kg per tonne crude steel.

Control of water consumption in a steel plant is also very important from the environmental point of view. All parts of the production operation involve the consumption of water, sometimes in very large quantities, e.g., for cooling the installations and the products. Attention has always been paid to the development and use of methods for saving water, e.g., the treatment and reuse of water in complex recirculating systems. In 1989, in a steelplant situated near the Rhine, only 3% of the process water used was fresh water, i.e., 2.5 m^3 fresh water per tonne crude steel (Figure 6.166) [318]; the remaining 97% came from the recirculation system. Some 83% of the water used in the steel industry is surface water.

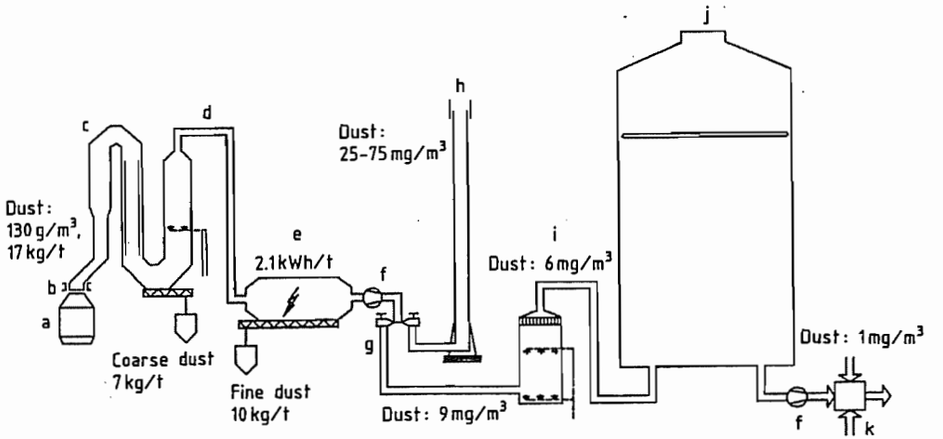

Figure 6.164: Converter gas cleaning and recovery system: a) Converter; b) Skirt; c) Steam boiler; d) Evaporation cooler; e) Dry electrostatic precipitator; f) Fan; g) Reversing valve; h) Flare stack; i) Gas cooler; j) Gasholder; k) Gas mixing station.

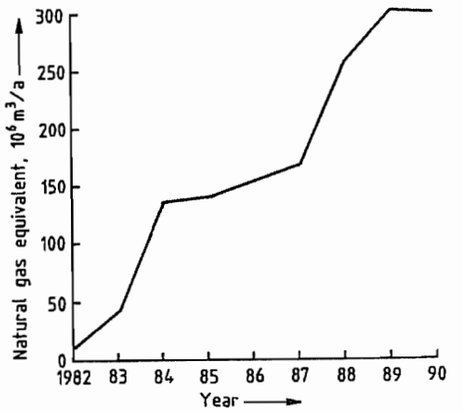

Figure 6.165: Energy production by the use of converter gas.

A high proportion of rolled steel production is cold-rolled or coated steel sheet, tinplate, black plate, and cold-rolled electric sheet. The hot-rolled strip for these finished products must be treated in continuous pickling lines to remove the adhering mill scale before the cold-rolling process. The used pickling solution is also treated in a recirculating system in which an iron salt, e.g., sulfate, crystallizes, and fresh acid is added, so that only a small fraction of the solution leaves the plant after neutralization. The iron hydroxide sludge, which contains gypsum, cannot be used any further. This also applies to the wash-water in the pickling line, but the amount of wash-water used can be much reduced by appropriate techniques.

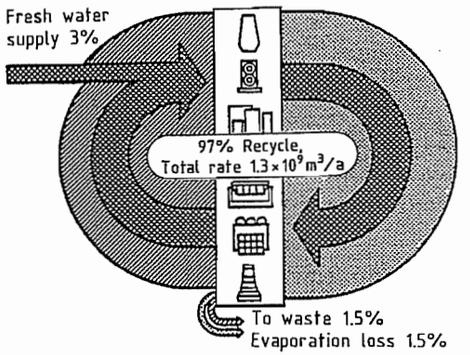

Figure 6.166: Internal water circulation.

6.7.1.2 Steel Processing and Steel in Use

Steel used in manufacturing as described in earlier sections, is environmentally a very friendly material.

The processing of steel can certainly involve sound emissions, e.g., during hammering, sheet metal working, and forging. Gases can result when flame cutting and welding steel. However, in both these cases, it is possible to protect personnel at the workplace without great cost and without causing too much inconvenience to the individual. In certain heat treatment processes, e.g., those using molten salt baths, the advice of the manufacturers of the salts or other substances used should be followed, and relevant legal requirements must be observed relating to their handling and disposal.

Environmental problems associated with the use of steel products are practically nonexistent, since steel is a highly recyclable material. Even tinplate is environmentally a friendly packaging material, as it can be separated from waste materials or residues, e.g., from garbage incineration plants, by virtue of the ferromagnetic properties of the steel, and can then be reused.

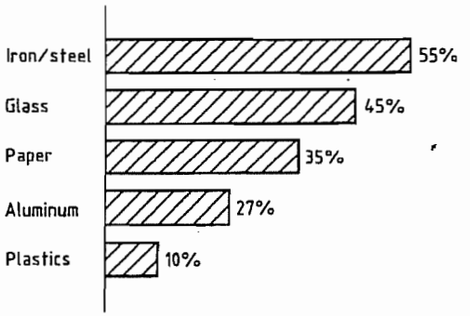

Figure 6.167: Extent of recycling of various materials.

Figure 6.167 illustrates the extent to which construction materials are recycled, and in the case of steel this can easily be increased further [323]. The reuse of steel scrap is of great importance for the overall economy. Approximately 60% less primary energy is required for melting scrap for steel production, than for the smelting of ores [323].

In the last 15 years, the use of sheet with a surface coating, mostly zinc, has increased considerably, both in automotive body manufacture and in other applications. Doubts about the use of zinc-coated steel scrap from these sources are unjustified. Most of the zinc vaporizes during crude steel production, and is recovered in the dust from the filters in the dedusting equipment. If manufacturers dispose of moderately zinc-rich scrap separately, this can be processed and used in suitable electric steel plants, and the zinc can be economically recycled. For this there must be at least 16% Zn in the filter dust [324].

6.7.2 Steel Recycling

6.7.2.1 The Tradition of Steel Recycling

More than 3000 years ago, iron had already been the material foundation for cultural development. It has given its name to an entire epoch. The industrialization is closely linked with the development of the iron and steel industry. Almost all other industries have been directly or indirectly dependent on advances in steel production.

On 28 October 1865, the first iron was smelted by the Siemens–Martin open hearth process using 70% scrap, so beginning the industrial utilization of scrap [325].

For over a hundred years, a technically and economically viable high-tonnage recycling system has existed for handling production waste and worn-out capital equipment and consumables made of steel and cast iron. For steel scrap, there is a completely closed system for recycling worn-out steel products, any number of times. The recycling process continually yields high quality steel grades without downgrading.

As industrialization progressed and steel production increased toward the 1890s, the demand for raw materials rose. By then, scrap was already an important substitute for the usual raw material in the iron- and steel-producing industry.

6.7.2.2 Types of Scrap

Listings. In order to provide precise descriptions of the physical and chemical properties required in reusable scrap, an agreed list of scrap grades has been prepared by the steel and steel recycling industry in Germany (Table 6.19).

Table 6.19: Extract from the German list of scrap grades (1 September 1993) (Source: Bundesverband der Deutschen Schrott-Recycling-Wirtschaft e.V., Düsseldorf).

Category	Specification	Description	Dimensions	Density	Steriles[a]
Old scrap	E3	Old thick steel scrap, predominantly more than 6 mm thick in sizes not exceeding 1.5 × 0.5 × 0.5 m, prepared in a manner to ensure direct charging. May include tubes and hollow sections. Excludes vehicle body scrap and wheels from light vehicles. Must be free of rebars and merchant bars, free of metallic copper, tin, lead (and alloys), mechanical pieces and steriles to meet the aimed analytical contents. Refer to points (B) and (C) of the general conditions.	Thickness ≥ 6 mm < 1.5 × 0.5 × 0.5 m	≥ 0.6	≤ 1%
	E1	Old thin steel scrap predominantly less than 6 mm thick in sizes not exceeding 1.5 × 0.5 × 0.5 m prepared in a manner to ensure direct charging. If greater density is required it is recommended that maximum 1 metre is specified. May include light vehicle wheels, but must exclude vehicle body scrap and domestic appliances. Must be free of rebars and merchant bars, free of metallic copper, tin, lead (and alloys), mechanical pieces and steriles to meet the aimed analytical contents. Refer to points (B) and (C) of the general conditions.	Thickness < 6 mm < 1.5 × 0.5 × 0.5 m	≥ 0.5	< 1.5%
New scrap (low residuals, uncoated)[b]	E2	Thick new production steel scrap predominantly more than 3 mm thick prepared in a manner to ensure direct charging. The steel scrap must be uncoated unless permitted by joint agreement and be free of rebars and merchant bars even from new production. Must be free of metallic copper, tin, lead (and alloys), mechanical pieces and steriles to meet the aimed analytical contents. Refer to points (B) and (C) of the general conditions.	Thickness ≥ 3 mm < 1.5 × 0.5 × 0.5 m	≥ 0.6	< 0.3%
	E8	Thin new production steel scrap predominantly less than 3 mm thick prepared in a manner to ensure direct charging. The steel scrap must be uncoated unless permitted by joint agreement and be free of unbound ribbons to avoid trouble when charging. Must be free of metallic copper, tin, lead (and alloys), mechanical pieces and steriles to meet the aimed analytical contents. Refer to points (B) and (C) of the general conditions.	Thickness < 3 mm 1.5 × 0.5 × 0.5 m (except bound ribbons)	≥ 0.4	< 0.3%
	E6	New production thin steel scrap (less than 3 mm thick) compressed or firmly baled in a manner to ensure direct charging. The steel scrap must be uncoated unless permitted by joint agreement. Must be free of metallic copper, tin, lead (and alloys), mechanical pieces and steriles to meet the aimed analytical contents. Refer to points (B) and (C) of the general conditions.		≥ 1	< 0.3%
Shredded	E40	Shredded steel scrap. Old steel scrap fragmentized into pieces not exceeding 200 mm in any direction for 95% of the load. No piece, in the remaining 5%, shall exceed 1000 mm. Should be prepared in a manner to ensure direct charging. The scrap shall be free of excessive moisture, loose cast iron and incinerator material (especially tin cans). Must be free of metallic copper, tin, lead (and alloys), and steriles to meet the aimed analytical contents. Refer to points (B) and (C) of the general conditions.		> 0.9	< 0.4%

Category	Specification	Description	Dimensions	Density	Steriles[a]
Steel turnings[c]	ESH	Homogeneous lots of carbon steel turnings of known origin, free from excessive bushy. Should be prepared in a manner to ensure direct charging. Turnings from Free Turning Steel must be clearly identified. The turnings must be free from all contaminants such as nonferrous metals, scale, grinding dust, and heavily oxidized turnings or other materials from chemical industries. Prior chemical analysis could be required.			[d]
	ESM	Mixed lots of carbon steel turnings, free from excessive bushy and free from turnings from Free Cutting Steel. Should be prepared in a manner to ensure direct charging. The turnings must be free from all contaminants such as nonferrous metals, scale, grinding dust, and heavily oxidized turnings or others materials from chemical industries.			[d]
High residual scrap	EHRB[e]	Old and new steel scrap consisting mainly of rebars and merchant bars prepared in a manner to ensure direct charging. May be cut, sheared, or baled and must be free of excessive concrete or other construction material. Must be free of metallic copper, tin, lead (and alloys), mechanical pieces and steriles to meet the aimed cnalytical contents. Refer to points (B) and (C) of the general conditions.	Max. 1.5 × 0.5 × 0.5 m	≥ 0.5	< 1.5%
	ENRM[f]	Old and new mechanical pieces and components not accepted in the other grades prepared in a manner to ensure direct charging. May include cast iron pieces (mainly the housings of the mechanical components). Must be free of metallic copper, tin, lead (and alloys), and pieces such as bearing shells, bronze rings, and others as well as steriles, to meet the aimed analytical contents. Refer to points (B) and (C) of the general conditions.	Max. 1.5 × 0.5 × 0.5 m	≥ 0.6	< 0.7%
Fragmentized scrap from incineration	E46	Fragmentized incinerator scrap. Loose steel scrap processed through an incinerating plant for household waste followed by magnetic separation, fragmentized into pieces not exceeding 200 mm in any direction and consisting partly of tin-coated steel cans. Should be prepared in a manner to ensure direct charging. The scrap shall be free of excessive moisture and rust. Must be free of excessive metallic copper, tin, lead (and alloys), and steriles to meet the aimed analytical contents. Refer to points (B) and (C) of the general conditions.		≥ 0.8	Fe content ≥ 92%

[a] Corresponds to the weight of steriles, not adhering to the scrap, remaining at the bottom of the vehicle after unloading by magnet.
[b] Coated Material must be notified.
[c] Free from all contaminants (nonferrous metals, scale, grinding dust, chemical materials, excess oil).
[d] To date, no clear method to determine these values.
[e] Rebar and Merchant Bar must be classified apart due essentially to the copper content which could place them out with old scrap and new scrap low residual grades.
[f] Mechanical and engine components must be classified apart principally due to their Ni, Cr, and Mo content which could place them out with the thick old scrap and heavy new scrap low residual grades.

These defined grades apply only to carbon steel scrap. The following general requirements are included in the European list of scrap grades of 1 July 1995. The scrap must be:

- Prepared in a manner to ensure direct charging
- Handleable magnetically
- Free from elements harmful to the smelting process

Plant Scrap. Plant scrap is produced in the manufacture of steel and of rolled finished products. It is directly reused in the steelworks.

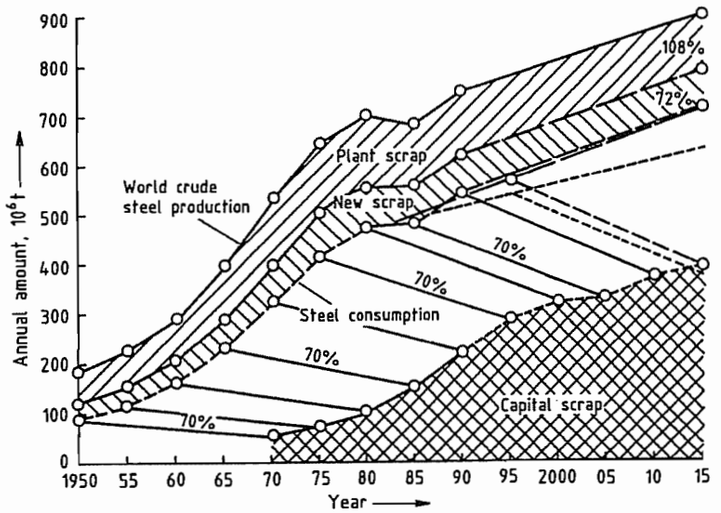

Figure 6.168: Development of arisings of plant scrap, new, and capital scrap, with estimated future figures.

New Scrap. New scrap arises in steel processing industries as production waste. It is usually returned to steelworks and foundries by the recycling industry.

Capital Scrap. Capital scrap is composed of steel, cast steel, and cast iron originating from used commodity and industrial goods. There are three types, classified according to origin:

- Demolition scrap
- Automobile scrap
- Collected scrap

The development of the amounts of plant scrap, new scrap, and capital scrap is illustrated in Figure 6.168, with estimated future figures, assuming that 70% of steel consumption is returned to the material cycle after a period of 20 years.

6.7.2.3 Scrap Processing

Separation

Steel is used in engineering, plant construction, vehicles, building industry, shipbuilding, household appliances, packaging, etc. When products that consist mainly of steel are no longer usable, they are usually processed by the steel recycling industry. The composition and dimensions of scrap are usually such that it cannot be used in steelworks and foundries in its original state. Appropriate processes must therefore be used for:

- Size reduction
- Separation from other materials
- Classification into grades

A unique characteristic of steel and iron scrap is that it can easily be recovered from accompanying materials by its magnetic properties, enabling the iron-containing constituents to be returned to steelworks and foundries in a high state of purity.

Shearing Machines

Large pieces of scrap can be size-reduced by shearing machines. Even before the World War I guillotine shears were used for this purpose.

Further developments led to the larger and faster alligator shears, and then to the hydraulic machines used today, where the scrap is charged by a crane into a feeding bed. The feeding bed is usually provided with a prepress which compresses the scrap so that even bulky material can be pushed under the blades of the shears. Size reduction of, e.g., freight cars industrial equipment, and large components, including material from shipbreaking and other heavy demolition work, is carried out with shears with a compression force of up to 2000 t and blades up to 2.50 m wide [326].

Presses

Scrap presses are used to densify clean steel scrap, e.g., production waste from rolling mills and steel processing industries, to facilitate transportation and charging, and to reduce it to the specified dimensions.

In the early 1920s, slow mechanical screw presses with large vertical boxes and small charging holes were developed. These were able to bale light collected scrap and new sheet scrap.

Mechanical baling presses were followed by high-pressure hydraulic presses with large charging boxes. This hydraulic equipment produces high-density bales of the size needed for steel production plants, e.g., converters and electric furnaces, and for the melting facilities of the foundry industry. The usual bale sizes are: 30 × 30 × 30 cm and 40 × 40 × 60 cm for the foundry industry, and 60 × 60 × 150 cm for the steel industry [327].

Shredders

Increasingly, scrap is no longer in pure form, but combined with other materials. Examples include old vehicles and household appliances, which contain considerable amounts of plastics, glass, rubber, nonferrous metals, and other materials. Shredders (Figure 6.169) have been used by the steel recycling industry since the mid 1960s to produce automobile and collected scrap that meets the requirements of the steelworks.

A shredder functions on the principle of the swing-hammer mill. The products fed to the shredder are broken down to pieces not larger than fist-sized, and are then fed to an air separator to remove the light waste fraction, which includes plastics, textiles, and cardboard. An electromagnetic drum or band separator separates the steel scrap from the nonferrous metals and coarse impurities (heavy waste fraction). The materials removed by the air separator, which cannot, at present, be recycled (shredder residues) must be disposed of. This is expensive, and is likely to become more so. Shredding provides a means of recovering the iron and steel from used products with purity ca. 98%, so that they can be returned to the raw material cycle.

6.7.2.4 Factors Influencing Recycling

Alloy Steels

In steel production, the properties of various grades of steel are achieved by adding alloying elements. Alloy steel can also be returned to the material cycle, if it is sorted according to chemical composition. The alloying elements are retained when the scrap is melted, and new alloy steels can be produced from this metal.

Surface Coatings

Steel is surface coated to give the properties required, i.e., surface quality, stress condition, and corrosion protection. Surface coatings can be either metallic (e.g., zinc) or nonmetallic. The latter include organic coatings (plastic or paints) and inorganic coatings (cement mortar or enamel) [328].

Smelting of zinc-coated steel scrap during steel production is the present state of the art. As zinc boils at 907 °C and steel melts at 1400–1500 °C, the zinc vaporizes from the melt and is collect ed as zinc oxide in dedusting plants. If the zinc content of the steelworks dust is ca. 16%, it is profitable to recover the zinc [329, 330].

Before scrap recovered from steel with a nonmetallic coating can be returned to steel production, it is usually processed by shredding, or cold shock treatment to remove adhering materials from the scrap, as these are harmful to the smelting process, or can lead to inadmissible emissions.

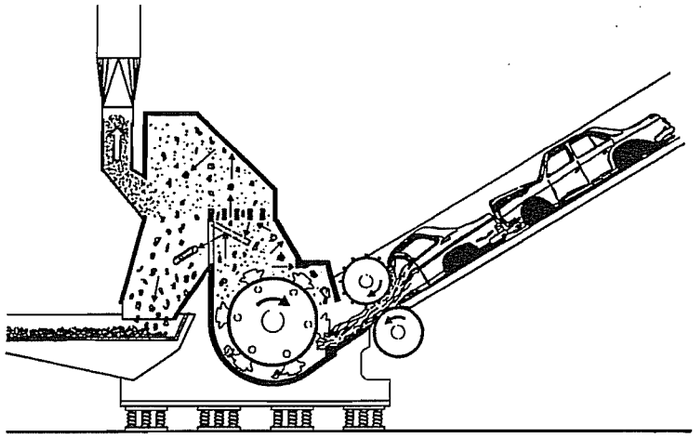

Figure 6.169: Operating principle of a shredder.

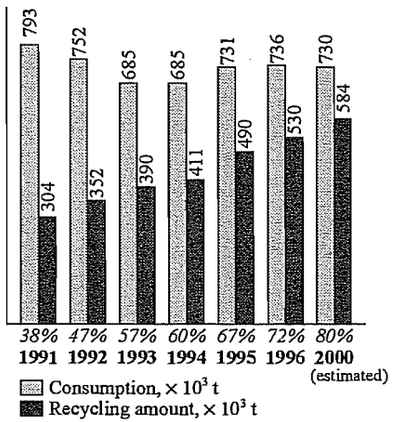

Figure 6.170: Consumption and partial recycling of tinplate packaging in Germany.

Pretreatment of Used Steel Products

Steel products and components at the end of their lives are often associated with impurities, or are attached to other materials. To prevent the unwanted materials from being returned to steel production along with the scrap, pretreatment and purification are necessary, e.g., removal of oil from chips arising from the processing of steel, which are classified as new scrap.

Pretreatment of used products that consist mainly of steel is often also necessary for disposing of or recycling the other materials in the products, e.g., the disposal of old cars. In the initial dismantling, the batteries of the old vehicles are removed to return the lead to a separate material cycle. This also prevents the lead from contaminating waste tips when the shredder residues are dumped. For the same reason, fuel, oil, gear, differential, and shock absorbers, and brake fluid and coolant are recovered before the old cars are shredded. In refrigerators, freezers, and air conditioning equipment, the cooling liquids are recovered to prevent their escape into the atmosphere.

Tinplate packaging, e.g., for foodstuffs, consists of very thin tinned steel sheet. The scrap from tinplate cans is processed by the steel recycling industry, and returned to steel production where it is used without problems. The consumption of tinplate packaging and the extent of its recovery for recycling in Germany is shown in Figure 6.170.

Steel sheet packaging for commercial use, e.g., barrels or canisters, can be contaminated with organic or inorganic residues from the filling (paints, varnishes, oils, or adhesives). They must be emptied as far as possible and then processed by, e.g., shredding, cold shock treatment, or centrifuging, enabling the scrap to remain in the material cycle, provided that the chemical and physical quality requirements of the steel industry are met.

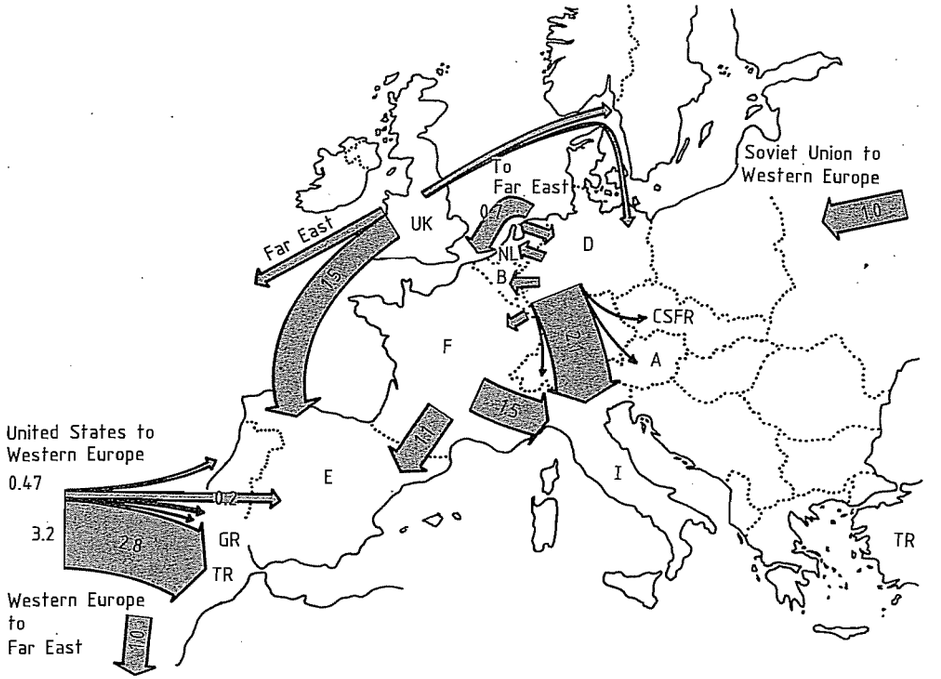

Figure 6.171: World trade in scrap 1990.

6.7.2.5 Economic and Logistic Aspects

Scrap Consumption

According to the International Iron and Steel Institute (IISI), total world consumption of scrap, including scrap used in foundries, was 360×10^6 t in 1994. Most of this (330×10^6 t) was used in steel production. In 1994, total world crude steel production was 728×10^6 t [331]. Hence, the average consumption of scrap per tonne crude steel produced was ca. 450 kg. Electric steel plants accounted for 223×10^6 t scrap. Thus, ca. 60% of scrap was consumed by electric steel plants.

World Market for Scrap

Scrap is an international commodity with a free price structure. Scrap arisings and consumption vary greatly from one country to another. The proportions of the various steel production processes in different countries have a considerable influence on scrap consumption, and hence on the flow of imports and exports. In electric steelworks, 100% scrap can be used for steel production. In 1995, the average usage of scrap in German electric steelworks was 1004 kg per tonne crude steel.

In oxygen steel production, pig iron produced in the blast furnace is oxidized together with scrap in a converter. The average usage of scrap in 1995 in Germany was 181 kg per tonne crude steel for this process [332]. In the production of high quality steel grades shredded scrap for cooling is preferred because of its high purity and the small lump size.

The most important flows of scrap in world trade in 1990 are illustrated in Figure 6.171.

Infrastructure and Logistics

The task of the steel recycling industry is to take responsibility for iron and steel scrap, i.e., to transport, store, process, and deliver to steelworks and foundries a high-quality raw material.

The recycling system offers one particular advantage: The collecting points are installed in all countries. They collect scrap according to its origin, lump size, and impurity levels. The structure of these organizations varies:

- Small-scale and collection service
- Medium-sized scrap wholesale traders
- Organizations supplying scrap to steelworks

Scrap is transported by rail, water, and road. To enable prompt delivery, the steel recycling industry has made considerable investments in handling and transportation facilities.

The demand for scrap is not constant, so the scrap recycling industry maintains stocks containing the equivalent of the purchasing requirements of steelworks for ca. 2 months. Thus, the industry has taken over an important function in balancing scrap arisings with consumption [333].

6.8 Economic Aspects

6.8.1 World Steel Production, Consumption, and Trade

From the World War II to the early 1970s, world crude steel production grew at an average annual rate of ca. 5.5%. Since then, the rate has been only 1% (Figure 6.172). The number of steel-producing countries increased from ca. 30 to ca. 90.

The largest steel-producing companies, with their 1992 production, are shown in Table 6.20.

Of the total world crude steel production, 721 × 10^6 t in 1992, 345 × 10^6 t (48%) was produced by 50 companies in the western world. There are also large steelworks in the countries of the former Soviet Union. Some of these are listed in Table 6.21.

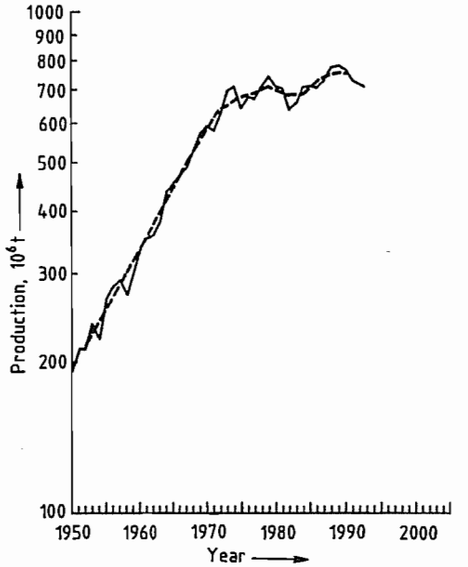

Figure 6.172: World steel production from 1950 (selected regions). Smooth curve is 5-year average. Data Supplied by the Statistisches Bundesamt (German Federal Bureau of Statistics) and the International Iron and Steel Institute (IISI).

Table 6.20: Leading steel producers 1992.

Company	Country	Production, 10^6 t
Nippon Steel	Japan	25.10
Usinor Sacilor	France	21.10
Posco	Korea	20.01
British Steel	United Kingdom	12.39
NKK	Japan	10.89
Ilva	Italy	10.60
Thyssen	Germany	10.13
Kawasaki	Japan	10.00
Sumitomo Metals	Japan	9.97
Sail	India	9.70
Bethlehem	United States	9.60
US Steel	United States	9.50

Table 6.21: Steel production in the former Soviet Union.

Steelworks	Country	Capacity, 10^6 t/a
Magnitogorsk	Russia	16.2
Chereporets	Russia	14.0
Krivoy Rog	Ukraine	13.9
Lipetsk	Russia	9.9
Nizhiny Tagil	Russia	8.3

After the political changes of the early 1990s, steel production in these countries decreased considerably, i.e., from 216 × 10^6 t in 1987 to 124 × 10^6 t in 1993.

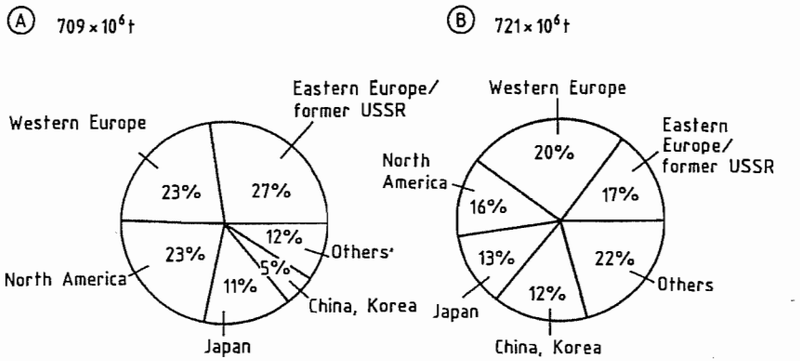

Figure 6.173: Steel consumption: A) 1974; B) 1992. Source: IISI, Brussels.

Table 6.22: Steel production and consumption 1970–1992.

Region	Production	Consumption	Balance, 10^6 t	Production	Consumption	Balance, 10^6 t	Production	Consumption	Balance, 10^6 t
	1970			1980			1992		
European Community	146.2	132.9	13.3	141.9	119.9	22.0	129.1	115.2	13.9
Western Europe	161.9	153.9	8.0	161.2	142.1	19.1	153.8	135.3	18.5
United States	119.3	127.3	–8.0	101.5	118.6	–17.1	84.3	100.3	–16.0
Japan	93.3	69.9	23.4	111.4	79.0	32.4	98.1	84.0	14.1
Industrialized countries	397.4	374.0	23.4	406.9	366.2	40.7	366.9	340.4	26.5
Developing countries	22.1	42.2	–20.1	56.7	94.4	–37.7	117.2	147.7	–30.5
Brazil	5.4	6.0	–0.6	15.3	14.3	1.0	23.9	9.1	14.8
Eastern Europe	40.1	41.5	–1.4	61.2	59.6	1.6	32.4	21.1	11.3
Former Soviet Union	115.9	110.2	5.7	147.9	150.4	–2.5	117.0	115.0	2.0
China	18.0	22.5	–4.5	37.1	43.2	–6.1	80.0	83.1	–3.1
World	595.7	592.8	2.9	715.9	718.8	–2.9	720.5	714.8	5.7

Table 6.23: World trade in steel 1991.

Country	Exports, 10^6 t	Country	Imports, 10^6 t
Germany	19.6	Germany	16.8
Japan	17.9	United States	14.3
Belgium/Luxembourg	14.3	France	10.3
France	12.0	Italy	10.3
Brazil	10.9	Japan	9.0
Italy	9.0	Taiwan	8.7
United Kingdom	8.0	South Korea	8.5
Korea	7.7	United Kingdom	5.6
United States	5.8	Iran	5.5
Netherlands	5.7	Netherlands	5.2
Soviet Union	5.4	Belgium/Luxembourg	4.7
Spain	4.8	Soviet Union	4.6

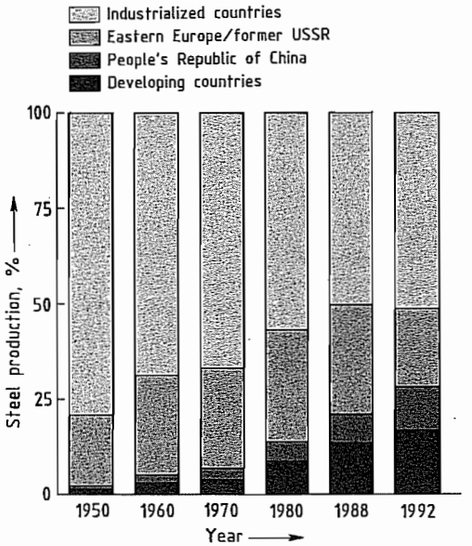

Figure 6.174: Crude steel production by region 1950–1992.

The strong growth of the world steel industry starting in the 1970s was due to the high demand for steel in western Europe, Japan, and eastern Europe. In these regions, steel consumption expanded by almost 7% per annum. In the United States, the rate was only 2%. Consumption by the developing countries grew rapidly from small beginnings, at > 8.5% per annum.

In the last 30 years, considerable regional changes in steel consumption and production have occurred. Approximately one-fifth of steel consumption and 15% of steel production is associated with the developing regions (Figure 6.173). China has also moved ahead. Japan improved its position until the early 1970s, but its share of the world volume has stagnated since then. Europe and the United States are producing a considerably lower proportion than 20 years ago.

Regional shifts have increased the extent to which the developing countries have become self-sufficient, but in recent years, demand has grown more rapidly than supply. The traditional exporters, e.g., Japan and the European Community, have relied more strongly on their domestic markets. The United States has been a net importer since 1959. The relationship between production and market supply has developed as shown in Table 6.22.

Brazil has become one of the largest net exporters. Meanwhile, the contribution by eastern Europe and the former Soviet Union to the world total has decreased since the end of the communist planned economy (Figure 6.174).

World steel exports have grown more rapidly than world production (Figure 6.175) because of variations in the regional distribution of demand and production. In the 1970s and early 1980s, the volume of international trade in steel tended to grow at the same rate as general world trade, but in recent years, the volume of steel trade has not increased. The increasing self-sufficiency of new producing countries tends to have a braking effect, but in the area of products and grades, and as a result of competition for customers by the manufacturing companies, active interchange across national boundaries is likely in future.

Steel exports from Japan have decreased from > 30×10^6 t in the mid-1980s to 18×10^6 t in 1991. Most significant is the collapse of trade among the former COMECON countries—ca. 15×10^6 t reduction in the exchange volume. As shown by the high uptake by China from the international market in late 1992/early 1993, relatively large fluctuations in world steel exports are likely.

A summary of the largest exporting and importing countries in 1991 is given in Table 6.23.

An important feature of the steel industry that affects investment decisions is the extent of export orientation of steel manufacturers. In the industrialized countries, the important steel consumers, e.g., engineering and motor vehicle manufacturers, export a high proportion of their steel-containing products (Table 6.24).

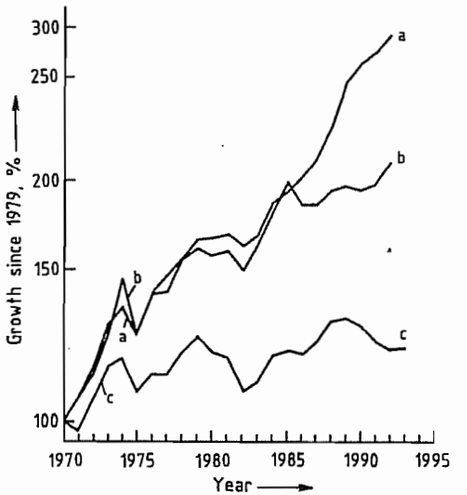

Figure 6.175: World steel exports, production, and trade from 1970. 1970 figures = 100%. a) World trade (all products); b) Steel exports; c) Crude steel production. Source: IISI; Dresdner Bank.

Table 6.24: Direct and indirect steel exports of selected regions.

	Direct export	Indirect export	Direct production, %	Indirect production, %
	10^6 t rolled steel			
European Community				
1979	65.7	32.0	53.4	32.4
1990	70.2	37.7	5839	35.8
Japan				
1979	30.7	12.0	30.8	17.1
1990	16.6	20.4	16.9	23.0

Table 6.25: Steel consumption in selected countries 1990.

Country	Consumption, kg rolled steel per capita
West Germany	482
France	285
United Kingdom	244
Sweden	336
Japan	751
Brazil	60

In countries with very high steel exports, e.g., Germany and Japan, the so-called indirect foreign steel trade affects the trend of development of steel consumption and per capita steel consumption considerably (Table 6.25). For these two countries in 1990, indirect exports and imports of rolled steel resulted in a net balance, estimated at 9.3 and 19.4×10^6 t. These examples show the importance of the basic conditions for fair international trade.

The demand for steel, the most important construction material for industry (including the construction industry) and handicrafts, is mainly determined by overall economic development, and hence by capital investment and external trade in steel-containing goods. The optimism which, in the early 1970s, led to investment in steel capacity was considerably dampened after the first oil crisis of 1974–75. The second large increase in the price of oil in 1979, and the increased attention to environmental problems slowed down the economic growth of the western industrialized countries, where the standard of living had reached a remarkably high level. Future growth is likely to be essentially calmer.

6.8.2 Steel Intensity and Weight Saving in Steel

Steel consumption depends on the state of the overall national economy, especially on investments and foreign trade. In the early stages of industrialization, steel consumption grows at a rate out of proportion to that of the national product. Later, the so-called steel intensity decreases, and steel consumption grows more slowly than the national product (Figure 6.176). The most important reasons include:

- Weight savings in steel manufacture by design optimization, making use of lighter and qualitatively superior steels. The 320 m Eiffel Tower was built of 7000 t steel in 1889, but today would require only 2000 t. A 165 m mast for a radio link station can be built today with only 210 t steel.
- The use of different materials within the broad area of rolled steel products, e.g., greater use of flat products in place of long products, and the use of increasingly thin sheet for flat products (Figure 6.177).

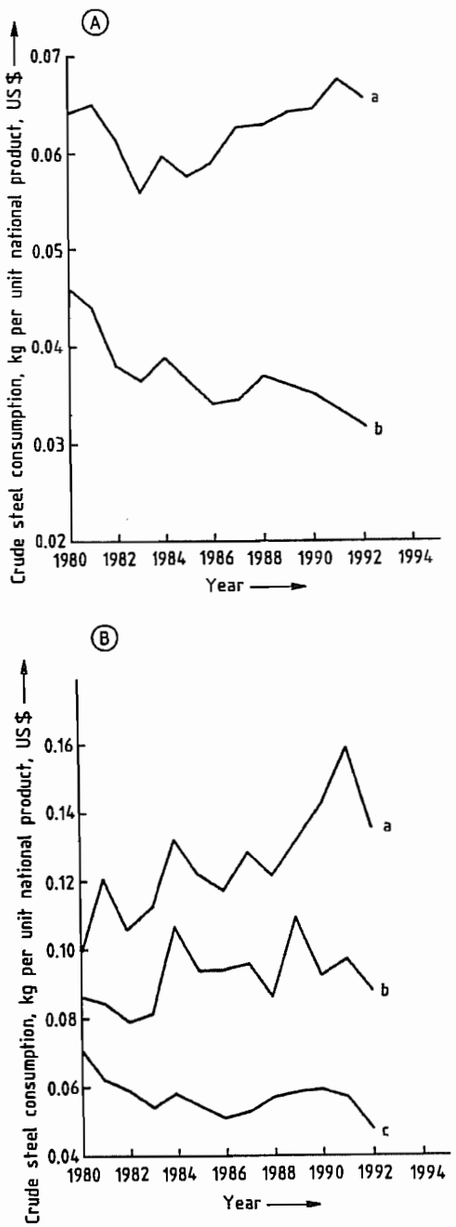

Figure 6.176: Steel consumption from 1980: A) Developing countries (a); Industrialized countries (b); B) Korea (a); Turkey (b); Japan (c). From calculations supplied by IISI.

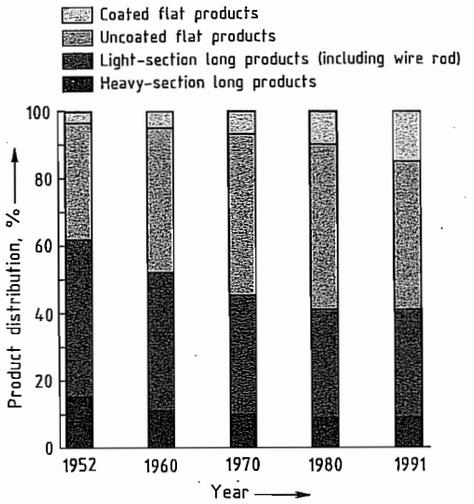

Figure 6.177: Distribution of rolled steel finished products in the European Community. Source: Eurostat.

- Replacement of steel by other materials, e.g., light metals or plastics, e.g., in automobiles. The proportion of steel and iron has decreased from 75% in the 1970s to 65% in the early 1990s. The aluminum content has grown from 3% to 5%, and plastics from 6% to 10%. It is likely that steel will continue to be the most important constituent of automobiles, remaining at ca. 60%.
- A combination of steel with other materials is often the best solution (e.g., sandwich construction).
- The reason for most of the reduction in specific steel consumption is the improved productivity of the steel industry itself, and not the replacement of materials.
- With increasing maturity of a national economy, the fraction of the total national product accounted for by commercial services increases, and the fraction accounted for by manufacturing and heavy basic materials decreases. In 1960, the proportion of the West German national product accounted for by manufacturing was 53%, in 1980 it was 43%, and in 1992, 37%. Mining, basic materials, and manufactured goods contributed 32%, 30%, and 23% to the turnover of manufacturing business in these years.

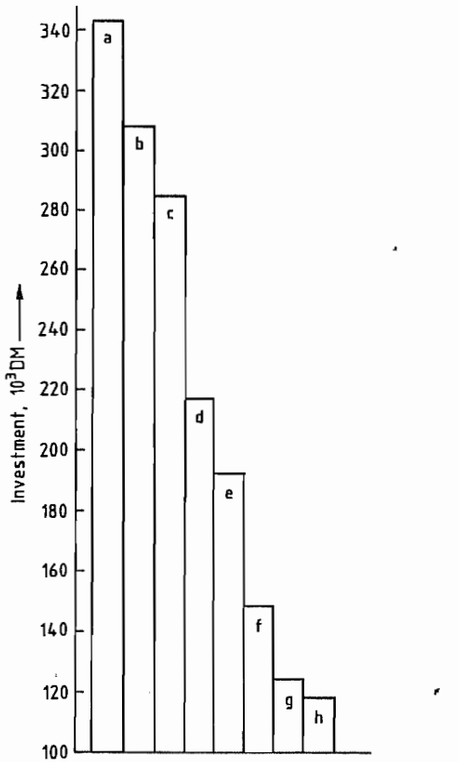

Figure 6.178: Capital investment per installation, West Germany 1990: a) Steel; b) Chemicals; c) Quarrying, extraction, and working up of stone and earths; d) Industry (total); e) Road vehicles; f) Food industry; g) Electrical industry; h) Mechanical engineering. Source: IW, Cologne.

6.8.3 Capital Investment and Subsidies

The steel industry, a capital-, energy-, and raw-material-intensive industry, has always striven to improve productivity and cost effectiveness. Improvements in industrial plant design production methods, and installations for recovering or recycling waste heat, waste gases, electricity, and water have been of central importance. The high intensity of capital investment brought steep cost reductions whenever it was possible to fully utilize the capacities of very large installations. Consequently, from the 1950s to the 1970s, large integrated steelworks were central to strategic planning. Optimization of locations with respect to raw material supplies (coastal steelworks) or large marketing regions (Rhine, Ruhr) was emphasized. Technical development at that time mainly provided the measurement and control techniques essential for large blast furnaces, large converters, strand casting plants, and large rolling mills, and the electronic support for the organization of production. Innovations and improvements have contributed to reductions in the capital cost per tonne steel produced, in specific energy consumption, in raw and auxiliary materials costs, and in general running costs.

In modern steelworks, the production of 1 tonne rolled steel requires 1.1 t crude steel, whereas 20 years ago it required 1.3 t. Consequent savings of raw steel are ca. 80×10^6 t/a worldwide. There is a further possible saving of 40×10^6 t by further modernization, assuming the same volume of rolled steel.

However, intensity of capital investment compared with other branches of industry is still relatively high. In 1990, it was 340 000 DM per installation, which compares with only 118 000 DM in engineering (Figure 6.178). Capital investment constitutes just 20% of the cost of steel produced in West Germany. Personnel costs account for ca. 25%. The sum of these costs is only slightly influenced by short-term market fluctuations. Large production units cannot be throttled back at will. However, as the steel market reacts extremely strongly to economic change (rising demand in boom periods, falling demand during recessions), suppliers have problems in matching supply to demand, especially in times of weak markets. The result is intense competition between suppliers for small market volumes at falling prices. As long as businesses can build up a financial reserve in good economic times, short-term falls in demand can be coped with. However, this becomes much more difficult if medium-term demand forecasts are over-optimistic.

For a long time, so-called mini-steelworks have become the cost and price leaders among producers of light-section steel products (e.g.,

rod and wire rod). For this product area, the favored production scheme is electrosteel processing of scrap and small rolling mills. This reduces capital costs, and gives flexibility in matching market fluctuations.

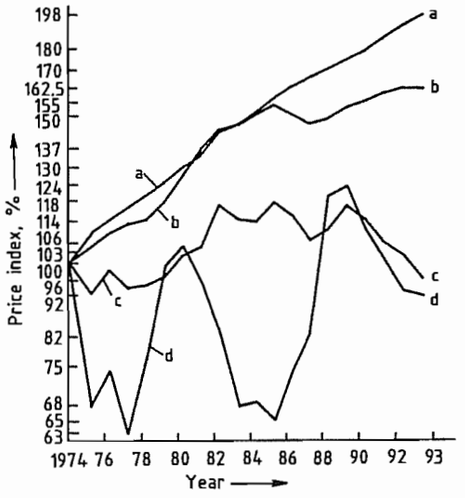

Figure 6.179: Price fluctuation in selected branches of the West German business economy 1974–1993. 1985 index recalculated to set 1974 figures = 100%. a) Producers' prices, motor vehicle construction; b) Commercial products (total); c) Rolled steel; d) Export prices, Western Europe (steel bars). Data supplied by the Statistisches Bundesamt (German Federal Bureau of Statistics).

New technology, organization systems, and the resulting increase in productivity and economic efficiency have also influenced price. Steel prices have risen considerably more slowly than those of the average industrial product. In recent years they have even fallen, and the severe fluctuations in international quotations during economic cycles have at least been no worse than those of 20 years ago (Figure 6.179).

There are very high barriers preventing steel making installations with overcapacity from getting out of the market. In western Europe since the mid 1970s these have become even higher, as state intervention distorts competition, making reduction in capacity very difficult. Large subsidies have ensured survival, especially of nationalized undertakings (Figure 6.180). Reduction in capacity is lagging behind the true need, and finance for capital investment in modernization has continued to be available (Table 6.26).

Private undertakings can only combat such subsidized competition for a limited period, if there is no countervailing policy to avoid subsidized companies increasing their market share.

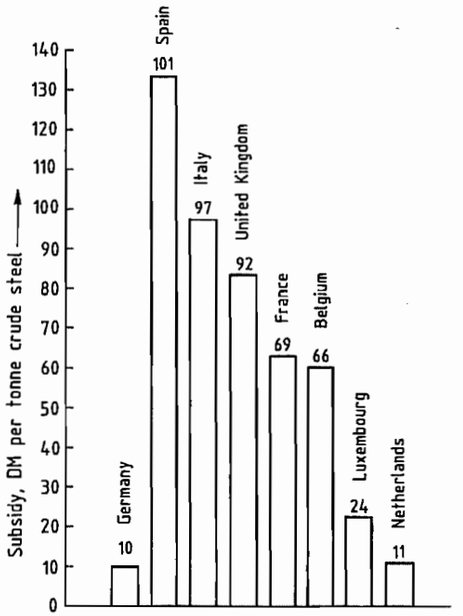

Figure 6.180: Distortion of competition by subsidies 1975–1993. Figures for Spain from 1984. Source: Wirtschaftsvereinigung Stahl (Industrial Association for Steel).

Table 6.26: Capital investment and subsidies in selected countries 1975–1991. Average figures, DM per tonne crude steel produced.

	West Germany	France	United Kingdom	Italy
Subsidies	10	69	92	97
Capital investment	47	63	70	67

The steel politics of the European Community since the middle 1970s exemplify the disastrous effects of state intervention in a market economy. The decisions of the European Commission and the Council of Ministers during the steel crisis of 1991–1993 show that there is a gulf between the broad political aims of a European Union and the real economic, financial, and structural politics of the member countries.

In some steel-producing countries (e.g., the United Kingdom and Brazil) governments have become unwilling to pay high subsidies, on the grounds that they block the possibilities for investment in alternative projects. Privatization of nationalized steel undertakings has gone ahead.

6.8.4 Future Prospects

New perspectives are opening up in the steel industry through further technical developments in casting and rolling technology. A new generation of continuous production lines, from crude steel to products close to final dimensions, may considerably reduce the specific capital costs both of flat steel products and of heavy profiles, increasing the flexibility of undertakings to match economic fluctuations. At the same time, productivity can be significantly improved. Different configurations of the supply structure are likely to become available to the large suppliers of flat steel products, who are themselves advancing these technical developments, i.e., independent small and medium manufacturing units, or a combination of several plants with an efficient source of crude iron and steel from large units.

In recent years, small and medium-sized steelworks, mainly based on scrap, have been in favor, but there are limits to this development. Increasing amounts of scrap are available for steel production, but growing world steel demand is likely to require the smelting of iron ore.

Thus, from the economic point of view, many opportunities present themselves for steel as a competitive material for the future.

6.9 References

1. H.-J. Engell: Stahl – *Prinzipien seines Aufbaus und Aufgaben künftiger Entwicklungen*, Jahrbuch der Akademie der Wissenschaften in Göttingen, 1982.
2. Verein Deutscher Eisenhüttenleute (ed.): "Fundamentals", *Steel—A Handbook for Materials Research and Engineering*, vol. 1, Springer Verlag, Berlin 1992.
3. International Iron and Steel Institute (IISI): *World steel in Figures*, Brussels 1992.
4. K. A. Zimmermann: "Renaissance der Eisenbahn – eine Realität?" *IISI – Jahrestagung*, Colorado Springs 1978.
5. R. Grundmann, H. M. Mozek, K. H. Michel, H. Mülders: "Warmband und Kaltband aus nichtrostenden Stählen", *Stahl u. Eisen* **107** (1987) 1221–1227.
6. J. G. L. Blumhof: *Versuch einer Encyklopädie der Eisenhüttenkunde*, vol. 1–4, G. F. Heyer, Gießen 1816–1821.
7. L. Beck: *Geschichte des Eisens*, vol. 1–5, Vieweg & Sohn, Braunschweig 1891–1903.
8. O. Johannsen: *Geschichte des Eisens*, 3rd ed., Verl. Stahleisen, Düsseldorf 1953.
9. R. F. Tylecote: *A History of Metallurgy*, 2nd ed., Inst. of Materials, London 1992.
10. A. Paulinyi: *Das Puddeln*, Oldenbourg, München 1987.
    K. C. Barraclough: "Blister Steel", vol. 1; "Crucible Steel", vol. 2; *Steelmaking Before Bessemer*, Metals Society, London 1984.
11. K. C. Barraclough: *Steelmaking 1850–1900*, Inst. of Metals, London 1990.
12. O. Johannsen: "Die geschichtliche Entwicklung der Walzwerkstechnik", in J. Puppe, G. Stauder (eds.): *Walzwerkswesen*, vol. 1, Verl. Stahleisen, Düsseldorf, Springer Verlag, Berlin 1929, pp. 252–337.
13. *Stahlfibel*, Verlag Stahleisen, Düsseldorf 1989, p. 135.
14. O. Johannsen: *Geschichte des Eisens*, 3rd ed., Verlag Stahleisen, Düsseldorf 1953, p. 331.
15. Valerius-Hartmann: *Handbuch der Stahleisen Fabrikation*, J. G. Engelhardt, Freiberg 1985, Figure 1.
16. W. Rosenbleck, H. W. Kreutzer, R. Steffen, W. Schäfer, R. Willeke, *Stahl u. Eisen* **101** (1981) no. 7, 463–471.
17. D. Springorum, *Stahl u. Eisen* **112** (1992) no. 12, 45.
18. H. M. W. Delport, *Ironmaking Steelmaking* **19** (1992) no. 3, 183–189.
19. H. W. Kreutzer: "Schrotteinsatz in der Eisen- und Stahlindustrie", paper presented at "Ruckstandsoptimierte Werkstoff- und Produktionstechnik am Beispiel des Automobils". RWTH, Aachen, Germany, Nov. 25, 1993.
20. R. Willeke, R. Ewers, H. W. Kreutzer, *Stahl u. Eisen* **114** (1994) no. 5, 83–88.
21. Verein Deutscher Eisenhüttenleute (VDEh) (eds.): *Jahrbuch Stahl 1994*, vol. 1, p. 216.
22. H. W. Kreutzer, *Stahl u. Eisen* **112** (1992) no. 5, 65–69.
23. W. Ullrich, H. Schicks, *Stahl u. Eisen* **111** (1991) no. 11, 85–92.
24. J. W. Brown, R. L. Reddy, P. J. Salomon: "Economic Problems Related to Creation of Steelplants Using Direct Reduction", Economic Commission for Europe (ECE), Seminar given at the Steel Committee, May 16–20, 1983, Nordwijkerhout, Report R30.
25. R. Steffen, H.-B. Lüngen, *Stahl u. Eisen* **114** (1994) no. 6, 85–92.

26. Midrex Corp.: Midrex News Release, Charlotte, N.C. 1993.
27. F. A. Stephens, *Steel Times Int.*, **March 1993**, 11–12.
28. K. H. Zepter, F. Daube, *Stahl u. Eisen* **103** (1983) no. 7, 319–324.
29. N. Bannenberg, *Stahl u. Eisen* **111** (1991) no. 7, 71–76.
30. E. Höffken: "Entwicklungstrend des Oxygenstahlverfahrens", *Freiberg. Forschungsh. B* **229** (1982) 57–66.
31. W. Florin, R. Hammer, E. Hoffken, W. Ullrich, H. Schicks, *Stahl u. Eisen* **105** (1985) no. 9, 531–536.
32. J. Geiseler, *Stahl u. Eisen* **111** (1991) no. 1, 531–536.
33. T. B. Massalski (ed.): *Binary Alloy Phase Diagrams*, 2nd ed., vol. 1, ASM Int. Materials Information Society, Ohio 1990.
34. F. Neumann, H. Schenck, *Arch. Eisenhüttenwes.* **30** (1959) 477–483.
35. M. G. Benz, J. F. Elliott, *Trans. Am. Inst. Min. Metall. Pet. Eng.* **221** (1961) 303–332.
36. G. K. Sigworth, J. F. Elliott, *Met. Sci.* **8** (1974) 298–310.
37. L. S. Darken, R. W. Gurry, *J. Chem. Soc. A* **68** (1946) 798–816.
38. C. R. Taylor, J. Chipman, *Trans. Am. Inst. Min. Metall. Pet. Eng.* **154** (1943) 228–247.
39. Z. Buzek, A. Hulta, *Freiberg. Forschungsh. B* **117** (1969) 59–73.
40. The Japan Society for the Promotion of Science, The 19th Committee on Steelmaking. Steelmaking Data Sourcebook, Gordon and Breach, New York 1988.
41. H. D. Kunze, E. Schürmann, *Gießereiforschung* **20** (1968) 35–48.
42. R. D. Pehlke, J. F. Elliott, *Trans. Am. Inst. Min. Metall. Pet. Eng.* **218** (1960) 1088–1101.
43. M. Ohtani, *Tetsu to Hagane* **54** (1968) 1381–1407.
44. E. Schürmann, F. Winterfeld, *Thyssenforschung* **4** (1972) 118-132.
45. F. Oeters: *Die physikalische Chemie der Eisen- und Stahlerzeugung*, Verlag Stahleisen, Düsseldorf 1964, 156–211.
46. R. D. Walker, D. Anderson, *Iron Steel* **45** (1972) 271–276.
47. S. Banya, S. Matoba in G. R. St. Pierre (ed.): *Physical Chemistry of Process Metallurgy*, part 1, Interscience Publisher, New York 1959, pp. 373–401.
48. P. Hammerschmid, D. Janke, H. W. Kreutzer, E. Reichenstein, R. Steffen, *Stahl u. Eisen* **105** (1985) 433–442.
49. M. Olette, C. Gatellier, R. Vasse: "Progress in Ladle Steel Refining", *Proc. Int. symp. Phys. Chem. Iron Steelmaking* **1982**, art. VII-1.
50. P. V. Riboud, C. Gatellier, *Ironmaking Steelmaking* **12** (1985) 79–86.
51. E. T. Turkdogan, *Arch. Eisenhüttenwes.* **54** (1983) 1–10.
52. E. Steinmetz, *Rodex Rundschau* 1969, 605–617.
53. F. Oeters: *Metallurgie der Stahlerzeugung*, Springer Verlag, Berlin, Verlag Stahleisen, Düsseldorf 1989.
54. V. G. Levitch: *Physicochemical Hydrodynamics*, Prentice Hall, Englewood Cliffs 1962.
55. A.-K. Bolbrinker in Verein Deutscher Eisenhüttenleute (ed.): *Stahlfibel*, Verlag Stahleisen, Düsseldorf 1989.
56. R. Weber, L.-A. Mersoletto, H.-W. Gudenau, F.-H. Gradien, *Stahl u. Eisen* **110** (1990) no. 12, 98.
57. Verein Deutscher Eisenhüttenleute (ed.): *Jahrbuch Stahl*, Verlag Stahleisen, Düsseldorf 1990.
58. H. Voge, E. Eickworth, *Stahl u. Eisen* 79 (1959) no. 23, 1716.
59. T. Shima in: *Proc. Sixth IJSC*, Nagoya 1990.
60. E. Plöckinger, W. Wahlster, *Stahl u. Eisen* **80** (1960) 407–416.
61. L.-P. Pesce, H. Todzy, H. Schnitzer, *Int. Steel Mat. Mag.* (1989) 591.
62. R. Heinke et al., *Steel Techn. Int.* **1988**.
63. ABB Publikation: "Direct Current Arc Furnace".
64. Verein Deutscher Eisenhüttenleute (ed.): *Eisenhütte*, 5th ed., Verlag Stahleisen, Düsseldorf 1961.
65. H .-U. Lindenberg, K.-H. Schubert, H. Zorcher, *Stahl u. Eisen* **107** (1987) 1192.
66. G. K. Sigworth, J. F. Elliott, *Metal Science* (1971), p. 298, 310.
I. Barin, O. Knacke: *Thermodynamical Properties of Inorganic Substances*, Springer-Verlag, Heidelberg 1973.
67. H. Legrand, M. Amblard in: *Int. Conf. Sec. Met.* 1987, p. 452.
68. F. Oeters, E. Görl, *Steel research* **61** (1990) no. 9.
69. G. Stolte, R. Teworte, *33 Met. Prod.* **11** (1991) 18/19.
70. D. Nolle, U. Eulenburg, A. Jahns, H. Miska in: *Int. Conf. Sec. Met.* **1987**, p. 275.
71. B. Chalmers: *Principles of Solidification*, J. Wiley & Sons, New York 1964.
72. M. C. Flemings: *Solidification Processing*, McGraw-Hill, New York 1974.
73. W. Kurz, D. J. Fisher: *Fundamentals of Solidification*, Trans Tech SA, Ædermannsdorf, Switzerland 1984.
74. B. W. Berry (ed.), "Solidification of Metals", *Proc. Int. Conf.*, Brighton, 4–7 December 1967, The Iron and Steel Institute, London 1968.
75. "Solidification and Casting of Metals", *Proc. Int. Conf. Solidifcation*, Sheffield, 18–21 July 1977, The Metal Society, London 1979.
76. The University of Sheffield and The Institute of Metals (eds.): "Solidification Processing 1987, Preprints", *Int. Conf.*, Sheffield, United Kingdom, Sept. 21–24, 1987.
77. G. Grünbaum et al.: *A Guide to the Solidification of Steels*, Jernkontoret, Stockholm 1977.
78. H. Jacobi, K. Schwerdtfeger, *Metall. Trans.* **7A** (1976) 811–820.
79. M. A. Taha, H. Jacobi, M. Imagumbai, K. Schwerdtfeger, *Metall. Trans.* **13A** (1982) 2131–2141.
80. E. Schürmann, S. Baumgartl, L. Nedeljkovic, M. Tripkovic, *Steel Research* **58** (1987) no. 11, 498–502.
81. K. Miyamura, I. Taguchi, H. Soga, *Trans. Iron Steel Inst. Jpn.* **24** (1984) 883–890.
82. K. Schwerdtfeger: *Metallurgie des Stranggießens, Gießen und Erstarren von Stahl*, Verlag Stahleisen, Düsseldorf 1992, pp. 171–202.
83. K. Wünnenberg, *Stahl u. Eisen* **98** (1978) no. 6, 254–259.

84. W. Dahl, H. Hengstenberg, C. Düren, *Stahl u. Eisen* **86** (1966) no. 13, 782–795.
85. E. Steinmetz, H.-U. Lindenberg, *Arch. Eisenhüttenwes.* **47** (1976) no. 9, 521–524; no. 12, 713–718.
86. K. Schwerdtfeger, *Arch. Eisenhüttenwes.* **41** (1970) no. 9, 923–937; 43 (1972) no. 3, 201–205.
87. F. Oeters, H.-J. Selenz, E. Förster, *Stahl u. Eisen* 99 (1979) no. 8, 389–397.
88. E. Steinmetz, H.-U. Lindenberg, W. Mörsdorf, P. Hammerschmid, *Stahl u. Eisen* 97 (1977) no. 23, 1154–1159.
89. E. Steinmetz, H.-U. Lindenberg, *Arch. Eisenhüttenwes.* **47** (1976) no. 4, 199–204.
90. *Ullmann*, 4th Ed., **22**, 14–16.
91. *The Making, Shaping and Treating of Steel*, 10th ed., United States Steel Corp., Pittsburgh, Ass. Iron Steel Eng. (1985) 691–740.
92. G. Lepie, H. Rellermeyer: "Untersuchungen über den Erstarrungsverlauf in Gußblöcken", *Arch. Eisenhüttenwes.* **37** (1966) no. 12, 925–934.
93. K.-K. Aschendorff, E. Köhler, H. Schroer, B. Abel: "Seigerungen in unberuhigten Stahlblöcken", *Stahl u. Eisen* **82** (1962) no. 20, 1356–1366.
94. H. F. Bishop, F. A. Brandt, W. S. Pellini: "Solidification Mechanism of Steel Ingots", *J. Met.* **4** (1952) 44–54.
95. A. Diener, A. Drastik, W Haumann: "Untersuchung über den Wärmeübergang zwischen Block und Kokille beim Erstarren von Stahl", *Arch. Eisenhüttenwes.* **43** (1972) 525–533.
96. F. Oeters, K. Sardemann: "Untersuchung zum zeitlichen Verlauf der Erstarrung in der Randzone und zur Spaltbildung zwischen Block und Kokille", *Int. Iron Steel Congr.*, Düsseldorf 1974, vol. 3 VDEh, Düsseldorf 1974.
97. H.-J. Langhammer, H. G. Geck: "Vorgänge beim Gießen und Erstarren von unberuhigtem Stahl", in: *Gießen und Erstarren von Stahl*, Verlag Stahleisen, Düsseldorf 1967, pp. 33–75.
98. W. Recknagel, H. Oppenhoff: "Was der Blasstahlwerker von seiner Arbeit wissen muß", *Stahleisen-Schriften*, 2nd ed., vol. 6, Verlag Stahleisen, Düsseldorf 1977, p. 120.
99. H. C. Vacher, E. H. Hamilton, *Trans. Am. Inst. Min. Metall. Eng. Iron Steel Div.* **95** (1931) 124–140.
100. A. Hultgren, G. Phragmén, *Trans. Am. Inst. Min. Metall. Eng. Iron Steel Div.* **135** (1939) 133–244.
101. H. Rellermeyer: "Vorgänge bei der Blockerstarrung", in: *Die physikalische Chemie der Eisen- und Stahlerzeugung*, Verlag Stahleisen, Düsseldorf 1964, pp. 350–376.
102. H. Rellermeyer, R. Hammer: "Metallurgische Fragen beim Vergießen und Erstarren von unberuhigtem Stahl", *Stahl u. Eisen* **78** (1958) no. 22, 1505–1513.
103. K. Asano, T. Otiashi, *Tetsu to Hagane* **54** (1968) 74–75, 643–673.
104. P. Nilles: "Theoretical Study of the Solidification of Rimming Steel", *J. Iron Steel Inst. London* **202** (1964) 601–609.
105. P. Nilles, F. Becker, A. Thill: "Untersuchung über die Erstarrung von unberuhigt vergossenem Stahl", *Stahl u. Eisen* **85** (1965) 1025–1032.
106. H.-J. Langhammer, H. G. Geck: "Vorgänge beim Gießen und Erstarren von unberuhigtem Stahl", in: *Gießen und Erstarren von Stahl*, Verlag Stahleisen, Düsseldorf 1967, pp. 33–75.
107. K. Kupzog, R. Hammer, H. Rellermeyer: "Untersuchungen zur Seigerung bei unberuhigtem Stahl", *Stahl u. Eisen* **82** (1962) no. 7, 394–401.
108. E. Schürmann, W Groetschel, O. Peter: "Untersuchung des Auskoch- und Erstarrungsverhaltens von unberuhigt vergossenem Stahl", *Arch. Eisenhüttenwes.* **36** (1965) 619–631.
109. R. Hammer, G. Lepie, Th. Kootz, K. Wick: "Einschlüsse im unberuhigten Stahl", in "Das Vergießen und Erstarren von Stahl zu Blöcken", *Freiberger Forschungsh. B* **137**, Leipzig 1968, pp. 56–77.
110. "Gemeinschaftsforschung über Grundlagen des Gießens und Erstarrens", *Stahl u. Eisen* **96** (1976) no. 17, 840–846.
111. F. Oeters: "Blockguß", *Z. Metallk.* **63** (1972) 301–306.
112. P. M. Macnair, *J. Iron Steel Inst. London* **160** (1948) 151–163.
113. A. Diener: "Strömungstechnische Probleme beim Vergießen von Stahl", *Stahl u. Eisen* 96 (1976) no. 25/26, 1337–1340.
114. J. R. Blank, E. B. Pickering: "The Effect of Solidification in Large Ingots on Segregation of Non-Metallic Inclusions", *The Solidification of Metals. Proc. of the Conf.*, Brighton 1967, Iron and Steel Inst., London 1968, pp. 370–376.
115. K. Schwerdtfeger: "Einfluß der Erstarrungsgeschwindigkeit auf die Mikroseigerung und die interdendritische Ausscheidung von Mangansulfideinschlüssen in einem Mangan und Kohlenstoff enthaltenden Stahl," *Arch. Eisenhüttenwes.* **41** (1970) no. 9, 923–937.
116. R. D. Doharty, D. A. Melford: "Solidification and Microsegregation in Killed Steel Ingots with Particular Reference to 1% C, 1.5% Cr Steel", *J. Iron Steel Inst. London* **204** (1966) 1131–1143.
117. F. Oeters, K. Rüttiger, A. Diener, G. Zahs: "Zur Theorie der metallurgischen Vorgänge bei der Erstarrung von Stahl", *Arch. Eisenhüttenwes.* **40** (1969) no. 8, pp. 603–613.
118. C. Roques, P. Martin, Ch. Dubois, P. Bastien: "Étude de l'hétérogénéité des gros lingots de forge", *Rev. Metall.* (Paris) **57** (1960) no. 12, 1091–1103.
119. A. Hultgren: "A and V Segregation in Killed Steel Ingots", *Scand. j. Meetall.* **2** (1973) 217–227.
120. H.-D. Pantke, H. Neumann: "Vorgänge beim Gießen und Erstarren von halbberuhigtem Stahl", in: *Gießen und Erstarren von Stahl*, Verlag Stahleisen, Düsseldorf 1967, pp. 76–90.
121. H. Knüppel, F. Eberhard: "Gesetzmäßigkeiten bei der Kohlenmonoxydentwicklung teilberuhigt erstarrender Stähle", *Arch. Eisenhüttenwes.* **34** (1963) no. 5, pp. 325–340.
122. J. Koenitzer, R. Hammer: "Der Sauerstoff im beruhigten und halbberuhigten Stahl", *Stahl u. Eisen* **83** (1963) no. 10, 569–577.
123. K. F. Behrens, R. Hammer: "Production of Aluminium-Killed Steel by Mold Additions of Aluminium", *Proc. Nat. Open Hearth Basic Oxygen Steel Conf.* **50** (1967) 112–115.
124. U. Petersen, K. G. Speith, A. Bungeroth, *Stahl u. Eisen* **86** (1966) no. 6, 333–353.
125. M. M. Wolf, *Steelmaking Conf.* **75** (1992) 83–137.

126. *Contin. Cast. Steel, Proc. Int. Conf.*, Biarritz, 31 May–2 June 1976, The Metals Society, London 1977.
127. "Continuous Casting", *Proc. Int. Iron Steel Congr. 4th*, London, May 12–14, 1982.
128. *Continuous Casting '85*, London, 22–24 May 1985, The Institute of Metals London 1985.
129. CRM and VDEh (eds.): *4th international Conference Continuous Casting*, ICC '88, Brussels, 17–19 May 1988, Stahleisen, Düsseldorf 1988.
130. AIM (ed.): *1st European Conference on Continuous Casting*, Florence, 23–25 Sept. 1991, Milano 1991.
131. H. Schrewe: *Stranggießen von Stahl*, Einführung und Grundlagen, Verlag Stahleisen, Düsseldorf 1987.
132. K. Schwerdtfeger: *Metallurgie des Stranggießens, Gießen und Erstarren von Stahl*, Verlag Stahleisen, Düsseldorf 1992.
133. L. J. Heaslip, A. McLean, 1. D. Sommerville: "Chemical and Physical Interactions During Transfer Operations", *Continuous Casting*, vol. 1, ISS-AIME, Warrendale 1983.
134. J. K. Brimacombe, I. V. Samarasekera, J. E. Lait: "Heat Flow, Solidification and Crack Formation", *Continuous Casting*, vol. 2, ISS-AIME , Warrendale 1984.
135. J. J. Moore: "The Application of Electromagnetic Stirring (EMS) in the Continuous Casting of Steel", *Continuous Casting*, vol. 3, ISS-AIME Warrendale 1984.
136. T. B. Harabuchi, R. D. Pehlke: "Design and Operations", *Continuous Casting*, vol. 4, ISS-TMS, Warrendale 1988.
137. R. A. Heard, A. McLean: "Horizontal Continuous Casting", *Continuous Casting*, vol. 5, ISS-TMS, Warrendale 1988.
138. H. Schrewe et al., *Stahl u. Eisen* **108** (1988) no. 9, 427–436.
139. "Progress of the Iron and Steel Technologies in Japan in the Past Decade, III: Steelmaking", *Transactions ISIJ* **25** (1985) 627–710.
140. E. Höffken et al., *Stahl u. Eisen* **105** (1985) no. 22, 1167–1175.
141. G. Holleis, R. Scheidl, W. Dutzler, *Fachber. Hüttenprax. Metallweiterverarb.* **25** (1987) no. 10, 959–967.
142. D. Kothe, F.-P. Pleschiutschnigg, F. Boehl, *MPT Metallurg. Plant and Technol.* **13** (1990) no. 1, 1226.
143. P. Nilles, A. Étienne, *1st European Conf. on Continuous Casting*, vol. 1, Florence 1991, pp. 1.1–1.16.
144. D. Schauwinhold, *Stahl u. Eisen* **102** (1982) no. 21, 1077–1082.
145. P. Riboud in K. Schwerdtfeger (ed.): *Metallurgie des Stranggießens, Gießen und Erstarren von Stahl*, Verlag Stahleisen, Düsseldorf 1992, pp. 233–255.
146. K. Wünnenberg, *Stahl u. Eisen* **98** (1978) no. 6, 254–259.
147. R. Thielmann, R. Steffen, *Stahl u. Eisen* **100** (1980) no. 7, 401–407.
148. P. Voss-Spilker, W. Reichelt, *Iron Steel Eng.* **1983** June, 32–38.
149. P. Stadler, J. von Schnakenburg, *Stahl u. Eisen* **109** (1989) no. 9, 463–469.
150. T. Nozaki, S. Itoyama, *Trans. Iron Steel Inst. Jpn.* **27** (1987) 321–331.
151. The Korean Institute of Metals, The Institute of Metals, UK, Preprints 2 (eds.): "SRNC-90 Near Net Shape Casting", Internat. Conf., RIST, Pohang, Korea, Oct. 14–19, 1990.
152. J.-P. Birat, R. Steffen, *MPT Metallurg. Plant Technol.* **14** (1991) no. 3, 44–57.
153. E. Höffken, P. Kappes, H. Lax, *Stahl u. Eisen* **106** (1986) no. 23, 1253–1259.
154. F. K. Iverson, K. Busse, *Stahl u. Eisen* **111** (1991) no. 1, 37–45.
155. W. Rohde, H. Wladika, *Stahl u. Eisen* **111** (1991) no. 1, 47–61.
156. H.-J. Ehrenberg, L. Parschat, F.-P. Pleschiutschnigg, C. Praßer, W Rahmfeld, *Stahl u. Eisen* **109** (1989) no. 9/10, 453–462.
157. F.-P. Pleschiutschnigg et al., *MPT Metallurg. Plant Technol.* **15** (1992) no. 2, 66–82.
158. E. Höffken, *Stahl u. Eisen* **113** (1993) no. 2, 49–54.
159. W. E. Duckworth, G. Hoyle: *Electro-Slag Refining*, Chapman and Hall, London 1969.
160. H. C. Child, G. E. Oldfield, R. Bakish, A. Lawley: "Vacuum Melting" in O. Winkler, R. Bakish (eds.): *Vacuum Metallurgy*, Chap. V, Elsevier, Amsterdam 1971, pp. 517–642.
161. W.H. Sutton: "Progress in the Vacuum (VIM, VAR) Melting of High Performance Alloys", *Proc. Int. Conf. Vac. Metall. 7th*, Nov. 26–30, 1982, Tokyo, The Iron and Steel Institute of Japan, Tokyo 1982, pp. 904–915.
162. L. W. Lherbier: "Melting and Refining", in C. T. Sims, N. S. Stoloff, W. C. Hagel (eds.): *Superalloys II*, Chap. 14, J. Wiley & Sons, New York 1987, pp. 387–410.
163. A. Choudhury: "State of the Art of Superalloy Production for Aerospace and Other Applications Using VIM/VAR or VIM/ESR", *ISIJ Int.* **32** (1992) no. 5, 563–574.
164. A. Choudhury, E. Hengsberger: "Electron Beam Melting and Refining of Metals and Alloys", *ISIJ Int.* **32** (1992) no. 5, 673–681.
165. J. Menzel, G. Stein, R. Dahlmann: "Manufacture of N-Alloyed Steels in a 20 t PESR-Furnace", in *High Nitrogen Steels HNS90*, Aachen, Oct. 10–12, 1990, Verlag Stahleisen, Düsseldorf 1990, pp. 365–375.
166. G. K. Bhat: "Plasma Arc Remelting" in J. Feinman (ed.): *Plasma Technology in Metallurgical Processing*, Chap. 13, Iron and Steel Society, Warrendale 1987, pp. 163–174.
167. K. Roesch, H. Zeuner, K. Zimmermann: *Stahlguß*, 2nd ed., Verlag Stahleisen, Düsseldorf 1982.
168. H. Wübbenhorst, G. Engels: *5000 Jahre Gießen von Metallen*, Gießerei-Verlag, Düsseldorf 1989.
169. F. Roll: *Handbuch der Gießerei-Technik*, Springer Verlag Berlin 1959.
170. H G. Gerhard, O. Nickel, K. Röhrig, D. Wolters: I.egiertes Gußeisen, vol. 1, 1970, vol. 2, 1974, Gießerei-Verlag, Düsseldorf.
171. G. Oehlstöter, J. Jäckel, *Stahl u. Eisen* **112** (1992) 53–60.
172. W Krämer, J. Schnyder, H. Feldmann, G. Kirchmann, *Stahl u. Eisen* **110** (1990) no. 6, 59–64.

173. A. Hensel, P. Poluchin (eds.): *Technologie der Metallformung*, Deutscher Verlag für Grundstoffindustrie, Leipzig 1991, p. 476.
174. W. Schupe, G. Thaler: "Überblick über den Entwicklungsstand der Ofenführung durch Rechnerunterstützung", *Stahl u. Eisen* **107** (1987) no. 20, 37–42.
175. L. Prümmer in VDEh (ed.): *Grundlagen des Beizens in Herstellung von kaltgewalztem Band*, Verlag Stahleisen, Düsseldorf 1970.
176. W. Bumbullis, G. Köhler, B. Schweinsberg: "Kaltwalzen auf flacher Bahn", *Beizeinrichtungen in Kontaktstudium Umformtechnik*, part II, 'seminar preprint, Verlag Stahleisen, Düsseldorf 1981.
177. B. Frisch, W. R. Thiele, *Stahl u. Eisen* **101** (1981) no. 9, 577–585.
178. B. Frisch, W. R. Thiele, D. Prediger, *Arch. Eisenhüttenwes.* **54** (1983) no. 8, 311–380.
179. B. Frisch, W. R. Thiele, C. Messerschmidt, *Arch. Eisenhüttenwes.* **54** (1983) no. 9, 375–380.
180. H. J. Heimhard, G. Hitzemann, *Stahl u. Eisen* **105** (1985) 1222–1228.
181. E. Neuschütz: "Planheitsmessung und -regelung beim Warm- und Kaltwalzen von Bändern", *Symposium DGM "Walzen von Flachprodukten"*, DGM-Informationsgesellschaft, Oberursel 1987.
182. B. Chatelain: "Einfluß der Glühparameter auf die Gas-Metall-Reaktion bei fest gewickelten Ringen", EGKS-Bericht EUR 12 115 FR.
183. B. Chatelain, V. Leroy: "Gas-Metall-Reaktionen beim Haubenglühen, Einfluß die Oberflächeneigenschaften des Blechs", EGKS-Abschlußbericht Nr. 7210/KB/204.
184. B. Chatelain et al.: "Beurteilung des Glühens von kohlenstoffarmen Stählen mit Wasserstoff–GasMetall-Reaktionen", *Rev. Metall.* CII, Feb. (1989) 173–180.
185. R. Pankert: "Durchlaufglühverfahren für Feinbleche im Vergleich", *Stahl u. Eisen* **105** (1985) 889 ff.
186. H. W Honervogt et al.: "Blankglühanlage für nichtrostende und säurebeständige Kaltbänder", *Stahl u. Eisen* **107** (1987) no. 9, 267.
187. J. Albrecht et al.: "Stand der Technik bei der Herstellung von Schmelztauchüberzügen", *Stahl u. Eisen* **107** (1987) no. 21, 973 ff.
188. J. H. Meyer zu Bexten, G. Gessner, K. F. Hüttebräucker, K. P. Mohr: "Elektrolytisch verzinktes Feinblech – Die Situation in Deutschland", *Stahl u. Eisen* **108** (1988) no. 21, 975 ff.
189. B. Meuthen, R. Pankert: "Stand der Breitbandverzinkung in Japan", *Stahl u. Eisen* **110** (1990) no. 6, 75 ff.
190. H. Lämmermann, K. Frommann: "Oberflächenveredelung von Band", Vakuumbeschichtung von Stahlband, Berichtsband, Verlag Stahleisen, Düsseldorf 1990.
191. W. Dürr, G. Höltzsch, J. Kuhn, W Schlump: "Aus der Dampfphase beschichtetes Blech und Band", *Stahl u. Eisen* **113** (1993) no. 5, 79–87.
192. P. von Laer, H. Hülsmann: *Herstellung von bandbeschichtetem Feinblech – Eigenschaften, Verarbeitung, Anwendung*, VDEh, DVV, Düsseldorf 1987.
193. P. Funke, H. R. Priebe, H. Buddenberg: "Die Untersuchung von Verfahrensparameters beim Walzplattieren", *Stahl u. Eisen* **110** (1990) no. 6, 67 ff.
194. H. Buddenberg, P. Funke, W. Gebel, R. Theile: "Herstellung und Eigenschaften NE-metallplattierter Stahlbänder für die Automobilindustrie", *Stahl u. Eisen* **111** (1991) no. 7, 93 ff.
195. Verein Deutscher Eisenhüttenleute (ed.): "Fundamentals", *Steel – A Handbook for Materials Research and Engineering*, vol. 1, Springer Verlag, Verlag Stahleisen, Düsseldorf 1992, p. 17.
196. G. Krauss in F. B. Pickering (ed.): *Microstructure and Transformations in Steel*, vol. 7, VCH Verlagsgesellschaft, Weinheim 1992, p. 1.
197. A. von den Steinen: *Gasturbinen, Probleme und Anwendungen*, Verlag Stahleisen, Düsseldorf,1967, pp. 131–146.
198. K. E. Heusler, *Z. Electrochem.* **62** (1958) 582.
199. T. Ramachandran, K. Bohnenkamp, *Werkst. Korros.* 30 (1979) 43.
200. E. G. Dafft, K. Bohnenkamp, H.-J. Engell, *Corros. Sci.* **19** (1979) 591.
201. M. Stratmann, *Ber. Bundesnges. Phys. Chem.* **94** (1990) 626.
202. U. R. Evans, C. A. J. Taylor, *Corros. Sci.* **12** (1972) 227.
203. K. Bohnenkamp, *Arch. Eisenhüttenwes.* **47** (1976) 751.
204. G. Schikorr, *Werkst. Korros.* **14** (1963) 69.
205. G. Herbsleb, H.-J. Engell, *Z. Elektrochem.* **65** (1961) 881.
206. C. Wagner, *Ber. Bunsenges. Phys. Chem.* 77 (1973) 1090.
207. N. Sato, G. Okamoto, *J. Electrochem. Soc.* **110** (1963) 605.
208. Y. M. Kolotyrkin, *Z. Elektrochem.* **62** (1958) 664.
209. K. Osazawa, H.-J. Engell, *Corros. Sci.* 6 (1966) 389.
210. K. J. Vetter, H.-H. Strehblow, *Ber. Bunsenges. Phys. Chem.* **74** (1970) 1024.
211. J. E. Truman in J. Foct, A. Hendry (eds.): *Proc. I. Int. Conf. High Nitrogen Steels*, Institute of Metals, London 1989, p. 225.
212. R. Stefec, F. Franz, A. Holecek, *Werkst. Korros.* **30** (1979) 189.
213. N. Lukomski, K. Bohnenkamp, *Werkst. Korros.* **30** (1979) 482.
214. J. W. Oldfield, W. H. Sutton, *Br. Corros. J.* **13** (1978) 13.
215. K. Bungardt, E. Kunze, E. Horn, *Arch. Eisen hüttenwes.* **29** (1958) 193.
216. J. J. Demo, A. P. Bond, *Corrosion (Houston)* **31** (1975) 21.
217. B. Strauß, H. Schottky, J. Hinnüber, *Z. Anorg. Chem.* **188** (1930) 309.
218. I. Class, H. Gräfe, *Werkst. Korros.* **11** (1960) 5–29.
219. G. Herbsleb, *Werkst. Korros.* **19** (1968) 406.
220. D. L. Davidson, F. F. Lyle, *Corrosion (Houston)* **31** (1975) 135.
221. H.-J. Engell in J. C. Scully (ed.): *The Theory of Stress Corrosion Cracking in Alloys*, published by NATO Scientific Affairs Division, Brussels 1971, p. 86.
222. E. Brauns, H. Ternes, *Werkst. Korros.* **19** (1968) 1.
223. M. Ahlers, E. Riecke, *Corros. sci.* **18** (1978) 21.
224. M. Marek, R. F. Hochmann, *Corrosion (Houston)* **27** (1971) 361.
225. H. E. Hänninen, *Int. Met. Rev.* **24** (1979) 85.
226. M. O. Speidel, *Corrosion (Houston)* **33** (1977) 199.

227. A. Bäumel, H.-J. Engell, *Arch. Eisenüttenwes.* **32** (1961) 379.
228. K. Bohnenkamp, *Arch. Eisenhüttenwes.* **39** (1968) 361.
229. E. Wendler-Kalsch, *Werkst. Korros.* **31** (1980) 534.
230. W. Rädecker, B. N. Mishra, *Werkst. Korros.* **17** (1966) 193.
231. J. Küpper, H. Erhart, H. J. Grabke, *Corros. Sci.* **21** (1981) 227.
232. E. Riecke, *Werkst. Korros.* **29** (1978) 106.
233. E. Riecke, *Met. Corros. Proc. Int. Congr. Met. Corros. 8th* **1981**, no. 1, 605.
234. J. P. Hirth, *Metall. Trans.* **11A** (1980) 861.
235. R. A. Oriani, *Ber. Bunsenges. Phys. Chem.* **76** (1972) 848.
236. L. S. Darken, R. W Gurry, *J. Am. Chem. Soc.* **67** (1945) 1398.
237. J. Spencer, O. Kubaschewski, CALPHAD *Comput. Coupling Phase Diagrams Thermochem.* **2** (1978) 147.
238. B. E. F. Fender, F. D. Riley, *J. Phys. Chem. Solids* **30** (1969) 793.
239. A. Rahmel: in *Chemical Metallurgy of Iron and Steel*, ISI Publ., no. 146, London 1973, p. 395.
240. H.-J. Engell, *Acta Metall.* **6** (1958) 439.
241. K. Hauffe, H. Pfeiffer, *Z. Metallkd.* **44** (1953) 27.
242. E. T. Turkdogan, W. M. McKewan, L. Zwell, *J. Phys. Chem.* **69** (1965) 327.
243. F. S. Pettit, R. Yinger, J. B. Wagner, Jr., *Acta Metall.* **8** (1960) 617.
244. H. I. Grabke, *Ber. Bunsenges. Phys. Chem.* **69** (1965) 48.
245. H. J. Grabke, K. J. Best, A. Gala, *Werkst. Korros.* **21** (1970) 911.
246. C. Wagner, *Z. Phys. Chem. Abt. B* **21** (1933) 25; **32** (1936) 447.
247. K. Bohnenkamp, H.-J. Engell, *Arch. Eisenhüttenwes.* **33** (1962) 359.
248. H. Meurer, H. Schmalzried, *Arch. Eisenhüttenwes.* **42** (1971) 87.
249. W. Koenigsmann, F Oeters, *Werkst. Korros.* **29** (1978) 10.
250. L. A. Morris, W. W. Smeltzer, *Acta Metall.* **15** (1967) 1591.
251. A. D. Dalvi, W. W. Smeltzer, *J. Electrochem. Soc.* **121** (1974) 386.
252. C. Wagner, *Corros. Sci.* **9** (1969) 91.
253. G. C. Wood, I. G. Wright, T. Hodgkiess, D. P. Whittle, *Werkst. Korros.* **21** (1970) 900.
254. K. A. Hay, F. G. Hicks, D. R. Holmes, *Werkst. Korros.* **21** (1970) 917.
255. W. C. Hagel, *Corrosion (Houston)* **21** (1965) 316.
256. P. Tomaszewicz, G. R. Wallwork, *Corrosion (Houston)* **40** (1984) 152.
257. M. J. McNallan, W. W. Liang, S. H. Kim, C. T. King in R. A. Rapp (ed.): "High Temperature Corrosion", NACE 1983, 316.
258. H. J. Grabke, E. M. Müller, *Werkst. Korros.* **41** (1990) 227.
259. D. Bramhoff, H. J Grabke, E. Reese, H. P. Schmidt, *Werkst. Korros.* **41** (1990) 303.
260. E. Reese, H. J. Grabke, *Werkst. Korros.* **43** (1992) 547.
261. G. H. Geiger, R. L. Levin, J. B. Wagner, Jr., *J. Phys. Chem. Solids* **27** (1966) 947.
262. B. Swaroop, J. B. Wagner, Jr., *Trans. Metall. Soc. AIME* **239** (1967) 1215.
263. K. Hauffe, A. Rahmel, *Z. Phys. Chem. (Leipzig)* **199** (1951) 152.
264. R. A. Meussner, C. E. Birchenall, *Corrosion (Houston)* **13** (1957) 677.
265. E. T. Turkdogan, *Trans. Metall. Soc. AIME* **242** (1968) 1665.
W. L. Worrell, E. T. Turkdogan, *Trans. Metall. Soc. AIME* **242** (1968) 1673.
266. W. Auer, *Met. Corros. Proc. Int. Congr. Met. Corros. 8th* **1981**, no. 2, 649.
267. A. Rahmel, *Oxid. Met.* **9** (1975) 401.
268. T. Flatley, N. Birks, *J. Iron Steel Inst.* **209** (1971) 523.
269. R. P. Salisburg, N. Birks, *J. Iron Steel Inst.* **209** (1971) 534.
270. B. A. Gordon, V. Nagarajan, *Oxid. Met.* **13** (1979) 197.
271. R. A. Perkins in R. A. Rapp (ed.): *High temperature corrosion*, NACE, Houston, Texas 1981.
272. F H. Stott, F. M. F. Chong in D. B. Meadowcroft, M. J. Manning (eds.): *Proc. Conf. Corrosion Resistant Materials for Coal Conversion Systems*, Applied Science, London 1983, p. 491.
273. J. Stringer, "Sulfidation as Industrial Problem and Limiting Factor", Workshop on The High Temperature Corrosion of Alloys in Sulfur Containing Environments, Petten, Dec. 1985.
274. R. E. Lobnig, H. J. Grabke, *Corros. Sci.* **30** (1990) 1045.
275. F. Neumann, U. Wyss, *HTM Härterei Tech. Mitt.* **25** (1970) 253.
276. C. A. Stickels, C. M. Mack, M. Brachaczek, *Metall. Trans.* **11B** (1980) 471
277. H. J. Grabke, U. Gravenhorst, W. Steinkusch, *Werkst. Korros.* **27** (1976) 291.
278. A. Schnaas, H. J. Grabke, *Oxid. Met.* **12** (1978) 387.
279. H. J. Grabke, *Arch. Eisenhüttenwes.* **46** (1973) 603.
280. H. J. Grabke, *HTM Härterei Tech. Mitt.* **45** (1990) 110.
281. H. J. Grabke, *Mater. Sci. Eng.* **42** (1980) 91.
282. J. Wünning, *Härterei Tech. Mitt.* **23** (1968) 101; *HTM Härterei Tech. Mitt.* **39** (1984) 50.
283. K. Ledjeff, A. Rahmel, M. Schorr, *Werkst. Korros.* **30** (1979) 767, **31** (1980) 83.
284. G. M. Lai in: *High Temperature Corrosion of Engineering Alloys*, American Society for Metals, Materials Park, Ohio 1990, pp. 68–71.
285. J. C. Nava Paz, H. J. Grabke, *Oxid. Met. 39* (1993) 437.
286. H. J. Grabke, R. Krajak, J. C . Nava Paz, *Corros. Sci.* **35** (1993) 1141.
287. H. J. Grabke, R. Krajak, E. M. Müller-Lorenz, *Werkst. Korros.* **44** (1993) 89.
288. H. J. Grabke, C. B. Bracho-Troconis, E. M. Müller-Lorenz, *Werkst. Korros.* **45** (1994) 215.
289. H. J. Grabke, *Ber. Bunsenges. Phys. Chem.* **72** (1968) 533, 541.
290. I. Aydin, H -E. Bühler, A. Rahmel, *Werkst. Korros.* **31** (1980) 675.
291. W. Steinkusch, *Werkst. Korros.* **27** (1976) 91.
292. K. Lücke, *Arch. Eisenhüttenwes.* **25** (1954) 181.
293. A. Mayer, *Stahl u. Eisen* **83** (1963) 1169.

294. W Oelsen, K.-H. Sauer, *Arch. Eisenhüttenwes.* **38** (1967) 141.
295. W.-D. Jentzsch, S. Böhmer, *Neue Hütte* **11** (1974) 647.
296. R. M. Hudson, *Trans. Metall. Soc. AIME* **230** (1964) 1138.
297. G. J. Kor, J. F. van Rumpt, *J. Iron Steel Inst.* **207** (1969) 1377.
298. G. A. Nelson: *Steels for Hydrogen Service at Elevated Temperatures and Pressures in Petroleum Refneries and Petrochemical Plants*, API Publication 941, Washington, May 1983.
299. W. Pepperhoff: "Physikalische Eigenschaften", in Verein Deutscher Eisenhüttenleute (ed.): *Werkstoffkunde Stahl*, vol. 1, "Grundlagen", Düsseldorf 1984, pp. 401–433.
W. Pepperhoff: "Physical Properties", in Verein Deutscher Eisenhüttenleute (ed.): *Steel*, vol. 1, "Fundamentals", Düsseldorf 1992, pp. 379--411.
300. *Landolt-Börnstein*, 6th ed., **4**, 2a, 131–300.
301. K. K. Kelley, *J. Chem. Phys.* **11** (1943) 16–18.
302. D. C. Wallace, P. N. Siddles, G. C. Danielson, *J. Appl. Phys.* **31** (1960) 168–176.
303. M. Braun: "Über die spezifische Wärme von Eisen, Kobalt und Nickel im Bereich hoher Temperaturen", Dissertation, Universität Köln 1964.
304. W. Bendick, W. Pepperhoff, *Acta Metall.* **30** (1982) 679–684.
305. H. M. Ledbetter, R. P. Reed, *J. Phys. Chem. Ref. Data* **2** (1974) 531–618.
306. K. M. Koch, W. Jellinghaus: *Einführung in die Physik magnetischer Werkstoffe*, Deuticke, Wien 1957.
307. E. Kneller: *Ferromagnetismus*, Springer Verlag, Berlin 1962.
308. R. Kohlhaus, F. Richter, *Arch. Eisenhüttenwes.* **33** (1962) 291–299.
309. W Oelsen, *Stahl u. Eisen* **69** (1949) 468–475.
310. R. M. Bozorth: *Ferromagnetism*, Van Nostrand, New York 1955.
311. Y. Endoh, Y. Ishikawa, *J. Phys. Soc. Jpn.* **30** (1971) 1614–1627.
312. L. Kaulman, M. Cohen, *J. Met.* **8** (1956) 1393–1400.
313. H.-H. Ettwig, W. Pepperhoff, *Phys. Status Solidi A* **23** (1974) 105–111.
314. W. Bendick, H.-H. Ettwig, F. Richter, W. Pepperhoff, *Z. Metallkd.* **68** (1977) 103–107.
315. F. Richter, W. Pepperhoff, *Arch. Eisenhüttenwes.* **47** (1976) 45–50.
316. H. P. Hougardy: Umwandlung und Gefüge unlegierter Stähle. Eine Einführung, Ind ed., Verlag Stahleisen, Düsseldorf 1990.
317. *Atlas zur Wärmebehandlung der Stähle*, vol. 1, Verlag Stahleisen, Düsseldorf 1961.
318. E. Schulz, Jahrestagung IISI, Montreal, Canada, 7 Oct. 1991, *Stahl u. Eisen* **112** (1992) no. 5, 43–51.
319. K. A. Zimmermann, *Stahl u. Eisen* **111** (1991) no. 12, 36–40.
320. J. A. Philipp et al., *Stahl u. Eisen* **112** (1992) no. 12, 75–86.
321. J. A. Philipp, *World Steel & Metalworking Annu.* **1988**, 101–104 (SPG-Coburg).
322. J. A. Philipp, *World Steel Rev.* **1** (1991) 62–73.
323. E. Schulz, *Stahl u. Eisen* **113** (1993) no. 2, 25–33.
324. E. Höffken, J. Wolf, P. Kühn, *Thyssen Tech. ber.* **24** (1992) 119–127.
325. Verein Deutscher Eisenhüttenleute (eds.): *Stahlfibel*, Verlag Stahleisen, Düsseldorf 1989, p. 134.
326. Bundesverband der Deutschen Schrott-Recycling-Wirtschaft e.V. (ed.): *Vom Schrott zum Stahl*, Düsseldorf 1984, pp. 37, 38, 39.
327. Bundesverband der Deutschen Schrott-Recycling-Wirtschaft e.V. (ed.): *Vom Schrott zum Stahl*, Düsseldorf 1984, pp. 36, 37.
328. W. Ullrich, H. Schicks: "Aspekte zum Recycling von metallisch beschichtetem Stahl", *Stahl u. Eisen* **111** (1991) no. 11, 85, 86.
329. J.-P. Kleingarn: "Ruckgewinnung von Zink aus verzinktem Stahlschrott", *Feuerverzinken* **15** (1986) no. 3, Beratung Feuerverzinken, Düsseldorf.
330. In [324] pp. 121, 124.
331. International Iron and Steel Institute, Brussels.
332. Bundesverband der deutschen Stahl-Recycling-Wirtschaft e.V., Düsseldorf.
333. Bundesverband der Deutschen Schrott-Recycling-Wirtschaft e.V. (ed.): *Vom Schrott zum Stahl*, Düsseldorf 1984, pp. 11, 12.

7 Ferroalloys

RUDOLF FICHTE (§§ 7.1, 7.5, 7.9); FATHI HABASHI (§ 7.2, INTRODUCTORY PARAGRAPH); FRED W. HALL (§ 7.2, EXCEPT INTRODUCTORY PARAGRAPH); BERND NEUER, GERHARD RAU (§ 7.3); PETER M. CRAVEN, JOHN W. WAUDBY, DAVID BRUCE WELLBELOVED (§ 7.4); DEREK G. E. KERFOOT (§ 7.6); HERBERT DISKOWSKI (§ 7.7); EBERHARD LÜDERITZ (§ 7.8); JOACHIM ECKERT (§ 7.10); VOLKER GÜTHER, OSKAR ROIDL (§§ 7.11–7.12); GÜNTER BAUER (RETIRED), HANS HESS, ANDREAS OTTO, HEINZ ROLLER, SIEGFRIED SATTELBERGER (§ 7.12); HARTMUT MEYER-GRÜNOW (§ 7.13)

7.1 Introduction

Ferroalloys are master alloys containing elements that are more or less soluble in molten iron and that improve the properties of iron and steel. These alloys usually contain a significant amount of iron. Ferroalloys have been used for the last 100 years, principally in the production of cast iron and steel [1]. As additives, they give iron and steel improved properties, especially increased tensile strength, wear resistance, and corrosion resistance. These effects come about through one or more of the following:

- A change in the chemical composition of the steel
- The removal or the tying up of harmful impurities such as oxygen, nitrogen, sulfur, or hydrogen
- A change in the nature of the solidification, for example, upon inoculation [2]

Ferroalloys are also used as starting materials in the preparation of chemicals and pure metal; as reducing agents (e.g., the use of ferrosilicon to reduce rich slags); as alloying elements in nonferrous alloys; as starting materials for special products such as amorphous metals. Table 7.1 lists some commercial ferroalloys.

Over the years, the binary ferroalloys have been modified by the addition of further components. For example, magnesium is regularly added to ferrosilicon, which, when used in cast iron, produces a spheroidal graphite; and manganese or zirconium can be added to calcium–silicon.

Production. Generally, ferroalloys are prepared by direct reduction of oxidic ores or concentrates with carbon (carbothermic), silicon (silicothermic), or aluminum (aluminothermic, closely related to the Goldschmidt reaction; see section 7.2). However, roasted ores (e.g., for ferromolybdenum) and pure technical-grade oxides (for ferromolybdenum and ferroboron) are also used as starting materials.

The large-volume ferroalloys — *ferrosilicon*, *ferromanganese*, *ferrochromium* — are prepared continuously by carbothermic reduction in large, submerged-arc furnaces. The carbon is provided by coke, and the power supply ranges from 15 to 100 MVA. Ferromanganese is also produced in blast furnaces. Both ferromanganese and ferrochromium, because of their affinity for carbon, contain high concentrations of carbon (7–8 %). In contrast, ferrosilicon contains little carbon; in fact, the carbon concentration decreases as the silicon concentration is increased, e.g., ferrosilicon containing 25 % Si contains 1 % C, while that containing 75 % Si contains only 0.1 % C.

Table 7.1: Ferroalloys.

Alloy	Composition, %
Calcium–silicon	28–35 Ca 60–65 Si 6 Fe
Calcium–silicon–aluminum	15–25 Ca 10–40 Al 35–50 Si
Calcium–silicon–barium	15–20 Ca 14–18 Ba 55–60 Si
Calcium–silicon–magnesium	25–30 Ca 10–15 Mg 50–55 Si
Calcium–manganese–silicon	16–20 Ca 14–18 Mn 58–59 Si
Calcium–silicon–zirconium	15–20 Ca 15–20 Zr 50–55 Si
Ferroboron	12–14 B
Ferrochromium	45–95 Cr 0.01–10 C
Ferrosilicochromium	40–65 Cr 45–20 Si
Ferromanganese	75–92 Mn 0.05–8.0 C
Ferrosilicomanganese	58–75 Mn 35–15 Si
Ferromolybdenum	62–70 Mo
Ferronickel	20–60 Ni
Ferroniobium	55–70 Nb
Ferroniobiumtantalum	55–70 Nb 2–8 Ta
Ferrophosphorus	ca. 25 P
Ferroselenium	ca. 50 Se
Ferrosilicon	8–95 Si
Ferrotitanium	20–75 Ti
Ferrotungsten	70–85 W
Ferrovanadium	35–80 V
Ferrozirconium	ca. 85 Zr
Ferrosilicozirconium	35–42 Zr ca. 50 Si

Low-carbon ferromanganese (0.1–2 % C) or ferrochromium (0.02–2 % C) is produced in the following way: a silicon-containing alloy, ferrosilicomanganese or ferrosilicochromium, is made by carbothermic reduction of an appropriate ore and quartzite in a submerged-arc furnace. Then this silicon alloy is used for the silicothermic reduction of an appropriate ore in an electric-arc refining furnace. Oxygen is seldom used to reduce the carbon content.

Ferrophosphorus is a by-product of the carbothermic production of phosphorus. *Ferrotungsten* is produced carbothermically in small, high-power electric furnaces. *Ferroboron* is produced from carbon, iron, and boron oxide or boric acid in one- and three-phase electric furnaces. *Zirconium-containing ferrosilicon* is made carbothermically in electric furnaces from zircon ($ZrSiO_4$) or baddeleyite (ZrO_2); ferrosilicon, with either 75 or 90 % Si, is added.

Silicothermic reduction, with the addition of some aluminum, is used to prepare *ferromolybdenum* in refractory-lined reaction vessels. The energy released in the reaction is adequate to melt both metal and slag, and the solidified block of ferromolybdenum can be recovered easily. *Ferronickel* is also mainly produced by silicothermic reduction. Aluminothermic reduction is the method of choice for the production of *ferrovanadium*. The starting materials are vanadium(V) oxide, aluminum, and iron turnings, chips, stampings, or nail bits. The reaction is carried out in refractory-lined reaction vessels. The reaction produces enough heat to melt both metal and slag. In fact, inert materials must be added to keep the peak temperature lower. Ferrotitanium and ferroboron are also produced aluminothermically.

The production and use of titanium as a large-volume construction material yields enough scrap for *ferrotitanium* containing ca. 70 % Ti to be made by melting iron and titanium scrap together. *Ferrozirconium* containing 80–85 % Zr is also made by melting metal scrap and iron together. *Ferroselenium* is produced by the exothermic reaction of iron and selenium powders.

The production of ferroalloys is of great economic importance, especially in countries that have the raw materials and the energy supply. Alloy steels constitute an ever growing fraction of total steel production because of their superior properties. As an example of the importance of ferroalloys, an estimated 1.8×10^9 DM (ca. $\$0.8 \times 10^9$) of ferroalloys were consumed in 1986 by the steel industry in Germany.

Environmental Aspects. During the production of ferroalloys, the emission of undesirable substances into the environment must be kept under control. There are guidelines for this, e.g., see [3].

7.2 Carbothermic and Metallothermic Processes

Carbothermic processes are mainly used for the large-scale production of ferrosilicon, ferromanganese, ferrochromium, ferronickel, and ferrotungsten. Ferrophosphorus is a by-product of elemental phosphorus production by the carbothermic reduction of phosphate rock. Carbothermic processes for the production of ferroboron, ferrotitanium, ferrovanadium, and ferromolybdenum have been largely replaced by metallothermic processes, mainly aluminothermic and silicothermic.

7.2.1 General Considerations

7.2.1.1 Introduction[1]

The usual method of reduction by carbon is inapplicable to the reduction of refractory oxides and ores. The products commonly covered under this title are usually required to be low in carbon and they are avid carbide formers. Also, no conventional refractories would stand up to the long reduction times at the high temperatures required. For such products, ad-

[1] For the production of chromium by the aluminothermic process, see Chapter 46.

vantage is taken of the high temperatures achieved and the rapidity of metallothermic reactions using reactive metals, notably Al.

Early examples of such reactions are BERZELIUS' reduction of K_2TaF_7 by Na and WÖHLER's reduction of $AlCl_3$ by Na, in 1825 and 1828, respectively. However, the father of aluminothermic processes was undoubtedly GOLDSCHMIDT who, in 1898. described the production of low-carbon, high melting-point metals, without extraneous heat, by feeding an exothermic mix into an already ignited first portion [4].

The term "aluminothermic processes" can cover a wide field. For the present purposes it is taken. as is generally understood, to be the manufacture, by Al reduction of refractory oxides or ores, of metals and alloys mainly used in the steel and superalloy industries. Because some important alloys are produced aluminosilicothermically, they are included in the survey.

The main alloys under discussion are FeB, FeMo, FeNb, FeTi, FeV, and FeW. There are many minor variations, such as CrC, where superior purity or the absence of Fe is required for alloys used in superalloy production, and FeNb from Nb_2O_5 instead of ore, where extra purity is required, again for superalloys.

Aluminothermic Mn, formerly of importance, has been superseded by electrolytic Mn, and aluminothermic production of FeTi has largely given way to induction furnace melting of Fe and Ti scraps. The latter method also now substitutes for the former, dangerous, highly exothermic production of 55–60% TiAl and 55–60% ZrAl. When possible, combined electroaluminothermic methods can be used.

Because most basic reactions require extra heat this is provided by Al and a vigorous oxidant. Aluminum is an expensive fuel. At an Al powder price of $1400/t and a small-scale electricity cost of 4.9 C/kWh the heating effect of Al combustion costs about three times that of electricity.

Although a minor proportion of production, some FeB, FeNb, FeTi, and FeV is produced in the arc furnace. In view of the small tonnages involved, such productions usually occur only where an arc furnace exists for other purposes.

Apart from the necessity of metallothermic reduction advantages of the process as compared to conventional reduction processes are:

- Very rapid reaction with less heat loss by radiation and convection
- Much less gas volume
- Easy accommodation of diverse productions
- Small plant investment (important, considering the small production).

A disadvantage of metallothermic production is that no refining of the metal is possible. It is important to leave the slag in situ to allow metal drops to settle into the regulus, so that one is faced with a large depth of slag quickly crusting over. Alternatively, if the slag is tapped, requiring subsequent ore dressing processes to recover included metal, the metal regulus quickly becomes sluggish. Therefore, the composition of the mix must be regulated very carefully to produce the optimum combination of oxygen and reactant metal levels in the product, and all ingredients must be low in harmful impurities. Obvious ones are C, S, and P. Other impurities in the various ores used for different products are As, Sn, Pb, Sb, and Cu. Nitrogen is not usually a problem because the metal regulus formed is protected by the slag layer. Chromium metal, used in superalloys and electric heating elements, is an extreme case, where, apart from low impurities generally, certain impurities, such as Ga, Pb, and B, must be kept down to a few parts per million.

Table 7.2: Production of metal and alloys by aluminothermic processes.

	t/a	Expressed as
FeB	1 350	18% B
FeMo[a]	40 500	65% Mo
FeNb	16 300	65% Nb
FeV	25 000	80% V
FeW	4 000	80% W

[a] The FeMo represents about one third of the total Mo used in the steel industry; the remaining two thirds are used as MoO_3.

The worldwide – excluding the former USSR and China – production of ferroalloys by aluminothermic processes is shown in Table 7.2.

7.2.1.2 Basic Metallurgy

A metallothermic reduction of a metal compound is possible when the reductant metal has a greater affinity for the nonmetal element of the compound than the desired metal. In various branches of metallurgy the nonmetal may be a halogen, sulfur, or oxygen. Aluminothermic processes, as previously defined, depend upon the high affinity of Al for oxygen as compared to that of many other metals.

Thermochemistry

Aluminum has a high affinity for oxygen, and the ease of reduction of a metal oxide depends on the difference in oxygen affinity of Al and the metal. The affinity for oxygen is indicated by its heat of formation, ΔH, expressed for comparison purposes as ΔH per mol/oxygen (kJ/mol O). Table 7.3 gives a selection of ΔH values at the standard temperature of 298 K.

A quantitative measure for the stability of an oxide is the Gibbs free energy of formation, ΔG, which is related to the heat of formation by the formula:

$$\Delta G_T^0 = \Delta H - T\Delta S$$

Table 7.3: Heats of formation of oxides [5].

Oxide	$-\Delta H_{298}$, kJ/mol oxide	$-\Delta H_{298}$, kJ/mol O
CaO	634.7	634.7
MgO	601.7	601.7
Al_2O_3	1678.5	559.4
ZrO_2	1101.5	550.6
TiO_2	945.4	472.7
SiO_2	911.0	455.5
B_2O_3	1272.8	424.1
Na_2O	415.3	415.3
Ta_2O_5	2047.3	409.5
Nb_2O_5	1900.8	380.2
Cr_2O_3	1130.4	376.8
V_2O_5	1551.6	310.2
WO_3	843.2	280.9
Fe_3O_4	1117.5	279.3
Fe_2O_3	821.9	273.8
FeO	264.6	264.6
MoO_3	745.7	248.7

where S is the entropy and is always zero or positive because it corresponds with the increasing atomic disorder of the system with temperature. Figure 7.1 shows the free energy of formation of the oxides of interest at high temperatures. All oxides become less stable as temperature increases. The more negative the free energy of formation at a given temperature the greater the tendency for that metal to reduce an oxide of less negative free energy.

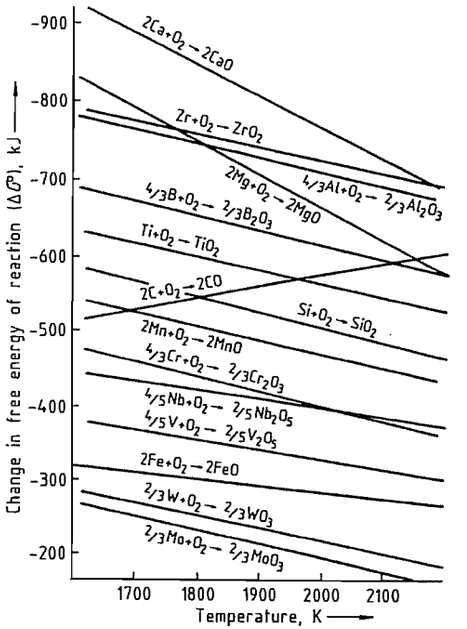

Figure 7.1: Change in free energy of oxide formation reactions [6].

The free energies of reaction of oxides with Al and Si are given in Figures 7.2 and 7.3.

Although the free energy of reaction is a quantitative measure, not all data necessary for such complex reactions as commercial metallothermic reactions are readily available and it is usual for the practicing metallurgist to rely on heats of formation for calculation of heats of reaction.

Fundamental Reactions

Although Ca and Mg may be the most suitable reactants, they are not used in the reduc-

tions under review. Their basic costs are high compared to Al and Si and 16 parts by weight O require 40 parts Ca, 24 parts Mg, 18 parts Al, or 14 parts Si. Furthermore, the boiling points of Ca and Mg are 1484 °C and 1090 °C, respectively. The heats of reaction of the oxides of interest with Al and Si are given in Table 7.4.

A guide for a successful aluminothermic reaction, permitting adequate separation of metal and slag, is a $-\Delta H_{298}$ higher than 300 kJ/mol [7]. This is confirmed in practice: additional heat is required for Cr production, whereas the reaction producing 80% FeV is so vigorous that it requires cooling. This guide does not apply to silicothermic reactions.

Auxiliary Reactions

Many reactions require additional heat to produce fully liquid metal and slag. Except for producing pure Cr, the first step is to make an addition of iron oxide plus reactant, giving a higher average heat of reaction. This also has the advantage of producing significantly lower melting points (Table 7.5).

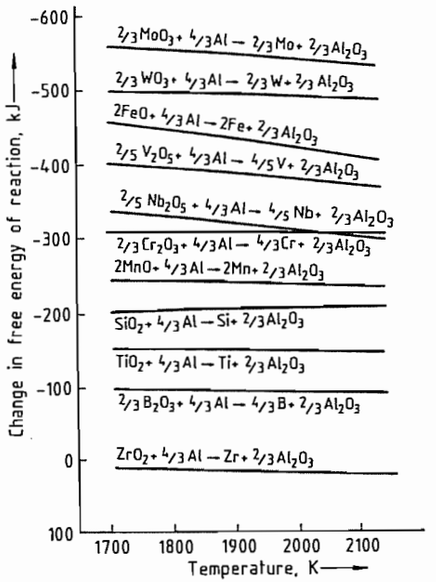

Figure 7.2: Change in free energy of reaction in the reduction of oxides by aluminum.

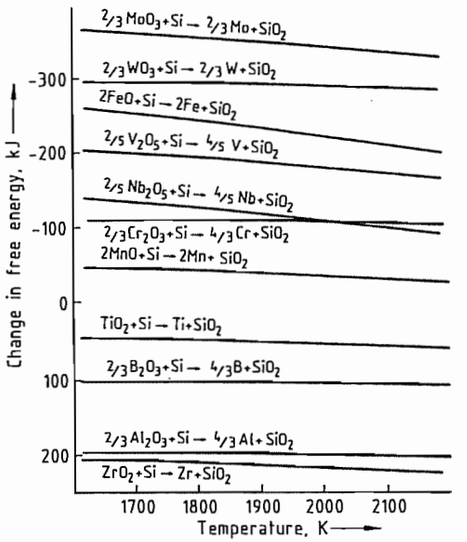

Figure 7.3: Change in free energy of reaction in the reduction of oxides by silicon.

Table 7.4: Heats of reaction per mole reductant.

	$-\Delta H_{298}$, kJ
$^3/_4TiO_2 + Al \rightarrow {}^3/_4Ti + {}^1/_2Al_2O_3$	130.2
$^3/_4SiO^2 + Al \rightarrow {}^3/_4Si + {}^1/_2Al_2O_3$	156.0
$^1/_2B_2O_3 + Al \rightarrow B + {}^1/_2Al_2O_3$	202.6
$^3/_{10}Nb_2O_5 + Al \rightarrow B + {}^1/_2Al_2O_3$	268.8
$^1/_2Cr_2O_3 + Al \rightarrow Cr + {}^1/_2Al_2O_3$	273.8
$^3/_{10}V_2O_5 + Al \rightarrow {}^3/_5V + {}^1/_2Al_2O_3$	373.9
$^1/_2WO_3 + Al \rightarrow {}^1/_2W + {}^1/_2Al_2O_3$	417.4
$^3/_8Fe_3O_4 + Al \rightarrow {}^9/_8Fe + {}^1/_2Al_2O_3$	420.2
$^1/_2Fe_2O_3 + Al \rightarrow Fe + {}^1/_2Al_2O_3$	428.3
$^3/_2FeO + Al \rightarrow {}^3/_2Fe + {}^1/_2Al_2O_3$	442.1
$^1/_2MoO_3 + Al \rightarrow {}^1/_2Mo + {}^1/_2Al_2O_3$	466.4
$^2/_3WO_3 + Si \rightarrow {}^2/_3W + SiO_2$	348.8
$^1/_2Fe_3O_4 + Si \rightarrow {}^2/_3Fe + SiO_2$	352.1
$^2/_3Fe_2O_3 + Si \rightarrow {}^4/_3Fe + SiO_2$	363.0
$2FeO + Si \rightarrow 2Fe + SiO_2$	381.8
$^2/_3MoO_3 + Si \rightarrow {}^2/_3Mo + SiO_2$	414.1

Table 7.5: Melting points of some metals (in °C) and of alloys of these metals with iron.

V	1902	80% FeV	1770
B	2180	16% FeB	1550
Nb	2468	65% FeNb	1560
Mo	2620	65% FeMo	1900
W	3410	80% FeW	2500

In silicothermic reactions, a proportion of Al is usually used to increase the exothermicity particularly, because the products, e.g., FeW and FeMo, have such high melting points.

Because the alloy specifications have become traditional, although not necessarily ideal, there is a limit to the amount of iron oxide and Al to be added, and, indeed, it may be more economical to increase the heat content of the mixture further, by using highly oxidic compounds plus Al. The reactions and the heats of reaction (in kJ/mol Al) for the additives most commonly used are:

$$K_2Cr_2O_7 + 4Al \rightarrow 2Cr + 2Al_2O_3 + K_2O$$
$$\Delta H_{298} = -422.0 \text{ kJ/mol Al}$$

$$3BaO_2 + 2Al \rightarrow 3BaO \cdot Al_2O_3$$
$$\Delta H_{298} = -812.0 \text{ kJ/mol Al}$$

$$NaClO_3 + 2Al \rightarrow Al_2O_3 + NaCl$$
$$\Delta H_{298} = -869.2 \text{ kJ/mol Al}$$

$$3KClO_4 + 8Al \rightarrow 4Al_2O_3 + 3KCl$$
$$\Delta H_{298} = -839.0 \text{ kJ/mol Al}$$

In some cases additional heat was applied formerly extraneously by preheating the charge. This has been given up because of practical difficulties of heating a mixture of low heat conductivity and the danger of premature ignition, with loss of the charge and damage to the preheating equipment.

The cheap nitrates are not used now because products low in nitrogen are required and the metals in question are avid nitride formers. BaO_2 is useful because it not only acts as an oxidant, but is a strong base and assists the progress of the reaction by combining with the Al_2O_3 produced. However, its high molecular mass and its one available oxygen atom make it a very expensive oxidant, and its use is confined to highly exothermic mixes, e.g., for TiAl and ZrAl, where it helps to smooth the reaction. The common oxidant is $NaClO_3$, but $KClO_4$ is to be preferred because it is more stable and $NaClO_3$ is hygroscopic. In Cr mixes, $K_2Cr_2O_7$ is used and is preferred to CrO_3 on health grounds as well as expense.

Fluxes

Both Al_2O_3 and SiO_2 have high melting points, 2050 °C and 1722 °C, respectively. The aim in metallothermic reactions is to produce a fluid slag, so as to permit good separation of slag and metal. In the case of aluminosilico reactions, residual iron oxide and Al_2O_3 are already good fluxes, and lime also is used because the strongly basic CaO, apart from fluxing, lowers the activity of Al_2O_3 and SiO_2.

In aluminothermic reactions residual oxides may play a part, the compound $Al_2O_3 \cdot TiO_2$ having a melting point of 1590 °C; Na_2O and K_2O, not completely vaporized, also assist. The usual flux is CaO which has a pronounced effect on the melting point of Al_2O_3. It is not used in Cr manufacture as it spoils the slag for use in refractories and calcium chromite is a stable compound.

Figure 7.4 shows the effect on melting point of additions of several oxides to Al_2O_3.

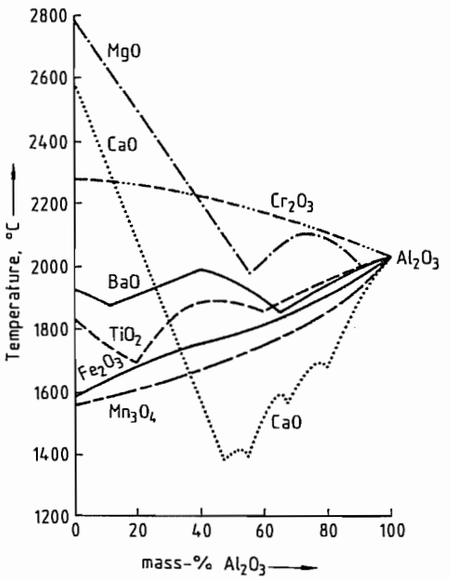

Figure 7.4: Melting point curves of binary alumina slags.

Table 7.6: Heats of formation of compound oxides.

Compound	$-\Delta H_{298}$, kJ/mol
$Al_2O_3 \cdot SiO_2$	192.6
$2Al_2O_3 \cdot B_2O_3$	69.5
$BaO \cdot Al_2O_3$	100.5
$CaO \cdot Al_2O_3$	15.1
$CaO \cdot SiO_2$	89.2

Table 7.7: Heats of formation of intermetallic compounds.

Compound	ΔH_{298}, kJ/mol
FeTi	40.6
FeB	29.3
$FeAl_3$	112.2
FeSi	77.0
TiAl	80.8
CaSi	150.7
AlB	67.0

The energy required to fuse the flux is partially compensated by the heats of formation of the compound oxide (Table 7.6).

Formation of Intermetallic Compounds

The heat of reaction of the mixture can be increased by the formation of intermetallic compounds. Table 7.7 gives some examples. However, this is restricted in that most of the higher heats of formation belong to unwanted compounds because the usual aim is to keep residual elements, such as Al and Si, to a minimum. Of the alloys considered it is only in the case of FeTi and to a lesser extent in that of FeB that aluminides have some significance.

All reactions are equilibria. Commercial alloys must be low in oxygen and most alloys can be produced at 1 % Al or Si without appreciable oxygen content. This is not the case with FeTi, where the equilibrium cannot be driven further than Al levels of 4–6 %.

Thermochemistry in Practice

A commercial metallothermic reaction must provide sufficient heat to drive the reaction as far to the right side of the equation as possible, plus that heat required to bring the products to a temperature sufficiently high to permit separation of metal and slag and to provide for heat losses. The amount of total heat must be the minimum required, because heat is expensive and because excess heat supplied to an exothermic reaction moves the equilibrium in the undesired direction.

Heats of formation have not always been determined at the high operating temperatures. Working on heats of formation at 298 K requires knowing the specific heats, latent heats, and, in charges employing sodium salts and chlorates, the heats of vaporization. Slags can be complex so that little idea can be had of their heats of formation. The amount of heat losses cannot be forecast and varies with the size of charge. Losses can be established and compensated for only by trial and error.

Therefore, available information is used as much as possible, accompanied by intelligent extrapolations of such information. Final adjustments to the charge are a matter of trial and error. A very simple example is:

$$Cr_2O_3 + 2Al \rightarrow 2Cr + Al_2O_3 \quad \Delta H_{298} = -548\ kJ$$

Heat required for products at 2000 °C:

Al_2O_3	$H_{2273} - H_{298}$	356 kJ
2Cr	$H_{2273} - H_{298}$	184 kJ
amounts to:		540 kJ

According to this, there is a heat balance, so there should be a satisfactory result. However, it is found in practice that 125 kJ extra heat are required, provided by Al plus $K_2Cr_2O_7$ and/or $KClO_4$. This 125 kJ (for a certain size of charge) is a measure of the heat losses. More would be required for small charges and less for bigger charges. It is interesting that this conforms with the guide.

Chemical composition of ores is some guide to improving the heat balance. Generally the higher the state of the oxide in the ore, the higher the heat of reaction with Al or Si. A classical example was that of Mn ore where the reaction $3MnO + 2Al \rightarrow 3Mn + Al_2O_3$ did not supply sufficient heat. A preoxidation to Mn_3O_4 produced a satisfactory result. Preoxidation also is found beneficial to some ilmenites.

There are many other factors affecting the fine control of an exothermic reaction, and it is not always economic to indulge in laboratory control of all of them. They mainly affect the

speed of the reaction, which should be an optimum to minimize heat losses but not to create excess heat with its adverse effect on the equilibrium.

Granulometry. If the charge is to be reacted in bulk then the ideal would be a charge of concrete-type granulometry, giving maximum contact and minimum air inclusion. However, to provide effective heat control, charges usually are fed. There should be an optimum particle size of the ingredients, therefore, coarse enough to minimize dust losses but fine enough to give an adequate speed of reaction. Aluminum powder can be controlled, because suppliers will supply within reasonable size ranges. In some cases, such as the highly exothermic FeV reaction, Al pellets and turnings can be used and they are used also to some extent in the very competitive production of the cheap alloy FeTi. These are crude raw materials and different parcels require slight adjustments to the mix. Ores are a different matter. These must usually be used as they arise; the coarser they are in any one production, the more the amount of heat required. Where ores are extremely fine, leading to high dust losses, it may be economical to pelletize.

Mineralogic Structure of Ores. Complex ores, such as pyrochlore, can vary widely in structure, and different parcels require adjustments to the mix.

Bulk Density. This is related to granulometry, but even in Cr_2O_3, which would be expected to be uniform from parcel to parcel and where grain sizes are of a few microns, variations in the supplier's final calcination temperature can affect the bulk density greatly and hence the recovery.

Mass of Charge. The percentage of heat losses varies inversely with the size of charge. These losses cannot be measured, but when the mass of a charge is increased, less heat per unit charge is required; this decrease can be obtained by an intelligent estimate finalized by trial and error.

Rate of Feeding. This is very much an art and efficient feeding can minimize some of the above mentioned difficulties. The general aim is to maintain a cover of unreacted mix on the surface of the liquid slag, so as to minimize radiation losses but not to feed too fast and produce too hot a reaction.

It can be seen from the above that whereas thermochemistry plays a vital role in providing the basic knowledge for any metallothermic production, there are other "fine tuning" adjustments that are a matter of experience.

7.2.1.3 Commercial Production

There are two methods of promoting the reaction. One is to fill the reaction vessel with the charge and ignite it via an easily ignitable mixture, such as BaO_2 or Na_2O_2 plus aluminum; the reaction then proceeds from top to bottom of the charge. This is a wasteful method because only approximately one third of the capacity of the reaction vessel is used. The mix calculation must be very accurate because no control of the speed of reaction can be exercised. Because the charge is always covered by liquid slag, dust losses should be low, but there can be considerable loss by splashing owing to the violence of the reaction. The short reaction time should mean low heat losses, but this advantage is counteracted by the intense radiation from an always liquid surface. This method is seldom used, but there are some reactions that are so exothermic that they are dangerous and practically impossible to feed, such as those for the minor products 55–60 % TiAl and ZrAl. This "firing down" method is used sometimes also for FeW production, where the extra heat supplied to achieve the high melting point requires a highly exothermic reaction near the limit of feedability.

The second method, almost universal, is to use a charge slightly more exothermic than that for "firing down", to ignite a small portion in the reaction vessel, and to feed the remaining charge. By doing so, the full capacity of the vessel is used so that vessel preparation costs per unit production are approx. one third those of the "firing-down" method. Another great advantage is that the speed of the reac-

tion can be controlled by varying the feeding rate so that it gets neither too hot nor too cold. As mentioned previously, this is quite an art, but it is surprising how soon a skilled worker becomes used to visual control of the temperature of the reaction.

There are also two types of reaction vessel. One is a mobile steel pot, lined with refractory. The other is a sand bed into which cylindrical holes are dug and lined with firebrick. This latter method usually is confined to alumino-silico reactions, such as those for FeW and FeMo.

Pot reactions are carried out in firing chambers, where the under pressure, as compared to that outside, is kept to the minimum required for complete exhaust of fume consistent with the charge feeder's need to observe the reaction but to keep dust losses to a minimum. *Sand bed reactions* are usually under a movable hood connected to the main flue. Whereas tall chimneys were once the solution to disposal of fume, modern conceptions of pollution control demand efficient dust collection. Owing to the volatility of MoO_3, this production demands its separate dust collector, the recovery from which makes the difference between profit and loss on the operation. For other productions, because of the small tonnage of individual products and because the fume is largely Al_2O_3, CaO, NaOH, etc., with low contents of valuable oxide, a communal collector is used. Collectors are of many types, but the most efficient is the reverse-jet filter. Because of the presence of CaO, NaOH, etc., the filter, when not in use, must always be kept above 100 °C to prevent caking of the fume on the bags.

Figure 7.5 shows the arrangement, in principle, for feeding, reaction in a chamber, and fume extraction. After firing, the reaction pots must be left to cool to allow final settling out of metal droplets and eventual solidification. Depending on the size of the reaction, solidification can take a long time, but 24 h, which often fits in with the overall routine of the production, is usually sufficient. The pot is then stripped, leaving a block of metal with adherent block of slag. The whole is then carefully quenched in a water tank, which causes the slag block to separate and embrittles the metal to some extent, facilitating subsequent crushing.

The sides of the metal block are surrounded by an adherent mixture of metal and slag created by penetration into the refractory lining. This easily breaks away and is consumed in the next reaction. The top surface, containing pockets of very adherent slag, requires removal by automatic hammers and, in the last resort, by hand chipping hammers. The bottom of the block usually requires less attention. Final cleaning of the whole block is by shot blasting.

The block is coarsely broken up by a mobile hammer of the pile driver type and crushed to desired size in jaw crushers and/or rotary crushers with intermediate screenings. There is immense variety in customer's size requirements, ranging from, say, 15-cm lumps for bulk users down to graded powders for welding rod manufacturers. An increasing demand is for bags of 6 mm and down alloy, each containing a fixed weight of the desired alloying element.

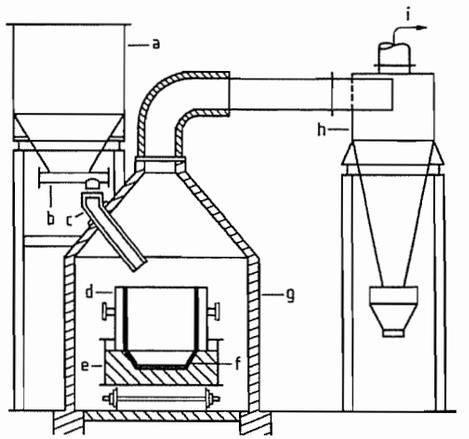

Figure 7.5: Reaction chamber with feeding hopper, reaction vessel, and dust collector: a) Feeding hopper; b) Feed-regulating valve; c) Feeding chute; d) Separable refractory-lined steel plate cylinder; e) Refractory-lined base; f) Optional magnesite inner lining; g) Firebrick-lined chamber; h) Filter; i) Offtake to chimney.

Pot Design and Construction

Although there is theoretically no limit to the size of the charge, as compared to steel production, the weights are small for the following reasons:

- *Costs.* Overall, raw materials are expensive. It is the aim of a producer to try to keep pace evenly with sales, holding modest stocks of raw materials and finished product. The total annual production of any one producer is small and diverse, with, in some cases, several specifications for one product.
- *Handling Facilities.* The total weight of a refractory-lined pot full of metal and slag is about three times that of the metal produced. Crane size is limited by cost and the small building required for carrying out the reactions, and for total operation lift trucks are convenient.
- *Preliminary Metal Breaking.* The small tonnages involved preclude a very expensive, large, preliminary breaking plant. Some alloys, particularly FeMo, are very tough and metal block thickness is usually limited to 30–35 cm.
- *Metal Specification.* Some residual specifications are very tight, notably that for Al in Cr metal. A mishap in the weighing of the charge can produce an off-grade block that may be in stock for a long time.
- *Refractory Failure.* Although rare, there can be an occasional failure of the refractory, producing breakout of metal and slag at high economic loss.

Therefore, metal block weights usually vary between 1000 and 2500 kg and, depending on the density of metal and slag, two pot sizes suffice. A small pot of ca. 200 kg metal capacity is useful for intermediate size investigations on new raw materials. A typical pot covering 1000–1750 kg metal would have internal dimensions of ca. 100 cm diameter and 125 cm height and one for 2500 kg would have the same height but be of 120 cm diameter in order to avoid too thick a metal block.

The outer construction consists of a plate steel cylinder attached to a heavy steel base by quick-acting lugs. The base may be on wheels or adapted for lift truck operation. The lining is of moistened, crushed slag from chromium or ferrovanadium production, because this is a reasonably pure corundum. To ease cleaning of the metal block, magnesite tiles may be used in the metal zone, particularly for the hotter reactions. After preparation of the refractory base, either from bricks or ramming of crushed slag, the sides are rammed around a tapered, withdrawable template. Ramming is by hand, by pneumatic or electric hammer, or by jolting on a foundy jolt molding machine. The lining must then be dried for several hours to remove moisture. It is taken up to a dull red heat.

Basic sand bed operation is to construct a well in the sand bed from unmortared firebricks which takes the whole molten charge. After sufficient time is allowed for metal to settle out, a channel is made through the sand at the slag–metal interface level and the slap tapped off. A variation is to use a similar well in the sand bed sufficient to accommodate only the metal, topped by a firebrick-lined steel shell to accommodate the slag, with ample sand seal at the junction. After the reaction, the slag is tapped at the junction and the shell used several times.

Charge and Charge Preparation

Ideally, there would be an optimum size for raw materials, fine enough for a successful reaction but as coarse as possible to minimize dust losses. Fortunately, most oxides and ores are of reasonable size in these respects. Wolfram ores may have to be ground sometimes and it is known that very fine ores, such as pyrochlore, have been pelletized. Chromium oxide, at a grain size of a few µm, can be expected to give high dust losses but the grains have a strong tendency to self-adherence so that the particles are much larger. Even so, there is a slightly noticeable difference in recovery when different oxides are used, this varying directly with the final calcining of the oxide during its manufacture. The calcination increases grain size and density.

Auxiliary oxidants are of satisfactory grain size with the proviso that $NaClO_3$ tends to agglomerate on storage and must be sieved down to max. 1 mm before use. The minimum size of Al is limited by dust losses and the risk of dust explosions. It should not be below ca. BSS 240 = 64 μm. The size used in exothermic reactions then depends on the reaction. For chromium it is on the order of average 0.25 mm, for FeB and FeNb, 0.45 mm, and the Al powder can be partially substituted by cheaper foil powder. In the highly exothermic FeV reaction, where the V_2O_5 is in the form of flakes or lumps, only a little coarse powder is used to assist the start of the reaction, the bulk being pellets, chopped wire, and/or pure turnings. Despite the fine size of ilmenite and rutile, the same applies to FeTi production. Owing to the relative cheapness of the ores, Al is the most expensive ingredient, and cheap aluminum is used at the expense of Ti recovery.

In aluminosilico reductions only powders are used, in the case of FeMo because the ore is fine, in the case of FeW to obtain maximum speed of reaction so as to achieve the high temperature required. The reductants are Al powder and 75% FeSi, on the order of 0.25 mm average.

The amount of flux used is kept to a minimum in aluminothermic charges. Where sodium salts are used as auxiliary oxidants, residual Na_2O already lowers the melting point of the slag. A calcium salt is the usual flux because it has such a significant effect on the melting point of Al_2O_3 (Figure 7.4). Instead of CaO, CaF_2 often is used as its low melting point of 1418 °C assists in promoting a smooth reaction. The amount used is often 1–2% of the total charge, never more than 5%.

Significant quantities of $CaO–CaF_2$ are used in aluminosilico thermic reactions because it is important for their success to tie the SiO_2 produced. As can be seen from Table 7.5, CaO has a strong affinity for SiO_2.

After the components have been weighed out accurately, they are mixed completely in a gently acting mixer, such as a drum with lifters, V blender, or rotating cube. Duration of mixing can be determined only by practice and can be determined initially by analyzing samples taken at intervals.

The charge is then dropped into a feeding hopper.

Feeding

When a charge has been prepared accurately to produce the desired result, success depends on the efficiency of feeding. The usual method is to control the exit valve of the feeding hopper according to the visual observation of the speed of the reaction, making slight adjustments to compensate for momentary coldness or hotness. Additional finer control is often applied by means of a handrake in the feeding chute. A fast reaction, such as that for FeV, often requires cooling, and a second small hopper may be used to feed a portion of crushed FeV slag. A FeW reaction is fed as fast as possible.

Further Processing

Pot stripping, block cleaning, and crushing require no further description than given earlier, except to emphasize the importance of avoiding cross contamination. This is particularly the case with FeB. A small amount of B is very beneficial to a steel designed for it but an unknown amount can be disastrous.

Safety Precautions

It must be realized that exothermic production, inadequately supervised, can be a very dangerous operation. Aluminum powder and oxidants are themselves fire hazards, and risk is magnified, when they are in contact, maybe to explosive proportions.

Aluminum powder and oxidants must be stored separately and the latter kept clear of carbonaceous material. Only sufficient for a single charge should be brought to the mixing department, and, during weighing, the oxide or ore should be sandwiched between the Al powder and the auxiliary oxidant to avoid direct, concentrated contact.

Mixing plants should be grounded to avoid buildup of static electricity. During firing, overfeeding can cause violent eruptions. Lumpy $NaClO_3$ can cause explosions. In case of an inadvertent lining failure, a large enough well should be provided to accept all the charge.

The main causes of disastrous explosions are Al dust explosions, either primary, because of careless handling, or secondary, over an overfed reaction. It also has been known for the metal and slag, apparently solid, to be quenched while still liquid internally, creating a disastrous explosion.

Employees must be protected from inhalation of dust and physical contact with charge components. This is particularly the case with hexavalent compounds of Cr, which can cause the well-known chrome ulcers.

Housekeeping must be exceptional. Fine dust accumulated on roof beams has been known to combust spontaneously.

7.2.1.4 Other Uses of Aluminothermic Processes

A significant use of an aluminothermic process is the welding of railway and tramway line joints, where the reaction takes place in a small crucible, and the steel produced is tapped onto the joint. In a similar manner, heavy cracked steel components, such as rolls, are welded and worn parts are built up and remachined. Developments over the last few years are the repair of ingot mold stools, where the steel stream has worn a cavity, and of cracked ingot mold lugs.

The use of exothermic reactions in incendiary bombs, where the intense Fe_2O_3-Al reaction ignites the magnesium casing, is well known. Other military uses are for flares, which in the case of sea rescue give off colored smokes.

Milder reactions, damped down by insulating materials, are used in feeder head compounds, which are spread over the surface of liquid steel ingots in order to conserve the heat and minimize piping. For steel castings, similar compositions are formed into sleeves inserted in the sand mold to insure liquidity over the whole of the pouring time. Where large amounts of alloying addition are made to steel in the ladle, the cooling effect of the addition may be counteracted by the use of exothermic briquettes composed of alloy, Al, and oxidant. Minor uses are for jointing of Al and Cu cables by a CuO–Al reaction, and as slow reactions for hand warmers and food cans for explorers.

7.2.1.5 Possible Further Developments

Wherever alloys with low content are required, aluminothermic processes are necessary, and they have been brought to such an efficiency that little further improvement can be foreseen. Improved refractories may permit further transfer of some reactions to the arc furnace, saving Al plus auxiliary oxidant, but at present, those which can be envisaged possibly to stand up to the longer exposure are very expensive and have to compete with the self-produced refractory from an exothermic reaction.

Plasma processes are a possibility, the very high temperatures encouraging the oxide carbon reaction, but up to now there has been no success in driving the reaction to low C levels. Here again, refractories are a problem.

A relaxation of maximum impurity levels would be of mutual economic benefit to alloy maker and steel maker. Stringent specifications for superalloys are obvious, but when the small proportion of alloy used in many steels and the wealth of purification methods used in bulk steel production are considered, then some relaxation in impurity levels should be possible, enabling use of cheaper, more impure ores. Higher Al and/or Si levels would give better recovery and, where present specifications are very low, lower oxygen levels.

7.3 Ferrosilicon [10, 11]

The term ferrosilicon refers to iron–silicon alloys with Si contents of 8–95%.

Table 7.8: Composition of ferrosilicons (ISO 5445).

Designation	Chemical composition									
	Si		Al		P (max.)	S (max.)	C (max.)	Mn (max.)	Cr (max.)	Ti (max.)
	Over	Up to and including	Over	Up to and including						
FeSi 10	8.0	13.0		0.2	0.15	0.06	2.0	3.0	0.8	0.30
FeSi 15	14.0	20.0		1.0	0.15	0.06	1.5	1.5	0.8	0.30
FeSi 25	20.0	30.0		1.5	0.15	0.06	1.0	1.0	0.8	0.30
FeSi 45	41.0	47.0		2.0	0.05	0.05	0.20	1.0	0.5	0.30
FeSi 50	47.0	51.0		1.5	0.05	0.05	0.20	0.8	0.5	0.30
FeSi 65	63.0	68.0		2.0	0.05	0.04	0.20	0.4	0.4	0.30
FeSi 75 Al 1	72.0	80.0		1.0	0.05	0.04	0.15	0.5	0.3	0.20
FeSi 75 Al 1.5	72.0	80.0	1.0	1.5	0.05	0.04	0.15	0.5	0.3	0.20
FeSi 75 Al 2	72.0	80.0	1.5	2.0	0.05	0.04	0.20	0.5	0.3	0.30
FeSi 75 Al 3	72.0	80.0	2.0	3.0	0.05	0.04	0.20	0.5	0.5	0.30
FeSi 90 Al 1	87.0	95.0		1.5	0.04	0.04	0.15	0.5	0.2	0.30
FeSi 90 Al 2	87.0	95.0	1.5	3.0	0.04	0.04	0.15	0.5	0.2	0.30

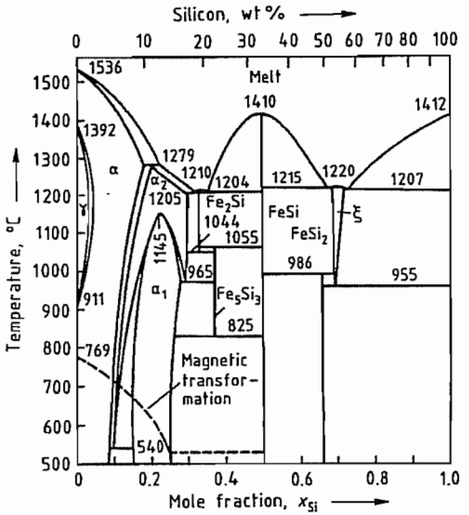

Figure 7.6: Iron–silicon phase diagram [12].

Table 7.8 lists the composition of commercial ferrosilicons.

FeSi75 is commercially the most important, although FeSi45 is still produced in large quantities for the North American market. Alloys containing > 95 % silicon are classified as silicon metal.

Physical Properties. The Fe–Si phase diagram (Figure 7.6) shows the existence of four compounds: Fe_2Si, Fe_5Si_3, FeSi, and $FeSi_2$ [12]. Commercial alloys differ from the compounds shown in the phase diagram with regard to their stoichiometry.

During solidification of the standard grade, FeSi75, silicon crystallizes initially, followed by solidification of the ξ-phase—the high-temperature phase of $FeSi_2$—at 1207 °C. FeSi45 is composed of initially separated FeSi and $FeSi_2$, which is stable below 955 °C [13].

Transformation of the ξ-phase to stable $FeSi_2$ is accompanied by an increase in volume, which can lead to disintegration of the alloy in the range of 45–65 % silicon. The transformation and thus the disintegration can be suppressed by supercooling (i.e., rapid solidification in shallow molds).

Structural data for the iron silicides are summarized in Table 7.9. Table 7.10 lists the densities and melting ranges of commercial alloys.

Table 7.9: Crystal structure of iron silicides.

Compound	Crystal structure	Lattice constants, pm
Fe_5Si_3	hexagonal	$a = 675.5$, $c = 471.7$
FeSi	cubic	$a = 448.9$
$FeSi_2$	tetragonal	$a = 269.2$, $c = 513.7$

Table 7.10: Density and melting range of commercial FeSi alloys.

Alloy	ρ, g/cm³	Melting range, °C
FeSi 10	7.3	1280–1350
FeSi 25	6.5	1270–1350
FeSi 45	5.1	1250–1350
FeSi 75	3.2	1250–1350
FeSi 90	2.5	1300–1400

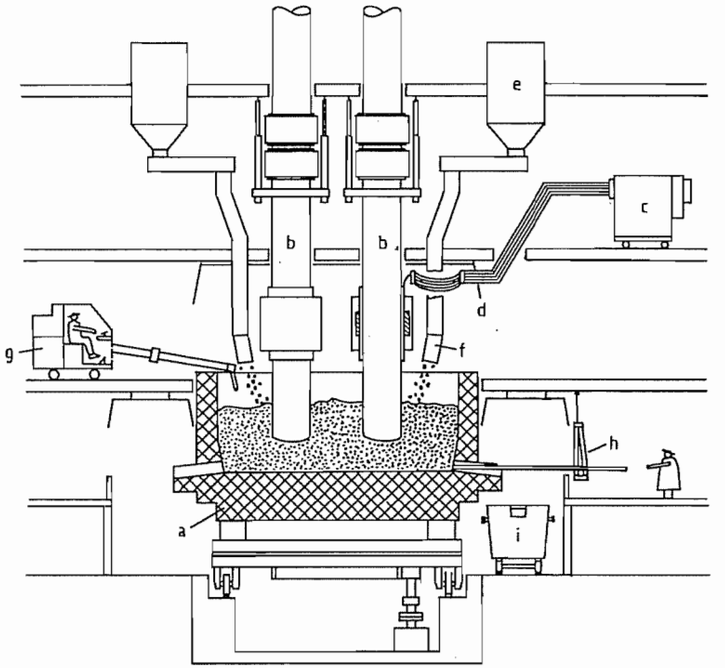

Figure 7.7: Submerged arc furnace: a) Furnace casing with lining (rotatable); b) Electrodes; c) Transformers; d) Secondary power supply; e) Raw material bunker; f) Charging pipes; g) Stoker machine; h) Burning-out unit; i) Tapping-off ladle.

Raw Materials. Pure quartzes with SiO_2 content > 98 % are used for the production of FeSi45 to FeSi90. Such quartzes occur naturally as pebbles or rock (vein quartz, quartzite). Quartz sands are processed into briquettes, in which the reducing coal required for a quasi-self-fluxing burden can be incorporated. For good gas flow through the furnace, the starting materials should be free of fine particles, which also requires that they remain dimensionally stable on heating and do not decrepitate too early.

Depending on the location, high-quality iron ore or scrap iron is used as the iron source. In industrialized countries, washed and dried unalloyed steel turnings are generally used.

Flaming coals with low ash content, metallurgical coke, high-temperature brown coal coke, petroleum coke, brown coal briquettes, or wood chips are employed as reducing agent, depending on availability. In calculating the amount of reducing agent required, the carbon resulting from consumption of the Söderberg electrodes must be taken into account; the electrodes supply 5–10 % of the total requirement.

The trend is toward the use of finer-grained quartz and coal. For quartz (previously 15–100 mm) the particle size now used is 8–40 mm; for coal, 2–20 mm.

Production. Ferrosilicon is produced in three-phase, submerged arc furnaces with power consumptions of 10–70 MW, corresponding to an annual capacity between 9×10^3 and 60×10^3 t per furnace.

Figure 7.7 shows a schematic of such a furnace. With few exceptions, production is carried out in open furnaces, which allow the burden surface to be poked with stoker machines to prevent crust formation and thus maintain uniform gas flow through the fur-

nace. In modern furnaces the furnace casing can be rotated to reduce encrustation in the lower areas.

Closed furnaces must be built with a rotating furnace vessel to avoid sintering of the burden, since stoker machines can no longer be used. Closed furnaces operate more efficiently (cheaper) because the carbon monoxide gas formed can be used. However, this requires a more elaborate construction of the furnace: with a rotatable hearth and extensive dedusting of the hot off-gases [14].

Generally, large furnaces with capacities of > 40 MW present additional construction and operational problems. The thermal stress of the refractory materials and the off-gas losses also increase because these furnaces have higher operating temperatures [15, 16].

Reactions in the furnace occur according to the simplified scheme:

$$SiO_2 + 2C \rightarrow Si + 2CO$$

$$Fe + Si \rightarrow FeSi$$

Side reactions also occur that result in a lower yield of the desired product, especially when insufficient carbon is used:

$$SiO_2 + C \rightarrow SiO + CO$$

$$SiO_2 + Si \rightarrow 2SiO$$

Gaseous SiO is oxidized by atmospheric oxygen at the burden surface to give SiO_2 dust, which is carried out of the furnace with the off-gas.

An excess of carbon leads to the formation of SiC, which also lowers the yield.

Specific material and energy requirements for the production of FeSi45 and FeSi75 are summarized in Table 7.11.

Table 7.11: Specific material and energy consumption for FeSi production.

	FeSi 45	FeSi 75
Quartz, kg/t	1200–1300	1800–2000
Iron turnings, kg/t	550–650	230–260
Carbon, kg/t	450–520	700–900
Söderberg paste, kg/t	40–50	55–70
Energy consumption, kWh/t	5800–6500	8500–10 000

Heating the batch to the reaction temperature of up to 1800 °C is achieved mainly by electrical energy (ca. 80%). The energy uptake of the batch depends on the so-called hearth resistance, whereby the conductivity of the FeSi burden is provided mainly by the coal. Thus, changing the type of coal influences the resistance. The grain size also plays a role: the smaller the grain, the higher is the resistance. The hearth resistance automatically regulates the depth of insertion of the Söderberg electrodes and thus the power consumption of the furnace. A uniformly high hearth resistance and low electrodes are desirable.

The liquid alloy, that accumulates in the hearth is tapped off to pouring ladles at regular intervals (about once an hour) and poured into shallow molds.

Ferrosilicon production is a slag-free process, which means that all the impurities present in the raw materials are transferred to the product. To obtain high purities the alloy must be purified by further treatment outside the furnace.

Aluminum and calcium impurities are removed by oxidation:

- By injection of gaseous oxygen through immersed lances or through nozzles or sparging blocks in the base of the pouring ladle
- By treatment with oxidizing siliceous slag, which can be stirred or blown in

Treatments used to obtain the lowest aluminum and calcium concentrations (in the extreme case, 0.02% max.) also result in silicon losses. The silicon content for these grades drops from 75 to ca. 65%.

Due to the low affinity of titanium for oxygen, the content of titanium impurities cannot be lowered metallurgically. Low Ti contents must be obtained by using raw materials that contain as little titanium as possible.

Environmental Protection. Silicon monoxide vapor is formed in the reduction process. The SiO is oxidized in air to produce extremely fine SiO_2 dust (particle size 0.1–1 μm), which is carried out of the furnace with the off-gas. Furthermore, small amounts of fine particles from the burden are also entrained. A total of 250–350 kg of dust is produced per tonne of FeSi75 [17].

The off-gas from the furnace can be cleaned in filter chambers (bag filters) to the maximum values allowed by TA Luft (20 mg/m^3). The collected dust is sometimes dumped but is now mainly sold as a raw material. Pure SiO_2 dusts are used as cement additives, for example [18, 19].

Since the FeSi process is slag free, it has the advantage of having no slag that must be disposed of.

Quality Specifications. Quality requirements and terms of delivery are summarized in ISO 5445 (see Table 7.8) and DIN 17560. In addition, numerous customer specifications exist, some of which require drastically reduced impurity contents. The sieve analysis of ferroalloys is set out in ISO 4551; sampling is described in ISO 4552; and chemical analysis, in ISO 4139 and ISO 4158. Recognized analysis methods are also described in [20–22].

Storage, Transport, and Toxicology. Ferrosilicons produce hydrogen on contact with water. Alloys containing 30–70% Si are classified as dangerous substances, Class 4.3, for transport by road and rail according to GGVS/GGVE and RID/ADR. Alloys with < 30% and > 70% Si are excluded from this regulation for land transportation. All commercial FeSi alloys are classified as dangerous goods, Class 4.3, for transportation by ship (IMDG Code) and by air (UN no. t408, IATA-DGR: Class 4.3).

Ferrosilicon itself is nontoxic. For handling the dust the general MAK values for fine dust (6 mg/m^3) are applicable [23], as well as the usual safety measures such as goggles and face masks.

On contact with water, traces of toxic gases such as phosphine can be formed by reaction with slag adhering to the ferrosilicon. However, if stored in ventilated rooms in accordance with regulations, the critical MAK concentrations are rarely attained (PH_3: MAK 0.1 ppm) [23].

Uses. Approximately 75% of the FeSi produced is used in the steel industry, where a requirement of 3–3.5 kg of FeSi75 per tonne of steel can be considered normal. For melting almost all grades of steel, silicon is added as a deoxidizer and alloying agent. Silicon binds oxygen dissolved in steel melts, leading to noncritical concentrations. To increase this effect, FeSi is generally added together with other deoxidizers such as aluminum, calcium, and manganese.

Silicon that is not consumed in deoxidation dissolves as an alloying element in the steel and increases its strength and yield point [24]. Conventional construction steels contain 0.2–0.4% silicon. More highly alloyed grades include tool steels, in which silicon improves the hardenability and wear resistance; hot-work steels that contain silicon for better tempering properties; spring steels (up to 2% Si); and transformer and electro steels (up to 4.5% Si). Low hysteris losses are characteristic of the latter materials. Since the magnetic losses depend on the purity of the steel, high-purity FeSi, with drastically reduced content of aluminum, carbon, and titanium, is used.

Foundries consume almost 25% of the ferrosilicon produced worldwide. Normal cast iron contains 2–3% silicon for improved precipitation of graphite and increased strength.

Ferrosilicon alloys are also used as carrier alloys for metals such as barium, strontium, calcium, and titanium, usually in amounts of 2–4%. These treatment alloys for gray cast iron are added to the ladle or mold to improve the precipitation of graphite. Ferrosilicon is also the prealloy for FeSiMg alloys; magnesium causes the formation of spherical graphite in spherulitic graphite iron.

Economic Aspects. In 1990, world consumption of ferrosilicon, calculated as FeSi75, was 3.4×10^6 t, which compared to a capacity of 5.5×10^6 t. Thus capacities were utilized only to ca. 62%. Usually, the rate of utilization varies between 65 and 75%. Thus, the economic situation at the beginning of the 1990s was characterized by marked pressure on prices and by the closure of unprofitable operations. However new capacities of ca. 250×10^3 t/a are now planned, with almost 200×10^3 t/a in Venezuela alone.

The choice of plant location depends less on the raw materials (quartz, coal) than on the availability of cheap electricity. Production is spread worldwide; the CIS and China are important producers (each with a capacity of ca. 10^6 t/a), followed by Norway, the United States and Brazil (each ca. 0.5×10^6 t/a).

7.4 Ferromanganese

A number of manganese-containing ferroalloys are manufactured which are used largely in the mild steel, foundry, and stainless steel industries [25–27]. The names and typical compositions of these alloys are given in Table 7.12, and the international standards for the most commonly used alloys, namely high-carbon ferromanganese HC FeMn and silicomanganese FeSiMn, are given in Table 7.13 [25]. These are generally classified as intermediate products and the range of their end uses is shown in Figure 7.8.

Table 7.12: Types of ferromanganese and their general compositions [27].

Alloy	Composition, %		
	Manganese	Carbon	Silicon
High-carbon ferromanganese (carburé)	72–80	7.5	< 1.25
Medium-carbon ferromanganese (affiné)	75–85	< 2.0	
Low-carbon ferromanganese (suraffiné)	76–92	0.5–0.75	
Silicomanganese	65–75	< 2.5	15–25
Ferromanganese silicon	58–72	0.08	23–35
Spiegeleisen	16–28	< 6.5	11–45

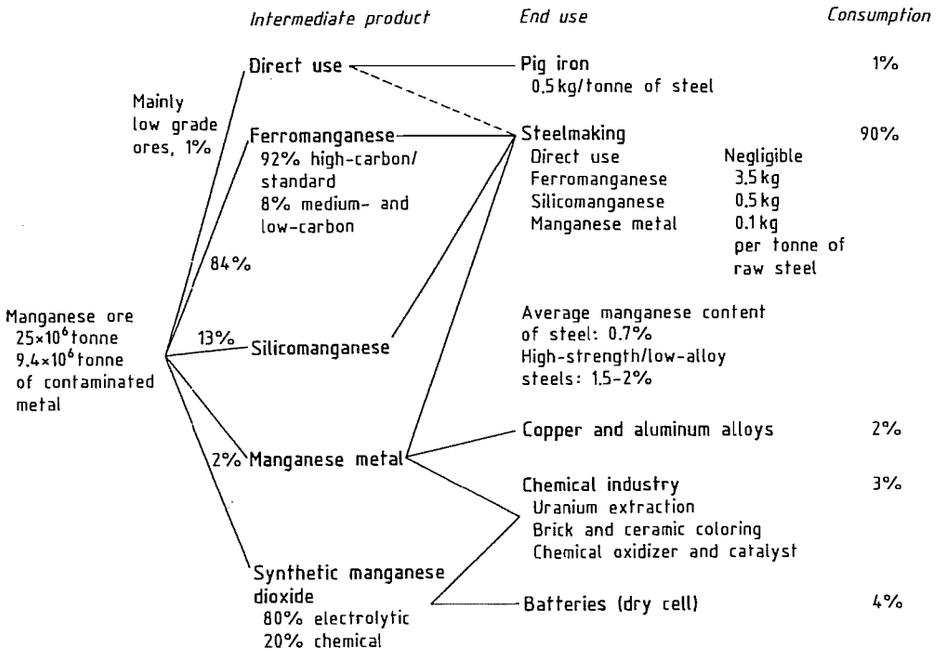

Figure 7.8: Manganese intermediate products and end uses.

Generally, high-carbon ferromanganese and silicomanganese are produced from a blend of manganese-containing ores, and in the case of silicomanganese, slags and silica are added. Ferromanganese can be produced in either electric submerged furnaces or blast furnaces, although only four blast furnace producers exist in the Western world [26], whereas silicomanganese is largely produced in submerged arc furnaces. Producers of high-carbon ferromanganese and silicomanganese are listed in Table 7.14. High-carbon ferromanganese can be converted to medium-carbon manganese by an oxygen blowing process, and silicomanganese can be further refined into medium- or low-carbon ferromanganese as well as manganese metal (Figure 7.9).

Table 7.13: Ferromanganese standards [25].

Alloy	Country or organization	Standard	Reference
FeMn	International Standards Organization	DIS	5446
	France	AFNOR NF	A-15-020
	Japan	JIS	G 2301
	United States	ASTM	A 99-66
	Former Soviet Union	GOST	4755-70
	Germany	DIN	17564
FeSiMn	International Standards Organization	DIS	5447
	France	AFNOR NF	A-13-030
	Japan	JIS	G 2304
	United States	ASTM	A 701
	Former Soviet Union	GOST	4756-70
	Germany	DIN	17564

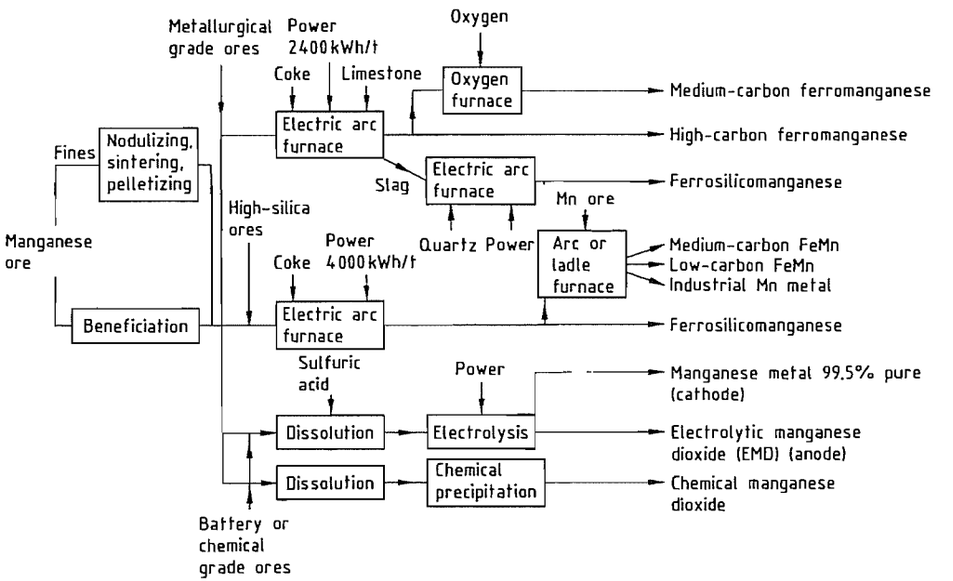

Figure 7.9: Summary of process routes.

Table 7.14: Producers of high-carbon ferromanganese and silicomanganese (producers of 10 000 t/a of either ferroalloy in 1988) [26].

Country	Company	Site	Capacity, × 10^3 t (1995)		Production, × 10^3 t (1995)	
			FeMn	SiMn	FeMn	SiMn
South Africa	Samancor	Meyerton	365	180	304	125
	Transalloys	Witbank	0	140	0	141
	Ferroalloys	Cato Ridge	170	0	129	0
India	Tisco	Keonjhar	18	12	13	9
	Facor	Shreeramnagar	21	0	12	0
	Khandelwal	Khandelwal Nagar	30	10	11	6
	Sandur Manganese	Hospet	40	5	36	3
	UF & A	Maneck Nagar	18	50	15	35
	Maharashtra Electrosmelt	Chandrapur	72	18	40	18
Japan	Nippon Denko	Hidaka	0	19	0	6
	Kobe Steel	Kakogawa	61	31	41	29
	Mizushima	Hurashiki	156	0	155	0
	Chuo Denki Kogyo	Kashima	85	57	71	33
	Nippon Denko KK	Tokushima	95	53	73	8
	JMC	Takaoka	85	7	55	3
Korea	Korea Ferroalloy	Pohang	37	48	37	27
	Dongil Chungong	Pohang	30	35	28	25
	Dongbu Industry	Tonghae	55	42	51	37
Taiwan	Chen Hsing Industrial	Taipei	30	20	15	0
Belgium	Sadaci	Gent	19	10	15	10
France	SFPO	Boulogne	390	0	337	0
	Pechiney	Dunkerque	0	60	0	55
Italy	Carlo Tassara	Breno	10	45	8	39
	Italghisa	Bagnolo Meila	15	33	11	32
Norway	Elkem	Porsgrunn	150	50	104	24
	Tinfos Jernverk	Kvinesdal	0	135	0	120
	Elkem	Sauda	150	60	127	65
Spain	Hidro Nitro	Monzón	0	40	0	10
	Fyesa	Boo de Guarnizo	35	46	30	30
	Carburos Metálicos	Cee	50	46	18	28
Argentina	Grassi	Malargue	27	24	10	20
Brazil	Paulista/Sibra	Various	163	255	122	230
	Maringa	Itapeva	20	30	10	24
Mexico	Minera Autlan	Teziutlan	0	28	0	19
	Minera Autlan	Tamos	86	65	78	65
Venezuela	Hevensa	Puerto Ordaz	0	70	0	52
USA	Elkem Metals	Marietta	120	80	112	56
Australia	Temco	Bell Bay	105	95	93	94
	Total, Africa		535	320	433	266
	Total, Asia		833	407	653	239
	Total, Europe		819	525	650	413
	Total, Latin America		296	472	220	410
	Total, North America		120	80	112	56
	Total, Australia		105	95	93	94
	World Total		2708	1899	2161	1478

Table 7.15: Composition of the former Soviet blast-furnace high-carbon ferromanganese [27].

Grade and official grade coke	Mn content, %	Si, %	Deleterious elements, not to exceed		
			P, % (group A[a])	P, % (group B[a])	S, %
Mn-5	75.0	2.0	0.35	0.45	0.03
Mn-6	70.0–75.0	2.0	0.35	0.45	0.03
Mn-7	70.0–75.0	1.0	0.35	0.45	0.03

[a] Furnace.

7.4.1 High-Carbon Ferromanganese

7.4.1.1 Production of Ferromanganese in Blast Furnaces [26–30]

Ferromanganese can be produced in blast furnaces in a manner similar to pig iron and spiegeleisen; however, in the Western world only four producers employ this method. These are Thyssen Stahl (Germany), BSC Cleveland (United Kingdom), SFPO (France), and Mizushima (Japan) (see Table 7.16, page 426), [26]. In the former Soviet Union, the majority of the high-carbon ferromanganese is produced in blast furnaces [27]. The choice of the use of blast furnaces over electric furnaces is based on the relative price of coke and electricity. Blast furnaces are usually used where the cost of power is high in relation to coke. In blast furnaces, coke is used both as a reductant and as the energy source. The coke rate in blast furnaces is higher than in submerged arc furnaces, which use electricity as the power source [28]. An exception to this is SFPO, where off-gases from the furnace are used to produce electricity, which is sold back to the local power supplier.

The product produced from blast furnaces generally contains 76% Mn and 16% Fe; the ferromanganese produced in the former Soviet Union is generally of a lower grade (Table 7.15) [27].

Raw Material Selection and Pretreatment. The raw materials required for the production of high-carbon ferromanganese are manganese ores, fluxes such as limestone, dolomite, or silica, and solid fuels and reductants such as coke.

In order to produce ferromanganese of the required grade a single ore is seldom suitable because the desired Mn/Fe ratio of the charge determines the Mn content of the final product [28]. Ores from various sources are therefore blended to achieve the ideal ratio and to limit the contents of the deleterious components silica, alumina, and phosphorus in the raw material mix.

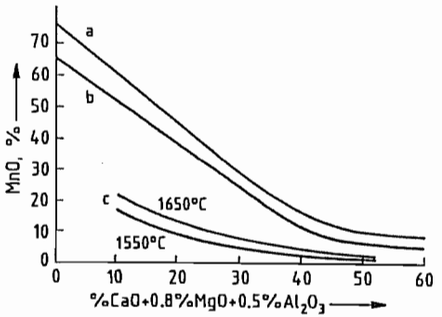

Figure 7.10: Variation of equilibrium MnO content of slag for high-carbon ferromanganese and silicomanganese production [31].

The raw material is crushed and screened to ca. 5–30 mm. Alternatively, sintered or pelletized fine ore can be used (see Section 47.4). Some deleterious components can be partially removed from the ore prior to melting by dense-medium separation or flotation. Slagging components (dolomite or limestone) can be added to the sintered or pelletized ore, which results in cost savings in the blast furnace. Partial reduction of the higher manganese oxides may also occur during sintering.

Blast Furnace Operation. In comparison to iron making, high gas temperatures are required in ferromanganese production because the reduction of manganese(II) oxide takes place at a higher temperature than is required for the reduction of wustite [29]. This is achieved by oxygen enrichment of the hot blast or, in the case of SFPO, by heating the blast with nontransferred arc plasma torches [30]. The plasma arc increases the flame temperature from 2200 to 2800 °C and considerably reduces the coke consumption, which usually ranges from 1270 to 2000 kg/t.

The recovery of manganese in the alloy is usually 75–85%. This is influenced by the MnO content of the slag, the slag-to-metal ratio, and losses in the flue gases. The MnO content of the slag is highly dependent on the basicity ratio (CaO + MgO)/SiO_2 (Figure 7.10) [31], which can be controlled by the choice of ore and addition of flux. Losses to the flue gas can generally be recovered in the gas cleaning section (see Section 7.4.5). These

materials can then be agglomerated and returned to the furnace.

At the Mizushima works, the double bell valve of the conventional blast furnace has been replaced with an arrangement incorporating a distribution chute (Figure 7.11) [32]. This results in a better distribution of the burden in the shaft and therefore a more even flow of gas through the burden (Figure 7.12). The incorporation of a distribution chute lowers the coke consumption of the furnace.

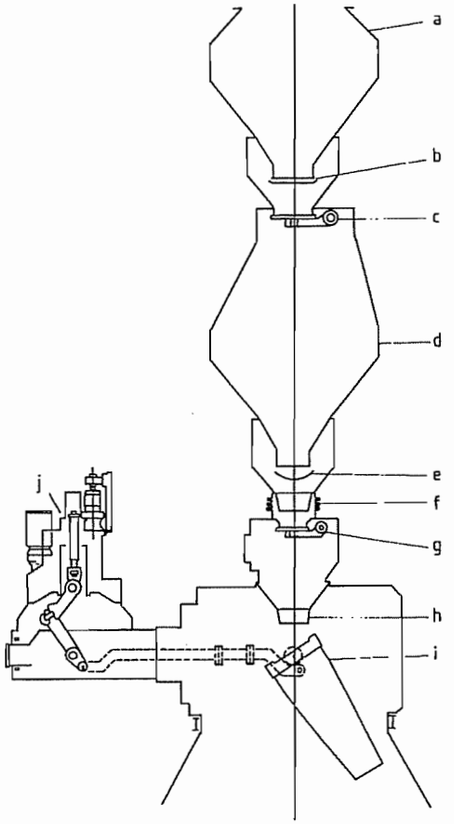

Figure 7.11: The cardan distributor on the blast furnace [32]: a) Upper bunker; b) Gate valve; c) Upper seal valve; d) Lower bunker; e) Material flow control gate; f) Expansion joint; g) Lower seal valve; h) Vertical chute; i) Distribution chute; j) Driving apparatus.

In spite of the innovations mentioned above the raw material costs of blast furnaces remain higher than those of submerged arc furnaces [26] due to the high cost of coke. With the exception of SFPO, blast furnace production costs are higher than the average production cost of ferromanganese in electric furnaces.

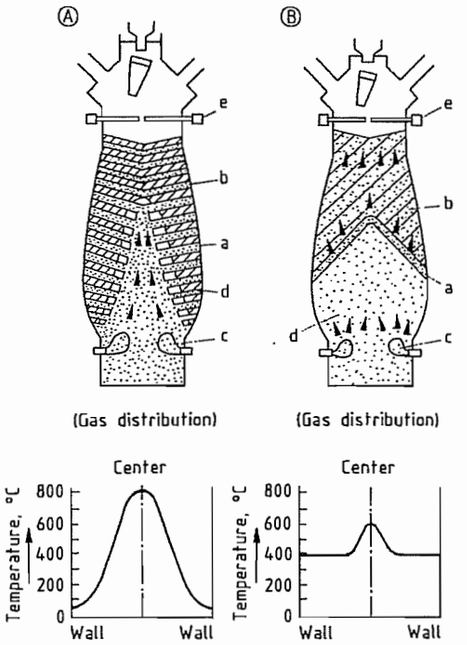

Figure 7.12: Effect of mixing on the distribution of gas in a blast furnace [32]. A) For layer by layer charging; B) For perfect-mixed charging. a) Cohesive zone; b) Lumpy zone; c) Raceway; d) Dead man; e) Throat sonde.

The Reduction Process in the Blast Furnace. The reduction of the higher manganese oxides to manganese(II) oxide takes place in the upper zone of the shaft according to the reactions given earlier. These generally occur below 900 °C and are indirect. The reactions are exothermic, and the heat generated causes high top temperatures and necessitates water cooling of the furnace top.

The reduction of manganese(II) oxide

$$MnO + C \rightarrow Mn + CO$$

is highly endothermic, in contrast to the weakly endothermic reduction of wustite. This requires higher temperatures and, consequently, higher coke rates are required for the smelting of ferromanganese in blast furnaces.

7.4.1.2 Production of Ferromanganese in Electric Arc Furnaces

The majority of producers of ferromanganese in the Western world use submerged arc electric furnaces (Table 7.16). Although electric furnaces have lower capacities than blast furnaces they have the advantage that the heat requirement is provided by electricity, and coke and coal are added to the feed only as reductants. Consequently the coke consumption is lower in electric furnaces than in blast furnaces, which is a considerable advantage in the light of dramatically increasing coke prices. An additional advantage is that the process is not entirely dependent on high-strength coke, unlike blast furnaces, and a portion of the carbon requirement can be supplied in the form of coal. In South Africa, where coking coal is in short supply, up to 70 % of the carbon for the production of ferro- and silicomanganese is supplied in the form of bituminous coal.

Originally electric furnaces were small (3–8 MVA); however, furnaces have grown progressively larger with time [33]. Recently built electric furnaces have capacities of 75–90 MVA. Smaller furnaces are still popular with producers because they offer flexibility in that they can be switched more easily between different products than their larger counterparts [34]. The larger size and more stable operation of modern electric furnaces, due largely to computer control, have resulted in lower electricity consumption. Electric furnaces used in the production of manganese alloys are generally circular and have three electrodes, each coupled to a separate electrical phase (Figure 7.13) [35]. The diameters of these furnaces range from 2 to 20 m.

In modern electric arc furnaces the raw material is usually fed by gravity from bunkers above the furnace. Fresh burden therefore automatically enters the furnace as the raw materials are melted and slag and metal are removed from the system. In older furnaces use is still made of charging cars to introduce raw materials to the top of the units.

As the raw materials move down the furnace, the higher oxides of manganese are reduced to MnO by the gas leaving the furnace. The reduction of manganese(II) oxide occurs by the contact of carbon with the molten oxide in the slag phase. The overall reaction is:

$$MnO + {}^{10}/_{7}C \rightarrow {}^{1}/_{7}Mn_7C_3 + CO$$

for which

$$G^0 = 265.7 - 0.18T \text{ kJ [36]}$$

The heat required for this endothermic reaction, for heating the burden, and to compensate for heat losses is supplied by the electrical input to the furnace. Heating takes place by the flow of electricity from the tips of the electrodes, which are submerged in the burden, through the burden and slag to the metal, as well as through the flow of electricity between the electrodes [36].

Design and Operation of Electric Furnaces

The degree of heating depends on the electrical current flow as well as the resistance provided by the burden and the slag to the flow of electricity. In the production of ferromanganese the resistivity of the burden is low, hence low voltages between the electrodes are necessary to maintain satisfactory penetration of the electrodes in the charge. The vapor pressure of manganese is high; therefore overheating of the charge must be avoided. The current densities on the electrodes should accordingly be lower for ferromanganese production than for other ferroalloys [37]. The diameters of the electrodes are therefore larger in ferromanganese furnaces than in other ferroalloy furnaces to facilitate the high currents required for low voltage operation. The distance between electrode centers is usually larger than in other furnaces, hence the furnace diameters tend to be greater. The values of these design parameters for a number of operating furnaces are given in Table 7.17.

Table 7.16: Profiles of manganese alloy producers [26].

Country	Company (location)	Furnaces utilized on ferromanganese	Furnaces utilized on silicomanganese
Argentina	Industrias Siderúrgicas Grassi (El Nihuil)	1 × 5 MVA	1 × 5 MVA
	(Blanco Encalada)	1 × 3 MVA	1 × 3 MVA
Australia	Temco (Bell Bay)	1 × 27 MVA	1 × 29 MVA
			1 × 35 MVA
			1 × 45 MVA
Belgium	Sadaci (Gent)	1 × 25 MVA	
Brazil	Companhia Ferroligas do Amapa (Santana)	1 × 13 MVA	
	Cia de Cimento Portland Maringa (Itapeva)	1 × 7 MVA	1 × 7 MVA, 1 × 3 MVA.
			1 × 15 MVA
France	Usinor Sacilor (Dunkirk)	102 × MVA	
	SFPO (Boulogne)	blast furnaces	
	Pechiney Électrométallurgie (Dunkirk)		1 × 45 MVA
Georgia	Zestafoni Ferroalloys (Zestafoni)	22 furnaces	1 × 600 MVA
India	Andhra Ferro Alloys (Kottavalasa)	1 × 4 MVA	
	Facor (Shreeramnager)	1 × 17 MVA	
	GMR Vasavi Industries (Tekkali)		2 × 19 MVA
	Nava Bharat Ferroalloys (Paloncha)		1 × 17 MVA
	Ispat Alloys (Balasore)	1 × 15 MVA	2 × 15 MVA
	Tata Iron & Steel Co. (Joda)	1 × 17 MVA	1 × 9 MVA
	Crescent Ferroalloys (Seoni)		1 × 3 MVA
	Hira Ferroalloys (Raipur)	1 × 7 MVA	
	Jain Carbide & Cehmicals (Raipur)		2 × 3 MVA
	Jalan Ispat Castings (Meghnagar)		1 × 9 MVA
	Nav Chrome (Raipur)	1 × 4 MVA	
	Quality Steel & Forging (Meghnagar)		1 × 4 MVA
	Shree Ganesh Ferroalloys (Raigarh)	1 × 4 MVA	interchangeable to SiMn
	Sri Girijia Smelters (Raipur)[a]	1 × 4 MVA	
	Srinivasa Ferroalloys (Raipur)[a]	1 × 4 MVA	
	Standard Ferroalloys (Raipur)		1 × 8 MVA
	Vika Ferroalloys (Raipur)	1 × 3 MVA	interchangeable to SiMn
	Dandeli Steel & Ferroalloys (Dandeli)	1 × 4 MVA	interchangeable to SiMn
	Sandur Manganese (Vyasankere)	1 × 18 MVA	interchangeable to SiMn
	Visvesvaraya Iron & Steel (Bhadravati)	2 × 22 MVA	
	Balaji Electro Smelters (Yeotmal)	1 × 4 MVA	interchangeable to SiMn
	Kandelwal Ferroalloys (Kanhan)	1 × 9 MVA	1 × 9 MVA
	Maharashtra Elektrosmelt (Chandrapur)	1 × 33 MVA	1 × 33 MVA
	Universal Ferro & Allied Chemicals (Tumsar)	1 × 17 MVA	1 × 17 MVA, 2 × 9 MVA
Italy	Italghisa (Bagnolo Mella)		1 × 15 MVA
	Fornileghe (Breno)	2 × 10 MVA	1 × 10 MVA
Japan	Chuo Denki Kogyo (Kashima)	1 × 40 MVA	1 × 50 MVA
	Kobe Steel (Kakogawa)	1 × 20 MVA	1 × 20 MVA
	Mizushima (Mizushima)	1 blasst furnace	
	Nippon Denko (Samani)		1 × 8 MVA
	(Miyako)		1 × 5 MVA
	(Tokushima)	1 × 40 MVA	
	Yahagi Iron (Nagoya)	1 blast furnace	
Kazakhstan	Yermak (Yermak)[a]		27 furnaces
Korea	Dongbu Corporation (Donghae City)	1 × 8 MVA	1 × 8 MVA
	Dongil Industries (Pohang)	1 × 8 MVA	1 × 12 MVA, 1 × 8 MVA
	Hanhap Corporation (Pohang)	1 × 13 MVA	1 × 16 MVA
Mexico	Minera Autlan (Tamos)	1 × 33 MVA	
		1 × 33 MVA, 2 × 15 MVA	
	(Teziutlan)		1 × 12 MVA, 2 × 6 MVA
			1 × 5 MVA
	Ferroalmex (Gómez Palacio)		2 × 15 MVA

Country	Company (location)	Furnaces utilized on ferromanganese	Furnaces utilized on silicomanganese
Norway	Elkem (Porsgrunn)	1 × 45 MVA, 1 × 39 MVA, 1 × 18 MVA	interchangeable to SiMn
	Elkem (Sauda)	1 × 5 MVA, 1 × 36 MVA, 1 × 30 MVA, 1 × 24 MVA, 1 × 10 MVA, 2 × 6 MVA	interchangeable to SiMn
	Tinfos Jernverk (Kvinesdal)		2 × 45 MVA
South Africa	Ferro Alloys (Cato Ridge)	2 × 24 MVA, 2 × 12 MVA	
	Samancor (Meyerton)	2 × 75 MVA, 1 × 81 MVA	2 × 18 MVA, 2 × 21 MVA, 3 × 10 MVA
	Transalloys (Witbank)		1 × 21 MVA, 1 × 23 MVA, 2 × 49 MVA
Spain	Ferroatlántica (Boo)	1 × 20 MVA	1 × 30 MVA, 2 × 13 MVA
	(Cee)	1 × 17 MVA	3 × 24 MVA
	(Monzón)		1 × 45 MVA
Taiwan	Chen Hsing Industrial (Hsi-Chih)	1 × 10 MVA	interchangeable to SiMn
Ukraine	Nikopol Ferroalloys (Nikopol)	16 furnaces	29 furnaces
	Zaporozhye Ferroalloys (Zaporozhye)	1 × 1050 MVA	
USA	Elkem Metals (Marietta)	2 × 40 MVA	1 × 50 MVA
Venezuela	Havensa (Matanzas)		1 × 11 MVA, 2 × 9 MVA, 2 × 3 MVA, 1 × 15 MVA

[a] Interchangeable to FeCr.

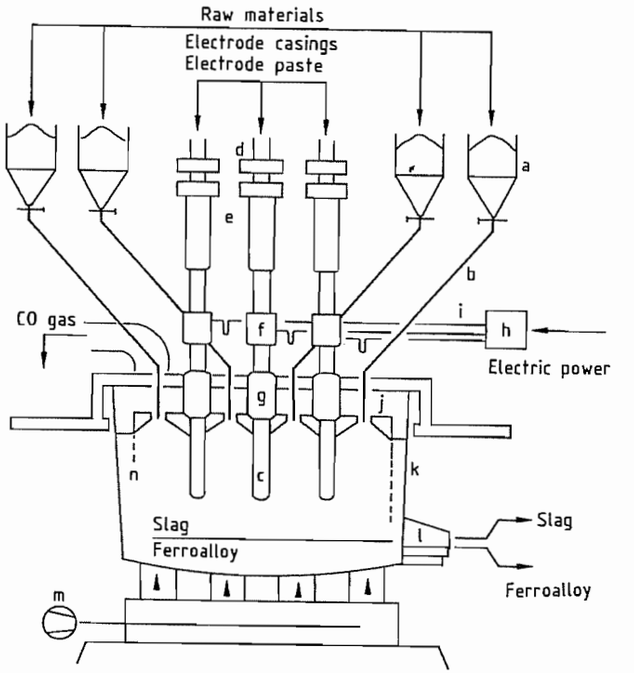

Figure 7.13: Layout of an electric arc furnace [35]: a) Charging bins; b) Charging tubes; c) Electrodes; d) Electrode slipping device; e) Electrode positioning devices; f) Current transmission to electrodes; g) Electrodes sealing; h) Furnace transformer; i) Current bus bar system; j) Furnace cover; k) Furnace shell; l) Tap hole; m) Furnace bottom cooling; n) Refractory material.

Table 7.17: Furnace design parameters.

	Elkem Beauharnois	Elkem Sauda	Temco Bellbay	Samancor Meyerton M 10	Samancor Meyerton M 4	Former Soviet Union PRO 2.5	Former Soviet Union PKZ 33
Inside shell diameter, m	15.1	12.5	10.0	16.0	9.8	2.7	6.7
Shell height, m	8.8	6.0	5.2	8.0	5.7	1.2	3.0
Electrode diameter, m	1.90	1.90	1.4	1.90	1.20	0.30	1.5
Tapholes	2 Metal, 2 Slag	2 Metal, 1 Slag	2 Metal, 1 Slag	2 Metal, 1 Slag	2 Metal, 1 Slag		
Megawatt rating	4.5	30	13	46	20	2.5	33

Most electric furnaces have two tapholes offset by 60 °C which are used alternately to tap both slag and metal. The slag and metal are then separated either in the ladle or by means of a skimmer plate in the runner between the furnace and the ladle [38]. In larger furnaces, separate tapholes are included for metal and slag [34]. Tapholes are usually opened by taphole drills and closed with automatic mud guns.

An important feature in the design of submerged arc furnaces is the Söderberg electrodes. These are used because the large electrode diameters required for the production of manganese alloys make the use of prebaked electrodes uneconomic. The Söderberg electrode consists of a mild steel or stainless steel casing which is stiffened with internal fins and is filled with a carbonaceous paste, consisting of a solid aggregate, usually calcined anthracite, and a binder of coal-tar pitch [34]. The paste becomes plastic when hot and fills the entire volume of the casing. On further heating of the electrode by the electric current and furnace heat, the paste is baked and becomes solid. As the electrode is consumed, additional casings are welded onto the top. The current carrying capacity and strength of an electrode is a function of the quality of the paste, the electrode baking rate, and the cross-sectional area. Breakages of Söderberg electrodes are a major cause of downtime in electric furnaces, and proper management of the electrodes is therefore essential for efficient production [34].

A number of devices are commercially available to control the electrodes' movement and slipping rate (rate at which the electrode is allowed to move through the rings to compensate for its consumption in the furnace). One of these is designed and manufactured by Elkem [38]. The electrode is clamped by hydraulically operated rings and is moved up and down on hydraulic cylinders. Current is fed to the electrode through brass contact shoes clamped around its diameter.

Large electric furnaces are usually completely closed at the top, and the CO-rich gas leaves the furnace at approximately 290 °C and is cleaned in cyclones and venturi scrubbers. The gas is then either flamed off to the atmosphere or, more recently, is used to generate electricity. This is the case of SFPO [26] and at Tinfos in Norway [39]. At Elkem's plant in Canada the off-gases are used to fuel auxiliary equipment in the plant [40]. Smaller furnaces are either open or closed. In the case of open furnaces the gas is usually withdrawn by fans and cleaned in a bag-filter plant. In this case the gases are completely burnt in the furnace and have no commercial value.

Raw materials are usually batch weighed and blended according to a predetermined recipe and are then fed to bunkers above the furnace. The mix then gravitates into the furnace through feed chutes. To ensure an even distribution of material over the furnace, up to ten feed chutes are radially distributed around each electrode and one is positioned in the center of the furnace.

After the metal is tapped from the furnace it is cast into molds formed from ferromanganese fines or cast iron and allowed to solidify. The alloy is then removed, crushed, and screened into various size fractions, depending on the requirements of the user. An alternative to this practice is the use of a casting machine. In this case the metal is tapped directly onto a moving train consisting of small molds. The metal then solidifies and is ejected from the mold at the end of the strand. The advantage of this process is that the product is more even in size and cubical in shape. The generation of fines (–6 mm), which are generally unsalable, is also minimized. To date Elkem, Samancor, Transalloys, Chuo Denki, and Mizushima use casting machines for a portion of their products.

Raw Materials Required for the Manufacture of High-Carbon Ferromanganese

Manganese ores from different sources vary widely in their contents of manganese, iron, silica, alumina, lime, magnesia, and phosphorus. To produce standard ferromanganese (78% Mn) and a slag containing 30% MnO, the manganese to iron ratio in the charge must be 6:5. Since a single manganese ore of this ratio is seldom available, blending of ores from different sources is common practice to reach the desired manganese to iron ratio and to control the level of deleterious elements, particularly phosphorus. The ore mixes used in some operations are shown in Table 7.18 [37]. The use of sinter as a source of manganese is becoming increasingly popular. In the sintering process a degree of prereduction is achieved, reducing the energy requirement in the furnace. The additional advantage of sinter is that fine ores, which are otherwise unusable, are agglomerated in the sintering process. Bag-house dust and sludge from gas cleaning plants can also be recycled to the furnace in the form of sinter. The maximum amount of sinter that can be fed to the furnace is a moot point and depends on its mineralogy and state of prereduction. When sinter replaces ore of high MnO_2 content, the energy required in the furnace increases because the highly exothermic reduction of MnO_2, Mn_2O_3, and Mn_3O_4, (see Section 47.5.2) no longer takes place in the furnace [37]. The use of Mamatwan sinter, in place of Mamatwan ore, results in power savings because the calcination of the carbonates in Mamatwan ore is energy consuming [41]. At the Zestafori ferralloy works in the former Soviet Union, up to 100% sinter is used in the furnaces [42]. The bottom size of ore is also important because close packing of the ore in the furnace must be avoided [37]. This can result in the formation of calcined bridges in the furnace, which disrupt the distribution of gas and can cause eruptions when the gas entrained under a bridge is suddenly released on its collapse [34]. Generally ores larger than 6 mm are used in large furnaces. The addition of small amounts of –6 mm material to small furnaces is possible. Generally, ore is screened prior to batch weighing of the furnace mix.

The carbon required in the furnace is generally added in the form of coke. The size of the reductant is important. Coke and coal of too small a size can also cause close packing as well as affecting the resistivity of the burden. To maintain electrode penetration at Elkem Sauda [43] coke nuts (10–20 mm) are used. This is a compromise between the resistivity and the necessity of maintaining a coke bed at the bottom of the furnace.

Limestone, dolomite, or silica are added to the process as fluxes to adjust the basicity of the slag. The amount and type of flux added depends on the blend of ores and whether a discard- or high-slag practice is used. At Elkem's operation in Beauharnois the use of alumina as a flux makes the operation of the furnace possible with 100% Moanda ore from Comilog [44].

Chemistry of the Process

A dig out of a 75 MVA ferromanganese furnace at the Metalloys operation in South Africa showed that nine distinct zones exist around each electrode (Figure 7.14) [45]. This study showed that material descends rapidly down the side of the electrode (a) into the semi-active zone (b), where prereduction of higher manganese oxides to MnO takes place. Thereafter, the material moves into the active zones of the furnace (e, f), where reactions

take place between the manganese(II) oxide in the melt and the coke particles in the coke bed:

$$7MnO + 10C \rightarrow Mn_7C_3 + 7CO$$

Equilibrium between the slag and metal was thought to exist under each electrode, and further from the electrode, layers of unreacted ore and coke were found to be present (h). This suggests that heat is concentrated under each electrode. The path of electrical transfer was deduced to be from the electrode tip through the coke bed and into the alloy layer (g).

The efficient production of high-carbon ferromanganese therefore depends on the degree of reduction of MnO by carbon as well as the prereduction that occurs in the upper region of the furnace. The ratio of CO and CO_2 in the off-gas is important and can be used to monitor the condition of the furnace. The higher the CO_2 content of the off-gas, the higher is the energy efficiency of the process, because the reducing potential of the gas is being more fully utilized (Figure 7.15) [43, 45]. Good operation of the furnace is indicated by a $CO_2/(CO_2 + CO)$ ratio of 0.55. This ratio, as well as the MnO content of the slag, can be used to control the coke rate of the furnace. Undercoking of the furnace is indicated by high MnO content of the slag and a low CO_2 content in the off-gas [43].

Table 7.18: Operating parameters of some ferromanganese electric arc furnaces.

			Temco Bellbay	Elkem Porsgrunn	Elkem Beauharnois	Facor Sheermnagar	Soman-cor M 10	Soman-cor M 2
Raw material additions, tonnes/tonne alloy								
Manganese ore:	Groote Eylandt		1.171	(18%)				
	South Africa:	high grade	0.780	(31%)			0.927	0.926
		medium						
		Mamatwan ore		(51%)			0.345	
		Mamatwan sinter					0.884	0.176
	Gabon:	Moanda ore			(78%)			
		Moanda sinter			(22%)			
	India:	average 44% Mn				2.18–2.23		
Operating results								
Average operating load, MW			13	25	34.4	5	45	16
Operating time, %				98	99		99	98
Specific energy consumption, kWh/t			2430	2399	2050	3100	2560	2710
Manganese recovery, %				77.3	75	79	77	74
Slag practice			high slag	high slag	high slag	discard slag	discard slag	discard slag
Slag composition, %								
MnO			40.4	43.1	44.7	20.0	20.0	20.0
MgO			1.8	4.4		2.5	7.3	7.4
Al_2O_3			13.8	11.1	28.8	9.00	4.3	3.8
CaO			15.2	11.9	1.0	32.5	35.6	34.8
SiO_2			28.2	24.2		30.5	32.4	31.5
Metal analysis, %								
Mn			78	78	78	74.5	76.5	76.5
Fe				14.6		17.6	15.4	15.4
Si			0.25	0.08		0.50	0.20	0.20
P			0.14	0.16		0.35	0.09	0.09
C			6.7	6.89		6.7	6.9	6.9
Ratios								
Slag/metal ratio			0.514				0.68	0.80
Basicity ratio (mass)			0.68			1.35	1.35	
Basicity ratio (molar)			1.9					

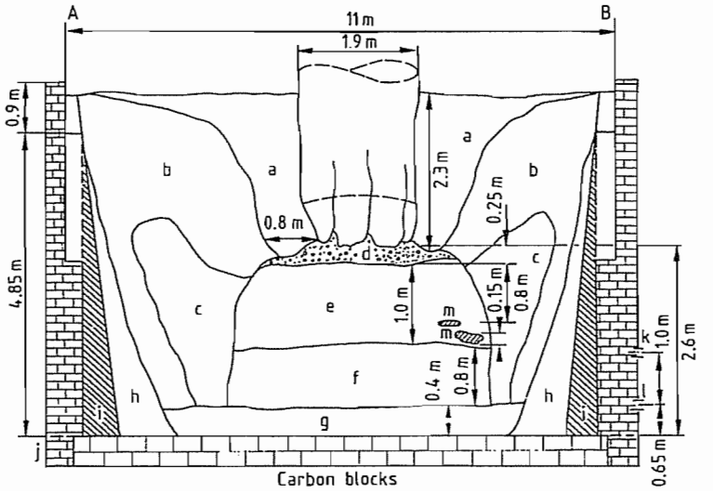

Figure 7.14: Zones in a ferromanganese furnace [36]: a) Loosely sintered burden; b) Loosely sintered material enriched in carbonaceous reducing agents; c) Coke and slag region, showing the active zone away from the electrode; d) Coke bed; e) Coke-enriched layer, with CaO–MnO–SiO2 slag; f) MnO melt layer with some slag, coke, and additional carbonaceous reducing agent; g) Ferromanganese alloy layer intermixed with MnO melt; h) Graphitized and carbon-rich material; i) Carbon lining; j) Brick lining; k) Slag taphole level; l) Metal taphole level; m) Pieces of electrode.

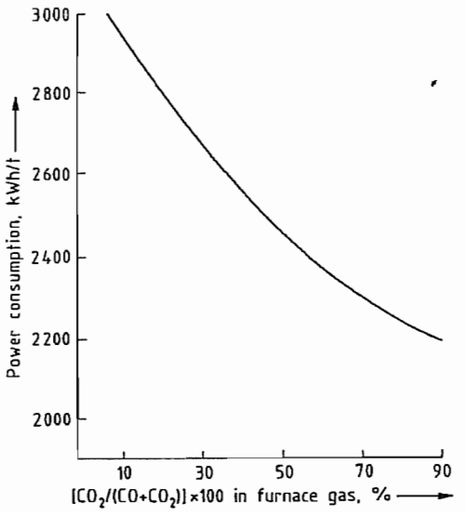

Figure 7.15: Relationship between off-gas composition and power consumption for ferromanganese production [43].

A further influence on the MnO content of the slag is the basicity ratio (CaO + MgO):SiO_2. Generally the addition of basic oxides increases the melting point of the slag. The hotter slag improves the reaction between the slag and the coke and, consequently, more MnO is reduced. Increasing the basicity of the slag thus decreases the residual MnO content (Figure 7.10). The MnO content of the slag is also reduced by increasing the penetration of the electrodes, which also increases the slag temperature. The target MnO content of the slag depends on whether a discard- or high-slag process is used.

Discard-Slag Practice

Discard slags generally have MnO contents of 8–12%. Slag is produced by the silica and other basic oxides entrained in the ore. Manganese(II) oxide is entrained in the silicate network and is released by addition of CaO or MgO. By increasing the basicity of the slag the recovery of manganese as metal is increased; however, consumption of carbon and electricity also increases. The discard-slag process is therefore only used where power is relatively cheap and the delivered cost of manganese ore is high [37]. The recovery of manganese to the metal is between 70 and 75% when this practice is used. The practice usu-

ally involves the addition of limestone or dolomite to the furnace. However, in South Africa where high proportions of Mamatwan ore are used, a basic slag is produced without the addition of limestone, due to the high CaO content of the ore. In India the discard-slag practice is used because high recoveries of manganese are necessary to produce 74% Mn from lower grade ores.

High-Slag Practice

In the high-slag practice less coke is required for reduction and little or no basic fluxes are used because the MnO content of the slag satisfies the requirement for basic oxides. Slags of this nature tend to contain more than 25% MnO. In the high MnO practice the power consumption is reduced because a higher proportion of the reduction occurs by the gases and less MnO is reduced by solid carbon. Maximum use is therefore made of the exothermic nature of the prereduction reactions. The recovery of manganese is low in the ferromanganese furnace, but the overall recovery of manganese is high because the slag is usually used for the production of silicomanganese [37].

An additional attraction of the high-slag process is that an artificial ore, with a manganese to iron ratio of up to 100:1, can be made from relatively low-grade ores. This artificial ore can then be used to produce the highest grade of ferromanganese without the need to purchase costly high-grade ores. An additional benefit is the extremely low phosphorus content of the slag, which hence lowers the phosphorus content of any mix in which it is used. In countries having only ores with high phosphorus contents, the first stage of the process is the production of a slag high in MnO and a low-manganese alloy [46].

Since the energy input in the production of ferromanganese by the high-slag process is lower than that of the discard-slag process, it is used by most producers. Slag compositions for various producers are shown in Table 7.18.

7.4.2 Production of Silicomanganese

Unlike ferromanganese, silicomanganese is only produced in electric arc furnaces, most of which can be used interchangeably to produce either of the manganese-containing alloys. Silicomanganese is used either as a substitute for ferromanganese and ferrosilicon in steelmaking or as a raw material for the production of medium- and low-carbon ferromanganese and industrial manganese metal. The composition of silicomanganese produced in the Western world is given in Table 7.12 and of that produced in the former Soviet Union in Table 7.19. Although silicomanganese generally contains 14–19% Si, grades containing up to 35% are produced for the production of extremely low-carbon alloys.

The solubility of carbon in the alloy decreases with increasing silicon content (Figure 7.16) [47]. On cooling, sparingly soluble SiC comes out of solution.

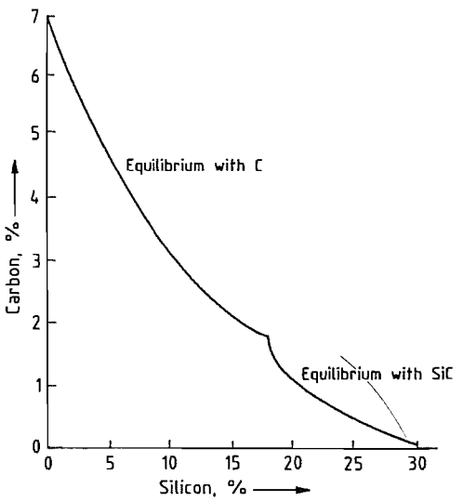

Figure 7.16: Carbon solubility in the Fe–Mn–Si–C system (50–80% Mn) at 1420 °C [47].

Table 7.19: Composition of Soviet silicomanganese [27].

Grade and official grade code	Si[a], %	Mn minimum, %	C, %	Deleterious elements, not to exceed		
				P, % (group A[b])	P, % (group B[b])	S, %
CMn26	26.0	60.0	0.2	0.1	0.05	0.03
CMn20	20.0–25.9	65.0	1.0	0.3	0.25	0.03
CMn17	17.0–19.9	65.0	1.7	0.3	0.35	0.03
CMn14	14.0–16.9	65.0	2.5	0.3	0.35	0.03
CMn10	10.0–13.9	65.0	3.5	0.3	0.35	0.03

[a] As reported.
[b] Furnaces.

Table 7.20: Operating parameters for silicomanganese production.

			Temco Bellbay	Elkem Porsgrunn	Elkem Beauharnois
Raw material additions, tonnes/tonne alloy					
Manganese ore:	Groote Eylandt		0.227		
	South Africa:	medium grade		0.536	0.942
		Mamatwan ore		0.647	
		Mamatwan sinter			0.754
Ferromanganese slag			0.227		
Remelt metal			0.091		
Reductants:	coke		0.141	0.198	
	coal			0.566	0.836
Fluxes:	limestone				
	magnesite				
	quartz		0.127	0.610	0.814
Operating results					
Average operating load, MW			28	46	11
Operating time, %			94	97	98
Specific energy consumption, kWh/t			4400	3870	3900
Manganese recovery, %			85	74	67
Slag composition, %					
MnO				78.0	15.0
MgO				3.9	4.5
Al_2O_3			29.7	7.7	6.1
CaO				20.9	21.1
SiO_2			33.8	48.5	47.0
Metal analysis, %					
Mn			65.9	67.7	65.5
Fe				16.0	15.5
Si			19.1	17.5	17.8
P				0.09	0.09
C			1.38	1.18	1.15
Ratios					
Slag/metal ratio				0.72	1.17
Basicity ratio			1.0	0.54	0.55

There are three general routes for the production of silicomanganese:

- Reduction of manganese ores and silica with coke and coal
- Reduction of MnO-rich slags from ferromanganese production and quartzite with coke and coal
- Reaction of standard ferromanganese and quartzite with coke

The first two processes are used for the production of alloys containing 15–25% Si and can be carried out in the same furnaces used for ferromanganese production. The third method is used to produce alloys containing 30–35% Si and is generally performed in smaller furnaces.

Raw Materials. The raw materials used in silicomanganese production are similar to those

used in making ferromanganese. Silica is added to the furnace as quartz or quartzite, and ferromanganese slag can be used as an alternative additional source of manganese instead of manganese ore or sinter. As in the case of ferromanganese, production advantages can be gained by using sintered ore (particularly from Mamatwan). At the Kashima works of Chuo Denki, 40% of the ore feed is in the form of sinter. The raw materials used to produce silicomanganese are given in Table 7.20.

Chemistry of the Process. In a dig out of a small electric arc furnace [48], four zones were distinguished: the burden zone, the zone of the coke bed, the melting zone, and the metal layer. In the burden zone, the higher oxides of manganese are reduced to MnO, while the higher oxides of iron are reduced to FeO and partially to metallic iron. Manganese(II) oxide is converted to complex silicates, which begin to melt at the bottom of the burden zone. Fine metallic particles exist in the coke bed zone, which are possibly caused by condensation of silicon and manganese in the hot areas under the electrodes. In the upper and lower parts of the melt zone, the reduction of manganese and silicon oxides occurs. The equilibrium is determined by the following reaction [31]:

$$SiO_2 + 2Mn \rightarrow Si + 2MnO$$

This equation is important in determining the silicon and manganese contents of the metal that collects in the lowest part of the furnace and is influenced by the slag chemistry and the temperature of the process. Increasing the CaO content of the slag reduces the silicon content of the metal. The basicity requirement of the slag is therefore better supplied in the form of MgO. Higher temperatures tend to drive Si into the metal at the expense of Mn. Higher temperatures are therefore required in the production of silicomanganese than in the production of ferromanganese.

Silicomanganese is produced by most manufacturers of manganese alloys, and the slag and metal compositions and operating parameters of some producers are given in Table 7.20. To produce manganese metal of 97% Mn by the silicothermic method, a silicomanganese containing 28% Si is required that is particularly low in phosphorus and iron. This is made from a manganese slag produced from the partial reduction of manganese ore.

Operation of the Furnace. The operation of the furnace for silicomanganese production is similar to that of ferromanganese production. However, deeper penetration of the electrodes is necessary to provide the higher temperature required to drive the reduction of silicon [31]. The resistivity of the burden is therefore important, and the size and the activity of the reductant is critical for stable operation of the furnace.

7.4.3 Production of Medium-Carbon Ferromanganese

Medium-carbon ferromanganese contains 1–1.5% carbon and has a manganese content of 75–85% (Table 7.12). Medium-carbon ferromanganese can be produced either by refining high-carbon ferromanganese with oxygen or by the silicothermic route, whereby the silicon in silicomanganese is used to reduce additional MnO added as ore or slag. The former process has considerable advantages [47] and is used by most producers. Elkem Metals in Norway and the United States use their patented manganese oxygen refining (MOR) process to refine high-carbon ferromanganese in plants having capacities of 5000 t/month and have closed their silicothermic plant in the United States. A similar facility was sold under license to the Torros plant of Minera Autlan in Mexico. Thyssen Stahl (Germany) uses a similar process to produce medium-carbon ferromanganese from the high-carbon ferromanganese produced in their blast furnaces. Samancor (South Africa) and Usinor Sacilor (France) have patented a similar process, but have not yet built a plant [49].

Transalloys (South Africa) produces 20 000 t/a of medium-carbon ferromanganese by the silicothermic route and appears to be the only producer in the Western world to do so. In the former Soviet Union, medium- and low-carbon ferromanganese are produced silicothermically with manganese recoveries of 59–63% [27]. The silicothermic and MOR processes are shown schematically in Figure 7.17.

7.4.3.1 Production of Medium-Carbon Ferromanganese by Oxygen Refining of High-Carbon Ferromanganese

In the MOR process patented by Union Carbide, high-carbon ferromanganese is decarburized in a similar manner to the steelmaking process in the basic oxygen furnace [47]. However, several distinctive differences are encountered in the case of ferromanganese:

- A final temperature of 1750 °C compared to 1550 °C
- Refractory attack is more severe
- Difficult casting of the final alloy
- The higher vapor pressure of manganese
- The higher volume and temperature of the off-gas

In the MOR process, oxygen is blown into the molten high-carbon ferromanganese and the temperature is increased from its tapping value of 1300 to 1750 °C. The heat required is supplied by the oxidation of manganese to manganese(II) oxide and carbon to carbon monoxide. The need to increase the temperature is shown by the carbon temperature relationship in Figure 7.18. In the early part of the blowing process, most of the oxygen is consumed by oxidation of manganese, and the temperature of the melt increases from 1300 to 1550 °C. Hereafter, carbon is rapidly oxidized and the temperature rises to 1650 °C. Above this temperature, the rate of carbon removal decreases and manganese is once again oxidized. The process is stopped at 1750 °C, which corresponds to a carbon content of 1.3%. Further reductions in carbon content result in unacceptably high losses of manganese. In the MOR process, the recovery of manganese is ca. 80% and the distribution of manganese can be broken down as follows [47]:

Alloy MC FeMn	80%
Fume formed by vaporization	13%
Slag formed by oxidation of Mn	5%
Other losses, splashing	2%

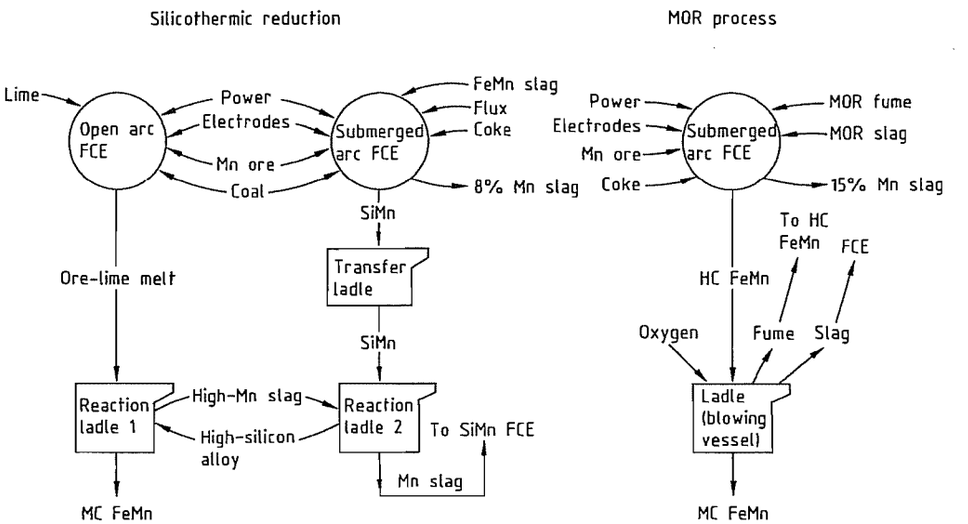

Figure 7.17: Process flow sheet comparison for silicothermic reduction and the MOR process [47].

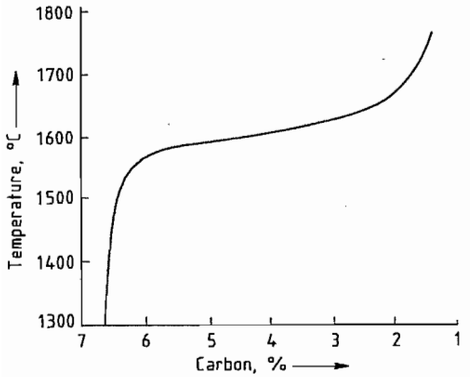

Figure 7.18: Dependence of carbon content on temperature for a ferromanganese alloy (Mn:Fe, 6:1) at 101.3 kPa [47].

The manganese lost in the fume is recovered in the gas cleaning plant and is then pelletized and returned to the high-carbon ferromanganese furnace. The slag, which contains about 65% MnO, is also returned to the high-carbon ferromanganese furnace. The successful operation of this process depends on the design of the blowing vessel and oxygen lance as well as giving careful attention to operational procedures. In the joint patent of Samancor and Usinor Sacilor, a bottom blown converter is used and steam is injected at the end of the blow as a coolant [49].

The MOR process has many advantages over the silicothermic process: lower energy consumption, lower capital investment, lower production cost, and greater flexibility.

The main disadvantage of the process is that its use is limited to production of medium-carbon ferromanganese because the carbon content cannot be reduced to below 1.3%.

7.4.3.2 Silicothermic Production of Medium-Carbon Ferromanganese

In the silicothermic production of medium-carbon ferromanganese, a high-grade slag or a melt containing manganese ore and lime is contacted with silicomanganese containing 16–30.1% silicon [50]. The silicon in the alloy acts as the reducing agent in the process, which reduces the manganese(II) oxide in the melt. Similarly to silicomanganese production, the equilibrium is determined by the reaction:

$$Si + 2MnO \rightleftharpoons SiO_2 + 2Mn$$

The purpose of the lime is to reduce the activity of the SiO_2 in the melt, thus forcing the above reaction as far to the right as possible. The ratio of CaO to SiO_2 in the slag should be greater than 1.4 to ensure a sufficient reduction in the activity of SiO_2. The carbon entering the process in the silicomanganese remains entirely in the metal phase and is therefore found in the product. Thus, to produce a medium-carbon ferromanganese containing 1% C, a silicomanganese containing 20% Si is necessary (Figure 7.16).

The heat produced by the silicothermic reduction is not sufficient to sustain the process; hence it is usually carried out in an electric arc furnace. These furnaces are usually small and, unlike ferromanganese furnaces, are lined with magnesite bricks, which are fairly resistant to the highly basic slag. The power consumption is between 1000 and 3000 kW. These furnaces can be tilted so that the slag can be separated from the metal. At Transalloys (South Africa) the process is carried out in a mixing ladle.

Although the silicothermic reduction process is more energy intensive than the decarburization of high-carbon ferromanganese, it has the advantage that the final carbon content is limited only by the carbon content of the initial silicomanganese. The silicothermic process can therefore be used to produce low-carbon ferromanganese and industrial manganese metal.

7.4.4 Production of Low-Carbon Ferromanganese

Low-carbon ferromanganese contains 76–92% Mn and 0.5–0.75% C (see Table 7.12). The production of low-carbon silicomanganese is not possible by the decarburization of high-carbon ferromanganese without incurring extremely high losses of manganese [50].

Use must accordingly be made of a silicothermic reduction process.

The process is similar to that used in the silicothermic production of medium-carbon ferromanganese. High-purity ores are used and in particular ores containing iron and phosphorus should be avoided. An artificial manganese ore, produced as a high-grade slag, is particularly suitable because of its low impurity level and because all the manganese is present as MnO. The reduction of the higher oxides of manganese is therefore unnecessary.

The operating figures for 1 t of ferromanganese containing 85–92% Mn, 0.1% C, and 1% Si with a manganese recovery of 75% are:

Calcied manganese ore	1250–1350 kg
Silicomanganese (32–33% Si)	800–850 kg
Quicklime	1000–1100 kg
Electrodes	10–12 kg
Electricity	1800–2500 kWh

Since the required silicon content of the metal is low, a slag high in MnO is necessary. The MnO content of the slag can, however, be reduced by the use of a two-stage refining operation. In the first stage, an excess of silicomanganese is maintained and a slag containing 6–8% Mn is teemed and discarded. The second refining stage with manganese ore and lime results in a slag containing 10–14% Mn, which is returned to the silicomanganese furnace.

7.4.5 Gas Cleaning

In all the processes described in this chapter, large volumes of gas are generated. These gases consist generally of CO, CO_2, and N_2, and contain large quantities of dust from the raw materials and condensed manganese droplets. These gases require cleaning prior to their venting to the atmosphere. In open furnaces, in which the gas is totally combusted, hoods are incorporated in the design through which the gas is removed. This gas is cooled in trombone coolers to ca. 200 °C and the dust is removed in bag filters. Ideally, after recovery the dust should be agglomerated and returned to the furnace. In closed furnaces, the gas is usually cleaned in cyclones and venturi scrubbers prior to combustion to the atmosphere or used in downstream processes. At Elkem Sauda in Norway, gas from the 36 MVA furnace is cleaned by two wet venturi scrubbers. The gas has an initial dust loading of 150 g/m3 which is reduced to a maximum of 50 mg/m^3 [38]. The dust recovered from the cleaning plant is filtered, sintered and returned to the process. At Samancor's Meyerton works in South Africa the gas from the 81 MVA and two 75 MVA closed furnaces is cleaned by a cyclone followed by two venturi scrubbers. A mist eliminator is included in the gas plant of the 81 MVA furnace to reduce the moisture content because the gas is used for heating in other areas of the plant. The emissions from the gas plants are less than 50 mg/m^3, which is the statutory maximum. The gas from the remaining open furnaces is cleaned in a bag filter plant. Investigations are under way to briquette the dust from this plant due to its high manganese content and high manganese to iron ratio.

It is expected that dust limits will be reduced to 25 mg/m^3. In addition to this the exposure limits allowed in the working environment in manganese producing facilities have been reduced due to the toxicity of manganese dust; the following limits apply:

United States, United Kingdom, Australia, Belgium, Brazil, Germany	5 mg/m^3
Yugoslavia	2 mg/m^3
Former Soviet Union, Poland	0.3 mg/m^3
Bulgaria	0.02 mg/m^3

7.4.6 Recent Developments and Future Trends

Energy-Saving Measures. In regions with high electricity prices recent developments have concentrated on the saving of energy. This is of particular importance to Japanese producers of manganese alloys that use electric furnaces. Developments include the use of the off-gas from the furnace to preheat and mildly prereduce the ore, either in a rotary kiln or in a shaft kiln above the furnace.

The former process is used at the Kashima Works of Chuo Denki, where the feed to the

40 MVA ferromanganese furnace is heated to 950 °C in a rotary kiln and the higher oxides of the manganese ore are partially reduced. The ore loses 23 % of its mass during this process [51]. The use of this system has resulted in savings in power, and an additional advantage is that coal can be used instead of coke to satisfy the carbon requirement of the furnace. Care must be taken to avoid rapid heating and consequent decrepitation of the ore in the kiln.

The process in which a shaft kiln is positioned above the furnace was invented by NASU [52]. In this process the gas from the furnace is burnt under the furnace roof and the hot burnt gas leaves the furnace through a vertical shaft. The raw ore mix is introduced to the top of the shaft and is heated in a countercurrent fashion by the exhaust gas. The ore is then fed to the furnace, where further heating takes place as the ore is exposed to the radiant heat produced by the burning gas in the roof. Two furnaces of this type are in operation at the Mizushima plant and their operation has resulted in power savings.

Computer Control of Electric Furnaces. Computer control of electric furnaces is practiced by Elkem at Suada in Norway, at Marietta in Ohio, and at Beauharnois in Canada. Temco in Tasmania and Samancor in South Africa also use computer control [53]. The following improvements in operating parameters have been realized by computer control at Elkem's plant at Beauharnois:

Operating power level (MV)	5 % improvement
Power cost reduction from increased load	3 % improvement
	9 % improvement
Manpower cost reduction	lower variaiton
Statistical process control	in product

Elkem is investigating the potential of enhancing their process control system by the incorporation of an expert system. This system, based on artificial intelligence, will incorporate the experience of the operator in the process control system and will be used to diagnose reasons for poor furnace performance. Possible changes to improve the operation will be suggested by the expert system [54].

Use of Plasma Furnaces. Non-transferred arc plasma furnaces have been used successfully in the production of charge chrome. Attempts to produce ferromanganese in plasma furnaces have not been economically successful due to the high losses of manganese caused by volatilization in the arc attachment zone. In addition, no preheating of the ore takes place in a plasma furnace, unlike in the burden zone of the submerged arc furnace. In an effort to solve these problems and to utilize the higher specific throughputs that are obtainable in a plasma unit, a combined plasma/shaft furnace is being jointly developed by Voest Alpina and Samancor [55].

7.5 Ferrochromium

Ferrochromium is a master alloy of iron and chromium, containing 45–95 % Cr and various amounts of iron, carbon, and other elements. The ferrochromium alloys are classified by their carbon content and are known by their French names because basic work in this field was carried out mainly in France:

- *High-carbon ferrochromium* (HC ferrochromium) with 4–10 % C, "ferrochrome carburé"
- *Medium-carbon ferrochromium* (MC ferrochromium) with 0.5–4 % C, "ferrochrome affiné"
- *Low-carbon ferrochromium* (LC ferrochromium) with 0.01–0.5 % C, "ferrochrome suraffiné"

The mechanical and chemical properties of steel can be improved by alloying it with ferrochromium. Chromium combined with nickel gives stainless steel excellent chemical resistance.

The first industrial use of ferrochromium in producing low-chromium alloy steels was in 1860–1870 in France. Previously P. Berthier (1821) and E. Fremy (1857) produced small quantities of high-carbon ferrochromium in crucibles by reducing chromite or combinations of chromium and iron oxides with charcoal. This direct reduction process was transferred to the blast furnace or cupola to

produce low-chromium alloys with 7–8 % Cr, and later on alloys with 30–40 % Cr. In the United States (1869), Sweden (1886), and Russia (1875), similar processes were developed for producing high-carbon ferrochromium [56, pp. 1–3; 57].

The fundamental work by Moissan (1893) on using the electric arc furnace and its industrial application for the direct carbothermic production of high-carbon ferrochromium by Héroult (1899) were major improvements over the blast furnace that led to the modern large-scale production.

The reduction of chromite by silicon for the production of low-carbon ferrochromium was developed by F. M. Beckett (1907) and improved by G. Jean (1909).

The aluminothermic production of low-carbon ferrochromium has proved to be too expensive and the method is seldom used now.

7.5.1 Physical and Chemical Properties

Low-carbon ferrochromium has a bright silvery appearance; as carbon content increases, the metal turns from gray to dark gray. The density and melting range for different grades of ferrochromium are summarized in Table 7.21 [58].

The Fe–Cr phase diagram (Figure 7.19, [59]) exhibits a continuous series of solid solutions at higher temperature and a σ-phase at lower temperature. This brittle σ-phase has a tetragonal structure ($a = 8.7995 \times 10^{-10}$ m, $c = 4.5442 \times 10^{-10}$ m).

Commercial ferrochromium contains mainly carbon as a constituent element because of the high affinity of chromium for the carbon used in the reduction process. The constitution and structure of the C–Cr–Fe system has been reviewed [60]. A projection of the liquidus temperatures and solid-phase equilibrium by isothermal sections from 1150 to 600 °C have been published [60].

7.5.2 Raw Materials

The only raw materials for the production of ferrochromium are chromite ores. The mineral chromite has a spinel structure and its formula may be written as $(Fe^{2+}, Mg)O \cdot (Cr, Al, Fe^{3+})_2O_3$. A high Cr:Fe ratio is advantageous to produce an alloy with high chromium content. Chromite ores are classified as follows [61]:

- Ores rich in chromium: > 46 % Cr_2O_3, Cr:Fe > 2:1; for the production of ferrochromium
- Ores rich in iron: 40–46 % Cr_2O_3, Cr:Fe < 2:1; for the production of charge chrome and for the chemical industry
- Ores rich in aluminum: > 60 % (Cr_2O_3 + Al_2O_3), > 20 % Al_2O_3; for refractories

Metallurgical-grade chromite ores are classified as hard lumpy or friable lump types, fines, and concentrates. Concentrates are produced by mechanical upgrading of lean ores or fines [62].

Table 7.21: Some physical properties of ferrochromium and ferrosilicochromium [58].

Alloy	Density ρ, g/cm³	Melting range, °C	
		Liquidus	Solidus
Chromium metal (electrolytic)	7.2	1900	
Chromium metal (aluminothermic)	7.2	1850	
Low-carbon ferrochromium (72 % Cr, 0.01 % C)	7.35	1690	1660
Low-carbon ferrochromium (72 % Cr, 0.05 % C)	7.35	1670	1639
Low-carbon ferrochromium (69 % Cr, 0.1 % C)	7.35	1604	1343
High-carbon ferrochromium (69 % Cr, 4–6 % C, 1 % Si)	7.2	1500	1350
High-carbon ferrochromium (64 % Cr, 5 % C, 1 % Si)	7.1	1450	1340
Ferrochromium, charge grade (63 % Cr, 5.5 % C, 7 % Si)[a]	6.7	1500	1400
Ferrochromium, charge grade (56 % Cr, 6 % C, 5 % Si)[a]	6.8	1493	1660
Ferrochromium silicon (36 %, 40 % Si)	5.3	1388	1360

[a] Charge chrome (see Table 7.27).

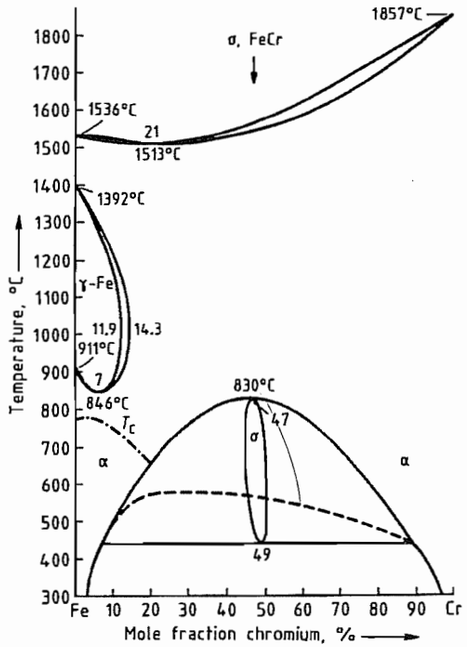

Figure 7.19: Fe–Cr phase diagram [59].

In the production of high-carbon ferrochromium, which is by far the alloy in greatest demand, generally a lumpy type of chromite ore is necessary. The submerged arc smelting of high-carbon ferrochromium by direct reduction of carbon in large low-shaft electric furnaces generally requires lumpy chromite ores to allow the reaction gases to pass from the lower reaction zone to the top of the furnace, where the burden (i.e., charge) is continuously charged.

About 80% of chromite ores in the western world are fines (< 10 mm). Therefore, efforts have been made to agglomerate these fines, by either sintering, briquetting, or pelletizing [63]. Fines of chromite ores can be used to produce low-carbon ferrochromium.

Typical analyses of some important metallurgical chromite ores are summarized in Table 7.22 [64].

The reducing agent for chromite is usually carbon in the form of coke (gas coke, coal, or charcoal); its contents of S and P should be low. Silicon as a reducing agent is used in the form of ferrosilicochromium or ferrosilicon to produce low-carbon ferrochromium. Fluxing agents, e.g., quartzite or alumina (corundum or bauxite) and lime, are charged with the burden for slag formation. In the carbothermic production of ferrosilicochromium, chromite and quartzite are used as the raw materials.

7.5.3 Production

The oxides of iron and chromium present in the chromite can be readily reduced at high temperature with carbon. Because of the tendency of chromium to form carbides, a carbon-containing alloy is always obtained. The oxides can also be reduced with silicon, aluminum, or magnesium. However, only carbothermic and silicothermic reductions are used commercially. The reducibility of chromite depends on its composition. A chromite rich in iron ($FeO \cdot Cr_2O_3$) can be reduced by carbon at lower temperature than one rich in magnesium ($MgO \cdot Cr_2O_3$) [65, 66]. Iron oxide is reduced by carbon at a lower temperature than chromium oxide.

A thermodynamic analysis of carbothermic reactions in the field of ferroalloys has been performed [67]. For the carbothermic reduction of FeO, Cr_2O_3, and SiO_2, equilibrium temperatures at different CO pressures were calculated. The values in Table 7.23 were found at 101.3 kPa. Carbides with higher carbon content formed initially at lower temperature react at higher temperature with Cr_2O_3 and form carbides with lower carbon content; finally, reduction of SiO_2 starts at higher temperature. Therefore, production of ferrosilicochromium alloys requires high temperature.

In practice the reactions are somewhat more complicated because iron-containing chromium carbides are formed. In high-carbon ferrochromium, the double carbide $(Cr, Fe)_7C_3$ is present. In this compound, two to four Cr atoms can be substituted by iron atoms. Equilibrium temperatures have been calculated for the FeO reduction in chromite [66]:

Table 7.22: Analyses of some chromite ores, metallurgical grade.

Compound	Chromite ore, %				
	Tranvaal lump[a]	Zimbabwe friable[b]	USSR lump[c]	Turkey lump[d]	Albania lump
Cr_2O_3	42.55	49.53	53.73	47.58	40.5
FeO	21.85	11.6	8.5	9.45	11.4
Fe_2O_3	4.85	2.2	4.3	3.1	—
MgO	9.26	17.52	17.3	18.7	23.3
Al_2O_3	15.5	7.3	9.4	8.8	7.3
SiO_2	5.54	5.14	4.3	8.33	12.6
L.O.I.[e]	0.2	2.3	2.1	2.25	3.4
Cr:Fe	1.43	3.20	3.81	3.42	3.13

[a] Bushveldmassiv [64].
[b] Great Dyke (friable lump) [64].
[c] Kempirsajski [64].
[d] Anatolia (Fethiye) [64].
[e] Loss on ignition.

Table 7.23: Equilibrium temperatures for various carbothermic reduction reactions [67].

Condensed reactants	Condensed products	Gases	Equilibrium temperature, °C
FeO, C	Fe	CO_2, CO	670
Cr_2O_3, C	Cr_3C_2	CO	1150
Cr_2O_3, Cr_3C_2	Cr_7C_3	CO	1190
Cr_2O_3, Cr_7C_3	$Cr_{23}C_6$	CO	1530
Cr_2O_3, $Cr_{23}C_6$	Cr	CO	1810
SiO_2, C	SiC	CO	1480
SiO_2	Si	CO, Si	1710

$$FeO \cdot Cr_2O_3 + C \rightleftharpoons Fe(\alpha, \beta, \gamma) + Cr_2O_3 + CO \quad t = 950\ °C$$

For the Cr_2O_3 reduction:

$$MgO \cdot Cr_2O_3 + {}^{13}/_{3}C \rightleftharpoons {}^{2}/_{3}Cr_3C_2 + MgO + 3CO \quad t = 1200\ °C$$

Because the difference in temperature between these two reactions is slight and because iron also facilitates reduction of chromium oxide, selective reduction of iron is difficult. In solid-state reduction studies on Transvaal chromite, the amount of iron and chromium found in the metallic state at 1000 °C was 11.0% of the iron and 1.3% of the chromium, and at 1200 °C was 98.3% of the iron and 38.5% of the chromium [64].

In the carbothermic reduction process, unreduced oxides from the chromite (MgO, Al_2O_3) and from the gangue (SiO_2 in serpentine and olivine) are collected in a slag, which generally contains 30% SiO_2, 30% MgO, and 30% Al_2O_3. The remaining 10% is composed of Cr_2O_3, CaO, MnO, and FeO [65]. Control of slag composition is important with respect to melting temperature and fluidity. The approximate melting temperature may be derived from the ternary diagram for MgO–Al_2O_3–SiO_2 [68].

Low-carbon ferrochromium is produced by the silicothermic reduction of chromite ore. Silicon is used in the form of ferrosilicochromium, which is produced in submerged arc furnaces (as is high-carbon ferrochromium) by carbon reduction of chromite ore and quartzite. The solubility of carbon in the FeSiCr alloy depends on the silicon content; if the silicon content is higher, the carbon content is lower. The carbon solubility at different silicon contents and temperatures is shown in Table 7.24 [69]. The reduction of Cr_2O_3 by Si is enhanced by addition of lime (CaO), which reduces the activity of SiO_2 in the slag. The reduction may be written as follows:

$$FeO \cdot Cr_2O_3 + 2Si + 4CaO \rightarrow (2Cr + Fe) + 2Ca_2SiO_4$$

Special chromium master alloys like CrMo, CrW, and CrNb are produced aluminothermically by coreduction of the relevant oxides together with chromium oxide.

Table 7.24: Solubility of carbon in ferrosilicochromium as a function of temperature, calculated from equations given in [69].

Silicon content[a], %	Carbon content, %			
	1550 °C	1450 °C	1350 °C	1300 °C
20	2.34	2.21	2.08	2.02
30	0.66	0.60	0.54	(solid)
40	0.07	0.05	0.03	0.02
50	0.03	0.02	(solid)	(solid)

[a] Cr:Fe = 2.67.

7.5.3.1 High-Carbon Ferrochromium

High-carbon ferrochromium is produced by direct reduction of chromite ores with carbon (coke, coal, or charcoal) in large, three-phase submerged arc furnaces with 10–50 MV A capacity (corresponding to 15 000–60 000 t/a of ferrochromium production). Elkem in Sweden operates the largest known electric arc furnace with 105 MV·A capacity. This furnace is used to produce high-carbon ferrochromium and ferrosilicochromium.

Submerged arc furnaces work continuously as a low-shaft electric furnace, where the burden is charged around the self-burning Söderberg electrodes. These electrodes are deeply immersed in the burden column and discharge to the reduced liquid products, i.e., the metal and slag, on the bottom of the furnace. Metal and slag are tapped at regular intervals through tapholes near the furnace bottom; they flow into a ladle with a slag overflow leading to another ladle or to a slag pan. After the slag has been skimmed, the metal is poured into heavy, flat cast-iron molds lined with sand or into sand molds. The furnace hearth and the walls in the reaction zone are normally lined with carbon blocks or a ramming mix; in special cases, magnesite is used. The walls of the shaft are lined with fireclay or magnesite.

In older plants with relatively small submerged arc furnaces, the CO reaction gas is burned at the top of the furnace and then scrubbed. Modern submerged arc furnaces with high capacities are totally closed, and the unburned reaction gas (ca. 90% CO) is scrubbed. Thus, the volume of the off-gas can be minimized (by a factor of 10–20 compared to that of the open top furnace), and the investment costs for the gas-cleaning plant are correspondingly lower. Furthermore, the combustible gas can be used as a fuel for processes, such as calcining the limestone and drying and preheating the ore or the whole burden, or for producing energy.

The coke rate is calculated on the basis of the stoichiometric requirement of the oxides and on the amount of dissolved carbon in the alloy; allowance is made for some combustion at the top of the furnace and for reaction with moisture. The slag composition is important to produce metal of desired quality and to maintain smooth furnace operation. Therefore, the slag is analyzed from tap to tap or once per shift, and the additives are altered accordingly. In modern plants, calculation of the burden and collection of data from the furnace are computerized [70].

The silicon content in high-carbon ferrochromium is dependent on the reduction temperature. High-melting slags lead to higher silicon content in the alloy (ferrochromium with 4–6% C). A typical slag composition is 30–33% SiO_2, 26–28% Al_2O_3, 20–25% MgO, 3–7% CaO, and 8–13% Cr_2O_3 for charge chrome containing 52–54% Cr, 6–7% C, and 2–4% Si produced from Transvaal ore or charge chrome containing 63–67% Cr, 5–7% C, and 3–6% Si produced from Zimbabwe ore.

The lumpiness of the ore and the coke quality are important to maintain a proper submerged arc process. Because of the high coke rate (ca. 25%), the coke properties (size, bulk density, volatile matter, and fixed carbon) are mainly responsible for the electrical resistance of the burden.

The current/potential ratio (*I/U*) is particularly important for large furnaces to maintain a reasonable power factor [71]; as a rule, *I/U* is approximately 200. Therefore, the electric power must be supplied at high current and low potential (e.g., 50 kA at 250 V). Specially constructed leads to the electrodes are necessary to carry the secondary current in order to avoid self-induction and energy losses [72].

Because more than 80% of chromite ores mined in the western world are finer than 10 mm, agglomeration processes have been adopted to provide a good burden porosity in the electric arc furnaces, especially in the larger ones [63]. In some ferrochromium plants, fines and lumpy ores are blended in ratios between 1:1 and 4:1. Thus, Union Carbide in Tubatse, South Africa, produces 120 000 t/a of charge chrome in three open submerged arc furnaces, each with a capacity of 30 MV·A. A blend of 80% fines and 20% lumpy ore is used. A submerged arc process can be maintained by using raking machines to break the crusts that are formed [73]. A Cr recovery of 75% was achieved for the production of a charge chrome containing 52.5% Cr, 6.4% C, 3.5% Si, 0.04% S, and 0.02% P, and a slag containing 38% SiO_2, 25.5% MgO, 4.5% CaO, 32% Al_2O_3, and 13% Cr_2O_3. The power consumption was 4000 kWh/t of alloy.

Middelburg Steel & Alloys in South Africa installed a briquetting plant with a capacity of 250 000 t/a. The use of briquettes improved the furnace performance and resulted in higher productivity and lower specific energy consumption. In two semiclosed submerged arc furnaces, each with a capacity of 30 MV·A, 100 000 t/a of charge chrome (53.5% Cr, 7.4% C, 2–3% Si, 0.015% S, and 0.015% P) was produced with a power consumption of 3800 kW h/t of alloy [74].

Pelletizing of chromite fines and concentrates as an agglomeration process has been adopted by Gesellschaft für Elektrometallurgie (GfE) in Germany using the Lepol (grate kiln) process [75], and by Ferrolegeringar in Trollhättan, Sweden, using the Cobo (cold bond) process [76]. These pellets can be used for the production of ferrochromium and silicochromium.

Sintered chrome ore fines were used successfully in Japan. However, briquetting is the main agglomeration method used [63].

Figure 7.20 shows the new process developed by Outokumpu Oy in Finland for the production of ferrochromium from their own chromite-containing deposit near the town of Kemi [77, 78].

The chromite concentrate is pelletized, using bentonite as a binder. After sintering in a shaft furnace, the pellets are blended with fluxes and coke. This burden is then preheated in a rotary kiln at 1000–1100 °C and charged to a fully closed 24 MV·A submerged arc furnace producing 60 000 t/a of charge chrome (53.5% Cr, 7% C, and 2.5% Si) and slag (30.2% SiO_2, 24.9% MgO, 6.8% CaO, 25.9% Al_2O_3, 6.8% Cr, and 1.8% Fe); Cr recovery is 84%. The off-gas from the furnace (ca. 90% CO) has a heat value of 3.07 kWh/m³ (STP) and is used as a fuel for the shaft furnace and for heating the kiln.

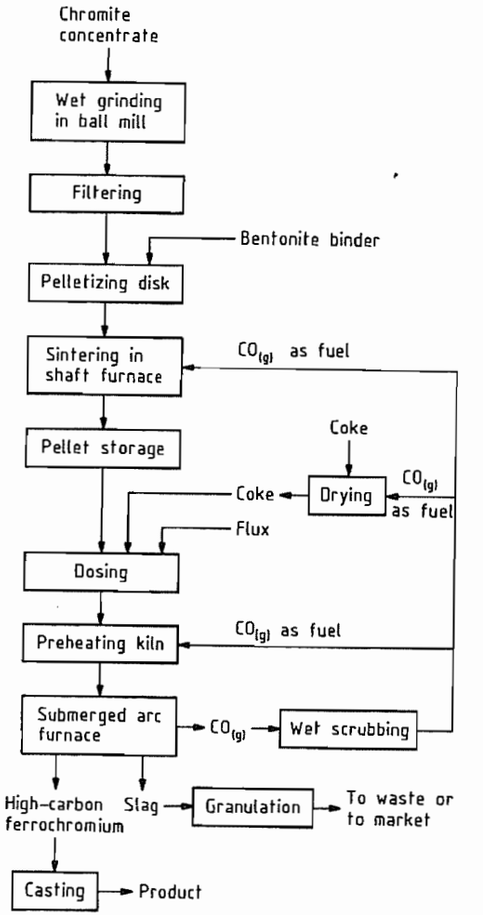

Figure 7.20: Outokumpu Oy high-carbon ferrochromium process [77, 78].

This technology results in a low specific energy consumption of 2600–2800 kWh/t of charge chrome. The process has been adopted in other countries (Orissa Mining in India, Elazig in Turkey, Hellenic Ferroalloys in Greece, and Ferrochrome Philippines in the Philippines). Ferrochrome Philippines successfully began production in 1984 in a 20 MV·A furnace rated for 50 000 t/a of high-carbon ferrochromium [79].

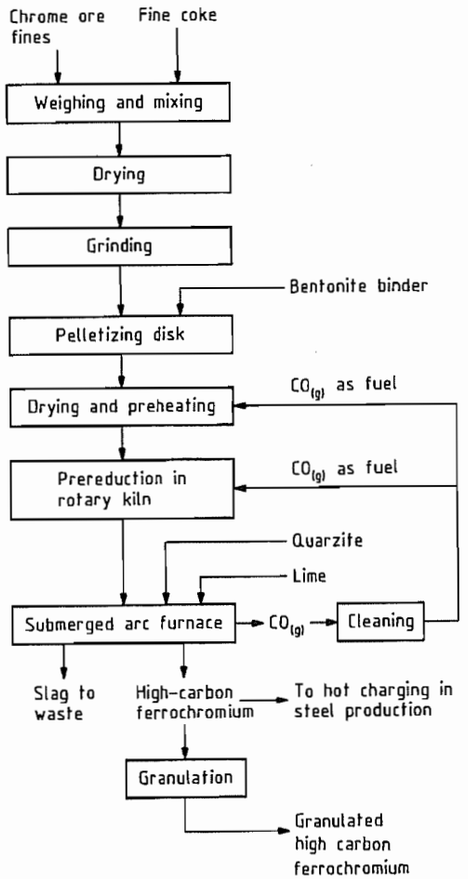

Figure 7.21: Showa Denko high-carbon ferrochromium process [80, 81].

A further improvement in specific energy consumption was achieved by the SRC process (solid-state reduction of chrome ores), developed by Showa Denko K. K. in Japan [80, 81]. This process is shown in Figure 7.21. The addition of carbon and flux during pelletizing resulted in a reduction of iron oxide and a partial reduction of chromium oxide during sintering in a rotary kiln at 1350–1450 °C. Hot charging a burden containing 60% prereduced pellets in a closed 18 MV·A submerged arc furnace required an energy consumption of 2000–2100 kWh/t of alloy for an annual production of 50 000 t high-carbon ferrochromium (57–60% Cr, ca. 8% C, and ca. 3% Si). This process was also adopted by Johannesburg Consolidated Investment (South Africa) in a 180 000 t/a ferrochromium plant.

A special ferrochromium 4–6% C grade with 60–72% Cr and max. 1.5% Si was used for many years in the steel industry before inexpensive charge chrome from South Africa became more attractive. This ferrochromium is not saturated with carbon. It is produced the same way as charge chrome in large submerged arc furnaces, but with a magnesite lining instead of a carbon lining. This process has been improved by using chromite ore mixes containing a definite fraction of hard and lumpy refractory ores with a high MgO content to produce a high-melting slag (e.g., 29–32% SiO_2, 32–35% MgO, 29–32% Al_2O_3, and 3.5–6.0% Cr_2O_3) [82, 83]. At a higher reduction temperature of 1500–1700 °C, the following refining reaction of the refractory ore takes place [66]:

$$3(Cr, Fe)_7C_3 + Cr_2O_3 \rightarrow (Cr, Fe)_{23}C_6 + 3CO$$

Because of the low sulfur specification (< 0.05%) in this grade, coke with low sulfur content is used as the reductant; 30–35% of the sulfur in the coke is transferred to the metal. Alternatively, desulfurizing slags may be used. The ferrochromium can be poured into a highly basic fluid slag, e.g., slag from the LC-ferrochromium process. The sulfur forms CaS, which is removed in the slag.

A new process for producing ferrochromium with 5% C and < 1% Si from unagglomerated chromite fines in a transferred arc plasma furnace has been developed by Tetronics Research & Development [84]. Commercialization of this process has been accomplished in South Africa, where a 10.8 MV·A plasma furnace has been built [85].

7.5.3.2 Medium-Carbon Ferrochromium

Medium-carbon ferrochromium with 0.5–4% C can be produced by refining high-carbon ferrochromium or by silicothermic reduction of chromite ores. Batch refining of high-carbon ferrochromium with refractory chromite ores in an electric arc furnace is no longer used because of the high power consumption of 8000–9000 kWh/t of ferrochromium [72].

Decarburization of high-carbon ferrochromium in an oxygen-blown converter is more economical, especially on a large scale. In the United States and Japan, a top-blowing process with oxygen using water-cooled lances to the metal surface was used. In Germany, a bottom-blowing process (OBM = oxygen bottom Maxhütte or Q-BOP) was introduced in the 1970s [86]. This process is characterized by oxygen injection from the bottom into the metal bath with the oxygen jet, resulting in a high decarburization rate of ca 0.3% C/min. Because of the high bath temperature (1800–1850 °C), mainly the carbon is oxidized. Chromium recovery is high; for example, recovery of product with 0.8–1% C is 85%, and it is improved to 90–93% by adding silicochromium and lime. A typical sequence for a blow is shown in Figure 7.22 [87].

Because demand for medium-carbon ferrochromium is small compared to demand for the high-carbon material, the decarburization processes are rarely used. However, reduction of chromite ores with silicon in the form of silicochromium is used and is an economical production method for medium-carbon ferrochromium because the low-carbon grade can be produced as well. To make ferrochromium with 1–2% C, a silicochromium alloy with a Si content of 25–30% can be used (see Table 7.24). The power consumption, including the energy for silicochromium, amounts to 5000–6000 kWh/t of ferrochromium.

7.5.3.3 Low-Carbon Ferrochromium

Low-carbon ferrochromium is produced mainly by silicothermic reduction of chromite ores. This process dates back to the Swedish three-step process introduced in 1920 by A. B. Ferrolegeringar in Trollhättan [72].

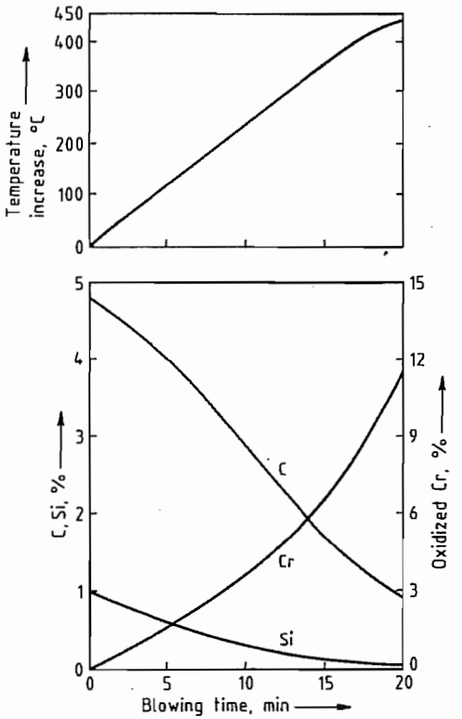

Figure 7.22: Sequence of an OBM-oxygen blow of carbon ferrochromium [87].

In step one, chromite ore was totally reduced with carbon in an electric arc furnace to an intermediate ferrochromium (Halbprodukt) with 60–65% Cr, 5–6% C, and 5–7% Si, and a discard slag. In step two, this intermediate ferrochromium was smelted with quartzite and coke in a slagless process to produce silicochromium (40–45% Si, ca. 40% Cr, and < 0.5% C). Finally, this silicochromium was used as a reductant in the third step; the crushed alloy was thrown onto the surface of a chrome ore-lime melt in an arc furnace. The tapped ferrochromium contained ca. 70% Cr, ca. 1% Si, and 0.03–0.05% C. The slag, which contained 20–25% Cr_2O_3, was returned to the first step to improve Cr recovery.

This Swedish process was modified, especially when the direct silicochromium production by carbothermic coreduction of chromite ore and quartzite in large submerged arc fur-

naces in one step proved more economical than the slagless process. Furthermore, the silicothermic conversion was improved by adding more lime to form a highly basic slag (CaO/SiO_2 ratio of ca. 2). Thus, ferrochromium with < 1.5% Si was produced with a lean slag (ca. 5% Cr_2O_3) in one step. Residual elements, i.e., S and N, were low (< 0.01% and < 0.02%, respectively). The power consumption was 3000–3500 kWh/t of ferrochromium for the silicothermic process (arc furnaces with 2–10 MV·A capacity) and, including the power consumption for the silicochromium production, was 8000–9000 kWh/t ferrochromium.

Currently, the most important process for the production of LC ferrochromium is the Perrin process, developed in 1937 by the Société Ugine in France [88]. This process combines the direct reduction of silicochromium in a submerged arc furnace with a countercurrent silicothermic reduction of a chrome ore-lime melt (produced in an arc furnace) in a reaction ladle.

Production of Silicochromium. Silicochromium is not only used as a reductant in the production of LC ferrochromium, but also as an alloying and deoxidizing agent in the steel industry.

Silicochromium is made in large three-phase submerged arc furnaces of 10–36 MV·A capacity. These furnaces are of the same type as those used to produce HC ferrochromium. The lower reaction zone is lined with carbon and the upper side walls of the furnace shaft are lined with fireclay bricks. Maintaining the Söderberg electrodes deep in the burden column (30–50 cm above the hearth) is important to reduce the SiO_2 to Si. Therefore, coke with low electric conductivity and low bulk density (< 400 kg/m^3) is used (e.g., gas coke).

The electrical conditions in silicochromium furnaces are somewhat different from those in furnaces used to produce HC ferrochromium; e.g., the current/potential ratio is higher (I/U = ca. 500) [72]. The volume of $CO_{(g)}$ from silicochromium production is much higher than from HC ferrochromium production. Therefore, a porous burden is essential. To scrub the huge volumes of $CO_{(g)}$ produced, modern silicochromium furnaces are closed systems, and the unburned gas is used as a fuel.

To produce an alloy composed of 45% Si, 40% Cr, and 0.02% C, a burden containing 100 parts of a refractory chromite (high Cr/Fe ratio of ca. 3 and a MgO/Al_2O_3 ratio of 1.2–1.4), 110 parts of quartzite, and 65 parts of coke (85% fixed C) is continuously charged to the submerged arc furnace. Metal and slag are tapped every few hours. The slag contains 48–50% SiO_2, 25–27% MgO, 19–21% Al_2O_3, and 1–3% Cr_2O_3. The Cr recovery is 93–95%, and the power consumption is 7500–8500 kWh/t of alloy (45% Si). The power consumption is primarily dependent on the Si content of the alloy. For a silicochromium with 40% Si and 45% Cr, the power consumption is 6500–7500 kWh/t.

Production of LC Ferrochromium by the Perrin Process. Single-stage silicochromium production is one portion of the Perrin process. This process requires two furnaces: a submerged arc furnace to produce silicochromium and an open-top electric arc furnace to melt a chromite ore-lime slag. A flow sheet of the entire process is shown in Figure 7.23.

The silicochromium and slag from the submerged arc furnace are tapped to a lined segregating ladle and are allowed to settle for 1–2 h. Dissolved SiC floats to the top. The separated alloy (40–45% Si, 45–40% Cr, and 0.05–0.02% C) is removed through a taphole at the bottom of the ladle. The alloy is reacted with an intermediate liquid slag (8–10% Cr_2O_3) in a second basic-lined reaction ladle to produce an intermediate alloy and a discard slag. The intermediate alloy (20–25% Si, 60–55% Cr, and 0.05–0.03% C) is allowed to solidify and is separated from the slag (< 1% Cr_2O_3). Because of its high basicity, the slag disintegrates to powder (falling slag).

The rich slag (chrome ore lime melt with 25–27% Cr_2O_3, 7–8% FeO, 2–3% SiO_2, and 45–48% CaO) is tapped from the open-top electric arc furnace in weighed amounts to another basic-lined reaction ladle. Crushed intermediate alloy from the first reaction ladle is added to form the desired LC ferrochromium (ca. 70% Cr, < 1.5% Si, and 0.02–0.05% C) and an intermediate slag (8–10% Cr_2O_3). This slag is reacted with silicochromium to lower the Cr_2O_3 content to < 1%.

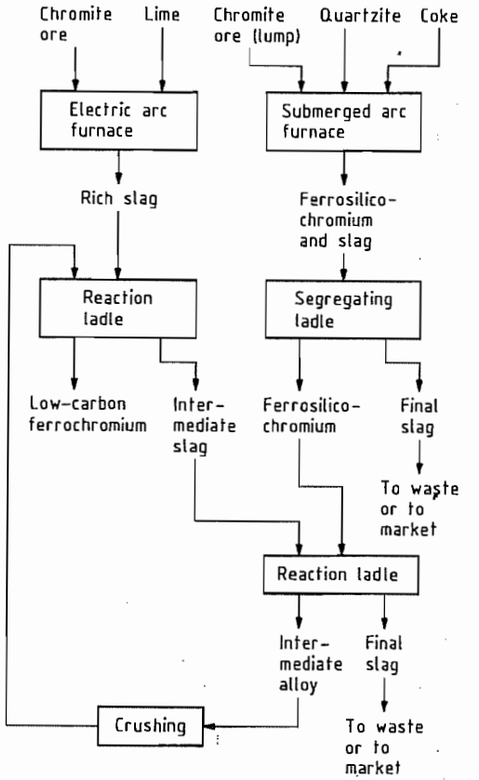

Figure 7.23: Low-carbon ferrochromium production by the Perrin process [88] (according to [65]).

Production of 1 t of silicochromium by this process typically requires 1450 kg of chrome ore, 1500 kg of quartzite, 870 kg of coke, 32–35 kg of electrodes, and 7700 kWh power [65]. Production of 1 t of ferrochromium requires 1440 kg of chrome ore, 1250 kg of lime, 660 kg of silicochromium (45% Si and 40% Cr), 22 kg of electrodes, and 3200 kWh power.

Therefore, the total energy consumed to produce 1 t of LC ferrochromium, including silicochromium production, is 8200 kW·h. The overall recovery of Cr by the Perrin process is 90–92%.

Low-carbon ferrochromium is tough and difficult to break. Therefore, it is poured into flat molds, sometimes filled with liquid slag to protect the mold. Quenching the hot alloy in water facilitates breaking it into small lumps, which is performed with heavy pneumatic hammers.

Many variations of the Perrin process have been developed. For example, chrome ore or lime have been added to the exothermic reactions, which occur in the two reaction ladles (Figure 7.23), to "dampen" the reaction and to save energy. Another variation is the selective reduction of FeO, producing an iron-rich alloy; the remaining slag, high in Cr_2O_3, is reacted with silicochromium high in Si, to give LC ferrochromium (80–90% Cr). By selectively reducing FeO, CoO is also reduced in the iron-rich alloy and a Co-free ferrochromium can be produced. This is used to produce alloyed steels for atomic energy plants.

Production of LC Ferrochromium by the Simplex Process. From 1943 to 1953 Union Carbide developed a new production process for LC ferrochromium, the so-called Simplex process, in which finely ground HC ferrochromium was decarburized in the solid state with oxidized ferrochromium by vacuum annealing [89–91]. The plant in Marietta, Ohio, went into production in 1953 and is now managed by Elkem Metals Co., Pittsburgh, Pennsylvania. The flow sheet of the process is shown in Figure 7.24.

High-carbon ferrochromium is crushed, pulverized in ball mills, and then oxidized in suspension in a vertical gas- or oil-fired shaft furnace [92]. The proper stoichiometric C/O ratio for decarburizing is attained by mixing the oxidized material with HC ferrochromium powder according to the following reactions:

$$3Cr_7C_3 + Cr_2O_3 \rightarrow Cr_{23}C_6 + 3CO$$

$$^1/_2Cr_{23}C_6 + Cr_2O_3 \rightarrow {}^{27}/_2Cr + 3CO$$

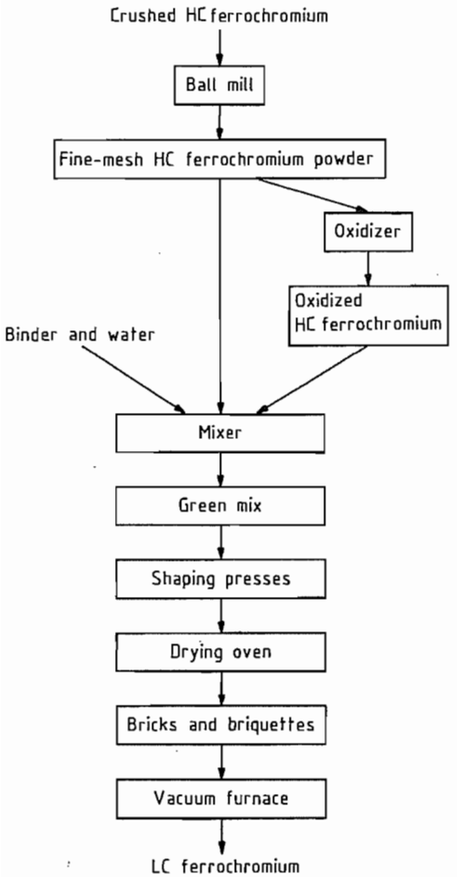

Figure 7.24: Production of low-carbon ferrochromium by the Simplex process [90].

The mixture is either formed into briquettes or loosely packed in corrugated pasteboard boxes, placed on a refractory topped bogie hearth (33.5 m × 3.35 m), and rolled into the vacuum chamber, which is a horizontal steel cylinder (43 m in length × 4.6 m in diameter). The graphite resistance heating elements are suspended above the charge from the refractory-lined roof. The vacuum (0.01–0.4 kPa) is generated by multistage steam ejectors. The process requires a special heating program up to 1370 °C, which follows the progress of decarburization. When the decarburization of the charge is complete, the power is shut off and the furnace is cooled by flooding with argon.

A complete reaction cycle requires 4–5 d; ca. 100 t of material is produced. A typical analysis of LC ferrochromium from the Simplex process is ca. 70% Cr, ca. 1% Si, and 0.008–0.010% C. Oxygen is higher (ca. 1%) than in LC ferrochromium from the Perrin process (ca. 0.2%).

7.5.3.4 Nitrogen-Containing Low-Carbon Ferrochromium

Chromium has a high affinity for nitrogen and forms the nitrides Cr_2N and CrN. Low-carbon ferrochromium can form nitrides either in the solid or in the liquid state. These alloys with up to 10% N are used in steel containing nitrogen as well as chromium [58]. The Simplex process is convenient for forming nitrides in LC ferrochromium in the solid state. During the cooling cycle, nitrogen is added to the vacuum vessel and the optimum temperature range of 1200–800 °C is held over a longer period to produce an alloy with 7–10% N.

Silicothermically produced LC ferrochromium can form nitrides when pulverized and heated in boxes in a continuous annealing furnace at 1000 °C under nitrogen [93]. The sintered product (ρ 5–6 g/cm³) contains 5–10% N as Cr_2N.

On the other hand, LC ferrochromium can form nitrides in the liquid state with nitrogen gas in a melting furnace, e.g., an induction furnace [94]. The tapped alloy contains 2–4% N and is very homogeneous (ρ 7.0 g/cm³) [95].

7.5.3.5 Other Chromium Master Alloys

Chromium master alloys other than ferrochromium are produced in much smaller amounts. They are used mainly to produce heat-resistant alloys, based on nickel or cobalt (superalloys), and abrasion-resistant materials, and are used to alloy small amounts of chromium to copper or aluminum.

Nickel–chromium master alloys containing 50–80% chromium may be made by aluminothermic processes or by melting chromium metal and nickel in induction-heated furnaces. The aluminothermic process must be performed in water-cooled molds in an inert atmosphere because of the high quality required of these master alloys [96]. For direct melting of chromium metal and nickel, a vacuum induction furnace or an inert gas atmosphere is also preferred; refining occurs simultaneously during melting [97].

Binary chromium master alloys, such as *chromium–molybdenum* (with 30% Mo) or *chromium–niobium* (with 30–80% Nb) [98, 99], are made by aluminothermic reduction of the corresponding oxides. Master alloys containing more than two metals, e.g., *cobalt–chromium–tungsten* (ca. 43% Co, ca. 37% Cr, ca. 16% W, ca. 3% C), or *cobalt–chromium–molybdenum* (26–30% Cr, 4–5% Mo, rest Co) [99], are made by direct melting of the metals in an inert atmosphere or in vacuum induction furnaces. *Copper–chromium* master alloys containing up to 10% Cr, e.g., V–CuCr 10 [100], are made by directly alloying chromium with an oxygen-free copper melt; the resulting alloy is quickly cast into flat pigs. The same method is used for the production of *aluminum–chromium* master alloys with 5, 10, or 20% Cr by alloying comminuted chromium metal with a superheated aluminum melt. The master alloy containing 5–6% Al is standard in Germany, i.e., V–AlCr 5 [101]. Another aluminum chromium master alloy containing ca. 50% Cr and 50% Al is made for special purposes [99].

7.5.4 Quality Specifications, Storage and Transportation, and Trade Names

International standards of specifications and conditions of delivery for ferrochromium and ferrosilicochromium are given in ISO 5448 [102] and ISO 5449 [103], respectively. The following specifications are contained in tables in reference [102]:

- Chromium content of ferrochromium alloys ranges from 45 to 95% [102, Table 1]; e.g., the designation is FeCr 50 for 45–55% Cr content.
- Composition of HC ferrochromiums with normal phosphorus [102, Table 2] and with low phosphorus content [102, Table 3]; e.g., FeCr 50 C 50 (45–55% Cr, 4–6% C, max. 1.5% Si, max. 0.050% P, and max. 0.10% S), or FeCr 60 C 50 Si 2 LP (55–65% Cr, 4–6% C, 1.5–3% Si, and max. 0.03–% P). HC ferrochromium is standardized to 10% C. Ferrochromium with low sulfur content is designated LS (low sulfur, i.e., max. 0.05%).
- Analysis of MC ferrochromiums with normal phosphorus [102, Table 4] and with low phosphorus [102, Table 5]; carbon content ranges from 0.5–1.0%, 1.0–2.0%, up to 2.0–4.0%, e.g., FeCr 70 C 20 (65–75% Cr, 1.0–2.0% C, max. 1.5% Si, max. 0.050% P, and max. 0.050% S); or FeCr 60 C 10 LP (55–65% Cr, 0.5–1.0% C, max. 1.5% Si, max. 0.03% P, and max. 0.050% S).
- Standard chemical composition of LC ferrochromium for normal [102, Table 6] and for low [102, Table 7] phosphorus alloys; carbon content ranges from less than 0.015%, 0.015–0.030%, up to 0.25–0.50%; e.g., FeCr 60 C 05 (55–65% Cr, 0.03–0.05% C, max. 1.5% Si, max. 0.050% P, max. 0.030% S, and max. 0.15% N) or FeCr 70 C 03 LP (65–75% Cr, 0.015–0.03% C, max. 1.5% Si, max. 0.03% P, max. 0.03% S, and max. 0.15% N).
- LC ferrochromium with high chromium content (75–95%) [102, Table 8]; e.g., FeCr 90 C 03 (85–95% Cr, 0.015–0.03% C, max. 1.5% Si, max. 0.020% P, max. 0.03% S, max. 0.02% Co, and max. 0.20% N).
- Nitrogenated LC ferrochromiums [102, Table 9]; the three given are smelted FeCr…C1 N3, sintered FeCr–C1 N7, and sintered FeCr…C1 N7 Si. The Cr contents given in [102, Table 1] are valid for these alloys. The nitrogen contents are 2–4% in the smelted qualities and 4–10% in the sintered qualities.

- Particle size ranges for ferrochromium deliveries [102, Table 9]; there are seven classes from 100–315 mm (Class 1) to ≤ 3.15 mm (Class 7).

ISO Standard 5448 [102] also covers testing (sampling and chemical analysis) as well as storage and transportation according to international regulations. ISO Standard 5449 [103] for ferrosilicochromium specifications and conditions of delivery recognizes 12 different compositions with increasing Si content, ranging from FeCrSi 15 (min. 55% Cr, 10%–18% Si, max. 6% C, max. 0.05% P, and max. 0.03% S) up to FeCrSi 50 (min. 20% Cr, 45–60% Si, max. 0.1% C, max. 0.03% P, and max. 0.03% S). Low-carbon and low-phosphorus grades are FeCrSi 50 LC (max. 0.05% C) and FeCrSi 48 LP (min. 35% Cr, 42–55% Si, max. 0.05% C, max. 0.02% P, and max. 0.01% S). The particle size of ferrosilicochromium deliveries is specified in seven classes as for ferrochromium. Ferrochromium and ferrosilicochromium are shipped in bulk or packaged in containers or steel drums.

In the United States, standards for ferrochromium and ferrosilicochromium are specified in ASTM A 101–73 [104] and ASTM A 482–76 [105]. Also recommended are methods for sampling (ASTM–E32) and chemical analyses (ASTM–E31). Comparisons between the standards in Germany for ferrochromium and ferrosilicochromium in DIN17565 [106] and the ISO standards are given in Tables 7.25 and 7.26 [107].

Internationally approved methods for sampling [108] and analytical determination of chromium in ferrochromium and ferrosilicochromium [109] and of silicon in ferrosilicochromium [110] are available as a draft.

Table 7.27 contains trade names and the relevant analyses of special and nonstandardized ferrochromium and ferrosilicochromium alloys. Charge chrome is a relatively cheap high-carbon ferrochromium with no definite specification. It can be added to a basic oxygen-blown stainless steel charge [65]. Extra-high-carbon (EHC) ferrochromium is supplied as a powder for abrasive surface-welding purposes. Simplex ferrochromium is a low-carbon ferrochromium produced by the Simplex process. Low-carbon and -nitrogen (LCN) and low-carbon, -nitrogen, and -silicon (LCNSi) ferrochromium are trade names for special grades used to manufacture corrosion- and heat-resistant steel. A low-carbon ferrochromium reactor grade is used to make corrosion- and heat-resistant steel for nuclear equipment. Cromax is a low-carbon, high-chromium ferrochromium used to produce heat-, corrosion-, and wear-resistant special steel. The high-chromium alloys can partly replace chromium metal in superalloys. Silicochrom 40 is mainly used for deoxidizing steel and for Cr_2O_3 reduction in slags; silicochrom 60 for alloying corrosion- and heat-resistant steel.

Table 7.25: Comparison of the chemical composition of ferrochromium ISO 5448 and DIN 17565 [107].

Designation	% Cr		% C		% Si		% P max.		% S max.	
	SIN	ISO	DIN	ISO	DIN	ISO	DIN	ISO	DIN	ISO
FeCr 70 C 5	60–72	—	4.0–6.0	—	< 1.5	—	0.030	—	0.50	—
FeCr 50/60/70 C 50	—	45–75[a]	—	4.0–6.0	—	< 1.5	—	0.050	—	0.10
FeCr 50/60/70 LSLP	—	45–75[a]	—	4.0–6.0	—	< 1.5	—	0.030	—	0.05
FeCr 70 C	65–75	—	0.5–4.0[b]		< 1.5		0.030	—	0.050	—
Fe 50/60/70 C	—	45–75[a]	—	0.5–4.0[b]	—	< 1.5	—	0.050	—	0.050
FeCr 70 C[c]	65–75	—	0.01–0.50[d]	—	< 1.5	—	0.030	—	0.010	—
FeCr 50/60/70 C	—	45–75[a]	—	0.015–0.50[e]	—	< 1.5	—	0.050	—	0.030

[a] FeCr 50 means 45–55% Cr, FeCr 60 means 55–65% Cr, FeCr 70 means 65–75% Cr.
[b] In four grades.
[c] 0.15% N.
[d] In seven grades.
[e] In six grades.

Table 7.26: Comparison of the chemical composition of ferrosilicochromium ISO 5449 and DIN 17565 [107].

Designation	% Cr		% C		% Si		% P max.		% S max.	
	SIN	ISO	DIN	ISO	DIN	ISO	DIN	ISO	DIN	ISO
FeCrSi 15	—	> 55.0	—	10.0–18.0	—	6.0	—	0.050	—	0.030
FeCrSi 20/22	55–65	> 55.0	25–20	20.0–25.0	0.50	0.05	0.020	0.030	0.010	0.030
FeCrSi 23	—	> 45.0	—	18.0–28.0	—	3.5	—	0.050	—	0.030
FeCrSi 26	—	> 45.0	—	24.0–28.0	—	1.5	—	0.030	—	0.030
FeCrSi 33	—	> 43.0	—	28.0–38.0	—	1.0	—	0.050	—	0.030
FeCrSi 40	40–45	> 35.0	45–35	35.0–40.0	0.050	0.2	0.020	0.030	0.010	0.030
FeCrSi 45	—	> 28.0	—	40.0–45.0	—	0.1	—	0.030	—	0.030
FeCrSi 50 LC	—	> 20.0	—	45.0–60.0	—	0.05	—	0.030	—	0.030
FeCrSi 55	—	> 28.0	—	50.0–55.0	—	0.03	—	0.030	—	0.030
FeCrSi 48 LP	—	> 35.0	—	42.0–55.0	—	0.05	—	0.020	—	0.010

Table 7.27: Special and nonstandardized ferrochromium and ferrosilicochromium alloys.

Trade name	Analysis, %							Producer
	Cr	C	Si	P	S	N	Co	
Charge chrome[a]	53–58	5–8	6–3	—	—	—	—	—
EHC ferrochromium	min. 66	min. 9.0	0.5–1.0	max. 0.03	max. 0.05	—	—	GfE/EWW[b]
Simplex ferrochromium	ca. 70	max. 0.01	ca. 1.0	—	—	—	—	Union Carbide/Elkem
LCN ferrochromium	ca. 70	max. 0.05	max. 1.5	—	—	max. 0.020	—	GfE/EWW[b]
LCNSi ferrochromium	ca. 70	max. 0.05 max. 0.03	max 0.30 max. 0.20	—	—	max. 0.020	—	GfE/EWW[b]
Ferrochromium reactor grade	80–85	max. 0.06 max. 0.05	max. 2.5 max. 1.50	—	—	max. 0.20	max. 0.02	ABF/FTA[c]
Cromax-90 chrome	85–90	max. 0.06 max. 0.03	max. 1.0 max. 0.5	max. 0.015 min. 0.007	max. 0.015 min. 0.007	—	—	Showa Denko
Silicochrom 40	35–40	max. 0.05	35–40	max. 0.03	—	—	—	GfE/EWW[b]
Silicochrom 60	55–65	max. 0.05	20–25	max. 0.03	—	—	—	GfE/EWW[b]

[a] Alloy has no definite specification.
[b] Gesellschaft für Elektrometallurgie/Elektrowerk Weisweiler.
[c] Aktiebolaget Ferrolegeringar/Trollhätteverken.

7.5.5 Uses

Ferrochromium is used principally as a master alloy to produce Cr-containing steel and cast iron [58]. Chromium alloyed in steel imparts oxidation and corrosion resistance because of the formation of a thin, continuous, impervious chromium oxide film on the steel surface.

Most ferrochromium is used to manufacture stainless steel. Martensitic grades with ca. 13% Cr are used for applications such as knives, whereas ferritic grades with 18–22% Cr are used as deep-drawing sheets. Austenitic CrNi steels exhibit especially good corrosion (acid) resistance and are used for equipment in the chemical industry as well as for food-processing machinery. The most widely known type is AISI 302, which contains 18% Cr and 8% Ni. A small amount of molybdenum further improves the acid resistance. Heat-resistant steel (24–26% Cr and 19–21% Ni) is used in power stations for steam boilers and heat exchangers; superalloys based on nickel or cobalt (ca. 30% Cr) are used for gas turbine parts.

Chromium addition to steel also improves its mechanical properties (ability to harden, wear resistance, and retention of strength at elevated temperature). Steel with 0.5–2.0% Cr is widely used in the automotive industry as

case-hardening steel (≤ 0.2% C and 1.4–2.1% Ni) and heat-treatable steel (0.2–0.5% C, 0.9–2.1% Ni, and 0.15–0.35% Mo). Abrasion-resistant steel for ball bearings is alloyed with 0.5–1.6% Cr (ca. 1% C and 0.2% Mo). Permanent magnetic steel contains 1–3% Cr (1.0–1.3% C). In tool steel for cold and hot working and high-speed steel, up to 14% Cr is alloyed as carbide (in addition to carbides of W, Mo, and V). Stellites (35–70% Co, 25–33% Cr, 10–25% W, and 2–4% C) are highly resistant to abrasion and are used for cutting tools.

Addition of up to 30% chromium to cast iron improves hardness and heat resistance. Powdered ferrochromium (mainly the high-carbon grade) is used for chromizing the surface of steel or cast iron parts (pack-chromizing or case-chromizing. A high-carbon ferrochromium with extra-high-carbon content is used in powdered form for abrasive surface welding (Table 7.27, EHC Ferrochromium).

7.5.6 Economic Aspects

Ferrochromium is mainly consumed in highly industrialized countries producing a major amount of high-grade (stainless) steel, e.g., the United States, Europe, and Japan. However, production is shifting from these consuming countries to those with large ore resources; 93% of the known potential chromite reserves of the world are in Africa, mainly in South Africa, and ca. 3% in the former USSR and Albania [111] (see Table 46.1). This shift is a consequence of modern oxygen-blowing processes in combination with argon and vacuum treatment, i.e., argon–oxygen decarburization and vacuum–oxygen decarburization, for the production of stainless steel. These processes allow the use of cheap HC ferrochromium (charge chrome) instead of LC grades. Formerly only LC ferrochromium could be used. Because power consumption for production of HC ferrochromium is only about half that of the LC grade, the availability of cheap hydroelectric power in Scandinavia is no longer as advantageous. The change in ferrochromium consumption from LC to HC grades first took place in the United States and later, in the 1970s, in Europe [112].

In 1984, world production of marketable, i.e., lumpy, ore and concentrates was 9.2×10^6 t, 11% of which was produced in Western Europe, Finland, Turkey, Greece, and Cyprus, 37% in Eastern Europe (former USSR and Albania), 4% in Latin America (Brazil and Cuba), 9% in Asia (Philippines, India, Iran, Vietnam, Japan, and Pakistan), and 38% in Africa (South Africa, Zimbabwe, Madagascar and Sudan) [113]. In 1984, the world production of chromite ore and concentrates was 9.9×10^6 t, 72% of which was consumed for metallurgical, 12% for refractory, and 17% for chemical purposes.

The metallurgical industry was the main user of chromium and consumed the following amounts in 1980 (based on United States statistics) [114]: 72% for wrought stainless and heat-resistant steels, 13% for wrought alloy steel, 3% for tool steel, 7% for cast iron and cast steel, and 5% for other uses. In 1984, the total consumption of primary chromium units (from ferrochromium) in the United States was 195 380 t of which 79% was for the production of stainless and heat-resisting steels, i.e., 96 kg of chromium units per ton of stainless and heat-resisting steels produced [115]. The ferrochromium consumption in Germany was 263 300 t in 1985. The change in consumption of LC to HC ferrochromium over the last 25 years is evident from Table 7.28.

In 1981, consumption of ferrochromium in the western world was estimated to be $(1.32–1.36) \times 10^6$ t; ca. 0.5×10^6 t of this was consumed in the European Economic Community (EEC). In 1982, consumption fell drastically because of the recession in the steel industry. Consumption in the western world has since increased to ca. 2×10^6 t [116]. In 1981, the production capacity for ferrochromium plants in the western world was 3.1×10^6 t [86].

Prices of ferrochromium and ferrosilicochromium are reported weekly in *Metal Bulletin* (London). *Erzmetall* (published monthly) reports prices twice a year for raw materials and for ferrochromium. *American Metal Market* is a daily publication that also gives chromium ore and alloy prices.

Because the United States does not possess chromite deposits, most of the ferrochromium consumed is imported, mainly from Africa [117].

7.5.7 Environmental Protection; Toxicology and Occupational Health

Considerable attention must be paid to environmental protection during ferrochromium production. Dust evolution from ores and raw materials must be controlled during transportation and storage, and also during preparatory processes.

The off-gas from the electric arc furnaces is cleaned by using devices, such as bag filters, scrubbers, and electrostatic precipitators [72]. Bag filters are mainly used in preparatory processes, e.g., grinding, drying, briquetting [74], and pelletizing [75], and in open or semiclosed submerged arc furnaces [73, 74]. Scrubbers (Venturi and disintegrators) are preferred for cleaning unburned CO gas from closed submerged arc furnaces [77]. Effluent water from the scrubber is treated to meet wastewater regulations. Electrostatic precipitators (Cottrell filters) are also used for cleaning the off-gas from submerged arc furnaces for HC ferrochromium [118] and ferrosilicochromium [119] production. Gas from the chrome ore-lime melting furnace and from the ladle reactions during the Perrin process are cleaned with bag filters [120]. The dust content can be lowered from 150 to 20 mg/m³ and the emission of Cr(VI) to < 1 mg/m³ by optimizing the working conditions.

Chromium(VI) is mainly responsible for the toxicity of chromium and its compounds. Chromic acid, CrO_3, is carcinogenic. Germany has enacted an emission protection law and a technical guidance for clean air (TA-Luft) [121]. The TA-Luft restricts the mass of carcinogenic substances, i.e., Cr(VI) compounds (specified as Cr), in respirative form to 1 mg/m³ (Class II). The total dust concentration in emissions is limited to 20 mg/m³, and other inorganic materials in dust form, i.e., chromium and its compounds (Class III), to 5 mg/m³. The maximum allowable concentration (MAK) of CrO_3 (measured as CrO_3) in the air at the workplace is 0.1 mg/m³ [122].

In the United States the Clean Air Act Amendments, enacted in 1970, mandated the states set standards to limit air pollution. In pursuing this amendment, the U.S. Environmental Protection Agency (EPA) in a joint effort with the Ferroalloys Association studied dust emissions from alloy plants to establish ambient air quality standards [123, 124]. The states enacted process weight regulations and applied them to ferroalloy furnaces. The EPA published their studies "Engineering and Cost Study of the Ferroalloy Industry" and proposed New Source Performance Standards (NSPS) for new furnaces. A comparison of the state regulations and the NSPS (promulgated October, 1974) limitations for HC ferrochromium, charge chrome, and ferrosilicochromium for a 30-MW furnace are shown in Table 7.29 [124].

Table 7.28: Ferrochromium consumption in Germany.

	Consumption, t/a					
	1960	1965	1970	1973	1983	1985
LC ferrochromium	43 450	34 650	44 500	33 550	13 000	14 350
MC ferrochromium	20 300	24 400	16 700	18 400	7 500	11 600
HC ferrochromium	7 500	17 550	70 600	113 150	210 000	237 350
Total	71 250	76 600	131 800	165 100	220 500	263 300

Table 7.29: Comparison of NSPS limitations and state regulations for ferrochromium dust emissions [124].

Material	NSPS limitation		State regulation	
	kg/(mw·h)	kg/h	Most stringent	Least stringent
HC ferro-chromium	0.23	6.94	13.00	17.55
Charge chrome	0.23	6.94	13.00	17.55
Ferrosilico-chromium	0.23	6.94	8.29	10.80

Regulations on water pollution control (the federal act was passed in 1972) were also proposed by the Ferroalloys Association Environmental Committee and EPA [124]. Finally, the disposal of solid waste (slags, dusts, etc.) is also subject to regulations.

The TLV–TWA (1985–1986), which have been adopted, are as follows [125]: 0.5 mg/m^3 for chromium metal and chromium(II) and chromium(III) compounds, and 0.05 mg/m^3 for chromite ore processing (chromate) as Cr and chromium(VI) compounds as Cr. Chromite ore processing and certain water-insoluble Cr(VI) compounds are listed in Appendix A1a as human carcinogens.

7.6 Ferronickel

The rotary kiln electric furnace smelting process is now used almost universally for the production of ferronickel from oxide ores. Nippon Mining shut down the last blast furnace producing ferronickel, at Saganoseki in Japan, in 1985 [131]. Variations on the electric furnace ferronickel process, which were developed in the 1950s by Ugine (France) and by Falconbridge in the 1960s, made it possible to achieve a more selective reduction of nickel, and thereby produce higher nickel grade products from lower grade ores.

The first commercial scale electric furnaces to produce ferronickel were the 10.5 MVA units installed by SLN at its Doniambo smelter in New Caledonia in 1958. The largest units currently (1989) in operation are a 51 MVA unit at Cerro Matoso in Colombia and a 60 MVA furnace at Pacific Metals at Hachinohe in Japan.

7.6.1 Rotary Kiln–Electric Furnace Process [130]

In the earliest plants, the function of the rotary kiln was limited to drying and dehydrating the ore, and furnace operating temperatures did not exceed 700 °C. The hot calcine was then blended with reductant, usually coal, and transferred to the electric furnace where reduction of the metals occurred.

In the electric furnace the calcined ore was smelted with the reductant to form immiscible layers of slag and ferronickel. The New Caledonian ores, with their high magnesia and silica contents (2.5% Ni, 10–15% Fe), require no additional flux for slag formation. Virtually all the nickel and 60–70% of the iron in the ore are reduced to metal to yield a ferronickel grading about 20% Ni; the slag contains only 0.1% Ni. The energy consumption in the electric furnace for this mode of operation is 2.0–2.2 GJ per tonne of dry ore (550–600 kWh/t).

As the process was developed and applied to a wider range of nickel laterite ores, several improvements in design and operating technique were made. The operating temperature of the rotary kiln was increased to 900–1000 °C, and reductant was added to the kiln feed to ensure a more complete dehydration of the ore and to allow a partial reduction of the metals to occur in the kiln. As a result energy consumption in the electric furnace was reduced to 1.8–2.0 GJ/t (500–550 kWh/t).

The degree of reduction achieved in the kiln depends on the composition of the ore and on the reactivity of the reductant. Iron and nickel silicate minerals are generally less reactive than nickel oxide minerals. Usually lignites and charcoal are the most reactive reductants, and high-volatile coals are more reactive than low-volatile coals, anthracite, or coke. Typically, under optimum conditions, up to 40% of the nickel is reduced to metal in the kiln, while the iron oxides are reduced to iron(II) oxide (FeO).

In the electric furnace the charge must be heated to 1400–1650 °C to permit the separation of distinct slag and metal phases. The energy input to the charge is provided by

radiation from the electric arcs around the tips of the electrodes and by the heat generated in the slag by resistance heating due to the flow of current through the slag layer between the electrodes. Since the electrical resistivity of the metal layer is much lower than that of the slag, very little heat is generated in the metal layer, which must therefore receive heat by conduction and convection transfer from the overlying slag layer. For satisfactory heat transfer, the temperature differential between slag and metal layers should be at least 100 °C.

The mode of operation of the electric furnace is largely determined by the melting temperature of the slag. Except for the limonitic ores, where the alumina and lime contents have a significant effect, the slag melting temperatures for a particular ore can be estimated from the FeO–MgO–SiO_2 equilibrium phase diagram (Figure 7.25) [132]. For SiO_2/MgO weight ratios of less than 2:1, the slag melting temperatures are essentially independent of the FeO content. At high SiO_2/MgO weight ratios the slags are close to saturation with SiO_2, and the slag melting temperatures are then a function of the FeO content (Figure 7.26) [129]. High iron contents, which normally occur with low-magnesia ores, result in the formation of highly corrosive low-melting (1350–1450 °C) slags. Since the use of magnesia or silica fluxes is usually uneconomic, the problem of low-melting slags must be overcome in the design and operating mode of the furnace [133].

Operation of the electric furnace is simplest when the slag melting temperature is higher than the metal melting temperature (1300–1400 °C). For such a system the furnace is operated with a covered bath (Figure 7.27A). The hot ore charge is allowed to build up on top of the molten slag, and the electrodes are not immersed in the slag layer. Under these conditions much of the reduction reaction occurs in the hot charge layer before it melts.

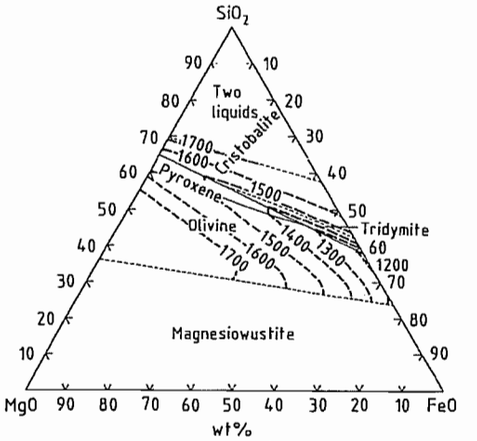

Figure 7.25: The FeO–MgO–SiO_2 phase diagram.

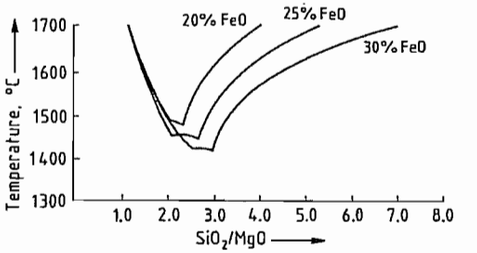

Figure 7.26: Slag melting point as a function of FeO content.

The high-iron limonite ores, which produce slags with melting points well below the melting point of the metal phase, can be smelted if the distance between the electrode tips and the slag–metal interface is reduced significantly. The electrodes must therefore penetrate deeply into the molten slag layer (Figure 7.27B). A vertical temperature gradient is then set up in the slag layer, with the highest temperature around the electrode tips. Under these conditions it is possible to operate the furnace with a metal tapping temperature higher than the slag tapping temperature. However the deep immersion of the electrodes in the slag results in a significant reaction between the carbon of the electrodes and metal oxides in the slag, with the evolution of carbon monoxide around the electrodes. The evolution of gases makes covered bath operation of the furnace impractical, and necessitates open bath

operation (Figure 7.27B) with the slag surface exposed around the electrodes [130].

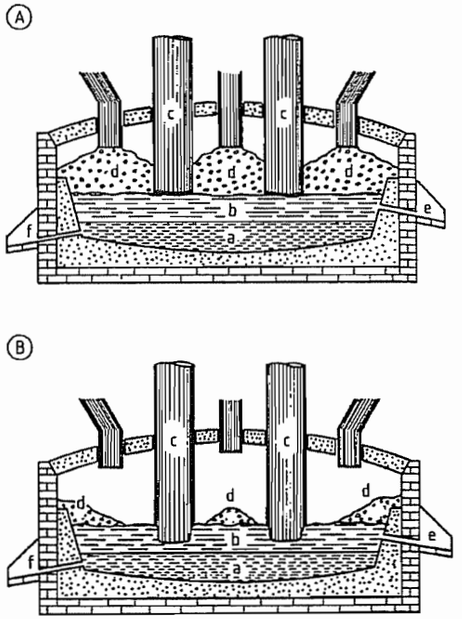

Figure 7.27: Electric furnace operation. A) Covered bath; B) Open bath. a) Metal pool; b) Slag bath; c) Electrodes; d) Solid charge; e) Slag tap hole; f) Metal tap hole.

The ferronickel grade produced in the electric furnace smelting operation can be closely controlled by the amount of solid reductant added to the process. For a given addition of reductant, nickel recovery is highest, followed by cobalt, and iron recovery to the metal phase is lowest. Generally as much as 60–70% of the iron is reduced from silicate ores, while only 10–15% of the iron is reduced from high iron limonitic ores.

Normal operating practice is to produce up to 25% Ni ferronickel from silicate ores and 15–20% Ni ferronickel from limonitic ores. Nickel losses to the electric furnace slag under these conditions are quite low (0.1% Ni in the slag). Nickel losses to slag increase with nickel grade, although grades with 35–45% Ni can normally be produced from most ores without excessive losses (0.15–0.20% Ni in the slag). Above 45% Ni in ferronickel, slag losses increase rapidly. Where higher grades are required, the ferronickel electric furnace product can be upgraded by removing iron by oxidation and slagging in an oxygen-blown converter, and the high Ni content slag is recycled to the electric furnace. Ferronickel grades as high as 90% nickel can be achieved with two stages of converter upgrading.

Current industrial practice is illustrated by the following descriptions of specific operations. In the Doniambo smelter of SLN in New Caledonia, which was built in 1958, the wet ores are carefully blended and screened to produce a smelter feed with an average composition of 2.5–3.0% Ni and Co, 20–28% MgO, 15–20% Fe_2O_3, and 30–40% SiO_2. The ore is blended with anthracite as a reductant and heated in a rotary kiln to 950 °C. Only a minor degree of reduction occurs in the kiln. The hot calcine is transferred to an electric furnace (one of eight 10.5 MVA or three 33 MVA units). Smelting is carried out with a charge covered bath, although the electrodes dip about 30 mm into the slag layer. Energy consumption is 90 MJ/kg Ni (2.35 GJ/t ore or 650 kWh/t ore) and electrode consumption is 1.5 kg/kg Ni (39 kg/t ore). Nickel and iron recoveries from ore to ferronickel product are 95 and 50%, respectively. The slag tapping temperature is 1550–1600 °C, while the metal is tapped at 1450 °C. The slag, which typically contains 0.1–0.2% Ni, is granulated and discarded [134, 135].

The crude ferronickel contains 24% Ni, 69% Fe, 2% C, 3% Si, 1.5% Cu, and 0.25% S. It is either cast into ingots for market, converted to nickel matte, or desulfurized and refined to higher quality ferronickel. Ferronickel is marketed by SLN as 25 kg ingots and as granules.

Much the same process is used by the three Japanese ferronickel smelters, Pacific Metals at Hachinohe [136], Sumitomo at Hyuga [137], and Nippon Mining at Saganoseki, by Morro do Niquel in Brazil [138], by PT Aneka Tambang in Indonesia, and by Cerro Matoso in Colombia [139, 140]. All these operations process ores with relatively low Fe/Ni ratios of 6:1 or less. Representative ore and slag compositions are given in Table 7.30.

Table 7.30: Silicate ore and slag compositions [129].

Smelter	Ore composition, %				Slag composition, %		
	Ni	Fe	MgO	SiO_2	FeO	SiO_2	MgO
SLN	2.7	14–15	20–28	35–40	12	45	30
Hyuga	2.4	9–14	22–29	35–43	8	52	36
Morro de Niquel	1.25	6.5	30	43	7	50	30
Aneka Tambang	2.25	13	24	45	5	56	29
Cerro Matoso	2.9	14	15	46	22	59	20

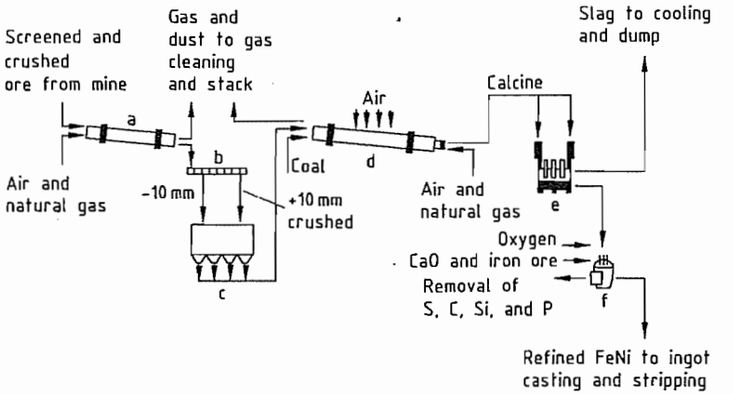

Figure 7.28: Flow sheet of the Cerro Matoso ferronickel smelter: a) Drying kiln; b) Screen; c) Batch bins; d) Reduction kiln; e) Electric furnace; f) ASEA/SKF Fe–Ni refining.

The most recently built plant is that of Cerro Matoso (1982) which treats an ore with the exceptionally high SiO_2/MgO ratio of 3:1. The resulting acid slags have proved to be highly corrosive to furnace refractories. The dried ore (12% moisture) is ground, blended with coal, and pelletized prior to entering the rotary kiln (Figure 7.28). The kiln is operated at 900–950 °C with an oxidizing atmosphere and a reducing bed to achieve prereduction of 20% of the nickel to metal, and up to 95% of the iron oxide to the divalent state (FeO). Smelting is carried out in a single 51 MVA electric furnace. The ferronickel, grading over 40% Ni, is tapped at 1420–1440 °C, while the slag, containing 0.2% Ni, is tapped at 1600–1630 °C. The ferronickel is refined and upgraded to 43% Ni prior to being cast into 22 kg ingots, or granulated [139].

The operation of LARCO at Larymna in Greece is an example of ferronickel production from a very low grade limonitic ore (1.2–1.3% Ni, 31–35% Fe). In this case a high degree of prereduction in the rotary kiln is essential. The ground ore is blended with lignite, coal, and heavy fuel oil, and heated to 920 °C in one of two countercurrently fired rotary kilns. The kiln discharge still contains about 3% carbon, but is reported to contain no metallic nickel, while most of the iron oxides are reduced to FeO. The calcine is smelted in one of four electric furnaces (13–16 MVA) to produce a metal phase containing 15% Ni, 0.02% C, and 0.25% S. The metal is tapped at 1520 °C and upgraded to 28% Ni in an oxygen-blown converter. This treatment also reduces the sulfur content to 0.06%. Energy consumption for the electric furnace is 125 MJ/kg Ni (1.6 MJ/t ore or 440 kWh/t ore) and electrode consumption is 0.4 kg/kg Ni (5 kg/t ore) [141].

7.6.2 Ugine Ferronickel Process

In the rotary kiln–electric furnace process excess carbon is normally added to the furnace charge to ensure quantitative reduction of nickel oxide. As a result more iron oxide is re-

duced to metal than is desirable, decreasing the ferronickel grade and leaving a high residual carbon level, typically 1–3% in the product. The excess iron and carbon are subsequently removed by oxidation with air or oxygen. Consequently the process is not particularly economical in terms of energy consumption.

A more selective method of nickel oxide reduction was developed by the French company Ugine in the early 1950s and applied commercially by Hanna Mining in their plant in Riddle, Oregon, in 1954. In this process the ore is dried and calcined in a rotary kiln and melted in an electric furnace without addition of reductant to produce a melt of iron and nickel oxides. No slag metal separation occurs in the electric furnace. The molten ore is transferred to a ladle furnace where it is reduced by reaction with ferrosilicon at 1650 °C. The two phases are mixed by repeated pouring of the mixture from one ladle furnace to another. The nickel oxide and some of the iron oxide are reduced to metal. The balance of the iron is removed as slag.

$$2Fe_2O_3 + FeSi \rightarrow 4FeO + SiO_2 + Fe$$

$$2NiO + FeSi \rightarrow 2Ni + SiO_2 + Fe$$

$$2FeO + FeSi \rightarrow 3Fe + SiO_2$$

The reduced ferronickel contains 30–50% Ni and very low levels of carbon and sulfur. The major impurity is phosphorus, which is removed by oxidation with iron ore and slagging with lime.

7.6.3 Falcondo Ferronickel Process [142]

The Falconbridge ferronickel operation in the Dominican Republic treats a low-grade ore (1.5% Ni, 17% Fe, 24% MgO, and 35% SiO_2) by means of a specially developed process designed to provide a more selective reduction of nickel relative to iron than is possible in the rotary kiln–electric furnace process. Reduction of briquetted ore is carried out in shaft furnaces fired with a reducing gas, generated by cracking low-sulfur naphtha. No solid or liquid reductants are added to the furnace feed. A high degree of reduction of the ore is achieved in the shaft furnace, and the subsequent electric furnace step is required to do little more than melt the reduced calcine to allow separation of the metal and slag phases. The ferronickel produced is high grade (38% Ni) and contains low impurity levels (< 0.04% C and Si).

The Falcondo plant, which has a capacity of 35 000 t/a Ni, was commissioned in 1971. The ore is carefully blended to maintain a constant chemical composition, particle size, and moisture content, so that it can be briquetted without a binder. The briquettes are calcined and reduced in twelve open-top shaft furnaces. Each furnace is equipped with its own gasification reactor in which low-sulfur naphtha is cracked by combustion with a deficiency of air to produce reducing gas ($CO + H_2$). The hot reducing gas at 1250 °C is first cooled to 1150 °C before being supplied to the shaft furnace through the primary tuyères. The gas flows upwards, countercurrent to the ore briquettes which are fed to the open top of the furnace. The gas reduces the nickel oxides to metal and the iron oxides to FeO. A portion of the partly reacted reducing gas is taken off from the top of the furnace, where it is mixed with a controlled amount of air and fed back into the furnace through secondary tuyères located 1.8 m above the primary tuyères. This stream provides the combustion fuel to dry and calcine the ore feed in the upper section of the shaft.

The hot reduced briquettes are discharged from the bottom of the shaft furnace at 800 °C and are transferred to one of three 55 MVA electric furnaces. The furnace operation consumes only 1.6 GJ/t (440 kWh/t) of charge. The crude ferronickel, which is tapped at 1475–1500 °C, contains 32–40% Ni. The slag, containing about 0.15% Ni, is tapped at 1500–1600 °C. The crude ferronickel, which typically contains only 0.15% S, 0.03% P, 0.04% Si, and 0.02% C, is refined to remove sulfur and phosphorus.

Table 7.31: Impurities in ferronickel [129].

Smelter	Crude Fe–Ni, %				Refined Fe–Ni, %			
	C	S	Si	P	C	S	Si	P
SLN	2.5	0.40	1.50	0.150	0.03	0.02	0.02	0.02
Cerro Matoso	0.17	0.45	1.45	0.024	0.03	0.03	0.70	0.03
Falcondo	0.02	0.15	0.04	0.030	0.06	0.08	0.30	0.01

7.6.4 Refining of Ferronickel

The refining of ferronickel resembles that of steel in that the principal impurities are sulfur carbon, silicon, phosphorus, and oxygen. Typical impurity levels in crude and refined ferronickel are shown in Table 7.31.

Crude ferronickel produced by the conventional rotary kiln–electric furnace process usually contains high levels of carbon and sulfur. These ferronickels are first treated under reducing conditions to remove sulfur and are then refined sequentially under oxidizing conditions with suitable fluxes to remove carbon, silicon, and phosphorus. Ferronickel produced by the selective reduction processes, such as the Ugine or Falcondo processes, which typically contain very low levels (< 0.04%) of carbon and silicon, are normally treated first for phosphorus and then for sulfur removal. The Falcondo ferronickel is not refined to remove carbon or silicon, and in fact the levels of these impurities increase during refining.

A variety of equipment is used for the refining of ferronickel, including electric arc furnaces, shaking ladles, and low-frequency induction furnaces for desulfurization, and oxygen-blown converters (both L-D and side-blown) for silicon, carbon, and phosphorus removal. The ASEA–SKF ladle furnace, which incorporates an electric arc furnace roof carrying three carbon electrodes and induction stirring of the melt, is used in a number of plants including Cerro Matoso and Falcondo.

Sulfur is generally removed under reducing conditions by adding soda ash, lime, or calcium carbide to the molten ferronickel. Good agitation of the melt is essential to ensure effective mixing of the reagent with the metal phase, and this can be achieved by adding the reagent to the ladle during furnace tapping, by using a shaking ladle, or by providing electrical induction stirring. In some plants poling with greenwood poles is used to provide additional agitation and reductant. Sulfur reacts with the fluxes to form sodium or calcium sulfides, which are slagged off with the silicates formed by reaction of flux with silicon:

$$3Na_2O + 2S + Si \rightarrow 2Na_2S + Na_2SiO_3$$

$$CaC_2 + S \rightarrow CaS + 2C$$

The melt cools during this treatment and oxygen is blown into the melt to reheat it to tapping temperature. Two stages of fluxing are often necessary to desulfurize the ferronickel to the required level (0.02%). The Falcondo smelter uses a complex combination of ferrosilicon, aluminum, silicocalcium, lime, and fluorspar to desulfurize its low-carbon ferronickel.

Removal of silicon, carbon, and phosphorus is normally conducted in an oxygen-blown converter or an oxygen lanced ladle. Carbon is removed simply by oxidation with oxygen to carbon monoxide. Silicon is removed by oxidation with oxygen and fluxing with lime and fluorspar. Phosphorus is oxidized either by blowing the melt with oxygen or by adding iron ore and fluxing the phosphorus(V) oxide with lime:

$$6P + 5Fe_2O_3 + 12CaO \rightarrow 10Fe + 3Ca_4P_2O_9$$

The slags are removed by skimming after each refining step. If necessary the ferronickel can be deoxidized by addition of ferrosilicon, although this practice increases the silicon content.

Ferronickel is not usually treated to remove cobalt, copper, or arsenic, which may be present in significant amounts. Refined nickel can be produced by the electrorefining of 90% ferronickel in a chloride sulfate electrolyte, but this process has not found wide application [141].

7.7 Ferrophosphorus

During the production of elemental phosphorus by reduction of phosphate rock in an electric furnace, ferrophosphorus collects under the slag. The ferrophosphorus is tapped off, usually once per day, through a hole in one of the carbon blocks, which is opened with an oxygen lance and closed again with a clay plug. The ferrophosphorus, together with some slag, flows into a crucible, from which the lighter slag overflows into a bed of sand. When the tapping off is completed the ferrophosphorus is poured from the crucible into a bed of sand, and, after cooling, is broken into pieces [143].

Every time the ferrophosphorus is tapped off, its radioactivity is measured. If a ^{60}Co source becomes dislodged as the furnace lining wears away, the ^{60}Co is transferred quantitatively into the ferrophosphorus. The radiation supervisor decides in each case whether the ferrophosphorus should be sold, placed in short term storage, or stored indefinitely.

Fume extraction operates in the areas surrounding the furnace tapping and sand beds. The waste gases are purified by wet methods. For new installations, the following emission levels are not exceeded [144]:

Dust	50 mg/m³
Phosphoric acid (as P_2O_5)	20 mg/m³

Depending on the method of furnace operation, the ferrophosphorus contains between 15 and 28% P, corresponding approximately to the formula Fe_2P. The more extensively the phosphate rock is reduced, the more silica is converted into silicon, which reduces the phosphorus content of the ferrophosphorus. The combined content of P and Si is 25–30%. Ferrophosphorus with a low silicon content (< 3%) has a fairly good market potential, and is used in the manufacture of phosphorus-containing alloys. The grades with a low phosphorus content are not in great demand, but can be used in smelting low-phosphorus iron ores or to increase the P_2O_5 content of basic Thomas slag.

Ferrophosphorus is stored in the open, and supplied either loose or in drums. The other metals present in the ferrophosphorus in addition to the Fe, P, and Si depend on the composition of the phosphate rock. Examples of compositions of ferrophosphorus are given in Table 7.32.

Valuable metals such as vanadium, can be recovered economically from the ferrophosphorus if they are present in unusually high concentrations. Vanadium is recovered together with chromium by blowing with oxygen. Both metals accumulate in the slag.

Older processes for treating ferrophosphorus, which are however no longer of importance, are described in [145].

Table 7.32: Composition of ferrophosphorus (%).

Process	P	Si	Ti	Cr	V	Mn
Hœchst high percentage	26.6	0.3	4.5	0.2	0.6	0.5
Hœchst low percentage	20.0	9.5	5.8	0.2	0.5	0.7
TVA	24.0	1.7	1.7	0.2	0.3	1.1
FMC	27.1	0.2	0.3	4.5	5.4	0.5

7.8 Ferrotungsten

7.8.1 Composition

Commercial ferrotungsten is a tungsten–iron alloy containing at least 75% W, and having a very fine-grained structure and a steel-gray appearance. It is supplied in 80–100 mm lumps in accordance with DIN/ISO standard specifications. Special sizes can be produced by further size reduction to suit customers' requirements. The standardized compositions are listed in Table 7.33 [146].

The binary phase diagram for Fe–W is shown in Figure 7.29. The phases Fe_7W_6 (μ) and FeW (δ) exist close to the edge phases. However, ferrotungsten occurs in the equilibrium state only after prolonged high-temperature treatment. Therefore, in commercial ferrotungsten, the phase Fe_2W (λ) should still be present alongside the δ-phase. The melting temperature of ferrotungsten containing ca. 80% W is very high, the liquidus temperature being > 2500 °C and the solidus temperature ca. 1640 °C. The density of ferrotungsten is 15.4 g/cm³.

7.8.2 Uses

Ferrotungsten and tungsten melting base are mainly used as alloying materials in the steel industry as they dissolve more readily than pure tungsten in molten steel, owing to their lower melting points, and are also cheaper.

Tungsten additions increase the hardness yield strength, and ultimate tensile strength of the steel without reducing the elongation, area reduction on breaking, and notched bar fracture toughness [148].

In steel, tungsten forms stable carbides that increase hot strength and wear resistance. Tungsten-containing alloys are therefore mainly used in the production of tool steels, especially high-speed steels [149].

High-speed steels represent the main application area for ferrotungsten. These steels are highly alloyed with tungsten, molybdenum, vanadium, and chromium. After the correct heat treatment, they have high hardness and wear resistance, and are mainly used for machining at high cutting rates and temperatures up to 600 °C. The alloying elements and the carbon form hard, wear-resistant carbides in a matrix with good hardness retention properties. The standard high-speed steels specified in DIN 17350 contain 6–18.5% tungsten [150].

Table 7.33: Specifications of the composition of ferrotungsten, DIN 17562 and ISO 5450 [146] (impurities: 0.6–1.0% Si; 0.6–1.0% Mn; 0.20–0.25% Cu; 0.05–0.06% S; 0.05–0.06% P).

	% W		% C max.	% Al max.	% Sn max.	% As max.	% Sb max.		% Mo max.	
	DIN	ISO	DIN/ISO	DIN/ISO	DIN/ISO	DIN/ISO	DIN	ISO	DIN	ISO
FeW 80	75–80		1.0		0.10	0.10	0.08			
FeW 80		70–85	1.0	0.10	0.10	0.10		0.05		1.0
FeW 80 LC		70–85	0.1	0.10	0.10	0.10		0.05		0.5

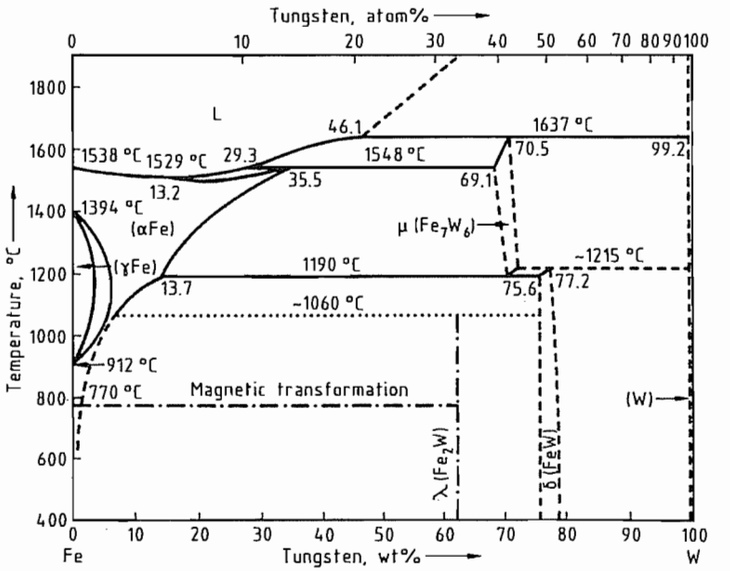

Figure 7.29: Binary phase diagram of the Fe–W system [147].

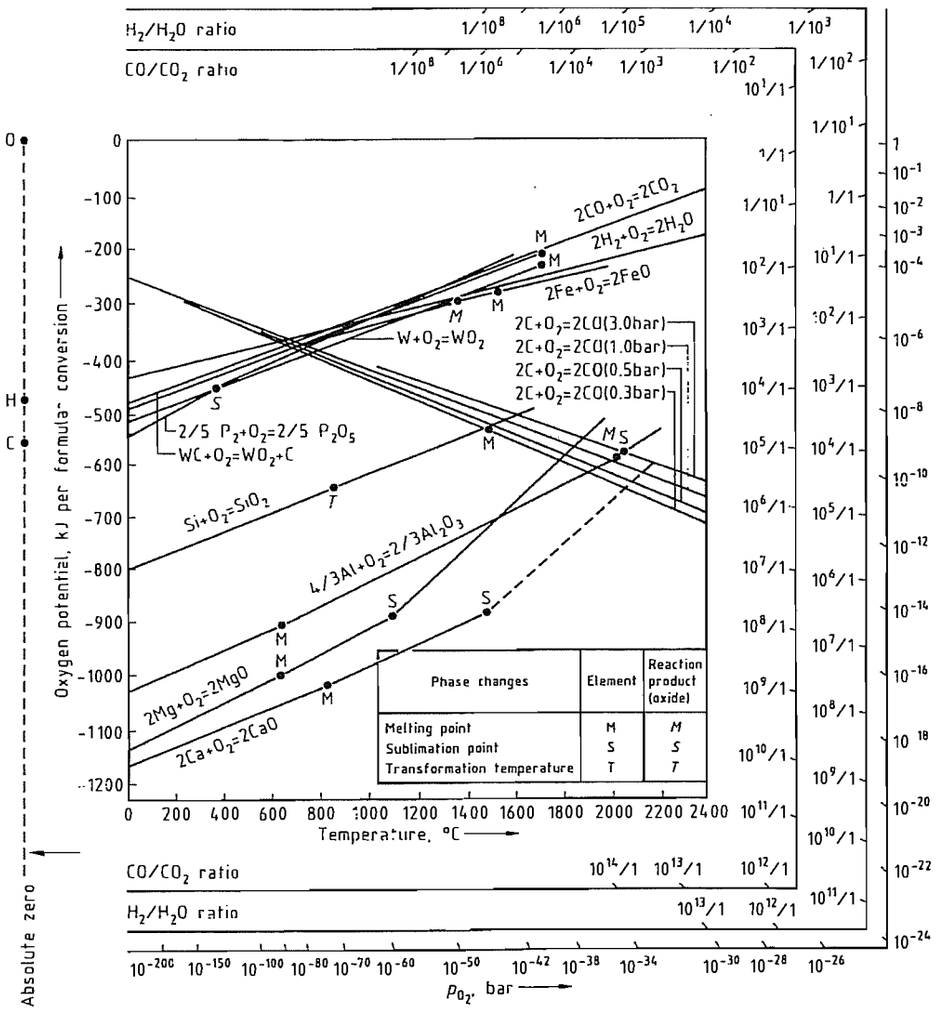

Figure 7.30: Effect of temperature on the oxygen potentials of oxides [151].

7.8.3 Production

The raw materials used for ferrotungsten production are rich ores or concentrates containing the minerals wolframite, hübnerite, ferberite, and scheelite. "Synthetic scheelite", a precipitated calcium tungstate, is also used.

These raw materials contain tungsten in the form of WO_3, which can be relatively easily reduced either with carbon or silicon and/or aluminum. Reduction with magnesium and calcium is also possible, but is of no industrial importance for cost reasons. Figure 7.30 shows the effect of temperature on the oxygen potentials of metal oxides. Although tungsten forms carbides with carbon, the formation of tungsten carbide in the finished product can be virtually prevented by suitably controlling the $CO:CO_2$ ratio, so that a low-carbon ferrotungsten with a maximum carbon content of 1 % is produced. Tungsten oxides are reduced in preference to iron oxides, so that ferrotungsten with a high tungsten content can be produced, even if the ore has a high FeO content.

Thus, ferrotungsten can be produced by carbothermic reduction in an electric arc furnace or by metallothermic reduction aluminum.

The carbothermic or silicocarbothermic method is preferred for cost reasons. Moreover, higher impurity contents (tin and arsenic) can be tolerated in the raw materials.

When high levels of arsenic and tin are present in the concentrates, these cab ne vaporized by roasting in rotary tube furnaces.

7.8.3.1 Carbothermic Production

Because of the high melting point of ferrotungsten, the so-called solid block melting process is normally used, as tapping off is not possible at the furnace temperatures that are required.

In this process, the ferrotungsten accumulates in the hearth of the furnace vessel, which is constructed in sections. After the desired weight has been produced, the furnace lining is removed and the metal ingot can be removed after cooling. The solid block is cleaned, crushed, and sorted. The cleaned-off material and skin of the ingot are returned to the furnace for remelting.

The use of several melting vessels enables the process to be semicontinuous.

The process is usually operated in two stages, as an excess of tungsten ore is used in the ingot melting process (refining stage), producing a WO_3-rich slag that must be processed in a second (reduction) stage to give ferrotungsten with a low W content and a low-WO_3 slag.

The low-W ferrotungsten is reused in the refining stage. The slag, which contains < 1 % WO_3, can be dumped. The flow diagram of this two-stage process is shown in Figure 7.31 [152].

In the three-phase electric arc furnaces usually used today, the pitch circle diameter of the electrodes is small to ensure adequate energy concentration. Typical furnace data for a three-phase electric arc furnace for the production of FeW 80 are [153]:

Power	2000–3000 kVA
Refractory lining	monolithic rammed carbon
Electrode material	
refining stage	graphite
reduction stage	Söderberg
Energy consumption per tonne FeW	7500–8500 kWh
FeW ingot weight	11–12 t

The electric arc furnaces are provided with waste-gas purification plants both for environmental reasons and to realize the value of the WO_3 in the flue dust. This dust, enriched in arsenic and tin vaporized from the concentrates is usually added to the reduction stage or processed in special batches. The resulting secondary dust must either be chemically processed to obtain tungsten compounds or disposed of as a special waste if it cannot be sold.

7.8.3.2 Carbothermic and Silicothermic Production

In 1937, V. N. Gusarov developed a continuous process for the production of ferrotungsten containing ca. 75 % W. This was used in the former Soviet Union and former Czechoslovakia [154, 155]. It is presumably now used in the Czech Republic.

This metallurgically interesting process is carried out in three successive stages in a three-phase electric arc furnace lined with magnesite. Of the oxygen in the WO_3, 60 % reacts with carbon and 40 % with silicon (as ferrosilicon containing 75 % Si). In the first stage, ferrotungsten (75 % W) is produced by substoichiometric carbon reduction. This ferrotungsten is formed in a pasty consistency under a WO_3-rich slag, and can be scooped out with ladles. Details of the individual processes are as follows:

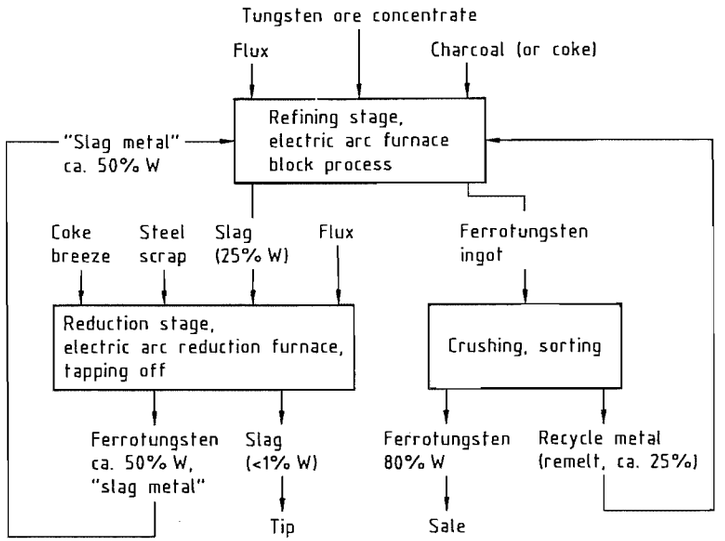

Figure 7.31: Carbothermic production of ferrotungsten.

Tungsten yields of 97–98% can be obtained in the solid block process.

Stage 1. Reduction of tungsten ore concentrates by carbon under a WO_3-rich slag (10–16% WO_3, 26–28% FeO, 15–17% MnO), and scooping out the ferrotungsten (e.g., 73.3% W, 0.4% Mn, 0.43% Si, 0.05% P, 0.06% S, 25.2% Fe).

Stage 2. Reduction of the WO_3-rich slag with FeSi 75 and addition of scrap iron (to reduce the tungsten content of the ferrotungsten produced). Tapping off the low-WO_3 slag (e.g., 0.3% WO_3, 20.8% MnO, 51% SiO_2, 2.7% FeO, 3.6% Al_2O_3, 21.1% CaO). The metal, with a reduced tungsten content (54–70% W, 3–8% Si, 1–2% Mn) remains in the furnace.

Stage 3. Refining of the low-tungsten metal by adding tungsten concentrates. A WO_3-rich refining slag (18–25% WO_3) is formed, and the tungsten content of the metal increases.

The advantage of the process is the continuous method of operation; thus the furnace can be operated for considerably longer periods without interruption for relining than in the solid block process. A further advantage is the lower energy consumption, i.e., ca. 4000 kWh per tonne of ferrotungsten. The tungsten yield is 98%, approximately the same as for the solid block process.

Disadvantages include the heavy labor of the scooping operation and the accumulation of some of the ferrotungsten in a "furnace sow" or "salamander". This ferrotungsten can be retrieved only after furnace relining, and is recovered as product after remelting.

7.8.3.3 Metallothermic Production

Tungsten oxide can be reduced by silicon and/or aluminum (Figure 7.30). Compared with carbothermic reduction, metallothermic production of ferrotungsten requires purer raw materials, as the reactions proceed very rapidly, and the impurities are chemically reduced as well as the raw materials. In this process, about 50% of the tin and arsenic present, most of which would be vaporized during the longer carbothermic process, end up in the ferrotungsten.

The tungsten concentrates in finely divided form are mixed with coarsely powdered aluminum and silicon. Pure silicon or ferrosilicon cannot be used, as these would not give a self-sustaining reaction, the heat evolved being insufficient to melt the ferrotungsten and slag formed. Aluminum and silicon in the ratio 70:30 are therefore used.

The reaction mixture is charged into a refractory-lined furnace vessel and preheated to 400–500 °C. The preheating can be omitted if Fe_2O_3 and Al are mixed into the reaction mixture as a booster.

The reaction is started at the top by igniting initiators, which are mixtures of, e.g., BaO_2 and aluminum powder. A purely aluminothermic mixture burns completely in a few minutes, but silicothermic–aluminothermic mixtures react more slowly. After cooling, the furnace vessel is removed, and the blocks of metal and slag are separated. This method produces ferrotungsten ingots of 700–2000 kg. The metal ingot is cleaned, crushed, and sorted. Pieces with adhering slag are sent back for remelting.

The metallothermic production process has lost much of its importance in recent years, owing to the high costs of the aluminum and silicon reducing agents, and the necessity for using pure and therefore expensive raw materials.

The process is suitable only for special customer requirements, and for operations which also produce other alloys by the aluminothermic principle.

Advantages of the process include the simple, low-cost plant, and the minimal tying-up of materials resulting from the short processing time. The tungsten yield is ca. 96%.

M. Riss and Y. Khodorovsky have described the electroaluminothermic production of ferrotungsten from scheelite [155]. The reaction time is extended by melting in an electric arc furnace, and separation of the metal from the slag is improved.

7.9 Ferroboron

Ferroboron is basically an iron–boron alloy containing 10–20% B. It is used mainly in the steel industry. Ferroboron was first produced in 1893, by Henri Moissan [156], from boric acid, iron, and carbon in a single-phase electric-arc furnace lined with carbon. Ferroboron produced in this way contains carbon. The introduction of the thermite reaction by Goldschmidt in 1898 led to the aluminothermic reduction of boric oxide to ferroboron, for years the main commercial method for producing ferroboron. Recently though the carbothermic process has again found use for the production of ferroboron, now as a raw material for the manufacture of amorphous metals. Aluminothermic ferroboron contains residual aluminum, which causes severe casting problems.

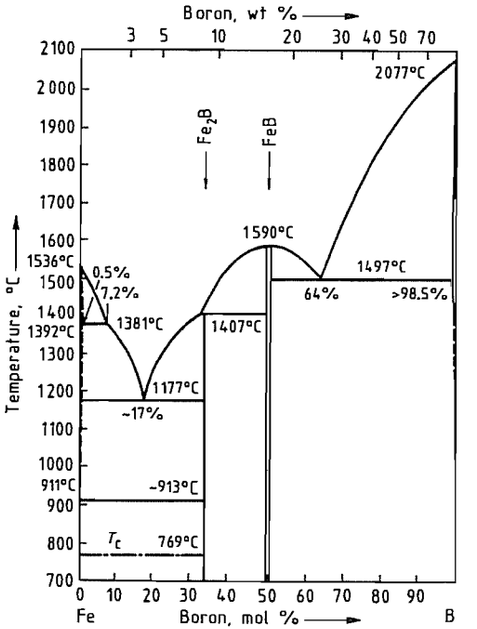

Figure 7.32: Phase diagram of iron–boron [157].

7.9.1 Physical Properties

In the system iron-boron, shown in Figure 7.32 [157], there are two intermetallic compounds, FeB and Fe_2B (ρ 6.3 and 7.3 g/cm^3, respectively). The crystal structure of FeB is orthorhombic (a = 0.5502, b = 0.2948, c = 0.4057 nm), whereas that of Fe_2B is tetragonal (a = 0.5109, c = 0.4249 nm). Additional physical properties of the two iron borides are summarized in Table 7.34. Also see [161].

The enthalpies of formation at 1385 K have been determined by high-temperature solution calorimetry [162]: –67.87 ± 8.05 kJ/mol for Fe_2B, and –64.63 ± 4.34 kJ/mol for FeB.

Commercial ferroboron alloys, either aluminothermic or carbothermic, are bright silver and brittle with a fine or coarse crystalline fracture. The density depends mainly on the boron content:

boron, %	20.2	17.9
aluminum, %	2.7	0.8
density, g/cm³	6.02	6.41

Table 7.34: Properties of Fe_2B and FeB [158–160].

Property	Fe_2B	FeB
Microhardness, Vickers, 100 g, kN/mm²	13.24	16.19
Thermal conductivity, $W cm^{-1} K^{-1}$	0.2–0.3	0.1–0.2
Electrical resistivity, at room temperature, μΩcm	≈ 10	≈ 20
Temperature coefficient of resistance, μΩ/K	0.18	0.4
Curie temperature, K	1015	598
Coefficient of linear expansion (300–1000 K), K^{-1}	8×10^{-6}	$10–16 \times 10^{-6}$

7.9.2 Chemical Properties

Commercial ferroboron changes in appearance over prolonged exposure to humid air; its bright silver disappears, the surface turning dull gray, with almost red "rusty" stains. Ferroboron dissolves in mineral acids (Section 7.9.7). Distilled hot water may react slightly with ferroboron [163]. Some contradictory statements about the chemical behavior of ferroboron in the literature are probably due to other elements in the alloy. Fe_2B dissolves in HCl (1:2), hydrogen and boranes evolving, the latter hydrolyzing into suboxides [164, 165]. FeB is resistant to HCl ($\rho = 1.19$ g/cm³) and H_2SO_4 ($\rho = 1.84$ g/cm³), both at room temperature and at their boiling point. FeB dissolves completely in HNO_3. Both FeB and Fe_2B react with nitrogen at temperatures above 350 °C to give boron nitride [158].

The behavior of boronized steels, i.e., steel with thin layers of FeB on the surfaces, was discussed by A. Matuschka [159]. Such steels are oxidation resistant up to 700–900 °C. The boronized steel CK45 (AISI 1042) is resistant to 20% HCl, 10% H_3PO_4, and 10% H_2SO_4 at 56 °C. Stainless steels, such as X10CrNiTi 18 9 (Werkstoff Nr. 1.4541, AISI 321, SAE 30321) can be made more resistant to attack by 20% HCl or 10% H_2SO_4 at 56 °C by boronizing the surface.

7.9.3 Raw Materials

The following boron minerals can be used for the manufacture of ferroboron: colemanite (51% B_2O_3), pandermite (48% B_2O_3), priceite (51% B_2O_3), and boracite (62% B_2O_3). However, the raw materials most commonly used are boric oxide (≈ 99% B_2O_3) and boric acid (≈ 57% B_2O_3).

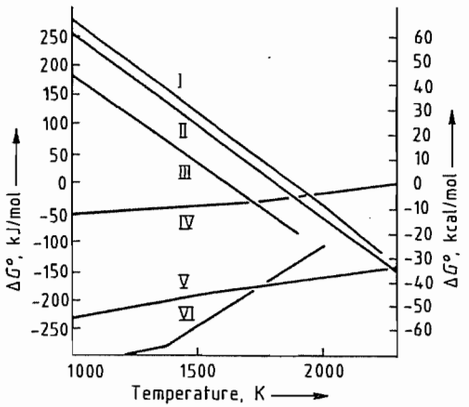

Figure 7.33: Free energies ΔG^0 of reactions reducing boric oxide as a function of temperature.
I — $^2/_3B_2O_3 + 2C \rightarrow {}^4/_3B + 2CO$
II — $^2/_3B_2O_3 + {}^7/_3C \rightarrow {}^1/_3B_4C + 2CO$
III — $^2/_3B_2O_3 + {}^4/_3Fe + 2C \rightarrow {}^4/_3FeB + 2CO$
IV — $^2/_3B_2O_3 + Si \rightarrow {}^4/_3B + SiO_2$
V — $^2/_3B_2O_3 + {}^4/_3Al \rightarrow {}^4/_3B + {}^2/_3Al_2O_3$
VI — $^2/_3B_2O_3 + 2Mg \rightarrow {}^4/_3B + 2MgO$

7.9.4 Production

Boric oxide can be reduced by carbon, aluminum, or magnesium. Reduction by silicon is incomplete. Figure 7.33 shows the calculated free energies of the corresponding reactions as a function of temperature [160]. For commercial production, either reduction by carbon (carbothermic or endothermic) or reduction by aluminum, sometimes with some magnesium (aluminothermic or exothermic) is usual. The coreduction of iron and boric oxide proceeds more readily than the reduction of either alone because of the formation of the borides Fe_2B and FeB. Iron can be replaced by other boride-forming metals, manganese, nickel, or cobalt. In carbothermic reduction there is a tendency to form boron carbide, thus leading to a carbon-containing ferroboron.

Aluminum and boron also form borides, and this results in residual aluminum in aluminothermic ferroboron.

7.9.4.1 Carbothermic Production

In order to produce a carbothermic ferroboron with a low carbon content the boron content must be high, i.e., the higher the boron content the lower the carbon solubility and thus carbon pick-up.

The reduction of boric oxide by carbon requires high temperature; therefore, the process is carried out in an electric-arc furnace (single- or three-phase type) of capacities up to 1500 kVA. These are relatively small production units, for the worldwide demand for ferroboron is low compared with that for other electrothermic ferroalloys.

The London & Scandinavian Metallurgical Co., United Kingdom, produces a ferroboron with 16–18% B, 0.5% C, and < 0.15% Al by carbothermic reduction of boric oxide.

In a Japanese patent [166] the carbothermic production of ferroboron from boric acid, iron powder, and charcoal in a Héroult-type electric-arc furnace with carbon lining is claimed. One example describes the production of an alloy with 10.3% B, 2% Si, and 0.98% C in a 350-kW three-phase electric-arc furnace. The mix is 100 parts boric acid, 135.8 parts iron powder (92.9% Fe), and 57 parts charcoal powder. The boron recovery is 81.7%, and the power consumption 4550 kWh per tonne of alloy. Another example describes the small-scale production of an alloy containing 15.3% B. Another Japanese patent [167] claims the carbothermic production of a B- and Si-containing alloy, e.g. 3.3% B, 2.9% Si, and 3.0% C, in a special vertical blast furnace. The ferroboron is intended for use in the manufacture of amorphous alloys.

The production of ferroboron from pig iron and boric acid in an electric-arc furnace with a final oxygen blow leads to an alloy with 16.3% B, 0.03–0.06% Al, and 0.03–0.06% C. The boron recovery in small-scale runs is said to be 60–65%; the power consumption, 16 500 kWh per tonne of alloy [168]. Silicon-containing boron alloy can be produced by carbothermic reduction. The process is described by K. D. Frank in [169]. A mixture of 100 parts colemanite, 100 parts quartzite, 40 parts iron turnings, and 60 parts low-temperature coke is charged to a 1000-kW electric-arc furnace. A metal containing 5.35% B, 37.2% Si, and 0.21% C is tapped. Boron recovery is 70%, and the power consumption is 6000 kWh per tonne of alloy.

Gesellschaft für Elektrometallurgie mbH, Düsseldorf, Germany, has developed a process for the carbothermic production of ferroboron containing 15–20% B and < 0.1% Al in a three-phase submerged arc furnace, whereby boric oxide and iron oxide are simultaneously reduced by charcoal and other low-density carbonaceous materials, e.g., wood chips [170].

Nickel boron can also be produced carbothermically. Boric oxide and/or boric acid and nickel are the raw materials. London and Scandinavian Metallurgical Co., London, United Kingdom, produces a nickel boron containing 15–18% B; 0.5 and 0.15% C (max.); and 0.20% Al (max.) in the electric-arc furnace by carbon reduction.

7.9.4.2 Aluminothermic Production

Ferroboron can be made batchwise in a convenient way by the reduction of boric oxide and iron oxide with aluminum powder. Some magnesium in the aluminothermic mix is beneficial: Magnesium is the stronger reducing agent at temperatures below its boiling point, whereas aluminum is more effective above the boiling point of magnesium, where such metallothermic reactions generally take place. The aluminothermic coreduction of boric oxide and iron oxide (Fe_2O_3) is highly exo-

thermic, and only a little additional energy is necessary for a self-propagating reaction. The thoroughly mixed compounds are charged into a refractory-lined pot and ignited, either the whole mix (top firing) or by igniting a starting mix, the rest then charged as the reaction proceeds over a few minutes. The liquid metal and slag separate on account of differing densities, and after cooling the metal button, up to 1500 kg, is removed. After mechanical cleaning, the metal button is broken and crushed to the desired size. The companies of the Metallurg Group [171], who produce ferroboron from boric oxide, iron oxide, and aluminum powder, obtain boron recoveries of 70–75% for the 18–20% B grade and 80–85% for the 15–18% B grade by optimizing process parameters. The aluminum consumption can be as low as 4.8–5 kg Al per kg of B.

N. A. Chirkov et al. [172] investigated heat balances for an electro-aluminothermic ferroboron process using either 1) boric oxide or 2) boric acid as the raw material. Three different mixes — igniting, main, and precipitation — are charged consecutively into a three-phase electric-arc furnace and reacted to produce a ferroboron melt with ≈ 20% B. The composition of the charges and the results are summarized in Table 7.35. The heat balances for these two cases are shown in Table 7.36. The investigators are convinced that the process can be optimized to improve the boron recovery and the consumption figures.

When borate ores such as boracite or colemanite are used as raw materials, instead of boric oxide, the aluminothermic process gives boron recoveries as low as 40–50% [173–175]. The specific aluminum consumption is normally higher because the process needs additional energy, in form of either a booster (peroxides or chlorates plus aluminum powder) or in the form of electricity by smelting the mix in the electric-arc furnace (electro-aluminothermic process).

Table 7.35: Charge composition during electro-aluminothermic production of ferroboron using boric oxide and boric acid raw materials [172].

	Mix 1			Mix 2		
	Igniting	Main	Precipitation	Igniting	Main	Precipitation
Raw materials						
Boric oxide, kg	—	1200	—	—	—	—
Boric acid, kg	—	—	—	—	1800	—
Iron ore, kg	200	200	1000	200	180	950
Al powder, kg	65	820	282	65	820	262
Lime, kg	70	100	170	70	450	170
Total, kg	335	2320	1452	335	3250	1382
Time, min	30	98	32	3	114	23
Power consumption, kWh		1130			1980	
Products						
Ferroboron, kg		1200[a]			1100[a]	
% B		20			18	
% Al		3			3.9	
% Si		1.13			1.7	
Slag, kg		2900[a]			2080[a]	
% B_2O_3		14–15[a]			10–12[a]	
Boron recovery, %		64			63	
Aluminum consumption, kg per tonne of ferroboron		973			1043	
Energy consumption, kWh per tonne of ferroboron		940			1800	

[a] Estimated.

Table 7.36: Heat balances for the electro-aluminothermic production of ferroboron using boric oxide and boric acid as raw materials [172].

Input and consumption	From B_2O_3		From H_3BO_3	
	ΔH, 10^6 J	%	ΔH, 10^6 J	%
1. Chemical reactions	13 182	69.0	12 345	58.3
2. Electric power	4 072	21.3	7 143	33.7
3. Side reactions	1 833	9.7	1 699	8.0
Total input	*19 087*		*21 186*	
1. Heat content of slag	9 515	49.3	9 237	42.9
2. Heat content of metal	3 235	16.7	2 907	13.5
3. Heat content of dust	63	0.3	125	0.6
4. Dehydration of acid	48	0.2	1 084	5.0
5. Decomposition of carbonates	60	0.3	98	0.5
6. Heat content of gases	141	0.7	2 805	13.1
7. Accumulation of heat by furnace brickwork	4 678	24.2	4 212	19.6
8. Radiation	1 581	8.3	1 045	4.8
Total consumption[a]	*19 319*		*21 514*	

[a] The discrepancies between input and consumption are 232×10^6 J (1.2%) and 328×10^6 J (1.5%).

Table 7.37: German Standards 17567 [180].

Designation	Composition							
	B, %	Al, max. %	Si	C	Mn	P	S	Co
FeB16	15–18	4.0	1.0	0.10	0.50	0.005	0.001	0.005
FeB18	18–20	2.0	2.0					
FeB12C	10–14	0.50	4.0	2.0	0.50	0.005	0.1	0.005
FeB17C	14–19							

Table 7.38: United States standards [181].

Grade	Composition, %				
	Boron		Carbon	Silicon	Aluminum
	min.	max.	max.	max.	max.
A1	12.0	14.0	1.5	4.0	0.5
A2	12.0	14.0	1.5	4.0	8.0
B1	17.5	19.0	1.5	4.0	0.5
B2	17.5	19.0	1.5	4.0	8.0
C1	19.0	24.0	1.5	4.0	0.5
C2	19.0	24.0	1.5	4.0	8.0

Complex boron additives for steel, which contain boron in a dilute alloy together with protective elements, are produced from ferroboron and other alloying elements by a melting process (see Table 7.39, and [176]). Other boron master alloys such as nickel boron and cobalt boron with ≈ 15% B and 0.1% or 1.0% Al (max.) can be produced aluminothermically using boric oxide and nickel or cobalt (as metal and/or oxide) [177]. Copper boron with ca. 2% B is commercially produced by Gesellschaft für Elektrometallurgie [178], using an electromagnesiothermic process with copper and boric oxide as raw materials. Aluminum master alloys with 2.5–4.5% B and 5% Ti + 1% B are produced in an induction furnace by adding potassium boron fluoride and potassium titanium fluoride to an aluminum bath [179].

7.9.5 Quality Specifications for Commercial Grades

Quality standards are specified in Germany by DIN 17567 [180], which also describes sizing, sampling, analytical methods, shipment, and storage. Analyses of the standard grades are summarized in Table 7.37. The American ASTM recognizes six grades of ferroboron; analyses are given in Table 7.38. Ferroboron is shipped in various sizes. In Europe pieces of fist size and in the United States sizes such as 2 in or 1 in x Down are commercial. Ferroboron can also be ground to powder of desired size (e.g., 20 mesh x D, i.e., less than 0.84 mm). In the United States, where the use of boron in steel is fast growing, and also in the United Kingdom, special boron alloys

have been developed as hardenability intensifiers (Table 7.39). These complex alloys contain elements to protect boron against oxidation (Al, Si) and boron nitride formation (Ti, Zr) [182]. Boron-containing aluminum master alloys (Table 7.40) are standardized in Germany [183]. Nickel boron, cobalt boron, and copper boron are not standardized. Typical analyses for commercial alloys are given in Table 7.40.

In the United States and the United Kingdom special boron additives for the steel industry have been developed. The *trade names*, e.g., BATS (abbreviation for boron–aluminum–titanium–silicon), are shown in Table 7.39.

7.9.6 Storage and Shipment

Ferroboron and other boron master alloys are generally not toxic, and there is no special legislation on use and handling. Ferroboron is generally packed in steel drums marked with material grade, size, lot number, and producer. The shipment is accompanied by a data sheet on safe handling including physical and chemical properties, sale storage, and handling directions, e.g., use of protective gloves or dust respirators. Ferroboron and other boron master alloys and additives should be stored in a dry area in their original containers.

7.9.7 Chemical Analysis

For the determination of boron in ferroboron the sample is dissolved in HCl (1:1) or H_2SO_4 (1:1) containing a few drops of HNO_3 and refluxed. Residues rich in boron are fused with sodium peroxide. The solution is passed through an ion-exchange column, neutralized, diluted with polyalcohol, and titrated with sodium hydroxide [184–186]. Small amounts of boron in steel are determined by special methods [182]. One photometric determination of boron in steel is the curcumin method. A fully automated determination of boron in ferroboron, aluminum, and complex ferroalloys by neutron transmission is a convenient method for routine analyses [187]. Standard analytical methods in the United States and the United Kingdom [188, 189] have been described.

Table 7.39: Complex boron alloy "hardenability intensifiers" [176, 182].

Designation	Composition[a], %						
	B	Al	Ti	Si	Zr	Mn	C
BATS 50[b]	0.50	13	20	7	5	8	—
BATS TT[b]	1.60	11	58	—	3.5	5	—
BATS 2Z[b]	2.50	11	36	8	6	—	—
BATS Wire	2.3	89.7	8	—	—	—	—
CARBOTAM[b]	2.0	3.0	15–20	4	—	—	0.50
BALCORE 101[c]	2.5	25	—	—	—	—	—
BALCORE 102[c]	3.4	34	—	—	—	—	—

[a] The remainder is iron.
[b] BATS 50, BATS TT, BATS 2Z, and CARBOTAM are registered trademarks of the Shieldalloy Corp., Newfield, NJ.
[c] BALCORE is a registered trademark of the LSM Co., London. The size of BALCORE 101 wire is 3.2 mm (34 g/m). The size of BALCORE 12 wire is 5 mm (75 g/m).

Table 7.40: Composition of boron master alloys [176–178].

Alloy	Analysis, %					
	B	Ti	Al	Si	C	Others
Aluminum boron V-Al B 3	2.5–3.4	—	rest	max. 0.2	—	[a]
V-Al B 4	3.5–4.5	—	rest	max. 0.2	—	[a]
Aluminum–titanium–boron V-Al Ti 5 B 1	0.9–1.4	5.0–6.2	rest	max. 0.2	—	[a]
Nickel boron	15–18	—	0.1–1.0	max. 0.8	0.1–0.5	rest Ni
Cobalt boron	15–18	—	max. 1.0	—	—	rest Co
Copper boron	≈ 2	—	—	—	—	rest Cu

[a] See DIN 1725 [183].

7.9.8 Pollution Control

During production the usual proscriptions on pollution have to be obeyed.

In both the carbothermic and the exothermic reduction processes the dust off-gases have to be cleaned, either dry in bag filters or electrostatic dust precipitators or wet in disintegrators or Venturi scrubbers (O. Renz in [169]). A special combined dry–wet cleaning plant for the off-gases of an aluminothermic plant is described by Seybold [190].

7.9.9 Uses

The main use of ferroboron is in steel [182, 191]. Very small amounts of boron improve the hardenability of both plain carbon and alloyed steels. Boron acts as a hardenability intensifier of other hardening elements, such as carbon, manganese, chromium, molybdenum, etc. The boron should be present in the concentration range of 5–15 ppm (max. 30 ppm). Thus the use of boron saves the expense of more costly alloying elements. Because of the high affinity of boron for oxygen and nitrogen, also that dissolved in steel, boron has to be protected from these two elements. Therefore, good predeoxidation by calcium, aluminum, or silicon and denitrification by titanium or zirconium are necessary. In the United States and the United Kingdom complex boron master alloys that contain these protective elements have been developed and have proved very effective for controlled boron addition to steels. In case-hardened steels, boron exhibits better hardenability and strength; in nonaging steels, especially for the automotive industry, the sheet-forming properties are improved. Boron also offers benefits in high-strength low-alloy (HSLA) steels, and it improves the cutting properties in high-speed steels.

In stainless steels of the chrome–nickel type (ASTM 316), 0.004–0.009% B significantly improves the ductility in the hot forming range (950–1250 °C). In very low concentration (0.002–0.005%) boron is beneficial to creep properties in austenitic heat-resistant stainless steels, as well as in ferritic steels, then in combination with titanium, molybdenum, or niobium. Steels with boron contents up to 2.5% are used for control rods in nuclear reactors because the thermal neutron cross section of boron is so high. Boron is also used in hardfacing and abrasion-resistant alloys; e.g., Colmonoy, a Ni–Cr–Si–B alloy containing up to 3% B, and Stellite, an abrasion-resistant Co–Cr–W alloy containing up to 2.5% B.

The copper–boron master alloy is the best agent for deoxidizing copper for the production of a highly conducting metal. Aluminum is treated with aluminum boron master alloy to increase the electrical conductivity and with aluminum–titanium–boron master alloy to refine the grain [179].

A new field of boron usage is the production of amorphous alloys or metallic glasses. Intensive development has been carried out by Allied Chemical Corp. [192]. These alloys consist of a transition metal (Fe, Ni, or Co) and about 20 mol% of a metalloid (B, C, Si, or P). They exhibit extraordinary physical properties, especially the magnetic properties, and may be used for low-hysteresis-loss transformer cores [193].

7.9.10 Economic Aspects

The consumption of ferroboron is relatively low due to the small concentrations necessary in steel. In the Western World and Japan, ferroboron production was ≈ 1400 t/a in 1982 and ≈ 2000 t/a in 1983, showing an increasing tendency. In 1981 only 2% of the total boron consumption in the United States was for the metallurgy and nuclear fields [194]. According to American Metal Market (28 Dec. 1983), ferroboron costs $3.89 per pound (one pound = 454 g); nickel boron, $5.57 per pound of the regular grade, $5.67 per pound for the low-aluminum grade, and $6.30 per pound for the low-carbon grade.

7.9.11 Toxicology and Industrial Hygiene

Ferroboron and boron master alloys are generally not toxic, but in the handling of raw materials for their production protective measures must be taken, e.g., the use of protective gloves and glasses as well as dust respirators when handling boric acid. In the production facilities the usual protective measures (clothing, glasses, dust respirators) must also be taken.

7.10 Ferroniobium

Approximately 85–90% of the total niobium production is used in the steel industry in the form of iron niobium alloy (ferroniobium) containing 40–70% niobium. Depending on the application, the alloy can also contain small amounts of Ta (ferroniobium tantalum), e.g., FeNb65Ta2, which contains 65% Nb and 2% Ta. Other alloy specifications are given in [195].

7.10.1 Production

Ferroniobium is usually produced by aluminothermic reduction of niobium oxide ores, with the addition of iron oxides if the niobium ore used contains insufficient iron. The starting materials are mainly columbites and pyrochlore concentrates.

The enthalpy of the reaction between Nb_2O_5 and Al is –276.1 kJ/mol Al, which is lower than the threshold value for self-sustaining aluminothermic reactions. The mixture must therefore either be preheated or mixed with oxygen-releasing compounds such as BaO_2, CaO_2, $KClO_4$, $KClO_3$ or $NaNO_3$.

Concentrates with lower percentages of niobium (ca. 40%) can also be treated by the aluminothermic process in an electric arc furnace. Also, a two-stage electroaluminothermic process for the production of ferroniobium from columbite has been developed [196].

The method of operation is to charge the mixture of niobium concentrate with the additives to refractory lined reaction vessels. Either the whole mixture is reacted, or a small amount is set aside, ignited with a special exothermic mixture, and added to the bulk mixture. The molten reaction product is allowed to solidify in the furnace, and the block of metal separates from the slag. After cooling, it is broken into pieces of the required size.

In the aluminothermic process operated at Araxa, Fe–Nb blocks of metal up to 11 t in weight are produced. The yield of niobium metal is 96–97%. The typical composition of a reaction charge is as follows:

Pyrochlore concentrate	18 000 kg (60% Nb_2O_5)
Iron oxide	4000 kg (68% Fe)
Aluminum powder	6000 kg
Fluorspar	750 kg
Lime	500 kg

The reaction gives ca. 11 000 kg of ferroniobium of composition:

Nb	66.0%
Fe	30.5%
Si	1.5%
Al	0.5%
Ti	0.1%
P	0.1%
S	0.04%
C	0.08%
Pb	0.02%

and ca. 20 000 kg of slag containing:

Al_2O_3	48%
CaO	25.0%
TiO_2	4.0%
BaO	2.0%
Re_2O_3	4.0%
Nb_2O_5	trace
ThO_2	2.0%
U_3O_8	0.05%

Special niobium alloys, e.g., nickel–niobium, cobalt–niobium, aluminum–niobium, and chromium–niobium, are also manufactured by the aluminothermic process. For these alloys, which have various niobium contents [197], niobium oxide is the only raw material used.

7.10.2 Uses of Ferroniobium

Niobium has very marked carbide and nitride forming properties and is therefore mainly used in the production of steels and gray iron [198]. The addition of niobium prevents intercrystalline corrosion in stainless austenitic chromium nickel steels and improves corrosion resistance, weldability, ductility, and toughness in ferritic chromium steels [199]. Ferroniobium is also used as a trace additive in large quantities for the production of high-strength low-alloy (HSLA) steels used in automobile body manufacture, structural steels, concrete reinforcing steel, and pipelines. Superalloys containing up to 5% niobium are used for gas turbine components. These materials have high hot strength [200, 201], and mostly have a nickel or copper base. The niobium is added in the form of nickel niobium or cobalt niobium.

7.11 Ferrotitanium

7.11.1 Composition and Uses

Ferrotitanium is described in DIN 17566 as a master alloy containing at least 28% Ti, obtained by reduction of the corresponding raw materials or their concentrates. The International Standard for ferrotitanium is ISO 5454-1980 (E), which specifies a Ti content of at least 20% and allows greater variation in the Al content (up to 10% Al) than DIN 17566. The Standards specify not only the chemical composition (Table 7.41) but the condition, testing methods (sampling and analysis), shipping, and storage. Ferrotitanium in "normal lump form" usually means lumps up to 25 kg in weight. Ferrotitanium can also be supplied on demand as crushed material and/or sieved as agreed. It is supplied in sealed steel drums.

Melting points and densities of some commercial ferrotitanium alloys are listed in Table 7.42.

The binary titanium–iron phase diagram is shown in Figure 7.34 [202].

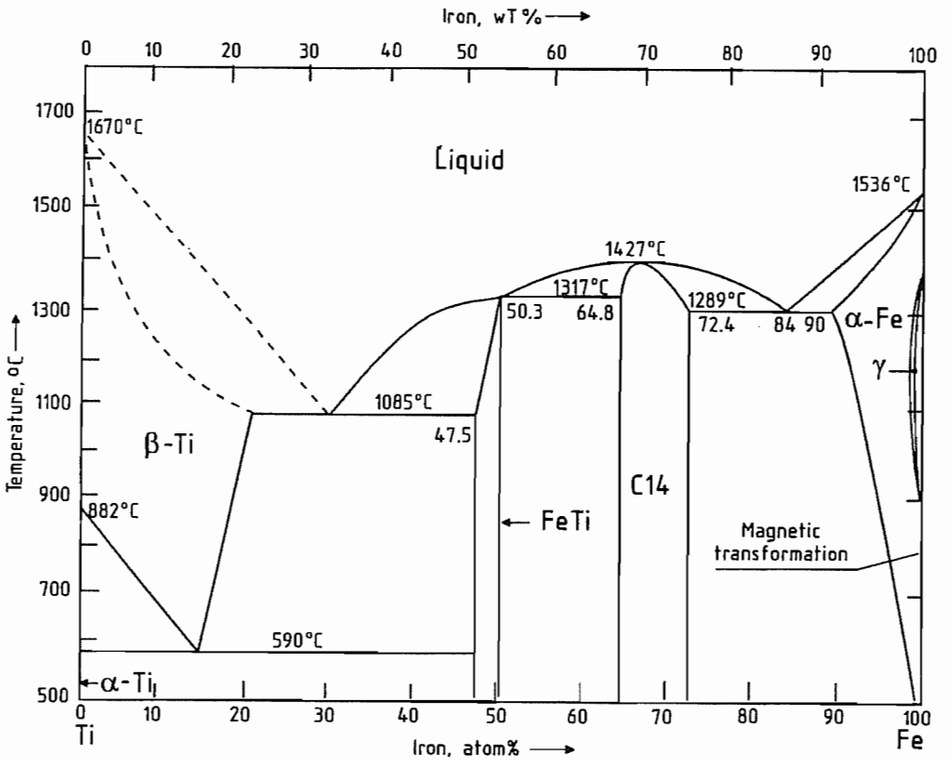

Figure 7.34: Ti–Fe phase diagram [202].

7.9.11 Toxicology and Industrial Hygiene

Ferroboron and boron master alloys are generally not toxic, but in the handling of raw materials for their production protective measures must be taken, e.g., the use of protective gloves and glasses as well as dust respirators when handling boric acid. In the production facilities the usual protective measures (clothing, glasses, dust respirators) must also be taken.

7.10 Ferroniobium

Approximately 85–90% of the total niobium production is used in the steel industry in the form of iron niobium alloy (ferroniobium) containing 40–70% niobium. Depending on the application, the alloy can also contain small amounts of Ta (ferroniobium tantalum), e.g., FeNb65Ta2, which contains 65% Nb and 2% Ta. Other alloy specifications are given in [195].

7.10.1 Production

Ferroniobium is usually produced by aluminothermic reduction of niobium oxide ores, with the addition of iron oxides if the niobium ore used contains insufficient iron. The starting materials are mainly columbites and pyrochlore concentrates.

The enthalpy of the reaction between Nb_2O_5 and Al is –276.1 kJ/mol Al, which is lower than the threshold value for self-sustaining aluminothermic reactions. The mixture must therefore either be preheated or mixed with oxygen-releasing compounds such as BaO_2, CaO_2, $KClO_4$, $KClO_3$ or $NaNO_3$.

Concentrates with lower percentages of niobium (ca. 40%) can also be treated by the aluminothermic process in an electric arc furnace. Also, a two-stage electroaluminothermic process for the production of ferroniobium from columbite has been developed [196].

The method of operation is to charge the mixture of niobium concentrate with the additives to refractory lined reaction vessels. Either the whole mixture is reacted, or a small amount is set aside, ignited with a special exothermic mixture, and added to the bulk mixture. The molten reaction product is allowed to solidify in the furnace, and the block of metal separates from the slag. After cooling, it is broken into pieces of the required size.

In the aluminothermic process operated at Araxa, Fe–Nb blocks of metal up to 11 t in weight are produced. The yield of niobium metal is 96–97%. The typical composition of a reaction charge is as follows:

Pyrochlore concentrate	18 000 kg (60% Nb_2O_5)
Iron oxide	4000 kg (68% Fe)
Aluminum powder	6000 kg
Fluorspar	750 kg
Lime	500 kg

The reaction gives ca. 11 000 kg of ferroniobium of composition:

Nb	66.0%
Fe	30.5%
Si	1.5%
Al	0.5%
Ti	0.1%
P	0.1%
S	0.04%
C	0.08%
Pb	0.02%

and ca. 20 000 kg of slag containing:

Al_2O_3	48%
CaO	25.0%
TiO_2	4.0%
BaO	2.0%
Re_2O_3	4.0%
Nb_2O_5	trace
ThO_2	2.0%
U_3O_8	0.05%

Special niobium alloys, e.g., nickel–niobium, cobalt–niobium, aluminum–niobium, and chromium–niobium, are also manufactured by the aluminothermic process. For these alloys, which have various niobium contents [197], niobium oxide is the only raw material used.

7.10.2 Uses of Ferroniobium

Niobium has very marked carbide and nitride forming properties and is therefore mainly used in the production of steels and gray iron [198]. The addition of niobium prevents intercrystalline corrosion in stainless austenitic chromium nickel steels and improves corrosion resistance, weldability, ductility, and toughness in ferritic chromium steels [199]. Ferroniobium is also used as a trace additive in large quantities for the production of high-strength low-alloy (HSLA) steels used in automobile body manufacture, structural steels, concrete reinforcing steel, and pipelines. Superalloys containing up to 5% niobium are used for gas turbine components. These materials have high hot strength [200, 201], and mostly have a nickel or copper base. The niobium is added in the form of nickel niobium or cobalt niobium.

7.11 Ferrotitanium

7.11.1 Composition and Uses

Ferrotitanium is described in DIN 17566 as a master alloy containing at least 28% Ti, obtained by reduction of the corresponding raw materials or their concentrates. The International Standard for ferrotitanium is ISO 5454-1980 (E), which specifies a Ti content of at least 20% and allows greater variation in the Al content (up to 10% Al) than DIN 17566. The Standards specify not only the chemical composition (Table 7.41) but the condition, testing methods (sampling and analysis), shipping, and storage. Ferrotitanium in "normal lump form" usually means lumps up to 25 kg in weight. Ferrotitanium can also be supplied on demand as crushed material and/or sieved as agreed. It is supplied in sealed steel drums.

Melting points and densities of some commercial ferrotitanium alloys are listed in Table 7.42.

The binary titanium–iron phase diagram is shown in Figure 7.34 [202].

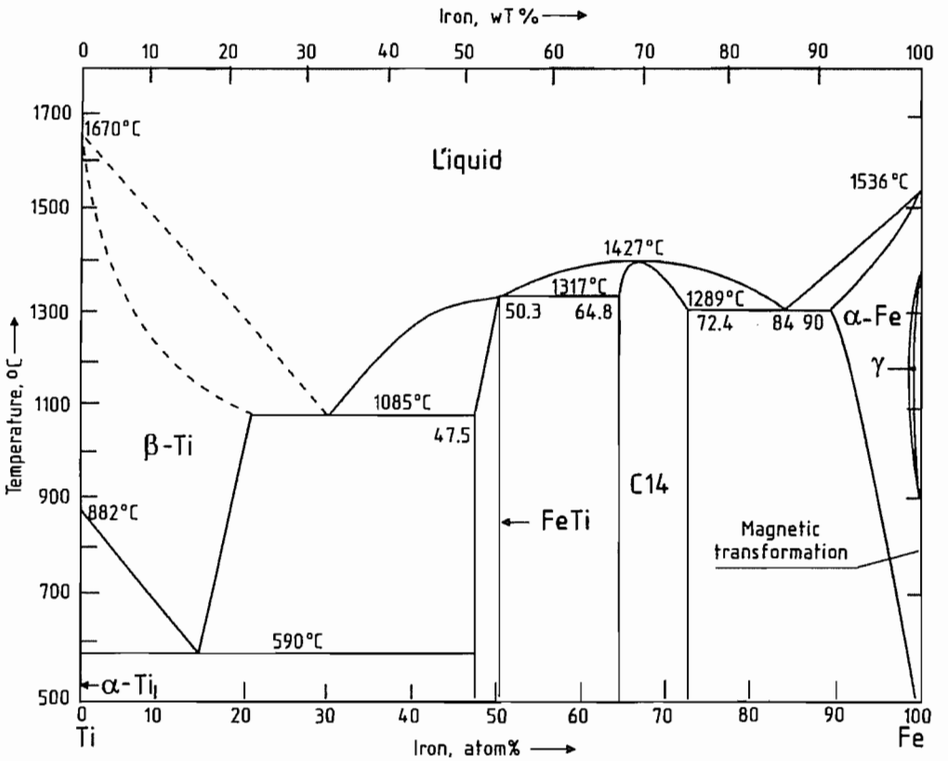

Figure 7.34: Ti–Fe phase diagram [202].

Table 7.41: Composition of commercial ferrotitanium alloys DIN 17566.

Alloy grade	Alloy number[a]	Chemical composition, %						
		Ti[b]	Total Al max.	Si max.	Mn Max.	C max.	P max.	S max.
FeTi 30	0.4530	28–32	4.5	4.0	1.5	0.10	0.050	0.060
FeTi 40	0.4540	36–40	6.0	4.5	1.5	0.10	0.10	0.060
FeTi 50	0.4550	46–50	75	4.0	1.0	0.10	0.10	0.060
FeTi 70	0.4570	65–75	2.0	0.20	1.0	0.20	0.040	0.030
FeTi 70 VB (vacuum treated)	0.4571	65–75	0.50	0.10	0.20	0.20	0.030	0.030

[a] In accordance with DIN 17007, Sheet 3 (draft).
[b] Variation within a batch must not exceed ±2%.

Applications in the Iron and Steel Industry. Compared with pure titanium, ferrotitanium has the advantages of better solubility (lower melting point and higher density) and lower price. Titanium is useful mainly because of its ability to form a carbide. However, as the affinity of titanium for oxygen is considerably higher than for carbon, the steel must be effectively deoxidized before titanium is added. Titanium is only used for this deoxidation in special cases. Titanium is also used for nitrogen removal and for bonding with sulfur [203].

Table 7.42: Melting points and densities of some commercial ferrotitanium alloys.

Composition, %			*mp*, °C	ρ, g/cm³
Ti	Al	Si		
30.6	4.0	3.7	1325–1500	6.2
39.1	5.8	4.0	1325–1480	5.9
46.6	7.6	3.2	1305–1480	5.5
70.0	0.1–0.5		1070–1135	5.4

In the production of stainless austenitic chromium–nickel steels, titanium is added to combine with the small amount of carbon present to form TiC ("stabilization"), thereby preventing intergranular corrosion (e.g., adjacent to welds).

Deoxidation of killed steel with titanium improves its quality by minimizing oxidic inclusions. Depending on the carbon content, it also reduces cracking tendency (grain refinement of austenite) and increases yield strength (titanium-containing ferrite). Titanium addition also minimizes segregation in the upper part of the ingot on casting, thus improving the yield.

Addition of titanium to tool steels gives a finer grain and reduces the depth of hardening and hence the cracking tendency. In sulfur-containing free-cutting steels, especially highly alloyed stainless chrome and chromium–nickel steels, the sulfur is bonded to the titanium. This prevents red shortness and improves ductility.

Some complex master alloys with boron contain titanium and other elements (BATS = boron–aluminum–titanium–silicon). The boron is added in small amounts to the steel to improve the hardening properties and grain refinement, and the titanium is added to protect the boron from nitrogen (by forming TiN).

High-temperature hardenable alloys based on iron and especially nickel (e.g., nimonic alloys) contain up to 4.5% Ti [204]. Here, the titanium reacts with the aluminum and nickel to form coherent particles with the composition $Ni_3(Ti, Al)$, which cause precipitation hardening. Titanium is also used as a microalloying element in high-strength, low-alloy (HSLA) steels [205].

The addition of titanium to cast iron causes the formation of finer graphite on supercooling, thereby improving the mechanical properties.

Powdered ferrotitanium and ferrosilicon–titanium alloys, sometimes with higher aluminum contents, are used as coatings on welding electrodes. Also, welding wires for HSLA steels are alloyed with ca. 0.5% Ti to give a fine-grained weld bead.

7.11.2 Production

The starting materials for the production of ferrotitanium are ilmenite, leucoxene, perovskite, and slag concentrates produced from ilmenite. Because of the increasing availability of titanium scrap, this also is used to an increasing extent for the production of ferrotitanium (mostly > 70% Ti) and other titanium master alloys.

Reduction with Carbon. Carbothermic production in electric arc furnaces leads to high carbon contents in the ferrotitanium. However, as the main use of ferrotitanium is to combine with the carbon in steel, the presence of carbon in the ferrotitanium is undesirable, and this production method is therefore now hardly used. The carbothermic production of ferrotitanium containing 15–18% Ti, 5–8% C, 1–3% Si, and 1–2% Al, and of ferrosilicon titanium containing ca. 30% Ti, ca. 30% Si, up to 0.3% C, and 1–3% Al is described in [206].

Metallothermic Production. DIN 17566 specifies grades of ferrotitanium containing 28–50% Ti and 4.5–7% Al. These are mainly produced by the aluminothermic process. The reduction of TiO_2 by Al proceeds via TiO.

$$3TiO_2 + 2Al \rightarrow 3TiO + Al_2O_3$$

$$3TiO + 2Al \rightarrow 3Ti + Al_2O_3$$

If there is too much TiO_2 in the reaction mixture, TiO can be formed as a third phase besides the metal and slag [207]. In the aluminothermic production of ferrotitanium there is a high consumption of aluminum, as it reacts both with the iron oxide in the ilmenite and with the oxygen-producing substances added to increase the exothermicity.

An aluminothermic mixture, consisting, for example, of 4320 kg Australian ilmenite (58.55% TiO_2), 480 kg rutile (96.7% TiO_2), 190 kg calcined limestone, 107 kg potassium perchlorate, and 1693 kg Al powder, is placed in a refractory-lined combustion vessel and ignited to start the reaction. After cooling, a 2250 kg block of ferrotitanium is obtained containing 39.8% Ti, 6.7% Al, 3.4% Si, and 0.02% C, which separates well from the slag. The titanium yield is 50%, and the specific consumption of aluminum (based on the Ti in the ferrotitanium) is 1.89 kg Al/kg Ti.

In the electro-aluminothermic process, which is carried out in an arc furnace, the raw materials contain as little iron oxide as possible, so that most of the aluminum is used to reduce titanium oxide. The consequent lack of exothermicity is compensated by electrical energy. A process developed in France is now widely used [208]. Here, an ilmenite concentrate, after addition of lime, is partially reduced with carbon in an electric-arc furnace to give a slag concentrate with a high concentration of titanium oxide, and the reduced iron is tapped off. The molten slag is then reduced in several stages by blowing in aluminum and iron, producing ferrotitanium of the desired composition.

In a process developed by the Gesellschaft für Elektrometallurgie [209], a calcium oxide/titanium oxide melt containing ca. 75% TiO_2 is first produced from prereduced ilmenite, from rutile and lime, or from perovskite with addition of iron scrap, and is reacted with a molten aluminum iron alloy containing 60–70% Al in a reaction ladle to give ferrotitanium and slag. Yields of titanium of 60–67% are obtained, and the specific aluminum consumption is 1.0–1.1 kg Al/kg Ti.

Production from Titanium Scrap and Sponge. As the availability of titanium scrap is increasing with the growth in the consumption of titanium, it is being increasingly used for the production of ferrotitanium (mainly high-grade material containing 65–75% Ti) and ferrotitanium–silicon. Because of its low melting point (ca. 1100 °C) the alloy containing 70% titanium melts comparatively readily when alloyed with iron in an induction furnace, in an arc furnace with consumable electrodes under vacuum or argon, or in an electroslag melting furnace. Contact of the melt with air must be prevented because of the strong affinity of titanium for oxygen and nitrogen. Ferrotitanium can also react with refractory crucibles [210]. The high-grade ferrotitanium alloys produced by melting under vacuum are designated FeTi 70 VB in DIN 17566.

Calcium–silicon–titanium alloys are produced by melting together commercial cal-

cium silicon and titanium sponge or scrap in an induction furnace [206, p. 579].

7.11.3 Economic Aspects

The prices of ferrotitanium are published in the London "Metal Bulletin", and the monthly average prices (from the Metal Bulletin), with the corresponding exchange rates, have been published since 1979 in the journal *Erzmetall* [211].

7.12 Ferrovanadium

According to DIN 17563 [212], ferrovanadium is "a master alloy with a vanadium content of at least 50% produced by reduction of the corresponding raw materials or their concentrates". In the United States alloys with lower vanadium contents are also commercially available. The iron vanadium and vanadium aluminum master alloys and the commercial grades of vanadium alloys are listed in Table 7.43.

Table 7.43: Commercial grades of vanadium master alloys [213, 214].

Ferrovanadium	% V	% C	% Si	% Al
FeV 40	35–48	0.5	2.0	0.5
FeV 50	48–60	0.5	2.0	0.3
FeV 60	50–65	< 0.15	< 1.5	< 2.0
FeV 80	78–82	0.15	1.5	< 1.5

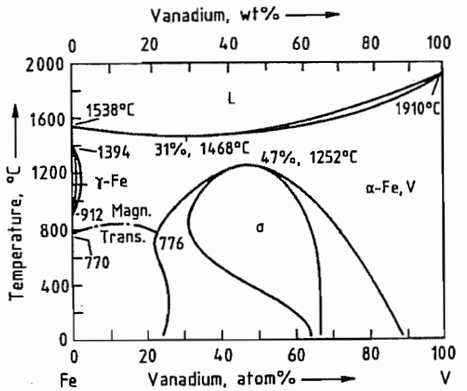

Figure 7.35: Phase diagram Fe–V [215].

The Fe–V phase diagram (Figure 7.35) shows almost complete mutual solubility of the elements. At compositions approximating to FeV below 1200 °C, a σ-phase exists which forms tetragonal crystals.

7.12.1 Production from Vanadium Oxides

The reduction of vanadium oxides is assisted by the presence of iron, as the activity of the vanadium is reduced, and the solubility of oxygen in vanadium–iron is much lower than in pure vanadium, because of the lower melting point [216]. The vanadium oxides can therefore be reduced with carbon, silicon, and aluminum in the presence of iron, the product being ferrovanadium.

Reduction with Carbon. The high affinity of vanadium for carbon leads to carbide formation, so that carbothermic reduction can only be used when there is no requirement for vanadium with low carbon content. The Union Carbide Corporation has developed a process that gives a V_2C-containing alloy known as Carvan [217], with a C content in the range 10–13% [213].

Reduction with Silicon. Under today's conditions for the processing of V_2O_5, silicothermic reduction is no longer generally profitable, as the process has multiple stages and gives a poor vanadium yield in the form of a low-vanadium ferrovanadium. The vanadium losses in this process are 10–25% [218].

Reduction with Aluminum. The high-vanadium grades of ferrovanadium, FeV 60, FeV 80, and FeV 90, are now usually produced by aluminothermic treatment of V_2O_5. The aluminothermic process can readily be controlled on a large scale. It is especially suitable for the treatment of vanadium pentoxide because it gives a high yield of high-grade ferrovanadium in a single process step.

After ignition, the reaction of V_2O_5 with aluminum is self-sustaining. Some of the mixture of V_2O_5 flakes, aluminum powder or granules, fine steel shot, and an initiating mixture (e.g., BaO_2 + Al powder) is ignited, and further quantities of the mixture are then added. The combustion time for the usual batch size (to produce 0.5–1 t metal) is only a few minutes. After cooling for 2–3 d, the furnace is dismantled, and the block of metal at the bottom is cleaned and crushed or ground to the commercially desired particle size.

As the reaction proceeds very rapidly, the aluminum in the metal and the vanadium oxide in the slag may not attain equilibrium, so that the vanadium content of the slag may be too high. To prevent this, an electric arc is ignited after completion of the aluminumothermic reaction to maintain the molten state of the melt and the slag until reaction is complete [219].

7.12.2 Direct Production from Slags and Residues

Enriched vanadium-containing oxidation slags can also be processed directly to a technical-grade ferrovanadium. In the method of Christiania Spigerverk [220], a 50% ferrovanadium is obtained in an electric arc furnace by a two-stage reduction process. In the first stage, the FeO fraction of the slag is reduced with ferrosilicon (FeSi 75) with addition of lime, and in the second stage the slag obtained in the first stage is reduced with 90% silicon to give a ferrovanadium alloy. The vanadium yield is 80%, and the FeV still contains traces of Si, Cr, Mn and Ti.

Ferrovanadium can be obtained by the electrosilicothermic treatment of high-vanadium boiler ashes and enriched fly ash, either alone or in combination with vanadium-containing oxidation slags, depending on their composition. As oil residues and fly ash contain only small amounts of iron, the iron removal stage normally necessary with oxidation slags can be omitted.

7.13 Ferromolybdenum

In the steel and foundry industry molybdenum is added to melts, either as technical oxide or in the form of ferromolybdenum. Table 7.44 summarizes the internationally standardized ferromolybdenum alloys; the typical molybdenum content ranges from 55 to 75%. Compared to pure molybdenum, ferromolybdenum dissolves much more easily in the steel melt and is cheaper to produce. Practical experience has shown that alloys with up to 75% molybdenum do not cause any dissolution problems. Nevertheless there is still a demand for 65% molybdenum alloys which are even less critical as regards dissolution characteristics. The Fe–Mo phase diagram is shown in Figure 7.36. Due to the limited information available, the melting temperatures of the alloy at high molybdenum concentrations can only be estimated. In practice they are likely to be considerably lower than indicated by the phase diagram because of significant concentrations of silicon and other impurities.

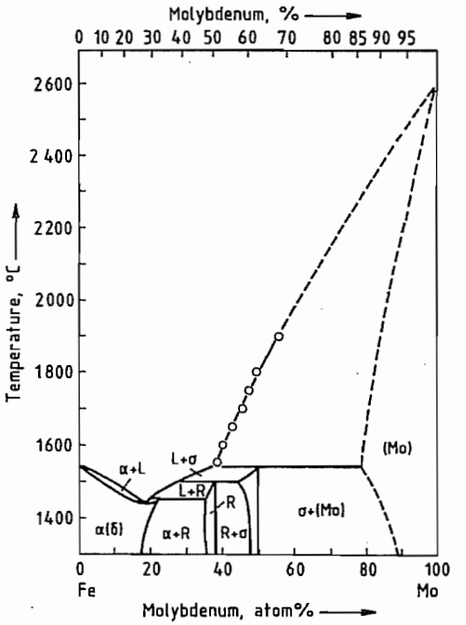

Figure 7.36: Fe–Mo phase diagram showing estimated liquidus (L) compositions at higher molybdenum concentrations [221]. α, δ, and R are intermetallic phases.

Table 7.44: International specifications for ferromolybdenum.

Specification	Symbol/designation	Composition, %							
		Mo	Si (max.)	C (max.)	S (max.)	P (max.)	Cu (max.)	Pb (max.)	Sn (max.)
ASTM A 132-74 (reapproved 1979)	Ferromolybdenum (formerly grade B)	60.0 min.	1.0	0.10	0.15	0.05	1.0	0.01	0.01
DIN 17561	FeMo 70 (0.4270[a])	60–75[b]	1.0	0.10	0.10	0.10	0.5		
	FeMo 62 (0.4262[a])	58–65[b]	2.0	0.50	0.10	0.10	1.0		
ISO 5452	FeMo 60	55.0–65.0[c]	1.0	0.10	0.10	0.05	0.5		
	FeMo 60 Cu 1	55.0–65.0	1.5	0.10	0.10	0.05	1.0		
	FeMo 60 Cu 1.5	55.0–65.0	2.0	0.50	0.15	0.05	1.5		
	FeMo 70	65.0–75.0[c]	1.5	0.10	0.10	0.05	0.5		
	FeMo 70 Cu 1	65.0–75.0	2.0	0.10	0.10	0.05	1.0		
	FeMo 70 Cu 1.5	65.0–75.0	2.5	0.10	0.20	0.10	1.5		
Japanese Industrial Standard, JIS G 2307 1978									
Class:									
High-carbon ferromolybdenum	FMoH	55.0–65.0[c]	3.0	6.0	0.20	0.10	0.5		
Low-carbon ferromolybdenum	FMoL	60.0–70.0[c]	2.0	0.10	0.10	0.06	0.5		

[a] Material numbers in preparation, proposed numbers.
[b] The range of variation within a lot may not exceed ±2%.
[c] The range of variation within a graded lot should not exceed 3% absolute.

The principal raw materials used for ferromolybdenum production are molybdenum concentrates and technical-grade molybdenum trioxide. One method proposed for the production of ferromolybdenum used molybdenum concentrates which were reacted with ferromanganese to form ferromolybdenum and manganese sulfide [222]:

$$MoS_2 + 2Mn \rightarrow Mo + 2MnS$$

Due to the high Gibbs free energy of manganese(II) sulfide formation, this reaction is claimed to yield ferromolybdenum with a relatively low sulfur concentration, but a further sulfur removal step appears to be necessary. This process is not, however, used on a commercial basis.

Technical-grade molybdenum trioxide is commonly used as the molybdenum raw material. Because of its high value and the fact that MoO_3 starts to sublime at 700 °C, electrostatic precipitators or bag houses must be used to collect the molybdenum dust and sublimates for recirculation. Good housekeeping is also essential to minimize molybdenum handling losses.

Two principal processes are used for molybdenum oxide reduction: carbothermic reduction in a submerged arc furnace and metallothermic reduction. The most commonly applied method is the silicothermic reduction, a type of metallothermic reduction.

7.13.1 Submerged Arc Furnace Carbothermic Reduction

The carbothermic reduction of MoO_3 can proceed as follows:

$$2MoO_3 + 2C \rightarrow 2MoO_2 + 2CO$$

$$MoO_2 + 2C \rightarrow Mo + 2CO$$

or with formation of molybdenum carbide:

$$MoO_2 + 2.5C \rightarrow 0.5Mo_2C + 2CO$$

The Gibbs free energies of oxide and carbide formation are shown in Figure 7.37 as a function of temperature. The reduction of MoO_3 starts at fairly low temperatures. If the process were run at these temperatures (i.e., < 600 °C) then Mo_2C would be formed because it is more stable than molybdenum. However, since the process is run at 1700–2000 °C, any intermediately formed molybdenum carbide reacts to form molybdenum metal:

$$2Mo_2C + MoO_2 \rightarrow 5Mo + 2CO$$

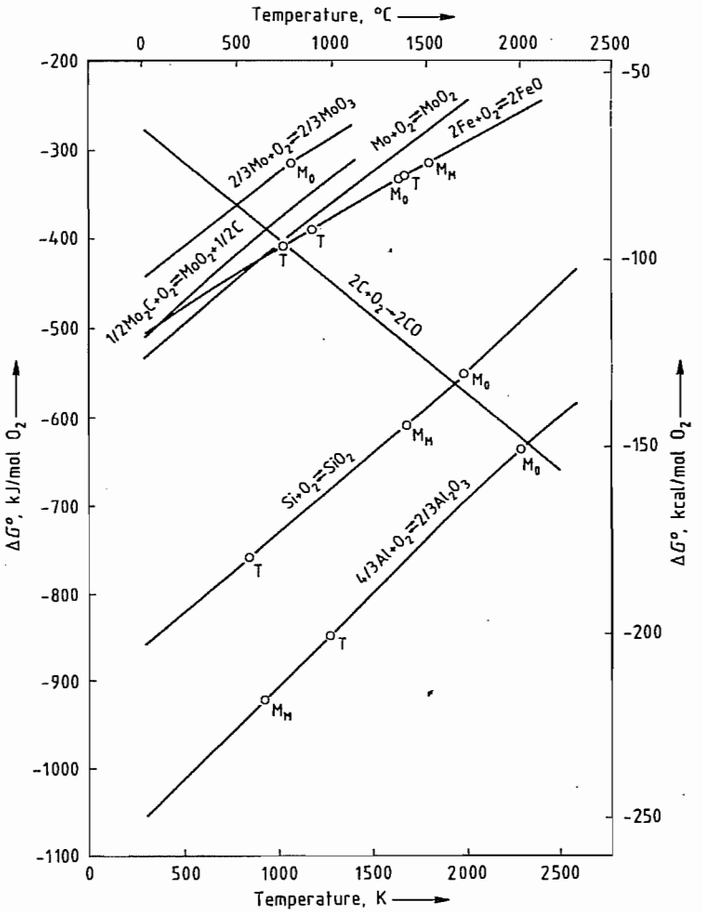

Figure 7.37: Gibbs free energy of oxide and carbide formation [223]. T = transformation point; M_M = melting point of metal; M_O = melting point of oxide.

Under practical conditions the resulting metal alloy is low in carbon.

Because of the commercial disadvantages of the process, detailed literature describing the process is limited [224–227]. The process was previously run in single-phase 300–500 kW and three-phase 1500–2000 kW electric arc furnaces. The use of the single-phase arc furnace seems to have been more successful because of its higher energy density within the furnace. A single-phase system with a cylindrical magnesite or carbon-based rammed furnace body and equipped with a bottom carbon electrode is shown in Figure 7.38. The top electrode is adjustable and the whole furnace arrangement runs on tracks so that it can easily be replaced with a new unit. The process is run batchwise, producing a semimolten metal block and a slag. The slag contains up to 10% molybdenum oxide and must be retreated by remelting. Melting of a 1.5–2 t metal block takes about 20–28 h. To separate metal and slag, the furnace assembly must be stripped and later rebuilt for reuse.

Raw materials are technical-grade molybdenum oxide; iron ore or millscale, steel

punchings, nail nips or turnings; lime and fluorspar as fluxing agents; and charcoal as reducing agent. To minimize MoO_3 sublimation, the concentrate and carbon material are briquetted. The reaction is started by melting slag from a previous reaction and adding the briquetted mixture to the slag to avoid molybdenum sublimation. Once the initial reduction to MoO_2 has taken place, sublimation is avoided. The resulting slag consists of some unreduced MoO_2 and FeO which has a higher Gibbs free energy than MoO_2 (Figure 7.37). To improve metal–slag separation, lime and fluorspar are added. The slag should be fluid and is tapped toward the end of the reduction cycle. The metal block is stripped while it is still red hot and quenched in water to aid subsequent crushing. The metal must be hand-sorted to recycle any parts of the block contaminated with slag. The resulting molybdenum-rich slag has to be remelted in a separate process into a low-molybdenum, high-carbon intermediate alloy which is recycled.

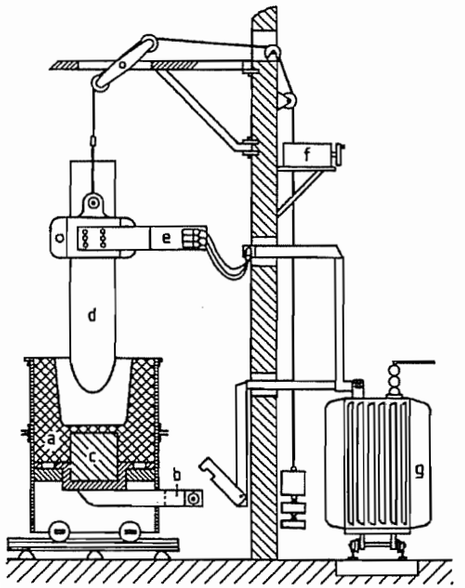

Figure 7.38: Single-phase submerged arc furnace [227]: a) Furnace with rammed lining; b) Bottom electrode power supply bar; c) Bottom electrode (carbon); d) Top electrode; e) Electrode clamp with power supply cables; f) Electrode control; g) Transformer.

Table 7.45: Consumables required to produce 1 t of ferromolybdenum in the carbothermic process [227].

Consumable	Single-phase furnace 300 kW	Three-phase furnace, 1500 kW
Roasted Mo concentrate, kg	1160	1420
Remelt material, kg	280	330
Slag treatment metal, kg	165	168
Nail nips, kg	172	230
Platescale, kg	290	102
Lime, kg	150	178
Fluorspar, kg	150	178
Charcoal, kg	255	310
Electrodes, kg	95	135
Power, kWh	4300	4450
Products		
Ferromolybdenum, kg	1000	1000
Remelt, kg	270	250
Dust, kg	66	

Table 7.45 shows the consumption of electric energy and ingredients required to produce ferromolybdenum using the carbothermic process.

7.13.2 Metallothermic Reduction

Metallothermic reduction in which silicon (or aluminum) is used to reduce the MoO_3 is the commonly used production process for ferromolybdenum today. Its advantages are that it is a single-step process which results in a saleable metal and a low-molybdenum slag and that it requires only basic process equipment. Due to the large difference in the Gibbs free energy for aluminum oxide and silicon dioxide formation compared to molybdenum oxide formation (Figure 7.37), the reduction process approaches 100% molybdenum reduction.

An aluminothermic or silicothermic reaction must be sufficiently exothermic to melt all the reaction constituents resulting in satisfactory separation of the liquid metal and liquid slag phases before cooling. According to SHEMTCHUSHNY, a minimum specific heat of reaction of –2700 kJ/kg is required for a reaction to be self-sustained [228]. This assumes that no additional heat is added to the reaction (e.g., by preheating the charge or by adding booster oxides and further reducing metal). Consideration of the specific heats of reaction shows that both aluminum and silicon can be used to reduce MoO_3 in self-sustained reactions:

$$^2/_3MoO_3 + Si \rightarrow {}^2/_3Mo + SiO_2 \quad -3241\ kJ/kg$$

$$^1/_2MoO_3 + Al \rightarrow {}^1/_2Mo + {}^1/_2Al_2O_3 \quad 4689\ kJ/kg$$

If aluminum is reacted with MoO_3, the resulting heat of reaction is very high, leading to excessive evaporation of MoO_3 and the danger of an explosion of the reaction mixture.

Consequently, silicon is the preferred reducing element. Furthermore, less silicon is necessary compared to aluminum (stoichiometric consumption is 0.439 kg silicon per kilogram of molybdenum, compared to 0.562 kg aluminum per kilogram of molybdenum) and silicon in the form of ferrosilicon is considerably cheaper than aluminum.

Practical experience, even when using charges much larger than a 200 kg, shows that silicon alone does not result in a self-sustained reaction. Some of the silicon must therefore be replaced with aluminum or other elements with a similar oxygen affinity. Some of the required iron is often added in the form of millscale or iron ore concentrates which react with silicon or aluminum to generate additional heat. Part of the iron remains as FeO in the slag and acts as a fluxing agent. Further fluxing agents are lime and fluorspar, which are necessary to ensure good separation of metal and slag and low molybdenum concentrations (typically < 1%) in the slag. The dust generated in the process can contain up to 5% of the molybdenum in the charge. Any dust and sublimed MoO_3 must be extracted, recovered, and recycled to achieve an overall molybdenum yield of 97–99%.

To achieve reproducible reactions, a homogeneous mixture of the precisely weighed reaction ingredients is required. All ingredients must be dry, well-calcined, and ideally their particle size should be < 1 mm. A typical firing arrangement is shown in Figure 7.39. The crucible unit consists of a circular or square, sand- or brick-lined base section and a cylindrical refractory-lined, steel section that contains the reaction slag. The mix feeding arrangement allows part of the reaction mixture to be placed into the well-dried crucible unit. The reaction is started by adding a small amount of a mixture of barium peroxide and aluminum to a special starter mix which tends to be more exothermic than the main mix. Once the main mix has started to react, the bulk of the reaction mix is continuously fed into the crucible arrangement. Total reaction times of 30–60 min for metal block weights of 1–4 t can be expected. After completion of the reaction, metal and slag are allowed to segregate for another 30–60 min before the bulk of the slag is tapped off. The red-hot metal block is then stripped off the furnace base and quenched in water to aid crushing. Jaw crushers are commonly used for crushing the metal. Considerable care has to be taken when sampling the metal for molybdenum content because the molybdenum tends to segregate within the block. Any highly segregated metal and metal contaminated with slag inclusions is recycled for remelting. Good housekeeping is necessary to recycle all splashings, floor sweepings, etc. and achieve a good total molybdenum yield.

In a process modification used by Duval Corporation, Duval Sierrita [230], the entire reaction mix is charged into the reaction crucible before ignition. The advantage is that controlled addition of the reaction mix is not required. The disadvantages are that the reaction speed cannot be controlled by varying the feed rate and that a larger crucible unit is required to contain the initial mixture.

Recent developments have centered on improving process economics. Automatic handling and weighing of the raw materials as well as finished metal and ferromolybdenum slag is one area of activity. Other activities center around the optimization of ingredient and consumable costs.

Metallothermic mixtures used to produce ferromolybdenum are summarized in Table 7.46. Mixtures A–D represent different possibilities of increasing the reaction heat by using aluminum or calcium in the form of a calcium–silicon or a ferrosilicon–aluminum alloy [227]. Reaction D can be regarded as a fairly typical ferromolybdenum reaction mix; it

gives 87 kg ferromolybdenum with 67–73% molybdenum, 0.05–0.08% carbon, 0.03–0.05% sulfur, 0.25–0.6% silicon and 5 kg remelt metal as well as a slag containing 0.34% MoO_3, 13.85% Fe_2O_3, 7.4% CaO, 9.9% Al_2O_3, and 64.5% SiO_2. The reaction mix also contains recycled dust and metal remelt which is normal practice when continuously producing ferromolybdenum.

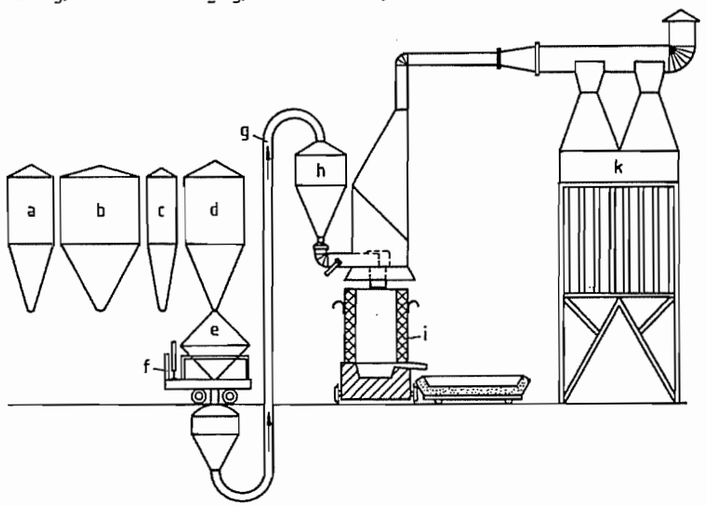

Figure 7.39: Metallothermic firing arrangement [229]: a) Storage hopper for iron ore or millscale; b) Storage hopper for roasted Mo concentrate; c) Storage hopper for fluorspar; d) Storage hopper for aluminum and ferrosilicon (75% Si) powder; e) Mixing hopper; f) Balance; g) Air lift system; h) Firing hopper; i) Reaction vessel; k) Electrostatic precipitator.

Table 7.46: Reaction mixtures used for ferromolybdenum production.

Component	Durrer, Volkert [227]				Climax Molybdenum			Literature from the former Soviet Union		
	A	B	C	D	[231] E	[232] F	[232] G	[233] H[a]	[234] I[b]	[235] J[c]
Roasted Mo concentrate, kg	100	100	100	100	100	100	100	100	100	100
MoO_3 concentration, %	ca. 90	ca. 90	ca. 90	ca. 90	85	85	85	81.7–84	80.3	85
Platescale, kg	29	16–18	35	51		24.2	22.5			
Fe ore, kg					26.9			26	22	29.6
Fe concentration, %					69				65.7	67.1
Fe turnings, kg	5–6	18						19.5		
Fe scrap, kg						17.3[d]	5.2[d]		19	19.2
Ferrosilicon, kg	31.5	21–23	65[e]	38	48.9	20.8	31.2	35.1	31.6	36.8
Si concentration, %	75	75	45	75	50	75	75	75	77	73.6
Ca–Si alloy, kg		17–18								
Al powder, kg	9.0			5	5.1	12.1	6.9	3.7	4.3	3.8
Al concentration, %	99.5			99.5	93				93	99
Lime, kg				2.5	7	8.7		3.0		3
Fluorspar, kg			7	7.5	2.2		5.2	2.0	3	2
CaF_2 concentration, %					95					
Dust, kg				9.5			5.2			
Remelt, kg				5.5			6.9			

[a] Up to 36 mixes used in one reaction.
[b] Mix preheated to 150 °C.
[c] Calculated mix.
[d] Fe shot.
[e] FeSi 45 Al 10 alloy.

Mixtures E–G have been reported to have been used by Climax Molybdenum in their Langeloth (USA) plant [231]. The mixtures are based on 100 kg technical molybdenum oxide input with 85% MoO_3 in the technical oxide. Reaction E can be regarded as a typical reaction mix for a ferromolybdenum with 58–64% molybdenum. The maximum impurity levels quoted were 0.1% carbon, 0.25% sulfur, 0.5% copper, and 1% silicon. Reaction G can be regarded as a typical reaction mix yielding an approximately 70% molybdenum alloy.

Mixtures H–J have been taken from literature from the former Soviet Union [233–235]. Mixture H gives ferromolybdenum containing 60–65% molybdenum, 0.15–0.9% silicon, 0.04% phosphorus, 0.08% sulfur, 0.05% carbon, and ca. 0.5% copper and slag containing 0.06–0.17% molybdenum, 67–70% SiO_2, 7–11% FeO, 10–13% Al_2O_3, 6–8% CaO, and 1–3% MgO. Mixture I uses a mix preheating to 150 °C, and should have resulted in a ferromolybdenum with ca. 56% molybdenum (calculated). Mixture J is part of a calculated formulation according to Elyutin [235]. The calculation is based on 96.8 kg ferromolybdenum containing 58.14% molybdenum, 0.53% silicon, and 0.07% carbon and 87 kg slag containing 65.65% silicon oxide, 10.06% aluminum oxide, and 24.28% iron(II) oxide. A heat balance has been calculated for this formulation. The total heat generated is 422.45 MJ. This heat is assumed to be consumed to provide the latent and melting heat for the metal (25%), the slag (50%), and to cover the heat losses of 25%.

7.14 References

1. R. Fichte, H.-J. Retelsdorf: "Stahlveredler" in *Winnacker-Küchler*, vol. 4, pp. 198–234.
   Durrer–Volkert: *Metallurgie der Ferrolegierungen*, 2nd ed., Springer Verlag, Berlin–Heidelberg–New York 1972.
   A. G. E. Robiette: *Electric Smelting Processes*, Griffin, London 1973.
   F. Leitner, E. Plöckinger: *Edelstahlerzeugung*, 2nd ed., Springer Verlag, Wien–New York 1965.
2. P. D. Deeley, K.-J. A. Kundig, H. R. Spendelow, Jr.: *Ferroalloys and Alloying Additives Handbook*, Shieldalloy Corp., Newfield, N. J., Metallurg Alloy Corp., New York 1981.
3. VDI-Richtlinien VDI 2576 (May 1983): *Emissionsminderung – Elektrothermische und metallothermische Erzeugung von Ferrolegierungen* (Emission Control – Electrothermic and Metallothermic Ferroalloy Production), vol. 2 of *VDI-Handbuch Reinhaltung der Luft*, Beuth Verlag, Berlin–Köln 1983.
4. H. Goldschmidt, *Justus Liebigs Ann. Chem.* **301**(1898) 19–28.
5. O. Kubaschewski, C. B. Alcock: *Metallurgical Thermochemistry*, 5th ed., Pergamon Press, London–New York 1979.
6. N. P. Elyutin et al.: *Production of Ferroalloys*, 2nd ed., Israel Programme for Scientific Translations, S. Monon, Jerusalem 1961.
7. W. Dautzenberg, in: Dürrer & Frank, (G. Volkert, K.-D. Frank, eds.): *Metallurgie der Ferrolegierungen*, 2nd ed., Springer Verlag, Berlin–Göttingen–Heidelberg–New York 1972.
8. E. M. Levin et al.: *Phase Diagrams for Ceramists*, American Ceramic Society Inc., Columbus, 1964, Supplement 1969.
9. W. G. Moffatt: *Handbook of Binary Phase Diagrams*, General Electric Corp, Schenectady 1973 (plus updates).
10. K. A. Feldmann, K. D. Frank in R. Durrer, G. Volkert (eds.): *Metallurgie der Ferrolegierungen*, Springer Verlag, Berlin 1972.
11. W. P. Eljutin, I. A. Palow, B. E. Levin: *Ferrolegierungen*, VEB Verlag Technik, Berlin 1953.
12. E. Schürmann, N. Hensgen, *Arch. Eisenhüttenwes.* **51** (1980) no. 1, 1–4.
13. J. A. De Huff, V. D. Coppolecchia, A. Lesnewich, *Electr. Furn. Proc.* **27** (1969) 167–174.
14. H. Krogrund, *ISLAFA Conference*, Acapulco 1978.
15. DEMAG company brochure, Submerged Arc Furnaces, Duisburg 1979.
16. T. W. Lopuszynski, J. P. Trunco, W. L. Wilbern, *Electr. Furn. Proc.* **30** (1972) 89–93.
17. U.S. Environmental Protection Agency Office of Air and Waste Management Research Triangle Park, N. C., 27711 EPA 450/2-74-008, 1974.
18. G. Rau, *Erzmetall* **44** (1991) no. 11, 557–559.
19. P. C. Aitcin, *Electr. Furn. Proc.* **42** (1984) 301–310.
20. ASTM Designation: *Annual Book of ASTM Standards*, E 360 – 70 T, ASTM, Philadelphia, 1970.
21. *Handbuch für Eisenhüttenlaboratorium*, vol. 2, Verlag Stahleisen mbH, Düsseldorf.
22. *Analyse der Metalle*, vol. 1, Springer Verlag, Berlin 1980.
23. DFG: *Maximale Arbeitsplatzkonzentration und Biologische Arbeitsstofftoleranzwerte*, VCH Verlagsgesellschaft, Weinheim 1991.
24. E. Houdremont: *Handbuch der Sonderstahlkunde*, Springer Verlag, Berlin 1956.
25. J. S. Stanko: *Steel Makers Guide to Manganese*, Mintek, Randburg 1989.
26. Commodities Research Unit: *The Costs of Producing Ferroalloys*, vol. 2, London 1989.
27. V. V. Strishkov, R. M. Levine: *The Manganese Industry in the U.S.S.R.*, U.S. Bureau of Mines, Washington 1986.
28. H. Bromet: "Technical and Economic Comparison of the Various Furnaces used for Ferro and Silico

Manganese", *INFACON 80. Proc. Int. Ferro-Alloys Congr.* **2nd**, 1980.
29. O. Kubaschewski, C. D. Alcock: *Metallurgical Thermochemistry*, 5th ed., Pergamon Press, Oxford 1979.
30. *Plasma Torches in Blast Furnaces*, Société du ferromanganèse de Paris, Outreau 1986.
31. W. J. Rankin: "Si–Mn Equilibrium in Ferromanganese Production", *J. S. Afr. Inst. Min. Metall.* **79** (1979) Sept., c167–c174.
32. S. Sakurai: *Recent Operational Results of the Shaft Type Ferro-Manganese Smelting Furnace*, Mizushima Ferro-Alloy Company Japan, Mizushima 1986.
33. A. G. Arnesen, B. Asphaug: "Computer Control of Electric Smelting Furnaces", *Proc. Int. Ferro Alloy Conf.*, Johannesburg 1974.
34. Z. Van der Walt, W A. Gericke: "The Effect of the Magnitude of Scale on Various Operating Characteristics in the Production of High-Carbon Ferromanganese", *Proc. Lat. Am. Inst. Iron and Steel*, Seminar Ferroalloys, 1975.
35. G. Glöckler, H. G. Müller: "A Comparison of the Electric Submerged Arc Furnace and the Plasma Smelting Furnace", *BHM Berg-Hüttenmänn. Monatsh.* **134** (1989) no. 5.
36. A. Kousaris, J. B. See: "Reactions in the Production of High Carbon Ferromanganese from Mamatwan Ore", *J. S. Afr. Inst. Min. Metall.* **19** (1979) 149–158.
37. R. T. Hooper, "The Production of Ferromanganese", *Electr. Furn. Conf Proc.* **24** (1967) 141–145.
38. L. Rossenmyr: "Manganese Alloy Production in Large Submerged Arc Furnaces", *Electr. Furn. Conf. Proc.* **27** (1970) 121–124.
39. Tinfos Company Brochure, Tinfos Jernwerk AS, Oyestronda, Norway 1989.
40. "Electric Furnaces Beats Pollution", *Mod. Power Eng.*, May 1974.
41. W. Gericke: "The Establishment of a 500 000 t/a Sinter Plant at Samancor's Mamatwan Manganese Ore Mine", *Proc. Int. Ferroalloys Congr.* **5th** (1987) April.
42. A. A. Tskilishvili: "Production of High-Carbon Ferromanganese from Manganese Iron Sinter", *Stal'* (1975) no. 9, 816–817.
43. E. Svana: "Ferro Manganese Smelting", *Elkem Seminar on Smelting*, New Delhi 1974.
44. R. G. Rotzlaff: "High Carbon Ferromanganese Production on the High Alumina Practice", *Electr. Furn. Conf. Proc.* **44** (1987) 169–173.
45. H. W. Wise: "High Carbon Ferromanganese Metallurgical Variables", *Electr. Furn. Conf. Proc.* **24** (1968) 88–92.
46. J. F. Dery: "Metallurgical Calculations for Ore Evaluation and Operational Planning in the Electric Furnace Smelting of High Carbon Ferromanganese", unpublished paper (1964).
47. D. S. Kozak, L. R. Matricardi: "Production of Refined Ferromanganese Alloy by Oxygen Refining of High Carbon Ferromanganese", *Electr. Furn. Conf. Proc.* **38** (1980) 123–127.
48. R. Ando, T. Yamagishi, T. F. Fukusima, K. Kawasaki: "A Study on the Silicomanganese Process", *Electr. Furn. Conf. Proc.* **34** (1974) 107–115.
49. Creusot-Loire and S. A. Manganese Amcor Ltd., FR 79 0169, 1979.
50. N. A. Barcza, D. P. O'Shaughnessy: "Optimum Slag – Alloy Relationships for the Production of Medium to Low Carbon Ferromanganese", *Can. Metall. Q.* **20** (1981) no. 3, 285–294.
51. T. Chisaki, K. Takervchi: "Electric Smelting of High Carbon Ferromanganese with Preheated Prereduced Materials at Kashima Works", Kashima 1971.
52. I. Tanabe: "Preheating of Ore for a Ferromanganese Furnace. A Recent Trend in Japan", *Electr. Furn. Conf. Proc.* **23** (1967) 131–138.
53. C. T. Ray, A. H. Olsen: "Computer Control of Four Furnaces in Tasmania", *Electr. Furn. Conf. Proc.* **44** (1987) 217–223.
54. T. K. Leonard: "Expert Systems Can Control Ferroalloy Processes", *Proc. Int. Ferroalloy Congr.* **5th** (1989) 267–279.
55. H. Muller, D. B. Wellbeloved: "Examples of Plasma Potential for Industrial Applications", *Symp. Proc. Int. Symp. Plasma Chem.* 1989.
56. A. H. Sully, E. A. Brandes: *Metallurgy of the Rare-Earth Metals – Chromium*, 2nd ed., Butterworth, London 1967.
57. A. Coutagne: *La fabrication des ferro-alliages*, Baillière Fils, Paris 1924.
58. P. D. Deeley, K. J. A. Kundig, H. R. Spendelow, Jr.: *Ferroalloys and Alloying Additives Handbook*, 1st ed., Shieldalloy Corp., Newfield, N.J., 1982 Metallurgy Alloy Corp., New York, NY, 1981.
59. O. Kubaschewski: *Iron–Binary Phase Diagrams*, Springer-Verlag, Berlin–Heidelberg–New York and Verlag Stahleisen mbH, Düsseldorf 1982, pp. 31–34.
60. V. G. Rivlin, *Int. Metal. Rev.* **29** (1984) no. 4, 299–327.
61. P. Wille, *Stahl Eisen* **103** (1983) no. 3, 127–132.
62. F. Ergunalp, *Trans. Inst. Min. Metall.* **89** (1980, Oct.) A179–A184.
63. D. P. O'Shaughnessy, *Mining Mag.* **147** (1982, Oct.) 291–299.
64. H. Fuchs: "Untersuchung des Petrographischen und Mineralogischen Aufbaus von Chromerzen für die Metallurgische Verwertung und ihrer Reduzierbarkeit mit dem Ziel der Aufstellung von Bewertungsrichtlinien", Dissertation Rheinisch-Westfälische-Technische-Hochschule (RWTH), Aachen 1962.
65. A. G. E. Robiette: *Electric Smelting Processes*, C. Griffin Co., London 1973, pp. 150–178.
66. K. Willand: "Untersuchungen zur Herstellung von Ferrochrom mit 4–6% Kohlenstoff", Dissertation RWTH, Aachen 1971.
67. J. H. Downing: "Theoretical Basis for Smelting Ferroalloys", *34th Electric Furnace Conference*, St. Louis, Miss., Dec., 1976.
68. E. M. Levin, C. R. Robbins, H. F. McMurdie in M. K. Reser (ed.): *Phase Diagrams for Ceramists*, 2nd ed., compiled at National Bureau of Standards, American Ceramic Society, Columbus, OH, 1969, p. 246 (Fig. 712).
69. F. Breuer: "Untersuchungen über das System Chrom–Eisen–Silizium–Kohlenstoff und ihre Nutzanwendung im Bereich der Technischen Silikochrom-Legierungen", Dissertation RWTH, Aachen 1961.

70. M. S. Rennie, *Electr. Furn. Conf. Proc.* **37** (1979), 202–209.
71. J. H. Downing, L. Urban, *J. Met.* **18** (1966) 337–344.
72. G. Volkert, W. Dautzenberg, J. Willems, G. Zieger et al.: "Ferrochrom und Chrommetall", in Durrer, G. Volkert, K.-D. Frank: *Metallurgie der Ferrolegierungen*, 2nd ed., Springer, Berlin–Heidelberg–New York 1972, pp. 292–365.
73. H. D. Rowley, D. M. Legg: "Construction and Operation of Charge Chrome Facilities at Tubatse Ferrochrome (Pty.), Steelport, Transvaal, South Africa", *35th Electric Furnace Conference*, Chicago, Dec. 1977, Special Arc Prepr.
74. W. D. Winship: "Briquetting – An Economic Solution for the Production of Ferro-Chrome in South Africa", *Proc. of the 15th Biennial Conf.*, Inst. for Briquetting and Agglomeration, Montréal, Québec, 1977, pp. 139–152.
75. E. Lankes, W. Böhm: "Experience Made and Operational Results Obtained with a Chrome Ore Pelletizing Plant Working on the LEPOL Process", *Int. Ferroalloy Conf. (INFACON)*, Johannesburg, South Africa, Apr., 1974.
76. N. G. Lindberg, T. S. Falk, *CIM Bull.* **69** (1976, Sept.) 117–126.
77. J. Relander, M. Honkaniemi: "Production of Ferrochrome from Low-Grade Ores", *Symposium on Extraction of Steel Alloying Metals*, Technical Univ. of Lulea, Sweden, Mar. 15–18, 1983, Prepr. pp. 295–301.
78. H. Tuovinen, J. Relander, M. Honkaniemi, *Electr. Furn. Conf. Proc.* **36** (1978) 127–133.
79. W. Schiffner, *Stahl Eisen* **104** (1984) no. 21, 1099–1101.
80. Y. Kanoh, *Met. Bull. (London)*, Ferro Alloys Special Issue, **1971**, 83–85.
81. K. Ichikawa, *Chem. Eng.* **81** (1974, Apr.) 36–37.
82. R. A. Leeper, T. J. Dyrdek, *Electr. Furn. Conf. Proc.* **23** (1965) 110–114.
83. H.-J. Retelsdorf, R. M. Fichte, F. Breuer, H. Zimmermann, *Metall (Berlin)* **36** (1982) 140–143.
84. N. A. Barcza, T. R. Curr, W. D. Winship, C. P. Heanley, *Electr. Furn. Conf. Proc.* **39** (1981) 243–260.
85. *Met. Bull. Mon.* **151** (1983, Jul.) 91–93.
86. Ges. f. Elektrometallurgie mbH, DE 2201388, 1972 (F. Breuer, K. Brotzmann, G. Duderstadt, R. Fichte et al.); DE 2 531034, 1975 (F. Breuer, G. Duderstadt, G. Nassauer, W. M. Dresler et al.); DE 2540290, 1975 (F. Breuer, G. Duderstadt, W. Dresler, R. Fichte et al.).
87. H. Franke, G. Duderstadt: "Production of Medium Carbon Ferrochromium in a Bottom Blowing Converter and its Application in Stainless Steel Production", *Int. Ferroalloy Conf. (INFACON)*, Johannesburg, South Africa, Apr. 1974.
88. Soc. d'électrochimie, d'électrométallurgie et aciéries électriques d'Ugine, US 2100265, 1932 (P. Perrin).
89. Electric Furnace Products Co., DE 860073, 1950 (H. de Wet Erasmus, H. R. Spendelow, Jr.).
90. C. G. Chadwick, *J. Met.* **13** (1961) 806–808.
91. J. Krüger in O. Winkler, R. Bakish (eds.): *Vacuum Metallurgy*, Elsevier, Amsterdam–London–New York 1971, pp. 265–268.
92. Union Carbide Corp., DE 1302764, 1961 (F. D. Hamilton, Jr., O. B. Chamberlain, Jr.).
93. Gesellschaft für Elektrometallurgie mbH, DE 1558500, 1967 (R. Fichte, H. Franke, H.-J. Retelsdorf).
94. V. P. Nemchenko et al., *Stal'* **1982**, no. 7, 37–39 (Engl. Transl. from Russ. BISI 21593).
95. GfE-Lieferprogramm, 1974.
96. Reading Alloys, US 4 331475, 1982 (F. H. Perfect).
97. R. Hähn, H. Andörfer, H.-J. Retelsdorf, *Erzmetall* **36** (1983) 459–465.
98. Shieldalloy Corp., Product Specifications MA-104, MA-106, Newfield, NJ, 1979.
99. GfF, Legierungen – Legierungsmetalle, Gesellschaft für Elektrometallurgie mbH, Düsseldorf, Mar., 1980.
100. DIN 17657, Kupfer-Vorlegierungen, 1973.
101. DIN 1725 Blatt 3, Aluminiumlegierungen – Vorlegierungen, 1973.
102. International Standard ISO 5448, Ferrochromium-Specification and Conditions of Delivery, International Organization for Standardization, 1981.
103. International Standard ISO 5449, Ferrosilicochromium-Specification and Conditions of Delivery, International Organization for Standardization, 1980.
104. ASTM Designation, A101-73, Standard Specification for Ferrochromium, American National Standard G68.1, American National Standards Institute, 1973.
105. ASTM Designation, A482.76, Standard Specification for Ferrochrome-Silicon, American National Standard G76.1, American National Standards Institute, 1976.
106. DIN 17565, Ferrochrom, Ferrochrom-Silizium und Chrom. Technische Lieferbedingungen, Arbeitsausschuß Ferrolegierungen im Deutschen Normenausschuß (DNA), 1968.
107. H.-J. Fischer, K.-D. Frank: *Erzmetall* **35** (1982) 403–409.
108. International Standard ISO 3713, Draft Proposal, Ferroalloys Sampling and Preparation of Samples, General Rules, ed. Dec., 1985.
109. Draft International Standard ISO/DIS 4140, Ferrochromium and Ferrosilicochromium Determination of Chromium Content Potentiometric Method, International Organization for Standardization, 1978.
110. Draft International Standard ISO/DIS 4158, Ferrosilicon, Ferrosilicomanganese and Ferrosilicochromium Determination of Silicon Content Gravimetric, International Organization for Standardization, 1977.
111. W.-H. Grebe, H. Kästner, C. Kippenberger, U. Krauß et al.: *Untersuchungen über Angebot und Nachfrage Mineralischer Rohstoffe, VII Chrom*, Bundesanstalt für Geowissenschaften & Rohstoffe, Hannover; Deutsches Institut fur Wirtschaftsforschung, Berlin 1975, 147 pp.
112. P. Wille, *Stahl Eisen* **103** (1983) 127–132.
113. B. M. Coope, "Chromite", *Mining Annual Review* **1984**, 65–68, published by *Min. J. (London)* **1984** (June).
114. *Chromium Review* (1983, Apr.) no. 1, 13.

115. D. P. O'Shaughnessy, *J. Met.* **37** (1985, July) 57–58.
116. *Erzmetall* **37** (1984) 478–479.
117. *Met. Bull. Mon.* **131** (1981, Nov.) 59–63.
118. J. W. Scott, *Electr. Furn. Conf. Proc.* **29** (1971) 80–82.
119. H.-J. Retelsdorf, E. Hodapp, N. Endell, *Electr. Furn. Conf. Proc.* **27** (1969) 109–114.
120. D. Liesegang, *Erzmetall* **37** (1984) 18–21.
121. Erste Allgemeine Verwaltungsvorschrift zum Bundes-Immissionsschutzgesetz, TA-Luft (Technische Anleitung zur Reinhaltung der Luft) Feb. 27, 1986.
122. D. Henschler (ed.): *Gesundheitsschädliche Arbeitsstoffe, Chrom und seine Verbindungen*, Verlag Chemie, Weinheim 1983, Part 9.
123. R. A. Person, *Electr. Furn. Conf. Proc.* **33** (1975) 39–46.
124. R. Wintersteen, *Electr. Furn. Conf. Proc.* **39** (1981) 221–225.
125. ACGIH (ed.): *Threshold Limit Values (TLV) for Chemical Substances in the Work Environment*, ACGIH, Cincinnati, OH, 1985–1986.
126. G. P. Tyroler, C. A. Landolt (eds.): *Extractive Metallurgy of Nickel and Cobalt*, The Metallurgical Society of AIME, Warrendale, PA, 1988.
127. D. J. I. Evans, R. S. Shoemaker, H. Veltman (eds.): *International Laterite Symposium*, SME-AIME, New York 1979.
128. Y. Ogura, I. Doi (eds.): "Proceedings of International Symposium on Laterite", *Int. J. Miner. Process.* **19** (1987) 1–4.
129. C. M. Diaz et al. in [126, pp. 211–239].
C. M. Diaz et al., *J. Met.* **40** (1988) no. 9, 28–33.
130. A. A. Dor, H. Skretting in [127, pp. 459–490].
131. K. Ishii in [128, pp. 15–24].
132. E. F. Osborn, A. Muan in M. K. Reser (ed.): *Phase Diagrams for Ceramacists*, American Ceramic Society, Columbus, OH, 1964, p. 236.
133. B. Wasmund, G. G. Hatch, "Systematic Approach to the Design of a High Power Electric Matte Furnace", *World Electrotechnical Congress*, Moscow 1977.
134. M. de Vernon in J. N. Anderson, P. E. Queneau (eds.): *Pyrometallurgical Processes in Non-Ferrous Metallurgy, TMS*, vol. 39, Gordon and Breach, New York 1967.
135. *Min. Mag.* **130** (1974) May, 336–349.
136. K. Yamada, T. Hiyama in [128, pp. 215–221].
137. T. Ogura, K. Kuwayama, A. Ono, Y. Yamada in [128, pp. 189–198].
138. E. Langer in [127, pp. 397–411].
139. S. C. C. Barnett, I. Patino, F. A. Perez, J. G. Schofield in *Extraction Metallurgy '85*, Inst. Min. Metall., London 1985.
140. R. R. Roberlson, I. P. Vargas, *Eng. Min. J.* **186** (1985) no. 5, 18–22.
141. *Min. Mag.* **129** (1973) July, 12–19.
142. I. H. Keith et al. in [127, pp. 123–242].
143. Knapsack, DE 2127251, 1971 (U. Thümmler, J. Rothkamp).
144. VDI-Richtlinie: *Phosphor und anorganische Phosphorverbindungen, ausgenommen Düngemittel*, VDI 3450, May 1989.
145. *Ullmann*, 3rd ed., **13**, 515.
146. H. J. Fischer, K.-D. Frank, *Erzmetall* **35** (1982) 403–409.
147. T. Massalski: *ASM Binary Alloy Phase Diagrams*, 2nd ed., American Society for Metals, Materials Park, OH, 1992.
148. *Ullmann*, 4th ed., **A22**, 54.
149. *Winnacker-Küchler*, 4th ed., **4**, 180–182.
150. J. Eube in: *Stahl, Tabellenbuch für Auswahl und Anwendung, DIN*, 1st ed., Verlag Stahleisen, Düsseldorf 1992.
151. VDEH (eds.): *Grundlagen des Hochofenverfahrens*, Verlag Stahleisen, Düsseldorf 1973.
152. A. G. E. Robiette: *Electric Smelting Processes*, Charles Griffin, London 1973.
153. R. Durrer, G. Volkert: *Metallurgie der Ferrolegierungen*, 2nd ed., Springer Verlag, Berlin–Heidelberg–New York 1972.
154. V. P. Elyutin, Y. A. Pavlov, B. E. Levin, E. M. Alekseev: *Production of Ferroalloys–Electrometallurgy*, 2nd ed., MIR Publ., Moscow 1957.
155. M. Riss, Y. Khodorovsky: *Production of Ferroalloys*, MIR Publ., Moscow 1967.
156. J. Escard: *Les fours électriques industriels et les fabrications électrothermiques*, 2nd ed., Dunod, Paris 1924, p. 458.
157. O. Kubaschewski: *Iron-Binary Phase Diagrams*, Springer Verlag, Berlin–Heidelberg–New York, Verlag Stahleisen, Düsseldorf 1982.
158. G. V. Samsonov: *Handbook of High Temperature Materials*, no. 2: *Properties Index*, Plenum Press, New York 1964.
159. A. Graf v. Matuschka: *Borieren*, Hanser Verlag, München–Wien 1977.
160. I. Barin, O. Knacke: *Thermochemical Properties of Inorganic Substances*, Springer Verlag, Berlin, Verlag Stahleisen, Düsseldorf 1973, supplement (authors: I. Barin, O. Knacke, O. Kubaschewski) 1977.
161. H. Pastor. F. Thevenot, *Inf. Chim.* 1978, no. 178, 151–170.
162. S. Sato, O. J. Kleppa, *Metall. Trans. B* **13B** (1982) 251–257.
163. *Gmelin*, Iron (system no. 59), main A2 (1929) 1177–1178.
164. L. Y. Markovskii, G. V. Kaputovskaja, *Zh. Prikl. Khim. (Leningrad)* **33** (1960) 569–577.
165. L. Y. Markovskii, E. T. Bezruk, *Zh. Prikl. Khim. (Leningrad)* **35** (1962) 491–498.
166. Mitsui Mining & Smelting Co., JP 60016/73, 1971 (T. Masuyama et al.).
167. Kawasaki Steel Corp., DE-OS 3228593, 1982, Prior. JP P174960-81 (T. Hamada et al.).
168. Mitsui Mining & Smelting Co., JP 5826025, 1981.
169. G. Volkert, K. D. Frank (ed.): *Metallurgie der Ferrolegierungen*, 2nd ed., Springer Verlag, Berlin 1972.
170. Gesellschaft für Elektrometallurgie, DE 3409311-7, 1984.
171. Metallurg Alloy Corp., New York, NY, USA; Shieldalloy Corp., Newfield, NJ; London & Scandinavian Metallurgical Co., Ltd., London, England; Gesellschaft für Elektrometallurgie mbH, Düsseldorf, Germany (private communication).
172. N. A. Chirkov et al., *Stal'* **1967**, 325–327, Transl. BISI 14535 (August 1976).

173. V. P. Elyutin, Y. A. Pavlov, B. E. Levin, E. M. Alekseev: *Production of Ferroalloys – Electrometallurgy*, 2nd ed., National Science Foundation, Washington, D.C., and the Department of the Interior; translated from Russian by the Israel Program for Scientific Translations (1961).
174. M. Riss, Y. Khodorovsky: *Production of Ferroalloys*, MIR Publishers, Moscow 1967 (transl. from the Russian by I. V. Savin).
175. G. V. Samsonov, *Vopr. Poroshk. Metall. Prochn. Mater.* **1960**, no. 8, 8–23; *Chem. Abstr.* **57** (1962) 8274c.
176. Shieldalloy Corp., Newfield, NJ: *Product Specification Data Sheet* (1979).
177. London & Scandinavian Metallurgical Co., London: *The Metallurg Companies, Products etc.* (July 1975).
178. Gesellschaft für Elektrometallurgie, Düsseldorf: *Legierungen und Legierungsmetalle*, Prospectus 1980.
179. G. P. Jones, J. Pearson, *Metall. Trans. B* **7B** (1976) 223–234.
180. DIN 17567: Ferrobor – Technische Lieferbedingungen (Jan. 1970).
181. ANSI/ASTM A 323-76: *Standard Specification for Ferroboron.*
182. P. D. Deeley, K. J. A. Kundig: *Review of Metallurgical Applications of Boron in Steel*, Shieldalloy Corp., Newfield, NJ, Metallurg Alloy Corp., New York 1982.
183. DIN 1725 Blatt 3: Aluminiumlegierungen – Vorlegierungen (June 1973).
184. Chemikerausschuß der GDMB: *Analyse der Metalle. I. Schiedsanalysen*, 3rd ed. (1966); *II. Betriebsanalysen*, 2nd ed. (1961), Springer Verlag, Berlin.
185. *Handbuch für das Eisenhütten-Laboratorium*, vol. 2a, Verlag Stahleisen, Düsseldorf 1982.
186. G. Wünsch, F. Umland in W. Fresenius, G. Jander (ed.): *Handbuch der analytischen Chemie*, 3rd part: *Quantitative Analyse*, vol. III: "Elemente der dritten Hauptgruppe, Bor", 2nd ed., Springer Verlag, Berlin–Heidelberg–New York 1971.
187. H. L. Giles, G. M. Holmes, *J. Radioanal. Chem.* **48** (1979) 65–72.
188. British Standard 1121: *Methods for the Analysis of Iron and Steel*, part 49: *Boron in Ferro-Boron. Volumetric*, 1966.
189. ASTM (E 31): *Chemical Analysis of Ferro-Alloys, Ferroboron.*
190. C. F. Seybold, *Electr. Furn. Proc.* **27** (1969) 99–108.
191. P. D. Deeley, K. J. A. Kundig, H. R. Spendelow Jr.: *Ferroalloys & Alloying Additives Handbook*, Shieldalloy Corp., Newfield, NJ, Metallurg Alloy Corp., New York, NY, 1981.
192. Allied, DE-OS 3011152, 1980.
193. W. Jaschinski, W. Wolf, *Metall (Berlin)* **36** (1982) 782–783.
194. E. W. Fajans: *Mining Annual Review – 1982*, Min. J., London, June, 1982, pp. 112–113.
195. R. Durrer, G. Volkert in G. Volkert, K.-D. Frank (eds.): *Metallurgie der Ferrolegierungen*, Springer Verlag, Berlin–Göttingen–Heidelberg 1972.
196. Vanadium Corp., US 2909427, 1958 (H. W Rathman, J. O. Staggers, H. K. Bruner).
197. Gesellschaft für Elektrometallurgie mbH, Düsseldorf, Lieferprogramm 1989.
198. A. J. DeArdo, J. M. Gray, L. Meyer: "Fundamental Metallurgy of Niobium in Steel" in H. Stuart (ed.): *Niobium–Proceedings of the International Symposium*, New York 1984, pp. 685–759.
199. S. R. Keown, F. B. Pickering: "Niobium in Stainless Steels" in H. Stuart (ed.): *Niobium–Proceedings of the International Symposium*, New York 1984, pp. 1113–1141.
200. C. T. Sims: "A Perspective of Niobium in Superalloys" in H. Stuart (ed.): *Niobium–Proceedings of the International Symposium*, New York 1984, pp. 1169–1220.
201. J. K. Tien, J. P. Collier: "Current Status and Future Developments of the Niobium and Tantalum Containing Supercalloys", *Proceedings of International Symposium on Tantalum and Niobium* 1988, Tantalum–Niobium International Study Center, Brussels, Belgium, pp. 657–679.
202. J. L. Murray, *Bull. Alloy Phase Diagrams* **2** (1981) no. 3, 393.
203. London & Scandinavian Metallurgical Co.: *Legierungselemente*, Ges. f. Elektrometallurgie, Düsseldorf 1962.
Leitner-Plöckinger in E. Plöckinger, H. Straube (eds.): *Die Edelstahlerzeugung*, 2nd Ed., Springer-Verlag, Berlin 1965.
204. T. Sims, W. C. Hagel: *The Superalloys*, Wiley, New York 1972.
205. "Micro Alloying" *75th Proceedings of an International Symposium on HSLA-Steels* 1975, Union Carbide Corp., New York 1977.
206. W. Dautzenberg, G. Volkert: "Ferrotitan", in G. Volkert, K. D. Frank (eds.): *Metallurgie der Ferrolegierungen*, 2nd ed., Springer-Verlag, Berlin 1972.
207. H.-G. Brandsleller, Ph.D. Thesis RWTH Aachen 1956.
208. Pêchiney Compagnie de produits chimiques et électrométallurgiques, FR 1321503, 1962; DE-AS 1245134, 1972.
209. Gesellschaft für Elektrometallurgie, DE 2242352, 1972.
210. G. Duderstadt, Ph.D. Thesis RWTH Aachen 1960.
211. *Erzmetall* **32** (1979) 107, 251, 354, 461; **33** (1980) 63, 241, 421, 521; **34** (1981) 50, 224, 439, 566; **35** (1982) 59, 212, 412, 549.
212. DIN 17563, Ferrovanadium, Technische Lieferbedingungen, Dec. 1965.
213. G. Roethe, W. Gocht: *Handbuch der Metallmärkte*, Springer Verlag, Berlin 1974.
214. GfE Gesellschaft für Elektrometallurgie mbH, company brochure, Nürnberg, Aug., 94.
215. J. F. Smith: *Phase Diagrams of Binary Vanadium Alloys*, American Society for Metals Int., Met. Park, OH, 1989.
216. W. Schmidt: "Untersuchungen an Vanadiummetall und seinen aluminothermisch hergestellten Legierungen mit Aluminium und Eisen", Ph. D. Thesis, RWTH Aachen 1969.
217. UCC, US 3334992, 1962.
218. O. Smetana: "Ferrovanadin und Vanadinmetall", in *Durrer-Volkert: Metallurgie der Ferrolegierungen*, 2nd ed., Springer Verlag, Berlin 1972.
219. F. Goebel, OE 169315, 1951.

220. Christiania Spigerverk, NO 115556, 1967.
221. J. K. Thorne, J. M. Dahle, L. H. Van Vlack, *Met. Trans.* **1** (1970) 2125–2132.
222. Ferrolegeringar Trollhætteverken AB, DE-OS 2716591, 1977 (J. Wallen).
223. I. Barin, O. Knacke: *Thermochemical Properties of Inorganic Substances*, Springer Verlag, Berlin and Verlag Slahleisen mbH, Düsseldorf 1973.
224. L. Northcott: *Molybdenum*, Butterworth, London 1956.
225. A. G. E. Robiette: *Electric Smelting Processes*, Charles Griffin & Co. Ltd., London 1973.
226. British Intelligence Objectives Sub-Committee: *The German Ferro-Alloy Industry*, B.I.O.S. Final Report No. 798, Trip No. RAT 71/72 Dec., 1945.
227. R. Durrer, G. Volkert in G. Volkert, K. D. Frank (eds.): *Metallurgie der Ferrolegierungen*, 2nd ed., Springer Verlag, Berlin 1972.
228. *Ullmann*, 4th ed. 7, 355.
229. H. Haag, *Erzmetall* **15** (1962) 229–234.
230. *Eng. Min. J.* **176** (1975) no. 6, 98–99.
231. M. W. Murphy, E. S. Wheeler, A. Linz, *Min. Metall* **27** (1946) 350–352.
232. J. H. Young Jr.: *Comparison of Electric Smelting Processes with Thermite Process*; Preprint von ILAFA–Latin American Seminar on Ferroalloys, Salvador de Bahia, June 22–27, 1975.
233. M. Riss, Y. Khodorovsky: *Production of Ferroalloys*, MIR Publishers, Moscow 1967.
234. V. I. Vasil'ev et al, *Sb. Tr. Chelyab. Elektrometall. Komb.* **4** (1975) 55–59; *Chem. Abstr.* **84** (1976) 138 836t.
235. V. P. Elyutin, Y. A. Pavlov, B. E. Levin, E. M. Alekseev: *Production of Ferroalloys Electrometallurgy*, 2nd ed, Israel Program for Scientific Translations, Jerusalem 1957.